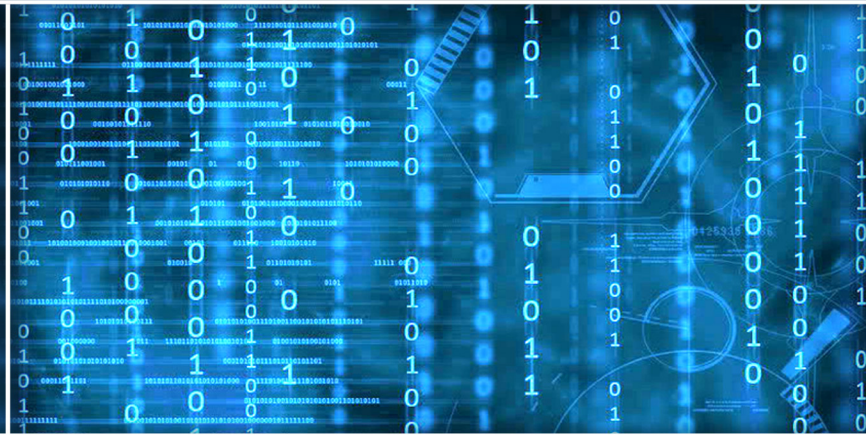


Volume 10 Issue 6

June 2019



ISSN 2156-5570(Online)

ISSN 2158-107X(Print)



# Editorial Preface

## *From the Desk of Managing Editor...*

It may be difficult to imagine that almost half a century ago we used computers far less sophisticated than current home desktop computers to put a man on the moon. In that 50 year span, the field of computer science has exploded.

Computer science has opened new avenues for thought and experimentation. What began as a way to simplify the calculation process has given birth to technology once only imagined by the human mind. The ability to communicate and share ideas even though collaborators are half a world away and exploration of not just the stars above but the internal workings of the human genome are some of the ways that this field has moved at an exponential pace.

At the International Journal of Advanced Computer Science and Applications it is our mission to provide an outlet for quality research. We want to promote universal access and opportunities for the international scientific community to share and disseminate scientific and technical information.

We believe in spreading knowledge of computer science and its applications to all classes of audiences. That is why we deliver up-to-date, authoritative coverage and offer open access of all our articles. Our archives have served as a place to provoke philosophical, theoretical, and empirical ideas from some of the finest minds in the field.

We utilize the talents and experience of editor and reviewers working at Universities and Institutions from around the world. We would like to express our gratitude to all authors, whose research results have been published in our journal, as well as our referees for their in-depth evaluations. Our high standards are maintained through a double blind review process.

We hope that this edition of IJACSA inspires and entices you to submit your own contributions in upcoming issues. Thank you for sharing wisdom.

**Thank you for Sharing Wisdom!**

**Managing Editor**  
**IJACSA**  
**Volume 10 Issue 6 June 2019**  
**ISSN 2156-5570 (Online)**  
**ISSN 2158-107X (Print)**  
**©2013 The Science and Information (SAI) Organization**

# Editorial Board

## Editor-in-Chief

**Dr. Kohei Arai - Saga University**

*Domains of Research: Technology Trends, Computer Vision, Decision Making, Information Retrieval, Networking, Simulation*

---

## Associate Editors

**Chao-Tung Yang**

**Department of Computer Science, Tunghai University, Taiwan**

*Domain of Research: Software Engineering and Quality, High Performance Computing, Parallel and Distributed Computing, Parallel Computing*

**Elena SCUTELNICU**

**"Dunarea de Jos" University of Galati, Romania**

*Domain of Research: e-Learning, e-Learning Tools, Simulation*

**Krassen Stefanov**

**Professor at Sofia University St. Kliment Ohridski, Bulgaria**

*Domains of Research: e-Learning, Agents and Multi-agent Systems, Artificial Intelligence, Big Data, Cloud Computing, Data Retrieval and Data Mining, Distributed Systems, e-Learning Organisational Issues, e-Learning Tools, Educational Systems Design, Human Computer Interaction, Internet Security, Knowledge Engineering and Mining, Knowledge Representation, Ontology Engineering, Social Computing, Web-based Learning Communities, Wireless/ Mobile Applications*

**Maria-Angeles Grado-Caffaro**

**Scientific Consultant, Italy**

*Domain of Research: Electronics, Sensing and Sensor Networks*

**Mohd Helmy Abd Wahab**

**Universiti Tun Hussein Onn Malaysia**

*Domain of Research: Intelligent Systems, Data Mining, Databases*

**T. V. Prasad**

**Lingaya's University, India**

*Domain of Research: Intelligent Systems, Bioinformatics, Image Processing, Knowledge Representation, Natural Language Processing, Robotics*

# CONTENTS

Paper 1: AHP-based Security Decision Making: How Intention and Intrinsic Motivation Affect Policy Compliance

*Authors: Ahmed Alzahrani, Christopher Johnson*

PAGE 1 – 8

Paper 2: Prediction of Visibility for Color Scheme on the Web Browser with Neural Networks

*Authors: Miki Yamaguchi, Yoshihisa Shinozawa*

PAGE 9 – 18

Paper 3: Application of the Scattering Bond Graph Methodology for Composite Right/Left Handed Transmission Lines

*Authors: Islem Salem, Hichem Taghouti, Ahmed Rahmani, Abdelkader Mami*

PAGE 19 – 24

Paper 4: Expert System for Milk and Animal Monitoring

*Authors: Todor Todorov, Juri Stoinov*

PAGE 25 – 30

Paper 5: Innovative Means of Medical Students Teaching through Graphical Methods for Cardiac Data Estimating and Serious Games

*Authors: Galya N. Georgieva-Tsaneva*

PAGE 31 – 39

Paper 6: Muscles Heating Analysis in Sportspeople to Prevent Muscle Injuries using Thermal Images

*Authors: Brian Meneses-Claudio, Witman Alvarado-Díaz, Fiorella Flores-Medina, Natalia I. Vargas-Cuentas, Avid Roman-Gonzalez*

PAGE 40 – 44

Paper 7: Advanced Metaheuristics-based Tuning of Effective Design Parameters for Model Predictive Control Approach

*Authors: Mohamed Loffi Derouiche, Soufiene Bouallègue, Joseph Haggège, Guillaume Sandou*

PAGE 45 – 53

Paper 8: Secure Medical Internet of Things Framework based on Parkerian Hexad Model

*Authors: Nidal Turab, Qasem Kharma*

PAGE 54 – 62

Paper 9: Two Dimensional Electronic Nose for Vehicular Central Locking System (E-Nose-V)

*Authors: Mahmoud Zaki Iskandarani*

PAGE 63 – 70

Paper 10: Forensic Analysis using Text Clustering in the Age of Large Volume Data: A Review

*Authors: Bandar Almaslukh*

PAGE 71 – 76

Paper 11: Internet of Things (IOT): Research Challenges and Future Applications

*Authors: AbdelRahman H. Hussein*

PAGE 77 – 82

Paper 12: Classification of Hand Movements based on Discrete Wavelet Transform and Enhanced Feature Extraction

Authors: Jingwei Too, Abdul Rahim Abdullah, Norhashimah Mohd Saad

PAGE 83 – 89

Paper 13: Modified Graph-theoretic Clustering Algorithm for Mining International Linkages of Philippine Higher Education Institutions

Authors: Sheila R. Lingaya, Bobby D. Gerardo, Ruji P. Medina

PAGE 90 – 95

Paper 14: Digital Preservation of Cultural Heritage: Terengganu Brassware Craft Knowledge Base

Authors: Wan Malini Wan Isa, Nor Azan Mat Zin, Fadhilah Rosdi, Hafiz Mohd Sarim

PAGE 96 – 102

Paper 15: Computer Students Attitudes on the Integration of m-Learning Applications

Authors: Abdulmohsin S. Alkhunaizan

PAGE 103 – 108

Paper 16: Exploring the Use of Digital Games as a Persuasive Tool in Teaching Islamic Knowledge for Muslim Children

Authors: Madihah Sheikh Abdul Aziz, Panadda Auyphorn, Mohd Syarqawy Hamzah

PAGE 109 – 113

Paper 17: Brain-Controlled for Changing Modular Robot Configuration by Employing Neurosky's Headset

Authors: Muhammad Haziq Hasbulah, Fairul Azni Jafar, Mohd. Hisham Nordin, Kazutaka Yokota

PAGE 114 – 120

Paper 18: Analysis of Spatially Modelled High Temperature Polymer Electrolyte Membrane Fuel Cell under Dynamic Load Conditions

Authors: Jagdesh Kumar, Jherna Devi, Ghulam Mustafa Bhutto, Sajida Parveen, Muhammad Shafiq

PAGE 121 – 130

Paper 19: A Collaborative Filtering Recommender System Model for Recommending Intervention to Improve Elderly Well-being

Authors: Aini Khairani Azmi, Noraswaliza Abdullah, Nurul Akmar Emran

PAGE 131 – 138

Paper 20: Forecasting Feature Selection based on Single Exponential Smoothing using Wrapper Method

Authors: Ani Dijah Rahajoe

PAGE 139 – 145

Paper 21: A Review on the Verification Approaches and Tools used to Verify the Correctness of Security Algorithms and Protocols

Authors: Mohammed Abdulqawi Saleh Al-humaikani, Lukman Bin Ab Rahim

PAGE 146 – 152

Paper 22: Performance Comparison of Detection, Recognition and Tracking Rates of the different Algorithms

Authors: Meghana Kavuri, Kolla Bhanu Prakash

PAGE 153 – 158

Paper 23: QoS-based Semantic Micro Services Discovery and Composition using ACO Algorithm

Authors: Ahmed ESSAYAH, Mohamed Youssfi, Omar Bouattane, Khalifa Mansouri, Elhocein Illoussamen

PAGE 159 – 168

**Paper 24: An Approach to Control the Positional Accuracy of Point Features in Volunteered Geographic Information Systems**

*Authors: Mennatallah H. Ibrahim, Nagy Ramadan Darwish, Hesham A. Hefny*

**PAGE 169 – 175**

**Paper 25: Android Security Development: SpywareDetection, Apps Secure Level and Data Encryption Improvement**

*Authors: Lim Wei Xian, Chan Shao Hong, Yap Ming Jie, Azween Abdullah, Mahadevan Supramaniam*

**PAGE 176 – 187**

**Paper 26: An Aspect Oriented Programming Framework to Support Transparent Runtime Monitoring of Applications**

*Authors: Abdullah O. AL-Zaghameem*

**PAGE 188 – 193**

**Paper 27: A Novel Intelligent Cluster-Head (ICH) to Mitigate the Handover Problem of Clustering in VANETS**

*Authors: A.H. Abbas, Mohammed I. Habelalmateen, L. Audah, N.A.M. Alduais*

**PAGE 194 – 203**

**Paper 28: Weld Defect Categorization from Welding Current using Principle Component Analysis**

*Authors: Hayri Arabaci, Salman Laving*

**PAGE 204 – 211**

**Paper 29: Moving Object Detection in Highly Corrupted Noise using Analysis of Variance**

*Authors: Asim ur Rehman Khan, Muhammad Burhan Khan, Haider Mehdi, Syed Muhammad Atif Saleem*

**PAGE 212 – 216**

**Paper 30: Smart Home Energy Management System Design: A Realistic Autonomous V2H / H2V Hybrid Energy Storage System**

*Authors: Bassam Zafar, Ben Slama Sami, Sihem Nasri, Marwan Mahmoud*

**PAGE 217 – 223**

**Paper 31: Evaluation of the Performance of the University Information Systems: Case of Moroccan Universities**

*Authors: Ayoub Gacim, Hicham Drissi, Abdelwahed Namir*

**PAGE 224 – 230**

**Paper 32: Immuno-Computing-based Neural Learning for Data Classification**

*Authors: Ali Al Bataineh, Devinder Kaur*

**PAGE 231 – 237**

**Paper 33: Predictive Method for Service Composition in Heterogeneous Environments within Client Requirements**

*Authors: Saleh M. Altowaijri*

**PAGE 238 – 244**

**Paper 34: Spectral Classification of a Set of Hyperspectral Images using the Convolutional Neural Network, in a Single Training**

*Authors: Abdelali Zbakh, Zoubida Alaoui Mdaghri, Abdelillah Benyoussef, Abdellah El Kenz, Mourad El Yadari*

**PAGE 245 – 250**

**Paper 35: Optical Recognition of Isolated Machine Printed Sindhi Characters using Fourier Descriptors**

*Authors: Nasreen Nizamani, Mujtaba Shaikh, Jawed Unar, Ehsan Ali, Ghulam Mustafa Bhutto, Abdul Rafay*

**PAGE 251 – 255**

Paper 36: Junction Point Detection and Identification of Broken Character in Touching Arabic Handwritten Text using Overlapping Set Theory

Authors: Inam Ullah, Mohd Sanusi Azmi, Mohamad Ishak Desa

PAGE 256 – 260

Paper 37: Implementation of Machine Learning Model to Predict Heart Failure Disease

Authors: Fahd Saleh Alotaibi

PAGE 261 – 268

Paper 38: Hyperparameter Optimization in Convolutional Neural Network using Genetic Algorithms

Authors: Nurshazlyn Mohd Aszemi, P.D.D Dominic

PAGE 269 – 278

Paper 39: New Method of Faults Diagnostic based on Neuro-Dynamic Sliding Mode for Flat Nonlinear Systems

Authors: O.Dhaou, L.Sidhom, A.Abdelkrim

PAGE 279 – 291

Paper 40: Big Data Technology-Enabled Analytical Solution for Quality Assessment of Higher Education Systems

Authors: Samiya Khan, Xiufeng Liu, Kashish Ara Shakil, Mansaf Alam

PAGE 292 – 304

Paper 41: A Novel Network user Behaviors and Profile Testing based on Anomaly Detection Techniques

Authors: Muhammad Tahir, Mingchu Li, Xiao Zheng, Anil Carie, Xing Jin, Muhammad Azhar, Naeem Ayoub, Atif Wagan, Muhammad Aamir, Liaquat Ali Jamali, Muhammad Asif Imran, Zahid Hussain Hulio

PAGE 305 – 324

Paper 42: Experimental Analysis of Color Image Scrambling in the Spatial Domain and Transform Domain

Authors: R. Rama Kishore, Sunesh

PAGE 325 – 333

Paper 43: Hijaiyah Letter Interactive Learning for Mild Mental Retardation Children using Gillingham Method and Augmented Reality

Authors: Irawan Afrianto, Agung Faishal Faris, Sufa Atin

PAGE 334 – 341

Paper 44: Causal Impact Analysis on Android Market

Authors: Hadiqa AmanUllah, Mishal Fatima, Umair Muneer, Sadaf Ilyas, Rana Abdul Rehman, Ibraheem Afzal

PAGE 342 – 350

Paper 45: Emotion Detection in Text using Nested Long Short-Term Memory

Authors: Daniel Haryadi, Gede Putra Kusuma

PAGE 351 – 357

Paper 46: Dynamic Matrix Control DMC using the Tuning Procedure based on First Order Plus Dead Time for Infant-Incubator

Authors: J. El Hadj Ali, E. Feki, A. Mami

PAGE 358 – 367

Paper 47: Dense Hand-CNN: A Novel CNN Architecture based on Later Fusion of Neural and Wavelet Features for Identity Recognition

Authors: Elaraby A. Elgallad, Wael Ouarda, Adel M. Alimi

PAGE 368 – 378

**Paper 48: Detection of Suspicious of Diabetic Feet using Thermal Image**

*Authors: Brian Meneses-Claudio, Witman Alvarado-Díaz, Fiorella Flores-Medina, Natalia I. Vargas-Cuentas, Avid Roman-Gonzalez*

**PAGE 379 – 383**

**Paper 49: Blind Image Quality Evaluation of Stitched Image using Novel Hybrid Warping Technique**

*Authors: Sanjay T. Gandhe, Omkar S. Vaidya*

**PAGE 384 – 389**

**Paper 50: Bio-inspired Think-and-Share Optimization for Big Data Provenance in Wireless Sensor Networks**

*Authors: Adel Alkhalil, Rabie Ramadan, Aakash Ahmad*

**PAGE 390 – 397**

**Paper 51: Fragile Watermarking based on Linear Cellular Automata using Manhattan Distances for 2D Vector Map**

*Authors: Saleh AL-ardhi, Vijey Thayanathan, Abdullah Basuhail*

**PAGE 398 – 403**

**Paper 52: A Watermarking System Architecture using the Cellular Automata Transform for 2D Vector Map**

*Authors: Saleh AL-ardhi, Vijey Thayanathan, Abdullah Basuhail*

**PAGE 404 – 410**

**Paper 53: Electromyography Signal Acquisition and Analysis System for Finger Movement Classification**

*Authors: Alvarado-Díaz Witman, Meneses-Claudio Brian, Roman-Gonzalez Avid*

**PAGE 411 – 416**

**Paper 54: Blood Vessels Segmentation in Retinal Fundus Image using Hybrid Method of Frangi Filter, Otsu Thresholding and Morphology**

*Authors: Wiharto, YS. Palgunadi*

**PAGE 417 – 422**

**Paper 55: A New Image Inpainting Approach based on Criminisi Algorithm**

*Authors: Nouho Ouattara, Georges Laussane Loum, Ghislain Koffi Pandry, Armand Kodjo Atiampo*

**PAGE 423 – 433**

**Paper 56: Improving Knowledge Sharing in Distributed Software Development**

*Authors: Sara Waheed, Bushra Hamid, NZ Jhanjhi, Mamoona Humayun, Nazir A Malik*

**PAGE 434 – 443**

**Paper 57: IRPanet: Intelligent Routing Protocol in VANET for Dynamic Route Optimization**

*Authors: Rafi Ullah, Shah Muhammad Emad, Taha Jilani, Waqas Azam, Muhammad Zain uddin*

**PAGE 444 – 450**

**Paper 58: Depth Limitation and Splitting Criteria Optimization on Random Forest for Efficient Human Activity Classification**

*Authors: Syarif Hidayat, Ahmad Ashari, Agfianto Eko Putra*

**PAGE 451 – 458**

**Paper 59: The Mathematical Model of Hybrid Schema Matching based on Constraints and Instances Similarity**

*Authors: Edhy Sutanta, Erna Kumalasari Nurnawati, Rosalia Arum Kumalasanti*

**PAGE 459 – 464**



**Paper 60: The Role of Technical Analysis Indicators over Equity Market (NOMU) with R Programming Language**

*Authors: Mohammed A. Al Ghamdi*

**PAGE 465 – 471**

**Paper 61: A Circular Polarization RFID Tag for Medical Uses**

*Authors: Nada Jebali, Ali Gharsallah*

**PAGE 472 – 479**

**Paper 62: Passenger and Luggage Weight Monitoring System for Public Transport based on Sensing Technology: A Case of Zambia**

*Authors: Apolinalious Bwalya, Jackson Phiri, Monica M. Kalumbilo, David Zulu*

**PAGE 480 – 489**

**Paper 63: Survey Energy Management Approaches in Data Centres**

*Authors: Bouchra Morchid, Siham Benhadou, Mariam Benhadou, Abdellah Haddout, Hicham Medromi*

**PAGE 490 – 495**

**Paper 64: Comparative Study of Methods that Detect Levels of Lead and its Consequent Toxicity in the Blood**

*Authors: Kevin J. Rodriguez, Alicia Alva, Virginia T. Santos, Avid Roman-Gonzalez*

**PAGE 496 – 499**

**Paper 65: Smart Smoking Area based on Fuzzy Decision Tree Algorithm**

*Authors: Iswanto, Kunnu Purwanto, Weni Hastuti, Anis Prabowo, Muhamad Yusvin Mustar*

**PAGE 500 – 504**

**Paper 66: A Comprehensive Collaborating Filtering Approach using Extended Matrix Factorization and Autoencoder in Recommender System**

*Authors: Mahamudul Hasan, Falguni Roy, Tasdikul Hasan, Lafifa Jamal*

**PAGE 505 – 513**

**Paper 67: Satellite Image Enhancement using Wavelet-domain based on Singular Value Decomposition**

*Authors: Muhammad Aamir, Ziaur Rahman, Yi-Fei Pu, Waheed Ahmed Abro, Kanza Gulzar*

**PAGE 514 – 519**

**Paper 68: Convolutional Neural Networks in Predicting Missing Text in Arabic**

*Authors: Adnan Soury, Mohamed Alachhab, Badr Eddine Elmohajir, Abdelali Zbakh*

**PAGE 520 – 527**

**Paper 69: Multi-Modal Biometric: Bi-Directional Empirical Mode Decomposition with Hilbert-Hung Transformation**

*Authors: Gavisiddappa, Chandrashekar Mohan Patil, Shivakumar Mahadevappa, Pramod KumarS*

**PAGE 528 – 537**

**Paper 70: Heuristics Applied to Mutation Testing in an Impure Functional Programming Language**

*Authors: Juan Guti´errez-C´ardenas, Hernan Quintana-Cruz, Diego Mego-Fernandez, Serguei Diaz-Baskakov*

**PAGE 538 – 548**

**Paper 71: Exploiting the Interplay among Products for Efficient Recommendations**

*Authors: Anbarasu Sekar, Sutanu Chakraborti*

**PAGE 549 – 556**

**Paper 72: An Assessment of Open Data Sets Completeness**

*Authors: Abdulrazzak Ali, Nurul A. Emran, Siti A. Asmai, Amelia R. Ismail*

**PAGE 557 – 562**

**Paper 73: Design and Application of a Smart Diagnostic System for Parkinson's Patients using Machine Learning**

*Authors: Asma Channa, Attiya Baqai, Rahime Ceylan*

**PAGE 563 – 571**

**Paper 74: An Effective Framework for Tweet Level Sentiment Classification using Recursive Text Pre-Processing Approach**

*Authors: Muhammad Bux Alvi, Naeem A. Mahoto, Mukhtiar A. Unar, M. Akram Shaikh*

**PAGE 572 – 581**

**Paper 75: Competitive Algorithms for Online Conversion Problem with Interrelated Prices**

*Authors: Javeria Iqbal, Iffikhar Ahmad, Asadullah Shah*

**PAGE 582 – 589**

**Paper 76: Introducing Multi Shippers Mechanism for Decentralized Cash on Delivery System**

*Authors: Hai Trieu Le, Ngoc Tien Thanh Le, Nguyen Ngoc Phien, Nghia Duong-Trung, Ha Xuan Son, Thai Tam Huynh, The Phuc Nguyen*

**PAGE 590 – 597**

**Paper 77: Content-based Automatic Video Genre Identification**

*Authors: Faryal Shamsi, Sher Muhammad Daudpota, Sarang Shaikh*

**PAGE 598 – 607**

**Paper 78: A Comparison of Sentiment Analysis Methods on Amazon Reviews of Mobile Phones**

*Authors: Sara Ashour Aljuhani, Norah Saleh Alghamdi*

**PAGE 608 – 617**

**Paper 79: Virtualizing a Cluster to Optimize the Problems of High Scientific Complexity within an Organization**

*Authors: Enrique Lee Huamaní, Patricia Condori, Avid Roman-Gonzalez*

**PAGE 618 – 622**

**Paper 80: School Manager System based on a Personal Information Architecture**

*Authors: Elena Fabiola Ruiz Ledesma, Elizabeth Moreno Galván, Juan Jesús Gutiérrez García, Chadwick Carreto Arellano*

**PAGE 623 – 629**

**Paper 81: Fusing Identity Management, HL7 and Blockchain into a Global Healthcare Record Sharing Architecture**

*Authors: Mohammad A. R. Abdeen, Toqeer Ali, Yasar Khan, M. C.E. Yagoub*

**PAGE 630 – 636**

**Paper 82: An Efficient Machine Learning Technique to Classify and Recognize Handwritten and Printed Digits of Sudoku Puzzle**

*Authors: Sang C. Suh, Aghalya Dharshni Manmatharaj*

**PAGE 637 – 642**

# AHP-based Security Decision Making: How Intention and Intrinsic Motivation Affect Policy Compliance

Ahmed Alzahrani<sup>1</sup>, Christopher Johnson<sup>2</sup>

School of Computing Science  
University of Glasgow  
Glasgow, UK

**Abstract**—Analytic hierarchy process is a multiple-criteria tool used in applications related to decision-making. In this paper, analytic hierarchy process is used as guidance in information security policy decision-making by identifying influencing factors and their weights for information security policy compliance. The weights for intrinsic motivators are identified based on self-determination theory as essential criteria, namely, autonomy, competence, relatedness, along with behavioural intention towards compliance; and use four awareness focus areas. A survey of cyber-security decision-makers at a Fortune 600 organisation provided data. The results suggest that behavioural intention (52% of the weight of influencing factors) is more important than autonomy (21%), competence (21%) or relatedness (6%) in influencing behaviour towards information security policy compliance. Determining weights of intrinsic motivation, intention, and awareness focus areas can help security decision-making and compliance with policy, and support design of effective security awareness programmes. However, these weights may in turn be affected by local organisational and cultural factors.

**Keywords**—Analytic Hierarchy Process; behavioural intention; autonomy; competence; relatedness; information security policy compliance

## I. INTRODUCTION

Policy decision making is one of the most challenging tasks in the field of information security and compliance. It must consider multiple aspects in a stable form to for appropriate decision making to deal with the actual situation as well as future planning.

Analytic Hierarchy Process (AHP), initially developed by Thomas L. Saaty in 1972 [1], is widely used in the Multi-Criteria decision-making method to solve complex decision problems. AHP quantifies related priorities for specific alternatives on a scale according to decision-makers' judgment [2]. It uses both mathematics and the psychology of human decision-making based on pair-wise comparisons to measure the criteria for a specific problem [3]. Moreover, it helps regulate tangible and intangible criteria in an organised way by providing a simple solution to the decision-making problem. It also provides a comparison of both quantitative and qualitative information based on decision-makers' judgements to obtain weights and priorities [2]. The AHP approach uses hierarchical levels for decomposing a complex problem into multiple sub-problems. The first level represents the goal of decision making, and the higher levels represent a set of criteria and alternatives [4] (see Section III, Fig. 2).

In this paper, the three essential elements of self-determination theory (SDT), autonomy, competence and relatedness have been extensively used. They were analysed for their potential to enhance the intrinsic motivation of employees and, their behavioural intention toward security policy compliance. SDT, developed by Deci and Ryan [5] helps to understand developmental and psychological requirements for analysing the roots of motivation and personality. This theory focuses on an individual's behaviour, self-motivation and determined for target behaviour. Motivation is divided into extrinsic and intrinsic motivation, along with the three psychological requirements of competence, autonomy and relatedness [5][6]. SDT has been chosen for two reasons: From a theoretical perspective, adoption of SDT in the field of information security is under-researched, even though SDT has successfully improved intrinsic motivation in fields like health and education. From a practical standpoint, the results of this study can help provide an organisation with a new perspective on the ability of intrinsic motivation to encourage compliance and, ultimately, address a wide range of potential security vulnerabilities.

Further, the AHP method for guiding policy decision-making was used to determine the factors and their weights for ensuring compliance with ISPs. This analysis indicates that determining weights of intrinsic motivation factors, and awareness focus areas, can potentially help decision-making on security compliance policy and designing proper security awareness programmes for an organisation, as discussed in Section 6.

This paper examines AHP as a method to support cyber security decision-making within a Fortune 600 organisation. The paper uses AHP to identify the weights for intrinsic motivation and behavioural intention to comply with the information security policy, which helps security decision-makers design suitable security awareness programmes.

The paper is organised as follows: Section II provides a review of related work in the field. Section III describes the methodology followed in conducting this study. Section IV presents the study analysis. The reporting results are presented and discussed in Section V, followed by recommendation in Section VI. Section VII presents the study limitations, avenues for future work and Section VIII presents the study conclusions.

## II. BACKGROUND

### A. Theoretical Foundation

Information security policy is a challenging field for decision makers, who face many dynamic aspects related to evolving cyber-security threats. Employee motivation plays an essential role in compliance with policy. An information security policy presents the acceptable practice of employees of an organisation and prescribes penalties for violations. There must be efforts to encourage employees toward compliance with the existing policy. This implies that the intrinsic motivation of employee to comply with information security policies can help to achieve long term advantages for the organisation. The significant factors involved in intrinsic motivation, in the SDT model, include autonomy, competence and relatedness, as described below.

1) *SDT component:* Autonomy refers to the desire of people to be able to choose a course of action that matches their inner beliefs [7]. It targets a personal desire for protecting their scope for action and decision-making [8]. A sense of autonomy supports an increase in intrinsic motivation to follow an organisation's rules, regulations and policies. Wall, Palvia, and Lowry [9] analysed the effect of autonomy as control-related motivation and the efficacy of employees' intentions toward policy compliance. The authors reported that an increased perception of autonomy increased the perception of efficacy, which improved employees' compliance with their organisations' policies.

Competence refers to the people's assessment of their ability to do the task at hand and their likelihood of obtaining the desired results [10]. It measures employees' perception of whether they have relevant skills to accomplish specific security tasks for compliance of information security policy. A sense of competence helps people feel confident in their ability to defend sensitive information of the organisation. Per SDT, competence is similar to self-efficacy for individuals' skills and abilities for performing a specific security task [11]. Thus, competence helps to reduce the stress and anxiety that are often related to information security policies like encryption and access control measures.

Relatedness measures an individual's requirement for remaining connected to others and being understood, valued and accepted by them. In SDT, relatedness is directly affected by the security culture within an organisation. Security culture involves employees' shared beliefs and values about cyber-security [12]. An increase in relatedness helps to increase the level of intrinsic motivation for compliance with information security policies. Organisational culture establishes the shared set of expectations and beliefs among members of the organisation, and partially determines the behaviour of each member of the organisation. Compliance is positively affected by a shared and accepted security culture [12].

2) *Behavioural intention:* Behavioural intention is a combined product of subjective norms, attitudes toward the behaviour, and perceived behavioural control [13]. A favourable opinion of a person towards behaviour and subjective norms leads to more perceived behavioural control

and a firmer intention of the person to perform the target behaviour. In addition, individuals are supposed to present their intentions for providing chances for a given level of actual control over the behaviour [13]. The theory of planned behaviour focuses the knowledge for required skills in performing the behaviour, experience with the behaviour, and environmental factors [14]. The behaviour intention is determined by perceived behaviour control along with attitude and subjective norms. The jointly-established intention can be directly interpreted as the amount of control over the behaviour. The combined determination of the behaviour and the intention is related to motivation and a sense of control over the behaviour and hence affects compliance with information security policy.

### B. Analytic Hierarchy Process

Analytic hierarchy process (AHP) is widely used as a multiple-criteria decision-making tool for applications in diverse fields such as planning, selecting the best alternative, resource allocation, resolving conflicts, and optimisation. AHP is an appropriate tool for this study as it addresses the hierarchical requirements of the proposed model.

The AHP method has been widely used in banking, manufacturing systems, education, healthcare, the military, information technology and many other areas for more than thirty years [15], [16]. AHP supports planning, resource allocation, evaluation, development and optimisation [2]. The study by Vaida and Kumar [16] provides a complete literary review.

In the context of information security, several studies have used AHP to evaluate information security policy from decision-making perspectives and for assessing information security awareness training.

Syamsuddin and Hwang [2], used the AHP approach to develop a framework for decision-makers to evaluate information security policy performance. To get decision-maker preferences, they used a survey based on AHP methodology prior to more detailed data analysis. The authors found that the availability of information security got the highest priority by decision makers, followed by confidentiality and integrity. Likewise, the authors used AHP to develop a model for information security policy decision making [17]. They used four security policy factors (management, technology, economy and culture) and three security components (confidentiality, integrity and availability) to develop their model. Their findings indicated that AHP helps policymakers make appropriate decisions by using qualitative and quantitative methods.

Syamsuddin [18] also evaluated information security policy decision-making in e-government systems via the AHP method. The results showed that decision-makers preferred management and technology as the essential aspects of information security and that availability of information was more important than other information security aspects. Also, the author stated that using AHP supported evaluation of the performance of information security policy in both qualitative and quantitative ways.

Kruger and Kearney [19] developed a prototype model for information security awareness measurement at an international gold mining company. The authors used AHP to determine the relative weights of information security awareness assessment across three dimensions (knowledge, attitude and behaviour). Also, their awareness programme used six focus areas (adhere to policies, keep password secret, email and internet, mobile equipment, incident reports and all actions carry consequences). A spreadsheet application was used to process importance weights based on the AHP method. In their findings, they stated that the effectiveness of measurement by the model relies on the importance weightings that must be obtained from key management’s professional judgement.

Kruger and Kearney [20] used AHP to determine the relative importance weights for knowledge, attitude and behaviour to implement an information-security awareness programme. They used AHP to determine the weights of alternative elements (the awareness programme topics were: adhere to policies, keep password secret, email and internet, mobile equipment, incident reports, and all actions carry consequences) in the AHP model. According to key managers’ professional judgements and opinions, behaviour had an importance weight of 50% compared to knowledge (30%) and attitude (20%). Whereas the main security principles (confidentiality, integrity and availability) focus on protecting information, security awareness helps the organisation create and sustain the positive security behaviour of employees [19]. Hence, the organisation will ensure that employees do not create expensive, avoidable mistakes concerning information security and that they will have a good understanding of their information security policy and procedures [21][22].

### III. METHODOLOGY

The flowchart of the proposed method is shown in Fig. 1. Further details are in the following sections.

#### A. Study Method Assessment and Refinement of Measurement Scales

Two independent researchers in the AHP field confirmed the study method. They also conducted a final validation of the AHP questionnaire before it was distributed. Their feedback helped to improve the questionnaire’s design.

#### B. Data Collection Procedure

The AHP questionnaire was shared with a Fortune 600 organisation to obtain responses from cyber-security managers and experts. The head of the information security awareness group was asked to send an email including the survey link and a description of the study objectives to security managers and experts. The participants were not asked to state their names or email addresses. As shown in Table I, an AHP preference scale [23] was used for this study to derive priorities for each factor in the form of questions such as, “How important is autonomy compared to competence?” (cf. Appendix 1, Section A.1).

#### C. The Proposed Decision Model

To determine the important weights for autonomy, competence, relatedness, and intention, a new model is proposed as seen in Fig. 2. The model is divided into a three-level hierarchy based on the previous literature study. Level

one shows the goal of this study, which is information security weight decision making, followed by three components of SDT with intention in level two and four security awareness focus areas in the third level. The security awareness focus areas were selected based on the incidents report from a Fortune 600 organisation and was validated by security managers and experts within the same organisation.

#### D. AHP Method

The AHP method can easily be applied to a complex decision problem in four steps [24], as given in the instructions below.

- Step 1: Define the decision problem as a hierarchy. This is the most important aspect of AHP; the problem is decomposed into a hierarchy of like elements as shown in Fig. 2. The model includes three levels (goal, criteria and alternatives).
- Step 2: Use pairwise comparisons of decision elements. Break down the problem into a hierarchy to obtain the local weight of each element. This step compares an element of a specific level in relation to an element in the level directly above it.
- Step 3: Calculate the local weights and consistency of comparison matrices. The local weights of all elements are determined using the eigenvalue method (EVM). “The normalised eigenvector corresponding to the principal eigenvalue of the judgement matrix provides the weights of the corresponding elements” [2].
- Step 4: Obtain the final weights of elements by aggregating the weights of decision elements across different levels. Here, the local weights of decision elements from all levels are aggregated to calculate the final weights of the alternatives (security awareness focus areas in the third level).

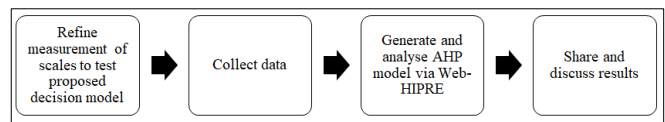


Fig. 1. Flowchart of the Proposed Method.

TABLE I. SAATY’S PAIRWISE COMPARISON SCALE

| Scale value              | Definition Criterion X in comparison to Y |
|--------------------------|---|
| Equal Importance         | 1   |
| Equally to Moderately    | 2   |
| Moderate Importance      | 3   |
| Moderately to Strong     | 4   |
| Strong Importance        | 5   |
| Strongly to very strong  | 6   |
| Very strong Importance   | 7   |
| Very strong to extremely | 8   |
| Extreme Importance       | 9   |

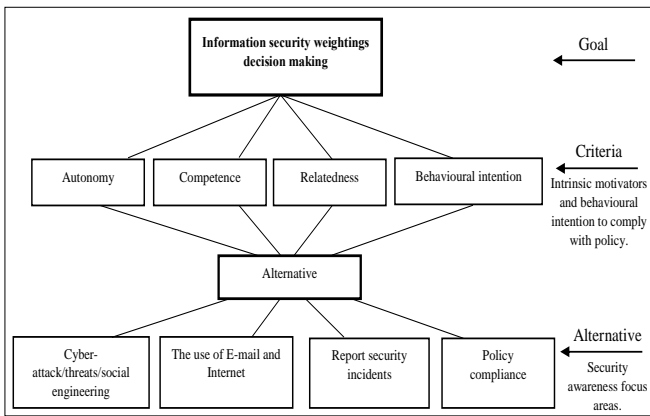


Fig. 2. Information Security Weighting Decision-Making Model.

#### IV. DATA ANALYSIS

This study makes use of the Web-HIPRE to generate and analyse the AHP model. Web-HIPRE is an adaptation of AHP which enables a decision maker to form a robust decision model [25]. The complex decision problem is entered by providing general labels in the decision tree, at each of the node levels. After that, the problem components need to be entered. Then, to make effective use of the Web-HIPRE algorithms, the user must enter pair-wise preferences at every node level for criteria, sub-criteria and alternatives. After this process has been carried out, the suitable analysis algorithm is used to determine the model’s recommendation. The algorithm of Web-HIPRE makes it possible to perform sensitivity analysis. This process ascertains the criteria or sub criteria which play a dominant role in the entire decision-making process. The algorithm is designed so it can be employed to a group mode as well. The algorithm of WebHIPRE allows an issue or problem to be structured based on specific criteria and alternatives. Then each of the critical decision-making components is linked with web pages so that the specific details relating to the criteria, sub-criteria and alternatives can be understood in a simpler manner. The Web-HIPRE software uses AHP to calculate the consistency measure (CM) using the formula shown in Fig. 3.

In this formula, “ $r(i,j)=\max a(i,k)a(k,j), k \in \{1,..,n\}$ ” stands for the extended bound of the comparison matrix element  $a(i,j)$ , and  $r(i,j)$  is the inverse of  $r(j,i)$ . Thus, the consistency measure is an indicator of the size of this extended region formed by the set of local preferences such that  $W_i \leq r(i,j)W_j$  for all  $i,j \in \{1,..,n\}$ ” [25]. For example, as shown in (Appendix 1, Section A.1: criteria comparisons), participating security decision-makers were asked to respond to pairwise comparison questions of autonomy, such as, “How important is the cyber-attack awareness focus area relative to the use of internet and email awareness focus area?” The decision-makers could use local organisational and cultural factors to choose the proper awareness focus area that would best address autonomy motivator needs. After that, Web-HIPRE was used to find the CM of the pairwise comparison of autonomy according to the decision-makers’ inputs. As shown in Table 3, the cyber-attack awareness focus area had the top priority consideration of 0.568, with a CM at an acceptable level of 0.060, which is less than Saaty’s maximum acceptable value of 0.10 [23].

$$CM = \frac{2}{n(n-1)} \sum_{i>j} \frac{\bar{r}(i,j) - \underline{r}(i,j)}{(1 + \bar{r}(i,j))(1 + \underline{r}(i,j))}$$

Fig. 3. Consistency Measure Formula.

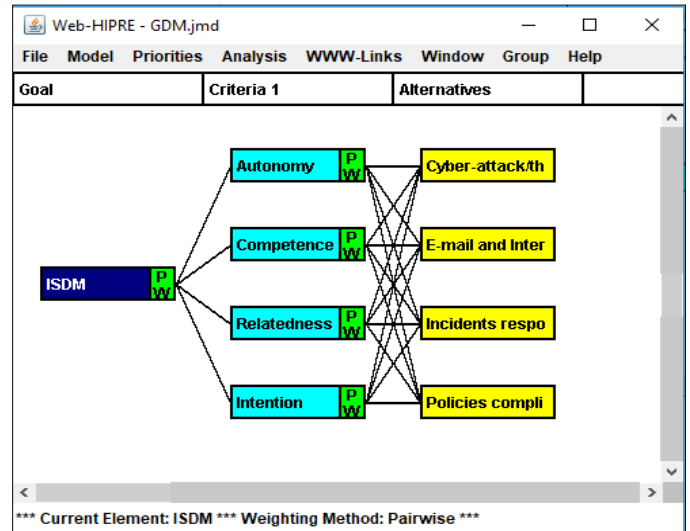


Fig. 4. Information Security Decision Making (ISDM) Model.

CM is a vital element of Web-HIPRE as it converts inconsistent decision elements or replies into an “extended” series of appropriate preference statements. It helps to mitigate the inconsistencies that could arise in the decision-making process and makes it more uniform in nature. The measure basically ranges between 0 and 1, and its value gets higher with an increase in the inconsistency of the comparison matrix elements. The algorithm establishes interconnections among the core decision-making elements. This helps to arrive at the final decision that can be implemented to solve the problem at hand. One of the unique aspects of the algorithm is the ability to structure the entire issue in smaller segments so that each of the core decision-making components can be critically considered by the software.

Fig. 4 shows the first step of the AHP analysis method, which defines the decision problem as a hierarchy. The figure shows the AHP model developed in Web-HIPRE, based on Fig. 2 that includes four criteria and four alternatives to achieve the study goal. Subsequently, all responses from respondents are inserted into the compression windows for each intrinsic motivator, as well as for intention to comply with ISP.

#### V. RESULTS AND DISCUSSION

Tables II to VII show the complete paired comparison matrix. Respondents’ inputs were used to make a pairwise comparison for each factor depicted in 3. Table II illustrates the pairwise comparison of criteria with respect to the goal, based on the second step of the AHP analysis method. It is clearly showed that intention is the most important factor among the three components of SDT and controls 57% of overall information security weighted decision making. Autonomy and competence factors controlled similar importance weights of

18.7% and 17.5% respectively. The relatedness factor had the lowest priority among all other factors, with 6.7% of local weight. As can be seen in Table II, the consistency ratio value is 0.081, which means good consistency since it's below Saaty's maximum acceptable value of 0.10 [23].

Tables III to VI explain the local weights of comparative alternatives based on four criteria that define the local weight value of the four security awareness focus areas (cyber-attack, the use of email and internet, incident response and policy compliance) according to the third step of the AHP analysis method. Respondents' inputs were used to make a pairwise comparison for each factor, as shown in (Appendix 1, Section A.2 to A.5). The consistency measure values of these factors are below the acceptable value of 0.10, showing very good consistency. To get the overall priorities of all decision factors, all factors' local weights were calculated and aggregated them into an overall weight value as shown in Table VI. Policy compliance is preferred as the top awareness focus area with the value of 0.293, followed by use of email and internet and

incident response, which have similar priority values of 0.255 and 0.259. Cyber-attack accounted for only 0.193. The final result indicated that intention, with 52%, is considered more important than the other three components of SDT. Autonomy and competence have similar importance priorities of approximately 21%. Relatedness accounted for 6%.

According to these findings, decision-makers in the organisation put the most emphasis on policy compliance as the top priority among all other alternatives or awareness focus areas (the others being cyber-attack, the use of email and internet and incident response). This also reflects the top priority of intention towards compliance in the organisation among the other three components of SDT. Hence, decision-makers believe that employees' intentions play an essential role in policy compliance in the organisation, along with autonomy and competence. On the other hand, decision-makers considered relatedness as the lowest priority among all elements, and that it had a minimal effect on employee behaviour towards policy compliance.

TABLE II. PAIRWISE COMPARISON OF CRITERIA

|                             | Autonomy | Competence | Relatedness | Intention | Local weight |
|-----------------------------|----------|------------|-------------|-----------|--------------|
| Autonomy                    | 1.0      | 1.0        | 3.0         | 0.33      | 0.187        |
| Competence                  | 1.0      | 1.0        | 3.0         | 0.25      | 0.175        |
| Relatedness                 | 0.33     | 0.33       | 1.0         | 0.14      | 0.067        |
| Intention                   | 3.0      | 4.0        | 7.0         | 1.0       | 0.571        |
| Consistency Measure = 0.081 |          |            |             |           |              |

TABLE III. PAIRWISE COMPARISON OF AUTONOMY

|                             | Cyber-attack | E-mail and Internet | Incidents response | Policies compliance | Local weight |
|-----------------------------|--------------|---------------------|--------------------|---------------------|--------------|
| Cyber-attack                | 1.0          | 4.19                | 4.22               | 3.52                | 0.568        |
| E-mail and Internet         | 0.24         | 1.0                 | 1.0                | 1.17                | 0.148        |
| Incidents response          | 0.24         | 1.0                 | 1.0                | 0.85                | 0.136        |
| Policies compliance         | 0.28         | 0.85                | 1.17               | 1.0                 | 0.148        |
| Consistency Measure = 0.060 |              |                     |                    |                     |              |

TABLE IV. PAIRWISE COMPARISON OF COMPETENCE

|                             | Cyber-attack | E-mail and Internet | Incidents response | Policies compliance | Local weight |
|-----------------------------|--------------|---------------------|--------------------|---------------------|--------------|
| Cyber-attack                | 1.0          | 0.3                 | 0.3                | 0.25                | 0.086        |
| E-mail and Internet         | 3.29         | 1.0                 | 1.04               | 0.83                | 0.288        |
| Incidents response          | 3.38         | 0.96                | 1.0                | 1.13                | 0.308        |
| Policies compliance         | 3.99         | 1.2                 | 0.88               | 1.0                 | 0.319        |
| Consistency Measure = 0.063 |              |                     |                    |                     |              |

TABLE V. PAIRWISE COMPARISON OF RELATEDNESS

|                             | Cyber-attack | E-mail and Internet | Incidents response | Policies compliance | Local weight |
|-----------------------------|--------------|---------------------|--------------------|---------------------|--------------|
| Cyber-attack                | 1.0          | 0.3                 | 0.32               | 0.29                | 0.093        |
| E-mail and Internet         | 3.28         | 1.0                 | 1.0                | 1.0                 | 0.303        |
| Incidents response          | 3.09         | 1.0                 | 1.0                | 0.91                | 0.291        |
| Policies compliance         | 3.4          | 1.0                 | 1.1                | 1.0                 | 0.313        |
| Consistency Measure = 0.018 |              |                     |                    |                     |              |

TABLE VI. PAIRWISE COMPARISON OF INTENTION

|                             | Cyber-attack | E-mail and Internet | Incidents response | Policies compliance | Local weight |
|-----------------------------|--------------|---------------------|--------------------|---------------------|--------------|
| Cyber-attack                | 1.0          | 0.34                | 0.39               | 0.3                 | 0.102        |
| E-mail and Internet         | 2.94         | 1.0                 | 0.83               | 0.97                | 0.284        |
| Incidents response          | 2.59         | 1.2                 | 1.0                | 0.84                | 0.291        |
| Policies compliance         | 3.31         | 1.03                | 1.19               | 1.0                 | 0.324        |
| Consistency Measure = 0.069 |              |                     |                    |                     |              |

TABLE VII. FINAL RESULT

| Goal           | Cyber-attack | E-mail and Internet | Incidents response | Policies compliance | Overall weight |
|----------------|--------------|---------------------|--------------------|---------------------|----------------|
| Autonomy       | 0.119        | 0.031               | 0.028              | 0.031               | 0.209          |
| Competence     | 0.018        | 0.060               | 0.064              | 0.066               | 0.207          |
| Relatedness    | 0.006        | 0.019               | 0.018              | 0.020               | 0.063          |
| Intention      | 0.051        | 0.145               | 0.148              | 0.176               | 0.521          |
| Overall weight | 0.193        | 0.255               | 0.259              | 0.293               |                |

## VI. RECOMMENDATION

The AHP results can be used to design a proper security awareness programme which may help to enhance policy compliance. Also, this results can be used for data processing and transform it into meaningful information using the matrices presented in Table VII such as [19][20]. As shown by the final results in Table VII, the following are recommended when designing an awareness programme based on intrinsic motivation on the basis of SDT:

### A. Autonomy

As shown in Table VII, cyber-attack has the highest priority value of 0.119 over other awareness focus areas toward autonomy. Since autonomy focuses on the desire to protect an individual's scope for action and decision-making [8], [20], it is recommended that the organisation develop suitable awareness programmes that focus on cyber-attacks, threats and social engineering to increase employees' decision-making ability when they face real-world attacks.

### B. Competence

As can be seen in Table VII, the awareness focus areas related to competence (use of email and internet, incident response and policy compliance) have similar priority values of 0.060, 0.064 and 0.066 while cyber-attack has only 0.018. As a result, since competence measures employees' perception of whether they possess the relevant skills to achieve particular security tasks, it is recommended that the organisation focus on those three areas to increase employees' security knowledge.

### C. Relatedness

While it has the lowest priority value among the other factors, it is still recommended that the organisation develop suitable awareness programmes that focus on the use of email and internet, incident response and policy compliance, because they have similar priority values of 0.019, 0.018 and 0.020. Cyber-attack has only 0.006. The awareness programme should meet the relatedness requirements: the individual's need to be understood, valued, accepted, and connected to others. This would be achieved either in class or online awareness courses to encourage involvement, participation, and discussion among

employees. If they share good security knowledge with each other, employees will be more likely to comply with their organisation's security policy.

### D. Intention

As shown in Table VII, the awareness focus areas related to intention (use of email and internet, incident response and policy compliance) have a similar priority value of 0.145, 0.148 and 0.176, while cyber-attack has only 0.051. Intention has the highest priority among the factors and it refers to activities employees must carry out to maintain information security as defined by their organisation's policy. Therefore, it is recommended that the organisation develop awareness programmes that focus on these areas to increase employees' intentions towards compliance. Employees who show less than suitable behaviour with regard to their organisation's policy might benefit from regular awareness sessions and training. The primary goals of security awareness are to enhance employees' behaviour towards policy compliance and to establish good security practices.

## VII. LIMITATIONS AND FUTURE WORK

Despite efforts to increase accuracy, this study has a notable limitation: it only used data collected from cyber-security managers and experts of a single large organisation in Saudi Arabia, which potentially undermines its generalisability. Future research may consider conducting the study with a different organisation or even in another country to explore the generalisability of its results and provide more evaluation of the information security weighing decision-making model.

This study demonstrates that AHP is powerful method to support decision-making about complex sustainability issues. Also, AHP helped participating decision makers recognise and outline complex problem in detail. However, despite the strengths of AHP, there are some issues with its methodology. Since AHP can divide a complex problem into a number of sub-levels, this may lead to very large number of pairwise comparisons that must be made. Processing the input for each sublevel can be time-consuming. Decision-makers who took part in this study had difficulty using the 9-point scale (see Table I). They reported that it was difficult to distinguish



between the nine points to decide, for example, whether one criteria or alternative was 6 or 7 times more important than another. The scale problem seems to be common and some researchers, such as Hajkovicz *et al.* [26] modified the procedure by using a 2-point scale, (more or less important or equally important) in the field of natural resources management. Hence, future work of this study may conduct more research into the applicability of an alternative to the 9-point scale in the field of security policy compliance. This may help participants provide their feedback with fewer restrictions and less confusion.

### VIII. CONCLUSION

In conclusion, this study attempts to help organisations determine the important factors and their weights for information security decision making by using the AHP method. Using AHP, this study proposes a model that uses four criteria (autonomy, competence, relatedness, and intention) and four alternative awareness focus areas (cyber-attack, the use of email and internet, incident response and policy compliance). The study demonstrates that intention represents the highest priority, followed by autonomy and competence while relatedness has the lowest weight. Also, the study concludes that policy compliance, the use of email and internet and incident response are the essential security awareness topics that should be addressed under the requirements of competence, relatedness, and intention. In contrast, the result recommends using only cyber-attack, threats and social engineering awareness topics to discuss the needs of autonomy to increase employees' decision-making ability when they face real-world attacks.

### REFERENCES

- [1] T. L. Saaty, "An eigenvalue allocation model for prioritization and planning," *Energy Manag. Policy Center, Univ. Pennsylvania*, pp. 28–31, 1972.
- [2] I. Syamsuddin, J. H.- JSW, and undefined 2010, "The Use of AHP in Security Policy Decision Making: An Open Office Calc Application.," Citeseer.
- [3] T. S.-I. journal of services sciences and undefined 2008, "Decision making with the analytic hierarchy process," *inderscienceonline.com*.
- [4] A. Fakouri, H. Pasha, P. Jalili, and S. Abdollahzadeh, "Ranking the captech technology strategies by integrating fuzzy ahp and fuzzy topsis methods."
- [5] R. Ryan and E. Deci, "Self-determination theory and the facilitation of intrinsic motivation, social development, and well-being.," *Am. Psychol.*, vol. 55, no. 1, pp. 68–78, 2000.
- [6] R. M. Ryan and E. L. Deci, *Self-determination theory: Basic psychological needs in motivation, development, and wellness*. Guilford Publications, 2017.
- [7] E. L. Deci and R. M. Ryan, "Hedonia, eudaimonia, and well-being: an introduction," *J. Happiness Stud.*, vol. 9, no. 1, pp. 1–11, Jan. 2008.
- [8] A. Alzahrani, C. Johnson, and S. Altamimi, "Information security policy compliance: Investigating the role of intrinsic motivation towards policy compliance in the organisation.," in *2018 4th International Conference on Information Management (ICIM)*, 2018, pp. 125–132.
- [9] J. Adie, J. Duda, and N. Ntoumanis, "Perceived coach-autonomy support, basic need satisfaction and the well-and ill-being of elite youth soccer players: A longitudinal investigation," *Psychol. Sport Exerc.*, 2012.
- [10] L. Vandercammen and J. Hofmans, "The mediating role of affect in the relationship between need satisfaction and autonomous motivation," *J. Occup.*, 2014.
- [11] P. Ifinedo, "Understanding information systems security policy compliance: An integration of the theory of planned behavior and the protection motivation theory," *Comput. Secur.*, vol. 31, no. 1, pp. 83–95, 2012.
- [12] G. Greene and J. D'Arcy, "Assessing the impact of security culture and the employee-organization relationship on IS security compliance," *Symp. Inf. Assur.*, 2010.
- [13] I. Ajzen, "Perceived Behavioral Control, Self-Efficacy, Locus of Control, and the Theory of Planned Behavior 1," *J. Appl. Soc. Psychol.*, vol. 32, no. 4, pp. 665–683, Apr. 2002.
- [14] M. S. Hagger and N. L. D. Chatzisarantis, "Integrating the theory of planned behaviour and self-determination theory in health behaviour: A meta-analysis," *Br. J. Health Psychol.*, vol. 14, no. 2, pp. 275–302, May 2009.
- [15] A. Ishizaka, A. L.-E. systems with applications, and undefined 2011, "Review of the main developments in the analytic hierarchy process," Elsevier.
- [16] O. Vaidya, S. K.-E. J. of operational research, and undefined 2006, "Analytic hierarchy process: An overview of applications," Elsevier.
- [17] J. Hwang, I. S.-& Simulation, 2009. AMS'09. Third, and undefined 2009, "Information Security Policy Decision Making: An Analytic Hierarchy Process Approach," *ieeexplore.ieee.org*.
- [18] I. Syamsuddin, J. H.-J. of Simulation, undefined Systems, S. and, and undefined 2009, "The application of AHP to evaluate information security policy decision making," *ijssst.info*.
- [19] H. A. Kruger and W. D. Kearney, "A prototype for assessing information security awareness," *Comput. Secur.*, vol. 25, no. 4, pp. 289–296, Jun. 2006.
- [20] H. Kruger and W. Kearney, "Measuring information security awareness: A West Africa gold mining environment case study," 2005.
- [21] P. Puhakainen and M. Siponen, "Improving employees' compliance through information systems security training: an action research study," *Mis Q.*, pp. 757–778, 2010.
- [22] C. Brodie, "The Importance of Security Awareness Training The Importance of Security Awareness Training The Importance of Security Awareness Training GIAC Gold Certification The Importance of Security Awareness Training."
- [23] T. L. Saaty and J. M. Katz, "How to make a decision: The Analytic Hierarchy Process," *Eur. J. Oper. Res.*, vol. 48, pp. 9–26, 1990.
- [24] F. Z.- interfaces and undefined 1986, "The analytic hierarchy process—a survey of the method and its applications," *pubsonline.informs.org*.
- [25] J. Mustajoki and R. P. Hämäläinen, "Web-Hipre: Global Decision Support By Value Tree And AHP Analysis," *INFOR Inf. Syst. Oper. Res.*, vol. 38, no. 3, pp. 208–220, Aug. 2000.
- [26] S. Hajkovicz, M. Young, D. H. MacDonald, and others, "Supporting decisions: Understanding natural resource management assessment techniques," 2000.

### APPENDIX I

The following example explains a paired comparison for participants:

Suppose you have two mobile phone brands Apple and Samsung. Which mobile phone brand do you like better than the other and how much better do you like it in comparison with the other? Use this relative scale to measure how much you like the mobile phone brand on the left (Apple) compared to the mobile device on the right (Samsung).

If you like the Apple better than Samsung, mark between number 1 and 9 on the left side; if you favour Samsung more than Apple, mark on the right side.

|       |   |   |   |   |   |   |   |   |   |   |   |   |   |   |   |   |   |         |
|-------|---|---|---|---|---|---|---|---|---|---|---|---|---|---|---|---|---|---------|
| Apple | 9 | 8 | 7 | 6 | 5 | 4 | 3 | 2 | 1 | 2 | 3 | 4 | 5 | 6 | 7 | 8 | 9 | Samsung |
|-------|---|---|---|---|---|---|---|---|---|---|---|---|---|---|---|---|---|---------|

A. Questionnaire

For each section, the participants indicated how important factor A is relative to factor B by using the scale from 1- 9 as explained in Table I.

1) Criteria comparisons.

|             |   |   |   |   |   |   |   |   |   |   |   |   |   |   |   |   |   |             |
|-------------|---|---|---|---|---|---|---|---|---|---|---|---|---|---|---|---|---|-------------|
| Autonomy    | 9 | 8 | 7 | 6 | 5 | 4 | 3 | 2 | 1 | 2 | 3 | 4 | 5 | 6 | 7 | 8 | 9 | Competence  |
| Autonomy    | 9 | 8 | 7 | 6 | 5 | 4 | 3 | 2 | 1 | 2 | 3 | 4 | 5 | 6 | 7 | 8 | 9 | Relatedness |
| Autonomy    | 9 | 8 | 7 | 6 | 5 | 4 | 3 | 2 | 1 | 2 | 3 | 4 | 5 | 6 | 7 | 8 | 9 | Intention   |
| Competence  | 9 | 8 | 7 | 6 | 5 | 4 | 3 | 2 | 1 | 2 | 3 | 4 | 5 | 6 | 7 | 8 | 9 | Relatedness |
| Competence  | 9 | 8 | 7 | 6 | 5 | 4 | 3 | 2 | 1 | 2 | 3 | 4 | 5 | 6 | 7 | 8 | 9 | Intention   |
| Relatedness | 9 | 8 | 7 | 6 | 5 | 4 | 3 | 2 | 1 | 2 | 3 | 4 | 5 | 6 | 7 | 8 | 9 | Intention   |

2) Pairwise comparisons of autonomy

|                            |   |   |   |   |   |   |   |   |   |   |   |   |   |   |   |   |   |                            |
|----------------------------|---|---|---|---|---|---|---|---|---|---|---|---|---|---|---|---|---|----------------------------|
| Cyber-attack               | 9 | 8 | 7 | 6 | 5 | 4 | 3 | 2 | 1 | 2 | 3 | 4 | 5 | 6 | 7 | 8 | 9 | Use of e-mail and Internet |
| Cyber-attack               | 9 | 8 | 7 | 6 | 5 | 4 | 3 | 2 | 1 | 2 | 3 | 4 | 5 | 6 | 7 | 8 | 9 | Incidents response         |
| Cyber-attack               | 9 | 8 | 7 | 6 | 5 | 4 | 3 | 2 | 1 | 2 | 3 | 4 | 5 | 6 | 7 | 8 | 9 | Policies compliance        |
| Use of e-mail and Internet | 9 | 8 | 7 | 6 | 5 | 4 | 3 | 2 | 1 | 2 | 3 | 4 | 5 | 6 | 7 | 8 | 9 | Incidents response         |
| Use of e-mail and Internet | 9 | 8 | 7 | 6 | 5 | 4 | 3 | 2 | 1 | 2 | 3 | 4 | 5 | 6 | 7 | 8 | 9 | Policies compliance        |
| Incidents response         | 9 | 8 | 7 | 6 | 5 | 4 | 3 | 2 | 1 | 2 | 3 | 4 | 5 | 6 | 7 | 8 | 9 | Policies compliance        |

3) Pairwise comparisons of competence

|                            |   |   |   |   |   |   |   |   |   |   |   |   |   |   |   |   |   |                            |
|----------------------------|---|---|---|---|---|---|---|---|---|---|---|---|---|---|---|---|---|----------------------------|
| Cyber-attack               | 9 | 8 | 7 | 6 | 5 | 4 | 3 | 2 | 1 | 2 | 3 | 4 | 5 | 6 | 7 | 8 | 9 | Use of e-mail and Internet |
| Cyber-attack               | 9 | 8 | 7 | 6 | 5 | 4 | 3 | 2 | 1 | 2 | 3 | 4 | 5 | 6 | 7 | 8 | 9 | Incidents response         |
| Cyber-attack               | 9 | 8 | 7 | 6 | 5 | 4 | 3 | 2 | 1 | 2 | 3 | 4 | 5 | 6 | 7 | 8 | 9 | Policies compliance        |
| Use of e-mail and Internet | 9 | 8 | 7 | 6 | 5 | 4 | 3 | 2 | 1 | 2 | 3 | 4 | 5 | 6 | 7 | 8 | 9 | Incidents response         |
| Use of e-mail and Internet | 9 | 8 | 7 | 6 | 5 | 4 | 3 | 2 | 1 | 2 | 3 | 4 | 5 | 6 | 7 | 8 | 9 | Policies compliance        |
| Incidents response         | 9 | 8 | 7 | 6 | 5 | 4 | 3 | 2 | 1 | 2 | 3 | 4 | 5 | 6 | 7 | 8 | 9 | Policies compliance        |

4) Pairwise comparisons of relatedness

|                            |   |   |   |   |   |   |   |   |   |   |   |   |   |   |   |   |   |                            |
|----------------------------|---|---|---|---|---|---|---|---|---|---|---|---|---|---|---|---|---|----------------------------|
| Cyber-attack               | 9 | 8 | 7 | 6 | 5 | 4 | 3 | 2 | 1 | 2 | 3 | 4 | 5 | 6 | 7 | 8 | 9 | Use of e-mail and Internet |
| Cyber-attack               | 9 | 8 | 7 | 6 | 5 | 4 | 3 | 2 | 1 | 2 | 3 | 4 | 5 | 6 | 7 | 8 | 9 | Incidents response         |
| Cyber-attack               | 9 | 8 | 7 | 6 | 5 | 4 | 3 | 2 | 1 | 2 | 3 | 4 | 5 | 6 | 7 | 8 | 9 | Policies compliance        |
| Use of e-mail and Internet | 9 | 8 | 7 | 6 | 5 | 4 | 3 | 2 | 1 | 2 | 3 | 4 | 5 | 6 | 7 | 8 | 9 | Incidents response         |
| Use of e-mail and Internet | 9 | 8 | 7 | 6 | 5 | 4 | 3 | 2 | 1 | 2 | 3 | 4 | 5 | 6 | 7 | 8 | 9 | Policies compliance        |
| Incidents response         | 9 | 8 | 7 | 6 | 5 | 4 | 3 | 2 | 1 | 2 | 3 | 4 | 5 | 6 | 7 | 8 | 9 | Policies compliance        |

5) Pairwise comparisons of intention

|                            |   |   |   |   |   |   |   |   |   |   |   |   |   |   |   |   |   |                            |
|----------------------------|---|---|---|---|---|---|---|---|---|---|---|---|---|---|---|---|---|----------------------------|
| Cyber-attack               | 9 | 8 | 7 | 6 | 5 | 4 | 3 | 2 | 1 | 2 | 3 | 4 | 5 | 6 | 7 | 8 | 9 | Use of e-mail and Internet |
| Cyber-attack               | 9 | 8 | 7 | 6 | 5 | 4 | 3 | 2 | 1 | 2 | 3 | 4 | 5 | 6 | 7 | 8 | 9 | Incidents response         |
| Cyber-attack               | 9 | 8 | 7 | 6 | 5 | 4 | 3 | 2 | 1 | 2 | 3 | 4 | 5 | 6 | 7 | 8 | 9 | Policies compliance        |
| Use of e-mail and Internet | 9 | 8 | 7 | 6 | 5 | 4 | 3 | 2 | 1 | 2 | 3 | 4 | 5 | 6 | 7 | 8 | 9 | Incidents response         |
| Use of e-mail and Internet | 9 | 8 | 7 | 6 | 5 | 4 | 3 | 2 | 1 | 2 | 3 | 4 | 5 | 6 | 7 | 8 | 9 | Policies compliance        |
| Incidents response         | 9 | 8 | 7 | 6 | 5 | 4 | 3 | 2 | 1 | 2 | 3 | 4 | 5 | 6 | 7 | 8 | 9 | Policies compliance        |

# Prediction of Visibility for Color Scheme on the Web Browser with Neural Networks

Miki Yamaguchi<sup>1</sup>

School of Science for Open and Environmental Systems  
Keio University, Kanagawa, Japan

Yoshihisa Shinozawa<sup>2</sup>

Faculty of Science and Technology  
Keio University, Kanagawa, Japan

**Abstract**—In this study, we propose neural networks for predicting the visibility of color schemes. In recent years, most of us have accessed websites owing to the spread of the Internet. It is necessary to design web pages that allow users to access information easily. The color scheme is one of the most important elements of website design and therefore, we focus on the visibility of the background and character colors in this study. The prediction methods of visibility of color scheme have been proposed. In one of the prediction methods, neural networks are used to forecast pairwise comparison tables that indicate the visibility of background and character colors. Our model employs neural networks for color recognition and visibility prediction. The neural networks used for color recognition include functions that forecast the color class name from a color and extract the features of the color. The neural networks used for visibility prediction include functions that employ the features of background and character colors extracted by neural networks for color recognition and forecast the visibility of a color scheme. Pairwise comparison tables are forecasted with the prediction results of neural networks for visibility prediction. We conducted pairwise comparison experiment on a web browser, as well as color recognition experiment and evaluated our model. The results of the experiments suggest that our model could improve the accuracy of pairwise comparison tables compared to existing methods. Thus, proposed model can be used to predict the visibility of color schemes.

**Keywords**—Visibility prediction; color recognition; pairwise comparison experiment; human color vision; neural networks

## I. INTRODUCTION

Websites on the Internet transmit and aggregate information. Therefore, they need to be created with consideration for content and ease of viewing (visibility). Elements that contribute to the visibility of a webpage include the color scheme, character size, and the overall layout, with the color scheme regarded as a particularly important aspect. This study focuses on the visibility of the background and character colors (henceforth referred to as the color scheme) displayed on a webpage.

As websites need to be designed considering color scheme visibility, standards or indices of ease of viewing are necessary. Consequently, the World Wide Web Consortium (W3C) recommends a brightness difference of at least 125 and a color difference of at least 500. However, an index that expresses the visibility of individual color schemes has not yet been devised. Therefore, many research attempts to clarify the color schemes of higher or lower visibility. Examples of these studies include attempts to clarify the color scheme visibility through

experiments [1]-[5] and the development of software that can judge color scheme visibility or change the scheme to increase visibility. In particular, the proposed method involves the use of pairwise comparison to collect data on the visibility of background and character colors, and subsequently employing the Thurstone pairwise comparison method to index color scheme visibility [6]. As this type of research attempts to clarify the color scheme visibility through the collection and analysis of experimental data, a large volume of data are required. In this context, experimental data was used to develop predictive devices that can judge visibility levels and subsequently use them to predict the visibility of unfamiliar color schemes [7], [8].

The objective of this study is to use experimental data to develop a predictive device capable of judging color scheme visibility, and then devise a method for predicting the visibility of unfamiliar color schemes. Previous research [6] proposed the use of the Thurstone pairwise comparison method on data collected from pairwise comparison experiments to create pairwise comparison tables (pairwise comparison scores) as an index of color scheme visibility. Other studies [7], [8] attempted to predict pairwise comparison tables for background and character colors, which are used as an index of the visibility of unfamiliar color schemes.

A study [7] on background and character color visibility proposed a method for deriving pairwise comparison tables that involve training a neural network and then employing it to predict the visibility of a color scheme that was not learned by the network. In this process, multiple color coordinate systems (RGB, HSV, XYZ, L\*a\*b\*) for each background and character color were used [7] as input features for the neural network. Furthermore, another study [8] introduced a model of human color perception (the Multi-Stage Color Model [9]) to reproduce the perceptual process, extract features that are factors related to visibility, and use these features to train a neural network in an attempt to improve the predictive precision with regard to color scheme visibility.

This study attempts to improve on previous research [7], [8] by training a neural network to make it capable of predicting color scheme visibility. This study does not utilize the features derived from color systems or existing color perception models while predicting color scheme visibility. We propose training a neural network capable of color recognition (color recognition refers to specifying the color name of a particular color), extracting features related to color scheme visibility, and then employing them in the prediction of color

scheme visibility. The proposed method is used to predict the pairwise comparison tables for unfamiliar color schemes. The predictions are then compared with the predictions made using the methods based on previous research [7], [8] to evaluate the validity of the proposed method.

This paper is structured as follows. Section 2 presents a review of the existing literature in the field. Section 3 discusses areas for improvement in the existing literature. Section 4 outlines the proposed method for collecting experimental data and predicting the visibility of unfamiliar color schemes. Section 5 discusses the experiment to evaluate the validity of the proposed method by comparing it with those in the existing literature. Section 6 discusses the results of the evaluation experiment. Finally, Section 7 presents a summary of the study and outlines future research directions.

## II. LITERATURE REVIEW

### A. Data Collection by Pairwise Comparison Experiment

To collect data on the visibility of color schemes displayed on browsers, this study utilized the Thurstone pairwise comparison method, which indexed color scheme visibility [6]. The data collection method, which involved a pairwise comparison experiment developed from the existing literature, is discussed below.

In the first step, the following pairwise comparison experiment was performed on twenty participants (individuals aged in their twenties and thirties, with normal color perception).

Fig. 1 shows that the participants were asked to select the easier to view of two character strings of the same color grouping but with different luminance, written horizontally next to each other (right side/left side) on a browser with the same background color for both strings. Microsoft Internet Explorer was used as a browser and was displayed in the center of the monitor at a size that allowed both screens to be seen at roughly the same time. The character strings displayed were the same sentence that could be read from left to right. The same monitor was used throughout the entire experiment. All other experimental conditions (lighting, the positioning of the monitor with respect to the participant) were similar for all participants.

The colors used in the experiment were limited to web-safe colors. For the background, four colors were selected from each of the ten color groups (red, green, blue, cyan, magenta, yellow, and four other web safe colors). For the character colors, five colors were selected from each of the same groups. The RGB values for the background and character colors used are presented in Table I and Table II (web safe colors are abbreviated as WSC1, WSC2, WSC3, WSC4). Consequently, for the case where the background color grouping was red, the R parameter of the RGB value was varied over four grades, #66, #99, #cc, and #ff. When the character color grouping was red, the R parameter of the RGB was varied over five grades, #33, #66, #99, #cc, and #ff. Fig. 2 shows the luminance of the background and character colors.

A total of 400 combinations were shown to each participant for pairwise comparison. When the character color was from

the red grouping, for example, a combination of 40 background colors (10 color groupings  $\times$  4 grades per grouping) and 10 character colors (two selections from the five grades within the red color grouping  ${}_5C_2$ ). Given that there are ten character color groupings, the number of observations per pairwise comparison experiment per person was 4000. Pairwise comparisons were not made between characters from different color groupings, and background/character colors were displayed in random order for each participant. Accordingly, four thousand observations of the following data were collected for each participant.

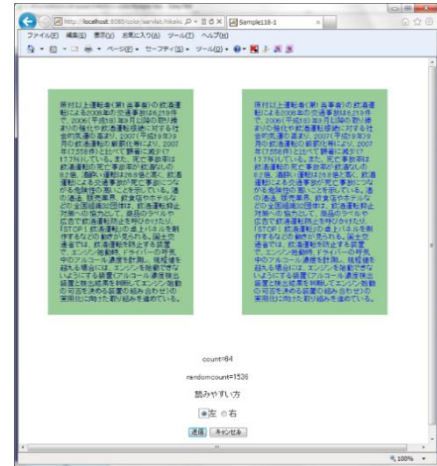


Fig. 1. Background Color and Character Color on the Browser.

TABLE I. BACKGROUND COLORS

| Background Colors |             |            |            |            |            |
|-------------------|-------------|------------|------------|------------|------------|
| <i>i</i>          | Color group | <i>j=1</i> | <i>j=2</i> | <i>j=3</i> | <i>j=4</i> |
| 1                 | Red         | #660000    | #990000    | #cc0000    | #ff0000    |
| 2                 | Green       | #006600    | #009900    | #00cc00    | #00ff00    |
| 3                 | Blue        | #000066    | #000099    | #0000cc    | #0000ff    |
| 4                 | Cyan        | #006666    | #009999    | #00cccc    | #00ffff    |
| 5                 | Magenta     | #660066    | #990099    | #cc00cc    | #ff00ff    |
| 6                 | Yellow      | #666600    | #999900    | #cccc00    | #ffff00    |
| 7                 | WSC1        | #ff6699    | #ff9999    | #ffcc99    | #ffff99    |
| 8                 | WSC2        | #669900    | #999900    | #cc9900    | #ff9900    |
| 9                 | WSC3        | #99cc66    | #99cc99    | #99cccc    | #99ceff    |
| 10                | WSC4        | #666666    | #996699    | #cc66cc    | #ff66ff    |

TABLE II. CHARACTER COLORS

| Character Colors |             |            |            |            |            |            |
|------------------|-------------|------------|------------|------------|------------|------------|
| <i>l</i>         | Color group | <i>l=1</i> | <i>l=2</i> | <i>l=3</i> | <i>l=4</i> | <i>l=5</i> |
| 1                | Red         | #330000    | #660000    | #990000    | #cc0000    | #ff0000    |
| 2                | Green       | #003300    | #006600    | #009900    | #00cc00    | #00ff00    |
| 3                | Blue        | #000033    | #000066    | #000099    | #0000cc    | #0000ff    |
| 4                | Cyan        | #003333    | #006666    | #009999    | #00cccc    | #00ffff    |
| 5                | Magenta     | #330033    | #660066    | #990099    | #cc00cc    | #ff00ff    |
| 6                | Yellow      | #333300    | #666600    | #999900    | #cccc00    | #ffff00    |
| 7                | WSC1        | #ff3399    | #ff6699    | #ff9999    | #ffcc99    | #ffff99    |
| 8                | WSC2        | #339900    | #669900    | #999900    | #cc9900    | #ff9900    |
| 9                | WSC3        | #99cc33    | #99cc66    | #99cc99    | #99cccc    | #99ceff    |
| 10               | WSC4        | #336633    | #666666    | #996699    | #cc66cc    | #ff66ff    |

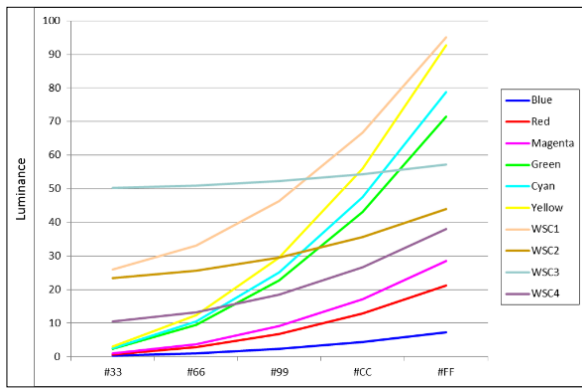


Fig. 2. Luminance of Background and Character Colors.

- Background Color, Left Character Color, Right Character Color, Direction that was easier to view
- #330000, #000066, #000099, Left

### B. Thurstone Pairwise Comparison Method

In the next step, the Thurstone pairwise comparison method was used to score the visibility of the background and character colors. In the pairwise comparison experiment, the luminance of the background colors in the  $i$  grouping ( $i=1,2, \dots, 10$ , where  $i=1$  is red,  $i=2$  is green, ...,  $i=10$  is WSC4) was varied over four grades. The change in the luminance value was represented by  $j$  ( $j= 1,2,3,4$ ) (see Table I). For example, for background colors in the red grouping ( $i=1$ ),  $j=1$  is #660000,  $j=2$  is #990000,  $j=3$  is #cc0000, and  $j=4$  is #ff0000 (expressed as background color  $j$  in color grouping  $i$ ). Similarly, the luminance of the character color in the  $k$  grouping ( $k=1,2, \dots, 10$ , where  $k=1$  is red,  $k=2$  is green, ...,  $k=10$  is WSC4) was also varied over five grades (see Table II). The change in the luminance of the left character color is represented by  $l$  ( $l=1,2, \dots, 5$ ) and the change in the luminance of the right character color is represented by  $r$  ( $r=1,2, \dots, 5$ ,  $l \neq r$ ) (expressed as character color  $l$  or  $r$  in color grouping  $k$ ).

Accordingly, when participant  $p$  ( $p=1,2, \dots, 20$ ) is presented with background color from group  $i$  with the  $j^{\text{th}}$  luminance value (background color  $j$  from color grouping  $i$ ) with the character color from group  $k$  with the  $l^{\text{th}}$  luminance value as the left-hand character color (character color  $l$  from color grouping  $k$ ) and the character color from group  $k$  with the  $r^{\text{th}}$  luminance value as the right-hand character color (character color  $r$  from color grouping  $k$ ), the value of the visibility of the color scheme will be  $x_{pijkl}$ . When participant  $p$  judges the right character color as easier to view,  $x_{pijkl}=1$  and when the left character color is judged as easier to view,  $x_{pijkl}=0$ . The mean value of all twenty participants will be  $y_{ijkl}$  (Equation (1)).

$$y_{ijkl} = \frac{1}{20} \sum_{p=1}^{20} x_{pijkl} \quad (1)$$

Specifically, for the background color  $j$  in the color group  $i$ ,  $y_{ijkl}$  will be the ratio of cases where the right-hand character  $r$  in color grouping  $k$  is judged to be easier to view than the left-hand character  $l$  from the same color grouping. Accordingly,  $y_{ijkl}=1.0-y_{ijkrl}$  (in the case where  $i=r$ ,  $y_{ijkl}=0.5$ ). Next, the inverse function of the cumulative distribution function of the standard normal distribution is derived with respect to  $y_{ijkl}$

( $Normsinv$  in Equation (2)). Subsequently, the mean values for all character colors are calculated, and the pairwise comparison scores  $z_{ijkr}$  are derived (Equation (2)).

$$z_{ijkr} = \frac{1}{5} \sum_{l=1}^5 Normsinv(y_{ijklr}) \quad (2)$$

For the background color  $j$  in color group  $i$ , the pairwise comparison score  $z_{ijkr}$  will be the index of the visibility of character color  $r$  in color group  $k$ .

According to the above process, the experimental data, for the ten background color groupings for each character color, 40 observations per person (4 grades of background color  $\times$  10 character color pairs) was employed to quantify the visibility levels of the combinations of the four background colors and five character colors. As an example, Table III presents the results for the case where the character color was from the red grouping, and the background color was from the green grouping.

The columns in Table III display the RGB values of the background colors (4 colors) and the rows display the RGB values of the character colors (5 colors). Higher pairwise comparison scores indicate color schemes that are easier to observe and vice versa, which yielded the number of background colors for each character color, ten pairwise comparison tables, for a total of 100 tables.

TABLE III. RESULTS OF THURSTONE PAIRWISE COMPARISON METHOD (CHARACTER COLOR RED, BACKGROUND COLOR GREEN)

| Background colors | Character colors |         |         |         |         |
|-------------------|------------------|---------|---------|---------|---------|
|                   | #330000          | #660000 | #990000 | #cc0000 | #ff0000 |
| #006600           | 0.157            | -0.497  | -0.714  | 0.221   | #0.833  |
| #009900           | 1.006            | 0.408   | -0.418  | -0.769  | -0.228  |
| #00cc00           | 1.064            | 0.633   | -0.156  | -0.730  | -0.810  |
| #00ff00           | 1.077            | 0.573   | 0.0     | -0.573  | -1.077  |

### C. Predicting the Visibility of a Color Scheme

If it were possible to predict the pairwise comparison tables even for unfamiliar color schemes, then these tables could be used to determine whether or not the combination of background and character colors on the webpage being currently viewed by the user is easy or difficult to view. Furthermore, if the color scheme was judged to be difficult to view, it would be possible to change it to a scheme that is easier to view by switching it to a combination of higher value. If this kind of feature could be implemented in a browser, it would be possible to determine the visibility of the page currently being viewed and to change it to a color scheme with higher visibility.

In this context, a previous study [7] proposed a method whereby a portion of the data collected from a pairwise comparison experiment is employed as color scheme data, with the remainder treated as unfamiliar data with a neural network (henceforth “network”) used to predict its pairwise comparison tables. For example, only the data where the character color is from the red, blue, and green groupings are used, with the pairwise comparison tables for character colors from the remaining seven color groupings being predicted (here, the character color groupings employed in the training of the

network are referred to as the basic color groupings). Consequently, the method attempts to teach the network using the basic color grouping data and then derive the pairwise comparison tables after using the trained network to predict the visibility of the unfamiliar color schemes.

Additionally, a previous study [7] used RGB, HSV, XYZ (Yxy) and L\*a\*b\* color system values for each of the background and character colors as input features for the network to predict the color scheme visibility. Furthermore, luminance difference and the color difference between the background and character colors may influence the visibility of the color scheme. In this context, a previous study [8] introduced a model of human color perception (Multi-Stage Color Model [9]) to reproduce the color perceptual process, extract features that are factors related to visibility, and use these features to train a neural network in an attempt to improve the predictive precision of color scheme visibility.

#### D. Overview of the Multi-Stage Color Model

This section presents an overview of the Multi-Stage Color Model (henceforth, MSC Model) [9]. The MSC Model is a color perception model comprised of a number of stages.

In the first stage of the MSC Model, visible light (RGB values) are converted into response values (spectral sensitivity values) for three types of cones (L, M, and S). In this study, RGB values (gamma-corrected, as the pairwise comparison experiment, carried out on a computer display) were transformed into XYZ values and then, Equation (3) was used to derive the response values  $L$ ,  $M$ ,  $S$  for each cone [10].

$$\begin{pmatrix} L \\ M \\ S \end{pmatrix} = \begin{pmatrix} 0.155 & 0.543 & -0.0329 \\ -0.155 & 0.457 & 0.0329 \\ 0.0 & 0.0 & 0.016 \end{pmatrix} \begin{pmatrix} X \\ Y \\ Z \end{pmatrix} \quad (3)$$

In the second stage, the response values of the opponent color cells are derived. There are opponent color cells that are stimulated by one cone and inhibited by the surrounding cones (on-center/off-surround type) and cells that are inhibited by one cone and stimulated by the surrounding cones (off-center/on-surround type). A total of six types of opponent color cells - ON-center/OFF-surround type cells centered on the L-cone (with a response value denoted by  $L_o$ ), the M-cone ( $M_o$ ), and the S-cone ( $S_o$ ) and OFF-center/ON-surround type cells centered on the L-cone ( $-L_o$ ), the M-cone ( $-M_o$ ), and the S-cone ( $-S_o$ ). The three types of cones are randomly connected to these cells in a ratio assumed to be 10:5:1. Furthermore, the ratio of the response values of the center and surrounding cells is assumed to be 1:1. The response values for all opponent color cells are expressed in Equation (4).

$$\begin{aligned} L_o &= 16L - (10L + 5M + S) = 6L - 5M - S \\ M_o &= 16M - (10L + 5M + S) = -10L + 11M - S \\ S_o &= 16S - (10L + 5M + S) = -10L - 5M + 15S \\ -L_o &= -16L + (10L + 5M + S) = -6L + 5M + S \\ -M_o &= -16M + (10L + 5M + S) = 10L - 11M + S \\ -S_o &= -16S + 10L + 5M + S = 10L + 5M - 15S \end{aligned} \quad (4)$$

In the third stage, the responses of the six types of color opponent cells are combined to set the way the color is seen. The basic combinations are the responses of  $L_o - M_o$  and  $M_o - L_o$  and adding or subtraction the  $S_o$  response will yield the response value that corresponds to the perception of red, yellow, green, and blue.

- Red ( $R_o$ ) is formed by  $L_o - M_o$  plus  $S_o$ .
- Yellow ( $Y_o$ ) is formed by  $L_o - M_o$  minus  $S_o$ .
- Green ( $G_o$ ) is formed by  $M_o - L_o$  minus  $S_o$ .
- Blue ( $B_o$ ) is formed by  $M_o - L_o$  plus  $S_o$ .

The number of each type of cell is considered in the addition and subtraction process. In the MSC Model, the ratio of  $L_o:M_o:S_o$  is assumed to be 10:5:2 with the color response being derived by Equation (5).

$$\begin{aligned} R_o &= 10L_o - 5M_o + 2S_o \\ Y_o &= 10L_o - 5M_o - 2S_o \\ G_o &= 5M_o - 10L_o - 2S_o \\ B_o &= 5M_o - 10L_o + 2S_o \end{aligned} \quad (5)$$

Thus, the luminance value  $V$  is derived from Equation (6) and concludes the process in the MSC Model.

$$V = L + M + S \quad (6)$$

### III. PROPOSAL

The aim of this study is to improve the existing research [7], [8] and increase the accuracy of visibility prediction by developing, through training, a network capable of predicting color scheme visibility. A previous study [8] used an existing color perception model while extracting features for visibility from background and character colors. Instead of using an existing model, in this study, data are collected from the color recognition experiment detailed in Section 4.2 and attempts to develop, through training, a color recognition network and then utilize it to extract features from background and character colors. Furthermore, this study proposes to use the extracted features to predict the color scheme visibility. Finally, the validity of the proposed method is evaluated by predicting the pairwise comparison tables for unfamiliar color schemes and then comparing them and their predictive precision with the tables predicted by existing methods [7], [8].

#### IV. A METHOD FOR PREDICTING THE VISIBILITY OF COLOR SCHEMES

##### A. Overview of the Proposed Method

Fig. 3 presents an overview of the proposed method, which consists of the color recognition neural network for feature extraction (henceforth color recognition network), the visibility prediction neural network for predicting color scheme visibility (henceforth visibility prediction network), and the pairwise comparison table prediction element. This section gives an overview of the proposed method, and further subsections provide details on its respective parts. The first aspect to be discussed is the color recognition network (see Section 4.3 for details).

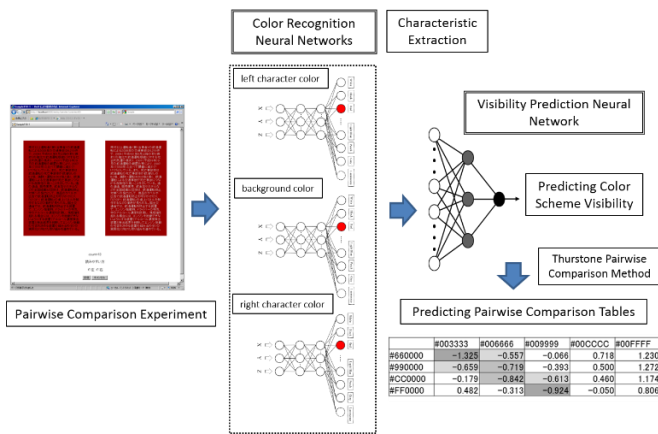


Fig. 3. Overview of the Proposed Method.

The existing color perception model employed in previous studies (MSC Model) has the ability to output the response value, which corresponds to the degree of luminance of the opponent color (red-green, blue-yellow) or the colors red, green, blue, or yellow, from the response value of the cone relating to an arbitrary color. To give the network in this study the same functionality as the existing color perception models, it was given the ability to output the color name and brightness of a particular color when its XYZ color system value is inputted. Thirteen colors that could be predicted were specified, white, black, red, green, yellow, orange, blue, purple, brown, yellow-green, light-blue, peach, and gray. Data concerning colors and their respective color names were collected through the color recognition experiment detailed in Section 4.2.

When predicting the visibility of a color scheme, three color recognition networks are prepared, the XYZ values for the background color and left/right character colors are entered, and the network is activated. The features to be entered into the visibility prediction network in the next step are then extracted. After the features of background color and left/right character colors extracted from the color recognition network are entered into the visibility prediction network, a prediction on which of the character colors has a higher level of visibility is made (see Section 4.4 for details). This network utilizes the three layer type neural network employed in the existing literature [7]. By combining these two network forms, the visibility of an unfamiliar color scheme can be predicted. In the element that predicts the pairwise comparison tables, the Thurstone pairwise comparison method is employed based on the results of the visibility prediction network to predict the pairwise comparison tables (see Section 4.5).

### B. Color Recognition Experiment

To develop a color recognition network, a color recognition experiment that collected data on colors and respective color names was carried out. The color recognition experiment involved showing color sample cards to participants to match colors with color names. The color sample cards used in this study were from the DIC Color Guide 19<sup>th</sup> Edition (652 colors) [11]. Sixty participants (aged in their twenties and thirties, with normal color perception) were involved. Participants were shown one card from the color guide and asked to match it

with one of thirteen color names (white, black, red, green, yellow, orange, blue, purple, brown, yellow-green, light-blue, peach, and gray). Berlin & Kay [12] defined eleven basic colors (white, black, red, green, yellow, orange, blue, purple, brown, peach, and gray). Furthermore, yellow-green and light-blue are often included in the colors that are generally perceived by Japanese people. Considering that the lack of colors can lead to difficulties in color recognition, too many will lead to the emergence of individual differences. This study included yellow-green and light-blue to make a total of thirteen colors. The XYZ values of the color sample cards were measured using a spectrophotometer (Konica Minolta CM-700d). At the time of data collection, the color sample cards were shown to the participants under fixed lighting (approximately 400 lux) in front of a stable background (white with an XYZ value of X = 68, Y = 72, Z = 71).

### C. Training the Color Recognition Neural Network

Using data collected from the color recognition experiment, a network capable of predicting the color name of an unfamiliar color was developed. The structure of this network is shown in Fig. 4. The color recognition network was set up as a four layer feedback type because the MSC Model involves inputting an XYZ value (LMS cone response value) and outputting the color name after passing through the opponent color response. The input value was the XYZ color system value of the color sample card (the number of neurons in the input layer was three). The output value was the color name and luminance value (Y-value) of the color that was inputted (there were 14 neurons in the output layer). Based on the preliminary experiment, the number of neurons for the first and second middle layers was set at twenty and all layers were connected.

For a given color sample card, the XYZ value of the color was the input, and a teaching signal was applied to the color name neuron to correspond to the ratio of the responses of the participants in the color recognition experiment. When the number of participants that responded "Blue" was 45 and "Light Blue" 15 for example, 45/60 was applied to the neuron corresponding to blue in the output layer, 15/60 was applied to the neuron corresponding to light blue and 0 was applied to the other neurons. For the luminance value, the Y-value was applied as the teaching signal. In this way, the 652 color sample cards were used as training data to train the color recognition network to output the teaching signals. The training algorithm is as follows.

- 1) Randomize the number of connections inside the color recognition network.
- 2) Training data  $\mathbf{x}_i$  (XYZ color system) ( $i=1,2,\dots,652$ , XYZ value is normalized to a value between 0 and 1).
- 3) Set  $i=1$ .
- 4) Input training data  $\mathbf{x}_i$  into the color recognition network. Set the teaching signal of the output layer neuron relating to the color name to the ratio of the responses of the 60 participants with normal color perception. Set the input value of the teaching signal for the neuron relating to luminance to the Y-value.
- 5) Activate the color recognition network.

6) Adjust the number of connections until the error sum of squares of the teaching signal and the output value from the output layer is minimized. Use backpropagation (method of moments) in the training.

7) Set  $i=i+1$ , select another training data  $x_i$  and then return to 4). When all of the training data has been taught, initiate the completion judgment in 8).

8) Repeat steps 3) through 7) until the total error sum of squares becomes constant. This kind of color recognition network can predict the color name and luminance of a particular color.

#### D. Training the Visibility Prediction Neural Network

Fig. 5 presents the structure of the visibility prediction network. Similar with the existing literature [7], the network is made up of three layers. The input is comprised of the features of the background colors and left and right character colors as extracted from the color recognition network, that is, the output value differences from the output layers of the three color recognition networks (the number of features being  $14 \times 2$ ). In this case, the luminance value difference and the color difference of the background and character colors may influence the color scheme visibility. Therefore, this study utilizes the difference in the output values of the background color and left and right character colors from the output layer of the color recognition network as features.

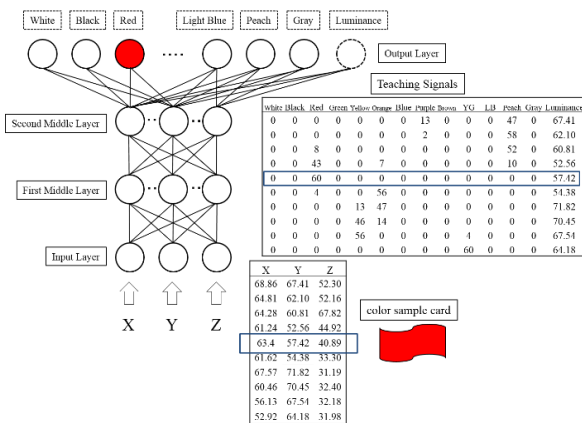


Fig. 4. Color Recognition Neural Network.

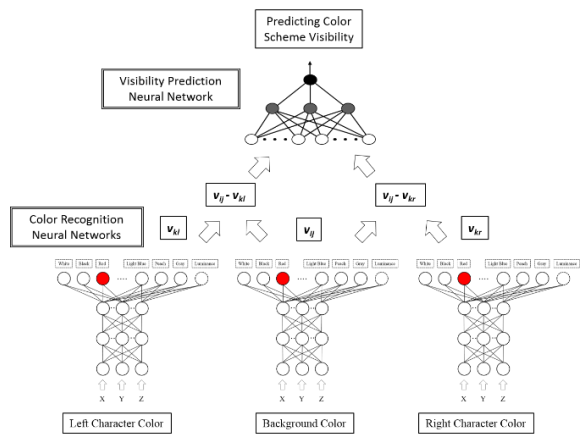


Fig. 5. Visibility Prediction Neural Network.

The number of input layer neurons for the visibility prediction network was the number of the above features. The number of middle layer neurons was set at 128, and the number of output layer neurons was set at one. When the right character color was easier to view in combination with the background and left and right character colors, a teaching signal was applied to fire the output layer neuron (output value of 1). Moreover, when the left character was easier to view, a teaching signal was applied to avoid firing the output layer neuron (output value of 0). In this way, the visibility prediction network was trained in line with the teaching signal.

Additionally, this study set the observations concerning the red, blue, and green character color groupings (1200 observations) as basic color groupings taken from 4000 observations per participant gathered from the pairwise comparison experiment data outlined in Section 2.1 and used them as training data to develop the visibility prediction network. The remaining seven character color groupings (cyan, magenta, yellow, and the four WSC) were used as evaluation data (2800 observations), and the color scheme visibility prediction was performed. The learning algorithm is as follows.

- 1) Randomize the number of connections within the visibility prediction network.
- 2) Input background color  $j$  ( $j=1,2,3,4$ ) of the color group  $i$  ( $i=1,2, \dots, 10$ ), and left character color  $l$  ( $l=1,2,3,4,5$ ) and right character color  $r$  ( $r=1,2,3,4,5, l \neq r$ ) of the basic color group  $k$  ( $k=1,2,3$ ) into the color recognition network, activate the network, and extract the respective features  $v_{ij}$ ,  $v_{kl}$ ,  $v_{kr}$  (the output values from the output layer). Set  $v_{ijklr}$  as the feature, which is the combination of these features. The feature to be inputted into the visibility prediction network will thus be  $v_{ijklr} = (v_{ij} - v_{kl}, v_{ij} - v_{kr})^T$ .
- 3) Input the feature  $v_{ijklr}$  into all of the neurons in the input layer of the visibility prediction network.
- 4) Set the teaching signal  $t_{ijklr}$ .
- 5) Activate the visibility prediction network and derive the output value  $o_{ijklr}$ .
- 6) Adjust the number of connections until the error sum of squares of the teaching signal  $t_{ijklr}$  and the output value  $o_{ijklr}$  is minimized. Use backpropagation (method of moments) in the training.
- 7) Make a new combination of background and left/right character colors and return to 2). When all of the combinations have been taught, perform the completion judgment in 8).
- 8) Repeat steps 2) through 7) until the total error sum of squares becomes constant.

#### E. Predicting the Pairwise Comparison Table of an Unfamiliar Color Scheme

Next, the trained network was used to predict the visibility of character colors that lie outside of the basic color groupings. For unfamiliar background color  $j$  in color grouping  $i$ , and left character color  $l$  and right character color  $r$  both in color grouping  $k$ , the feature  $v_{ijklr}$  will be extracted from the color recognition network. Thus, when the feature  $v_{ijklr}$  is entered into the visibility prediction network and the network activated, the



output value  $o_{ijklr}$  can be treated as the probability that the right-hand character color will have higher visibility for the color scheme. If the output value from the visibility prediction network is the threshold (set at 0.5 or higher), then for that color scheme, the right-hand character color will be judged as easier to view. If it is less than the threshold, then the left-hand character color will be judged as easier to view.

The element for predicting the pairwise comparison tables utilized the visibility scores for the background and character colors derived by the Thurstone pairwise comparison method (Section 2.2), which employed the output values from the visibility prediction network. For example, when predicting the pairwise comparison tables for the case where the character colors are from the cyan grouping and the background color is from the red, the features of the 40 combinations of character color (5 colors, #003333, #006666, #009999, #00cccc, #00ffff) and background color (4 colors, #660000, #990000, #cc0000, #ffff00) shown in Table I and Table II are entered into the network and 40 output values are derived. Next, taking the output value from the network,  $o_{ijklr}$ , as the probability that the right-hand character was predicted as being easier to see ( $y_{ijklr}$ ), the value of the inverse function of the cumulative distribution function of the standard normal distribution was derived, mean values for all colors were calculated, and the pairwise comparison scores  $z_{ijklr}$  were derived. For every other color scheme, the above process was carried out in the same way for all 40 combinations to create the pairwise comparison tables. The above process yielded a total of 70 pairwise comparison tables for seven character color groupings.

## V. EVALUATION

### A. Evaluation Method

The red, green, and blue character colors were set as basic color groupings, and the proposed method was constructed from the corresponding data from the pairwise comparison experiment (1200 observations). The data from the remaining seven color groupings (2800 observations) were treated as unfamiliar color schemes, and a pairwise comparison table prediction was performed.

The evaluation method was as follows. To investigate whether it was possible to use the proposed method to predict the visibility of unfamiliar color schemes, visibility predictions for these schemes were performed for each participant, the predictions were compared to the actual pairwise comparison data, and the predictive precision was derived. Similarly, to investigate whether it was possible to predict pairwise comparison tables, the pairwise comparison tables predicted by the proposed method and the tables created with actual experimental data were compared. In the final step, the validity of the proposed method was investigated by comparing the input features of the visibility prediction network as produced by the proposed method and the two methods (outline below) in the existing literature [7], [8].

- Existing Method-1 [7]: All RGB, HSV, XYZ, and L\*a\*b\* color system values for the background and left/right character colors were used. In this case, there were 36 features denoting that the number of neurons in

the input layer of the visibility prediction network was also 36.

- Existing Method-2 [8]: For the background and left/right character colors, in line with the Multi-Stage Color Model, response values of the LMS cones (Equation (3)), the response values ( $R_0, B_0, G_0, Y_0$ ) corresponding to the red, blue, green, and yellow responses (Equation (5)), and luminance values  $V$  (Equation (6)) were derived and used as features. In addition, the difference in luminance between the background color and left/right character colors and the difference in the response value of the opponent colors ( $R_0 G_0, B_0 Y_0$ ) were also considered as features. In this case, there were 30 features denoting that the number of neurons in the input layer of the visibility prediction network was also 30.

Setting the structure (number of middle and output layers) and training conditions of the visibility prediction networks, the same characters were inputted, and the visibility prediction networks were constructed (networks were constructed for each participant).

### B. Results of the Color Scheme Visibility Prediction

Using the trained network, predictions on whether the left or right character would be more visible against the background were made by each participant for the seven non-basic character color groupings. The results were then compared to the actual pairwise comparison experiment data (2800 observations). Table IV presents the results of the two existing methods and the proposed method. Furthermore, the table also shows the mean values of the predictive precision (the ratio of correct answers for the 2800 observations) for each color for the 20 participants and the mean values of the predictive precision with respect to all character colors for each of the existing and proposed methods.

Table IV shows that the mean value of the predictive precision for the 20 participants with respect to all character colors using the proposed method was 82.16%. For the Existing Method-1, the result was 79.58%, and for the Existing Method-2, the value was 81.52%. Using the proposed method returns a level of predictive precision that is higher than the Existing Method-2 (MSC Model), which has higher predictive accuracy of the two existing methods.

TABLE IV. RESULTS OF THE COLOR SCHEME VISIBILITY PREDICTION

| Character color | Existing Method-1 | Existing Method-2 | Proposed Method |
|-----------------|-------------------|-------------------|-----------------|
| Cyan            | 86.20%            | 89.97%            | 88.36%          |
| Magenta         | 82.48%            | 87.55%            | 86.67%          |
| Yellow          | 88.16%            | 89.71%            | 89.46%          |
| WSC1            | 78.17%            | 80.97%            | 81.87%          |
| WSC2            | 80.65%            | 78.93%            | 82.02%          |
| WSC3            | 58.68%            | 57.41%            | 60.35%          |
| WSC4            | 82.75%            | 86.08%            | 86.41%          |
| Mean            | 79.58%            | 81.52%            | 82.16%          |

C. Results of the Prediction of Pairwise Comparison Tables

In this stage, pairwise comparison tables for the seven non-basic color groupings were predicted and compared to those created from actual experimental data. As an example, Table V presents the pairwise comparison tables predicted using the proposed method for the case where the character colors were from the cyan grouping, and the background color was from the red grouping. The upper values show the actual pairwise comparison scores and the values shown in parentheses are the predicted pairwise comparison scores.

With regard to the predictive precision of the pairwise comparison tables, it is sufficient to evaluate them by using the difference between the predicted value and the actual pairwise comparison score. The evaluation index employs the error sum of squares between these two values. Specifically, as shown in Table V, when using the pairwise comparison tables to change a color scheme for easier viewing, it is sufficient to change to a color scheme with a high score. Therefore, when using pairwise comparison tables to compare color scheme visibility, the magnitude relationship of adjacent scores should be assessed. In this context, the actual and predicted values of the magnitude relationship between the score of an arbitrary color scheme in the table and the scores of its eight adjacent (above/below, left/right, and diagonal) color schemes were tested for consistency for all color schemes. The ratio of these values (referred to as the accuracy rate) was used as the predictive precision of the pairwise comparison tables. Table VI and Table VII present the accuracy rate for each of the character colors for the 20 participants as well as the mean of the error sum of squares and the mean value for all character colors for each of the existing and proposed methods.

TABLE V. PREDICTION OF THURSTONE PAIRWISE COMPARISON METHOD (CHARACTER COLOR CYAN, BACKGROUND COLOR RED)

| Background color | Character colors   |                    |                    |                   |                  |
|------------------|--------------------|--------------------|--------------------|-------------------|------------------|
|                  | #003333            | #006666            | #009999            | #00cccc           | #00ffff          |
| #660000          | -1.352<br>(-1.325) | -0.676<br>(-0.557) | 0.071<br>(-0.066)  | 0.761<br>(0.718)  | 1.196<br>(1.230) |
| #990000          | -0.621<br>(-0.659) | -1.163<br>(-0.719) | -0.172<br>(-0.393) | 0.723<br>(0.50)   | 1.233<br>(1.272) |
| #cc0000          | -0.092<br>(-0.179) | -0.894<br>(-0.842) | -0.608<br>(-0.613) | 0.361<br>(0.460)  | 1.233<br>(1.174) |
| #ff0000          | 0.534<br>(0.482)   | -0.461<br>(-0.313) | -0.671<br>(-0.924) | -0.012<br>(-0.05) | 0.611<br>(0.806) |

TABLE VI. RESULTS OF THE PREDICTION OF PAIRWISE COMPARISON TABLES (ACCURACY RATE)

| Character color | Existing Method-1 | Existing Method-2 | Proposed Method |
|-----------------|-------------------|-------------------|-----------------|
| Cyan            | 82.28%            | 86.61%            | 84.55%          |
| Magenta         | 78.39%            | 82.68%            | 81.50%          |
| Yellow          | 85.21%            | 87.03%            | 85.84%          |
| WSC1            | 74.86%            | 77.19%            | 78.02%          |
| WSC2            | 75.61%            | 74.14%            | 76.86%          |
| WSC3            | 59.49%            | 59.39%            | 61.55%          |
| WSC4            | 77.70%            | 81.08%            | 79.81%          |
| Mean            | 76.22%            | 78.30%            | 78.30%          |

TABLE VII. RESULTS OF THE PREDICTION OF PAIRWISE COMPARISON TABLES (MEAN OF THE ERROR SUM OF SQUARES)

| Character color | Existing Method-1 | Existing Method-2 | Proposed Method |
|-----------------|-------------------|-------------------|-----------------|
| Cyan            | 0.424             | 0.269             | 0.340           |
| Magenta         | 0.633             | 0.354             | 0.395           |
| Yellow          | 0.361             | 0.286             | 0.306           |
| WSC1            | 0.748             | 0.559             | 0.543           |
| WSC2            | 0.626             | 0.656             | 0.557           |
| WSC3            | 1.496             | 1.568             | 1.401           |
| WSC4            | 0.617             | 0.422             | 0.426           |
| Mean            | 0.701             | 0.588             | 0.567           |

The results in Table VI and Table VII are as follows: proposed method 78.30% (0.567), Existing Method-1 76.22% (0.701), and Existing Method-2 78.30% (0.588). The accuracy rate for the proposed method was approximately the same as that for the Existing Method-2 (MSC Model), but the value of the error sum of squares shows that there has been an improvement in predictive precision. The above results indicate that, with regard to the prediction of pairwise comparison tables, the proposed method realizes an improvement in predictive precision when compared to the methods in the existing literature.

VI. DISCUSSION

A. Predictive Precision of the Color Recognition Network

This section considers the predictive precision of the color recognition network. When actually predicting color scheme visibility, all results of the color sample cards (652 colors) were utilized in constructing the color recognition network. From the perspective of network evaluation, the color sample cards were divided into training data and evaluation data. Two patterns for the data (2-cross validation) were created, one where the even-numbered colors (of the 652 total colors) were used for training data and the odd-numbered colors were used for the evaluation data and another where the odd-numbered colors were used for the training and even numbered colors for evaluation. Under the conditions described in Section 4.3, the training data was used to develop the color recognition network. Color name prediction was performed on the evaluation data of sixty participants, and the level of predictive precision was derived. Table VIII presents the results of this process.

Table VIII presents the mean value, standard deviation, and maximum and minimum values for the accuracy rate for the sixty participants. For comparison purposes, the results of the nearest neighbor algorithm are also shown. Table VIII shows that the color recognition network can be used to predict the color recognition of individual participants with a predictive precision level of approximately 75% (compared to the nearest neighbor algorithm, an increase of 10.5% in the predictive precision level can be expected).

B. Features Utilized in the Training of the Visibility Prediction Network

In this study, the output values from the output layer of the color recognition network (referred to as Feature-1) were

utilized as features for training the visibility prediction network. The output values of the middle layers of a network trained through backpropagation can be used as valid features after the output of output values in line with the teaching signal. In this context, the output values of every middle layer in the color recognition network were trialed as a feature in the visibility prediction network (referred to as Feature-2). In this case, given that differences in the output values of all of the middle layers of the three color recognition networks were taken as features, the number of features to be entered into the visibility prediction network was 80 ( $40 \times 2$ ).

TABLE. VIII. PREDICTIVE PRECISION OF THE COLOR RECOGNITION NETWORK

|                  | Mean   | Standard Deviation | Maximum | Minimum |
|------------------|--------|--------------------|---------|---------|
| Proposed Method  | 75.47% | 3.66%              | 81.90%  | 65.34%  |
| Nearest Neighbor | 64.98% | 3.16%              | 70.55%  | 57.21%  |

TABLE. IX. RESULTS OF THE COLOR SCHEME VISIBILITY PREDICTION WITH FEATURE-1 AND FEATURE-2

| Character color | Proposed Method |           |
|-----------------|-----------------|-----------|
|                 | Feature-1       | Feature-2 |
| Cyan            | 88.36%          | 89.48%    |
| Magenta         | 86.67%          | 88.95%    |
| Yellow          | 89.46%          | 92.01%    |
| WSC1            | 81.87%          | 83.16%    |
| WSC2            | 82.02%          | 83.90%    |
| WSC3            | 60.35%          | 60.96%    |
| WSC4            | 86.41%          | 89.17%    |
| Mean            | 82.16%          | 83.95%    |

TABLE. X. RESULTS OF THE PREDICTION OF PAIRWISE COMPARISON TABLES WITH FEATURE-1 AND FEATURE-2 (ACCURACY RATE AND MEAN OF THE ERROR SUM OF SQUARES)

| Character color | Proposed Method   |                   |
|-----------------|-------------------|-------------------|
|                 | Feature-1         | Feature-2         |
| Cyan            | 84.55%<br>(0.340) | 86.14%<br>(0.30)  |
| Magenta         | 81.50%<br>(0.395) | 84.22%<br>(0.317) |
| Yellow          | 85.84%<br>(0.306) | 89.47%<br>(0.217) |
| WSC1            | 78.02%<br>(0.543) | 79.19%<br>(0.508) |
| WSC2            | 76.86%<br>(0.557) | 79.34%<br>(0.464) |
| WSC3            | 61.55%<br>(1.401) | 61.80%<br>(1.362) |
| WSC4            | 79.81%<br>(0.426) | 84.40%<br>(0.325) |
| Mean            | 78.30%<br>(0.567) | 80.65%<br>(0.499) |

The results of the color scheme visibility and pairwise comparison table predictions after training the visibility prediction network with Feature-2 are presented in Table IX and Table X. The training conditions were similar for Feature-1.

Table IX shows that Feature-2 has an accuracy level of 83.95% when predicting color scheme visibility results, which is 1.8 percentage point improvement over the result for Feature-1 (82.16%). Furthermore, Table X shows that using Feature 2 when predicting pairwise comparison tables yields an accuracy level of 80.65% with an error sum of squares of 0.499, which is an improvement over the result for Features-1 (accuracy rate of 78.30%, error sum of squares of 0.567). Accordingly, when predicting color scheme visibility, the output values of the color recognition network and the output values of the middle layer are important. Specifically, the results confirm the validity of the color recognition network.

## VII. CONCLUSION AND FUTURE WORK

Based on the research into the prediction of pairwise comparison tables as an index of the visibility of background and character colors, this study constitutes an attempt to improve the predictive precision of these tables by training a neural network capable of predicting color scheme visibility. The proposed method consists of a color recognition neural network for extracting features and a visibility prediction neural network for predicting color scheme visibility. For the feature extraction element, the data collected from the color recognition experiment was used to develop a color recognition neural network, which extracted features related to color scheme visibility. The prediction element used the extracted features to train the visibility prediction neural network. In the final step, data collected from the pairwise comparison experiment was used to predict the pairwise comparison tables of unfamiliar color schemes.

The results of this study show that the proposed method can produce higher levels of predictive precision than those used in previous studies, and that it is possible to develop a neural network that can be trained to be capable of predicting color scheme visibility. Future research plans include the collection of more data through color recognition experiments and improving the color recognition network by attempting to increase the predictive precision through the extraction of color scheme visibility features with higher validity.

### REFERENCES

- [1] J. Ling and P. Schaik, "The effect of text and background colour on visual search of web pages," *Displays*, Vol. 23, No. 5, pp.223-230, 2002.
- [2] R. H. Hall and P. Hanna, "The impact of web page text-background colour combinations on readability, retention, aesthetics and behavioural intention," *Behaviour and Information Technology*, Vol. 23, No. 3, pp.183-195, 2004.
- [3] N. Nishiuchi, K. Yamanaka, and K. Beppu, "A Study of Visibility Evaluation for the Combination of Character Color and Background Color on a Web Page," 2008 Second International Conference on Secure System Integration and Reliability Improvement, pp.191-192, 2008.
- [4] D. Bhattacharyya, B. Chowdhury, T. Chatterjee, M. Pal, and D. Majumdar, "Selection of character/background colour combinations for onscreen searching tasks: An eye movement, subjective and performance approach," *Displays*, Vol. 35, No. 3, pp.101-109, 2014.
- [5] M. Grozdanovic, D. Marjanovic, G. L. Janackovic, and M. Djordjevic, "The impact of character/backgroundcolour combinations and

- exposition on character legibility and readability on video display units," Transactions of the Institute of Measurement and Control, Vol. 39, No. 10, pp.1454-1465, 2017.
- [6] D. Saito, K. Saito, K. Notomi, and Masao Saito, "A Study on Visibility Rating of Several Representative Web-Safe Color," IEEJ Transactions on Electronics, Information and Systems, Vol. 125, No. 6, pp.892-897, 2005 (in Japanese).
- [7] T. Oikawa and Y. Shinozawa, "Prediction of visibility for background and character colors on the web browser," Transactions of Human Interface Society, Vol. 14, No. 2, pp.75-86, 2012 (in Japanese).
- [8] M. Yamaguchi and Y. Shinozawa, "Prediction of Visibility for Color Schemewith a Multi-stage Color Model," Transactions of Information Processing Society of Japan, Vol. 54, No. 3, pp.1230-1241, 2013 (in Japanese).
- [9] R. L. De Valois and K. K. De Valois, "A multi-stage color model," Vision Research, Vol.33, No.8, pp.1053-1065, 1993.
- [10] F. Vi'eno't, H. Brettel, and J. D. Mollon, "Digital video colourmaps for checking the legibility of displays by dichromats," COLOR research and application, Vol.24, No.4, pp.243-252, 1999.
- [11] DIC Color Guide 19th Edition, [http://www.dic-graphics.co.jp/products/cguide/dic\\_color\\_guide.html](http://www.dic-graphics.co.jp/products/cguide/dic_color_guide.html) (2019/06/17 author checked).
- [12] B. Berlin and P. Kay, "Basic Color Terms: Their Universality and Evolution," Berkeley & Los Angeles: University of California Press, 1969.

# Application of the Scattering Bond Graph Methodology for Composite Right/Left Handed Transmission Lines

Islem Salem<sup>1</sup>, Hichem Taghouti<sup>2</sup>, Ahmed Rahmani<sup>3</sup>, Abdelkader Mami<sup>4</sup>  
UR-LAPER, University of Tunis El Manar, Tunis, Tunisia<sup>1,2,4</sup>  
CRISAL, Centrale Lille, Lille, France<sup>3</sup>

**Abstract**—The approach of the metamaterials based on the theory of transmission lines has an influence on the development of the radiofrequency domain, so the types and techniques of elaboration of these artificial lines are quite diversified. This paper will present two models of Artificial Transmission Line CRLH (Composite Right Left Handed) composed of a combination of resonators OSRR (Open Split Ring Resonators) and OSCRR (Complementary Open Split Ring Resonators). This paper will also show how the Scattering Bond Graph (SBG) study methodology allows to provide electromagnetic simulation results (Scattering parameters, phase response) more conducive to Bond Graph (BG) modeling, and will prove the possibility of having the most perfect line (solved the problem of impedance adaptation) and better understanding of the behavior of radiofrequency systems.

**Keywords**—Scattering Bond Graph (SBG); metamaterials; wave matrix [W]; modelization; transmission line; scattering matrix [S]; CRLH; OSCRR; OSRR

## I. INTRODUCTION

The development of the communication system imposes the evolution of the modeling and study techniques of hyperfrequency systems. As well as, the exploitation of metamaterials technology [1] (periodic structure characterize by wave propagation with opposite phase and group speed) to play an important role in reducing the size of electronic circuits. Among the applications used by this technology are the waveguide structures (filter) and the radiant devices (antenna) which seems to have more advantage compared to the old structures.

Despite the many advantages of the metamaterials techniques [2], the analysis of microwave circuits remains difficult and has problems especially adaptation and modeling that requires manufacturers to redo the complete study to change some parameters which plays a role negative role on the effectiveness of the results obtained.

In [3] and [4], the CRLH (Composite Right Left Handed) structures were introduced by the classical technique which possesses indeterminate equations with several unknowns, thus the resolution of non-homogeneous differential equations.

Since the appearance of the bond graph theory [5] research in the field of dynamic physical systems has been developed, but this theory has remained limited only for low frequency

systems. Until 2009 [6], where researchers have developed an analytical method that makes it possible to classify two-port network (at only one lumped element) in microwave, we apply the conjunction between the scattering formalism and the bond graph approach.

In this study, two types of CRLH transmission line structures inspired by the combination of OSCRR (Complementary Open Split Ring Resonators) and OSRR (Open Split Ring Resonators), will be presented and studied and analyzed with the Scattering Bond Graph methodology.

The first part is dedicated to the modulation and deduction of the parameters of the different system circuits by the scattering bond graph method.

The second part is reserved for the development of two new CRLH transmission line structures, and to study the physical characteristics of each structure from the [W] wave matrix. Where this matrix describes the relations between the incident waves and reflects whatever the complexity of the system.

Finally, the reliability of the methodology is determined from the level of adaptation of the transmission lines and the total transfer of the incident waves

## II. SCATTERING BOND MODELING

The bond graph tool appeared for the first time by Pynter [5], which is a unified graphical language for all domains. This approach is based on the phenomenon of energy exchange (flow and effort) in the system that allows to model and simulate systems that can be multidisciplinary.

The concept of the scattering matrix (generally noted [S]) which was invented for the first time by Wheeler [7], is the study of the n-pole hyper frequency linear system through the parameters of this matrix  $S_{ij}$

The conjunction between the two approaches gives birth to a new methodology called Scattering Bond Graph [8], this methodology proved its efficiency of modelling of the microwave system [9]. This method goes through three phases, first is to model the system by the bond graph approach and apply the causality (notion allows to highlight the cause-effect relationship (flow and effort) of the system and to release an associated mathematical model). Secondly

find the parameters of the wave matrix (denoted [W]) (each subsystem has a wave matrix). Third, find the scattering matrix [S] by applying (1) [7].

$$[S] = \begin{bmatrix} \frac{W_{11}}{W_{22}} & \frac{1}{W_{22}} (W_{22}W_{11} - W_{21}W_{12}) \\ \frac{1}{W_{22}} & \frac{-W_{21}}{W_{22}} \end{bmatrix} \quad (1)$$

The SBG technique is based on the translation of the electrical circuit based in lumped elements into a graphic diagram [10]. But in radio frequency each element admits its own electrical and magnetic characteristics (electric and magnetic fields). In the case of study with the BG approach we can consider that the whole system is a resonant element, which allows us to have more precision.

As shown in Fig. 1, the circuit in “π” is composed by the combination of a shunt admittance “Y” in parallel with a series impedance “Z” in parallel with another shunt admittance “Y”.

Using the bond-graph approach definitions, the “π” causal circuit model (present of a causal link between a potential input and output of the model) can be represented by Fig. 2 (0-1-0 junction).

From the causal model bond graph 0-1-0 junction we can directly extract the wave matrix [W]<sub>010</sub>

$$[W]_{010} = \frac{1}{2} \begin{bmatrix} zy^2 + 2yz + 2z + y + 2 & zy^2 - z + 2y \\ -zy^2 + z - 2y & -zy^2 + 2yz - 2y - z + 2 \end{bmatrix} \quad (2)$$

As shown in Fig. 3 the circuit in “T” is composed by the combination of a series impedance “Z” in parallel with a shunt admittance “Y” in parallel with another series impedance “Z” [9] [11].

Using the bond-graph approach definitions, the “T” causal circuit model can be represented by Fig. 4 (1-0-1 junction).

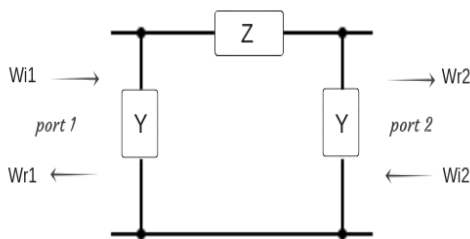


Fig. 1. Model of a Circuit in “π”.

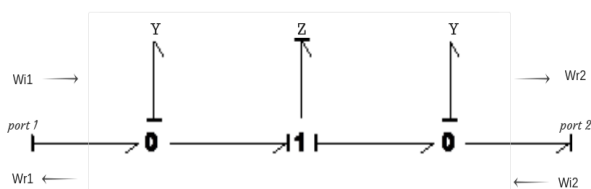


Fig. 2. Causal Bond Graph Model of Circuit in “π”.

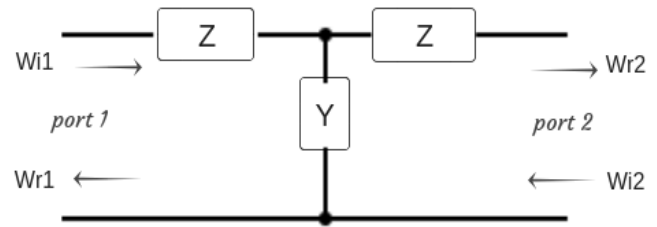


Fig. 3. Model of a Circuit in “T”.

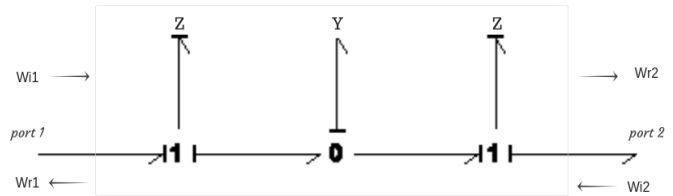


Fig. 4. Causal Bond Graph Model of Circuit in “T”.

From the causal model bond graph 0-1-0 junction can directly extract the wave matrix [W]<sub>101</sub>

$$[W]_{101} = \frac{1}{2} \begin{bmatrix} yz^2 + 2yz + 2z + y + 2 & yz^2 + y - 2z \\ yz^2 - y + 2z & -yz^2 + 2yz - 2z - y + 2 \end{bmatrix} \quad (3)$$

### III. ANALYSIS COMPOSITE RIGHT/LEFT HANDED (CRLH) TRANSMISSION LINE BY SCATTERING BOND GRAPH METHODOLOGY

The CRLH line introduced for the first time by the American Cloz in 2003 [12], and as its name indicates, the CRLH is transmission line has a right handed wave propagation (admits a positive permittivity and permeability ( $\epsilon_r > 0$  and  $\mu_r > 0$ )), but also a wave propagation left handed (also called artificial doubly negative materials ( $\epsilon_r < 0$  and  $\mu_r < 0$ )). Several researches have shown that the exploitation of CRLH has the advantage of being able to reduce the size and the number of the electrical components for the systems of wireless communication.

In the rest of this study, will be interested in the development of the CRLH transmission line modeling technique based on the combination of the OSRR resonator introduced by J. Martel and Al in 2004 [13] and OCSRR resonator, produced by A.Velz and Al in 2009 [14]. This contribution will be made by the proposed methodology Scattering Bond Graph.

The CRLH line is composed of three sub-systems in cascade, from which the choice of the SBG approach wasn't arbitrary since among the advantages of this methodology it solved the problem of adaptation between subsystems, in other words will haven't to redo the calculations or add parameters to reach the adaptation between the different subsystems (OSRR and OCSRR resonators) before having the adaptation to the complete system (CRLH line).

The solution is to apply the product of the wave matrices [W] extract directly from the equivalent diagram Bond Graph before finding the scattering parameter (through the relation (1))

The first sub-system is the OSRR resonator. Fig. 5 represents its equivalent Bond Graph model (circuit T) where it is composed by a capacitance element C (parasitic capacitance will be taken into account in the design) in serie (1-junction) with C<sub>serie</sub> and L<sub>serie</sub>, then in parallel with a second capacitance element C.

By applying the laws of the BG approach and causality obtain the wave matrix [W]<sub>OSRR</sub>

$$[W]_{OSRR} = \frac{1}{2} \begin{bmatrix} z_s y^2 + 2 y z_s + 2 y + z_s + 2 & z_s y^2 - z_s + 2 y \\ -z_s y^2 + z_s - 2 y & -z_s y^2 + 2 y z_s - 2 y - z_s + 2 \end{bmatrix} \quad (4)$$

Where, z<sub>s</sub> and y represent respectively the normalized series impedance and the normalized admittance (s: represents the Laplace operator).

$$z_s = \left( \frac{1}{\tau_{cserie}} + \tau_{Lserie} \right) s \quad (5)$$

$$y = \tau_c s \quad (6)$$

The second sub-system is the OCSRR resonator. Fig. 6 represents its equivalent Bond Graph model (circuit π) where it is composed by an inductance element L (parasitic inductance will be taken into account in the design) in parallel (0-junction) with C<sub>parallel</sub> and L<sub>parallel</sub>, in series with a second inductance element L.

By applying the laws of the BG approach and causality obtain the wave matrix [W]<sub>OCSRR</sub>

$$[W]_{OCSRR} = \frac{1}{2} \begin{bmatrix} y_p z^2 + 2 y_p z + 2 z + y_p + 2 & y_p z^2 + y_p - 2 z \\ y_p z^2 - y_p + 2 z & -y_p z^2 + 2 y_p z - 2 z - y_p + 2 \end{bmatrix} \quad (7)$$

Where, y<sub>p</sub> and z represent respectively the normalized parallel admittance and the normalized impedance.

$$y_p = \left( \frac{1}{\tau_{Lparallel}} + \tau_{Cparallel} \right) s \quad (8)$$

$$z = \tau_L s \quad (9)$$

#### A. OCSRR-OSRR-OCSRR Line Model

The first proposal for a CRLH transmission line is represented by Fig. 7 where it consists of two OCSRR resonators and an OSRR resonator that are cascading.

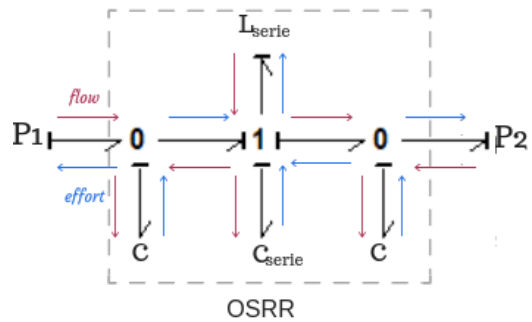


Fig. 5. Representation of the Model by Bond Graph of the Resonator OSRR.

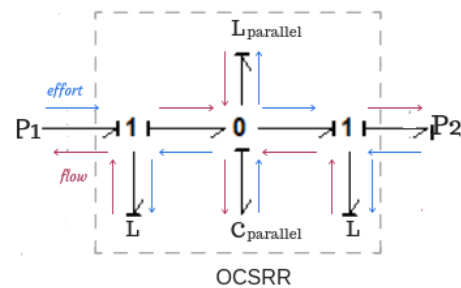


Fig. 6. Representation of the Model by Bond Graph of the Resonator OCSRR.

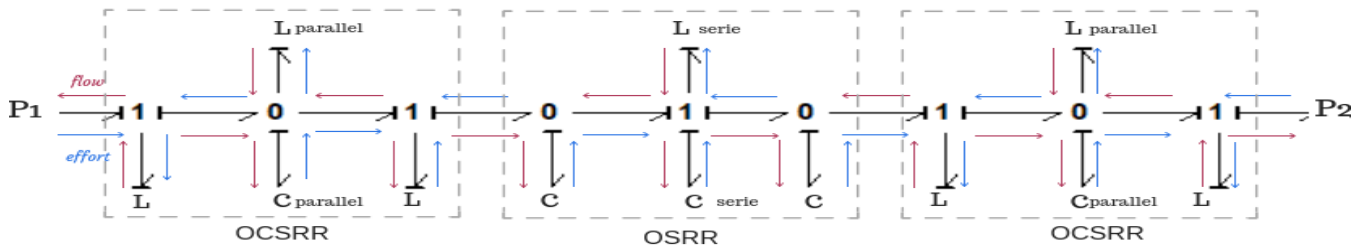


Fig. 7. Representation of the Model by Bond Graph of the CRLH Line.

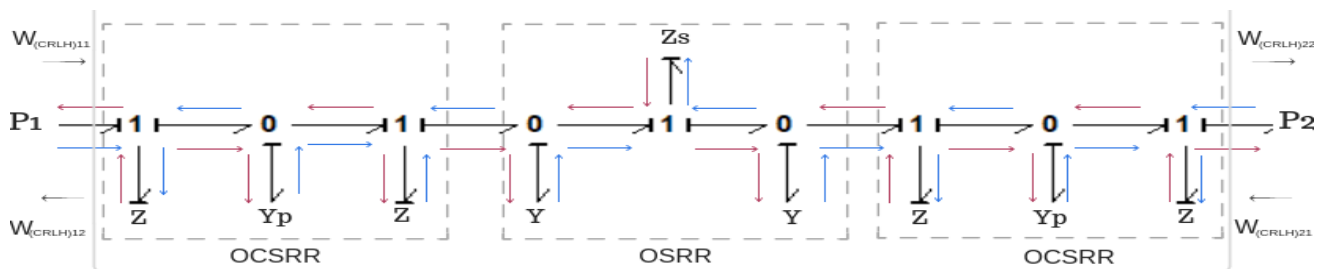


Fig. 8. Representation of the Reduced Model by Bond Graph of the CRLH Line.

By applying the properties of the bond graph approach to the representation of CRLH, the reduced model is presented by Fig. 8.

The wave matrix  $[W_{CRLH}]_A$  of the CRLH line can be written as follows (by (4) and (6)).

$$[W_{CRLH}]_A = [W]_{OCSRR} * [W]_{OSRR} * [W]_{OCSRR} \quad (10)$$

$$[W_{CRLH}]_A = \begin{pmatrix} W_{CRLH11A} & W_{CRLH12A} \\ W_{CRLH21A} & W_{CRLH22A} \end{pmatrix} \quad (11)$$

$$W_{CRLH11A} = \frac{1}{8} \left( -(y^2z_s + 2y - z_s)(y_pz^2 + y_p - 2z) + (y^2z_s + 2yz_s + 2y + z_s + 2)(y_pz^2 + 2y_pz + y_p + 2z + 2) - (y^2z_s + 2y - z_s)(y_pz^2 + 2y_pz + y_p + 2z + 2) + (y_pz^2 + y_p - 2z)(y^2z_s - 2yz_s + 2y + z_s - 2) \right) (y_pz^2 - y_p + 2z) \quad (12)$$

$$W_{CRLH12A} = -\frac{1}{8} \left( (y^2z_s + 2y - z_s)(y_pz^2 + y_p - 2z) - (y^2z_s + 2yz_s + 2y + z_s + 2)(y_pz^2 + 2y_pz + y_p + 2z + 2) + (y_pz^2 + y_p - 2z) + (-y^2z_s + 2y - z_s)(y_pz^2 + 2y_pz + y_p + 2z + 2) + (y_pz^2 + y_p - 2z)(y^2z_s - 2yz_s + 2y + z_s - 2) \right) (y_pz^2 - y_p + 2z) \quad (13)$$

$$W_{CRLH21A} = \frac{1}{8} \left( (y^2z_s + 2y - z_s)(y_pz^2 - y_p + 2z) + (y^2z_s - 2yz_s + 2y + z_s - 2)(y_pz^2 - 2y_pz + y_p + 2z - 2) + (y_pz^2 - y_p + 2z) + (y^2z_s + 2y - z_s)(y_pz^2 + 2y_pz + y_p + 2z + 2) + (y_pz^2 - 2y_pz + y_p + 2z - 2) + (y_pz^2 - y_p + 2z)(y^2z_s + 2yz_s + 2y + z_s + 2) \right) (y_pz^2 + 2y_pz + y_p + 2z + 2) \quad (14)$$

$$W_{CRLH22A} = -\frac{1}{8} \left( (y^2z_s + 2y - z_s)(y_pz^2 - y_p + 2z) + (y^2z_s - 2yz_s + 2y + z_s - 2)(y_pz^2 - 2y_pz + y_p + 2z - 2) + (y_pz^2 - 2y_pz + y_p + 2z - 2) + (y^2z_s + 2y - z_s)(y_pz^2 + 2y_pz + y_p + 2z + 2) + (y_pz^2 - 2y_pz + y_p + 2z - 2) + (y_pz^2 - y_p + 2z)(y^2z_s + 2yz_s + 2y + z_s + 2) \right) (y_pz^2 + y_p - 2z) \quad (15)$$

According to the equivalent diagram of the assembly of the three proposed resonators, have obtained the characteristic wave matrix  $[W_{CRLH}]_A$ . To obtain the electromagnetic responses of this system, it is necessary to directly deduce the scattering matrix  $[S_{CRLH}]_A$  from the whole system.

$$[S_{CRLH}]_A = \begin{bmatrix} \frac{W_{CRLH11A}}{W_{CRLH22A}} & \frac{W_{CRLH22A}W_{CRLH11A} - W_{CRLH21A}W_{CRLH12A}}{W_{CRLH22A}} \\ 1 & \frac{-W_{CRLH21A}}{W_{CRLH22A}} \end{bmatrix} \quad (16)$$

Fig. 9 represents the frequency response of the proposed CRLH<sub>A</sub> line (transmission and reflection coefficient) and Fig. 10 represents the phase response.

According to the result of the simulation obtained, the CRLH<sub>A</sub> admits two spades of frequencies at resonance frequencies 2.2 GHz and 3.8GHz and at most -23 dB, which proves that the system is adapted to a bandwidth of 3.4 GHz. But the incident wave isn't totally transmitted.

### B. OSRR-OCSRR-OSRR Line Model

The second proposal for a CRLH transmission line is represented by Fig. 11 where it consists of two OSRR resonators and an OCSRR resonator that are cascading.

By applying the properties of the bond graph approach to the representation of CRLH, the reduced model is presented by Fig. 12.

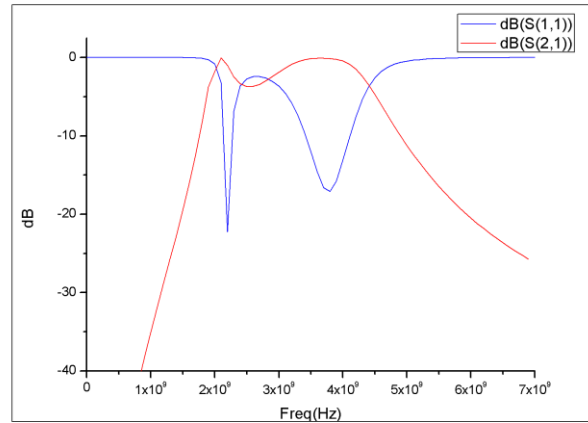


Fig. 9. The Frequency Response of the Proposed CRLH<sub>A</sub> Line.

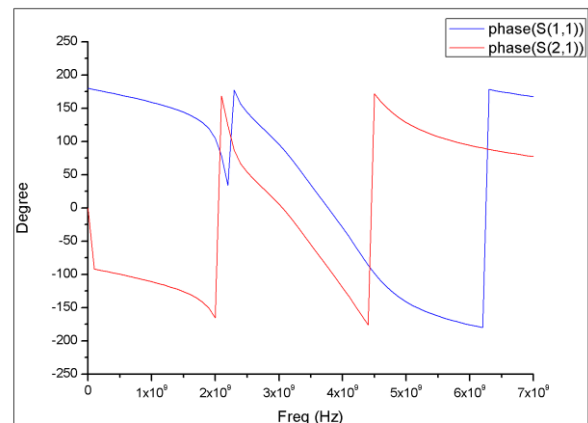


Fig. 10. The Phase Response.

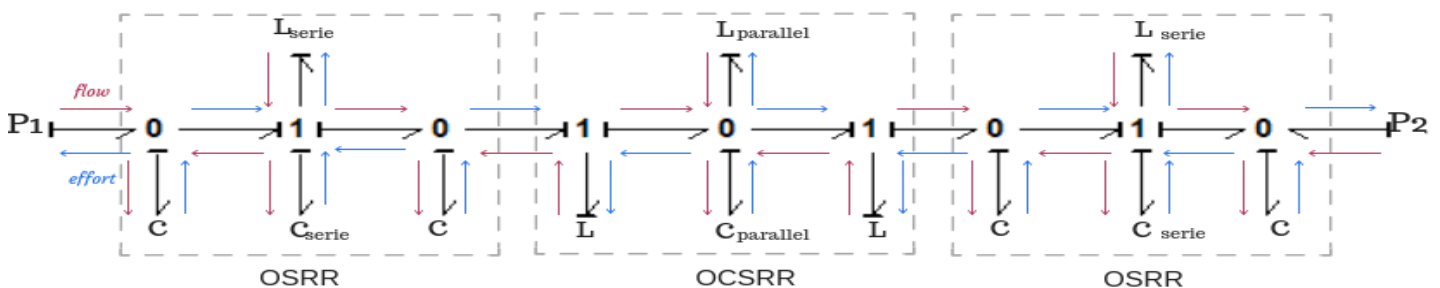


Fig. 11. Representation of the CRLH<sub>B</sub> Model by Bond Graph.



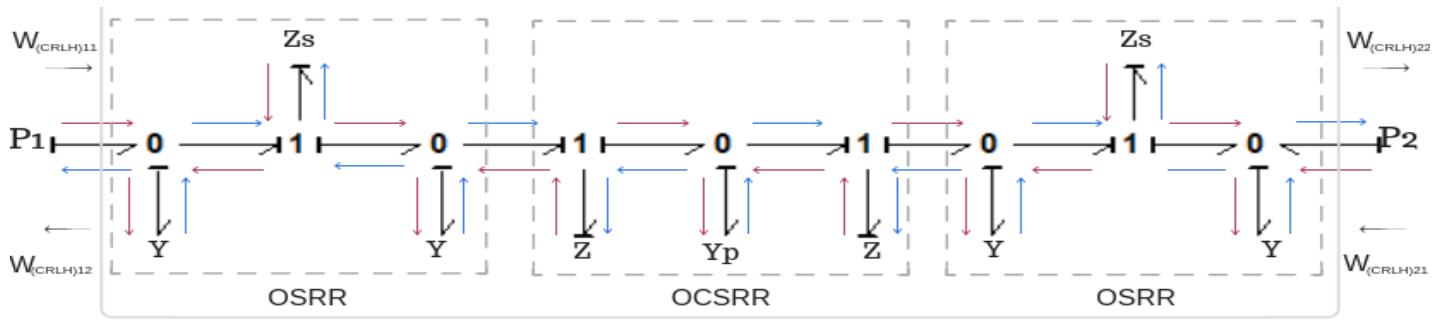


Fig. 12. Representation of the CRLH<sub>B</sub> Reduced Model by Bond Graph.

The wave matrix  $[W_{CRLH}]_A$  of the CRLH line can be written as follows (by (4) and (6)):

$$[W_{CRLH}]_B = [W]_{OCSRR} * [W]_{OSRR} * [W]_{OCSRR} \quad (17)$$

$$[W_{CRLH}]_B = \begin{pmatrix} W_{CRLH11B} & W_{CRLH12B} \\ W_{CRLH21B} & W_{CRLH22B} \end{pmatrix} \quad (18)$$

$$[W_{CRLH}]_{11B} = \frac{1}{8} ((y^2 z_s + 2y - z_s)(y_p z^2 - y_p + 2z) + (y^2 z_s + 2y z_s + 2y + z_s + 2)(y_p z^2 + 2y_p z + y_p + 2z - 2) - (y^2 z_s + 2y - z_s)(y_p z^2 - 2y_p z + y_p + 2z - 2) + (y_p z^2 + y_p - 2z)(y^2 z_s + 2y z_s + 2y + z_s + 2))(y^2 z_s + 2y - z_s) \quad (18)$$

$$[W_{CRLH}]_{12B} = \frac{1}{8} ((y^2 z_s + 2y - z_s)(y_p z^2 - y_p + 2z) + (y^2 z_s + 2y z_s + 2y + z_s + 2)(y_p z^2 + 2y_p z + y_p + 2z - 2) - (y^2 z_s + 2y - z_s)(y_p z^2 - 2y_p z + y_p + 2z - 2) + (y_p z^2 + y_p - 2z)(y^2 z_s + 2y z_s + 2y + z_s + 2))(y^2 z_s - 2y z_s + 2y + z_s - 2) \quad (19)$$

$$[W_{CRLH}]_{21B} = \frac{1}{8} ((y^2 z_s + 2y - z_s)(y_p z^2 + y_p - 2z) - (y^2 z_s - 2y z_s + 2y + z_s - 2)(y_p z^2 - 2y_p z + y_p + 2z - 2) + (y_p z^2 - y_p + 2z)(y^2 z_s - 2y z_s + 2y + z_s - 2))(y^2 z_s + 2y z_s + 2y + z_s - 2) \quad (20)$$

$$[W_{CRLH}]_{22B} = \frac{1}{8} ((y^2 z_s + 2y - z_s)(y_p z^2 + y_p - 2z) - (y^2 z_s - 2y z_s + 2y + z_s - 2)(y_p z^2 - 2y_p z + y_p + 2z - 2) + (y_p z^2 - y_p + 2z)(y^2 z_s - 2y z_s + 2y + z_s - 2))(y^2 z_s + 2y - z_s) \quad (21)$$

According to the equivalent diagram of the assembly of the three proposed resonators, have obtained the characteristic wave matrix  $[W_{CRLH}]_B$ . To obtain the electromagnetic responses of this system, it is necessary to directly deduce the scattering matrix  $[S_{CRLH}]_B$  from the whole system.

$$[S_{CRLH}]_B =$$

$$\begin{bmatrix} W_{CRLH11B} & (W_{CRLH22B} W_{CRLH11B} - W_{CRLH21B} W_{CRLH12B}) \\ W_{CRLH22B} & W_{CRLH22B} \\ 1 & -W_{CRLH21B} \\ W_{CRLH22B} & W_{CRLH22B} \end{bmatrix} \quad (22)$$

Fig. 13 represents the frequency response of the proposed CRLH<sub>B</sub> line (transmission and reflection coefficient) and Fig. 14 represents the phase response.

According to the result of the simulation obtained, the CRLH<sub>B</sub> admits two spades of frequencies at resonance frequencies 2.1 GHz and 4.4 GHz and at most -35 dB, which proves that the system is adapted to a bandwidth of 3.4GHz. And the incident wave is totally transmitted.

### C. Discussion

The choice of the most perfect model type is made according to the highest adaptation. This model must also consider the need to have the minimum loss.

It is noted that the line CRLH<sub>B</sub> is more preferment than the line CRLH<sub>A</sub>. Because according to the results of simulation the line CRLH<sub>B</sub> is more adaptable is possesses a wider bandwidth and does not admit of loss. So for the realization of line CRLH one proposes the second solution.

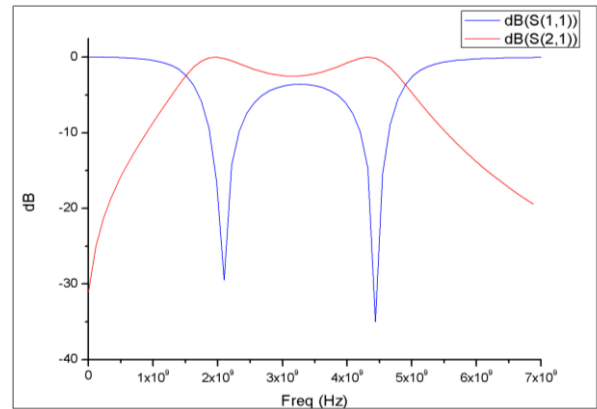


Fig. 13. The Frequency Response of the Proposed CRLH<sub>B</sub>.

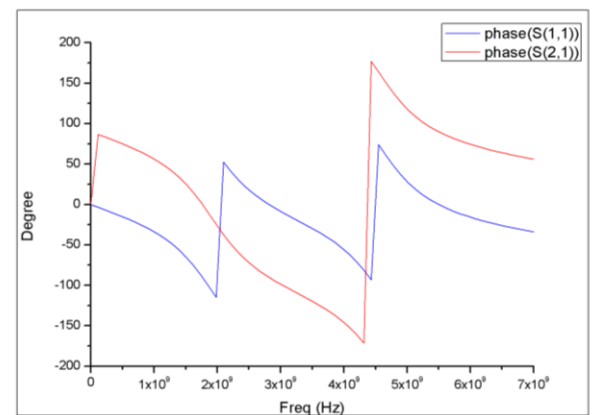


Fig. 14. The Phase Response.

#### IV. CONCLUSION

In the first part, we modeled the equivalent circuits of the resonators OCSRR and OSRR, and then we developed the wave matrix [W] by applying the properties of the bond graph.

In the second part, we proposed two new CRLH transmission line structures based on the combination of OCSRR and OSRR.

In the third part, we analyzed the characteristics of each transmission line from its scattering parameters deduced from the diagram bond graph.

Finally, we proved by simulation that the scattering bond graph methodology is a useful tool to check the performance of radiofrequency models before the implementation phase. We also validated that SBG is a simpler and more reliable technique for complex communication systems.

In the study of the future, we use the efficiency of the scattering bond graph methodology in the study of the more complex system that is the Dual Composite Right/Left Handed Transmission.

#### REFERENCES

- [1] Grbic, G. V Eleftheriades, A. Grbic, and G. V Eleftheriades, "Experimental verification of backward-wave radiation from a negative refractive index metamaterial Experimental verification of backward-wave radiation from a negative refractive index metamaterial," vol. 5930, 2002.
- [2] W. Hong, B. Liu, Y. Wang, Q. Lai, and H. Tang, "Half Mode Substrate Integrated Waveguide : A New Guided Wave Structure for Microwave and Millimeter Wave Application," vol. 152, p. 4244, 2006.
- [3] A. A. Chaudhry, J. K. Arif, Z. Ahmed, M. A. Chaudhary, and M. Bin Ihsan, "Parameter Extraction of Composite Right / Left Handed ( CRLH ) Transmission Line Unit Cell Using Off Resonance Method," pp. 779–781, 2017.
- [4] P. Fathi, Z. Atlasbaf, and K. Forooraghi, "Compact Dual-Wideband Bandpass Filter Using CSRR Based Extended Right / Left-Handed Transmission Line," vol. 81, no. January, pp. 21–30, 2018.
- [5] H. Paynter and M. M. I. T. Press, "Analysis and design of engineering systems : class notes for M . I . T . course 2 . 751 / by Henry M . Paynter ; with the assistance of Peter Briggs . not subject to copyright . Users are free to copy , use , " 1961.
- [6] H. Taghouti, A. Mami, and B. Graph, "Extraction , Modelling and Simulation of the Scattering Matrix of a Chebychev Low-Pass Filter with cut-off frequency 100 MHz from its Causal and Decomposed Bond Graph Model," vol. 10, no. 1, pp. 29–37, 2010.
- [7] "Constructing the scattering matrix for optical microcavities as a nonlocal boundary value problem," vol. 5, no. 6, pp. 20–28, 2017.
- [8] S. Dridi, I. Ben Salem, and L. El Amraoui, "A Multi-Energetic Modeling Approach based on Bond Graph Applied to In-Wheel-Motor Drive System," vol. 9, no. 10, pp. 422–429, 2018.
- [9] I. Salem, H. Taghouti, and A. Mami, "Modeling CSRR and OCSRR loaded transmission line by bond graph approach methodology," 2018 9th Int. Renew. Energy Congr. IREC 2018, no. Irec, pp. 1–6, 2018.
- [10] J. Sabri, N. Omrane, T. Hichem, M. Abdelkader, and G. Ali, "Miniaturized Meander Slot Antenna Tor RFID TAG with Dielectric Resonator at 60 Ghz," Int. J. Adv. Comput. Sci. Appl., vol. 7, no. 4, pp. 373–380, 2016.
- [11] S. Khmailia, "Impedance Matching of a Microstrip Antenna," vol. 8, no. 7, pp. 19–23, 2017.
- [12] F. S. Paper, C. Caloz, T. Itoh, and L. Angeles, "TU2C-3 Invited - Novel Microwave Devices and Structures Based on the Transmission Line Approach of Meta-Materials," pp. 195–198, 2003.
- [13] J. Martel et al., "A New LC Series Element for Compact Bandpass Filter Design," vol. 14, no. 5, pp. 210–212, 2004.
- [14] A. Vélez et al., "Open Complementary Split Ring Resonators ( OCSRRs ) and Their Application to Wideband CPW Band Pass Filters," vol. 19, no. 4, pp. 197–199, 2009.

# Expert System for Milk and Animal Monitoring

Todor Todorov<sup>1</sup>, Juri Stoinov<sup>2</sup>

Institute of Mathematics and Informatics, BAS Sofia, Bulgaria<sup>1</sup>  
Faculty of Mathematics and Informatics  
St. Cyril and St. Methodius University of Veliko Tarnovo  
Veliko Tarnovo, Bulgaria<sup>1,2</sup>

**Abstract**—Expert systems (ES) are one of the prominent research domains of artificial intelligence (AI). They are applications developed to solve complex problems in a particular domain, at the level of extra-ordinary human intelligence and expertise. In the paper is presented design and development of expert system for data collection, analysis and decision making for early mastitis detection. It focuses on both milk quality and animals health.

**Keywords**—Expert system; milk quality; animal health

## I. INTRODUCTION

Expert systems (ES) are characterized with high performance, high responsiveness and reliability combined with ease of use and ease of understanding, which makes developing of such system challenging and involves different type of specialists [1]. The ES are capable of:

- advising and instructing humans in decision making
- demonstrating, explaining and interpreting inputs
- deriving solutions, diagnosing problems, predicting results and justifying conclusions
- suggesting different options for solving the problems in their domain

Despite their capabilities, they also have all kinds of limitations, most significant of them being that they cannot refine their own knowledge base, and that they cannot produce accurate output for inadequate knowledge base. This makes them incapable of substituting human decision making. Expert systems are well integrated in the animal health management [2], [3], [6], [7], [8].

## II. COMPONENTS OF EXPERT SYSTEM

In Fig. 1 are shown components of an ES. It is composed of three main parts that are responsible for different things and are interacting in a different ways [9]. They are the knowledge base, the interface engine and the user interface.

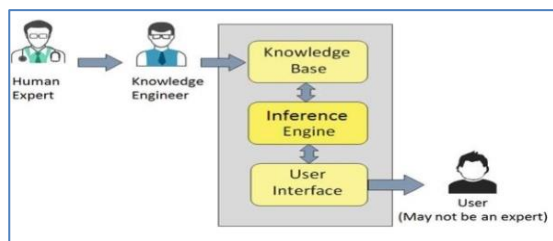


Fig. 1. Components of ES.

## A. Knowledge Base

Knowledge is termed as data, information and past experience combined together. The data is a collection of facts, and the information is organized as data and facts about the task domain. The knowledge base should contain domain-specific and high-quality knowledge. The success of an ES majorly depends upon the collection of highly accurate and precise knowledge. The knowledge base in ES is stored of both factual and heuristic knowledge. Heuristic knowledge is about practice, accurate judgment, and ability of evaluation and informed guessing.

Knowledge representation is the method used to organize and formalize the knowledge in the knowledge base, usually in the form of if-then-else rules [4]. The success of any ES majorly depends on the quality completeness and accuracy of the information stored in the knowledge base. The knowledge base is formed by collecting information from different experts in the specific domain, scientists and the knowledge engineers. The knowledge engineer is a person with case analyzing skills and a quick learner. Knowledge engineer is responsible of categorization and organization of the information in a meaningful way, often in the form of if-then-else constructs to be used by the inference machine. He also monitors the development of the ES and is responsible for the quality control.

## B. Inference Engine

The use of efficient procedures and rules by the inference engine is essential in deducting a correct and flawless solution. In case of knowledge based ES the inference engine acquires and manipulates the data in the knowledge base to arrive in particular solution. In case of rule based ES it applies rules repeatedly to the facts, which are obtained from earlier rule execution. It might also add new knowledge to the knowledge database if required and resolve rule conflicts when multiple rules are applicable to a particular case. In order to recommend a solution, the engine might use forward chaining or backward chaining strategy.

Forward chaining is a strategy based on the question “What can happen next?” The Inference engine runs the chain of conditions and derivation in order to deduce the outcome. It considers all the facts and rules, and sorts them before concluding a solution. This strategy is preferred when the ES is trying to make a conclusion, calculate result or prediction of a result as an effect of changes of some system parameter. For example: trying to predict the effect of increases of greenhouse gasses to the climate.

With backward chaining strategy the ES is trying to find the answer of the question “Why this happened?” On the basis of what has already happened, the Inference tries to find out which conditions could have happened in order to end up with this result. It is used to find the cause for a reason. For example reasons for the increasing rates for type 2 diabetes.

As expert systems evolved, many new techniques were incorporated into various types of inference engines. Some of the most important are:

1) *Truth maintenance*: These systems record the dependencies in a knowledge base so that when facts are altered, dependent knowledge can be altered accordingly. For example, if the system learns that Socrates is no longer known to be a man it will revoke the assertion that Socrates is mortal.

2) *Hypothetical reasoning*: In this, the knowledge base can be divided up into many possible views, a.k.a. worlds. This allows the inference engine to explore multiple possibilities in parallel. For example, the system may want to explore the consequences of both assertions, what will be true if Socrates is a Man and what will be true if he is not?

3) *Fuzzy logic*: One of the first extensions of simply using rules to represent knowledge was also to associate a probability with each rule. So, not to assert that Socrates is mortal, but to assert Socrates may be mortal with some probability value. Simple probabilities were extended in some systems with sophisticated mechanisms for uncertain reasoning and combination of probabilities.

4) *Ontology classification*: With the addition of object classes to the knowledge base, a new type of reasoning is possible. Along with reasoning simply about object values, the system could also reason about object structures.

### C. User Interface

The user interface (UI) provides an interaction between user of the ES and the ES itself. The user of the ES does not need to be an expert to use the system. The UI needs to have some clear and user friendly way to display how the system reached to a particular conclusion.

The UI should also make it easy for the user to trace the credibility of the deductions that lead to the final decision. It should be designed towards the users, in order to allow them to accomplish their goals in the shortest possible way, to work with their existing or desired work practices, and makes efficient use of the users input. The technology should be adapted to the user’s requirement and no the other way around.

### D. Applications, Limitations, Benefits

Expert systems like any other technology have its limitations. Large systems are costly, because they require significant development time and compute resources. Basic limitation can be classified in four basic categories:

- Limitation of the technology.
- Difficult knowledge acquisition.
- They are difficult to maintain.
- High development costs.

Expert systems are widely used in design, medicine, monitoring systems, process control systems, knowledge domain, finance and commerce, for things like camera lens design, automobile design, diagnosis systems to deduce cause of disease from observed data, leakage monitoring in long petroleum pipeline, finding out faults in vehicles, computers, detection of possible fraud, suspicious transactions, stock market trading, airline scheduling, cargo scheduling.

Main benefits from such systems include their availability, less production cost, often they provide great speed, and are able to reduce the amount of work, their error rate is less compared to human errors, they reduce risk, since they can work in environment that is not human friendly and they provide a steady response with-out getting motional tensed or fatigued.

### III. DEVELOPMENT OF ANIMAL MONITORING EXPERT SYSTEMS

The process of ES development is iterative. Steps in developing the ES include:

1) *Identify a problem domain*: This includes checking if the domain is suitable for an expert system to solve it, if there is an access to experts in the area of the domain, determine the cost-cost-effectiveness of the system in the given domain.

2) *Design the system*: This includes identifying the ES technology, establishing a degree of interaction with other systems and databases, investigation how the concepts can represent the domain knowledge best.

3) *Develop a prototype*: This includes acquiring the domain knowledge from the experts and representing it the needed format for the inference engine.

4) *Test and refine the prototype*: This includes using sample cases to test the prototype for any deficiencies in performance

5) *Develop and complete the ES*: This includes tests to ensure that the interaction of the ES with all elements of its environment, including end users, databases, and other information systems, documenting the ES project, training the users to use the ES.

6) *Maintain the system*: This includes keeping the knowledge base up to date by regular review and updates, search for integrations with other information systems as those systems evolve.

The animal monitoring system is planned as expert system for the dairy industry. It is mainly targeted for cows but with adaptation of the algorithm should be able to work with goats and buffalos. It focuses on both milk quality and animals health. It tries to detect early symptoms of mastitis, based on specific physical qualities of the milk samples and start early treatment of the animal and early separation of infected milk, preventing it from mixing with other milk in the tanks which can potentially lead to infecting the whole tank with pathogens and cause significant loses for the farmers from the order of thousands of euro depending on the tank size. In worst case it can reach the market and have an effect on the public health since milk and other dairy products have the potential to transmit pathogenic organisms to humans [5].

Cost effective equipment is used to feed the data into the system. The selected equipment for field measurements is EkoMilk Horizon hybrid mid-infrared and ultrasound analyzer. Clustered version of it with sample feeder is able achieve 350 milk samples per hour for price 0.04 euro per test, which makes it perfect choice for a mini lab. Milking robot version that is also available can work fully unattended as in farm setup controlled by the milking robot automation software [10]. With the partners from BulTeh 2000 Wi-Fi module to all modifications of the EkoMilk Horizon analyzer is added and is connected to the Internet. That allowed us to feed the system with real-time raw data from each measurement made with the analyzer.

#### A. Communication and Data Storage

Communication between the analyzer and the expert system is made possible over internet with the integrated ESP8266 Wi-Fi module from Olimex [11]. Wi-Fi connection has to be set up from the analyzer menu. Once the connection is made, and instrument have the connection to the internet, HTTP protocol is used for communication with the system, since it is widely used and all network equipment including firewalls are preconfigured to allow this kind of traffic.

Cryptographic hashes are used for signing every message. This ensures the message integrity and validates and authenticates the sender instrument in the system. Each instrument has to be registered in the system using its AMP identification code that is printed on the box and on the instrument label. Four digit pin is also associated with it. This gives us another layer of security and guarantees that fake data could not enter the system and compromise its operation and results.

Once the data is received and all signatures checked, it is stored securely in the system database. Blockchain proof-of-work technology and smart contracts based on the Ethereum API [12] is used to additionally secure the measurements data, in a way that any further modification of any of the parameters of the measurement can be detected and the affected measurements and decisions that are made based on them invalidated.

Combined with the secure data transfer methodology from the analyzer to the system, it can guarantee that the origin of the data is genuine and no external modifications are possible. This ensures that the input data is correct and prevent the system working with incorrect data which is one of the main problems of the expert systems, because working with corrupted data not only will produce wrong output, but it can contaminate the knowledge base with wrong data and compromise future predictions.

The extra defense mechanisms that check that all parameters are in normal operation ranges additionally ensures the reliability of the system, and also helps detecting malfunctions in the analyzing equipment. This bad measurement is excluded from the blockchain and does not contribute to the final system decisions.

Using the same communication channel the analyzer sends all errors and log messages that happened during operations. They are also stored in the system for future analysis, and to find some correlation between them and problems in the measured results. The information system uses them for notifying the users or warns them about missed procedures that might have negative effect on the measurements and break the warranty of the analyzer. Notifications are especially helpful when the instrument is working in unattended mode paired with milking robot. This way the operator will know when it is time for maintenance or when his attention is needed because of errors.

Another important part of collecting the data is the identification of the sample and the animal or tank from where the sample is taken. In most cases the animal identification code comes with the measurement. In rare cases, when the animal or tank identification data is missing by the time of the measurement, user will need to interact with the system and do the identification manually via appropriate template that he can download, fill with the animal or the tank identification number next to the measurement sequence number, and upload back to the system. Using the unattended or the manual identification process, the system needs this identification data, because it later plays important role connecting the newly made measurement with the existing knowledge base.

#### B. Knowledge Base

The system keeps a big knowledge base consisted of different types of data. Some of the important entities are the instruments and their full history of raw measurements, their logs and errors and also their location. As it turns out the location is very important parameter, since there are different practices in the dairy industry in the different countries. The cultural, technological and legal differences in the different countries give significant changes in the results calibration and treatment of the animals. The difference is mostly noticed between Western farms and the farms in the developing countries in Asia. There are sometime differences between farms in the same country. That is why information about the farm is stored in the knowledge base. At the end the hope is that the decisions of the expert will be consistent with the local practices and compliant with local market and best practices of the vets that are serving the given farm.

Each animal has a lot of metadata initially entered and later collected in the system. The animal species is also tracked but for now the research is based on cows. The inference engine takes into account parameters such as breed, herd, the barn that the animal lives in, full history of previous treatments and previous measurements when it is deducting treatments or calibrating the results. Often the parents of the animal and their full history are known when the cow is born in the farm under the control of the expert system.

The system also distinguishes between tank and animal milk and keeps different parameters for the tanks. For example it knows the location - the country and region, the volume, the milk origin by animal and also it has full history of previous measurements over time and all the tank maintenance data.

The most important information in the knowledge base is the old measurements. There is a lot of meta data connected to each measurement, starting with the raw data about physical properties of the sample from the analyzer, the official lab milk quality results for the same sample, the exact analyzer used, is it cow or tank sample and which, and in case of cow we store also information for the udder quarter of the animal, the time that he sample is taken and some others.

The first decision that the expert system needs to do on every measurement is how to properly calibrate it.

### C. Measurement Calibration

Once we receive the data from the measurement and we have the sample identified, the expert system can start a process that we call calibration. This is process of deduction of the basic milk quality parameters based on the physical milk properties that the analyzer reads. Example data of the process is shown in Fig. 2.

Milk quality parameters include Fat, Protein and the main milk quality indicator-somatic cells count [13]. The analyzer has ultrasonic, infra-red, conductivity and other sensors and also measures the flow time at a given temperature.

The inference engine gets various types of data from the knowledge base in order to calibrate the measurement correctly. It uses the instrument measurements count to account for sensors wearing, the country, the farm and the animal but mostly the physical properties mapped to the official lab milk quality results, which are constantly updated. Every value that the inference engine pulls from the knowledge base is checked against the normal operating ranges of the system.

The operating ranges are also stored in the knowledge base in the form of rules. These rules are added by the experts in the area and the analyzer manufacturers, and if such abnormal conditions are detected the inference engine is marking the sample as unreliable and attach a warning message to the measurement with a suggested maintenance procedure that needs to be performed on the analyzer. In Fig. 3 is shown the interface for adding such rules to the system.

This flow as many others trigger an action in the notification engine in the expert system.

The notification subsystem is used for notifying the users and other external systems for circumstances that the expert system detects. It uses various channels including API calls to external systems, SMS, e-mail messages and in system UI notifications.

If all parameters are in normal working ranges, the engine starts checking its if-then-else constructs in order to select the right calibration table for the given conditions. As shown in Fig. 4 the calibration tables are stored in the knowledge base, and are added by experts in the area of milk analysis and chemistry. The system has appropriate user interface for adding, exporting, importing and modifying calibration tables. Once the right calibration table is selected, it is used to calculate the final values for the milk quality parameters that are added to the measurement and back to the knowledge base.

### D. Health and Treatment Analysis

The expert system analysis about heard health status is based mainly on the somatic cells count in the milk samples for the given animal over time. The inference engine is working with another set of predefined if-then-else statements, but from different kind of experts - veterinarians. In Fig. 5 is presented how the current set of rules categorizes the animals in four categories: healthy, clinical mastitis, chronicle mastitis and no data available.

If the health status of an animal changes, it triggers an action in the notification engine, and notification to the farmer or veterinarian is sent. The notification contains the appropriate treatment plan for the animal, based on the country or region best practices and law regulations.

The local veterinarian experts are consulted for the creation of the rules for each farm, in order to match the best practices so far for the given farmer and heard. In the modern farms the notification engine sends an API call to the milking robot, notifying it that the milk from this animal should not be mixed with the other milk, in order to limit the contamination and limit the losses.

|            |   |   |   |      |      |     |      |      |      |      |
|------------|---|---|---|------|------|-----|------|------|------|------|
| Farm1 Tank | - | - | A | 22.9 | 22.9 | 140 | 4.64 | 4.17 | 5.50 | 9.04 |
| Farm1 Tank | - | - | A | 22.7 | 21.0 | 146 | 4.63 | 3.54 | 5.48 | 9.02 |

Fig. 2. Calibrated and uncalibrated Measurement.

**Create Rule**

Farm: All farms

Type: User Defined

Result Type: Viscosity (LT[s])

Compare Type: Greater (>)

Value: 5

Message: blockage is possible

Fig. 3. Adding a Rule to Inference Engine.

| Name                      | Created At          | Updated At          | Farms | Instruments |  |  |  |
|---------------------------|---------------------|---------------------|-------|-------------|--|--|--|
| Initial                   | 2018-04-16 07:32:43 | 2018-07-02 09:13:36 | 0     | 13          |  |  |  |
| Africa March 18           | 2018-05-02 15:46:02 | 2018-05-24 08:38:36 | 0     | 0           |  |  |  |
| Africa 24May18            | 2018-05-24 08:37:18 | 2018-05-29 11:09:57 | 0     | 1           |  |  |  |
| 06Jun18                   | 2018-06-05 14:22:52 | 2018-07-09 13:52:10 | 0     | 0           |  |  |  |
| SCC corr for UHT and past | 2018-09-26 09:23:09 | 2018-09-26 09:23:36 | 0     | 1           |  |  |  |
| EHE(R) Initial            | 2019-02-08 08:56:43 | 2019-02-08 08:58:25 | 0     | 2           |  |  |  |

Fig. 4. UI for Managing Calibration Tables.



Fig. 6. Revenue Calculator.

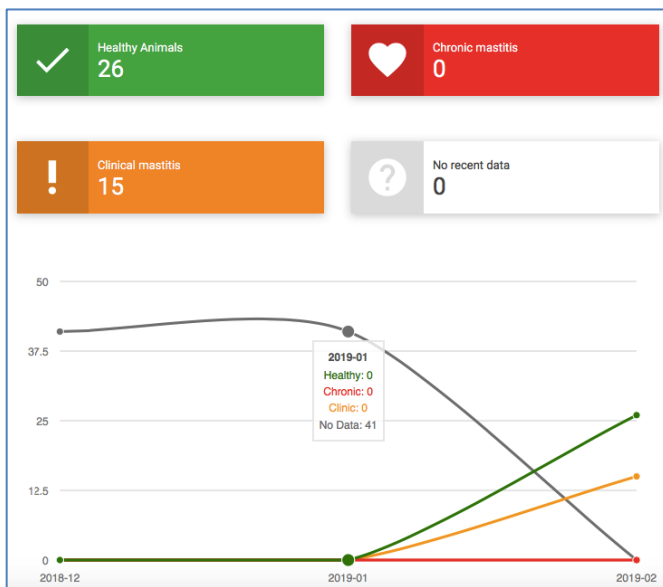


Fig. 5. Health Categories.

Treatment plans are stored back to the knowledge base, and the animal somatic cell count monitored and if the condition does not improve, the farmer should consult with a veterinarian. The inference engine rules are not still well tested in different control groups in order for the expert system to change the current treatment based on the old treatment plan and the somatic cell count readings after the start of the treatment. Tank milk condition is also monitored, but the data is used just for creating a tank dashboard where specialist can monitor the tank condition over time, work with the current collected data and try to create rules for the tank maintenance.

In Fig. 6 is shown the revenue calculator included in the system. It indicates approximately how much money the farmer saved by the early mastitis detection by calculating the amount of milk that will be lost due contamination and late animal treatment.

#### IV. CONCLUSION AND FUTURE WORK

Most of the work already done so far was focused on the data collection and measurement calibrations techniques. Even that the calibration mechanism in the inference engine works stable with if-then-else statements and the calibrations tables, another approach based on fuzzy logic and neural networks can be implemented. The first layer on the network will get all the inputs including the milk physical properties, the identified animal, the breed, location, instrument and so on and the output layer will produce the milk quality parameters including fat, protein and somatic cell count. The network will be constantly retrained with the samples from the official laboratories.

The knowledge base about treatment plans and early mastitis diagnosis based on the somatic cell count could be updated with more rules, so the system can prescribe more accurate treatments, and also give it the ability to change treatment plans and suggest termination of animals that have chronicle mastitis that is not affected by the treatments prescribed. The system should have ability to work with more complex rules based on the old treatment plans and recent somatic cell counts, suitable UI for managing these rules per farms from veterinarians and UI for explaining the end decision for treatment, especially valuable in cases when the system is suggesting the termination of the animal.

The expert system should be also expanded toward decisions about the tank milk, because of the large amount of milk collected there it can prevent tremendous losses of production. Revenue calculator also can be improved. There is not enough statistical data in the knowledge base that gives indications how much the milk production is increased when early mastitis detection techniques are used. It varies from one farm to another, but correctly estimating these values will give very clear indications of the benefits of using the expert system. The reduced cost per sample analysis could also be considered here.

Another not directly connected area with the early mastitis detection in which the system could be expanded is related to the support and maintenance of the milk analyzers. With all the data collected the system can monitor important deadlines for maintenance and also detect the common failures in the analyzers by catching drifts in the data. It can then make use of its built in notification subsystem to notify the support or the manufacturer. The system is already monitoring the instrument logs and errors and notifies the users if the measurement process is halted. This is especially useful for the unattended installations. More milk analyzers could be also integrated with the system.

#### REFERENCES

- [1] M. Benson, Handbook of Expert Systems, Clanrye international, 2015.
- [2] A. Dagnino, J. I. Allen, M. N. Moore, "Development of an expert system for the integration of biomarker responses in mussels into an animal health index", Biomarkers, vol. 12(2), 2007, pp. 155-72.
- [3] J. Enting, R.B.M. Huirne, "A knowledge documentation methodology for knowledge-based system development: an example in animal health management", Computers and Electronics in Agriculture, vol. 22, Issues 2-3, pp. 117-129, 1999.
- [4] W. Ertel, Introduction to Artificial Intelligence, Springer International Publishing, 2017.
- [5] K. Hameed, G. Sender, A. Kossakowska, "Public health hazard due to mastitis in dairy cows", Animal Science Papers and Reports vol. 25, no. 2, 2006, pp.73-85.
- [6] M. Jampour, "A Fuzzy Expert System to Diagnose Diseases with Neurological Signs in Domestic Animal", In proceedings of Eighth International Conference on Information Technology: New Generations (ITNG), 2011.
- [7] R. Michele, F. Scioscia, E. Di Sciascio, "A knowledge-based framework enabling decision support in RFID solutions for healthcare", International Journal of Recent Trends in Engineering, vol. 1, no. 4, 2009, pp. 68-71.
- [8] P.L. Nuthall, G.J. Bishop-Hurley, "Expert systems for animal feeding management", Computers and electronics in agriculture, vol. 14, no 1, 1996.
- [9] Artificial Intelligence-Expert Systems: [https://www.tutorialspoint.com/artificial\\_intelligence/artificial\\_intelligence\\_expert\\_systems.htm](https://www.tutorialspoint.com/artificial_intelligence/artificial_intelligence_expert_systems.htm)
- [10] Ekomilk Horizon: <https://www.bulteh.com/ekomilk-horizon-unlimited-hybrid-analyzer.html>
- [11] MOD-WIDI-ESP8266: <https://www.olimex.com/Products/ToT/ESP8266/MOD-WIFI-ESP8266/open-source-hardware>
- [12] Contract APIs: <https://etherscan.io/apis#contracts>
- [13] Somatic Cell Count: <https://dairy.ahdb.org.uk/technical-information/animal-health-welfare/mastitis/symptoms-of-mastitis/somatic-cell-count-milk-quality-indicator/#.XHJ-zS2B1QI>



# Innovative Means of Medical Students Teaching through Graphical Methods for Cardiac Data Estimating and Serious Games

Galya N. Georgieva-Tsaneva  
Institute of Robotics, Bulgarian Academy of Sciences  
Sofia, Bulgaria

**Abstract**—Now-a-days non-traditional methods and tools are introduced in the training of medical students which are mediated by the rapid development of information technologies: software training systems, Serious Games, and video materials. The paper presents a software system for the processing and analysis of physiological data, which is suitable for use in the medical students' training process and a study has been made of the use of serious games in medical education. For optimal work with a software system, a database of cardiac data has been created for healthy individuals and individuals with various cardiac diseases. The established system and the cardiology database can be used by medical doctors to study statistical parameters and graphical cardiac data representation in various diseases. The results obtained from the analysis of the data through graphical methods can be used as an effective visual means for increasing the success of medical students' training. The paper presents the results of a survey of the interest of medical students in higher education Universities in Bulgaria to the inclusion of Serious Games in their medical training. The results show a high interest in game-based learning: by including serious games such as innovative training, it will be possible to build on theoretical education and to increase the efficiency of the education process.

**Keywords**—*Serious games; medical education; cardiovascular disease; heart rate variability; time domain analysis; spectrogram*

## I. INTRODUCTION

According to the World Health Organization, cardiovascular diseases are one of the most common causes of death in humans-most often by heart attacks, strokes, and hypertension. Average in the year over 17 million people die of cardiovascular disease, this is over 30% of all deaths worldwide (in 2015: 17.7 million people, representing 31% of all global deaths). In America, on average every 40 seconds, one person dies as a result of heart disease [1].

Healthy people have a heart rate that ranges from 60 to 100 beats per minute. On the activity of the heart, it affects the human brain, which activates the autonomic nervous system (ANS) with its 2 partitions-sympathetic and parasympathetic. The autonomic nervous system is a system that controls blood pressure, glands with internal secretion and body muscles. The sympathetic part of the nervous system accelerates heart rhythm, and the heart needs about 5 seconds to respond to this impact. Parasympathetic part of the nervous system reduces heartbeat and the heart responds is very quickly to this effect.

ANS is influenced by factors of various character – internal nature (age, body temperature, health status) and external nature (climatic conditions, body position, physical workload, stress factors). The nervous system stimulates the production of 2 hormones-cortisol and adrenaline. Adrenaline (acts quickly) increases heart rate, increases blood pressure, mobilizes energy reserves. Cortisol (acting more slowly) helps to supplement our energy resources, helps memory, and supports the immune system. There are many factors influencing heart activity: nervous system activity, day/night cycle, thermoregulation, etc. All external and internal factors affect heart activity, striving to achieve an inner balance in heart activity.

In the healthy heart, cardiac pulsations occur as a result of the operation of the sinus (sinoatrial) node, which permanently creates action potential, setting the rhythm of the heart. Therefore, in the normal functioning of the cardiovascular system of the human body, the heart rhythm is named a normal sinus rhythm.

Heart Rate Variability (HRV) is a tool for effective non-invasive ANS testing and the effect of ANS that has on cardiovascular system performance. The statistical and geometric parameters of HRV are the most commonly used means of HRV analyzing by researchers and physicians of cardiologists. The main purpose of this material is to study the parameters of HRV in the time domain of cardiac data of healthy and diseased individuals, comparative analysis and summaries.

The evaluation of the HRV parameters was carried out through a software program created by the author. The established software system and the base of various cardiac data can be used by medical students to study the impact of many cardiac diseases on statistical parameters of Heart Rate Variability and graphical depiction of HRV by histograms and spectrograms. A cardiological software system can be the basis for developing a serious game for the purpose of training students in medicine.

### A. Serious Games in the Education

The use of serious educational games in student education is an innovative method by which learners are challenged to improve their knowledge, build up the learning material and seek new knowledge in the field they are studying. Serious games incorporated software and history that are united for learning purposes. Serious games have a dynamic character

and are able to keep the attention of their users for a long time. Serious games can enhance students' creativity, improve users' ability to take decisions in critical situations, and promote risk-taking in decision-making. Like all other games and serious games cannot be played twice in the same way that allows for the development of creative and logical thinking. Much of the serious games are designed to be played in a team that helps develop the work of a team.

Rest of the paper is summarized as follow: Literature survey is shown in Section II. In Sections III Heart Rate Variability is presented. The use of serious games in medical education is presented in Sections IV. The experimental results are discussed in Sections V and VI respectively. Conclusion and future directions are presented in Section VII.

## II. RESEARCH BACKGROUND

The interest of researchers in the study of Heart Rate Variability in recent years has grown exponentially. The HRV is not a separate physiological signal, it is derived from the electrocardiogram signal, recorded using various specialized devices: an electrocardiograph (used constantly in cardiology and recording short ECG signals-usually from 3 to 5 minutes); a Holter monitoring device (used less frequently when short records fail to show the nature of the cardiac problem and recording 24-hour long data). Historically, the first human electrocardiogram was published in 1887 by Augustus D. Waller, the first paper on paper was carried out in 1903 by the Dutch physiologist Willem Einthoven.

Lee [2] examines the HR variability in healthy people and patients with abnormal cardiograms. Studies of the HRV in the time domain make Drawz et al. [3], observing patients with chronic kidney disease and diabetic patients [4]. Surveys on 24-hour Holter Records of influence of the Age and Gender on the HRV are given in work [5]. The authors of [6-8] study the change in HRV due to various diseases.

A detailed overview of the results of several researchers' studies on HRV is presented in the book [9]. Detection and classification of cardiac intervals, statistical analysis of ECG and HRV in MATLAB environment are presented in [10]. The works [11, 12] are dedicated to the overall analysis of the HRV.

The analysis of ECG records is always preceded by a pre-processing of the data. The input cardiac records are subjected to the following treatments: denoising of the overlaid additional noise that hinders the next signal processing [13], reduction of the baseline drift, QRS complex detection. The authors of [14, 33] present effective methods of reducing noise and suppressing the drift of the baseline by methods of Empirical Mode Decomposition [14] and adaptive bionic wavelet transform [33].

A cardiac monitoring system for patients with cardiovascular diseases using a GSM module that transmits information on a risky situation is described in the work [15].

For research purposes, have been developed methods to simulate HRV sequences on which new algorithms can be tested for cardiac data processing and analysis [16].

The use of innovative Serious Games in education is a process that has grown in recent years around the world and is supported by technology development. Today, modern technology enters the classroom and offers new, interesting tools to improve the learning process, one of which is the use of serious learning games.

Annetta [17] gives the following definition of a serious game: "serious games are electronic/computer-access games that are not designed for commercial purposes but rather for training users on a specific skill set". According to Zuda [18], a serious game is състезания, "with specific rules, that uses entertainment to further government or corporate training, education."

Serious games in education have one of two purposes [19]: solving a problem or simulating events from the real world, thanks to which different skills develop.

According to Presky [20], serious games are a very good opportunity to engage learners in the training process.

Serious games evolve over time; they can now be used on different platforms [21].

## III. HEART RATE VARIABILITY

Heart Rate Variability is a modern diagnostic parameter that is produced by non-invasive methods on human subjects. Its application in clinical medical practice is regulated through the adoption of an HRV standard by the European Society of Cardiology and the North American Society of Pacing and Electrophysiology (1996) [22].

The reducing of the Heart Rate Variability after acute myocardial infarction is a sign of a serious health disorder in the individual's body [23] The authors of [24] found a link between the severely reduced HR variability and the increased probability of death after myocardial infarction. In the scientific literature, a correlation between the significantly reduced values of the statistical parameters of the HRV has been found [25] and sudden cardiac death [26]. Studies of various diseases of the cardiovascular system (heart failure, Ventricular arrhythmia, coronary artery disease, diabetes neuropathies, arterial hypertension, etc.) often include HRV analysis. Studies on the causes of Chronic Atrial Fibrillation include HRV analysis [8]. Not least, the ANS response to various physiological stresses and psychological effects can be assessed by HRV analysis. Hence, HRV research can provide valuable information to cardiological doctors about the impact of the patient's treatment process and on the body's internal abilities to cope with the illness problem.

The HRV analysis is based on determining the time sequences between the adjacent highest P peaks in the graph of the ECG signal. This analysis can provide information on the

functional state of the person and to monitor the dynamics of his change. Surveys in the time domain are divided into calculating statistical parameters and determining geometric parameters. There are two approaches to calculating the time parameters: calculations on the entire continuous record and calculations on small parts of it [22]. The statistical parameters to be determined on the basis of long - term Holter ECG records are [22]:

- Parameters calculated directly from normal intervals.
- Parameters based on differences between successive NN intervals.

For purposes of this study, the input HRV data were obtained through a Holter monitoring performed on sick and healthy individuals. Holter devices retain continuous 24-hour ECG recordings. Before the data are used, these records are decompressed and pre-processing. This includes noise reduction [27], reduction of the drift of the baseline, localization of the QRS complex [28]. Then RR time intervals are obtained, ectopic intervals are excluded and NN time intervals (derived from sinus node depolarizations [29]) are obtained.

Time domain analysis measures changes in heart rate depending on the time parameter or measures the intervals between consecutive normal heart cycles. The calculated time domain parameters are as follows:

- RR intervals minimum, maximum and mean values;
- heart rate minimum, maximum and mean values;
- standard deviation calculated on the lengths of normal cardiac intervals: SDNN, SDANN, SDindex;
- the standard deviation of heart rate SDhr;
- the parameters RMSSD, NN50, pNN50, and others.

From the statistical parameters, the standard for HR variability recommends the study of SDNN, SDANN, and RMSSD [22]. The formulas for calculating the statistical parameters, as well as explanations of their character are presented in Table I.

In the geometric analysis of HRV, the normal intervals are represented by a histogram of the distribution of the density of the differences between the successive normal intervals [22]. From the distribution represented on the corresponding histogram, it can be judged about the length of the more frequent intervals in the HRV sequence. Intervals, which are much shorter or longer than normal intervals, can easily be seen on the histogram - they fall outside the main peak of the triangular histogram and can thus be identified.

Geometric parameters are:

- HRVTi: HRV triangular index;
- TINN: triangular index of normal NN intervals;
- Lorenz plot of normal intervals.

Geometric parameters of HRV are presented in Table I. From the geometric parameters, the HR variability standard recommends the HRVTi study [22]. Reference (normal) values of parameters (Statistical and Geometrical) in the time domain for healthy individuals [22] are presented in Table II.

In the time domain, apart from calculating the above-mentioned parameters, histograms of normal cardiac intervals and heart rate histograms are also drawn. The histogram is a graphical representation of HRV: time-dependent distribution of duration of RR sequences. Fig. 1 shows a graph of normal cardiological intervals and an individual with normal sinus rhythm, and Fig. 2 shows a graph of an individual with cardiovascular disease. The lengths of the HRV intervals of the healthy individual are distinguished by a higher variation than the lengths of the intervals in the diseased individual. The lengths of the intervals in Fig. 2 are located in a narrower overall width, the series looks more even, and the adjacent intervals are of a near length. The cardiac rhythm of patients with cardiovascular disease has small variations. When an unexpected event occurs, the body reacts by increasing or decreasing its heart rate and in this way it adapts to the changes. In the presence of stress or fright, the healthy heart reacts by accelerating its rhythm, but soon the rhythm returns to its normal values. In ill individuals, the accelerated rhythm is retained and is usually required medication to reduce heart rhythm.

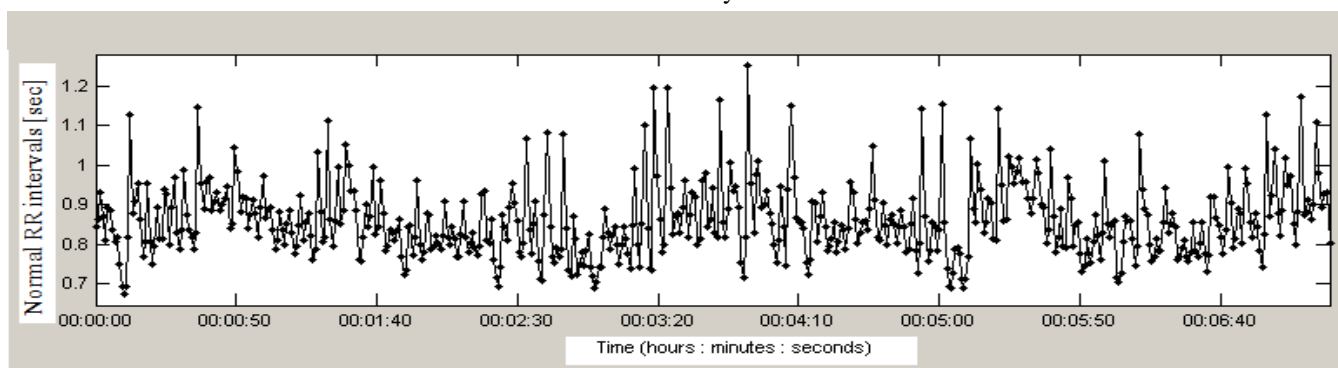


Fig. 1. Normal Cardiological Intervals (an Individual with Normal Sinus Rhythm).

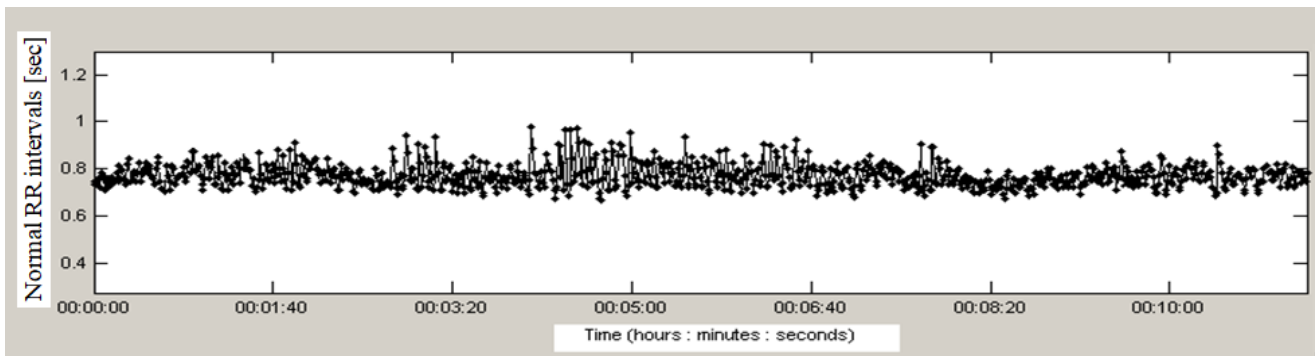


Fig. 2. Normal Cardiological Intervals (an Individual with Cardiovascular Disease).

TABLE I. STATISTICAL AND GEOMETRICAL PARAMETERS IN THE TIME DOMAIN [22], [ 30]

| Parameter [units ]   | Formula  | Description and relations  |
|--|--|--|
| <b>Statistical parameters</b>  |  |  |
| RR Mean [ms]   | $\overline{RR} = \frac{1}{N} \sum_{i=1}^N RR_i$  | Mean value of RR intervals.  |
| HR Mean [bpm]  | $HR\ Mean = \sqrt{\frac{1}{N-1} \sum_{i=1}^N (HR_i - \overline{HR})^2}$                  | Standard deviation (SD) of heart rate over the entire measurement period.  |
| SDNN [ms]  | $SDNN = \sqrt{\frac{1}{N} \sum_{i=1}^N (RR_i - \overline{RR})^2}$                        | Estimates NN-intervals standard deviation in the whole ECG record or parts of it. Estimates overall HRV.Gives information about all cyclical components that affect the dynamics of normal intervals in ECG over the estimated period of the record. Also reflects the slow reaction of the heart to the hormones. Parameter values grow as the record length increases. |
| SDANN[ms]  | $SDANN = \sqrt{\frac{1}{N} \sum_{i=1}^N (\overline{RR}_i - \overline{\overline{RR}})^2}$ | SD of the averages normal time intervals over five-minute segments calculated. Estimates long-term fluctuation. Reflects circadian rhythmicity of autonomic function.  |
| RMSSD[ms]  | $RMSSD = \sqrt{\frac{1}{N-1} \sum_{i=1}^{N-1} (RR_{i+1} - \overline{RR}_i)^2}$           | The square root of the mean of the sum of the squares of successive differences between NN intervals [31].Short-term records obtaining. Measured short term variation. Reflects high-frequency variations and parasympathetic regulation of the heart.   |
| SDNN index [ms]  | $SDNN_{index} = \frac{1}{N} \sum_{i=1}^N SDNN_i$   | It is the mean of the standard deviations of all NN intervals for each five-minute segments of the entire recording. The Index is measured autonomic influence on HRV.   |
| NN50 [count]   | -  | Represents the number of adjacent NN intervals differing by more than 50ms It gives an idea of the dynamics between adjacent normal intervals-measured short term variation.   |
| pNN50 [%]  | $pNN50 = \frac{NN50}{NN} \cdot 100\%$  | Percentage of successive normal intervals > 50 ms. The ratio of the number of adjacent NN intervals differing by more than 50 ms (NN50) to the total number of NN intervals multiplied by 100.   |
| <b>Geometric parameters</b>  |  |  |
| HRVTi [-]  | $HRVTi = \frac{\sum_{i=1}^{N_b} b(t_i)}{\max_i b(t_i)} = \frac{N-1}{\max_i b(t_i)}$      | Calculated on the basis of the previously constructed histogram. Overall Heart Rate Variability estimation. Dependent on the length of the bin [32].   |
| TINN [ms]  | Interpolation procedure.   | Overall Heart Rate Variability estimation.   |
| <p><i>N</i>- number of all intervals; <i>i</i>-index;<br/> <math>\overline{RR}</math> - an average of all RR intervals; <math>\overline{RR}_i</math>- mean value of RR intervals in the segment;<br/> <i>b</i> –bin corresponding to time <i>t<sub>i</sub></i>; <i>N<sub>b</sub></i> – number of bins;<br/> <math>\overline{\overline{RR}}</math> - mean value of all RR averages overall 5-minute segments, M-number;<br/> <math>\overline{HR}</math> - an average of all HR.</p> |  |  |

TABLE II. REFERENCE VALUES OF PARAMETERS IN THE TIME DOMAIN [22]

| Parameter            | Normal values (mean±sd) | Units | Note   |
|----------------------|-------------------------|-------|--|
| HRmin                | >50                     | bpm   | High levels are a symptom of high HRV, low levels – of low HRV |
| HRmax                | <120                    | bpm   |  |
| SDNN                 | 141±39 (102-180)        | ms    |  |
| SDANN                | 127± 35 (92-162)        | ms    |  |
| RMSSD                | 27±12 (15-39)           | ms    |  |
| HRV Triangular Index | 37±15 (22-52)           | -     |  |

#### IV. USING SERIOUS GAMES IN MEDICAL EDUCATION

Serious games are competition, story, art, and software. In medical education, serious games are tools to reinforce the learning material, to test the learning and to acquire new knowledge. The use of simulation games in medical training makes it possible to learn new skills in a safe environment, to create an experience for a given medical manipulation or activity (for example, injection, blood pressure measurement, diagnosis, the appointment of laboratory tests). The use of serious games in medical education enables students to place themselves in a virtual environment close to the real environment one in which to examine a patient, identify his disease, and arrange treatment. The purpose of such a serious game is the virtual healing of the patient by the virtual physician. The mistakes that a student can make will not affect a real patient, so the game is also safe for patients, and it is a valuable experience that students can acquire in their training and then use it in their practice of medicine.

The serious medical game can be created in a way, that allows increasing the level of complexity in the game, when established user progress. When a user successfully make the treatment of a virtual patient and the patient is healing, the student may be faced with a more complex situation—a clinical case for which greater skill is required, and the consideration of more objective facts. Some of the medical training games offer the opportunity to take different roles from the user (student, trainee, specialist, and head of the hospital ward) and so the user learns how to act, what are his responsibilities, according to the role he has taken.

Serious education games in medical training offer the opportunity to acquire valuable experience, increase student motivation, and give feedback quickly to the knowledge and skills of their users.

#### V. RESULTS

The created cardiac record database contains over 1100 records of patients with various cardiological diseases and records of healthy individuals. The records are 24-hour records of heart activity obtained with Holter monitoring and received from the Multiprofile Regional Hospital for Active Treatment “Dr. Stephen Cherkov”, Veliko Tarnovo, Bulgaria.

*Characteristics of patients.* Investigations were performed on 116 Holter Records of 3 groups of Individuals (Individuals with Sinus Bradycardia, Ventricular Fibrillation, and Individuals with Normal Sinus Rhythm). Their demographic characteristic (the age and gender distribution, the mean age of subjects) is shown in Table III. Values of parameters are expressed as mean  $\pm$  standard deviation (SD) or in percent (%). There is no significant difference between the different groups according to Gender and Age.

The heart rate variability analysis is done in the time domain using an author's software program. Analyzed records were obtained during the daily life of individuals using the Holter monitoring method. Individual recordings can be recorded locally on the computer or downloaded from a remote server. The software is implemented in a MATLAB programming environment. The tested parameters were

determined according to the formulas shown in Table I and following the recommendations of the standard for the HRV.

Fig. 3 shows the histograms made on the recordings of healthy subjects with normal sinus rhythm. The distribution of normal cardiac intervals is central, with the largest percentage of the intervals being located in a few columns around the tachogram mod (with cardiac intervals of 0.45 to 1 sec). At the same time, there are intervals of different sizes, located in both the smaller values and the larger values of the interval lengths.

Fig. 4 shows histograms of patients with Ventricular Fibrillation. The distribution of intervals is a wider range, the basis of the histogram is of normal width.

Sinus bradycardia (heart rate > 100 bpm) is presented in Fig. 5, there is a shifting of the histogram mod (the most frequent value of intervals in the histogram) to the right and a presence of a small number of high columns.

TABLE III. DEMOGRAPHIC CHARACTERISTIC

| Parameter     | SB<br>n= 48       | VF<br>n= 36       | NSR<br>n=32       | P value |
|---------------|-------------------|-------------------|-------------------|---------|
| Gender, Men % | 51.06             | 54.48             | 53.13             | NS      |
| Age $\pm$ SD  | 63.11 $\pm$ 22.08 | 63.94 $\pm$ 28.46 | 52.46 $\pm$ 24.18 | NS      |

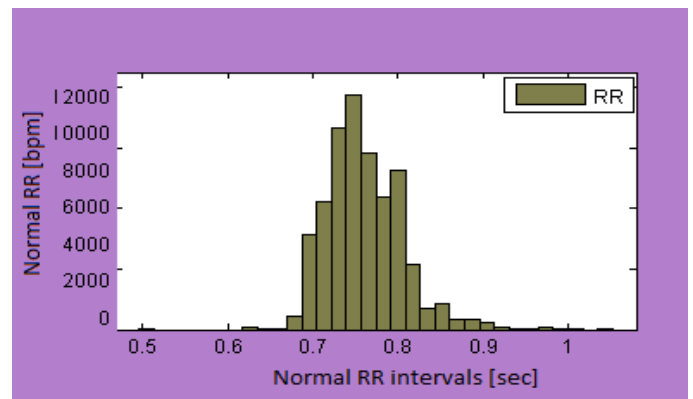


Fig. 3. A Healthy Individual.

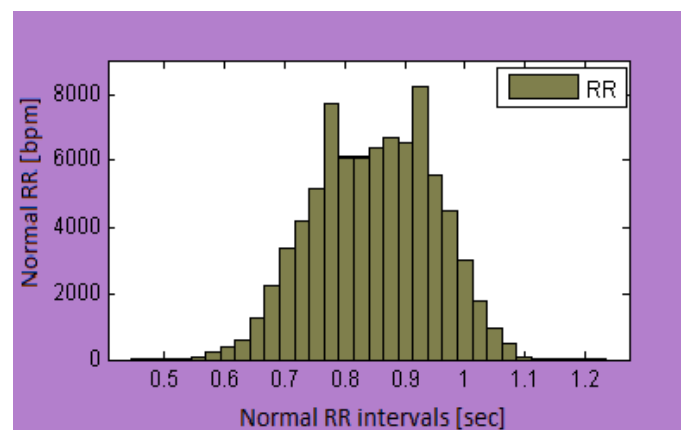


Fig. 4. Ventricular Fibrillation.

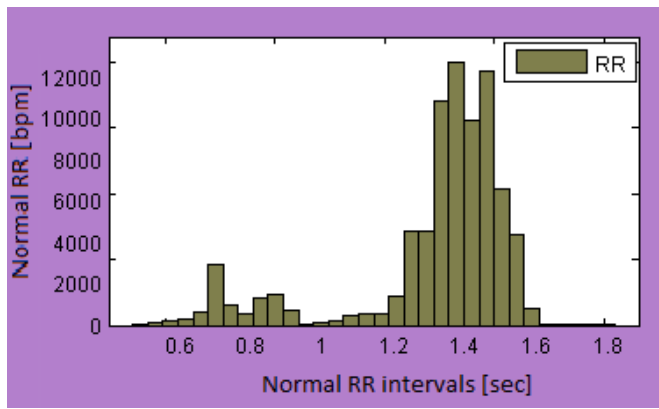


Fig. 5. Sinus Bradycardia.

Table IV presents the average results of the defined statistical and geometric parameters of HRV analysis obtained from the study of several groups of Individuals (total number 116): Individuals with normal sinus rhythm (NSR); Individuals with Ventricular Fibrillation (VF), Sinus Bradycardia (SB). The results are presented as mean  $\pm$  standard deviation (mean  $\pm$  sd). The values of the parameters of the study groups were tested by the ANOVA test.

The assessments of the mean value of normal cardiac intervals and the mean heart rate indicate that these parameters are not statistically significant ( $p > 0.05$ ). Their mean values, however, are determinant in the diagnosis of sinus bradycardia (mean HR  $< 60$ , mean RR  $> 1000$  ms). From time domain parameters studied, the values of statistical deviations SDNN ( $p = 0.026$ ), SDANN ( $p = 0.019$ ) have statistical significance ( $p < 0.05$ ). In the studied groups of patients, there was a tendency to decrease of these two parameters compared to individuals with normal heart rhythm and compared to the reference values recommended by the standard. In individuals with sinus bradycardia, the opposite trend is observed - the SDNN and SDANN values are higher than those of normal sinus rhythm individuals. Therefore, there is an increase in HRV in patients with sinus bradycardia. RMSSD values are significantly reduced in individuals with Ventricular Fibrillation while those with Sinus Bradycardia are significantly elevated. Studies have shown that the pNN50 parameter has statistical significance, and in individuals suffering from different diseases, it has higher values than in healthy individuals. Of the two studied geometric parameters, HRVTi has statistical significance. TINN values are not statistically significant ( $p = 0.117$ ) and are highest in healthy controls.

The results of the study groups of individuals are also depicted using a spectrogram method-a graphical method of displaying the spectrum of frequencies of a signal dependent of the time. Three methods are used in the training software program to generate a spectrogram: Burg Periodogram; Lomb-Scargle Periodogram and Wavelet method.

Fig. 6 shows a spectrogram of a healthy individual obtained by the wavelet method. Heart Rate Variability in healthy individuals is high and indicates their ability to respond appropriately to environmental changes, stress, and other adverse effects. In Low Frequency (0.04-0.15 Hz, LF) and

High Frequency (0.15-0.4 Hz, HF) area (in the spectrogram) predominate the following colors: yellow, orange and red, which represent the high power values of the studied signal. Fig. 7 and Fig. 8 show spectrograms of individuals with cardiovascular disease. The signal power at LF and HL area is low (depicted using large blue fields): low heart rate variability, the indicator for of poor health of the individual.

- Application of the software system in the medical education process

Students' training, including a graphical presentation of the results of various cardiac disease records, aims to develop students' creative thinking and to create visual imagination related to different types of cardiac diseases, which will increase their motivation for learning and will be another a method of strengthening knowledge and increasing the success rate of the discipline.

TABLE IV. PARAMETERS IN THE TIME DOMAIN

| Parameter     | SB n= 48<br>(mean $\pm$ sd) | VF n= 36<br>(mean $\pm$ sd) | NSR n=32<br>(mean $\pm$ sd) | P value<br>mean $\pm$ sd |
|---------------|-----------------------------|-----------------------------|-----------------------------|--------------------------|
| Mean RR [ms]  | 1016.01 $\pm$ 424.87        | 841.07 $\pm$ 294.92         | 840.14 $\pm$ 387.68         | NS (0.053)               |
| Mean HR [bpm] | 59.82 $\pm$ 26.64           | 72.65 $\pm$ 32.92           | 73.48 $\pm$ 28.73           | NS (0.061)               |
| SDNN [ms]     | 142.32 $\pm$ 11.08          | 132.97 $\pm$ 14.93          | 139.4 $\pm$ 21.17           | <0.05 (0.026)            |
| SDANN [ms]    | 136.8 $\pm$ 19.06           | 124.43 $\pm$ 18.72          | 129.02 $\pm$ 22.51          | <0.05 (0.019)            |
| SDindex [ms]  | 62.17 $\pm$ 4.13            | 61.99 $\pm$ 6.14            | 62.13 $\pm$ 3.78            | NS (0.985)               |
| RMSSD [ms]    | 32.47 $\pm$ 6.09            | 29.62 $\pm$ 8.73            | 29.07 $\pm$ 2.03            | <0.05 (0.035)            |
| pNN50 [%]     | 24.4 $\pm$ 18.6             | 25.71 $\pm$ 12.06           | 16.39 $\pm$ 11.04           | <0.05 (0.023)            |
| HRVTi         | 21.43 $\pm$ 4.06            | 19.4 $\pm$ 6.7              | 22.27 $\pm$ 2.02            | <0.05 (0.034)            |
| TINN [ms]     | 448.2 $\pm$ 171.4           | 485.7 $\pm$ 181.43          | 516.37 $\pm$ 109.63         | 0.172                    |

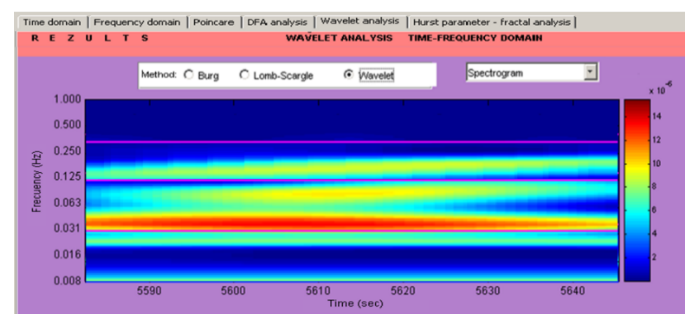


Fig. 6. Spectrogram of Normal HRV.

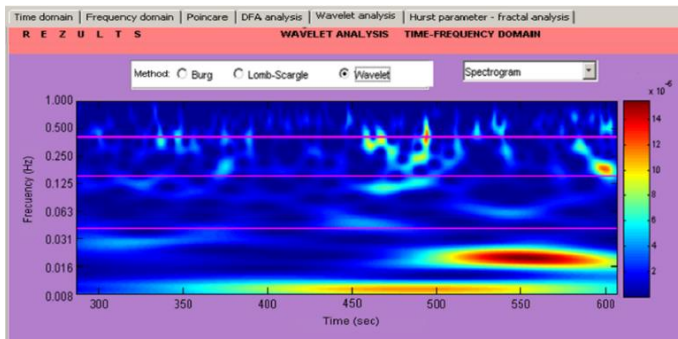


Fig. 7. Spectrogram of abnormal HRV (Ventricular Fibrillation).

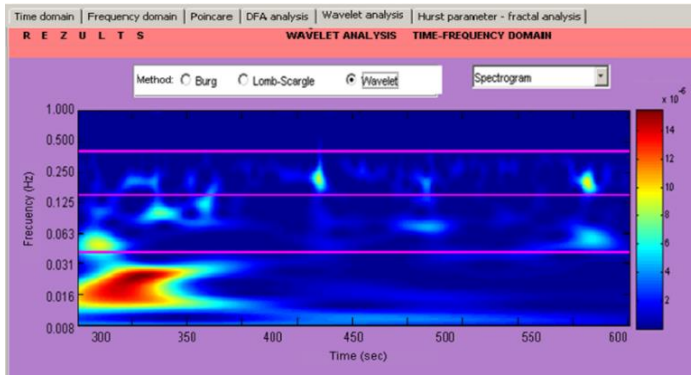


Fig. 8. Spectrogram of abnormal HRV (Sinus Bradycardia).

The created software system allows the selection of data records of patients with various diseases, calculation of the statistical parameters of cardiac records (time domain parameters of HRV) and the graphic results of the research results. The resulting histograms and spectrograms illustrate the heart rate variability through the rich-colored figures.

- Results of research on the use of Serious Games in medical education in Bulgaria

The use of serious games in the education process is a relatively new direction in the pedagogical aspect. Traditional education needs a change to meet the requirements of the modern technological age and the requirements of the students themselves, whom today work freely with new technologies, process varied information in a short time and are oriented towards technological innovation. A very good idea is the presentation of the medical material through serious games, which will give a different view of the taught knowledge. Technological approach to education is inevitable, given the pervasive introduction of technology into people's everyday lives.

The established software system is a tool for effective medical students' training, which makes it possible, through repeated use, to remember imperceptibly and long lasting many basic parameters of the HRV, which can help future medical specialists to diagnose patients. Additionally, the established system having cardiac storage and distribution module based on their underlying diagnosis can be used to store actual patient data and refer to a subsequent visit to create an electronic history of the disease in which also store Holter records and numerical and graphical results.

The presented software system can also be developed in the form of a serious game to be used by students in their preparation for their cardiology specialty. The creation of a serious training game is one of the goals of a program that works to create effective training tools for medical students.

A survey was conducted among 162 medical students in Universities in Bulgaria, which aims to explore the interest of students in the inclusion of serious education games in their training. The survey was conducted among a small number of respondents, but the results obtained were interesting and indicative.

Fig. 9 shows the results of the answer to the question "Do you want serious games to be used in university training?" Most respondents (96.3%) have answered YES, only 1 respondent has answered NO, and 2.1% said: "I cannot decide". The results obtained show a great interest of the students to include serious games in the educational process as an opportunity for further build on of the learning material and improving the knowledge and skills of the subjects.

Fig. 10 shows the results of the survey of respondents about their preferences for various types of serious games. The question makes it possible to indicate more than 2 responses. A predominant percentage of respondents want to use competitive games (69.1%), which shows a striving for development in a competitive environment. 50.6% prefer to play adventure games, which is an indication of interest in learning with creative, entertaining elements. 40.7% of respondents want to playtest games, believing that they will help to better learn the learning material.

The answers of respondents to this question show a great interest in various types of serious games that enable teachers to choose the appropriate Serious Games among a wide range of type of learning games by matching what kind of serious game is best suited to the specific pedagogical goals in the learning process.

The survey conducted included a question about the possibility of including serious games with virtual reality in student education (see Fig. 11). Most respondents (140 of all 162 students) has answered YES, 18 has answered: "I cannot decide", and only 1 student has answered NO. The answers to this question indicate students' readiness to use serious games with virtual reality in their training. These serious educational games can improve a number of medical skills of students through virtual simulations.

### Do you want serious games to be used in the university training?

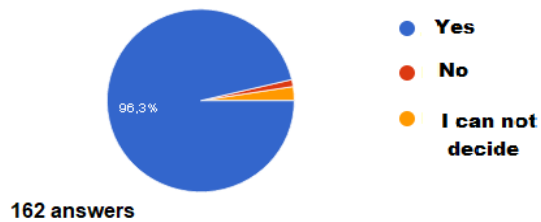
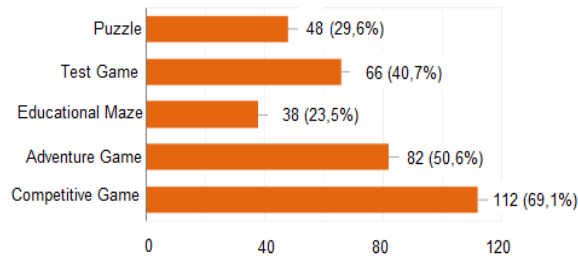


Fig. 9. Exploring the Interest in Serious Educational Games.

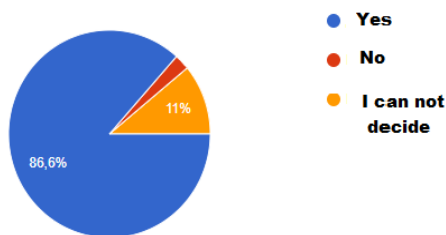
### What serious games you prefer to play?



162 answers

Fig. 10. Exploring the Interest in the Types of Serious Educational Games.

### Do You want to be given the opportunity to learning through Serious Games with virtual reality?



162 answers

Fig. 11. Exploring the Interest in Serious Games with Virtual Reality.

The study shows a high interest from students to various types of serious educational games, which shows the possibility of introducing various innovative games in the medical education, according to the study material and the medical skills that the students have to acquire.

The survey and its results can be used to improve the education process in Universities with medical specialties. The study shows that the inclusion of serious educational games in medical training is an innovative method provided by the development of information technology that students will use with interest.

## VI. DISCUSSION AND FUTURE SCOPE ON THE USE OF SERIOUS GAMES IN TRAINING

Serious educational games today are the focus of many researchers and lecturers. The study conducted among medical students in Universities in Bulgaria shows great interest in the use of serious educational games for the purposes of their medical education. Research on the use of serious games in student education in the medical learning process in many countries around the world shows that serious games play a significant role studying them and in teaching new materials. At the same time, the study conducted among Bulgarian

students shows a considerable interest in the use of serious games and their inclusion in the learning education process.

The author's future work in this direction may include exploring the possibilities for including serious games in medical education in Bulgaria: is there a necessary material and technological base in medical Universities in order for serious games to be brought into the learning process in medical higher education.

An important issue in using serious games is whether teachers themselves are willing and willing to use serious games in the learning process, and what pedagogical impacts may be in using serious games. The interest of Bulgarian students of serious games, the increase in the use of serious games in the world's Universities shows an inevitable tendency: serious games are entering into the learning process, the prerequisites for this are present, technologies are constantly developing and marking high growth in recent years, that the necessary technical resources for the use of serious games will be available.

In conclusion, the following can be noted: the use and consolidation of the serious educational games in the educational process is a significant trend that will mark a new direction in the development of education both in the world and in Bulgaria.

## VII. CONCLUSION

The paper presents a software system for processing and analyzing cardiac data that can be used in medical education to extend students' knowledge and learn additional information about HRV statistical parameters. The software system enables the study of cardiac data of healthy individuals and patients with various cardiac diseases. The results obtained are presented graphically and numerically. The graphical way allows for the visual perception of the results obtained and the creation of links between visual methods of acquiring knowledge and traditional learning methods.

The survey among 162 students in Bulgaria shows an increased interest of respondents to include serious educational games in medical education in Bulgaria. The results show that the inclusion of serious games in training seems attractive to students. A high percentage of respondents declare their preference to use serious games in their education that have a competitive (69.1%) and adventure (50.6%) element. Having a predefined scenario (story) is an additional element to increase the attractiveness of the serious game.

## ACKNOWLEDGMENT

This work was supported by the Bulgarian Ministry of Education and Science under the National Research Program "Young scientists and postdoctoral students" approved by DCM # 577 / 17.08.2018 and NSF of Bulgaria under the Research project № DM 12/36/20.12.2017, "Investigation of Mathematical Techniques of Analysis of Physiological Data with Functionality for People with a Visual Deficit."



REFERENCES

- [1] E. Benjanim, S. Vinary, C. Callaway, A. Chamberlain, A. Chang, S. Cheng, etc. "AHA Statistical Update Heart Disease and Stroke Statistics—2018 Update. A Report From the American Heart Association Circulation". 2018; Vol.137, 20.03, pp.:e67–e492.
- [2] R.-G. Lee, I.-C. Chou, C.-C. Lai, M.-H. Liu, M.-J. Chiu, "A Novel QRS detection algorithm to the analysis for heart rate variability of patients with sleep apnea," Biomed. Eng. Appl. Basis Comm., Vol.17, 2005, No 5, pp. 258-262.
- [3] P. Drawz, D.C. Babineau, C. Brecklin, J. He, R. Kalle, E. Soliman, etc. "Heart Rate Variability is a Predictor of Mortality in CKD - A Report from the CRIC Study," American Journal of Nephrology, 2013, No 38, pp. 517–528.
- [4] T. Benichou, B. Pereira, M. Mermillod, I. Tauveron, D. Pfabigan, etc. "Heart rate variability in type 2 diabetes mellitus: A systematic review and meta analysis," PLoS ONE, 2018, Vol. 13, No 4, pp. 1-19.
- [5] K. Umetani, D. H. Singer, R. Mcrcraty, M. Atkinson, K. Umetani, D. H. Singer, R. Mcrcraty, M. Atkinson, "Twenty-Four Hour Time Domain Heart Rate Variability and Heart Rate: Relations to Age and Gender Over Nine Decades," JACC, Vol. 31, 1998, No. 3, pp. 593–601.
- [6] V. Barauskiene, E. Rumbinaite, A. Karuzas, E. Martinkute, A. Puodziukynas, V. Barauskiene, E. Rumbinaite, A. Karuzas, E. Martinkute, A. Puodziukynas, "Importance of Heart Rate Variability in Patients with Atrial Fibrillation," J Cardiol Clin Res, Vol. 4, 2016, No. 6, pp. 1080-1086.
- [7] B. Erynucu, M. Bilge, N. Guler, "Comparison of Heart Rate Variability and Treadmill Exercise Score in Patients with Stable Coronary Artery Disease," International Journal of Angiology IO, 2001, pp.178-182.
- [8] Ö. Akyürek, E. Diker, M. Güldal, D.Oral, "Predictive Value of Heart Rate Variability for the Recurrence of Chronic Atrial Fibrillation after Electrical Cardioversion," Clin. Cardiol. Vol. 26, 2003, pp.196–200.
- [9] M. Malik, A. J. Camm. Dynamic Electrocardiography. Blackwell Publ. Inc./Futura Division, New York, 2004.
- [10] B. Malia S. Zuljb, R. Magjarevic, D. Miklavcic, T. Jarma, "Matlab-based tool for ECG and HRV analysis," Biomedical Signal Processing and Control, Vol. 10, 2014, pp. 108-116.
- [11] G. Ernst, Heart Rate Variability. Springer-Verlag, London, 2014.
- [12] D. M. Kumar, S.C. Prasannakumar, B. G. Sudarshan, D. Jayadevappa. "Heart Rate Variability Analysis: A Review" International Journal of Advanced Technology in Engineering and Science, Vol. 1, No. 6, 2013, pp. 9-24.
- [13] V.S.B. Geetha, S. Sudha, "QRS complex detection in ECG of rescued victims in disaster zones," International Journal of Applied Engineering Research Vol. 10, 2015, No. 55, pp. 230-235.
- [14] L. Murali, T. Manigandan, D. Chitra, S. V. Gopeka, "Mixed domain VLSI approach for ECG QRS complex detection," International Journal of Applied Engineering Research, Vol. 9, 2014, 24, pp. 27067-27081.
- [15] M. Sibinagalingam, S. Vijayprasath, "Survey on ECG based heart rate variability analysis," International Journal of Applied Engineering Research, Vol. 10, 2015, No 20, pp.15305-15310.
- [16] G. Georgieva-Tsaneva, M. Gospodinov, E. Gospodinova, "Simulation of Heart Rate Variability Data with Methods of Wavelet Transform," in B. Rachev, A. Smrikarov, Proc of 13th International Conference on Computer Systems and Technologies-CompSysTech'12, Vol. 630, ACM Press, New York, 2012, pp.306-312.
- [17] L. Annetta, „The ‘I’s’ Have It: A Framework for Serious Educational Game Design;“ Review of General Psychology. American Psychological Association 2010, Vol. 14, No. 2, 105–112.
- [18] M. Zyda, „From visual simulation to virtual reality to games,“ Computer, 2005, IEEE Computer Society, pp. 25-32.
- [19] P. Noemí, S. Máximo „Educational Games for Learning. Universal Journal of Educational Research,“ 2014, Vol. 2, No 3, pp. 230-238.
- [20] M. Prensky. "Digital game-based learning," ACM Computers in Entertainment, 2003, Vol 1 (1), Book Two.
- [21] P, Vorderer, U. Ritterfeld, "Digital games," In Nabi R, Oliver M, eds. The SAGE handbook of media processes and effects. Thousand Oaks, CA: Sage, 2009.
- [22] M. Malik, "Task Force of the European Society of Cardiology and the North American Society of Pacing and Electrophysiology. Heart rate variability: standards of measurement, physiological interpretation, and clinical use" Circulation, Vol. 93, 1996; pp. 1043-1065.
- [23] N. Dey, A. Ashour, "Classification and Clustering in Biomedical Signal Processing," Advances in Bioinformatics and Biomedical Engineering, book series, IGI, 2016.
- [24] H. Huikuri, P. Stein, "Clinical Application of Heart Rate Variability after Acute Myocardial Infarction," Frontiers in Physiology, 2012, Vol. 3, pp. 3-41.
- [25] H.V. Huikuri, M.K. Linnaluoto, T. Seppanen, K.E. Airakinen, K.M. Kessler, J.T. Takkenen, R.J. Myerburg, "Circadian rhythm of heart rate variability in survivors of cardiac arrest," Am J Cardiol., Vol. 70, 1992, pp. 610-615.
- [26] C. Raab, N. Wessel, A. Schirdewan, J. Kurths, "Large-Scale Dimension Densities for Heart Rate Variability Analysis," Computers in Cardiology, 2005, Vol.32, pp.985–987.
- [27] G. Georgieva-Tsaneva, "QRS Detection Algorithm for long term Holter records," in B. Rachev, A. Smrikarov, Proc 14th International Conference on Computer Systems and Technologies-CompSysTech'13, Vol. 767, ACM, New York, 2013, pp. 112-119.
- [28] G.Georgieva-Tsaneva, K. Tcheshmedjiev, "Denoising of Electrocardiogram Data with Methods of Wavelet Transform, "in B. Rachev, A. Smrikarov, Local Proceedings of 14th International Conference on Computer Systems and Technologies-CompSysTech'13, Ruse, Bulgaria, 2013, pp. 9 – 16.
- [29] G. Georgieva-Tsaneva, Application of Mathematical Methods for Analysis of Digital ECG Data. Information Technologies and Control, Year XIV, 2/2017, SAI, 2017, pp. 35-43.
- [30] M. Malik, "Time-domain measurement of heart rate variability," Cardiac Electrophysiology Review, Vol. 3, 1997, pp. 329–334.
- [31] H.-G. Kim, E.-J. Cheon, D.-S. Bai, Y. H. Lee, and B.-H. Koo, "Stress and Heart Rate Variability: A Meta-Analysis and Review of the Literature," Psychiatry Investig., 2018, Vol 15, No3, pp. 235–245.
- [32] I. Gussak, C. Antzelevitch, Electrical Diseases of the Heart: Genetics, Mechanisms, Treatment, Prevention, Springer Science & Business Media, 2008.
- [33] L. Wang, X.Zhou, Y.Xing, S. Liang, "A Fast and Simple Adaptive Bionic Wavelet Transform: ECG Baseline Shift Correction", Cybernetics and Information Technologies, Vol. 16, 2016, No 6, pp. 60-68.

# Muscles Heating Analysis in Sportspeople to Prevent Muscle Injuries using Thermal Images

Brian Meneses-Claudio<sup>1</sup>, Witman Alvarado-Díaz<sup>2</sup>, Fiorella Flores-Medina<sup>3</sup>

Natalia I. Vargas-Cuentas<sup>4</sup>, Avid Roman-Gonzalez<sup>5</sup>

Image Processing Research Laboratory (INTI-Lab)  
Universidad de Ciencias y Humanidades, Lima, Perú

**Abstract**—Muscle heating is the process that every athlete follows before any physical activity or sport which are the legs where greater force is exerted and in case a good heating routine is not practiced, the muscles can suffer tears, cramps or fractures due to sudden movements while the muscles are cold. According to the National Institute of Arthritis and Musculoskeletal and Skin Diseases of the United States, the most common injuries occur in the ankles because it is a central point where greater force is exerted by the induced weight of the athletes, in addition if excessive muscle care is important. That is why the evaluation of muscle heating in athletes to prevent muscle damage was raised in this research work, first two thermal images of the before and after heating will be obtained using the FLIR ONE Pro thermal camera following a protocol of distance, position and temperature range, then the images are processed in the MATLAB software to map them in the temperature range and then subtract them to obtain the zones where the temperature variations are found indicating where an adequate heating has been carried out. As a result, the areas where the subtraction of both images was positive were obtained, this new image of the subtraction is superimposed on the real image, showing the real image with the areas where it has proceeded with an optimal heating.

**Keywords**—Thermal image; muscle heating; heat map; muscle injuries, temperature range

## I. INTRODUCTION

The heating or stretching of the muscles is important when doing any physical activity or sports, as explained in [1], it does not matter that it is for a short time [2] because when practicing any activity, it is required that all the muscles have been respectively activated. In addition, heating is important because it prevents sprains, tears and cramps that could cause fractures.

According to the National Institute of Arthritis and Musculoskeletal and Skin Diseases of the United States [1], the most common lesion is the ankle because it is where the weight of the body is centered and more physical activity is practiced in the body which is not well trained.

The heating consists in performing a variety of exercises that cause the progressive increase of the muscular temperature, it is recommended that the intensity of the exercises increase with the heating means at the beginning you start with low intensity exercises and then with high intensity exercises.

In [2], it explains that they did tests with young people of 13-15 years of age, in both genders, these young people made a muscle heating of 12 minutes, finishing the heating, they made thermal tests and a variation between the 0.43°C and 1.13°C were obtained, being the optimal temperatures for athletes. The main objective of this research was the verification of muscle heating in the legs, arms, face and neck, where 1.69°C was obtained in the arms, face and neck and 0.72°C in the legs and feet, standardizing ranges for the practice of sport.

In [3], it indicates that the main damages that the athletes suffer are in the muscular zones, of which they are considered as muscular pathologies that are responsible in the rehabilitation of the skeletons, for that reason, they made a thermographic study to identify the zones of higher temperature sectoring the muscles of greater importance, in addition, classify the muscle damage to know the ranges of the mildest and the most deadly in which it can reach a muscle breakdown.

There are intensity phases of heating that consist of: a) Cardiovascular heating: it is known as full trot because the muscles require to reach a minimum temperature; b) Joint mobility: they are more complete movements following an order, sequence and starting ascending or descending (ankle, knees, hips, shoulders, neck, etc); c) Global Stretches: it is the final stage of a regular heating where the muscles are stretched and previously having a heating, these stretches can be maintained in a specific position of 6 to 12 seconds avoiding pain [4]. In addition, it is important to have a prudent stretch time in heating because it affects the contractile capacity of the muscles [5].

The physical consequences of not doing muscle heating or bad practice of muscle heating are tears, joint injuries, cramps, ligament injuries being progressive and fractures due to sudden movements in sports where high muscle strength is required [6], in addition, knowing that Athletes tend to care for their muscles and that's why you need an adequate heating and a heating routine where all the muscles of the body are stimulated [7].

The main objective of the research work is the evaluation of the heating of muscles in athletes to prevent muscle damage and indicate if another routine of additional heating is required to that already applied. The evaluation is done before and after doing a muscle heating to check if an optimal heating routine has been done.

The thermal images show the thermal composition of a body or objective, in addition to differentiating in which zones there is a higher temperature index, also, these images can be processed with image processing software because they are compatible. In addition, it is now known that the use of thermal images serves to verify the variation of temperature in internal maladies and to know if in case a body is sufficiently heat to make a physical effort.

The following research work is structured as follows: In section II, the development of thermal image processing before and after the athlete's heating will be presented. In section III, the results will be shown by the 2 thermal images referring to the before and after the heating and the subtraction of the image superimposed in the real image to identify the areas that have been heated. Finally, in section IV, it presents the discussion and conclusions of the research work.

## II. METHODOLOGY

In the methodology, each part of the segmentation of the temperature variation of the images before and after the heating is developed for the prevention of muscular injuries of the leg, which consist of the acquisition of the thermal images before and after the heating, Segmentation of the zones of higher temperature in both images, subtract both images and finally superimpose the subtraction of both images to the real image to obtain where it has been heated and also identify if an optimal heating has been done.

The steps of the system are shown in Fig. 1, where the processes by which the images are submitted are indicated to end with the superposition of the differentiation of the thermal image in the image where the highest temperature is presented.

### A. Image Acquisition

At the stage of image acquisition, a thermal camera called FLIR ONE Pro was used, it is a camera capable of capturing thermal images and compatible with Android and IOS mobile devices. This camera has 2 lenses [8] as shown in Fig. 2, where the upper lens captures images and the lens of the lower camera captures the thermal image. In addition, this device has a software called as its name, where you can process those thermal images received, for example: change the temperature range, change the colors of the heat map and among other things. For the process of capturing thermal images, it used a converter from Connector C to Micro USB because the thermal camera has a connector C from factory and, in this case, it used an Android mobile device. In Fig. 2, the thermal camera and the connector C to Micro USB connector converter are shown.

In the following Table I, the characteristics of the FLIR ONE Pro thermal camera are shown.

The FLIR ONE Pro is a device capable of capturing thermal images, as well as its complement in heat map, it is also capable of viewing at a distance the temperature distribution of complete surfaces where a temperature variation is identified. This camera was born based on an idea to identify electronic problems in industrial equipment because, manually, it took too much time, on the other hand, with thermal imaging, it could identify where the problems were and solve it in a period of less time, currently, is used in the medical field to

know the distribution of body temperature as well as for different projects where the temperature variation data is required.

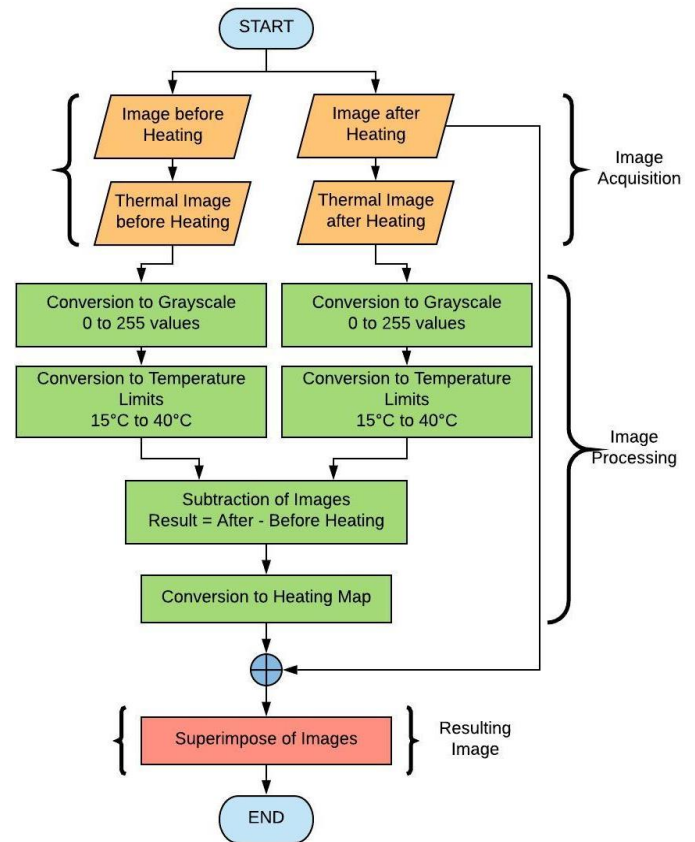


Fig. 1. Flowchart for the Evaluation of Muscle Heating



Fig. 2. FLIR ONE Pro Thermal Camera and Type C to Micro USB Connector Adapter.

TABLE I. CHARACTERISTICS OF THE FLIR ONE PRO

| FLIR ONE Pro       |                          |
|--------------------|--------------------------|
| Temperature Range  | -20 °C – 400 °C          |
| Compatibility      | IOS y Android Devices    |
| Maximum Distance   | 8 meters                 |
| Weight             | 36.5 g.                  |
| Dimensions         | 68 x 34 x 14 millimeters |
| Thermal Resolution | 160 x 120                |
| Work Time          | 1 hour                   |

**B. Image Processing**

The images follow a processing as shown in Fig. 3, where it can observe the thermal images before and after heating, these images are processed according to the flow diagram described above; Fig. 3(d) represents the heat map conversion section, in which the warmest areas of the leg can be observed.

The MATLAB software reads the images received by the FLIR ONE Pro, being the images before and after the heating, each pixel read represented by each dimension.

Then, it converts the thermal images to gray scale so the software uses the following multiplications to give values to each pixel, as shown below:

$$0.2989 * R + 0.5870 * G + 0.114 * B \tag{1}$$

This process is done for the thermal images and thus obtain it between the ranges from 0 to 255 in two dimensions. This process is important because in this way it can be converted to a temperature scale.

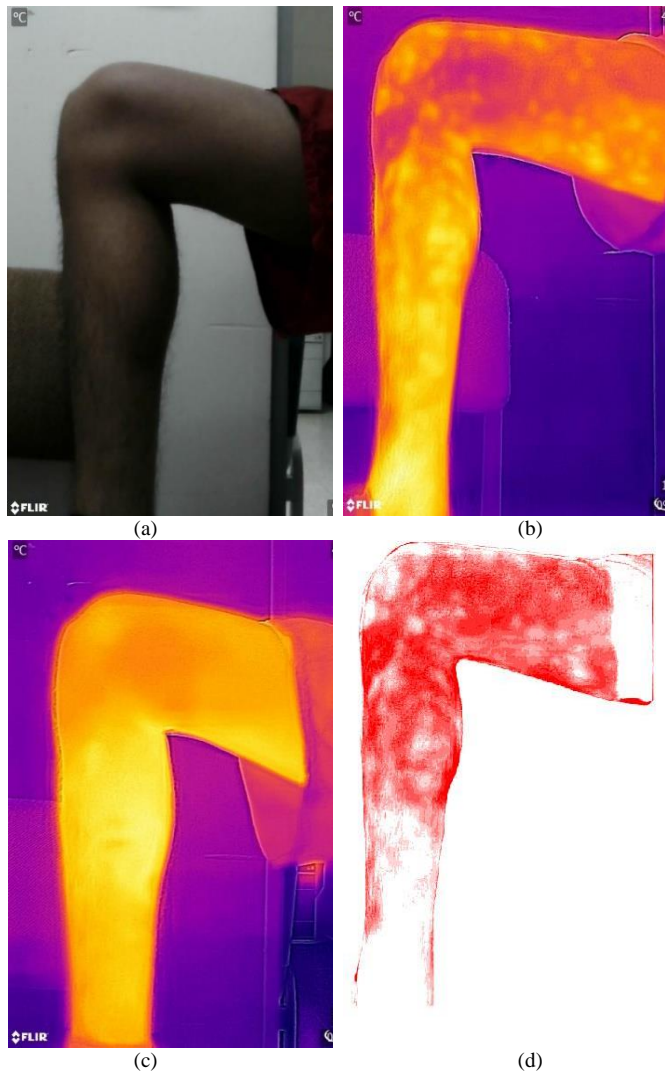


Fig. 3. (a) Real Image. (b) Thermal Image before Heating. (c) Thermal Image after Heating. (d) Difference of Thermal Images in Heat Map.

Then, convert the images in gray scale to temperature scale with the following formula:

$$\text{output1} = ((\text{Pixel\_Image} - \text{FromLow}) * (\text{ToHigh} - \text{ToLow}) / (\text{FromHigh} - \text{FromLow})) + \text{ToLow} \tag{2}$$

Where:

- FromLow and FromHigh = 0 y 255 (Gray Scale)
- ToLow and ToHigh = Temperature Range to which will convert the image.

As it wants to convert from gray scale to temperature map, it uses the maximum and minimum ranges in the formula, then get the following formula:

$$\text{output1} = ((\text{Pixel\_Image} - 0) * (40 - 15) / (255 - 0)) + 15$$

Next, it is to subtract the thermal images in temperature scale to obtain the zones where a temperature difference has taken place [9] indicating that it has proceeded with a correct heating. Therefore, a simple subtraction of both thermal images is performed in which the thermal image after heating must predominate.

$$\text{Subtraction} = \text{Thermal\_After} - \text{Thermal\_Before} \tag{3}$$

This result will be converted to heat map, obtaining as a result Fig. 3(d) where the hottest zones are shown and where there has been a more noticeable differentiation of temperature change, in addition, it is identified that some areas have more intense red indicating that it is where the subtraction of temperature is much greater.

Finally, this image will be superimposed on the real image to identify the areas where it has proceeded with a correct heating.

**III. RESULTS**

The thermal images were captured based on a protocol because all the images are required to be homogeneous in that sense, they are captured with the same physical characteristics for further processing. In Table II, the characteristics to which the thermal images were captured are represented.

TABLE II. CHARACTERISTICS OF THERMAL IMAGES

| Thermal Images                  |   |
|---------------------------------|---|
| Distance                        | 40 cm                                       |
| Temperature Range               | 15 °C – 40 °C                               |
| Connected Device                | Moto E5                                     |
| Place where the Image was taken | -Before Tibialis.<br>-Tibialis.<br>-Soleus. |
| Rest Time                       | 0   |

In [10], the study was conducted in a group of 12 people, divided into 2 randomly selected groups. it was to include heating exercises at the beginning of the training and at the end with the aim of pre-activating (improving the work produced to store elastic energy and using it in later actions) the extensor muscles of the foot and see if they produce difference or improvements in the actions in the game, mainly in the jump.

The new heating was performed for 3 weeks. Athletes perform heating before training, but rarely, heating helps to pre-activate the muscles. The results obtained were an improvement in the speed of physical actions.

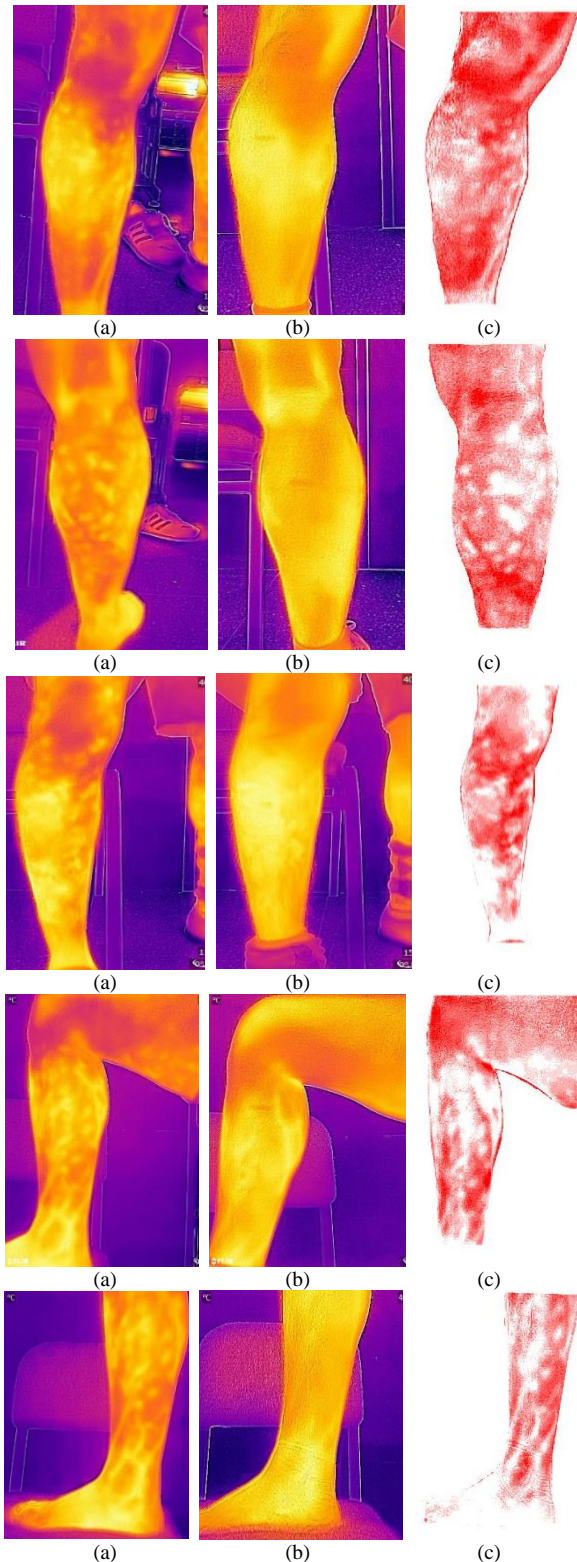


Fig. 4. (a) Thermal Image before Heating. (b) Thermal Image after Heating. (c) Subtraction of Thermal Images in Heat Map.

In [11], the research tells us about the need for heating and proposes a heating by measuring the type of activity, intensity, recovery time and duration. The author considers the routine of heating very essential to obtain an optimal performance in training or competitions where exercises of power, agility, aerobics and strength should be considered. The heating consists of routine prior to the realization of physical exercise that wants to prepare the athlete to perform to the maximum during training and / or competition. An increase in body temperature causes the glycolytic metabolism and phosphagens in the muscle to be activated more rapidly for a competition; an improvement of the nerve impulse transmission speed is also achieved. There are many studies that indicate that stretching causes very positive effects on performance, but there are 2 that say otherwise these studies indicate that stretching prior to a competition or training harms performance. Except for a stretch of less than 60 seconds (in this case, it does not harm or favor).

Fig. 4 shows the results obtained with a database of 10 soccer athletes, where the thermal images of the before and after heating up will be shown and then the subtraction of the images on the heat map.

#### IV. DISCUSSION

The research work confirms the use of thermal images to detect the areas of the body that an athlete must heating, with this information the athlete can avoid injuries due to lack of heating.

The device to which the FLIR ONE Pro will connect is not important because it will only work as thermal image storage because the thermal camera does not contain internal storage.

It tried to capture the thermal images at the precise moment where they had just finished heating up because in several research studies indicate that the human body cools very quickly when no action is taken.

While the reception of thermal images, it needs a protocol where the reader must follow. The protocol must focus on the thermal images and the position where was taken the images.

Some of the sportspeople didn't want to make any analysis because the zone where the images was taken are the most sensible parts of them so it informed about the study and the benefits which brings it.

#### V. CONCLUSIONS

It is concluded that the areas with more temperature can be detected through thermal images in an efficient and fast way because only the images need to be captured and then the software will segment it automatically obtaining the zone where the important activated muscles are located for physical activity.

It is concluded that a protocol was established because it was adjusted to the size of the user's leg in addition to having the same characteristics for each image and also to calibrate the FLIR ONE Pro in the required temperature range.

As future work, it wants to create a preventive measure of muscle damage suffered by athletes and also elderly people

because it knows that their bones and ligaments are worn out over time and could detect muscle damage and follow a healing process avoiding more serious injuries.

As future work, it wants to have a clinic historical of the sportspeople to enforce this study and could improve the performance of them. Also, applying this study when they are training at the gym because there is where they heat all the body and it could sectorized the zones where they don't train.

#### REFERENCES

- [1] G. Contreras Landgrave, E. J. Camacho Ruiz, S. C. Manzur Quiroga, O. D. Patiño Casas, and L. Ruano Casado, *La obesidad en el Estado de México: Interfaces y ocurrencias*, vol. 5, no. 1. Universidad Nacional Autónoma de México, Facultad de Estudios Superiores Iztacala, Unidad de Investigación Interdisciplinaria en Ciencias de la Salud y la Educación, 2014.
- [2] B. Flores Chico, E. Buendía Lozada, and J. Reynoso Morales, "Dinámica térmica de la piel de adolescentes después del trote," *Rev. Ciencias del Ejerc.*, vol. 10, pp. 16–35, 2016.
- [3] M. Schmitt and Y. Guillot, "Thermography and Muscular Injuries in Sports Medicine," in *Recent Advances in Medical Thermology*, Boston, MA: Springer New York, 1984, pp. 439–445.
- [4] B. Meneses-Claudio, W. Alvarado-Díaz, and A. Roman-Gonzalez, "Detection of Suspicious of Varicose Veins in the Legs using Thermal Imaging," 2019.
- [5] A. D. Galera, "Orientaciones Didácticas sobre el Calentamiento previo a la Actividad Física," Barcelona, 2018.
- [6] C. A. P. Martínez, J. E. F. Soto, and O. A. M. Barrera, "Procedimientos para prevenir las lesiones físicas en la disciplina de Karate-do," *Rev. Boletín Redipe*, vol. 6, no. 3, pp. 212–219, Mar. 2017.
- [7] J. C. Ruíz Quiñonez, "La flexibilidad corporal y su importancia en el desarrollo de actividades físicas / deportivas," Mar. 2019.
- [8] S. Agarwal, H. S. Sikchi, S. Rooj, S. Bhattacharya, and A. Routray, "Illumination-invariant Face recognition by fusing thermal and visual images via gradient transfer," Nueva York, Feb. 2019.
- [9] J. Azzeh, Z. Alqadi, H. Alhatamleh, and M. Abuzalata, "Creating a Color Map to be used to Convert a Gray Image to Color Image," *Int. J. Comput. Appl.*, vol. 153, no. No 2, pp. 31–34, 2016.
- [10] J. M. ; Saenz and B. Y. Ureña, "Effect of a Learning Work of the Eccentric-Concentric Cycle on the Jump Capacity in Volleyball."
- [11] A. Pérez-López and D. Valadés, "Bases fisiológicas del calentamiento en voleibol: propuesta práctica (Physiological Basis of Volleyball Warm-Up: Practical Proposal)," *Cultura\_Ciencia\_Deporte*, vol. 8, no. 22, pp. 31–40, Mar. 2013.

# Advanced Metaheuristics-based Tuning of Effective Design Parameters for Model Predictive Control Approach

Mohamed Lotfi Derouiche<sup>1</sup>, Soufiene Bouallègue<sup>\*2</sup>, Joseph Haggège<sup>3</sup>, Guillaume Sandou<sup>4</sup>

Laboratoire de Recherche en Automatique (L.A.R.A), École Nationale d'Ingénieurs de Tunis (ENIT)<sup>1,3</sup>

Université de Tunis EL Manar, BP 37, Le Belvédère, 1002 Tunis, Tunisia

Institut Supérieur des Systèmes Industriels de Gabès, Université de Gabès, Rue Salaheddine EL Ayoubi, 6011 Gabès, Tunisia<sup>2</sup>

L2S, CentraleSupélec, CNRS, Université Paris Sud, Université Paris-Saclay<sup>4</sup>

3 rue Joliot Curie, 91192 Gif-sur-Yvette Cedex, France

**Abstract**—This paper presents a systematic tuning approach for Model Predictive Control (MPC) parameters' using an original LabVIEW-implementation of advanced metaheuristics algorithms. Perturbed Particle Swarm Optimization (pPSO), Gravitational Search Algorithm (GSA), Teaching-Learning Based Optimization (TLBO) and Grey Wolf Optimizer (GWO) metaheuristics are proposed to solve the formulated MPC tuning problem under operational constraints. The MPC tuning strategy is done offline for the selection of both prediction and control horizons as well as the weightings matrices. All proposed algorithms are firstly evaluated and validated on a benchmark of standard test functions. The same algorithms were then used to solve the formulated MPC tuning problem for two dynamical systems such as the magnetic levitation system MAGLEV 33-006, and the three-tank DTS200 process. Demonstrative results, in terms of statistical metrics and closed-loop systems responses, are presented and discussed in order to show the effectiveness and superiority of the proposed metaheuristics-tuned approach. The developed CAD interface for the LabVIEW implementation of the proposed metaheuristics is given and freely accessible for extended optimization puposes.

**Keywords**—Model predictive control; parameters tuning; advanced metaheuristics; MAGLEV 33-006; DTS200 three-tank process; LabVIEW implementation

## I. INTRODUCTION

In recent decades, the Model Predictive Control (MPC) has emerged as a leading control strategy due to its effectiveness and robust performance on complex systems under operational constraints. Such a control approach is one of the most used and successfully implemented in a large variety of industrial applications. As an advanced robust control strategy, the MPC approach is used to drive renewable energy systems [1]. By controlling the bidirectional buck-boost converters of the PV-battery based AC micro-grid system, the fluctuating output from the solar energy sources is smoothed. In [2], Rahimi & Moghaddam proposed an extended MPC approach for maximizing the absorbed power of a point absorber wave energy converter. In [3], a new information-theoretic based MPC approach has been developed and applied to autonomous vehicles in the aggressive driving around a dirt test track. Worthmann et al. [4] proposed a tailored nonquadratic stage cost-based MPC scheme is proposed to the steering problem of

the nonholonomic unmanned ground vehicles. Other several various developments and applications of MPC approach can be found in [5-8].

In the MPC formalism, the tuning of effective design parameters, i.e. control and prediction horizons as well as the weighting matrices [6,7], remains a hard problem and a serious drawback. Indeed, the successful implementation of a MPC algorithm in practical applications requires appropriate tuning of the controller parameters which specify the performance of the closed-loop dynamics. This parameters' tuning, difficult and not systematic, becomes more and more tedious and time-consuming. To overcome such a problem, various techniques have been proposed and investigated. In [9], an intelligent deep-learning based mechanism is proposed for the implementation of a MPC algorithm for a mode-locked fiber laser system. The introduced recurrent neural network allows the classic MPC predicting of the birefringence and the laser states task. Yamashita, Zanin & Odloak [10] formulated the MPC tuning task as a multi-objective optimization problem. Two methods based on the lexicographic and compromise optimization algorithms have been proposed and successfully applied to a shell heavy oil fractionator benchmark. Another similar tuning approach based on the Pareto multi-objective optimization has been proposed for drinking water networked systems [11]. In [12], the authors present a reverse-engineering tuning method for the MPC strategy and applied for a binary distillation column system. In a pole placement framework, an analytical MPC tuning strategy has been proposed for a class of industrial systems described by first order plus dead time models [13]. Shah & Engell [14] present a semi-definite programming based approach to determine MPC parameters for MIMO systems thanks to a specification of the desired behavior of the closed-loop for small changes.

All these related works lack the systematic aspect and simplicity of the MPC parameters tuning. Indeed, most of these techniques are restrictive, and/or time-consuming in real-world implementation scenarios. Far from these analytical and restrictive tuning methods, the use of soft computing concepts, in particular the optimization by metaheuristics algorithms, seems a promising solution for this kind of hard problems, often non-convex and non-smooth [15-17]. Up to date, there

have been a few research works that successfully integrated the metaheuristics-based optimization and MPC approach. Most of these given works use classic and old metaheuristics such as the Genetic Algorithms (GA), standard Particle Swarm Optimization (PSO), Ant Colony Optimization (ACO) and so on [18-23]. Unfortunately, all these algorithms for the formulated problems present limitations in terms of premature convergence and unbalanced exploitation/exploration mechanism. These drawbacks affect the quality and optimality of the found solutions.

Recently, many advanced and global metaheuristics have been proposed in the literature with easier to implement algorithms and less control parameters in comparison with the old ones. The perturbed Particle Swarm Optimization (pPSO) [24], Gravitational Search Algorithm (GSA) [25], Teaching-Learning Based Optimization (TLBO) [26] and Grey Wolf Optimizer (GWO) [27] are have attracted considerable interest due to their effectiveness and wide range of applicability. Their suitability to solve the MPC parameters' tuning, formulated as a constrained optimization problem, presents a promising alternative for reducing the complexity of the MPC strategy. In this paper, an original LabVIEW-based implementation of these advanced metaheuristics algorithms is investigated. The tuning stage of all effective MPC parameters, i.e. weighting filters and prediction/control horizons, is formulated as a nonlinear optimization problem under operational constraints. Numerical validation and comparison studies are given for two different benchmarks process such as the suspended sphere MAGLEV-33-006 and the DTS200 three interconnected tanks DTS200 systems. All the proposed metaheuristics have been firstly experimented and validated on a benchmark of standard test problems [15,16].

The main contributions of the paper are, on the one hand, the development of a systematic metaheuristics-based method of easy and fast tuning of the MPC parameters' for dynamical systems. The classical trials-errors methods are no longer used and the design time is further reduced. On the other hand, a software CAD interface for the implementation of the proposed metaheuristic algorithms, in particular for the resolution of the MPC tuning problem, is developed under the LabVIEW graphical programming environment. Such a software tool is freely accessible.

The remainder of this paper is organized as follows. In Section II, a preliminary survey on the MPC approach is firstly presented. The effective control parameters' tuning problem is formulated as a constrained optimization problem. Section III presents a theoretical background of the proposed pPSO, GSA, TLBO and GWO metaheuristics as well as their original implementation under the graphical programming LabVIEW software. All given algorithms are numerically validated through various test functions from the optimization literature. Section IV is dedicated to the application of the proposed metaheuristics-tuned MPC approach for the position control of a suspended sphere in the didactic MAGLEV-33-006 benchmark as well as the level control of the three DTS200 plants. All demonstrative simulation results are presented and discussed. Section V concludes this paper.

## II. TUNING PROBLEM FORMULATION

### A. Formalism and basic Concepts

In the MPC framework, the human behavior is reproduced according to which it is a question of selecting control actions for the system to be controlled on a finite horizon [5-7]. To achieve the control performances under operational constraints, a digital model of the plant is used and decisions are constantly updated as depicted in Fig. 1.

In Fig. 2, both prediction and control horizons, denoted as  $N_p$  and  $N_c$ , respectively, are shown as ones of the main and effective design parameters of the MPC approach. The discrete-time control signals, system outputs and reference trajectories are  $u$ ,  $y$ , and  $r$ , respectively. The MPC algorithm assumes that  $u(k-1+i) = u(k+N_c-1)$  for  $N_c < i \leq N_p$ .

A MPC algorithm leads to compute the control laws  $\{u(k-1+i), i=1, 2, \dots, N_c\}$  where only the first element  $u^*(k)$  of such an optimized control sequence is applied to the system. These control laws are updated at each sampling time  $k$  in order to minimize the cost function (1) under various operational constrains [5,6,23]:

$$J(k) = \sum_{i=1}^{N_p} \hat{e}^T(k+i|k) Q \hat{e}(k+i|k) + \sum_{i=0}^{N_c-1} [\Delta u^T(k+i|k) R \Delta u(k+i|k)] \quad (1)$$

where  $r(k+i|k)$ ,  $\hat{y}(k+i|k)$  and  $\Delta u(k+i|k)$  denote respectively the setpoint trajectories, predicted outputs and increments of control laws at the time  $k+i$ , given all measurements up to and including those at sampling-time  $k$ . The terms  $Q = Q^T > 0$  and  $R = R^T > 0$  are the weighting matrices of the MPC technique, and  $\hat{e}(\cdot) = \hat{y}(\cdot) - r(\cdot)$ .

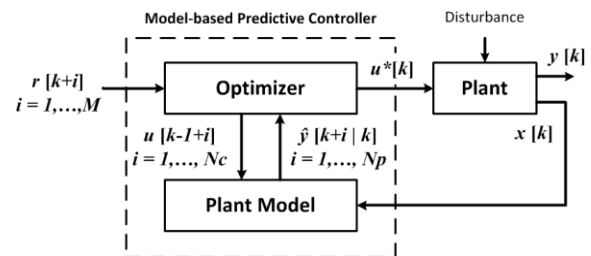


Fig. 1. Model Predictive Control Structure.

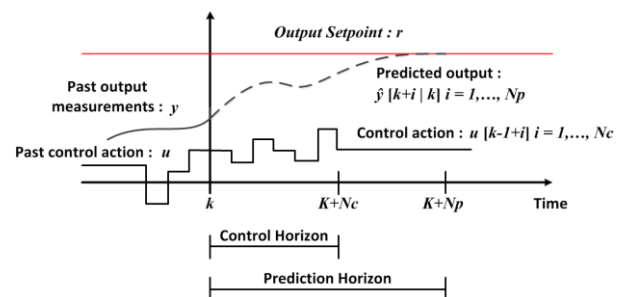


Fig. 2. Prediction and Control Horizons in MPC Framework.



Such an optimization process is repeated at the next sampling-time based on the measured system state  $x(k)$  and under operational constraints specified on the control actions, plant output signals and states as follows:

$$\begin{aligned} u_{\min} &\leq u(k) \leq u_{\max} \\ \Delta u_{\min} &\leq \Delta u(k) \leq \Delta u_{\max} \\ y_{\min} &\leq y(k) \leq y_{\max} \\ x_{\min} &\leq x(k) \leq x_{\max} \end{aligned} \quad (2)$$

### B. Optimization Problem Formulation

Since the operational constraints of the MPC are specified, the effective design parameters, i.e. prediction/control horizons ( $N_p, N_c$ ) and the weighting matrices ( $\mathbf{Q}, \mathbf{R}$ ), need to be tuned appropriately to improve the performances and robustness of the predictive controllers. In this paper, all these control parameters are considered as decision variables of the following formulated optimization problem:

$$\begin{cases} J_1(N_p, N_c, \mathbf{Q}, \mathbf{R}) = \sum_{\tau=0}^{+\infty} [y(\tau) - r(\tau)]^2 \\ s.t: & N_c \leq N_p \\ & u_{\min} \leq u(\tau) \leq u_{\max}, \\ & \Delta u_{\min} \leq \Delta u(\tau) \leq \Delta u_{\max}, \\ & y_{\min} \leq y(\tau) \leq y_{\max}, \\ & x_{\min} \leq x(\tau) \leq x_{\max} \end{cases} \quad (3)$$

where  $\tau$  is the simulation time.

Schematically, the principle of the proposed metaheuristics-tuned MPC parameters' is illustrated in Fig. 3.

The problem formulation (3) takes into account the operational constraints given by Equation (2). The prediction horizon  $N_p$  is always higher than the control one  $N_c$ . For simplicity purposes, only constraints on the control laws are considered as follows:

$$\max_{0 \leq \tau < +\infty} |u(\tau)| \leq u_{\max} \quad (4)$$

where  $u_{\max}$  is the maximum value of the control signal.

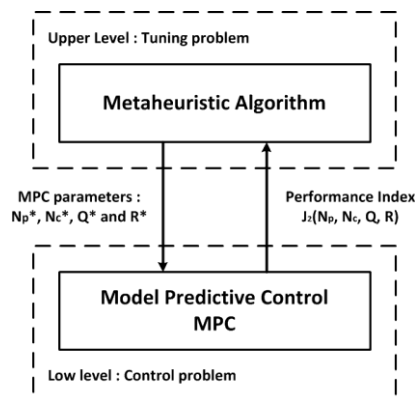


Fig. 3. Proposed Metaheuristics-based MPC Tuning Approach.

Since the optimization problem (3) is constrained, the following static penalty-based method is proposed to handle with the inequality type of operational constraints:

$$\begin{aligned} J_2(N_p, N_c, \mathbf{Q}, \mathbf{R}) &= \sum_{\tau=0}^{+\infty} [y(\tau) - r(\tau)]^2 \\ &+ \exp\left(1000 \frac{N_c - N_p}{N_p}\right) \\ &+ \exp\left(1000 \frac{\max_{0 \leq \tau < +\infty} |u(\tau)| - u_{\max}}{u_{\max}}\right) \end{aligned} \quad (5)$$

## III. PROPOSED METAHEURISTICS

### A. Perturbed PSO Algorithm

Originally proposed by Xinchao [24], the perturbed variant of the PSO algorithm, abbreviated pPSO, maintains a population of  $n_{PART}$  particles in the D-dimensional research space. The  $i^{\text{th}}$  particle of the swarm is characterized by its current position  $\mathbf{x}_i^j = (x_i^{j,1}, x_i^{j,2}, \dots, x_i^{j,D})$  and velocity  $\mathbf{v}_i^j = (v_i^{j,1}, v_i^{j,2}, \dots, v_i^{j,D})$  at the iteration  $t \in [1, n_{GENE}]$ . In the pPSO formalism, the trajectory of the  $i^{\text{th}}$  particle is updated according to the following motion equations:

$$\mathbf{x}_{t+1}^i = \mathbf{x}_t^i + \mathbf{v}_{t+1}^i \quad (6)$$

$$\mathbf{v}_{t+1}^i = w\mathbf{v}_t^i + c_1 r_{1,t}^i (\mathbf{p}_t^i - \mathbf{x}_t^i) + c_2 r_{2,t}^i (\hat{\mathbf{p}}_t^g - \mathbf{x}_t^i) \quad (7)$$

where  $w$  is the inertia factor,  $c_1$  and  $c_2$  are the cognitive and social factors respectively,  $r_{1,t}^i$  and  $r_{2,t}^i$  are random numbers uniformly distributed in the interval  $[0,1]$ , and  $\mathbf{p}_t^i$  is the best previously position, obtained by the  $i^{\text{th}}$  particle in the swarm and the global best position  $\hat{\mathbf{p}}_t^g$  is now defined by:

$$\hat{\mathbf{p}}_t^g = N(\mathbf{p}_t^g, \sigma) \quad (8)$$

where  $\sigma$  is the degree of uncertainty about the optimality of the global best position  $\mathbf{p}_t^g$  in the standard PSO algorithm.

### B. Gravitational Search Algorithm

The Gravitational Search Algorithm (GSA), initially proposed by Rashedi, Nezamabadi & Saryazdi [25], considers agents as objects of different masses to solve difficult and hard optimization problems. Thanks to the gravity forces, each object will be influenced by their neighbors. Every object position is updated using the concepts of Newton's laws of gravity and motion, as follows:

$$\mathbf{F}_t^{ij} = G_t \cdot \left( \frac{m_{a,t}^i m_{p,t}^j}{r_{ij,t}^2} \right); \quad \mathbf{a}_t^i = \frac{\mathbf{F}_t^i}{m_t^i} \quad (9)$$

where  $\mathbf{F}_t^{ij}$  denotes the gravitational force between two entities,  $G_t$  is the gravitational constant,  $m_{a,t}^i$  is the active mass and  $m_{p,t}^j$  is the passive mass,  $r_{ij,t}$  is the distance between the  $i^{\text{th}}$  and  $j^{\text{th}}$  entities, and  $\mathbf{F}_t^i$ ,  $\mathbf{a}_t^i$  and  $m_t^i$  represent the force applied to the  $i^{\text{th}}$  particle, its acceleration and mass, respectively.

### C. Teaching-Learning based Optimization Algorithm

Introduced Rao, Savsani & Vakharia [26], the Teaching-Learning Based Optimization (TLBO) method is based on the influence effect of a teacher on the output of learners, i.e. the potential solutions of the optimization problem. The TLBO algorithm is divided in two phases: teaching and learning. In the first stage, the teacher tries to bring his learners up to his level in terms of knowledge. The new vector of decision variables is updated as follows:

$$\mathbf{x}_{t+1}^i = \mathbf{x}_t^i + \text{Difference\_Mean}_i \quad (10)$$

where  $\text{Difference\_Mean}_i$  denotes the difference between the existing and new means  $M_t$  and  $M_{t+1}$ , computed as follows:

$$\text{Difference\_Mean}_i = \text{rand}_i (M_{t+1} - T_F M_t) \quad (11)$$

where  $\text{rand}_i$  is a random number in the interval [0,1] and  $T_F$  is the teaching factor that selects the value of mean as follows:

$$T_F = \text{round} [1 + \text{rand} (0,1)] \quad (12)$$

In the second phase, the increasing knowledge is done randomly through the interaction between learners using the following computation steps:

$$\text{If } f(\mathbf{x}_t^i) < f(\mathbf{x}_t^j), \text{ then } \mathbf{x}_{t+1}^i = \mathbf{x}_t^i + \text{rand}_i (\mathbf{x}_t^j - \mathbf{x}_t^i), \text{ else} \\ \mathbf{x}_{t+1}^i = \mathbf{x}_t^i + \text{rand}_i (\mathbf{x}_t^j - \mathbf{x}_t^i) \quad (13)$$

### D. Grey Wolf Optimizer Algorithm

Recently proposed by Mirjalili, Mirjalili & Lewis [27], the Grey Wolf Optimizer (GWO) tries to mimic the social hierarchy and behavior of wolves where the fittest solution, denoted as  $\alpha$ , is the leader of the troupe. Subsequently, the second and third best solutions are named as  $\beta$  and  $\delta$ , respectively. All remaining candidate solutions are presumed to be  $\omega$ . The related algorithm has the following four phases:

- Encircling prey sub-model:

$$\mathbf{D}_t^i = |\mathbf{C}_t^i \mathbf{x}_t^p - \mathbf{x}_t^i| \quad (14)$$

$$\mathbf{x}_{t+1}^i = \mathbf{x}_t^p - \mathbf{A}_t^i \mathbf{D}_t^i \quad (15)$$

where  $\mathbf{x}_t^p$  is the prey position, and  $\mathbf{x}_t^i$  indicates the position of a grey wolf,  $\mathbf{A}_t^i$  and  $\mathbf{C}_t^i$  are control parameters defined as:

$$\mathbf{A}_t^i = 2a_t \mathbf{r}_{1,t}^i - a_t \quad (16)$$

$$\mathbf{C}_t^i = 2\mathbf{r}_{2,t}^i \quad (17)$$

where  $a_t$  are linearly decreasing in the interval [2, 0] and  $\mathbf{r}_{1,t}^i$  and  $\mathbf{r}_{2,t}^i$  are random vectors in [0,1].

- Hunting sub-model:

$$\begin{cases} \mathbf{D}_{\alpha,t}^i = |\mathbf{C}_{1,t}^i \mathbf{x}_{\alpha,t}^i - \mathbf{x}_t^i| \\ \mathbf{D}_{\beta,t}^i = |\mathbf{C}_{2,t}^i \mathbf{x}_{\beta,t}^i - \mathbf{x}_t^i| \\ \mathbf{D}_{\delta,t}^i = |\mathbf{C}_{3,t}^i \mathbf{x}_{\delta,t}^i - \mathbf{x}_t^i| \end{cases} \quad (18)$$

$$\begin{cases} \mathbf{x}_{1,t}^i = \mathbf{x}_{\alpha,t}^i - \mathbf{A}_{1,t}^i \cdot \mathbf{D}_{\alpha,t}^i \\ \mathbf{x}_{2,t}^i = \mathbf{x}_{\beta,t}^i - \mathbf{A}_{2,t}^i \cdot \mathbf{D}_{\beta,t}^i \\ \mathbf{x}_{3,t}^i = \mathbf{x}_{\delta,t}^i - \mathbf{A}_{3,t}^i \cdot \mathbf{D}_{\delta,t}^i \end{cases} \quad (19)$$

$$\mathbf{x}_{t+1}^i = \frac{\mathbf{x}_{1,t}^i + \mathbf{x}_{2,t}^i + \mathbf{x}_{3,t}^i}{3} \quad (20)$$

- Attacking prey step: this is done by decreasing  $a_t$  over the course of iterations which enhances the exploitation capacity of the algorithm.
- Search for prey: this is done by giving  $\mathbf{A}_t^i$  random values greater than 1 or less than -1 which enhances the exploration mechanism.

### E. Numerical Experimentation and Analysis

All proposed pPSO, GSA, TLBO and GWO metaheuristics algorithms are graphically implemented and executed under LabVIEW software in such a manner to insure modularity and scalability using the Sub-Virtual Instruments (VIs) formalism (see Fig. A1 and A2 of Appendix A). All these algorithms have been coded in MATLAB 7.8 and executed on a PC computer with Core 2 Duo-2.20 GHz CPU and 2.00 GB RAM. After the software implementation phase, various optimization tests are used to compare the obtained results with the published ones. To do so, the optimization test functions of Appendix B have been implemented as new libraries in the LabVIEW Functions palette.

A benchmark of eight standard test functions [15-17], with various properties for the optimization framework, is adopted for the numerical experimentation stage. Each of these functions has a different set of features representative of a different class of single-objective optimization problems. All proposed metaheuristics algorithms have been evaluated and validated thanks to this benchmark. The related statistical results in terms of the best, mean and worst cases of the optimization as well as the standard deviation (STD) are summarized in Table I for independent 30 runs. From Table I, the validity of the LabVIEW-based implementation is checked. The convergence of all algorithms is usually guaranteed in a reasonable computation time and with remarkable superiority. Roughly, the STD metric has a small value which means that the according algorithms are repeatable over the independent 30 runs, especially for the GWO one. From such a graphical-based implementation of advanced metaheuristics, it is observed that there is no algorithm that excels in solving all considered functions. This is already mentioned by the well-known ‘‘No Free Lunch’’ theorem which stipulates that ‘‘for any algorithm, any elevated performance over one class of problems is offset by performance over another class’’.

TABLE I. NUMERICAL OPTIMIZATION RESULTS OVER 30 RUNS

| Function |        | pPSO     | GSA      | TLBO     | GWO      |
|----------|--------|----------|----------|----------|----------|
| $f_1$    | Best   | 5.55e-06 | 1.30e-16 | 1.45e-06 | 1.44e-30 |
|          | Mean   | 7.50e-06 | 4.03e-16 | 1.75e-04 | 1.07e-27 |
|          | STD    | 8.97e-07 | 3.97e-16 | 3.69e-04 | 1.10e-27 |
|          | Median | 7.48e-06 | 2.51e-16 | 3.75e-05 | 5.92e-28 |
| $f_2$    | Best   | 1.09e-02 | 4.48e-08 | 1.85e-06 | 1.07e-17 |
|          | Mean   | 6.87e-01 | 1.13e-01 | 4.74e-04 | 1.08e-16 |
|          | STD    | 1.51e+00 | 3.77e-01 | 1.30e-03 | 7.59e-17 |
|          | Median | 9.39e-02 | 9.27e-08 | 3.54e-05 | 7.56e-17 |
| $f_3$    | Best   | 3.75e-03 | 4.62e+02 | 5.44e+01 | 9.02e-09 |
|          | Mean   | 9.69e-01 | 1.02e+03 | 2.42e+02 | 1.26e-05 |
|          | STD    | 1.29e+00 | 3.22e+02 | 2.14e+02 | 2.98e-05 |
|          | Median | 3.82e-01 | 1.01e+03 | 1.78e+02 | 1.34e-06 |
| $f_4$    | Best   | 1.82e+01 | 2.74e+01 | 1.28e+01 | 2.64e+01 |
|          | Mean   | 2.70e+01 | 4.24e+01 | 1.08e+02 | 2.81e+01 |
|          | STD    | 3.37e+00 | 2.95e+01 | 3.86e+01 | 7.61e-01 |
|          | Median | 2.68e+01 | 3.00e+01 | 9.45e+01 | 2.81e+01 |
| $f_5$    | Best   | 1.00e+00 | 0.00e+00 | 4.20e+01 | 0.00e+00 |
|          | Mean   | 2.57e+01 | 1.32e+01 | 1.59e+02 | 0.00e+00 |
|          | STD    | 3.07e+01 | 2.57e+01 | 1.14e+02 | 0.00e+00 |
|          | Median | 1.65e+01 | 4.00e+00 | 1.26e+02 | 0.00e+00 |
| $f_6$    | Best   | 3.87e-03 | 4.05e-02 | 2.33e-02 | 6.76e-04 |
|          | Mean   | 1.11e-02 | 8.19e-02 | 5.59e-02 | 2.12e-03 |
|          | STD    | 3.62e-03 | 3.26e-02 | 2.52e-02 | 1.08e-03 |
|          | Median | 1.05e-02 | 8.04e-02 | 5.13e-02 | 1.96e-03 |
| $f_7$    | Best   | 4.08e+01 | 1.49e+01 | 1.79e+01 | 0.00e+00 |
|          | Mean   | 8.82e+01 | 2.93e+01 | 2.80e+01 | 3.44e+00 |
|          | STD    | 2.69e+01 | 8.62e+00 | 4.88e+00 | 3.70e+00 |
|          | Median | 8.61e+01 | 2.59e+01 | 2.74e+01 | 2.21e+00 |
| $f_8$    | Best   | 2.38e-07 | 1.74e+01 | 1.54e-06 | 0.00e+00 |
|          | Mean   | 1.21e-02 | 2.74e+01 | 8.59e-02 | 3.37e-03 |
|          | STD    | 1.50e-02 | 6.97e+00 | 1.15e-01 | 7.33e-03 |
|          | Median | 7.40e-03 | 2.60e+01 | 3.95e-02 | 0.00e+00 |

#### IV. APPLICATIONS TO THE CONTROL OF DYNAMIC SYSTEMS

##### A. Case-Study 1: Magnetic Levitation System

The magnetic levitation system MAGLEV 33-006 from the Feedback Company (see Fig. 4) is a SISO process example used to validate the proposed metaheuristics-tuned MPC approach. Demonstrative results and analyses are given and discussed through this subsection.

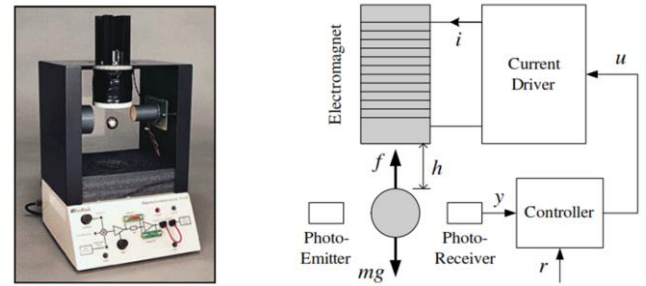


Fig. 4. Schematic Set-up of the MAGLEV 33-006 System.

The position dynamics of the metal sphere of MAGLEV system is modeled as follows [28, 29]:

$$m \frac{d^2 y}{dt^2} = \gamma mg_a - K \frac{(\rho u + i_0)^2 \gamma^3}{(y - y_0)^2} \quad (21)$$

where  $y$  is the voltage reflecting the distance between the coil and the metal sphere,  $\gamma > 0$ ,  $\rho > 0$  and  $K$  are the sensor gain, coil resistor and electromechanical conversion gain, respectively,  $y_0$  and  $i_0 > 0$  are the voltage and the offsets current, respectively, and  $g_a$  is the acceleration of gravity.

Taking  $x = [y \quad \dot{y}]^T$  as a state vector, the continuous-time state-space representation of the system is given by:

$$\begin{cases} \dot{x}_1 = x_2 \\ \dot{x}_2 = \gamma g_a - K \frac{(\rho u + i_0)^2 \gamma^3}{m(x_1 - y_0)^2} \end{cases} \quad (22)$$

With a sampling period of 5ms and while using the numeric values of the physical model parameters, a discrete-time model of the MAGLEV 33-006 plant is derived as follows:

$$\begin{cases} x_{k+1} = \begin{bmatrix} 1.0108 & 0.0050 \\ 4.3185 & 1.0108 \end{bmatrix} x_k + \begin{bmatrix} -0.0142 \\ -5.6779 \end{bmatrix} u_k \\ y_k = [1 \quad 0] x_k \end{cases} \quad (23)$$

Since that the MAGLEV 33-006 system is SISO type, the unknown weighting matrices  $Q$  and  $R$  of the MPC approach are scalars. Therefore, the formulated optimization problem (5) has four decision variables, i.e. two horizons ( $N_p, N_c$ ) and two weighting coefficients ( $Q = q_1, R = r_1$ ). For all proposed pPSO, GSA, TLBO and GWO algorithms, a maximum number of iterations equal to 100 and a population size of 40 are considered as common control parameters. For the algorithms with specific control parameters, i.e. pPSO and Genetic Algorithm (GA), the following set of coefficients is used:

- pPSO [24]:  $c_1 = 0.5$ ;  $c_2 = 0.3$ ;  $w = 0.9$ ;  $\sigma_{\max} = 0.15$   
 $\sigma_{\min} = 0.001$  and  $\alpha = 0.5$ ;
- GA [30]: crossover probability 0.85; mutation rate 0.005; Min mutation rate 0.0005 and Max rate 0.25.

TABLE II. OPTIMIZATION RESULTS FOR THE MAGLEV SYSTEM OVER 30 RUNS

|             | GA       | pPSO     | GSA      | TLBO     | GWO      |
|-------------|----------|----------|----------|----------|----------|
| Best        | 1.95e+01 | 7.68e+00 | 7.68e+00 | 7.67e+00 | 7.67e+00 |
| Mean        | 3.02e+01 | 7.68e+00 | 7.68e+00 | 7.68e+00 | 7.68e+00 |
| STD         | 1.62e+01 | 9.33e-04 | 1.98e-03 | 1.35e-03 | 1.27e-03 |
| Median      | 2.37e+01 | 7.68e+00 | 7.68e+00 | 7.68e+00 | 7.68e+00 |
| Duration    | 01:53:14 | 06:10:42 | 00:44:00 | 01:30:55 | 02:20:54 |
| $N_p^*$     | 2.00e+01 | 2.00e+02 | 8.30e+01 | 2.70e+01 | 2.60e+01 |
| $N_c^*$     | 1.10e+01 | 5.20e+01 | 3.90e+01 | 1.40e+01 | 1.40e+01 |
| $Q^* = q_1$ | 3.21e+00 | 1.85e+02 | 9.59e+01 | 5.77e+01 | 8.56e+01 |
| $R^* = r_1$ | 2.57e+00 | 1.72e+02 | 8.92e+01 | 5.26e+01 | 7.74e+01 |
| $u_{max}$   | 2.29e+00 | 2.29e+00 | 2.29e+00 | 2.29e+00 | 2.29e+00 |

The resolution of the constrained optimization problem (5) leads to the results of Table II.

From a practical point of view, when exceeding the value  $u_{max} = 2.3 V$ , the ball will stack immediately to the coil which creates a constraint on the control action. For all numerical experimentations, a comparison with the GA metaheuristic [30] is investigated. From these results, all metaheuristics improve high performances in terms of stability, trajectories tracking and handling of constraints. All proposed algorithms have almost reached the same solutions quality in terms of time computation and optimality, except the GA one. The plant output and control action signals have similar shapes and one representation is shown in Fig. 5 and Fig. 6, respectively.

An evaluation of the time-domain performances of the metaheuristics-tuned MPC for the MAGLEV process is given in Table III. It is shown that the TLBO-based method leads to high performance in terms of fastness and damping responses as well as the precision of the steady-state dynamics.

### B. Case-Study 2: Hydraulic System

As depicted in Fig. 7(a), the DTS200 three-tank system is used to validate the proposed metaheuristics-tuned MPC approach for MIMO systems.

Setpoint and Plant Outputs

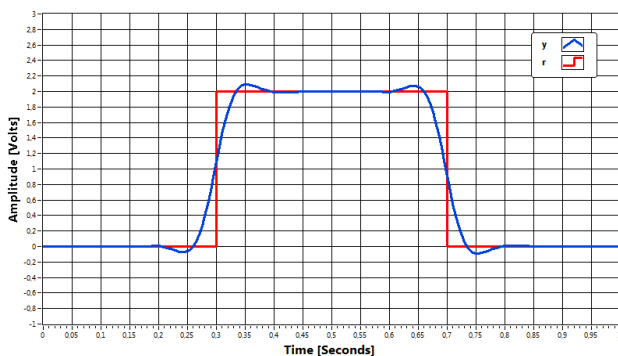


Fig. 5. MAGLEV 33-006 System Response: TLBO-based Approach.

Control Action

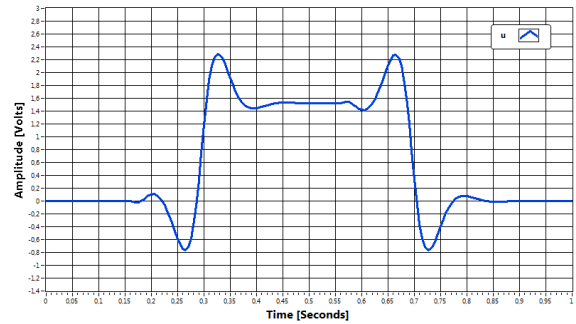


Fig. 6. Metaheuristics-Tuned MPC Signal: TLBO-based Approach.

TABLE III. TABLE. PERFORMANCE EVALUATION OF THE TUNED MPC OF MAGLEV SYSTEM

| Algo. | Settling time (ms) | Overshoot (%) | Steady-state error |
|-------|--------------------|---------------|--------------------|
| pPSO  | 135.00             | 10            | 0.00               |
| GSA   | 150.00             | 5             | 0.00               |
| TLBO  | 100.00             | 5             | 0.00               |
| GWO   | 120.00             | 8             | 0.00               |
| GA    | 090.00             | 12            | 0.00               |

A simplified dynamic model for such a system is given as follows [31-33]:

$$\begin{cases} \frac{dh_1}{dt} = Q_1 - k_1 \sqrt{|h_1 - h_3|} \text{sign}(h_1 - h_3) \\ \frac{dh_2}{dt} = Q_2 - k_3 \sqrt{|h_2 - h_3|} \text{sign}(h_2 - h_3) - k_2 \sqrt{h_2} \\ \frac{dh_3}{dt} = k_1 \sqrt{|h_1 - h_3|} \text{sign}(h_1 - h_3) + k_3 \sqrt{|h_2 - h_3|} \text{sign}(h_2 - h_3) \end{cases} \quad (24)$$

where  $h_1$ ,  $h_2$  and  $h_3$  are the liquid heights inside the tanks.

The interconnection parameters  $k_i$  and  $Q_i$  are defined as:

$$k_i = a_i \frac{S_n \sqrt{2g a}}{A}; Q_j = \frac{Q'_j}{A}, \forall i = 1, 2, 3 \text{ and } j = 1, 2 \quad (25)$$

where  $A$  and  $S_n$  are the cross section of the tanks and the valves, respectively,  $a_i$  are the outflow coefficients,  $Q'_1$  and  $Q'_2$  are the flow rates of the two pumps  $P_1$  and  $P_2$ .

A linearization of (24) around the point ( $h_{1op} = 0.4m$ ,  $h_{2op} = 0.2m$ ,  $h_{3op} = 0.3m$ ,  $Q'_{1op} = 32.24e-6 m^3/sec$ ,  $Q'_{2op} = 27.91e-6 m^3/sec$ ) leads to the discrete-time model:

$$\begin{cases} x_{k+1} = \begin{bmatrix} 0.9503 & 0.0012 & 0.0484 \\ 0.0012 & 0.9065 & 0.0462 \\ 0.0484 & 0.0462 & 0.9041 \end{bmatrix} x_k + \begin{bmatrix} 316.472 & 0.1359 \\ 0.1359 & 309.2 \\ 8.0659 & 7.7682 \end{bmatrix} u_k \\ y_k = \begin{bmatrix} 1 & 0 & 0 \\ 0 & 1 & 0 \end{bmatrix} x_k \end{cases} \quad (26)$$

To achieve a smooth pump control, the saturation behavior is avoided. The operational constraint  $u_{\max} = 10^{-4} \text{ m}^3/\text{sec}$  is used as the maximum pumps flow rate. Since the DTS200 is a MIMO system, the decision variables  $\mathbf{Q}$  and  $\mathbf{R}$  of problem (5) are matrices and chosen with the following expressions:

$$\mathbf{Q} = \begin{bmatrix} q_{11} & 0 \\ 0 & q_{22} \end{bmatrix} > 0, \quad \mathbf{R} = \begin{bmatrix} r_{11} & 0 \\ 0 & r_{22} \end{bmatrix} > 0 \quad (27)$$

So, the formulated MPC tuning problem for the system (24) is solved to optimize the following decision variables:

$$\mathbf{x} = (N_c, N_p, q_{11}, q_{22}, r_{11}, r_{22})^T \in \mathbb{R}_+^6 \quad (28)$$

While using the same control parameters of the proposed algorithms, 30 independent runs of problem (5) lead to the statistical results of Table IV and dynamical responses of Fig. 7(b), Fig. 8 and Fig. 9. These demonstrative results show the superiority and effectiveness of the proposed metaheuristics in terms of damping responses, tracking capabilities and robustness under the operational constraints. All proposed algorithms have almost reached the same solution qualities. In the GA-based strategy, the MPC algorithm creates pump saturation, i.e. at pump 2, by reaching the constraint  $u_{\max}$  as shown in Fig. 8 and Fig. 9. However, the GWO-based method achieves more efficient and smooth control without using an anti-windup mechanism.



(a) Synoptic Schema of the DTS200 Three-Tank System.

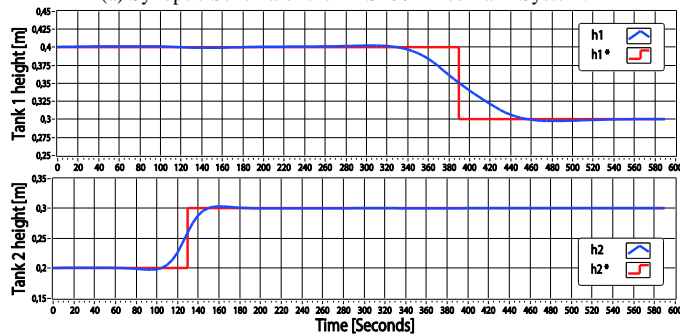


Fig. 7. (b) DTS200 Process Responses: GWO-based Approach.

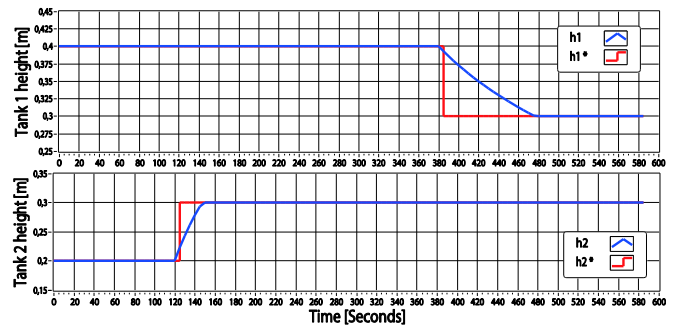


Fig. 8. DTS200 Process Responses: GA-based Approach.

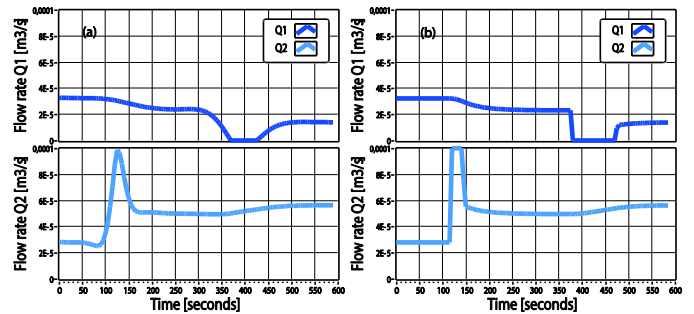


Fig. 9. Metaheuristics-Tuned MPC Signals: (a) GWO-based Approach and (b) GA-based Approach.

The performances of the metaheuristics-tuned MPC for the DTS200 process are summarized in Table V. One can observe the superiority of the GWO-tuned MPC in terms of fastness and smoothness of time-domain responses. The steady-state errors remain null for all algorithms. For the GA-tuned MPC case, the predictive behavior of the control law is not observed. The system outputs' variations are not smooth which presents a major drawback in the real-world implementation. In addition, the steady-state error for this tuning algorithm is not null in comparison with all others tuning metaheuristics.

TABLE IV. NUMERICAL OPTIMIZATION RESULTS FOR THE DTS200 SYSTEM OVER 30 RUNS

|            | GA       | pPSO     | GSA      | TLBO     | GWO      |
|------------|----------|----------|----------|----------|----------|
| Best       | 5.51e+00 | 3.58e-02 | 2.85e-02 | 2.13e-02 | 2.13e-02 |
| Mean       | 5.95e+00 | 3.58e-02 | 4.50e-01 | 2.62e-02 | 2.81e-02 |
| STD        | 2.88e-01 | 7.69e-07 | 4.12e-01 | 3.37e-03 | 5.49e-03 |
| Median     | 5.98e+00 | 3.58e-02 | 2.50e-01 | 2.85e-02 | 2.85e-02 |
| Duration   | 04:47:28 | 03:38:04 | 04:11:17 | 10:02:29 | 04:52:11 |
| $N_p^*$    | 1.00e+00 | 1.10e+01 | 6.00e+00 | 9.50e+01 | 1.00e+02 |
| $N_c^*$    | 1.00e+00 | 1.00e+00 | 1.00e+00 | 2.80e+01 | 2.70e+01 |
| $q_{11}^*$ | 5.27e+00 | 5.12e+01 | 4.64e+01 | 1.00e-08 | 3.14e-08 |
| $q_{22}^*$ | 1.72e+00 | 7.88e+00 | 9.16e+01 | 1.00e-08 | 1.11e-07 |
| $r_{11}^*$ | 9.04e+01 | 2.22e+01 | 4.21e+01 | 5.56e-01 | 1.66e+00 |
| $r_{22}^*$ | 2.85e-02 | 4.88e+00 | 3.54e+01 | 1.56e-02 | 1.73e-01 |
| $Q_{\max}$ | 1.00e-04 | 6.60e-05 | 8.35e-05 | 9.88e-05 | 9.88e-05 |

TABLE V. TABLE PERFORMANCE EVALUATION OF THE TUNED MPC OF DTS200 SYSTEM

| Algo. | Settling time (sec) | Overshoot (%) | Steady-state error |
|-------|---------------------|---------------|--------------------|
| pPSO  | 98/T1; 27/T2        | 0             | 0.00               |
| GSA   | 60/T1; 52/T2        | 4             | 0.00               |
| TLBO  | 64/T1; 58/T2        | 5             | 0.00               |
| GWO   | 70/T1; 50/T2        | 1             | 0.00               |
| GA    | 92/T1; 23/T2        | 0             | 0.01               |

### V. CONCLUSIONS

In this paper, an advanced metaheuristics-based approach for MPC parameters' tuning has been proposed and successfully applied for SISO and MIMO systems. The proposed pPSO, GSA, TLBO and GWO algorithms are originally implemented under LabVIEW graphical software. These algorithms are firstly evaluated on a benchmark of standard test functions in order to be numerically validated for the formulated MPC tuning problems. All optimization results are discussed and compared in order to show the validity of such a LabVIEW-based implementation. The MPC tuning problem, involving the choice of the well-known prediction and control horizons as well as the weighting matrices, is formulated as a constrained optimization problem and solved using the proposed advanced metaheuristics. All demonstrative results are compared with those obtained by the classical GA-based implementation. Applications to the position control of the MAGLEV system and level regulation of the three-tank DTS200 plants are successfully achieved.

Future works deal with the real-world implementation of the metaheuristics-tuned MPC approaches using a compatible CompactRIO-RT board. The formulation of the proposed metaheuristics algorithms in an online tuning framework is also investigated for the hydraulic DTS200 process.

### REFERENCES

[1] Y. Shan, J. Hu, Z. Li, and J.M. Guerrero, "A Model Predictive Control for Renewable Energy Based AC Microgrids Without Any PID Regulators", IEEE Transactions on Power Electronics, vol. 33, no. 11, pp. 9122-9126, 2018.

[2] N. Rahimi, R.K. Moghaddam, "Maximizing the Absorbed Power of a Point Absorber using an FA-based Optimized Model Predictive Control", China Ocean Engineering, vol. 32, no. 6, pp. 696-705, 2018.

[3] G. Williams, P. Drews, B. Goldfain, J.M. Rehg, and E.A. Theodorou, "Information-Theoretic Model Predictive Control: Theory and Applications to Autonomous Driving", IEEE Transactions on Robotics, vol. 34, no. 6, pp. 1603-1622, 2018.

[4] K. Worthmann, M.W. Mehrez, M. Zanon, G.K. I. Mann, R.G. Gosine, and M. Diehl, "Model Predictive Control of Nonholonomic Mobile Robots Without Stabilizing Constraints and Costs", IEEE Transactions on Control Systems Technology, vol. 24, no. 4, pp. 1394-1406, 2016.

[5] D. Bao-Cang, Modern Predictive Control, 1<sup>st</sup> ed. USA CRC Press, 2010.

[6] D. Q. Mayne, "Model predictive control: Recent developments and future promise", Automatica, vol. 50, no. 12, pp. 2967-2986, 2014.

[7] J. B. Rawlings and D. Q. Mayne, Model Predictive Control: Theory and Design. Madison, USA.: Nob Hill Publishing, 2013.

[8] S. Bouallègue and R. Fessi, "Rapid Control Prototyping and PIL Co-Simulation of a Quadrotor UAV Based on NI myRIO-1900 Board", International Journal of Advanced Computer Science and Applications, vol. 7, no. 6, pp. 26-35, 2016.

[9] T. Baumeister, S.L. Brunton, and J.N. Kutz, "Deep Learning and Model Predictive Control for Self-Tuning Mode-Locked Lasers", Journal of the Optical Society of America B, vol. 35, no. 3, pp. 617-626, 2018.

[10] A. S. Yamashita, A. C. Zanin, and D. Odloak, "Tuning of Model Predictive Control with Multi-objective Optimization", Brazilian Journal of Chemical Engineering, vol. 33, no. 02, pp. 333-346, 2016.

[11] Q. N. Tran, R. Octaviano, L. Ozkan and A.C.P.M. Backx, "Generalized Predictive Control tuning by controller matching", In Proceedings of the 2014 American Control Conference, pp. 4889-4894, Portland, Oregon, USA, 2014.

[12] P. Bagheri, A.K. Sedigh, "Analytical approach to tuning of model predictive control for first-order plus dead time models", IET Control Theory & Applications, vol. 7, no. 14, pp. 1806-1817, 2013.

[13] R. Toro, C.Ocampo-Martinez, F. Logist, J.V. Impe and V. Puig, "Tuning of Predictive Controllers for Drinking Water Networked Systems", In Proceedings of the 18th World Congress of the International Federation of Automatic Control, pp. 14507-14512, Milano-Italy, 2011.

[14] G. Shah and S. Engell, "Tuning MPC for Desired Closed-Loop Performance for MIMO Systems", In Proceedings of the 2011 American Control Conference, San Francisco, CA, USA pp. 4404-4409, 2011.

[15] X.-S. Yang, Engineering optimization :an introduction with metaheuristic applications, 1st ed. New Jersey, USA: John Wiley & Sons, Inc., 2010.

[16] J. Dréo, A. Pétrowski, P. Siarry, and E. Taillard, Metaheuristics for Hard Optimization, 1st ed. Berlin-Heidelberg: Springer-Verlag, 2006.

[17] M. Gendreau and J.-Y. Potvin, Handbook of Metaheuristics, 2nd ed., vol. 146. Boston, MA: Springer US, 2010.

[18] G. Sandou and S. Oлару, Particle Swarm Optimization Based NMPC: An Application to District Heating Networks, in Nonlinear Model Predictive Control, D.M.R.L. Magni and F. Allgöwen, Eds. Berlin Heidelberg: Springer Verlag, 2009.

[19] G. Sandou and S. Oлару, Ant Colony and Genetic Algorithm for Constrained Predictive Control of Power Systems, in Hybrid Systems: Computation and Control, A. Bemporad and A. B. Buttazzo, Eds. Berlin Heidelberg: Springer Verlag, 2007.

[20] G. Sandou, Metaheuristic strategy for the hierarchical predictive control of large scale energy networks, Control Eng. Appl. Informatics, vol. 11, no. 3, pp. 32-40, 2009.

[21] H.M. Albeahdili, T. Han and N.E. Islam, Hybrid Algorithm for the Optimization of Training Convolutional Neural Network, Int. Jour.of Advanced Comp. Science and Applications, vol.6, no.10,pp.79-85,2015.

[22] R. Suzuki, F. Kawai, H. Ito, C. Nakazawa, Y. Fukuyama, and E. Aiyoshi, Automatic Tuning of Model Predictive Control Using Particle Swarm Optimization, In Proceedings of the 2007 IEEE Swarm Intelligence Symp. Honolulu, pp. 221-226, 2007.

[23] M. L. Derouiche, S. Bouallègue, J. Haggège, and G. Sandou, LabVIEW Perturbed Particle Swarm Optimization Based Approach for Model Predictive Control Tuning, In Proceedings of the 4th IFAC International Conference on Intelligent Control and Automation Sciences, vol. 49, no. 5. Reims, pp. 353-358, 2016.

[24] X. Zhao, A perturbed particle swarm algorithm for numerical optimization, Appl. Soft Comput., vol. 10, no. 1, pp. 119-124, 2010.

[25] E. Rashedi, H. Nezamabadi-pour, and S. Saryazdi, GSA: A Gravitational Search Algorithm, Inf. Sci. (Ny.), vol. 179, no. 13, pp. 2232-2248, 2009.

[26] R. V. Rao, V. J. Savsani, and D. P. Vakharia, Teaching-learning-based optimization: A novel method for constrained mechanical design optimization problems, Comput. Des., vol. 43, no. 3, pp. 303-315, 2011.

[27] S. Mirjalili, S. M. Mirjalili, and A. Lewis, Grey Wolf Optimizer, Adv. Eng. Softw., vol. 69, pp. 46-61, 2014.

[28] H. Yaghoubi, The Most Important Maglev Applications, J. Eng., vol. 2013, pp. 1-19, 2013.

[29] M. Santos, R. K. H. Galvao, and T. Yoneyama, Robust Model Predictive Control for a Magnetic Levitation System Employing Linear Matrix Inequalities, ABCM Symp. Ser. Mechatronics, vol.4, pp.147-155, 2010.

[30] W. Golebiowski, Waptia-genetic optimization algorithm-General-LAVA. [Online]. Available: <https://lavag.org/files/file/94-waptia-genetic-optimization-algorithm/>. [Accessed: 08-Jan-2017].

[31] J. Ivanka and P. Navratil, Multiestimation Scheme for Adaptive Control of Three Tank System DTS200, In Proceedings of the 48th International Scientific Conference on Experimentalni Analiza Napeti 2010 Experimental Stress Analysis. Velke Losiny, pp. 123-130, 2010.

[32] P. Chalupa and J. Novak, Modeling and model predictive control of a nonlinear hydraulic system, *Comput. Math. with Appl.*, vol. 66, no. 2, pp. 155–164, 2013.

[33] L. Wang, *Model Predictive Control System Design and Implementation Using MATLAB*, 1st ed. London: Springer London, 2009.

APPENDIX A: LABVIEW FRONT PANELS FOR MPC PARAMETERS' TUNING

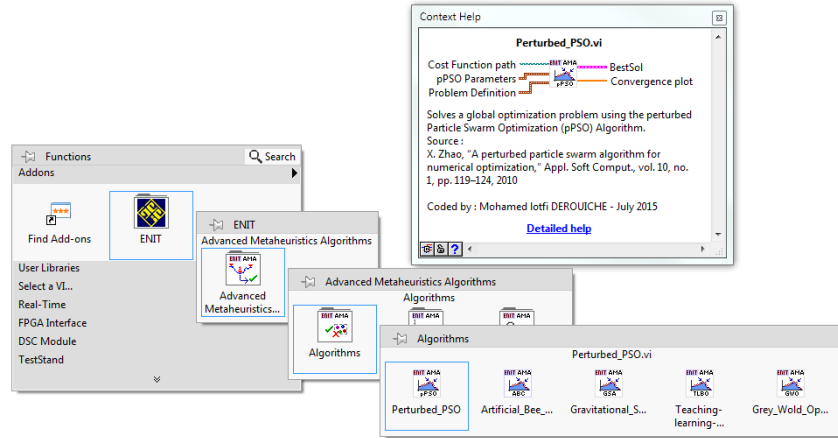


Fig. A1 Advanced Metaheuristic Algorithms as Part of the Lab view Functions Palette.

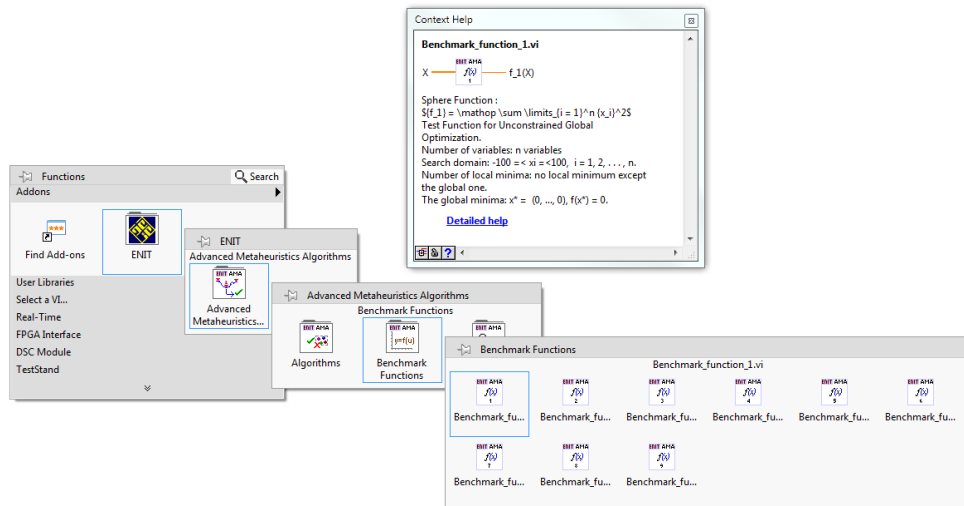


Fig. A2 Benchmark Functions as Part of the Lab view Functions Palette.

APPENDIX B: BENCHMARK OF TEST FUNCTIONS

All LabVIEW implementations of optimization functions are available for free access and download through the following National Instruments web site: [HTTP://SINE.NI.COM/NIPS/CDS/VIEW/P/LANG/EN/NID/216789](http://sine.ni.com/nips/cds/view/P/LANG/EN/NID/216789)

| Optimization functions   | Domain          | $f_{\min}$ | Optimization functions  | Domain            | $f_{\min}$ |
|--|-----------------|------------|---|-------------------|------------|
| $f_1 = \sum_{i=1}^n x_i^2$   | $[-100, 100]^n$ | 0          | $f_5 = \sum_{i=1}^n (x_i + 0,5)^2$  | $[-100, 100]^n$   | 0          |
| $f_2 = \sum_{i=1}^n  x_i  + \prod_{i=1}^n  x_i $                       | $[-10, 10]^n$   | 0          | $f_6 = \sum_{i=1}^n i x_i^4 + \text{random}[0, 1]$  | $[-1.28, 1.28]^n$ | 0          |
| $f_3 = \sum_{i=1}^n \left( \sum_{j=1}^i x_j \right)^2$                 | $[-100, 100]^n$ | 0          | $f_7 = \sum_{i=1}^n [x_i^2 - 10 \cdot \cos(2\pi x_i) + 10]$   | $[-5.12, 5.12]^n$ | 0          |
| $f_4 = \sum_{i=1}^{n-1} [100 \cdot (x_{i+1} - x_i^2)^2 + (x_i - 1)^2]$ | $[-30, 30]^n$   | 0          | $f_8 = \frac{1}{4000} \sum_{i=1}^n x_i^2 - \prod_{i=1}^n \cos\left(\frac{x_i}{\sqrt{i}}\right) + 1$ | $[-600, 600]^n$   | 0          |

# Secure Medical Internet of Things Framework based on Parkerian Hexad Model

Nidal Turab<sup>1</sup>

Networks & information security Dept, Faculty of IT  
Al-Ahliyya Amman University, Amman-Jordan

Qasem Kharma<sup>2</sup>

Computer Science Dept, Faculty of IT  
Al-Ahliyya Amman University, Amman-Jordan

**Abstract**—Medical Internet of Things (MIoT) applications enhance medical services by collecting data using devices connected to the IoT. The collected data, which may include personal data and location, is transmitted to mobile device and to health care provider via Internet Service Provider (ISP). Unfortunately, connecting a device to a network or sending data via wide network may make those devices and data vulnerable to unauthorized access. In this research, a secure 3-tier MIoT framework is proposed. Tier 1 includes the devices and sensors that will collect data. Those devices and sensors are based upon limited resources; therefore, they cannot apply complex security and privacy algorithms. Tier 2 includes the devices that will collect data from Tier 1 and submit it to Tier 3 via Internet Service Provider (ISP). Tier 3 includes the Health Information System. The framework defines the controls that are needed between layers to secure user privacy and data based on the Parkerian Hexad Model.

**Keywords**—MIoT; Parkerian Hexad; PRMS; Lightweight Encryption

## I. INTRODUCTION

IoT is defined as a network that enables every object or device on the planet to interact, connect, and exchange data with other objects. The concept of IoT began in 1998, where Brave, et al. [1] designed a haptic prototype to support distance-communication between people. Also, the term "Internet of Things" was first used by Kevin Ashton in 1998 to describe the system that connects different objects using sensors [2]. Since that time, the IoT has numerous promising application domains such as in smart homes, smart Cities, smart power grids, farming, transport systems, wearable clothes and devices, industrial Internet, and healthcare.

One important application of IoT is in healthcare due to the rapid increase in world population, along with increased life expectancy and chronic diseases. Hence, it is vital to develop medical electronics and wearable devices that improve healthcare services by reducing cost, reducing the frequency of clinic visits, reducing the length of hospitalization, reaching patients in distant places, and monitoring patients continuously.

The term MIoT (Medical Internet of Things) means the applications of Internet of Things technologies in the medical field including the integration of healthcare devices with IoT enabled technologies (sensors, Wi-Fi, etc.) and applications to communicate with health care systems. MIoT can reduce the frequency of hospital visits by allowing patients to connect remotely and transfer data to their physicians. According to

the Frost & Sullivan analysis, the global MIoT market was worth \$22.5 billion in 2016, and is expected to reach \$72.02 billion by 2021 [3]. Today, there are many applications based on MIoT. Some current MIoT applications include:

- Patient Remote Monitoring System (PRMS): the use of IoT based technologies helps to monitor patients and record their vital signs through medical sensors in real time. Pulse oximeters and other sensors collect vital signs including blood pressure, body temperature, pulse, breathing rate, blood glucose, and patients' height, weight, and body mass index [4] [5] [6]. The aforementioned data are collected and sent to medical care centers where they are analyzed, and relevant medical information is extracted and forwarded to the intended physicians.
- Healthcare for elderly and disabled persons: The number of elderly and disabled people is increasing each year. Smart homes can provide comfortable and independent living for elderly and disabled people rather than staying in dedicated facilities (elderly or disabilities nursing homes). They can utilize wearable devices utilizing wireless technology to control home appliances, light sources, climate control, etc. In addition, sensors placed in different locations at home can track movements and other information for family member(s), or even send any urgent vital signs and health alerts to physicians immediately [7].
- Healthcare for rustic public health monitoring and control: Many patients living in rural areas encounter the problem of a lack of nearby healthcare centers. Using IoT based health monitoring and control technologies can help to overcome this problem by monitoring patients' health symptoms and urgent information. RFID sensors are used to record the patient health information. These data are sent through the Internet to the nearest health care center, or send alert messages to doctors directly [8] [9].
- Ingestible Sensor: The ingestible sensor developed by Proteus Digital Health helps to monitor patients' behavior of taking prescribed medication. The Proteus ingestible sensor can be consolidated with any pharmaceutical products to reach the stomach (via swallowing) where it powers up and sends signals through the patient's tissue to a patch on the skin that detects the signal and records the exact time the



medication has been taken. Furthermore, the patch can record heart rate, body position, and other activity. Using wireless technology, the patch sends information to a mobile phone application, which in turn can send the collected data to a physician or health care center [10] [11].

- IoT based Healthcare automated patient records system: The use of MIoT based technologies enables doctors to reduce time spent on daily routine tasks such as documenting patient history and medication rather than physical examinations and monitoring. These technologies are based upon using smart glasses accompanied with voice command systems to transmit data to hands-free, encrypted HIPAA-certified systems [12] [13].
- Adverse Drug Reaction System: Adverse drug reaction (ADR) is any harm caused by taking a medication. It can result from lengthy treatments or even a single drug dosage. In a typical IoT based ADR system [13], healthcare applications using NFC-enabled devices read data about drugs and compares them against patients' allergy profiles and medical histories, utilizing unified health data located at national health care centers. If a patient has an ADR, an alarm will be triggered [14].
- Heart disease monitoring system: The time it takes to arrive at a health care center is life-or-death for persons suffering from a heart attack; in some cases, patients are unconscious and unable call the healthcare center. This delay in notifying healthcare professionals could result in death. MIoT solutions can send real time (instant) patient vital signs (electrocardiography, blood pressure, pulse rate) to physicians. Additionally, they can send the patients' location, facilitating reaching them at the appropriate time [8].
- Compliance with Guidelines on Hand Hygiene in Health Care: according to the WHO Guidelines on Hand Hygiene in Health Care, infections are caused by various factors related to human behavior or systems and processes of health care suppliers [15]. Fortunately, infections are preventable; one basic measure to reduce infection is hand hygiene. MIoT hand-hygiene compliance monitoring (HHCM) systems would detect the degree of cleanliness in a healthcare worker by transmitting information about when the person enters or leaves a healthcare facility sterilization unit [15].
- Hearing Aids IoT based technologies: studies show that over 5 percent of the world's population starts having hearing difficulties after the age of 25. MIoT created wearable ear hearing aid devices. They can connect to and control a variety of household devices and mechanical tools [16].
- Oxygen Saturation Monitoring: Oxygen saturation monitor displays the percentage of blood saturated with oxygen. It is a wearable sensor placed on a thin part of

the patient's skin, allowing it to determine the oxygen absorbance due to the pulsing arterial blood [17].

- Although having a variety of medical devices connected to MIoT to increases its efficiency and reduces the cost of medical services, connecting devices to a wider network makes those devices more vulnerable to attacks. Therefore, any devices connected to IoT must be controlled in order to protect those devices from unauthorized access [18]. In this paper, a secure MIoT is proposed to protect patient data and privacy. The structure of this paper is organized as follows: Section 2 reviews related work on securing e-health systems. The challenges of the Medical IoT are discussed in Section 3. Section 4 presents a proposed secure structure of the e-health system in which there is a set of security criteria related to each user of a health system. Finally, the paper conclusions are in Section 5.

## II. RELATED WORK

- A lot of work has been done to address the issues of medical IoT safety and privacy. D. Salvi, E. V. Mora and M. T. A. Waldmeyer [19] listed all of the security problems related to patents' remote monitoring systems with some possible solutions. They proposed a security architecture based upon the legal basis of European Recommendation No R(97)5, the architecture based on renowned technologies such as web services for patients monitoring devices and service providers. D. Lake, R. M. R. Milito, M. Morrow and R. Vargheese [20] have identified some emerging standards and regulatory bodies for e-health. P. Gope and T. Hwang [21] described some security and privacy issues in BSN based healthcare systems. Further, they proposed a secure IoT based healthcare security system called BSN-Care, which mitigates some security issues of the BSN based healthcare system. S. Khoja, H. Durrani, R. E. Scott, A. Sajwani, and U. Piryani [22] have developed tools that cover all aspects of the Khoja-Durrani-Scott [KDS] framework for e-health systems. The proposed tools have been developed for healthcare governance, healthcare providers, and patients to understand their e-health programs. F. Rezaeibagha, K. T. Win, and W. Susilo [23] investigate the requirements of security and privacy of e-health from a technical perspective. The conducted literature is compared with ISO/IEC 27002:2013 and ISO/IEC 29100:2011 standards. They concluded that access control policies should be mandated to provide patient privacy. W. Leister, M. Hamdi, H. Abie and S. Poslad [24] presented an evaluation framework for adaptive security of e-health applications. The framework is based on security and QoS requirements for a generic e-health model, and a generic assessment framework. They presented three scenarios: home, hospital, and emergency scenarios.
- O. Olakanmi, I. Kamil and S. Ogundoyin [25] proposed a recommendation security and privacy framework to achieve anonymous authentication during the recommendation process and a trust model for efficient

selection of health care specialists. In Lee J the authors proposed a service-oriented security framework for remote medical services. The proposed framework supports dynamic security elements in accordance with demands of remote medical services. It enables confidentiality, integrity, and availability for all parties of remote medical systems.

- D. Y. Weider, L. Davuluri, M. Radhakrishnan and M. Runiassy [26] evaluated the gaps in security-oriented (SOD) enterprise frameworks especially Australian and the US frameworks reviewing existing frameworks and compared their risk-based methodologies. They established a guide to develop adequate threat mitigations that meet the needs of the healthcare stakeholders. W. Leister, M. Hamdi, H. Abie and S. Poslad [24] developed a framework to validate and assess the context-aware adaptive security eHealth solutions. They developed scenarios for patients with chronic diseases who use biomedical sensors. D. P. Mirembe [27] investigated the current trend in Telemedicine, E-health and Wellness (TEW) research and development, including their technologies, standards, services, and security implementations. In addition, they developed a framework that describes any TEW system. B. Ondiege, M. Clarke and G. Mapp [28] reviewed remote patient monitoring RPM they used Microsoft threat modelling tool, to explore current threats in IEEE 11073 standard devices then they propose a new security framework for remote patient monitoring devices. B. Mozzaquatro, C. Agostinho, D. Goncalves, J. Martins and R. Jardim-Goncalves [29] proposed an ontology-based framework for securing e-health composed of two approaches: design time and run time. H. Mora, D. Gil, R. M. Terol, J. Azorín and J. Szymanski [30] proposed a distributed framework for monitoring human biomedical signals. the proposed framework can be applied to other mobile environments, with high processing and have high data volumes. L. Catarinucci, D. De Donno, L. Mainetti, L. Palano, L. Patrono, M. L. Stefanizzi and L. Tarricone [31] proposed IoT-aware architecture, for Smart Hospital System (SHS) for RPM, network infrastructure relying on a CoAP, 6LoWPAN, and REST paradigms has been implemented for UHF RFID and WSN.

R. Piggin [32] explains ways to resolve issues concerning safety and security, also they highlights approaches that medical devices' manufacturers should take to improve security throughout lifecycle of their products.

### III. CHALLENGES OF MEDICAL IOT

One of the most significant threats that IoT poses is to data security and privacy. Healthcare records contain various types of private information, including a patient's name, email address, date of birth, social insurance number, and medical history. That information is valuable to hackers and is usually stored in one place, rarely changed (not as credit card numbers), and can be sold at higher prices on the black market

(dark web). Hence, MIIoT applications must take in consideration data security and privacy.

Unfortunately, most of the IoT sensors and devices lack data protocols and standards. In addition to that, there is significant ambiguity regarding data ownership regulation. All these factors make the data highly susceptible to cybercriminals who can hack into the system and compromise Personal Health Information (PHI) of both patients as well as doctors. Moreover, continuous access to health records is essential for the safety of patients because if the healthcare provider loses access to medical records, patients' lives could be at risk. Some security vulnerabilities that can compromise healthcare systems are:

- Data forgery or corruption: the attacker can modify or delete medical records to achieve some illegal purpose. Modifying vital health records may result in system failure and cause patient death.
- Medical staff: doctors, nurses and medical staff at the health care centers have easy access to medical records and patient files. This can be used for identity theft or other purposes such as blackmail.
- Unsecured medical sensors and devices: medical devices with access to healthcare centers' devices must meet security standards so they do not leave networks vulnerable to malware, eavesdropping, and phishing.
- Stolen medical devices or sensors: Any stolen medical device can be used to access the healthcare provider network if no security measures are applied.
- The risk of revealing or stealing personal data of patients and their medical history for the purposes of extortion or defamation might be one of the largest security threats to health care systems.
- Unrestricted access to healthcare provider devices and systems: systems and devices with no restricted areas can easily and altered be accessed by unauthorized personnel [33].

### IV. SECURE STRUCTURE MODEL FOR MIIoT SYSTEMS

The most crucial aspect in the medical field is to preserve the privacy of health care records and systems. Patients must be confident that their data is stored and processed in a secure manner, with no security breaches. If the trust relationship between patients and health care systems is broken, they will not reveal information necessary to deliver the health care they need. Medical records at healthcare providers contain sensitive and personal information about patients. Therefore, healthcare providers should ensure the privacy of information, especially because the patients' data can be increasingly stored accessed remotely. Protecting patients' medical records and information, and weighing sharing this information with different medical users is the main challenge of health service providers. Consequently, it is pivotal for healthcare service providers to have well structured, secured, and reliable system for storing electronic medical records in their health information systems.

In this paper, a three-tier layered network architecture is used to secure the medical records transferred from the patient to the healthcare provider. The three tiers are:

**Tier 1:** This consists of medical sensors, devices, and scales that measure the vital signs of the human body, whether or not they are wearable. Examples include BPM, ECG, glucose meters, hearing aid devices, weight scales, brain activity monitors, and so on. The aforementioned devices and sensors have constrained resources (memory processing power and power supply), thus they cannot perform complex algorithms required for security and privacy implementations. Compact hardware and software implementations with low power, RAM, and ROM usage are desirable.

**Tier 2:** This includes smart phones, PDAs, tablets, and wireless access points. Tier 2 devices receive wireless signals from tier 1 devices and transmit them to the MIoT provider via ISP or cloud service provider.

**Tier 3:** This can be considered as the MIoT, consists of health record servers, medical database servers, and storage devices. Physicians can access data stored on the MIoT provider's infrastructure to track and diagnose patient health. Tier 3 devices require complex security measures as they represent the medical data and records repository.

The three-tier network architecture is illustrated in Fig. 1.

The CIA Triad composed only of the three elements: Confidentiality, Integrity and Availability, but does not adequately address and satisfy the requirements of ownership and continuity of the medical records and health care systems. Therefore, the Parkerian Hexad model is a more suitable model than the CIA triad, since the Parkerian Hexad model

adds three extra elements to the CIA triad: Possession or Control, Authenticity, and Utility [32] [34]. The rationale of using Parkerian Hexad model as central structure of this study is that its attributes cannot be broken down into further ingredient; and not overlap with each other. The following subsection addresses each facet of the Parkerian Hexad model as related to three-tier architecture:

**Facet 1: Authentication:** Authentication means to identify a person or device to another person or device, usually by using usernames and passwords. The three-tier network authentication takes place at two points: between tier 1 and tier 2 devices, and between tier 2 and tier 3 devices. For authentication between tier 1 and tier 2, authentication protocols are limited to lightweight authentication protocols that give a reasonable level of authentication while preserving the constrained device resources. There are a variety of lightweight authentication protocols that provide authentication; they vary according to data size, key size and application:

- 1) *LMAP*: 896-bits authentication protocols designed for resource constrained RFID tags [35].
- 2) *ALIKE*: 80-bits and above asymmetric key based on RSA scheme for resource constrained RFID tags [36].
- 3) *ELLI*: Elliptic Curve-based authentication scheme: Elliptic curve cryptography offers the same security level as RSA with smaller key sizes and less processing power, and can offer authentication for resource constrained devices [37].
- 4) *IBS*: Identity-Based Signatures: verifying users' digital signatures using only public users' identifiers or any other public information [38].

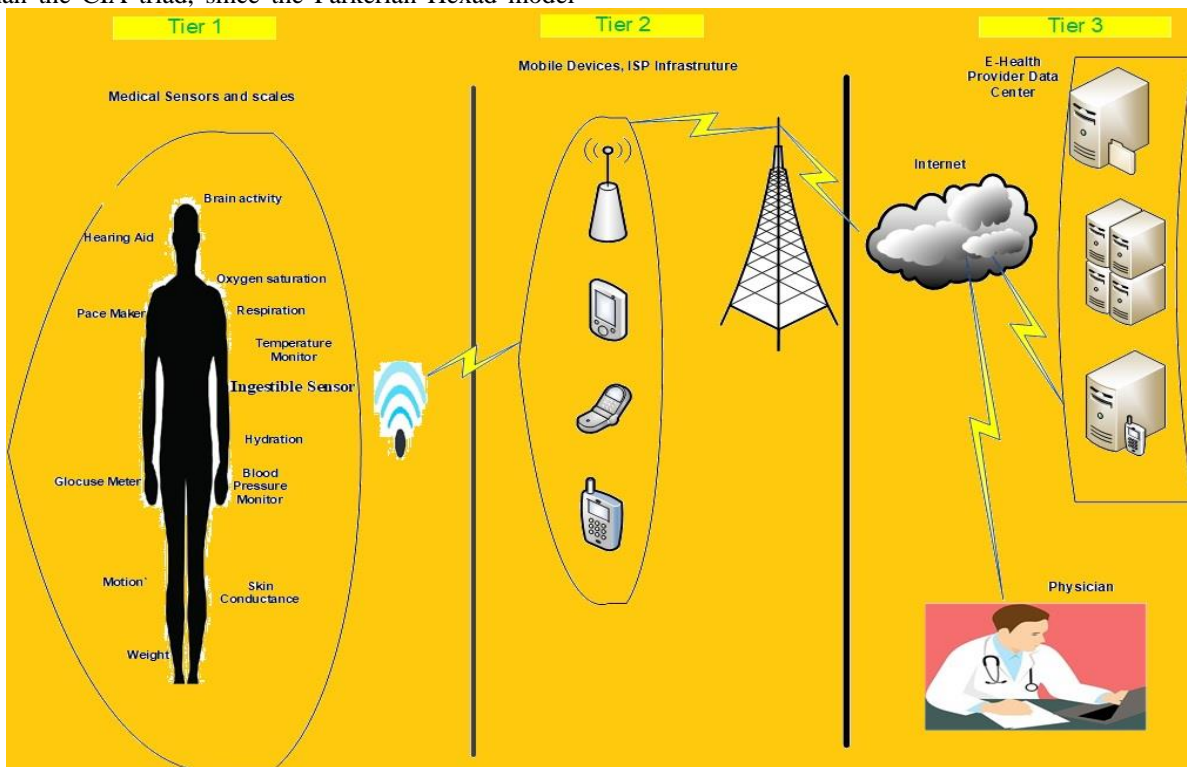


Fig. 1. The Proposed Secure three-Tier MIoT Architecture.

Regarding tiers 2 and 3, any authentication protocol (either PPP or AAA) could be used as there are no constrained resources. Any PPP authentication such as Password Authentication Protocol (PAP), Challenge-handshake Authentication Protocol (CHAP), Extensible Authentication Protocol (EAP), and any AAA authentication such as TACACS, Remote Authentication Dial-In User Service (RADIUS), and Diameter and Kerberos can be deployed.

**Facet 2: Integrity:** Data integrity technique means data generated by a medical device is transmitted and stored in the healthcare center but neither altered nor tampered with [39]. Integrity between tiers 1 and 2 is limited to lightweight integrity designed for constrained device resources. There is a variety of lightweight integrity that varies according to hash functions and permeation size; some of them are described briefly below:

- Photon: is 256 bits hash function with permutation sizes up to 288 bits [40].
- Spongint: is 256 bits hash function with permutation sizes up to 272 bits [41].
- Lesamnta: is 256 bits hash function with permutation size 384 bits [42].

Between tiers 1 and 2, Public Key Infrastructure (PKI) can be used for medical data integrity but the requirements of key management and public keys distributions on large environments such as Medical IoT make it difficult to adopt. Thus, another promising choice is the use of blockchain technology to provide medical data integrity. Keyless Signature Infrastructure (KSI) provides integrity and identity associated with medical digital assets. By integrating KSI into healthcare systems, regardless of whether medical data is transmitted or stored, every medical device, system configuration, and digital health record can be verified. KSI hash is a one-way function such that there is no mathematical formula or process to recover the file from the hash. KSI forms a unique distributed database across the medical servers. Records can only be added to the database, never removed. The KSI Infrastructure consists of a distributed network of devices configured as cores, aggregators, and gateways. Hierarchical structure works as follows: low-level aggregation servers collect and process requests from clients and then send them to the upper level servers. Each server receives the request from the downstream server, adds them to the hash tree, and sends the local root hash to its preceding upstream server [43] [44] [45].

**Facet 3: Confidentiality:** Only authorized parties can explore the information, this can be achieved through the process of encryption involving encoding information into a new, ciphered form that can be understood only by authorized parties who have the secret key. An interceptor may illegally interfere with the information in unencrypted form. As with authentication, encryption takes place at two points: between tier 1 and tier 2 devices, and between tier 2 and tier 3 devices.

Encryption between tier 1 and tier 2 is limited to lightweight encryption protocols that offer a reasonable level of encryption while preserving the constrained device resources. There are a number of lightweight encryptions that vary according to data size, key size, and application. Some of them are briefly described below:

- 1) *Camellia*: Camellia block cipher has key sizes of 128-bit, 192-bit, and 256-bit, and can be implemented either by hardware or software [46].
- 2) *TWINE*: A Lightweight, Versatile Block Cipher, has key sizes of 80-bit and 128-bit, and can be implemented either by hardware or software [47].
- 3) *Trivium*: Hardware oriented synchronous stream ciphers with 80-bits key length [48].
- 4) *SIMON and SPECK*: are two families of block cipher with 80-bit, 96-bit, and 128-bit that are implemented on both hardware and software [49].
- 5) *PRESENT*: Block cipher with 80-bit and 128-bit key lengths. PRESENT is suitable for RFID tags and sensor networks [50].
- 6) *PICALO*: A block cipher that supports 80-bit and 128-bit keys. PICALO can be implemented in hardware and it is suitable for RFID tags and sensor networks [51].
- 7) *LEX*: A 128-bit key stream cipher. LEX is based on AES [52].
- 8) *LED*: 64-bit and 128-bit key block cipher encryption is based on AES and is dedicated for hardware implementation [53].
- 9) *CLEFIA*: a block cipher with 128-bit, 192-bit, and 256-bit key sizes, CLEFIA supports AES. [54]
- 10) *Enocoro*: 80-bit key stream cipher encryption dedicated to hardware implementation [55].

Regarding tier 2 and tier 3, any encryption protocol (either symmetric key or public key) could be used because there are no constrained resources. Some of encryption algorithms are Triple DES, RSA, Blowfish, AES, Elliptic curve, and more.

Another emerging category of encryption is the authenticated encryption that provides authentication besides message integrity; it consists of encrypting the plain text then computing the hash value. Authenticated encryption requires fewer resources than a serial operation of encrypt and authentication. Some of authenticated encryption schemes are:

- 1) *The Hummingbird-2*: An authenticated encryption algorithm that has a 128-bit key. Hummingbird-2 is a good choice for passive RFID systems [56].
- 2) *Phelix*: An authenticated encryption that combines stream cipher and MAC function. Phelix uses a 256-bit key [57].
- 3) *Fides*: A single pass block cipher authenticated encryption algorithm, FIDES uses either 80-bit or 96-bit keys [58].

4) *ACRON*: 128-bit authenticated encryption algorithm efficient in both hardware and software implementations [59].

5) *Grain-128a*: 128-bit stream authenticated encryption algorithm that uses non-linear functions of authentication and encryption [60].

6) *SCREAM and iSCREAM*: 128-bit tweakable block ciphers with authenticated encryption [61].

7) *ALE*: a 128-bit key based on AES, an online single-pass lightweight authenticated encryption that uses Nonces. [62]

8) *LAC*: 80-bit key block cipher authenticated encryption, and has a similar structure to ALE [63].

9) *ASC-1*: Stream cipher authenticated encryption with key size of 128-bit [64].

10) *Quark*: A family of lightweight authenticated encryption algorithms that support 256-bit key size, dedicated for constrained hardware security [65].

11) *Ascon*: A family of lightweight block cipher authenticated encryption algorithms that support key lengths of 96 and 128 bits. [66].

12) *Joltik*: 64-bit and 128-bit tweakable block cipher authenticated encryption algorithm [67].

13) *Ketje*: 182-bit cipher authentication and encryption algorithm based on sponge structure [68].

14) *Sablier*: 80 and 256 bits key authenticated encryption that is hardware-efficient [69].

**Facet 4: Possession or Control:** Medical records and data obtained by medical sensors, diagnoses, and laboratory tests are valuable because any breach can infringe upon patients' privacy. Rightful ownership of medical records varies from country to country. In the United States, there is no federal law regarding ownership of medical records; the Health Insurance Portability and Accountability Act (HIPAA) gives patients the right to access and modify their Medical records, but do not specify ownership of the medical records. In the United Kingdom, the Secretary of State for Health owns NHS's medical records. In Canada, the patient owns the information contained in the medical records, but the healthcare provider owns the records themselves [70] [71]. Broadly speaking, as no data is stored in the medical sensors located at tier 1, controlling data is the responsibility of the healthcare provider in tier 3.

**Facet 5: Utility or Usability:** ISO defines usability as "The extent to which a product can be used by specified users to achieve specified goals with effectiveness, efficiency, and satisfaction in a specified context of use" [72]. In tier 1, the medical device (or sensor) must have a measure or procedure to ensure that any health information or data (measured or collected) by it remains usable and useful across the lifetime

of the medical device, and can be transferred to any successor medical device(s) [32].

The international standard ISO/IEC 62366: Medical Devices Application of Usability Engineering to Medical Devices assures that medical device manufacturers follow a systematic usability process. Besides medical devices design, manufacture and development process manufacturers will need to change the way they design, manufacture, and develop in order to comply with the standard.

Some of the important usability concerns defined by the standard are:

1) The design and manufacture of the medical devices must assure that when it used under the intended purpose and under the suitable operating conditions, it will not harm the safety of patients. Moreover, this shall include:

a) Reducing the risk of use error due to the required levels of technical knowledge, experience, and training required to achieve the required operation of the device

b) Considering the physical conditions of intended patient (normal or disabled users)

2) The measurement, monitoring and display scale must be indicative, easy to understand and simple to use, while maintaining the intended purpose of the medical device

3) Operating instructions must avoid misuse for devices emitting radiation

4) Device instructions are in layman's terms easy to understand by patients [73] [74].

From the tier 3 prospective, usability of computer software and applications described in the ISO 9241 ISO/TR 16982:2002 standard that provides information on usability methods used for design and evaluation of any objects such as software, computer, tool, website, and process [75].

**Facets 6: Availability:** It is beneficial for any health service provider to affirm that health records are available to the authorized people at the proper time. Lack of availability could decrease the health service quality, and increase the risk of litigation for the health service provider.

Confidentiality, Authentication and Integrity of electronic health records are basic elements of availability. In addition, health care systems must have backup components, such as fault-tolerance systems. Thus, if a software or hardware component goes down or malfunctions, the system can switch to a backup component. Moreover, healthcare providers must apply ISO/IEC 24762:2008 standard guidelines for providing the provision of information and communications technology disaster recovery services to ensure business continuity [76] [77].

TABLE I. LAYERED NETWORK ARCHITECTURE AND ITS RELATION TO PARKERIAN HEXAD FACETS

| Facet  | Supporting Protocols/Standards  | Recommend implementation   | Network tier(s)   |
|--|---|--|---|
| Authentication                                       | <ol style="list-style-type: none"> <li>1. Lightweight Authentication protocols (LMAP, ALIKE, ELLIE ,IBS)</li> <li>2. PPP &amp; AAA authentication (PAP, CHAP, EAP, TACACS, RADIUS, Diameter and Kerberos)</li> </ol>                                      | LMAP, ALIKE, ELLIE ,IBS  | Between Tier1 & Tier2 devices<br>BetweenTier2/Tier3 devices     |
| Integrity  | <ol style="list-style-type: none"> <li>1. lightweight integrity: Photon, Spongent: Lesamnta:</li> <li>2. PKI and KSI</li> </ol>   | Photon, Spongent (approve by Lightweight Cryptography Working Group [37])                              | Between Tier1 & Tier2 devices<br>BetweenTier2/Tier3 devices     |
| Confidentiality                                      | <ol style="list-style-type: none"> <li>1. Lightweight encryption protocols: Camellia, TWINE, Trivium, SIMON, RESENT, PICALO,LEX, LED, CLEFIA, Enocoro</li> <li>2. Symmetric key or public key: Triple DES, RSA, Blowfish, AES, Elliptic curve.</li> </ol> | PRESENT, CLEFIA, SIMON and SPECK (all with key size of 128 bits minimum to meet NIST requirements)     | Between Tier1 & Tier2 devices<br>BetweenTier2/Tier3 devices     |
| Integrity/Confidentiality (authenticated encryption) | The Hummingbird-2, Phelix. Fides, ACRON, Grain-128a. SCREAM and iSCREAM, ALE, LAC, ASC-1, Quark , Ascon, Joltik, Ketje, Sablier:  | ALE: 128<br>Photon:<br>Quark<br>Grain-128a<br>(approve by Lightweight Cryptography Working Group [37]) | Between Tier1 & Tier2 devices                                   |
| Possession or Control                                | Possession of medical sensors and devices plus medical records.<br>Possession of health records and data  |  | Tier 1 Devices<br>Tier3 component and devices                   |
| Utility  | Comply with (ISO/IEC 62366)<br>ISO/TR 16982:2002 standard   |  | Tier 1 devices<br>Tier 3 network components and devices         |
| Availability   | ISO/IEC 62366<br>Comply with ISO/IEC 24762:2008   |  | Tier 1 devices<br>Tier2 & Tier 3 network components and devices |

## V. CONCLUSIONS

Advances in mobile devices, medical sensors, and IoT technologies are expected to provide revolutionary innovations in healthcare. However, connecting devices that collect data from patients to wide network are vulnerable to unauthorized access, and patient data must be protected. Therefore, Medical IoT (MIoT) must take in consideration data security and privacy when collecting data and sending data from a device to another.

This paper proposes 3-tier architecture to ease the process of transmitting, storing, and transferring medical data. The lowest layer in the architecture, tier 1, it consists of sensors and devices collecting data from the patient. The middle layer, tier 2, includes smart devices and wireless access points. The last layer, tier 3, contains the servers maintaining healthcare databases.

In order to handle the security issues in the architecture, the architecture is based on the Parkerian Hexad model, which adds three levels of security to the traditional CIA Triad to address the special requirements of health records and data. Sets of algorithms were investigated to recommend the appropriate security level for each layer in the architecture based on capabilities of the devices in that layer to maintain

the QoS since the devices have different capabilities in each layer in terms of processing, memory, and power. Table I summarizes those algorithms and recommends the appropriate algorithm in each tier according to Parkerian Hexad model.

Some of the limitations of the study are concerning patient safety and privacy. In addition, more details of the proposed framework needs to be studied in the future.

## REFERENCES

- [1] S. Brave and A. Dahley, "inTouch: a medium for haptic interpersonal communication," in CHI'97 Extended Abstracts on Human Factors in Computing Systems, 1997.
- [2] K. Ashton, "That 'internet of things' thing," RFID journal, vol. 22, no. 7, pp. 97-114, 2009.
- [3] D. V. Dimitrov, "Medical internet of things and big data in healthcare," Healthcare informatics research, vol. 22, no. 3, pp. 156-163, 2016.
- [4] H. Banaee, M. Ahmed and A. Loutfi, "Data mining for wearable sensors in health monitoring systems: a review of recent trends and challenges," Sensors, vol. 13, no. 12, pp. 17472-17500, 2013.
- [5] A. Pantelopoulos and N. G. Bourbakis, "A survey on wearable sensor-based systems for health monitoring and prognosis," IEEE Transactions on Systems, Man, and Cybernetics, Part C (Applications and Reviews), vol. 40, no. 1, pp. 1-12, 2010.
- [6] K. Zeitz and H. McCutcheon, "Observations and vital signs: ritual or vital for the monitoring of postoperative patients?," Applied Nursing Research, vol. 19, no. 4, pp. 204-211, 2006.

- [7] R. Das, A. Tuna, S. Demirel, K. NETAS AS and M. K. Yurdakul, "A Survey on the internet of things solutions for the elderly and disabled: applications, prospects, and challenges," *International Journal of Computer Networks and Applications*, vol. 4, no. 3, pp. 1-9, 2017.
- [8] C. Li, X. Hu and L. Zhang, "The IoT-based heart disease monitoring system for pervasive healthcare service," *Procedia Computer Science*, vol. 112, pp. 2328-2334, 2017.
- [9] B. Singh, S. Bhattacharya, C. L. Chowdhary and D. S. Jat, "A review on internet of things and its applications in healthcare," *Journal of Chemical and Pharmaceutical Sciences*, vol. 10, no. 1, pp. 447-452, 2017.
- [10] E. Rich and A. Miah, "Mobile, wearable and ingestible health technologies: towards a critical research agenda," *Health sociology review*, vol. 26, no. 1, pp. 84-97, 2017.
- [11] P. Belluck, "First Digital Pill Approved to Worries About Biomedical 'Big Brother'," *New York Times*, 2017.
- [12] A. J. Jara, F. J. Belchi, A. F. Alcolea, J. Santa, M. A. Zamora-Izquierdo and A. F. Gómez-Skarmeta, "A Pharmaceutical Intelligent Information System to detect allergies and Adverse Drugs Reactions based on internet of things," in *Pervasive Computing and Communications Workshops (PERCOM Workshops)*, 2010 8th IEEE International Conference on, 2010.
- [13] M. Kang, E. Park, B. H. Cho and K.-S. Lee, "Recent patient health monitoring platforms incorporating internet of things-enabled smart devices," *International neurourology journal*, vol. 22, no. Suppl 2, p. S76, 2018.
- [14] V. Kalaiselvan, P. Kumar, P. Mishra and G. Singh, "System of adverse drug reactions reporting: What, where, how, and whom to report?," *Indian Journal of Critical Care Medicine*, vol. 19, no. 9, p. 564, 2015.
- [15] M. A. Ward, M. L. Schweizer, P. M. Polgreen, K. Gupta, H. S. Reisinger and E. N. Perencevich, "Automated and electronically assisted hand hygiene monitoring systems: a systematic review," *American journal of infection control*, vol. 42, no. 5, pp. 472-478, 2014.
- [16] U. Lindqvist and P. G. Neumann, "The future of the Internet of Things," *Communications of the ACM*, vol. 60, no. 2, pp. 26-30, 2017.
- [17] U. K. Anaesthesia, "Principles of pulse oximetry," *Anaesthesia UK*, 2004.
- [18] R. Rutherford, "Internet of Things—striking the balance between competition and security," *Network Security*, vol. 2019, no. 2, pp. 6-8, 2019.
- [19] D. Salvi, E. V. Mora and M. T. A. Waldmeyer, "An architecture for secure e-Health systems," *Universidad Politecnica de Madrid, Spain*, vol. 1, pp. 2-4, 2010.
- [20] D. Lake, R. M. R. Milito, M. Morrow and R. Vargheese, "Internet of things: Architectural framework for ehealth security," *Journal of ICT Standardization*, vol. 1, no. 3, pp. 301-328, 2014.
- [21] P. Gope and T. Hwang, "BSN-Care: A secure IoT-based modern healthcare system using body sensor network," *IEEE Sensors Journal*, vol. 16, no. 5, pp. 1368-1376, 2016.
- [22] S. Khoja, H. Durrani, R. E. Scott, A. Sajwani and U. Piryani, "Conceptual framework for development of comprehensive e-health evaluation tool," *Telemedicine and e-Health*, vol. 19, no. 1, pp. 48-53, 2013.
- [23] F. Rezaeibagha, K. T. Win and W. Susilo, "A systematic literature review on security and privacy of electronic health record systems: technical perspectives," *Health Information Management Journal*, vol. 44, no. 3, pp. 23-38, 2015.
- [24] W. Leister, M. Hamdi, H. Abie and S. Poslad, "An evaluation framework for adaptive security for the iot in ehealth," *International Journal on Advances*, 2014.
- [25] O. Olakanmi, I. Kamil and S. Ogundoyin, "Secure and privacy-preserving referral framework for e-health system," *Internal Journal of Information Science*, vol. 6, no. 2, pp. 11-25, 2017.
- [26] D. Y. Weider, L. Davuluri, M. Radhakrishnan and M. Runiassy, "A security oriented design (SOD) framework for ehealth systems," in *2014 IEEE 38th International Computer Software and Applications Conference Workshops*, 2014.
- [27] D. P. Mirembe, "Design of a secure framework for the implementation of telemedicine, eHealth, and wellness services," 2006.
- [28] B. Ondiege, M. Clarke and G. Mapp, "Exploring a new security framework for remote patient monitoring devices," *Computers*, vol. 6, no. 1, p. 11, 2017.
- [29] B. Mozzaquatro, C. Agostinho, D. Goncalves, J. Martins and R. Jardim-Goncalves, "An Ontology-Based Cybersecurity Framework for the Internet of Things," *Sensors*, vol. 18, no. 9, p. 3053, 2018.
- [30] H. Mora, D. Gil, R. M. Terol, J. Azorín and J. Szymanski, "An IoT-based computational framework for healthcare monitoring in mobile environments," *Sensors*, vol. 17, no. 10, p. 2302, 2017.
- [31] L. Catarinucci, D. De Donno, L. Mainetti, L. Palano, L. Patrono, M. L. Stefanizzi and L. Tarricone, "An IoT-aware architecture for smart healthcare systems," *IEEE Internet of Things Journal*, vol. 2, no. 6, pp. 515-526, 2015.
- [32] Richard Piggin, "Cybersecurity of medical devices," 2017.
- [33] M. Al Ameen, J. Liu and K. Kwak, "Security and privacy issues in wireless sensor networks for healthcare applications," *Journal of medical systems*, vol. 36, no. 1, pp. 93-101, 2012.
- [34] W. H. Organization, S. P. f. Research, T. i. T. Diseases, W. H. O. D. o. C. o. N. T. Diseases, W. H. O. Epidemic and P. Alert, *Dengue: guidelines for diagnosis, treatment, prevention and control*, World Health Organization, 2009.
- [35] P. Peris-Lopez, J. C. Hernandez-Castro, J. M. Estévez-Tapiador and A. Ribagorda, "LMAP: A real lightweight mutual authentication protocol for low-cost RFID tags," in *Proc. of 2nd Workshop on RFID Security*, 2006.
- [36] Sandrine Agagliate, "ALIKE: Authenticated Lightweight Key Exchange," 2010.
- [37] K. McKay, L. Bassham, M. Sönmez Turan and N. Mouha, "Report on lightweight cryptography," *National Institute of Standards and Technology*, 2016.
- [38] D. Galindo and F. D. Garcia, "A schnorr-like lightweight identity-based signature scheme," in *International Conference on Cryptology in Africa*, 2009.
- [39] M. N. Aman, B. Sikdar, K. C. Chua and A. Ali, "Low Power Data Integrity in IoT Systems," *IEEE Internet of Things Journal*, 2018.
- [40] J. Guo, T. Peyrin and A. Poschmann, "The PHOTON family of lightweight hash functions," in *Annual Cryptology Conference*, 2011.
- [41] A. Bogdanov, M. Knežević, G. Leander, D. Toz, K. Varıcı and I. Verbauwhede, "SPONGENT: A lightweight hash function," in *International Workshop on Cryptographic Hardware and Embedded Systems*, 2011.
- [42] S. Hirose, K. Ideguchi, H. Kuwakado, T. Owada, B. Preneel and H. Yoshida, "A lightweight 256-bit hash function for hardware and low-end devices: lesamnta-LW," in *International Conference on Information Security and Cryptology*, 2010.
- [43] A. Buldas, A. Kroonmaa and R. Laanoja, "Keyless Signatures' Infrastructure: how to build global distributed hash-trees," in *Nordic Conference on Secure IT Systems*, 2013.
- [44] A. Buldas, R. Laanoja and A. Truu, "Keyless signature infrastructure and PKI: hash-tree signatures in pre-and post-quantum world," *International Journal of Services Technology and Management*, vol. 23, no. 1-2, pp. 117-130, 2017.
- [45] J. M. Roman-Belmonte, H. De la Corte-Rodriguez and E. C. Rodriguez-Merchan, "How blockchain technology can change medicine," *Postgraduate medicine*, vol. 130, no. 4, pp. 420-427, 2018.
- [46] J. Nakajima and S. Moriai, *A Description of the Camellia encryption Algorithm*, Aug, 2000.
- [47] T. Suzaki, K. Minematsu, S. Morioka and E. Kobayashi, "Twine: A lightweight, versatile block cipher," in *ECRYPT Workshop on Lightweight Cryptography*, 2011.
- [48] C. De Canniere and B. Preneel, "Trivium," in *New Stream Cipher Designs*, Springer, 2008, pp. 244-266.
- [49] R. Beaulieu, S. Treatman-Clark, D. Shors, B. Weeks, J. Smith and L. Wingers, "The SIMON and SPECK lightweight block ciphers," in *Design Automation Conference (DAC)*, 2015 52nd ACM/EDAC/IEEE, 2015.

- [50] A. Bogdanov, L. R. Knudsen, G. Leander, C. Paar, A. Poschmann, M. J. B. Robshaw, Y. Seurin and C. Vikkelsoe, "PRESENT: An ultra-lightweight block cipher," in International Workshop on Cryptographic Hardware and Embedded Systems, 2007.
- [51] K. Shibutani, T. Isobe, H. Hiwatari, A. Mitsuda, T. Akishita and T. Shirai, "Piccolo: an ultra-lightweight blockcipher," in International Workshop on Cryptographic Hardware and Embedded Systems, 2011.
- [52] A. Biryukov, "A new 128-bit key stream cipher LEX," eSTREAM, ECRYPT Stream Cipher Project, Report, vol. 13, p. 2005, 2005.
- [53] M. R. Jian Guo, Thomas Peyrin, Axel Poschmann, "The LED Block Cipher," in Selected Areas in cryptography , 2011.
- [54] T. Shirai, K. Shibutani, T. Akishita, S. Moriai and T. Iwata, "The 128-bit blockcipher CLEFIA," in International Workshop on Fast Software Encryption, 2007.
- [55] D. Watanabe, K. Ideguchi, J. Kitahara, K. Muto, H. Furuichi and T. Kaneko, "Enocoro-80: A hardware oriented stream cipher," in The Third International Conference on Availability, Reliability and Security, 2008.
- [56] D. Engels, M.-J. O. Saarinen, P. Schweitzer and E. M. Smith, "The Hummingbird-2 lightweight authenticated encryption algorithm," in International Workshop on Radio Frequency Identification: Security and Privacy Issues, 2011.
- [57] D. Whiting, B. Schneier, S. Lucks and F. Muller, "Fast encryption and authentication in a single cryptographic primitive," ECRYPT Stream Cipher Project Report, vol. 27, no. 200, p. 5, 2005.
- [58] B. Bilgin, A. Bogdanov, M. Knežević, F. Mendel and Q. Wang, "Fides: Lightweight authenticated cipher with side-channel resistance for constrained hardware," in International Workshop on Cryptographic Hardware and Embedded Systems, 2013.
- [59] P. Dey, R. S. Rohit and A. Adhikari, "Full key recovery of ACORN with a single fault," Journal of Information Security and Applications, vol. 29, pp. 57-64, 2016.
- [60] M. ? gren, M. Hell, T. Johansson and W. Meier, "Grain-128a: a new version of Grain-128 with optional authentication," International Journal of Wireless and Mobile Computing, vol. 5, no. 1, pp. 48-59, 2011.
- [61] V. Grosso, G. Leurent, F.-X. Standaert, K. Varici, F. Durvaux, L. Gaspar and S. Kerckhof, "SCREAM & iSCREAM side-channel resistant authenticated encryption with masking," Submission to CAESAR, 2014.
- [62] J. Jean, T. Peyrin, S. M. Sim and J. Tourteaux, "Optimizing implementations of lightweight building blocks," IACR Transactions on Symmetric Cryptology, vol. 2017, no. 4, pp. 130-168, 2017.
- [63] L. Zhang, W. Wu, Y. Wang, S. Wu and J. Zhang, "LAC: A lightweight authenticated encryption cipher," Submitted to the CAESAR competition, 2014.
- [64] G. Jakimoski and S. Khajuria, "ASC-1: an authenticated encryption stream cipher," in International Workshop on Selected Areas in Cryptography, 2011.
- [65] J.-P. Aumasson, L. Henzen, W. Meier and M. Naya-Plasencia, "Quark: A lightweight hash," in International Workshop on Cryptographic Hardware and Embedded Systems, 2010.
- [66] C. Dobraunig, M. Eichlseder, F. Mendel and M. Schläffer, "Ascon v1. 2," Submission to the CAESAR Competition, 2016.
- [67] J. Jean, I. Nikolić and T. Peyrin, "Joltik v1. 3," CAESAR Round, vol. 2, 2015.
- [68] G. Bertoni, J. Daemen, M. Peeters, G. Van Assche and R. Van Keer, "CAESAR submission: Ketje v1, March 2014," URL <http://ketje.noekeon.org/Ketje-1.1.pdf>. [cited at p. 44, 48, 49, and 67].
- [69] B. Zhang, Z. Shi, C. Xu, Y. Yao and Z. Li, "Sablier v1," Candidate for the CAESAR Competition. See also <https://competitions.cr.yp.to/round1/sablierv1.pdf>, 2014.
- [70] K. Judson, "Law & ethics for medical careers," 2002.
- [71] D. A. Grant, "MDs still confused about patient access to medical records," CMAJ: Canadian Medical Association Journal, vol. 158, no. 9, p. 1126, 1998.
- [72] I. I. O. f. Standardization, ISO/TS 20282-2: 2013 (en). Usability of consumer products and products for public use—Part 2: Summative test method, 2013.
- [73] P. Hodgson, "Usability for medical devices: A new international standard," URL <http://www.userfocus.co.uk/articles/ISO62366.html>, 2010.
- [74] M. E. Wiklund, J. Kendler and A. Y. Strohlic, Usability testing of medical devices, CRC press, 2015.
- [75] N. Bevan, "Guidelines and standards for web usability," in Proceedings of HCI international, 2005.
- [76] A. Tsohou, S. Kokolakis, C. Lambrinouidakis and S. Gritzalis, "Information systems security management: a review and a classification of the ISO standards," in International Conference on e-Democracy, 2009.
- [77] N. Innab, "Availability, Accessibility, Privacy and Safety Issues Facing Electronic Medical Records".



# Two Dimensional Electronic Nose for Vehicular Central Locking System (E-Nose-V)

Mahmoud Zaki Iskandarani

Faculty of Engineering, Al-Ahliyya Amman University, Amman, Jordan

**Abstract**—A new approach to vehicle security is proposed, tried, tested. The designed and tested system comprises an odor detection system (E-Nose) that sends signals corresponding to selected odors to the smart vehicle Electronic Control Unit (ECU), which is interfaced to a smart system with neural networks. The signal is interpreted in time and space, whereby a certain ordered number of samples should be obtained before the vehicle functions are unlocked. Correlation of rise and decay times and amplitudes of the signal is carried out to ensure security. The proposed system is highly secured and could be further developed to become a vital and integrated part of Intelligent Transportation Systems (ITS) through the addition of driver's body odor smell as an extra measure of security and in cases of accidents to auto call emergency services with driver identification and some diagnostics. Such system can be utilized in smart cities.

**Keywords**—Odors; E-Nose; neural networks; security; correlation; smart vehicles; intelligent transportation systems; smart cities

## I. INTRODUCTION

An E-nose is generally recognized as a device that encompasses array of electrochemical sensors with specification capabilities and adaptable pattern recognition system, able to classify individual vapors components or combination of vapors. An electronic nose recognizes an odor through fingerprinting of its chemical elements using an array of sensors backed by intelligent software for pattern recognition. Such technology is already in use across many industries, including agricultural, environmental, food, manufacturing, and the military. Also, E-Noses are increasingly playing an important role in disease detection such as diabetes by means of blood sniffing and can detect lung diseases through sucking up vapors and sniffing the breath [1-5].

The E-Nose is a modular sensor system made for detection of odors, odor mixtures, aromas, and gaseous substances in both open and closed environments. It uses chemical sensors for detection and artificial intelligence for treatment of the measured data. Such a device is regarded as fingerprint one that analyze the odor as a whole. By processing the obtained fingerprint of the odor, that constituent substance(s) would be recognized and classified. Such functionality is important in many quality and security control systems [6-10].

There are two main components in the E-Nose; the sensing part and the intelligent pattern recognition part. The combination of broad sensing elements coupled with intelligent information processing algorithms makes the E-Nose such a

promising tool for odor related applications. The sensing part comprises an array of chemical sensing elements with each sensing element capable of measuring a different part of the odor spectrum. Each odorant produces a unique characteristic (signature) of its own, once exposed to the sensing array. By presenting many different odorants to the sensor array, a database is built up. This database of odorants with each odorant unique characteristics is used to train an intelligent classification system, such as Neural Networks [11-20].

The way E-noses sense odorant molecules is similar to human olfactory system. The odors interact with a responsive materials making up the sensor array, resulting in a change in the material characteristics and producing a unique response related to the specific smelled odorant. The software processes the obtained signals, and filter out unnecessary information and performs pattern recognition. Some commonly used sensing materials are: metal oxides, conducting polymers and composites. Pattern recognition can be successfully performed using an Artificial Neural Networks (ANN) algorithm.

ANN is a learning and classification algorithm which is based on operation of the human brain. It deduces meaning from the data which is complex or difficult to mathematically represent in order to identify patterns and enable decision making. Weight Elimination Algorithm (WEA) is based on Backpropagation (BP) algorithm, which is an iterative gradient algorithm aims at decreasing the root mean square error. Input and output layers are interconnected through hidden layers.

Traditionally, systems are vulnerable to those armed with the right equipment and willing to intrude. Sometimes passwords are unchanged and left as the default ones. Access to these gives the power to the fraudster's to hack. The power of neural network- odor sensing based technology together with the traditional strengths of conventional rules-based fraud detection technologies is a crucial and very effective solution to intrusion, as adaptive neural analysis techniques allow high levels of security; while conventional rules-based technologies provide a high level of detail [21-30].

In this paper, a fresh approach to the use and application of E-Nose system is proposed which utilizes odor sensing together with artificial neural networks interfaced to the ECU of the vehicle. Such approach will support both driver and vehicle functionality in terms of driver identification for secure access and mobility. The system can be further developed to support driver health and status monitoring while driving and driver vanning, support and intervention under critical conditions if integrated with other vehicular systems and interfaced to wireless communication systems.

## II. RELATED WORK

The last few years seen a rapid development of Intelligent Transportation Systems (ITS), Intelligent Vehicles and Vehicular Ad Hoc Network (VANET) with the tendency to change the way we drive by providing a safe, secure, and reliable ubiquitous computing systems capable of covering many roads.

Due to the advancement in electronics and its interface and integrated into the automotive industry and modern transportation, there has been a marked change in road vehicle technology. In smart vehicles there are over 90 devices equivalent to microcomputers placed in each smart vehicle, which provide services to drivers by controlling vehicle operation, comfort, support, security and safety. Electronic devices are used control almost every function inside the vehicle and supervise complex and complicated.

An intelligent or smart vehicle, is a vehicle that is capable of sensing its environment by combining a variety of sensor inputs, such as Radio Detection And Ranging (RADAR), LIDAR Light Detection And Ranging (LIDAR), Global Positioning Systems (GPS), Computer vision devices such as Cameras, and other safety, mobility, comfort, and security related applications. Such applications are performed through continuous monitoring of the performance and status of the vehicle and driver. Such sensors can be classified under different categories such as; safety sensors, diagnostics sensors, multimedia and comfort sensors, environmental sensors, driver/driving monitoring sensors, and traffic monitoring sensors. There is no doubt that intelligent or smart vehicles will play a central role in personal mobility, driver safety and vehicle security in the future. Highly automated driving systems will relieve the drivers from stressing tasks ensuring safer and sustainable mobility [31].

Three main operational levels of sensor based electronic computing systems are realized within an intelligent vehicle system [32]:

- 1) Warning: To inform the driver about potentially dangerous situations without support or intervention.
- 2) Support: To inform and support the driver and provide guidance in facing a risky and threatening situation.
- 3) Intervention: An automated intervention into the vehicle control is carried out at this level.

In intelligent vehicles, the objective is to fuse and aggregate data from different sensors according to the following criteria:

- a) Data source.
- b) Data type.
- c) Data architecture.
- d) Data level of abstraction.

Data type and sources are critical in facing many challenges related to transportation systems, such as smooth integration independent data sources in real-time to meet requirements.

Data integration techniques must be integrated with Artificial Intelligence algorithms (AI) to allow the vehicle to

understand the current state similar to human understanding and interpretation, and to react accordingly.

The privacy and security of vehicles highly depend on reducing intrusiveness by including security and privacy protocols into the communication devices that are supported by the communication networks to protect drivers, vehicles, passengers, and passengers within the vehicular network environment. Hackers have penetrated, modified, corrupted or taken control of vehicle systems through sensors monitoring systems and internal and external vehicle communication systems. Threats exist to identity data in vehicles with intrusion with malicious intent. In-vehicle software can have millions of lines of code which executes on both the primary computer board(s) and over 80 microprocessor-based electronic control units (ECUs) networked throughout the body of the car [33-43].

It is envisaged in this work that it could be very useful to produce mobile E-Noses that could also be mounted within a vehicular structure (On Board Units OBU), which is interfaced to the rest of the vehicle via an ECU unit and can work in collaboration with the rest of the vehicle sensory system. An E-nose device attached to an intelligent car is considered a sensory source similar to on board cameras, radar and other sensor data sources, which all need specialized software for data collection and interpretation. Adding E-noses to the system of available sensors will lead to improvement of the overall security model on the three mentioned operational levels of the vehicle computing system aiding in both driver identification, health diagnostics such as stress levels, heart attacks, accidents, and vehicle security.

## III. MATERIALS AND METHODS

Three Odor keys are inserted and form a complex odor key by combining the sequential sampling of the three separate odor keys into one correlated odor key. The odor detection system employs Figaro TGS (Metal Oxide Semiconductor) Sensors shown in Fig. 1. The keys inserted in a certain order as an extra measure of security. The sampling process is shown in Fig. 2. The system will sample the odor keys until it returns back to its original base signal after completing three-key scan, before unlocking.

Weight Elimination Algorithm (WEA) is used to carry out training of the Neural Networks system in order to enable unlocking and locking of the vehicle as shown in Fig. 3.

WEA works by minimizing a modified error function which is formed by adding an overhead term to the original error function used in the algorithm. The overhead variable in weight decay applies cost values to large weights, hence, causes weights under consideration to converge to smaller absolute values. Large weights can adversely affect generalization according to their position in the network. When large weight values lie between input layer and hidden layer, they affect smoothness of the output function, with possible near discontinuities. However, if they lie between the hidden layer and the output layer, they can lead to out of range outputs. Hence, large weights can cause excessive variation in the output and instability of the neural structure, as their values and instability will be outside the range of the output activation

function. Weights size is critical and in some cases will have marked effect in determining generalization.



Fig. 1. Figrao TGS (MOS) Sensor.

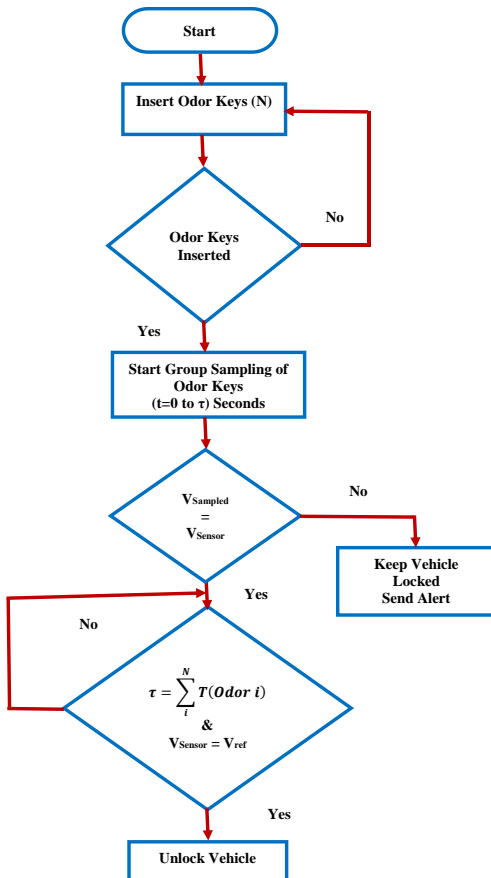


Fig. 2. Odor Key Unlocking System

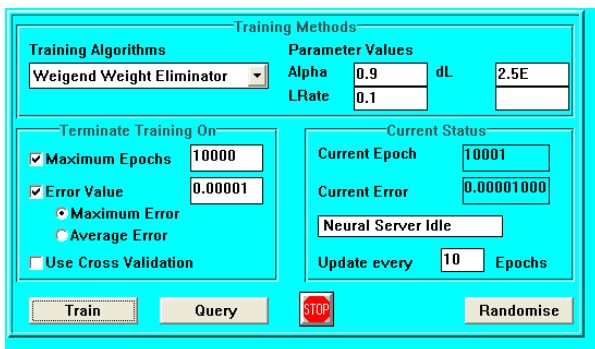


Fig. 3. Neural Networks (WEA) Training System

Weight elimination describes the dynamic changes in neural network convergence through error functions. The overall weight elimination error function is shown in equation (1):

$$E_{WE} = E_{Initial} + E_{Overhead} \quad (1)$$

Where;

$$E_{initial} = \frac{1}{2} \sum_k (d_k - o_k)^2 \quad (2)$$

$$E_{Overhead} = \beta \left( \sum_{jk} \frac{\left( \frac{w_{jk}}{w_N} \right)^2}{1 + \left( \frac{w_{jk}}{w_N} \right)^2} \right) \quad (3)$$

Where;

$E_{WE}$  : The combined overhead function that includes the initial overhead function,  $E_{Initial}$  and the weight-elimination term  $E_{Overhead}$ .

$\beta$  : The weight-reduction factor,

$w_{jk}$  : Represents the individual weights of the neural network model

$w_N$  : A scale parameter computed by the WEA.

$d_k$  : The desired Output.

$o_k$  : The actual Output.

The dynamic weight changes is calculated as shown in equation (4)

$$\Delta w_{jk} = \left( -\alpha \frac{\partial E_{Initial}}{\partial w_{jk}} \right) - \left( \beta \frac{\partial E_{Overhead}}{\partial w_{jk}} \right) \quad (4)$$

Where;

$\alpha$  : The Learning Rate (between 0 and 1)

The parameter,  $w_N$ , is a scale parameter computed by the WEA, and selected to be the smallest weight from the last epoch or set of epochs to converge small weights to zero.  $w_N$  plays a fundamental role so that the network will converge with either small number of large weights or large number of small weights.

#### IV. RESULTS

Tables I to III show the used odor keys used in validating the designed system, while Fig. 4 shows the Neural Network model used for training with distributed weights.

TABLE I. USED ODOR KEY 1

| Odor Key 1              |              |
|-------------------------|--------------|
| Response Time (Seconds) | VSensor/VRef |
| 0                       | 1            |
| 1                       | 1.3          |
| 2                       | 1            |

TABLE II. USED ODOR KEY 2

| Odor Key 2              |              |
|-------------------------|--------------|
| Response Time (Seconds) | VSensor/VRef |
| 0                       | 1            |
| 1                       | 1.4          |
| 2                       | 2.6          |
| 3                       | 2.7          |
| 4                       | 2.55         |
| 5                       | 1.9          |
| 6                       | 1.6          |
| 7                       | 1.4          |
| 8                       | 1.25         |
| 9                       | 1            |

TABLE III. USED ODOR KEY 3

| Odor Key 3              |              |
|-------------------------|--------------|
| Response Time (Seconds) | VSensor/VRef |
| 0                       | 1            |
| 1                       | 1.3          |
| 2                       | 2            |
| 3                       | 3.2          |
| 4                       | 3.7          |
| 5                       | 3.7          |
| 6                       | 3.7          |
| 7                       | 3.7          |
| 8                       | 3.7          |
| 9                       | 2.7          |
| 10                      | 2            |
| 11                      | 1.8          |
| 12                      | 1.6          |
| 13                      | 1.5          |
| 14                      | 1.4          |
| 15                      | 1.25         |
| 16                      | 1.1          |
| 17                      | 1.05         |
| 18                      | 1            |

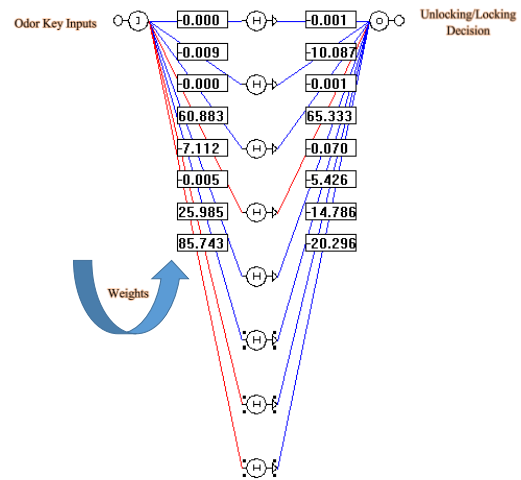


Fig. 4. Neural Networks Model used for Training and Decision Making.

#### V. ANALYSIS AND DISCUSSION

Fig. 5 shows the signal characteristics of odor coded key, which consists of three separate odor keys combined.



Fig. 5. Used Odor Coded Key in System Testing.

Table IV shows used training Odor keys data for the Neural Networks model shown in Fig. 4, while Table V shows the testing results of the Neural System assuming the correct Odor Keys are used.

Tables VI and VII shows testing data obtained as a result of incorrect odor keys 2 and 3 with Table VIII and Fig. 6 showing areas of pattern change and difference between correct and incorrect odor keys.

As the sampled odor keys that form the complex odor key change in pattern, the inputs to the neural network will change, causing a different actual output which when compared with desired output will result in a unique value that causes the system to stop sampling and raise an alarm and send an alert to the vehicle owner that an unauthorized key is being used. The vehicle system will stay locked and a time stamp will register the date and time the incident occurred.

Under normal operating conditions, the sampling system should fulfill both time cycle scanning, amplitude cycle scanning, and order cycle scanning to allow unlocking of the vehicle and its functions, hence, the result is a three dimensional function as prescribed by equation (5).

$$f_{unlocking} = f(\text{time, amplitude, position}). \quad (5)$$

TABLE IV. ODOR KEYS TRAINING DATA

| Training Data Set {Odor 1, Odor 2, Odor 3} |                                  |                                   |
|--|----------------------------------|-----------------------------------|
| Response Time (Seconds)                    | Training Data Input VSensor/VRef | Training Data Output VSensor/VRef |
| 0  | 1                                | 0                                 |
| 1  | 1.3                              | 1                                 |
| 2  | 1                                | 0                                 |
| 3  | 1                                | 0                                 |
| 4  | 1.4                              | 1                                 |
| 5  | 2.6                              | 1                                 |
| 6  | 2.7                              | 1                                 |
| 7  | 2.55                             | 1                                 |
| 8  | 1.9                              | 1                                 |
| 9  | 1.6                              | 1                                 |
| 10   | 1.4                              | 1                                 |
| 11   | 1.25                             | 1                                 |
| 12   | 1                                | 0                                 |
| 13   | 1                                | 0                                 |
| 14   | 1.3                              | 1                                 |
| 15   | 2                                | 1                                 |
| 16   | 3.2                              | 1                                 |
| 17   | 3.7                              | 1                                 |
| 18   | 3.7                              | 1                                 |
| 19   | 3.7                              | 1                                 |
| 20   | 3.7                              | 1                                 |
| 21   | 3.7                              | 1                                 |
| 22   | 2.7                              | 1                                 |
| 23   | 2                                | 1                                 |
| 24   | 1.8                              | 1                                 |
| 25   | 1.6                              | 1                                 |
| 26   | 1.5                              | 1                                 |
| 27   | 1.4                              | 1                                 |
| 28   | 1.25                             | 1                                 |
| 29   | 1.1                              | 1                                 |
| 30   | 1.05                             | 1                                 |
| 31   | 1                                | 0                                 |

TABLE V. ODOR KEYS TESTING DATA: CORRECT KEYS

| Testing Data Set 1 {Odor 1, Odor 2, Odor 3} |                                 |                                  |                |
|---|---------------------------------|----------------------------------|----------------|
| Response Time (Seconds)                     | Testing Data Input VSensor/VRef | Testing Data Output VSensor/VRef | Rounded Output |
| 0   | 1                               | 0                                | 0              |
| 1   | 1.3                             | 1.00197                          | 1              |
| 2   | 1                               | 0.00006                          | 0              |
| 3   | 1                               | 0.00006                          | 0              |
| 4   | 1.4                             | 1.00197                          | 1              |
| 5   | 2.6                             | 0.99917                          | 1              |
| 6   | 2.7                             | 0.99959                          | 1              |
| 7   | 2.55                            | 0.99943                          | 1              |
| 8   | 1.9                             | 0.99987                          | 1              |
| 9   | 1.6                             | 0.99917                          | 1              |
| 10  | 1.4                             | 1.00197                          | 1              |
| 11  | 1.25                            | 0.99788                          | 1              |
| 12  | 1                               | 0.00006                          | 0              |
| 13  | 1                               | 0.00006                          | 0              |
| 14  | 1.3                             | 1.00197                          | 1              |
| 15  | 2                               | 0.99877                          | 1              |
| 16  | 3.2                             | 1.00003                          | 1              |
| 17  | 3.7                             | 1.00045                          | 1              |
| 18  | 3.7                             | 1.00045                          | 1              |
| 19  | 3.7                             | 1.00045                          | 1              |
| 20  | 3.7                             | 1.00045                          | 1              |
| 21  | 3.7                             | 1.00045                          | 1              |
| 22  | 2.7                             | 0.99959                          | 1              |
| 23  | 2                               | 0.99877                          | 1              |
| 24  | 1.8                             | 0.99862                          | 1              |
| 25  | 1.6                             | 0.99917                          | 1              |
| 26  | 1.5                             | 1.00021                          | 1              |
| 27  | 1.4                             | 1.00197                          | 1              |
| 28  | 1.25                            | 0.99788                          | 1              |
| 29  | 1.1                             | 1.00180                          | 1              |
| 30  | 1.05                            | 0.99867                          | 1              |
| 31  | 1                               | 0.00006                          | 0              |

TABLE VI. ODOR KEYS TESTING DATA-CHANGE IN ODOR KEY 2

| Testing Data Set 2 {Odor 1, Odor 2, Odor 3}<br>Incorrect Odor Key 3 |                                 |   |                |
|---|---------------------------------|---|----------------|
| Response Time (Seconds)   | Testing Data Input VSensor/VRef | Actual Testing Data Output VSensor/VRef | Rounded Output |
| 0   | 1                               | 0                                       | 0              |
| 1   | 1.3                             | 1.00197                                 | 1              |
| 2   | 1                               | 0.00006                                 | 0              |
| 3   | 1                               | 0.00006                                 | 0              |
| 4   | 1.4                             | 1.00197                                 | 1              |
| 5   | 0.6                             | -0.09999                                | 0              |
| Time Stamp  | Stop Sampling and Send Alert    |   |                |

TABLE VII. ODOR KEYS TESTING DATA-CHANGE IN ODOR KEY 3

| Testing Data Set 3 {Odor 1, Odor 2, Odor 3}<br>Incorrect Odor Key 3 |                                 |   |                |
|---|---------------------------------|---|----------------|
| Response Time (Seconds)   | Testing Data Input VSensor/VRef | Actual Testing Data Output VSensor/VRef | Rounded Output |
| 0   | 1                               | 0                                       | 0              |
| 1   | 1.3                             | 1.00197                                 | 1              |
| 2   | 1                               | 0.00006                                 | 0              |
| 3   | 1                               | 0.00006                                 | 0              |
| 4   | 1.4                             | 1.00197                                 | 1              |
| 5   | 2.6                             | 0.99917                                 | 1              |
| 6   | 2.7                             | 0.99959                                 | 1              |
| 7   | 2.55                            | 0.99943                                 | 1              |
| 8   | 1.9                             | 0.99987                                 | 1              |
| 9   | 1.6                             | 0.99917                                 | 1              |
| 10  | 1.4                             | 1.00197                                 | 1              |
| 11  | 1.25                            | 0.99788                                 | 1              |
| 12  | 1                               | 0.00006                                 | 0              |
| 13  | 1                               | 0.00006                                 | 0              |
| 14  | 1.3                             | 1.00197                                 | 1              |
| 15  | 2                               | 0.99877                                 | 1              |
| 16  | 3.2                             | 1.00003                                 | 1              |
| 17  | 3.7                             | 1.00045                                 | 1              |
| 18  | 3.7                             | 1.00045                                 | 1              |
| 19  | 3.7                             | 1.00045                                 | 1              |
| 20  | 3.7                             | 1.00045                                 | 1              |
| 21  | 3.7                             | 1.00045                                 | 1              |
| 22  | 2.7                             | 0.99959                                 | 1              |
| 23  | 2                               | 0.99877                                 | 1              |
| 24  | 1.8                             | 0.99862                                 | 1              |
| 25  | 1.6                             | 0.99917                                 | 1              |
| 26  | 0.5                             | -0.09999                                | 0              |
| Time Stamp  | Stop Sampling and Send Alert    |   |                |

TABLE VIII. COMPARISON BETWEEN ODOR KEYS TESTING DATA

| All Data Sets {Odor 1, Odor 2, Odor 3} |                                |                                   |                                   |
|--|--------------------------------|-----------------------------------|-----------------------------------|
| Response Time (Seconds)                | Correct Odor Keys VSensor/VRef | Incorrect Odor Key 2 VSensor/VRef | Incorrect Odor Key 3 VSensor/VRef |
| 0                                      | 1                              | 1                                 | 1                                 |
| 1                                      | 1.3                            | 1.3                               | 1.3                               |
| 2                                      | 1                              | 1                                 | 1                                 |
| 3                                      | 1                              | 1                                 | 1                                 |
| 4                                      | 1.4                            | 1.4                               | 1.4                               |
| 5                                      | 2.6                            | 0.6                               | 2.6                               |
| 6                                      | 2.7                            |                                   | 2.7                               |
| 7                                      | 2.55                           |                                   | 2.55                              |
| 8                                      | 1.9                            |                                   | 1.9                               |
| 9                                      | 1.6                            |                                   | 1.6                               |
| 10                                     | 1.4                            |                                   | 1.4                               |
| 11                                     | 1.25                           |                                   | 1.25                              |
| 12                                     | 1                              |                                   | 1                                 |
| 13                                     | 1                              |                                   | 1                                 |
| 14                                     | 1.3                            |                                   | 1.3                               |
| 15                                     | 2                              |                                   | 2                                 |
| 16                                     | 3.2                            |                                   | 3.2                               |
| 17                                     | 3.7                            |                                   | 3.7                               |
| 18                                     | 3.7                            |                                   | 3.7                               |
| 19                                     | 3.7                            |                                   | 3.7                               |
| 20                                     | 3.7                            |                                   | 3.7                               |
| 21                                     | 3.7                            |                                   | 3.7                               |
| 22                                     | 2.7                            |                                   | 2.7                               |
| 23                                     | 2                              |                                   | 2                                 |
| 24                                     | 1.8                            |                                   | 1.8                               |
| 25                                     | 1.6                            |                                   | 1.6                               |
| 26                                     | 1.5                            |                                   | 0.5                               |
| 27                                     | 1.4                            |                                   |                                   |
| 28                                     | 1.25                           |                                   |                                   |
| 29                                     | 1.1                            |                                   |                                   |
| 30                                     | 1.05                           |                                   |                                   |
| 31                                     | 1                              |                                   |                                   |

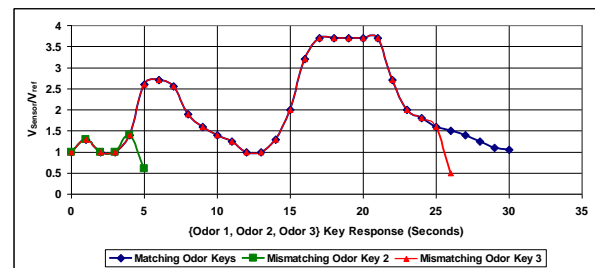


Fig. 6. System Testing with Incorrect Odor Keys.

Any deviation in any of the parameters in equation (5) will cause the system to halt and alert. The order or keys position relative to each other can periodically be change, by retraining the system again for different order of the same odorant, which is a standard security practice as changing a password every few weeks. Also, the types of odorants can also be changed and the system retrained to use the new odorants, which is a fourth security dimension.

The sampling system could be placed in a remote device held by the person concerned or in the vehicle itself with regular but random interchanging of odor keys.

Neural Engine will initially be trained to recognize the odor keys and only unlocks the vehicle if the random combination of the three keys falls within the space-time domains of the training key sets. Any other keys will not be able to unlock the system and will raise a remote call to the user.

## VI. CONCLUSIONS

The proposed system is a good step towards a new type of vehicular security systems, which can be made as simple and as complex as necessary by increasing the number of odorants or the process of sampling. Future developments could include smelling of the driver body odorant in a combination with an external odorant or on its own, which means that body odor can be used as a biometric identification for vehicles, similar to fingerprinting. More stable and integrated sensors with temperature compensation and high level of noise isolation will contribute to a great deal in refining the system and improve its reliability.

## REFERENCES

- [1] J. Yan, X. Guo, S. Duan, P. Jia, L. Wang, C. Peng, S. Zhang, "Electronic nose feature extraction methods: A review," *Sensors*, vol. 15, pp. 27804–27831, 2015.
- [2] S. Vishesh, M. Srinath, K. Gubbi, H. Shivu, N. Prashanta, "Portable Low Cost Electronic Nose for Instant and Wireless Monitoring of Emission Levels of Vehicles Using Android Mobile Application," *IJARCCCE*, vol. 5, no. 9, pp. 134–140, 2016.
- [3] R. Suganya, R. Uthayakumar "Electronic nose for accident prevention and vehicleblack box system," *IJARECE*, vol. 4, no. 5, pp. 1206–1209, 2015.
- [4] A. Guentner, V. Koren, K. Chikkadi, M. Righettoni, S. Pratsinis, "E-nose sensing of low-ppb formaldehyde in gas mixtures at high relative humidity for breath screening of lung cancer?" *ACS Sensors*, vol. 1, no. 5, pp. 528–535, 2016.
- [5] A. Loutfi, S. Coradeschi, G. Mani, P. Shanker, J. Rayappan, "Electronic noses for food quality: a review," *Journal of Food Engineering*, vol. 144, pp. 103–111, 2015.
- [6] A. Gongora, J. Monroy, J. Gonzalez-Jimenez, "An Electronic Architecture for Multipurpose Artificial Noses," *Journal of Sensors*, vol. 2018, pp. 1-9, 2018.
- [7] H. Zhiyi, H. Chenchao, Z. Jiajia, H. Guohua, "Electronic nose system fabrication and application in large yellow croaker (*Pseudosciaena crocea*) freshness prediction," *Journal of Food Measurement and Characterization*, vol. 11, no. 1, pp. 33–40, 2017.
- [8] M. Castrica, S. Panseri, E. Siletti, F. Borgonovo, L. Chiesa, C. Balzaretta, "Evaluation of Smart Portable Device for Food Diagnostics: A Preliminary Study on Cape Hake Fillets (*M. capensis* and *M. paradoxus*)," *Journal of Chemistry*, vol. 2019, Article ID 2904724, pp. 1–7, 2019.
- [9] S. Chiu, K. Tang, "Towards a chemiresistive sensorintegrated electronic nose: a review," *Sensors*, vol. 13, no. 10, pp. 14214–14247, 2013.
- [10] J. Guti´errez, M. Horrillo, "Advances in artificial olfaction: Sensors and applications," *Talanta*, vol. 124, pp. 95–105, 2014.
- [11] S. Marco, A. Guti´errez-G´alvez, A. Lansner et al, "A biomimetic approach to machine olfaction, featuring a very large-scale chemical sensor array and embedded neuro-bio-inspired computation," *Microsystem Technologies*, vol. 20, no. 4-5, pp. 729–742, 2014.
- [12] L. Xu, J. He, S. Duan, X. Wu, Q. Wang, "Comparison of machine learning algorithms for concentration detection and prediction of formaldehyde based on electronic nose," *Sensor Review*, vol. 36, no.2, pp. 207–216, 2016.
- [13] S. Radi, S. Ciptohadijoyo, W. Litananda, M. Rivai, M. Purnomo, "Electronic nose based on partition column integrated with gas sensor for fruit identification and classification," *Computers and Electronics in Agriculture*, vol. 121, pp. 429–435, 2016.
- [14] S. Sarkar, A. Bhondekar, M. Macas et al., "Towards biological plausibility of electronic noses:A spiking neural network based approach for tea odour classification," *Neural Networks*, vol. 71, pp. 142–149, 2015.
- [15] Y. Sun, D. Luo, H. Li, C. Zhu, O. Xu, H. Hosseini, "Detecting and Identifying Industrial Gases by a Method Based on Olfactory Machine at Different Concentrations," *Journal of Electrical and Computer Engineering*, vol. 2018, Article ID 1092718, pp. 1–9, 2018.
- [16] E. Ordukaya, B. Karlik, "Quality Control of Olive Oils Using Machinem Learning and Electronic Nose," *Journal of Food Quality*, vol. 2017, Article ID 9272404, pp. 1–7, 2017.
- [17] A. Tiele, S. Esfahani, J. Covington, "Design and Development of a Low-Cost, Portable Monitoring Device for Indoor Environment Quality," *Journal of Sensors*, vol. 2018, Article ID 5353816, pp. 1–14, 2018.
- [18] A. Iosifidis, A. Tefas, and I. Pitas, "Approximate kernel extreme learning machine for large scale data classification," *Neurocomputing*, vol. 219, pp. 210–220, 2017.
- [19] K. Yan, D. Zhang, "Calibration transfer and drift compensation of e-noses via coupled task learning," *Sensors and Actuators B: Chemical*, vol. 225, pp. 288–297, 2016.
- [20] Z. Ma, G. Luo, K. Qin, N. Wang, W. Niu, "Weighted Domain Transfer Extreme Learning Machine and Its Online Version for Gas Sensor Drift Compensation in E-Nose Systems," *Wireless Communications and Mobile Computing*, vol. 2018, Article ID 2308237, pp. 1–17, 2018.
- [21] A. Di Gilio, J. Palmisani, G. de Gennaro, "An Innovative Methodological Approach for Monitoring and Chemical Characterization of Odors around Industrial Sites," *Advances in Meteorology*, vol. 2018, Article ID 1567146, pp. 1–8, 2018.
- [22] A. Hassan, A. Bermak, "Biologically Inspired Feature Rank Codes for Hardware Friendly Gas Identification with the Array of Gas Sensors," *IEEE Sens. J.*, vol. 16, pp. 5776–5784, 2016.
- [23] Y. Jing, Q. Meng, P. Qi, M. Cao, Z. Ming, S. Ma, "A Bioinspired Neural Network or Data Processing in an Electronic Nose," *IEEE Trans. Instrum. Meas.*, vol. 65, pp. 2369–2380, 2016.
- [24] L. Zhang, F. Tian, G. Pei, "A novel sensor selection using pattern recognition in electronic nose," *Measurement*, vol. 54, pp. 31–39, 2014.
- [25] H. Ray, N. Bhattacharyya, A. Ghosh, B. Tudu, R. Bandyopadhyay, S. Biswas, S. Majumdar, "Fragrance profiling of Jasminum sambac Ait. flowers using electronic nose," *IEEE Sens. J.*, vol. 17, pp. 160–168, 2017.
- [26] H. Liu, Q. Li, B. Yan, L. Zhang, Y. Gu, "Bionic Electronic Nose Based on MOS Sensors Array and Machine Learning Algorithms Used for Wine Properties Detection," *Sensors*, vol. 19, no. 45, pp. 1–11, 2019.
- [27] W. Cao, C. Liu, S. Duan, P. Jia, "Feature Extraction and Classification of Citrus Juice by Using an Enhanced L-KSVD on Data Obtained from Electronic Nose," *Sensors*, vol. 19, no. 916, pp. 1–17, 2019.

- [28] Y. Wu, T. Liu, S. Ling, J. Szymanski, W. Zhang, S. Su, "Air Quality Monitoring for Vulnerable Groups in Residential Environments Using a Multiple Hazard Gas Detector," *Sensors*, vol. 19, no. 362, pp. 1–16, 2019.
- [29] X. Zhan, X. Guan, R. Wu, Z. Wang, Y. Wang, G. Li, "Discrimination between Alternative Herbal Medicines from Different Categories with the Electronic Nose," *Sensors*, vol. 18, no. 2936, pp. 1–15, 2018.
- [30] C. Deng, K. Lv, D. Shi, B. Yang, S. Yu, Z. He, J. Yan, "Enhancing the Discrimination Ability of a Gas Sensor Array Based on a Novel Feature Selection and Fusion Framework," *Sensors*, vol. 18, no. 1909, pp. 1–17, 2018.
- [31] Juan Guerrero-Ibáñez, S. Zeadally, Juan Contreras-Castillo, "Sensor Technologies for Intelligent Transportation Systems," *Sensors*, vol. 18, no. 1212, pp. 1–24, 2018.
- [32] J. Contreras-Castillo, S. Zeadally, J. Guerrero -Ibáñez, "A seven-layered model architecture for Internet of Vehicles," *Journal of Information and Telecommunication*, vol. 1, no. 1, pp. 4–22, 2017.
- [33] R. Dhall, V. Solanki, "An IoT Based Predictive Connected Car Maintenance Approach," *Machines*, vol. 4, no. 3, pp. 16–22, 2017.
- [34] E. Hamida, H. Noura, W. Znaidi "Security of Cooperative Intelligent Transport Systems: Standards, Threats Analysis and Cryptographic Countermeasures," *Electronics*, vol. 4, pp. 380–423, 2015.



# Forensic Analysis using Text Clustering in the Age of Large Volume Data: A Review

Bandar Almaslukh

Department of Computer Science, College of Computer Engineering and Sciences  
Prince Sattam bin Abdulaziz University, Al-Kharj 11942, Saudi Arabia

**Abstract**—Exploring digital devices in order to generate digital evidence related to an incident being investigated is essential in modern digital investigation. The emergence of text clustering methods plays an important role in developing effective digital forensics techniques. However, the issue of increasing the number of text sources and the volume of digital devices seized for analysis has been raised significantly over the years. Many studies indicated that this issue should be resolved urgently. In this paper, a comprehensive review of digital forensic analysis using text-clustering methods is presented, investigating the challenges of large volume data on digital forensic techniques. Moreover, a meaningful classification and comparison of the text clustering methods that have been frequently used for forensic analysis are provided. The major challenges with solutions and future research directions are also highlighted to open the door for researchers in the area of digital forensics in the age of large volume data.

**Keywords**—Digital investigation; forensic analysis; text clustering

## I. INTRODUCTION

Digital Forensic Investigation (DFI) is the process of exploring digital devices in order to generate digital evidence related to an incident being investigated [1]. The six steps of the Digital Forensic Investigation (DFI) process as stated by DFRWS (Digital Forensic Research Workshop) illustrated in Fig. 1. First, the identification phase where all the components, devices, and data related to the incident are determined. After that, the preservation phase is conducted by avoiding any activities that can damage the collected digital information.

The next step is collecting the digital information that could be related to the incident under investigation, named the collection phase. Then, the examination phase is used for in-depth systematic search of evidence related to the incident being investigated. In the analysis phase, the investigator derives a conclusion for the evidence collected in the examination phase. Finally, the findings are summarized and presented to the court of law in the presentation phase.

However, over several years, the issue of digital investigation in large volume data has been raised increasingly. Many studies indicated that this issue should be addressed to find efficient solutions. For example, in [2] authors state that the coming digital forensic crisis is the growing size of storage devices since the tasks of collecting and analyzing and presenting a terabyte of data in a short report is more

challenges. In addition, the ever growing in storage number and capacity with lack of adequate automated analyzing techniques are considered as one of the main current challenges in digital forensics filed [3-6]. In [7] the challenges posed to the digital forensics by the problem of big data are discussed.

The problem of big data can lead to wrong decision-making, falling to find evidence or loss of life in dangerous cases [7]. Specifically, the task of examination and analysis become more challenges in the age of big data since the current forensics tools cannot cope with large volumes of data. The limitation of these tools is designed for a relatively small volume of data (up to 1 Terabyte).

However, it is common in the age of big data that the volume of data that need to be analyzed can extend from a number of terabytes up to a couple of petabytes. To cope with the large volumes of data researchers have used clustering algorithms as an alternative approach to speed up the examination and analysis phases. Since a great deal of the stored data is linguistics in nature (textual) [8], specifically the text clustering techniques have been utilized.

Text clustering is thematically assigning the text documents to separate groups where documents in the same group are more similar than other groups. Clustering methods are usually used for data analysis in which there is no prior or little knowledge about the data [9]. This is specifically the case in numerous applications of computer digital forensics addressed in this work.

In this paper, we conduct a comprehensive review for the state of the art research works that utilizing text clustering in the digital forensics investigation process. The main objective of the paper is to provide the reader with the recent text clustering techniques used in the context of digital forensics and benchmarking these techniques. In addition, the ideas of where the research might go next for the researchers who are interesting in this filed are provided.

The rest of the paper is structured as follow: Section II states the literature review of text clustering algorithms. Problem statement and motivation are presented in Section III, as well as, the summary of related works is shown in Section IV. Section V gives the applicability of clustering techniques in the literature that are utilized for large textual data. Conclusion is drawn in Section VI. Finally, future trends are presented in Section VII.

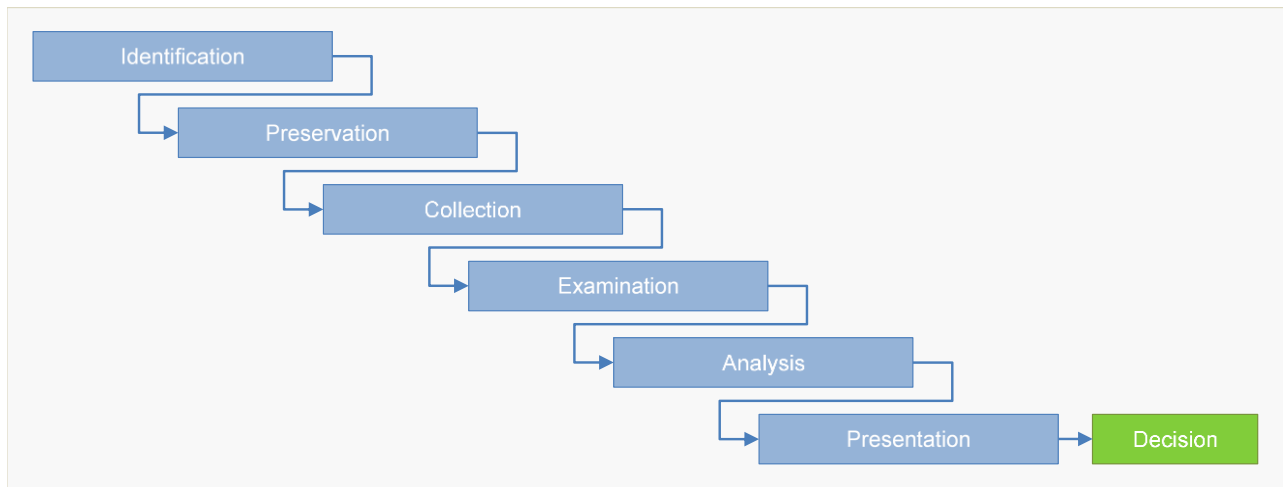


Fig. 1. The Digital Forensic Investigation (DFI) Process as Stated by the Digital Forensic Research Workshop (DFRWS).

## II. LITERATURE REVIEW

Clustering algorithms have been studied since 1990; the literature on this subject is enormous. However, only few researchers have utilized the text clustering algorithms in the digital forensics context. The main algorithms used are SSOM (scalable self-organizing map), k-means, kernel k-means, hierarchical clustering, and Latent Dirichlet Allocation (LDA). Essentially, we can classify the related works to fifth classes based on the clustering techniques used, as follow:

### A. Scalable Self-Organizing Map (SSOM)

A Kohonen self-organizing map (SOM) [18] is a type of unsupervised learning based on neural network approaches. This network consists of two layers: an input layer and an output layer (normally two-dimensional map). The input layer considered as a distributed layer, where the number of nodes in this layer as many as the input object features. After that, the network is trained to transform high-dimensional objects (input layer) to two-dimensional objects (output layer). However, in [19], scalable self-organizing map (SSOM) takes advantage of sparsity in the text document feature vector to improve the computational complexity of the SOM.

In the context of digital forensics analysis, the conceptual documents clustering using SSOM have utilized. For example, in [10], the SSOM clustering algorithm was used to cluster the search hits retrieved by the computer forensics tools. The software named Grouper was developed to evaluate the proposed method. Despite the required computer processing time, the proposed method reduced the examiner analytical time by around 80%. The limitation of this research is that testing the proposed method on a relatively small dataset (40 gigabytes) which is not the case in the age of big data.

### B. Subject-based Clustering

The study offered in [11] proposed a novel subject-based semantic document clustering approach. This approach clustering the documents stored on seized devices according to the subjects provided by the investigator. The main intuition behind this algorithm is to extend semantically the subjects provided by the investigator using WordNet [20] and a list of forensic specific synonyms. To model the proposed algorithm,

a new subject vector space model (SVSM) was formulated. This model based on the vector space model (VSM) [21] and topic-based vector space model (TVSM) for information retrieval [22]. SVSM is an n-dimensional space model. Each dimension in the space characterizes one subject, where each dimension is orthogonal from each other (independent from each other). Terms and documents representation in SVSM is similar to their representation in TVSM.

However, the limitation of this research work is that the produced clusters based on the investigator experience to provide the appropriate subjects. In addition, it seems unlikely that the expert investigator can know all the criminals' events occurred in seized devices. To overcome this limitation, the work in [12] applies the same subject-based clustering algorithms in [11], with the help of subject suggestion that provided to the investigator. The provided subject suggestion improves the task of an investigator in terms of accuracy and speed. However, the subject-based semantic document clustering method in [11] assigns each document to the appropriate cluster, and all documents that do not belong to any subject are grouped in a separate cluster (named "general"). The problem is that the documents in the "general" cluster are belonging to different subjects. Therefore, the research work in [13] solves this problem by clustering the documents in the "general" cluster using bisection k-means algorithm.

### C. Kernel K-mean

The "k-means" term was used first time by James Macqueen in 1967 [23]. It has been using intensively in the field of data mining as an unsupervised learning technique. K-mean grouping the set of observation  $\mathcal{D} = \{D_i; i = 1, \dots, N\}$  into a set of  $K$  clusters, where  $K \leq N$ . The  $N$  observations are grouped in  $K$  disjoint clusters where the intra-cluster similarity between observation more than inter-cluster. The limitation of conventional k-means, it cannot detect the non-linear separable clusters accurately. Therefore, the kernel version of k-means was proposed in [24], to detect the non-linear separable clusters. The intuition of kernel k-means is to map all observation,  $D_i$  to another space using one of the will know kernel function such as the sigmoid kernel. By mapping to the new space, the observation clusters will be linearly separable.

However, the research work in [17] utilized the kernel-based version of k-means to clustering the documents stored on suspect devices. It adopts the method in [25] to measure the similarity between documents, where the Euclidian distance and term base on stylistic information used. Enron dataset used to measure experimentally the performance of the proposed work. The weakness of this research is that evaluating the proposal using the email dataset only which not reflect the real world cases where the textual data from different resources.

#### D. LDA (Latent Dirichlet Allocation)

LDA is a generative probabilistic model of a discrete data collection such as text corpus [26]. Essentially, it represents the documents as random mixtures over latent topics, and each topic is considered as a distribution over words. LDA has been considering as one of the best text modeling approaches, which automatically discover hidden topics from document corpus.

However, Authors in [14] showed how the topic modeling approaches could be applied to the forensic data. Specifically, the LDA clustering algorithm used to facilitate the examination and analyses phases in DFI process. In addition, the challenges posed by digital forensic data to the topic modeling algorithms mentioned. They conclude that topic modeling is beneficial for realizing the semantic of text documents in forensic data as well as summarizing the content of the documents.

In addition, a profound comparison between keyword-based search techniques and LDA is accomplished in [7]. The comparison was conducted on Real Data Corpus (RDC), which was collected from 2400 disks belonging to a real user. They conclude that LDA topic analysis should not be considered as a replacement of keyword-based search techniques, but it offers some benefits. The first benefits are relaxing the condition to match the keyword with the exact word appeared in the document. In addition, facilities the documents browsing by grouping documents based on the topic.

#### E. Benchmarking different Clustering Algorithms

The research works under this section was proposed to benchmark diverse clustering algorithms for forensic analysis. For instance, in [15] authors have proposed an approach that utilizes document clustering algorithms for the forensic analysis of seized digital devices. They realized that the majority of the related works in digital forensics assumes that the number of clusters is prior known, but in reality, the number of clusters varies from one case to the other. Thus, the relative validity index such as Silhouette [27] has used to estimate the number of clusters from the data automatically. The proposed approach is demonstrated by carrying out an extensive comparative study of the six well-known clustering

algorithms (k-means, k-medoids, hierarchical clustering (Single/Average/complete link) and cluster ensembles (CSPA)), with a different mixture of parameters. In order to make the comparison more realistic, these algorithms applied to five real-world investigation cases seized by the Brazilian Federal Police Department. They conclude that the hierarchal algorithms (Average Link, complete Link) produce the best result in term of accuracy and stability. In addition, it had been shown how the hierarchal algorithms could be used to facilitate the digital examination task. However, we believe that hierarchal clustering techniques are not some good choices when the datasets are very large since they have a high computation cost. Another interesting research to benchmark some of the clustering algorithms in the context of digital forensic analysis proposed in [16]. In order to analyze the text string search output, k-means, SOM, LDA followed by k-means, and LDA followed by SOM clustering algorithms were used and evaluated. It realized that LDA follows by k-means accomplished the best performance; also, k-means and SOM achieve a better performance when they combined with LDA. Unfortunately, the poor evaluation was achieved since only small size synthetic data is used (up to 10 gigabytes), which is not the case in real-world data. To improve the performance of document clustering algorithms for criminal news, the authors in [28] proposed to use a Memetic Algorithm Feature Selection (MAFS) method with k-means and Spherical k-means (Spk) clustering algorithms. They achieved in somehow good clustering labels. In [29], the authors used a hierarchical clustering algorithm to distribute the chunks of a certain file type from memory into their corresponding files. This method does not need any information about the number of clusters. However, the dataset size used in this work is very small. Moreover, the hierarchical clustering algorithm is more sensitive to noise and outliers, as well as it is difficult to handle different sized clusters and clusters with convex shapes.

### III. SUMMARY OF THE LITERATURES

In order to provide the reader with the main characteristics of the related work, a summary is provided in this section. The main features used to designate the related work are the size of the datasets used, including the semantic between words and identifying the cluster label. The size of datasets is considered as an important feature since it reflects the scalability in term of time complexity, and considering semantic between words provide a more accurate result. In addition, good cluster labeling helps the investigator to identify the semantic content of the clusters. Based on text clustering techniques that are used for digital forensics, the related works are classified into five classes as shown in Table I.

TABLE I. RELATED WORKS SUMMARY

| Clustering Algorithms  | Paper (Publication Year)  | Is semantic between words is included | Good Cluster Labeling | Achieved Accuracy (%) | Dataset Size                             |                                  |
|--|---|---------------------------------------|-----------------------|-----------------------|--|----------------------------------|
| SSOM (Scalable Self-Organizing Map)  | [10] (2011)   | No                                    | No                    | 70.9                  | Small (up to 40 gigabytes)               |                                  |
| Subject-based Clustering<br>(Actually this in not unsupervised clustering techniques since the clustering here based on the subjects provided by investigator) | [11] (2013)   | Yes                                   | Yes *                 | 72                    | Small (up to 3893 documents)             |                                  |
|  | [12] (2014)   | Yes                                   | Yes *                 | 80                    | Very Small (up to 100 documents)         |                                  |
|  | [13] (2014)   | Yes                                   | Yes *                 | 65                    | Small (up to 3893 documents)             |                                  |
| Kernel k-means   | [2] (2009)  | No                                    | No                    | -                     | Small (up to 3331 documents)             |                                  |
| LDA (Latent Dirichlet Allocation)<br>(topic modeling)  | [7] (2014)  | Yes                                   | Yes                   | -                     | Relatively Large (up to 98529 documents) |                                  |
|  | [14] (2008)   | Yes                                   | Yes                   | -                     | Very Small (up to 837 documents)         |                                  |
| Benchmarking Different Clustering Algorithms   | k-means, k-medoids, hierarchical clustering (Single/Average/complete link) and cluster ensembles (CSPA) | [15] (2013)                           | No                    | No                    | 91                                       | Very Small (up to 131 documents) |
|  | K-mean, SOM, LDA + K-mean and LDA+ SOM  | [16] (2014)                           | Yes                   | Yes                   | 67                                       | Small (up to 40 gigabytes)       |
| Memetic Algorithm Feature Selection with k-means and Spherical k-means (Spk)   | [28] (2018)   | No                                    | No                    | -                     | Small (up to 4195 documents)             |                                  |
| Hierarchical clustering algorithm  | [29] (2018)   | No                                    | No                    | 84.9                  | Very Small (20 files)                    |                                  |
| Yes *: means that the cluster labeling based on the subjects provided by investigator.   |   |                                       |                       |                       |  |                                  |

#### IV. PROBLEM STATEMENT AND MOTIVATION

In recent years, a major challenge to digital forensic examination and analysis phases is the ever growing in the number and volume of digital devices seized by the digital forensic agencies for investigation. This is a consequence of the ongoing development of storage capacity and computing technologies, as well as the number of devices seized per case has increased. In addition, the number of backlogs of seized devices waiting for analysis (regularly many months to years) has increased rapidly.

However, in order to reduce the overall examination time, many digital forensic tools such as FTK<sup>1</sup>, Encase<sup>2</sup>, etc. have been developed. The main techniques utilized in these tools are keyword search, regular expression search, and approximate matching search. These tools are designed to accomplish 100% query recall to retrieve all relevant documents, regardless of the extremely high proportion of non-relevant documents retrieved (very low precision). The limitations of these techniques are applied against the entire stored data (e.g., email document, internet history, instant message, word documents PDF files, etc.) without prior knowledge about the similarity amongst the documents. In addition, they are limited to the background knowledge about the case as well as the used search terms from the investigator's personal experience. Thus, the search hit of these techniques suffers from a large number of false negative and false positive. Therefore, the examiners still have to analyze the data manually in order to find potential evidence. However, this process is time-consuming, exceed the expert examiner ability and prone to human error.

Indeed, these challenges have led many researchers [10,11,12,13,14,7,15,16,17] to intentionally use different approaches such as machine learning and data mining in digital forensics for semi-automatic data analysis, in particular algorithms for document clustering. The clustering algorithms normally utilized for exploratory data analysis, when there is no prior knowledge about the data. This is exactly the case in the majority of digital investigation cases. However, the main idea behind document clustering algorithms is to group the objects from different clusters where the similarity between these objects within a cluster is more than the similarity between the objects in different clusters. Therefore, the examiner can perform preliminary analysis by investigating the representative documents of each produced cluster; making the task of examining the entire documents is avoided. Moreover, the investigator has the ability to prioritize the analysis of each cluster based on the relationship strength with the case under investigation.

The encouraging results of text clustering techniques in many fields are motivated the researchers to discover the usability of these techniques as a substitute approach to finding evidence in digital forensics filed. This encourages us to conduct a comprehensive review of the research works that addressing the problem of analyzing digital textual data in digital forensics using document-clustering techniques. However, this work is considered as a starting point for the researchers who interested in improving the accuracy and speed up the analyzing of large-scale textual data in digital forensics.

<sup>1</sup> <http://accessdata.com/products/computer-forensics/ftk>

<sup>2</sup> <https://www.guidancesoftware.com/>

V. APPLICABILITY OF CLUSTERING TECHNIQUES UTILIZED IN THE LITERATURE FOR LARGE TEXTUAL DATA

Analyzing large volumes of text data in the digital forensics fields, we develop a set of criteria to evaluate these techniques as shown in Table II. These criteria are time complexity, tackling high dimensionality, number of input parameters.

Time complexity is very important since we deal with a large volume of data. Tackling high dimensionality is very important criteria since the data type is text, which is high dimensional data. In addition, the number of input parameters is very important because a large number of parameters might reduce the cluster quality. Finally, for large datasets, the main strength and weakness of each technique are presented in Table II.

TABLE II. PROPOSED EVALUATION CRITERIA

| Text Mining Method  | Technique                | Time Complexity  | Tackling High Dimensionality | Number of Input Parameters                        | Strength  | Weakness   |
|---|--------------------------|--|------------------------------|---|---|--|
| <b>Traditional Clustering Methods</b>   | k-means                  | $O(NKd)$   | No                           | 1<br>(number of clusters)                         | Scalable  | only discovering cluster with spherical shape  |
|   | Kernel k-means           | If sampling is used<br>$O(NmK + Nmd)$<br>Otherwise<br>$O(N^2K + N^2d)$ | Yes                          | 1<br>(number of clusters)                         | Detect the non-linear separable clusters                                  | Not Scalable   |
|   | Hierarchical Clustering  | $O(N^2)$   | No                           | 0   | Can provide clusters at different levels of granularity                   | Not Scalable   |
|   | SOM                      | $O(N^2)$   | Yes                          | 5   | It makes similarities between data easier to be observed and interpreted. | Similar objects could be split to more than one cluster  |
| <b>Topic Modeling</b>   | LDA                      | $O(NWKd)$<br>[24]  | Yes                          | 1<br>(number of topics)                           | Topics in corpus is identified clearly                                    | It is hard to know interpretable topics when LDA is working and difficult when the design is not balanced. |
| <b>Clustering Based on Information Retrieval Model</b>  | Subject-based Clustering | $O(N)$   | Yes                          | Many set of words each set represents one subject | Assume that user has prior knowledge about data                           | Based on subjects provided by user   |
| N: Number of document in the corpus      K: Number of clusters      D: Number of iteration      W: Number of words in the document. |                          |  |                              |   |   |  |

VI. CONCLUSION

The literature survey identified the potential future works remain in relation to forensic analysis using text clustering in the age of large volume data; for instance, validating text clustering on real world and large scale data, investigating the automatic approach for cluster labeling and bilingual clustering, etc. The related works are classified to fifth categories base on clustering techniques. The categories are SSOM, Kernel k-means and subject-based clustering, LDA, and benchmarking different clustering algorithms. In the last categories, more than one clustering techniques are compared in the context of digital forensics. However, the applicability of the clustering techniques utilized in the literature to analyze a large volume of text data is investigated.

VII. FUTURE TRENDS

In this section, we stated several promising venues for future works. It is important to note that some of these future works are addressed partially in the literature and others not addressed at all. However, we can summarize the promising spots for the future works as follows:

1) Since the majority of the related works are validated on a relatively small dataset (up to 1 terabyte) or synthetic data, it is important to investigate the applicability of these methods on real-world as well as large datasets (from a number of terabytes up to a couple of petabytes).

2) Investigating the applicability of other clustering techniques, such as density-based clustering and bisection k-means.

3) Exploring the automatic approaches for cluster labeling to facilitate the analyzer task by identifying the semantic content of clusters.

4) In some country, it is common that seized devices have a document from two different languages such as English and Arabic. Therefore, the task of bilingual clustering needs to be investigated in the context of digital forensics analysis.

5) The majority of the related works represent document features as a bag of words that do not represent semantic relations between words. Therefore, it is beneficial to integrating the WorldNet [20] ontology with clustering

algorithms to enhance document-clustering quality. The WorldNet uses to find the semantic relation between words. In addition, it is useful to use the state-of-the-art deep learning technique called words embedding. Word embedding is considered as one of the most robust representations of document vocabulary. It is capable of capturing context of the words, semantic and syntactic similarity with other words in a document [30-32].

6) Parallel and distributed processing methods might be used to speed up the analysis of digital forensic data.

#### REFERENCES

- [1] Montasari, Reza, Richard Hill, Victoria Carpenter, and Amin Hosseinian-Far. "The Standardised Digital Forensic Investigation Process Model (SDFIPM)." In *Blockchain and Clinical Trial*, pp. 169-209. Springer, Cham, 2019.
- [2] Garfinkel, Simson, et al. "Bringing science to digital forensics with standardized forensic corpora." *digital investigation* 6 (2009): S2-S11.
- [3] Raghavan, Sriram. "Digital forensic research: current state of the art." *CSI Transactions on ICT* 1.1 (2013): 91-114.
- [4] Kazem, Craig. "Extracting Hidden Topics from Texts using LDA Model" A.I. Optify (2014): <http://www.aioptify.com/lda.php>.
- [5] W. Anwar, I. S. Bajwa, M. A. Choudhary, and S. Ramzan, "An Empirical Study on Forensic Analysis of Urdu Text Using LDA-Based Authorship Attribution," *IEEE Access*, vol. 7, pp. 3224-3234, 2019.
- [6] I. Al-Jadir, K. W. Wong, C. C. Fung, and H. Xie, "Enhancing digital forensic analysis using memetic algorithm feature selection method for document clustering," in *2018 IEEE International Conference on Systems, Man, and Cybernetics (SMC)*, 2018, pp. 3673-3678.
- [7] Noel, George E., and Gilbert L. Peterson. "Applicability of Latent Dirichlet Allocation to multi-disk search." *Digital Investigation* 11.1 (2014): 43-56.
- [8] Beebe, Nicole Lang, and Jan Guynes Clark. "Digital forensic text string searching: Improving information retrieval effectiveness by thematically clustering search results." *Digital investigation* 4 (2007): 49-54.
- [9] B. S. Everitt, S. Landau, and M. Leese. "In book: Cluster Analysis, London: Arnold." (2001): 128.
- [10] Beebe, Nicole Lang, et al. "Post-retrieval search hit clustering to improve information retrieval effectiveness: Two digital forensics case studies." *Decision Support Systems* 51.4 (2011): 732-744.
- [11] Dagher, Gaby G., and Benjamin CM Fung. "Subject-based semantic document clustering for digital forensic investigations." *Data & Knowledge Engineering* 86 (2013): 224-241.
- [12] Mascarnes, Sweedle, and Joanne Gomes. "Subject based Clustering for Digital Forensic Investigation with Subject Suggestion." *International Journal of Computer Applications* 102.11 (2014).
- [13] Thilagavathi, G., and J. Anitha. "Document Clustering in Forensic Investigation by Hybrid Approach." *International Journal of Computer Applications* 91.3 (2014).
- [14] de Waal, Alta, Jacobus Venter, and Etienne Barnard. "Applying topic modeling to forensic data." *IFIP International Conference on Digital Forensics*. Springer US, 2008.
- [15] da Cruz Nassif, Luís Filipe, and Eduardo Raul Hruschka. "Document clustering for forensic analysis: An approach for improving computer inspection." *IEEE transactions on information forensics and security* 8.1 (2013): 46-54.
- [16] Beebe, Nicole L., and Lishu Liu. "Clustering digital forensic string search output." *Digital Investigation* 11.4 (2014): 314-322.
- [17] Decherchi, Sergio, et al. "Text clustering for digital forensics analysis." *Computational Intelligence in Security for Information Systems*. Springer Berlin Heidelberg, 2009. 29-36.
- [18] Kohonen, Teuvo. "The self-organizing map." *Proceedings of the IEEE* 78.9 (1990): 1464- 1480.
- [19] Roussinov, Dmitri G., and Hsinchun Chen. "A scalable self-organizing map algorithm for textual classification: A neural network approach to thesaurus generation." *Communication and Cognition in Artificial Intelligence Journal*(1998).
- [20] Miller, George A. "WorldNet: a lexical database for English." *Communications of the ACM* 38.11 (1995): 39-41.
- [21] Salton, Gerard. "Automatic text processing: The transformation, analysis, and retrieval of." Reading: Addison-Wesley (1989).
- [22] Becker, Jörg, and Dominik Kuropka. "Topic-based vector space model." *Proceedings of the 6th international conference on business information systems*. 2003.
- [23] MacQueen, James. "Some methods for classification and analysis of multivariate observations." *Proceedings of the fifth Berkeley symposium on mathematical statistics and probability*. Vol. 1. No. 14. 1967.
- [24] Girolami, Mark. "Mercer kernel-based clustering in feature space." *IEEE Transactions on Neural Networks* 13.3 (2002): 780-784.
- [25] Decherchi, Sergio, et al. "Hypermetric k-means clustering for content-based document management." *Proceedings of the International Workshop on Computational Intelligence in Security for Information Systems CISIS'08*. Springer Berlin Heidelberg, 2009.
- [26] Blei, David M., Andrew Y. Ng, and Michael I. Jordan. "Latent dirichle t allocation." *Journal of machine learning research* 3.Jan (2003): 993-1022.
- [27] Kaufman, Leonard, and Peter J. Rousseeuw. *Finding groups in data: an introduction to cluster analysis*. Vol. 344. John Wiley & Sons, 2009.
- [28] Al-Jadir, Ibraheem, Kok Wai Wong, Chun Che Fung, and Hong Xie. "Enhancing digital forensic analysis using memetic algorithm feature selection method for document clustering." In *2018 IEEE International Conference on Systems, Man, and Cybernetics (SMC)*, pp. 3673-3678. IEEE, 2018.
- [29] Al-Sharif, Ziad A., Attaa Y. Al-Khalee, Mohammed I. Al-Saleh, and Mahmoud Al-Ayyoub. "Carving and Clustering Files in Ram for Memory Forensics." (2018).
- [30] Duan, Tiehang, Qi Lou, Sargur N. Srihari, and Xiaohui Xie. "Sequential embedding induced text clustering, a non-parametric bayesian approach." In *Pacific-Asia Conference on Knowledge Discovery and Data Mining*, pp. 68-80. Springer, Cham, 2019.
- [31] Wu, Songze, Huaping Zhang, Chengcheng Xu, and Tao Guo. "Text Clustering on Short Message by Using Deep Semantic Representation." In *Advances in Computer Communication and Computational Sciences*, pp. 133-145. Springer, Singapore, 2019.
- [32] Ihm, Sun-Young, Ji-Hye Lee, and Young-Ho Park. "Skip-gram-KR: Korean Word Embedding for Semantic Clustering." *IEEE Access* (2019).

# Internet of Things (IoT): Research Challenges and Future Applications

AbdelRahman H. Hussein

Department of Networks and Information Security  
Faculty of Information Technology / Al-Ahliyya Amman University

**Abstract**—With the Internet of Things (IoT) gradually evolving as the subsequent phase of the evolution of the Internet, it becomes crucial to recognize the various potential domains for application of IoT, and the research challenges that are associated with these applications. Ranging from smart cities, to health care, smart agriculture, logistics and retail, to even smart living and smart environments IoT is expected to infiltrate into virtually all aspects of daily life. Even though the current IoT enabling technologies have greatly improved in the recent years, there are still numerous problems that require attention. Since the IoT concept ensues from heterogeneous technologies, many research challenges are bound to arise. The fact that IoT is so expansive and affects practically all areas of our lives, makes it a significant research topic for studies in various related fields such as information technology and computer science. Thus, IoT is paving the way for new dimensions of research to be carried out. This paper presents the recent development of IoT technologies and discusses future applications and research challenges.

**Keywords**—Internet of Things; IoT applications; IoT challenges; future technologies; smart cities; smart environment; smart agriculture; smart living

## I. INTRODUCTION

The Internet can be described as the communication network that connects individuals to information while The Internet of Things (IoT) is an interconnected system of distinctively address able physical items with various degrees of processing, sensing, and actuation capabilities that share the capability to interoperate and communicate through the Internet as their joint platform [1]. Thus, the main objective of the Internet of Things is to make it possible for objects to be connected with other objects, individuals, at any time or anywhere using any network, path or service. The Internet of Things (IoT) is gradually being regarded as the subsequent phase in the Internet evolution. IoT will make it possible for ordinary devices to be linked to the internet in order to achieve countless disparate goals. Currently, an estimated number of only 0.6% of devices that can be part of IoT has been connected so far [2]. However, by the year 2020, it is likely that over 50 billion devices will have an internet connection.

As the internet continues to evolve, it has become more than a simple network of computers, but rather a network of various devices, while IoT serves as a network of various “connected” devices a network of networks [3], as shown in Fig. 1. Nowadays, devices like smartphones, vehicles, industrial systems, cameras, toys, buildings, home appliances, industrial systems and countless others can all share information over the Internet. Regardless of their sizes and

functions, these devices can accomplish smart reorganizations, tracing, positioning, control, real-time monitoring and process control. In the past years, there has been an important propagation of Internet capable devices. Even though its most significant commercial effect has been observed in the consumer electronics field; i.e. particularly the revolution of smartphones and the interest in wearable devices (watches, headsets, etc.), connecting people has become merely a fragment of a bigger movement towards the association of the digital and physical worlds.

With all this in mind, the Internet of Things (IoT) is expected to continue expanding its reach as pertains the number of devices and functions, which it can run. This is evident from the ambiguity in the expression of “Things” which makes it difficult to outline the ever-growing limits of the IoT [4]. While commercial success continues to materialize, the IoT constantly offers a virtually limitless supply of opportunities, not just in businesses but also in research. Accordingly, the understudy addresses the various potential areas for application of IoT domains and the research challenges that are associated with these applications.

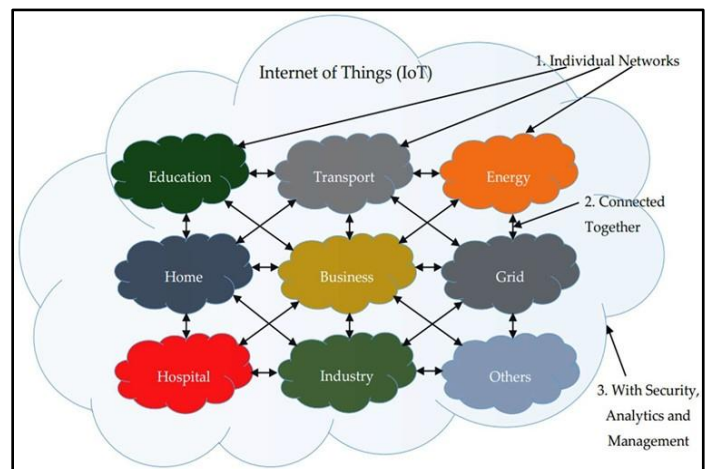


Fig. 1. IoT can be viewed as a Network of Networks [3].

## II. POTENTIAL APPLICATION DOMAINS OF IoT

Potential applications of the internet of Things are not only numerous but also quite diverse as they permeate into virtually all aspects of daily life of individuals, institutions, and society. According to [5], the applications of IoT cover broad areas including manufacturing or the industrial sector, health sector, agriculture, smart cities, security and emergencies among many others.

### A. Smart Cities

According to [6], the IoT plays a crucial role in improving the smartness of cities and enhancing general infrastructure. Some of IoT application areas in creating smart cities include; intelligent transportation systems [7], smart building, traffic congestion [7, 8] waste management [9], smart lighting, smart parking, and urban maps. This may include different functionalities such as; monitoring available parking spaces within the city, monitoring vibrations as well as material conditions of bridges and buildings, putting in place sound monitoring devices in sensitive parts of cities, as well as monitoring the levels of pedestrians and vehicles. Artificial Intelligence (AI) enabled IoT can be utilized to monitor, control and reduce traffic congestions in Smart Cities [6]. Moreover, IoT allows installation of intelligent and weather adaptive street lighting and detection waste and waste containers by keeping tabs of trash collection schedules. Intelligent highways can provide warning messages and important information, such as access to diversions depending on the climatic conditions or unexpected occurrences like traffic jams and accidents.

Application of IoT to achieve smart cities would require using radio frequency identification and sensors. Some of the already developed applications in this area are the Aware home and the Smart Santander functionalities. In the United States, some major cities like Boston have plans on how to implement the Internet of Things in most of their systems ranging from their parking meters, streetlights, sprinkler systems, and sewage grates are all scheduled to be interlinked and connected to the internet. Such applications will offer significant break throughs in terms of saving money and energy.

### B. Healthcare

Most healthcare systems in many countries are inefficient, slow and inevitably prone to error. This can easily be changed since the healthcare sector relies on numerous activities and devices that can be automated and enhanced through technology. Additional technology that can facilitate various operations like report sharing to multiple individuals and locations, record keeping and dispensing medications would go a long way in changing the healthcare sector [10].

A lot of benefits that IoT application offers in the healthcare sector is most categorized into tracking of patients, staff, and objects, identifying, as well as authenticating, individuals, and the automatic gathering of data and sensing. Hospital workflow can be significantly improved once patients flow is tracked. Additionally, authentication and identification reduce incidents that may be harmful to patients, record maintenance and fewer cases of mismatching infants. In addition, automatic data collection and transmission is vital in process automation, reduction of form processing timelines, automated procedure auditing as well as medical inventory management. Sensor devices allow functions centered on patients, particularly, in diagnosing conditions and availing real-time information about patients' health indicators [6].

Application domains in this sector include; being able to monitor a patient's compliance with prescriptions, telemedicine solutions, and alerts for patients' well-being. Thereby, sensors

can be applied to outpatient and inpatient patients, dental Bluetooth devices and toothbrushes that can give information after they are used and patient's surveillance. Other elements of IoT in this capacity include; RFID, Bluetooth, and Wi-Fi among others. These will greatly enhance measurement and monitoring techniques of critical functions like blood pressure, temperature, heart rate, blood glucose, cholesterol levels, and many others.

The applications of Internet of Things (IoT) and Internet of Everything (IoE) are further being extended through the materialization of the Internet of Nano-things (IoNT) [3]. The notion of IoNT, as the name implies, is being engineered by integrating Nano-sensors in diverse objects (things) using Nano networks. Medical application, as shown in Fig. 2, is one of the major focuses of IoNT implementations. Application of IoNT in human body, for treatment purposes, facilitates access to data from in situ parts of the body which were hitherto inaccessible to sense from or by using those medical instruments incorporated with bulky sensor size. Thus, IoNT will enable new medical data to be collected, leading to new discoveries and better diagnostics.

### C. Smart Agriculture and Water Management

According to [11], the IoT has the capacity to strengthen and enhance the agriculture sector through examining soil moisture and in the case of vineyards, monitoring the trunk diameter. IoT would allow to control and preserve the quantity of vitamins found in agricultural products, and regulate microclimate conditions in order to make the most of the production of vegetables and fruits and their quality. Furthermore, studying weather conditions allows forecasting of ice information, drought, wind changes, rain or snow, thus controlling temperature and humidity levels to prevent fungus as well as other microbial contaminants.

When it comes to cattle, IoT can assist in identifying animals that graze in open locations, detecting detrimental gases from animal excrements in farms, as well as controlling growth conditions in offspring to enhance chances of health and survival and so on. Moreover, through IoT application in agriculture, a lot of wastage and spoilage can be avoided through proper monitoring techniques and management of the entire agriculture field. It also leads to better electricity and water control.

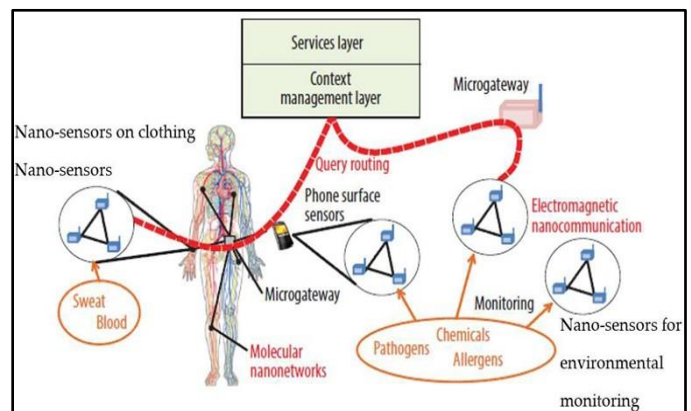


Fig. 2. The Internet of Nano-Things [3].



As [11] explain, in water management, the role of IoT includes studying water suitability in seas and rivers for both drinking and agriculture use, detecting pressure variations in pipes, and liquid presence outside tanks as well as monitoring levels of water variation in dams, rivers and reservoirs. These IoT applications utilize Wireless sensor networks. Examples of existing IoT applications in this domain include; SiSviA, GBROOS, and SEMAT.

#### D. Retail and Logistics

Executing the IoT in Supply Chain or retail Management has many benefits. Some include; observing storage conditions throughout the supply chain, product tracking to enable trace ability purposes, payment processing depending on the location or activity period in public transport, theme parks, gyms, and others. Inside the retail premises, IoT can be applied to various applications such as direction in the shop based on a preselected list, fast payment processes like automatically checking out with the aid of biometrics, detecting potential allergen products and controlling the rotation of products on shelves and warehouses in order to automate restocking procedures [12].

The IoT elements mostly used in this setting include; wireless sensor networks and radio frequency identification. In retail, there is a current use of SAP (Systems Applications and Products), while in logistics numerous examples include quality consignment conditions, item location, detecting storage incompatibility issues, fleet tracking among others. In the industry domain, IoT helps in detecting levels of gas and leakages within the industry and its environs, keeping track of toxic gases as well as the oxygen levels within the confines of chemical plants to ensure the safety of goods and workers and observing levels of oil, gases and water in cisterns and storage tanks. Application of IoT also assists in maintenance and repair because systems can be put in place to predict equipment malfunctions and at the same automatically schedule periodic maintenance services before there is a failure in the equipment. This can be achieved through the installation of sensors inside equipment or machinery to monitor their functionality and occasionally send reports.

#### E. Smart Living

In this domain, IoT can be applied in remote control devices whereby one can remotely switch appliances on and off hence preventing accidents as well as saving energy [1, 3]. Other smart home appliances include refrigerators fitted with LCD (Liquid Crystal Display) screens, enabling one to know what is available inside, what has over stayed and is almost expiring as well as what needs to be restocked. This information can also be linked to a smartphone application enabling one to access it when outside the house and therefore buy what is needed. Furthermore, washing machines can allow one to remotely monitor laundry. In addition, a wide range of kitchen devices can be interfaced through a smartphone, hence making it possible to adjust temperature, like in the case of an oven. Some ovens which have a self-cleaning feature can be easily monitored as well. In terms of safety in the home, IoT can be applied through alarm systems and cameras can be installed to monitor and detect window or door openings hence preventing intruders [3].

#### F. Smart Environment

The environment has a vital role within all aspects of life, from people, to animals, birds and also plants, are all affected by an unhealthy environment in one way or another. There have been numerous efforts to create a healthy environment in terms of eliminating pollution and reducing wastage of resources, but the existence of industries, as well as transportations wastes coupled with reckless and harmful human actions are common place elements which consistently damage the environment. Consequently, the environment requires smart and innovative ways to help in monitoring and managing waste, which provide a significant amount of data that forces governments to put in place systems that will protect the environment.

Smart environment strategies integration with IoT technology should be created for sensing, tracking and assessment of objects of the environment that offer potential benefits in achieving a sustainable life and a green world. The IoT technology allows observing and managing of air quality through data collection from remote sensors across cities and providing round the clock geographic coverage to accomplish better ways of managing traffic jams in major cities. Additionally, IoT technology can be applied in measuring pollution levels in water and consequently enlighten decisions on water usage. In waste management, which consists of various types of waste, like chemicals and pollutants being detrimental to the environment and to people, animals, and plants as well, IoT can also be applied. This can be achieved by environmental protection by means of controlling industrial pollution through instantaneous monitoring and management systems combined with supervision in addition to decision making networks. This serves to lessen waste [13].

In weather forecasting, IoT can be used to deliver a significant accuracy and high resolution for monitoring the weather by information sharing and data exchange. Through IoT technology, weather systems can collect information such as barometric pressure, humidity, temperature, light, motion and other information, from vehicles in motion and transmit the information wirelessly to weather stations. The information is attained by installing sensors on the vehicles and even on buildings after which it is stored and analyzed to assist in weather forecasting. Radiation is also a threat to the environment, human and animal health as well as agricultural productivity. IoT sensor networks can control radiation through constant monitoring of its levels, particularly around nuclear plant premises for detecting leakage and propagating deterrence.

### III. RESEARCH CHALLENGES

For all the above potential applications of IoT, there has to be proper feasibility into the different domains to ascertain the success of some applications and their functionality. As with any other form of technology or innovation, IoT has its challenges and implications that must be sorted out to enable mass adoption. Even though the current IoT enabling technologies have greatly improved in the recent years, there are still numerous problems that require attention, hence paving the way for new dimensions of research to be carried out. Since the IoT concept ensues from heterogeneous

technologies that are used in sensing, collecting, action, processing, inferring, transmitting, notifying, managing, and storing of data, a lot of research challenges are bound to arise. These research challenges that require attention have consequently spanned different research areas [14].

#### A. Privacy and Security

Owing to the fact that IoT has become a vital element as regards the future of the internet with its increased usage, it necessitates a need to adequately address security and trust functions. Researchers are aware of the weaknesses which presently exist in many IoT devices. Furthermore, the foundation of IoT is laid on the existing wireless sensor networks (WSN), IoT thus architecturally inherits the same privacy and security issues WSN possesses [3, 15]. Various attacks and weaknesses on IoT systems prove that there is indeed a need for wide ranging security designs which will protect data and systems from end to end. Many attacks generally exploit weaknesses in specific devices thereby gaining access into their systems and consequently making secure devices vulnerable [16, 17]. This security gap further motivates comprehensive security solutions that consist of research that is efficient in applied cryptography for data and system security, non-cryptographic security techniques as well as frameworks that assist developers to come up with safe systems on devices that are heterogeneous.

There is a need for more research to be conducted on cryptographic security services that have the capability to operate on resource constrained IoT devices. This would enable different skilled users to securely use and deploy IoT systems regardless of the inadequate user interfaces that are available with almost all IoT devices. In addition to the protection and security aspects of the IoT, additional areas like confidentiality in communication, trustworthiness, and authenticity of communication parties, and message integrity, and supplementary safety requirements should also be incorporated. These may include features like being able to prevent communication of various parties. As an example, in business transactions, smart objects must be prevented from facilitating competitors' access to confidential information in the devices and thus using this information maliciously.

#### B. Processing, Analysis and Management of Data

The procedure for processing, analysis and data management is tremendously challenging because of the heterogeneous nature of IoT, and the large scale of data collected, particularly in this era of Big Data [18]. Currently, most systems utilize centralized systems in offloading data and carrying out computationally intensive tasks on an international cloud platform. Nevertheless, there is a constant concern about conventional cloud architectures not being effective in terms of transferring the massive volumes of data that are produced and consumed by IoT enabled devices and to be able further support the accompanying computational load and simultaneously meet timing constraints [19]. Most systems are therefore relying on current solutions such as mobile cloud computing and fog computing which are both based on edge processing, to mitigate this challenge.

Another research direction as regards data management is applying Information Centric Networking (ICN) in the IoT. Since these information centric systems offer support in the efficient content retrieval and access to services, they appear to be quite valuable not just in accessing but also transferring as well as managing generated content and its transmission. This solution, however, brings about various challenges such as; how to extend the ICN paradigm competently over the fixed network edge, how to take in IoT's static and mobile devices as well as how to apportion the functionality of ICN on resource constrained devices [19].

Data analysis and its context not only plays a crucial role in the success of IoT, it also poses major challenges. Once data has been collected it has to be used intelligently in order to achieve smart IoT functions. Accordingly, the development of machine learning methods and artificial intelligence algorithms, resultant from neural works, genetic algorithms, evolutionary algorithms, and many other artificial intelligence systems are essential in achieving automated decision making.

#### C. Monitoring and Sensing

Even if technologies concerned with monitoring and sensing have made tremendous progress, they are constantly evolving particularly focusing on the energy efficiency and form aspect. Sensors and tags are normally expected to be active constantly in order to obtain instantaneous data, this aspect makes it essential for energy efficiency especially in lifetime extension. Simultaneously, new advances in nanotechnology/biotechnology and miniaturization have allowed the development of actuators and sensors at the Nano-scale.

#### D. M2M (Machine to Machine) Communication and Communication Protocols

While there are already existing IoT oriented communication protocols like Constrained Application Protocol (CoAP) and Message Queuing Telemetry Transport (MQTT), there is still no standard for an open IoT. Although all objects require connectivity, it is not necessary for every object to be made internet capable since they only need to have a certain capability to place their data on a particular gateway. Additionally, there are a lot of options in terms of suitable wireless technologies such as LoRa, IEEE 802.15.4, and Bluetooth even though it is not clear whether these available wireless technologies have the needed capacity to continue covering the extensive range of IoT connectivity henceforth.

The communication protocols for devices are the driving force in actualizing IoT applications, and they form the main support of data flow between sensors and the physical objects or outer world. While various MAC protocols have been projected for several domains with Frequency Division Multiple Access, Time Division Multiple Access and Carrier Sense Multiple Access (FDMA, TDMA and CSMA) for low traffic efficiency that is collision free, more circuitry in nodes are required respectively. The main objectives of the transport layer include guaranteeing an end-to-end reliability as well as performing end-to-end control of congestion. In this aspect, most protocols are unable to cooperate appropriate end to end reliability [20].

### E. Blockchain of Things (BCoT): Fusion of Blockchain and Internet of Things

Similar to IoT, blockchain technologies have also gained tremendous popularity since its introduction in 2018. Even though blockchain was first implemented as an underlying technology of Bitcoin cryptocurrency, it is now being used in multifaceted nonmonetary applications [21]. Miraz argues that both IoT and Blockchain can strengthen each other, in a reciprocal manner, by eliminating their respective inherent architectural limitations [22]. The underlying technology of IoT is WSN. Therefore, analogous to WSN, IoT also suffers from security and privacy issues. On the contrary, the primary reasons for blockchain's implementation trend in non-monetary applications is due to its inbuilt security, immutability, trust and transparency. These attributes are powered by blockchain's consensus approach and utilization of Distributed Ledger Technologies (DLTs) which require extensive dependency on participating nodes. Therefore, the fusion of these two technologies Blockchain and Internet of Things (IoT) conceives a new notion i.e. the Blockchain of Things (BCoT) where blockchain strengthens IoT by providing extra layer of security while the "things" of IoT can serve as participating nodes for blockchain ecosystems [22]. Thus, blockchain enabled IoT ecosystems will provide enhanced overall security [23] as well as benefit from each other.

### F. Interoperability

Traditionally as regards the internet, interoperability has always been and continues to be a basic fundamental value because the initial prerequisite in Internet connectivity necessitates that "connected" systems have the ability to "speak a similar language" in terms of encodings and protocols. Currently, various industries use a variety of standards in supporting their applications. Due to the large quantities and types of data, as well as heterogeneous devices, using standard interfaces in such diverse entities is very important and even more significant for applications which support cross organizational, in addition to a wide range of system limitations. Therefore, the IoT systems are meant towards being designed to handle even higher degrees of interoperability [24].

## IV. CONCLUSION

The IoT can best be described as a CAS (Complex Adaptive System) that will continue to evolve hence requiring new and innovative forms of software engineering, systems engineering, project management, as well as numerous other disciplines to develop it further and manage it the coming years. The application areas of IoT are quite diverse to enable it to serve different users, who in turn have different needs. The technology serves three categories of users, individuals, the society or communities and institutions. As discussed in the application section of this research paper, the IoT has without a doubt a massive capability to be a tremendously transformative force, which will, and to some extent does already, positively impact millions of lives worldwide. According to [25], this has become even more evident, as different governments around the world have shown an interest in the IoT concept by providing more funding in the field that is meant to facilitate further research. A good example is the Chinese Government.

Countless research groups have been, and continue to be, initiated from different parts of the world, and their main objective is to follow through IoT related researches. As more and more research studies are conducted, new dimensions to the IoT processes, technologies involved and the objects that can be connected, continue to emerge, further paving way for much more application functionalities of IoT. The fact that IoT is so expansive and affects practically all areas of our lives, makes it a significant research topic for studies in various related fields such as information technology and computer science. The paper highlights various potential application domains of the internet of things and the related research challenges.

## REFERENCES

- [1] M. H. Miraz, M. Ali, P. S. Excell, and R. Picking, "A Review on Internet of Things (IoT), Internet of Everything (IoE) and Internet of Nano Things (IoNT)", in 2015 Internet Technologies and Applications (ITA), pp. 219–224, Sep. 2015, DOI: 10.1109/ITechA.2015.7317398.
- [2] P. J. Ryan and R. B. Watson, "Research Challenges for the Internet of Things: What Role Can OR Play?," Systems, vol. 5, no. 1, pp. 1–34, 2017.
- [3] M. Miraz, M. Ali, P. Excell, and R. Picking, "Internet of Nano-Things, Things and Everything: Future Growth Trends", Future Internet, vol. 10, no. 8, p. 68, 2018, DOI: 10.3390/fi10080068.
- [4] E. Borgia, D. G. Gomes, B. Lagesse, R. Lea, and D. Puccinelli, "Special issue on" Internet of Things: Research challenges and Solutions", Computer Communications, vol. 89, no. 90, pp. 1–4, 2016.
- [5] K. K. Patel, S. M. Patel, et al., "Internet of things IOT: definition, characteristics, architecture, enabling technologies, application future challenges," International journal of engineering science and computing, vol. 6, no. 5, pp. 6122–6131, 2016.
- [6] S. V. Zanjali and G. R. Talmale, "Medicine reminder and monitoring system for secure health using IOT," Procedia Computer Science, vol. 78, pp. 471–476, 2016.
- [7] R. Jain, "A Congestion Control System Based on VANET for Small Length Roads", Annals of Emerging Technologies in Computing (AETiC), vol. 2, no. 1, pp. 17–21, 2018, DOI: 10.33166/AETiC.2018.01.003.
- [8] S. Soomro, M. H. Miraz, A. Prasanth, M. Abdullah, "Artificial Intelligence Enabled IoT: Traffic Congestion Reduction in Smart Cities," IET 2018 Smart Cities Symposium, pp. 81–86, 2018, DOI: 10.1049/cp.2018.1381.
- [9] Mahmud, S. H., Assan, L. and Islam, R. 2018. "Potentials of Internet of Things (IoT) in Malaysian Construction Industry", Annals of Emerging Technologies in Computing (AETiC), Print ISSN: 2516-0281, Online ISSN: 2516-029X, pp. 44-52, Vol. 2, No. 1, International Association of Educators and Researchers (IAER), DOI: 10.33166/AETiC.2018.04.004.
- [10] Mano, Y., Faical B. S., Nakamura L., Gomes, P. G. Libralon, R. Meneguete, G. Filho, G. Giancristofaro, G. Pessin, B. Krishnamachari, and Jo Ueyama. 2015. Exploiting IoT technologies for enhancing Health Smart Homes through patient identification and emotion recognition. Computer Communications, 89,90, (178-190). DOI: 10.1016/j.comcom.2016.03.010.
- [11] V. Sundareswaran and M. S. null, "Survey on Smart Agriculture Using IoT," International Journal of Innovative Research in Engineering & Management (IJIREM), vol. 5, no. 2, pp. 62–66, 2018.
- [12] P. Tadejko, "Application of Internet of Things in logistics-current challenges," Ekonomia i Zarz{a}dzanie, vol. 7, no. 4, pp. 54–64, 2015.
- [13] S. Rajguru, S. Kinhekar, and S. Pati, "Analysis of internet of things in a smart environment," International Journal of Enhanced Research in Man-agement and Computer Applications, vol. 4, no. 4, pp. 40–43, 2015.
- [14] H. U. Rehman, M. Asif, and M. Ahmad, "Future applications and research challenges of IOT," in 2017 International Conference on Informa-tion and Communication Technologies (ICICT), pp. 68–74, Dec 2017.

- [15] Z. Alansari, N. B. Anuar, A. Kamsin, M. R. Belgaum, J. Alshaer, S. Soomro, and M. H. Miraz, "Internet of Things: Infrastructure, Architecture, Security and Privacy", in 2018 International Conference on Computing, Electronics Communications Engineering (iCCECE), pp. 150–155, Aug 2018, DOI: 10.1109/iCCECOME.2018.8658516.
- [16] J. A. Chaudhry, K. Saleem, P. S. Haskell-Dowland, and M. H. Miraz, "A Survey of Distributed Certificate Authorities in MANETs," Annals of Emerging Technologies in Computing (AETiC), vol. 2, no. 3, pp. 11–18, 2018, DOI: 10.33166/AETiC.2018.03.002.
- [17] A. S. A. Daia, R. A. Ramadan, and M. B. Fayek, "Sensor Networks Attacks Classifications and Mitigation", Annals of Emerging Technologies in Computing (AETiC), vol. 2, no. 4, pp. 28–43, 2018, DOI: 10.33166/AETiC.2018.04.003.
- [18] Z. Alansari, N. B. Anuar, A. Kamsin, S. Soomro, M. R. Belgaum, M. H. Miraz, and J. Alshaer, "Challenges of Internet of Things and Big Data Integration", in Emerging Technologies in Computing (M. H. Miraz, P. Excell, A. Ware, S. Soomro, and M. Ali, eds.), (Cham), pp. 47–55, Springer International Publishing, 2018, DOI: 10.1007/978-3-319-95450-9\_4.
- [19] J. Cooper and A. James, "Challenges for database management in the internet of things" IETE Technical Review, vol.26, no.5, pp.320–329, 2009.
- [20] D. B. Ansari, A.-U. Rehman, and R. Ali, "Internet of Things (IoT) Protocols: A Brief Exploration of MQTT and CoAP," International Journal of Computer Applications, vol. 179, pp. 9–14, 03 2018.
- [21] M. H. Miraz and M. Ali, "Applications of Blockchain Technology beyond Cryptocurrency", Annals of Emerging Technologies in Computing (AETiC), vol. 2, no. 1, pp. 1–6, 2018, DOI: 10.33166/AETiC.2018.01.001.
- [22] Miraz, M.H., "Blockchain of Things (BCoT): The Fusion of Blockchain and IoT Technologies", Advanced Applications of Blockchain Technology, Studies in Big Data 60, 2019, DOI: 10.1007/978-981-13-8775-3\_7, [https://doi.org/10.1007/978-981-13-8775-3\\_7](https://doi.org/10.1007/978-981-13-8775-3_7).
- [23] Miraz, M. H. and Ali, M., 2018. Blockchain Enabled Enhanced IoT Ecosystem Security, Proceedings of the International Conference on Emerging Technologies in Computing 2018, London Metropolitan University, UK, Part of the Lecture Notes of the Institute for Computer Sciences, Social Informatics and Telecommunications Engineering (LNICST), vol. 200, pp. 38-46, Online ISBN: 978-3-319-95450-9, Print ISBN: 978-3-319-95449-3, Series Print ISSN: 1867-8211, Series Online ISSN: 1867-822X, DOI: 10.1007/978-3-319-95450-9\_3, Springer-Verlag, [https://link.springer.com/chapter/10.1007/978-3-319-95450-9\\_3](https://link.springer.com/chapter/10.1007/978-3-319-95450-9_3).
- [24] A. Mazayev, J. A. Martins, and N. Correia, "Interoperability in IoT Through the Semantic Profiling of Objects," IEEE Access, vol. 6, pp. 19379–19385, 2018.
- [25] R. Porkodi and V. Bhuvanawari, "The Internet of Things (IoT) Applications and Communication Enabling Technology Standards: An Overview," in 2014 International Conference on Intelligent Computing Applications, pp. 324–329, March 2014.

# Classification of Hand Movements based on Discrete Wavelet Transform and Enhanced Feature Extraction

Jingwei Too<sup>1</sup>, Abdul Rahim Abdullah<sup>2</sup>, Norhashimah Mohd Saad<sup>3</sup>

Fakulti Kejuruteraan Elektrik, Universiti Teknikal Malaysia Melaka, Melaka, Malaysia<sup>1,2</sup>

Fakulti Kejuruteraan Elektronik dan Kejuruteraan Komputer, Universiti Teknikal Malaysia Melaka, Melaka, Malaysia<sup>3</sup>

**Abstract**—Extraction of potential electromyography (EMG) features has become one of the important roles in EMG pattern recognition. In this paper, two EMG features, namely, enhanced wavelength (EWL) and enhanced mean absolute value (EMAV) are proposed. The EWL and EMAV are the modified version of wavelength (WL) and mean absolute value (MAV), which aims to enhance the prediction accuracy for the classification of hand movements. Initially, the proposed features are extracted from the EMG signals via discrete wavelet transform (DWT). The extracted features are then fed into the machine learning algorithm for classification process. Four popular machine learning algorithms include *k*-nearest neighbor (KNN), linear discriminate analysis (LDA), Naïve Bayes (NB) and support vector machine (SVM) are used in evaluation. To examine the effectiveness of EWL and EMAV, several conventional EMG features are used in performance comparison. In addition, the efficacy of EWL and EMAV when combine with other features are also investigated. Based on the results obtained, the combination of EWL and EMAV with other features can improve the classification performance. Thus, EWL and EMAV can be considered as valuable tools for rehabilitation and clinical applications.

**Keywords**—*Electromyography; feature extraction; discrete wavelet transform; classification; pattern recognition*

## I. INTRODUCTION

As a biomedical signal, electromyography (EMG) signal is playing an important role in developing the human machine interaction devices. Naturally, EMG signal recorded from the muscle contraction contains rich muscle information, which is beneficial in describing the muscle behavior and condition, as well as the hand movement [1], [2]. In recent days, the myoelectric control has been received much attentions from the biomedical researchers. The correlation between amplitude and motion grants the EMG signal to become one of the most powerful sources in controlling the prosthesis [3].

Thanks to current technology, the usage of pattern recognition based myoelectric control has become viable. Needless to say, the type of classifier does not significantly affect the classification performance, while the quality of extracted features has shown a great impact in EMG signals classification [4]. Without loss of generality, feature extraction is a technique to extract the valuable information from the signal itself, which should contain much information as possible [4], [5]. Feature extraction can be categorized into time domain (TD), frequency domain (FD) and time-frequency domain (TFD). Among the EMG features, TD features are the most commonly used. In a past study, Hudgins et al. [6]

introduced five EMG features for pattern recognition. The authors indicated that proposed features are good in discriminating the EMG patterns. Later, Khushaba et al. [7] developed a subset of features based on time-dependent spectral moments to classify the multiple hand movements at different limb positions. Moreover, Samuel et al. [8] proposed three new EMG features for arm movements classification. The author showed that proposed features outperformed other conventional features in EMG pattern recognition. However, TD features assume the EMG data from stationary signals and there is no frequency information provided [9]. On one hand, FD features only contains spectral information, in which the time information is limited. For these reasons, the TFD features are utilized in this work.

In the past studies, time-frequency methods such as short time Fourier transform (STFT) and wavelet transform (WT) are widely used in EMG signal processing [10]–[12]. However, STFT cannot provide satisfactory performance due to its fixed window size [13], [14]. From the previous works, it is reported that spectrogram or short time Fourier transform (STFT) was not very effective in EMG pattern recognition system [10], [13]. As compared to STFT, wavelet transform (WT) provides changeable time and frequency resolution, which is more formidable for extracting the high quality signal information [14]. In this regard, we focus on WT in current work.

Generally, WT decomposes the signal into detail and approximation coefficients at different sub-bands, in which the time information at different frequency ranges can be obtained [14]. Previous works indicated that the features extracted based on discrete wavelet transform (DWT) were showing good discriminate power in describing the target concept. Phinyomark et al. [15] extracted the mean absolute value (MAV) feature via DWT transformation for patterns classification. Doulah et al. [16] applied the DWT and root mean square (RMS) feature for neuromuscular diseases classification. Moreover, Xing et al. [9] proposed the wavelet packet node energy as the features for EMG pattern recognition. Previous findings showed that the feature extraction based on WT transformation was more capable in achieving a high classification performance.

Among the existing EMG features, wavelength (WL) and mean absolute value (MAV) are the most frequently used. This is mainly due to their efficiency and simplicity in EMG pattern recognition [1], [15]. Based on WL and MAV features, we propose the enhanced wavelength (EWL) and enhanced mean absolute value (EMAV) features in this paper. The proposed features are tested by using the EMG data acquired from the

publicly access EMG database. Four popular machine learning algorithms include  $k$ -nearest neighbor (KNN), Naïve Bayes (NB), linear discriminate analysis (LDA) and support vector machine (SVM) are used in evaluation. In addition, several conventional EMG features are used in performance comparison. Moreover, the effectiveness of EWL and EMAV when combine with other features are also investigated. The experimental results show that EWL and EMAV can be valuable tools for rehabilitation and clinical applications.

The organization of paper as follows: Section II describes the proposed EMG pattern recognition system. Meanwhile, the proposed feature extraction methods are also presented. Section III discusses the experimental results. At last, the conclusion is pointed in Section IV.

## II. MATERIAL AND METHOD

Fig. 1 illustrates the flow diagram of proposed EMG pattern recognition system. Firstly, the EMG signals are acquired from the publicly access EMG database. Afterward, DWT is applied to decompose the signals into multiresolution wavelet coefficients. Next, the features are extracted from each coefficient to form an EMG feature set. The feature set that consists of several features are then fed into the classifiers (machine learning algorithms) for the classification of six hand movement tasks.

### A. EMG Data

The EMG data is acquired from the sEMG for Basic Hand Movements Data Set via UCI Machine Learning Repository [17]. Note that only the first database is utilized in this work. This dataset consists of the EMG signals of six different hand movement tasks recorded from five healthy subjects (two males and three females). In the experiment, two channels were used in the process of recording. The subject was instructed to perform each hand movement for 6 seconds. Additionally, each movement was repeated for 30 times, and the EMG signals were sampled at 500 Hz [18]. The hand movement tasks are listed in Table I.

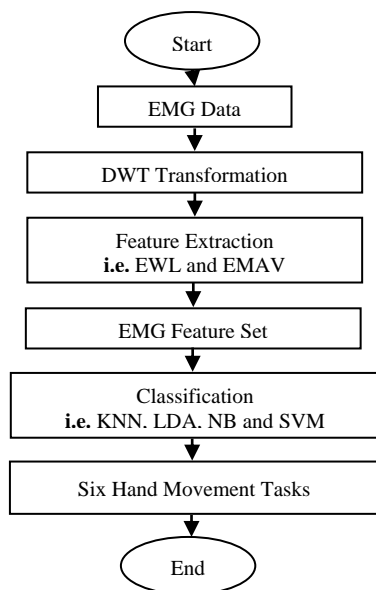


Fig. 1. Flow Diagram of Proposed EMG Pattern Recognition System.

TABLE I. LISTED HAND MOVEMENTS

| No | Hand movement task |
|----|--------------------|
| 1  | Spherical          |
| 2  | Tip                |
| 3  | Palmar             |
| 4  | Lateral            |
| 5  | Cylindrical        |
| 6  | Hook               |

### B. Discrete Wavelet Transform

Basically, EMG signal is presented in time domain (TD). However, in TD, the frequency and spectral information are limited. Thus, the time-frequency method is applied in this research. Due to the efficiency and reliable of discrete wavelet transform (DWT) in biomedical signal processing, the DWT has become our major focus in this work. Briefly, DWT decomposes the EMG signals into multiresolution wavelet coefficients, which exhibits the signal in both time and frequency representations. By this way, the extracted features contain the time information at different frequency sub-bands [19]. This in turn will improve the time-frequency information, thus leading to high prediction accuracy.

The wavelet decomposition involves two digital filters, which are low-pass and high-pass filters. Mathematically, the first decomposition level of DWT can be expressed as:

$$A[k] = \sum_n x[n] \cdot g[2k - n] \quad (1)$$

$$D[k] = \sum_n x[n] \cdot h[2k - n] \quad (2)$$

where  $x[n]$  represents the signal,  $D[k]$  is the detail and  $A[k]$  is the approximation. Note that detail and approximation are the outputs of high pass and low pass filters, respectively. The decomposition process is repeated until the desired level is satisfied [11], [20]. According to the findings in [21], the DWT with Biorthogonal 3.3 at fourth decomposition level is utilized in this paper. An illustration of wavelet decomposition of DWT at fourth decomposition level is shown in Fig. 2.

### C. Conventional Feature Extraction

Feature extraction is a process that reforms the raw EMG data into a reduced expression set of features. A quality feature shall comprise of meaningful information that can best describe the target concept in the classification process [22]. In this study, 14 popular and commonly used EMG features are utilized. These features are selected due to their simplicity and promising performances in previous works.

Mean absolute value (MAV) is one of the most popular EMG features, and it is defined as the average of the summation of absolute value of signal [6], [23]. MAV can be expressed as:

$$MAV = \frac{1}{L} \sum_{i=1}^L |x_i| \quad (3)$$

where  $x$  is the wavelet coefficient and  $L$  is the length of coefficient.

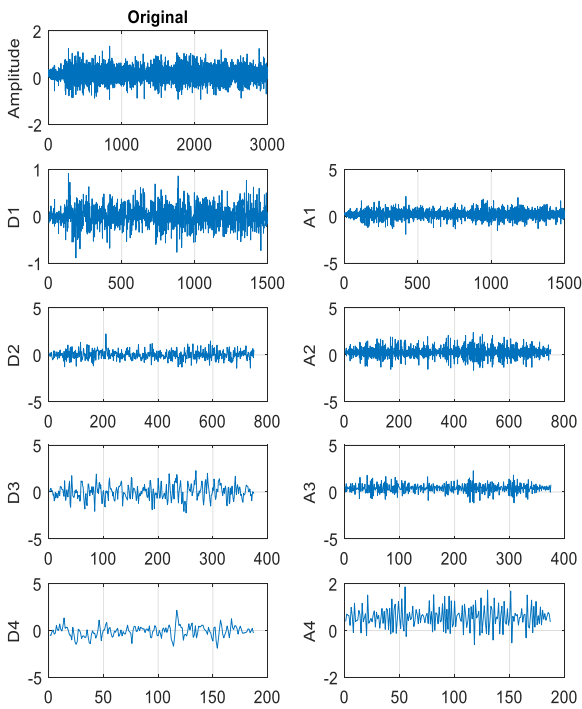


Fig. 2. Wavelet Decomposition of DWT at Fourth Decomposition Level.

Wavelength (WL) is another popular EMG feature, and it can be calculated by simplifying the cumulative length of waveform summation [6], [24]. The WL can be defined as:

$$WL = \frac{1}{L} \sum_{i=2}^L |x_i - x_{i-1}| \quad (4)$$

where  $x$  is the wavelet coefficient and  $L$  is the length of coefficient.

Zero crossing (ZC) is an EMG feature that measures the frequency information [6], [23]. Mathematically, ZC can be expressed as:

$$ZC = \sum_{i=1}^{L-1} f(x_i)$$

$$f(x_i) = \begin{cases} 1, & \text{if } \{(x_i > 0 \& x_{i+1} < 0) \mid (x_i < 0 \& x_{i+1} > 0)\} \\ & \& |x_i - x_{i+1}| \geq T \\ 0, & \text{otherwise} \end{cases} \quad (5)$$

where  $x$  is the wavelet coefficient,  $T$  is the threshold value and  $L$  is the length of coefficient.

Slope sign change (SSC) is a traditional EMG feature that determines the number of times in which the number of waveform changes sign [6], [23]. SSC can be calculated as:

$$SSC = \sum_{i=2}^{L-1} f(x_i)$$

$$f(x_i) = \begin{cases} 1, & \text{if } \{(x_i > x_{i-1} \& x_i > x_{i+1}) \mid (x_i < x_{i-1} \& x_i < x_{i+1})\} \\ & \& \{|x_i - x_{i+1}| \geq T \mid |x_i - x_{i-1}| \geq T\} \\ 0, & \text{otherwise} \end{cases} \quad (6)$$

where  $x$  is the wavelet coefficient,  $T$  is the threshold value and  $L$  is the length of coefficient.

Average amplitude change (AAC) is another popular EMG feature, and it can be formulated as [24]:

$$AAC = \sum_{i=1}^{L-1} |x_{i+1} - x_i| \quad (7)$$

where  $x$  is the wavelet coefficient and  $L$  is the length of coefficient.

Log detector (LD) is a feature that is good at estimating the exerted force, and it can be defined as [25]:

$$LD = \exp\left(\frac{1}{L} \sum_{i=1}^L \log(|x_i|)\right) \quad (8)$$

where  $x$  is the wavelet coefficient and  $L$  is the length of coefficient.

Root mean square (RMS) is one of the popular features which is useful in describing the muscle information [26]. In mathematics, RMS can be calculated as:

$$RMS = \sqrt{\frac{1}{L} \sum_{i=1}^L (x_i)^2} \quad (9)$$

where  $x$  is the wavelet coefficient and  $L$  is the length of coefficient.

Difference absolute standard deviation value (DASDV) is another frequently used EMG feature, and it can be expressed as [26]:

$$DASDV = \sqrt{\frac{\sum_{i=1}^{L-1} (x_{i+1} - x_i)^2}{L-1}} \quad (10)$$

where  $x$  is the wavelet coefficient and  $L$  is the length of coefficient.

Myopulse percentage rate (MYOP) is defined as the mean of Myopulse output in which the absolute value of EMG signal exceeds the pre-defined threshold value [24]. MYOP can be given as follows:

$$MYOP = \frac{1}{L} \sum_{i=1}^L f(x_i)$$

$$f(x_i) = \begin{cases} 1, & \text{if } x_i \geq T \\ 0, & \text{otherwise} \end{cases} \quad (11)$$

where  $x$  is the wavelet coefficient,  $T$  is the threshold value and  $L$  is the length of coefficient.

Willison amplitude (WA) is an EMG feature that acts as an indicator of the firing of motor unit potentials, and it can be computed as [25]:

$$WA = \sum_{i=1}^{L-1} f(x_i)$$

$$f(x_i) = \begin{cases} 1, & \text{if } |x_i - x_{i+1}| \geq T \\ 0, & \text{otherwise} \end{cases} \quad (12)$$

where  $x$  is the wavelet coefficient,  $T$  is the threshold value and  $L$  is the length of coefficient.

Simple square integral (SSI) is defined as the summation of square values of EMG signal amplitude, and it can be computed as [24]:

$$SSI = \sum_{i=1}^L (x_i)^2 \quad (13)$$

where  $x$  is the wavelet coefficient and  $L$  is the length of coefficient.

Variance of EMG signal (VAR) is good at measuring the signal power, and it can be expressed as [25]:

$$VAR = \frac{1}{L-1} \sum_{i=1}^L (x_i)^2 \quad (14)$$

where  $x$  is the wavelet coefficient and  $L$  is the length of coefficient.

Modified mean absolute value (MMAV) is an extension of MAV feature by assigning the weight window function. Mathematically, MMAV can be computed as [24]:

$$MMAV = \frac{1}{L} \sum_{i=1}^L w_i |x_i|$$

$$w_i = \begin{cases} 1, & \text{if } 0.25L \leq i \leq 0.75L \\ 0.5, & \text{otherwise} \end{cases} \quad (15)$$

where  $x$  is the wavelet coefficient and  $L$  is the length of coefficient.

Modified mean absolute value 2 (MMAV2) is another extension of MAV feature by assigning the continuous weight window function, and it can be expressed as [24]:

$$MMAV2 = \frac{1}{L} \sum_{i=1}^L w_i |x_i|$$

$$w_i = \begin{cases} 1, & \text{if } 0.25L \leq i \leq 0.75L \\ 4i/L, & \text{if } i < 0.25L \\ 4(i-L)/L, & \text{otherwise} \end{cases} \quad (16)$$

where  $x$  is the wavelet coefficient and  $L$  is the length of coefficient.

#### D. Proposed Enhanced Feature Extraction

In this paper, two features namely enhanced mean absolute value (EMAV) and enhanced wavelength (EWL) are proposed for EMG signals classification. In the first step, the motivation of this work is briefly explained. Fig. 3 demonstrates an example of EMG signal. As can be seen, most of the information is found within the middle region of the signal. On one hand, the signal presented at the early and final stages are

less informative due to slow reaction of the subject in the experiment.

To overcome the issues above, EMAV and EWL features are proposed. The proposed features are formulated as follows:

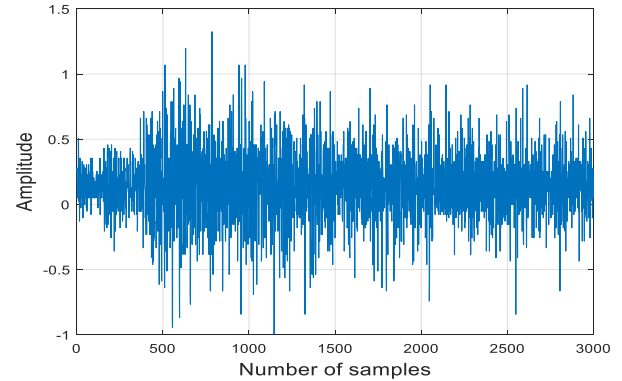


Fig. 3. Sample of EMG Signal.

#### Enhanced Mean Absolute Value (EMAV)

$$EMAV = \frac{1}{L} \sum_{i=1}^L |(x_i)^p|$$

$$p = \begin{cases} 0.75, & \text{if } i \geq 0.2L \text{ \& } i \leq 0.8L \\ 0.50, & \text{otherwise} \end{cases} \quad (17)$$

#### Enhanced Wavelength (EWL)

$$EWL = \sum_{i=2}^L |(x_i - x_{i-1})^p|$$

$$p = \begin{cases} 0.75, & \text{if } i \geq 0.2L \text{ \& } i \leq 0.8L \\ 0.50, & \text{otherwise} \end{cases} \quad (18)$$

where  $x$  is the wavelet coefficient and  $L$  is the length of the coefficient. As can be seen in Eq. (17) and (18), the parameter  $p$  is used to identify the influence of sample within the signal. In EMAV and EWL, a greater number of  $p$  is utilized for 20% to 80% of regions. This is because by strengthening the information content at the middle region, more valuable information can be obtained. In this way, the quality of features can be improved. Furthermore, it is seen that EMAV and EWL are the extension of MAV and WL with simple modification, and thus no much additional computational time is required in the evaluation.

#### E. Machine Learning Algorithm

After feature extraction, the EMG feature set is built. Four popular machine learning algorithms include  $k$ -nearest neighbor (KNN), Naïve Bayes (NB), linear discriminate analysis (LDA) and support vector machine (SVM) are employed to evaluate the effectiveness of proposed features in EMG pattern recognition. These machine learning algorithms are chosen due to their promising performances in previous works.

KNN is one of the famous learning algorithms, which performs faster than other modern algorithms in classification tasks [27]. Briefly, KNN is categorized into learning and



classification phases. The former gathers the training data for training work, whereas the latter predicts the test data with all the training data according to the  $k$  most similar training data [23]. In this work, the  $k$ -value of KNN is set at 1.

NB is a simple machine learning algorithm, and it is good at measuring the density of the dataset. Generally, NB employs the Bayes theorem to determine the probability of data by assuming all the features are independent [28]. It predicts the most probable class by examining the probability of test features. In this paper, NB with Gaussian kernel distribution is utilized.

LDA is the most robustness learning algorithm in EMG studies. Additionally, LDA is high speed training and computationally less expensive [29]. In LDA, the data is assumed to be normally distributed with equal covariance matrices. The main idea of LDA is to discriminate the observed features to the target class in which the posteriori probability can be maximized [25]. In this study, the LDA with pseudo-linear function is utilized.

SVM is a well-known and powerful learning algorithm in EMG pattern recognition. The general idea of SVM is to seek out the hyperplane that partitions the data into desired class in which the data is transformed into high dimensional space [30]. However, SVM is designed for binary class, but not the multi-class problems. Therefore, the SVM with one-versus-all approach and radial basis kernel (RBF) function is applied in this paper [31].

### III. RESULTS AND DISCUSSIONS

Remark, the features are extracted from the EMG signals via DWT transformation. For each feature type, 16 features (1 feature  $\times$  2 channels  $\times$  8 coefficients) are extracted from each movement from each subject. Afterward, the extracted features are fed into the KNN, NB, LDA and SVM for the classification process. In this work, 10-folds cross-validation method is applied. In 10-folds cross-validation manner, the data is equally divided into 10 folds, where each fold is used for testing in succession, and the remainder 9 folds are used to train the classifier. Finally, the mean accuracy obtained from 10 folds is recorded.

In the first part of the experiment, the performance of single feature (EWL and EMAV) is examined, and the result is compared with other 14 conventional EMG features. Table II outlines the average accuracy of 16 features over five subjects. Note that the best result for each classifier is bolded. From Table II, the average accuracy achieved by the proposed features (EMAV and EWL) were much better than other conventional features for all learning algorithms. From the result obtained, it can be inferred that EMAV and EWL are powerful features in EMG signals classification.

Among the KNN, NB, LDA and SVM, the optimal learning algorithm is found to be LDA, which contributed the highest classification accuracy in this work. Inspecting the result on LDA, it is seen that EMAV and EWL contributed competitive performance in current work. Consequently, EWL and EMAV scored high average accuracy of 95.11% and 96.89%. The result obtained indicates that EMAV and EWL

features were able to provide promising performance in this research.

In the second part of the experiment, the efficacy of the combination of EWL and EMAV with other features is investigated. Table III demonstrates the average accuracy of 14 different feature combinations over five subjects. In this table, the best result for each classifier is highlighted with bold text. As can be observe, instead of using a single feature, the combination of EWL and EMAV with other features can effectively improve the prediction accuracy. By applying LDA, it is seen that the combination of EWL+EMAV+MAV+WL contributed the optimal average accuracy in differentiating the six different hand movements. Moreover, it is observed that EMAV+EWL+ZC+SSC achieved the best average accuracy when KNN, NB and SVM are utilized. On the whole, it can be inferred that the combinations of EMAV and EWL with other features were beneficial in improving the classification performance of EMG pattern recognition system.

Based on the result obtained, the best average accuracy is achieved by using the proposed combined EMG feature set (EWL+EMAV+MAV+WL) with LDA classifier, 97.56%. In comparison with other conventional feature sets, the proposed feature set is highly capable in discriminating the EMG patterns, which leads to better classification result. On the other hand, the experimental results show the superiority of LDA against KNN, NB and SVM. This might because the extracted features consist of high linearity, thus resulting in high prediction accuracy.

TABLE II. AVERAGE ACCURACY OF 16 FEATURES OVER 5 SUBJECTS

| Feature | Average accuracy (%) |              |              |              |
|---------|----------------------|--------------|--------------|--------------|
|         | KNN                  | LDA          | SVM          | NB           |
| MAV     | 94.56                | 96.33        | 95.11        | 93.22        |
| WL      | 94.56                | 94.56        | 95.89        | 93.78        |
| ZC      | 94.22                | 95.11        | 95.00        | 92.56        |
| SSC     | 83.89                | 87.22        | 89.00        | 83.67        |
| AAC     | 92.56                | 94.56        | 94.44        | 93.78        |
| LD      | 90.22                | 91.78        | 92.78        | 91.56        |
| RMS     | 94.00                | 95.67        | 95.11        | 93.78        |
| DASDV   | 93.56                | 95.89        | 95.11        | 93.22        |
| MYOP    | 81.00                | 86.33        | 86.89        | 84.33        |
| WA      | 75.67                | 81.56        | 79.67        | 80.78        |
| SSI     | 93.00                | 90.00        | 94.78        | 92.44        |
| VAR     | 90.56                | 90.00        | 92.44        | 92.44        |
| MMAV    | 94.33                | 95.44        | 95.44        | 93.00        |
| MMAV2   | 91.44                | 93.56        | 93.56        | 92.11        |
| EWL     | <b>95.00</b>         | 95.11        | <b>96.22</b> | 93.56        |
| EMAV    | 94.67                | <b>96.89</b> | 96.11        | <b>93.89</b> |

TABLE III. AVERAGE ACCURACY OF 14 FEATURE COMBINATIONS OVER 5 SUBJECTS

| Feature combination | Average accuracy (%) |              |              |              |
|---------------------|----------------------|--------------|--------------|--------------|
|                     | KNN                  | LDA          | SVM          | NB           |
| EMAV+EWL            | 95.00                | 96.89        | 96.22        | 94.56        |
| EMAV+EWL+MAV+WL     | 94.44                | <b>97.56</b> | 96.22        | 94.22        |
| EMAV+EWL+SSC+ZC     | <b>96.00</b>         | 95.22        | <b>97.22</b> | <b>96.56</b> |
| EMAV+EWL+MYOP+WA    | 95.22                | 95.11        | 96.33        | 93.89        |
| EMAV+EWL+RMS+DASDV  | 95.00                | 96.67        | 96.22        | 94.78        |
| WL+MAV+SSC+ZC       | 95.33                | 96.11        | 96.78        | 96.44        |
| MYOP+WA+SSI         | 93.00                | 89.78        | 94.67        | 93.67        |
| MAV+WL+MYOP+WA      | 94.67                | 95.33        | 96.11        | 93.67        |

|                    |       |       |       |       |
|--------------------|-------|-------|-------|-------|
| MAV+MMAV+MMAV2     | 94.22 | 94.56 | 95.67 | 93.67 |
| AAC+LD+RMS+DASDV   | 94.22 | 96.11 | 95.22 | 94.00 |
| WL+MAV             | 94.56 | 96.33 | 95.89 | 94.11 |
| AAC+LD+MYOP+WA     | 77.00 | 94.22 | 81.00 | 92.78 |
| SSI+VAR+MMAV+MMAV2 | 93.00 | 95.44 | 94.67 | 93.56 |
| MYOP+WA            | 75.78 | 85.78 | 79.67 | 86.67 |

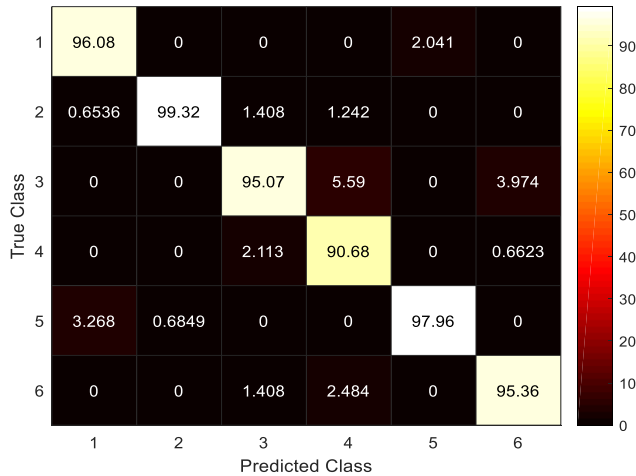


Fig. 4. Confusion Matrix of Combined Feature Set (EMAV+EWL+MAV+WL) with LDA over 5 Subjects (%).

Furthermore, the result of class-wise accuracy (accuracy of each hand movement task) is discussed. Fig. 4 illustrates the confusion matrix of proposed combined feature set (EMAV+EWL+MAV+WL) with LDA over five subjects. Note that the number 1 to 6 in both axes represents the hand movement types. From Fig. 4, it is observed that the tip movement (2<sup>nd</sup> hand movement task) has been perfectly recognized (99.32%), followed by cylindrical movement (97.96%). The results obtained evidently show the efficacy of EWL and EMAV in EMG signals classification. Hence, EWL and EMAV features can be appropriate choices for EMG feature extraction in clinical and rehabilitation applications.

#### IV. CONCLUSION

The quality of feature is one of the important factors that can greatly affect the accuracy in EMG signals classification. In this paper, two modified versions of WL and MAV features, namely EWL and EMAV are proposed for efficient EMG signals classification. The proposed features are tested with the EMG data of five healthy subjects, and the results are further compared with other conventional EMG features. In addition, the performance of the combinations of EWL and EMAV with other features are also investigated. Our results showed that the best classification performance was achieved by the LDA and combined feature set (EWL+EMAV+MAV+WL). In short, EWL and EMAV can be the valuable tools in EMG pattern recognition.

There are several limitations in this work. First, only five combinations of feature sets (with EMAV and EWL) are applied. However, it is worth noting that the combination of EMAV and EWAL with other EMG features can be also considered for performance enhancement. Second, the scope of this study is limited to one time-frequency method, DWT. However, other popular time-frequency methods such as wavelet packet transform (WPT) and empirical mode

decomposition (EMD) are also applicable to EMG signal processing. In the future, the EWL and EMAV can be extracted directly from EMG signals without performing the transformation. Therefore, more effective EMG pattern recognition system can be developed in future work.

#### ACKNOWLEDGMENT

The authors would like to thank the Ministry of Higher Education (MOHE), Malaysia for funding research under grant GLuar/STEVIA/2016/FKE-CeRIA/100009.

#### REFERENCES

- [1] Y. Gu, D. Yang, Q. Huang, W. Yang, and H. Liu, "Robust EMG pattern recognition in the presence of confounding factors: features, classifiers and adaptive learning," *Expert Syst. Appl.*, vol. 96, pp. 208–217, Apr. 2018.
- [2] M. F. Wahid, R. Tafreshi, M. Al-Sowaidi, and R. Langari, "Subject-independent hand gesture recognition using normalization and machine learning algorithms," *J. Comput. Sci.*, vol. 27, pp. 69–76, Jul. 2018.
- [3] N. Wang, K. Lao, X. Zhang, J. Lin, and X. Zhang, "The recognition of grasping force using LDA," *Biomed. Signal Process. Control*, vol. 47, pp. 393–400, Jan. 2019.
- [4] G. Gaudet, M. Raison, and S. Achiche, "Classification of Upper limb phantom movements in transhumeral amputees using electromyographic and kinematic features," *Eng. Appl. Artif. Intell.*, vol. 68, pp. 153–164, Feb. 2018.
- [5] Y. Ning and Y. Zhang, "A new approach for multi-channel surface EMG signal simulation," *Biomed. Eng. Lett.*, vol. 7, no. 1, pp. 45–53, Feb. 2017.
- [6] B. Hudgins, P. Parker, and R. N. Scott, "A new strategy for multifunction myoelectric control," *IEEE Trans. Biomed. Eng.*, vol. 40, no. 1, pp. 82–94, Jan. 1993.
- [7] R. N. Khushaba, M. Takruri, J. V. Miro, and S. Kodagoda, "Towards limb position invariant myoelectric pattern recognition using time-dependent spectral features," *Neural Netw.*, vol. 55, no. Supplement C, pp. 42–58, Jul. 2014.
- [8] O. W. Samuel et al., "Pattern recognition of electromyography signals based on novel time domain features for amputees' limb motion classification," *Comput. Electr. Eng.*, vol. 67, pp. 646–655, Apr. 2018.
- [9] K. Xing, P. Yang, J. Huang, Y. Wang, and Q. Zhu, "A real-time EMG pattern recognition method for virtual myoelectric hand control," *Neurocomputing*, vol. 136, no. Supplement C, pp. 345–355, Jul. 2014.
- [10] K. Englehart, B. Hudgins, P. A. Parker, and M. Stevenson, "Classification of the myoelectric signal using time-frequency based representations" *Med. Eng. Phys.*, vol. 21, no. 6, pp. 431–438, Jul. 1999.
- [11] A. Subasi, "Classification of EMG signals using combined features and soft computing techniques," *Appl. Soft Comput.*, vol. 12, no. 8, pp. 2188–2198, Aug. 2012.
- [12] J. Too, A. R. Abdullah, N. Mohd Saad, and N. Mohd Ali, "Feature Selection Based on Binary Tree Growth Algorithm for the Classification of Myoelectric Signals," *Machines*, vol. 6, no. 4, p. 65, Dec. 2018.
- [13] J. Too, A. R. Abdullah, N. M. Saad, N. M. Ali, and T. N. S. T. Zawawi, "Exploring the Relation Between EMG Pattern Recognition and Sampling Rate Using Spectrogram," *J. Electr. Eng. Technol.*, vol. 14, no. 2, pp. 947–953, Mar. 2019.
- [14] M. R. Canal, "Comparison of Wavelet and Short Time Fourier Transform Methods in the Analysis of EMG Signals," *J. Med. Syst.*, vol. 34, no. 1, pp. 91–94, Feb. 2010.
- [15] A. Phinyomark, C. Limsakul, and P. Phukpattaranont, "Application of Wavelet Analysis in EMG Feature Extraction for Pattern Classification," *Meas. Sci. Rev.*, vol. 11, no. 2, pp. 45–52, 2011.
- [16] A. B. M. S. U. Doulah, S. A. Fattah, W. P. Zhu, and M. O. Ahmad, "Wavelet Domain Feature Extraction Scheme Based on Dominant Motor Unit Action Potential of EMG Signal for Neuromuscular Disease Classification," *IEEE Trans. Biomed. Circuits Syst.*, vol. 8, no. 2, pp. 155–164, Apr. 2014.

- [17] "UCI Machine Learning Repository." Website: <https://archive.ics.uci.edu/ml/index.php>.
- [18] C. Sapsanis, G. Georgoulas, A. Tzes, and D. Lymberopoulos, "Improving EMG based classification of basic hand movements using EMD," in 2013 35th Annual International Conference of the IEEE Engineering in Medicine and Biology Society (EMBC), 2013, pp. 5754–5757.
- [19] A. Subasi, "Classification of EMG signals using PSO optimized SVM for diagnosis of neuromuscular disorders," *Comput. Biol. Med.*, vol. 43, no. 5, pp. 576–586, Jun. 2013.
- [20] E. Gokgoz and A. Subasi, "Comparison of decision tree algorithms for EMG signal classification using DWT," *Biomed. Signal Process. Control*, vol. 18, pp. 138–144, Apr. 2015.
- [21] J. Too, A. R. Abdullah, and N. M. Saad, "A Comparative Analysis of Wavelet Families for the Classification of Finger Motions," *Int. J. Adv. Comput. Sci. Appl. IJACSA*, vol. 10, no. 4, 2019.
- [22] A. Phinyomark, F. Quaine, S. Charbonnier, C. Serviere, F. Tarpin-Bernard, and Y. Laurillau, "EMG feature evaluation for improving myoelectric pattern recognition robustness," *Expert Syst. Appl.*, vol. 40, no. 12, pp. 4832–4840, Sep. 2013.
- [23] W.-T. Shi, Z.-J. Lyu, S.-T. Tang, T.-L. Chia, and C.-Y. Yang, "A bionic hand controlled by hand gesture recognition based on surface EMG signals: A preliminary study," *Biocybern. Biomed. Eng.*, vol. 38, no. 1, pp. 126–135, Jan. 2018.
- [24] A. Phinyomark, P. Phukpattaranont, and C. Limsakul, "Feature reduction and selection for EMG signal classification," *Expert Syst. Appl.*, vol. 39, no. 8, pp. 7420–7431, Jun. 2012.
- [25] D. Tkach, H. Huang, and T. A. Kuiken, "Study of stability of time-domain features for electromyographic pattern recognition," *J. NeuroEngineering Rehabil.*, vol. 7, p. 21, May 2010.
- [26] K. S. Kim, H. H. Choi, C. S. Moon, and C. W. Mun, "Comparison of k-nearest neighbor, quadratic discriminant and linear discriminant analysis in classification of electromyogram signals based on the wrist-motion directions," *Curr. Appl. Phys.*, vol. 11, no. 3, pp. 740–745, May 2011.
- [27] L.-Y. Chuang, C.-H. Yang, and J.-C. Li, "Chaotic maps based on binary particle swarm optimization for feature selection," *Appl. Soft Comput.*, vol. 11, no. 1, pp. 239–248, Jan. 2011.
- [28] P. A. Karthick, D. M. Ghosh, and S. Ramakrishnan, "Surface electromyography based muscle fatigue detection using high-resolution time-frequency methods and machine learning algorithms," *Comput. Methods Programs Biomed.*, vol. 154, no. Supplement C, pp. 45–56, Feb. 2018.
- [29] D. Rivela, A. Scannella, E. E. Pavan, C. A. Frigo, P. Belluco, and G. Gini, "Analysis and Comparison of Features and Algorithms to Classify Shoulder Movements From sEMG Signals," *IEEE Sens. J.*, vol. 18, no. 9, pp. 3714–3721, May 2018.
- [30] A.-C. Tsai, J.-J. Luh, and T.-T. Lin, "A novel STFT-ranking feature of multi-channel EMG for motion pattern recognition," *Expert Syst. Appl.*, vol. 42, no. 7, pp. 3327–3341, May 2015.
- [31] T. Lorrain, N. Jiang, and D. Farina, "Influence of the training set on the accuracy of surface EMG classification in dynamic contractions for the control of multifunction prostheses," *J. NeuroEngineering Rehabil.*, vol. 8, p. 25, May 2011.

# Modified Graph-theoretic Clustering Algorithm for Mining International Linkages of Philippine Higher Education Institutions

Sheila R. Lingaya<sup>1</sup>, Bobby D. Gerardo<sup>2</sup>, Ruji P. Medina<sup>3</sup>  
Technological Institute of the Philippines - Quezon City, Philippines<sup>1,3</sup>  
Tarlac Agricultural University<sup>1</sup>  
West Visayas State University<sup>2</sup>

**Abstract**—Graph-theoretic clustering either uses limited neighborhood or construction of a minimum spanning tree to aid the clustering process. The latter is challenged by the need to identify and consequently eliminate inconsistent edges to achieve final clusters, detect outliers and partition substantially. This work focused on mining the data of the International Linkages of Philippine Higher Education Institutions by employing a modified graph-theoretic clustering algorithm with which the Prim's Minimum Spanning Tree algorithm was used to construct a minimum spanning tree for the internationalization dataset infusing the properties of a small world network. Such properties are invoked by the computation of local clustering coefficient for the data elements in the limited neighborhood of data points established using the von Neumann Neighborhood. The overall result of the cluster validation using the Silhouette Index with a score of .69 indicates that there is an acceptable structure found in the clustering result – hence, a potential of the modified MST-based clustering algorithm. The Silhouette per cluster with .75 being the least score means that each cluster derived for  $r=5$  by the von Neumann Neighborhood has a strong clustering structure.

**Keywords**—MST-based clustering; Small World Network; von Neumann Neighborhood; internationalization; Prim's MST

## I. INTRODUCTION

Internationalization and partnership development undertakings pave way to establish identity in the international arena. As such, data in the field of internationalization as mirrored by students and international partnerships established by education institutions is growing to be a good interest of researches [1]–[4]. This is since the rate of internationalization increases with the unhindered channels of communications and affordable travel expenses. Universities seek to seize the opportunities from global partnerships and foster relationships with other organizations or institutions. Internationalization is also described to transform into mainstream strategy in higher educations and is increasingly seen as adding value to the life of universities through improving their quality [5]. The definition of internationalization being the process of integrating international, intercultural, or global dimensions into the purpose, functions or delivery of post-secondary education [6] is by common knowledge, the most frequently cited and widely accepted.

Meanwhile, methods and techniques in data mining allow analysis of very large datasets (i.e. big data) to extract and discover previously unknown structures and relations out of huge amount of details [7] for the purpose of knowledge extraction. As such, clustering in the data mining arena aims to establish high intra-cluster and low inter-cluster similarity in data. The high intra-cluster similarity should be based on the derived measurement from the data while the low inter-cluster similarity should maintain that elements in the different clusters should have maximum distance. These are intended to achieve beneficial knowledge from the data [8] for decision making and strategizing. Among different types of clustering, the most conventional distinction is whether the set of clusters is hierarchical or partitional [9] where hierarchical is a set of nested clusters while partitional clustering divides the set of data objects into non-overlapping clusters such that each object is in exactly a single cluster [10]. However in the real world, clusters come in arbitrary shapes, varied densities and unbalanced sizes that is why there is no universal clustering method which can deal with all problems [11].

Since most clustering algorithms' performance is affected by the shape and size of the detectable clusters [12], the requirement of an *a priori* knowledge about the actual number of clusters and the setting of a threshold to obtain adequate clustering results; a number of modifications to the clustering algorithms have emerged and are being explored to cope with said problems. Among which are graph-theoretic or graph-based clustering algorithms where data is represented in an undirected graph denoted as  $G=\{V,E\}$  where the set of all data points is  $V$  and the set of connections between two distinct data objects (i.e. edges or links are contained in  $E$ . This is associated with a distance measure resulting to a connected subgraph or clusters. The use of Minimum Spanning Tree (MST) is one of said methods which either uses the Prim's [13]–[15] or Kruskal's [16], [17]. An MST is constructed for the whole data with a threshold value being set along with a number of steps to terminate the process to form clusters resulting from removing an inconsistent edge whose value is greater than the threshold value. However, this strategy is constrained by the identification and elimination of the inconsistent edge [17], detection of outliers [18], as well as insufficiently evidenced partitioning—hence, having the same weaknesses as other clustering methods that are based on distance measures [19].

This work aims to perform data mining in the data of the international linkages of Philippine Higher Education Institutions (PHEIs) using a proposed modified Prim's MST-based clustering algorithm producing a minimum spanning tree for the dataset infusing the computation of local clustering coefficient for the data points in the limited neighborhood generated by von Neumann Neighborhood.

This paper is organized as follows. Section II presents the conceptual framework of the modified Prim's MST-based clustering algorithm invoking the properties of the small-world network of graph theory. It also highlights the preparation of the International Linkages data. Section III includes the results of the simulation and the cluster validation. Section IV highlights the conclusions and future works of the study.

## II. MODIFIED PRIM'S MST-BASED CLUSTERING ALGORITHM

Clustering can be used on many problems as it is helpful to seek and see relationships. It aims to congregate into clusters unlabeled data elements with high similarity based on a measure obtained solely from the data itself [20]. The distance measure defines the radius of membership depending on the type of data on hand. A good cluster is associated with high clustering value in terms of distance so the selection of distance metric is essential in clustering [21] while another clustering algorithm approach is to represent a target data set as a weighted undirected graph [20].

### A. Prim's MST-based Clustering Algorithm

Prim's MST Algorithm uses a distance function to specify the closeness of data objects to establish the weight between them by choosing an arbitrary point to the next adjacent point of minimum weight. For clustering, an edge inconsistency measure is defined to identify an inconsistent edge to be removed to partition the whole dataset into clusters. Prim's MST is modified for efficient construction of spanning tree based on the k-nearest neighbor search mechanism during which a new edge weight is defined to maximize the intra-cluster similarity and minimize the inter-cluster similarity [13]. The algorithm can be used for a complete graph while using Fibonacci Heap [19], [22].

In this work, the traditional Prim's MST Algorithm for clustering defined by [18] as shown in Fig. 1 is modified by infusing the local neighborhood search by the von Neumann Neighborhood in order to facilitate the computation of the local clustering coefficients of the data elements in said neighborhood.

Higher clustering coefficient indicates the robustness on an average shortest path between any pair of nodes [23]–[25]. As such, small world networks [26] have the properties of having a small mean of shortest path length and high clustering coefficient. The Local Clustering Coefficient (LCC) quantifies the closeness of the neighbors of a vertex in becoming a clique. A concept in graph theory, LCC is basically computed as the number of triangles connected to a vertex over the number of

triples around a given vertex. It is the probability that duos of neighbors of a vertex are connected by an immediate connection – the value is  $0 \leq LCC \leq 1$ . Thus,

$$LCC = \frac{\text{number of connected neighbors}}{\text{number of neighbors}} \quad (1)$$

Meanwhile, the von Neumann Neighborhood is one of the most commonly used types of neighborhood for cellular automata of two dimensions [27]. It is also used in pattern generation [28] and operations research [29] as it has been proven to have better performance than other topologies to further improve the quality of local search [30]. It can be extended by taking the set of data objects at Manhattan distance  $r$  where  $r > 1$  which yields a result of a diamond-shaped region – hence, the neighborhood of data objects. The two-dimensional square lattice is composed of the central cell and the four adjacent cells around achieved through traversing North, East, West and South (NEWS) derived at a Manhattan distance 1. The number of neighbors (i.e. cells) in 2-dimensional by von Neumann Neighborhood of the cellular evolutionary algorithm for range  $r$  is defined as:

$$2r(r + 1) + 1 \quad (2)$$

As such, the modified Prim's MST-based Clustering Algorithm establishes the adjacency of the data facilitated by the suitable cellular automaton, the von Neumann Neighborhood which simulates the establishment of neighborhood. This precludes the computation of local efficiency or local clustering coefficient. Thus, the modified Prim's MST construction for clustering is defined by  $(u, v, LCC(v), d(u,v))$  such that  $u$  is the initial data point and  $v$  is the terminal data point.

While the traditional Prim's MST considers only the next minimum distance  $d(u,v)$  between data  $u$  in the MST being built  $T$  and the adjacent data point  $v$  in  $V$ ; the modified algorithm initially considers the LCC of the adjacent data point  $LCC(v)$  to ensure a high clustering coefficient for the whole cluster – hence, pursuing clusters of density. As Prim grows the MST one edge at a time, it should be noted that the next candidate edge or connection of data point must respect the partition or cut of the set of points in the minimum spanning tree  $T$  and  $V$  to avoid having a cycle.

```
Pseudocode for FMST for Clustering  
  
procedure MST Clustering (V: set of data points v )  
construct a fully connected graph G of V such that  
the  
    edge weights are the distances between data  
    points  
construct Prim's minimum spanning tree T of G  
maintain disjoint sets V and T  
select minimum d(v,u) where v ∈ V and u ∈ V  
check for cycle  
find all inconsistent edges of T  
remove inconsistent edges to get a set of connected  
    components  
define the connected components as clusters
```

Fig. 1. Prim's Minimum Spanning Tree for Clustering.

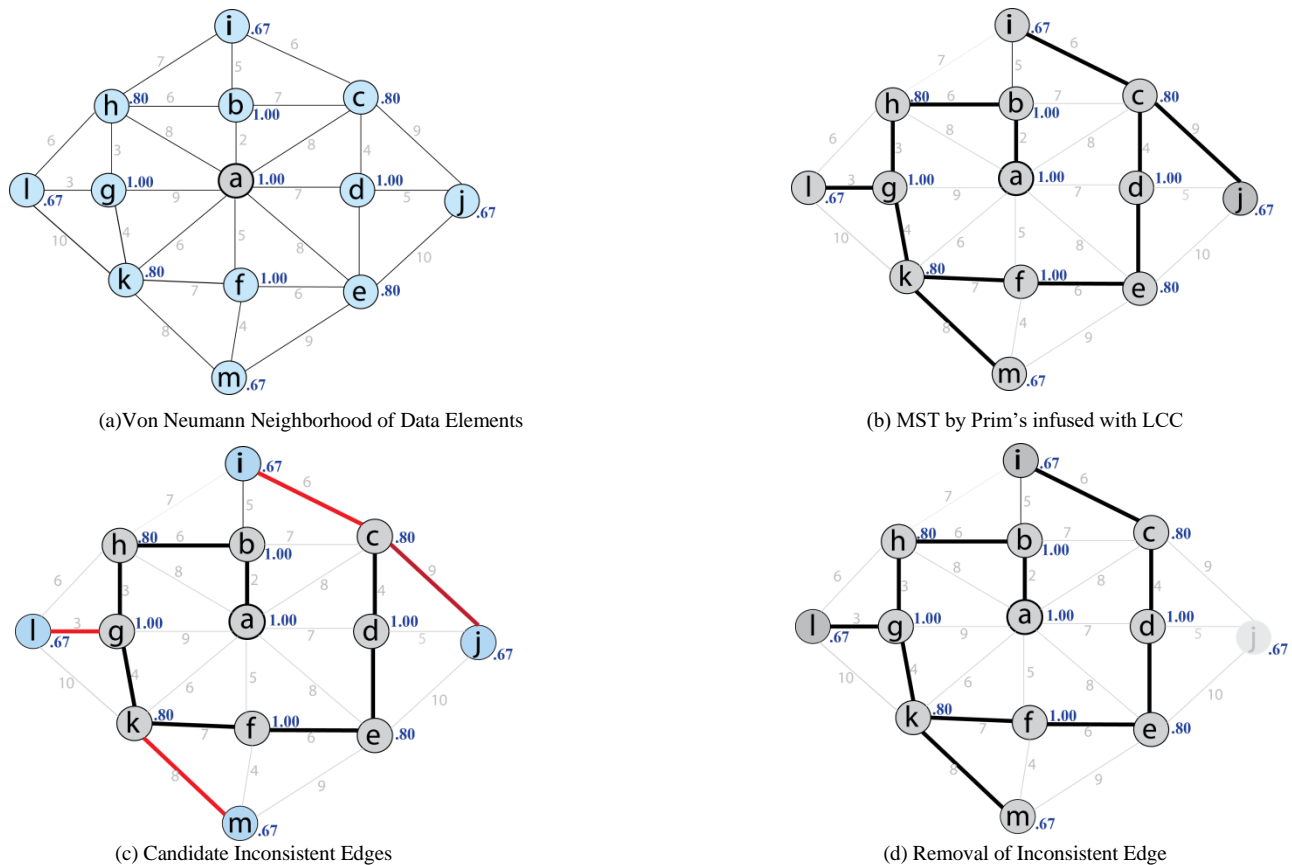


Fig. 2. Prim's Minimum Spanning Tree Construction for a Local Neighborhood Established using Von Neumann.

Being the data element having the least  $LCC(v)$  and maximum distance  $d$  is the criterion set for identifying the inconsistent edge. Data elements  $l, j, k$  and  $m$  in Fig. 2(a) are all  $LCC=.67$  – hence, their distances to the data points in the MST were considered as indicated in Fig. 2(b). As such,  $d(c,j)=9$  indicated in Fig. 2(c) as the connection with the greatest distance is the inconsistent edge. The algorithm will herein iterate and continue on the other data points of the data set. The resulting MST must have  $N-1$  edges for  $N$  number of data points without cycle – hence, the cluster as seen in Fig. 2(d).

**B. Data Cleaning and Preparation**

The PHEI International Linkages data contains the actual and essential records for the international linkages of Philippine Higher Education Institutions. It is consist of partnerships entered by PHEIs with foreign universities and/or organizations transpiring into different internationalization activities including student exchange, faculty exchange, academic collaboration, research collaboration and other activities across different disciplines. The dataset is summarized in Table I.

An integral part of the data mining process is the data to which knowledge discovery is applied. The International Linkages data contains instances of inconsistencies, incompleteness and variations in the essence of data mining. As such, entries or values were simplified and prepared such that the proposed algorithm is able to process it. In the original

data, the field for partnership form has duplicative entries and no defined options. A particular discipline is mentioned in several groups with each specific to a particular partnership. A similar case can be observed with an area of partnership (e.g. Faculty Exchange) being included and specific in a number of partnerships. Hence, in Table II are the disintegrated attributes rooted from the form of linkages attribute of the original data.

TABLE I. LIST OF PHEI LINKAGES DATASET FEATURES AND DESCRIPTION

| Name         | Definition   | Example          |
|--------------|--|------------------|
| country      | where foreign university or organization partnered is located            | Indonesia        |
| continent    | where country of foreign university or organization partnered is located | Asia             |
| phei         | the Philippine Higher Education Institution (e.g. SUC, HEI)              | TAU              |
| partner      | name foreign university or organization partnered                        | CRRU             |
| p_form       | form of partnership  | Bilateral        |
| p_area       | area of internationalization activities                                  | Faculty Exchange |
| p_discipline | field of discipline covered by the partnership                           | Education        |
| d_signed     | date when partnership was signed   | 02/06            |
| p_year       | year when partnership was signed   | 2017             |
| p_status     | if active or inactive  | Active           |

TABLE II. CONTENT RELATED FEATURE OF ATTRIBUTES DISINTEGRATED FROM FIELD

| Name         | Definition   |
|--------------|--|
| p_type       | Bilateral; Multilateral  |
| p_area       | Faculty Exchange; Student Exchange; Research(er) Exchange/Collaboration; Academic Collaboration; Joint Publication |
| p_discipline | Accounting, Arts, Education, Fashion and Textiles, Social Studies  |

The conversion of the textual values was necessary since most instances are texts and multiple values are specific to one entry. The data cleaning and preparation executed is where each distinct group is coded. For instance, in the area of partnership terms, the PHEI can either use its own nomenclature but certainly, it may also use the terms of reference by the prospect foreign partner university or organization. Hence, all attributes were coded and assigned a numerical value to discretize the data so that the clustering algorithm will be able to process it.

### III. RESULTS AND DISCUSSION

The cluster analysis of the data on international linkages of PHEIs aimed to gain valuable insights of the data to see what groups the data elements belong to while having the modified clustering algorithm to define instances with similar properties as a group. Data may come into mix type in the real world such that one attribute may be expressed in ration and others in terms of categorical that adjustment may be hard in terms of the algorithm because some specific algorithms can only be applicable to certain types of data. There may be a need for some data transformation or preprocessing to do so that the algorithm will work. Data cleaning and preprocessing was an integral part of the data mining process to make adjustments and the data be made suitable with the proposed algorithm as it cleaned and prepared the data for the algorithm to be able to process it.

#### A. Simulation

The algorithm was implemented through the following Pseudocode in Fig. 3 and simulated on the discretized Internationalization data set.

```
Pseudocode for Modified Prim's MST-based Clustering with Local Efficiency  
  
procedure MST Clustering (V: set of data points v )  
  Remove all redundant data  
  set arbitrary data point  
  get arbitrary data point's Neighborhood  
  generate connection for each data point in neighborhood;  
  set LCC for each data point in neighborhood  
  construct Prim's minimum spanning tree T of G  
  maintain disjoint sets V and T  
  set data point with least LCC and maximum distance as  
  inconsistent edge  
  remove inconsistent edges to get a set of connected  
  components  
  define the connected components as clusters
```

Fig. 3. Modified Prim's MST-based Clustering with Local Efficiency.

The International Linkages data set is composed of 12 attributes with 748 instances. With a random value  $r=5$ , seven clusters were generated. The attributes with only at most 2 possible values were not used for the experiment.

Two attributes (e.g. continent, pheI) were used to define an instance-hence to illustrate, data point  $(x, y)$  defines one data element by its value on attributes continent and pheI as  $x$  and  $y$ , respectively. The neighborhood of said data points determined by NEWS was derived with the nearest higher value in  $x$  for north, nearest lower value in  $x$  for south, nearest higher value in  $y$  for east, and nearest lower value in  $y$  for south until the prescribed number of neighbors of the arbitrarily chosen value through von Neumann's Neighborhood is derived.

An observation on the result of the presented data mining procedure is that the generation of edge or connection between the data points to form the neighborhood impacts the processing time of the algorithm. The complexity of this part of the modified algorithm is also challenged when the data points are not linear. The choice of value for  $r$  also is also critical as a minimum choice will produce more clusters which impact the inter-cluster separation.

#### B. Cluster Validation

As there is no optimal clustering algorithm [31], it is necessary to evaluate the generated clusters of the mining process on the International Data. One approach is an internal validation with which the concentration is the partitioned data such that the compactness and separation of the clusters are measured. The Silhouette index [32] is where the silhouettes show which objects lie well within their partition and which are somewhere between clusters. The silhouettes herein were formed basically by knowing the clusters or partitions generated by the modified clustering algorithm and the distance between the data points-hence, a data point  $i$ 's distance to other points within the cluster it belongs to and to other data points in other clusters.

The average distance  $a(i)$  of a data point  $i$  to all other objects in the cluster it belongs to is computed in the same manner that the average distance  $b(i)$  to other objects in other clusters is also derived. Hence, the silhouette score is derived as:

$$s(i) = \frac{b(i)-a(i)}{\max\{a(i),b(i)\}} \quad (3)$$

The Silhouette index is chosen for the validation of the resulting clusters of the proposed graph-theoretic clustering algorithm in order to observe how well the algorithm partitioned the data set [33]. The focus is also on the quality of the clustering structure being measured only using information or feature intrinsic to the data set [34]. Another salient point in choosing the Silhouette index for cluster validity is because it measures attributes taken from the data, itself and the clusters found [35]. The silhouette scores ranging from  $-1 \leq s(i) \leq 1$  can be interpreted in Table III.

The validation on the clustering result generated by the modified graph-theoretic clustering algorithm infused with small-world network structure based on the Silhouette score is presented in Table IV which presents the silhouette score of the clustering result. The average intra-cluster distance was derived

from calculating the distance of a random point (x, y) in a cluster towards all other data points in the same cluster to which it belongs to. Inter-cluster distance is the distance of this (x, y) towards the other data points in other clusters.

TABLE III. SILHOUETTE SCORE INTERPRETATION

| Range       | Description     | Interpretation                             |
|-------------|-----------------|--|
| 0.71 – 1.00 | Strong          | A strong structure has been found.         |
| 0.51 – 0.70 | Reasonable      | Reasonable structure has been found.       |
| 0.26 – 0.50 | Weak            | Structure is weak and could be artificial. |
| ≤ 0.25      | Not Substantial | No substantial structure has been found.   |

TABLE IV. SILHOUTTE VALIDATION ON CLUSTERING RESULT

| Cluster ID | Average Intra-Cluster Distance | Average Inter-Cluster Distance | Silhouette Score |
|------------|--------------------------------|--------------------------------|------------------|
| 1          | 2.57                           | 14.65                          | 0.81             |
| 2          | 2.46                           | 9.65                           | 0.75             |
| 3          | 3.09                           | 15.82                          | 0.80             |
| 4          | 3.20                           | 19.83                          | 0.84             |
| 5          | 2.86                           | 16.64                          | 0.83             |
| 6          | 2.70                           | 15.82                          | 0.83             |
| 7          | -                              | 15.11                          | 0.00             |

The average Silhouette score derived as 0.69 indicates an acceptable structure was found which is also manifested in the scores of all the clusters which derived scores not lower than 0.75 which means that each cluster has a strong structure except for Cluster 7 which has only one (1) data point – hence, silhouette score is 0. Such constraint is present to prevent the number of groups from significantly increasing [36]. Consequently, when a clustering result is interpreted based on Table III, the clustering is acceptable when the score is at least 0.50 [37].

#### IV. CONCLUSION

This work performed data mining in the international linkages of Philippine Higher Education Institutions (PHEIs) data using a proposed modified Prim’s MST-based clustering algorithm producing a minimum spanning tree for the data set infusing the computation of local clustering coefficient for the data points in the limited neighborhood generated by von Neumann’s Neighborhood.

An integral part of this work was the preparation of the raw data to achieve the dataset that is ready for processing by the modified Prim’s MST-based clustering algorithm. The numerical attributes of the International Linkages dataset were used for the clustering to work on similarity on a particular parameter.

The results of the study show that there is an acceptable structure found in the clustering result with silhouette score 0.69 and 0.75 being the least score for the 6 out of 7 clusters derived for r=5 of the von Neumann Neighborhood.

However, the algorithm is still bound by the *a priori* input value of r which dictates the number of possible neighbors in one cluster for the von Neumann Neighborhood. As such the

optimum number of clusters and most ideal value of r for a particular size of data are interesting.

Also for future works, the interest is also centered on the cluster validation utilizing external validity indices particularly those which works or are specific to graph-theoretic clustering algorithms. The data can also be refined more and subjected to clustering process to compare the performance of the traditional and the modified clustering algorithm.

#### ACKNOWLEDGMENT

The authors would like to extend gratitude to the Commission on Higher Education International Affairs Staff (Philippines) for cooperation in the realization of this work by providing the data necessary for the study. Appreciation is also extended to the Tarlac Agricultural University as well as the Technological Institute of the Philippines – Quezon City.

#### REFERENCES

- [1] U. Teichler, “Internationalisation of higher education: European experiences,” *Asia Pacific Educ. Rev.*, vol. 10, no. 1, pp. 93–106, 2009.
- [2] J. Lawrence, “Internationalization of Higher Education in the United States of America and Europe: A Historical, Comparative, and Conceptual Analysis (review),” *Rev. High. Educ.*, vol. 27, no. 2, pp. 281–282, 2004.
- [3] D. Dutschke, “Campus Internationalization Initiatives and Study Abroad,” *Coll. Forum*, vol. 45, no. October, pp. 67–73, 2009.
- [4] W. Green and C. Whitsed, “Critical perspectives on internationalising the curriculum in disciplines,” *Crit. Perspect. Int. Curric. Discip. Reflective Narrat. Accounts from Business, Educ. Heal.*, no. February, 2015.
- [5] A. Aerden, F. De Decker, J. Divis, M. Frederiks, and H. de Wit, “Assessing the internationalisation of degree programmes: Experiences from a Dutch-Flemish pilot certifying internationalisation,” *Compare*, vol. 43, no. 1, pp. 56–78, 2013.
- [6] J. Knight, “Internationalization Remodeled: Definition, Approaches, and Rationales,” *J. Stud. Int. Educ.*, vol. 8, no. 1, pp. 5–31, 2004.
- [7] V. Vijay, V. P. Raghunath, A. Singh, and S. N. Omkar, “Variance based moving k-means algorithm,” *Proc. - 7th IEEE Int. Adv. Comput. Conf. IACC 2017*, no. i, pp. 841–847, 2017.
- [8] B. Kenidra, M. Benmohammed, A. Beghriche, and Z. Benmounah, “A Partitional Approach for Genomic-Data Clustering Combined with K-Means Algorithm,” *2016 IEEE Intl Conf. Comput. Sci. Eng. IEEE Intl Conf. Embed. Ubiquitous Comput. 15th Intl Symp. Distrib. Comput. Appl. Bus. Eng.*, pp. 114–121, 2016.
- [9] J. Chang, J. Luo, J. Z. Huang, S. Feng, and J. Fan, “Minimum Spanning Tree Based Classification Model for Massive Data with MapReduce Implementation,” *2010 IEEE Int. Conf. Data Min. Work.*, pp. 129–137, 2010.
- [10] P.-N. Tan, M. Steinbach, and V. Kumar, “Chap 8: Cluster Analysis: Basic Concepts and Algorithms,” *Introd. to Data Min.*, p. Chapter 8, 2005.
- [11] R. Xu and D. Wunsch II, “Survey of clustering algorithms for MANET,” *IEEE Trans. Neural Networks*, vol. 16, no. 3, pp. 645–678, 2005.
- [12] C. Zhong, D. Miao, and R. Wang, “A graph-theoretical clustering method based on two rounds of minimum spanning trees,” *Pattern Recognit.*, vol. 43, no. 3, pp. 752–766, 2010.
- [13] X. Wang, X. L. Wang, and J. Zhu, “A new fast minimum spanning tree-based clustering technique,” *IEEE Int. Conf. Data Min. Work. ICDMW*, vol. 2015–Janua, no. January, pp. 1053–1060, 2015.
- [14] L. Galluccio, O. Michel, P. Comon, M. Klinger, and A. O. Hero, “Clustering with a new distance measure based on a dual-rooted tree,” *Inf. Sci. (Ny)*, vol. 251, pp. 96–113, 2013.
- [15] G. W. Wang, C. X. Zhang, and J. Zhuang, “Clustering with Prim’s sequential representation of minimum spanning tree,” *Appl. Math. Comput.*, vol. 247, pp. 521–534, 2014.



- [16] P. Das and K. A. A. Nazeer, "A novel clustering method to identify cell types from single cell transcriptional profiles," *Procedia Comput. Sci.*, vol. 132, no. Iccids, pp. 983–992, 2018.
- [17] D. R. Edla, S. Machavarapu, and P. K. Jana, "An Improved MST-based Clustering for Biological Data," pp. 42–47, 2012.
- [18] N. Paivinen, "Clustering with a minimum spanning tree of scale-free-like structure," vol. 26, pp. 921–930, 2005.
- [19] C. Zhong, D. Miao, and P. Fränti, "Minimum spanning tree based split-and-merge: A hierarchical clustering method," *Inf. Sci. (Ny)*, vol. 181, no. 16, pp. 3397–3410, 2011.
- [20] A. Singh, A. Yadav, and A. Rana, "K-means with Three different Distance Metrics," *Int. J. Comput. Appl.*, vol. 67, no. 10, pp. 13–17, 2013.
- [21] C. B. Abhilash, K. Rohitaksha, and S. Biradar, "A Comparative Analysis of Data sets using Machine Learning Techniques," *Adv. Comput. Conf.*, pp. 24–29, 2014.
- [22] D. Elsayad, A. Khalifa, M. E. Khalifa, and E. S. El-Horbaty, "An Improved Parallel Minimum Spanning Tree Based Clustering Algorithm for Microarrays Data Analysis," no. Infos, pp. 66–72, 2012.
- [23] L. H. Yen and Y. M. Cheng, "Clustering coefficient of wireless ad hoc networks and the quantity of hidden terminals," *IEEE Commun. Lett.*, vol. 9, no. 3, pp. 234–236, 2005.
- [24] M. R. Brust, D. Turgut, C. H. C. Ribeiro, and M. Kaiser, "Is the clustering coefficient a measure for fault tolerance in wireless sensor networks?," *IEEE Int. Conf. Commun.*, pp. 183–187, 2012.
- [25] C. H. Zeng and K. C. Chen, "Clustering coefficient analysis in large wireless ad hoc network," 2017 IEEE/CIC Int. Conf. Commun. China, ICC 2017, vol. 2018–Janua, no. Iccc, pp. 1–6, 2018.
- [26] Q. K. Telesford, K. E. Joyce, S. Hayasaka, J. H. Burdette, and P. J. Laurienti, "The Ubiquity of Small-World Networks," vol. 1, no. 5, 2011.
- [27] D. A. Zaitsev, "A generalized neighborhood for cellular automata," *Theor. Comput. Sci.*, vol. 666, no. November, pp. 21–35, 2017.
- [28] U. Sahin, S. Uguz, H. Akin, and I. Siap, "Three-state von Neumann cellular automata and pattern generation," *Appl. Math. Model.*, vol. 39, no. 7, pp. 2003–2024, 2015.
- [29] N. Y. Soma and J. P. Melo, "On irreversibility of von Neumann additive cellular automata on grids," *Discret. Appl. Math.*, vol. 154, no. 5 SPEC. ISS., pp. 861–866, 2006.
- [30] X. Min, X. Xu, and Z. Wang, "Combining von neumann neighborhood topology with approximate-mapping local search for ABC-based service composition," *Proc. - 2014 IEEE Int. Conf. Serv. Comput. SCC 2014*, pp. 187–194, 2014.
- [31] O. Arbelaitz, I. Gurrutxaga, and J. Muguerza, "An extensive comparative study of cluster validity indices," vol. 46, pp. 243–256, 2013.
- [32] P. J. Rousseeuw, "Silhouettes: A graphical aid to the interpretation and validation of cluster analysis," *J. Comput. Appl. Math.*, vol. 20, no. C, pp. 53–65, 1987.
- [33] J. Shen, S. I. Chang, E. S. Lee, Y. Deng, and S. J. Brown, "Determination of cluster number in clustering microarray data," *Appl. Math. Comput.*, vol. 169, no. 2, pp. 1172–1185, 2005.
- [34] A. Thalamuthu, I. Mukhopadhyay, X. Zheng, and G. C. Tseng, "Evaluation and comparison of gene clustering methods in microarray analysis," *Bioinformatics*, vol. 22, no. 19, pp. 2405–2412, 2006.
- [35] D. N. Campo, G. Stegmayer, and D. H. Milone, "A new index for clustering validation with overlapped clusters," vol. 64, pp. 549–556, 2016.
- [36] F. Wang, J. D. Kelleher, J. Pugh, and R. Ross, "An Analysis of the Application of Simplified Silhouette to the Evaluation of k-means Clustering Validity," 2017.
- [37] R. C. De Amorim and C. Hennig, "Recovering the number of clusters in data sets with noise features using feature rescaling factors," vol. 324, no. 2015, pp. 126–145, 2016.

# Digital Preservation of Cultural Heritage: Terengganu Brassware Craft Knowledge Base

Wan Malini Wan Isa<sup>1</sup>, Nor Azan Mat Zin<sup>2\*</sup>, Fadhilah Rosdi<sup>3</sup>, Hafiz Mohd Sarim<sup>4</sup>  
Faculty of Information Science and Technology, University Kebangsaan Malaysia, Malaysia<sup>1,2,3,4</sup>  
Faculty of Informatics and Computing, University Sultan Zainal Abidin, Malaysia<sup>1</sup>

**Abstract**—Early exposure to cultural heritage is necessary to preserve it from extinction. One form of cultural heritage that is now on the brink of extinction is the Terengganu brassware craft. Current young generations are mostly not interested in this heritage. Furthermore, intangible heritage in the form of knowledge and skills are only stored in the memory of the practitioners. Lack of documentation has led to the sole reliance on practitioners such that the knowledge is lost upon their demise. Hence, intangible heritage knowledge has to be acquired and stored in a knowledge base system to keep them in a systematic and permanent form. Manipulating and transferring the knowledge and skills will also ensure the continuity of this heritage, and ensure it can be accessed by future generations. This paper discusses the development of the knowledge base of Terengganu Brassware Craft as a digital preservation of cultural heritage. Knowledge acquisition was carried out using interview and observation techniques. Then, the knowledge is represented using ontology. This knowledge, in digital form, can be manipulated and disseminated to the community to ensure the continuity of the knowledge.

**Keywords**—Cultural heritage; digital preservation; intangible cultural heritage; knowledge acquisition; knowledge base; knowledge representation; ontology

## I. INTRODUCTION

Cultural heritage is a treasure that has been or is owned by a person or a group of societies or people who collectively share responsibilities for protection and retention. Cultural heritage can be divided into tangible and intangible cultural heritage. Tangible cultural heritage is something that can be perceived and held, either static or mobile. Examples include monuments, buildings, and textiles. Intangible cultural heritage, on the other hand, refers to knowledge and expertise that are interpreted through oral tradition, customary values, and culture, language, and writing. Examples of intangible cultural heritage are festive events, rituals and beliefs, performing arts, visual arts, and traditional medical art. Terengganu brassware craftsmanship is an example of intangible heritage that can be categorized under traditional craftsmanship.

Recent technological developments enable the digital preservation of knowledge. One of the goals of digital preservation is to gather, refine, maintain, and share cultural resources that can subsequently be used by scholars, members of the community, and younger generations [1]. The use of current technology such as a knowledge base has improved the knowledge management of cultural heritage, particularly

intangible heritage, to be more efficiently and effectively managed. Furthermore, the development of a knowledge base has enabled the storing of this knowledge in a digital and systematic form to preserve it and ensure the sustainability of this cultural heritage in the future. The stored knowledge can then be used to develop applications such as websites, games or mobile applications for the dissemination of intangible cultural heritage.

Currently, cultural heritage, especially intangible heritage such as Terengganu brassware craft, is dying out because most of the younger generation is no longer interested in learning and preserving the heritage. Lack of young people becoming apprentices contributes to the slow extinction and maybe eventual loss of this heritage to the society, unless effort to preserve the knowledge is carried out. Moreover, according to previous work [2], the traditional method of transferring intangible heritage knowledge has been done through personal and verbal information exchange, specifically by imitating, observing and listening to the master craftsman. This traditional way of transferring knowledge lead to heritage knowledge not properly preserved and the absence of documentation cause sole reliance on the practitioners' knowledge, thus causing the knowledge to be forgotten and lost with the death of individual practitioners. Therefore, some preservation efforts are needed to ensure the continuity of the cultural legacy.

This paper discusses the development of a knowledge base for Terengganu brassware craft cultural heritage as a digital preservation effort for dying craft. The remaining of the paper is organized as follows: Section II discusses the background and related works on cultural heritage and their preservation; Section III describes the method used for this study; Section IV presents the results and discussion; and Section V presents the conclusion.

## II. BACKGROUND AND RELATED WORK

### A. Terengganu Brassware Craft

Terengganu is a State located on the East Coast of Malaysia. There are various types of well-known cultural heritage in Terengganu such as batik, wicker, and woodcarving. One famous heritage in the State is the brassware craft founded 300 years ago. In the past, the production of brassware craft was very active in Kampung Ladang and Kampung Tanjung, Kuala Terengganu. The brassware craft produced by the Terengganu craftsmen is a Peninsula Malay art that has a high-quality artistic identity and shape [3]. Study

\* Corresponding Author

The research is funding by Universiti Kebangsaan Malaysia under the Grand Challenge Fund (DCP-2017-007/2).

from [4] states that the symbols and identities highlighted in the brassware craft have artistic elements and aesthetic values that reflect the identity and culture of the Malay community.

Although the craft was popular in the local community in the past, presently, the brassware craft industry is in a critical phase, as the market and production of brassware-based craft products have decreased. A recent study stated that this craft is almost extinct due to the lack of sustainability, skills, and interests of the younger generation, and limited modern technology applications [5]. Therefore, this craft should be preserved and maintained to ensure its sustainability for future generations.

### B. Digital Preservation of Cultural Heritage

Cultural heritage encompasses the whole environment that reflects the activities and successes of the past that cannot be interchanged [6]. This makes the preservation of cultural heritage very important and shows that efforts need to be taken to ensure its sustainability for future generations. According to *Kamus Dewan*, preservation means maintaining, defending, and caring while another study [7] defined it as an action that preserves cultural heritage objects and historical objects. Besides that, another definition of preservation from [8] is an act or process of taking action to defend the existing form, integrity, and material of a building or structure and the protective plant of a site.

One study [9] listed four key reasons for cultural heritage preservation, which are, cultural memory, convenient proximity, environmental diversity, and economic gain. The importance of cultural heritage as a cultural memorial is that the preservation is able to maintain a historical material in physical form and to transfer valuable knowledge and skills from the past generations to the present and future generations. As convenient proximity, preservation can support interaction among the environment, people, and community activities. Meanwhile, through the diversity of the environment owing to the different or similar identities of the local community, the preservation of cultural heritage will ensure that domestic artifacts and craftsmen are preserved amidst urban expansion. Lastly, preservation can benefit the community in terms of economic growth, namely, the cost of building new buildings and turning them into tourist attraction spots can be saved.

Digital preservation is one of the methods to keep the history of a country alive. Technological advancement has led to digital preservation being more widely used in libraries, museums, and information centers. Digital preservation can be defined as a proper architecture that consists of packages that are commonly implemented by archivists to ensure that the information is always available, as well as to ensure its usability and interpretability [10]. Digital preservation does not only preserve culture and legacy; it also enables easy documentation of the materials, which can be used as an educational reference for the future generation [11]. Furthermore, digitalization offers a platform for existing users and the upcoming generation to access cultural information, so that they can learn, comprehend, and even create digital resources using the Internet [1].

There are various methods of digital preservation that can be carried out such as three-dimensional modeling [10], [12], virtual reality [13], [14], augmented reality [15], and so on. In addition, a knowledge base is also an effective method for digital preservation. A knowledge base is defined as a collection of knowledge about the world that is processed by computers [16]. Besides, it also acts as a centralized warehouse for information or as a database on a particular subject [17]. A knowledge base is an essential element in knowledge-based systems for optimizing information gathering, organizing information, and perusing certain information. Since cultural heritage has a lot of knowledge to be preserved, especially intangible cultural heritage, the use of a knowledge base is significant as a medium of digital preservation and documentation.

## III. METHOD

This section would discuss the activities involved in developing the knowledge base for Terengganu brassware craft such as knowledge acquisition and knowledge representation. Fig. 1 shows the process flows for developing a knowledge base for Terengganu brassware craft. The development of the Terengganu brassware craft knowledge base consists of three main activities- knowledge acquisition, analysis and knowledge representation. The first activity is the knowledge acquisition which involves the process of gathering and obtaining knowledge from the domain experts using interview and observation techniques. Next, the knowledge obtained from the previous activity is analyzed by coding, clustering and identifying the knowledge to be used for subsequent activities. The third activity is the knowledge representation process whereby an ontology was developed and then stored in a knowledge base. This knowledge base is developed in Malay language, since the knowledge to be preserved is a Malay cultural heritage. The description of each activity is described in the next section.

### A. Knowledge Acquisition

Knowledge acquisition is a process of obtaining knowledge from sources such as experts, books, documents, or computers [18]. The knowledge gained includes specific knowledge of a problem domain or problem-solving in general or meta-knowledge, or information about how experts use their knowledge to solve problems. Author [19] mentions there are several techniques used in the process of acquiring knowledge such as manual methods (e.g. interview, surveys, observation), automated tools (e.g. traditional machine learning techniques), interactive computer-based tools, or combinations of these.

In this study, the knowledge acquisition part involved exploring and acquiring knowledge from Terengganu brassware craft experts about this valuable heritage. Knowledge about craftsmanship is a tacit knowledge, which is shared through socialization (tacit to tacit) from generation to generation. Tacit knowledge is a knowledge that is based on an individual's experience, is deeply embedded, hard to express and explain, not yet articulated, and is equal to the practical know-how knowledge [1].

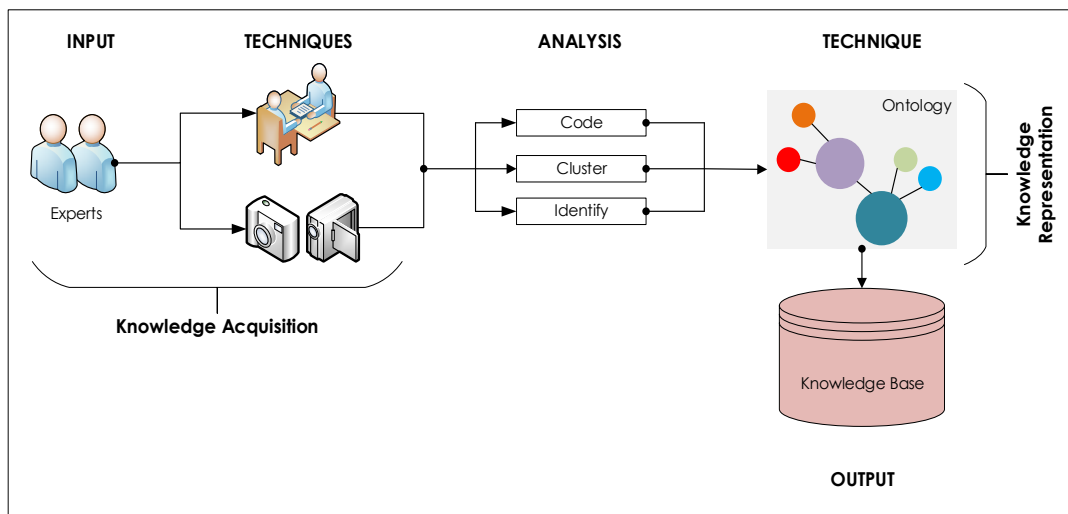


Fig. 1. Overview of Processes in Developing the Knowledge base for Terengganu Brassware Craft.

Since the knowledge investigated is tacit, interview and observation methods were used to acquire this knowledge from the experts i.e. the brassware craftsmen. These methods were employed to extract the knowledge because the craftsmen usually keep this knowledge in their memory and pass them down through personal exchanges and oral tradition. For this study, three craftsmen were selected for the interview, as they are considered experts by virtue of being involved in the brassware craft industry for more than 10 years. In addition, interviews were also conducted with Terengganu Museum officers and a Terengganu Branch officer from Perbadanan Kemajuan Kraftangan Malaysia, to get more information on the brassware artifacts and products.

Before the fieldwork was carried out, an extensive review of the literature was performed to explore the basic knowledge of brassware craft and to help frame the interview questions. An extensive review was done by obtaining information from books, journals, and online sources. While for the interview, a semi-structured interview approach was selected as the means for knowledge gathering. This interview format allowed for specific questions and topics to be addressed while offering the respondents an opportunity to give additional feedback and elaborate further on any aspect of their experience they considered relevant to this study [20]. Semi-structured interview questions were developed, consisting of 20 questions that can be categorized into three main categories: a) history of brassware, b) brassware artifacts or products, and c) brassware producing process.

Apart from that, an observation method was carried out after the interview sessions to obtain a better understanding of the process of making brassware craft. The outputs from the interview were transcribed into textual format while the findings from the observations were recorded in the form of images and videos. The data were then transferred to a computer. These data from the knowledge acquisition activities were then analyzed following several steps such as coding and clustering. Then, the important knowledge was identified and extracted for the implementation of knowledge representation activities.

### B. Knowledge Representation

Knowledge representation is a process of understanding, designing, and implementing ways to represent the information acquired so that it can be used by the computer [21]. It is to find the mapping between knowledge and representation and then choosing a suitable form to express knowledge, that is to make the facts, rules, concepts of the world coded into a suitable data structure, then representing them in an acceptable form using the computer [22].

In this study, knowledge was represented in the form of ontology because ontology provides a clear organization of specialized knowledge and multidimensional representation. Ontology also permits people or software agents to share a common understanding of the information structure and enables the reuse of the developed domain knowledge. Besides, study from [1] states that ontology is one of the alternatives used to represent the domain of knowledge, where this method helps us to perform the semantic modeling of concepts, and to represent axioms in ontology in logic languages.

There is a well-known ontology for the cultural heritage domain, namely CIDOC CRM. The CIDOC CRM allows integration, mediation, and interchange of information of diverse cultural heritage and their association with the digital library and archive data. It is used to summarize various schemata (80 classes and 130 relationships) under different museum fields as well as to enhance the knowledge semantic from distributed databases of cultural heritage [23]–[25]. Nevertheless, several studies [26], [27] have revealed that the CIDOC CRM approach was considered too focused on museums with only less than 5% of the ideas of CIDOC CRM actually being utilized by the museums.

Ontology development can be carried out either by reusing and integrating with existing ontology or developing from scratch [28], [29]. However, some researchers claim that it is better to develop a new ontology from scratch rather than correcting the existing ontology, especially in terms of costing [30]. For this study, the ontology for brassware craft was developed from scratch since there is no existing ontology that

is suitable for the traditional craftsmanship domain. Ontology Development 101 [31] was selected as a method to develop the brassware craft ontology. This method consists of five phases, namely specification, integration, conceptualization, implementation, and evaluation, as shown in Fig. 2.

The first phase is the specification phase in which the domain, purpose, and scope of the ontology were defined. The domain for this ontology is an intangible cultural heritage that focuses on brassware craft while the purpose of the ontology development is to model the brassware craft knowledge base. The integration phase is not relevant in this development, as this ontology is not integrated with other ontologies. Next is the conceptualization phase where all possible terms and properties related to the terms of the domain were listed down. Then, class, properties, and instances were defined based on the terms.

In the implementation phase, a software, i.e. Protégé version 5.2 was selected as the ontology engineering environment and the Web Ontology Language (OWL) was set as the ontology language. The final phase is the evaluation phase that was carried out to evaluate and debug the performance of the ontology model. SPARQL query was used to verify the accuracy and correctness of the knowledge representation.

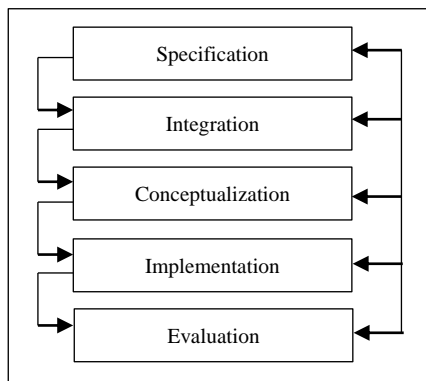


Fig. 2. Ontology Development 101 [31].

#### IV. RESULTS AND DISCUSSION

This section discusses the results from the knowledge acquisition and knowledge representation activities.

##### A. Knowledge Acquisition Result

Based on the interviews, it was found that there are different opinions regarding the origin of the Terengganu brassware industry; it could have originated from China, India or Patani, Thailand. In addition, there is no written evidence as to when the industry began in Terengganu, but based on the estimation of the industry, it has been operating in Terengganu for more than 300 years. Respondents also stated that the past glory of the craft industry in Terengganu reached its peak when the Sultan's palace court recognized and encouraged the people to study the art.

Knowledge of the artifacts was obtained from Muzium Terengganu while knowledge about the products was obtained from the craftsmen and Perbadanan Kemajuan Kraftangan Malaysia, Terengganu Branch. The knowledge acquired

includes the artifacts or product names, the function of each product, the motifs or design, and the manufacturing year and size. Table I shows examples of brassware artifact knowledge.

Furthermore, the most important knowledge gained was the traditional method of producing brassware craft including the materials and equipment used, which is known as the lost wax brass casting technique. From the interviews and observations, it can be concluded that there are 11 major processes involved in the production of brassware craft, as shown in Fig. 3. Besides that, knowledge was also acquired on the main materials used, which include the metal mixture consisting of copper, zinc, tin, nickel, aluminum, and other materials used such as wax, clay, sand, and others. The types of equipment used were crucibles, ground furnaces, grinder machines, and many others.

##### B. Knowledge Representation Result

The result of knowledge representation from the previous activities was presented in the form of a list of all the terms and properties related to the terms as, well as the examples of the terms, such as the name of the artifacts, the list of motifs, the usage, the materials, and the equipment. Based on these terms, the concepts were identified; however, the concepts alone were not enough to provide comprehensive information. Therefore, the properties of the concepts were defined, for example, the concepts of the artifacts and their properties such as name, motifs, and usage was further defined. The instances for the concepts were also identified based on the terms. Ontology was also applied to the process of brassware production, broken down into properties such as sub-processes, materials, and equipment. The representation of knowledge was stored in the knowledge base. Table II shows the basic terms of the concepts and properties of brassware ontology. Meanwhile, Table III lists the relationship between the concepts and the properties.

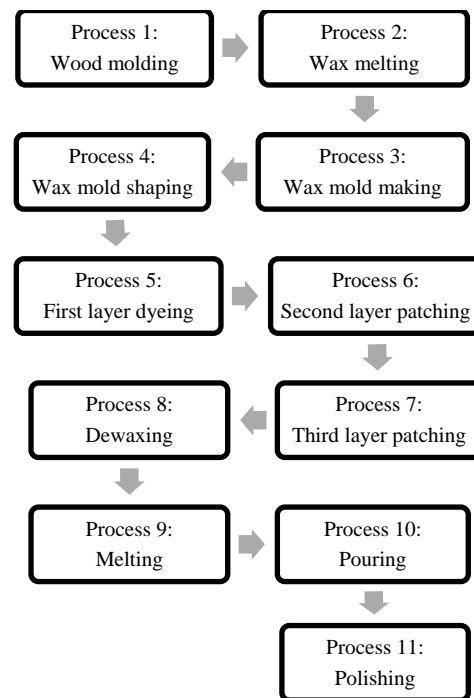


Fig. 3. The main Process in Producing Terengganu Brassware Craft.

TABLE I. BRASSWARE ARTIFACT KNOWLEDGE

| Name   | Function   | Motifs   | Size   | Year of manufacture |
|--|--|----------|--|---------------------|
| Rectangular betel leaf holder (Tepak sirih biasa 4 segi) | Used as a place for storing gobek, betel leaf, gambier, betel nut, and other requirements while eating betel | Geometry | Length: 20.2 cm<br>Width: 10.2 cm<br>Height: 5.0 cm                    | Around the 90s      |
| Brassware pitch (Kendi tembaga)                          | Used as a tool for storing water for drinking purposes, washing hands and so on                              | Floral   | Length: 27.0 cm<br>Width: 19.5 cm<br>Height: 22.4 cm<br>Weight: 2.4 kg | Around the 70s      |
| Brassware wok (Kuali Tembaga)                            | Used as a tool for cooking dishes and stirring cakes   | Geometry | Diameter: 45 cm<br>Height: 21 cm                                       | Around the 80s      |

Then, the result of the implementation was obtained and illustrated in Fig. 4 and Fig. 5. Fig. 4 shows the visualization part of the Terengganu brassware craft ontology. This ontology has eight main classes which are Artifik, Kategori, Motif, Sejarah, Bahan, Peralatan, Proses and LangkahProses. There are twelve subclasses under the main classes such as Logam and PasirPantai under Bahan class. Instances are created under appropriate class with the relation name has individual, for example, the instance Proses01\_Pembentukan\_Acuan\_Kayu belongs to the Proses class. Object property is used to link instances such as Proses01\_Pembentukan\_Acuan\_Kayu has property hasLangkah; whereby Melarik\_kayu and Melicinkan\_acuan\_kayu are two instances of LangkahProses class.

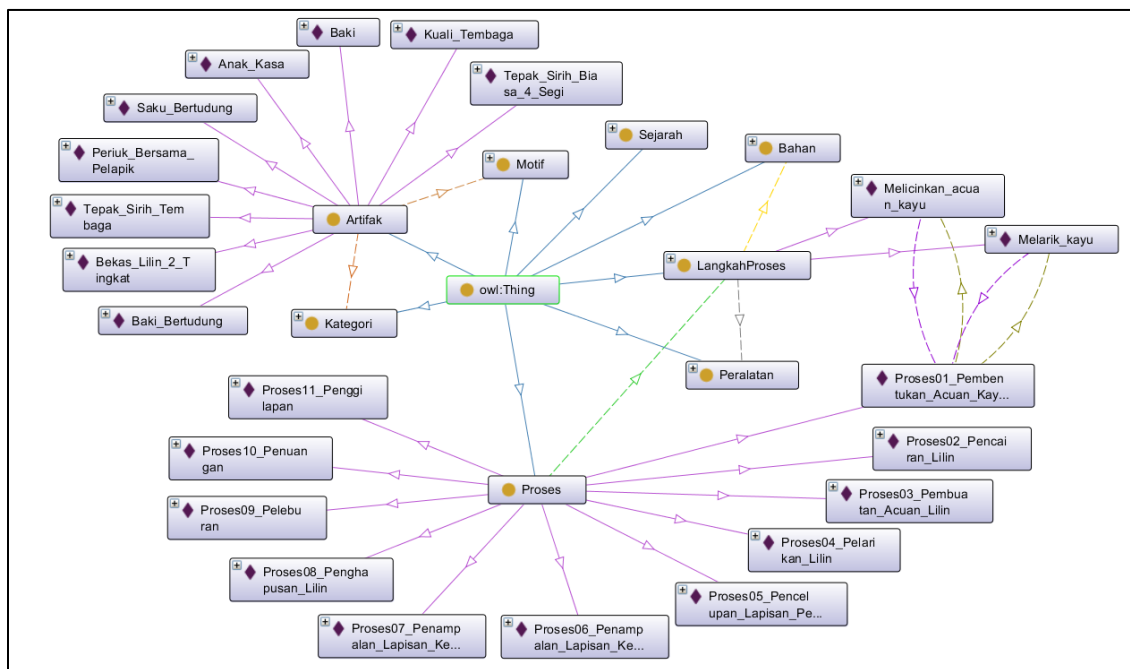


Fig. 4. Visualization Part of the Terengganu Brassware Craft Ontology.

Fig. 5 shows an excerpt of the OWL representation of brassware ontology in OWL/XML syntax serialization (.owl). *Kuali\_Tembaga* and *Tepak\_Sirih\_Biasa\_4\_Segi* are declared as individual instances. Class *LangkahProses* is created and has *Melarik\_kayu* as its instance. Object property *hasBahan* is linked to *Melarik\_kayu* and material *Kayu\_Cengal*. While, data property, *Keterangan* is linked to the instances *Melarik\_Kayu* with data value such as *Acuan kayu diperbuat dari bongkah kayu dan dibentuk dengan melarik kayu tersebut mengikut bentuk yang dikehendaki. Acuan kayu dilarik menggunakan mesin pelarik dan pahat pelarik kayu.*

TABLE II. BASIC TERMS OF CONCEPTS AND PROPERTIES FOR TERENGGANU BRASSWARE CRAFT ONTOLOGY

| Concepts                     | Properties   |
|------------------------------|--------------|
| Artifik (Artifact)           | -            |
| Proses (Process)             | hasLangkah   |
| LangkahProses (ProcessSteps) | isLangkahOf  |
| Bahan (Material)             | hasBahan     |
| Peralatan (Equipment)        | hasPeralatan |
| Kategori (Category)          | hasKategori  |
| Motif (Motif)                | hasMotif     |
| Sejarah (History)            | -            |

TABLE III. RELATIONSHIP BETWEEN CONCEPTS AND PROPERTIES

| Concept Name                 | Instance Name                   | Property     | Value         |
|------------------------------|---------------------------------|--------------|---------------|
| Artifik (Artifact)           | Tepak sirih biasa 4 segi        | hasMotif     | Geometri      |
|                              |                                 | hasKategori  | Adat istiadat |
| Proses (Process)             | Proses1: Pembentukan Acuan kayu | hasLangkah   | Melarik kayu  |
| LangkahProses (ProcessSteps) | Melarik kayu                    | hasBahan     | Kayu seraya   |
|                              |                                 | hasPeralatan | Mesin Pelarik |

```

<?xml version="1.0"?>
<Ontology xmlns="http://www.w3.org/2002/07/owl#"
xml:base="http://www.kraftembaga.com/TembagaOnto"
xmlns:rdf="http://www.w3.org/1999/02/22-rdf-syntax-ns#"
xmlns:xml="http://www.w3.org/XML/1998/namespace"
xmlns:xsd="http://www.w3.org/2001/XMLSchema#"
xmlns:rdfs="http://www.w3.org/2000/01/rdf-schema#"
ontologyIRI="http://www.kraftembaga.com/TembagaOnto">
<Prefix name="owl" IRI="http://www.w3.org/2002/07/owl#" />
<Prefix name="rdf" IRI="http://www.w3.org/1999/02/22-rdf-syntax-ns#" />
<Prefix name="xml" IRI="http://www.w3.org/XML/1998/namespace" />
<Prefix name="xsd" IRI="http://www.w3.org/2001/XMLSchema#" />
<Prefix name="rdfs" IRI="http://www.w3.org/2000/01/rdf-schema#" />
<Declaration>
  <NamedIndividual IRI="#Kuali_Tembaga" />
</Declaration>
<Declaration>
  <NamedIndividual IRI="#Tepak_Sirih_Biasa_4_Segi" />
</Declaration>
  <ClassAssertion>
    <Class IRI="#LangkahProses" />
    <NamedIndividual IRI="#Melarik_kayu" />
  </ClassAssertion>
  <ObjectPropertyAssertion>
    <ObjectProperty IRI="#hasBahan" />
    <NamedIndividual IRI="#Melarik_kayu" />
    <NamedIndividual IRI="#Kayu_Cengal" />
  </ObjectPropertyAssertion>
  <DataPropertyAssertion>
    <DataProperty IRI="#Keterangan" />
    <NamedIndividual IRI="#Melarik_kayu" />
    <Literal datatypeIRI="http://www.w3.org/1999/02/22-rdf-syntax-ns#PlainLiteral">Acuan kayu diperbuat dari bongkah kayu dan dibentuk dengan melarik kayu tersebut mengikut bentuk yang dikehendaki. Acuan kayu dilarik menggunakan mesin pelarik dan pahat pelarik kayu.</Literal>
  </DataPropertyAssertion>

```

Fig. 5. An Excerpt of the Terengganu Brassware Craft Ontology in OWL Representation.

Evaluation was performed using SPARQL query based on competency questions that were constructed in the first phase. Examples of the evaluation are as follows:

Competency Question 1: What is the process for producing Terengganu brassware craft?

SPARQL query:  
 SELECT ?Proses  
 WHERE {  
 ?class rdfs:subClassOf\* krafTem:Proses .  
 ?Proses rdf:type ?class .  
 } ORDER BY ?Proses

Answer:

```

Proses01_Pembentukan_Acuan_Kayu
Proses02_Pencairan_Lilin
Proses03_Pembuatan_Acuan_Lilin
Proses04_Pelarikan_Lilin
Proses05_Pencelupan_Lapisan_Pertama
Proses06_Penampalan_Lapisan_Kedua
Proses07_Penampalan_Lapisan_Ketiga
Proses08_Penghapusan_Lilin
Proses09_Peleburan
Proses10_Penuangan
Proses11_Penggilapan

```

Competency Question 2: What are the steps involved in every process?

SPARQL query:  
 SELECT ?Proses ?NoLangkah ?Langkah  
 WHERE {  
 ?Proses krafTem:hasLangkah ?Langkah .  
 ?Langkah krafTem:NoLangkahProses ?NoLangkah .  
 } ORDER BY ?Proses ?NoLangkah

Answer:

| Proses                              | NoLangkah  | Langkah                                    |
|-------------------------------------|--|--|
| Proses01_Pembentukan_Acuan_Kayu     | "1"^^<http://www.w3.org/2001/XMLSchema#decimal>  | Melarik_kayu                               |
| Proses01_Pembentukan_Acuan_Kayu     | "12"^^<http://www.w3.org/2001/XMLSchema#decimal> | Melinkan_acuan_kayu                        |
| Proses02_Pencairan_Lilin            | "2"^^<http://www.w3.org/2001/XMLSchema#decimal>  | Mencampurkan_lilin_dan_damar               |
| Proses02_Pencairan_Lilin            | "22"^^<http://www.w3.org/2001/XMLSchema#decimal> | Memasak_lilin                              |
| Proses03_Pembuatan_Acuan_Lilin      | "3"^^<http://www.w3.org/2001/XMLSchema#decimal>  | Membasahkan_acuan_kayu                     |
| Proses03_Pembuatan_Acuan_Lilin      | "32"^^<http://www.w3.org/2001/XMLSchema#decimal> | Mencelup_acuan_kayu_dalam_lilin_ganas      |
| Proses03_Pembuatan_Acuan_Lilin      | "33"^^<http://www.w3.org/2001/XMLSchema#decimal> | Mencelup_acuan_lilin_dalam_air             |
| Proses04_Pelarikan_Lilin            | "4"^^<http://www.w3.org/2001/XMLSchema#decimal>  | Melarik_acuan_lilin                        |
| Proses04_Pelarikan_Lilin            | "42"^^<http://www.w3.org/2001/XMLSchema#decimal> | Menanggalkan_acuan_lilin                   |
| Proses04_Pelarikan_Lilin            | "43"^^<http://www.w3.org/2001/XMLSchema#decimal> | Merendam_acuan_lilin_dalam_air             |
| Proses05_Pencelupan_Lapisan_Pertama | "5"^^<http://www.w3.org/2001/XMLSchema#decimal>  | Membanuh_banohan_pertama                   |
| Proses05_Pencelupan_Lapisan_Pertama | "52"^^<http://www.w3.org/2001/XMLSchema#decimal> | Mencelup_acuan_lilin_dalam_banohan_pertama |
| Proses05_Pencelupan_Lapisan_Pertama | "53"^^<http://www.w3.org/2001/XMLSchema#decimal> | Mengeringkan_acuan_lapisan_pertama         |
| Proses06_Penampalan_Lapisan_Kedua   | "6"^^<http://www.w3.org/2001/XMLSchema#decimal>  | Membanuh_banohan_kedua                     |
| Proses06_Penampalan_Lapisan_Kedua   | "62"^^<http://www.w3.org/2001/XMLSchema#decimal> | Menampal_acuan_dengan_banohan_kedua        |
| Proses06_Penampalan_Lapisan_Kedua   | "63"^^<http://www.w3.org/2001/XMLSchema#decimal> | Mengeringkan_acuan_lapisan_kedua           |

## V. CONCLUSION

In this paper, knowledge acquisition and representation for the development of a knowledge base for Terengganu brassware craft were discussed. The knowledge acquisition activities involved interviews with brassware experts and

observation. Meanwhile, ontology was selected as the knowledge representation method since it can represent knowledge for a specific domain. The development of this knowledge base was a significant effort towards the digital preservation of cultural heritage. This study focuses on the development of a knowledge base for intangible cultural heritage of the process of producing Terengganu brassware craft and tangible cultural heritage of artifacts such as design motif and category. Future studies can explore other similar intangible heritage knowledge, besides expanding this knowledge base.

Future works will involve the validation of this knowledge in the knowledge base with a domain expert. This validation is important to verify the knowledge of the brassware craft before it can be applied to other applications such as semantic search or games to disseminate the knowledge to the young generations and thus increase awareness of the preservation and conservation of cultural heritage.

#### ACKNOWLEDGMENT

The author would like to acknowledge Universiti Kebangsaan Malaysia for funding this research under the Grand Challenge Fund (DCP-2017-007/2). We also thank the Skim Latihan Akademik (SLAB)/ Skim Latihan Akademik IPTA (SLAI), Ministry of Education Malaysia and Ahmad Zaidi Abd. Wahab from The Society of Terengganu Brassware Entrepreneurs (TEMAGA).

#### REFERENCES

- [1] Pramarta and J. G. Davis, "Digital preservation of cultural heritage: Balinese Kulkul artefact and practices," *Lect. Notes Comput. Sci. (including Subser. Lect. Notes Artif. Intell. Lect. Notes Bioinformatics)*, vol. 10058 LNCS, pp. 491–500, 2016.
- [2] F. M. Dagnino et al., "Serious Games to Support Learning of Rare 'Intangible' Cultural Expressions," 9th Int. Technol. Educ. Dev. Conf. (INTED 2015), no. March, pp. 7184–7194, 2015.
- [3] Syed Ahmad Jamal, *Form & Soul*. Kuala Lumpur: Dewan Bahasa dan Pustaka, 1994.
- [4] A. B. Sabran et al. *Fusion 'Eksplorasi Bentuk Kraf Tembaga Melalui Integrasi Teknologi*," vol. 3, pp. 114–126, 2015.
- [5] S. A. Mohamad, K. A. A. Abd Rahman, and M. F. A. Abdullah, "Problem Analysis and Challenges of Terengganu Brassware Industry," *Teren. Int. Tour. Conf.* 2013, vol. 2013, pp. 1–7, 2013.
- [6] J. Feilden, B. M., & Jokilehto, *Management guidelines for world cultural heritage sites*. Paris: ICCROM, 1993.
- [7] H. Kurniawan, A. Salim, H. Suhartanto, and Z. A. Hasibuan, "E-Cultural Heritage and Natural History Framework: an integrated approach to digital preservation," *Int. Conf. Telecommun. Technol. Appl.*, vol. 5, no. November 2015, pp. 177–182, 2011.
- [8] E. L. Howe, B. J., Fleming, D. A., & Kemp, *Houses and Homes: Exploring Their History*, Vol 2. Rowman Altamira, 1997.
- [9] S. Prompayuk and P. Chairattananon, "Preservation of Cultural Heritage Community: Cases of Thailand and Developed Countries," *Procedia - Soc. Behav. Sci.*, vol. 234, pp. 239–243, 2016.
- [10] A. Belhi, A. Bouras, and S. Fofou, "Digitization and preservation of cultural heritage: The CEPROQHA approach," 2017 11th Int. Conf. Software, Knowledge, Inf. Manag. Appl., pp. 1–7, 2017.
- [11] M. Z. Idris, N. B. Mustafa, and S. O. Syed Yusoff, "Preservation of Intangible Cultural Heritage Using Advance Digital Technology: Issues and Challenges," vol. 16, no. 1 OP-Harmonia: Journal of Arts Research & Education; 2016, Vol. 16 Issue 1, p1-13, 13p, p. 1, 2016.
- [12] H. Shishido, Y. Ito, Y. Kawamura, T. Matsui, A. Morishima, and I. Kitahara, "Proactive preservation of world heritage by crowdsourcing and 3D reconstruction technology," *Proc. - 2017 IEEE Int. Conf. Big Data, Big Data 2017*, pp. 4426–4428, 2017.
- [13] M. G. Abdelmonem, G. Selim, S. Mushatat, and A. Almogren, "Virtual Platforms for Heritage Preservation in the Middle East: the Case of Medieval Cairo" *Int.J. Archit. Res ArchNet-IJAR*, vol.11, no.3, p.28, 2017.
- [14] Y. Yi and E. J. Shutao, "The Application of Virtual Reality Technology to Heritage Conservation in Famagusta's Armenian Church," 2017, pp. 313–323.
- [15] L. W. Shang, T. G. Siang, M. H. Bin Zakaria, and M. H. Emran, "Mobile augmented reality applications for heritage preservation in UNESCO world heritage sites through adopting the UTAUT model," *AIP Conf. Proc.*, vol. 1830, 2017.
- [16] T. Rebele, F. Suchanek, J. Hoffart, J. Biega, E. Kuzey, and G. Weikum, "YAGO: A Multilingual Knowledge Base from Wikipedia, Wordnet, and Geonames," in *ISWC 2016, Part II, LNCS 9982*, vol. 9982, 2016, pp. 177–185.
- [17] A. T. Imam, T. Rousan, and S. Aljawarneh, "An expert code generator using rule-based and frames knowledge representation techniques," 2014 5th Int. Conf. Inf. Commun. Syst. ICICS 2014, pp. 1–6, 2014.
- [18] Turban, J. E. Aronson, and T.-P. Liang, *Knowledge Acquisition, Representation, Reasoning*. 2007.
- [19] J. H. Boose, "A survey of knowledge acquisition techniques and tools," *Knowl. Acquis.*, vol. 1, no. 1, pp. 3–37, 1989.
- [20] A. Louise Barriball, K., While, "Collecting Data using a semi-structured interview: a discussion paper," *J. Adv. Nurs.*, vol 19, pp. 328–335, 1994.
- [21] S. C. Shapiro, "Knowledge representation," in *Encyclopedia of Cognitive Science*, John Wiley Sons, Ltd, 2006.
- [22] G. Jiang and X. Cheng, "Building Knowledge Base for Consulting System on Agricultural Practical Techniques," pp. 303–307.
- [23] G. Tan, T. Hao, and Z. Zhong, "A Knowledge Modeling Framework for Intangible Cultural Heritage Based on Ontology," 2009 Second Int. Symp. Knowl. Acquis. Model., pp. 304–307, 2009.
- [24] H. Liu, H. Bao, J. Wu, and J. Feng, "An Information Flow Based Approach To Semantic Integration Of Distributed Digital Museums," no. August, pp. 4430–4437, 2006.
- [25] H. Z. Liu, "Global ontology construction for heterogeneous digital museums," *Proc. Sixth Int. Conf. Mach. Learn. Cybern. ICMLC 2007*, vol. 7, no. August, pp. 4015–4019, 2007.
- [26] M. Doerr, "The Dream of a Global Knowledge Network — A New Approach," vol. 1, no. 1, pp. 1–23, 2008.
- [27] R. Brownlow, S. Capuzzi, L. Martins, I. Normann, and A. Poulouvasilis, "An Ontological Approach to Creating an Andean Weaving Knowledge Base," vol. 8, no. 2, pp. 1–31, 2015.
- [28] M. Cristani and U. Verona, "A Survey on Ontology Creation Methodologies," vol. 1, no. June, pp. 48–68, 2005.
- [29] A. Gómez-pérez and M. D. Rojas-amaya, "Ontological Reengineering for Reuse," pp. 139–156, 1999.
- [30] H. S. Pinto and J. P. Martins, "Ontologies: How can They be Built?," *Knowl. Inf. Syst.*, vol. 6, no. 4, pp. 441–464, 2004.
- [31] N. F. Noy and D. L. McGuinness, "Ontology Development : A Guide to Creating Your First Ontology." 2001.



# Computer Students Attitudes on the Integration of m-Learning Applications

Abdulmohsin S. Alkhunaizan<sup>1</sup>

Department of Information Systems, College of Computer and Information Sciences  
Majmaah University, Majmaah 11952, Saudi Arabia

**Abstract**—Technology has an important role in the lives particularly in the field of education nowadays because of its accessibility and affordability. Mobile learning (m-Learning) which is form of e-learning is a novel approach in the arena of educational technology that offers personal, informal, blended learning and flexible learning opportunities to learners and instructors. The present study is an attempt to determine the computer students' attitudes on the integration of m-Learning app (WhatsApp). A total numbers of 143 student participants participated in the experiment. The study used quasi-experimental research design. The learners were performed intact groups of a public university. They were asked to complete the assignments through WhatsApp application. Two questionnaires were used to gather the data. The data was analyzed descriptively. Findings of the data showed that learners had positive attitudes towards the integration of m-Learning apps. The study also reports the suggestions for the future research and implications for the teachers.

**Keywords**—e-Learning; m-Learning; mobile applications; computer science; WhatsApp

## I. INTRODUCTION

21st century has derived the mode of e-Learning to m-Learning. Mobile phones are being replaced with computers. There is a transition from Computer Assisted Instruction [1] to Mobile Assisted Instruction (MAI) Smartphones have gained the popularity in the teaching instructions and these have gained an important position in the daily life particularly for learning purposes. The key reason behind this notion is that these gadgets are the source of gateway for global interaction. Because of the rapid progression and innovation, the use of computer technology is persistently used in education institutions [2]. Now the teachers have access to computer labs in the shape of mobile learning ubiquitously. The importance of computer and mobile technology has become so important and increasingly utilized in classroom. Thus, its importance cannot be ignored for the computer science students.

The modern classrooms are now equipped with flipped classes, computer labs and integrated learning around the globe [3]. Most of the educational institutions require a model that facilitates its teaching and academic faculty with the necessities to develop the learning process and better involvement of the blended learning. These higher educational institutions incorporate e-Learning in the shape Web-based teaching (WBT), virtual learning (VL) and learning management system (LMS) or some other e-Learning apps and educational technologies for various types of teaching and learning process [4]. Educational technology offers a valuable

assistance to learners to make learning process easy and understandable in its capacity. The schools are persistently in state of doubt by increased availability, presence, ubiquity, and role of educational technology in classroom setting.

The use of technology greatly relies on the teachers, students and in particular educational institutions' environments. Numerous studies [3, 5, 6] have recommended that the incorporation of technology can foster the learning abilities, develop motivation and aid overall learning efficiently. The integration of E-learning and ICT courses with the formal discourse requires the key skills those could be evaluated, measured and shifted from teachers to students; teacher to teachers and other academic professional for its effective transformation. These skills can develop the use and integration of E-learning more effectively and naturally. Moreover, this will lead to the development of the performance of various learning pursuits as compared to bizarre integration of computers or mobile phones with the formal classroom.

E-Learning is also marked as the process of learning by the use of electronic means and developed online learning sources which present material with the assistance of computer, tabs and mobile phones [7]. The success of E-learning is quite optimal for the computer education as the basic need of the learner is the access to material and educational software and applications. The access to learning material is just one click away from the learners as instructors just need to upload the material and learners can download it anywhere. The fact is that nowadays online learning has replaced the formal classroom rooms and distance learning which are also cost effective for many different types of learners [8]. The progression of information technology (IT), Computers, global communication and present teaching environment stimulate the integration of E-learning. Several fields of education are equipped with these sorts of IT inventions and are envisioned for, teaching, training, research and innovations purposes and for educational consultancy as well. Furthermore, the support and planning for academic institutions to develop the capacity of e-Learning also requires the key developments and innovations of the apps and the environment of the institution [9].

## II. M-LEARNING

From the last few years, instructors and institutions have been supporting instructive paradigms that encourage formal and well-balanced learning. The teaching material and work is retained for the concerned people who administer the

presentation of knowledge and information to the learners in these paradigms. Presently, the concentration in higher studies has shifted from the concept of instruction to blended learning that fosters the process of learning. The universities are using m-Learning apps to deliver the instruction for communication and teaching. The norm of teaching has started on focusing on paradigm shift instead of skills and capacities and institutions are analyzing the capabilities of learning applications [10]. The integration of smartphones is one of the key aspects of the educational transition. Mobile phones have directed a developed learning method, which is now in every learner's hand, and it is operative to use for educational purposes. The smartphones have the capacity of connectivity and dynamic methods of teaching and presenting material as well as information.

By evoking, the notion of "m-Learning" the individual contemplates impulsively about the prospect of learning beyond the fixed or predetermined environment [11]. It would be better to argue that m-Learning is not mere operation of mobile or smartphone devices in an e-learning field, but an expedient function of a dynamic and intricate process of learning [12]. To attain the full benefits of m-Learning, the knowledge of its innovation is essential. This needs stepping further than the apparent definition, concept definition and observing the proficiencies of smartphone devices and the background in which the students gain access to the learning material and instruction [13]. It is a re-evaluating of learning that stem from the learners' perspective. Referring to this notion, m-Learning is an addition of e-learning. In general, e-learning implies to a learning and instruction accompanied with various types of electronic tools and gadgets. In the e-learning instruction, there is always a variance in learning process between the applications and learning process. Even though electronic apparatus are utilized in m-Learning, the application and the learning as a whole, take place simultaneously. The primary purpose is to provide the important information and instruction in a precise time. m-Learning offers an opportunity to a rapid and relevant and important material and instruction for the particular task to be achieved to the learners.

m-Learning can be interrupted from different aspects to different context and people. Apparently, it seems from beyond the formal learning with mobile gadgets such as tablets, laptops, smartphones and Mp3 players. Without any doubt these devices are necessary for the mobile phone-based learning and instruction. Broadly mentioning m-Learning is not more than only a device to attain the access to material, content and collaboration for the learning purposes as well as it is around the mobility of the learning process and learners. The author in [14] marked mobile learning as "the processes (both personal and public) of coming to know through exploration and conversation across multiple contexts amongst people and interactive technologies". In this regard, he further added that the key point in the arena of m-Learning is the context. m-Learning offers a clear and understandable context for the learning and instruction that is impracticable with the desktops and other computing devices [15]. m-Learning is better illustrated as the ubiquitous learning that involves the use of wireless network, handheld mobile devices and support that extend and enhance the hold of learning and instruction.

Educational organization both desire social revolution and have to act on it. In the view of GSMA (2011) an assessment conducted by Blackboard realized that "virtually all students own a mobile phone or smartphone." In reality, GSMA refers to statistics from Ofcom indicating, "99% of people aged between 15 and 24 have a mobile phone, the highest penetration rate for any age group." Whereas, in 2000 the presence of mobile phone ownership was restricted to few people in the world and this was the problem for social connectivity that time. This conversion of "societal notions of discourse and knowledge" [16] is the milieu which institutions should both realize and control to stay relevant.

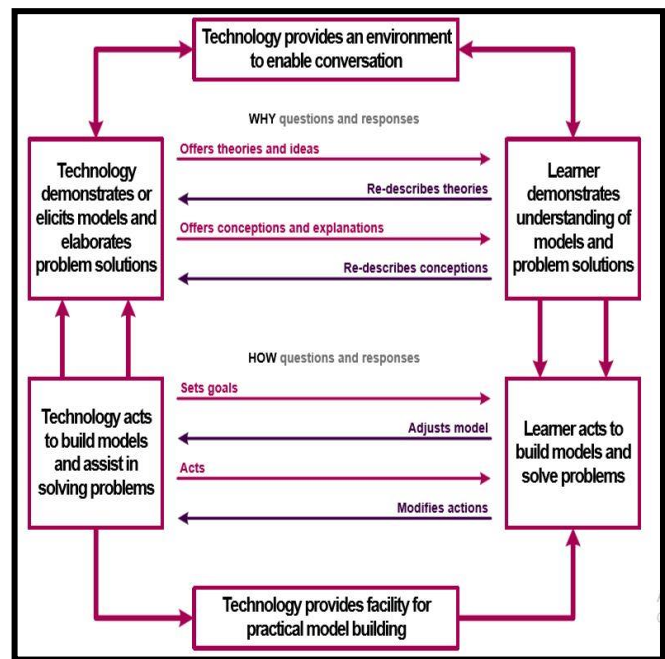


Fig. 1. Development Model of M-Learning [17]

Effective use of conversational Technology: Adopted from [17]

The essential functions of m-technology in developing the 'conversational learning' supported by Laurillard are as follows:

- offering a background and setting to assist conversation
- allowing learners to develop models with intentions of solving problems

This model includes both m-Learning and e-learning that allows the effective learning with the assistance of mobile devices, computer gadgets and applications.

### III. LITERATURE REVIEW

Numerous researchers have put their attention on m-Learning and its background recently. The literature is expanding on the notion of integration of m-Learning. An immediate search for the mobile application stores presents hundreds of free downloadable applications that can be used for learning and teaching. Nevertheless, m-Learning has the possibility to aid task-based learning and collaborative learning [2, 3, 5, 18, 19] the importance dedicated in m-

Learning has been primarily on the delivery of the content that followed teacher mediated technology integration. Early research focused on the sending SMS for quizzes, vocabulary, instruction receiving, and few have focused on the content and its incorporation for teaching.

The advantages of m-Learning apps are being investigated in different learning perceptives. The author in [20] carried out a study to develop learners' experiences and performance of the use of multimedia design. The researcher used numerous mobile phone apps for presentation and feedback session from the learners. The findings endorsed that the m-Learning is operative and successful for the participants and they enjoyed the m-Learning integration. Likewise, the study of [21] focused the mobile based application of Blackboard. The researchers used the mobile based application and desktop-based Blackboard learning for browsing Facebook, email and presenting posts on Facebook. The results indicate that learners remained neutral with the type of technology used as integration with the formal classroom. Furthermore, they added that even the learners didn't show any differences on the use of iPods for the learning. The only positive claim was made that the integration of technology has increased learners' engagement in the learning process.

Similarly, [22] established a conceptual model to investigate the aspects of the m-Learning that affect the presence of the adoption of m-Learning in Malaysian context. The findings of the study endorsed that learners perceived the usefulness of the MALL application. The gender difference didn't show any difference in the attitudes on the integration of MALL in traditional discourse. In another study [3] learners exhibited the positive perception on the use of m-Learning. Results indicated that learners liked the idea of using MALL application as an aid with the formal classroom learning. The author in [23] explored the use of social media for learning and teaching. The findings of the study indicated that social media apps had a positive impact on the learners' performance.

The author in [24] carried out a descriptive analysis of 18 research studies on the use of laptops for the learning purposes. In the analysis of the data presented in the empirical studies, it was found that most of the studies have indicated the positive attitudes in the integration of laptops. However, researchers also indicated some challenges on the integration of technology with the traditional discourse. The author in [25] investigated the effects of m-Learning in fostering learners listening skill among Korean EFL undergraduate learners. The primary purpose of the study was to explore the learners' attitudes on the integration of mobile apps. The analysis of the findings indicated that most of the participants exhibited positive attitudes. On contrary the study of [26] didn't present the positive attitude towards the integration of m-Learning. The differences in the result can be deemed by the fact that study was conducted in two different countries and cultures.

The use of m-Learning apps is still infancy and its developing. Many researchers in language learning and teaching perspective investigated the role of m-Learning apps. There is very little on the use of MALL application for science

subjects and other arena of the teaching and learning. In a study carried out by [27], for illustration, indicated the participants of their experiment were, at first, mainly unaware of how smartphones could be utilized to develop and foster the process of learning but rapidly they have accepted the idea of integrating m-Learning. To sum up, learners need to be helped to indicate the advantages of m-Learning app and how to integrate and use the m-learning with traditional classroom discourse.

Therefore, the present study is an attempt to explore the attitudes of computer students on the use of mobile applications for learning purposes. For this purpose, following research questions were devised to gather the data for the present study:

- 1) Do computer students use m-Learning application for learning purposes?
- 2) What are the attitudes of computer students on the integration of m-Learning application in their formal learning?

#### IV. RESEARCH METHODOLOGY

The present exploratory attempt is an effort to determine the perceived use of m-Learning application among university students in the context of integration with formal classroom. The use of mobile phone is quite vibrant in daily life of the people of Saudi Arabia. Accordingly, the study is designated to focus on the exploration of learners' attitudes towards the integration of m-Learning application in education pursuit. The study adopted the quasi-experimental design to explore the learners' attitudes. The learners were selected on the basis of their registration. The study used 3 experimental group only to investigate their attitudes on m-Learning application.

##### A. Participants

The participants of the present study were (N=143) learners who were enrolled in the second semester of the academic year 2018. All the learners were enrolled at the Preparatory Year Program where they had to study computer skills course for a period of 14 weeks. Their major was computer science and computer engineering. The age of the participants was ranging between 17 and 22.

##### B. Instruments

The study used two questionnaires to collect the data for the present study. One questionnaire was administered before the experiment and the second one was distributed after 7 weeks of the study experiment. Pre-questionnaire consisted of two main parts (the use of application and the use of application for educational purposes) with responses from sometimes to rarely. The second questionnaire was based on 5-point Likert-scale questionnaire from strongly agree to strongly disagree. Both questionnaires were devised by the researcher and then sent to expert in the field of m-Learning to check the face validity of the items. The expert suggestions were incorporated in the questionnaires. Then Google form was created to collect the responses of the participants. The reliability of the questionnaire was checked during the pilot period of the study. The reliability of the questionnaire was (.81 and .79) respectively which indicated that the instrument was reliable to gather the data.

C. Procedure

On the onset of the study, learners were asked to response a questionnaire. In this questionnaire, they were asked to indicate their usage of m-Learning applications in general and for educational purposes. Based on the responses of the participants' usage of m-Learning application, WhatsApp was chosen to send and discuss the material for computer skills course. The participants were asked to do solve the one-page assignments and send them in the groups. The researcher who was also the instructor of these groups sent assignment titles in the group. Participants were asked to check the responses of other members of the groups and they were encouraged to correct the mistakes they saw in the group. The discussion was continued for 6 weeks with two times weekly exposure to the application. The material sent in the group was taken from the course. Finally, in 7<sup>th</sup> week of the experiment, post questionnaire was sent to learners to underpin their attitudes. Their responses were transported into SPSS 22 software after coding them. The descriptive analysis was used to calculate the mean scores and standard of the responses of learners' attitudes.

V. RESULTS

Table I displays the participants' usage of mobile phone application in their everyday life. They were asked to choose from the given 5 applications.

Table I displays the computer students use of mobile phone application daily. It is obvious from Fig. 1 that almost all students use mobile application daily. Some of them use multiple applications. Most of the learners (n=119, 83%) use WhatsApp application for the communication and other purposes whereas Twitter (n=115, 73%) and YouTube (n=115, 80%) are also being used frequently.

A. Computer Students' usage of Mobile Apps for Learning Purposes

Table II given below display the computer students' use of the m-Learning application for academic purposes. For this purpose they were asked to rate the frequency (Always, Frequently, Sometimes, rarely, Never) of the usage of m-Learning applications.

TABLE I. COMPUTER STUDENTS' USAGE OF MOBILE APPLICATIONS

| S.No | Applications | Numbers of users | Percentages |
|------|--------------|------------------|-------------|
| 1    | WhatsApp     | 119              | 83%         |
| 2    | Twitter      | 105              | 73%         |
| 3    | Soma         | 33               | 23%         |
| 4    | Sanpchat     | 25               | 17%         |
| 5    | FB Messenger | 20               | 14%         |
| 6    | youtube      | 115              | 80%         |

TABLE II. CURRENT USE OF MOBILE APPS FOR LEARNING PURPOSES

| S.No | Frequency  | Use of apps | Percentages |
|------|------------|-------------|-------------|
| 1    | Always     | 5           | 3%          |
| 2    | Frequently | 14          | 10%         |
| 3    | Sometimes  | 30          | 21%         |
| 4    | Rarely     | 43          | 30%         |
| 5    | Never      | 61          | 43%         |

It is obvious from Table II that computer students' usage of mobile application is very low. They hardly use the m-Learning applications for learning purposes. A considerable high number (n=61, 43%) never used m-Learning applications for learning purposes. This is followed by (n=43, 30%) participants had rarely used m-Learning applications. Only 21% learners used m-Learning applications for learning and 3% had exposure to m-Learning applications for learning purposes.

B. Computer Students' Attitudes on the Integration of Learning Applications

Table II illustrates the computer students' attitudes on the usage of m-Learning application as an aid with their formal classroom teaching. They were exposed to m-Learning application WhatsApp for solving assignments and discussion, which they were supposed to share in the WhatsApp group. Their responses were recorded and illustrated in the table.

TABLE III. COMPUTER STUDENTS' ATTITUDES ON THE INTEGRATION OF LEARNING APPLICATIONS

| m-Learning Usage   | SD  | D   | N   | A   | SU  |
|--|-----|-----|-----|-----|-----|
| m-Learning app are beneficial for my learning.                                 | 3%  | 5%  | 10% | 36% | 46% |
| m-Learning have the potential of group work and offer rapid communication.     | 4%  | 7%  | 11% | 41% | 47% |
| m-Learning can assist me in looking for my study resources.                    | 2%  | 6%  | 13% | 30% | 49% |
| m-Learning can open many opportunities to develop learning process.            | 3%  | 7%  | 8%  | 32% | 50% |
| m-Learning has the ability to access the study –material anytime and anywhere. | 4%  | 6%  | 7%  | 28% | 55% |
| m-Learning is an easy and quick way to get instructions from the teachers.     | 4%  | 3%  | 6%  | 40% | 47% |
| m-Learning is a good tool of sharing study-material with classmates.           | 2%  | 5%  | 10% | 39% | 44% |
| m-Learning apps have helped me to manage my learning effectively.              | 7%  | 10% | 5%  | 30% | 48% |
| m-Learning had the potential to do the home homework and classwork.            | 10% | 8%  | 11% | 28% | 43% |
| m-Learning can assist me to foster learning skills.                            | 9%  | 7%  | 12% | 40% | 32% |
| m-Learning is a good source of interaction with the teachers.                  | 2%  | 6%  | 8%  | 45% | 39% |
| m-Learning is useful for feedback from classmates and instructors.             | 8%  | 5%  | 7%  | 31% | 49% |
| m-Learning increased my group discussion.                                      | 2%  | 8%  | 6%  | 42% | 42% |
| I will continue using m-Learning applications for learning other subjects      | 3%  | 5%  | 4%  | 38% | 51% |
| m-Learning causes distraction.   | 50% | 29% | 10% | 7%  | 4%  |

Table III presents the learners' attitudes on the integration of m-learning applications. It is viable from the results that learners acknowledged the idea of using m-Learning application as a support in computer skills learning. A large number of participants (36% strongly agree and 47%) regarded m-Learning as beneficial for the learning purposes as compared to only 3% who didn't endorse the idea. The maximum proportion (28% agree and 55% strongly agree) of the m-Learning aspect was item no 5, where learners indicated that the m-Learning has the potential to deliver study material anywhere effectively. Moreover, it is also evident that participants showed positive attitudes on the aspect of m-Learning. They marked that this would also be beneficial for learning other skills and subjects. As they portrayed this in item no. 10 where 40% of the participants indicated it useful for other learning other skill and 32% of the participants marked it strongly agree. This shows their positive perception on the integration of the m-Learning application.

It is also notable that a large number (38% agree and 51% strongly agree) of participants indicated positive attitude towards the behavioral intention. This indicates their positive attitudes towards the m-Learning applications. Only a small proportion (4% strongly agreed) of the experiment indicated that m-Learning is source of distraction when they are used for learning purposes.

## VI. DISCUSSION

The incorporation of technology is not infancy now in the institutions, and m-Learning applications have attained a special place in teaching and learning process. The ubiquity of mobile devices allows learners to integrate it pervasively for learning purposes. Thus, it is important to recognize the effect of technology integration as an option for learning. Currently, mobile learning devices have had a great impact on the daily life, as most of the people are having modern mobile phone devices, which offer learning opportunities. These assist users to interact with other people and sometimes to the device itself. Various studies have endorsed the idea of integration of the m-Learning application for the learning purposes. The review of literatures presents that the focus of the utility of the m-Learning apps was main on the language learning and teaching.

The analysis of the data shows that most the learners had the mobile phone devices and they did not use any of these devices for the learning purposes. Some of them were even not aware of the fact that these can be used for learning purposes. However, when they were exposed to the m-Learning application, they showed enthusiasm in taking part in the WhatsApp discussion. Their attitudes towards the m-Learning application integration were positive and they regarded it a useful learning tool.

The findings of the present study are in the line with [20] who investigated learners' experiences and performance of the use of multimedia design. The findings endorsed that the m-learning is operative and successful for the participants and they enjoyed the m-Learning integration. Likewise, the study result of the present study also endorsed the findings of [21]. The researchers used the mobile based application and desktop-based Blackboard learning for browsing Facebook,

email and presenting posts on Facebook. The results indicated that learners remained neutral with the type of technology used as integration with the formal classroom.

Similarly, [22] endorsed that learners perceived the usefulness of the MALL application. In another study [3] learners exhibited the positive perception on the use of m-Learning. Results indicated that learners liked the idea of using MALL application as an aid with the formal classroom learning. The author in [23] explored the use of social media for learning and teaching. The findings of the study indicated that social media apps had a positive impact on the learners' performance. The positive attitudes of m-Learning in the present study endorsed the findings of the previous studies [3, 5, 24, 25, 27]. However, the findings of the present attempt did not establish a link with the study of [26] The findings of their study didn't present the positive attitude towards the integration of m-Learning. The differences in the result can be deemed by the fact that study was conducted in two different countries and cultures.

## VII. CONCLUSION AND IMPLICATIONS

Mobile-based instruction is gaining popularity and this technology is attracting the attention of researchers to determine its usefulness. This is because of the wide spectrum of its positive and useful traits like ubiquity, flexibility and connectivity. The reviewed literature showed that most of the researchers have focused on the integration of m-Learning application in teaching language skills or other language related aspects. There is lack of literature that presents the effectiveness of m-Learning applications for computer students. This constructs the need of an investigation to gauge the learners' attitudes and effectiveness of m-Learning applications. The findings of the data analysis indicated that participants showed positive attitudes towards the integration-learning applications. The use of m-Learning application attracted their attention.

The results indicated that the integration of m-Learning application could be very handy for the computer students. This asserts that the m-Learning application can be beneficial for other subjects. Instructor need to integrate with sending and receiving assignments and homework. Moreover, m-Learning can also be utilized to evaluate the learners' performance. With less effort, teachers can get the desired results. Like many other studies, this study has some limitations. The study is limited to on male learners; a study is operational to compare the gender differences and performances of male and female learners. The present study is also limited to only one university a comparison can be made with other university locations. Finally, a comparison with other subjects is also necessary to measure the effectiveness of m-Learning application.

## REFERENCES

- [1] Cairo, J., Reading comprehension on the Internet: Expanding our understanding of reading comprehension to encompass new literacies. *The Reading Teacher*, 2003. 56(5): p. 458-464.
- [2] Qian, Y., Technology-Enabled Innovation for Academic Transformation in Higher Education, in *Technology Leadership for Innovation in Higher Education*. 2019, IGI Global. p. 132-164.

- [3] Khan, R.M.I., et al., EFL Instructors' Perceptions on the Integration and Implementation of MALL in EFL Classes. *International Journal of Language Education and Applied Linguistics*, 2018: p. 39-50.
- [4] Kizza, J.M., *Evolving Realities: Ethical and Secure Computing in the New Technological Spaces*, in *Ethical and Secure Computing*. 2019, Springer. p. 209-228.
- [5] Shahbaz, M. and R.M.I. Khan, Use of mobile immersion in foreign language teaching to enhance target language vocabulary learning. *MIER Journal of Educational Studies, Trends and Practices*, 2017. 7(1).
- [6] Taj, I.H., et al., Impact of Mobile Assisted Language Learning (MALL) on EFL: A meta-analysis. *Advances in Language and Literary Studies*, 2016. 7(2): p. 76-83.
- [7] Clark, R.C. and R.E. Mayer, *E-learning and the science of instruction: Proven guidelines for consumers and designers of multimedia learning*. 2016: John Wiley & Sons.
- [8] Burbules, N., *Watch IT: The risks and promises of information technologies for education*. 2018: Routledge.
- [9] Huda, M., et al., *Innovative teaching in higher education: the big data approach*. TOJET, 2016.
- [10] Zabit, M.N.M., *Problem-Based Learning on Students' Critical Thinking Skills in Teaching Business Education in Malaysia: A Literature Review*. *American Journal of Business Education*, 2010. 3(6): p. 19-32.
- [11] Zmuda, A., *Breaking free from myths about teaching and learning: Innovation as an engine for student success*. 2010: ASCD.
- [12] Guri-Rosenblit, S. and B. Gros, *E-learning: Confusing terminology, research gaps and inherent challenges*. *International Journal of E-Learning & Distance Education/Revue internationale du e-learning et la formation à distance*, 2011. 25(1).
- [13] Idrus, R.M., *Mobile learning in distance education: SMS application in a physics course*. *Mobile learning: Malaysian initiatives and research findings*. Malaysia: Centre for Academic Advancement, Universiti Kebangsaan Malaysia, 2013.
- [14] Sharples, M., et al., *Mobile learning*, in *Technology-enhanced learning*. 2009, Springer. p. 233-249.
- [15] Suki, N.M. and N.M. Suki, *Using Mobile Device for Learning: From Students' Perspective*. Online Submission, 2011.
- [16] Koole, M., J. Letkeman McQuilkin, and M. Ally, *Mobile learning in distance education: Utility or futility*. 2010.
- [17] Laurillard, D., *Rethinking university teaching: A conversational framework for the effective use of learning technologies*. 2002: Routledge.
- [18] Burston, J., *MALL: The pedagogical challenges*. *Computer Assisted Language Learning*, 2014. 27(4): p. 344-357.
- [19] Chinnery, G.M., *Emerging technologies going to the MALL: Mobile assisted language learning*. *Language learning & technology*, 2006. 10(1): p. 9-16.
- [20] Garaj, V., *m-Learning in the education of multimedia technologists and designers at the university level: A user requirements study*. *IEEE Transactions on Learning Technologies*, 2009. 3(1): p. 24-32.
- [21] Kinash, S., J. Brand, and T. Mathew, *Challenging mobile learning discourse through research: student perceptions of Blackboard Mobile Learn and iPad*. *Australasian journal of educational technology*, 2012. 28(4): p. 639-655.
- [22] Tan, G.W.-H., et al., *Determinants of mobile learning adoption: An empirical analysis*. *Journal of Computer Information Systems*, 2012. 52(3): p. 82-91.
- [23] Gikas, J. and M.M. Grant, *Mobile computing devices in higher education: Student perspectives on learning with cellphones, smartphones & social media*. *The Internet and Higher Education*, 2013. 19: p. 18-26.
- [24] Fleischer, H., *What is our current understanding of one-to-one computer projects: A systematic narrative research review*. *Educational Research Review*, 2012. 7(2): p. 107-122.
- [25] Nah, K.C., P. White, and R. Sussex, *The potential of using a mobile phone to access the Internet for learning EFL listening skills within a Korean context*. *ReCALL*, 2008. 20(3): p. 331-347.
- [26] Khaddage, F. and G. Knezek, *iLearn via mobile technology: A comparison of mobile learning attitudes among university students in two nations*. in *2013 IEEE 13th International Conference on Advanced Learning Technologies*. 2013. IEEE.
- [27] Woodcock, B., A. Middleton, and A. Nortcliffe, *Considering the Smartphone Learner: an investigation into student interest in the use of personal technology to enhance their learning*. *Student Engagement and Experience Journal*, 2012. 1(1): p. 1-15.

# Exploring the Use of Digital Games as a Persuasive Tool in Teaching Islamic Knowledge for Muslim Children

Madiah Sheikh Abdul Aziz<sup>1</sup>, Panadda Auyphorn<sup>2</sup>, Mohd Syarqawy Hamzah<sup>3</sup>  
Kulliyah of Information and Communication Technology  
International Islamic University Malaysia (IIUM), Selangor, Malaysia

**Abstract**—Various digital games have been developed that focus on providing a sense of enjoyment and excitement for their players in order to be a modern tool for releasing stress or simply for pleasure. In recent years, digital games were also used for teaching and learning. For example, in History subject, games were used for retelling historical stories; at the same time, to preserve the history for the next generation to learn, understand and appreciate. Similarly, Digital games with Islamic values have also been developed to teach Islamic values or knowledge among players, in other words to persuade players to learn or improve their knowledge on Islam. Many designers assumed that games could be used as a persuasive tool to influence players, to learn and understand Islam as a way of life. However, no prior research has been done on the perception of players before and after playing Islamic digital games. To this end, this paper investigates and reports if Islamic Digital Games could persuade gamers to understanding Islam by exploring the use of these games among gamers. A total of 20 school children voluntarily participated in the experiment and the findings are reported in this paper. The study found positive effects on the users' perception toward playing digital games embedded with Islamic values.

**Keywords**—Digital games; persuasive tool; Islamic knowledge; Islamic values

## I. INTRODUCTION

Games vary from computer-delivered interventions by aspiring to be highly enjoyable, attention-captivating and intrinsically motivating [1, 2]. Serious games differ from mere entertainment games in their aim to educate or promote behaviour change. Similarly, serious digital games with religious elements in this context, religion of Islam, are a type of computer-delivered intervention considered to be both educational and fun. Elaborating further, the main aim of these games is to educate or promote behaviour change towards knowing, understanding, and practicing Islam as a way of life. In the context of promoting Islam, this may be achieved via the provision of Islamic-related information, teaching and learning Qur'an (the Islamic sacred book for the Muslims), modeling of positive behaviours, the creation of opportunities to practice Islamic lifestyle; by reading du'a (say a prayer) before and after sleeping; eating or learning. Sitzmann [3] and Wouters, Van Nimwegen, Van Oostendorp, & Van Der Spek [4] highlighted that, serious games may furthermore create sustained effects by being intrinsically motivating to play longer and repeatedly. For example, in the context of this

research, religious digital games with Islamic elements like mobile Qur'an, should be played longer in the effort to memorize Quranic verses in the Qur'an.

## II. RELATED WORK

Serious games are formulated to derive their learning effects from at least three sources: 1) by creating immersion or engagement, a state in which the player becomes absorbed in the play without disbelief, while creating personally relevant experiences and deep affection for the characters; 2) by establishing flow, a state of high concentration in which the player experiences a balance between skills and challenge; and 3) by meeting the individuals' needs for mastery, autonomy, connectedness, arousal, diversion, fantasy, or challenge [5-9].

According to the literature, there are a few studies uses serious digital games with religious elements to inculcate Islamic knowledge among children. For instance, Lotfi, Amine, Fatiha, and Mohammed [10] developed a serious game for teaching ablution and praying correctly. They have tested the game with children and adult students. The results suggest that the players were satisfied with the game and express their intentions to practice in the daily life. In another similar research, Paracha, Jehanzeb, & Yoshie [11] used a serious game to teach Islamic values in school children. During the experiment, they were asked to play the game, and upon completion, they were asked with a series of interview questions. The results showed that the game increased moral values, empathy and awareness on intimidation that children have to overcome.

In relation to persuasion, Fogg [12] coined a model named *Fogg Behaviour Model* that focuses on behaviour change and it has been used as a tool for analyzing behaviour change. The Fogg model proposed three fundamental elements which are motivation, ability and trigger (behaviour trigger) and stated that to contribute a target behaviour, "a person must have sufficient motivation, sufficient ability, and an effective trigger. All three factors must be present at the same instant for the behaviour to occur."

For example, Ponnada, Ketan, & Yammiyavar [13] developed a digital game to persuade players based on the three elements of Fogg in order to change the diffidence of players to become more sociable. The game motivates players by offering rewards and enhances a player's ability by asking new friends to help them in fighting off bullies and the game's

signals on the interface act when acted upon i.e. triggers behavioural change.

This idea of using game as a persuasive tool was also explained by King, Delfabbro, & Griffiths [14] revealing that; presentation (i.e., graphic or sound in a game), social (i.e., share button), manipulation and control (i.e., loading screen or control keys), narrative (i.e., story in a game), reward and punishment features (i.e., bonus point or star) are often important in developing a serious digital game. In addition, narrative features can cause long-term player or addiction, while reward and punishment features evoked a sense of enjoyment.

Recent research shows that serious games with religious elements can be used to instill Islamic knowledge, practices and values for players, for example in changing and shaping people’s mindset towards a certain Islamic topic. They added that the games can instill the positive attitude on players such as compassion, forgiveness, responsibility and sociability [11].

Shelton & Scoresby [15] highlighted that the important features that could directly affect and effect high school students include narrative feature and instructional goals. Elaborating further, a narrative feature (or game story) embedded lessons and simulated situations to players. Meanwhile, instructional goals were designed in such a way to encourage players to be able to comprehend lessons in a game. Lotfi et al., [10] also emphasized on adding narrative feature(s) to gain attention of the players and develop main character(s) to facilitate learning process such as ablution and praying. These features played a significant role in increasing awareness and perception for players. Another example, Paracha et al., [11] use story (narrative feature) in a game such as a bully situation in order to simulate situations and provide solutions. According to the results, the players gained encouragement, empathy and Islamic moral after playing the game [11]. Shelton et al. also showed that the reward and punishment features like getting extra point or life can enhance the challenge and brings out the fun in games. However, focusing on too much fun may not allow the game players to achieve game’s objectives.

Players can learn a lesson when interacting with the game elements such as goals and role-playing. For instant, Muslim Kid in Evil Land game simulates the pre-Islamic Persia and requires a player to act as a practicing Muslim kid. The player is challenged to achieve the game’s goals which are calling and guiding people to Islam by fighting magician’s evil animals and the dark forces [16]. Therefore, it is safe to conclude that the narrative feature, reward and punishment, goals and role-play among others are significant factors for developing effective digital games with religious elements.

Although various research have been carried out relating to religious elements in games, no prior research explored on the perception of players before and after playing these games. This paper seeks to evaluate games with Islamic elements as a persuasive tool to teach Islamic Knowledge among children with Islam religion, also known as the Muslim. The next section explains the method used in this study.

### III. METHOD

Twenty primary school students (11 female, ranging from 6 to 12 years of age) voluntarily participated in the evaluation. Out of 20, ten participants were from English-based learning school in Gombak, Malaysia and another ten were from Thai-based learning school in Bangkok, Thailand. Participants were asked to play with the games in individual sessions taking between 15-30 minutes each. Instructions to participants, the informed consent form, and a demographic information form were provided and given to them. All sessions were audio recorded with permission and transcribed verbatim.

For this study, three games were selected from the Al-Qur’an category [17]. This category was selected, at least for a start, considering that the Holy Qur’an as the root of Islamic knowledge and as the main reference for all Muslim in the world. The three games selected were listed in Table I.

Upon arrival in the test venue, participants were welcomed and briefed about the experiment. Next, they were asked to play each game, they were asked to verbalize their thoughts as they went. At the end of each game, participants were asked to fill out a survey questions CEQE Questionnaire (CEQE). The CEQE was adopted evaluating the ten core elements of gaming experiences which cover sound, graphics, general environment, rules, story, enjoyment, goal, time, and rewards [18]. CEQE was a paper-based with 7-point Likert scale questions with (1) being strongly disagree and (7) being strongly agree as depicted in Table II. It consisted of two parts: the first part generally asked about the background details of each participant, and the second asked about their experiences toward playing digital games with Islamic values.

TABLE I. LIST OF GAMES SELECTED IN THIS STUDY

|   |   |
|---|---|
| <p><i>Ali and Sumaya let's Read</i></p> |  |
| <p><i>Noor Quest</i></p>                |  |
| <p><i>Mable Learns Qur'an</i></p>       |  |



TABLE II. CEGE QUESTIONNAIRE (CEGEQ) GIVEN TO PARTICIPANTS AFTER EACH GAME

| Questionnaire Questions                                | Elements            |
|--|---------------------|
| I enjoyed playing the games                            | Enjoyment           |
| I like the games                                       | Enjoyment           |
| I would play this game again                           | Enjoyment           |
| I like to spend a lot of time playing this game        | Time                |
| I understood the rules of the games                    | Rules               |
| The game was fair                                      | Rules               |
| The game was interesting                               | Enjoyment           |
| The game was difficult                                 | Rules               |
| I knew what to do to win the game                      | Goals               |
| The graphics were proper for the game                  | Graphic             |
| The graphics and sound effects of the game were proper | General Environment |
| The sound effects of the game were appropriate         | Sound               |
| The sound of the game affected the way I was playing   | Sound               |
| The story of the game was interesting                  | Story               |
| The game kept motivating me to keep playing            | Rewards             |

TABLE III. INTERVIEW QUESTIONS

| No. | Interview Questions   |
|-----|---|
| 1   | Which game do you think is the best?                        |
| 2   | Why do you like the game?                                   |
| 3   | What did you learn from the game?                           |
| 4   | Can you apply the Islamic knowledge learned in your life?   |
| 5   | Would you like to play Islamic digital games in the future? |

A semi-structured interview questions were also used after they completed the survey to further investigate and identify the perception of players towards playing these digital games. Table III summarized the interview questions. All sessions were audio recorded with permission and transcribed verbatim.

#### IV. RESULTS AND DISCUSSION

##### A. Pilot Study

It is important to note here that prior to the actual test; a pilot study was conducted first with 2 primary school students aged 6 and 7 years old following the exact procedure as mentioned earlier. Based on the study, we found that some corrections need to be made on the questions used for example, some vocabularies used were difficult for the children to understand, and therefore, the questions were then corrected with simpler wordings.

##### B. Actual Study

1) *Survey data:* In relation to their demographic background, the participants were separated based on English literacy into Thai and International groups. For an international group, it consisted of various nationalities which are 2 Malaysian, 3 Nigerian, 2 Somalian, 1 Syrian, 1 Indonesian and 1 Sri Lankan. The average age for participants from Thailand and other International participants were 7 and 8 years old, respectively.

In the survey, when asked if they have played with any Islamic Digital Games before, fifteen out of 20 (75 %) said

This research is fully sponsored by International Islamic University Malaysia through Research Initiative Grant Schemes (RIGS15-072-0072)

never. Others mentioned only rarely for both groups of participants; Thai and others. The genre that they like the most was Action game with 40% (Thai participants), and 50% (other participants) said they have no preferences. Based on the demographic of both groups, the Thai group had problem to understand the games due to language barrier and lack of Islamic knowledge related to the content of the games (Al-Quran) as compared to the other group of participants with different nationalities.

Based on Table IV, the international participants enjoyed and would like to keep playing compared to Thai participants as shown in the mean values of users' perception. For user's abilities, the mean values of international participants are ranged between 2.1 to 7.0, higher than the Thai participants. However, in terms of the game as being interactive, the mean values of both participant groups were similar at over 6.1. For P-value, the significant is 0.01 level for difficult content and at  $p < 0.05$  level on graphic and sound relation for both groups i.e. it is highly significant.

In Table V, the mean values of Users' perception are ranged between 5.6 and 6.8. For Users' abilities, the *Noor Quest* game is more difficult for Thai respondents (mean = 3.3) compared to International respondents (mean = 1.8). However, for the game interaction, the mean values of both groups are quite similar with the value of over 6.0.

Table VI shows that both groups have similar mean value for users' perceptions; although, the game was more difficult for the Thai participants. Furthermore, the game interaction section was similar in mean values for both groups which surpassed 5.9. For P-value, the significant was at 0.02 level based on how difficult the content of the game was for both groups.

TABLE IV. SURVEY RESULTS FOR THE ALI AND SUMAYA'S GAME

| Construct                  | Mean        |                      | P value |
|----------------------------|-------------|----------------------|---------|
|                            | Thai (n=10) | International (n=10) |         |
| <i>Users' perception</i>   |             |                      |         |
| Enjoyment                  | 6.3         | 6.9                  | .103    |
| Favorite                   | 6.6         | 6.5                  | .795    |
| Continuance                | 6.2         | 6.7                  | .299    |
| Time                       | 5.9         | 5.5                  | .649    |
| <i>Users' abilities</i>    |             |                      |         |
| Understanding              | 5.6         | 7.0                  | .077    |
| Fairness                   | 6.2         | 6.5                  | .536    |
| Interesting                | 6.4         | 6.8                  | .363    |
| Difficult content          | 5.3*        | 2.1*                 | .001    |
| Accomplishment             | 5.2         | 6.7                  | .084    |
| <i>Interactive game</i>    |             |                      |         |
| Graphic                    | 6.8         | 6.1                  | .080    |
| graphic and sound relation | 7.0**       | 6.2**                | .037    |
| Sound suitability          | 6.8         | 6.7                  | .696    |
| Sound effect               | 6.8         | 6.5                  | .177    |
| Story                      | 6.3         | 6.8                  | .216    |
| Motivation                 | 6.3         | 6.4                  | .856    |

TABLE V. SURVEY RESULTS FOR THE NOOR QUEST'S GAME

| Construct                  | Mean        |                      | P value |
|----------------------------|-------------|----------------------|---------|
|                            | Thai (n=10) | International (n=10) |         |
| <i>Users' perceptions</i>  |             |                      |         |
| Enjoyment                  | 6.7         | 6.8                  | .736    |
| Favorite                   | 6.4         | 6.8                  | .324    |
| Continuance                | 6.3         | 6.4                  | .836    |
| Time                       | 6.6         | 5.6                  | .216    |
| <i>Users' abilities</i>    |             |                      |         |
| Understanding              | 5.9         | 6.9                  | .156    |
| Fairness                   | 6.5         | 6.8                  | .331    |
| Interesting                | 6.3         | 6.4                  | .886    |
| Difficult content          | 3.3         | 1.8                  | .142    |
| Accomplishment             | 6.9         | 6.8                  | .662    |
| <i>Interactive game</i>    |             |                      |         |
| Graphic                    | 6.8         | 6.5                  | .382    |
| graphic and sound relation | 6.8         | 6.1                  | .146    |
| Sound suitability          | 6.8         | 6.6                  | .556    |
| Sound effect               | 6.8         | 6.7                  | .696    |
| Story                      | 6.6         | 7.0                  | .168    |
| motivation                 | 6.6         | 6.7                  | .749    |

TABLE VI. SURVEY RESULTS FOR THE MABLE LEARNS QUR'AN'S GAME

| Construct                  | Sample (n=20) |                      | P value |
|----------------------------|---------------|----------------------|---------|
|                            | Thai (n=10)   | International (n=10) |         |
| <i>Users' perceptions</i>  |               |                      |         |
| Enjoyment                  | 6.1           | 6.9                  | .247    |
| Favorite                   | 6.0           | 6.3                  | .666    |
| Continuance                | 6.0           | 6.4                  | .600    |
| Time                       | 5.9           | 5.5                  | .675    |
| <i>Users' abilities</i>    |               |                      |         |
| Understanding              | 6.6           | 6.7                  | .844    |
| Fairness                   | 6.7           | 6.2                  | .472    |
| Interesting                | 6.7           | 6.2                  | .274    |
| Difficult content          | 5.1*          | 2*                   | .002    |
| Accomplishment             | 6.1           | 6.2                  | .909    |
| <i>Interactive game</i>    |               |                      |         |
| Graphic                    | 7.0           | 6.5                  | .138    |
| graphic and sound relation | 6.9           | 5.9                  | .081    |
| Sound suitability          | 7.0           | 6.4                  | .111    |
| Sound effect               | 6.9           | 6.8                  | .660    |
| Story                      | 6.6           | 6.7                  | .714    |
| Motivation                 | 6.6           | 6.5                  | .845    |

Tables IV, V and VI show that both groups enjoyed playing the three games. Moreover, the three games kept motivating the students by providing efficient interactive game elements such as graphic, sound and story.

In relation to the games as a persuasive tool, the targeted behaviour of the three games as suggested by Fogg Behavioural Model (Fogg, 2009) is to persuade players to complete learning the Qur'anic verses, and answer the quiz that follows in order to unlock and proceed to the next level. The three games substantially motivated the respondents by integrating some interesting elements such as animation, graphic and rewards to motivate players. Those elements may drive pressure to the players and can simultaneously boost up the hope in gaining virtues of learning and reading Al-Qur'an.

In terms of ability, the *Ali and Sumaya* as well as *Mable learn Qur'an* games require the players to answer the Qur'anic questions correctly and collect rewards for passing to the next level. The *Noor Quest* game requests players to find missing Arabic letters by dragging the rocket to catch them in order to unlock the basic Surah. So, the three games are quite simple for the players to achieve the target. However, the games do not considerably focus on using either notification or sound to persuade their players to achieve all the Qur'anic lessons and quizzes. The games should motivate players by using Qur'anic verses or hadeeths (saying of the prophet) regarding the virtues of reading Al-Qur'an such as "The best of you are those who learn the Qur'an and teach it to others." (Al-Bukhari) to remind them in learning as a daily task.

Hence, it can be summarized that the three games provide high motivation but moderate trigger to persuade player to achieve the game's targets while players' ability is high when playing.

### C. Opinion Data

The results suggest that all three games have a positive influence on the perception of the participants because of the contents and graphical user interface provided. All students from both groups were interested to play with the Islamic games again and request more time for playing. Moreover, some students asked for the name of the games for them to download, and for future use later.

When asked about their most favorite game, nearly half preferred *Ali and Sumaya* which consisted of Islamic lessons and animation. The participants commented that the game was fun and challenging. Moreover, they liked the animation, the interface as well as Islamic knowledge embedded in the game. Upon completion of the game, they were able to read the surah correctly, as they have learnt how to read Al-Qur'an with the right Islamic manner, rules of *Tajweed* and pronunciation. For example, participants said, "I will use the game as an alternative way to learn Qur'an" and "the game encouraged me to be a Qur'an lover and I can read the Qur'an correctly". For the Thai participants, many said that for them the game is the basic knowledge for reciting Qur'anic verses correctly and encourages love and appreciation during the recitation.

In addition, 30% of the participants prefer *Noor Quest* as the best game due to the narrative element, graphic, engagement and physical movement in the game. The participants expressed that memorizing the Arabic alphabet and the basic Surah for kids can be easy, if they keep playing the game. The participants indicated that the Islamic knowledge in the game can be of benefit to them in the real life because remembering the Arabic letters is the first step to become closer to memorizing and knowing Al-Qur'an. For instant, "the game help me to memorize the Arabic letters and basic Surah", a participant said. Likewise, all thirty percent would like to play the game and other Islamic games in the nearest future.

Similarly, all participants also like the *Mable learn Qur'an* because of the knowledge, humor and graphic elements. The participants enjoyed playing with the learning rules of *Tajweed* just to complete the required goal and collect the

rewards. At that point, players can use the rewards to buy items for decorating their characters. Many participants said that they know Arabic vowel and pronunciation of the Arabic letters that help in reciting the Qur'an correctly through this game. For example, "I can apply the knowledge about Quran in my life", a participant said. Moreover, they expressed that the game can be used as a tool for understanding and memorizing the Qur'an easily and they would like to play the Islamic game again.

## V. CONCLUSION

The overall results show that the Islamic digital games may have positive effects on the users' perception toward playing Islamic games. Majority of the participants were interested in playing the games and have the intention to play more. The chosen Islamic digital games have discovered the participants' perceptions toward playing Islamic games and persuade them in terms of reading Al-Qur'an. Also, the research findings suggest that the content, rules, graphic, story and sound can be the major elements to be considered for increasing the attractiveness and enjoyment of the game from the Islamic perspectives. Using English as the main language is not a barrier for enjoyment but, can be a barrier in gaining knowledge and values in games. There should be an option for players to switch the language.

The findings of this research may benefit the game designers to venture more into the development of education-based games embedded with Islamic knowledge, principles or values for the gamers to learn, understand and apply in their daily life. In addition, a game-based learning that teaches Islamic principles or knowledge can be a great tool particularly for the non-Muslim or the new-Muslim to get to know Islam. This conclusion supports our findings, in our recent paper, on the benefits of digital games from the Muslims scholars' perspectives, as reported and discussed in [19].

## VI. FUTURE WORK

The study only focused on the three games for children from Al-Qur'an genre on mobile platforms. Hence, it is suggested that the future research to include games in different Islamic genres to explore further on the effect if these games as well as to ascertain the common and unique design elements to improve Islamic digital games.

The sample size covered 20 participants from different countries which cannot represent the perception of entire gamers toward playing the Islamic digital games. Conducting more research with greater number of participants would yield more insight.

## ACKNOWLEDGMENT

The authors would like to thank the International Islamic University of Malaysia for funding this research under the Research Initiatives Grant Scheme RIGS15-072-0072.

## REFERENCES

- [1] Graesser A, Chipman P, Leeming F, Biedenbach S. Deep Learning and Emotion in Serious Games. In: Ritterfeld U, Cody M, Vorderer P, editors. *Serious Games, Mechanisms and Effects*. New York and London, Routledge: 2009.
- [2] Prensky, M. *Don't bother me, Mom, I'm learning! How computer and video games are preparing your kids for 21st century success and how you can help!* 2009, St. Paul, MN: Paragon house.
- [3] Sitzmann, T. A meta-analytic examination of the instructional effectiveness of computer-based simulation games. *Personnel psychology* 64.2, 2011, pp. 489-528.
- [4] Wouters, P., Van Nimwegen, C., Van Oostendorp, H., & Van Der Spek, E. D. A meta-analysis of the cognitive and motivational effects of serious games. *Journal of educational psychology* 105, no. 2, 2013, 249.
- [5] Annetta LA. The I's Have It: A Framework for Serious Educational Game Design. *Review of General Psychology*. 2010, 14(2), pp. 105-112
- [6] Boyle EA, Connolly TM, Hainey T, Boyle JM. Engagement in Digital Entertainment Games: A Systematic Review. *Computers in Human Behaviour*. 2012, 28, pp. 771-780.
- [7] Connolly TM, Boyle E, Macarthur E, Hainey T, Boyle JM. A Systematic Literature Review of Empirical Evidence on Computer Games and Serious Games. *Computers & Education*. 2012, 59, pp. 661-686.
- [8] Kapp KM. *The Gamification of Learning and Instruction: game-based methods and strategies for training and education*. San Francisco, CA: John Wiley & Sons; 2012.
- [9] Lu, Amy Shirong, Tom Baranowski, Debb Thompson, and Richard Buday. "Story immersion of videogames for youth health promotion: a review of literature." *Games For Health: Research, Development, and Clinical Applications* 1, no. 3, 2012, pp. 199-204.
- [10] Lotfi, E., Amine, B., Fatiha, E., & Mohammed, B. Learning to pray, islamic children's game. In *International Conference on Multimedia Computing and Systems (ICMCS)*, 2014, pp. 622-627. IEEE.
- [11] Paracha, S., Jehanzeb, S., & Yoshie, O. A serious game for inculcating islamic values in children. In *Taibah University International Conference on Advances in Information Technology for the Holy Quran and Its Sciences*, 2013, pp. 172-177. IEEE.
- [12] Fogg, B. A behaviour model for persuasive design. *Proceedings of the 4th International Conference on Persuasive Technology*, 2009, 1.
- [13] Ponnada, A., Ketan, K. V., & Yammiyavar, P. A Persuasive game for social development of children in Indian cultural context. *4th International Conference on Intelligent Human Computer Interaction (IHCI)*, 2012, pp. 1-6.
- [14] King, D., Delfabbro, P., & Griffiths, M. Video game structural characteristics: A new psychological taxonomy. *International journal of mental health and addiction*, 2010, 8(1), pp. 90-106.
- [15] Shelton, B. E., & Scoresby, J. Aligning game activity with educational goals: Following a constrained design approach to instructional computer games. *Educational Technology Research and Development*, 59(1), 2011, pp. 113-138.
- [16] Tobergte, D. R., & Curtis, S. Assessment in Game-Based learning. *Journal of Chemical Information and Modeling*, 2013, Vol. 53.
- [17] Aziz, M. S. A., Auyphorn, P., Hamzah, M. S., & Othman, R. Types of Digital Games with Islamic Values. *Journal of Computational and Theoretical Nanoscience*, 16(3), 2019, pp. 1100-1103.
- [18] Calvillo Gamez, E. H. On the core elements of the experience of playing video games. 2009. UCL (University College London).
- [19] Aziz, M. S. A., Hamzah, M. S., & Othman, R. The Benefit of Digital Games from the Islamic Perspectives: Views from the Muslim Scholars. *Journal of Computational and Theoretical Nanoscience*, 16(3), 2019, pp. 1104-1107.

# Brain-Controlled for Changing Modular Robot Configuration by Employing Neurosky's Headset

Muhammad Haziq Hasbulah<sup>1</sup>, Fairul Azni Jafar<sup>2</sup>, Mohd. Hisham Nordin<sup>3</sup>, Kazutaka Yokota<sup>4</sup>

Faculty of Manufacturing Engineering, University Teknikal, Hang Tuah Jaya, 76100, Durian Tunggal, Melaka, Malaysia<sup>1,2,3</sup>  
Research Div. of Design and Eng. for Sustainability, Graduate School of Engineering, Utsunomiya University<sup>4</sup>  
7-1-2 Yoto, Utsunomiya-shi, 321-8585, Japan

**Abstract**—Currently, the Brain Computer Interfaces (BCI) system was designed mostly to be implemented for control purpose or navigation which are mostly being employed for mobile robot, manipulator robot and humanoid robot by using Motor Imagery. This study presents an implementation of BCI system to Modular Self-Reconfigurable (MSR) Dtto robot so the robot able to propagate multiple configurations based on EEG-based brain signals. In this paper, a Neurosky's Mindwave Mobile EEG headset is being used and a framework of controlling the Dtto robot by EEG signals, processed by OpenViBE software are built. The connection being established between Neurosky's headsets to the OpenViBE, where a Motor Imagery BCI is created to receive and process the EEG data in real time. The main idea for system developed is to associate a direction (Left, Right, Up and Down) based on Hand and Feet Motor Imagery as a command for Dtto robot control. The Direction from OpenViBE were sent via Lab Streaming Layer (LSL) and transmitted via Python software to Arduino controller in the robots. To test the system performance, this study was conducted in Real time experiments. The results are being discussed in this paper.

**Keywords**—Dtto robot; motor imagery; OpenVibe; modular robot; configuration; communication

## I. INTRODUCTION

In 1970s, a system for communication between human brain and external application being established by Jacques where the raw data obtained based on human brain signals being manipulated into a data vector [1]. The system basically revolves around an electroencephalogram (EEG) which is the brain electrical field measurement where it is being acquired by electrode (head placement) during tasks performing and widely used for diagnosis of mental disease and research in bioengineering [2].

One of the main motivations of BCI research is to help the disabled or elderly. According to the World Health Organization (WHO), 15 million people suffer stroke every year, with one third of them left permanently disabled [3]. Anyhow, with the advancement of technologies nowadays, the BCI implementation has been comprehend for individuals who non-disabled or at normal conditions. The extended BCI implementation is in 3D virtual environment, gaming, research, entertainment and in robotic study. Basically, the robots normally being controlled by using a typical input device for robot control which could be a mouse, a keyboard or a joystick by a normal healthy person. Same goes to Modular Self-

reconfigurable (MSR) robot which being controlled by conventional input interfaces. Unfortunately, that kind of input interfaces is inconvenient for people who have physical disabilities where most of the cases the person is unable to use their arm, unable to walk or even speak. Hence, the person who in that condition unable to effectively use the robot by the conventional input interfaces. This is the cases where the brain-controlled robot is being very useful. The development of brain-controlled robots would be very useful in such cases and this implementation has a potential to be employed to MSR robot. As a robot could be sent to places that inaccessible to humans, MSR robot is one of the robot which can used and it is possible to be controlled by brain.

Now-a-days, BCI system design is based on the exploitation of three categories of brain signals, which include event related desynchronization/event related synchronization (ERD/ERS), steady state visually evoked potential (SSVEP), and P300. There are certain disadvantages and advantages of the brain signals mentioned. Basically, the signals acquired based on the external stimulations of the user and the electrode positions on the head scalp.

In robotic field, BCI system that exploits the ERD/ERS brain signals basically being developed in order for robot control with EEG signals recorded during mental task performance, such as Motor Imagery (MI) and Motor Execution (ME) [4]. ERD/ERS control signals does not require any external stimulus. Hence, users or subject only need to focus their whole attention on controlling the MSR robot.

Even though, the other brain signal type able to be manipulated without substantial training, and it has capabilities to provide a several number control command possibilities, according to Al-Neheimish [5] cited by Malki et al. [6], Motor Imagery provides results with faster feedback. It is due to the asynchronous type of BCI system (ERD/ERS) which independent to the cue-based manner unlike synchronous BCI system (P300 and SSVEP). It is because this system manner make it possible for the EEG features to be process without waiting for the instruction to be completed as it can be process one after another [7][8][9][10]. However, the ERD/ERS BCI system also can be operated based on Cue-based system. Besides that, cue based Motor Imagery (MI) BCI is suitable for our research because it can be used without muscle involvement which is the purpose of BCI system and it gives a certain period for execution of the MSR robot to change configuration.

MSR robot capability for having multiple configurations is being tested by MI BCI system in this study. It acquires EEG signals from human brain and classifies them into two user mental states, left-hand and right-hand motor imagery. To ensure MSR robot is able to propagate multiple configurations based on MI BCI system, another two mental states for the user will be classified so the system will have 4 control input for the robot to change its configuration into 4 types of configurations. Besides that, the Neurosky Mindwave Mobile EEG headset is being used to obtain the EEG signals from the user. It is only have 1 electrode and a non-invasive EEG acquisition device. An expensive EEG headset device was mostly being considered in order to exploiting ERD/ERS brain signals because of the number of electrodes which is more and based on 10-20 electrode positions.

As a preliminary framework that this paper describes, the system of MI BCI system is capable of operating independently and being incorporated into larger platform which is controlling MSR robot. The capabilities of Neurosky for incorporated with MI BCI is expected to produce a poor result as Neurosky only have 1 electrode, meanwhile for MI system, the EEG data has to be acquired by multiple electrodes, positioned based on 10-20 electrode placement system. However, this study is being to show and prove that MSR robot can be controlled and changed for multiple configurations through MI BCI system by communication establishment from OpenViBE to Python for robot control. Hence, since the efficiency for the MSR robot to change its configuration based on the EEG signal is low, this study will not being concluded based on the signal accuracy only. This study will be concluded based on the results of communication establishment based on MI BCI system. Therefore, this study will provide a new perspective for the types of robot to be controlled by EEG.

In the next sections onwards, this paper discussed about the background for each one of the necessary element implemented to achieve this study objectives. Then, there is Section III where this experimental methodology for this study is being discussed. The system performance result is presented and discussed in Section IV and Section V is the conclusion drawn from the result of this study. Discussion on future work is being discussed in Section VI.

## II. BACKGROUND

### A. Electroencephalogram (EEG)

Billions number of neurons made up the brains where each of them is connected to thousands of nerves by axons. As an action potential merged in the dendrites, a stimulus is conveyed through axons in order to communicate. Hence, an electrical field will be generated based on synaptic current produced. According to Ala et al. [11], EEG is a technique for neural sources being localized with a high time resolution as electric scalar measurements is being exploited. Besides that, as researcher involved in EEG study, The International 10-20 standard is need to be known as it is used for positioning electrode on the user head scalp and multiple channels are used because the EEG signals are difference both in term of temporally and spatially.

The electrical signal generated by a single neuron in the human nervous system is too small to be assessed by an electrode on the head scalp [12]. Hence, the measurement of electrical activity is able to be recorded as it comes from the summation of the activity of hundreds of neurons with the electrode based on the closeness of electrode position to the head scalp. Neurons in a group electrify more by collectively and reflecting immediately as a signal being measured by becoming stronger and more collectively to the electrify frequency [12]. The value of the electrical field measured which produced by a group of neuron as overall is known as EEG signal [13].

### B. Neurosky's Mindwave Mobile

Neurosky's [14] device is one of the commercialized EEG devices which being developed to have the acquisition of the EEG based on one-channel of electrode. The electrode position for this device is designed to be at user forehead for frontal recording. Besides that, the type of electrode being used for this device is dry electrode. Reference point of Neurosky is being placed at the earclip. The EEG data from Neurosky transmitted wirelessly using Bluetooth. This device targeting low-end consumer market as it is low cost. Neurosky's headset is used to acquire the EEG data from user head scalp in this study. In Fig. 1, Neurosky's headset and the position of Neurosky's electrode based on 10-20 system are shown.

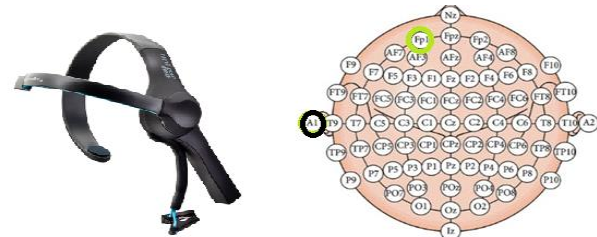


Fig. 1. Neurosky Mindwave Mobile (Left) [14] and the 10-20 System with the Neurosky Electrode Placement in Green-Colored Circle (Right).

### C. OpenViBE

An EEG processing software known as Open ViBE is a free to be downloaded software as it is an open source platform. This software is being developed so that it can be used for designing and testing of the BCI system. Besides that, it is a software where the developed BCI system can be used in real-time event. This software can be used for processing the EEG brain signals from signal acquisition, feature extraction, classification and this software also capable to visualize the data in real time [15]. This software provides a virtual display for convenient user interaction and can be connected with various EEG headsets for data acquisition. In addition, this software also provided with Classifier Trainer box which will be used for training models to classify input data. The available classifiers in OpenVibe processing tools are LDA, SVM and MLP [16].

### D. Dtto-Modular Self-Reconfigurable Robot

Hybrid-type of MSR robot known as M-TRAN is being a concept example for the development of Dtto MSR robot. Dtto robot is being designed in order to provide free space in half of the robot as much as possible. It is because so that it can be used by users to set up their preferred sensor such as Infrared

(IR) sensor or install more actuators. It is 3D printable and at low cost. Dtto is a robot module being designed which consists of two boxes, rounded on one side, connected by a bar. Multiple Dtto robot can join with each other by magnet attraction and able to propagate multiple configuration. It can be fully printed with 3D printer and has been designed using FreeCad software. The robot communicate to each other by Bluetooth and radio communication. Dtto Modular robot built with the idea of male and female part [17].

#### E. Event-Related Desynchronization/Event-Related Synchronization (ERD/ERS)

ERD/ERS is one of the brain signal which commonly being implemented for the BCI system. It is generated when mental tasks are being performed such as by Mental Arithmetic or Motor Imagery (MI) [18]. It is highly frequency band specific where ERD/ERS is able to be displayed at different locations on the head scalp [19]. Actually, there is a slightly differences between ERD and ERS. ERD happened to exhibit power of frequency band in a decreasing manner and meanwhile, ERS happened to exhibit power of frequency band in an increasing manner. The differences for the power spectrum of frequency bands generated show that there are changes occur for a group of neurons in firing patterns which happened during, before or after a motor task event. According to Manca [20], ERD/ERS generated as there are specific frequency changes where the amplitude of the brain signals is based directly on the number of synchronously active neurons. Hence, the increase and decrease for the power spectrum of frequency band can be considered as synchronization and desynchronization. The correlations of synchronization and desynchronization of cortical rhythms indicated to be as ERD/ERS [21]. Analysis of ERD/ERS brain signals recorded has to be done in frequency domain, where the frequency band responds prior to movement. According to Durka [22], the classical evaluation of ERD/ERS have categorized the brain signal into three frequency bands which are mu-band (10-12 Hz), beta-band (14-30 Hz) and gamma-band (30-40 Hz). Decreasing and increasing of frequency band in term of power percentage is evaluated for desynchronization/synchronization of the ERD/ERS brain signals. As prior to movement commencement, mu-ERD can be notable over sensory-motor cortex. Meanwhile, the beta-ERD as the beta band contralateral to the movement and beta-ERS ipsilateral [18]. The gamma-frequency band gave an information of maximum oscillations shortly before beginning of movement and while movement execution. It is shown as in Fig. 2.

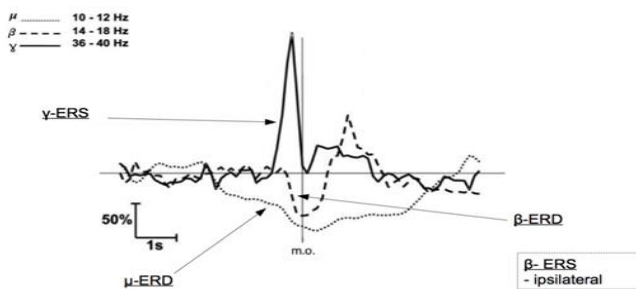


Fig. 2. The Classical Evaluation of ERD/ERS have Categorized the Brain Signal Into three Frequency Bands which are Mu-Band (10-12 Hz), Beta-Band (14-30 Hz) and Gamma-Band (30-40 Hz) [22].

### III. EXPERIMENTAL METHODOLOGY

#### A. Neurosky's Mindwave Mobile Set-up

The acquisition of EEG data is being done by Neurosky's headset. The headset is connected firstly to Open VIBE acquisition server so the BCI system designed by Open VIBE can be deployed. The "COM Port" need to be set correctly. The "Play" button is clicked and if the connection is successful, the acquisition signal will be displayed as in Fig. 3. As Neurosky's implemented dry electrode, it does not need to be moisturized.

#### B. Design of the Motor Imagery BCI System

Graz Motor Imagery is a standard of the mental state discrimination paradigm based on event related potentials. This system is designed by depending on the visually presented cue stimulus. It also based on discrete feedback which involving a symbol of cross ("+") that will be presented at the center of the monitor screen. Depending on the cue stimulus, the subject's task is to focus on their mental states for Motor Imagery to be classified into four control inputs to be visualized in OpenViBE (Right, Left, Up and Down) as in Fig. 4.

The user was asked to concentrate and to fixate to the computer monitor where the fixation cross will starting to be presented at the center of the monitor screen including a short 'beep' cue tone. An arrow will overlaid the fixated cross at the center of the monitor, pointing either between 4 directions. Subject or users will be given an instruction so that the subject is able to have four different movement imaginations. The direction of the arrow at the monitor interface will depends on it.

To train the classifier that will discriminate Right, Left, Up and Down direction by ERD/ERS brain signals, the EEG data is needed to be acquired. An online acquisition scenario is developed to detect both Motor Imagery stimulus and record regular EEG brain signal data. It will acquire the brain signal and all the data needed to train classifier and spatial filter to detect ERD/ERS signal for Motor Imagery system. The data collected from this online acquisition scenario can be used to other developed scenarios. A Common Spatial Pattern (CSP) trainer scenario is developed to compute spatial filter coefficients according to the Common Spatial Pattern algorithm. A third offline developed scenario is used to train the classifier to differentiate for ERD/ERS signal classification. The trained classifier finally being applied to the online Motor Imagery scenario created.

There are 3 Classifiers that can be employed in the scenario which are Linear Discriminant Analysis (LDA), Support Vector Machine (SVM) and Multilayer Perceptron. However, in this study, SVM classifier is implemented. SVM classifier used to differentiate between Motor Imagery signal classes during the scenario online. A probability value provided by SVM classifier will show where the signal belongs in classes [23]. Prior to the classification, before proceeding to the "classifier trainer" box in Classifier Trainer Scenario, pre-processed of the data is done by filtering the data to frequency between 8-30 Hz. Then, the data is decimated and segmented into epoch. Data features extraction is done by the epoch of EEG data acquire being used for trained the classifier. Prior to classifier trainer scenario, same process being through for

trained Common Spatial Pattern (CSP) spatial filter. Before training for the CSP spatial filter, it should first filter the data with respect to the desired band which is 8-30Hz. As stated from Open VIBE, CSP spatial filter is only implemented for two classes [16]. Hence, the implementation that had been done is to have two CSP spatial filter trainer boxes to train four epochs classes. Then the Stimulation multiplexer box algorithm merges several stimulation streams into one stimulation stream. The CSP algorithm work by minimized one condition of signal variance and increasing the other condition.

As for the Online Motor Imagery BCI system, the trained CSP spatial filter and classifier is employed in real time for it to be used online. The “Feature aggregator” box allows these features to be aggregated into a feature vector. Then, the classification step is done by using the “Classifier” box which is implemented with the trained classifier from the previous scenario. The processed data is sent to “Matrix Transpose” box and “Graz Visualization” box. Finally, the “Matrix Transpose” output is sent to the “LSL export (Gipsa)” box that interact by establishing communication with Python after the processed data being translated into a command for controlling the robots. The instruction for the subject to start Motor Imagery is generated by the “Graz Motor Imagery BCI Simulator” box at the early stage in this real-time online scenario.



Fig. 3. OpenVibe acquisition Server Connected with Neurosky’s Mindwave Mobile.

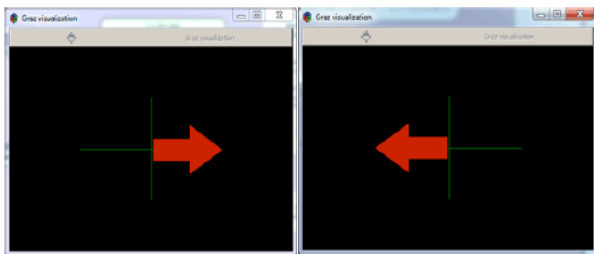


Fig. 4. Graz Motor Imagery Stimulation.

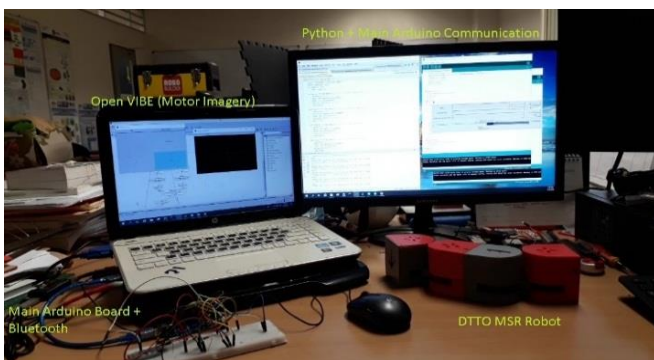


Fig. 5. Experimentation Setup (Neurosky’s Headset had been Wear).

The Dtto MSR robot is supposed to have 4 configurations, thus, 4 control inputs are needed for MI BCI system to determine the configurations for the Dtto MSR robot to change. The main idea is to associate the classified control output to the configuration number for the Dtto MSR robot.

As mentioned, the output data from OpenViBE being sent to the “LSL export (Gipsa)” box that interact by establishing communication with Python. Python programming language is needed in this implementation as there is no other way for direct communication between OpenViBE to Arduino unless there is intermediary programming language. A while-loop concept of Python coding is designed so the communication between Python and V-REP is maintained. The multiple robot configurations are able to change from time to time based on the input for the predetermined modular robot configuration. Those configurations were established by maintaining Python coding loop without changing the coding every time the configuration is changing. Then, the data from Python will be sent to main Arduino board. Bluetooth is being established so the main Arduino will transmit the data wirelessly to Dtto MSR robot and propagate multiple configurations. Fig. 5 shows the experimentation setup for controlling MSR robot by EEG brain signals.

#### IV. PERFORMANCE’S RESULT AND DISCUSSION

The data collected is based on 2 subjects that control the robot which are before training to control the robot (Untrained) and after training to control the robot (Trained). Hence, there are 4 performance results. Each data is based on 30 trials with predetermined configuration for the user to control the robot. The gender of the user is same as well as the age. It is because, to ensure this study is not influenced by gender or age factor. Based on Graz Motor Imagery generated based on EEG, the Left arrow represent Left hand movement for 1st configuration. The Right arrow represents Right hand movement for 2nd configuration. The Up arrow represents Left foot movement for 3rd configuration and the Down arrow represent Right foot movement for 4th configuration. This study is focusing on the establishment of EEG control for the Dtto robot to propagate multiple configurations. The modular robot control attempt results are summarized in Fig. 6.

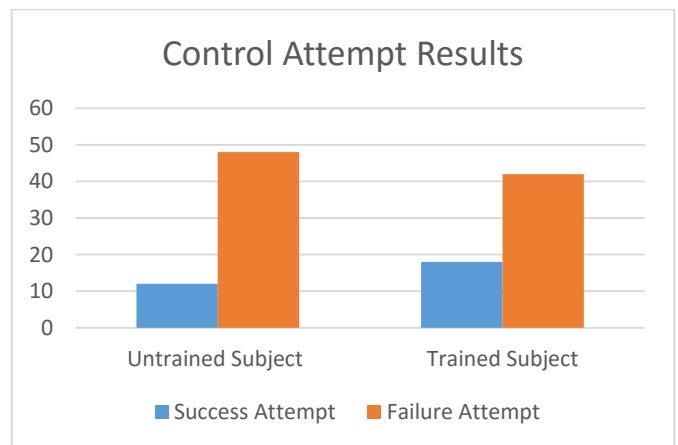


Fig. 6. Results for Dtto Robot Controlled by Brain.

Two 19 years old subject is participate in this study as EEG user where both of them are untrained subject initially. After the first experiment, both subject being trained for Motor Imagery. In this Motor Imagery study, the Motor Imagery system used is Cue-based BCI manner. This is mainly due to the asynchronous type is not depending to the cue-based manner of BCI system, so it might produce the output control signal that results based on the users unintended control as undefined mental task will be classified as control signals. They were asked for 30 control attempts of the robot where the configuration of the robot is based on the configuration instructed. As conclusion, the results obtained as in Fig. 6 (for both subjects) shows that the success rate for untrained subjects is 20% and the success rate for trained subject is 30%. In term of both subjects, the results in Fig. 6 can be detailed for both subject (Subject A and Subject B). The result is shown in Fig. 7.

Regarding the results of Fig. 6 and Fig. 7, the failures can be mainly resulted from the signal quality. It is because of the EEG device equipment where the signal acquisition is done by Neurosky's Mindwave Mobile device. As the BCI system developed is Motor Imagery system where ERD/ERS brain signal is exploited, the used of Neuroky's EEG where it only have one electrode may not be really suitable for Motor Imagery system. Unless for a system that only exploited the signal for concentration and meditation, it is necessary to use an EEG acquisition device where there are several electrodes, place on the head scalp based on 10-20 electrode placement. Besides that, the results could also be affected by how good the subject is trained. We can see a little improvement in the result of trained subject compared to untrained subject. Compared to P300 and SSVEP brain signals, Motor Imagery require an extensive training. Basically, trained subject give a better results as they are becoming better in concentration. Even though the subject is being trained, the results might be improved better if other type EEG acquisition device is being used.

Basically, the overall system is based around data transmission from OpenViBE to Dtto robot (master and slave). These data are transferred then trigger each command. If the right signal trigger is achieved, then if the failure still happened, it might be due to Noise error or Robot error. For better understanding, the results of modular robot configuration control can be seen in Fig. 8.

Fig. 8 shows the percentage of successful attempt with the indication of error probability. The 3% of Noise error happened as it involves the communication among the robot. As Dtto robot use NRF24L01 for communication with each other, noise error might happen during communication and the robot unable to propagate intended configuration. For 8% robot error, it happened as the robot unable to move at all. It might due to servo or low power supply for the robot that need to be further investigate.

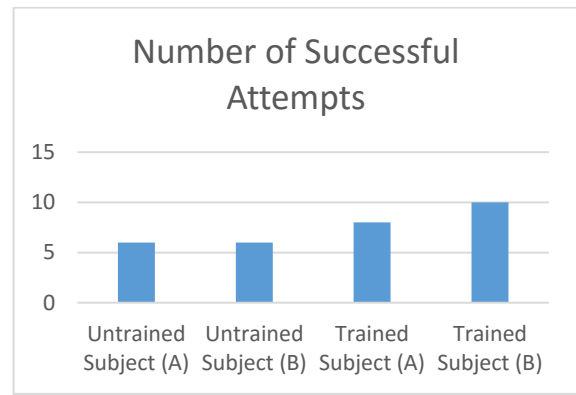


Fig. 7. Results for Trained and untrained Subjects.

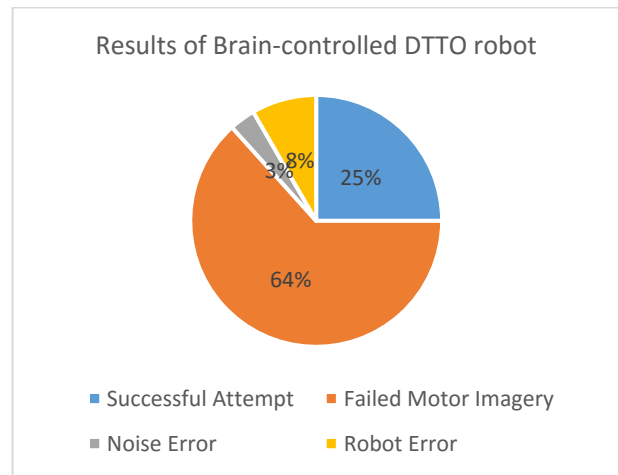


Fig. 8. Results for Modular Robot Configuration Control.

Besides that, for the Dtto robot ability of change the configuration based on EEG brain signal, the subject instructed the robot to change the robot configuration based on the Motor Imagery. All the robot configurations desired is shown as in Fig. 9, Fig. 10, Fig. 11 and Fig. 12 as follows.

The results of this experiment (out of number of successful attempt) in term of robot multiple configurations can be seen in Table I.



Fig. 9. Desired 1<sup>st</sup> Configuration (Straight Line-up).



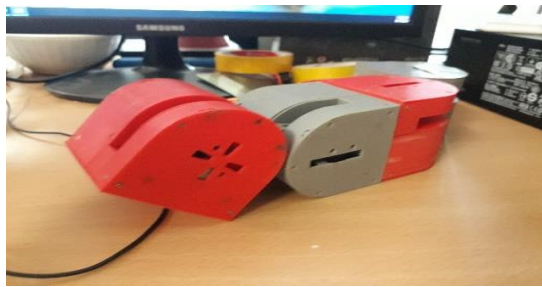


Fig. 10. Desired 2<sup>nd</sup> Configuration (Snake-like Propagation).



Fig. 11. Desired 3<sup>rd</sup> Configuration (Compact-shaped).



Fig. 12. Desired 4<sup>th</sup> Configuration (Separataion of Modular Robot).

TABLE I. SUCCESSFUL ATTEMPTS IN TERM OF ROBOT RECONFIGURATION

| Subjects            | Issued Commands (based on Successful Attempt within the Subjects) |                         |                         |                         |
|---------------------|---|-------------------------|-------------------------|-------------------------|
|                     | Configuratio<br>n A (%)   | Configurati<br>on B (%) | Configurati<br>on C (%) | Configurati<br>on D (%) |
| Untrained Subject A | 33.33   | 0                       | 33.33                   | 33.33                   |
| Untrained Subject B | 16.67   | 33.33                   | 50.00                   | 0                       |
| Trained Subject A   | 37.50   | 25.00                   | 25.00                   | 12.50                   |
| Trained Subject B   | 30.00   | 30.00                   | 20.00                   | 20.00                   |

This data shows that even though the efficiency for Neurosky's EEG device to control multiple Dtto MSR robot is low, it is possible to control MSR robot with brain as shown by the result in Table I. Most of the configurations are able to be achieved by the MSR robot when instructed by the subjects through the developed BCI system. It also able to change multiple type of configurations as intended by user through brain control.

The result obtained in this study is as expected and it might be due to a limitation. The available EEG device during this study is the Neurosky's Mindwave headset. Even though it is

possible to obtain a better EEG device, we believe that as a preliminary study on the Brain-controlled MSR robot subject, the result will help us to obtain the necessary information and it will be used for future research work. Besides that, the other limitation is the number of MSR Dtto robot used in this study. In this study, only 2 modules of Dtto robot are available to be used in our experiment. Each configuration can be in more complex shape if more robot modules are being used.

Overall, the communication system establishment from OpenViBE to Dtto robot can be said as successful with low error probability in term of Noise error and Robot error. The high probability of error in term of Motor Imagery signal is based on the ERD/ERS brain signal acquirement. However, the performance obtained for Motor Imagery BCI system may be improved by using OpenViBE-compatible EEG acquisition device and with the subject that undergo intensive Motor Imagery training. Hence, it is possible for MSR robot to be controlled by brain and perform multiple configurations.

## V. CONCLUSION

Most BCI system implemented to robot is for the robot control, which the command according to Motor Imagery. Results produced in this study provide an insight of implementing BCI system to multiple MSR robots for changing multiple configurations. It can be concluded that the potential for implementation of BCI and MSR robot can be achieved. Even though there are still many technical problems with the robot and the existing BCI system, it still has the potential to be successful in future, and the research and development for both of it are still ongoing for further improvement. Although the Motor Imagery BCI system may executes more than two commands, as MSR robot, more command to be executed should be a lot more advantages for MSR robot to have more configurations to be propagated. P300 or SSVEP might make it possible as they may offer more degree of freedom.

Besides that, the system designed is employed by a low-cost EEG headset device which still proves that the communication from OpenViBE to Dtto robot can be established. The data recorded from EEG device is obtained in real time. Experiments with subjects shows the framework introduced can achieve a better result in multiple MSR robot control in real time.

Overall, the objective of this paper to show that multiple MSR robots can be controlled by brain is achieved even though the results of the experiments are not really good as expected. However, the results show that the establishment of control communication between OpenVibe to Python language for robot control is achievable.

## VI. FUTURE WORK

There are some improvements that are possible to do for future work. Motor Imagery scenario could be improved to obtained better result. Besides that, there could be a more efficient way possible to establish communication from OpenViBE to Dtto MSR robot. Besides that, the number of robot module will be added in future research work so that it can be prove that the system is capable to control a lot more robot module to perform more complex configurations.

REFERENCES

- [1] J. J. Vidal, "Toward Direct Brain-Computer Communication," Annual Review on Biophysics and Bioengineering, vol. 2, pp. 57-80, 1973.
- [2] X. Hou, Y. Liu, O. Sourina, Y. R. E. Tan, L. Wang and W. Mueller-Wittig, "EEG based Stress Monitoring," IEEE International Conference on Systems, Man, and Cybernetics, pp. 3110-3115, 2015.
- [3] M. X. Cohen, "Where Does EEG Come From and What Does It Mean?," Trends Neuroscience, vol. 40, no. 4, pp. 208-218, 2017.
- [4] Z. Tang, S. Sun, S. Zhang, Y. Chen, C. Li and S. Chen, "A Brain-Machine Interface Based on ERD/ERS for an Upper-Limb Exoskeleton Control," Sensors, vol. 16, no. 12, pp. 1-14, 2016.
- [5] H. Al-Negheimish, L. Al-Andas, L. Al-Mofeez, A. Al-Abdullatif, N. Al-Khalifa and A. Al-Wabil, "Brainwave typing: Comparative study of P300 and motor imagery for typing using dry-electrode EEG devices, International Conference on Human-Computer Interaction, pp. 569-573, 2013.
- [6] A. Malki, C. Yang, N. Wang, and Z. Li, "Mind Guided Motion Control of Robot Manipulator Using EEG Signals," 2015 5<sup>th</sup> International Conference on Information Science and Technology (ICIST), pp. 6, 2015.
- [7] Q. Bin Zhao, L. Q. Zhang, and A. Cichoki, "EEG-based Asynchronous BCI control of a car in 3D Virtual Reality Environments," Chinese Science Bulletin, vol. 54, no. 1, pp. 78-87, 2009.
- [8] F. Lotte, H. Mouchere, and A. Lécuyer, "altern rejection strategies for the design of self-paced eeg-based brain-computer interfaces," International Conference on Pattern Recognition, pp. 1-5, 2008.
- [9] G. Pfurtscheller, T. Solis-Escalante, R. Ortner, P. Linortner, and G. R. Muller-Putz, "Self-paced operation of an SSVEP-based orthosis with and without an imagery-based 'brain switch': A feasibility study towards a hybrid BCI," IEEE Transactions on Neural Systems and Rehabilitation Engineering, vol. 18, no. 4, pp. 409-414, 2010.
- [10] A. Satti, D. Coyle, and G. Prasad, "Continuous EEG classification for a self-paced BCI," 2009 4th International IEEE/EMBS Conference on Neural Engineering, NER '09, pp. 315-318, 2009.
- [11] G. Ala, G. Fasshauer, E. Francomano, S. Ganci and M. McCourt, "The Method of Fundamental Solutions in Solving Coupled Boundary Value Problems for M/EEG," SIAM Journal on Scientific Computing, vol. 37, no. 4, pp. 570-590, 2015.
- [12] D. Cohen, and E. Halgren, "Magnetoencephalography," Encyclopedia of Neuroscience. Oxford: Academic Press, pp. 615-622, 2009.
- [13] J. Ward, "The Student's Guide to Cognitive Neuroscience," Psychology, Press Release, University of Rochester, 2000.
- [14] P. D. Girase, and M. P. Deshmukh, "Mindwave Device Wheelchair Control," International Journal of Science and Research (IJSR), vol. 5, no. 6, pp. 2172-2176, 2016.
- [15] K. V. Singala and K. R. Trivedi, "Connection Setup of Openvibe Tool with EEG Headset, Parsing and Processing of EEG signals," International Conference on Communication and Signal Processing (ICCSP), pp. 902-906, 2016.
- [16] Y. Renard, F. Lotte, G. Gibert, M. Congedo, E. Maby, V. Delannoy, O. Bertrand, and A. Lécuyer, "OpenViBE: An Open-Source Software Platform to Design, Test, and Use Brain-Computer Interfaces in Real and Virtual Environments," Presence Teleoperators Virtual Environment, vol. 9, no. 1, pp. 35-53, 2010.
- [17] Alberto, "Dtto - Explorer Modular Robot," Hackaday, 2016. [Online]. Available: <https://hackaday.io/project/9976-dtto-explorer-modular-robot>. [Accessed: 04-Jul-2017].
- [18] G. Pfurtscheller, and F. H. Lopes, "Event-related EEG / MEG synchronization and desynchronization: basic principles," Clinical Neurophysiology, vol. 110, no. 11, pp. 1842-1857, 1999.
- [19] D. R. Freitas, A. V. Inocência, L. T. Lins, E. A. Santos and M. A. Benedetti, "A Real-Time Embedded System Design for ERD/ERS Measurement on EEG-Based Brain-Computer Interfaces," XXVI Brazilian Congress on Biomedical Engineering, pp.25-33, 2019.
- [20] L. Manca, "Master Thesis Proposal: Comparison between ERD / ERS and MRCP based movement prediction on EEG-data," 2013.
- [21] C. Neuper, and G. Pfurtscheller, "Evidence for distinct beta resonance frequencies in human EEG related to specific sensorimotor cortical areas," Clinical Neurophysiology, vol. 112, no. 11, pp. 2084-2097, 2001.
- [22] P. J. Durka, "From wavelets to adaptive approximations: time-frequency parametrization of EEG. Biomedical Engineering Online," vol. 2, no. 1, pp. 1, 2003.
- [23] K. R. Muller, M. Tangermann, G. Dornhege, M. Krauledat, G. Curio, and B. Blankertz, "Machine learning for real-time single-trial EEG-analysis: From brain - computer interfacing to mental state monitoring," Journal Neuroscience Methods, vol. 167, no. 1, pp. 82-90, 2008.

# Analysis of Spatially Modelled High Temperature Polymer Electrolyte Membrane Fuel Cell under Dynamic Load Conditions

Jagdish Kumar<sup>1</sup>

School of Technology and Innovations  
University of Vaasa, Finland, Department of Electrical  
Engineering, Quaid-e-Awam  
University of Engineering Science & Technology, (QUEST)  
Nawabshah, 67480, Sindh, Pakistan

Jherna Devi<sup>2</sup>

Institute of Technology for Nanostructures (NST) and  
Center for Nano Integration Duisburg-Essen (CENIDE),  
University Duisburg-Essen, Duisburg D-47057, Germany,  
Department of Information Technology, Quaid-e-Awam  
University of Engineering Science & Technology, (QUEST)  
Nawabshah, 67480, Sindh, Pakistan

Ghulam Mustafa Bhutto<sup>3</sup>

Department of Electrical Engineering, Quaid-e-Awam  
University of Engineering Science & Technology, (QUEST)  
Nawabshah, 67480, Sindh, Pakistan

Sajida Parveen<sup>4</sup>

Department of Computer Systems Engineering, Quaid-e-  
Awam University of Engineering Science & Technology,  
(QUEST) Nawabshah, 67480, Sindh, Pakistan

Muhammad Shafiq<sup>5</sup>

School of Technology and Innovations  
University of Vaasa, Finland

**Abstract**—This paper presents an interesting approach to observe the effects of the load variations on the performance of high temperature polymer electrolyte membrane fuel cell system, such as: hydrogen and air flow rate, output voltage, power and efficiency. The main advantage of this approach is to analyse the internal behaviour of the fuel cell like current-voltage characteristics during energy conversion, when the load is varying dynamically. This approach of power system simulation models fuel cell system by integrating 3D-COMSOL model of high temperature polymer electrolyte membrane fuel cell with MATLAB/Simulink model of the fuel cell system. The MATLAB/Simulink model for the fuel cell system includes the fuel cell stack (single cell), load (sequence of currents), air supply system (air compressor), fuel supply system (hydrogen tank), and power-efficiency block. The MATLAB/Simulink model is developed in such a way that one part behaves as an input model to the 3D-COMSOL model of the fuel cell system, whereas second part behaves as an output model that recovers the results obtained from the 3D-COMSOL of the fuel cell. This approach of power system modelling is useful to show the performance of high temperature polymer electrolyte membrane fuel cell in much better and accurate way.

**Keywords**—Current-voltage characteristics; energy conversion; fuel cells; power system modeling; power system simulation

## I. INTRODUCTION

The exponential growth in electricity demand, depletion in fossil fuel and production of environmental pollutions, global concerns regarding environmental pollution, and deregulation in the electrical power market have driven the application of distributed energy resources to experience a boost in the power systems as a mean of producing electrical energy [1]–[6]. A Distributed generation (DG) is available in different forms,

which provide the customers a wide range of costs and reliability. A DG technology commonly consists of micro-scale to large-scale power generating resources [7] [8], like small gas turbines, micro turbines, mini hydro, bio-mass, wind, photovoltaic, and fuel cells. Among the distributed energy sources, fuel cells having high power density have gained a great attraction due to its environment friendly operation and can be promising alternative for internal combustion engines [9]. It can be a suitable and an economical option for rural electrification in developing countries.

A fuel cell energy is the results of an electrochemical process in which chemical energy of reaction is directly converted into electrical energy. The popularity of fuel cells as a mean for producing electrical energy increased from last two decade due to many advantages possessed by them. Fuel cells developed today are frequently used in zero-emission electric transportation of vehicles and vessels, off-grid and distributed power generation and in portable consumer electronics [2] [5] [9]–[13]. The wide range applications of fuel cell power system varies from few watts to megawatts make them unique energy converters as compared to any other energy conversion technology. Fuel cells have many characteristics such as they are environmental friendly because they do not use fossil fuels and hence do not produce emissions. They have higher efficiency in the range of 60-80%, they require low maintenance because they are static source of electric power [14] [15] they have comparatively higher efficiency than diesel or gas engines and operate noiselessly. They are sometimes more suitable than batteries because they provide continuous supply of electric power whereas the batteries face the charging and discharging processes. Fuel cells are categorised into different types based on electrolytes, cell material, operating

temperature, and fuel diversity. High Temperature Polymer Electrolyte Membrane Fuel Cell (HT-PEMFC) is considered to be the next generation fuel cell [16], because the electrochemical kinetics for electrode reactions is enhanced as compared to Low Temperature Polymer Electrolyte Membrane Fuel Cell (LT-PEMFC). The HT-PEMFC uses phosphoric acid doped polymer membranes and typically operates above 120°C up to 200°C [5].

LT-PEMFC is already a well-established technology whereas a little research work has been done so far on the development of HTPEMFC system. Despite many advantages, the main problem lies in the modelling of fuel cell to analyse their behaviour. Mathematical models for the fuel cells have attained a great attention in recent years. In [17], PEMFC mathematical model is developed with MATLAB/Simulink and the results are compared with the real test system. It has been found that the developed model is suitable to predict characteristics of the fuel cell as well as analyse, design optimization and real-time control of the PEMFCs. The performance of PEMFC under a constant current and constant power mode has also been analysed and different characteristics have been experimentally found and compared with theoretical calculation in [18]. The semi-empirical model of HT-PEMFC is developed in [19], which can predict the dynamic response at various random loads and fuzzy controller is designed or scheduling the purging process. The performance of 3D-COMSOL model of HT-PEMFC, based on three parameters: operating temperature, catalyst layer thickness, and proton exchange membrane thickness, has been investigated in [20]. The PEMFC having high energy density has been used in different hybrid energy systems and different control algorithms have been applied for optimal and efficient use of energy storage systems [14] [21] [22]. The several methods of starting up of HT-PEMFC from room temperature to the operating temperature are investigated in [23].

The most of the modelling of fuel cell are used in MATLAB/Simulink or COMSOL environment separately. These separate modelling in separate simulation tools has their own relative merits and demerits. COMSOL has the advantage that it can show the internal behaviours of the fuel cell. However, it has limitation that it cannot provide a facility to test fuel cell for dynamic load variations. On the other hand, MATLAB/Simulink has the ability to change the various parameters of the fuel cell but internal behaviours cannot be observed. To address this issue, this paper propose a new method which aims to identify the effect of load variation on performance of the HT-PEMFC by integrating HT-PEMFC model of COMSOL with the fuel cell system model of the MATLAB/Simulink by using MATLAB programming. This approach is suitable to find the internal behaviour of the HT-PEMFC while analysing the variation in load. The rest of the paper is organised as follows: Section II explains methodology of modelling the HT-PEMFC system, Section III presents the results obtained by the MATLAB/Simulink as well as COMSOL, and Section IV presents conclusion and future work follow.

## II. MODELLING OF HT-PEMFC SYSTEM

This section describes the modelling of HT-PEMFC system that consists of HT-PEM fuel cell (fuel cell stack), load profile (sequence of currents), air supply system (air compressor), H<sub>2</sub> supply (hydrogen tank), and power block for measuring total power, net power and hence the efficiency. All the subsystems of HT-PEMFC system are modelled in MATLAB/Simulink, except HT-PEM fuel cell for which 3D-COMSOL model is used. Subsections A, B, and C explain in detail the MATLAB/Simulink modelling, 3D-COMSOL modelling and integration of MATLAB/Simulink model with 3D-COMSOL model respectively.

### A. HT-PEMFC System Model in MATLAB/Simulink

The objective of the MATLAB Simulink model is to observe the effects of the load variation on HT-PEMFC performance, output power and efficiency as well as to regulate HT-PEMFC system dynamically to meet the desired load variations. The following are the subsystems are used to model the fuel cell system model.

1) *Air supply system*: A good performance of a fuel cell stack is based on the required air mass flow rate and air pressure. The mass flow rate and the pressure of the air in many fuel cell system designs are varied to control the oxygen partial pressure, depending on the electrical power output required from the fuel cell stack. The energy requirement of compression process is the main part of the energy consumption of the auxiliary systems in fuel cell system. A realistic air supply model is necessary for use in fuel cell system development particularly for two reasons. First for accurately analysing the fuel cell system performance. Secondly, it is important for maximizing the performance of a particular fuel cell system configuration. The Mass flow rate (kg/sec) of air is changed in this model in accordance with the dynamic variation in load current. The air flow rate in litter per minute is calculated by the equation (1).

$$V_{lpm(air)} = \frac{60000RT i_{fc}}{U_{f(O_2)} z F P_{(air)} y\%} \quad (1)$$

Where,

$R$ : Universal gas constant, 8.3145 [J·mol<sup>-1</sup>·K<sup>-1</sup>],

$T$ : Operating temperature, 453.13 [K],

$i_{fc}$ : fuel cell operating current, [A]

$U_{f(O_2)}$ : Oxygen utilization [set to be 0.593],

$z$ : Number of moving electrons 2 for hydrogen,

$F$ : Faraday's constant, 96485 [A·s·mol<sup>-1</sup>],

$P_{(air)}$ : Air Pressure 1.1 [bar]

$y\%$ : Air composition [set to be 0.21]

As in this model, the air pressure is varied with respect to the mass flow rate in kg/sec, so we have to convert this expression considering the air density of air as 1.225 kg/m<sup>3</sup> (sea level, 15°C).

The pressure ratio of an air varies in accordance with the mass flow rate and in this model; a look up table is used to evaluate the pressure ratio by considering the values of mass flow rate and pressure ratio from the compressor performance map. The minimum and maximum set points for mass flow rate are used as 1e-7 and 0.09 kg/sec respectively by considering the values used in look up table. In the same way, the minimum and maximum values for pressure ratio used are 1.1 and 4. Here one thing is very important to notice that minimum set point value of pressure ratio should be greater than 1. Otherwise, power consumption by the air compressor will be zero at pressure ratio equal to one.

In an adiabatic (no heat loss), the pressure changes from P2 to P1, then the temperature will change from T1 to T2' as shown in equation (2).

$$T_2' = T_1 \left( \frac{P_2}{P_1} \right)^{(\gamma-1)/\gamma} \quad (2)$$

Where,  $\gamma$  is the ratio of the specific heat capacities of the gas that is  $C_p/C_v$  and its value is 1.4 at 20°C. Where P1 and T1 are the applied pressure and temperature of the incoming air that are 1.1 bar and 298 K and P2 is the output pressure of the air compressor.

The actual temperature change will be higher than the isentropic temperature change because some of the motion of the moving blades and vanes in compressor can raise the temperature of the gas. It can be obtained by using the following equation (3).

$$\Delta T = T_2 - T_1 = \frac{T_1}{\eta_c} \left( \left( \frac{P_2}{P_1} \right)^{\frac{\gamma-1}{\gamma}} - 1 \right) \quad (3)$$

Where  $\eta_c$ : Compressor efficiency [%]

Keeping in view, the safe operation and optimum efficiency, a look up table is used to obtain the compressor efficiency in correspondence with the pressure ratio.

The power consumed to drive a compressor can be easily calculated from the change in temperature by using the equation (4).

$$Power = W' = Cp\Delta Tm' \quad (4)$$

Where  $m'$  is the mass flow rate in kg/sec, and change in temperature  $\Delta T$  can be obtained by using equation (3), so we have another equation in terms of pressure ratio as shown in equation (5).

$$Power = Cp \frac{T_1}{\eta_c} \left( \left( \frac{P_2}{P_1} \right)^{(\gamma-1)/\gamma} - 1 \right) m' \quad (5)$$

Where,

$$Cp: 1004 \text{ [J} \cdot \text{Kg}^{-1} \cdot \text{K}^{-1}]$$

$$\gamma: 1.4$$

$$\eta_c: \text{Isentropic efficiency}$$

To find the power needed from the motor or turbine driving the compressor, the equation 5 is divided by the mechanical efficiency  $\eta_m$ , which is taken 0.98 in this model.

2) *Fuel supply system (Hydrogen Tank)*: The hydrogen is fed to the anode in dead ended mode, so that there is no venting or circulation of the gas, but it is consumed by the fuel cell. The hydrogen is supposed to be stored in a tank at a pressure of 300 bars. It can be further reduced through the pressure reduction valves to a value comparable to the compressed air pressure that is approximately in the range of 1.1 to 4 bars as mentioned in the earlier section.

The anode inlet flow rate can be adjusted instantaneously by a valve to keep the pressure difference between the cathode and anode as minimum as possible. Here it is supposed that the anode flow resistance is negligible as compared to the cathode flow so that pressure difference can be maintained for the sufficient amount of flow of hydrogen for fuel cell reaction. The temperature of flow is supposed to be equal to the fuel cell temperature and the condition of the gas namely pressure, temperature of anode outlet flow is the same as the condition of the gas in the anode flow channel. The partial pressure of hydrogen can be determined by balancing the mass flow of hydrogen in anode. The model contains anode inlet total mass  $m_{H_2,in}$ , inlet flow pressure  $p_{H_2,in}$ , inlet flow temperature  $T_{an,in}$ , fuel cell current  $I_{st}$ , fuel cell temperature  $T_{st}$ . The state of hydrogen mass  $m_{H_2,an}$  inside the anode volume can be obtained by equation 6.

$$\frac{dm_{H_2,an}}{dt} = \dot{m}_{H_2,an,in} - \dot{m}_{H_2,reacted} \quad (6)$$

The other parameter of mass balance equation is to calculate the consumed hydrogen reaction rate is function of stack current given by equation 7.

$$\dot{m}_{H_2,react} = M_{H_2} \cdot \frac{N_{cell} \cdot I_{st}}{2F} \quad (7)$$

The mass of hydrogen calculated is used to determine hydrogen partial pressure  $p_{H_2,an}$  given by equation 8.

$$p_{H_2,an} = \frac{m_{H_2,an} \cdot R_{H_2} \cdot T_{opr}}{V_{an}} \quad (8)$$

Whereas, the anode pressure is given by equation 9.

$$p_{an} = p_{H_2,an} \quad (9)$$

The mass flow rate of hydrogen is controlled by at anode inlet by proportional control, which follows the changes in cathode pressure ( $p_{ca}$ ) and given by equation 10.

$$\dot{m}_{an,in} = k_1 \cdot (p_{ca} - p_{an}) \quad (10)$$

Table I represents the physical parameters, which are used in the equations of hydrogen fuel supply.

TABLE I. PHYSICAL PARAMETERS OF HYDROGEN GAS

| Symbol     | Definition                             | Value                                       |
|------------|--|---|
| $R_{H_2}$  | Hydrogen gas constant                  | 8.3145 J·mol <sup>-1</sup> ·K <sup>-1</sup> |
| $T_{opr}$  | Operating temperature                  | 453.13 K                                    |
| $V_{an}$   | Anode volume                           | 0.005 m <sup>3</sup>                        |
| $M_{H_2}$  | Hydrogen molar mass                    | 2.016e-3 Kg/mole                            |
| $N_{cell}$ | Number of cell in fuel cell stack      | 1   |
| $F$        | Faraday constant                       | 96485 C/mole                                |
| $k_1$      | Proportional gain for the supply valve | 2.1 Kg/(s·kPa)                              |

The fuel flow rate of hydrogen is changed in accordance with the dynamic variation in load current. The fuel flow rate is in litre per minute and calculated by the equation 11.

$$V_{lpm(fuel)} = \frac{60000RTifc}{U_{f(H_2)}zFP_{(fuel)}x\%} \quad (11)$$

Where:

R: Universal gas constant, 8.3145 [J·mol<sup>-1</sup>·K<sup>-1</sup>],

T: Operating temperature, 453.13 [K],

i<sub>fc</sub>: fuel cell operating current, [A]

U<sub>f(H<sub>2</sub>)</sub>: Hydrogen utilization [set to be 0.99556],

z: Number of moving electrons 2 for hydrogen,

F: Faraday's constant, 96485 [A.s.mol<sup>-1</sup>],

P<sub>(fuel)</sub>: Fuel pressure, calculated from equation 8,

X%: Hydrogen composition [set to be 0.9995]

In this model, hydrogen stored in a tank is considered at a pressure of 300 bar and at ambient room temperature of 298 K. Now adiabatic changes in output temperature T<sub>2</sub>' can be found by using equation 12.

$$T_2' = T_1 \left( \frac{P_2}{P_1} \right)^{(Y-1)/Y} \quad (12)$$

Where:

T<sub>1</sub>: 298 K for hydrogen to be at room temperature

Y: C<sub>p</sub>/C<sub>v</sub>= 1.405 for hydrogen

P<sub>1</sub>: 300 bar

P<sub>2</sub>: Partial pressure of hydrogen (P<sub>f</sub>)

3) *Dynamic load profile*: The load in the model is considered as sequence of currents applied at different time steps. The total time of simulation is 4 seconds with the 400 time steps, means each time step is of 0.01 second and the value of the load current is assigned to each time step. The sequence of current is applied in such a way that for each 80-time steps the load current is changed. For the first 80 time steps, the load current 0.06 A is considered, and for the remaining each 80 steps 0.04 A, 0.05 A, 0.07 A, and 0.03 A of the load current is considered.

4) *Power block*: The power block is used to measure fuel cell input and output power, net power, and the overall system efficiency. The Stack power is also known as output power obtained from the fuel cell. It is defined as the product of fuel cell voltage and the current drawn by the load from the fuel cell. It is given by equation 13.

$$P_{out} = V_{cell}I_{load} \quad (13)$$

The input power of the fuel cell is obtained by dividing fuel cell output power divided by the fuel cell stack efficiency, given by the equation 14.

$$P_{in} = \frac{P_{out}}{\eta_{stack}} \quad (14)$$

Where  $\eta_{stack}$  is fuel cell stack efficiency and given by the equation 15.

$$\eta_{stack} = \left( \frac{N_c I_{fc}}{zFU_{fH_2}} \right) \cdot \Delta_{H_0} \quad (15)$$

Where

N<sub>c</sub>: Number of cells=1;

I<sub>fc</sub>: Fuel cell current;

z: Number of moving electrons=2;

U<sub>fH<sub>2</sub></sub>: Utilization of hydrogen,

Δ<sub>H<sub>0</sub></sub>: Reaction Enthalpy, [241830 J·mol<sup>-1</sup>]

The net power obtained from the fuel cell stack is equal to the total stack power generated minus the power consumed by auxiliary equipment. In this model, the air compressor is used as auxiliary equipment that consumes the power, so the net power here will be the total power minus the compressor power given by equation 16.

$$P_{net} = P_{out} - P_{comp} \quad (16)$$

Thus, the overall fuel cell system efficiency is in this model is obtained by simply dividing the net power P<sub>net</sub> by the total power input P<sub>in</sub> to the fuel cell stack.

### B. Spatial modelling of HT-PEMFC in COMSOL

COMSOL is a flexible platform that allows users to model all relevant physical aspects of their designs. It is compatible for different application with different physics and interfaces their combinations. COMSOL Multi-physics provides finite element methods (FEM) solution for spatial modelling. A HT-PEMFC is based on phosphoric acid doped polymer membranes that usually operates in a temperature range of 160°C to 180°C, and this section describes the 3D spatial modelling of HT-PEMFC in COMSOL as shown in Fig. 1.

It contains flow channels for the fuel (Hydrogen) and air (oxygen), gas diffusion layers (GDLs) on each side of the electrodes for the proper distribution of gases, porous electrodes (anode and cathode) where the electrochemical reactions (oxidation and reduction) takes place, membrane used as an electrolyte for ionic current flow, inlets and outlets for incoming and outgoing of hydrogen and air. The electrochemical reactions produce water on the cathode side in the cell, which lowers both partial pressures of hydrogen and oxygen on the anode and cathode, respectively and the rate of the cell reactions. The local water concentration in the cell is sometimes have positive impact because it can increase the ion conductivity, but on other hand if water condenses in the cell can cause leaching of phosphoric acid out from the polymer matrix, which can reduce the ion conducting capabilities of the membrane as well as affect performance of the whole cell. Normally water does not condensate in the cell when temperature is above 100°C, but information about water content in the porous electrodes is required to optimize shut-down procedures, during operation [6].

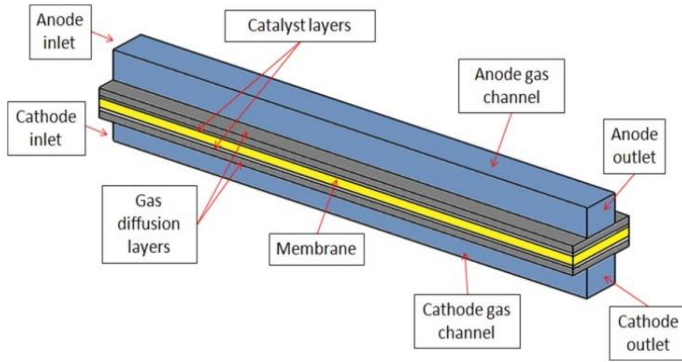
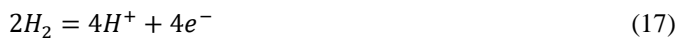


Fig. 1. Model Geometry of HT-PEMFC [6].

The electrochemical and thermal model of HT-PEMFC consists of many sub models such as current distribution model, mass transport models in both fluid channels and in porous media, and temperature distribution model. The anode and cathode potentials are obtained by using Butler-Volmer equation and the ionic and electronic currents are calculated by Ohm's law. The mass transfer of the both reaction species in flow channels and in porous diffusion layers are calculated by Maxwell-Stefan equation. The momentum transfer in flow channels is described by the Nernst-Stokes equation whereas the momentum transfer in porous gas diffusion layers is described by the Brinkman equation. In this modelling, the different unknown variables such as electronic potential, ionic potential, hydrogen mass fraction, water mass fraction, oxygen mass fraction, nitrogen mass fraction velocity field vectors in the anode compartment, cathode compartment and also in porous media, pressure in the anode compartment cathode compartment and porous media are determined by using the above physical laws and equations. Keeping in view the system modelling as discussed in Section A, only the parameters required to be evaluated are hydrogen and air mass flow rate, which are changing with respect to change in load current. Besides this, the model is used to evaluate the performance of current distribution and potential distribution inside HT-PEMFC. The different physics used in the model to determine the unknown variables are given in the following subsections.

1) *Secondary current distribution*: This physics is added for modelling the electrochemical currents using Ohm's law and solving for electronic potential  $\Phi_s$  in the porous electrodes (anode and cathode) and in the GDLs, ionic potential  $\Phi_l$  in the porous electrodes (anode and cathode), and in the electrolyte membrane. The local current densities in the porous electrodes depend on the ionic and electronic potentials, and local reactant concentrations. The hydrogen oxidation reaction occurs on the anode is given in equation 17.



The following local current density expression (linearized concentration dependent Butler-Volmer expression) is used when no water molecules are supposed to be involved in the proton transport and the for the hydrogen oxidation reaction, then anode current density is given in equation 18.

$$i_{loc} = i_o \left( \frac{\alpha_a + \alpha_c F}{RT} \right) \eta \quad (18)$$

Where

$F$ : Faraday's constant,  $96485 [A \cdot s \cdot mol^{-1}]$ ,

$R$ : Universal gas constant,  $8.3145 [J \cdot mol^{-1} K^{-1}]$ ,

$T$ : Operating temperature of fuel cell,  $453.13 [K]$ ,

$\alpha_a = 1$  (Anode charge transfer coefficient),

$\alpha_c = 1$ , (Cathode charge transfer coefficient),

$i_o$  = Exchange current density at anode, and it is determined by equation 19.

$$i_o = 1e^5 [A/m^2] \left( \frac{C_{H_2}}{C_{H_2,ref}} \right)^{0.5} \quad (19)$$

Where

$C_{H_2,ref}$ : Hydrogen reference concentration,  $40.88 [mol \cdot m^{-3}]$ ,

$C_{H_2}$ : Local hydrogen concentration  $[mol \cdot m^{-3}]$ ,

Whereas,  $\eta$  is an activation over potential at anode and is given by equation 20.

$$\eta = \phi_s - \phi_l - E_{eq} \quad (20)$$

Where

$\Phi_s$  = Electronic potential [V]

$\Phi_l$  = Electrolyte potential [V]

$E_{eq}$  = Equilibrium potential

The oxygen reduction reaction occurs on the cathode, known as cathode reaction in which water is produced and is given in equation 21.



For the oxygen reduction reaction, the following current density expression (Cathodic Tafel Equation) is used as given by equation 22.

$$\eta = A_c \times \log_{10} \left( \frac{-i_{loc}}{i_o} \right) \quad (22)$$

From above equation, current density at cathode ( $i_{loc}$ ) is determined. Whereas  $\eta$  is an activation over potential at cathode and is calculated in the same as given by equation 20. The  $A_c$  is Cathodic Tafel constant and its value should be less than 1, and here -0.095 V is considered.

The exchange current density at cathode ( $i_o$ ), can be determined by equation 23.

$$i_o = 1 [A/m^2] \left( \frac{C_{O_2}}{C_{O_2,ref}} \right) \quad (23)$$

Where,

$C_{O_2,ref}$ : Oxygen reference concentration,  $40.88 [mol \cdot m^{-3}]$

$C_{O_2}$ : Local oxygen concentration

The boundaries of anode GDL facing towards the flow pattern ribs are fixed to zero electronic potential, and the corresponding boundaries towards the cathode side are fixed to

the cell potential. All the other external boundaries are electrically isolating.

2) *Transport of concentrated species*: The Maxwell-Stefan equations are used to solve for the mass transport in the flow channels, GDLs and porous electrodes. Two Transport of Concentrated Species interfaces are used here, one for each electrode compartment. Hydrogen and water species are present on anode electrode compartment whereas oxygen, nitrogen and water are present on the cathode electrode compartment.

3) *Maxwell-Stefan diffusion equations*: When using Maxwell-Stefan Diffusion Model, the mass fraction of the species ( $w_i$ ) can be determined by equation 24.

$$\nabla \cdot j_i + \rho(\mathbf{u} \cdot \nabla)w_i = R_i \quad (24)$$

Where  $R_i$  is source term caused by chemical reactions,  $\mathbf{u}$  is velocity field which is determined in the next physics (Free and Porous Media Flow),  $\rho$  is gas density, and can be determined by ideal gas law equation as given in equation 25.

$$\rho = \frac{pA M_n}{RT} \quad (25)$$

Where  $M_n$  is molar mass of the species measured in Kg/mole,  $R$  is universal gas constant,  $T$  is operating temperature of the fuel cell and  $pA$  is the absolute pressure, and is determined by equation in equation 26.

$$p_A = p + p_{ref} \quad (26)$$

Where  $p$  is pressure which is also determined in the next physics (Free and Porous Media Flow) and  $p_{ref}$  is the reference pressure, which is taken as  $101e3$  [Pa] for the fuel cell. The relative mass flux vector  $j_i$  for the equation 24 is calculated by using equation 27.

$$j_i = -\left(-\rho w_i \sum_k D_{ik} d_k + D_i^T \frac{\nabla T}{T}\right) \quad (27)$$

Where  $D_{ik}$  is the Maxwell-Stefan diffusivity matrix, measured in  $m^2/s$ , and its coefficients are already described in the parameters of the fuel cell. The  $D_i^T$  represents the thermal diffusion coefficients of the species, measured in  $Kg/(m.s)$  but here they are not considered so their values are zero. The  $dk$  is diffusional driving force, and can be determined by equation 28.

$$d_k = \nabla x_k + \frac{1}{p_A} [(x_k - w_k)] \nabla p_A \quad (28)$$

Where  $x_k$  (mole fraction of species  $k$ ) and  $w_k$  (mass fraction of species  $k$ ) are determined by using the equations 29 and 30.

$$x_k = \frac{w_k M_n}{M_k} \quad (29)$$

$$M_n = \left(\sum_i \frac{w_i}{M_i}\right)^{-1} \quad (30)$$

For determining the mass sources and sinks, the couplings are made to the secondary current distribution interface and in the same way the couplings are made to the Free and Porous Media Flow interface for evaluating the velocity field and

pressure. The mass fractions are specified at the channel inlets, whereas the outflow conditions are used at channel outlets.

4) *Free and porous media flow interface*: The Navier-Stokes equations are used to model the velocity field and pressure (Pa) in the flow channels and Brinkman equations are used to model velocity field and pressure (Pa) in the porous gas diffusion layers (GDLs) and electrodes. The laminar inlet flow velocity profiles are considered while at the flow channel outlet boundaries, a pressure is considered. In this physics, anode and cathode compartment are made which consist of the corresponding flow channel, GDL and electrode domains. These compartments are named with "Fluid Properties" and follow the Navier-Stokes equations because of flow channels.

5) *Navier-Stokes equations*: The Navier-Stokes equations describe the motion of fluid substances and are derived by applying Newton's second law to fluid motion, along with the assumption that fluid stress is the sum of diffusing viscous term (proportional to the gradient of velocity) and a pressure term hence describing viscous flow. These equations explain velocity field or flow field of the fluid at a given point in space and time. The equation 31 describes how the velocity field  $\mathbf{u}$  is calculated.

$$\nabla \cdot (\rho \mathbf{u}) = 0 \quad (31)$$

Where  $\rho$  is density of species, and the dynamic viscosity  $\mu$  can be taken from the material properties of the species. The pressure in flow channels can obtain by using equation 32.

$$\rho(\mathbf{u} \cdot \nabla) \mathbf{u} = \nabla \cdot [pI + \mu((\nabla \mathbf{u}) + (\nabla \mathbf{u})^T) - \frac{2}{3}\mu(\nabla \cdot \mathbf{u})I + F] \quad (32)$$

Where,

$I$ : unity matrix of order  $3 \times 3$

$F$ : Influence of gravity and other volume forces, [ $Kg/(m^2.s^2)$ ]

$p$ : Pressure [Pa]

6) *Brinkman equations*: Brinkman equations have two dependent variables: the directional velocities and pressure. A combination of the continuity equation and momentum balance equation form the Brinkman equations and govern the flow in porous media. The Brinkman equations define fast-moving fluids in porous media with the kinetic potential from fluid velocity, pressure, and gravity to drive the flow. These equations are extended from Darcy's law to describe the dissipation of the kinetic energy by viscous shear as with the Navier-Stokes equations. Subsequently, this physics interface suits transitions in the best way between slow flow in porous media governed by Darcy's law and fast flow in channels described by the Navier-Stokes equations.

Porous flow is considered in "Porous Matrix Properties", which consist of anode GDL, anode electrode, cathode GDL and cathode electrode and follows the Brinkman equations. The velocity field  $\mathbf{u}$  of the species in the porous flow is determined by equation 33.

$$\nabla \cdot (\rho \mathbf{u}) = Q_{br} \quad (33)$$



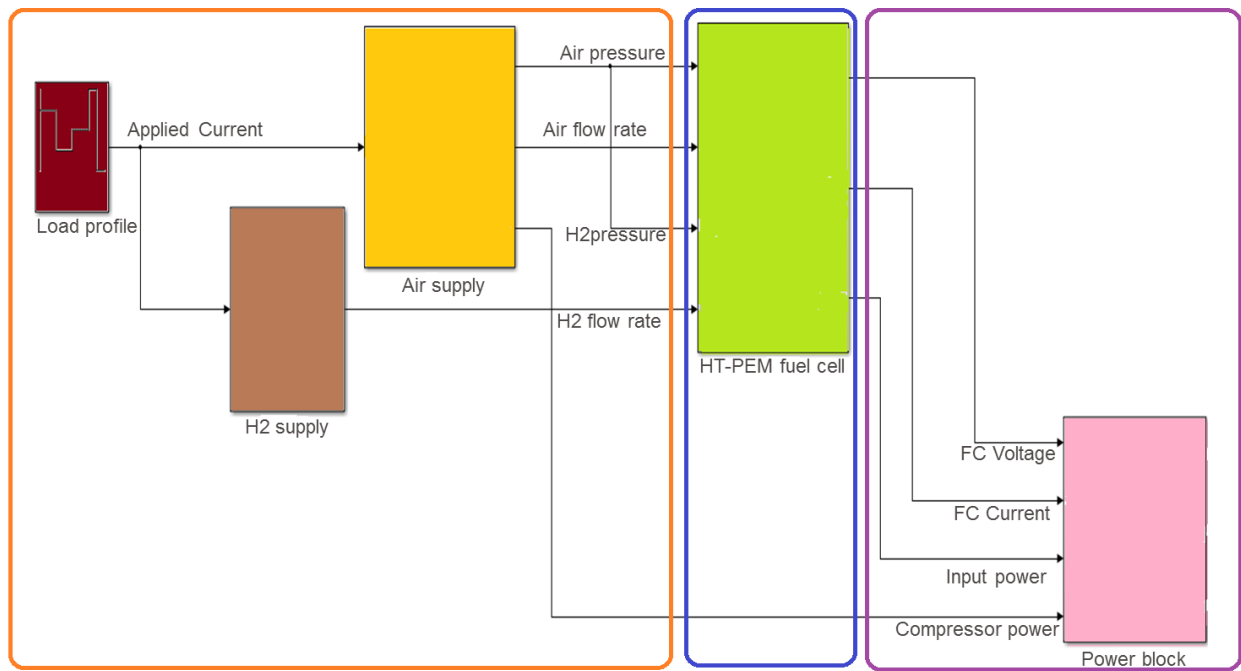


Fig. 2. Modelling of HT-PEMFC System.

Where,

$Q_{br}$ : Mass source or sink measured in  $\text{Kg}/(\text{m}^3.\text{s})$

By considering the porosity  $\epsilon_p$  and the permeability  $K_{br}$  [ $\text{m}^2$ ] of the material, the pressure of species in porous flow can be evaluated by using equation 34.

$$\frac{\rho}{\epsilon_p} \left( (u \cdot \nabla) \frac{u}{\epsilon_p} \right) = \nabla \cdot \left[ pI + \frac{\mu}{\epsilon_p} ((\nabla u) + (\nabla u)^T) - \frac{2\mu}{3\epsilon_p} (\nabla \cdot u) I \right] - \left( \frac{\mu}{K_{br}} + \beta_F |u| + \frac{Q_{br}}{\epsilon_p^2} \right) u + F \quad (34)$$

where  $\beta_F$  is Forchheimer drag option [ $\text{Kg}/\text{m}^4$ ], which adds a viscous force proportional to the square of the fluid velocity

### C. Integration of spatial model with fuel with system in MATLAB/Simulink

In this section, the procedure of integration of 3D-COMSOL model with FC system is described in steps. The Fig. 2 shows the integration of 3D-COMSOL model of HT-PEMFC with the inputs and outputs blocks modelled in MATLAB/Simulink. The main objective of integration of 3D-COMSOL Model of HT-PEMFC with FC System is to observe the internal behaviours of fuel cell like voltage distribution and current distribution with the variation of load demand. First of all 3D-COMSOL model of HT-PEMFC is saved as mph file. Afterwards, the FC system model of MATLAB/Simulink is broken in to two parts in such a way that one part behaves as an input model to the 3D-COMSOL model of HT-PEMFC, whereas second part behaves as an output model that recovers the results obtained from the 3D-COMSOL of HT-PEMFC. Based on the sequence of currents and time steps taken, “for” and “if” loops are applied and the corresponding changes in voltage, power, hydrogen flow rate and air flow rate are made in the simulation results of 3D-COMSOL model of HT-

PEMFC. These results are post processed from the workspace of MATLAB in the second part of Simulink model through the same MATLAB programming. Finally, we are now able to integrate the HT-PEMFC spatial model with fuel cell (FC) System model in MATLAB/Simulink by using COMSOL LiveLink for MATLAB.

### III. SIMULATION RESULTS OF HT-PEMFC SYSTEM

This section describes the results into the following two subsections as obtained from MATLAB/Simulink model of the HT-PEMFC system model and internal behaviours of 3D-COMSOL model of HT-PEMFC.

#### A. MATLAB Results

These results are obtained from MATLAB by integrating the HT-PEMFC COMSOL Model. Since the integration process is already mentioned that consists of input and output models. The results of both the models are given in Fig. 3 and Fig. 4, respectively.

Fig. 3 represents four parameters namely load current [A], current density [ $\text{A}/\text{m}^2$ ], H2 flow rate [ $\text{m}^3/\text{sec}$ ] and O2 flow rate [ $\text{m}^3/\text{sec}$ ] from top y-axis to bottom y-axis respectively. It shows that how the parameters like hydrogen flow rate and air flow rate are varied as the load current changes with respect to time on x-axis. The load in the model is considered as a dynamic load applied at different time steps. The total time of simulation is 4 seconds with the 400 time steps, means each time step is of 0.01 second and the value of the load current is assigned to each time step. The dynamic load current is applied in such a way that for each 80 time steps it varies with time. For the first 80 time steps, the load current 0.06 A is considered, and for the remaining each 80 steps 0.04 A, 0.05 A, 0.07 A, and 0.03 A of the load current is considered. The current density is obtained by simply dividing the load current

by the fuel cell current collecting area. The air and hydrogen flow rates change from the air compressor and fuel supply system respectively in accordance with change in load current as described in Section II. Here the important thing to be noticed is the compressor dynamics of the air compressor, which is considered here as 0.1 second.

Fig. 4 illustrates the results achieved from the COMSOL after integrating as described above. The output voltage, output power, utilization and efficiency of the fuel cell are presented on y-axis from top to bottom respectively. As the load current changes shown in the input model results in Fig. 3, the corresponding changes in output voltage, output power, utilization and efficiency of the fuel cell occurs as shown in Fig. 4. An increase in load current is followed by an increase in output power because the output power of the fuel cell is multiplication of the load current drawn from the fuel cell and output voltage of the fuel cell. In the same way higher the output power obtained from the fuel cell, higher will be the input power required. On the other hand the sudden increase in load current causes decrease in the output voltage and efficiency of the fuel cell, because the delay of compressor causes depletion of oxygen for the reaction so the output

voltage and hence the efficiency of fuel cell decrease. While the hydrogen utilization of the fuel cell is almost constant because as the load current changes, so the fuel flow rate changes.

### B. COMSOL Results

These results are very important and interesting too because they show the internal behavior of the fuel cell varying with respect to the dynamics of load current. The COMSOL results are obtained by putting the values as an input values to the COMSOL model of HT-PEMFC. Four case studies have been done for observing the distribution of electric potential and current density on cathode at time 2.39 seconds, and 2.45 seconds. These time steps are further marked with red circle for clear understanding of time steps taken for simulation in Fig. 4. These time steps are taken in such a way to observe the changes occurring in the internal behaviour of the fuel cell when there occurs a sudden increase in the load current from 0.05 A (at  $t=2.39$  seconds) to 0.07 A (at  $t=2.45$  seconds). In all these figures of COMSOL results, the cut plane view of cathode electrode of 3D-COMSOL model of HT-PEMFC is taken. The x-axis and y-axis of this 2D plot represent the width and length of cathode electrode.

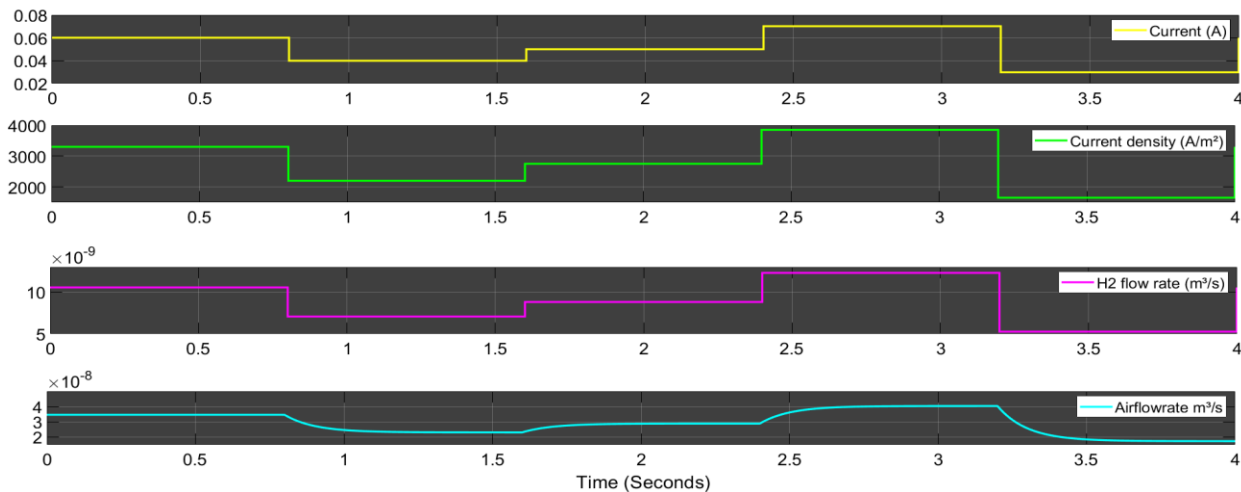


Fig. 3. Inputs from MATLAB model to HT-PEMFC CSOMSOL Model

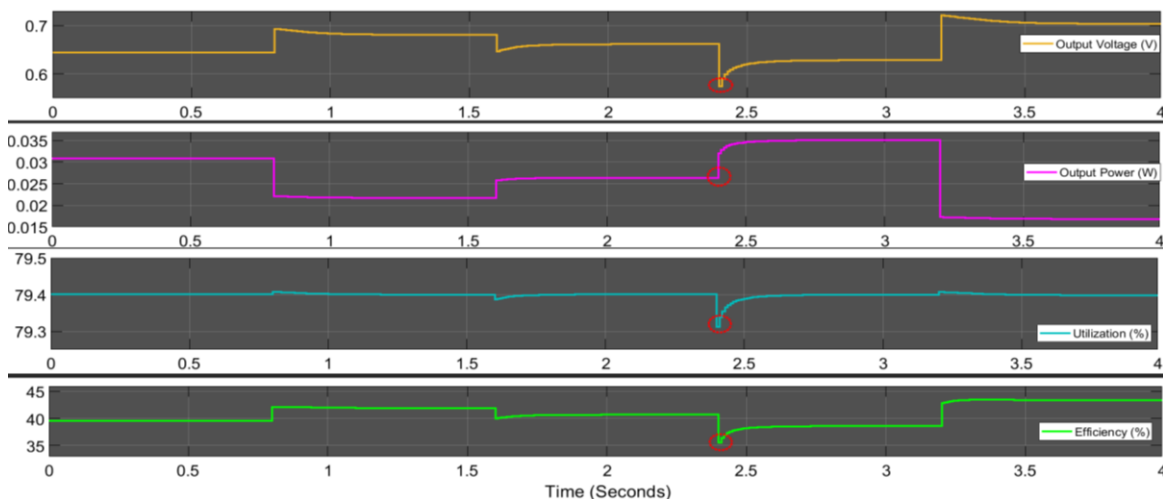


Fig. 4. Outputs from HT-PEMFC CSOMSOL Model.

1) *Case 1: electric potential (At t=2.39 seconds):* In Fig. 5, the minimum value of electric potential is 0.6608 V and the maximum value is 0.6644 V. The maximum value is at the centre of the x-axis and it decreases along the y-axis as moving from the inlet to outlet. The value does not change so much at the centre of the x- but changes very rapidly at the edges. As we move away from the centre of x-axis towards the left or right side the value of electric potential decreases because the concentration of the reactant is higher at the centre and lower at the edges.

2) *Case 2: electric potential (at t=2.45 seconds):* In Fig. 6, the minimum value of electric potential is 0.6118 V and the maximum value is 0.6173 V. The value of electric potential decreases along the y-axis as moving from the inlet to outlet. The value does not change so much at the centre of the x-axis and is maximum that is 0.6173 V but changes very rapidly at the edges. As we move away from the centre of x-axis towards the left or right side the value of electric potential decreases because the concentration of the reactant is higher at the centre and lower at the edges. Here the electric potential is lower as compared to case 1; the reason is same that is a sudden increase in current causes decrease in the electric potential. On the other hand electric potential in this case is almost same as compared to case 2 because at this time step, the same current is drawn which is 0.07 A.

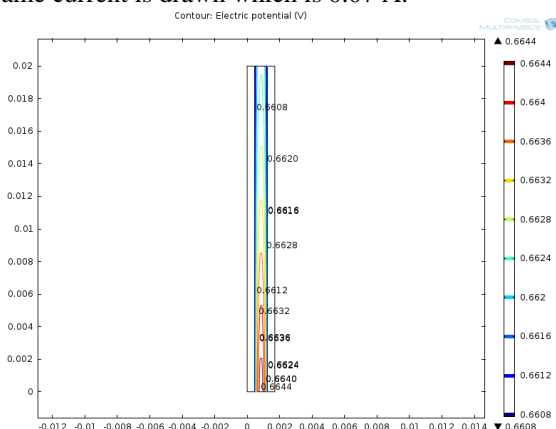


Fig. 5. Case 1: Electric Potential.

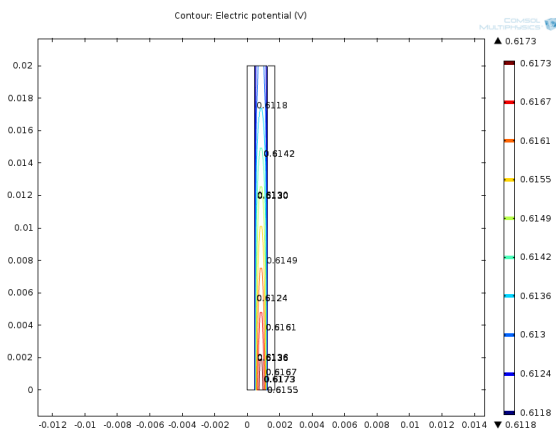


Fig. 6. Case 2: Electric Potential.

3) *Case 3: electrode current density (at t=2.39 seconds):* In Fig. 7, the minimum value of electrode current density is 471.82 A/m<sup>2</sup> at the centre of the x-axis. If we move away from the x-axis towards the left or right side from the centre of x-axis, the value of electrode current density increases up to the maximum value that is 6347.4 A/m<sup>2</sup> and afterwards it again decreases up to the average value of 2675.2 A/m<sup>2</sup> at the edges of the electrodes. The important point to be noted here is that the current distribution at the inlet is too much whereas at the outlet is very low. The maximum current distribution at the outlet is at the centre of the x-axis that is 3409.6 A/m<sup>2</sup> and 1206.3 A/m<sup>2</sup> at outlet edges.

4) *Case 4: electrode current density (at t=2.45 seconds):* In Fig. 8, the minimum value of electrode current density is 672.93 A/m<sup>2</sup> at the centre of the x-axis. As we move away from the x-axis towards the left or right side from the centre of x-axis, the value of electrode current density increases up to the maximum value that is 9763.6 A/m<sup>2</sup> and afterwards it again decreases up to the average value of 7490.9 A/m<sup>2</sup> at the edges of the electrodes. The important point to be noted here is that the current distribution at the inlet is too much whereas at the outlet is very low. The current distribution at the outlet of the centre of the x-axis is 1809.3 A/m<sup>2</sup>.

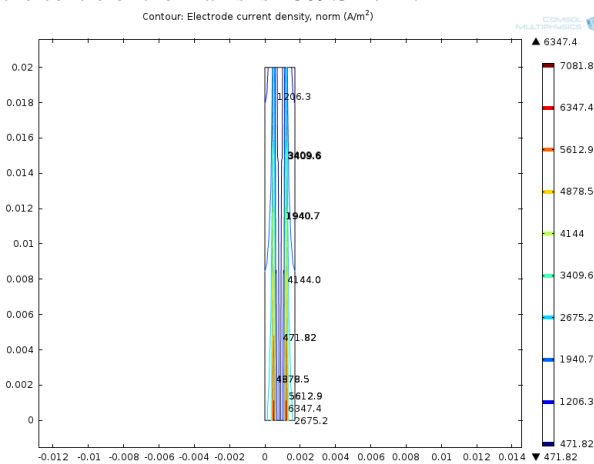


Fig. 7. Case 3: Electrode Current Density.

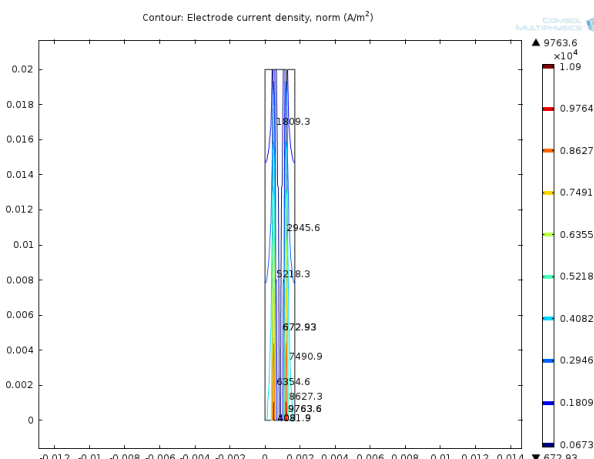


Fig. 8. Case 4: Electrode Current Density.

#### IV. CONCLUSION

This paper proposes a solution to observe the internal behaviour of fuel cell like voltage distribution, current distribution with the variation of load demand integration of 3D-COMSOL Model of HT-PEMFC with FC System. The task of achieving the effects of the load variation on HT-PEMFC has been achieved along with the internal behaviour of the fuel cell. The current findings with this approach of modelling can be useful to examine performance of HT-PEMFC in a better and accurate way. Moreover integration of HT-PEMFC with MATLAB allows more flexibility of changing any parameter with the M-script file, thus helps to find out more results as required. The result shows that concentration of electric potential and electrode current density distribution have adverse effects at the centre and edges cathode electrode of HT-PEMFC. The HTPEM-FC system does not include the thermal model, so thermal effects are not considered. In future work the thermal model can be added into HTPEM-FC system and the effects of temperature distribution on performance of the HTPEM-FC can be achieved. Since in practice HTPEM-FC contains stack were number of cells are connected together in series and parallel combination to obtain the desired power. This research work can be further helpful to replace the single cell with stack, and also replace single channels of gases with multiple channels to achieve the required power.

#### ACKNOWLEDGMENT

The work was supported with research grants by Quaid-e-Awam University of Engineering Science & Technology, Nawabshah, Sindh, Pakistan and University of Vaasa, Finland.

#### REFERENCES

- [1] J. Zhang et al., "High temperature PEM fuel cells," *Journal of Power Sources*, vol. 160, no. 2 SPEC. ISS., pp. 872–891, 2006.
- [2] Y. Wang, K. S. Chen, J. Mishler, S. C. Cho, and X. C. Adroher, "A review of polymer electrolyte membrane fuel cells: Technology, applications, and needs on fundamental research," *Applied Energy*, vol. 88, no. 4, pp. 981–1007, 2011.
- [3] S. Sharma and B. G. Pollet, "Support materials for PEMFC and DMFC electrocatalysts - A review," *Journal of Power Sources*, vol. 208, pp. 96–119, 2012.
- [4] A. Chandan et al., "High temperature (HT) polymer electrolyte membrane fuel cells (PEMFC)-A review," *Journal of Power Sources*, vol. 231, pp. 264–278, 2013.
- [5] R. E. Rosli et al., "A review of high-temperature proton exchange membrane fuel cell (HT-PEMFC) system," *International Journal of Hydrogen Energy*, vol. 42, no. 14, pp. 9293–9314, 2017.
- [6] R. K. Abdul Rasheed, Q. Liao, Z. Caizhi, and S. H. Chan, "A review on modelling of high temperature proton exchange membrane fuel cells (HT-PEMFCs)," *International Journal of Hydrogen Energy*, vol. 42, no. 5, pp. 3142–3165, 2017.
- [7] A. YMERI and S. MUJOVIC, "Impact of Photovoltaic Systems Placement, Sizing on Power Quality in Distribution Network," *Advances in Electrical and Computer Engineering*, vol. 18, no. 4, pp. 107–112, Dec. 2018.
- [8] J. A. Laghari, S. Ahmed, J. Kumar, and H. Mokhlis, "A Smart Under-Frequency Load Shedding Scheme based on Takagi-Sugeno Fuzzy Inference System and Flexible Load Priority," *Int. J. Adv. Comput. Sci. Appl.*, vol. 9, no. 3, 2018.
- [9] Q. Yan, H. Toghiani, and H. Causey, "Steady state and dynamic performance of proton exchange membrane fuel cells (PEMFCs) under various operating conditions and load changes," *Journal of Power Sources*, vol. 161, no. 1, pp. 492–502, 2006.
- [10] W. Andari, S. Ghozzi, H. Allagui, and A. Mami, "Design, Modeling and Energy Management of a PEM Fuel Cell / Supercapacitor Hybrid Vehicle," *Int. J. Adv. Comput. Sci. Appl.*, vol. 8, no. 1, pp. 273–278, 2017.
- [11] H. CHAOUALI, H. OTHMANI, M. Selméne, D. MEZGHANI, and A. MAMI, "Energy Management Strategy of a PV/Fuel Cell/Supercapacitor Hybrid Source Feeding an off-Grid Pumping Station," *Int. J. Adv. Comput. Sci. Appl.*, vol. 8, no. 8, pp. 250–257, 2017.
- [12] B. Mebarki, B. Allaoua, B. Draoui, and D. Belatrache, "Study of the energy performance of a PEM fuel cell vehicle," *International Journal of Renewable Energy Research*, vol. 7, no. 3, 2017.
- [13] J. Kumar, L. Kumpulainen, and K. Kauhaniemi, "Technical design aspects of harbour area grid for shore to ship power: State of the art and future solutions," *International Journal of Electrical Power & Energy Systems*, vol. 104, no. June 2018, pp. 840–852, Jan. 2019.
- [14] A. TOFIGHI and A. KALANTAR, "Adaptive Passivity-Based Control of PEM Fuel Cell/Battery Hybrid Power Source for Stand-Alone Applications," *Advances in Electrical and Computer Engineering*, vol. 10, no. 4, pp. 111–120, 2010.
- [15] Y. K. RENANI, B. VAHIDI, and H. A. ABYANEH, "Effects of Photovoltaic and Fuel Cell Hybrid System on Distribution Network Considering the Voltage Limits," *Advances in Electrical and Computer Engineering*, vol. 10, no. 4, pp. 143–148, 2010.
- [16] Y. Wang, J. Kowal, and D. U. Sauer, "Modeling of HTPEM Fuel Cell Start-Up Process by Using Comsol Multiphysics Principle of PEM fuel cell," *Comsol Conference*, no. June 2015, 2012.
- [17] Q. Li, W. Chen, Y.-T. Cham, M. Han, and J. Jia, "Dynamic characteristic modeling and control of proton exchange membrane fuel cell," *Xinan Jiaotong Daxue Xuebao/Journal of Southwest Jiaotong University*, vol. 44, no. 4, pp. 604–608, 2009.
- [18] I. P. Sahu, G. Krishna, M. Biswas, and M. K. Das, "Performance study of PEM fuel cell under different loading conditions," *Energy Procedia*, vol. 54, pp. 468–478, 2014.
- [19] C. Zhang, Z. Liu, X. Zhang, S. H. Chan, and Y. Wang, "Dynamic performance of a high-temperature PEM (proton exchange membrane) fuel cell - Modelling and fuzzy control of purging process," *Energy*, vol. 95, pp. 425–432, 2016.
- [20] L. Xia et al., "Investigation of parameter effects on the performance of high-temperature PEM fuel cell," *International Journal of Hydrogen Energy*, vol. 3, 2018.
- [21] J. Ma and M. Baysal, "Online Energy Management Strategy Based on Adaptive Model Predictive Control for Microgrid with Hydrogen Storage," vol. 8, no. 2, 2018.
- [22] Y. Allahvirdizadeh, M. Mohamadian, and M.-R. Haghifam, "A comparative study of energy control strategies for a standalone PV/WT/FC hybrid renewable system," *International Journal of Renewable Energy Research (IJRER)*, vol. 7, no. 3, pp. 1463–1475, 2017.
- [23] Y. Wang, D. U. Sauer, S. Koehne, and A. Ersöz, "Dynamic modeling of high temperature PEM fuel cell start-up process," *International Journal of Hydrogen Energy*, vol. 39, no. 33, pp. 19067–19078, 2014.

# A Collaborative Filtering Recommender System Model for Recommending Intervention to Improve Elderly Well-being

Aini Khairani Azmi<sup>1</sup>, Noraswaliza Abdullah<sup>2</sup>, Nurul Akmar Emran<sup>3</sup>

Faculty of Information and Communication Technology  
Universiti Teknikal Malaysia Melaka Hang Tuah Jaya  
76100 Durian, Tunggal, Melaka, Malaysia

**Abstract**—In improving elderly well-being nowadays, people at home or health care centre are mostly focusing on guarding and monitoring the elderly using tools, such as CCTV, robots, and other appliances that require a great deal of cost and neat fixtures to prevent damage. Elderly observations using the recommender system are found to be implemented, but only focusing on one aspect such as nutrition and health. However, it is important to give interventions to an elderly by concentrating more on the multiple aspects of successful ageing such as social, environment, health, physical, mental and other so that it can help the elderly people in achieving successful ageing as well as improving their well-being. In this paper, two recommender system models are proposed to recommend interventions for improving elderly well-being in the multiple aspects of successful ageing. These models using a Collaborative Filtering (CF) technique to recommend interventions to an elderly based on the interventions given to other elderly who have similar conditions with the user. The process of recommending interventions involves the generation of user profiles presenting the elderly conditions in multiple aspects of successful ageing. It also applying the k-Nearest Neighbor (kNN) method to find users with similar conditions and recommending interventions based on the interventions given to the similar user. The experiment is conducted to determine the performance of the proposed Collaborative Filtering (CF) recommender system and Collaborative Filtering and Profile Matching (CFS) compared to the Basic Search (BS). The results of the experiment showed that Collaborative Filtering (CF) recommender system and Collaborative Filtering and Profile Matching (CFS) outperformed Basic Search (BS) in terms of precision, recall and F1 measure. This result showed that the proposed models are efficient to recommend interventions using elderly profiles based on many aspects of successful ageing.

**Keywords**—Collaborative filtering; elderly well-being; k-nearest neighbor; recommender system; successful ageing

## I. INTRODUCTION

The significant increase in life expectancy at birth has been achieved over the last century. A combination of medical advances, escalating health and social care costs, and higher expectations for older age have brought international interest in promoting healthier elderly and achieving "successful" ageing. According to [1], successful ageing includes three main components which are; 1) low probability of disease and disease-related disability, 2) high cognitive and physical

functional capacity, and 3) active engagement in social and productive activities. A missing component to this three-factor model of successful ageing is identified in [1] which is positive spirituality which then became the fourth factor proposed in [3] to strengthen the model. Some consider health and functioning in old age as a prerequisite when striving for successful ageing [2]. Nutrition and environmental factors are also needed for elderly to age well, as well as achieving successful ageing [4]-[6]. Spiritual nowadays become more important to elderly in order to improve the quality of their life [7]-[8]. Therefore, it can be concluded that in order to achieve successful ageing, there are many aspects that need to be focused on for improving elderly well-being such as socialization, health, cognitive, physical, environment, nutrition and spirituality.

Elderly observations using the recommender system are found to be implemented, but only focusing on one aspect such as nutrition and health. There are some research works on recommender systems to improve elderly well-being such as recommending food and monitoring users' nutritional state by using user nutritional profile. According to [1], [2] and [3], multiple aspects must be considered in order for the elderly people to achieve successful ageing, as well as to improve their well-being. It is important to consider all the aspects or factors that contribute to successful ageing such as socialization, health, cognitive, physical, nutrition, spiritual and environment [1]-[8]. Those that achieve successful ageing have good conditions in all these aspects with no chronic illness, high levels of resilience, low rates of depression, good social network and also high levels of life satisfaction into their golden years. The elderly are most likely to age successfully with continuous monitoring and providing interventions for all these aspects. Therefore, a recommender system to recommend interventions by considering multiple aspects of successful ageing is required in order to improve elderly well-being and to help them achieve successful ageing.

In this paper, a recommendation model for recommending intervention in multi aspects of successful ageing for elderly people has been suggested by using the collaborative filtering technique. This technique utilized the elderly profiles created from the results of assessments conducted on various aspects of successful ageing such as socialization, health, cognitive, physical, nutrition, spiritual and environment. The k-Nearest Neighbor (kNN) algorithm was used for finding similar users or elderly based on the profiles of their conditions on these

aspects. Finally, interventions were recommended for the elderly based on the interventions that have been given to other elderly who have the same conditions or profiles.

This paper comprises five sections, where Section II describes the review of previous studies on the interventions for elderly, and Section III presents the methodologies which discussed the proposed user profiling and recommendation approach. In Section IV, experiment and evaluation results are discussed and this paper is concluded in Section V.

## II. LITERATURE REVIEW

### A. Related Work

The recommender system exists in many types of domains such as health, e-Commerce, movies, elderly well-being and many others. Usually, the Collaborative Filtering (CF) approach is used to recommend items to the user based on items that have been highly rated by similar users. There are many researches on recommender systems that have been conducted in each domain especially for frequently purchased items such as books and movies. This is because a large amount of ratings data can be easily accumulated and used by the recommender system to recommend these items for a new user. For recommending interventions, a large amount of ratings data is not available to be used by recommendation approaches to predict user's preferences. Thus, methods that can learn users' profiles without the availability of user's ratings are needed to be utilized by the recommendation approach.

A recommendation approach does exist for recommending interventions for elderly. There are some researches done on recommendation techniques for other types of items or services such as for recommending a recommendation related to the health [9] and nutrition [10]-[14]. In [9], the main focus of this recommender system is to build a digital platform focusing on people with dementia problem which most of this problem having by elderly. This recommender system provides interventions to caregivers and people living with dementia.

There are other recommender systems related with nutrition aspect. The nutritional semantic recommender system recommends a healthy diet plan to the elderly following expert guidelines [10]. It retrieves reliable and complete nutritional information from expert sources and manages this information by providing it to the users in the form of recommendations. A food recommendation proposed by [12] provides a healthy plan of diet for the elderly following expert guidelines which recommend the correct amount of nutrition to an elderly. It retrieved complete and reliable nutritional information from expert sources, such as people (nutritionists and gerontologists) or computerized systems (information systems and nutritional databases from the World Health Organization and, Spanish Society of Parenteral and Enteral Nutrition) and users in the context of these recommendations are offered to manage this information.

Another proposed intervention recommendation approach was focused on a demographic recommender system for the elderly [15]. This recommender system focused on the demographic aspect to provide elderly with information about services of health, recreation, household, etc. The purpose of

this study is to enable older people to live longer, determine their choices at home by providing useful information on comprehensive resources and providing personal information about available services in the surroundings of the user.

Lifestyle of the elderly was also being looked into which provide support in the context of recommendations to help users cope with typical issues of everyday life and contributing positively to their welfare [16]. The development of an Ambient Assisted Living (AAL) system called CARE that serves as a test-bed for user studies is focusing on recommendations and interventions. The two potential peer groups of users were recruited. Structured interview among a batch of 20 Greek seniors, and a batch of 27 German seniors, which were formed earlier were conducted. The seniors' lifestyle, medical needs, attitude towards AAL technologies were focused on, and more specifically, the desired functions and system configurations of a recommendation given by the CARE system. The interview's results were discussed and the primary CARE prototype that emerged as an add-on digital image frame that duplicated photo exposure with reserves and interventions has been drawn to enhance the lifestyle and welfare of seniors. Enhancing the lifestyle of elderly improves their social skills, thus making them happier when talking to others.

From this previous research works, most of the research works on recommending interventions for elderly are focusing on only one aspect of successful ageing such as health or nutrition. To the best of our knowledge, there is no recommender system model that integrates various aspects of successful ageing as well as recommends interventions based on the elderly conditions of these aspects. This shows that, most of elderly did not get enough quality of the life when they not get proper intervention from each of every aspect towards the successful of their age. To improve the well-being of elderly and help them to age successfully, many other aspects should be considered such as socialization, health, cognitive, physical, nutrition, spiritual and environment. Therefore, a recommendation system that can recommend interventions based on various aspects of successful ageing is proposed. This recommendation is based on elderly profiles generated from the assessment of these aspects. The next section will discuss the proposed approach in more details.

## III. PROPOSED APPROACH

For this experiment, in recommending the interventions to a new user, the following processes have been followed in order to make sure that the experiment went well and the detailed explanation are discussed in the section below:

- **User Profiling:** Building user profiles by using the assessment results of 7 aspects of successful ageing for identifying the elderly conditions.
- **Neighborhood Formation:** Collaborative Filtering was applied for selecting k number of nearest neighbors, based on the comparison of the new user's profile with the existing users' profiles.
- **Recommendations:** Selecting interventions and recommending interventions to the new user.

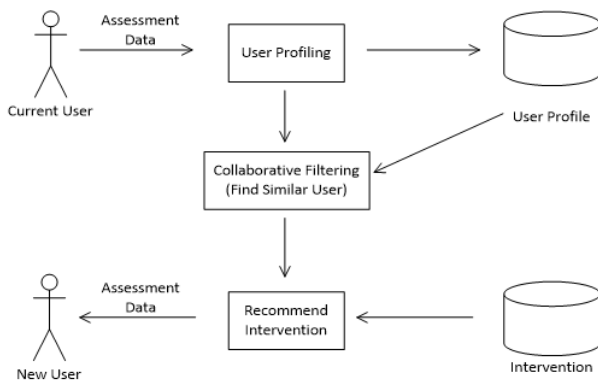


Fig. 1. A General Framework of the Interventions Recommendation.

Fig. 1 shows the framework for recommending interventions to the new users. A detailed explanation will be discussed in the section below.

### A. User Profiling

User profiling is the process of gathering information about the topics or subjects in which a user is interested in. User profiles are the main source of information through which personalization systems can learn about users' interests or preferences. The accuracy and effectiveness of user profiling affects the performance of recommender systems. The crucial aspect of user profiles is their ability to represent users' current interests. In this research, the elderly assessment profiles are important and always being considered to recommend interventions that are suitable for their conditions. Therefore, the proposed recommender system must take the user assessment result for each aspect into consideration when making interventions recommendation for the elderly. The user assessment profile will be used by the proposed recommendation techniques to recommend interventions for improving elderly well-being.

User profiling process consists of two main phases. The first phase of user profiling is to collect information about the user. To be able to identify the needs of users, the recommender system needs to know something about the user. For this research, the first step in gathering information about elderly people was by collecting their assessment data to identify the level of their successful ageing. In order to measure the level of successful ageing, they went through a few assessments twice a year. There were 7 different aspects assessed for each elderly which are socialization, health, cognitive, physical, nutrition, spiritual and environment to determine their conditions. Therefore, we considered these 7 aspects in creating user profiles and intervention recommendations. From these assessments, the results were collected and used to construct user profiles.

The second phase in user profiling was profile construction and representation. An essential process of the personalized recommender systems is how to a build user profile, which represents the information needs and preference of a user and has great impact on the performance of recommendations. One important consideration when constructing a user profile is that more accurate user profiles need to be generated in order to

provide more effective recommendations. For this step, each elderly will have his or her own user profile which consisted of 7 assessment results for each aspect. The user profiles were generated based on the information given by the experts from one of the elderly institution in Malaysia. Each aspect had different methods to calculate the assessment result in order to identify the elderly condition for the aspect. Then, the assessment result for each aspect was used to calculate the overall result based on the weightage given for each aspect. Finally, the user was classified into 3 different categories which are successful, semi-successful and non-successful based on the overall result of the assessments.

Basically, a user profile for elderly consisted of a vector of items and their ratings. User profile was used in suggesting an intervention for elderly. Below are the sample of user profiling for each user for this research.

$$P_i = \{A_{i1}, A_{i2}, A_{i3}, A_{i4}, A_{i5}, A_{i6}, A_{i7}\} \quad (1)$$

where A is assessment aspect, P is user profile and i represents different users or elderly. There are 7 variables or aspects that present a user profile which are  $A_{i1}$ ,  $A_{i2}$ ,  $A_{i3}$ ,  $A_{i4}$ ,  $A_{i5}$ ,  $A_{i6}$  and  $A_{i7}$ .  $A_{i1}$  represent the socialization aspect,  $A_{i2}$  represent the health aspect,  $A_{i3}$  represent the cognitive aspect,  $A_{i4}$  represent the physical aspect,  $A_{i5}$  represent the nutrition aspect,  $A_{i6}$  represent the spirituality aspect and  $A_{i7}$  represent the environment aspect for user i. The assessment method for each aspect was provided by the expert. The weightage was collected from the experts of each aspect in order to calculate the overall condition of the elderly. The weightages for each aspect are as follows: socialization (10), health (30), cognitive (15), physical (15), nutrition (10), spiritual (10) and environment (10). Below is the formula to calculate the weightage for each aspect based on the assessment data collected from the elderly.

- Socialization

A set of true and false questions (T=1/F=0) were given to elderly. They were given 15 questions in order to identify their social condition. The following formula was used to calculate the result for the elderly social condition.

$$A_{i1} = \frac{\sum QS}{\sum TQ} \times 10\% \quad (2)$$

where QS is the total number of correct answers given by the elderly from the socialization assessment and TQ is the total number of questions needed to be answered correctly.

- Health

There were 6 sections of the question consisting of 36 true and false questions (T=1/F=0) given to the elderly to answer in order to identify their health condition. The following formula was used to calculate the result for the elderly health condition.

$$A_{i2} = \frac{\sum QH}{\sum TQ} \times 30\% \quad (3)$$

where QH is the total number of correct answers given by the elderly from the health assessment and TQ is the total number of questions needed to be answered correctly.

- Cognitive

There were 2 types of tests given to the elderly to answer which were the Mini Mental State Examination (MMSE) and Barthel test. MMSE test comprises of 11 sets of multiple choice questions while Barthel test comprises of 10 sets of multiple choice questions. The following formula was used to calculate the result for the elderly cognitive condition.

$$A_{i3} = \left( \frac{\sum QC_1}{\sum TQ_1} \times 7.5\% \right) + \left( \frac{\sum QC_2}{\sum TQ_2} \times 7.5\% \right) \quad (4)$$

where  $QC_i$  is the total scores that have been answered by the elderly from the cognitive assessment (MMSE) and  $TQ_i$  is the total number of questions needed to be answered correctly in the cognitive assessment (MMSE). Meanwhile,  $QC_2$  is the total scores that have been answered by the elderly from the cognitive assessment (Barthel Index) and  $TQ_2$  is the total number of questions needed to be answered correctly in the cognitive assessment (Barthel Index).

- Physical

There were 2 types of tests conducted which were the Armcurl test and Time Up and Go (TUG) test. TUG test comprises of 12 true and false questions (T=1/F=0). However, an elderly was required to answer only one test according to their physical conditions. The following formula was used to calculate the result for the elderly physical condition.

$$A_{i4} = \left( \frac{\sum QP_1}{\sum TQ_1} \times 15\% \right) \text{ OR } A_{i4} = \left( \frac{\sum QP_2}{\sum TQ_2} \times 15\% \right) \quad (5)$$

where  $QP_i$  is the total scores that have been answered by the elderly from the physical assessment (Armcurl) and  $TQ_i$  is the total number of questions needed to be answered correctly in the physical assessment (Armcurl). Meanwhile,  $QP_2$  is the total number of correct answers given by the elderly from the physical assessment (TUG) and  $TQ_2$  is the total number of questions needed to be answered correctly in the physical assessment (TUG).

- Nutrition

There were 6 types of menus that the elderly must take in one day and the menu intake was checked daily by an assigned staff. Each menu taken by the elderly was given a score of 10 and for each menu not taken by the elderly was deducted by 5. If an elderly has taken 6 menus in a day, he or she was given a full mark of 60 per day. For each session, the score was given based on 6 months per session. Each elderly was being assessed based on the menu taken for 6 months only per session.

$$A_{i5} = \frac{\sum QN}{\sum TQ} \times 30\% \quad (6)$$

where  $QN$  is the total amount of menus taken by the elderly all day in one session (Session 1 is from January until June and Session 2 is from July until December) and  $TQ$  is the total number of nutrition menus needed to be taken per session in the nutrition assessment.

- Spiritual

This aspect was divided into 2 sets of questions which were for Muslims and non-Muslims. 5 sections of questions for

Muslims elderly comprised 54 multiple choice questions whereas 4 sections of questions for non-Muslims elderly is comprised 31 multiple choice questions to be answered. The following formula was used to calculate the result for the elderly spiritual condition.

$$A_{i6} = \frac{\sum QI}{\sum TQ} \times 10\% \quad (7)$$

where  $QI$  is the total number of correct answers given by the elderly from the spiritual assessment (Islam / Moral) and  $TQ$  is the total number of questions needed to be answered correctly.

- Environment

There were 4 sections of questions given to the elderly to answer which included 25 questions. The following formula was used to calculate the result for the elderly environment condition.

$$A_{i7} = \frac{\sum QE}{\sum TQ} \times 10\% \quad (8)$$

where  $QE$  is the total number of correct answers given by the elderly from the environment assessment and  $TQ$  is the total number of questions needed to be answered correctly.

Finally, the overall result was calculated by summing up the results of all aspects and the elderly was categorized into successful, semi-successful and non-successful based on their overall result. The following formula was used to calculate the overall result.

$$O_i = \sum_{i=j}^j A_{ij} \quad (9)$$

where  $O$  is the overall result of assessment for each aspect taken by an elderly, while  $i$  and  $j$  are the aspects of successful ageing.

### B. Collaborative Filtering and k-Nearest Neighbor (kNN)

The Collaborative Filtering (CF) recommendation approach is the earliest approach used in the recommender system and also the most popular and widely implemented technique. Collaborative Filtering methods are based on the accumulation and analysis on large amounts of information about user behavior, activity or preferences and prediction of what users want based on their similarity to other users.

A key advantage of the Collaborative Filtering approach is that it does not rely on machine analyzable content and therefore it is capable of accurately recommending complex items such as movies without requiring an understanding of the item itself. Many algorithms have been used in measuring user similarity or item similarity in recommender systems. In this paper, the k-nearest neighbor (kNN) approach and the cosine similarity were used in conducting the experiment. The key technique of kNN is to calculate the similarity between target user and the others, and then find the k nearest neighbors to predict the target user's interest or intervention.

The working kNN can be described, in the case of any unknown items as test items. The kNN classifier finds information from the training data that are almost similar; or almost close items as the test items. Among them, the k



number of items that are closest to the test items is selected as the nearest neighbors of the test items. For this research, cosine similarity method was used to find the similarity. In this case, two users were regarded as two vectors in the n dimensional item space. The similarity between them was measured by computing the cosine of the angle between these two vectors. Formally, similarity between users A and B is given as below where A and B represent the n dimensional vectors those users accumulated on the n items.

$$\text{similarity}(A, B) = \frac{A \cdot B}{\|A\| \times \|B\|} = \frac{\sum_{i=1}^n A_i \times B_i}{\sqrt{\sum_{i=1}^n A_i^2} \times \sqrt{\sum_{i=1}^n B_i^2}} \quad (10)$$

For this experiment, equation (10) was used in order to get the similarity value between two users. A represents the profile of existing user while B represents the profile of new user as discussed in section III. Each profile had 7 different values representing the result for each aspect. The Cosine Similarity values were calculated for other user profiles and the values were sorted to choose the selected (n) number of the most similar profiles. The number of k-NN that has been chosen for this experiment was 5 because it achieved better results.

### C. Recommendation

In this experiment, the interventions for each elderly profile were recommended based on the selected similar users. The profiles of the selected users were chosen based on the calculation of the 5 nearest neighbors. After the 5 neighbors were selected, the lists of all interventions of each neighbor were gathered accordingly. For the Basic Search (BS) approach, only interventions on the first nearest neighbor from 5 neighbors were selected to be recommended to the new active elderly, while for the Collaborative Filtering (CF) approach, all interventions from 5 nearest neighbor were ranked according to the frequency of interventions calculated from the intervention gathered from 5 neighbors. The highest number of interventions gathered for each aspect was selected to be recommended to the new or active elderly. For Collaborative Filtering with Profile Matching (CFS) approaches, the similarity of the user profile to the new user was calculated by matching each one of the 7 aspects of the nearest profile from 5 neighbors to the active or new one. The profile that matched or was nearest to the active or new profile was selected and the existing interventions given for that profile were selected to be recommended to the new or active one.

## IV. EXPERIMENT

This section focuses on the evaluation of the proposed user profiling and recommendation models. Firstly, the experiment design and the evaluation methods will be given. The experiments were conducted to see how the proposed user profiling and recommendation approaches performed by comparing them to the baseline approaches. Then, the results of experiments will be discussed and illustrated.

### A. Dataset

A case study has been conducted for the elderly well-being domain. Data on the results of assessment for elderly was collected from one of the elderly institutions in Malaysia which

is responsible for taking care of elderly people well-being. The data used in this research is an assessment data for seven (7) aspects of successful ageing collected from experts who conducted assessments to each elderly in each aspect of successful ageing. The intervention data were also collected from the interventions suggested by the experts. There were 139 samples of users involved in this research which were elderly aged above 60 living in this institution. The Collaborative Filtering recommender system prototype was also constructed to implement the interventions recommendations using user profiles constructed based on the assessment data. There were 139 user profiles created to be used by Collaborative Filtering; however, the user profiles can be accumulated for every assessment session which is conducted twice a year. The interventions were given to the elderly after each assessment session; therefore, the intervention data can also be collected for every assessment session.

There were 3 different recommendation approaches implemented in this experiment in order to compare the intervention recommendations given to an elderly by using each approach. The approaches were Basic Search (BS), Collaborative Filtering (CF) and Collaborative Filtering with Profile Matching (CFS). The BS approach represented the approach that is still widely used by the users which is to search based on the keyword they used. In this research, the keyword for the BS was represented by the value of each aspect in the user profile. The CF approach was used to recommend interventions based on the profiles of similar users which is by recommending frequent interventions given for the similar users. Meanwhile, in CFS, this approach recommended interventions based on the nearest profile to the active user profile which is by recommending interventions given to the user with the most similar profile for each aspect. The experiment results for these three approaches were compared to see their performance.

In this experiment, the 139 profiles of users were grouped into 3 which were A, B and C and each group had 46, 46 and 47 profiles respectively. Each run of experiment used one of the groups as the testing data and other groups as the training data. For the Basic Search (BS) approach, the profile of a user in the testing data was compared with other profiles in the training data and only interventions on the first nearest neighbor were selected to be recommended to the new active elderly. For CF and CFS approaches, the nearest 5 neighbors were chosen and the interventions gathered from these 5 neighbors will be selected and recommended to the new user. For the CF approach, the total number of each intervention was calculated and the highest number of interventions for each aspect was selected to be recommended to the new user. Meanwhile, for the CFS approach, the interventions were chosen and recommended to the new one by finding similar user profiles or the nearest user profile matching the 7 aspects from 5 neighbors to the active or new one. The results of these different approaches were then compared and evaluated using precision and recall to see whether the proposed approach performed better than other approaches. Further explanation on this method of evaluation is discussed in the next section.

**B. Evaluation Metrics**

In this experiment, Precision, Recall and F1 Measurement metrics were used to evaluate the performance of the proposed models. Recall and Precision are the measures for measuring the efficiency and the suitability of the recommendation obtained by the recommender system.

Recall measures the ability of the system to present all the relevant items and it can be seen as the measure of completeness. Recall also refers to the percentages of the relevant recommendation that were retrieved, out of the total relevant recommendations. Precision measures the ability of the system to present only those items that are relevant, and it can be seen as the measure of exactness. It is also refers to the percentages of the relevant recommendation that were retrieved, out of the total retrieved recommendations.

$$Recall = \frac{NM}{NT} \tag{11}$$

$$Precision = \frac{NM}{NR} \tag{12}$$

where *NM* is the number of suggested interventions matching the testing interventions, *NT* is the number of interventions that should be returned and *NR* is the number of returned suggested interventions. Finally, the average recall and precision for all profiles were calculated for each approach.

The F1 metric was used to provide a general overview of the overall performance. F1 metric was used to provide a general overview of the overall performance. The F1 measure combined the recall and precision results with an equal weight.

$$f1 = \frac{2 \times Precision \times Recall}{Precision + Recall} \tag{13}$$

**C. Experimental Setup**

In order to evaluate the effectiveness of the proposed user profiling approach and the recommendation approaches, this paper implemented the proposed user profiling, recommendation approaches, and the baseline models. For this experiment, 139 profiles of users were used as testing and training datasets. There were three runs of experiment conducted and the 139 profiles were divided into 3 groups (A, B and C). The division of dataset contained two (2) parts which were Training and Testing as illustrated in Fig. 2, 3 and 4.

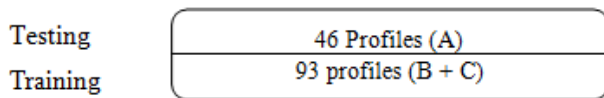


Fig. 2. The Division of Dataset for the Experiment (Run 1).

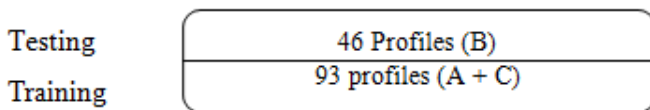


Fig. 3. The Division of Dataset for the Experiment (Run 2).

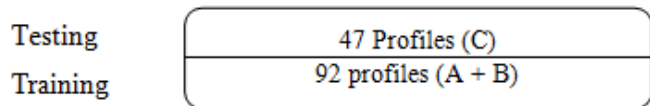


Fig. 4. The Division of Dataset for the Experiment (Run 3).

The testing dataset was considered as the target users or new users while the training dataset was considered as previous users. Training dataset was used to generate previous user’s profiles which were used to find neighbors by using the neighborhood formation method. Finally, the average result for the 3 runs was calculated. The experiments were conducted to test if the proposed method was able to suggest interventions according to the current user’s profile based on similar user profiles or neighbors. The interventions recommended for an elderly should improve the elderly well-being as the interventions were recommended based on the profiles of other elderly who have received the same interventions given by their caretakers.

**V. RESULTS AND DISCUSSION**

Results of recommendations based on user profiles were examined and the results on Basic Search (BS), Collaborative Filtering (CF) and Collaborative Filtering with Profile Matching (CFS) approaches were compared. The objective of this set of experiments was to verify that the result of interventions by using Collaborative Filtering with Profile Matching (CFS) approaches can generate more accurate recommendations compared to BS approaches and CF.

The table below shows the result of precision and recall for 3 different approaches. For these 3 approaches, the profile has been divided into 3 groups of runs and the results are been showed in the table. Table I shows the results of precision and recall for the BS approach. The results showed that precision for runs 1 and 3 was lower compared to recall at about 0.004 and 0.018. For run 2, it showed that the precision got higher at 0.002 compared to recall. Table II shows the results of precision and recall for the CF approach. Each group of runs had higher precision results compared to recall about at 0.125, 0.057 and 0.077. Meanwhile, Table III shows the results of precision and recall for the CFS approach and for this approach, the result was inverted with the CF approach in which the result of recall were more higher compare to precision at about 0.120, 0.107 and 0.091. The differences in results of recall in this approach were much higher compared to the CF approach while the results of precision in this approach were much lower compared to the CF approach. Table IV shows the average results of precision and recall as well as the result for F1 measure for 3 experiment runs including basic search (BS), Collaborative Filtering (CF) and Collaborative Filtering with Profile Matching (CFS) based on different groups.

TABLE I. RESULTS OF PRECISION AND RECALL (BS)

| Category | Precision | Recall |
|----------|-----------|--------|
| Run 1    | 0.494     | 0.498  |
| Run 2    | 0.455     | 0.453  |
| Run 3    | 0.498     | 0.516  |

TABLE II. RESULTS OF PRECISION AND RECALL (CF)

| Category | Precision | Recall |
|----------|-----------|--------|
| Run 1    | 0.586     | 0.461  |
| Run 2    | 0.606     | 0.549  |
| Run 3    | 0.575     | 0.498  |

TABLE III. RESULTS OF PRECISION AND RECALL (CFS)

| Category | Precision | Recall |
|----------|-----------|--------|
| Run 1    | 0.508     | 0.628  |
| Run 2    | 0.524     | 0.631  |
| Run 3    | 0.506     | 0.597  |

TABLE IV. AVERAGE RESULTS OF PRECISION, RECALL AND F1 MEASURE FOR BS, CF, CFS APPROACHES

| Category   | Precision | Recall | F1 Measure |
|--|-----------|--------|------------|
| Basic search (BS)                                  | 0.482     | 0.489  | 0.485      |
| Collaborative Filtering (CF)                       | 0.589     | 0.503  | 0.543      |
| Collaborative Filtering and Profile Matching (CFS) | 0.513     | 0.619  | 0.561      |

From the results of these 3 different approaches shown in Table IV, it can be seen that BS approach has the lowest precision and recall values compared to the others. This is because the BS approaches only used the basic searching which only focused on the result gathered from only one neighbor who had the most match profile with the active user. Some of the recommended interventions were not matched with the active elderly profile. For CF approach, it can be seen that the precision is the higher compared to BS and CFS. The highest precision of CF shows that the interventions recommended by CF approach are accurate and suitable according to the new elderly profile or condition. The recall of CF is higher than BS but lower than CFS. This is because there are many other similar recommendations that can be given to an elderly but not necessarily recommended by the CF. Meanwhile, the result of CFS approach are inverted with the CF approach. CFS has the highest recall but lower precision than CF which is about 0.106. It shows that in term of recall, the CFS approach is able to recommend more interventions needed by the active elderly because the interventions recommended were based on the interventions of the aspects that were most similar to the active elderly aspect. However, in terms of precision, CFS is lower than CF. It shows that, not all recommended interventions matched with the interventions given to the previous user. This is because there were many similar interventions that can be given to an elderly for each aspect and the interventions were not just fixed to only interventions provided to the previous elderly, even though the interventions were also accurate.

In terms of F1 Measure, the results also show that CF performs better than the BS which is about 0.058. This is because for Basic Search (BS), it just considered interventions for only the most matching profile which led to inaccurate and not similar interventions being recommended. This shows that, when more similar profiles were being considered, the results were more precise and accurate. This is because many interventions can be recommended based on existing user profiles that may contribute to more accurate recommendations result of assessment or profile of user. However, the F1 Measure results show that CFS performs better than CF with 0.018 value difference. This is because the CF approach only took interventions that are most frequently given for each aspect among the 5 neighbors while the CFS approach considered the interventions for each aspect that had the most similar aspect value of the profiles among the 5 neighbors.

## VI. CONCLUSION

Problem of ageing has been recognized as a major social problem by sociologists all over the world. In order to ensure that the elderly continue to flourish, it is important to give some interventions to them following the multiple aspects of successful ageing which are social, health, physical, cognitive, nutrition, spiritual, nutrition and environment. We have proposed a recommender system for recommending suitable interventions to the elderly based on interventions given to other elderly who have similar profiles or assessment results. The results of the experiment showed that the more accurate recommendation of interventions can be provided to the new elderly by using the Collaborative Filtering approach. The results showed that CF and CFS performed better than BS in terms of precision, recall and F1 Measure. However, recall for CF approach was lower than CFS because CF recommended interventions based on frequent interventions suggested for some similar users. In term of precision, CF was the highest which showed that the recommended interventions by this approach were accurate and suitable for the new elderly with the same profile or condition. The CFS had higher recall than CF and lower precision than CF. However the CFS gave the best result for F1 Measure which showed that this approach was the best approach among the other. This is because CF approach only took interventions that were most frequently given for each aspect among the 5 neighbors while CFS approach considered the interventions for each aspect that had the most similar aspect value of the active elderly profiles among the 5 neighbors. Thus, CFS suggested interventions that were most suitable for each aspect of active elderly profile. To conclude, the CF and CFS were able to recommend interventions based on user profiles generated from the assessment results, therefore the recommended interventions may improve the elderly well-being in multiple aspects of successful ageing.

## VII. LIMITATION

There are a few limitations that can be identified throughout this experiment in term of data collections. Data has been collected from only 2 sessions of evaluation and intervention for each of elderly throughout the year. This data limitation may restrict the possible interventions that can be given to the new elderly. To address this limitation, we plan to propose a hybrid recommender system model by combining knowledge-based and collaborative filtering for recommending more accurate intervention for an elderly. A knowledge-based recommender system can be applied to recommend interventions based on the knowledge gathered from the domain expert. After the user profiles and interventions have been accumulated, the collaborative filtering approach can be used to recommend interventions for the new elderly based on the intervention given for other elderly who have similar profiles.

## ACKNOWLEDGMENT

The authors would like to express their sincere appreciation for those who have participated in this research study. The authors of this paper are also appreciative to the Department of Information and Communication Technology at Universiti Teknikal Malaysia Melaka (UTeM) in supporting this work.

REFERENCES

- [1] Wahl, H., Deeg, D., & Litwin, H., "Successful ageing as a persistent priority in ageing research," *European Journal of Ageing*, vol. 13, pp. 1-3, 2016.
- [2] Cosco, T. D., K. Howse, and C. Brayne., "Healthy ageing, resilience and wellbeing," *Epidemiology and Psychiatric Sciences*, vol.26, no.6, pp. 579-583, 2017.
- [3] Zimmer, Z., Jagger, C., Chiu, C. T., Ofstedal, M. B., Rojo, F., & Saito, Y., "Spirituality, religiosity, aging and health in global perspective: A review," *SSM-population health*, vol.2, pp. 373-381, 2016.
- [4] Aleksandrova, K., Pounis, G., & di Giuseppe, R., "Diet, Healthy Aging, and Cognitive Function," In *Analysis in Nutrition Research*, pp. 321-336, 2019.
- [5] Costa, A., Carrión, S., Puig-Pey, M., Juárez, F., & Clavé, P., "Triple Adaptation of the Mediterranean Diet: Design of A Meal Plan for Older People with Oropharyngeal Dysphagia Based on Home Cooking," *Nutrients*, vol.11, no.2, pp. 425, 2019.
- [6] Oyeyemi, A. L., Kolo, S. M., Oyeyemi, A. Y., & Omotara, B. A., "Neighborhood environmental factors are related to health-enhancing physical activity and walking among community dwelling older adults in Nigeria," *Physiotherapy theory and practice*, vol.35, no.3, pp. 288-297, 2019.
- [7] Gautam, S., Neville, S., & Montayre, J. "What is known about the spirituality in older adults living in residential care facilities? An Integrative review" *International journal of older people nursing*, 2019.
- [8] Ali, J., Marhemat, F., Sara, J., & Hamid, H., "The relationship between spiritual well-being and quality of life among elderly people," *Holistic nursing practice*, vol.29, no.3, pp 128-135, 2015.
- [9] Oliva-Felipe, Luis, et al. "Health Recommender System design in the context of CAREGIVERSPRO-MMD Project." *Proceedings of the 11th Pervasive Technologies Related to Assistive Environments Conference. ACM,2018.*
- [10] V. Espín, M. V. Hurtado, and M. Noguera, "Nutrition for Elder Care: A nutritional semantic recommender system for the elderly," *Expert Syst.*, vol. 33, no. 2, pp. 201–210, 2016.
- [11] G. Agapito et al., "DIETOS: A recommender system for adaptive diet monitoring and personalized food suggestion," *Int. Conf. Wirel. Mob. Comput. Netw. Commun.*, 2016.
- [12] S. Bundasak and K. Chinnasarn, "EMenu recommender system using collaborative filtering and Slope One Predictor," *Proc. 2013 10th Int. Jt. Conf. Comput. Sci. Softw. Eng. JCSSE 2013*, pp. 37–42, 2013.
- [13] V. Espín, M. V. Hurtado, and M. Noguera, "Nutrition for Elder Care: A nutritional semantic recommender system for the elderly," *Expert Syst.*, vol. 33, no. 2, pp. 201–210, 2016.
- [14] T. Rist, A. Seiderer, S. Hammer, M. Mayr, and E. André, "CARE - Extending a Digital Picture Frame with a Recommender Mode to Enhance Well-Being of Elderly People," *Proc. 9th Int. Conf. Pervasive Comput. Technol. Healthc.*, 2015.
- [15] C. Stiller, F. Roß, and C. Ament, "Demographic recommendations for WEITBLICK, an assistance system for elderly," *Isc. 2010 - 2010 10th Int. Symp. Commun. Inf. Technol.*, pp. 406–411, 2010.
- [16] S. Hammer et al., "Design of a lifestyle recommender system for the elderly: Requirement Gatherings in Germany and Greece," In *Proceedings of the 8th ACM International Conference on Pervasive Technologies Related to Assistive Environments*, pp. 80, 2015.

# Forecasting Feature Selection based on Single Exponential Smoothing using Wrapper Method

Ani Dijah Rahajoe

Faculty of Engineering, University of Bhayangkara Surabaya  
Surabaya, Indonesia

**Abstract**—Feature selection is one way to simplify classification process. The purpose is only the selected features are used for classification process and without decreasing its performance when compared without feature selection. This research uses new feature matrix as the base for selection. This feature matrix contains forecasting result using Single Exponential Smoothing (FMF(SES)). The method uses wrapper method of GASVM and it is named FMF(SES)-GASVM. The result of this research is compared with other methods such as GA Bayes, Forward Bayes and Backward Bayes. The result shows that FMF(SES)-GASVM has maximum accuracy when compared of FMF(SES)-GA Bayes, FMF(SES)-Forward Bayes, FMF(SES)-Backward Bayes, however the number of selected features are more than if compared with FMF(SES)-GA Bayes and FMF(SES)-Forward Bayes.

**Keywords**—Single exponential smoothing; forecasting; feature selection; genetic algorithm

## I. INTRODUCTION

The number of variables of features would influence the time and performance in data mining process. One of the techniques to improve efficiency of mining data result especially in terms of process time was by selecting feature. In feature classification process, the selected features were those which had a better classification result or the same with the classification result without feature selection. The other benefit was faster process time because not all features were used. Feature selection had several methods namely filter, embedded and wrapper [1]. In filter method, the process of its feature selection was separated with its classification process. The qualified features were sought with the purpose to be able to influence the training result without looking at the mechanism of the training. Only the relevant features were used in the training. In wrapper method, learning machine was used as a black box to count feature-subset based on the level of its prediction [2],[3]. In embedded method, the evaluation process was to connect or link to a task (for example classification) from algorithm learning. In this embedded method, a sub-algorithm feature selection explicitly or implicitly was an integrated part in a more general algorithm learning [4].

In the field of forecasting, when there were more features were used, it certainly would influence its access time. Only feature with better accurate time would be selected. The research in this paper was different because the feature selection was conducted using machine learning process or wrapper method where the features were previously placed in a matrix of forecasting result. If the research [5] conducted

forecasting from the result of the selected features, in this research we used the forecasting result to select relevant features which resulted in a better accuracy than without feature selection. In this research, data daily demand forecasting orders from UCI machine learning repository was also used.

The use of Single Exponential Smoothing (SES) was especially to form its feature matrix. Feature selection method used wrapper method. The idea was how to transform forecasting data into a feature matrix which then was continued with feature selection process of wrapper method. Forecasting Algorithm of this research used Single Exponential Smoothing (SES) while its wrapper method used Genetic Algorithm – Support Vector Machine (GASVM). The use of wrapper method was because the accuracy was better compared with filter method, although the process time of filter method was faster compared with wrapper method [6]-[11]. The selection of GASVM Algorithm was because it was better than PSOSVM [12]. This research was also compared with other feature selection algorithm such as algorithm-Naive Bayes, forward-Naive Bayes approach, backward-Naive Bayes approach, and also without feature selection. The comparison without through feature selection meant that after through feature matrix formation, classification process was directly conducted.

The contributions of this research were:

- a) A proposal to form feature matrix through forecasting result was called Feature Matrix of Forecasting (FMF) using Single Exponential Smoothing (SES).
- b) Feature Selection using wrapper GASVM method was conducted after feature matrix formation called FMF(SES)-GASVM.
- c) The comparison of classification result with or without feature selection, and algorithm of other feature selections.

The rest of this paper was organized as follows: Section 2 presented the related work and Section 3 provided the materials and the proposed research method. Section 4 presented the experimental result and Section 5 concluded the paper.

## II. RELATED WORK

Several studies have used neural network to find the result of the selected features [5], [13]-[17]. However, the feature selection process is different, some use filter method, wrapper method and hybrid method.

Feature selection using filter method tends to process the original data first. The first feature with original data is conducted with clustering or classification using certain algorithm to select features [5], [13]. Then the selected features are classified to find their accurate result. For example, in the research [5] where the research used feature selection of filter method. The feature selections by using relief, PCA, discrete transformation of data (ReliefF, Information Gain, and Clustering K-means). The result of the selected features from different algorithm in the ranking has many similarities to the selected features, then the process using Elman Network (EN), Fuzzy System (Subtractive Clustering) (FSSC), Adaptive Neuro-Fuzzy Inference System. (ANFIS), FasArt (FART) is conducted. While the research with forecasting used multilayer perceptron (MLP) from selected features as its node [15]. Mutual information and K-nearest neighbors was also used as features selection process which would be predicted using neural network [15].

In [14], features selection research was conducted for time series forecasting using combination of filter wrapper. An interactive neural filter was proposed for feature evaluation to automatically identify the frequency of the time series, embedded in wrappers for feature construction, feature transformation and architecture selection. Time series data was conducted to calculate penalized Euclidean distance and the result was applied in wrapper method neural network to identify its seasonality. The use of neural network would require longer access time so that the combination between feature selections of filter method could cover the lack of access time. This was because the features used were less so that it can reduce the access time. Selection of features with a neural network is included in the wrapper method [18]. The use of neural network could also be used in the research of [13]. The research uses Improved Principal Component Analysis (IPCA) and the selected features were conducted through forecasting process using Neural Network Ensemble (NNE) and it was called NNEIPCABag. The feature selection process was done first so that the method was filter method, while the forecasting process uses NNE, because if the method was wrapper, the feature selection process was included in its learning machine.

The hybrid method can be a combination of a filter-wrapper method or wrapper-filter method. In [19], The hybrid method used is the filter-wrapper method. ACF combination (AutoCorrelation Function) and LSSVM (Least Squares Support Vector Machines) are used to build the electricity load forecast. In [20], researchers proposed a hybrid model based on features of WOA for the prediction of  $PM_{2.5}$  concentration.

### III. MATERIALS AND METHODS OF RESEARCH PROPOSED

Feature selection of wrapper method means that the selected features use machine learning as black box to count the level of its prediction [2], [3]. Therefore, it requires a process related to its machine learning.

#### A. Feature Selection of Wrapper Method

In this research, its wrapper method uses GASVM algorithm. Generally, the researchers select features from first data and then the result is conducted with forecasting process.

This kind of research, its selected features are not based on the result of forecasting accuracy but the result of feature selection is based on variables which may be considered relevant. In this paper, the result of forecasting is used as the bases of feature selection

#### B. Dataset

This research used data daily demand forecasting orders from VCI Machine learning repository (<https://archive.ics.uci.edu/ml/datasets/DailyDemandforecastingOrders>). The dataset was collected during 60 days; this is a real database of a Brazilian logistics company. This dataset has 13 attributes / features and 60 data. The dataset has 12 predictive attributes and a target that is the total of orders for daily treatment. The variable is week of month, day of the week, non-urgent order, urgent order, order type A, order type B, order type C, fiscal sector, orders from the traffic controller sector, banking orders 1, banking orders 2, banking orders 3, and target (total orders). Variable week of the month and day of the week are the data of observing day, while other variables contain value and target orders. Variables of days and months are extracted into data per day. Variable means the same as feature.

#### C. Single Exponential Smoothing

Forecasting is an action to read a behavior of future time from observation of the past time. Forecasting the value of the future time nowadays is extensively required to prepare anything happens, like in forecasting population, energy, economy. In civil population, the forecasting is conducted to estimate the number of people for several years in the future. For energy, estimation is needed to be able to know how much energy reserve available. In economy, global or local economy trend is needed to predict market behavior is the future time. Various techniques of forecasting except classical statistic, many now use soft computing [21]-[23].

Exponential Smoothing is simple method in its operation, low cost, extensive in adaptability and good in performance [24]. The exponential Smoothing method is frequently used as prediction method. Exponential Smoothing is a simple approach for forecasting. Forecasting is built from an average weight exponentially from past observations [25].

Principally, there are 3 techniques of exponential smoothing [26]. Exponential Smoothing technique is simple exponential technique [27], Holt's exponential smoothing [27], and Holt-Winters method [28]. Simple exponential smoothing needs a little computation and is used at the time of data pattern neither have not a cyclic variation nor trend in the historical data [29], [26]. Holt's method is known as double exponential smoothing method, using time series contains a trend. Holt-Winters technique can capture trend and seasonality in historical data [26].

Single Exponential Smoothing Method gets smoothing curve using one past data and one prediction of past data. Let an observed time series be  $y_1, y_2, \dots, y_n$ . The equation of simple exponential smoothing is shown as follows:

$$\hat{y}_{i+1} = \alpha y_i + (1-\alpha) \hat{y}_i \quad (1)$$

Where  $\hat{y}_{i+1}$  represents the predicted value at the time that  $i+1$ .  $\hat{y}_i$  is forecast value of variable  $Y$  at the time of period  $i$  and  $y_i$  is actual value at the time of period  $i$ ,  $\alpha$  is smoothing constant [27]. When starting algorithm, it needs initial forecast namely an actual value and a smoothing constant [25]. Smoothing constant has value between 0 and 1. This is because  $\alpha = 1$ , so the actual value and smoothed version of series are identical, while if  $\alpha = 0$ , the series is smoothed flat. When there is a difference between forecast value during the period of  $i + 1$  and the period of  $i$ , so it is shown in the following (2).

$$\hat{y}_{i+1} - \hat{y}_i = \alpha(y_i - \hat{y}_i) \quad (2)$$

When residual  $e_i = y_i - \hat{y}_i$  is forecast error during  $i$ , so it is shown on the equation as follows (3):

$$\hat{y}_{i+1} = \hat{y}_i + \alpha e_i \quad (3)$$

Therefore, exponential smoothing is old forecast plus an adjustment for error that occurred in the last forecast [30][31][25]. Then with the past forecasting value, so it is shown in the following:

$$\begin{aligned} \hat{y}_{i+1} &= \alpha y_i + (1-\alpha)[\alpha y_{i-1} + (1-\alpha)\hat{y}_{i-1}] = \\ \hat{y}_{i+1} &= \alpha y_i + \alpha(1-\alpha)y_{i-1} + (1-\alpha)^2 \hat{y}_{i-1}, \\ \hat{y}_{i+1} &= \alpha y_i + \alpha(1-\alpha)y_{i-1} + \alpha(1-\alpha)^2 y_{i-2} + (1-\alpha)^3 \hat{y}_{i-2}, \\ \hat{y}_{i+1} &= \alpha y_i + \alpha(1-\alpha)y_{i-1} + \alpha(1-\alpha)^2 y_{i-2} \\ &+ \alpha(1-\alpha)^3 y_{i-3} + (1-\alpha)^4 \hat{y}_{i-3} \dots \end{aligned}$$

So that forecasting equation in general is as follows (4):

$$\hat{y}_{i+1} = \alpha \sum_{k=0}^{i-1} (1-\alpha)(1-\alpha)^k y_{i-k} \quad (4)$$

Where  $\hat{y}_{i+1}$  is the forecast value of Variable  $y$  during the period of  $i+1$  so that  $\hat{y}_{i+1}$  is the weighted moving average of all past observations [25].

#### D. Forecast Error Management

In forecasting result, it is certainly not always the same with the reality or in the real condition, however, from this forecasting result supporting factors can be prepared to anticipate the risky things. The difference between forecasting result and the result of the real condition is called forecasting error. The comparison of mass difference between forecasting and real result can be used as a reference to determine the needs in the future. Small mass difference shows that the forecasting result comes near the real condition. One of the methods is by using Mean Squared Error (MSE). MSE is a computation of the total forecasting data difference with the real data. MSE is shown as follows:

$$MSE = \frac{1}{n} \sum_{i=1}^n (f_i - y_i)^2 \quad (5)$$

Where  $f_i$  is value of forecasting result. Variable  $y_i$  is real value and  $n$  is number of data. MSE is generally used as criteria to select its smoothing constant [30].

#### E. Feature Matrix of Forecasting

Feature selection is based on feature columns which are ready to be used for prediction. In time series research involving many dimensions such as multivariate time series (MTS), data dimension reduction is needed in order to be fit in

the feature columns which then continued by feature selection process. The transformation process into this feature columns is called vectorization [32]. Various ways have been used in order to be fit into that vectorization such as common principle component analysis (CPCA), using matrix correlation [33]. This is because the use of the word "matrix vectorization" refers to long calculation of vector in the research, while the research of [32] mentioned about feature matrix because it is a matrix which contains feature columns. In this research uses the term feature matrix because those matrix contains the selected features.

Feature matrix contains forecasting result of each feature using single exponential smoothing which then the combination of features with high accuracy are selected using wrapper GASVM method. Therefore, preprocessing from dataset is conducted to form its feature matrix.

#### F. Feature Selection of Wrapper GASVM Method

GASVM is a feature selection method which has two steps conducted repeatedly until a certain limit. The first step is feature selection step at random (using genetics algorithm) and the second step is classification process with the calculation of accuracy level from the combination of selected features (using Support Vector Machine). At the time the limit of feature selection process has been fulfilled, so the final result is the selected features which have maximum accuracy value when compared without feature selection.

Genetics Algorithm (GA) used for the application of feature selection has different way with algorithm used for optimization [34]. In the application of feature selection, GA is aimed to select features which will be used for classification process using SVM. Genetics Algorithm has several processes namely encoding of chromosomes, population initialization, fitness function, parents selection, crossover, mutation, population replacement and criteria limit. Population in one generation is the collection of some chromosomes containing the selected and unselected features. The selected features are represented by 1 and 0 if not selected. In this research, fitness function in genetics algorithm for feature selection uses the accuracy value of SVM classification result like the following (6).

$$\text{fitness}(x) = \text{accuracy}(x) \quad (6)$$

Accuracy value is from classification calculation using SVM. When  $a$  is the total of data which has label according to the real data and  $n$  is the whole total of testing data, so the accuracy equation is as follows (7):

$$\text{accuracy}(x) = \left(\frac{a}{n}\right) * 100\% \quad (7)$$

One of classification techniques is by using Support Vector Machines. Its classification usually involves collection of data with several features or attributes and there is a class label [35]. This SVM finds and makes use of margin or optimal separating hyper plane which separates two classes and maximize the closest distance from point to point from different class [35], [36]. A hyper plane which separates two classes with the following (8) [36][37][32]:

$$g(x) = w'x + w_0 \quad (8)$$

Where  $w$  is vector hyper plane  $g(x)$  and  $w_0$  or  $\|w\|$  is the distance from the point of origin to its hyperplane. The details is in [36], [37].

Feature Selection of GASVM Wrapper method starts from the separated data from testing and training data. On the first data, there is initialization data which contains the selected features. Then this feature build classifier model uses SVM. The calculation of its accuracy value uses training data. Fitness evaluation in genetic algorithm process is based on maximum accuracy value (then the selected feature is used as parents), next using crossover process, mutation, population replacement to get a new generation and so on. The process will stop when the criteria restrictions have been fulfilled.

G. Feature Selection of GASVM Wrapper Method from Forecasting Feature Matrix

Before feature selection is conducted, forecasting feature matrix is needed. In every feature, the result of forecasting for some time in the future ( $\hat{y}_{i+1}$ ) is calculated. In one dataset there must be one feature representing the class/label to determine the relevant feature when using GASVM. This is because algorithm support vector machine is a classification which evaluates the selected features based on the highest accuracy value. The steps of this research are:

Step 1. Preparing class/label feature: GASVM is a feature selection method based on the result of SVM classification. Therefore, features containing class/label data are needed.

Step 2. Forecasting of every feature for  $\hat{y}_{i+1}$ : In every feature, forecasting process using single exponential smoothing is conducted. Therefore, there is forecasting feature matrix with one column as a label column. In this research, normalization data are used.

Step 3. Forming forecasting feature matrix: Feature matrix of forecasting is a matrix containing features which will be selected, in which the forecasting data are the result of forecasting.

Step 4. Selection of features with high accuracy level: The selection of features uses GASVM wrapper method. Feature matrix of forecasting contains the result of forecasting using SES. During the process of feature selection with GASVM, it means that the data used is the result of SES forecasting. These selected features will show the accuracy value from the highest classification. Therefore, to know the performance of the selected features, the comparison with the result of classification is required if without the selection of features. The description of this research process is shown in Fig. 1.

IV. RESULT AND DISCUSSION

Single Exponential Smoothing selects smoothing constant with the smallest MSE. In the dataset, there are 11 features with one feature containing label for classification with label value of 0 and 1 (see sub-chapter III.B). Therefore, 10 features which are joined in the selection of features use GASVM. Prior to feature selection process, the dataset needs to be prepared.

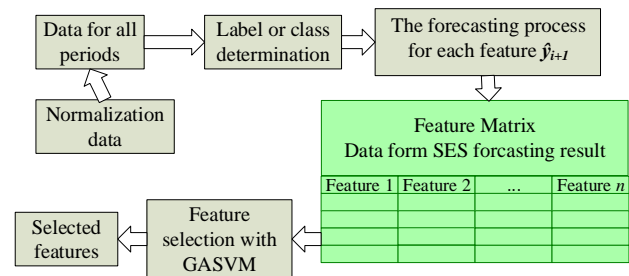


Fig. 1. The Proposed Work Block Diagram.

A. Preparation of Data

The dataset consists of the data of ordering for 5 weeks and 5 days (from Monday to Friday). The dataset is collected within 60 days. This is a real database of a Brazilian Logistic Company. Therefore, all data are used and prepared. This preparation of data includes data preprocessing and data normalization. The preparation of data is necessary because it is possible that the data without being processed first won't be complete and noisy, like there is field of redundancy, zero value or null, there is Outliner or inconsistent value with the valid rule [38]. In this research, the process of data preprocessing when features have no complete data, the empty data will be filled with average data from minimum value with maximum value of the same column data, while the normalization of the data uses MinMax data normalization.

B. Preparation of Class or Label Features

In this research, there are 11 features. One feature is a target or total orders. Feature or attribute of total orders is used as class/label. The selection of attribute or feature of total orders as label is because the attribute is the result of total orders at that time. Therefore, the total orders determine the amount of order which will be executed. The method used in the formation of class/label is by looking at values above or below average. The value of total orders below average is 0 and above average is 1. So there are 10 features left which will be processed for feature selection.

C. Forecasting with Single Exponential Smoothing

All data on features are calculated for their forecasting for some time in future  $\hat{y}_{i+1}$  (see sub-chapter III.G). Then smoothing constant is selected with the smallest MSE value. Table I shows the result of all features calculated their forecasting value using SES. The result can be seen from Fig. 2 to Fig. 6. Fig. 2 shows training data and the forecasting result using SES with smoothing constant having been selected for features of Non Urgent Order and Urgent Order. Fig. 3 shows training data and forecasting result using SES for feature data of Order Type A, Order Type B and Order Type C. Fig. 4 shows training data and forecasting result using SES for feature data of Fiscal Sector Orders and Orders from the traffic. Fig. 5 shows training data and forecasting result using SES for feature data of Banking Orders 1 and Banking Orders 2. Fig. 6 shows training data and forecasting result using SES for feature data of Banking Orders 3 and Target (Total Orders).



TABLE I. THE RESULT OF SMOOTHING CONSTANT AND MSE OF EACH FEATURE

| Features                    |                         |              |              |              |              |                     |
|-----------------------------|-------------------------|--------------|--------------|--------------|--------------|---------------------|
|                             | Non Urgent Order        | Urgent Order | Order type A | Order Type B | Order Type C | Fiscal Sector Order |
| Smoo-thing constant (Alpha) | 0.1                     | 0.1          | 0.1          | 0.1          | 0.1          | 0.1                 |
| MSE                         | 0.02772                 | 0.0357       | 0.0279       | 0.038        | 0.0313       | 0.0159              |
| Features                    |                         |              |              |              |              |                     |
|                             | Orders from the traffic | B. Orders 1  | B. Orders 2  | B. Orders 3  | Total Orders |                     |
| Smoo-thing constant (Alpha) | 0.1                     | 0.5          | 0.1          | 0.6          | 0.1          |                     |
| MSE                         | 0.0363                  | 0.0276       | 0.0515       | 0.0200       | 0.0318       |                     |

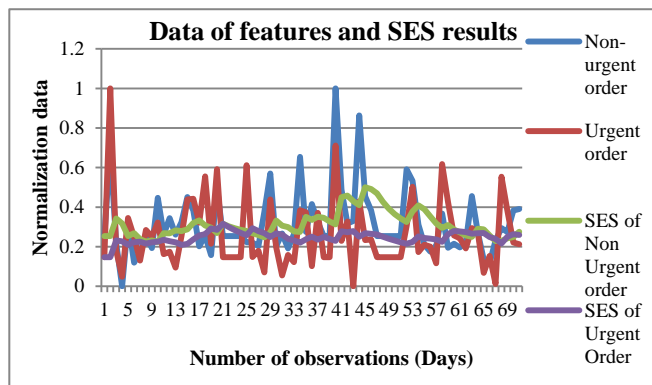


Fig. 2. Training Data and the Forecasting Result using SES with Smoothing Constant having been Selected for Features of Non urgent Order and urgent Order.

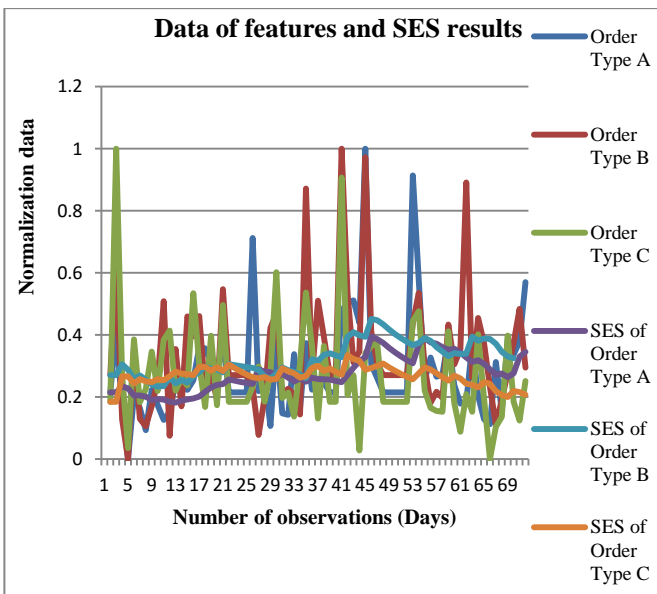


Fig. 3. Shows Training Data and Forecasting Result using SES for Feature Data of Order Type A , Order Type B and Order Type C.

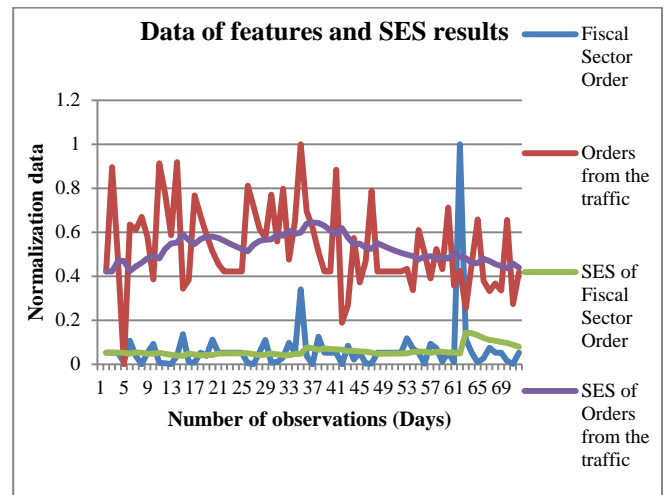


Fig. 4. Training Data and Forecasting Result using SES for Feature Data of Fiscal Sector Orders and Orders from the Traffic.

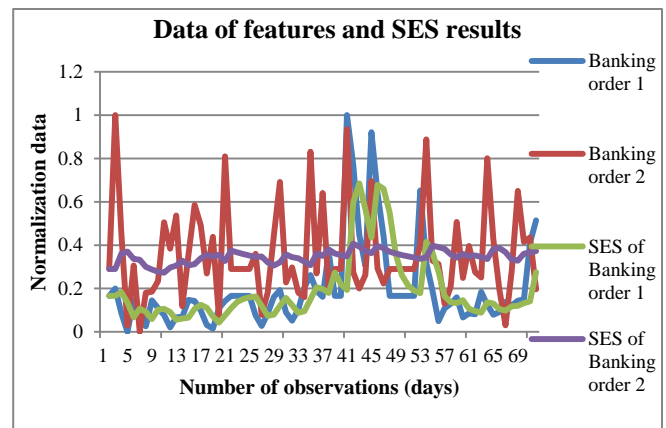


Fig. 5. Training Data and Forecasting Result using SES for Feature Data of Banking Orders 1 and Banking Orders 2.

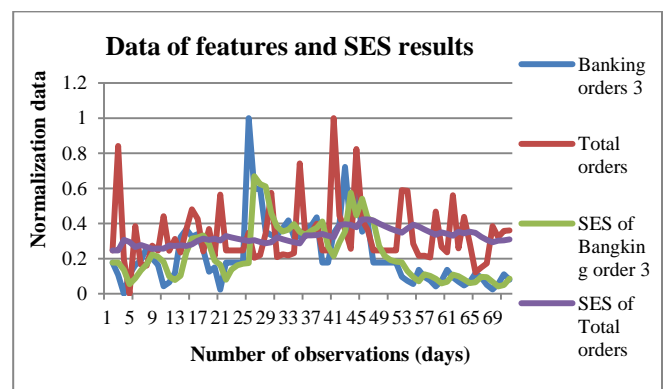


Fig. 6. Training Data and Forecasting Result using SES for Feature Data of Banking Orders 3 and Target (Total Orders).

#### D. Feature Matrix of Forecasting

Feature Matrix of forecasting here is a matrix containing the result of forecasting except for the result of feature forecasting used for label or class. Thus there are 10 features where lines/rows are observation days and the columns are features and one feature of total order is as class or label. The formation of class or label has been stated in sub-chapter IV.B.

### E. Selection of GASVM Feature

Several Parameters of genetic algorithm used in this research are as follows:

- 1) Population uses binary number where 0 is an unselected feature and 1 is the selected one.
- 2) Elitism is conducted in 2 ways, if the number of chromosomes is in odd population, so one duplicate of the best chromosome is kept, but if it is in even number two duplicates of the best one are kept.
- 3) The selection method used is roulette wheel weighting with rank weighting technique.
- 4) Crossover uses one-point crossover with crossover probability equal to 0.8.
- 5) Mutation probability used is 0.05. Mutation is done to all genes in chromosomes for random number GA grown smaller than the mutation probability.
- 6) New population for the next generation is the population as the result of GA process.
- 7) Maximum total of generation is 100; the size of population is 50.
- 8) The condition of terminal is used based on the maximum amount of population or generation evaluated and the maximum level of accuracy (100%).
- 9) The calculation of accuracy level with SVM is based on classification with two classes.

Special for Naïve Bayes on GA Bayes is helped by WEKA application version 3.6.11, whereas FSBLF and GASVM use Matlab version R211b. Parameter for Naïve Bayes uses default Weka, namely, fold 5, seed 1, threshold 0.01, start set-, and for genetic algorithm in Weka application uses the same parameter with the one in Matlab.

This reasearch uses algorithm and comparative method to know the result of several methods of feature selection. Feature selection of wrapper method used in this research is GASVM, GABayes, ForwardBayes and BackwardBayes. GASVM has been previously explained. GABayes is feature selection of wrapper method where features at random are selected using genetic algorithm and their Fitness is based on forward approach. This forward approach is an approach started from first feature in which its classification result is counted using naïve Bayes, then the combination of first feature and second, next is first feature, second and third. After that the features selected are only those with the highest accuracy value. On the contrary with ForwardBayes, on BackwardBayes the features counted, their accuracy starts from combination of all features, then decreasing one by one.

FMF(SES)-GASVM has the most maximum accuracy among the other four methods (without selection of feature, GABayes, ForwardBayes, Backward Bayes), even though the total of the selected features is more than GABayes and ForwardBayes. Table II shows accuracy value of 100 % for FMF(SES)-GASVM with five total number of selected features namely features 3,4,5,6 and 8. If without selection of feature, so there are 10 features with accuracy value of 97.2%. FMF(SES)-GABayes and FMF(SES)-ForwardBayes have less number of selected features that are 3 features, but the accuracy

value is lower for 97%. The less number of features, the faster the classification process, however, the accuracy is more emphasized. The lowest accuracy value is obtained from FMF(SES)-BackwardBayes with accuracy value 96%. Therefore, only features 3,4,5,6 and 8 are used to predict the future. This FMF-GASVM Method can be used in all forecasting dataset and has feature as class or label.

TABLE II. THE RESULT OF FEATURE SELECTION AND ITS ACCURACY PERCENTAGE

| Feature selection method                       | Selected features | Number of selected features | Accuracy (%) |
|--|-------------------|-----------------------------|--------------|
| FMF(SES)-GASVM                                 | 3,4,5,6,8         | 5                           | 100          |
| Without feature selection (SVM classification) | -                 | -                           | 97.2         |
| FMF(SES)-GaBayes                               | 1,4,5             | 3                           | 97           |
| FMF(SES)-ForwardBayes                          | 1,4,5             | 3                           | 97           |
| FMF(SES)-BackwardBayes                         | 1,3,4,5,9         | 5                           | 96.9         |

### V. CONCLUSION AND SUGGESTION

Features Matrix of Forecasting (FMF) is one of many ways to form features matrix of forecasting result as the first basis of the process of feature selection. So the purpose is to produce selected features with better accuracy value if without selection of feature. The other benefit is faster process time because not all features are used. This research used Single Exponential Smoothing (SES) to determine forecasting value in the future and is used the value on features matrix. The selection of its features used method of Wrapper Genetic Algorithm Support Vector Machine (GASVM). In this research, FMF(SES)-GASVM is compared with several other methods, namely, FMF(SES)-GABayes, FMF(SES)-FowardBayes, FMF(SES)-BackwardBayes and without selection of features. FMF(SES)-GASVM has maximum accuracy (100%) compared with the other four, however the number of selected features is more than FMF(SES)-GABayes and FMF(SES)-ForwardBayes. The result shows that only with features 3.4.5.6 and 8 can be used as forecasting features for future value with 100 % accuracy compared to the other four algorithms.

In this research, forecasting algorithm can be used besides Single Exponential Smoothing such as Double Exponential Smoothing. But it is still forming its matrix forecasting as the basis of feature selection. In addition, it can also use other methods of feature selection like filter or embedded method.

### ACKNOWLEDGMENT

Thank you to the University of Bhayangkara Surabaya for supporting this research.

### REFERENCES

- [1] H. Chouaib, O. R. Terrades, S. Tabbone, F. Cloppet, N. Vincent, and B. P. Nancy, "Feature selection combining genetic algorithm and Adaboost classifiers," in 1th International Conference on Pattern Recognition, 2008, vol. 5, no. Ea 2517, pp. 1-4.
- [2] I. S. Oh, J. S. Lee, and B. R. Moon, "Hybrid Genetic Algorithms for Feature Selection," IEEE TRansaction on Pattern Analysis And Machine Intelligence, vol. 26, no. 11, pp. 1424-1437, 2004.

- [3] R. Kohavi and H. John, "Artificial Intelligence Wrappers for feature subset selection," *Artificial Intelligence*, vol. 97, no. 97, pp. 273–324, 2011.
- [4] I. Witten and E. Frank, *Data Mining: Practical Machine Learning Tools and Techniques*, 2nd ed. Morgan Kaufmann, 2005.
- [5] R. G. Pajares, "Feature Selection for Time Series Forecasting: A Case Study," in *International Conference on Hybrid Intelligent Systems*, 2008, pp. 555–560.
- [6] R. Kohavi and G. John, "Wrappers for feature subset selection," *Artificial Intelligence*, vol. 97, pp. 273–324, 1997.
- [7] C. L. Huang and W. C. J., "A GA-based feature selection and parameters optimization for support vector machines," *Expert Systems with Applications*, vol. 31, pp. 231–240, 2006.
- [8] K. Z. Mao, "Feature subset selection for support vector machines through discriminative function pruning analysis," *IEEE transactions on systems, man, and cybernetics. Part B, Cybernetics*, vol. 34, no. 1, pp. 60–67, 2004.
- [9] E. Yu and S. Cho, "Ensemble based on GA wrapper feature selection," *Computers and Industrial Engineering*, vol. 51, no. 1, pp. 111–116, 2006.
- [10] J. Bi, K. P. Bennett, M. a Embrechts, and C. M. Breneman, "Dimensionality Reduction via Sparse Support Vector Machines," *Journal of Machine Learning Research*, vol. 1, pp. 1–16, 2002.
- [11] R. Sikora and S. Piramuthu, "Framework for efficient feature selection in genetic algorithm based data mining," *European Journal of Operational Research*, vol. 180, no. 2, pp. 723–737, 2007.
- [12] E. Alba, L. Jourdan, and E. Talbi, "Gene Selection in Cancer Classification using PSO / SVM and GA / SVM Hybrid Algorithms," *IEEE Congress on Evolutionary Computation (CEC)*, vol. 07, pp. 284–290, 2007.
- [13] L. Jian, "Neural Network Ensemble Based on Feature Selection," in *IEEE International Conference on Control and Automation*, 2007, vol. 00, pp. 1844–1847.
- [14] S. F. Crone and N. K. Å, "Neurocomputing Feature selection for time series prediction – A combined filter and wrapper approach for neural networks," *Neurocomputing Elsevier*, vol. 73, no. 10–12, pp. 1923–1936, 2010.
- [15] S. F. Crone and S. Häger, "Feature Selection of Autoregressive Neural Network Inputs for Trend Time Series Forecasting," in *International Joint Conference on Neural Networks*, 2016, pp. 1515–1522.
- [16] L. I. U. Tianhong, W. E. I. Haikun, Z. Kanjian, and G. U. O. Weili, "Mutual information based feature selection for multivariate time series forecasting," in *Proceedings of the 35th Chinese Control Conference*, 2016, pp. 7110–7114.
- [17] M. Maca and L. Lhotsk, "Wrapper Feature Selection Significantly Improves Nonlinear Prediction of Electricity Spot Prices," in *IEE International Conference on Systems, Man, and Cybernetics*, 2013, pp. 1171–1174.
- [18] M. Rana, I. Koprinska, and A. Khosravi, *Artificial Neural Networks*, Springer S., vol. 4. Switzerland: Springer International Publishing, 2015, pp. 445–446.
- [19] A. Yang, W. Li, and X. Yang, "Knowledge-Based Systems Short-term electricity load forecasting based on feature selection and Least Squares Support Vector Machines," *Knowledge-Based Systems*, vol. 163, pp. 159–173, 2019.
- [20] P. M. Concentration, F. Zhao, and W. Li, "A Combined Model Based on Feature Selection and WOA for PM2.5 Concentration Forecasting," *Atmosphere, MDPI*, no. 2, pp. 1–20, 2019.
- [21] L. A. M, M. Beni, D. Nieto, C. Di, and F. A. Sa, "Forecasting airborne pollen concentration time series with neural and neuro-fuzzy models," *Elsevier*, vol. 32, pp. 1218–1225, 2007.
- [22] D. Sonika, S. D. S, and K. Daljeet, "Long-Term-Load-Forecasting-Using-Soft-Computing-Techniques," *International Journal of Scientific & Engineering Research*, vol. 6, no. 6, pp. 450–457, 2015.
- [23] S. Chen, S. Member, and J. Hwang, "Temperature Prediction Using Fuzzy Time Series," in *IEEE Transactions on system, Man, and Cybernetics*, 2000, vol. 30, no. 2, pp. 263–275.
- [24] A. M. Systems, "Variable smoothing parameter of the double exponential smoothing forecasting model and its application Chen Feiyan, Li Qian, Liu Junhong and Zhang Jiuyong," in *International Cobference on Advance Mechatronic Systems*, 2012, pp. 386–388.
- [25] E. Ostertagova and O. Ostertag, "The simple Exponential Smoothing Model," in *The 4th International conference Modelling of Mechanical and Mechatronic Systems*, 2011, pp. 380–384.
- [26] L. Abderrezak, "Very Short-Term Electricity Demand Forecasting using Adaptive Exponential Smoothing Methods," in *15th International Conference on Science and Techniques of Automatic Control and Computer Engineering*, 2014, pp. 553–557.
- [27] R. G. Brown, *Statistical forecasting for inventory control*. New York: McGraw-Hill, 1959.
- [28] P. R. Winters, "Forecasting Sales by Exponentially Weighted Moving Average," *Management Science*, vol. 6, no. 3, pp. 231–362, 1960.
- [29] M. Mordjaoui, B. Boudjema, and M. Bouabaz, "Electric load consumption prediction using statistical approaches," *International Conference on Applied Analysis and Algebra*, pp. 20–24, 2012.
- [30] A. D. Azcel, *Complete Business Statistics*. Irwin, 1989.
- [31] E. Ostertagova, *Applied Statistic (in Slovak)*. Elfa, Kosice, 2011.
- [32] K. Yang, H. Yoon, and C. Shahabi, "A Supervised Feature Subset Selection Technique for Multivariate Time Series," in *International Workshop on Feature Selection for Data Mining*, 2005.
- [33] H. Yoon, K. Yang, and C. Shahabi, "Feature Subset Selection and Feature Ranking for Multivariate Time Series," *IEEE Transactions on Knowledge and Data Engineering*, vol. 17, no. 9, pp. 1186–1198, 2005.
- [34] A. D. Rahajoe, E. Winarko, and S. Guritno, "A Hybrid Method for Multivariate Time Series Feature Selection," *International Journal of Computer Science and Network Security*, vol. 17, no. 3, pp. 103–111, 2017.
- [35] V. Vapnik, "Statistical Learning Theory," *Adaptive and learning Systems for Signal Processing, Communications and Control*, pp. 1–740, 1998.
- [36] T. Hastie, R. Tibshirani, and J. Friedman, *The Elements of Statistical Learning: data mining, inference and prediction*. New York: Springer-Verlag, 2001.
- [37] R. . Duda, P. . Hart, and D. . Stork, *Pattern Classification*, Second. Wiley Interscience, 2001.
- [38] D. T. Larose, *An Introduction to Data Mining*. Canada: A John Wiley & Sons, Ltd, 2005.

# A Review on the Verification Approaches and Tools used to Verify the Correctness of Security Algorithms and Protocols

Mohammed Abdulqawi Saleh Al-humaikani<sup>1</sup>, Lukman Bin Ab, Rahim<sup>2</sup>

Department of Computer & Information Science, Universiti Teknologi Petronas Bandar Seri Iskandar, Malaysia

**Abstract**—Security algorithms and protocols are typical essential upgrades that must be involved within systems and their structures to provide the best performance. The protocols and systems should go through verification and testing processes in order to be more efficient and accurate. In the testing of software, traditional methods are used for accuracy check-up. However, this could not fulfill the measurement of all the testing requirements. The usage of formal verification approaches in checking security properties considers their best environment to be applied. The available literature discussed several approaches on developing the most robust formal verification methods for addressing and analyzing errors that face systems. This could be during the implantation process, unknown attacks, and nondeterministic adversary on the security protocols and algorithm. In this paper, a comprehensive review of the main formal verification approaches such as model checking and theorem proving has been conducted. Moreover, the use of verification tools was briefly presented and explained thoroughly. Those formal verification methods could be involved in the design, redesign of security protocols, and algorithms based on standards and determined sizes that is decided by these techniques' analysis. The critical analysis of the methods used in verifying the security of systems showed that model checking approaches and its tools were the most used approaches among all the reviewed methods.

**Keywords**—Security algorithms; security protocols; formal verification approaches; model checking; theorem proving

## I. INTRODUCTION

The number of technology users has increased rapidly on a daily basis all over the globe. This requires developers and researchers to conduct and invent algorithms and protocols that can provide a high level of security. For instance, in [1] stated that security and protection level that can be involved with a variety of information technology platforms include users and users data. Security in the form of security algorithms [2] and protocols [3] can achieve security purposes and provides authentication, data confidentiality, secrecy, and secured communication. One of the well-known security, cryptographic algorithms, and protocols are RSA, SSL/TLS [4]. These protocols and algorithms can be used to provide a level of security and confidentiality for different types of technology's users. However, the level of security offered will be associated with the risk of algorithms / protocols failures, third man attack, or other types of risks that can face users and applications. In [5] mentioned that there are different methods able to ensure the effective performance of these protocols and

algorithms by using testing, simulators, or formal verification approaches. The use of simulations to test or measure the security protocols and algorithms' properties is not fully trusted as stated in [6]. Meanwhile, there are some challenges in security protocols and algorithms introduced in the work done by Rosenberg [7] such as the increase number of cyber-attacks. Then, the measurement of results produced by simulators are not the proper tool to evaluate or analyse the properties and in verifying the correctness. Therefore, formal verification methods are considered as one of the approaches that can be used to verify the correctness of high-technologies and complex systems which include security algorithms and protocols [8].

To the authors' best of knowledge there is no available critical review on the methods used for the security verification protocols and algorithms. In this paper, a comprehensive review was conducted in order to describe, compare, and analyse the two formal verification approaches of security and their tools. This included model checking and theorem proving approaches. Hence, this paper would provide a platform for individuals and companies working on the security checking during the early stages of building the security systems.

## II. FORMAL VERIFICATION APPROACHES OF SECURITY ASPECTS

This section provides a review on the selected formal verification approaches that can be used in security aspects. These approaches aim to verify two different types of security methods that are security algorithms and security protocols. Besides, those approaches were classified into their uses and purposes. Among the most popular security verifications methods, two methods can be used to verify the correctness of security algorithms and protocols. These two methods are symbolic model checking [9] and theorem proving methods [10]. In the aforementioned formal verification methods, different tools and approaches are used by the researchers in their experiments. The following sections will explain these two approaches with their tools.

### A. Verification Approaches for Security Algorithms

In this subsection, the verification approaches that can be applied on security algorithms and a check on their validity are explained. Besides, the selected verification process for security algorithms was reviewed. Finally, all the selected verification approaches were compared in terms of their differences and usages.

1) *Overview on the verification approaches for security algorithms:* There are two formal approaches found in the literature to verify the correctness of the security algorithms which are symbolic model checking and theorem proving methods. First, the symbolic model checking is basically a model checking that is implemented as a symbolic representation. Symbolic model checking contains two main approaches; binary decision diagrams (BDD)-based model checking [11] and SAT-based model checking [12]. Symbolic model checking is considered as one of the efficient formal verification approaches that can be implemented in software and hardware systems. In [13, 14] stated that using model checking approach requires to build a model of the system from scratch that will have the desired properties to be verified by using model checkers. Otherwise, the model checker will not be useful to check the absence of error within systems without their models.

Secondly, theorem proving is another approach that can verify the correctness of systems in logic mathematical formulas. The properties of the system are formed as mathematical formulas and solved by finding the proof of presuppositions from the system. Lastly, these selected approaches were reviewed by other authors and will be discussed thoroughly in the next section.

### III. REVIEW ON THE SELECTED VERIFICATION APPROACHES FOR SECURITY ALGORITHMS

Schnepf et al. [15] proposed an automated alternative method that can support the verification process of the security in chains at the early stages. The proposed strategy considered control and data planes to be analysed, which contained different security algorithms formed as security functions in chains. First, the security specification of chains were translated into formal models to verify them using verification methods. The security specification translated into formal models using a presented method called Synaptic checker. Two categories supported the verification process and the first category was SMT solver based. The second category was model checking, at which the properties of the security functions were translated to a finite state machine to elaborate on the number of states. After that, the security properties were expressed in the form of temporal logic CTL. Together the FSM states with temporal logic CTL could be verified using the model checking nuXmv. The main benefit of this study was the ability to propose a method that designed as a packet of SDN language. This made it easy to be extended for further formal languages that could check simple invariants properties. Finally, the proposed method needed more improvements to support more complex security functions. Slind [16] presented the verification process of the Rijndael security algorithm. Rijndael block cipher is an algorithm that can encrypt and decrypt data with key sizes of 128, 192, and 256 bits and number of the rounds based on the block sizes. The security algorithm was approved using theorem proving method called HOL. The results showed that the security algorithm was easy to be verified because of the simplicity of its specification. The main advantage of this study was the simplicity of the algorithm when it was coded into SML language, which can be

easier to be understood and taught. Besides, the absence of verifying the security rules in case of hybrid security algorithms, or how the difficulties that can face verification process.

Moreover, Keerthi et al. [17] have provided an overview of using formal verification approaches to verify the correctness in the implementation of several security algorithms. The author used formal verification approaches differently based on the desired properties of IoT security algorithms. Cryptographic algorithms, such as ECC and RSA are used as a case study to verify their implementation by using model checking. The cryptographic algorithms were translated to SAT-based model checking in order to verify it by using a model checking approach CBMC (ANSI-C Bounded Model Checking). CBMC checks the verification of cryptographic algorithms with the help of SAT solver to specify the correctness in counter-example whether they failed or verified by showing the fail part, in case of any failure. The benefits of this work were the ability to prove the correctness of two of the most used cryptographic algorithms, by approving the ability of model checking to verify different extendable cryptographic algorithms. On the other hand, it was better to apply multiple cryptographic algorithms to be proved and to confirm the capability of verification approaches.

Furthermore, Arpit et al. [18] have verified one of the cryptographic algorithms called the ElGamal algorithm. ElGamal cryptographic is asymmetric keys based for encryption and decryption. ElGamal cryptographic provided a public key (PK) and secret key (SK) to add enhanced security on the exchanged data between the communicator parties. The author followed specific steps to represent the cryptographic algorithm safety properties and to get them verified. In addition, a transition system was built using a Kripke structure to describe the transitions system of the cryptographic algorithm. The Kripke structure was considered as a model system for the cryptographic algorithm and translated into the form of logic temporal language (LTL). The LTL defined the behaviour or the properties of the model system in the form of formulas. After that, the model system was verified using the model checking. The author has represented all the steps required for LTL syntax and behaviours in the case for any future studies for other cryptographic algorithms. Moreover, the usage of the model checking with the help of LTL showed the simplicity of verifying cryptographic algorithms using tools and formulas together. The drawbacks in this study were that no statistical analysis for future usages was provided which is considered a disadvantage. Chen et al. [19] proposed a formal verification methodology to verify the correctness of a cryptographic algorithm called Curve25519. Curve25519 is high-speed elliptic-curve cryptography that computed up to 18-bit of security keys. The authors have verified the Curve25519 using hybrid methodology consisted of SMT solving and theorem proving tools assistant. The authors believed that this approach could be computed or verified in low-level optimisation for actual cryptographic algorithms and protocols. The tools that have been used for verification were portable assembly, qhasm, the Boolector SMT solver, and the Coq proof assistant. Curve25519 wrote in an assembly language called qhasm using portable assembly qhasm that saved

development time for assembly software. This study presented new verification approach methodology that consisted different tools, which can offer low-level optimisation to verify real-world cryptographic algorithms. The disadvantage of using this methodology was because of the translation from a different language into assembly language qhasm, which cannot be accurate for most of the times.

#### A. Verification Approaches for Security Algorithms

In this subsection, the verification approaches used to assist in the security protocol verification and correctness are demonstrated. Besides, selected verification approaches for security protocols were reviewed and all the chosen verification approaches were compared based on their different usages. Formal verification methods / approaches that are usually used to verify the correctness of security algorithms was found to be similar to the formal verification approaches used to verify security protocols [20,21]. However, different tools are used in order to verify the security protocol properties such as SAMTC. The following sub-section briefly highlights the main security approaches of both theorem proving and model checking.

1) *Review of the selected verification approaches for security protocols:* Armando et al. [22] presented a formal verification approach called SAT-based Model-Checker (SATMC) to verify the correctness of critical security systems. This included security protocols business processes and security Application programming interfaces (APIs). SATMC has involved different verifying security protocols such as the security assertion markup language (SAML) 2.0, single sign-on (SSO) protocol, and OpenID. SATMC is SAT-based model checking that uses LTL formulas to format the properties of the requested protocol for verification purposes with the help of SAT-solver. The authors used ASLAN language to model and identify the problems and errors that could face any application with security protocols. This tool was successfully applied in verifying variety of security protocols that is considered as one of the useful tools in supporting model checking methods during the verification process. However, this tool lack to test security aspect sectors and it did not find any statistical analysis for optimising this approach. Paolo and Riccardo [23] have verified the properties of a security protocol called Needham-Schroeder public key authentication protocol. Needham-Schroeder public key authentication protocol was invented in 1978 and it is considered as one of the well-known security protocols. This protocol aimed to provide a level of security by using a trusted key server and public key to establish mutual secured authentication. The authors used the spin model checking approach in this study to verify the security properties of the protocol and to find any known attacks. However, the authors suggested developing a Promela model for the cryptographic protocol to help with the verification of the spin model checker approach. The developed model was built to identify the rules and behaviour of the protocol that need to be checked using the model checker. Lastly, the results show that there were no possible additional attacks that could be detected on

the protocol rather than the well-known attack that is called the Lowe's attack. This study investigated all the details to explain the procedure of the verification for the security protocol, which is considered as an excellent reference for future usages. The drawbacks of this study was the lack to provide a proper comparison between all the security properties such as time synchronisation, secrecy, and equivalences. Moreover, Schaller et al. [24] have proposed a formal verification model that can verify the cryptographic properties of three different security protocols on the network. The three protocols that have been verified in this study were; authenticated ranging, ultrasonic distance-bounding, and TESLA broadcast authentication. A model was formalised with Isabelle and higher-order logic (Isabelle/HOL) theorem proving methods. After that, the rules were defined and modeled to verify the physical characteristics that were found on each cryptographic protocol. The proposed formal model was able to capture the relay attacks, broadcast authentication, and other physical properties that were related to each security protocol. The proposed formal method enabled the capturing and verification for variety of cryptographic properties for three protocols, that are considered as helpful references for future works. Unfortunately, the study has not made any statistical comparison with other formal methods at the same level of functionalities. Cremers [25] had presented an overview of one of the efficient verification tool based on the graphics user interface (GUI) that can verify different security protocols. It is a model checking based tool that uses security protocol description language (SPDL) as an input language to write protocols that need to be analysed. The Scyther tool can identify the possible security protocols properties, attack and generates graphs for each attack based on proposed claims. The properties and attacks of the security protocols are analysed with the assistance of a backward search algorithm method that provides a set of infinite pattern traces to approve the correctness of events that must occur. The advantages of this study was its ability to explain the functionality of the Scyther verification tool in short form.

Finally, El-Madhoun et al. [26] have proposed a new security protocol used in near field communication (NFC) payment systems instead of Europay Mastercard Visa (EMV) security protocols. The new security protocol helped to overcome the vulnerabilities found in the EMV protocol. This protocol was based on an online communication and asymmetric cryptography that allow the connection with an authentication server to execute security functions for NFC transactions. The Scyther tool was used to verify the correctness of the proposed security protocol based on specific claims for verification purposes. The Scyther tool is a model checking-based tool and it supports infinite of traces that help to provide the correctness of the requested claimed. Security protocol description language (SPDL) was also used in this study to write the proposed protocol model into the Scyther tool and this helped to scale the number of claims and tests which simplified the verification procedure. The inputs of the claims provided for the verification were authentication and

confidentiality. Then, Scyther will approve the claims and check whether the protocol holds the claims or not. The results showed that the protocol had successfully passed the test and the tool approved the holdings of the claims. In conclusion, this study was able to provide a real example of using the Scyther model checking tool, but there was no statistical comparison of using different verification methods to verify the correctness of the proposed protocol.

#### IV. VERIFICATION TOOLS

There are various formal verification tools used to verify different security systems. However, an overview is listed below for some of the most popular formal verification tools that have been studied by the authors in previous discussed sections to verify the correctness of different security algorithms and protocols:

New symbolic model verifier (NuSMV) [27] is an extensive model checker of symbolic model verifier (SMV) and it is a formal verification and reliable tool to verify finite state systems. NuSMV is based on binary decision diagrams (BDDs). It interacts with the user by using a textual interface and it needs to implement or input the properties of finite state systems by using computational tree logic (CTL) or logic temporal language (LTL) formulas to help with the verification procedure. Some researchers used this tool as a formal verification tool to verify the properties of security protocol as in Panti et al. [28] who used the NuSMV model checker to verify the security properties of the Kerberos protocol [29]. The authors built a transition states diagram model to represent the Kerberos protocol flow in an understandable method. The security properties of the protocol were expressed by the temporal logic CTL in order to be verified in the NuSMV model checker. Besides, Panti et al. [30] have proposed to use the symbolic model checker NuSMV to verify the correctness of secure electronic transaction (SET) protocol. This protocol provides secure transactions process for the users in the open networks. The protocol was modeled as a transition diagram model and the security properties in the model were described to be verified in the NuSMV model checker. The results showed that there were two different possible attacks found during the verification process and this allowed attackers to attack users of this protocol. Moreover, Massimo and Fausto [31] used NuSMV model checker to be part of the verification process of Andrew Protocol [32]. The author built a model for the protocol by using multiagent finite state machine (MAFSM) to reform the protocol as finite states and converted it to NuSMV language to be verified.

C-bounded model checker (CBMC) [33] is one of the model checkers used to verify the security protocols. It needs two inputs in order to process the verification. The first input is that the system or the program needs to be verified and the second input is the formal specific properties that need to be verified as well. Various studies used this tool in their research experiments. For instance, Keerthi et al. [17] used CBMC to verify the implementation of cryptographic algorithms such as ECC and RSA. CBMC checks the verification of cryptographic algorithms with the help of satisfiability (SAT) solver to specify the correctness in counter-example. The result of the verification process will show two outputs either pass or fail

and in the case of failure, the failed parts will be expressed. Sosnovich et al. [34] have proposed a formal approach that helped to automatically discover any security vulnerabilities or attacks that can be found in the network protocol OSPF. The authors modelled the protocol on a concrete model form to expose the desired property to the model checker CBMC. Attacks occurred on OSPF were detected by using CBMC. Satisfiability modulo theories (SMT) [35] solvers use different types of methods to reason about the built theories on SMT solvers. Those solvers check in specific theory to solve satisfiability problems. Schnepf et al. [15] proposed an algorithm that assists to verify the security in chains. The algorithm went through two verification processes; one was model checking and the other one was SMT solvers. The SMT solver was used to check the satisfiability of the model that was designed for the proposed algorithm in order to verify the correctness of the algorithm's constraints. The algorithm was modelled by using SMTlib input language of SMT solvers for verification purposes. Chen et al. [19] have presented a formal verification approach to verify the correctness of Curve2551 cryptographic algorithm. The formal verification approach consisted of Boolector SMT solver and theorem proving tools assistant such as portable assembly (qasm). NuXmv is an evolution of NuSMV model checker and it is a new symbolic model checker that works on checking finite and infinite-state transition systems. It was extended from NuSMV with new data types. It provides advanced model checking techniques based on the SMT [36]. Chen et al. [19] verified the correctness of the cryptographic algorithm Curve2551 by using the model checker NuXmv with other verification approaches. The authors expressed the security properties of Curve2551 in the temporal logic CTL to be verified. However, Guanjie and Shigong [37] had verified the properties of one of the famous protocols of radio-frequency identification (RFID) protocol called hash-lock protocol. NuXmv model checker was used to check the security properties of the hash-lock protocol. A model was built for the hash-lock protocol and attack model to help in verifying the hash-lock protocol.

Spin tool [38] is a verification tool that is used for verifying the concurrent systems. It is considered as one of the robust model checkers used to verify security protocols. Paolo and Riccardo [23] have proposed to use the spin model checker to verify the security properties of Needham-Schroeder public key authentication protocol. The author built a model in the format of a Promela model for the cryptographic protocol to verify the protocol in the spin model checker. Besides, Li et al. [39] have used the spin model checker tool to verify one of the Ultralight-weight authentication protocols. Rfid authentication protocol with permutation (RAPP) is the proposed ultralight-weight authentication protocol that needs to be verified using the spin model checker. Modelling the ultralight-weight authentication protocol by using a protocol abstract modelling method to verify the authenticity and consistency of the protocol was suggested in this study. In addition, Scyther is a model checking tool that verifies the correctness of the claimed requests with the help of an infinite set of traces. The tool can help the protocol to suspect and analysis any attacks that can occur and identify the protocol behaviour [40]. Moreover, El Madhoun et al. [26] have verified a new proposed security protocol that was used in NFC payment systems instead of

Europay Mastercard Visa (EMV) security protocols. A model was built for the new protocol based on security protocol description language (SPDL) to input it into Scyther tool for verification purposes. The inputs of the claims that were provided for verification are authentication and confidentiality. Cas [25] proposed a new verification approach that was implemented on Scyther tool. The refinement proposed algorithm can verify and provide unbounded verification, falsification, and characterisation correctness of different type of security protocols such as TLS protocols. SATMC or SAT-based model checker [41, 42, 43] is a new formal verification approach that has a flexible platform of SAT-based checker. SATMC can verify the correctness of security sensitive protocols. It proposed a translation method that can help model checker to construct the required security protocols for verification purposes. The proposed method was implemented in SATMC checker using the features of SATMC combined with the proposed method. Besides, Armando et al. [22] had used SATMC as a formal model checker to verify different critical systems such as security systems in business processes and security APIs that include security protocols. The security protocols; SAML 2.0 single sign-on (SSO) protocol and OpenID were used as a case study. Furthermore, the ASLan language was used to model and input the properties of the security protocols into the model checker SATMC and NuSMV.

### V. DISCUSSION

In the previous sections, the described formal verification methods and tools have been grouped into two main groups; symbolic model checking, and theorem proving. Several papers have been reviewed based on the formal verification methods and tools, and further elaborated them in Tables I, II and III. Tables I and II explain the most used formal approaches among the two well-known described approaches. It can be observed that model checking methods were adopted by many researchers and it has the highest number of studies. This shows that model checking is the most acceptable tool in verifying security algorithm and protocols with a percentage of 70% compared with other tools as stated in Fig. 1. The percentage of studies that used theorem proving is considered low as this method is hard to be used. Theorem proving usually involves complicated formulas and multiple processes in order to get it done and its percentage was 30% which is considered acceptable as show in Fig. 1.

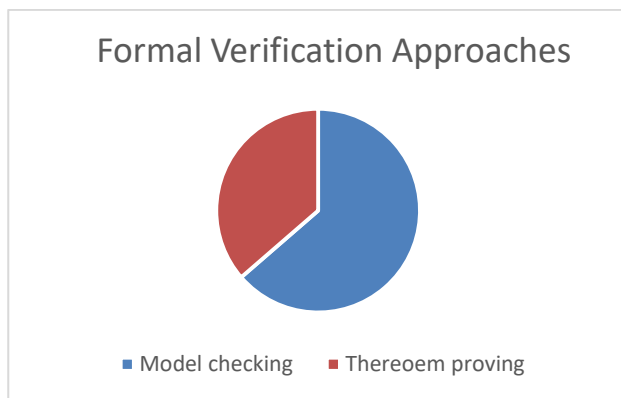


Fig. 1. Formal Verification Approaches.

Table III shows the most used tools that have been suggested by various researchers in order to help in the process of verifying security protocols and algorithms. The tools that have been used were NuSMV model checker that was used by two different researchers in the past sections. Moreover, NuSMV model explore the properties of system model using LTL and CTL. However, different researchers used different tools in the past section to assist the verification of their approaches or systems. They used spin tool, SATMC checker tool, NuXmv updated model checker of NuSMV, CBMC checker, Scyther tool and SMT solvers.

TABLE I. COMPARISON OF SYMBOLIC MODEL CHECKING APPROACHES

| Ref. | Main idea  | Formal verification method  |
|------|--|---|
| [15] | A method that was designed as a packet of SDN language which makes it easy to be extended for further formal languages to check simple invariants properties | The security properties were expressed to form temporal logic CTL. The FSM states together with temporal logic CTL could be verified using the model checking nuXmv.  |
| [17] | An overview of using formal verification approaches to verify the correctness in the implementation of serval security algorithms such as ECC and RSA.       | Verified using model checking approach CBMC (ANSI-C Bounded Model Checking).  |
| [18] | Verified one of the cryptographic algorithms called the ElGamal algorithm  | Built a transition system using a Kripke structure to describe the transitions system of the cryptographic algorithm and translated it into the form of logic temporal language (LTL). This was also checked using NuSMV                      |
| [22] | Verified the correctness of critical security systems that included security protocols business processes and security APIs.                                 | Used ASLan language to model and identify the problems and errors that could face the application that included security protocols and was verified using SATMC mode checker.   |
| [23] | Verified the properties of a security protocol called Needham-Schroeder public key authentication protocol.  | Developed a Promela model for the cryptographic protocol in order to help with the verification in the spin model checker approach.   |
| [25] | Presented an overview of one of the most efficient GUI based tools that can verify different security protocols.   | The properties and attacks of the security protocols were analysed with the help of a backward search algorithm method that provided a set of infinite pattern traces to approve the correctness of events by using the Scyther model checker |
| [26] | Proposed a new security protocol that was able to overcome the vulnerabilities found in the EMV protocol.  | Used protocol description language (SPDL) to write the proposed protocol model into the Scyther tool and helped to scale the number of claims and tests.  |



TABLE II. COMPARISON OF THEOREM PROVING APPROACHES

| Ref. | Main Idea  | Formal Verification Method   |
|------|--|--|
| [15] | A method that was designed as a packet of SDN language. This make it easy to be extended for further formal languages that can check simple invariants properties                            | Uses SMT solver to check the satisfiability of the model that made out the proposed algorithm in order to verify the correctness of the algorithm's constraints. The algorithm modelled by using SMTlib input language of SMT solvers for verification purposes. |
| [16] | Verified the security properties of the Rijndael security algorithm.   | Approved the security algorithm by using theorem proving method called HOL.  |
| [19] | Verified the correctness of a cryptographic algorithm called Curve25519.   | Verified the Curve25519 by using hybrid methodology that consisted of SMT solving and theorem proving tools assistant, qhsm, and Boolector SMT solver.   |
| [24] | Verified the cryptographic properties of three different security protocols on the network, such as authenticated ranging, ultrasonic distance-bounding, and TESLA broadcast authentication. | Formed models of the protocols with Isabelle/HOL formalization theorem proving methods. Besides, the rules were defined and modeled based on the physical characteristics found on each cryptographic protocol.  |

TABLE III. COMPARISON OF THEOREM PROVING APPROACHES

| Ref.       | Tool             | Formal verification type |
|------------|------------------|--------------------------|
| [28,30,31] | NuSMV            | Model checking           |
| [17,32]    | CBMC             | Model checking           |
| [15,19]    | SMT solvers      | Theorem proving          |
| [16,37]    | NuXmv            | Model checking           |
| [23,39]    | The spin checker | Model checking           |
| [24,26]    | Scyther tool     | Model checking           |
| [22,35]    | SATMC            | Model checking           |

## VI. FUTURE WORK

This paper illustrated two main verification methods to verify the correctness of security algorithms and protocols. The two main methods are model checking and theorem proving. Moreover, this paper presented the verification tools that used along with verification methods; tools such as, NuSMV, CBMC and SMT solvers. Future work can be done on verification methods that can be used to verify the different types of algorithms and protocols.

## VII. CONCLUSION

This paper presented a comprehensive literature review of the most used formal verification methods and approaches used to verify and analyse the correctness of security properties for the cryptographic protocols and algorithms. Various studies were extensively reviewed that involved the security protocols, algorithms and formal verification methods. Those studies were classified based on two main formal verification types; model checking and theorem proving. The reviewed literature was explained and analyzed in general based on the formal

verification approaches, proposed approaches, builds models for verification, advantages, and disadvantages.

The results showed that majority of the reviewed studies used model checking tools and approaches to verify their works and experiments. NuSMV is one of the formal verification tools that was used frequently by many researchers and this verification tool used LTL and CTL to format models for verification process. Therefore, the result of the discussion of the reviewed studies showed that there is still a gap in security aspects that could be studied intensively in the future studies.

## ACKNOWLEDGMENT

The authors acknowledge the generous financial support provided by Universiti Teknologi PETRONAS (UTP) using the Graduate Assistantship Scheme (GA). The authors would like to express their gratitude and appreciation to UTP for the generous support.

## REFERENCES

- [1] Y. Sun, J. Zhang, Y. Xiong, G. Zhu, "Data security and privacy in cloud computing", *Int. J. Distrib. Sens. Networks*, Vol. 10, No. 7, 2014.
- [2] G. Singh, S. Supriya, "A study of encryption algorithms (RSA, DES, 3DES and AES) for information security", *Int. J. Comput. Appl.*, Vol. 67, No. 19, 2013.
- [3] A. W. Roscoe, "Intensional specifications of security protocols", *Proceedings of the 9th IEEE Computer Security Foundations Workshop*, 1996.
- [4] T. Dierks, E. Rescorla, "The transport layer security (TLS) protocol version 1.2", *RFC 5246*, August 2008.
- [5] P. Bjesse, "What is formal verification?", *ACM SIGDA Newsletter*, Vol. 35, No. 24, 2005.
- [6] Q. Zhang, L. Cheng, R. Boutaba, "Cloud computing: state-of-the-art and research challenges", *J. Internet Serv. App*, Vol. 1, No 1, 2010.
- [7] J. Rosenberg, "Security in embedded systems", *Rugged Embed. Syst. Comput. Harsh Environ.*, Vol. 3, No. 3, 2017.
- [8] T. Coffey, R. Dojen, T. Flanagan, "Formal verification: an imperative step in the design of security protocols", *Comput. Networks*, Vol. 43, No. 5, 2003.
- [9] J. Edmund, M. Clarke, O. Grumberg, D.A. Peled, "Model Checking", *MIT Press*, 1999.
- [10] S.A. Cook, "The complexity of theorem-proving procedures", *Proceedings of the third annual ACM symposium on Theory of computing*, 1971.
- [11] F. Al-Saqqar, J. Bentahar, K. Sultan, W. Wan, E. K. Asl, "Model checking temporal knowledge and commitments in multi-agent systems using reduction", *Simul. Modell. Pract. Theory*, Vol. 51, No. 2, 2015.
- [12] W. Farn, "Formal verification of timed systems: a survey and perspective", *Proc. IEEE*, Vol. 92, No. 8, 2004.
- [13] S.P. Miller, M.W. Whalen, D.D. Cofer, "Software model checking takes off", *Commun. ACM*, Vol. 53, No. 2, Feb. 2010.
- [14] Alur, Rajeev, D. Dill, "Automata for modeling real-time systems", *Proc. International Colloquium on Automata Languages and Programming*, 1990.
- [15] N. Schnepf, R. Badonnel, A. Lahmadi, S. Merz, "Automated verification of security chains in software-defined networks with synaptic", *Proc. IEEE Conference on Network Softwarization (NetSoft)*, 2017.
- [16] K. Slind, "A verification of rijndael in HOL", *NASA conference publication*, 2002.
- [17] K. Keerthi, I. Roy, A. Hazra, and C. Rebeiro, "Security and fault tolerance in internet of things", *Springer International Publishing*, 2019.
- [18] Arpit, A. Kumar, "Verification of elgamal algorithm cryptographic protocol using linear temporal logic" *2011 Int. Conf. Multimed. Technol. IEEE*, 2011.

- [19] Y. Fang, Chen et al., "Verifying Curve25519 Software", Pro. of the 2014 ACM SIGSAC Conference on Computer and Communications Security, 2014.
- [20] Marrero, Will, E. Clarke, J. Somesh, "Model checking for security protocols", Carnegie-mellon univ pittsburgh pa dept of computer science, No. CMU-CS-97-139, 1997.
- [21] Subramanyan, Pramod, S. Ray, S. Malik, "Evaluating the security of logic encryption algorithms", In Proc. 2015 IEEE International Symposium on Hardware Oriented Security and Trust (HOST), 2015.
- [22] A. Armando, R. Carbone, L. Compagna, "SATMC: a SAT-based model checker for security protocols, business processes, and security APIs", Int. J. Softw. Tools Technol. Transf., Vol. 18, No. 2, 2016.
- [23] P. Maggi and R. Sisto, "Using SPIN to verify security properties of cryptographic protocols", International SPIN Workshop on Model Checking of Software, 2002.
- [24] P. Schaller, B. Schmidt, D. Basin, and S. Capkun, "Modeling and verifying physical properties of security protocols for wireless networks", Proc. IEEE Comput. Secur. Found. Symp., 2009.
- [25] C. Cremers, "The Scyther tool: verification, falsification, and analysis of security protocols", International Conference on Computer Aided Verification, Vol. 5123, 2008.
- [26] N. El-Madhoun, F. Guenane, G. Pujolle, "An online security protocol for NFC payment: Formally analyzed by the scyther tool", Proc. of the 2nd Conf. Mob. Secur. Serv., 2016.
- [27] A. Cimatti, E. Clarke, F. Giunchiglia, M. Roveri, "NUSMV: A new symbolic model checker," Int. J. Softw. Tools Technol. Transf., Vol. 2, No. 4, 2000.
- [28] M. Panti , L. Spalazzi , S. Tacconi, "Using the NuSMV model checker to verify the kerberos protocol", Proc. of the International Conference on Simulation and Multimedia in Engineering Education, Vol. 34, 2002.
- [29] Abdelmajid, T. Nabih, et al., "Location-based kerberos authentication protocol", Proc. of the 2010 IEEE Second International Conference on Social Computing, 2010.
- [30] M. Panti, L. Spalazzi, S. Tacconi, "Verification of security properties in electronic payment protocols", in Proc. ACM SIGPLAN IFIP WG, 2002.
- [31] M. Benerecetti, F. Giunchiglia, "Model checking security protocols using a logic of belief", International Conference on Tools and Algorithms for the Construction and Analysis of Systems, Vol. LNCS, No. 1785, 2000.
- [32] M. Burrows, M. Abadi, R.M. Needham, "A logic of authentication", ACM Transactions on Computer Systems, Vol. 8, No. 1, 1990.
- [33] C. Baier, C.T. Eds, "Tools and algorithms for the construction and analysis of systems", 21st International Conference TACAS, 2015.
- [34] O. Grumberg, A. Sosnovich, G. Nakibly, "Finding security vulnerabilities in a network protocol using parameterized systems", In Proceedings of CAV, 2013.
- [35] O. Demir, W. Xiong, F. Zaghoul, J. Szefer, "Survey of approaches for security verification of hardware / software systems", IACR Cryptol. ePrint Arch., 2016.
- [36] R. Cavada et al., "The NUXMV symbolic model checker", International Conference on Computer Aided Verification, Vol. 8559, 2014.
- [37] G. Yuan, S. Long, "Formal verification of RFID protocols using nuXmv", Proc. of the 10th IEEE Int. Conf. Anti-Counterfeiting, Secur. Identification (ASID), 2017.
- [38] G. J. Holzmann, "The spin model checker", IEEE Trans. Softw. Eng., Vol. 23, No. 5, 1997.
- [39] Li, Wei, et al, "Formal analysis and verification for an ultralightweight authentication protocol RAPP of RFID", National Conference of Theoretical Computer Science, 2017.
- [40] G. Goss, J. Hartmanis, J. Van Leeuwen, "Stabilization, safety, and security of distributed systems", proc. of the 14th International Symposium, Vol. 9, No. 3, 2012.
- [41] A. Armando, R. Carbone, L. Compagna, "SATMC: a SAT-based model checker for security critical systems", Proc. of the 20th International Conference on Tools and Algorithms for the Construction and Analysis of Systems (TACAS' 14), Vol. 8413, 2014.
- [42] S. P. Johnson, G. W. Wilson, Y. Tang, K. S. Scott, "SATMC: Spectral energy distribution Analysis Through Markov Chains", Monthly Notices of the Royal Astronomical Society, Vol. 436, No. 3, 2013.
- [43] A. Armando, R. Carbone, L. Compagna, "SATMC: a SAT-based Model Checker for Security-critical Systems", International Conference on Tools and Algorithms for the Construction and Analysis of Systems, 2014.

# Performance Comparison of Detection, Recognition and Tracking Rates of the different Algorithms

Meghana Kavuri<sup>1</sup>, Kolla Bhanu Prakash<sup>2</sup>

Department of Computer Science and Engineering, Koneru Lakshmaiah Education Foundation, Guntur, India

**Abstract**—This article discusses the approach of human detection and tracking in a homogeneous domain using surveillance cameras. This is a vast area in which significant research has been taking place from more than a decade and the paper is about detection of a human and its face in a given video and stores Local Binary Pattern Histogram (LBPH) features of the detected faces. Once a human is detected in the video, that person will be given a label and him/her is tracked in different video taken by multiple cameras by the application of machine learning and image processing with the help of OpenCV. Many algorithms were used for detecting, recognizing and tracking till date, thus in this paper, main thing is the comparison of the proposed algorithm with some among the state-of-the-art algorithms. And also shows how the proposed algorithm is better than the other chosen algorithms.

**Keywords**—Detection; recognition; tracking; local binary pattern histogram; Kalman filter; particle filter

## I. INTRODUCTION

The observation or monitoring of activity, behavior and other information by a system which includes several Closed Circuit Television (CCTV) cameras for observation and a set of algorithms to track a person is called Surveillance system. Technology has evolved a lot in the last few decades, previously there were no security cameras neither in Banks, Railway Station nor in other places. There were only security guards which protect these areas. Once the security cameras came into existence, it became easy to find people passing within the range of CCTV camera by simply searching through the videos recorded. Inventions increase people's expectations, although security camera reduces the human effort one has to search for an individual through the entire video which takes a considerable amount of time. So people thought what if the searching task can be accomplished by machine, it would save both human effort and time. A combination of machine learning algorithms with image processing is used to make a machine learn to reorganize a person and track that person in the given footage. The project is all about a system which has been designed to track a human in given videos.

Detecting a face from a video and tracking a person in that video is a very challenging task as there will be several changes including the resolution when a surveillance camera is used, and also the processing and computation of the frames taken from a surveillance camera in a real-time environment will be a critical and very challenging task because of many reasons. Some of the reasons where the difficulties arise are because of poor image quality, set up areas, limited networks, and compression of digital video, incorrect configuration, and

weather changes. Apart from these, there are some more serious problems that need to be taken into consideration are:

1) *Features*: Features of the person (spectacles, eyes, facial features, different hairstyles, body changes, facial hair) matter a lot while he/she is being tracked. Thus even after a period of time, the person who is already recognized earlier should be detected and recognized. Even if the person loses weight; if they have changed their hairstyle; if they are with/without beard and mustache; on the application of make-up and with/without spectacles, the person needs to be detected, recognized and tracked.

2) *Timings of the day*: Even if it is Morning/Afternoon/Evening/Night, the person needs to be detected and tracked.

3) *Occlusion*: If too many persons or even if a crowd is passing by, then also it should be able to identify and track the person.

4) *Weather*: Whatever may be the weather condition, detection and tracking should be efficient.

5) *Facial coverage*: Nowadays men and women cover their faces due to high temperatures, dust, and pollution.

6) *Age*: As a person ages too, facial features change due to the reduction of muscle and formation of wrinkles as the skin loosens.

7) *Twins/Triplets*: It is a bit tough for humans only to differentiate between twins/triplets.

These are some of the serious problems that are needed to be taken into consideration while implementing the algorithms [6]. Suspicious behaviours in shopping malls is also another serious problem, which also has to be considered [5].

Focusing on Face detection, there are many algorithms which had evolved from time to time. As the difficulties, objectives, and requirements increase, more efficient algorithms are being generated for accuracy and effectiveness as outcomes. Some of the detection algorithms by Colour, Motion, Model-based face tracking, Edge-Oriented Matching [1], Hausdorff Distance [2], Weak Classifier Cascades [3], Histogram of Oriented Gradients (HOG) and Deep Learning [4], etc. Many approaches are also there for the detection of a face like the frame-based detection, which is designed for still images and Typical Approaches, Real-Time & Multi-View Approaches [7], [8].

In this paper, the main point is comparison of different tracking algorithms from the state-of-the-art with the proposed algorithm which uses Local Binary Pattern Histograms

(LBPH) [9] and Tensorflow for detecting, recognizing and tracking the recognized person in other videos. LBPH approach is compared with Principal Component Analysis (PCA), Linear Discriminant Analysis (LDA) for animal recognition previously [10], which showed efficient results for a small test dataset. Tensorflow can be used in heterogeneous and large scale environments; it is mainly an advantage when it comes to the performance of an algorithm [11].

### II. APPROACH

Firstly, the human detection phase takes place, then face detection and then face recognition. As soon as the detection is performed in the video, the rectangle will be drawn and tracking will be done through the video. It doesn't mean that the faces detected in the video is similar to humans detected because, only the trained faces will be recognized and if there are untrained faces, they will just be detected as humans, but the face cannot be detected. After training some people on the machine, it now tries to recognize the individuals. After all these steps are successfully completed, then it moves to the next phase i.e., tracking of the recognized individual in the video.

After taking the video as input, it then sets a Histogram of Oriented Gradients (HOG) [12] descriptor for the human detection using the help of Support Vector Machine (SVM) and OpenCV libraries. Non-maximum suppression is used to reduce false positive cases.

Then, in the second phase, Haar features are used to detect human faces. The detected faces will be shown separately in another window. After the face detection phase, a person should be mainly recognized before his face gets recognized. Local Binary Pattern Histograms (LBPH) and Haar cascades are used for training the machine. Detected faces are considered as datasets and are used to train the machine and the LBPH values for the respective faces are stored in a YAML file.

### III. FLOW CHART

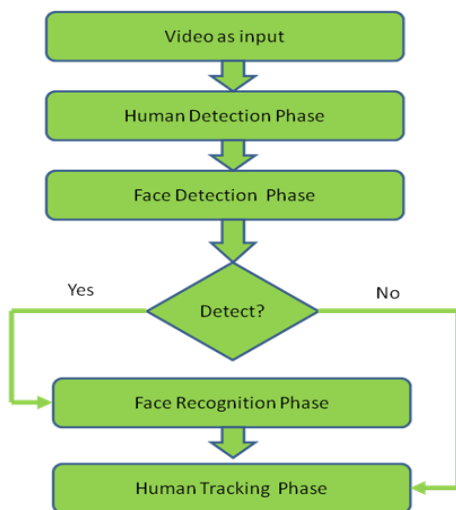


Fig. 1. Describes the Various Algorithms used in different Phases.

### IV. DATA FLOW DIAGRAM

Faces can be recognized by importing the values stored in the YAML file into the memory and LBPH face recognizer program tries to recognize the faces using the LBPH features. After the recognition of a face, a label will be given to the person. As soon as a person gets recognized in camera 1, he/she is labeled as subject1, and will be tracked with the same label even if he/she passes through camera 2. The step by step procedure involved in all the phases is displayed through the Fig. 2 and the flow of data is shown from one phase to another.

Main aim is to compare the proposed algorithm with the Kalman filter and Particle filter and compare the results. Kalman Filter is moderately consistent in tracking. And it was only tested for tracking a single person [14]. Kalman filter predicts the present state variables and their uncertainties, and after the outcome of the next state, previously predicted values will be updated with some weighted average. But in real-world applications, Particle filter [15] can also be used for non-linear systems and non-Gaussian systems as Kalman Filter is not that efficient to handle the non-linear systems. Now comparison of these algorithms with the proposed algorithm is done.

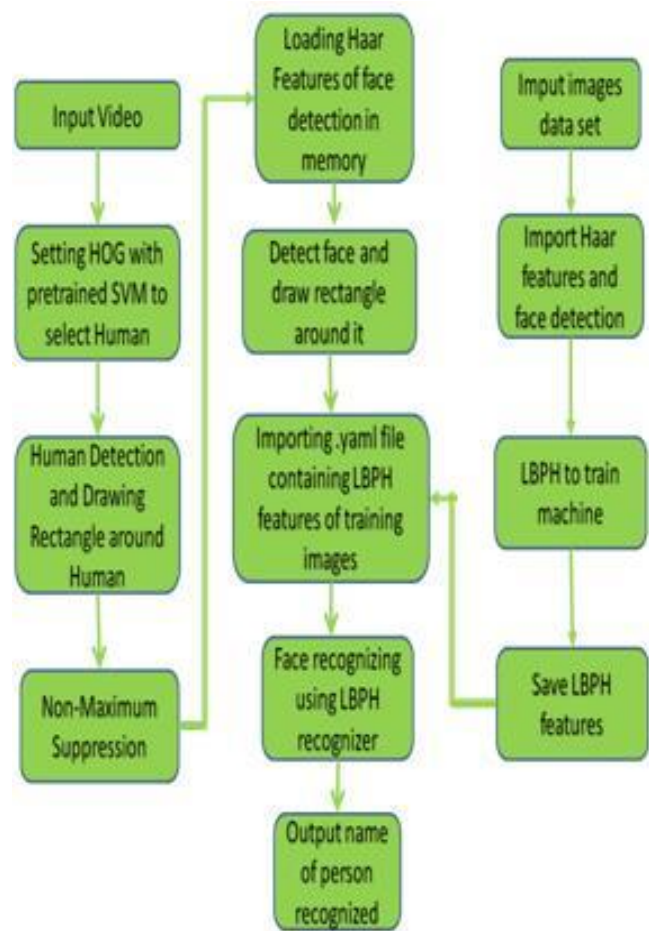


Fig. 2. Data Flow Diagram Showing the Flow of the Algorithm.

## V. EXPERIMENTAL RESULTS

The proposed algorithm has been tested within some video sequences captured by a camera. Its purpose is to detect humans, recognize and track them throughout the sequence. Below are the tables which give the results of the performance of the proposed algorithm when compared to the other chosen algorithms.

TABLE. I. THE COMPARISON OF DETECTION RATE

| Sequences | Algorithms    |                 |                    |
|-----------|---------------|-----------------|--------------------|
|           | Kalman Filter | Particle Filter | Proposed Algorithm |
| Sequence1 | 89.8%         | 90.3%           | 91.4%              |
| Sequence2 | 76.5%         | 77.1%           | 78.7%              |
| Sequence3 | 66.2%         | 82.4%           | 84.3%              |

TABLE. II. THE COMPARISON OF RECOGNITION RATE

| Sequences | Algorithms    |                 |                    |
|-----------|---------------|-----------------|--------------------|
|           | Kalman Filter | Particle Filter | Proposed Algorithm |
| Sequence1 | 82.4%         | 82.5%           | 87.6%              |
| Sequence2 | 72.6%         | 70.6%           | 74.7%              |
| Sequence3 | -             | 71.4%           | 73.8%              |

TABLE. III. THE COMPARISON OF TRACKING RATE

| Sequences | Algorithms    |                 |                    |
|-----------|---------------|-----------------|--------------------|
|           | Kalman Filter | Particle Filter | Proposed Algorithm |
| Sequence1 | 77.3%         | 79.6%           | 82.9%              |
| Sequence2 | 65.6%         | 69.7%           | 72.1%              |
| Sequence3 | -             | 62.5%           | 71.2%              |

From Table I, II and III, comparison of the performance of the three algorithms can be clearly seen. Kalman filter algorithm had given less performance when compared to other two, because Kalman filter in rapid situations, it showed very slow reaction speed and was unable to recognize the person and also couldn't track them. But if Extended Kalman Filter, Unscented Kalman Filter [13] were used, then could get some positive results and Kalman Filter has the inability to manage dynamic background pixels. On the other hand, Particle Filter showed better results when compared to Kalman Filter, but it is not effective in occlusion environments and also when fast rotations take place computational time increases.

## VI. RESULTS

As the methodology, working of the program are discussed and shown in the data flow diagram and the flow chart above, now showcasing the results against some test cases. The output of each and every test case using the screen shots of the output is provided. The program will require more computation as the training dataset size increases and also depends on the system configuration. After trying the program on two systems which were available with us, one of which

had the following specifications: AMD A4 2.2 GHz dual-core processor and 4GB RAM and the other system had the following specifications: Intel i5 2.4 GHz Quad-core processor 8 GB RAM. For an input video of 30 frames per second, the 1<sup>st</sup> system gave an output speed of just 4-5 fps. On the other hand, the 2<sup>nd</sup> system gave an output with a speed of 10-12 fps.

Initially, we tested the performance of the algorithms by considering the homogeneous environment. So the recognition of faces can be done only if training is done only for those faces beforehand. So the machine is trained for two people. One of them is labeled as 1 and the other one is labeled as 2. The output for four videos is shown, where each of the test videos represents different scenarios. Different stages of face detection and face recognition are shown in the results provided by the program. Here are the following screen shots of the different stages of the output obtained accordingly to the given input test videos.

The screen shots of the output provided by the program for the first video are shown in Fig. 1. In this video, only one person will be seen. The machine is trained to recognize that person and label him as 1. Initially, the frame is empty as seen in Fig. 3(a). When the person enters the frame, the program correctly detects the presence of a person and draws a rectangle around him. The program has correctly recognized the presence of person 1 as seen in Fig. 3(c) and it continues to track his face and correctly label it as 1. A false positive is triggered due to the sleeve of person 1 and the program has incorrectly detected it as a face and labeled as 1 as it can be seen in Fig. 3(o). Then again, the program has removed the false positive and correctly recognized person 1 in the upcoming figures until the person 1 goes out of the frame. In most of the cases, the human body is not detected because the full human body is not present in those frames.

The screen shots of the output provided by the program for the second person given in Fig. 4. Similar to video 1 in this video too only one person will be seen. The machine is trained to recognize him and label him as 2. Initially, the frame is empty seen in Fig. 4(a). As the person enters the frame, the program correctly detects the presence of a person in the upcoming frames as it can be seen in the figures. The program recognizes the person 2 and labels him for the first time in Fig. 4(m). The person continues to correctly label the face of a person 2 as 2 till the person moves out of the frame.

The screen shots of the output provided by the program for the third video are given in Fig. 3. Unlike previous videos, person 1 and person 2 both appear in this video, but they enter the frame one after the other and not together. Initially, the frame is empty as seen in Fig. 5(a). Then the person who is labeled as 1 in our training samples enters the frame. In Fig. 5(d), the program has recognized the presence of person 1 for the first time and has even successfully detected the face of person 1. Since in the frame, as they enter the body of person 1 is visible, the program has correctly drawn a rectangle around him as seen in Fig. 5(e). The system is successful in detecting the face of person 1 and labeling it as 1 till the time he is present in the frame.

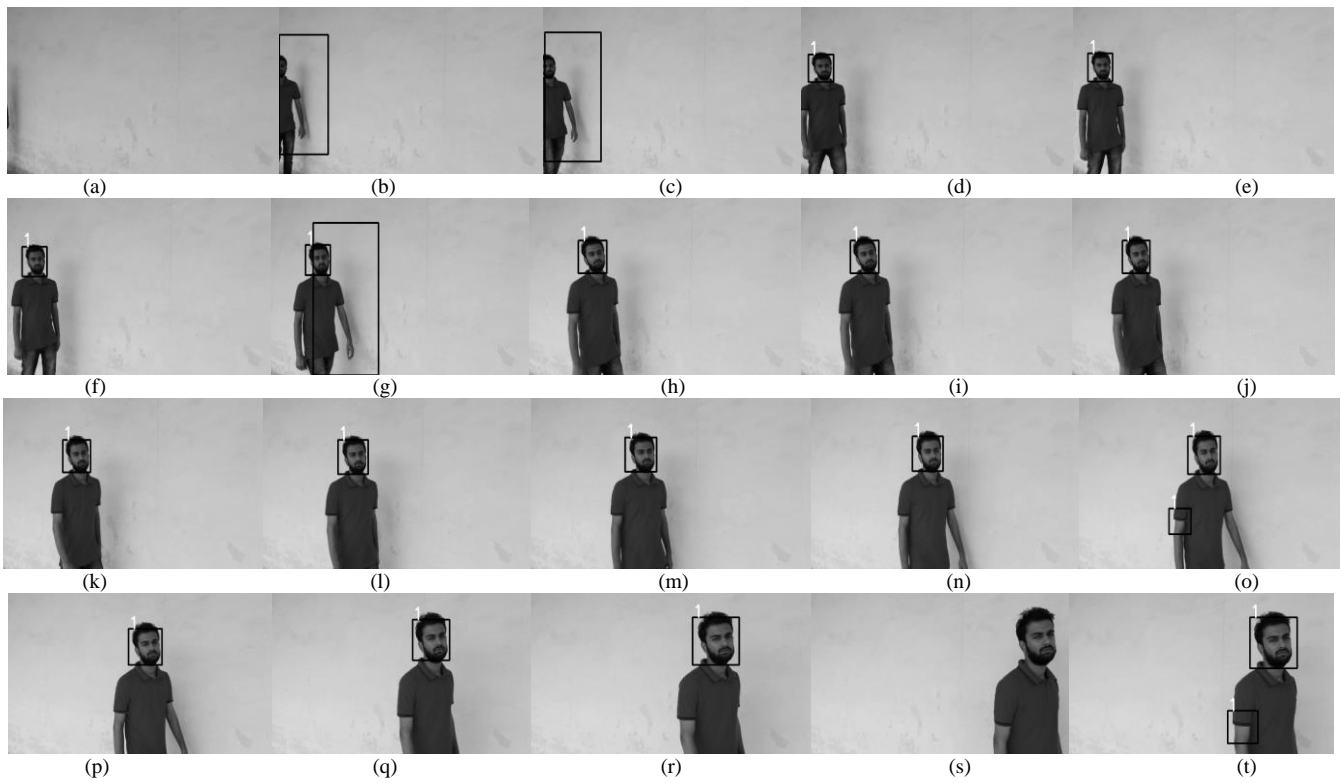


Fig. 3. Output of Video 1: Single Person Video; Frames o, True False Face Detected Cases, no Face Detected in Frame s, in many Images Human is not Detected Due to the Absence of Full Human Body.

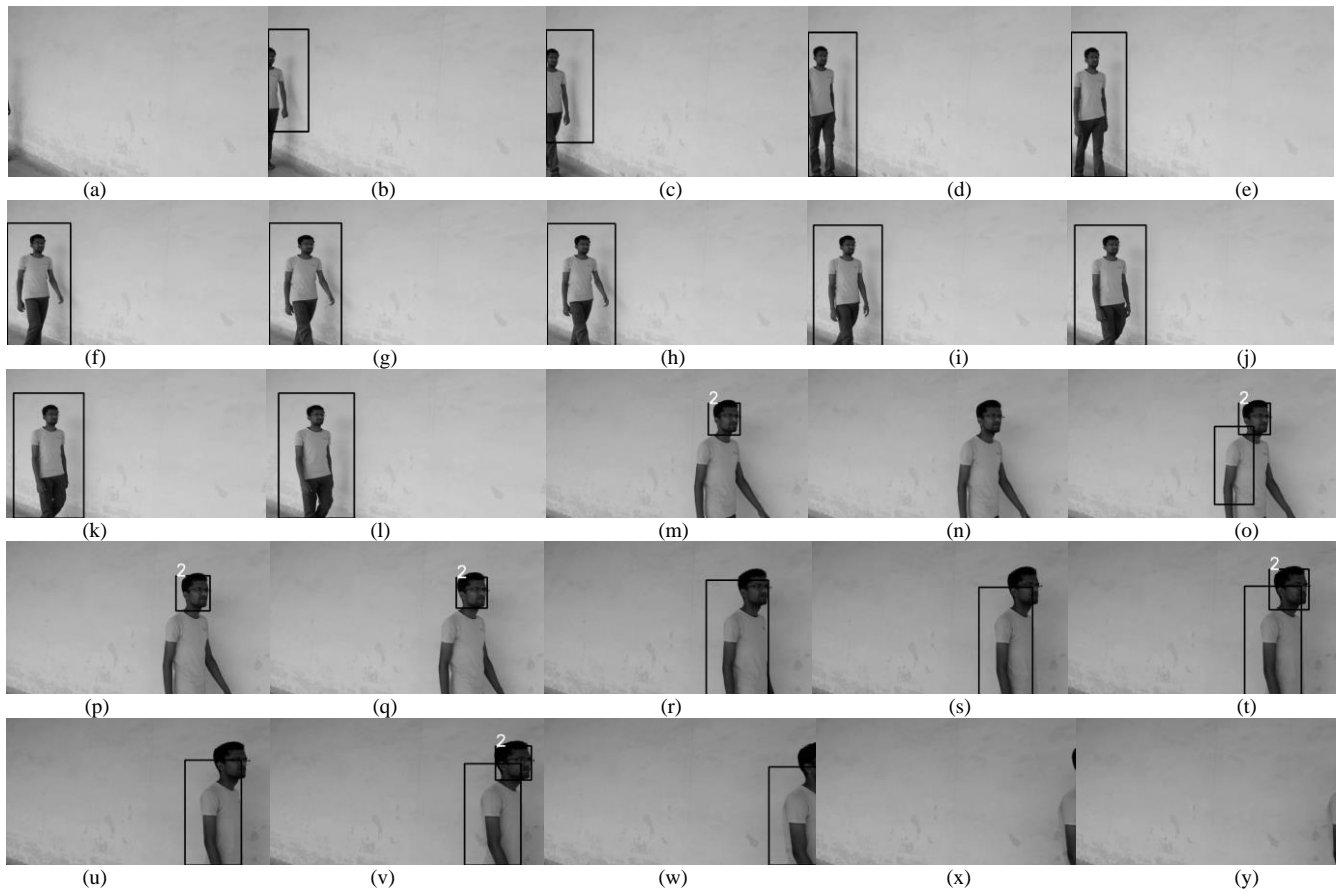


Fig. 4. Output of Video 2: Single Person Video; no Face Detected in many Images due to unclear Face.

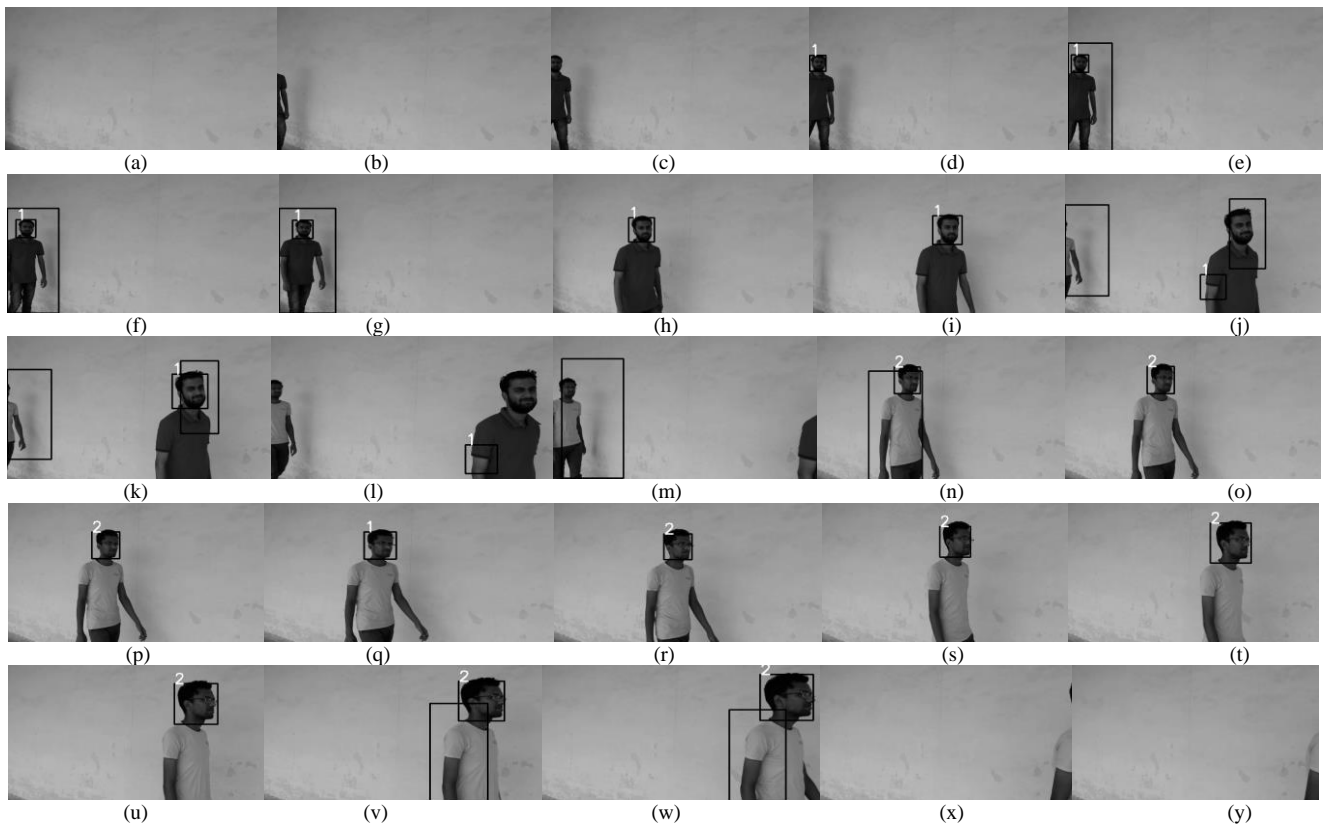


Fig. 5. Output of Video 3: Multiple Person Video, Walking One after other; False Faces are Detected in Frame g, j, l, and Frame q is Wrongly Detected as Subject 1.

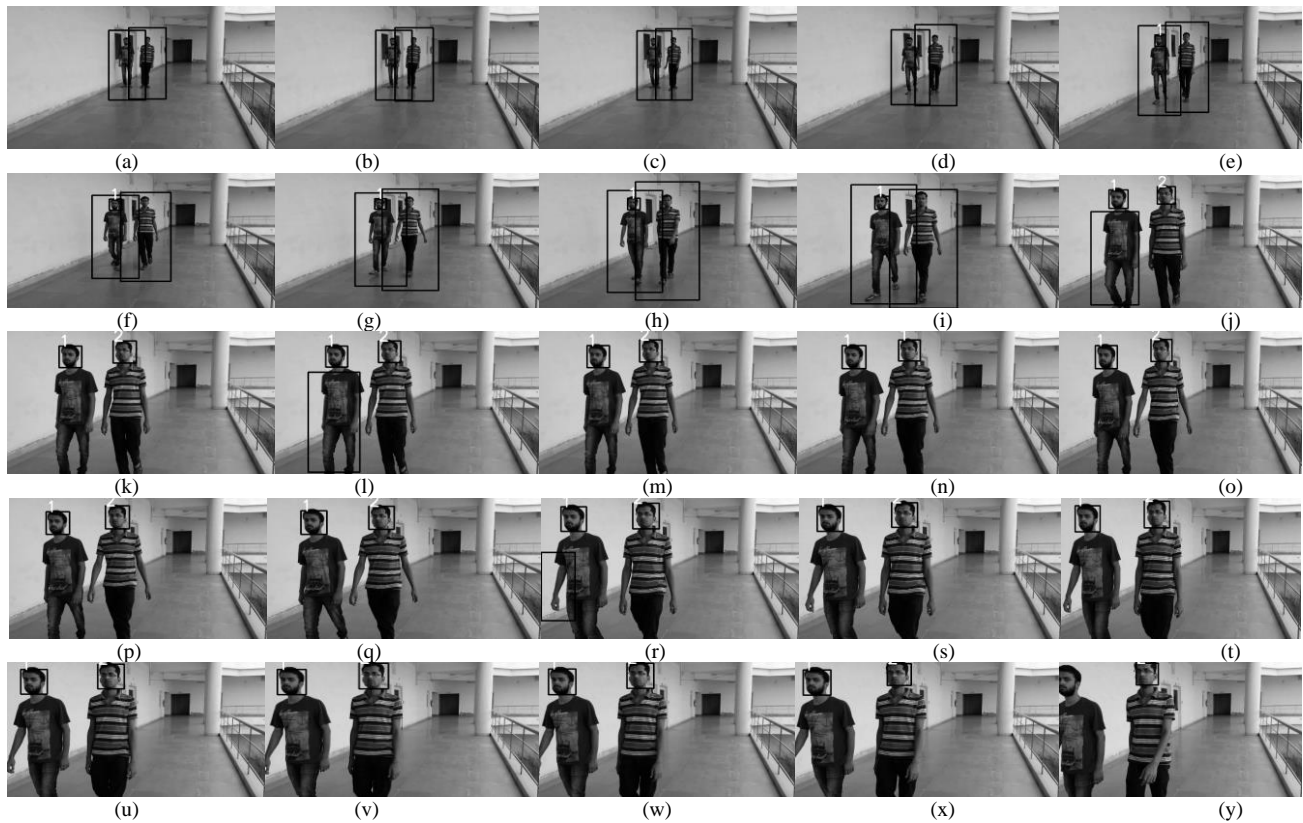


Fig. 6. Output of Video 4: Multiple Person Video, Walking Together; no Face Detected in Frames. a-d Due to the Larger Distance from the Camera.

Although, a false positive was detected by the system in Fig. 5(j) where the system false fully detects the sleeve of person 1 as a face. In the same frame, since the person 2 also enters the frame, a rectangle is drawn around him. Till Fig. 5(l), the presence of a person is correctly detected by the program and is shown by drawing a rectangle around that person. Now in Fig. 5(m), we see that person 1 is completely out of the frame and person 2 is correctly detected. The program was successful in detecting a face in Fig. 5(n) and has correctly labeled it as 2. The program then again fired a false positive as we can see in Fig. 5(q), it has incorrectly labeled person 2 as 1. In Fig. 5(r), the program has recognized and labeled the person 2 correctly as person 2 rectifying the false positive. The program continues to label the person 2 correctly until the person goes out of the frame.

The screen shots of the output provided by the program for video 4 are shown in Fig. 6. In this video, both person 1 and person 2 appear together in the same frame. We can see here since the first frame, the program has correctly detected both the persons. It has drawn a rectangle around both the humans as it can be seen in the figures given above. As they are moving towards the camera, the rectangle is drawn around them, also move with them in one way tracking them. In Fig. 6(e), the program has successfully recognized the person 1 and labeled him as 1. And it continues to track both of them until it finally recognizes the person 2, also as seen in Fig. 6(j). In this and the following figures, it can be seen how the program has successfully recognized both the persons and has correctly labeled them. As it can be seen in Fig. 6(n), the program false fully recognized the person 2 as person 1 and thus labeled person 2 also like 1, but in the following figures, the program has correctly recognized the person 1 as 1 and the person 2 as 2 and it continues to recognize them till the last frame. In this video, we can get better human detection because, in many frames, the full body of a human is present.

## VII. CONCLUSION

The proposed algorithm focuses mainly on human detection, recognition, and tracking, given a video as input to the program and can get the labels of the identified persons in the video. Only the limitation is that the user needs to train the machine beforehand, and then it will recognize the persons. A train.py program is used to train the machine for the people to be tracked. It took 30 fps when the input is given and we got 15 fps as the output. Also as the system configuration increases, better results will be shown. At some point of severe occlusion conditions, it doesn't give such accurate results. In future addition of a feature that the program itself

learns how to detect a new person whenever they appear and thus a label generation should be done automatically. So that whenever same person re-appears next time, he/she would be easily identified on its own and thus it implies the reduction of computational speed and also false positives.

## REFERENCES

- [1] B. Froba, Ch. Kulbeck, "Real-time face detection using Edge-Orientation matching", in the Conference on Audio- and Video-Based Biometric Person Authentication, 2001.
- [2] O. Jesorky, K. J. Kirchberg, and R. W. Frischholz, "Robust face detection using the Hausdorff distance", in the proceedings of the Third International Conference on Audio- and Video-Based Biometric Person Authentication, pp.90-95, 2001.
- [3] P. Viola, "Robust real-time face detection", in the International Journal of Computer Vision, pp. 137-154, 2004.
- [4] S. Chang, D. Xiaoqing, F. Chi, "Histogram of the oriented gradient for face recognition", Tsinghua science and technology, vol. 16, pp. 216-224, April 2011.
- [5] R. Aroyo, J. J. Yebes Luis, M. B. Selvan, G. D. J. Almazan, "Expert video-surveillance system for real-time detection of suspicious behaviors", in Expert systems with Applications, vol. 42, pp. 7991-8005, November 2015.
- [6] T. Nagaria, Dh. Chourishi, "A comprehensive survey and detailed study on various face recognition methods", in the International Research Journal of Engineering and Technology (IRJET), vol. 5, December 2018.
- [7] S. Rakesh, S. Abhishek, Deepak Agarwal, "Analysis of different face recognition algorithms", in the International Journal of Engineering Research and Technology (IJERT), vol. 3, November 2014.
- [8] K. Sunil Reddy, "Comparison of various face recognition algorithms", in the International Journal of Advanced Research in Science, Engineering and Technology, vol. 4, February 2017.
- [9] S. Ranganatha, Y. P. Gowramma, "Image training and LBPH based algorithm for face tracking in different background video sequence", in the International Journal of Computer Science and Engineering (JCSE), vol. 6, September 2018.
- [10] P Kamencay, T Tmovszky, M Benco, R Hudec, P Sykora, A Satnik, "Accurate wild animal recognition using PCA, LDA, and LBPH", IEEE, 2016.
- [11] M Abadi, P Barham, J Chen, Zh Chen, et al, "Tensorflow: A system for large-scale machine learning", OSDI, Savannah, GA, USA, November 2016.
- [12] N Dalal, Bill Triggs, "Histogram of oriented gradients for human detection", 2005.
- [13] Ch Liu, P Shui, Song Li, "Unscented extended Kalman filter for target tracking", in the Journal of Systems Engineering and Electronics, vol. 22, pp. 188-192, April 2011.
- [14] C Suliman, C Cruceru, Florin M, "Kalman filter based tracking in a video surveillance system", in the proceedings of the 10<sup>th</sup> International Conference on Development and Application Systems, Suceava, Romania, May 2010.
- [15] F Wang, "Particle filter for visual tracking", G. Shen and X. Huang, CSIE 2011, part I, CCIS 152, pp. 107-112, 2011.



# QoS-based Semantic Micro Services Discovery and Composition using ACO Algorithm

## Case Study: e-Learning Platform

Ahmed ESSAYAH<sup>1</sup>, Mohamed Youssefi<sup>2</sup>, Omar Bouattane<sup>3</sup>, Khalifa Mansouri<sup>4</sup>, Elhocein Illoussamen<sup>5</sup>

Laboratory SSDIA, ENSET Mohammedia, Hassan II University of Casablanca  
Mohammedia 28999, Morocco

**Abstract**—In this paper, we present a new model of e-Learning platforms based on semantic micro services using discovery, selection and composition methods to generate learning paths. In this model, each semantic micro service represents an elementary educational resource that can be a course, an exercise, a tutorial or an evaluation implementing a precise learning path objective. The semantic micro services are described using ontologies and deployed in multi-instances in a cloud environment according to a load balancing and a fault tolerance system. Learners' requests are sent to a proxy micro service having learning paths abstract structures represented as an oriented graph. Proxy micro service analyses the request to define the learner profile and context in order to provide him with the semantic micro services responsible of the educational resources satisfying his functional and non-functional needs. In this model, to achieve an optimal learning path generation a two steps process is employed, where local optimization uses semantic discovery and selection based on a matchmaking algorithm and a quality of service measurement, and global optimization adopts an ant colony optimization algorithm to select the best resource combination. Our experimental results show that the proposed model can effectively returns optimized learning paths considering individual, collective and pedagogical factors.

**Keywords**—*Semantic micro service; quality of service; learning path; e-learning platform; service discovery and composition; ant colony optimization algorithm*

### I. INTRODUCTION

Information technologies have brought significant progress to companies' information systems. In the last few years, web technologies, virtualization architectures and cloud computing have contributed to the dimension development of information systems and have forced the companies to restructure to adapt to these new technologies and be in a position to innovate constantly in order to remain competitive. Mobile geo-localized systems like smart phones and tiny embedded systems as Raspberry and Arduino have opened a new era for universal objects interconnection.

The Web 3.0 is starting to take shape and Internet of Things (IoT) has become a reality that information systems have to take into consideration. In fact, our environment objects can embed processing units making them able to perform complex tasks, take decisions while permanently connected to the internet allowing them to take advantage of massive collective intelligence. The huge quantity of data (Big Data) produced by the connected objects and mobile applications, requires new

data storage and processing technologies. In the computer-assisted learning, the e-Learning is an educational mode that has to benefit from the conjunction of all these new information technologies and from all presential classes capabilities.

To tackle the massification of higher education, the automation of learning process has become crucial; it allows the autonomous and remote learning and the individualization of learning paths. Many research works have been interested in improving educational content presented in e-Learning platforms [1, 3, 10, 15]. Other researches have proposed approaches for learning paths optimization [6, 11]. In another stage, some researchers have interested in learners behavior modeling in order to enhance the e-Learning platform performances [23, 25, 26]. In a rapidly changing and increasingly challenging environment, educational material description, discovery and composition require efficient strategies for better reuse. Micro services [8, 14, 20, 27] is an architecture style emerged in last few years that corresponds most closely to the massive distributed systems. The main idea is to break down a huge application to many tiny components loosely coupled and independent called "Micro Services". Each micro service should be responsible of one functionality, developed and deployed independently.

Different semantic languages allow describing functionalities of a micro service in a machine interpretable form using Semantic Web technologies [9, 22, 31, 16, 21]. The main purpose of semantic Web service technologies is to minimize the manual discovery and usage of Web services, by allowing software agents and applications to automatically discover, select, and invoke these Web resources to achieve the user needs. Many researches have interested in Semantic Web service discovery algorithms [5, 13, 24, 32] and proposed several matchmaking techniques to measure similarity score between user requirements and service capabilities.

Semantic micro service architecture seems to represent a great opportunity for learning management systems (LMS) [26, 7]. In this context, we propose a new model of e-Learning platform based on semantic micro services using semantic description, discovery, selection and composition for learning paths. In this model, each semantic micro service represents an elementary educational resource that can be a lesson, an exercise, a tutorial or an evaluation implementing a precise learning path purpose. Learners' requests are sent to a proxy micro service having learning paths abstract structures

represented as an oriented graph. Proxy micro service analyses the request to define the learner profile and context in order to provide him with the semantic micro services responsible of the educational resources satisfying his functional and non-functional needs. In this model, to achieve an optimal learning path generation a two steps process is employed, where local optimization uses semantic discovery and selection based on a matchmaking algorithm and QoS measurement [28], and global optimization adopts an ant colony optimization algorithm [2, 11, 12, 33] to select the best resource combinations.

The remainder of this paper is organized as follows. First, some related work about learning path and e-Learning platforms personalization and optimization is discussed. In the second section we present our e-Learning platform model architecture considering a learning path presented by an oriented graph. We then describe different components making up our model. Next, we discuss QoS normalization and aggregation for various non-functional characteristics of micro services. This is followed by a description of the semantic micro service discovery and selection algorithm. We then apply the Ant Colony Optimization algorithm to the learning path in order to obtain the optimal solution for each learner according to his profile and context. An application of our model and results are discussed in the next section. Finally, we present some conclusions and future works.

## II. RELATED WORK

Research efforts in learning paths generation and optimization in e-Learning platforms try to automate the learning process by generating personalized learning paths according to learners' profiles and preferences. The author in [35] proposes an adaptive learning path method that applies Ant Colony Optimization method and Ausubel Meaningful Learning Theory to find the best learning path for a group of learners according to their functional needs. The author in [30] uses a prediction method based on pattern recognition technique to identify dynamically the best learning style. In [34, 36] authors used artificial intelligent techniques to perform automatic personalization in e-learning systems. Bayesian networks are used in [37] to provide a solution of adaption of learning activities. In addition, service oriented architectures and ontologies are proposed in [38] to generate personalized learning resources. Most of existing approaches do not consider individual factors such as excellence, history, language, and motivation. In this paper, we present a model considering individual, collective and pedagogical factors in order to provide learners with the best learning experience.

## III. E-LEARNING PLATFORM MODEL ARCHITECTURE

We consider a learning path represented by an oriented graph  $G(O_i, E_j)$  where nodes  $O_i$  represent precise objectives, ( $i=1$  to  $N$ , where  $N$  is the total number of objectives), and  $E_j$  are edges representing all the possible paths a learner can use to complete the training goals, ( $j=1$  to  $M$ , where  $M$  is the total

number of edges). For each node  $i$ , various implementations for educational resources can be proposed  $R(i, k)$ , ( $k=1$  to  $H$ , where  $H$  is the number of resources associated to a node). There may be multiple teachers proposing relevant educational content for the same node  $i$ . The educational resource may be an entire course, a chapter, an exercise, a tutorial or an evaluation as a form of multiple choice or true/false quizzes. During learning process, a learner explore one educational resource for each node in the learning path, we use a local optimization method based on semantic matchmaking calculation and QoS measurements to select the right resources according to learner profile. Over the time, we use learners feedbacks and evaluations results to assign to each educational resource  $R(i, k)$ , of a node  $i$  a score  $S_i$  and to each edge  $E_j$  a weight  $W_j$  reflecting its pertinence. Our proposed platform use a metaheuristic optimization algorithm to choose the optimal learning path that provides the best results. Fig. 1 shows an example of a learning path composed by eight nodes and nine edges.

To reach an objective  $O_i$  we define multiple possible implementations of an educational resource  $R(i, k)$ . In this model, we present each implementation of an educational resource as a semantic micro service  $SMS-R_{i,k}$  described using ontologies and deployed in multi-instances in a cloud infrastructure. The motivation behind this choice is that each teacher may respond to an objective  $O_i$  according to his pedagogical approach. All resources semantic micro services  $SMS-R$  are registered in a special micro service called  $SMS-D$  representing the platform semantic repository.  $SMS-D$  uses an Ontology Web Language OWL-S [21] to describe properties and capabilities of  $SMS-R$  in unambiguous and computer-interpretable form. In our model, we also define a special micro service called  $SMS-C$ , designed to centralize and expose configuration of all the platform' micro services. All learners requests are sent to a proxy micro service  $SMS-P$  having learning paths abstract structures represented as an oriented graph.  $SMS-P$  communicates with  $SMS-D$  to define the learner profile and context and provide him with the  $SMS-R$  responsible of the educational resources satisfying his functional and non-functional needs. In some cases, the proxy service needs to send an information to all or most of the platform micro services, in this particular case a high-performance communication system based in AMQP protocol is used by implementing one of its brokers such as Rabbit MQ. Fig. 2 shows the technical architecture of all micro services in our platform.

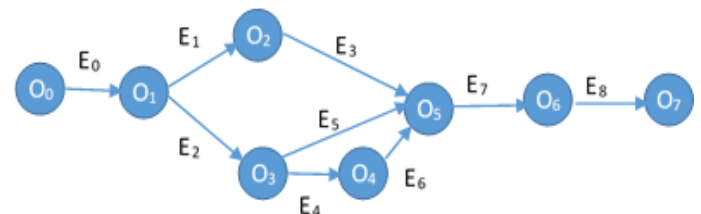


Fig. 1. Representation of a Learning Path as an Oriented Graph.

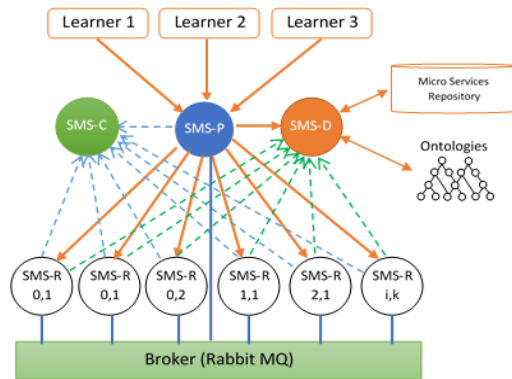


Fig. 2. e-Learning Platform Model Architecture.

#### IV. E-LEARNING PLATFORM MODEL COMPONENTS DESCRIPTION

##### A. Educational Resource Semantic Micro Services SMS-R

This semantic micro service is the main component of our e-Learning platform; it allows learners to access to educational resources. When an SMS-R is started, it looks firstly for the configuration micro service SMS-C, then, it connects to the discovery micro service SMS-D to register its location and publish its description to the semantic micro service registry. Technically, an educational resource micro service has three layers:

- Data access layer ensures educational content structuration and persistence in a lightweight data storage system such as micro DBMS or simple XML files. Generally, the educational resource content is an aggregate of a course presented as media content (text, images, audio, video, animation), an exercise, a tutorial and an evaluation.
- Business access layer defines the treatments required to manage the educational resource content. Operations in this layer guarantee the coherence of the data stored during interactions with the learner. It is the case of an initial assessment of a learner's skills for example.
- Web access layer allows exposing the business treatments via a REST API or through other remote access components such as web services based on SOAP protocol. Access rights of this layer are limited to the proxy micro service that manages learners' access to resources efficiently.

Educational resource semantic micro service evolves inside a container assuring the Inversion of Control (IoC) principle using an IoC micro framework. This framework manages implicitly the technical aspects of SMS-R such as security, transactions management, persistency, logs, monitoring, migration in order to expose the micro service capabilities through HTTP or SOAP protocol, a web container is used. Fig. 3 shows an educational resource semantic micro service structure.

Educational resource semantic micro services functional and non-functional properties are described using an Ontology Web Language OWL-S [17, 18] in unambiguous and computer-interpretable form. An OWL-S description is

composed of three parts, which are service profile, service model and service grounding. The service profile describes service functional and non-functional properties and it is the part used in the discovery process. The service model describes how the service works (internal processes), and the service grounding specifies the details of how the service can be accessed.

##### B. Proxy Micro-Service SMS-P

As mentioned in the previous section, we send all learners' requests to the proxy micro service, SMS-P analyze the request and extract information about learner profile and context, learning path id and current objective id. SMS-P send a discovery request with the objective description to the discovery micro service SMS-D in order to get a sorted list of SMS-R responsible of the educational resources matching exactly the current learning path objective and learner preferences. Using a matchmaking algorithm combined with a QoS measurement model, the proxy micro service selects the convenient SMS-R and send it the learner request in order to get the educational resource. Based on learner feedback and evaluation results a pertinence score is assigned to the educational resource. This score will be used in addition to other parameters to calculate the weight of the edge linking the current resource with the previous nodes in the learning path. This process is a part of learning path optimization using a metaheuristic algorithm called Ant Colony Optimization Algorithm ACO. Our proposed optimization algorithm will be presented in Section 6, it proposes to the learner the optimal learning path from all paths defined in the training plan. Communication diagram in Fig. 4 shows the interactions between different platform actors.

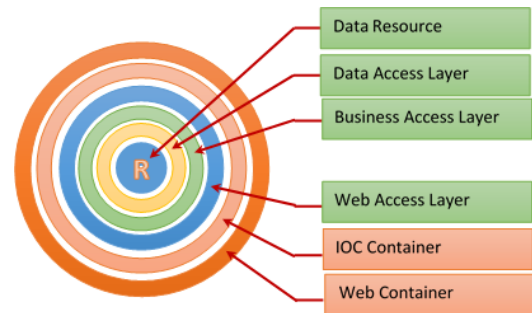


Fig. 3. Educational Resource Semantic Micro Service Structure.

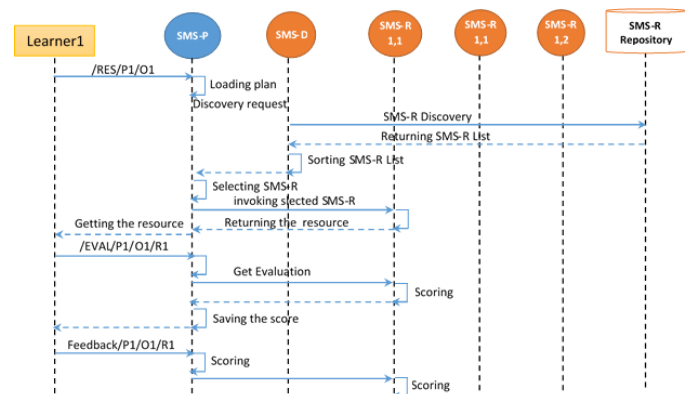


Fig. 4. Communication Diagram, Showing the Platform Actors' Interactions.

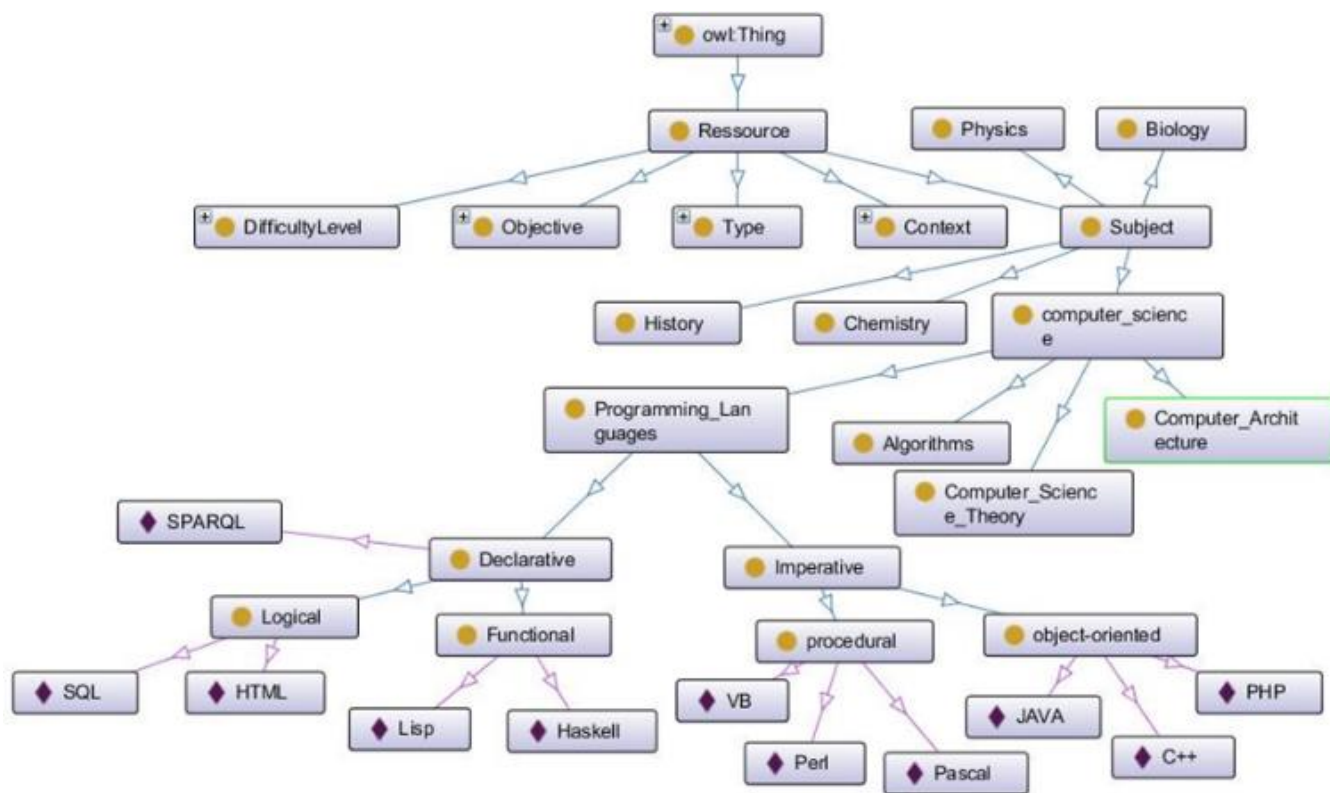


Fig. 5. Fragment from our Platform' Ontology for Educational Resource.

### C. Semantic Discovery and Selection Micro Service SMS-D

All SMS-R are described using OWL-S in unambiguous and computer-interpretable form allowing semantic discovery and selection micro service SMS-D first to compute semantic matchmaking of SMS-R capabilities (which are expressed in service profile in terms of inputs and outputs) and the learning path objective description. Semantic matchmaking is performed by calculating the semantic distance between concepts that are defined in an ontology and used to describe SMS-R and learning path nodes objectives. Matching degree and QoS attributes scores are used by SMS-D to sort the discovered SMS-R list before returning it to the proxy micro service. QoS of a SMS-R refers to non-functional properties including availability, security, language, response time, price and reputation. Fig. 5 shows a fragment from our e-Learning platform ontology.

### D. Configuration Micro Service SMS-C

In a micro service architecture, each micro service have its own configuration. This can result in duplication of a single property value across multiple micro services. Configuration micro service SMS-C is designed to externalize, centralize and expose configuration of all micro services in one place. SMS-C allows us to save time and effort when one or multiple properties values need to be changed.

## V. QoS ATTRIBUTES NORMALIZATION

QoS refers to non-functional properties of learning resources, including availability, security, language, response time, price and reputation. QoS attributes hold two different directions of their values; if the direction of the attribute is

positive, it means that a bigger value is better. On the contrary, if the direction is referred as negative, it means that smaller values are better. For example, for attribute response time the smaller value is usually preferred, so the direction of this parameter is negative, whereas for attribute availability the bigger value indicates a better quality for the specified parameter, so the direction is positive. To address this issue, all QoS attributes need to be normalized to the same scale [28]. Generally, all QoS attributes value will be normalized into a range from 0 to 1. The normalization is given by:

$$q'_1 = \begin{cases} \frac{q-min}{max-min}, & max \neq min \\ 1, & max = min \end{cases} \quad (1)$$

$$q'_2 = \begin{cases} \frac{max - q}{max - min}, & max \neq min \\ 1, & max = min \end{cases}$$

If the direction of attribute  $q$  is positive, use  $q'_1$  for normalization, otherwise use  $q'_2$ .

Each QoS attribute in Table I represents one aspect of quality of service, to evaluate the resource micro service QoS score we adopt an utility function given by formula 2 where  $q_i$  represents the normalized value of  $i^{th}$  QoS attribute and  $w_i$  is the corresponding weight. By using weight  $w_i$  for each QoS attribute, the system becomes able to calculate the resource QoS score according to each learner preferences. This method was proposed by [19], and is one of the widely used approaches in service selection and composition.

$$QoS(SMS-R) = \sum_{i=1}^n q_i w_i \quad (2)$$

TABLE I. TYPICAL QoS ATTRIBUTES OF A RESOURCE MICRO SERVICE

| QoS attribute      | Description  | Unit    |
|--------------------|--|---------|
| Response time (RT) | the duration between request submission and response reception | ms      |
| Availability (A)   | the probability that a service is operating and accessible     | percent |
| Price (P)          | The money that a learner has to pay to use the micro service   | Euro    |
| Reputation (R)     | The quality of being trustworthy                               | percent |

In our platform, we sort the candidate micro services according to their QoS score and semantic matching score, which reduces significantly the computational overhead of the overall optimization process.

A learning path is composed by multiple resources micro services to respond to a training pedagogical objective. Its QoS level for a precise learner is the addition of all QoS scores resource micro services composing it.

$$QoS(P) = \sum_{j=1}^N QoS(SMS-R_j) \quad (3)$$

While  $N$  represents the total number of nodes for the learning path  $P$  and  $QoS(SMS-R_j)$  is the quality of service score for the node  $j$ .

### VI. SEMANTIC MICRO SERVICE DISCOVERY AND SELECTION

Semantic micro service discovery is the process of locating existing Web services based on the semantic description of their functional and non-functional properties. In our platform, semantic micro service discovery is used to select the best candidate resource micro services  $SMS-R$  satisfying a precise objective described semantically in the learning path. Fig. 6 shows how the discovery and selection process is performed.

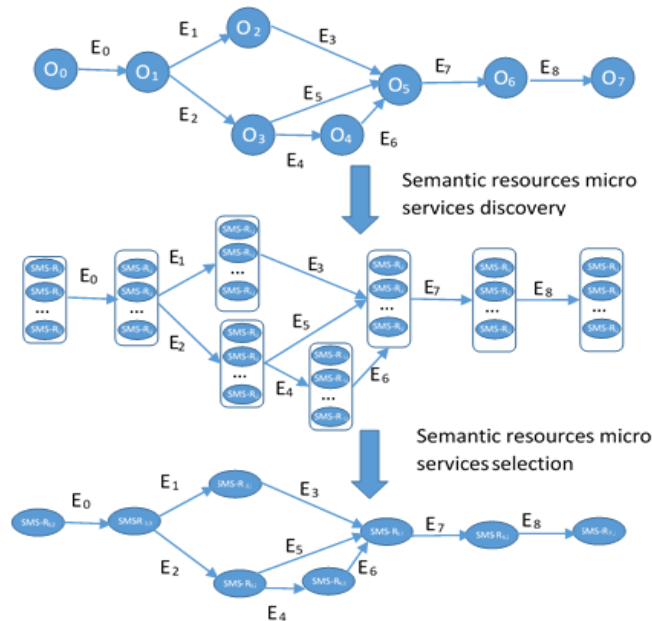


Fig. 6. Semantic Micro Service Discovery and Selection Process.

In this paper, we use our own domain ontology have been shown in Fig. 5 to calculate semantic distance [4, 29] between concepts composing  $SMS-R$  description and learning path objectives description. Our semantic matchmaking algorithm uses an edge-based approach to measure the semantic distance between two ontological concepts. In [18], the author computes the similarity between two concepts by finding the least common subsume ( $LCS$ ) node that connects their senses. For example, we can see in Fig. 5, the  $LCS$  of SQL and JAVA is Programming languages.

Once the  $LCS$  is identified, the distance between two senses is computed by:

$$Sim(c_1, c_2) = \frac{2d}{L_1 + L_2 + 2d} \quad (4)$$

Where  $d$  is the depth of the  $LCS$  from the root,  $L_1$  is the path length between  $c_1$  and  $LCS$ , and  $L_2$  is the path length between  $c_2$  and  $LCS$ .

Without considering the levels of nodes in the ontology hierarchy, the similarity measurement of this method could be misleading [32]. For example, the similarity between SQL and Java using this method is 0.57 and the similarity between Java and algorithms, which is a higher-level node, is 0.54. We define a modified measure based on this method that takes into account the position of concept nodes in the ontology.

$$levelSim(c_1, c_2) = \frac{2d+S}{L_1 + L_2 + 2d+S} \quad (5)$$

$$S = \log \frac{2 * \max(L_1) * \max(L_2)}{\max(L_1) + \max(L_2)} \quad (6)$$

Where  $d$  is the depth of the  $LCS$ ,  $L_1$  and  $L_2$  are the path lengths between semantic node  $c_1$ ,  $c_2$  and the  $LCS$  respectively,  $\max(L_1)$  is the maximum path length of semantic node  $c_1$ ,  $\max(L_2)$  is the maximum path length of semantic node  $c_2$ ,  $S$  is the logarithm of the harmonic mean between  $\max(L_1)$  and  $\max(L_2)$ . Formula (5) represents that the distance between any two nodes  $c_1$  and  $c_2$  is reduced if their parent node lies in the lower level of the hierarchy.

The similarity score between the micro service  $SMS-R_i$  set of concepts  $SC_R$  and a learning path' objective set of concepts  $SC_O$  is computed as follows:

$$SimScore(SC_O, SC_R) = \sum_{c_O \in SC_O} \frac{levelSim(c_O, SC_R)}{SC_O + SC_R} + \sum_{c_R \in SC_R} \frac{levelSim(c_R, SC_O)}{SC_O + SC_R} \quad (7)$$

### VII. LEARNING PATHS OPTIMIZATION USING ANT COLONY OPTIMIZATION ALGORITHM

Ant colony optimization (ACO) algorithms [11] are bio-inspired population-based metaheuristic algorithms modeling ants' behaviors. Ant system (AS) was the first ACO algorithm to be proposed in the literature by Marco Dorigo [2], in the 1920s to find approximate solutions in a graph, the first algorithm was inspired by ants' behavior in searching a path between nest and food source. The original idea was diversified to tackle large-scale problems and several new algorithms have been created, inspired of multiple aspects of ants behavior. The first algorithm was originated of observation of food resources' exploitation by ants. In facts, an

ant has a limited cognitive capability and by taking advantage of collective intelligence, it is able to find the shortest path between its nest and a food source.

The ants construct the solutions as follows:

- An ant explores randomly environment around the nest
- If this ant finds a food source, it returns directly to the nest, laying pheromone on its path.
- Pheromone is attractive; nearby ants tend to follow this path.
- Returning to the nest, these ants will increase pheromone in this path.
- If two paths are possible to reach the same food source, the shortest one will be followed, at the same time by more ants.
- The short path is increasingly promoted, becoming more and more attractive.
- The long path finished by disappearing because pheromone evaporates at certain rate in each iteration.
- Finally, all ants in the colony choose the shortest path.

In our case, we consider our learning path represented as an oriented graph in Fig. 1. Each node represents a precise objectives and each edge a possible navigation between two nodes. Each edge has a weight  $W$  initialized firstly by pedagogical team to express a relative importance for different possible paths leaving the same node. Each learner exploring the graph represents an ant. While following a path  $E_j$  to reach a node  $O_E$  proposing knowledge evaluation, the ant lays pheromones  $C$  which quantity depends on the score  $\alpha$  obtained.

To reflect back-propagation phenomena, pheromones are not simply laid on the edge that leads the ant to the current node but on the  $n$  previous edges that the ant has followed. This represents the pedagogical effect that the success of fail in a precise node is conditioned by learner prerequisites. Of course, this influence decreases with time and distance: more the node is far in the path history  $P(a)$  of the ant  $a$  less importance it has. To do, the quantity of pheromone lied decreases while the back-propagation moves backward. In our algorithm, we propose that the quantity  $\alpha$  of pheromones that will be added to the edge  $E_k$  in history  $P(a)$  will be equal to  $\alpha$  divided by  $d(k)$ , while  $d(k)$  is the distance between the evaluation node  $O_E$  and original node.

$$C_k = C_k + \frac{\alpha}{d_k} \tag{8}$$

Fig. 7 shows an example of back-propagation of pheromones for a learner passed an evaluation in node 7 and obtained a score  $\alpha_1$ . To reach the evaluation node  $E_7$ , he followed this learning path  $P = \{O_0, O_1, O_3, O_7\}$ . Quantities of pheromones laid on edges  $E_7, E_3, E_1$ , and  $E_0$  will be respectively  $\alpha_1, \alpha_1/2, \alpha_1/3$  and  $\alpha_1/4$ .

The fact that pheromones evaporate biologically with time is extremely important, it allows the ant colony to update regularly the information used to define the optimal path. In

our platform, it is important to implement an evaporation form to prevent our algorithm from being stuck in local optimum also to allow dynamic adaptability options.

Formula 9 shows the evaporation form of pheromones.  $\tau$ , the evaporation rate is a key feature in our system. The evaporation duration  $x$  represents a range when the evaporation should be recalculated. Typically,  $\tau = 0.999$  and  $x = 1$  day.

$$C_t = \tau^x C_{t-1} \tag{9}$$

In addition to evaluation results, learners review and submit feedbacks about educational resources. Each educational resource get a score  $\beta$  from learners. This score is multiplied by a credibility factor  $\mu$  associated to each learner by the system and pedagogical team according to learner' attendance rate and honesty. Appreciation score  $\beta$  is transformed to pheromone  $A$  laid on previous edges that the learner has followed to reach the current resource while respecting the back-propagation principal as follows:

$$A_k = A_k + \frac{\mu\beta}{d_k} \tag{10}$$

Evaporation of pheromones  $A$  is calculated the same way as formula 9.

$$A_t = \tau^x A_{t-1} \tag{11}$$

Values of  $W, C$  and  $A$  are considered as collective factors, they are used by all learners to construct their own path.  $W$  is an external factor given by pedagogical team to the learners/Ants community.  $C$  and  $A$  are internal factors created by individuals to serve the community. Our system should be able to consider individuals factors, related to learner profile and preferences, in order to achieve the desired compromise between individual, community and environment.

Individual factors that we may consider are numerous (preferences, excellence, history, language). The idea is to allow the system to propose solutions according to learner profile. In our case, we choose  $H$  the history factor.

The history factor  $H$  contains information about nodes visited previously with the learner, because it is an individual factor, there is an  $H$  value per node for each learner. Default value of  $H$  is 1, when a node is visited, corresponding value of  $H$  will be multiplied by a factor  $h$  inversely proportional to the evaluation score. For example, we can choose these values:

- $h=0.25$  if the score is between 75% and 100%
- $h=0.5$  if the evaluation score is between 50% and 75%
- $h=0.75$  if the evaluation score is between 25% and 50%
- $h=0.95$  if the evaluation score is less than 25%

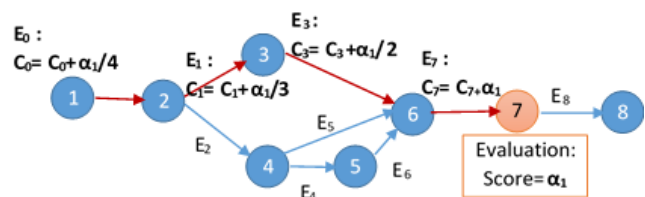


Fig. 7. Pheromones Back-Propagation Principal.

The role of  $H$  is to decrease the probability that a visited node will be proposed again. Of course, if a node gets a bad evaluation score ( $h=0.95$ ) it will be proposed very fast than if it gets a high score ( $h=0.25$ ).

With time, learners forget what they had seen. It is for this reason that  $H$  tends to return naturally to one. This anti-evaporation of pheromones phenomena is described as follows:

$$H_t = H_{t-1} \left( 1 + \frac{1-H_{t-1}}{H_{t-1}} \frac{1-e^{\gamma x}}{1+e^{\gamma x}} \right) \quad (12)$$

$\gamma$  is a constant of time that sets the anti-evaporation speed, it should be adjusted to correspond to learner' memory volatility. It is a pedagogical constant, which should be the subject of a discussion with teachers. Formulas 12 and 13 allow an easy calibration of  $\gamma$ . Formula 14 have shown how to compute  $\gamma$  value using  $H$  in the moments  $t$  and  $t - 1$  and the period  $x$  during which a learner may eventually forget a viewed resource.

$$\gamma = \frac{1}{x} \ln \left( \frac{1+\tau}{1-\tau} \right) \quad (13)$$

$$\tau = \frac{H_t - H_{t-1}}{1 - H_{t-1}} \quad (14)$$

All factors described previously  $W, C, A$  and  $H$  are unified in a form of a function called "Fitness", by analogy with literature of genetics algorithms. Formula 15 shows the expression of the fitness value of edge  $E_{i,j}$  linking node  $i$  with node  $j$  for a learner  $a$ .  $H$  is the memory factor,  $W$  is the pedagogical weight,  $C$  is evaluation score pheromones and  $A$  is the feedback score pheromones.  $\omega_H, \omega_w, \omega_c$  et  $\omega_A$  are weights allowing giving more emphasis to a factor compared to others. This function calculates excellence and desirability of an edge, and privileges it in the selection process.

$$f(a, E_{i,j}) = \omega_H H(j, a) (\omega_w W + \omega_c C + \omega_A A) \quad (15)$$

We can say that an edge is desirable if:

- The pedagogical team reinforces it (high  $W$ ).
- It is a source of good evaluation scores (high  $C$ )
- It has a good feedback score (high  $A$ )
- The next node had never been visited by the learner or estimated forgotten ( $H$  near to 1)

When a learner validates a node, he needs to choose between the available edges the suitable one. It is in this level where fitness measurements are used. A selection process chooses an edge randomly but most likely, it has a high fitness value. Thus, it appears clearly that effective edges become dominating but not exclusively. There is always place of chance and exploration. This chance is a crucial characteristic of selection process we talk here about "selective pressure"  $s$ . More  $s$  has a big value, more the fitness value is considered in selection process and strong edges tend to dominate weak ones. There are various methods to create the selection algorithm and consequently setup the parameter  $s$ . In our platform, the used common methods are:

- Roulette-wheel selection strategy-the probability to select each edge is strictly proportional to its fitness value; this strategy is entirely automatic, there is no way to setup the selective pressure. Roulette-wheel selection ensures that better edges have higher chance to be chosen and weak edges will be disappeared, and exploration will be replaced by a leaded exploitation. Formula 16 expresses the probability of selection of an edge  $E_{i,j}$  linking node  $i$  by node  $j$  using roulette-wheel strategy.

$$p(a, E_{i,j}) = \frac{f(a, E_{i,j})}{\sum_{k \in E} f(k, E_{k,j})} \quad (16)$$

- Tournament selection: It is a method of selecting randomly  $s$  individuals from a population and the winner of each tournament (the one with the best fitness) is selected. We can see clearly that  $s$  influences selection pressure. If the tournament size is larger, weak individuals have a smaller chance to be selected, because, if a weak individual is selected to be in a tournament, there is a higher probability that a stronger individual is also in that tournament. This method has the advantage of being easily configurable.
- Stochastic tournament selection: In this method, the weaker edge is selected by default.  $s_1$  challengers are selected randomly from a population, successive edges are compared and the edge with higher fitness value is inserted in the new population. The process continues until the population is full.

## VIII. APPLICATION AND MODEL EVALUATION

In this section, we discuss experimental results corresponding to an application implemented in the proxy micro service that lunches randomly HTTP clients representing each a learner. Each learner follows his learning path navigating from a node to another in the learning path graph (Fig. 8). We have chosen as an example a portion of a learning path about learning oriented-object programming OOP with Java language, having the following structure.

This learning path is an oriented graph composed by the following nodes:

- Nodes 1, 2, 5, 9 and 13 represent courses.
- Nodes 3, 6, 10 and 14 represent exercises.
- Nodes 4, 7, 11 and 15 represent tutorials.
- Nodes 5, 8, 12, 16 and 17 are evaluations.

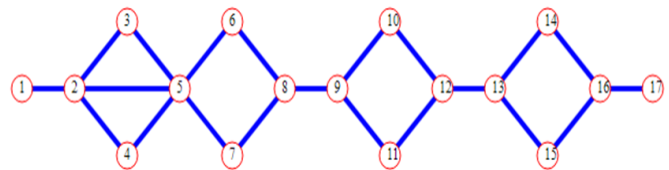


Fig. 8. The Structure of Proposed Learning Path.

Static data of this pedagogical structure has been implemented in an XML file, which the structure is shown in Fig. 9.

In this simulation, we consider that in node 2, that is a lesson, discovery algorithm found four semantic micro services SMS-R matching exactly the objective description but with different QoS values. Table II shows different qualities of service values discovered in node 2.

Three learners expressed their QoS preferences in Table III, allowing the system to rank selected resources micro services according to learners' profiles.

```
<?xml version="1.0" encoding="UTF-8" ?>
<Ontology xmlns="http://www.w3.org/2002/07/owl#"
owl: "http://www.w3.org/2002/07/owl#"
elearning: "http://www.w3.org/elearningOntology.owl" ?>
<path name="POO" subject="Computer Science" field="Programming
Languages" >
<node id="1" type="course" x="100" y="200">
<name>Introduction</name>
<description>Introduction to oriented-object programming
</description >
</node>
<node id="2" type="course" x="150" y="200">
<name>POO Basic Concepts</name>
<description>oriented-object programming basic </description>
</node>
...
<node id="17" type="evaluation" x="700" y="200">
<name>Final Evaluation</name>
<description> Quiz oriented-object programming basic
</description>
</node>
<link source="1" destination="2">
<w>100</w>
</link>
<link source="2" destination="3">
<w>35</w>
</link>
...
<link source="3" destination="5">
<w>20</w>
</link>
<link source="2" destination="5">
<w>50</w>
</link>
...
<link source="16" destination="17">
<w>100</w>
</link>
</path>
</ontology>
```

Fig. 9. XML File Representing the Application Learning Path Structure.

TABLE II. QoS VALUES OF SMS-R IN NODE 2

|               | SMS-R <sub>2,1</sub> | SMS-R <sub>2,2</sub> | SMS-R <sub>2,3</sub> | SMS-R <sub>2,4</sub> |
|---------------|----------------------|----------------------|----------------------|----------------------|
| Response time | 3 ms                 | 10ms                 | 5ms                  | 20ms                 |
| Availability  | 90%                  | 70%                  | 98%                  | 80%                  |
| Price         | 15 Euros             | 9 Euros              | 50 Euros             | 29 Euros             |
| Reputation    | 60%                  | 40%                  | 80%                  | 50%                  |

TABLE III. LEARNERS QoS PREFERENCES

|               | Learner <sub>1</sub> | Learner <sub>2</sub> | Learner <sub>3</sub> |
|---------------|----------------------|----------------------|----------------------|
| Response time | 0.2                  | 0.1                  | 0.4                  |
| Availability  | 0.1                  | 0.6                  | 0.1                  |
| Price         | 0.3                  | 0                    | 0.4                  |
| Reputation    | 0.4                  | 0.3                  | 0.1                  |

TABLE IV. QoS SCORES ACCORDING TO LEARNERS PREFERENCES

|                      | SMS-R <sub>2,1</sub> | SMS-R <sub>2,2</sub> | SMS-R <sub>2,3</sub> | SMS-R <sub>2,4</sub> |
|----------------------|----------------------|----------------------|----------------------|----------------------|
| Learner <sub>1</sub> | 0.72                 | 0.41                 | 0.67                 | 0.28                 |
| Learner <sub>2</sub> | 0.67                 | 0.05                 | 0.88                 | 0.28                 |
| Learner <sub>3</sub> | 0.86                 | 0.63                 | 0.55                 | 0.26                 |

We notice that invoked resource in node 2 change according to learners' preferences (Table IV). For learner<sub>1</sub> and learner<sub>3</sub> who are interested more about service price and response time the resource micro service SMS-R<sub>2,1</sub> with QoS scores equal to 0.72 and 0.86 is the best match. The SMS-R<sub>2,3</sub> with QoS score equal to 0.88 is the most suited to learner<sub>2</sub> who has more interest in the micro service availability and reputation.

In this simulation, scoring system is on 100. When multiple edges leave the same node, we choose pedagogical pertinence values W allowing the recommendation of tutorials instead of exercises, it is the case in edges (2=>3), (2=>4) and (2=>5) having respectively the values W: 35, 45 and 20. Which means that the pedagogical team recommends to follow the course by the tutorial 4 (45%) or the exercise 3 (35%) or as a last choice the next course 5 (20%).

By visiting a knowledge evaluation node, the ant lays pheromones C which quantity depends on the result obtained by the learner (Formula 7). In addition, a feedback score representing the quantity of pheromones A (Formula 9) corresponding to the learner feedback. Before moving to the next node, we activate the evaporation process (Formula 8 and 10).

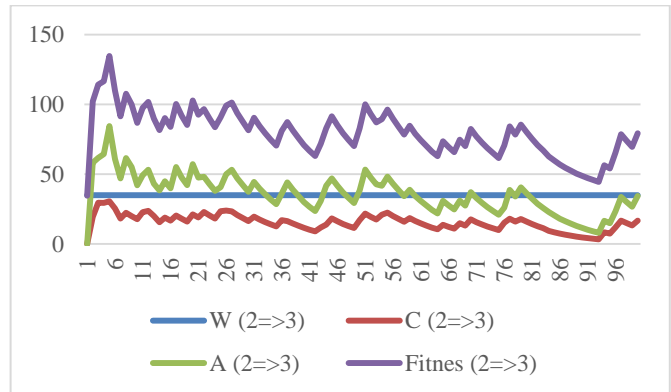


Fig. 10. Evolution of W, C, A and Fitness Values for the Edge 2=>3.

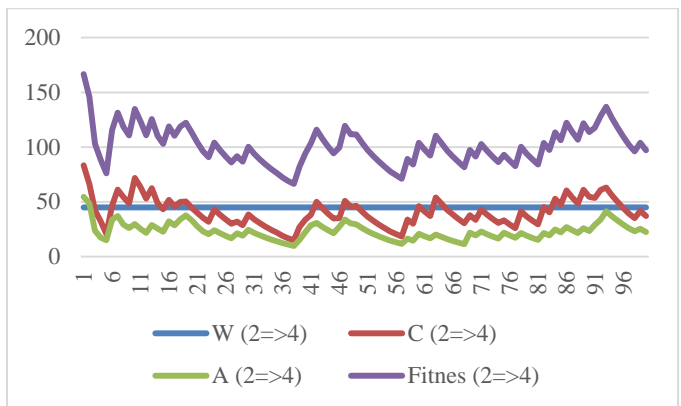


Fig. 11. Evolution of W, C, A and Fitness Values for the Edge 2=>4.



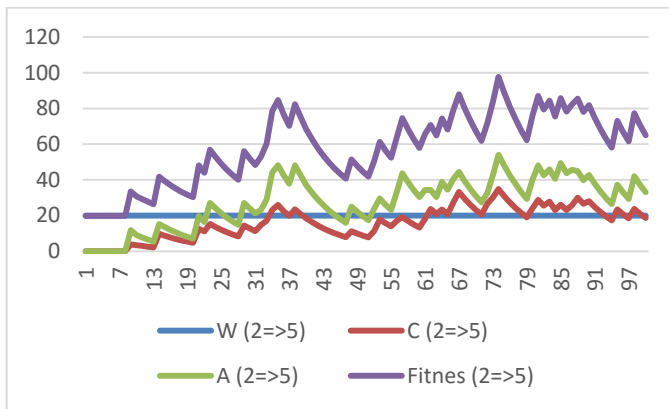


Fig. 12. Evolution of W, C, A and Fitness Values for the Edge 2=>5.

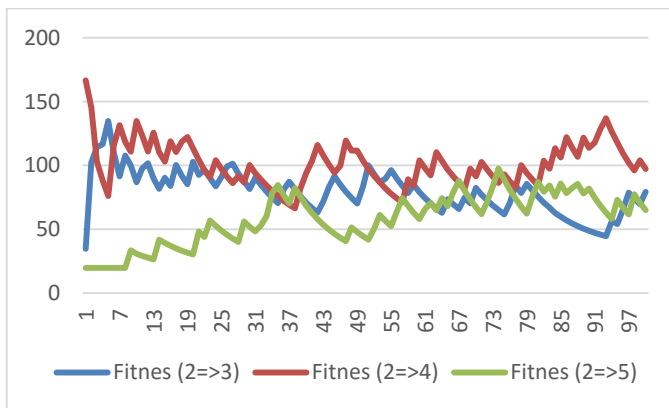


Fig. 13. Fitness Values Comparison for Edges 2=>3, 2=>4 and 2=>5.

To calculate the fitness value for each edge, C and A pheromones quantities are normalized with the W quantity putting them at 100.

Fig. 10, 11 and 12, respectively shows evolution curves of parameters W, C, A and Fitness while learners are following this learning path.

Fig. 13 represents a comparison between fitness values of three edges 2=>3, 2=>4 and 2=>5. We notice that the edge (2=>4) is the most followed, which reinforces the pedagogical team recommendation. Since the system uses many random selection methods, domination can changes with time. It is the case for learner number 57 who makes the edge (2=>3) temporary a dominating one. It is the case also for learner 73 who followed the edge (2=>5) making it temporary dominating instead of the recommended one. This allows new parameters difficult to take into consideration to appear such as excellence, learners serenity and evaluations pertinence. Despite all of that, our model allows to get at the end, very interesting results resisting all mentioned aleatory phenomena.

## IX. CONCLUSION

In this paper, we presented a new model for e-Learning platform based on semantic micro services and using discovery, selection and composition methods to create high quality learning paths responding to learners' preferences.

In this model, to achieve an optimal learning path selection a two steps process are employed, where local optimization

uses semantic discovery and selection based on a matchmaking algorithm and QoS measurement, and global optimization adopts an ant colony optimization algorithm to select the best resources combination. We consider individual, collective and pedagogical factors in order to provide learners with the best learning experience.

The achieved results are promising but there are still many potential extensions, which can enhance the platform reliability and performance. We are planning to improve the model by adding new advanced factors to the global optimization algorithm, and to enrich the resources micro services with additional semantic description approaches in order to improve the semantic matchmaking algorithms results.

## REFERENCES

- [1] Albano, G., M. Gaeta & S. Salerno (2006) E-learning: a model and process proposal. International Journal of Knowledge and Learning, 2, 73-88.
- [2] Colorni, A., M. Dorigo & V. Maniezzo (1992) DISTRIBUTED OPTIMIZATION BY ANT COLONIES. Toward a Practice of Autonomous Systems: Proceedings of the First European Conference on Artificial Life, 134-142.
- [3] Comendador, B. E. V., L. W. Rabago, B. T. Tanguilig & Ieee (2016) An Educational Model Based on Knowledge Discovery in Databases (KDD) to Predict Learner's Behavior Using Classification Techniques. 2016 Ieee International Conference on Signal Processing, Communications and Computing (Icspcc), 6.
- [4] Cui, J. & H. Yasuhara (1995) Calculating word similarity based on common attributes, total semantic distance and concept frequency. Symbiosis of Human and Artifact: Future Computing and Design for Human-Computer Interaction, 20, 729-734.
- [5] Gmati, F. E., N. Y. Ayadi, A. Bahri, S. Chakhar & A. Ishizaka (2016) A Framework for Parameterized Semantic Matchmaking and Ranking of Web Services. Proceedings of the 12th International Conference on Web Information Systems and Technologies, Vol 1 (Webist), 54-65.
- [6] Govindarajan, K., V. S. Kumar & Kinshuk. 2016. Dynamic Learning Path Prediction - A Learning Analytics Solution. In IEEE 8th International Conference on Technology for Education (T4E), 188-193. Indian Inst Technol Bombay, Mumbai, INDIA: Ieee.
- [7] Hegde, V. & H. S. S. Rao. 2017. A Framework to Analyze Performance of Student's in Programming Language Using Educational Data Mining. In 8th IEEE International Conference on Computational Intelligence and Computing Research (IEEE ICCIC), 632-635. Tamilnadu Coll Engn, Coimbatore, INDIA.
- [8] Jaramillo, D., D. V. Nguyen, R. Smart & Ieee. 2016. Leveraging microservices architecture by using Docker technology. In SoutheastCon. Norfolk, VA.
- [9] Jensen, J. (2019) A systematic literature review of the use of Semantic Web technologies in formal education. British Journal of Educational Technology, 50, 505-517.
- [10] Juhanak, L., J. Zounek & L. Rohlikova (2019) Using process mining to analyze students' quiz-taking behavior patterns in a learning management system. Computers in Human Behavior, 92, 496-506.
- [11] Kamsa, I., R. Elouahbi, F. El Khoukhi, T. Karite, H. Zouiten & Ieee. 2016. Optimizing collaborative learning path by ant's optimization technique in e-learning system. In 15th International Conference on Information Technology Based Higher Education and Training (ITHET). Istanbul, TURKEY: Ieee.
- [12] Klasnja-Milicevic, A., B. Vesin, M. Ivanovic & Z. Budimac (2011) E-Learning personalization based on hybrid recommendation strategy and learning style identification. Computers & Education, 56, 885-899.
- [13] Kumar, V. (2018) Selecting an Appropriate Web-Scale Discovery Service: A Study of the Big 4's. Desidoc Journal of Library & Information Technology, 38, 396-402.
- [14] Malavalli, D. & S. Sathappan. 2015. Scalable Microservice Based Architecture For Enabling DMTF Profiles. In 11th International

- Conference on Network and Service Management (CNSM), 428-432. Barcelona, SPAIN.
- [15] Miranda, S. & P. Ritrovato (2014) Automatic extraction of metadata from learning objects. 2014 International Conference on Intelligent Networking and Collaborative Systems (IncOS), 704-709.
- [16] Moussallem, D., M. Wauer & A. C. N. Ngomo (2018) Machine Translation using Semantic Web Technologies: A Survey. *Journal of Web Semantics*, 51, 1-19.
- [17] Pan, S. L., Y. X. Zhang & Ieee (2009) Ranked Web Service Matching for Service Description Using OWL-S. *Wism: 2009 International Conference on Web Information Systems and Mining*, Proceedings, 427-431.
- [18] Paolucci, M., T. Kawamura, T. R. Payne & K. Sycara (2002a) Semantic matching of Web services capabilities. *Semantic Web - Iswc 2002*, 2342, 333-347.
- [19] Paulraj, D., S. Swamynathan & M. Madhaiyan (2011) PROCESS MODEL ONTOLOGY-BASED MATCHMAKING OF SEMANTIC WEB SERVICES. *International Journal of Cooperative Information Systems*, 20, 357-370.
- [20] Peng, S. J., Z. T. Zhang & C. L. Wu. 2016. Geological Cloud Platform Based on Micro Service Architecture. In *Proceedings of the 3rd International Conference on Wireless Communication and Sensor Networks*, eds. J. Wang, H. Wang, B. Cheng & T. Chen, 566-568.
- [21] Rozsa, V., A. F. G. Viera & M. Dutra (2019) Semantic Web Technologies Applied to Internet Search Engines. *Investigacion Bibliotecologica*, 33, 165-191.
- [22] Shafin, S. H., L. Zhang & X. Xu. 2012. Automated Testing of Web Services System Based on OWL-S.
- [23] Singh, H. & S. J. Miah (2019) Design of a mobile-based learning management system for incorporating employment demands: Case context of an Australian University. *Education and Information Technologies*, 24, 995-1014.
- [24] Somasundaram, T. S., R. A. Balachandar, V. Swaminathan, A. Kumar, V. Paramasivan & Ieee. 2007. Semantic description and discovery of grid services using WSDL-S and QoS based matchmaking algorithm.
- [25] Tseng, J. C. R., H. C. Chu, G. J. Hwang & C. C. Tsai (2008) Development of an adaptive learning system with two sources of personalization information. *Computers & Education*, 51, 776-786.
- [26] Turker, Y. A., K. Baynal & T. Turker (2019) The Evaluation Of Learning Management Systems By Using Fuzzy Ahp, Fuzzy Topsis And An Integrated Method: A Case Study. *Turkish Online Journal of Distance Education*, 20, 195-218.
- [27] Wang, B., S. L. Yang, X. L. Ren, G. Y. Wang & M. Assoc Comp (2017) Research on Digital Publishing Application System Based on Micro-Service Architecture. *Proceedings of 2017 Vi International Conference on Network, Communication and Computing (Icncc 2017)*, 140-144.
- [28] Wang, H. B., D. R. Yang, Q. Yu & Y. Tao (2018) Integrating modified cuckoo algorithm and creditability evaluation for QoS-aware service composition. *Knowledge-Based Systems*, 140, 64-81.
- [29] Wei, T. T. & H. Y. Chang (2015) Measuring Word Semantic Relatedness Using WordNet-Based Approach. *Journal of Computers*, 10, 252-259.
- [30] Yang, J., Z. X. Huang, Y. X. Gao & H. T. Liu (2014) Dynamic Learning Style Prediction Method Based on a Pattern Recognition Technique. *Ieee Transactions on Learning Technologies*, 7, 165-177.
- [31] Zhang, L. & Ieee (2014) OWL-S Based Web Service Discovery in Distributed System. 2014 Ieee Workshop on Electronics, Computer and Applications, 882-885.
- [32] Zhang, N., J. Wang, Y. T. Ma, K. Q. He, Z. Li & X. Q. Liu (2018) Web service discovery based on goal-oriented query expansion. *Journal of Systems and Software*, 142, 73-91.
- [33] Zhao, Q., Y. Q. Zhang, J. Chen & Ieee (2016) An Improved Ant Colony Optimization Algorithm for Recommendation of Micro-learning Path. 2016 Ieee International Conference on Computer and Information Technology (Cit), 190-196.
- [34] Markowska-Kaczmar U, Kwasnicka H. , Paradowski M. Intelligent Techniques in Personalization of Learning in e- Learning Systems. *Studies in Computational Intelligence, Computational Intelligence for Technology Enhanced Learning*, Vol. 273, 2010.
- [35] Brusilovsky P. , Peylo C. Adaptive and intelligent Web-based educational systems. In P. Brusilovsky and C. Peylo (eds. ), *International Journal of Artificial Intelligence in Education* 13 (2-4), Special Issue on Adaptive and Intelligent Web-based Educational Systems, pp. 159-172, 2007.
- [36] Ahmad, K., Maryam, B. I., & Molood, A. E. (2013). A novel adaptive learning path method. 4th International Conference on e-Learning and e-Teaching (ICELET 2013), 2013.
- [37] Almohammadi, Khalid; Hagrass, Hani; Alghazzawi, Daniyal; et al. A zSlices-based general type-2 fuzzy logic system for users-centric adaptive learning in large-scale e-learning platforms. *SOFT COMPUTING* Volume: 21 Issue: 22 Pages: 6859-6880, 2017.
- [38] Zaharescu, EZaharescu, GA; Semantic Web Technologies Integrated in a SOA-Based E-Learning System, proceedings of the 6th international conference on virtual learning, icvl, 2011

# An Approach to Control the Positional Accuracy of Point Features in Volunteered Geographic Information Systems

Mennatallah H. Ibrahim<sup>1</sup>, Hesham A. Hefny<sup>3</sup>  
Computer Science,  
Faculty of Graduate Studies for Statistical Research  
Cairo University, Cairo, Egypt

Nagy Ramadan Darwish<sup>2</sup>  
Information Systems and Technology  
Faculty of Graduate Studies for Statistical Research  
Cairo University, Cairo, Egypt

**Abstract**—Volunteered geographic information (VGI) is a huge source of user-generated geographic information. There is an enormous potential to use VGI in different mapping activities due to its significant advantages. VGI is found to be richer and more up-to-date than authoritative geographic information. However, VGI quality is an obvious challenge that needs to be addressed in order to get the full potential of VGI. Positional accuracy is one of the important aspects of VGI quality. Although VGI positional accuracy can be high in some contexts, VGI datasets are characterized by a large spatial heterogeneity. This paper proposes an approach for controlling positional accuracy as well as decreasing the spatial heterogeneity of point features in VGI systems. A case study has been conducted in order to ensure the applicability and effectiveness of the proposed approach.

**Keywords**—Volunteered geographic information; quality control; positional accuracy; point features

## I. INTRODUCTION

The proliferation of GPS enabled hand-held devices, the advances of communication technology, as well as, the development of Web 2.0 and collaborative mapping applications have dramatically extended the role of Geographic Information (GI) consumers. GI consumers are not only able to use and share GI, but also to create it as well. Consequently, a new phenomenon termed as volunteered geographic information has emerged. The term VGI has been coined by [1].

VGI is considered as an important source of user-generated geographic information. Nowadays, citizens who are not professional cartographer are able to participate in developing large and sophisticated cartographic projects. VGI not only creates new GI datasets, it can also enrich the traditional authoritative datasets as well. Furthermore, VGI is being studied as an alternative to authoritative data as it has been concluded that authoritative spatial datasets are often out-of-date, incomplete, maintained expensively and their quality is inconsistent [2]. The author in [3] ensures that in some contexts, VGI can replace experts' data.

VGI has significant advantages that can overcome authoritative data limitations: (1) VGI can be accessed and obtained easily; (2) VGI is available over large areas either

freely or at low cost; (3) VGI can be updated and maintained quickly by its users. Moreover, VGI is the only source of spatial data in certain regions due to security and/or financial issues [2].

As a result, there is an enormous potential to use VGI in different mapping activities and to integrate VGI with the authoritative datasets. However, VGI quality represents clear challenge to users who are concerned about quality assurance and quality validation of spatial data [4], [5]. Moreover, there are also many concerns about VGI quality that act as main barriers to integrate VGI with authoritative GI datasets [6].

As a result, VGI quality is an important research area that gains much interest [7]. One of the important aspects of VGI quality is the positional accuracy. As mentioned by [3], VGI with high quality is often associated with positional accuracy. VGI positional accuracy is characterized by a large spatial heterogeneity. The previous literature has shown little effort for controlling positional accuracy of volunteered point features in VGI systems. This paper proposes an approach to control positional accuracy of point features in VGI systems, in order to increase positional accuracy and decrease positional accuracy heterogeneity of such features across VGI datasets and maps within VGI systems.

The paper is structured as follows; it is divided into six sections. Section II presents an overview of VGI quality and positional accuracy. Section III presents the related work. Section IV introduces the proposed approach. Section V introduces the proposed algorithm. Section VI presents the conducted case study. Section VII, Shows the result of the case study. Finally, Section VIII summarizes the main points discussed in the paper.

## II. VGI QUALITY AND POSITIONAL ACCURACY

Nowadays, private citizens provide online databases with vast amount of VGI through different websites and mobile applications. The provided VGI can be used in various disciplines as urban planning, public health, hydrology and disaster/risk management. As a result, VGI quality is critical especially if VGI will be used in spatial decision making processes. VGI quality is composite where it includes aspects dealing with data characteristics, volunteers' characteristics, and application context [8].

Generally, spatial data quality has eleven elements including lineage, positional accuracy, attribute accuracy, logical consistency, completeness, semantic accuracy and others [9]. Positional accuracy is one of the important elements of VGI quality. Positional accuracy is defined by [10] as the nearness of values that describe the position of a real-world entity in an appropriate coordinate system to the entity's true position in that system.

Generally, the main issues of VGI quality are the inconsistency of coverage and accuracy [2]. Although, VGI can reach in some contexts a high positional accuracy, a high spatial heterogeneity in positional accuracy has been indicated [12], [13]. As mentioned by [11], VGI is fundamentally imperfect with unknown and heterogeneous imperfection. From the reasons that lead to heterogeneity of VGI quality:

- Volunteers have different abilities, nature, expertise, motivation and priorities;
- Volunteers as well as VGI are not distributed equally over space;
- Volunteers may use different methods in VGI creation process (e.g. GPS and image tracing);
- Volunteers may use low accuracy devices in VGI creation process;
- There is no central coordination among volunteers;
- There are no systematic procedures for VGI creation or verification processes.

### III. RELATED WORK

As mentioned before, inaccurate VGI may lead to significant implications. In [14], the authors concluded that quality control during VGI creation process is important. There are several previous studies that are concerned about analysis and assessment of VGI accuracy. Unfortunately, such studies give useful insights about VGI accuracy, but only assist indirectly in identifying an approach to control VGI accuracy.

The attempts to assess VGI quality have concluded that data heterogeneity is an intrinsic characteristic of VGI [15]. Fortunately, there are a number of earlier studies that are concerned about VGI quality control and assurance in general. Those previous studies can be categorized into three categories which are intrinsic, extrinsic and hybrid as shown in Table I. Intrinsic category includes studies that depend on internal factors for controlling and assuring VGI quality which are volunteers and/or volunteered data characteristics. Extrinsic category includes studies that depend on external factors such as gatekeepers and geographic contexts. Hybrid Category includes studies that rely on both internal and external factors together.

In [5], the authors propose an intrinsic approach that follows Linus's law [16]. The authors suggest that VGI holds an intrinsic quality assurance measure which is the number of contributors who works on a certain spatial unit. It is concluded that there is a positive relationship between VGI positional accuracy and number of volunteers; where beyond 15

volunteers within a square kilometer the positional accuracy becomes very good.

However, in [11], it is indicated that the practical implementation of the approach proposed in [5] can be challenging where, if the volunteered information is of poor quality data, increasing the number of volunteers may negatively affect VGI quality. Furthermore, in [17], it is indicated that Linus's law is more suitable for prominent geographic facts than for obscure ones. The authors in [11] also added that by following Linus's law, it is difficult to know how the single correct contribution can be chosen against the majority agreement of other volunteers.

In [17], the authors describe three VGI quality assurance approaches. First, the crowdsourcing approach which also relies on the assumption that the quality increase when more volunteers work on one area (considered as intrinsic approach). Second, the social approach which relies on a hierarchy of trusted individuals; act as gatekeepers to control VGI quality (considered as extrinsic approach). Third, the geographic approach which relies on geography knowledge to detect the reasonability of VGI (considered as extrinsic approach). Unfortunately, the approaches described in [17] cannot be adopted in all contexts as social approach is limited by the quality of the gatekeepers and the geographic approach is limited by the available contextual information [11].

In [11], the authors propose an intrinsic method based on latent class to characterize volunteers' quality relying on their contributions. The proposed method enables choosing only the appropriate volunteers for a specific VGI creation processes leading to highly accurate VGI. Such method filter volunteers before proceeding in VGI creation process leading to the possibility of losing volunteers who may help in the specified volunteering task because they are not classified as appropriate volunteers.

In [18], conceptual VGI quality assurance model for species occurrence observations is proposed. In the proposed model, VGI trustworthiness is a function of three contexts which are consistency with habitat, consistency with neighbors and volunteers' reputation where the level of trustworthiness is quantified by fuzzy set theory. The proposed model is considered to be hybrid as it depends on both internal factors (volunteer reputation) and external factors (consistency with habitat and consistency with neighbors). Unfortunately, the proposed model depends on extrinsic factors that may not be available all the time; moreover, such approach is appropriate only for certain contexts.

TABLE I. RELATED WORK CATEGORIZATION

| Study                          | Category  |           |        |
|--------------------------------|-----------|-----------|--------|
|                                | Intrinsic | Extrinsic | Hybrid |
| [5]                            | ✓         |           |        |
| [17] - Crowd-sourcing Approach | ✓         |           |        |
| [17] - Social Approach         |           | ✓         |        |
| [17] - Geographic Approach     |           | ✓         |        |
| [11]                           | ✓         |           |        |
| [18]                           |           |           | ✓      |

As mentioned by [2], the issue of VGI quality is a trending research topic because of the vast amount of data and the inapplicability of Linus's law. The previous related work was concerned about controlling and assuring VGI quality with almost no efforts directed specifically to control positional accuracy of volunteered point features in VGI systems. The aim of this paper is to propose an approach that controls the positional accuracy of volunteered point features in VGI systems.

#### IV. PROPOSED APPROACH

The proposed approach aims to control the positional accuracy of point features in VGI systems in order to increase the positional accuracy and decrease the spatial heterogeneity of such features; it helps to create highly accurate and consistent volunteered geographic maps and datasets that contain no outliers. The proposed approach aims also to overcome the limitations of the previous related work. The proposed approach is hybrid where it depends on both internal and external factors for controlling VGI positional accuracy.

First, as shown in Fig. 1, we characterized the positional accuracy of the volunteered point features through three main dimensions which are volunteers, contributions and content. Each dimension is concerned about number of elements as follows:

- **Volunteer.** Concerned about the volunteers themselves; whether the volunteer is trained or not, volunteer's local knowledge and volunteer's location during his/her contribution.
- **Content.** Concerned about the volunteered point (VP); volunteers' density which reflects the number of volunteers in a specific area, volunteers' agreement which reflects the agreement of volunteers on a specific VP and the geographic context of the VP.
- **System Design.** Concerned about the environment through which the volunteers perform their volunteering task; task definition, the instructions given to the volunteers in order to accomplish their tasks accurately, the user interface through which the volunteers provide their VPs.

##### A. Volunteer Dimension

The first dimension to characterize the positional accuracy of VPs is the volunteer dimension. Volunteer dimension describes three aspects concerning the volunteers themselves which are training, local knowledge and location.

1) *Training:* Training is one of the important aspects that affect VGI quality [19], [8]. With appropriate training, volunteers are able to improve more than domain's expert [20]. Contributions from volunteers who have no formal geographic training may lead to inaccurate VGI [21]. Even remote volunteers when they get trained their contribution errors could be minimized [22]. In the proposed approach, all citizens will be allowed to volunteer; however, volunteers who got a training or had a training material will be tagged as trained volunteers.

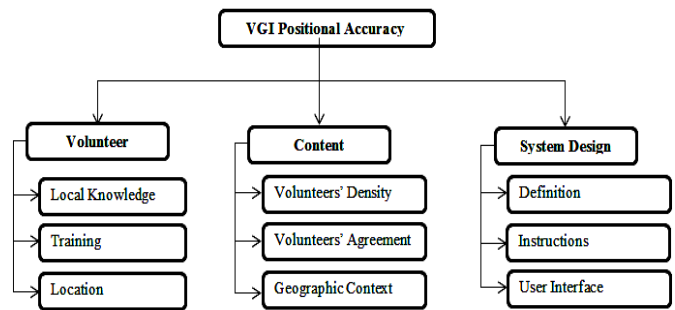


Fig. 1. Characterization of Positional Accuracy of Volunteered Point Features.

2) *Local knowledge:* One of VGI quality indicators is the volunteers' local knowledge [23]. Local Knowledge can lead to highly accurate and up-to-date local maps which sometimes provide information with quality higher than the experts' maps [20], [8], [17]. Volunteers are more familiar with their own area than distant authoritative experts, so volunteers with their local knowledge could create a map of their area more effectively. In the proposed approach, the volunteers are asked to determine their residence place before proceeding in VGI creation process. We assumed that the volunteers' local knowledge is related to their residence city and region.

3) *Location:* We have observed through our case study that if a point feature is located inside a building, only the volunteers who are located in the same area of the VP are able to determine the VP location accurately. Consequently, our proposed approach will automatically collect metadata about the volunteers' location during performing their volunteering task. If the VP is inside a building, the distance between the volunteer and the VP will be calculated using Euclidean distance. The volunteer has to be at a distance of 100 meters or less from his/her VP.

In the proposed approach, the volunteers are classified according to their local knowledge and training skills (i.e. whether they got trained or not). Volunteer are assigned a weight according to their class, as shown in Fig. 2. The proposed approach classifies volunteers according to their local knowledge with respect to their created VGI as follows:

- **Local volunteers.** Volunteering in their residence city (called city volunteer) or in their residence regions (called region volunteer). Local volunteers will be assigned a  $W_1$  up to 1, where  $W_1=1$ , if city-volunteer or  $W_1=0.75$ , if region-volunteer.
- **Remote volunteers.** Volunteering in their residence country but not their residence region (called country volunteers) or in other country (called other-country volunteers). Remote volunteers will be assigned  $W_1$  up to 0.35.  $W_1=0.35$ , if country-volunteers or  $W_1=0$ , if other-country-volunteers.

All volunteers except city-volunteers are further classified into trained or not trained volunteers and assigned  $W_2$  ( $W_2$ ). For trained volunteers,  $W_2 = 0.25$  and for untrained volunteers,  $W_2=0$ .

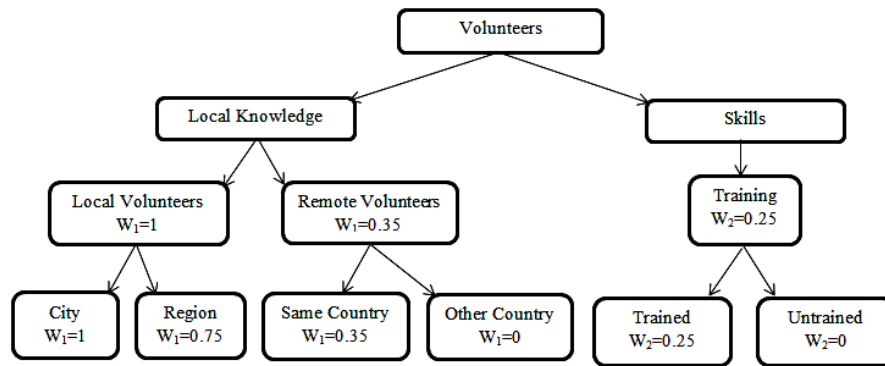


Fig. 2. Volunteers' Classification According to their Local Knowledge and Training.

Consequently, we have seven types of volunteers which are city, region-trained, region-untrained, country-trained, country-untrained, other-country-trained, and other-country-untrained. Each volunteers' type is assigned a Volunteer's Weight (VW) which is the summation of  $W_1$  and  $W_2$  (as shown in Table II).

The highest weight is assigned to city-volunteers due to their high local knowledge and also to region-trained volunteers; VW for both will be 1. Followed by region-trained volunteers (VW=0.75). Then VW decreases for country volunteers as the local knowledge of the volunteers respecting other regions and cities decreases (VW=0.35) and if country volunteer is trained VW will be increased to 0.55. Other-country volunteers are assigned the lowest weight if they are trained VW will be 0.25 and zero if they are not trained.

**B. Content Dimension**

The second dimension is content dimension which is concerned about the characteristics of the VPs. Firstly, the volunteers' density which reflects the number of volunteers who have volunteered within a specific area around the VP. Secondly, the volunteers' agreement that indicates whether there is an agreement on a specific VP or not. Thirdly, the geographic context is concerned about the suitable geographic content of the VPs. The VP will be assigned a weight according to the satisfied characteristics as shown in Fig. 3.

1) *Volunteers' density:* In [5], it is concluded that there is a positive relationship between VGI positional accuracy and number of volunteers. [24] and [25] also ensures that positional accuracy positively correlate with number of volunteers. In our approach the number of volunteers who volunteered within a distance of one kilometer around each VP is counted. If the number of volunteers exceeded 15, the volunteered point will be assigned a weight of 0.30.

2) *Volunteers' agreement:* Majority agreement provides confidence in the VP. According to standard consensus-based approach, if contributions from multiple volunteers are available, the majority view is followed, unfortunately, such approach may cause the one in million correctly volunteered information to be lost [11]. In our proposed approach, agreement on a specific VP is considered without losing the unique VP that has no agreement by assigning weight, instead of excluding VPs. A buffer zone of radius 15 meters is created around each VP. The number of volunteers within the created

buffer is counted; indicating the number of volunteers who agreed that there is a true point in the specified location. If the number of volunteers is two or more, the volunteered point will be assigned 0.40 for its weight.

3) *Geographic context:* According to Tobler's first law in [26], a location is likely to be more similar to its surrounding area than distant area. In other word, Tobler's law suggests that information about a location should be consistent with what is already known about its surrounding area [17]. As mentioned by [12], VGI quality can be enhanced by studying the geographic context of the map's objects, however little work has been done using such an approach. Our proposed approach will consider the VPs' geographic context. Two kinds of geographic context rules are allowed to be set before VGI creation process for including and excluding VPs. Any volunteered point that violates any of the exclusion rules will be excluded. On the other hand, any volunteered point that meets the inclusion rules will be assigned 0.30 for its weight.

The VP is assigned Content Weight (CW) as shown in Table III, in case that a VP satisfied all aspects of content dimension,  $CW = 1$ . If the VP satisfied the volunteers' density aspect with any other aspect, the  $CW = 0.70$ . If the VP satisfied the volunteers' density and geographic contexts aspects,  $CW=0.60$ . If none of the aspects are satisfied the CW will be equal to zero.

**C. System Design Dimension**

Important aspects that affect VGI quality are the definition provided to volunteers about their volunteering tasks, instructions of how to create the targeted VGI accurately and the interface through which volunteers perform their volunteering tasks.

TABLE II. WEIGHT OF DIFFERENT VOLUNTEERS' TYPES

| Volunteer's Type        | VW   |
|-------------------------|------|
| City                    | 1    |
| Region-Trained          | 1    |
| Region-Untrained        | 0.75 |
| Country-Trained         | 0.55 |
| Country-Untrained       | 0.35 |
| Other-Country-Trained   | 0.25 |
| Other-Country-Untrained | 0    |

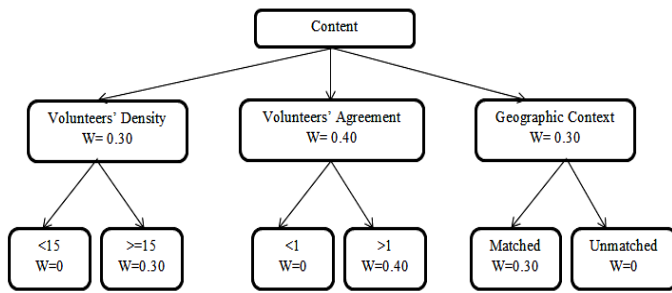


Fig. 3. Volunteered Points' Weight.

TABLE III. WEIGHT ASSIGNED TO VPS

| Content Dimension Satisfied Aspects           | Weight |
|---|--------|
| All aspects                                   | 1      |
| Volunteers' Density and Volunteers' Agreement | 0.70   |
| Volunteers' Density and Geographic Context    | 0.60   |
| Volunteers' Agreement                         | 0.40   |
| Volunteers' Density or Geographic Context     | 0.30   |
| None of the aspects                           | 0      |

1) *Definition and instructions:* In order to avoid confusing volunteers, before proceeding in and also during VGI creation process: (1) the task, its purpose and it's nature is defined and explained in a clear statement to all volunteers; (2) instructions about how to perform the volunteering task is provided to volunteers; and (3) the task's requirements and constraints is clearly specified.

2) *User interface:* A simple well-designed user interface is adopted by the proposed approach. Such design makes the VGI system clear and easy to use in order to avoid demotivating the targeted volunteers and to help them to perform their volunteering tasks accurately.

V. PROPOSED ALGORITHM

Once a volunteer inserted a VP's location on the map, the volunteer is assigned a weight according to Table II and the VP is checked against geographic context exclusion rules. If the VP violates any of the exclusion rules, it will be excluded from the VGI dataset. Otherwise, the VP will be checked if it is located inside a building or not. If the VP is located in a building, it will be included in the VGI dataset only if its volunteer is located at a distance of 100 meter or less from it. The VP is then assigned a weight according to Table III.

Volunteer's and VP's weight are then checked against each other, as shown in Table IV. The volunteers with VW equals to 1, all his/her VPs will be accepted. If VW equals to 0.75, only VPs with CW equals to (1, 0.7, 0.6, 0.4 or 0.3) will be accepted. If the VW equals to 0.55, only VPs with CW equals to (1, 0.7, 0.6 or 0.4) will be accepted. If VW equals to 0.35, only VPs with CW equals to (1, 0.7 or 0.6) will be accepted. If VW equals 0.25, only VP with CW equals to (1 or 0.7) will be accepted. Finally, if VW equals to 0, only VP with CW equals to 1 will be accepted. VP will be included in VGI dataset only if it follows Table IV, otherwise, it will be excluded.

As mentioned before, each VP is assigned two weights which are VW and CW. VW reflects the local knowledge and training skills of the volunteer, while CW reflects the volunteers' density, volunteers' agreement and if inclusion geographic context rule has been met.

The locations of all VPs which gained the weight of volunteers' agreement will be replaced by an Estimated Volunteered Point's latitude and longitude (EVP (x,y)). The EVP (x,y) is calculated as the center of area, as shown in Fig. 4, based on a computed generalized weight (wi) as follows:

$$EVP(\bar{x}) = VP \text{ latitude } x = \frac{\sum_{i=1}^n VP(y_i) w_i}{\sum_{i=1}^n w_i} \quad (1)$$

$$EVP(y) = VP \text{ longitude } y = \frac{\sum_{i=1}^n VP(x_i) w_i}{\sum_{i=1}^n w_i} \quad (2)$$

$$w_i = (VW_i + PW_i + NW_i)/3 \quad (3)$$

Where  $NW_i$  is the normalized number of VPs around each  $VP_i$  within a buffer zone of 5 meters.

$$NW_i = \frac{\text{Number of VPs around } VP_i \text{ within 5 m}}{\text{Number of VPs around } VP_i \text{ within 15 m}} \quad (4)$$

TABLE IV. VOLUNTEER WEIGHT AND CONTENT WEIGHT JOINING

| VW   | CW  |      |      |      |      |     |
|------|-----|------|------|------|------|-----|
|      | 1   | 0.70 | 0.60 | 0.40 | 0.30 | 0   |
| 1    | yes | yes  | yes  | Yes  | yes  | yes |
| 0.75 | yes | yes  | yes  | Yes  | yes  | x   |
| 0.55 | yes | yes  | yes  | Yes  | x    | x   |
| 0.35 | yes | yes  | yes  | X    | x    | x   |
| 0.25 | yes | yes  | x    | X    | x    | x   |
| 0    | yes | x    | x    | X    | x    | x   |

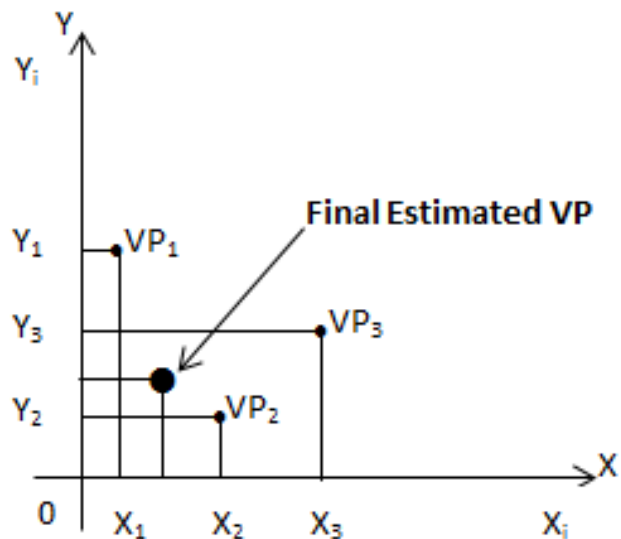


Fig. 4. Estimated Volunteered Point's Location in Case of Agreement.

The steps of the proposed algorithm are listed as follows:

| The Proposed Algorithm |   |
|------------------------|---|
| 1.                     | Volunteer inserts a VP's location on the map  |
| 2.                     | Volunteer is assigned a weight (VW) according to Table II   |
| 3.                     | IF (VP violates any geographic context rule) THEN   |
| 4.                     | Exclude VP from VGI dataset   |
| 5.                     | END IF  |
| 6.                     | IF (VP is located inside a building) AND (Volunteer is within a distance of 100 m or less from the VP) THEN |
| 7.                     | Include VP in VGI dataset   |
| 8.                     | ELSE  |
| 9.                     | Exclude VP from VGI dataset   |
| 10.                    | END IF  |
| 11.                    | VP is assigned a weight (PW) according to Table III   |
| 12.                    | IF (VW and PW follow Table IV) THEN   |
| 13.                    | Include VP in VGI dataset   |
| 14.                    | ELSE  |
| 15.                    | Exclude VP from VGI dataset   |
| 16.                    | END IF  |
| 17.                    | IF (there is volunteers' agreement on a certain point feature)  |
| 18.                    | FOR each agreed VP <sub>i</sub>   |
| 19.                    | Compute NW <sub>i</sub> according to (4)  |
| 20.                    | Compute w <sub>i</sub> according to (3)   |
| 21.                    | END FOR   |
| 22.                    | END IF  |
| 23.                    | Compute EVP ( $\bar{x}$ ) according to (1)  |
| 24.                    | Compute EVP ( $\bar{y}$ ) according to (2)  |
| 25.                    | Replace all agreed VPs' longitude and latitude with EVP( $\bar{x}$ , $\bar{y}$ ) in VGI dataset             |

## VI. CASE STUDY

In order to prove the feasibility and the applicability of the proposed approach a case study has been conducted. A VGI mobile application that adopts the proposed approach and algorithm has been developed and published on Google play store, see Fig. 5. The aim of the developed application is to collect volunteered data about the locations of automated teller machines (ATMs) for a specific bank in Cairo, Egypt. The volunteers were asked to locate the ATMs on the application's map. The developed application has a user friendly interface which is clear, simple and easy to use. Before proceeding in their tasks, the volunteers were provided detailed information about the aim and the purpose of the application. A detailed instructions before and during using application were available to volunteers.

First, we identified rules for the geographic context of the targeted point features (ATMs) as follows:

### A. Exclusion Rules

- Rule 1: The ATMs are within Cairo boundaries.
- Rule 2: The ATMs is not within the location of any other banks' buildings.
- Rule 3: The ATMs is not within the location of other bank's ATM.

- Rule 4: The ATMs is not within any water surfaces (e.g. rivers, and seas).

### B. Inclusion Rules

- Rule 5: The ATMs are within the location of the specified bank.
- Rule 6: The ATMs are within area that is categorized as a business area (e.g. shops centers).

The volunteers were then invited to register to the application and while registering they were asked to indicate their residence location. Before proceeding to contribute, an instruction page was displayed to the volunteer in order to identify exactly the volunteering task and it's purposes and also to indicate the requirements needed for that task (to turn on GPS and Wi-Fi).

Once registered, the volunteers were able to contribute by adding the location of the ATMs that they know or deal with on the map. A volunteer was also able to view, edit and delete other volunteers' contributions. Each function that can be performed on the application (contribute, view, edit or delete) has an instruction page to guide the volunteers how to perform it accurately. While volunteering the volunteer's position was caught and saved in the application's database. We had around 300 VPs from 45 volunteers. Ten volunteers have been trained before using the application on how to use the application efficiently, how to locate ATMs on the map accurately, and some illustrative examples were shown to them.

## VII. RESULTS AND DISCUSSION

We compared the VPs' dataset with a reference dataset that contain the real positions of the investigated point feature (ATMs). First, a buffer zone of radius 50 meters was created around each VP in the VGI dataset. Second, the distance between the VP and ATMs in the reference dataset within the created buffer, is measured using Euclidean distance and the nearest ATM is detected as a matched point. We evaluated the spatial errors for each VP and matched ATM, see Table V.



Fig. 5. Part of VPs on Application's Map.

TABLE V. SPATIAL ERRORS STATISTICS OF VOLUNTEERED ATMS

| Spatial Error (m) |          |          |                    |                          |
|-------------------|----------|----------|--------------------|--------------------------|
| Min.              | Max.     | Mean     | Standard Deviation | Coefficient of Variation |
| 0                 | 5.761835 | 2.410364 | 1.336997           | 55.46868 %               |



The minimum spatial error is zero which means that ATM's position has been located accurately. The maximum spatial error is 5.761835; indicating that our VPs' data set has no outliers. The mean of spatial errors is 2.410364; by considering the average accuracy of GPS devices (6-10 meters), all VPs' location can be considered as highly accurate. Finally, the standard deviation is 1.336997 and coefficient of variation is 55.46868 %.

We compared our results with the results of a previous study that aimed to assess the positional accuracy of point features in other VGI systems which is OpenStreetMap [14], the coefficient of variation shows that our approach has significantly decreased the spatial heterogeneity of the final VPs' dataset and the mean shows that our proposed approach increased the positional accuracy of VGI point features.

Unlike previous related work, our proposed approach is concerned specifically about controlling positional accuracy of point features; it increases positional accuracy and decreases spatial heterogeneity of such features. Furthermore, our proposed approach overcomes the limitations of the previous related work: (1) the proposed approach does not mainly depend on linus law, where it is concerned also about volunteers' quality and geographic context; (2) It does not depend on an external factor as a gatekeeper or a moderator; (3) It provides the flexibility of adding any suitable and available geographic contexts rules to get the benefit of using geographical knowledge to detect the reasonability of VGI; (4) It provides also the flexibility to deal with various types of volunteers regardless their experience or reputation without excluding any volunteers' contribution; (5) the proposed approach can be adapted to be suitable for various contexts.

### VIII. CONCLUSIONS

VGI quality is an obvious challenge that limits VGI usage and integration with authoritative datasets. The previous literature primarily focuses on assessing and evaluating VGI quality with few efforts concerned about VGI quality assurance and control. The previous literature lacks effort to control positional accuracy of point features in specific. In order to fill this gap an approach to control the positional accuracy of VGI has been proposed and a case study has been conducted to prove the applicability and effectiveness of the proposed approach.

### REFERENCES

- [1] M. Goodchild, "Citizens as sensors: the world of volunteered geography," *GeoJournal*, vol. 69, pp. 211-221. 2007.
- [2] H. Zhang, and J. Malczewski, "Quality evaluation of volunteered geographic information: The case of OpenStreetMap," *Volunteered Geographic Information and the Future of Geospatial Data*, pp. 19-46, 2017.
- [3] J. Meier, "An analysis of quality for volunteered geographic information," thesis, Wilfrid Laurier University, Waterloo, Canada, 2015.
- [4] M. Eshghi, and A. Alesheikh, "Assessment of completeness and positional accuracy of linear features in Volunteered Geographic Information (VGI)," in *International Conference on Sensors & Models in Remote Sensing & Photogrammetry*, 2015, p. 169.

- [5] M. Haklay, S. Basiouka, V. Antoniou and A. Ather. "How many volunteers does it take to map an area well? The validity of Linus' law to volunteered geographic information," *The Cartographic Journal*, vol. 47, pp. 315-322. 2010.
- [6] A. Flanagan, and M. Metzger, "The credibility of volunteered geographic information," *GeoJournal*. vol. 72, pp. 137-148. 2008.
- [7] L. See, et al. "Crowdsourcing, citizen science or volunteered geographic information? The current state of crowdsourced geographic information," *ISPRS International Journal of Geo-Information*, vol. 5 .2016.
- [8] L. Criscuolo, et al., *Handling quality in crowdsourced geographic information*. European Handbook of Crowdsourced Geographic Information. London: Ubiquity Press,2016.
- [9] P. Van Oort, "Spatial data quality: from description to application", thesis, Wageningen University, Wageningen, Netherlands. 2006.
- [10] J. Drummond, J. "Positional accuracy," *Elements of spatial data quality*, pp. 31-58. 1995.
- [11] G. Foody, et al. "Accurate attribute mapping from volunteered geographic information: issues of volunteer quantity and quality," *The Cartographic Journa*, vol. 52, pp. 336-344. 2015.
- [12] A. Vandecasteele, and R. Devillers, "Improving volunteered geographic information quality using a tag recommender system: The case of OpenStreetMap," *OpenStreetMap in GIScience*, pp. 59-80, 2015.
- [13] M. Haklay, "How good is volunteered geographical information? A comparative study of OpenStreetMap and Ordnance Survey datasets," *Environment and planning B: Planning and design*, vol. 37, pp. 682-703. 2010.
- [14] S. Jackson, et al. "Assessing completeness and spatial error of features in volunteered geographic information," *ISPRS International Journal of Geo-Information*, vol. 2, pp. 507-530. 2013.
- [15] D. Bégin, R. Devillers and S. Roche, "Assessing Volunteered Geographic Information VGI quality based on contributors' mapping behaviours," in *Int. Arch. Photogramm. Remote Sens. Spat. Inf. Sci*, 2013, p. 149.
- [16] E. Raymond, "The cathedral and the bazaar," *Knowledge, Technology & Policy*, vol. 12, pp. 23-49. 1999.
- [17] M. Goodchild, and L. Li, "Assuring the quality of volunteered geographic information," *Spatial statistics*, vol. 1, pp. 110-120. 2012.
- [18] H. Vahidi, B. Klinkenberg,, and W. Yan, "A fuzzy system for quality assurance of crowdsourced wildlife observation geodata," In *IEEE 2017 International Electronics Symposium on Knowledge Creation and Intelligent Computing (IES-KCIC)* , 2017, P. 55.
- [19] S. Ghosh, et al. "Crowdsourcing for rapid damage assessment: The global earth observation catastrophe assessment network (GEO-CAN)," *Earthquake Spectra*, vol. 27, pp. 179-198. 2011.
- [20] L. See, et al. "Comparing the quality of crowdsourced data contributed by expert and non-experts," *PloS one*, vol. 8. 2013.
- [21] M. Schwind., K. Davis, and P. Baldrige. "Analyzing volunteer geographic information accuracy and determining its capabilities for scientific research data," *Honors and Undergraduate Research*. 2014. Available electronically from <http://hdl.handle.net/1969.1/152055>.
- [22] M. Eckle, and P. de Albuquerque, "Quality assessment of remote mapping in OpenStreetMap for disaster management purposes," in *ISCRAM conference*. 2015.
- [23] M. Van Exel, E. Dias, and S. Fruijtier, "The impact of crowdsourcing on spatial data quality indicators," in *Proc. of the GIScience*, 2010, p.14.
- [24] V. Antoniu, "Volunteered geographic information measuring quality, understanding the value," *GEOmedia*, vol. 20, pp. 38-45, 2016.
- [25] P. Neis, D. Zielstra and A. Zipf, "Comparison of volunteered geographic information data contributions and community development for selected world regions," *Future Internet*, vol. 5, pp. 282-300. 2013.
- [26] H. Miller, "Tobler's first law and spatial analysis," *Annals of the Association of American Geographers*, vol. 94, pp. 284-289. 2004.

# Android Security Development: Spyware Detection, Apps Secure Level and Data Encryption Improvement

Lim Wei Xian<sup>1</sup>, Chan Shao Hong<sup>2</sup>, Yap Ming Jie<sup>3</sup>, Azween Abdullah<sup>4</sup>, Mahadevan Supramaniam<sup>5</sup>  
Taylor's University Lakeside Campus, School of Computing & IT (SoCIT), Subang Jaya, Selangor, Malaysia<sup>1, 2, 3, 4</sup>  
Research and Innovation Management Center, SEGi University, 47810 Petaling Jaya, Selangor Darul Ehsan, Malaysia<sup>5</sup>

**Abstract**—Most Android users are unaware that their smartphones are as vulnerable as any computer, and that permission by Android users is an important part of maintaining the security of Android smartphones. We present a method that uses manifest files to determine the presence of spyware and the security level of apps. Furthermore, to ensure that no leaked data occurs in Android smartphones, we propose new method for the encryption of data from Google Suite applications.

**Keywords**—Android; spyware detection; security level index; data encryption

## I. INTRODUCTION

In 2017, Android accounted for 85% of the smartphone market, and the Android operating system was also the most popular. However, Android is an open-source operating system that is often targeted by malicious software. In 2017, there were more than 3.5 million malware applications [1]. Since the development of Android 6.0 in 2015, Android has required permission for apps considered dangerous, and users can revoke this permission at any time [2].

The aim of the “Android Security Development” project is to provide a safer environment for Android smartphone users by detecting spyware more efficiently and effectively, prevent the leakage of personal information from Android smartphones, and raise awareness regarding permission for apps downloaded by Android users. Personal information in smartphones may include contacts, calendar schedule, and location, to name a few.

The first goal of this project was to prevent users from having spyware implanted in their smartphones and to prevent users from downloading malicious applications that cause their personal information to be leaked. As users may not be aware when their smartphones have been implanted with spyware or when they are downloading a malicious application, requiring permission does not effectively protect Android users' smartphones. As such, a spyware detection system is urgently needed that can detect and prevent malicious applications from being downloaded. We developed a Spyware Detection System that can alert users that a specific application has been implanted with spyware.

The second project goal was to provide an application security level index for users to access details about applications. With this index, users can assess the level of risk associated with using applications and be more informed regarding the permission request. The Application Security

Level Index is a software program that can produce a report about the type of permission required, as well as the risk of specific data being leaked if permission is given for the application. The Application Security Level Index will be in place before the application is available at the Google Play store.

The third goal was to implement Hybrid, which encrypts data from Google Suite to Google's server. We called it Hybrid because the process of encryption uses two encryption methods, both the Advanced Encryption Standard (AES) and the RSA encryption method. AES performs symmetric-key algorithm encryption and RSA asymmetric key algorithm encryption. With these two encryption methods, the data being transferred can be made sufficiently secure. Hence, users need not worry that their data is being leaked during its transmission.

In summary, the “Android Security Development” target audience is all those who use Android smartphones. With these three implementations, we provide our target audience with a safe and more secure environment for their Android smartphones. This paper is presents in ten sections, including the Introduction, Related Work, Architecture Diagram, Method for Detecting Android Spyware, Method for Implement Application Security Level Index, Method for Hybrid-Cryptosystem, Experiment Setup, Experiment Results, Critical Analysis and Conclusion and Future Work.

## II. RELATED WORK

### A. Android Permission Mechanism

Android is an operating system which used widely on billions of different devices, such as smartphones, tablets, wearable devices and intelligent appliances. However, such flexible supply of applications which causes vulnerable applications and malware easily obtains by users [3].

Various security mechanisms used in Android such as sandbox and permissions to solve Android related security threats. However the results of these security mechanisms are not satisfactory, as the malicious activities still targeting the Android applications. Android has improved the permission scheme since Android version 6 Marshmallow benefiting Android current users [3].

The permission mechanism in Android is to achieve a better security to Android platform. The permission mechanism is designed to separate the system and the

applications, which application have limited access to the system. The permission mechanism is essentially mandatory in Android control system based on permission labels, which will check the specific application, have the specific permission when attempting to access the protected resources such as gallery, phone and contact. Therefore the applications which needed 35 permissions is require to declare in its AndroidManifest.xml files and is mandatory to receives approval from the users to use the protected resources [3].

Furthermore, there is around 140 standard permissions in Android for protecting corresponding resources in an Android device. All the 140 permissions are classified into several categories which based on its sensitivities. Dangerous permissions are further grouped based on the functional relationship, for example, "READ\_SMS" and "RECEIVE\_SMS" permissions are comprise of "SMS" group. Moreover, permission system is workable on third party applications if their developers self-created permissions or apply standard to the interface of their applications [3].

Although, Android have permission system, permission protected resources are still contains vulnerabilities. Permission leak vulnerabilities is quite normal in third party applications, since the application is written by developers which are insufficient security background [3].

### B. Android Request App Permissions

According to the Android developer website [2], every Android mobile application that requires a permission must put a <user-permission> element in the app manifest at the top level in the project view as a <manifest> element. For example, an app that requires permission to send SMS messages would have a code in the manifest such as that shown in Fig. 1.

Basically, the Android permission system is divided into various protection levels based on the sensitivity of the app requiring permission. Some permission that are considered "normal" or that must use permissions is not affected very much by the system. However, if permission is listed as "dangerous," the system will prompt the user to explicitly grant the app access. The protection levels of Android permissions that affect third party apps are categorized as either normal, signature, or dangerous. These protection levels are also affected whether or not a runtime permission request is required.

The ability of users to revoke their permission for any app at any time became available only with the introduction of Android 6.0 (API Level 23). For example, if gallery permission was given by a user for an application yesterday, it would only be valid for that day. If the application wanted to access the gallery again, it must request permission once again.

In another example, if an application wanted to request permission to access the calendar, a method known as the "ContextCompat.checkSelfPermission ()" method is called, as shown in Fig. 2.

If the corresponding app has permission to access the calendar, the method shown in the figure above will return PERMISSION\_GRANTED, and only then can the application proceed to make changes in the calendar. However, if the

corresponding application does not have permission, this method will return PERMISSION\_DENIED, and the application must explicitly ask for user permission.

The reason Android has implemented this permission mechanism in the developer is to allow users to know which information apps are accessing their data and why corresponding apps need to access it. For example, if a user frequently denies permission requests by an app, this probably means that the user does not understand the reason the application is requesting such permission, and the user considers that the app does not need this access.

### C. Android Permission Groups

The Android web area [4] shows that Android categorizes all of its permissions group by group. With our proposed system, permission requests are in charge at the group level and single permission groups correspond to several permission declarations in the app manifest. For example, the CALENDER group includes both READ\_CALENDER and WRITE\_CALENDER declarations. Fig. 3 shows an architectural view of how a permission group works [4].

```
<manifest xmlns:android=  
    "http://schemas.android.com/apk/res/android"  
    package="com.example.snazyapp">  
  
    <uses-permission android:name=  
        "android.permission.SEND_SMS"/>  
  
    <application ...>  
        ...  
    </application>  
  
</manifest>
```

Fig. 1. Code to Request Permission [2].

```
if (ContextCompat.checkSelfPermission(thisActivity,  
    Manifest.permission.WRITE_CALENDAR)  
  
    != PackageManager.PERMISSION_GRANTED) {  
    //Permission is not granted  
}
```

Fig. 2. Code to Check for Permission [2].

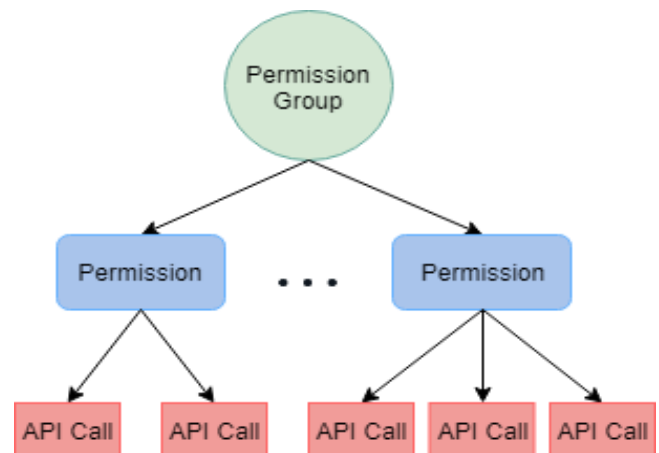


Fig. 3. Permission Group Architecture [4].

Permission groups in Android include all dangerous permissions. Although any permission that can belong to a permission group is assigned a protection level, a permission group only affects dangerous permissions that might affect the user experience, such that the system will protect the user's privacy.

#### D. Structure of Android Application Packages

Android applications are in APK file format. Fig. 4 shows that each APK file contains four important files, which include AndroidManifest.xml, classes.dex, META-INF, and resource files. Of these files, AndroidManifest.xml and classes.dex are often used in evaluating and analyzing threats and vulnerabilities [5].

The AndroidManifest.xml file contains application information described in XML, which is stored in binary form. Android Studio and Apktool can extract information from the AndroidManifest.xml file. Table I shows the main information stored in AndroidManifest.xml [5].

Android permissions in AndroidManifest.xml are categorized into three levels: normal, dangerous, and signature. Dangerous permissions will require approval from users. The version of Android operating system being used will determine the number of permissions requested [5]. Forty-four Android apps are in Java language and compiled in Java bytecode. These Java bytecodes are translated into Dalvik bytecode and stored in Dalvik executable format (DEX), for example in classes.dex. Dalvik bytecode enables code analysis without the use of source code, and it is also reverse-engineer friendly. APK files are stored in binary and since they are zip files, APK files cannot be analyzed directly. The Apktool has the ability to convert AndroidManifest.xml into text. So the bytecode in classes.dex can be reverse engineered to produce Smali code, a type of bytecode that is in human readable style and is useful for analysis [5].

#### E. Sandbox

Sandbox is a security mechanism for isolating app resources from each other to reduce system failures or the spread of malicious applications and to protect apps and the system from other malicious applications [6][7]. In general, a sandbox will allow an application to run in an isolated computing environment with limited resources. To use sandbox, Android assigns a unique user ID for each Android application and allows it to run its own process.

Sandbox is frequently used to run untrusted code or unverified programs obtained from third market applications that may contain malware. Typically, to run unfamiliar applications, sandbox will control resources, such as limiting the space for memory and permission access. In Android, the programmer must manually code the application that runs within the sandbox, so that the application will not be able to perform any unpermitted actions such as reading smartphone information without permission or any other malicious actions.

For example, if application A is downloaded from an untrusted source and tries to perform a malicious action, such as accessing a smartphone contact or gallery without permission, the Android operating system will prohibit this

action since application A does not have the required permission.

#### F. SafeGuard

Safeguard is a real time anti-malware application that detects and blocks suspicious or malicious actions and behaviors. The SafeGuard database frequently updates types of malware threats and blocking rules. In general, SafeGuard monitors all applications that are running on the Android operating system in real time. If the SafeGuard library detects behavior that uses an API or combination of APIs, the database will detect it and alert the user [8].

As Android is an open-source operating system, its security is weaker and more vulnerable to attack. Most Android applications use Java as the official programming language, which makes it easier to use reverse engineering to allow the injection of malicious code and rewriting of code. This means Android users are at greater risk than those who use Apple's App Store [8]. Although normal signature-based detection can be used to easily detect malware from source code, malware is evolving rapidly. In addition, Android has developed and applied a new security model called Sandbox that prevents access by one application to other applications, based on the unique share ID created for all applications and those running in the virtual environment.

SafeGuard detects suspicious APIs such as accesses to GPS, conversation histories, galleries, private information etc. in real time. It then instructs users to block those malicious behaviors to protect their personal information. In addition, SafeGuard expands the reach of the behavior detection mechanism corresponding to the malicious behavior type against the target application and API behaviors. Moreover, SafeGuard is constantly being updated via the Internet to keep the database up to date and able to deal with the limitations of anti-virus software and prevent malicious activity by malicious applications. To deal with new malware that dynamically fetches codes, a heuristic detection method has been proposed that detects both original and dynamic codes. In existing mobile anti-virus software, old malware can be easily detected, but new malware is difficult to screen. To address this problem, SafeGuard monitors application behavior and the calling of malicious APIs in real time. If an application breaks a behavior-based rule, SafeGuard will block the application from running.

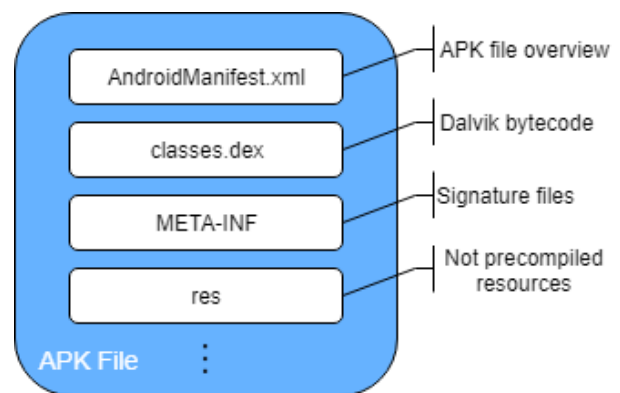


Fig. 4. APK File Structure [5].

TABLE I. ANDROID PERMISSION

| Tag Name        | Content  |
|-----------------|--|
| Application     | General configuration of application, such as icons, labels, and display theme |
| Uses-sdk        | Range of API levels needed to run the application                              |
| Uses-permission | Permissions requested by the application                                       |
| Uses-library    | Libraries used by the application  |

### G. Types of File Analysis

There are two main major file analysis method, which are static analysis and dynamic analysis, which combine can become hybrid analysis. Static file analysis can inspect the files inside an APK file. AndroidManifest.xml and classes.dex contain data which are suitable use for analysis. The permission request information which are in Android Manifest.xml and can be extracted [5][9].

Static analysis is focus on application's code analyses without executing the code [10]. There are already quite many static analysers that can analyse Java source code, as we know that Android mobile application is wrote in Java language. Nevertheless, most of the static analysers are based on syntactical analyses or will use theorem providing some simplifying hypotheses. Unfortunately, most of the static tools do not support technologies such as XML, which will affect the control flow graph of an Android app, as we know that Android Manifest is a XML file type. However, Julia static analyser performs a semantic sound analysis. First of all, the apps are reverse engineer using dex2jar to able to extract the Java bytecode and will have apktool to extract the Android Manifest. The Android Manifest is use to determine the entry points for parsing the Java bytecode of the app [11].

The Julia analyser library provides a representation of Java bytecode which is suitable for interpretation (Mandal, Cortesi, Ferrara, Panarotto, & Spoto, 2018). Julia analyses the Java source code, which are already compiled into Java bytecode inside Android Studio [12].

Dynamic analysis is the analysis that analyses the executing application on real time. It mainly focus on the behaviour of the application [8]. A dynamic analysis which presented by Taint Droid which it monitors the privacy of Android devices at real time by using privacy-sensitive data sources. Droid Box has extended the functionality of Taint Droid by modifying the Android framework; it can monitor the interesting API calls invoked by an application. It executes the application, and produce log of the behaviour that in the host operating system. After the executing which produces a more accurate analysis, however these approaches still contain problems which are overhead and require modification in the operating system and can cause a large part of Android users cannot use the system [13].

A type of Hybrid analysis called FlowSlicer, mixes a conservative static analysis with a dynamic analysis. The FlowSlicer allows a control over Android malicious applications with lower overhead and high accuracy. The idea behind FlowSlicer is that the static analysis use in filter elements that are important, while the dynamic analysis is use

during the executing of application. The techniques used in the static analysis are instrumentation and program slicing are used while the techniques used in dynamic analysis is a tagging architecture [13].

Program slicing is a type of static analysis that has been used in many different purposes, such as information flow, software maintenance, program analysis and optimization. Program slicing is used in FlowSlicer with the objective of filtering and identifying the possible information-flow leaks in order to do a better analysis. Program slicing is a technique that creates an executable slice of the original program. Only the needed statement from the original program will be slice out, known as slicing criterion. FlowSlicer will discover the dependencies of each statement present in the reachable methods [13].

### H. Advanced Encryption Standard (AES)

AES is a popular and widely used algorithm [14] that replaced DES following a public call in 1997 by the U.S. National Institute for Standards and Technology (NIST). The reason Triple-DES was replaced is that it required that DES be run three times to complete the encryption process, which it is not efficient, so a new and more efficient standard was needed. AES is a symmetric-key algorithm that uses the same key for both the encryption and decryption of data. The security of AES is directly proportional to the size of the key and the security level. This means that the longer the length of the key, the stronger the security. However, when the key is long, it also becomes slower.

### I. Rivest-Shamir-Adleman (RSA)

RSA is a cryptosystem that is popular for securing the transmission of data by generating a public and a private key that are mathematically linked to each other but cannot be derived from each other [15]. It is an asymmetric algorithm, meaning that it consists of two different keys, one public and the other private. The public key can be given to everyone, whereas the private key must be kept private or given only to authorized personnel. Public keys encrypt data that can only be decrypted by the matching private key.

RSA works by multiplying two large prime numbers to produce a difficult form such that decryption is infeasible. Even with the best computers or super computers today, breaching the security of data being transmitted remains infeasible due to its complexity and large size. As technology continues to improve day by day, the ability to factor larger and larger numbers has also increased. As such, increasing the strength of data security becomes directly proportional to the size of the key, whereby the larger the size of the key, the stronger the security.

J. Objective

In Google Play Protect, there are still many flaws in their machine learning in terms of Spyware Detection. Spyware might not always be active as there passively infecting in the system without doing anything harmful at all to the infected system. However, once given command, the Spyware will only send the file to outside system. Because of this, the Spyware Detection is to be implemented. Secondly, the main idea of implement Application Security Level Index, is because of the current Android application's permission is not obvious on the application page; hence the implementation of Application Security Level Index is to create awareness for all the Android users, which the current system have not implemented. Thirdly, the reason why this hybrid-cryptosystem is to be implemented is mainly because, they were only a simple encryption using Application Level Transport Security (ALTS) between the transmission channels of Android user's phone to the server of Google. And so hybrid-cryptosystem is to make sure that the transmission channels between Android user's phone and the server of Google to be secure, so that the information and data being transmitted through the transmission channel will be able to be secured also to be able to prevent any man-in-the-middle to be listening and stealing information and data.

III. ARCHITECTURAL DIAGRAM

Based on Fig. 5, starting from the left, which shows the developer of an app or apps, an app is published on the Google developer console via the Internet, is then connected and configured with the Google Services Cloud Server. The

app is in the file format of .apk file. The app will then go through our implementation, which is a software of combine the Application Security Level Index and Spyware Detection mechanism.

Next, our software will use Apktool to reverse engineer the apk file, after the reverse engineer the apk file will produce few files, but in our implementation, we just used the AndroidManifest.xml file for our Android Security Level Index and Spyware Detection mechanism.

Furthermore, will have two separate parts which are Application Security Level Index and Spyware Detection mechanism. Regarding to Application Security Level Index, the Android uses permission is extracted out from the AndroidManifest.xml, and our program will analyses the extracted uses-permission and produce a permission report. For the Spyware Detection mechanism, the program will extract specific information from the AndroidManifest.xml. The program will then compare with a list of keyword list and produce a result which identify whether the apps is benign or malignant from spyware.

After completing this process, it will produce a permission report and download approve for the app, and the app with permission report and download approve will be passed on to Google Play and then be published in the Google Play Store. The Google Play Store in the end user's devices is connected to Google Play Services. So, if the application requires updates, it will provide information to Google Play Services, which is connected to the Google Developer Console so the app developer can update the application.

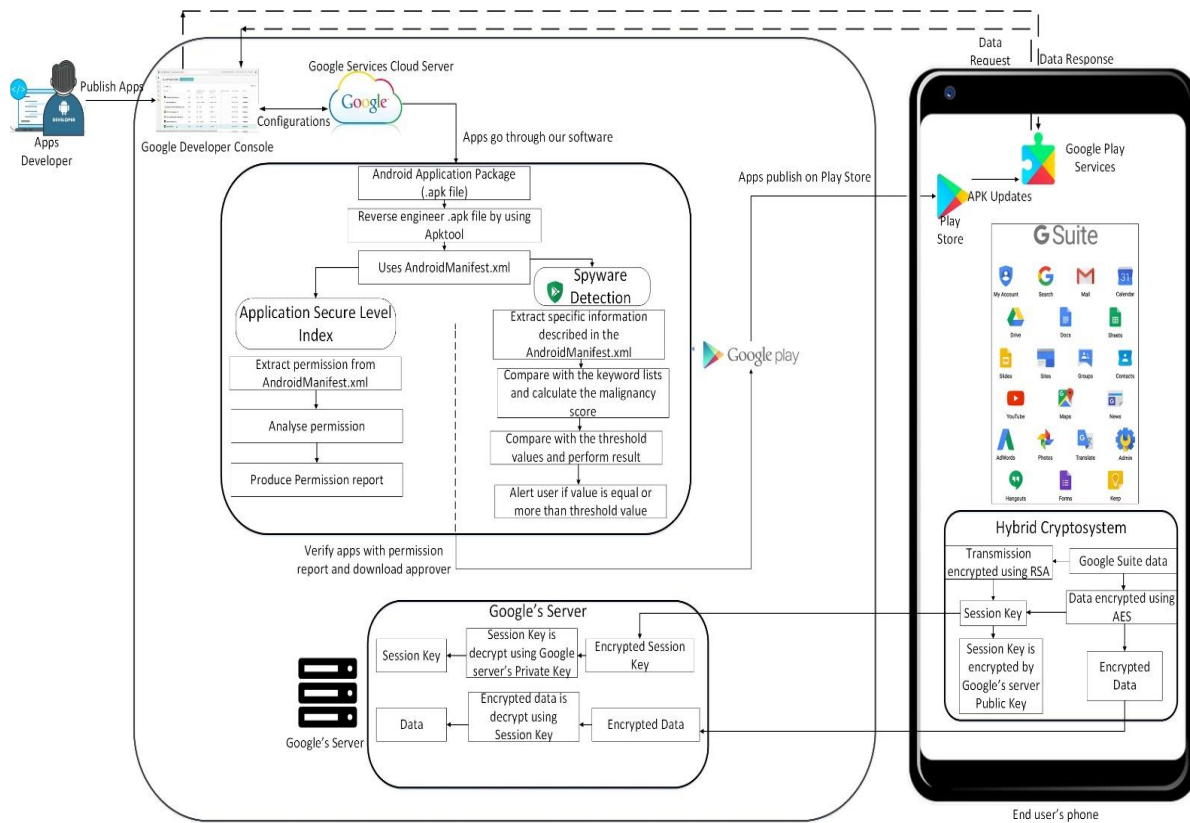


Fig. 5. Architectural Diagram of our System.

The last implementation, Hybrid Cryptosystem, is invoked when there are quite a number of Google Suite apps in Android OS devices that contain Google Search, Gmail, Google Account, YouTube, etc. These apps contain important information about the user of the smartphone. Hence, the Hybrid Cryptosystem will encrypt messages sent from the end user phone to Google’s server.

IV. METHOD FOR DETECTING ANDROID SPYWARE

Our proposed method for detecting Android spyware analyzes AndroidManifest.xml files. The Android application package known as an APK file (.apk) contains the manifest file, application program for the Dalvik virtual machine (VM), and application resources. The manifest file takes the form of “AndroidManifest.xml,” which occurs in all Android applications, while the application program is known as “classes.dex.” Application resources contain pictures, music, and some xml files that provide layout information.

Android malware is detected by following the steps shown in Fig. 6:

- Extract specific information in the AndroidManifest.xml of the APK file.
- Compare the extracted information with that in the keywords list provided by our new method. Then, calculate the malignancy score of the sample by comparing the information in Step 1 with the list.
- Compare the malignancy score in Step 2 with the threshold values established by this new method. If the malignancy score exceeds the threshold value, the sample is judged to be malware.

A. Extraction of Information Items

Manifest files contain essential information about Android applications, such as the version number of the application, the name of a package, required permission, and the API level. The format of the manifest file is identical in benign and malicious applications. However, there are certain differences in the characteristics of several information items. In our research phase, we investigated benign and malware samples and obtained a total number of samples. We then selected specific information items that showed a wide variety of spyware as compared to benign applications. Based on our results, Table II shows six information items that are extracted from manifest files and used by our proposed method to detect Android malware. The items are represented as text strings or numbers.

B. Keyword Lists and Malignancy Score

With this new method, several keyword lists are compiled for an application. Benign or malicious strings in a manifest file are recorded in the keyword list. We generate four types of keyword lists: (1) permission, (2) intent filter (action), (3) intent filter (category), and (4) process name, as shown in Table III. Because items (5) intent filter (priority) and (6) number of redefined permissions are represented by an integer and not a text string, they have no associated keyword lists.

After we obtain the keyword lists, the malignancy score for the above four information items are calculated. This process is performed by classifying the keywords as either benign or malicious. The malignancy score is calculated using

Formula (1):

$$P = \frac{M-B}{E} \tag{1}$$

where P is the malignancy score, M is the number of malicious strings, B is the number of benign strings, and E is the total number of information items.

Of the five permissions listed in Table IV, READ\_SMS, RECEIVE SMS, and SEND SMS are recorded in the keyword list and are classified as malicious strings, as shown in Table IV. Then, the malignancy score of this sample is calculated using

Formula (2):

$$P = \frac{3-0}{5} = 0.6 \tag{2}$$

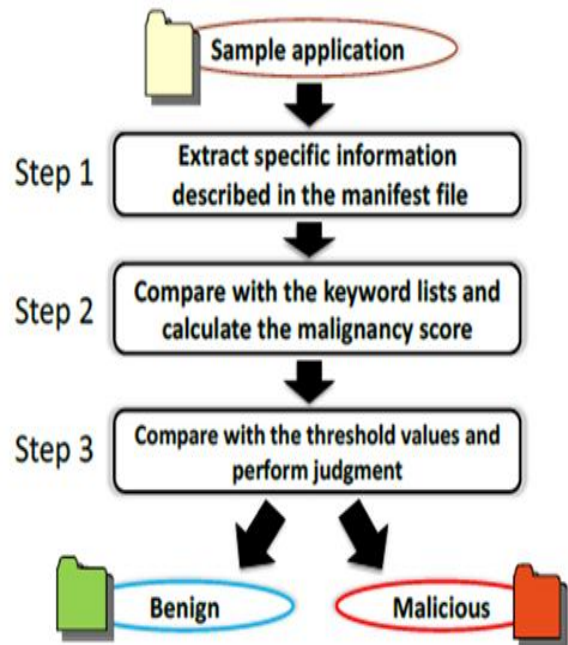


Fig. 6. Flowchart for Detecting Android Spyware.

TABLE II. LIST OF EXTRACTED INFORMATION ITEMS

| No. | Extracted information Items     |
|-----|---------------------------------|
| 1   | Permission                      |
| 2   | Intent filter (action)          |
| 3   | Intent filter (category)        |
| 4   | Process name                    |
| 5   | Intent filter (priority)        |
| 6   | Number of redefined permissions |

TABLE III. KEYWORDS LISTS

|                                   |                            |
|-----------------------------------|----------------------------|
| (List 1) Permission               |                            |
| 1. READ_SMS                       | 7. READ_HISTORY_BOOKMARKS  |
| 2. SEND_SMS                       | 8. Write_HISTORY_BOOKMARKS |
| 3. RECEIVE_SMS                    | 9. READ_LOGS               |
| 4. WRITE_SMS                      | 10. INSTALL_PACKAGES       |
| 5. PROCESS_OUTGOING_CALLS         | 11. MODIFY_PHONE_STATE     |
| 6. MOUNT_UNMOUNT_FILESYSTEMS      |                            |
| (List 2) Intent-filter(action)    |                            |
| 1. BOOT_COMPLETED                 | 8. Install_SHORTCUT        |
| 2. SMS_RECEIVED                   | 9. left_up                 |
| 3. CONNECTIVITY_CHANGE            | 10. right_up               |
| 4. USER_PRESENT                   | 11. left_down              |
| 5. PHONE_STATE                    | 12. right_down             |
| 6. NEW_OUTGOING_CALL              | 13. SIG_STR                |
| 7. UNINSTALL_SHORTCUT             | 14. VIEW (benign keyword)  |
| (List 3) Intent-filter (category) | (List 4) Process name      |
| 1. HOME                           | 1. remote2                 |
| 2. BROWSABLE (benign keyword)     | 2. main                    |
|                                   | 3. two                     |
|                                   | 4. three                   |

TABLE IV. PERMISSION KEYWORDS IN A SAMPLE

|  |
|--|
| <pre> &lt;uses-permission android:name="android.permission.INTERNET" /&gt; &lt;uses-permission android:name="android.permission.READ PHONE STATE" /&gt; &lt;uses-permission android:name="android.permission.READ SMS" /&gt; &lt;uses-permission android:name="android.permission.RECEIVE SMS" /&gt; &lt;uses-permission android:name="android.permission.SEND SMS" /&gt; </pre> |
|--|

### C. Thresholds and Judgement

The proposed method provides threshold values for the malignancy score. We use a data mining tool, Weka, to determine these threshold values. As with the four categories of information, the threshold values are set using the Weka J48 algorithm, which is based on a decision tree. We use both benign and malicious samples in the machine learning process.

Making a judgment about the safety of an application sample is based on conditions 1 and 2 and Formula (3), which are shown below. Condition 1 describes the characteristics of malware. Condition 2 is used to avoid incorrect judgments. In Formula (3), SCORE refers to the final malignancy score of the sample.

C1 and C2 are the number of items satisfied by a sample in conditions 1 and 2, respectively.

#### Condition 1:

- Malignancy score is greater than the threshold value determined by Weka.

- Count of intent filter (priority) is greater than the threshold value.
- Count of redefined permissions is greater than the threshold value.

#### Condition 2:

- Malignancy score of (2) intent filter (action) is negative (< 0)
- Malignancy score of (3) intent filter (category) is negative (< 0)

Criteria formula (3):  $SCORE = C1 - C2$

If the final score is greater than or equal to 1, the sample application is considered to be malware.

### V. METHOD FOR IMPLEMENTING APPLICATION SECURITY LEVEL INDEX

Fig. 7 demonstrates on how "Application Security Level Index" works. Fig. 7 shows in a simple way to illustrate the main process of Application Security Level Index.



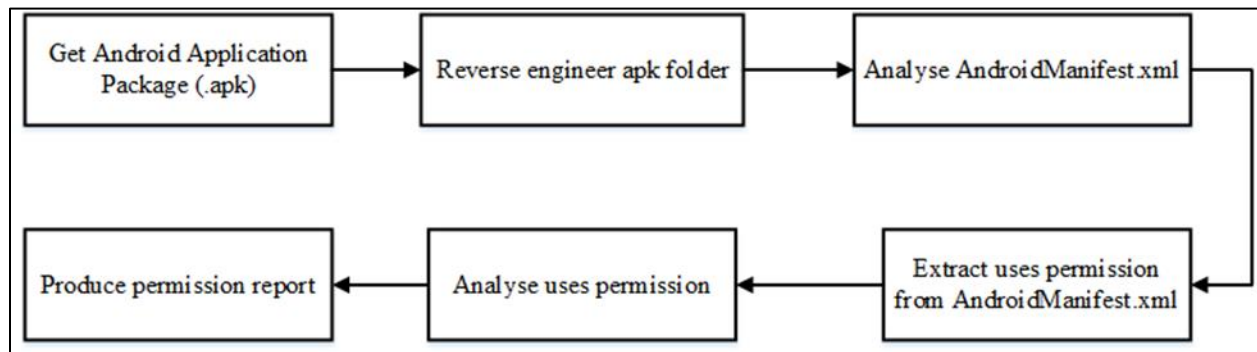


Fig. 7. Application Security Level Index's System Flow.

First of all, we will take the apk folder as an input to our system, the first step will be reverse engineer the apk folder, this is because apk folder is similar to zip folder, and cannot be unzip in a normal way, hence the purpose of reverse engineers the apk folder is to get the AndroidManifest.xml. The tool we used for reverse engineer the apk file is Apktool, which Apktool will produce the original folder, res folder, smali code folder, apktool.yml, assets folder, lib folder and AndroidManifest.xml. However, based on my system, I only need AndroidManifest.xml to analyses the Android uses permission of the apps. Hence, I will extract the Android uses permission from AndroidManifest.xml and yet analyses the permission uses. Based on the permission uses, the permission report will be ready to produce.

The purpose of permission report is to raise the awareness of Android users regarding to the permission uses for application that installed to their device. This is because based on my research, I found out that, majority of the users does not care about the permission requested from the app, as long the users can use the application. Furthermore, the nature of Google play store is also a problem. Apps description that in Google play store, does contain the permission that the specific apps require, however it is not easily to find the app permission from the description, users need to scroll all the way down to read more only can see the app permission. Moreover, the app permission does not tell the users that is the permission dangerous or normal. Hence users are not aware of dangerous permissions, such as calendar. Basically, with the app that request calendar permission, the particular app knows the schedule of users, if the users schedule is saved in the phone calendar. Here comes a bigger problem, with the technology today, people desire to make everything that around us to be simplified and convenient. Some of the smartphone users, store important data in their smartphone, for example, password, schedule, personal information such as identity card number, house address and etc. The examples above are important data

to users. That's why in Application Security Level Index's system, is to raise the awareness of smartphone' users, we cannot prevent users from saving important data with their phone, but what we can do is, to provide a solution to the users, let them conscious about the permission uses in their smartphone.

If our system is implemented, the users can see the permission report at a glance of the app description in the Google play store. With the use of our system, we basically highlighted the uses permission in Google play store, to achieve our objective.

## VI. METHOD FOR HYBRID-CRYPTOSYSTEM

Fig. 8 is the flow of the hybrid-cryptosystem. The hybrid-cryptosystem will be using Advanced Encryption Standard (AES) and RSA (Rivest-Shamir-Adleman).

The client will first generate a secret key using the AES program automatically. Then, the client will be request for a public key of their partner, so that they will be able to encrypt the secret key that is generated which will be then to be sent to their partner.

The process of sending the secret key will be encrypted by the RSA program using the formula  $CT = PT^E \text{ mod } N$  where  $N = p \times q$ , and  $p$  and  $q$  are 2 large prime number. The public key will have its value produced by the formula  $\text{gcd}(\phi(n), E) = 1; 1 < E < \phi(n)$  where  $\phi(n) = (p - 1)(q - 1)$ . Then the secret key received by their partner will be decrypted by their own private key using the formula  $PT = CT^D \text{ mod } N$ , where value of the private key is produced by the formula  $(D \times E) \text{ mod } \phi(n) = 1$ .

After the secret key has been received by the partner, the data that is needed to be sent to their partner will be encrypted using the secret key, and when the partner received the data, they will be decrypting it using the secret key.

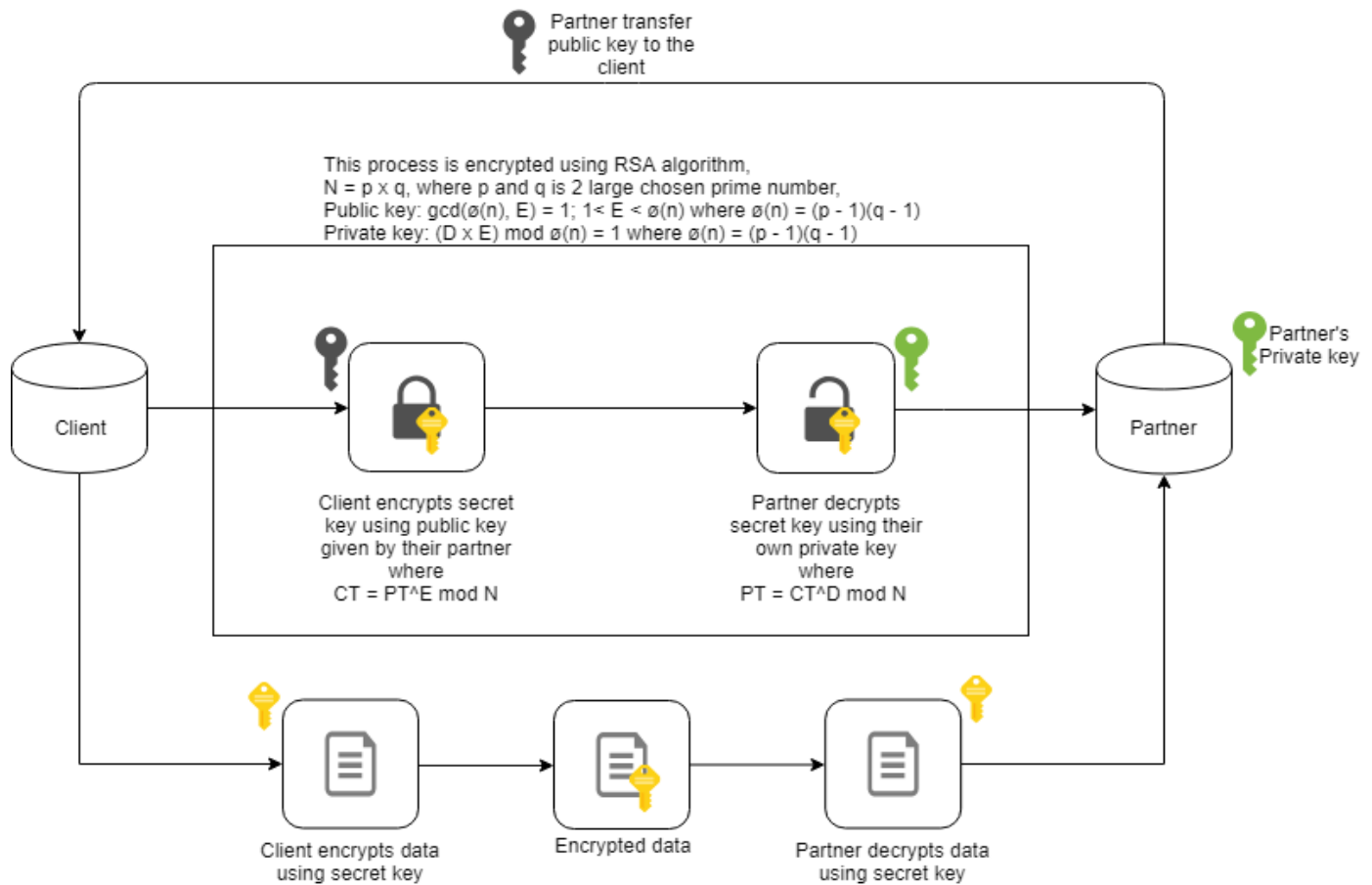


Fig. 8. The Flow of the System.

## VII. EXPERIMENTAL SETUP

### A. Experimental Setup for Second Implementation "Application Security Level Index"

For this setup we used NetBeans and Apktool [16], [17]. NetBeans is an integrated development environment for Java and Apktool is a tool for reverse engineering Android apk files. Hence, the language for our program is Java.

First, we installed Apktool on our computer via the Internet, and performed a setup on our computer to ready it for use. Next, we downloaded some popular applications used in Android devices, including WhatsApp, WeChat, Twitter, Subway Surf, Starbucks, Snapchat, Instagram, Clean Master, Clash of Clans, Google Chrome and Telegram [18] [19] [20]. These are the apps we used to test the program in this experiment.

The next step was to use the command prompt to run Apktool to reverse engineer the downloaded apps. Since the Android application package (.apk) file is actually a zip file, for our experiment, we needed to extract the AndroidManifest.xml from the apk file to analyze the Android permission used.

Fig. 9(i) shows an example of how Apktool reverse engineers the Telegram application. After the reverse engineering is complete, Apktool creates a folder name for the application, which in this case is telegram, and this folder contains res, smali, assets, lib, original, unknown, AndroidManifest.xml and apktool.yml, as shown above in Fig. 9(ii).

In our experiment we needed only the AndroidManifest.xml file. The AndroidManifest.xml file has plenty of lines of code, but our experiment requires only the Android use permissions.

First, we coded our program to analyze the AndroidManifest.xml file. This program extracted all of the Android use permissions from AndroidManifest.xml and compared them with the Android permission database we constructed of the permissions taken from Android [4]. After the comparison, we categorized the Android use permissions as either normal or dangerous. At the end of the program, two files are produced, i.e., Use-permissions.txt and report.txt. The Use-permissions file contains all the extracted Android Use permissions, and report.txt categorizes these permissions as either dangerous or normal, provides the number of permissions used, and shows the security level index. Fig. 9(iii) shows the generated Clash of Clans's report.txt.

```
C:\apktool>apktool d telegram.apk
I: Using Apktool 2.4.0 on telegram.apk
I: Loading resource table...
I: Decoding AndroidManifest.xml with resources...
S: WARNING: Could not write to (C:\Users\csh0698\AppData\Local\apktool\framework)
S: Please be aware this is a volatile directory and frameworks could go missing,
I: Loading resource table from file: C:\Users\csh0698\AppData\Local\Temp\1.apk
I: Regular manifest package...
I: Decoding file-resources...
I: Decoding values */* XMLs...
I: Baksmaling classes.dex...
I: Copying assets and libs...
I: Copying unknown files...
I: Copying original files...
```

(i) Apktool Reverse Engineer Telegram.Apk.

| Name                | Type        |
|---------------------|-------------|
| res                 | File folder |
| smali               | File folder |
| assets              | File folder |
| lib                 | File folder |
| original            | File folder |
| unknown             | File folder |
| AndroidManifest.xml | XML Docu    |
| apktool.yml         | YML File    |

(ii) Telegram Folder.

```
INTERNET,NORMAL
ACCESS_NETWORK_STATE,NORMAL
WAKE_LOCK,NORMAL
CHANGE_WIFI_STATE,NORMAL
ACCESS_WIFI_STATE,NORMAL
FOREGROUND_SERVICE,NORMAL
WRITE_EXTERNAL_STORAGE,DANGEROUS
READ_EXTERNAL_STORAGE,DANGEROUS

Total uses-permission is 8.
Total number of normal permission is 6.
Total number of dangerous permission is 2.

The application secure index is 87.0
```

(iii) Report.txt for Clash of Clans.

Fig. 9. (i) Apktool Reverse Engineer Telegram.Apk. (ii) Telegram Folder. (iii) Report.txt for Clash of Clans.

### B. Experimental Setup of Advanced Encryption Standard (AES)

An AES encryption is a symmetric-key encryption, and like the traditional door, it uses the same key to lock and unlock itself, which is also known as encrypt and decrypt in cryptosystems. The following steps show how AES Encryption works.

- Generate a key using “javax.crypto.KeyGenerator;” and “KeyGenerator”
- Encode key into files using “writeKey,” “FileOutputStream” and “write(key.getEncoded())”
- Receive the key using “getSecretKey,” “SecretKeySpec” and “Files.readAllBytes(file.toPath())” from “javax.crypto.spec.SecretKeySpec;” to be encoded as a key.
- Encrypt using “Cipher,” “SecretKey” and “Cipher.ENCRYPT\_MODE.”
- Decrypt using “Cipher,” “SecretKey” and “Cipher.DECRYPT\_MODE.”

1) *Testing:* To test that the encryption and decryption were working, we used messages “message” and “getBytes(),”

as well as “encrypted” and “decrypted,” then printed out the original message and the encrypted and decrypted messages.

a) Secret Key generated using “SecretKey” and “generateKey()”

b) Encryption and Decryption using the same key as “encrypted” and “decrypted”

c) IF (original, encrypted and decrypted message printed out without error)

Testing complete and successful

ELSE

Testing incomplete and unsuccessful.

### C. Experimental Setup of RSA (Rivest-Shamir-Adleman) Encryption

- Generate pairs of keys using “generateKey” and “KeyPairGenerator”
- Encode the pair of keys named “Public Key” and “Private Key” using “DataOutputStream” and “getEncoded()”
- Encryption method using “PublicKey,” “Cipher” and “ENCRYPT\_MODE.”

- Decryption method using “PrivateKey,” “Cipher” and “DECRYPT\_MODE”
- Re-create “PublicKey” from serialized key using “getInstance,” “KeyFactory” and “generatePublic” for “publicKeyPath”
- Re-create “PrivateKey” from serialized key using “getInstance,” “KeyFactory” and “generatePrivate” for “privateKeyPath”
- Re-create “PublicKey” from public key byte array using “getInstance,” “KeyFactory” and “generatePublic” as “encryptedPublicKey”
- Re-create “PrivateKey” from private key byte array using “getInstance,” “KeyFactory” and “generatePrivate” as “encryptedPrivateKey”.

1) *Testing*: To determine if the encryption and decryption works, a message using are working, we used the messages “data” and “getBytes()” will be used,(),” as well as “encrypted” and “decrypted” will also be used,,” then a message of printed out the original message, and the encrypted and decrypted message will be printed out messages.

a) Public Key and Private Key generated using “generateKey()”

b) “publicKey” encoded using “getPublicKey” as encrypted

c) “privateKey” encoded using “getPrivateKey” as decrypted

d) IF (original, encrypted and decrypted message printed out without error)

Testing complete and successful

ELSE

Testing incomplete and unsuccessful.

### VIII. EXPERIMENTAL RESULTS

#### A. Test Results for Application Security Level Index

TABLE V. APPLICATION SECURITY LEVEL INDEX’S TEST RESULTS

| Apk file       | AUP | NP | DP | SLI    |
|----------------|-----|----|----|--------|
| WhatsApp       | 30  | 18 | 12 | 31.00% |
| WeChat         | 30  | 19 | 11 | 35.50% |
| Twitter        | 18  | 9  | 9  | 50.50% |
| Subway Surf    | 6   | 5  | 1  | 92.50% |
| Starbucks      | 9   | 6  | 3  | 82.00% |
| Snapchat       | 20  | 12 | 8  | 54.00% |
| Instagram      | 18  | 10 | 8  | 55.00% |
| Clean Master   | 21  | 14 | 7  | 58.00% |
| Clash of Clans | 8   | 6  | 2  | 87.00% |
| Google Chrome  | 23  | 15 | 8  | 52.50% |
| Telegram       | 25  | 14 | 11 | 38.00% |

AUP = Total Number of Android Use Permissions

NP = Total Number of Normal Permissions

DP = Total Number of Dangerous Permissions

SLI = Security Level Index (where 100% is no permission use)

Table V shows the results of our program, with the apk files that we tested via our program in the left column. The results include the total number of Android use permissions, the total number of normal and dangerous permissions, and the security level index. The fewer permission requests by the application, the safer is that application. However, this does not mean that a larger number of permission requests by an application means that it is dangerous. More permission requests by an application simply mean that the specific application can access most of your phone utilities or data, which can but may not necessarily harm the end user.

Based on the above results, we found communications apps to require the most permission compared to other applications. These are apps such as WhatsApp, WeChat, and Instagram. The security level index of these applications is less than 50%, whereas the apps that request less permission include Subway Surf, the Starbucks app, and Clash of Clans, whose security level indexes are greater than 80%. By the color indicator, green indicates fewer use permissions with an index higher than 80%, yellow indicates a moderate number of use permissions with an index between 50% and 79%, and red indicates a high number of use permissions with an index less than 50%.

### IX. CRITICAL ANALYSIS

Based on the above test result from the Application Security Level Index, where shows the outcome result are expected from what we plan in the system flow. The SLI in the Table V is the index where is use to alert the end user about the specific apps that the end users installed in their device. The apps that we tested are the apps which is popular in the market and most of the public are using these apps. Although, if the SLI is indicate red color where a lot of data is used by the app, which doesn’t mean that the specific apps is dangerous, the index is indicate to the users the how much of data privacy are they exposing to the specific app developer, whether the app developer is trusted or not.

Then from the experiment test and test result from the Advanced Encryption Standard (AES) and RSA (Rivest-Shamir-Adleman) above, we use a line of text as a simulation of the real data because that we wanted to test and experiment if the cryptosystem is working. Not only that, in our experiment test, all keys included “Secret Key”, “Public Key”, “Private Key” will be generated automatically as a simulation of different key that will be used by the real application. By doing this, we assure that the code will be running successfully even with different keys. Then for the cryptography, as if the code has run successfully, meaning that the original text has been encrypted into cipher text, and the cipher text has been decrypted into plain text, it means that the code has been running successfully and the encryption and decryption is also running smoothly without errors. In the real form of data, it is

much more complicated, and then it is why we perform the simulation of data using a line of text. With our testing and results, we assure that, by just convert the text into the form of a real data, the real data will also be able to be encrypted and decrypted.

## X. CONCLUSIONS AND FUTURE WORK

In this paper, we proposed a spyware detection method for determining the security level of Play Store applications and the data encryption of Google Suite applications. Both spyware detection and apps security use only manifest files to process the results. Since manifest files are required in all Android applications, the proposed method is applicable to all Android applications. The cost of analyzing the manifest file is quite low and combined with Google Play Protect; it provides a more precise detection method. These two implementations will ensure the security of smartphones, even those free of any malware. In response to the global concern about data privacy, we have provided a data encryption method for the Google Suite applications used by most Android users.

In future work, we plan to fix those APK files that cannot be reverse engineered to obtain useful information, such as the Facebook application, to ensure that our method is applicable to all Android applications. We will closely follow trends in hacking methods to ensure that our data encryption method provides sufficient data security.

### REFERENCES

- [1] A. Arora and S. K. Peddoju, "NTPDroid: A Hybrid Android Malware Detector Using Network Traffic and System Permissions," Proc. - 17th IEEE Int. Conf. Trust. Secur. Priv. Comput. Commun. 12th IEEE Int. Conf. Big Data Sci. Eng. Trust. 2018, pp. 808–813, 2018.
- [2] "Request App Permissions | Android Developers." [Online]. Available: <https://developer.android.com/training/permissions/requesting#java>. [Accessed: 07- Nov- 2018].
- [3] Xu, Y., Wang, G., Ren, J., & Zhang, Y. (2019). An adaptive and configurable protection framework against android privilege escalation threats. Future Generation Computer Systems,92, 210–224. <https://doi.org/10.1016/j.future.2018.09.042>
- [4] "Permissions overview | Android Developers," Android Developers. [Online]. Available: <https://developer.android.com/guide/topics/permissions/overview>. [Accessed: 07- Nov- 2018].
- [5] T. Takahashi and T. Ban, "Android Application Analysis Using Machine Learning Techniques," Springer Link, 2018. [Online]. Available: [https://link.springer.com/chapter/10.1007%2F978-3-319-98842-9\\_7](https://link.springer.com/chapter/10.1007%2F978-3-319-98842-9_7). [Accessed: 05- Apr- 2019].
- [6] "Application Sandbox | Android Open Source Project," Android Open Source Project. [Online]. Available: <https://source.android.com/security/app-sandbox>. [Accessed: 11- Nov- 2018].
- [7] A. Bryk, "Sandbox-Evading Malware: Techniques, Principles, and Examples", Apriorit, 2018. [Online]. Available: <https://www.apriorit.com/dev-blog/545-sandbox-evading-malware>. [Accessed: 06- Mar- 2019].
- [8] Jeong E. S., Kim I. S. and Lee D. H., "SafeGuard: a behavior based real-time malware detection scheme for mobile multimedia applications in android platform," 2017. [Online]. Available: <https://link.springer.com/article/10.1007%2Fs11042-016-4189-1>. [Accessed: 05- Apr- 2019].
- [9] F. Shen, "Android Security via Static Program Analysis", Proceedings of the 2017 Workshop on MobiSys 2017 Ph.D. Forum - Ph.D. Forum '17, 2017. Available: <https://dl.acm.org/citation.cfm?doi=3086467.3086469>. [Accessed 7 March 2019].
- [10] L. Tuan, N. Cam and V. Pham, "Enhancing the accuracy of static analysis for detecting sensitive data leakage in Android by using dynamic analysis", Cluster Computing, vol. 22, 2017. Available: <https://link.springer.com/article/10.1007%2Fs10586-017-1364-8>. [Accessed 10 March 2019].
- [11] A. Mandal, A. Cortesi, P. Ferrara, F. Panarotto and F. Spoto, "Vulnerability analysis of Android auto infotainment apps", Proceedings of the 15th ACM International Conference on Computing Frontiers - CF '18, 2018. Available: <https://dl.acm.org/citation.cfm?doi=3203217.3203278>. [Accessed 10 March 2019].
- [12] R. Salvia, P. Ferrara, F. Spoto and A. Cortesi, "SDLI: Static Detection of Leaks Across Intents", 2018 17th IEEE International Conference On Trust, Security And Privacy In Computing And Communications/ 12th IEEE International Conference On Big Data Science And Engineering (TrustCom/BigDataSE), 2018. Available: <https://ieeexplore.ieee.org/document/8456010>. [Accessed 10 March 2019].
- [13] L. Menezes and R. Wismuller, "Detecting information leaks in Android applications using a hybrid approach with program slicing, instrumentation and tagging", 2017 International Carnahan Conference on Security Technology (ICCST), 2017. Available: <https://ieeexplore.ieee.org/document/8167856>. [Accessed 10 March 2019].
- [14] "Advanced Encryption Standard," tutorialspoint. [Online]. Available: [https://www.tutorialspoint.com/cryptography/advanced\\_encryption\\_standard.htm](https://www.tutorialspoint.com/cryptography/advanced_encryption_standard.htm). [Accessed: 10- Nov- 2018].
- [15] "RSA Cryptography Demo Applet | Holowczak.com Tutorials," Holowczak.com. [Online]. Available: <https://holowczak.com/rsa-cryptography-demo-applet/2/>. [Accessed: 27- Mar- 2019].
- [16] "Apktool - A tool for reverse engineering 3rd party, closed, binary Android apps." [Online]. Available: <https://ibotpeaches.github.io/Apktool/>. [Accessed: 27- Mar- 2019].
- [17] "Welcome to NetBeans." [Online]. Available: <https://netbeans.org/>. [Accessed: 27- Mar- 2019].
- [18] "AndroidAPKsFree - Free Apps (apk) Download for AndroidTM." [Online]. Available: <https://androidapkfree.com/>. [Accessed: 27- Mar- 2019].
- [19] "APKMirror - Free APK Downloads - Download Free Android APKs #APKPLZ." [Online]. Available: <https://www.apkmirror.com/>. [Accessed: 27- Mar- 2019].
- [20] "Download software about - Android ()." [Online]. Available: <https://en.uptodown.com/android/top>. [Accessed: 27- Mar- 2019].

# An Aspect Oriented Programming Framework to Support Transparent Runtime Monitoring of Applications

Abdullah O. AL-Zaghameem

Department of Computer and Information Technology  
Faculty of Science, Tafila Technical University, Tafila, Jordan

**Abstract**—Monitoring the runtime state and behavior of applications is very important to evaluate the performance of these applications and to inspect their behavior. In case of legacy applications that have been developed without monitoring capabilities, there is a real challenge to accomplish runtime state monitoring. This research redefines runtime monitoring concept, and then presents an Aspect Oriented Programming (AOP) framework to equip applications with the capabilities to monitor their runtime state transparently. The framework, called RM Framework, supports three monitoring modes; Invasive-mode, Controlled-mode/(Functionality and Attribute), and Controlled-mode/Selective. The framework is applied on a Java application as a case study. The results show smooth integration between application and runtime monitoring capabilities without affecting the target application consistency.

**Keywords**—Runtime state monitoring; application behavior; aspect oriented programming technique; statistical analysis; bytecode transformation

## I. INTRODUCTION

Runtime monitoring has been defined in [1] as “the act of observing an executing system in order to learn something about its dynamic behavior”. In this research, runtime monitoring, as a term, will be used to point out the state of executing application at a specific moment or during a period of time. The runtime state of an application includes information about components, amount of data processed during execution, and resource consumption; like CPU time and memory. Monitoring the runtime state of applications has several benefits like understanding and analyzing of software behavior [2, 3], detection of performance problems and bottlenecks [4-6], and building applications’ execution history and datasets [7].

Monitoring the runtime state of legacy applications is a very challenging mission. From one side, the source code of these applications most probably is unavailable, which makes it hard to perform white-box monitoring. From the other, a modular and systematic mechanism is required to perform smooth monitoring without violating the functionality and structure consistency of application. In this context, the Aspect Oriented Programming (AOP) [8] is vital and efficient technique. Because its capability to intersect the execution of

application at several points, the behavior and runtime state of that application could be inspected. In this research, the runtime state monitoring is presented as an AOP aspect, and a framework is developed to serve monitoring the runtime state of applications developed using Java™ programming language. The research is partially guided by the fundamentals of runtime monitoring presented in [3].

The paper is organized as follows: Section 2 discusses the runtime state of object-oriented applications and redefines the term “runtime state monitoring”. In Section 3, the term “Runtime Monitoring Aspect” is introduced, and a framework called Runtime Monitoring Framework is presented in Section 4. The section presents the details of framework. Section 5 applies RM framework on application as a case study. Section 6 discusses some related works. Finally, Section 7 concludes research results and lists some limitations.

## II. RUNTIME STATE OF OBJECT-ORIENTED APPLICATIONS

The “runtime state” points out the statistical and behavioral measurements of software execution at a given point of time, or during a period of time. As for statistical measurements, countable amounts of data (e.g. counters, data sizes, etc) during application execution need to be recorded and stored for further analysis. Collecting data will help answering questions like “How many times ..?” and “How much data ..?” For behavioral measurements, collecting specific data and observing links between components could facilitate the description of application behavior.

Inspecting runtime state of applications assists monitoring their performance, detecting any possible structural deformations or functional bottlenecks, and establishing execution history and test cases. In order to enable applications to record runtime state measurements, either they had been programmed to do so, or they should be *modified* and provided with the capabilities to record runtime state measurements. A real challenge arises for the second case; especially for legacy applications which their source code is missing. Providing these applications with the capability to record runtime state requires *injecting* the necessary monitoring code; taking into account not to violate application structure or functionality consistency.

### III. RUNTIME MONITORING ASPECT

To emphasize the runtime state concept and highlight its importance to software applications, the term “Runtime Monitoring” will be introduced as an AOP *Aspect*. The aspect represents the process of recording runtime state measurements. Fig. 1 illustrates a pseudo code for the Runtime Monitoring Aspect (RMA). As shown in the figure, the aspect defines four pointcuts that determine the locations (join points (JPs)) at application code where runtime state measurements need to be recorded. The first location is just before any method call. In RMA definition, JP1 represents this case. JP1 aims to collect information about the called method and the arguments passed to it to calculate the amount of data flow.

The second location is when a call to the method is completed. Information about the returned value(s) could be recorded. JP2 represents this case, where **ret** identifier points to the value returned after executing method **m**. In addition, recording successful execution of methods, as well as failed executions, is important to observe application behavior. The third important part in code that affects the runtime state of application is when new objects are instantiated. Collecting information about objects’ creation is not only important for statistical analysis, but also for monitoring application behavior and resources consumption. For this purpose, JP3 represents this concern.

In object oriented software, it is important to monitor the access of object’s fields (or attributes). In order to monitor fields’ access operations, type of access (either read or write) and the points in code at which a specific field is accessed need to be determined. For this purpose, JP4 in RMA inspects the occurrence of access operations and their types.

The definition of RMA listed in Fig. 1 is a generic case of interception. In other words, it defines how to apply runtime state monitoring overall the application functionality and behavior. For more applicability options of RMA, we suggest applying the following monitoring modes:

1) *The invasive mode*: In this mode (the default) all application components are put to monitoring. The mode represents the comprehensive monitoring if all functionalities are to be monitored.

2) *The controlled mode*: In this mode, we can monitor partial parts of runtime state. In this case, more concentration is oriented toward specific functionalities. In practice, this mode could be divided further into the following sub-modes:

a) *The Functionality Mode*: In which only objects’ methods are monitored for the sake of recording statistical data about application behavior and data flow.

b) *The Attribute Mode*: This mode targets the monitoring of object’s fields. It records measurements about fields’ access operations. This mode can help tracking the access of objects’ fields and how their values changed over runtime.

c) *The Selective Mode*: This mode could be considered as a custom mode. It supports the monitoring of the access of specific fields, and the execution of specific methods. This specialized mode provides the flexibility to monitor complex and large-scale applications as individual parts.

```

Aspect Runtime_Monitoring_Aspect
{
    JP1: before *.call(m, args) →updateRuntimeState(m, args);
    JP2: after *.call(m, ret) →updateRuntimeState(m, ret);
    JP3: after newobj →updateRuntimeState(obj);
    JP4: on field access f →updateRuntimeState(acc, f);
    Advice1: updateRuntimeState(Method m, Args[]) { .. }
    Advice2: updateRuntimeState(Method m, Object ret) { .. }
    Advice3: updateRuntimeState(Object obj) { .. }
    Advice4: updateRuntimeState(AccessType acc, Field f) { .. }
}
    
```

Fig. 1. Runtime Monitoring Aspect (RMA)–A Pseudo Code.

### IV. RM FRAMEWORK (RMF)

In this research, the static bytecode transformation approach is used to realize the RMA concepts. The static bytecode transformation performs the necessary bytecode modifications on the target software to produce a new version of that software by injecting the RMA mechanism. In this section, a detailed description of the realization of RMA as a framework will be presented.

#### A. Framework General Overview

Fig. 2 illustrates the general structure of RM Framework. The framework works at two main phases where a set of operations are performed. At the first one, called static phase, the target application (i.e. the software to be monitored) is given as input to the RMA Injection Unit (see Fig. 2), which performs three main operations:

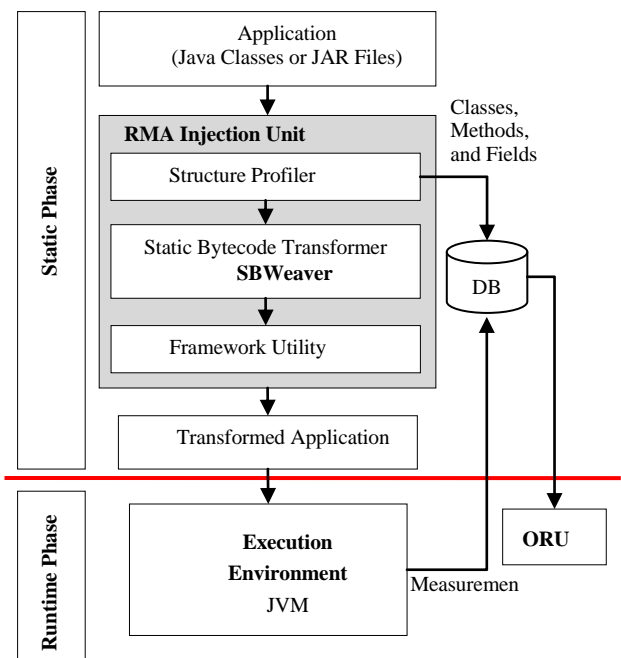


Fig. 2. The Structure of Runtime Monitoring (RM) Framework.

1) *Analyzing the input software:* At this point, the bytecode of the target software is inspected and analyzed. In other words, the structural units of the software (i.e. Java classes) are enclosed, and for each recognized class the member methods, member attributes (fields), and class constructors are inspected. The “Structure Profiler” is responsible of building a structure database for the entire software. This step is very important as it gives a road map that assists describing software classes, and helps manipulating classes easily. A full application profile is generated and stored in the database as a result.

2) *Once the structural database of the software is built:* The bytecode of software classes is then transformed. The “SBWeaver” transforms software classes and, for each class, it injects the necessary code required to realize the RMA at the specific join-points.

3) *To facilitate gathering the measurements of runtime state:* The framework utility code is added to the transformed application. The utility code serves mainly connection to database.

The output of static phase is a transformed version of the original application. In this context, it is important to assure the consistency of application structure and functionality transformation. This is to say, application should perform what it has been developed for without knowing it has been transformed.

The second phase is the runtime phase. The transformed application is executed, as normal, on top of its executing environment. During execution, the environment will gather and store the measurements of application runtime state in database.

### B. SBWeaver

The SBWeaver is the centric component in RM framework. It performs code transformation. It follows the algorithm depicted in the pseudo code of Fig. 3.

As this research targets Java applications, the Byte Code Engineering Library (BCEL) [9] is used. BCEL is an open source framework for Java bytecode transformation. The RM framework uses BCEL version 6.2.

```
1 SBWeaver(ApplicationPath appPath)
2 {
3   For each class clazz in the appPath do
4     If not already transformed(clazz) then
5       For each method m implemented by clazz do
6         Inject advices 1,2, and 3in method m according to
          joint-points declarationsJP-1, JP-2, and JP-3
          respectively
7       For each field f declared in class clazz do
8         Determine access operations (get or set) on fin
          method m, and injectadvice4 properly
9       End For
10      End For
11      Mark clazz as transformed
12    End For
13  }
```

Fig. 3. A Pseudo Code of SB Weaver at the Invasive-Mode.

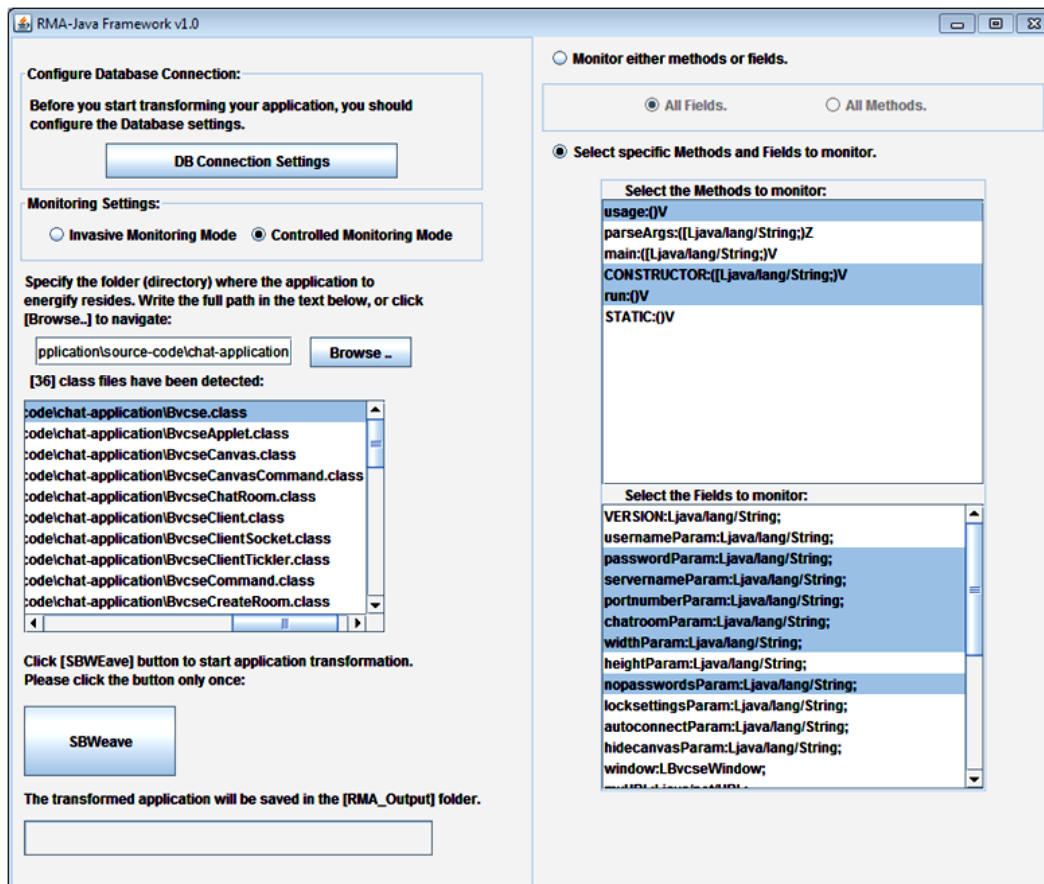


Fig. 4. The RMA Framework in Action.



The SBWeaver needs to know only where application classes reside. The BCEL is used to facilitate inspection of Java bytecode instructions in easy and powerful way. Therefore, the SBWeaver can traverse, for example, all access operations of specific fields. In Fig. 3, the SBWeaver enumerates the access operations on a field, and then injects the necessary code to collect the measurements of field access. The pseudo code shown in Fig. 3 depicts the SBWeaver at the Invasive-Mode. As for the step at line 11, transformed classes are marked *transformed* so they will not be transformed twice. For this purpose, the SBWeaver adds an implementation of the empty interface *ITTU\_SBWeaverMark*, which is used as a marking interface.

The output of SBWeaver is a transformed version of the application that is ready to be monitored at runtime. Fig. 4 illustrates the RMA framework GUI in action. The framework has been implemented totally using Java. Note the options of monitoring. In Controlled-Mode, users can select to perform monitoring (per class) either on methods or fields only. For fine-grain selection, users can select subset methods and subset fields to be involved in runtime monitoring. This flexibility in selection can increase target application suitability for monitoring.

### C. Output Representation Unit

During the execution of transformed application, runtime measurements and behavioral measurements are recorded. The Output Representation Unit (ORU) is part of RM framework and is responsible of representing these measurements in various ways. The ORU makes it easy to browse the results in proper and compatible way. However, users of RM framework can issue their customized reports as they have access to the database.

## V. CASE STUDY: MONITORING A CHATTING APPLICATION

An experiment has been conducted to test the RMA concepts on an object-oriented application. The application, called *Bvcse*, is a chatting application in Java. It is open source and free to download from the Internet.

### A. The “Bvcse” Chatting Application

The application consists of two parts; the server program, which coordinates and organize connections between clients. The second part is the client program, which allows users to chat in public global rooms or privately in user rooms. It allows chatters to share a drawing panel that provides a simple drawing toolbox to draw colorful sketches. Both programs are having GUI to facilitate chatting features. In total, “Bvcse” application includes (36) Java classes.

The application is an interactive application that broadcasts global chat messages and syncs the drawing board to all clients. Therefore, it has been selected to check monitoring applications with intensive interaction with different monitoring modes. Next section discusses how we apply the RMA monitoring modes on “Bvcse” application.

### B. Applying RMA on “Bvcse”

The RM Framework is used to augment “Bvcse” application with runtime state monitoring capability several

times; each time with a specific monitoring mode. For each case, the application is then deployed on five machines; four for clients (chatters) who do not know that the application is being monitored, and one for server.

1) *Invasive monitoring mode*: In this round, all the 36 classes of “Bvcse” application have been transformed. The SBWeaver excludes automatically all Interface and Enumeration classes. The direct impact of applying this mode is the inflation of application classes. Depending on the number of fields defined and methods implemented, the SBWeaver injects new code chunks. For example, the size of class “Bvcse.class” before transformation was (4,351 Bytes) and after transformation becomes (8,881 Bytes). All in all, the more fields defined by application class the more increasing in transformed class size. This is expected because SBWeaver injects for each field two methods; one to get field’s value and one to set a new value. In addition, all field access operations (gets and sets) in the original code will be replaced by calls to getter and setter methods.

2) *Controlled mode [functionality and attribute]*: The experiment is performed twice in this round; the first one to monitor method executions and the other to monitor field access operations. As for monitoring methods executions, the application works fine and all statistics have been recorded and stored in the database during the experiment duration (one hour). For field access monitoring, the application performance suffers from periodic congestion at clients and server sides; especially when syncing the drawing panel. Once again, a large number of fields need to be accessed upon message sending or drawing panel synchronization; which causes these congestions.

3) *Controlled mode [selective]*: In this round, three fields and three methods from each class have been randomly selected for monitoring (a customized set of fields and methods could be selected per class). The transformed application is then deployed for execution. As expected, the application works fine without any “stutters” as clients experience no delays. The statistical information gathered for the monitored fields and methods are recorded and stored in the database during experiment. Fig. 5 shows a short snippet for statistical field access as appeared in the database.

### C. Results and Discussion

According to experiment results, it is obvious that monitoring in the Invasive-Mode is improper for interactive and dense applications. As expected, the connection traffic was very dense and the performance of all five copies suffers strong bottlenecks. Technically, the experiment of round one comes out with the worst results; because large set of fields need to be accessed at the server and client programs each time a new message or new drawing panel update arrive. For RM framework, this means a connection to the database is required to execute update query for the corresponding accessed field; which means extra runtime.

| fieldID | classID | appID | fieldName        | fieldSignature     | fieldACC | Put | Get |
|---------|---------|-------|------------------|--------------------|----------|-----|-----|
| 18      | 2       | 5     | windowWidth      | I                  | V        | 39  | 6   |
| 19      | 2       | 5     | windowHeight     | I                  | V        | 34  | 6   |
| 23      | 2       | 5     | showCanvas       | Z                  | V        | 7   | 120 |
| 17      | 2       | 5     | room             | Ljava/lang/String; | V        | 7   | 79  |
| 22      | 2       | 5     | autoConnect      | Z                  | V        | 5   | 5   |
| 21      | 2       | 5     | lockSettings     | Z                  | V        | 5   | 5   |
| 20      | 2       | 5     | requirePasswords | Z                  | V        | 5   | 5   |

Fig. 5. Statistical Measurements of Some Fields as Appeared in the Database.

However, in all rounds, application consistency (structure and hierarchy) has been preserved. In addition, users give no comments on differences in application functionality; as they use the original application before applying RMA. Therefore, RM framework supports the monitoring transparency claimed in this research.

## VI. RELATED WORKS

Several researches have been conducted to deal with application runtime states. In the context of applications behavior, the authors in [10] have presented *blended program analysis* as a new paradigm to analyze large framework-based Java applications. The researchers have designed a blended escape analysis for approximating the effective lifetimes of objects. The approach was supposed to help explain how temporary structures are built and used. We found a relevancy between our work and their work from the purpose. This research collects information about the creation of objects statistically, while blended analysis inspects objects' lifetime lines.

A new metric to measure the degree of cohesion in relation to objects of a class at runtime has been presented in [11]. A runtime cohesion metric called LCOM-Desouky has been defined and experimented on Rhino 1.7R4 – an open source JavaScript framework written in Java. The study results in a large negative correlation between the metric and tested data. The author did not mention how they collect statistics for metric calculations at runtime. Our framework explains this step in details, and provides a modular and cohesion method for collecting runtime statistics. We do believe that more metrics could be constructed according to runtime statistics collected by RM framework.

A runtime state fetching method has been proposed in [5]. The authors designed a language called State Fetching Description Language (SFDL) to express monitoring requirements, and implemented a framework to compile SFDL rules into monitor probes which gather information and store them. The approach has been applied on distributed software and some performance bottlenecks have been detected. The approach is similar to RM framework from the point that both of them present runtime monitoring as a separate concern. Our approach, however, is transparent; there is no need to a description language such as SFDL to describe what to monitor. Instead, RM framework provides three monitoring modes.

The work proposed in [12] presents a similar approach to the one in [5]. The proposed technique uses Online Evolution

Module (OEM) which receives monitoring information and compares state event to pre-defined evolution rules. It performs evolution actions and real-time corrections if these rules are triggered. In [13], the author presented a performance analysis of large-scale object-oriented software by finding repeated patterns of dynamic behavior in calling context tree (CCT) extracted from software profile data. In the tested application with over 64 thousand unique calling contexts, 10 patterns account for over 50% of application execution.

The authors in [3] presented a survey of software runtime monitoring. The research introduced the fundamentals of runtime monitoring; which include the architecture of a monitoring system, and the monitoring levels. The study introduced, classified, analyzed, and compared the typical software runtime monitoring methods. The research presented some problems related to runtime monitoring methods, and gave some future directions.

## VII. CONCLUSIONS AND FUTURE WORK

Monitoring the runtime state of applications is important to study the behavior of these applications. Collecting runtime measurements is one of the vital methods to perform this task. In this research, Runtime Monitoring Aspect (RMA) has been presented, which describes how and when to collect statistical data about runtime state of object-oriented applications transparently. The research introduced the RM Framework as an implementation to RMA. The framework suggests three monitoring modes; the Invasive-Mode to monitor the overall application runtime state. The Controlled-Mode/(Functionality and Attribute) monitors method executions, which helps inspecting application behavior and tracks field access operations. Finally, the Controlled-Mode/Selective allows monitoring customized set of fields and methods.

An experiment has been conducted to apply RMA on a chatting application written in Java. In the experiment, all monitoring modes have been applied. Because the chatting application is highly interactive, bottlenecks and congestion problems appear when applying Invasive-Mode and Controlled-Mode/Attribute.

The RM framework has some limitations. First, it injects extra code into target applications, which may inflate their sizes. If verification on class sizes is an issue, then RM framework causes a violation. The framework is limited in scope because it targets applications developed in Java. For future work, more applications need to be monitored by RM framework.

REFERENCES

- [1] Nusayr and J. Cook, "AOP for the Domain of Runtime Monitoring: Breaking Out of the Code-Based Model", DSAL'09, March 3, 2009, Charlottesville, Virginia, USA, ACM. (2009)
- [2] J. Sundararaman and G. Back, "HDPV: interactive, faithful, in-vivo runtime state visualization for C/C++ and Java", SOFTVIS 2008, Herrsching am Ammersee, Germany, September 16–17, 2008. (2008)
- [3] L. Gao, *et. al.*, "A Survey of Software Runtime Monitoring". The 8th IEEE International Conference on Software Engineering and Service Science (ICSESS), Beijing, 2017, pp. 308-313. IEEE. (2017)
- [4] G. Franks, *et. al.*, "Layered Bottlenecks and Their Mitigation", Third International Conference on the Quantitative Evaluation of Systems (QEST'06), IEEE. (2006)
- [5] G. Changguo and W. Tao, "A Method and Framework for Fetching Software Runtime State", International Conference on Computer, Mechatronics, Control and Electronic Engineering (CMCE), IEEE. (2010)
- [6] J. Xu, "Rule-based Automatic Software Performance Diagnosis and Improvement", WOSP'08, June 24–26, 2008, Princeton, New Jersey, USA, ACM. (2008)
- [7] H. Rajan and K. Sullivan, "Aspect Language Features for Concern Coverage Profiling", In Proceedings of the 4th international conference on Aspect-oriented software development (AOSD '05). ACM, New York, NY, USA, 181-191. (2005)
- [8] G. Kiczales, *et. al.*, "Aspect-Oriented Programming", In proceedings of the European Conference on Object-Oriented Programming (ECOOP), Finland. Springer-Verlag LNCS 1241. June 1997. (1997)
- [9] M. Dahm, "Byte Code Engineering with the BCEL API", Freie Universitaat Berlin, Institut fur Informatik, (Technical Report B-17-98), April 3, 2001. (2001)
- [10] B. Dufour, B. Ryder, and G. Sevitsky, "Blended Analysis for Performance Understanding of Framework-based Applications", ISSTA'07, July 9–12, 2007, London, England, United Kingdom. ACM. (2007)
- [11] A. Desouky and L. Etzkorn, "Object Oriented Cohesion Metrics: A Qualitative Empirical Analysis of Runtime Behavior", ACM SE '14, March 28 - 29 2014, Kennesaw, GA, USA. (2014)
- [12] L. Zhen-Dong, *et. al.*, "Bytecode-based Software Monitoring and Trusted Evolution Programming Framework", 2012 IEEE Symposium on Robotics and Applications (ISRA), Kuala Lumpur, 2012, pp. 494-497. IEEE. (2012)
- [13] D. Maplesden, "Performance Analysis of Object-Oriented Software", ICSE Companion'14, May 31 – June 7, 2014, Hyderabad, India. ACM 978-1-4503-2768-8/14/05. ACM. (2014)

# A Novel Intelligent Cluster-Head (ICH) to Mitigate the Handover Problem of Clustering in VANETs

A.H. Abbas<sup>\*1</sup>, Mohammed I. Habelalmateen<sup>2</sup>, L. Audah<sup>3</sup>, N.A.M. Alduais<sup>4</sup>

Wireless and Radio Science Centre (WARAS) Faculty of Electrical and Electronic Engineering  
Universiti Tun Hussein Onn Malaysia 86400 Parit Raja, Batu Pahat, Johor, Malaysia<sup>1,2,3,4</sup>  
Department of Computer Technical Engineering, College of Technical Engineering  
The Islamic University, 54001 Najaf, Iraq<sup>2</sup>

**Abstract**—The huge development in the number of Vehicle factories have resulted in many people having lost their life due to accident, which has made vehicular Ad-hoc networks (VANETs) hot topic to enable improved communication between vehicles aimed at reducing the loss of life. The main challenge in this area is vehicle mobility, which has direct effect on network stability. Thus, most previous studies that discussed clustering focused on cluster formation, cluster-head selection and the stability of cluster to reduce the impact of mobility in the network, with little attention given to the clusters when passing from base-station to neighbor base-station. Therefore, this study focused on handover problem that occurs after cluster formation and cluster-head election during cluster passing from base station to base station, known as overlapping area. As the cluster in an overlapping area receives two signals from different base stations, the signal arriving at the cluster becomes weak due to interference between two frequencies resulting in loss of cluster information in the overlapping area. In this study, proposed a novel method named Intelligent Cluster-Head (ICH), which is a controller on two clusters that are used to change uplink between clusters to solve the handover problem in the overlapping area. The proposed method was evaluated with VMaSC-1hop method. The proposed method achieved percentage of packet loss up to 0.8%, percentage of packet delivery ratio (PDR) 99%, percentage of number of disconnected links 0.12% and percentage of network efficiency 99% in the cells edge.

**Keywords**—Vehicular Ad-Hoc networks; ITS; clustering; overlapping area; handover; ICH

## I. INTRODUCTION

This template, Vehicular Ad-hoc Networks (VANETs) is a sub-part of mobile Ad-hoc networks (MANETs). The main idea of VANETs is to establish communication between vehicles for the personal safety of the vehicle's occupants. VANETs has two main types of communication: 1) vehicle to vehicle (V2V), which allows vehicles to communicate between others in point to point link by using IEEE802.11p standard protocol. The advantages of this type are free of cost, no infrastructure required and easy network deployment. However, it triggers some issues when there are an insufficient number of vehicles, which result in disconnect problem and packet loss [1], [2]; 2) vehicle to infrastructure (V2I), which solves this issue by making sure that the vehicles are directly connected to the base station (BS). BS coverage is large because the higher transmission range decreases disconnect problem [3], [4]. However, there are still some issues that arise in this type, such as cost, difficult deployment network and

network load. All of the above issues result from high vehicle mobility. High speed of vehicles causes a change in topology, which results in an unstable network. Therefore, clustering is used to reduce the above issues by combining vehicles in a group called cluster. Cluster means connecting a number of vehicles that are in the same transmission range. One of these vehicles is called cluster-head (CH) and the remaining vehicles are called cluster-members (CMs), with the CH responsible for managing intra and inter-cluster communication [5]. The benefit of clustering enhancement network performance is that it reduces connection congestion at the base-stations in the network. Nevertheless, vehicle mobility is still the main challenge in the clustering according to [6]–[9]. Most of the previous studies focused on reducing the effect of mobility by increasing cluster stability since VANETs is sub-part of MANETs. However, although the maximum nodes speed are 8 km/h [10], the handover between neighboring base-stations (BS) in MANETs is a big challenge. Therefore, handover has become a huge challenge in VANETs. According to the National Speed Limits of Malaysia, the speed limit in urban areas is 90 km/h. In addition, according to local cellular networks in Malaysia, the average coverage area of LTE-BS in the city is between 300 and 400 meters, which leads to vehicles passing from one BS to another in short time duration, resulting in more vehicle information required during handover. Therefore, this paper has proposed a new method to solve the handover in the overlapping area, a method called Intelligent Cluster-Head (ICH). This paper is organized as follows; section II is focused on handover problem, section III described previous work related to a heterogeneous network, section IV describes the new method (ICH) and theoretical analysis, section V presents simulation and result analysis, section VI presents the conclusion and future work.

The introduction should briefly place the study in a broad context and highlight why it is important. It should define the purpose of the work and its significance. The current state of the research field should be reviewed carefully, and key publications cited. Please highlight controversial and diverging hypotheses when necessary. Finally, briefly mention the main aim of the work and highlight the principal conclusions. As far as possible, please keep the introduction comprehensible to scientists outside your particular field of research. References should be numbered in order of appearance and indicated by a numeral or numerals in square brackets, e.g., [1] or [2,3], or [4–6]. See the end of the document for further details on references.

\*Corresponding Author

## II. HANDOVER PROBLEM STATEMENT

This section discussed the handover problems in VANETs. Handover, which has been studied in cellular networks, occurs in the area between two neighbors BSs known as overlapping area [24]. This area resulted from overlap in the transmission range of both BSs and the signal in this area is weak because of interference in the frequencies of neighbor BSs, as shown in Fig. 1. Interference occurs between two neighbor BSs in the mobile cellular network, as proposed in [25]. Based on a literature review, no previous work has focused on handovers that occur in the overlapping area in the clustering of VANETs. Handover problem in clustering of VANETs is a more serious problem than in mobile devices because vehicles have ten times higher speed than mobile devices according to [10]. Vehicles in the overlapping area received two frequencies, one frequency from each BS, therefore vehicles are confused about sending its information to which base-station, while at the same time, the signal in this area has become weaker due to interference frequencies [25]. Three reasons why the handover problem occurs more frequently in VANETs is because vehicles are moving in high mobility, the vehicles are capable to move quickly from one BS to another, and vehicles require link established when moving, which cause increased handover in the network. According to Malaysian local cellular networks, the transmission range of BS in the urban city is limited so as to reduce the effect on people's health, and this has resulted in a high number of BSs, which is another reason to increase handover in the city. The use of clustering in this research has led to handover becoming a serious problem because communication with BS is done by cluster-head. In addition, the information that is sent to BSs consists of both CH and its CMs information, which may cause loss of cluster information when CHs is in the overlapping area. This is another reason that motivates us to solve this problem. Fig. 2 shows the handover problem in the overlapping area of clustering in VANETs.

From Fig. 2, CH2 is in the overlapping area, therefore it received two weak signals from two neighbor base-stations. Thus, during the handover with CH 2, information of cluster is lost. The proposed method aimed to solve the above problem by using intelligent cluster-head (ICH) as discussed in the next section.

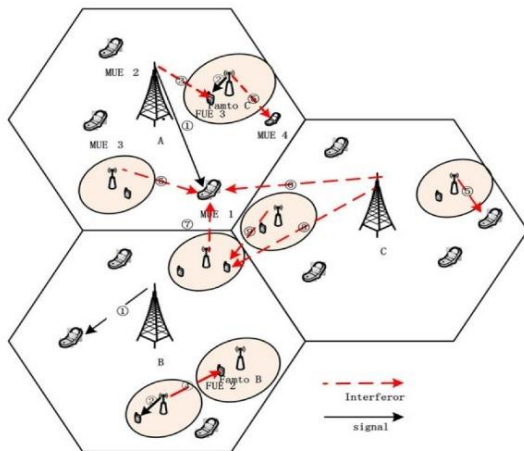


Fig. 1. Interference between Two BSs in the Mobile Network [25].

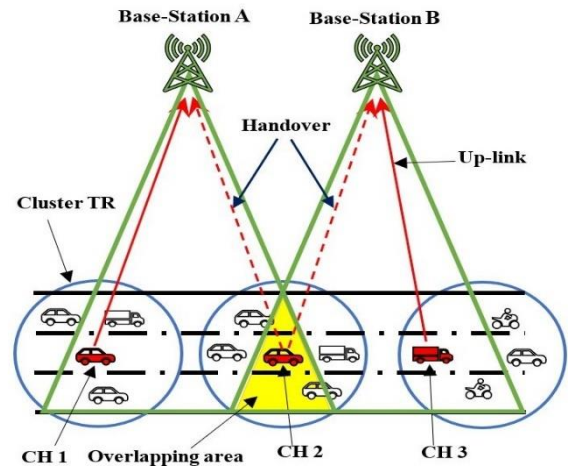


Fig. 2. Handover Problem in the Overlapping Area of Clustering in VANETs.

## III. RELATED WORKS

This part introduced previous works that used clustering with cellular networks (heterogeneous networks) in VANETs. The main challenge in this area is high vehicle mobility that results in a dynamic topology change. This has raised several issues, which are the stability of the cluster, overhead, delay, and disconnect problem. In previous work, [11] proposed centralized clustering-based hybrid vehicular networking architecture (CC-HVNA) that combines both IEEE 802.11p and LTE in VANETs to enhance data dissemination by creating roadside units (RSUs) or BS to elect and form a cluster. This method resulted in improved delay and packet delivery ratio (PDR). The authors in [12] proposed hierarchical cluster-based location service in city environments (HCBLs) to reduce overhead and increase cluster stability. Overhead is reduced by reducing the update location costs. Stability is enhanced by the selection of vehicle in the centric of neighbor's vehicles, known as CH. The outcome of this method is reduced location updates and increased cluster lifetime. In previous work, [13] proposed a novel multi-hop moving zone (MMZ) clustering scheme CH selection based on average relative speed, relative distance, and link life. The result of this method is increased CH lifetime and reduced delay. Moreover, authors in [14] proposed a new Vehicular Cloud (VC) model to enhance data dissemination by using LTE with IEEE802.11p, leading to increased PDR and reduced delay. Other authors in [15] proposed intelligent naïve Bayesian probabilistic estimation practice for traffic flow to form a stable clustering in VANET (ANTSC) algorithm to increase cluster stability by selected cluster head from the lane that has the heaviest traffic flow. In addition, authors in [16] proposed a novel destination and interest-aware clustering (DIAC) mechanism to reduce link failures between vehicles and LTE network based on the vehicle having the highest link-quality becoming the CH. The authors in [17] proposed a hybrid vehicular multi-hop algorithm for stable clustering (VMaSC) with LTE and IEEE802.11p multi-hop clustering. LTE was used to increase PDR and reduce delay, while VMaSC was used to form a stable cluster by selecting CH based on the relative speed of vehicles in the same transmission range (TR). The combination of VMaSC with

LET in a hybrid network, known as (VMaSC -LTE), was intended to reduce load at BS by reducing the number of clusters in the merge mechanism. However, while reduction in the number of clusters will reduce load at BS, the handover problem remains in the overlapping area. Other previous works focused on the use of gateway (GW) to reduce the load at BSs by a reduced number of CHs in the network. The GW is a normal node has two types based on the location of GW. The first type is the GW that is positioned between more than one CHs. This type of GW is used to send the CH information to other CHs that are within its transmission range with the aim to make each CH know about the neighboring CHs [18]–[20]. However, these CHs are still connected to the BSs even though GW is available. The second type of GW is the GW has a location at the beginning and end of the transmission range of CH. This type is not used to exchange information between CHs but is responsible for inter-cluster communication and used to inform its CH about new neighbor CH for merge mechanism [21]. The main goal of both types of GW is to achieve merge mechanism to merge several CHs in one CH to decrease the number of CH in the network according to a specific condition. The disadvantage of GW is that this re-broadcast caused flooding in the network. However, most researches used GW in multi-hop to increase cluster scalability and reduce the number of CH in the network. There is no procedure to select GW based only on the location of the node, therefore more than one GWs between two CHs caused more flooding and only one GW can do the same work of all the GWs. The concept of relay node (RN) is that a normal node is used to rebroadcast CH message to reach all CMs according to [22], [23]. The RN also caused flooding in the network. None of the previous related works have focused on handover problem that occurs in the overlapping area during using clustering in VANETs, therefore this study has proposed a new method call Intelligent Cluster-Head (ICH) to solve this problem. The concept of ICH is completely different from GW and RN. Table I shows the difference between GW, RN, and ICH. Summary of related works is presented in Table II.

#### IV. PROPOSED METHOD

This section discusses the proposed new method to solve the handover problem that occurs after cluster formation mentioned in the previous section. The aim of this new method, known as Intelligent Cluster-Head (ICH), is to control the connection link between CHs as discussed in section (C).

##### A. Features of ICH are

- ICH works as a controller on CHs and has the capability to move connection between CH and BS from one CH to another CH, thereby reserving signal strength (RSS) of CHs to prevent handover in the overlapping area because the proposed method can control on CHs by changing connection from CH has weak signal to another CH has good signal from BS.
- ICH is not a broadcast beacon that CHs use to broadcast for CMs to reduce flooding in the networks. However, ICH checks RSS in the beacons and when RSS of one CHs becomes weak, the ICH sends a notification to this CH about moving the connection to another CH during

ICH to guarantee the information of vehicles in the CH that has weak RSS is not consumed by overhead.

- ICH reduced the number of up-links between CH and BS by allowing only one CH to communicate with BS, and another CH sends its vehicle information during ICH to the CH that has a connection with BS. With this method, the number of up-link connections is reduced by half as compared to that available in all previous methods that used a heterogeneous network.
- ICH calculated dynamic threshold speed for both clusters according to simple Equation. ICH elected in accurate method. The details of this point are presented in the next sub-section.

##### B. Elected ICH

Should note, in this study clusters formation and CH election based on same method used in VMaSC-1hop in [17]. This study focuses on electing ICH after clusters formation and CH elected. When a vehicle received two beacon messages from different CHs, it does not change its state directly like GW. This vehicle checks the direction of new CH; if it is in the opposite direction, the vehicle drops the beacon and continues as CM in its original CH. However, if a beacon message is in the same direction, there are two cases according to Fig. 3.

**In the first case**, if the original CH (OCH) is in front of new CH (NCH), the vehicle that received a new beacon from NCH first checks the NCH speed; if the speed is less than OCH speed, the vehicle drops beacon and continues as CM. However, if NCH has a higher speed than OCH speed, the vehicle calculates dynamic threshold speed (Dthr) from Equation (1) and (2), then calculates the speed difference between NCH and OCH according to Equation (3). Table III shows the symbols of this paper.

$$D_{thro} = |OCH - VS| \tag{1}$$

$$D_{thrN} = |OCH - VS| \tag{2}$$

$$DCHs = NCH - OCH \tag{3}$$

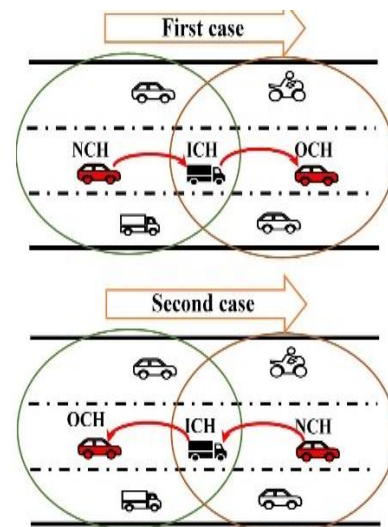


Fig. 3. Two Cases of CH.

TABLE. I. DIFFERENCE BETWEEN GW, RN AND ICH

| NO. | GW [18]–[21]                             | RN [22], [23]                         | Proposed ICH   |
|-----|--|---------------------------------------|--|
| 1   | Broadcast beacon and merge clusters      | Only for broadcast beacon             | Controller by moving connection link between CHs based on RSS    |
| 2   | Increased flooding in the network        | Increased flooding in the network     | Avoid flooding beacon problem                                    |
| 3   | Reduced number of up-link if merge occur | Does not reduce the number of up-link | Reduce the number of up-link without need for merge mechanism    |
| 4   | Increased network scalability            | Not did                               | Increased network scalability                                    |
| 5   | Elected based on location or CH elect GW | CH elect RN                           | Elected according to a special procedure as shown in section (B) |
| 6   | Not used                                 | Not used                              | Used DDthr and DSthr to increase link lifetime between CHs       |
| 7   | More than one in each CH or between CHs  | More than one in each CH              | Only one between CHs   |

TABLE. II. SUMMARY OF RELATED WORKS

| Ref. | Method  | Problem                    | Domain  | Outcome   | Solve handover problem |
|------|---------|----------------------------|---------|---|------------------------|
| [11] | CC-HVNA | • Data dissemination       | Highway | • Reduce Delay.<br>• Increase PDR.  | NA                     |
| [12] | HCBLs   | • Overhead.<br>• Stability | Urban   | • Increase cluster lifetime.<br>• Reduce location update.   | NA                     |
| [13] | MMZ     | • Overhead                 | Highway | • Increase CH lifetime.<br>• Reduce delay   | NA                     |
| [14] | VC      | • Data dissemination       | NA      | • Increase PDR.<br>• Reduce delay.  | NA                     |
| [16] | DIAC    | • Link Failures            | Urban   | • Increase CH and CM duration.<br>• Reduce overhead.<br>• Increase PDR.   | NA                     |
| [17] | VMaSC   | • Stability<br>• Overhead  | Highway | • Increase CH duration.<br>• Reduce the number of cluster in the network.<br>• Increase PDR.<br>• Reduce delay. | NA                     |

TABLE. III. LIST OF SYMBOLS

| NO. | Symbol             | Description                             | NO. | Symbol           | Description                               |
|-----|--------------------|---|-----|------------------|---|
| 1   | OCH                | Original cluster-head                   | 13  | $LLT_{O,I}$      | Link lifetime between OCH and ICH         |
| 2   | NCH                | New cluster-head                        | 14  | $LLT_{N,I}$      | Link lifetime between NCH and ICH         |
| 3   | $D_{thrO}$         | Dynamic threshold speed of OCH          | 15  | $\Delta D_{O,N}$ | The relative distance between OCH and NCH |
| 4   | $D_{thrN}$         | Dynamic threshold speed of NCH          | 16  | $P_O$            | Position of OCH                           |
| 5   | VS                 | Vehicle speed                           | 17  | $P_I$            | Position of ICH                           |
| 6   | DCHs               | Different CH speed                      | 18  | $P_N$            | Position of NCH                           |
| 7   | $\Delta D_{CH,CM}$ | The relative distance between CH and CM | 19  | $\Delta V_{O,N}$ | The relative speed between OCH and NCH    |
| 8   | $\Delta V_{CH,CM}$ | The relative speed between CH and CM    | 20  | $V_O$            | Speed of OCH                              |
| 9   | $V_{CH}$           | Speed of CH                             | 21  | $V_I$            | Speed of ICH                              |
| 10  | $V_{CM}$           | Speed of CM                             | 22  | $V_N$            | Speed of NCH                              |
| 11  | $LLT_{CH,CM}$      | Link lifetime between CH and its CM     | 23  | $TR_O$           | Transmission range of OCH                 |
| 12  | $LLT_{O,N}$        | Link lifetime between OCH and NCH       | 24  | $TR_I$           | Transmission range of ICH                 |

When the difference in speed between OCH and NCH is less than dynamic threshold speed according to Equation (4), the vehicle sends message to OCH that contains all previous details. The OCH then checks how many vehicles have received beacon message from NCH, then the Competing vehicles be made ICH (CICH); if there is only one vehicle, the CH sends a confirmation message to the vehicle and the vehicle becomes ICH. If there is more than one vehicle proposed to be ICH, the OCH calculates the different dynamic threshold for each vehicle according to Equation (5). Vehicles with low different dynamic threshold speed, distance near to the half of transmission range (TR) become ICH. The remaining CICH vehicles are arranged in the table ranged from low different dynamic threshold speed to high, with the benefit that when ICH loses connection in any way, the vehicle in the second row of the table directly becomes ICH in order to not repeat the process again for more flexibility in the network.

$$DCHs \leq D_{thro} \tag{4}$$

$$ICH = |D_{thro} - D_{thrN}| \tag{5}$$

**In the second case**, the vehicle's original CH (OCH) backs off new CH (NCH). The vehicle that received a new beacon from NCH first checks NCH speed, and if this speed is greater than OCH speed, the vehicle drops the beacon and continues as CM. However, if NCH has a lower speed than OCH speed, the vehicle calculates dynamic threshold speed (Dthr) from Equation (1) and (2), then calculates different speed between NCH and OCH according to Equation (6). The same step above is used for Equation (4) and (5).

$$DCHs = OCH - NCH \tag{6}$$

In the above cases, in this study, assume the vehicle that received a new beacon from another CH belongs to the OCH. However, if vehicles belong to NCH, the same above cases occur but the main difference is that validation will be with the value of NCH. This means that in all cases, the validation is done with the value of CH that owned the ICH. Fig. 4 shows the flowchart for elected ICH in both cases.

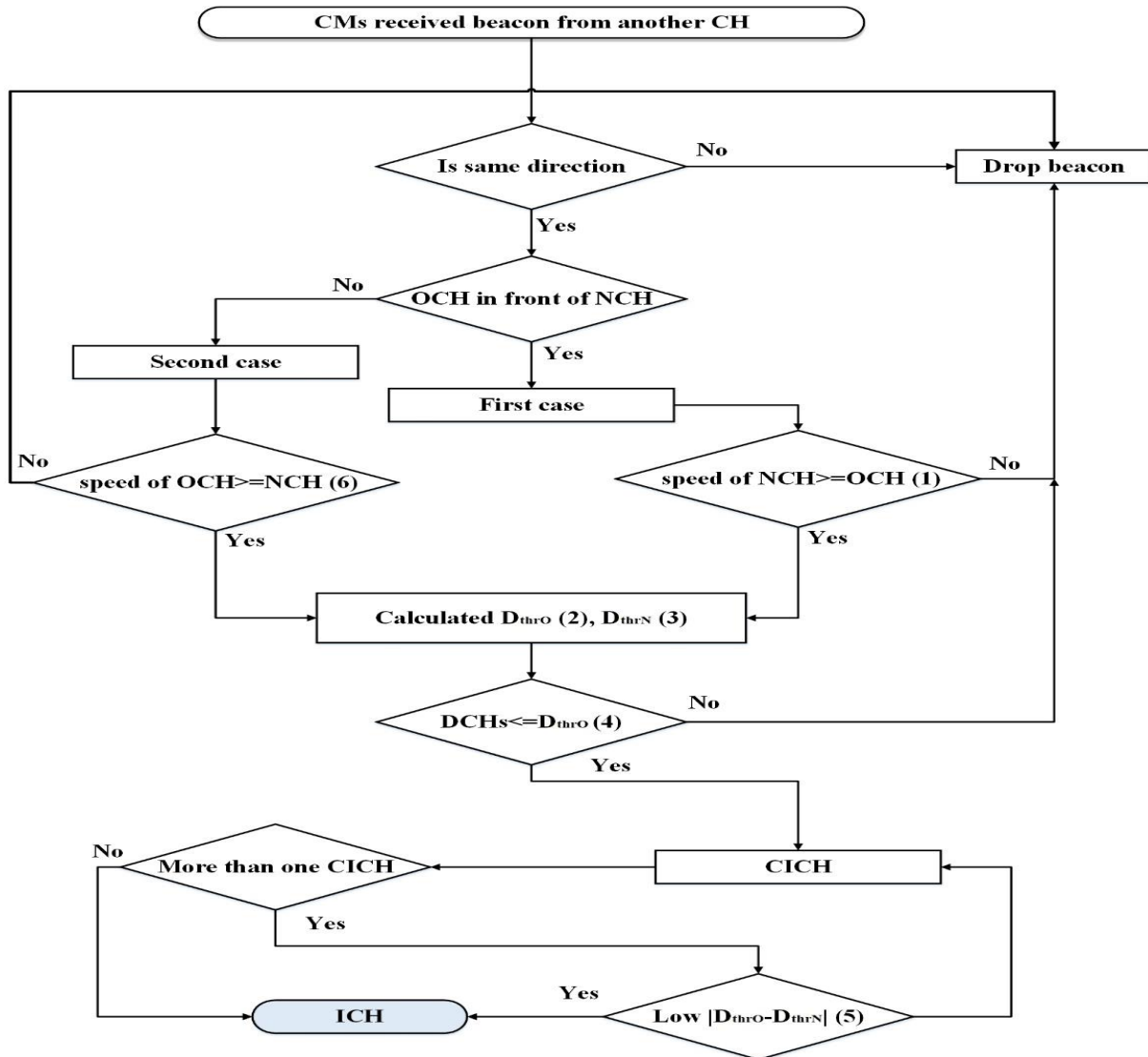


Fig. 4. Flowchart of ICH Election Process.



### C. Solve Handover Problem by Applying ICH Method

This section introduced how ICH manages neighbor clusters and changes up-link from one CH to another to solve the handover problem in the overlapping area. After CH sends a confirmation message to the proposed vehicle that has high qualification according to the previous section, the vehicle changes its state from CM to ICH then informs another cluster of this change. ICH begins to listen to both messages coming from CHs, and this message has CH-ID, direction of CH, speed of CH, number of CMs in the CH, different relative speed between CH and each CM, different relative distance between CH and its CMs, location of all clusters (location of each CM in addition to location of CH itself) and RSS of CH. The ICH compares the RSS of both CHs, and the CH having the highest RSS sends vehicle information for both clusters to the BS, while the CH that has low RSS sends its cluster information directly by using IEEE802.11p standard to ICH. The ICH sends this information to CH having the highest RSS. During this process, the CH that is connected in the BS remains connected in the BS until it has received two RSS from two BSs (this means the CH has arrived at the overlapping area). The CH then sends a weak signal message to ICH to change uplink connection with the BS to another CH in order not to lose vehicles' information. When ICH received a weak signal from CH, the ICH sends a message to another CH to establish a link with the BS. The ICH sends vehicle information of CH having two signals to another cluster, and then another cluster begins to send information to the BS while CH that received two signals disconnects the uplink with BS. Fig. 5 shows how ICH works.

As shown in Fig. 5, CH 2 received two signals because it is in the overlapping area. Thus, CH2 sends a weak signal message to ICH, which then sends a message to CH 1 to establish a link with the BS to send vehicle information. After the link has been established, the ICH sends CH 2 information to CH1, which is then sent to BS. By using ICH, the handover problem that occurs in the overlapping area is solved. Also, the use of ICH reduced the number of up-link connections with the BS, thereby increasing the cluster stability in the network. Fig. 6 shows the flowchart of vehicles that work as ICH.

Based on previous work [26], the LLT between CH and CM is collected from the following equation.

$$\Delta D_{CH,CM} = |P_{CH} - P_{CM}| \quad (7)$$

$$\Delta V_{CH,CM} = |V_{CH} - V_{CM}| \quad (8)$$

Collected LLT between CH and CM has two cases according to the following:

1) *First case:* When CM is in back of CH, LLT is collected according to Equation (9) in [26]

$$LLT_{CH,CM} = \frac{\Delta V_{CH,CM} * \Delta D_{CH,CM} + \Delta V_{CH,CM} * TR_{CH}}{(\Delta V_{CH,CM})^2} \quad (9)$$

2) *Second case:* When CM is in front of CH, LLT is collected according to Equation (10) in [26].

$$LLT_{CH,CM} = \frac{-\Delta V_{CH,CM} * \Delta D_{CH,CM} + \Delta V_{CH,CM} * TR_{CH}}{(\Delta V_{CH,CM})^2} \quad (10)$$

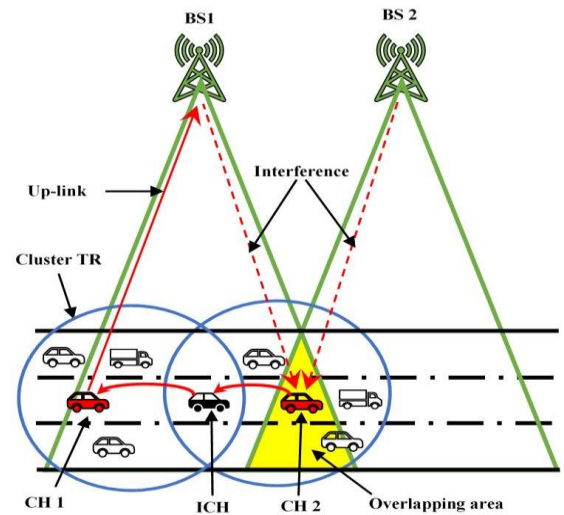


Fig. 5. Work of Intelligent Cluster-Head (ICH).

In this method, LLT is collected between two CHs during ICH. Also, there are two cases to collect LLT according to Fig. 3. The total LLT between OCH and NCH in this study was calculated according to Equation (11), while the different distance and different velocity were calculated according to Equation (12) and (13), respectively.

$$LLT_{O,N} = LLT_{O,I} + LLT_{N,I} \quad (11)$$

$$\Delta D_{O,N} = |P_O - P_I| + |P_N - P_I| \quad (12)$$

$$\Delta V_{O,N} = |V_O - V_I| + |V_N - V_I| \quad (13)$$

3) *The first case according to Fig. 3:* each case has two LLTs, one between OCH and ICH, while another LLT is between NCH and ICH. This means this method that the ICH must be in front of one CH and behind another CH. In Fig. 3, in this study, assume ICH belongs to OCH, only in both cases the purpose is to validate with the value of OCH only. The same scenario applies when ICH belongs to NCH exactly but validated with the value of NCH. According to Fig. 3, the ICH is behind OCH; therefore the LLT is collected according to Equation (14). In the same case where the ICH is in front of NCH, the LLT is collected according to Equation (15).

When ICH is behind OCH, LLT is collected according to Equations (8), (9) and (10).

$$LLT_{O,I} = \frac{\Delta V_{O,I} * \Delta D_{O,I} + \Delta V_{O,I} * TR_O}{(\Delta V_{O,I})^2} \quad (14)$$

$$LLT_{N,I} = \frac{-\Delta V_{N,I} * \Delta D_{N,I} + \Delta V_{N,I} * TR_I}{(\Delta V_{N,I})^2} \quad (15)$$

To get the total LLT between two CHs (OCH and NCH), substitute Equations (14) and (15) in Equation (11).

$$LLT_{O,N} = \frac{\Delta V_{O,I} * \Delta D_{O,I} + \Delta V_{O,I} * TR_O}{(\Delta V_{O,I})^2} + \frac{-\Delta V_{N,I} * \Delta D_{N,I} + \Delta V_{N,I} * TR_I}{(\Delta V_{N,I})^2} \quad (16)$$

Simplify equation (16) to get the best equation to collect LLT between two CHs in Equation (17).

$$\begin{aligned}
 LLT_{O,N} &= \frac{\Delta V_{O,I} * (\Delta D_{O,I} + TR_I)}{(\Delta V_{O,I})^2} + \frac{\Delta V_{N,I} * (-\Delta D_{N,I} + TR_I)}{(\Delta V_{N,I})^2} \\
 &= \frac{\Delta D_{O,I} + TR_I}{(\Delta V_{O,I})} + \frac{-\Delta D_{N,I} + TR_I}{(\Delta V_{N,I})} \\
 &= \frac{(\Delta V_{N,I}) * (\Delta D_{O,I} + TR_I) + (\Delta V_{O,I}) * (-\Delta D_{N,I} + TR_I)}{(\Delta V_{O,I}) * (\Delta V_{N,I})} \\
 &= \frac{\Delta V_{N,I} * \Delta D_{O,I} + \Delta V_{N,I} * TR_I - \Delta D_{N,I} * \Delta V_{O,I} + \Delta V_{O,I} * TR_I}{(\Delta V_{O,I}) * (\Delta V_{N,I})} \quad (17)
 \end{aligned}$$

4) The second case according to Fig. 3: this case is different than other cases in that the signals are based on the location of ICH according to OCH and NCH as shown in Equation (18).

$$LLT_{O,N} = \frac{-\Delta V_{O,I} * \Delta D_{O,I} + \Delta V_{O,I} * TR_O}{(\Delta V_{O,I})^2} + \frac{\Delta V_{N,I} * \Delta D_{N,I} + \Delta V_{N,I} * TR_I}{(\Delta V_{N,I})^2} \quad (18)$$

#### D. Theoretical Analysis and a Numerical Example

Based on the real-data collected from local cellular networks in Batu Pahat, Johor, Malaysia, the transmission range of LTE-base-station is between 300 to 400 meters. Therefore, there are many BSs on the road, which leads to a lot of overlapping areas that resulted in more handovers as vehicles move on the road. Handover caused serious problems, especially in clustering, because each cluster represents the CH of each vehicle, and passing CH in the overlapping area caused loss of all CMs information resulted from handover between two BSs. [17] proposed VMaSC-LTE that is closest to the idea of this study, where the load on the BS is reduced due to a number of clusters in the network. However, reduction in the

number of clusters will reduce load at BS but not solve handover problem because the remaining clusters still have a handover. Also, there has been no focus on the overlapping area. In this paper, we proposed ICH to solve handover problems by positioning the ICH at the end of clusters-transmission range. Thus, the front CH that received two signals from two different BSs is directed to stop sending vehicle information to the BS in order to not lose its cluster information and sends this information to ICH and then to another CH that is not in the overlapping area. Also, ICH reduced uplink by half because every two clusters that have ICH use only one uplink to connect both clusters in the BS. This is because of the use of IEEE802.11p protocol to connect inter and intra cluster and this protocol has data rate 27 Mbps according to [27]. This study focuses on broadcast safety message that has a size between (512 and 1000) byte according to [10], [14], [17], [28], therefore the link between CH and BS can send both CHs information during IEEE502.11p. For example, if each CH has a maximum number of CMs, this means 20 CMs according to [29], therefore the total number of both clusters within the CHs becomes 42 vehicles. According to above, each vehicle sends safety message 1000 bytes in size, therefore the total size of safety message for both clusters become (42x1000= 42,000 bytes. Divided by 1000 to convert to KB, the size becomes 42 Kbps and the link can send up to 27 Mbps). Also, a reduced number of up-link results in reduced overhead cost and increased cluster stability in the network. Since VMaSC-LTE is used in highway scenario, in order to evaluate this method with VMaSC-LTE, the idea of this method was applied in this paper, scenario in the numerical example.

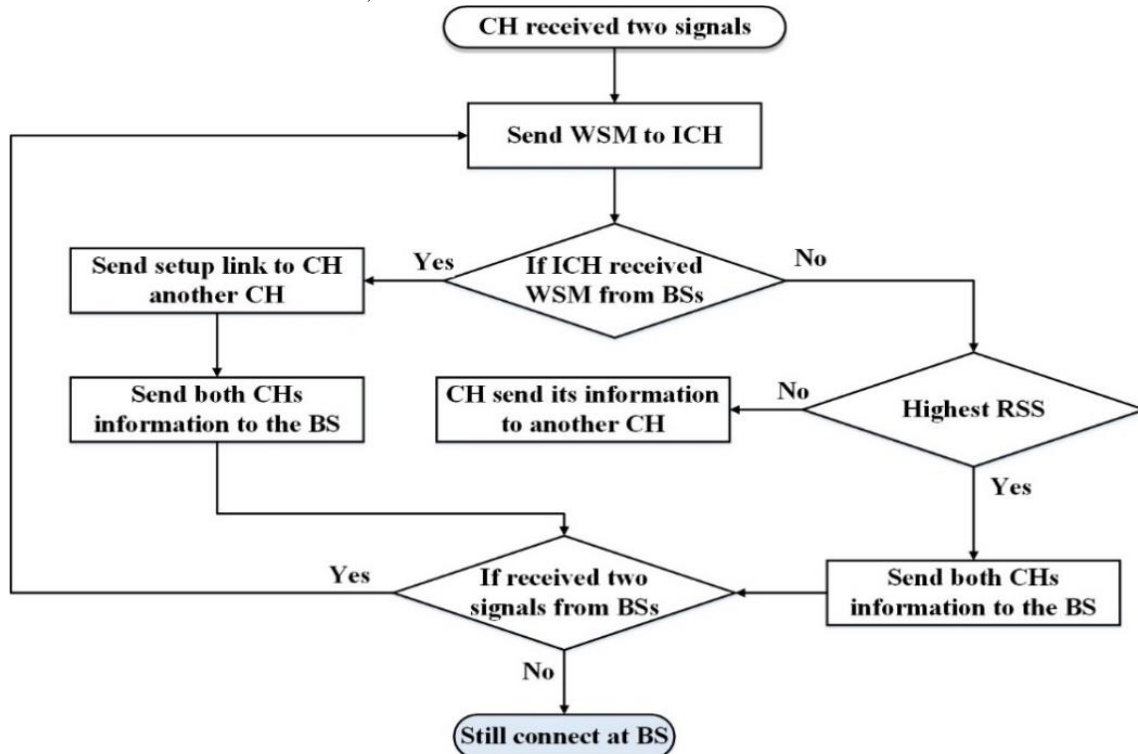


Fig. 6. Flowchart of Vehicles that Work as ICH.

If assumed length of road to be 10 km in urban Batu Pahat, Johor, Malaysia, and number of vehicles (N-V) to be 100 according to real-data of local cellular network in Batu Pahat, the TR of BS 300 m, the number of BSs (N-BS) is closer to 33 BS according to the real-data collected from local cellular networks. This resulted in 32 overlapping area (OA), the number of CMs (N-CMs) in each cluster is 20; therefore the total number of CHs (N-CHS) in this road is 5. These clusters in VMaSC-LTE have handover (HO) in each overlapping area. Therefore, a number of handovers in VMaSC-LTE are  $32 \times 5 \times 20 = 3200$  handovers for total cluster according to the number of CMs in each cluster over a 10 km road from 100 vehicles. However, in this method, no handover occurs in the clusters having ICH, but the handover occurs if the cluster does not have ICH. However, most of the clusters in proposed method have ICH because of high vehicle density in the urban area, especially in Batu Pahat city. From the above example and because the ICH connects only two CHs, in the above example one of five CH has handover in the overlapping area. Therefore, the number of packets lost in this cluster is calculated according to  $32 \times 1 \times 20 = 640$  handover in the network on the same road.

As shown in Fig. 7(A), there is no handover in the overlapping area because ICH changed the up-link when CH 2 received two signals from BS1 and BS2. However, in Fig. 7(B), the CH2 has no other choice than to send its cluster information, therefore the probability of handover occurrence is high. The number of handovers increases as road length and number of vehicles on the road increases. Table IV shows the result of a numerical example.

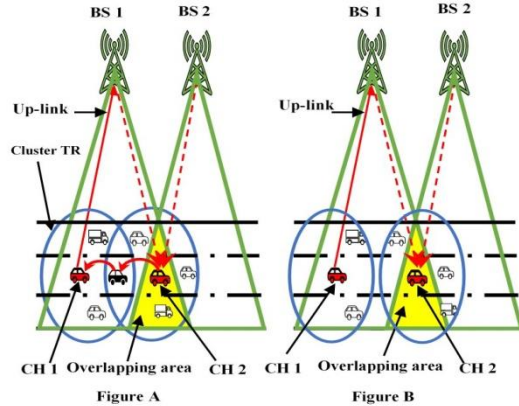


Fig. 7. Illustration of the difference between ICH and VMaSC-LTE Methods.

TABLE IV. RESULT OF A NUMERICAL EXAMPLE.

| Method         | Road | N-V | N-CH | N-BS | OA | HO   |
|----------------|------|-----|------|------|----|------|
| VMaSC-LTE [17] | 10km | 100 | 5    | 33   | 32 | 3200 |
| ICH            | 10km | 100 | 5    | 33   | 32 | 640  |

## V. SIMULATION MODELING

In this section, evaluated and validated ICH method with VMaSC-1hop method [17]. The evaluation was done by applying the concept of VMaSC-1hop on the scenario. VMaSC-1hop method has been selected for evaluation because it is close to the proposed idea. The VMaSC-1hop used GW to

merge clusters to reduce load at BSs, which consist of packet loss, packet delivery ratio, disconnect problem and number of uplink connection. Unfortunately, this method did not discuss the handover problem that occurs in the overlapping area. Therefore, the proposed method reduces the load at BSs in the overlapping area. Both methods are applied by using MATLAB-a 2018 in the simulation. The simulation parameters used in this study are shown in Table V.

### A. Performance Metrics

- Packet loss: This is defined as the number of CHs that failed in sending the cluster information to the BSs. In this study, the packet loss is measured in the overlapping area (cell edges) only. Also, the information related to CHs loss in this area consists of information of CH and its CMs. The packet loss increased when the number of clusters increased and the number of CMs in each CH increased.
- Packet delivery ratio (PDR): This is defined as the number of CHs that successfully sent its cluster information to the BS during cell edge. The PDR increased when the number of CH that successfully sent its cluster information in the cell edge increased and the number of CMs in each CH increased.
- A number of disconnections: It is the number of CH that lost connection with BS during cell edges from the total number of CH that successfully connects with the BS in this area.
- Network efficiency: The average ratio of a number of packet loss to the total number of PDR in the cells edge. Increased percentage of packet loss during cells edge result in reduced network efficiency.

### B. Performance Comparison between ICH Method and VMaSC-1hop Method

Table VI shows the ICH method has less packet loss than VMaSC-1hop method in cells edge because of the ICH transfer communication up link from CH that received two signals from different BSs to another CH. By this process, the number of packet loss is reduced. The VMaSC method used GW to make the connection between neighbors' CHs for merge mechanism without any permission to move up link connection because it is a normal node; therefore, the packet loss occurs in the cells edge. From the table, the ICH method also has packet loss, but much less than VMaSC method. The packet loss in the proposed method results from CH that had no neighbor CH. Therefore, in this case, the packet loss occurred in ICH method. The average percentage of packet loss at a cell edge in the ICH method and VMaSC-1hop method is 0.8% and 84%, respectively.

Fig. 8 shows the ICH method has higher packet delivery ratio than the previous method, and the reason is that proposed method can deliver packets even in cell edge by changing uplink from CH that has weak signal or confused single to CH that has good signal or only one signal. Thus, the percentage of PDR in proposed method is greater than the previous method. The average percentage of PDR at the cell edge in ICH method and VMaSC-1hop method is 99% and 15%, respectively.

TABLE V. SIMULATION PARAMETERS

| Parameters                       | Value               |
|----------------------------------|---------------------|
| Simulation time                  | 300 s in each run   |
| MAC protocol                     | IEEE 802.11p        |
| Transmission range               | 300 m               |
| Number of vehicles               | 100,200,300,400,575 |
| Road length                      | 17.8 km             |
| Number of lanes in the road      | 3                   |
| Length of car                    | 3 m                 |
| Maximum lane speed               | 10-100 km/h         |
| Number of hops                   | One hope            |
| maximum number of CMs in each CH | 20                  |
| Number of iterations             | 100                 |
| Number of runs                   | 10                  |

TABLE VI. NUMBER OF PACKET LOSS IN BOTH METHODS IN THE CELLS EDGE

| Number of Vehicles                                 | Proposed | VMaSC-1hop [17] |
|--|----------|-----------------|
| 100 Vehicles                                       | 181      | 6920            |
| 200 Vehicles                                       | 167      | 16422           |
| 300 Vehicles                                       | 151      | 25314           |
| 400 Vehicles                                       | 190      | 34466           |
| 575 Vehicles                                       | 149      | 50467           |
| The average number of packet loss in the cell edge | 167.60   | 26717.8         |

Fig. 9 shows the number of disconnect in the cells edge between ICH method and VMaSC-1hop method. The ICH method resulted in fewer disconnect than the previous method because the ICH allows CH to connect in the BS, even the CH in the cell edge, while the previous method during cell edge has disconnect because the CH received two signals from different BS and GW cannot transfer uplink connection to neighbor CH.

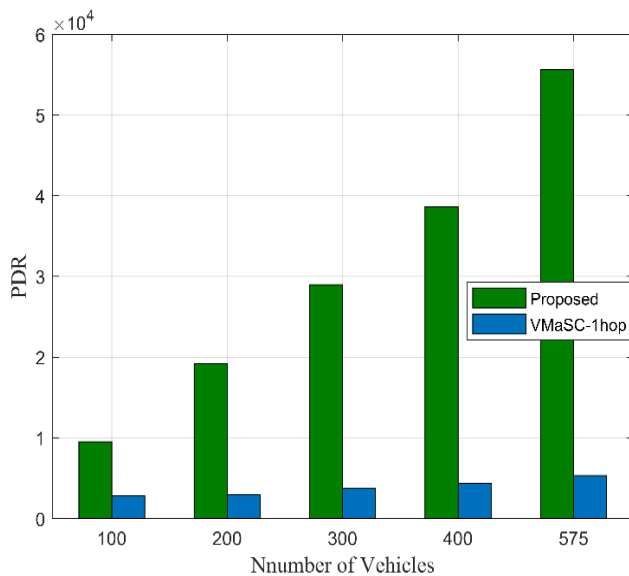


Fig. 8. PDR in the Cells Edge.

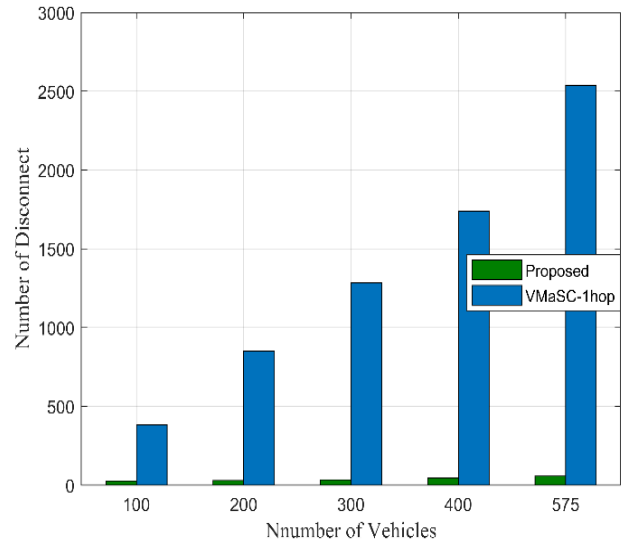


Fig. 9. Disconnect Problem During Cells Edge.

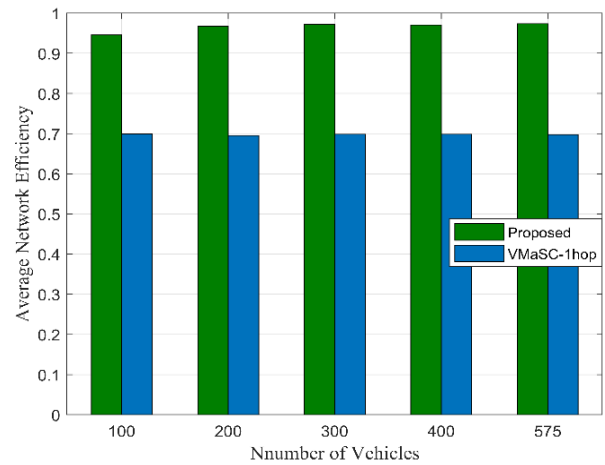


Fig. 10. Network Efficiency in the Cells Edge.

Fig. 10 shows the network efficiency of ICH and VMaSC-1hop method. From the figure, the ICH method results in a higher percentage of network efficiency than VMaSC-1hop method because ICH method has less percentage of packet loss, less percentage of disconnect problem and a higher percentage of PDR than VMaSC-1hop method. Therefore, the network efficiency in ICH method is higher than in VMaSC-1hop method. The average percentage of network efficiency in the ICH method and VMaSC-1hop method is 96% and 70%, respectively.

## VI. CONCLUSION

This paper has proposed a novel method known as Intelligent Cluster-Head to solve the handover problem that occurs in the overlapping area (cell edge) when the cluster is passed from one BS to another neighbor BS. ICH is a controller vehicle that controls a neighbor's CHs and specifies the cluster having the higher RSS to send vehicle information of both clusters to BS. Also, ICH has the ability to change uplink from one cluster to another to solve handover problem of CH receiving two signals from different BSs in direct

contact with ICH, and the ICH then changes the uplink to another cluster. The evaluation was done by using MATLAB software during evaluating the ICH method with the concept of VMaSC-1hop and the result shows the ICH method and VMaSC-1hop have an average percentage of packet loss of 0.8% and 84%, respectively. The percentage of PDR in ICH method and VMaSC-1hop is 99% and 15%, respectively. The number of disconnect in ICH method is less than VMaSC-1hop method and the network efficiency in ICH method VMaSC-1hop method is 96% and 70%, respectively. In future work, will analyse and evaluate the effect of delay and overhead when using the proposed method. Also, we will apply this method on a highway scenario.

#### REFERENCES

- [1] V. Vukadinovic, K. Bakowski, P. Marsch, I. D. Garcia, H. Xu, M. Sybis, P. Sroka, K. Wesolowski, D. Lister, and I. Thibault, "3GPP C-V2X and IEEE 802.11 p for Vehicle-to-Vehicle communications in highway platooning scenarios," *Ad Hoc Networks*, vol. 74, pp. 17–29, 2018.
- [2] G. Yan and D. B. Rawat, "Vehicle-to-vehicle connectivity analysis for vehicular ad-hoc networks," *Ad Hoc Networks*, vol. 58, pp. 25–35, 2017.
- [3] E. Ndashimye, S. K. Ray, N. I. Sarkar, and J. A. Gutiérrez, "Vehicle-to-infrastructure communication over multi-tier heterogeneous networks: a survey," *Comput. Networks*, vol. 112, pp. 144–166, 2017.
- [4] J. Hoefl Michal and Rak, "How to provide fair service for V2I communications in VANETs?," *Ad Hoc Networks*, vol. 37, pp. 283–294, 2016.
- [5] Y. A. Shah, H. A. Habib, F. Aadil, M. F. Khan, M. Maqsood, and T. Nawaz, "CAMONET: Moth-flame optimization (MFO) based clustering algorithm for VANETs," *IEEE Access*, vol. 6, pp. 48611–48624, 2018.
- [6] S. Vodopivec, J. Bešter, and A. Kos, "A survey on clustering algorithms for vehicular ad-hoc networks," in *Telecommunications and Signal Processing (TSP), 2012 35th International Conference on*, 2012, pp. 52–56.
- [7] S. M. AlMheiri and H. S. AlQamzi, "MANETs and VANETs clustering algorithms: A survey," in *GCC Conference and Exhibition (GCCCE), 2015 IEEE 8th*, 2015, pp. 1–6.
- [8] M. Gerla and J. T.-C. Tsai, "Multicluster, mobile, multimedia radio network," *Wirel. networks*, vol. 1, no. 3, pp. 255–265, 1995.
- [9] G. V. Rossi, Z. Fan, W. H. Chin, and K. K. Leung, "Stable clustering for ad-hoc vehicle networking," in *Wireless Communications and Networking Conference (WCNC), 2017 IEEE*, 2017, pp. 1–6.
- [10] A. Abuashour and M. Kadoch, "Performance improvement of cluster-based routing protocol in VANET," *IEEE Access*, vol. 5, pp. 15354–15371, 2017.
- [11] C. Shi, Y. Zhou, W. Li, H. Li, N. Lu, N. Cheng, and T. Yang, "A Centralized Clustering Based Hybrid Vehicular Networking Architecture for Safety Data Delivery," in *GLOBECOM 2017-2017 IEEE Global Communications Conference*, 2017, pp. 1–6.
- [12] R. Aissaoui, A. Dhraief, A. Belghith, H. Menouar, H. Mathkour, F. Filali, and A. Abu-Dayya, "Hebbs: A hierarchical cluster-based location service in urban environment," *Mob. Inf. Syst.*, vol. 2015, 2015.
- [13] Z. Khan and P. Fan, "A multi-hop moving zone (MMZ) clustering scheme based on cellular-V2X," *China Commun.*, vol. 15, no. 7, pp. 55–66, 2018.
- [14] S. A. Khawatreh and E. N. Al-Zubi, "Improved Hybrid Model in Vehicular Clouds based on Data Types (IHVCDT)," *Int. J. Adv. Comput. Sci. Appl.*, vol. 8, no. 8, pp. 114–118, 2017.
- [15] A. Mehmood, A. Khanan, A. H. H. M. Mohamed, S. Mahfooz, H. Song, and S. Abdullah, "ANTSC: An intelligent naive Bayesian probabilistic estimation practice for traffic flow to form stable clustering in VANET," *IEEE Access*, vol. 6, pp. 4452–4461, 2018.
- [16] I. Ahmad, R. M. Noor, I. Ahmady, S. A. A. Shah, I. Yaqoob, E. Ahmed, and M. Imran, "VANET LTE based heterogeneous vehicular clustering for driving assistance and route planning applications," *Comput. Networks*, vol. 145, pp. 128–140, 2018.
- [17] S. Ucar, S. C. Ergen, and O. Ozkasap, "Multihop cluster based IEEE 802.11 p and LTE hybrid architecture for VANET safety message dissemination," *IEEE Trans. Veh. Technol.*, vol. 65, no. 4, pp. 2621–2636, 2016.
- [18] R. S. Bali, N. Kumar, and J. J. P. C. Rodrigues, "An efficient energy-aware predictive clustering approach for vehicular ad hoc networks," *Int. J. Commun. Syst.*, vol. 30, no. 2, p. e2924, 2017.
- [19] S.-S. Wang and Y.-S. Lin, "PassCAR: A passive clustering aided routing protocol for vehicular ad hoc networks," *Comput. Commun.*, vol. 36, no. 2, pp. 170–179, 2013.
- [20] M. Song and F. Cuckov, "A Mobility-Aware General-Purpose Vehicular Ad-Hoc Network Clustering Scheme," *J. Inf. Sci. Eng.*, vol. 26, no. 3, pp. 897–911, 2010.
- [21] M. Ren, L. Khoukhi, H. Labiod, J. Zhang, and V. Vèque, "A mobility-based scheme for dynamic clustering in vehicular ad-hoc networks (VANETs)," *Veh. Commun.*, vol. 9, pp. 233–241, 2017.
- [22] D. Al-Terri, H. Otrok, H. Barada, M. Al-Qutayri, R. M. Shubair, and Y. Al-Hammadi, "Qos-olsr protocol based on intelligent water drop for vehicular ad-hoc networks," in *Wireless Communications and Mobile Computing Conference (IWCMC), 2015 International*, 2015, pp. 1352–1357.
- [23] E. Dror, C. Avin, and Z. Lotker, "Fast randomized algorithm for 2-hops clustering in vehicular ad-hoc networks," *Ad Hoc Networks*, vol. 11, no. 7, pp. 2002–2015, 2013.
- [24] S. Sbit, M. B. Dadi, and B. C. Rhaimi, "Comparison of Inter Cell Interference Coordination Approaches," *World Acad. Sci. Eng. Technol. Int. J. Electr. Comput. Energ. Electron. Commun. Eng.*, vol. 11, no. 7, pp. 865–870, 2017.
- [25] Y. Li, C. Niu, F. Ye, and R. Q. Hu, "A universal frequency reuse scheme in LTE-A heterogeneous networks," *Wirel. Commun. Mob. Comput.*, vol. 16, no. 17, pp. 2839–2851, 2016.
- [26] Z. Y. Rawashdeh and S. M. Mahmud, "A novel algorithm to form stable clusters in vehicular ad hoc networks on highways," *EURASIP J. Wirel. Commun. Netw.*, vol. 2012, no. 1, p. 15, 2012.
- [27] D. Roy, M. Chatterjee, and E. Pasiliao, "Video quality assessment for inter-vehicular streaming with IEEE 802.11 p, LTE, and LTE Direct networks over fading channels," *Comput. Commun.*, vol. 118, pp. 69–80, 2018.
- [28] L. Rui, Y. Zhang, H. Huang, and X. Qiu, "A New Traffic Congestion Detection and Quantification Method Based on Comprehensive Fuzzy Assessment in VANET," *KSII Trans. Internet Inf. Syst.*, vol. 12, no. 1, 2018.
- [29] S. Asoudeh, M. Mehrjoo, N.-M. Balouchzahi, and A. Bejarzahi, "Location service implementation in vehicular networks by nodes clustering in urban environments," *Veh. Commun.*, vol. 9, pp. 109–114, 2017.

# Weld Defect Categorization from Welding Current using Principle Component Analysis

Hayri Arabaci<sup>1</sup>

Electric-Electronics Engineering Department  
Selçuk University Konya, Turkey

Salman Laving<sup>2</sup>

Mechatronics Engineering Department  
Selçuk University Konya, Turkey

**Abstract**—Real time welding quality control still remains a challenging task due to the dynamic characteristic of welding. Welding current of gas metal arc welding possess valuable information that can be analyzed for weld quality assessment purposes. On-line monitoring of motor current can be provided information about the welding. In this study, current signals obtained during welding in the short-circuit metal transfer mode were used for real-time categorization of deliberately induced weld defects and good welds. A hall-effect current sensor was employed on the ground wiring of the welding machine to acquire the welding current signals during the welding process. Vector reduction of the current signals in time domain was achieved by principle component analysis. The reduced vector was then classified by various classification techniques such as support vector machines, decision trees and nearest neighbor to categorize the arc weld defects or pass it as a good weld. The proposed technique has proved to be successful with accurate classification of the welding categories using all three classifiers. The classification technique is fast enough so it can be used for real time weld quality control as all the signal processing is carried out in the time domain.

**Keywords**—Arc weld defects; feature extraction; PCA; classification techniques; on-line monitoring

## I. INTRODUCTION

Welding is an integral process in manufacturing in the metal industry. Gas Metal Arc Welding (GMAW) is usually chosen over other welding techniques due to its various advantages. A few major advantages are high productivity, can be used for automation, is mobile and the welding can be carried out from various angles and positions. Due to its exponential growth and vital importance in the industry, the need for evaluating any defects present on the welded parts arose. A lot of research has been carried out to overcome this challenge but due to the complexity of the physics involved in arc welding [1] the challenge has not been successfully overcome. The complexities arise from the various variables/parameters that define the dynamic welding process such as gas flow rate, welding intensity, welding speed, electrode feed rate, material composition, arc length, weld seam geometry etc. All these variables are interrelated by a highly non-linear and interdependent process [2], making it difficult to come up with a valid theoretical model to define the process. Therefore, many researchers in the area have focused on studying the welding parameters individually or combining a few together to get feedback on the final weld quality.

Several undesired scenarios can appear during the welding processes which may directly affect the quality of the final welds. Some of the known factors of weld defect and irregularities during GMAW are; Instantaneous short circuits, failure of arc re-ignition and wire feed rate variations [3]. These factors, if kept under steady control, can lead to achieving a good final weld. Other factors which cannot be directly controlled like contamination and environmental conditions in the welding area need to be kept optimal to ensure quality welding. Commonly used off-line techniques to identify welding quality include destructive (macrographs) and non-destructive testing like x-ray, ultrasounds, penetrant liquids, magnetic particles, etc. [4]. These off-line techniques, although being accurate, have many drawbacks so research work has mostly focused on developing an on-line sensing and welding path determination by using feedback and adaptive control [5]. On-line monitoring of the welding process reduces the effects of the uncontrollable factors and also saves on the otherwise resource consuming quality control inspection. Several sources such as welding sound, voltage signal, current signal, power, weld-pool image, electric arc are found to have a correlation with weld quality [6]. Therefore the most commonly used methods of on-line quality inspection derive from the use of welding voltage and current [7], welding sound [8] and high-speed photography [9].

Multiple studies have been carried out to analyze the sound produced for the purpose of on-line weld defect. It is common knowledge that the human welder combines both audible sound and vision to control the welding process [10]. The knowledge of the behavior of acoustic signals generated during the welding process is important for inspection of the consistency of the process [11]. The sound signals produced during GMAW carry information about the transfer mode, behavior of the arc column and the molten pool [8]. A mathematical relationship that relates the sound produced during the welding, the arc voltage and the welding current was formulated by [12]. A study by [13] showed that the short circuit transfer mode of the GMAW produces discernible sound which makes it easier to capture and analyze compared to the other two modes; Globular mode and spray mode. Despite the vast research on this area, industrial use of sound signals for on-line quality monitoring of GMAW is still not realized. This is due to the fact that in the industrial environment background noise is a great hindrance to the acquisition of the welding sound. Usually research is carried out in laboratories using welding trolleys or a moving

workpiece that is usually not the case in the industries. The background noise in these laboratories is from the shielding gas and the welding machine which is not a hindrance since their magnitude is very low compared to the actual welding sound [14]. In addition, the sound signals require some signal processing before being able to use which makes the on-line defect detection slower. Some of the basic signal processing includes filtering the sound signal in time domain and then converting the filtered signal to frequency domain for further processing [15].

High-speed photography is another method some researchers have used to develop on-line weld defect detection. It is not a very common technique due to the fact that it is expensive, can be affected by splatter which can damage the acquisition equipment which is closely placed to the welding torch and requires high bandwidth for acquisition and processing. Measuring the arc voltage and welding current is a common method researchers have been using for defect detection in the welding process [7]. This method is simple and relatively reliable and most of the signal processing can directly be carried out in the time domain. Welding equipment usually keep one of the parameters constant; constant voltage or constant current welding equipment. It is common to take the parameter that is variable for weld quality control purposes.

Several time domain processing techniques have been suggested by researchers. Some have successfully used welding voltage or welding current to detect a defect in the welding process. Control charts have been used by [16] on the welding voltage to identify porosity in the final weld. They confirmed their study using radiographic test. Hilbert–Huang transform and time–frequency entropy was used by [17] on preprocessed current signals to estimate the stability of short-circuiting GMAW. The author in [18] proposed using regression modeling using all the three parameters; sound, current and voltage to predict two main weld quality measures; welding defects and bead shape factor. A technique of Wavelet packet coefficients of current signal in back-propagation Artificial Neural Network (ANN) was used by [19] to monitor weld defects in Pulsed Metal Inert Gas Welding. The authors achieved an error rate of 11% using this technique. ANN together with PCA feature extraction was successfully employed by [20] to monitor arc-welding systems. They presented several examples of weld seams that showed that, once the ANN has been properly trained, it can efficiently discriminate different welding defects, lack of penetration and gas flow reduction among others. Many similar approaches have been used in research and theoretically the results are promising. However, a universal on-line system that will detect weld defect and categorize them immediately is still lacking. Some approaches require too much time to process and give results which may be a hinder for on-line control. Some approaches tend to be complex so implementation cannot be realized. For example acquiring voltage, current and sound at the same time complicates the system and may lose versatility where it may work for some applications and be erroneous on others.

This study presents a technique for detecting a weld defect and categorizing the cause of the weld defect. Current signals

were acquired from deliberately induced weld defects as well as from good welding. The weld faults were induced by:

- Deliberate fast welding
- Welding carried out without shielding gas
- Deliberate slow welding
- Increasing the wire feed rate
- Decreasing the wire feed rate

The captured current signals in time domain are then processed using PCA for vector reduction. The reduced vector samples are then divided into train and test samples for classification. A total of three classifiers were used to identify which classifier is the fastest and most accurate. This technique aims to reduce the complexity of the system, be versatile and give results fast enough so they can be used for on-line defect detection and categorize the cause of faulty welds.

## II. EXPERIMENTAL PROCEDURE

Standard industrial, constant voltage, welding equipment, OZEN GDC360 V was used in this study. The experiments were carried out on mild steel plates which were 4 mm thick using an electrode wire with a diameter of 1.0mm. The shielding gas used was a mixture of Argon (80%) and Carbon 20(%). The welding current is sampled at 20 kHz from a Hall effect current sensor using a data acquisition card. The photograph of the welding set-up and components used are shown in Fig. 1 while the data acquisition system photograph is shown in Fig. 2. The block diagram of the used experimental system is given in Fig. 3. An experienced welder carried out the welding and varied the parameters for deliberate faulty welding. The parameters for a good weld are shown in Table I. Eight runs for each welding class were made with a run time of approximately 5 seconds for each run. feature extraction and classification were made for each data. Flow chart of the technique used in this study was given in Fig. 4.



Fig. 1. Welding Set-Up.

TABLE I. WELD CLASS DATA ROW PLACEMENT IN A MATRIX

| Parameter              | Value      |
|------------------------|------------|
| Wire Feed Rate         | 350 cm/min |
| Approximate Weld Speed | 30 cm/min  |



Fig. 2. Data Acquisition System.

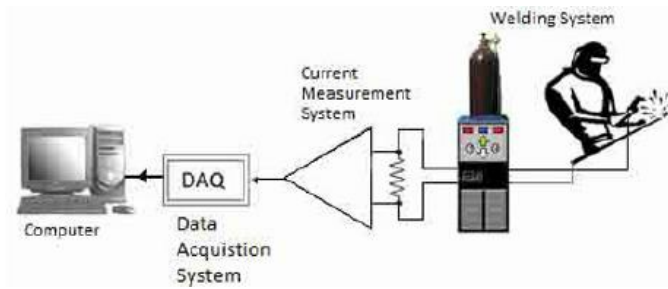


Fig. 3. Block Diagram of the Experimental Set-up [21].

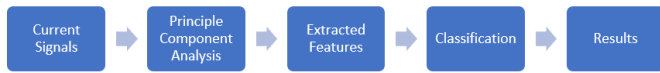
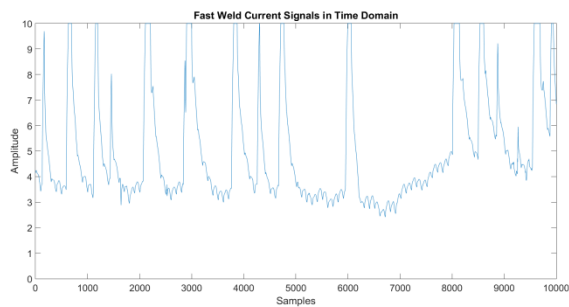


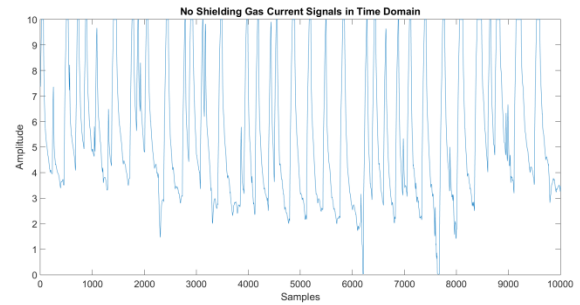
Fig. 4. Flow Chart of the Technique used in this Study.

### III. EXPERIMENTAL RESULTS AND DATA PROCESSING

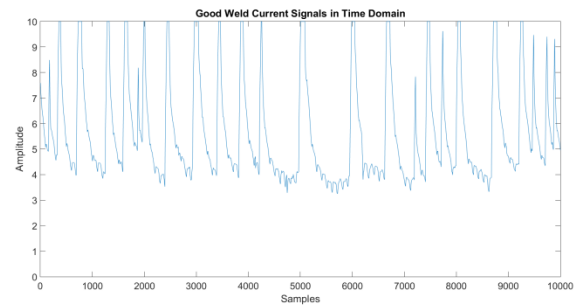
The Current signals of each weld run acquired on the data acquisition system were exported in excel format to a PC for the processing. Each signal had around 100,000 samples so the first part of the processing was to truncate the signals to 10,000 samples. To get accurate results, the truncation was done randomly on different parts of the signal. Several truncation runs were made from different parts of the signal each time to ensure legitimacy of the results. The plots on Fig. 5(A-F) show the signals truncated from sample 30,001 to 40,000 from the first test runs of the different weld types plotted versus time.



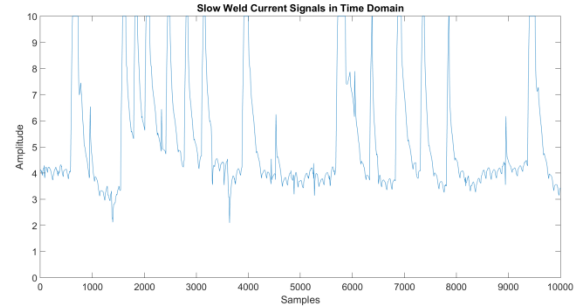
(A) Current Signals Obtained from Fast Welding.



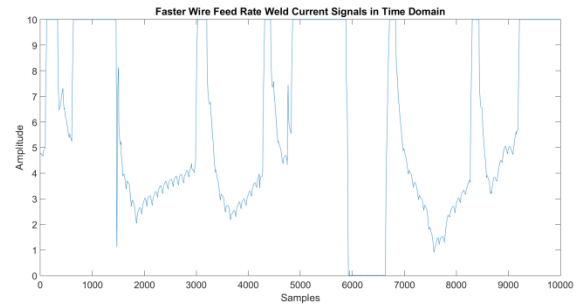
(B) Current Signals Obtained from Welding without Shielding Gas.



(C) Current Signals Obtained from Good Welding.



(D) Current Signals Obtained from Slow Welding.



(E) Current Signals Obtained from Fast Wire Feed Rate Welding.



Fig. 5. (F) Current Signals Obtained from Slow Wire Feed Rate Welding.



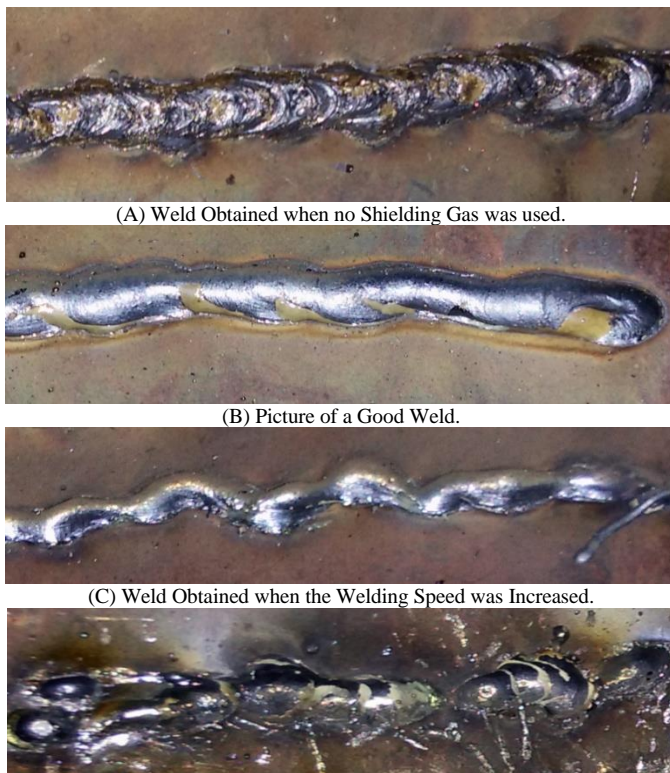


Fig. 6. (D) Weld Obtained when the Wire Feed Rate is reduced.

The rising and falling of the welding current in a well-defined pattern usually signifies a good weld. This can clearly be seen on Fig. 5C where the peaks are in a good pattern and well spread out with little difference between peak gaps. A photograph of the good weld is shown in Fig. 6B. Notice the few peaks in Fig. 5A; the welding process was too fast therefore short circuits took place far apart resulting in a bad weld. Fig. 6C shows a photograph of a fast weld where it can be seen that the material deposition is less. Rapid peak currents can be noticed on the weld carried out without shielding gas as shown on Fig. 5B. Fig. 6A shows the weld carried out without using shielding gas. The porosity of the final weld can be seen. With a fast wire feed rate shown on Fig. 5E, the electrode is vigorously fed to the workpiece leading to constant contact (short circuit) therefore the current is almost always peaked. From Fig. 5F it can be deduced that with a slow wire feed rate, there is little metal deposition with time therefore short circuits that are very far apart. Fig. 6D shows the corresponding photograph where the weld is basically just splatter.

From Fig. 5(A-F) it is clear that welding current signals possess valuable data that can be used to categorize weld defects. Statistical methods like Peak to Peak, Standard Deviation, Root Mean Square, Skewness and Kurtosis etc. could directly be used on this raw data to identify the weld defects with some success. But in the real industrial environment such deliberately induced weld defects would not exist. The variation of the short circuit peaks may be little when a defect comes across so statistical methods may be left wanting. Therefore Principal Component Analysis (PCA) was chosen for this study. PCA not only finds the variance in data, but it also carries out dimensional reduction which gets rid of

redundant data. This is especially useful when using a classifier to classify the data.

#### A. Principle Component Analysis

Principle Component Analysis (PCA) is one of the most important methods used in pattern recognition and compression. In the works of [22], fault detection applications in industries using PCA have been presented. The authors reviewed cases where PCA was successfully implemented in the various industries coming up with a conclusion that it is feasible to use PCA for successful fault detection. Despite this fault detection success in the industry, PCA is more commonly known for its role in facial recognition applications. Many researchers on facial recognition techniques choose to use PCA for feature extraction from the facial images. In PCA method, the 2-Dimensional face image matrices are transformed into a 1-Dimensional vector [23]. Since signals are already in a 1-Dimensional vector, it simplifies the data processing even further as there is no need to concatenate the vector before applying the PCA method. The main steps to be carried out in the PCA approach are summarized below:

- 1) Standardize the scale of the data into d-dimensional vector (d is the different classes of data).
- 2) Compute the covariance matrix for the data. The covariance matrix is the scatter matrix.
- 3) Obtain the Eigenvectors and Eigenvalues from the covariance matrix or alternatively perform Singular Vector Decomposition. Eigenvectors and Eigenvalues exist in pairs: every eigenvector has a corresponding eigenvalue. An eigenvector can simply be thought of as a direction while an eigenvalue is a number showing how much variance there is in the data in that direction.
- 4) Sort the eigenvectors in order of decreasing eigenvalues and choose k eigenvectors with the largest eigenvalues to form a d by k dimensional matrix W in which every column represents an eigenvector. W is our new projection matrix
- 5) Finally, the projection matrix is used to transform the samples onto the new subspace.

In our case, we had 8 test runs for each of the 6 weld groups (5 faulty welds and 1 good weld). To make processing much faster only the last 5 test runs were used for PCA. Therefore, a total of 30 different classes were used for the feature extraction each having 10,000 samples. The data was standardized into one matrix of 30 by 10,000. The first five samples were of Fast welding followed by No Shield Gas welding. The Good weld data was on classes 11-15 followed by Slow welding, Rapid Wire Feed weld and Slow Wire Feed Rate weld at classes 26-30 as shown in Table II.

Then the covariance of this matrix was computed. This resulted in a 10,000 by 10,000 matrix. This was followed by obtaining the eigenvectors and corresponding eigenvalues from the covariance matrix and choosing 100 eigenvectors from the 10,000 obtained with largest eigenvalues in a descending order. Projecting onto the subspace leaves us with a matrix of just 30 by 100. Taking fewer Eigenvectors will increase the speed of the process but may affect the performance. Taking more eigenvectors would lead to slow processing with a slight

increase in performance up to a certain point. In our case 100 was found to be optimal. The data at this point was ready to be used for classification.

TABLE II. WELD CLASS DATA ROW PLACEMENT IN A MATRIX

| Type of Weld             | Row Placement |
|--------------------------|---------------|
| Fast Welding             | 1 to 5        |
| No Shielding Gas Welding | 6 to 10       |
| Good Welding             | 11 to 15      |
| Slow Welding             | 16 to 20      |
| Fast Wire Feed Welding   | 21 to 25      |
| Slow Wire Feed Welding   | 26 to 30      |

Classification is a supervised learning approach in which the computer program trains from the data input given to it and then uses this training to classify new observation. The most commonly used classifiers are;

- 1) Naive Bayes Classifier
- 2) Support Vector Machines
- 3) Decision Trees
- 4) Boosted Tress
- 5) Random Forest
- 6) Artificial Neural Networks
- 7) Nearest Neighbor

For this study SVM, Decision Tress and Nearest Neighbor classifiers were used.

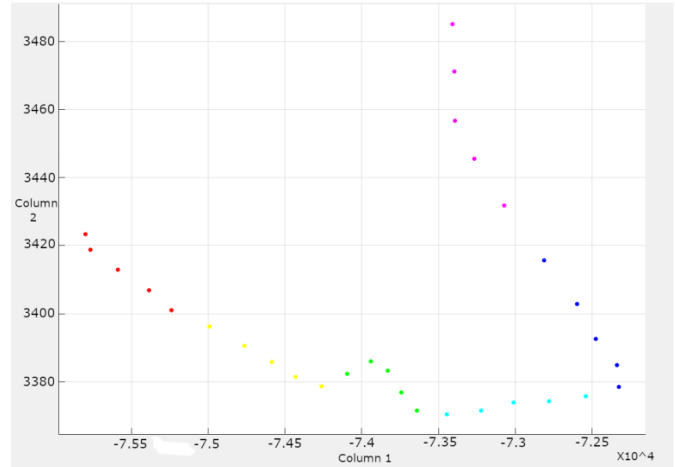
### B. Support Vector Machines

Support Vector Machines (SVM) classifier makes use of the special function called the kernel, with which the experimental data set is converted from the original space of characteristics into the higher dimension space with the construction of a hyperplane that separates classes [24]. SVM is one of the most popular classification systems in data mining and pattern recognition applications, due its high classification rates [25]. It gives very good results in terms of accuracy when the data are linearly or non-linearly separable. When the data are linearly separable, the SVMs result is a separating hyperplane, which maximizes the margin of separation between classes. If data are not linearly separable, the algorithm works by mapping the data to a higher dimensional feature space using an appropriate kernel function [26].

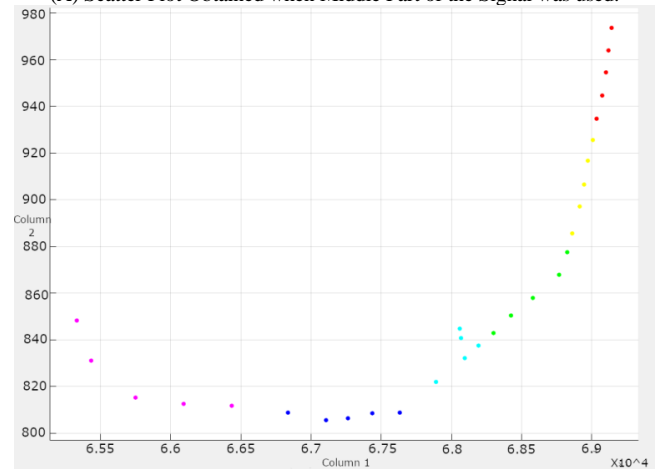
### C. Classification Results and Discussion

The Projection vector was tested with the three mentioned classification techniques. To decide on which runs of the weld classes to choose for training and testing, two methods can be used; Cross Validation and Holdout. Holdout simply takes a percentage of the data for training and tests the rest with that trained data. This method is good for large data sets. Since each weld class had just five runs in the reduced vector, using holdout method was not feasible so cross validation method was used. Cross validation method selects a number of divisions to partition the data into. Each division is then held out in turn for testing. The classifier trains each division using data outside the division and the data to be tested is within the division and the average test error over all division is

calculated. In this way all data is used for both training and testing thus classifying more accurately. This method takes longer to classify compared to holdout but the overall efficiency of the results is better. The classifier results are presented in three different figures to give a good idea of the accuracy of each classifier and show which weld class was misclassified. The three figures show Percentage Accuracy, Confusion Matrix and Scatter Plots.



(A) Scatter Plot Obtained when Middle Part of the Signal was used.



(B) Scatter Plot Obtained when Random Part of the Signal was used.

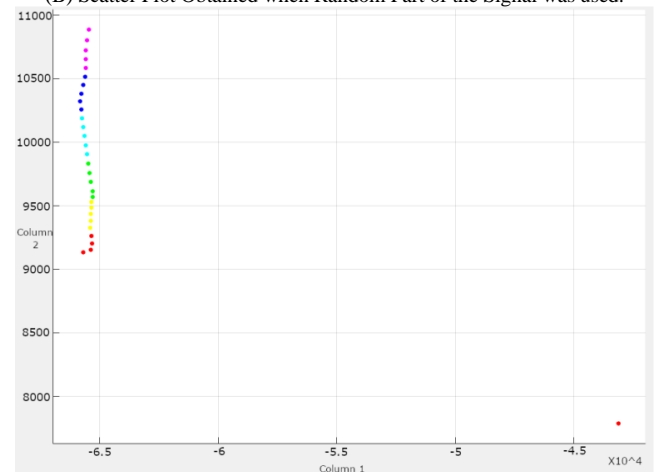


Fig. 7. (C) Scatter Plot Obtained when the First Part of the Signal was used.

Fig. 7(A-C) shows the scatter plots of the projected vector data. The different color dots represent the weld types. A scatter plot gives an idea of how successful PCA was on a certain data set. Well spread out data means that the feature extraction was successful and high success rates in classification. Data points of different classes close to each other on the scatter plot will usually lead to a less accurate classification but that also depends on the classification algorithm used as well. Figures 8A and 8B show the scatter plot from PCA conducted on the middle parts of the signal. The data is well scattered and the features from the different weld types are discernible. Fig. 7C shows the scatter plot from PCA conducted on the first part of the signals, which is from sample 1 to 10,000. Although the different weld types can be differentiated, the feature points are not so well spread out compared to when the middle parts of the signal are used.

Fig. 8 (A-D) shows the percentage accuracy of the three classifiers used on the projected vector from different parts of the signal. Fig. 9A and 9B, whose corresponding scatter plot is 8A and 8B, are the results of when the middle part of the signal was used. Fig. 8C resulted from the same projected vector as 9B but in this case Quadratic SVM was used instead of Linear SVM to see the effect on the final accuracy. Fig. 8D, whose corresponding scatter plot is Fig. 8C, is the accuracy when the first part of the signal was used. From the accuracy plots it is clear that using the first parts of the signal can result in lesser accuracy. This may be due to the fact that during the first few seconds of the welding process the process is not very stable and the current readings may fluctuate abnormally. It is also clear that k-nearest-neighbors is by far more accurate and reliable for classification on our dataset. It achieved 100% accuracy in all runs except for the first part of the signals where an accuracy of 90% was realized. SVM is also a reliable classifier for our data set and using Quadratic SVM increased the accuracy as depicted from Fig. 9B and 9C. Decision Trees classifier performed poorly and is unreliable for our data set. Overall speed of all the classifiers was very fast. In a matter of milliseconds we had the accuracy results. Generally the accuracy results portray the success of using PCA on current signals for weld defect detection.

Fig. 9 (A-D) shows the confusion matrix of the classifiers. A confusion matrix is a table that is often used to describe the performance of a classifier on a set of test data for which the true values are known. As the green shade gets darker the percentage accuracy increases while darkening shade of red implies increasing percentage error in classification. The Legend for Confusion matrix is presented in Table III. Fig. 9A shows the confusion matrix of the k-nearest-neighbors classifier (almost all runs from different parts of the signals had the same result). The k-nearest-neighbors classifier accurately categorized the weld defects and can tell whether it was a good weld or not. Fig. 9B shows confusion matrix of the SVM classifier when the first part of the signal was used. The classifier could not tell the difference between fast welding, no-gas welding and good welding in some of the weld test runs.

It misclassified 2 good weld runs as being no-gas weld runs and 2 no-gas weld runs as being fast weld runs. When other parts of the signals were used SVM had 100% accuracy in categorization. Confusion matrix for decision trees is shown in Fig. 10C and 10D. Decision tree classifier struggled in categorizing the welding types. In some cases, it totally misclassified the weld types as can be seen from Fig. 9D where it entirely misclassified the good weld and slow wire feed rate weld. Overall accuracy of categorization by Decision Tree was around 80% when the whole signal is considered.

|              |       |
|--------------|-------|
| Tree         |       |
| Complex Tree | 71.4% |
| SVM          |       |
| Linear SVM   | 100%  |
| KNN          |       |
| Fine KNN     | 100%  |

(A) Classification Accuracy when Middle Part of Signal was used.

|              |       |
|--------------|-------|
| Tree         |       |
| Complex Tree | 100%  |
| SVM          |       |
| Linear SVM   | 93.3% |
| KNN          |       |
| Fine KNN     | 100%  |

(B) Classification Accuracy when Random Part of Signal was used.

|               |      |
|---------------|------|
| Tree          |      |
| Complex Tree  | 100% |
| SVM           |      |
| Quadratic SVM | 100% |
| KNN           |      |
| Fine KNN      | 100% |

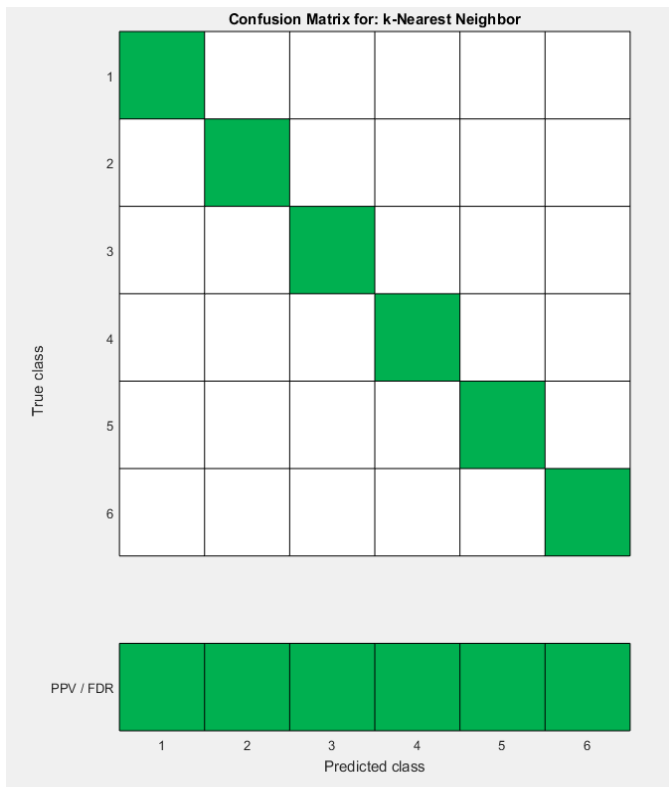
(C) Classification Accuracy when Quadratic SVM was used Instead of Linear SVM.

|              |       |
|--------------|-------|
| Tree         |       |
| Complex Tree | 63.3% |
| SVM          |       |
| Linear SVM   | 86.7% |
| KNN          |       |
| Fine KNN     | 90.0% |

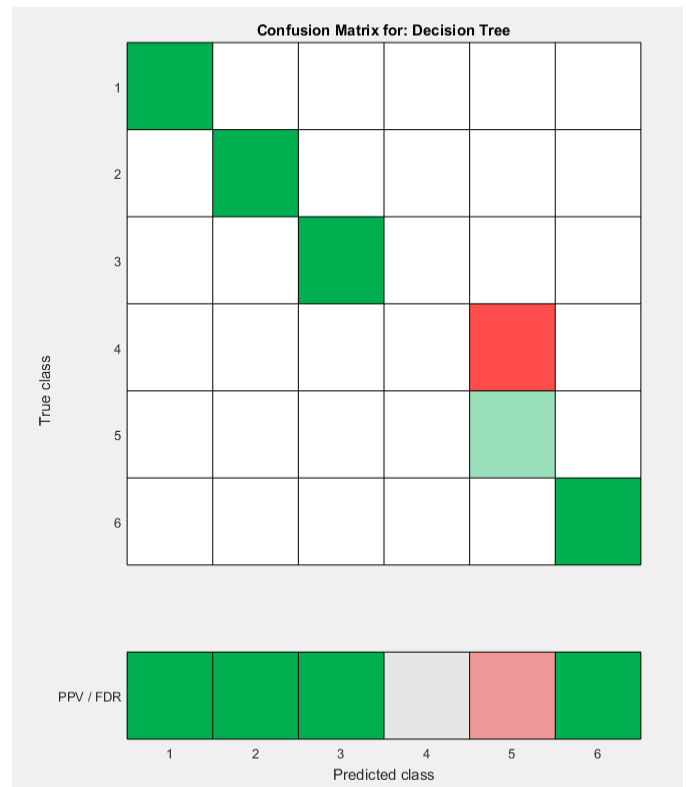
Fig. 8. (D) Classification Accuracy when First Part of Signal was used.

TABLE III. LEGEND FOR CONFUSION MATRIX

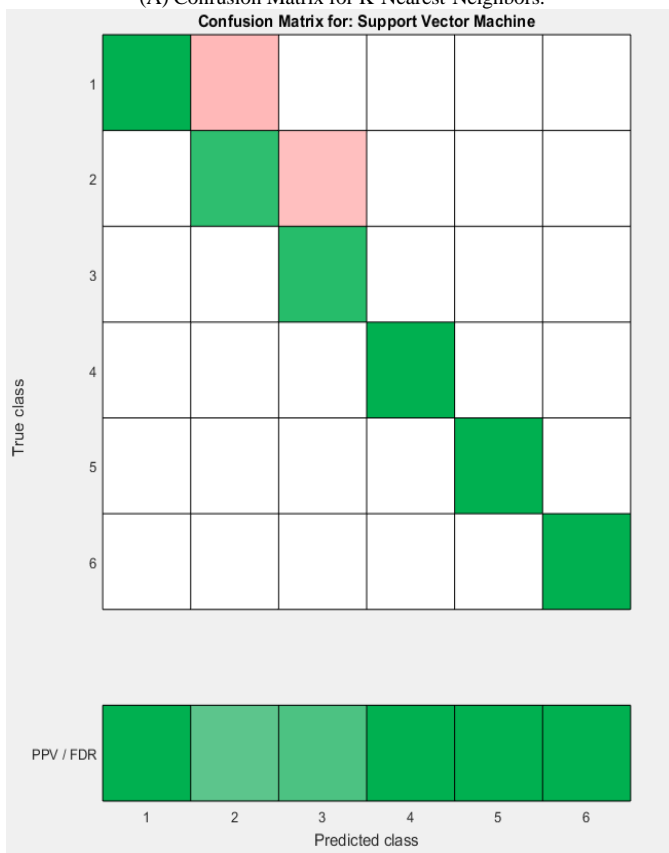
| Class Number | Weld Class Represented   |
|--------------|--------------------------|
| 1            | Fast Welding             |
| 2            | No Shielding Gas Welding |
| 3            | Good Welding             |
| 4            | Slow Welding             |
| 5            | Fast Wire Feed Welding   |
| 6            | Slow Wire Feed Welding   |



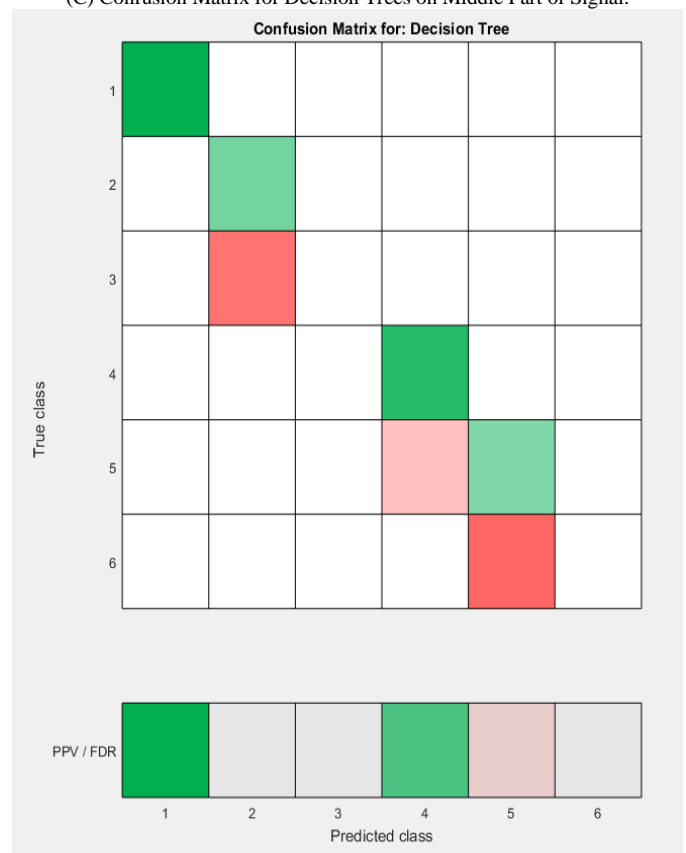
(A) Confusion Matrix for K-Nearest-Neighbors.



(C) Confusion Matrix for Decision Trees on Middle Part of Signal.



(B) Confusion Matrix for SVM on First Part of Signal.



(D) Confusion Matrix for Decision Trees on First Part of Signal.

#### IV. CONCLUSION

In this paper, an attempt was made to categorize weld defects from current signals using PCA and a suitable classifier. Current signals were obtained from deliberately defected welding and good welds. Defected welding was obtained by either changing the welding speed, changing the wire feed rate or carrying out welding without shielding gas. Features from the obtained current signals were extracted using PCA. The extracted features were then used to classify the weld defects or pass it as a good weld. Three classifiers were used namely SVM, Decision Trees and Nearest Neighbor. The results showed that Nearest Neighbor classifier was the most accurate with 100% accuracy in categorizing the weld defects in almost all cases. SVM classifier followed closely with high accuracy in most of the runs. Decision Trees classifier did not perform as well as the other classifiers but its overall classification accuracy was around 80%. The total time taken from data acquisition to feature extraction and classification is very low. Since this set-up did not immediately process the welding signals on-line, only an estimate of the processing and classification time of less than a minute can be given. This little time taken and the few resources required proves that the method proposed in this study could successfully be employed for on-line weld defect detection and categorization in the GMAW process. For future work, this technique could be improved by employing a robot to carry out the welding and carrying out the research on-line to prove the efficiency of this technique.

#### REFERENCES

- [1] Wu, C. S., M. Ushio, and M. Tanaka. "Analysis of the TIG welding arc behavior." *Computational Materials Science* 7.3 (1997): 308-314.
- [2] Cary HB. *Modern welding technology*. New Jersey: Prentice Hall; 1989.
- [3] Hermans, M. J. M., and G. Den Ouden. "Process behavior and stability in short circuit gas metal arc welding." *Welding Journal-New York* (1999): 137-s.
- [4] Mirapeix, J., et al. "Real-time arc-welding defect detection and classification with principal component analysis and artificial neural networks." *NDT & e International* 40.4 (2007): 315-323.
- [5] Saini, D., and S. Floyd. "An investigation of gas metal arc welding sound signature for on-line quality control." *Welding Journal-New York-77* (1998): 172-s.
- [6] Zhang, Zhifen, et al. "Online welding quality monitoring based on feature extraction of arc voltage signal." *The International Journal of Advanced Manufacturing Technology* 70.9-12 (2014): 1661-1671.
- [7] Polajnar, Ivan, Zoran Bergant, and Janez Grum. "Arc Welding Process Monitoring by Audible Sound." *12th International Conference of the Slovenian Society for Non-Destructive Testing: Application of Contemporary Non-Destructive Testing in Engineering*. 2013.
- [8] Grad, Ladislav, et al. "Feasibility study of acoustic signals for on-line monitoring in short circuit gas metal arc welding." *International Journal of Machine Tools and Manufacture* 44.5 (2004): 555-561.
- [9] Wang, Qi Long, Pen Jin LI, and Masaaki Naka. "Arc light sensing of droplet transfer and its analysis in pulsed GMAW process." *Quarterly Journal of the Japan Welding Society* 15.3 (1997): 415-424.
- [10] Čudina, Mirko, Jurij Prezelj, and Ivan Polajnar. "Use of audible sound for on-line monitoring of gas metal arc welding process." *Metalurgija* 47.2 (2008): 81-85.
- [11] Roca, A. Sánchez, et al. "New stability index for short circuit transfer mode in GMAW process using acoustic emission signals." *Science and Technology of Welding and Joining* 12.5 (2007): 460-466.
- [12] Cayo, E. H., and SC Absi Alfaro. "Weld transference modes identification through sound pressure level in GMAW process." *Journal of Achievements in Materials and Manufacturing Engineering* 29.1 (2008): 57-62.
- [13] Cayo, E. H., and SC Absi Alfaro. "Welding quality measurement based on acoustic sensing." *Proceedings of 19th International Congress of Mechanical Engineering*. 2007.
- [14] Schiebeck, E. "Audible range acoustic diagnosis of the MAG welding arc." *Welding international* 5.7 (1991): 572-576.
- [15] Ghofrani, Mohsen, Hamid Shahabi, and Farhad Kolahan. "Evaluate and control the weld quality, using acoustic data and artificial neural network modeling." *Indian Journal of Scientific Research* 1 (2014).
- [16] Thekkuden, Dinu Thomas, et al. "Assessment of Weld Quality Using Control Chart and Frequency Domain Analysis." *ASME 2018 Pressure Vessels and Piping Conference*. American Society of Mechanical Engineers, 2018.
- [17] Huang, Yong, et al. "Feature extraction for gas metal arc welding based on EMD and time-frequency entropy." *The International Journal of Advanced Manufacturing Technology* 92.1-4 (2017): 1439-1448.
- [18] Shahabi, Hamid, and Farhad Kolahan. "Regression modeling of welded joint quality in gas metal arc welding process using acoustic and electrical signals." *Proceedings of the Institution of Mechanical Engineers, Part B: Journal of Engineering Manufacture* 229.10 (2015): 1711-1721.
- [19] Srivastava, Mr Shashank, and Mr Samuel Debbarma. "Artificial Neural Network based monitoring of Weld Quality in Pulsed Metal Inert Gas Welding using Wavelet Packets of Current Signal." (2017).
- [20] Mirapeix, J., et al. "Real-time arc-welding defect detection and classification with principal component analysis and artificial neural networks." *NDT & e International* 40.4 (2007): 315-323.
- [21] Akinci, Tahir Çetin, Hidir Selçuk Noğay, and Gökhan Gökmen. "Determination of optimum operation cases in electric arc welding machine using neural network." *Journal of mechanical science and technology* 25.4 (2011): 1003-1010.
- [22] Shaikh, Shakir M., et al. "Data-driven based Fault Diagnosis using Principal Component Analysis." *INTERNATIONAL JOURNAL OF Advanced Computer Science and Applications* 9.7 (2018): 175-180.
- [23] Barnouti, Nawaf Hazim, et al. "Face Detection and Recognition Using Viola-Jones with PCA-LDA and Square Euclidean Distance." *International Journal of Advanced Computer Science and Applications (IJACSA)* 7.5 (2016): 371-377.
- [24] Demidova, Liliya, Evgeny Nikulchev, and Yu Sokolova. "The svm classifier based on the modified particle swarm optimization." *International Journal of Advanced Computer Science & Applications* 7.2 (2016): 16-24.
- [25] Kadh, Mustafa S., and Asst Prof Dr Alia Karim Abdul. "Handwriting Word Recognition Based on SVM Classifier." *International Journal of Advanced Computer Science & Applications* 1 (2015): 64-68.
- [26] Afifi, Ashraf. "Laguerre kernels-based SVM for image classification." *International Journal of Advanced Computer Science and Applications* 5.1 (2014).

# Moving Object Detection in Highly Corrupted Noise using Analysis of Variance

Asim ur Rehman Khan<sup>1</sup>, Muhammad Burhan Khan<sup>2</sup>, Haider Mehdi<sup>3</sup>, Syed Muhammad Atif Saleem<sup>4</sup>

Multimedia Lab

National University of Computer and Emerging Sciences (NUCES)  
Pakistan

**Abstract**—This paper implements three-way nested design to mark moving objects in a sequence of images. Algorithm performs object detection in the image motion analysis. The inter-frame changes (level-A) are marked as temporal contents, while the intra-frame variations identifies critical information. The spatial details are marked at two granular levels, comprising of level-B and level-C. The segmentation is performed using analysis of variance (ANOVA). This algorithm gives excellent results in situations where images are corrupted with heavy Gaussian noise  $\sim N(0, 100)$ . The sample images are selected in four categories: ‘baseline’, ‘dynamic background’, ‘camera jitter’, and ‘shadows’. Results are compared with previously published results on four accounts: false positive rate (FPR), false negative rate (FNR), percentage of wrong classification (PWC), and an F-measure. The qualitative and quantitative results prove that the technique out performs the previously reported results by a significant margin.

**Keywords**—Analysis of variance (ANOVA); image motion analysis; object detection

## I. INTRODUCTION

Tracking of objects in a sequence of images has several applications in robotics and computer graphics. A few real life applications are security, traffic control, medical applications, animation, and automation. The broader research area covers several scenarios, like object detection by having more than one camera, a moving camera, changing luminance level, etc. Here, however, only the simplest situation is considered with a single camera in a fixed position. The luminance of the surrounding area is assumed to be unchanged. Any change in the gray level is attributed to the moving object in the foreground, while the non-changing pixel values are considered as regions with the stationary background. There are generally two research directions to handle this situation; first is the pixel-based approach where each pixel is identified as either the part of moving object or the stationary background area. The second approach is region-based which considers a group of pixels for identifying regions with an overall common pattern.

One of the simplest pixel-based approach for identifying moving object is by taking the absolute difference of two consecutive frames [1]. In region-based approach, the pixel interrelations are also considered [2]. Recent research proposed several techniques of object detection. The object-detection using histogram based background subtraction and fuzzy logic is examined in [3] and [4]. A generic algorithm based on real-time traffic surveillance scheme has been

proposed in [5]. Reference [6] studied the use of K-nearest neighbor clustering method to identify vehicles that come dangerously close while driving. Several researchers have considered the robust principal component analysis (RPCA) as a method for object detection [7]-[10]. A Gaussian-based model is employed to identify moving objects in the presence of atmospheric turbulence in [11]. Other researchers proposed a hierarchical modeling [12] and saliently fused sparse decomposition approaches [13]. In addition [14] explores combined shape and feature-based non-rigid object tracking algorithm for object detection. All of the above approaches essentially considered noise-free images.

The real images are generally corrupted with various levels of noise. The noise is more prominent when raw images needed to be transmitted to another location where the processing is performed. This noise may have any distribution; but for simplicity it is assumed that the noise is additive, and have Gaussian distribution. This assumption has been proved to be valid through several tests. The analysis of variance (ANOVA) exhibits strong resilience under heavy Gaussian noise [15]. This paper extends a previously published paper [16]. In the previous paper statistical comparison was made to identify edges of an object. Here, the objective is to identify both the temporal information based on inter-frame statistical analysis, as well as the spatial details based on intra-frame information. A comprehensive mathematical background of ANOVA is presented in [17]. Consequently, this paper implements three-way nested design to segment image frames having both the temporal as well as the spatial information. The suggested algorithm performed effectively in both the noise-free situations as well as in the presence of heavy Gaussian noise of  $\sim N(0, 100)$ . The algorithm was validated through rigorous simulations performed on standard image sequence. Section II reviews the essential mathematical background for three-way nested design, Section III presents the simulation results. Section IV concludes this study.

## II. THREE-WAY NESTED DESIGN

A three-way nested design comprises of levels A, B, and C such that the level-C is nested within level-B and the level-B is nested through level-A. This is given as A, B(A), and C(B). The level-A is based on inter-frame temporal information, whereas the level-B and level-C identify intra-frame pixel variations highlighting the important features. The level-B identifies regions with slowly moving objects, and the level-C

identifies motion at a smaller granular level. Fig. 1 explains the distribution of pixels into various levels. Following parametric model has been used:

$$\Omega: y_{ijkl} = \mu + a_i + b_{ij} + c_{ijk} + e_{ijkl} \quad (1)$$

where  $\mu$  represents general mean of pixels. The inter-frame effect (factor-A) is represented by  $a_i, i = 1, \dots, I$ , the intra-frame feature (factor-B) is represented by  $b_{ij}, j = 1, \dots, J_i$ , and the sub-intra-frame feature (factor-C) is represented by  $c_{ijk}, k = 1, \dots, K_{ij}$ . Here, the value of  $I$  is equal to 2, while the values of  $J_i$  and  $K_{ij}$  are equal to 4. The parameters,  $a_i, b_{ij}$ , and  $c_{ijk}$  are unknown, having fixed-effect. The model, in essence, assumes no randomness in any of these parameters. All variations are included in the error,  $e_{ijkl}, l = 1, \dots, L_{ijk}$ . The value of  $L_{ijk}$  is 4. The error is assumed to have uncorrelated, Gaussian distribution  $\sim N(0, \sigma^2 I)$ .

The objective is to test the hypothesis  $H_\Omega$  for the presence of a particular effect against the null hypothesis  $H_0$ , where null hypothesis confirms the absence of that particular effect. The test is first performed for inter-frame feature  $a_i$ . In case the null hypothesis is rejected, then there is a sufficient justification to assume that a significant moving area is present within the mask region. Next, the selected image window is tested for the presence of sufficient variation at two gray levels B and C. This test is performed on single frame for intra-frame feature extraction.

Under the  $\Omega$ -model of (1), the net effect is the sum of mean  $\mu$ , various parameters  $a_i, b_{ij}, c_{ijk}$ , and error  $e_{ijkl}$ . The effect of mean and parameters is combined in  $\eta_{ijk}$  as,

$$\eta_{ijk} = \mu + a_i + b_{ij} + c_{ijk} \quad (2)$$

We impose the side conditions,

$$\begin{aligned} \sum_i u_i a_i &= 0 & \sum_j v_{ij} b_{ij} &= 0 \text{ for all } i \\ \sum_k w_{ijk} c_{ijk} &= 0 \text{ for all } i, j \end{aligned} \quad (3)$$

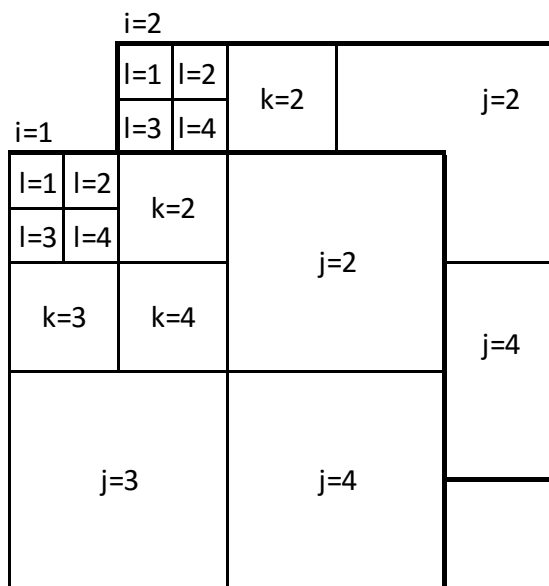


Fig. 1. Mask used for Effects A, B(A), and C(B).

where  $\{u_i\}, \{v_{ij}\}, \{w_{ijk}\}$  are nonnegative weights such that

$$\sum_i u_i = 1; \sum_j v_{ij} = 1 \text{ for all } i; \sum_k w_{ijk} = 1 \text{ for all } i, j \quad (4)$$

The mean-square error is defined as  $\Lambda$ ,

$$\Lambda = \sum_i \sum_j \sum_k \sum_l^{L_{ijk}} (y_{ijkl} - \eta_{ijk})^2 \quad (5)$$

The objective is to minimize the parameter  $\Lambda$  with respect to each of the desired effects. To derive the sums of squares of various effects we consider the following hypothesis:

$$H_A : \text{all } a_i = 0; H_B : \text{all } b_{ij} = 0; H_C : \text{all } c_{ijk} = 0 \quad (6)$$

The regions  $\Omega_A, \Omega_B$ , and  $\Omega_C$  corresponds to the intersection of the overall hypothesis space  $\Omega$  with each of the specific hypothesis sub-spaces identifying various effects represented by parameters,  $a_i, b_{ij}$ , and  $c_{ijk}$ .  $n_{ijkl}$  represents each pixel. The value of  $L_{ijk}, n_{ij}, n_i$ , and  $n$  are equal to 4, 16, 64, and 128, respectively. The weights are found from,

$$w_{ijk} = L_{ijk}/n_{ij}; v_{ij} = n_{ij}/n_i; u_i = n_i/n \quad (7)$$

The dot notation in the subscript signifies aggregation or averaging over the index represented by the dot, like  $y_{ijk.} = \sum_l y_{ijkl}$ . A bar on  $y_{ijk}$  represents weighed sum, as  $\bar{y}_{ijk} = y_{ijk.}/n$ . The least square (LS) estimate of parameter space,  $\eta_{ijk}$  is given by  $\hat{\eta}_{ijk} = \hat{\mu} + \hat{a}_i + \hat{b}_{ij} + \hat{c}_{ijk}$ , where  $\hat{\mu}, \hat{a}_i, \hat{b}_{ij}$  and  $\hat{c}_{ijk}$  are LS estimates of the corresponding parameters, which are  $\mu, a_i, b_{ij}$  and  $c_{ijk}$ . By adding the LS estimate  $\hat{\eta}_{ijk}$  and subtracting the LS estimate of various parameters as given above, (5) is rearranged as,

$$\Lambda = \sum_i \sum_j \sum_k \sum_l [(y_{ijkl} - \hat{\eta}_{ijk}) + (\hat{\mu} - \mu) + (\hat{a}_i - a_i) + (\hat{b}_{ij} - b_{ij}) + (\hat{c}_{ijk} - c_{ijk})]^2 \quad (8)$$

By solving the above equation and also using the side conditions, the operator  $\Lambda$  is given by,

$$\begin{aligned} \Lambda = & \sum_i \sum_j \sum_k \sum_l (y_{ijkl} - \hat{\eta}_{ijk})^2 + n (\hat{\mu} - \mu)^2 + \\ & \sum_i n_i (\hat{a}_i - a_i)^2 + \sum_i \sum_j n_{ij} (\hat{b}_{ij} - b_{ij})^2 + \\ & \sum_i \sum_j \sum_k L_{ijk} (\hat{c}_{ijk} - c_{ijk})^2 \end{aligned} \quad (9)$$

TABLE. I. SUM OF SQUARE OF VARIOUS EFFECTS

|     |   |   |
|-----|---|---|
| SSA | = | $\sum_i n_i \bar{y}_{i...}^2 - n \bar{y}^2$   |
| SSB | = | $\sum_i \sum_j n_{ij} \bar{y}_{ij.}^2 - \sum_i n_i \bar{y}_{i...}^2$                    |
| SSC | = | $\sum_i \sum_j \sum_k L_{ijk} \bar{y}_{ijk}^2 - \sum_i \sum_j n_{ij} \bar{y}_{ij.}^2$   |
| SSE | = | $\sum_i \sum_j \sum_k \sum_l y_{ijkl}^2 - \sum_i \sum_j \sum_k L_{ijk} \bar{y}_{ijk}^2$ |
| SST | = | $\sum_i \sum_j \sum_k \sum_l y_{ijkl}^2 - n \bar{y}^2$                                  |
| SST | = | SSA + SSB + SSC + SSE   |

All cross-product terms become zero due to the selection of weights (4) in the side conditions (3) as illustrated by the last two terms [17],

$$\begin{aligned} \sum_i \sum_j \sum_k \sum_l (\hat{b}_{ij} - b_{ij})(\hat{c}_{ijk} - c_{ijk}) &= \\ \sum_i \sum_j (\hat{b}_{ij} - b_{ij}) \sum_k L_{ijk} (\hat{c}_{ijk} - c_{ijk}) &= 0 \end{aligned} \quad (10)$$

Similarly, other cross-product terms also vanish. In (9), the first term on the right is  $\sum_i \sum_j \sum_k \sum_l (y_{ijkl} - \hat{\eta}_{ijkl})^2$  which is the sum of squares of error (SSE). The total sum of square (SST) is equal to the sum of squares due to each effect and the sum of square of error. This, in essence, is the partitioning of the SST into sums of squares of various effects and the sum of square of error (SSE) as given in Table I. The corresponding degrees of freedom (d.f.) are outlined in Table II.

The sums of squares of various factors and the error have a chi-square distribution  $\chi_r^2$  where ‘r’ is the d.f. The mean square of factors A, B, and C and the error are equal to the sum of square divided by their corresponding degrees of freedom.

$$\begin{aligned} MSA &= \frac{SSA}{(I-1)} & MSB &= \frac{SSB}{\sum_i (J_i - 1)} \\ MSC &= \frac{SSC}{\sum_i \sum_j (K_{ij} - 1)} & MSE &= \frac{SSE}{\sum_i \sum_j \sum_k (L_{ijk} - 1)} \end{aligned} \quad (11)$$

The various effects are tested through the F-test using the corresponding hypotheses, where the interest is in testing the null hypotheses against the alternate hypotheses. As mentioned, the significance of effects A, B, and C is found by partitioning the total space  $H_\Omega$  into sup-spaces for individual effect, corresponding to  $\Omega_A, \Omega_B,$  and  $\Omega_C$ . Mathematically this is similar to finding the ratio of mean square of a particular effect {e.g. MSA, MSB, or MSC} with respect to the mean square of error (MSE) as given in Table III.

TABLE II. DEGREES OF FREEDOM

| Effect | Degree of Freedom (d.f.)                               |
|--------|--|
| A      | $(I - 1) = 2 - 1 = 1$                                  |
| B(A)   | $\sum_i (J_i - 1) = 2(3) = 6$                          |
| C(B)   | $\sum_i \sum_j (K_{ij} - 1) = 2(4)(3) = 24$            |
| Error  | $\sum_i \sum_j \sum_k (L_{ijk} - 1) = 2(4)(4)(3) = 96$ |

TABLE III. THRESHOLDS FOR HYPOTHESIS TESTING

| Effect | Space for various effects      | Threshold       |
|--------|--------------------------------|-----------------|
| A      | $\Omega_A = H_A \cap H_\Omega$ | $f_A = MSA/MSE$ |
| B      | $\Omega_B = H_B \cap H_\Omega$ | $f_B = MSB/MSE$ |
| C      | $\Omega_C = H_C \cap H_\Omega$ | $f_C = MSC/MSE$ |

The mean square of A (MSA) corresponds to chi-square distribution,  $\chi_{I-1}^2$  with (I-1) degree of freedom. The mean square of error (MSE) also corresponds to a chi-square distribution  $\chi_p^2$  with ‘p’ degree of freedom. Here, ‘p’ is equal to  $\sum_i \sum_j \sum_k (L_{ijk} - 1)$ . The ratio of two chi-square distributions is equal to an F-distribution,  $F_{\alpha, v_1, v_2}$  where  $\alpha$  is the upper  $100\alpha\%$  point. Statistically,  $\alpha$  is defined as  $P\{F_{v_1, v_2} > F_{\alpha, v_1, v_2}\} = \alpha$  where  $v_1$  and  $v_2$  are the degrees of freedom of MSA, and MSE respectively. In this particular case,  $v_1$  is equal to (I-1) and  $v_2$  is equal to  $\sum_i \sum_j \sum_k (L_{ijk} - 1)$ . The null hypothesis,  $H_0$  is rejected against the alternate,  $H_A$  if  $f_A > F_{\alpha, (I-1), IJK(L-1)}$ . The test is repeated for effect-B by comparing ratio  $f_B > F_{\alpha, I(J-1), IJK(L-1)}$ . Similarly, the threshold  $f_C > F_{\alpha, IJ(K-1), IJK(L-1)}$  is tested.

### III. SIMULATION RESULTS

The test was performed on two consecutive image frames selected in four categories: baseline, dynamic background, camera jitter, and shadows. It was assumed that the frames were captured at a small time interval with sufficient overlapping area. A mask size of 8 x 8 pixels was used for the statistical comparison. It was expected that the masks were sufficiently overlapped to preserve regions of objects having some kind of motion.

The template for three-way nested design is shown in Fig. 1. Level-A compared inter-frame pixels and identified regions with some kind of motion. The other two levels, B(A) and C(B) provided intra-frame pixel analysis, using mask sizes of 4 x 4 and 2 x 2 pixels, respectively. Furthermore, regions with both the temporal as well as the spatial information were marked. The threshold for the three levels,  $f_A, f_B,$  and  $f_C$ , were equal to 8.49, 3.49, and 2.29 respectively with the value of ‘ $\alpha$ ’ selected as 0.001 for  $f_A$  and 0.005 for both  $f_B$  and  $f_C$  [16].

MATLAB routine ‘bwperim’ using an 8-level connected neighborhood was used to identify the contours. A preprocessing stage reduced the original 256 gray shades using (12).  $I_{in}$  is the input image,  $I_1$  is an intermediate image with smaller range of gray shades,  $I$  is the image used in the algorithm and ‘ $\alpha$ ’ is a scaling factor; its value is arbitrarily selected as 40.

$$I_1 = \frac{1}{\alpha} I_{in} \quad \text{and} \quad I = \alpha \times I_1 \quad (12)$$

The sample images were taken from the CDnet database [18]. These images have been tested previously in [19]. Fig. 2 shows first frame of an image, the noisy image by the addition of Gaussian noise  $\sim N(0, 100)$ , the processed clean image, processed noisy image, and the contour of processed noisy image.

An overall observation is that the algorithm performed better in case of noisy images. Further, the algorithm performed exceptionally well in case of ‘dynamic background’. It was found that the algorithm was extremely sensitive to the slightest gray level change in area comprising of roads.



By reducing the granular level using (12), the number of quantization levels are reduced, thus significantly improving the F-measure. The quantitative analysis include false positive rate (FPR), false negative rate (FNR), percentage of wrong classification (PWC), and F-measure. The first three parameters were expected to have smaller value, while the overall quality measure, F-measure was expected to be closer to 1. The result of this algorithm is compared with previously published results for clean images. To the best of our knowledge, the results for noisy images are not available. It was observed that higher value of PWC in case of ‘shadow’

were due to the fact that the shadow constituted a larger area and the algorithm had mistakenly identified this area as the moving object. The algorithm was tested using MATLAB 2014, on a core i7 processor. The processing time was roughly equal to 2.5 seconds. A better result is expected by using faster computers employing parallel processing. By looking at the F-measure, it is clear that the algorithm is able to detect moving objects in both the noise-free as well as the noisy images. Comparison of proposed algorithm with recently published results is shown in Table IV.



Fig. 2. Original and Processed Images in Four Categories.

TABLE IV. COMPARISON OF PROPOSED ALGORITHM WITH RECENTLY PUBLISHED RESULTS

| S.No. | Image Category     | Noise Level | Previous Results [19] |      |     |           | Proposed Algorithm |        |        |           |
|-------|--------------------|-------------|-----------------------|------|-----|-----------|--------------------|--------|--------|-----------|
|       |                    |             | FPR                   | FNR  | PWC | F-Measure | FPR                | FNR    | PWC    | F-Measure |
| 1.    | Baseline           | no noise    | 0.003                 | 0.13 | 0.9 | 0.87      | 0.545              | 0.0004 | 1.526  | 0.986     |
|       |                    | w/ noise    | -                     | -    | -   | -         | 0.293              | 0.001  | 0.896  | 0.943     |
| 2.    | Dynamic Background | no noise    | 0.009                 | 0.20 | 1.2 | 0.65      | 0.033              | 0.0347 | 3.418  | 0.919     |
|       |                    | w/ noise    | -                     | -    | -   | -         | 0.096              | 0.0073 | 3.280  | 0.982     |
| 3.    | Camera Jitter      | no noise    | 0.018                 | 0.27 | 2.9 | 0.69      | 0.553              | 0.0029 | 4.259  | 0.962     |
|       |                    | w/ noise    | -                     | -    | -   | -         | 0.161              | 0.0043 | 1.647  | 0.949     |
| 4.    | Shadows            | no noise    | 0.011                 | 0.17 | 2.1 | 0.78      | 0.399              | 0.0183 | 13.018 | 0.956     |
|       |                    | w/ noise    | -                     | -    | -   | -         | 0.231              | 0.0873 | 12.937 | 0.789     |

#### IV. CONCLUSION

This paper outlines a novel approach employing a three-way nested design using the analysis of variance (ANOVA). The sample images comprised of only two frames recorded within a short time interval with sufficient overlapping of pixels. The pixels identified to contain some kind of motion were combined to become part of the moving object. The temporal part was identified by statistical analysis of pixels at the two image frames. Spatial information at two granular levels were used to identify important details. The simulations were formed first in noise-free situation, and then in the presence of heavy Gaussian noise  $\sim N(0, 100)$ . The algorithm response was tested using the qualitative as well as the quantitative methods. The qualitative response was based on images taken in four categories: baseline, dynamic background, camera jitter, and images containing shadows. The quantitative analysis was based on false positive rate (FPR), false negative rate (FNR), percentage of wrong classification (PWC), and F-measure. The results were compared with a previously published results of clean images. The proposed algorithm performed better compared to the previous results. The proposed algorithm performed excellent in case of noisy images. In our view, the technique has great potential. The limitation of this approach is relatively longer processing time, and therefore not appropriate for real-time applications. One promising future extension is the analysis of covariance (ANCOVA).

#### REFERENCES

- [1] K. K. Hati, P. K. Sa, and B. Majhi, "Intensity range based background subtraction for effective object detection," *IEEE Signal Process. Lett.*, vol. 20, no. 8, pp. 759-762, Aug. 2013.
- [2] P. Chiranjeevi and S. Sengupta, "Detection of moving objects using multi-channel kernel fuzzy correlogram based background subtraction," *IEEE Trans. Cybernetics*, vol. 44, no. 6, pp. 870-881, Jun. 2014.
- [3] D. K. Panda and S. Meher, "Detection of moving objects using fuzzy color difference histogram based background subtraction," *IEEE Signal Process. Lett.*, vol. 23, no. 1, pp. 45-49, Jan. 2016.
- [4] Z. Wang, K. Liao, J. Xiong, and Q. Zhang, "Moving object detection based on temporal information," *IEEE Signal Process. Lett.*, vol. 21, no. 11, pp. 1403-1407, Nov. 2014.
- [5] G. Lee, R. Mallipeddi, G. Jang, and M. Lee, "A genetic algorithm-based moving object detection for real-time traffic surveillance," *IEEE Signal Process. Lett.*, vol. 22, no. 10, pp. 1619-1622, Oct. 2015.
- [6] J. Park, J. H. Yoon, M. Park, and K. Yoon, "Dynamic point clustering with line constraints for moving object detection in DAS," *IEEE Signal Process. Lett.*, vol. 21, no. 10, pp. 1255-1259, Oct. 2014.
- [7] L. Zhu, Y. Hao, and Y. Song, " $L_{1/2}$  norm and spatial continuity regularized low-rank approximation for moving object detection in dynamic background," *IEEE Signal Process. Lett.*, vol. 25, no. 1, pp. 15-19, Jan. 2018.
- [8] X. Zhou, C. Yang, and W. Yu, "Moving object detection by detecting contiguous outliers in the low-rank representation," *IEEE Trans. Patt. Anal. Mach. Intell.*, vol. 35, no. 3, pp. 597-610, Mar. 2013.
- [9] F. Shang, J. Cheng, Y. Liu, Z. Luo, and Z. Lin, "Bilinear factor matrix norm minimization for robust PCA: algorithms and applications," *IEEE Trans. Patt. Anal. Mach. Intell.*, vol. 40, no. 9, pp. 2066-2080, Sep. 2018.
- [10] S. Javed, A. Mahmood, S. Al-Maadeed, T. Bouwmans, and S. K. Jung, "Moving object detection in complex scene using spatiotemporal structured-sparse RPCA," *IEEE Trans. Image Process.*, vol. 28, no. 2, pp. 1007-1022, Feb. 2019.
- [11] O. Oreifej, X. Li, and M. Shah, "Simultaneous video stabilization and moving object detection in turbulence," *IEEE Trans. Patt. Anal. Mach. Intell.*, vol. 35, no. 2, pp. 450-462, Feb. 2013.
- [12] L. Li, Q. Hu, and X. Li, "Moving object detection in video via hierarchical modeling and alternating optimization," *IEEE Trans. Image Process.*, vol. 28, no. 4, pp. 2021-2036, Apr. 2019.
- [13] W. Hu, Y. Yang, W. Zhang, and Y. Xie, "Moving object detection using tensor-based low-rank and saliently fused-sparse decomposition," *IEEE Trans. Image Process.*, vol. 26, no. 2, pp. 724-737, Feb. 2017.
- [14] T. Kim, S. Lee, and J. Paik, "Combined shape and feature-based video analysis and its application to non-rigid object tracking," *IET Image Process.*, vol. 5, iss. 1, pp. 87-100, Feb. 2011.
- [15] J. F. Y. Cheung, M. C. Wicks, C. Genello, and L. Kurz, "A statistical theory for optimal detection of moving objects in variable corrupted noise," *IEEE Trans. Image Process.*, vol. 8, no. 12, pp. 1772-1787, Dec. 1999.
- [16] A. U. R. Khan, S. M. A. Saleem, H. Mehdi, "Detection of edges using two-way nested design," *International Journal of Advanced Computer Science and Applications (IJACSA)*, vol. 8, no. 3, pp. 136-144, March 2017.
- [17] H. Scheffe, "The Analysis of Variance," New York, Wiley, 1959.
- [18] Image Database, CDnet: <http://www.changedetection.net/>
- [19] N. Goyette, P. Jodoin, F. Porikli, et. al., "A novel video dataset for change detection benchmarking," *IEEE Trans. on Image Processing*, vol. 23, no. 11, pp. 4663-4679, 2014.

# Smart Home Energy Management System Design: A Realistic Autonomous V2H / H2V Hybrid Energy Storage System

Bassam Zafar<sup>1</sup>

Information System Department, FCIT  
King Abdulaziz University, Jeddah  
Saudi Arabia

Ben Slama Sami<sup>2</sup>

Jeddah Community college, JCC  
King Abdulaziz University, Jeddah  
Saudi Arabia

Sihem Nasri<sup>3</sup>

Department of Physics,  
Analysis and Treatment of Electrical and Energy Systems  
Unit, Faculty of Sciences of Tunis Tunisia

Marwan Mahmoud<sup>4</sup>

Jeddah Community college, JCC  
King Abdulaziz University, Jeddah  
Saudi Arabia

**Abstract**—The hybrid fuel cell electric vehicle powered by household power during peak use is another opportunity to reduce emissions and save money. For this reason, Vehicle-to-Home (V2H) and Home-to-Vehicle (H2V) systems were proposed as a new method of exchanging smart energy and a new method of exchanging smart energy. The main goal of this paper is to develop a smart home energy management based on IoT, generate more energy efficiency and share production between home and vehicle. In fact, the Hybrid Fuel cell electric vehicle will be used simultaneously to power household appliances during peak demand for electricity to solve energy consumption. The household's energy is derived from an accurate Autonomous hybrid power system. Several technologies such as Proton Exchange Membrane Fuel Cell, solar panel, Supercapacitor (SC) device and water electrolyzer are incorporated into the proposed system. Two-way electrical energy from the PEMFC-Hybrid Electric Vehicle and household power will be exchanged by discharging vehicle energy storage to balance energy demand and supply. To this end, a smart energy management unit (EMU) will be developed and discussed in order to meet the estimated fuel consumption mitigation goals during peak periods when demand is highest, coordinating between household power and vehicle energy storage. The Matlab / Simulink software based on an experimental database extracted from household power to demonstrate the effectiveness of the proposed strategy and its effects on V2H / H2V operations will simulate the presented design for one day. The Matlab / Simulink software based on an experimental database extracted from household power to demonstrate the effectiveness of the proposed strategy and its effects on V2H / H2V operations will simulate the presented design for one day.

**Keywords**—Home energy management system; fuel cell; super-capacitor; solar power; vehicle to home; home to vehicle

## I. INTRODUCTION

### A. Motivations

The rapid development of a new economic hybrid electric vehicle and renewable energy, including solar photovoltaic

and wind energy, has enhanced energy demand and environmental crises [1-2]. Hybrid Fuel Cell Electric vehicles have been selected as an attractive potential for reducing demand for oil, emissions and becoming a grid-capable electric vehicle (loading and/or discharging via grid or home). Indeed, to replace conventional ICE vehicles, these new generations of electric vehicles (EVs) have been developed. The household power has attracted a lot of attention in both academia and industry, according to the rapid evolution of clean energy production and the new economic EVs [3-4]. Different home energy management systems (HEMS) were designed and developed to control household fuel consumption power during peak periods. The HEMS was used as tools for sharing and reducing energy demand based on energy consumption and home profiles of production. In general, HEMS creates optimal schedules for consumption and production through multiple goals such as load profiles, energy demand and costs [5]. EVs are seen as attractive sources for household power during peak consumption using newly introduced HEMS technologies. In a sophisticated home energy system, various projects on the smart home have considered H2V and V2H a novelty. The V2H was described as an energy storage system in which the EV was used during peak periods when demand is highest to provide the home with electricity. Besides renewable energy sources such as solar energy, wind turbines, etc., it is also possible to consider vehicles as an energy source to meet the home energy demand [6]. Besides renewable energy sources such as solar energy, wind turbines, etc., it is also possible to consider vehicles as an energy source to meet the home energy demand [7]. Moreover, several methods and platforms, such as Intelligent Sensor Technologies, Home Network, and Smart Home Appliance [8-9], have been studied and developed for the smart home. Furthermore, due to the complexity and diversity of systems, as well as repeated control strategies without the problem of optimum level, the full potential of smart homes is still present. The purpose of intelligent home energy management was to control application and data acquisition,

production, transmission, and network electricity [10]. Moreover, this smart management has attracted more interest from the research community to use a modern automation technology in the smart house promises. In order to share energy demand, performance and an intelligent network economy, it is essential to reconcile EVs and renewable energy to optimize the energy balance. As a result, researchers recently focused on developing advanced platforms for smart energy management to integrate electric vehicles and renewable energies into household and grid loads, as well as new materials and renewable energy structure considering the efficiency of power conversion [11].

Several works with Home-to-Vehicle and Vehicle-to-Home Technologies have been presented in the literature. Several platforms have been put in place and tested. The designed systems were reviewed to demonstrate that the energy supplied to the electric charge is sufficient depending on the demand or load power. During peak consumption, different scenarios were added to control the household power to share the required energy. Different methods and techniques have been used as mathematical optimization to create an efficient hour of operation, accurate production decisions and good consumption.

The rest of this article will be organized as follows: Home Energy Management System (HEMS); (HEMS) System Design; the energy management section will explain the proposed smart and the concluding remarks will be discussed in the conclusion and future work section.

#### B. Summary of Home Energy Management System (HEMS) using the Smart Home (Home Automation)

The developed HEMS were selected as a new energy management approach to ensure energy savings and peak demand [12]-[13]. Broadly speaking, HEMS can be defined as a precise approach system that allows households to control their energy demand by adding various network-wide hardware / software connections [14]. HEMS were also taken in various forms, for example:

- HEMS can provide consumers with information on how to use energy at home and/or provide incentives for changing consumption [15].
- HEMS can provide the ability of the household to control energy processes consumed at home through a smart phone or Web service. Home Appliances can be managed or implemented either manually using rule sets that can be planned or optimized based on the behavior of the user [16].

HEMS has emerged as an effective control of household appliances which, on the one hand, can provide power and, on the other, reduce peak loads. Using the most relevant technologies, energy savings and demand savings can be grouped into four categories: home automation, integrated wireless technology, smart home micro-computers, and home energy management system.

The Internet of Things (IoT) was selected to communicate between appliances. Communication can be enabled to the remote devices via selected interfaces such as gateways.

Several projects have been developed in this context (such as: Baywatch, Fiemser, Smart House / Smart Grid, etc...) to meet the needs of consumers or industrialists.

Making smart homes, simplifying household life, ensuring home security and maximizing occupant comfort with minimal energy use are the main goals for developing these projects.

#### C. Summary of IoT-Based Smart Home Automation System

Because of its various interests, wireless sensor networks (WSN) are selected as an attractive potential. The WSNs aim to offer several advantages over traditional approaches for different new applications such as: environmental monitoring; health security; smart homes, etc. [17]. The Internet protocol (IPv4 or IPV6) was used as an accurate solution to develop the Internet of Things (IoT) to connect appliances [18]. WSN therefore faces many obstacles that include different challenges such as:

- How to use a small and low power node effectively?
- How to implement the security required when data is transmitted between nodes?
- How to solve environmental conditions when transmitting data?

Several studies conducted WSN with IP to develop IoT without interruption to ensure real-time connectivity between different nodes. For example, the author proposed and developed a precise IoT-based WSN platform in [19]. The WSN-Platform developed is aimed at collecting the data detected in real time [20]. The results obtained were demonstrated based on low power consumed by each node. In, the authors proposed a WSN framework for controlling smart home appliance devices requiring energy. According to a given experimental database, the proposed platform deals with monitoring and control of house equipment [21]-[22]. The WSNs were shared data via an internet connection to ensure real - time connectivity between appliances.

#### D. The Problematic

The emergence of sophisticated electrical systems and high popular inflation strengthened rising electricity demand. Therefore, today the world faces a major challenge in finding a radical solution to the problem of energy deficit that stems mainly from the imbalance in demand-production. Indeed, the power grid is facing the balance that maintains the issue of climate change-influenced peak management of demand and supply and demand. In addition, ancient housing technology supported heavy energy consumption. The house is therefore seen as a complex node of energy linked to many energy flows.

The imminent integration of renewable sources and electric vehicles will strengthen this node and exacerbate the management problem that rests on monitoring and optimizing all these flows to enable proper distribution of energy to household equipment. Electricity users are also faced with costly tariffs on energy caused by massive energy consumption and unlimited user demand.

### E. Contributions

The principle commitment anticipated from this work is to build up a savvy home administration exploiting Home-to-Vehicle (H2V) and Vehicle-to-Home (V2H) innovation techniques with a smart supervision control methodology so as to achieve a few upgrades:

- Ensure the storage process in positive conditions.
- Energy request fulfillment whatever the conditions: stand up to fuel and energy needs.
- Vehicle fuel charging from home mulling over the energy request.
- System elements security:
  - Avoid the Supercapacitor cheating and overproduction of H<sub>2</sub> gas fuel
  - Be confronting profound Supercapacitor release and overwhelming fuel utilization.

## II. SYSTEM DESIGN

The given system aims to maintain the power balance between demand and production considering the energy storage and recovery phenomenon and the control of the energy flows transferred between the vehicle and the house. Hence, the described system deals with several main duties:

- Home production and demand control.
- Vehicle demand control and charging.
- Fuel distribution way control.

Thus, the two-way energy exchange phenomena insured by the vehicle and the smart home is highlighted. Indeed, the given system is operated according to two modes depending on the distribution way nature. These two modes are provided by set of energy equipments as PV source, Electrolyzer, Supercapacitor and Fuel Cell.

The first distribution way is ensured from the house to the parked vehicle "H2V". Indeed, in case of excess energy, the system uses the amount of hydrogen generated at home to electrify the vehicle after checking its lack and storage capacity. While there is need of energy in the house, the second distribution way is highlighted. In this case the house production equipment are unable to meet the energy needs, which requires the use of the car reserve to remedy the energy shortage "V2H" (see Fig.1). The system therefore requires an intelligent control unit for distribution and consumption in order to ensure the system's ideal functioning and protect it against any constraint that may lead to its corruption.

- **The energy production:** This constitutes the energy issued from the photovoltaic module located at the house roof, the expression of the PV generated current is described as [23]:

$$I_{PV} = I_{ph} - I_s e^{\frac{(N_s \cdot V_{PV} + N_p \cdot I_{PV} \cdot R_s)}{V_T}} - \frac{N_s \cdot V_{PV} + N_p \cdot I_{PV} \cdot R_s}{R_{sh}} \quad (1)$$

- **The energy consumption:** It is defined by the total installed appliances consumption, this energy may be used for lighting, heating, leisure,

$$I_{LD} = \sum_{i=0}^n I_{AP_i} \quad (2)$$

- **Electrolyzer equipment:** It is an electrochemical device that, in the presence of an excess power current, produces hydrogen by decomposing the water molecule into H<sub>2</sub> and O<sub>2</sub> gas. The generated hydrogen flow is calculated from the Faraday law as [24]:

$$Q_p = \frac{\eta_{EL} \cdot N_{EL} \cdot I_{EL}}{2 \cdot F} \quad (3)$$

- **Supercapacitor equipment:** It is an electrical device that through its discharge can accomplish the energy recovery process. So, to ensure its protection against the deep discharge, the Supercapacitor is controlled by its state of charge described by the expression [25]:

$$SOC_{SC} = \left[ \frac{I_{SC}}{I_{SC_{max}}} \right]^2 \quad (4)$$

Instead of battery, Supercapacitor is used as a short term energy storage device which is intervening in a period when excess generated power is lower than that nominal of electrolyzer.

- **H<sub>2</sub> Station:** It is equipment dedicated to the storage of the produced hydrogen flux. The storage process made under high pressure follows the law described by the equation below [26]:

$$P_{st} = \frac{R \cdot T_{st}}{V_{st}} \cdot Q^S \quad (5)$$

The hydrogen flow storage control is made by state of charge verification that is expressed as:

$$SOC_{H_2} = \frac{Q^S}{Q_{max}^S} \quad (6)$$

- **Fuel Cell equipment:** It is a generator which, in the presence of hydrogen, generates an electric current in order to assist in the load demand satisfaction. The hydrogen consumption is described according the Faraday law as [27]:

$$Q_C = \frac{N_{FC} \cdot I_{FC}}{2 \cdot F \cdot \eta_{FC}} \quad (7)$$

- **Electric Vehicle:** It is an electric vehicle based on fuel cell that requires hydrogen as fuel to be running.

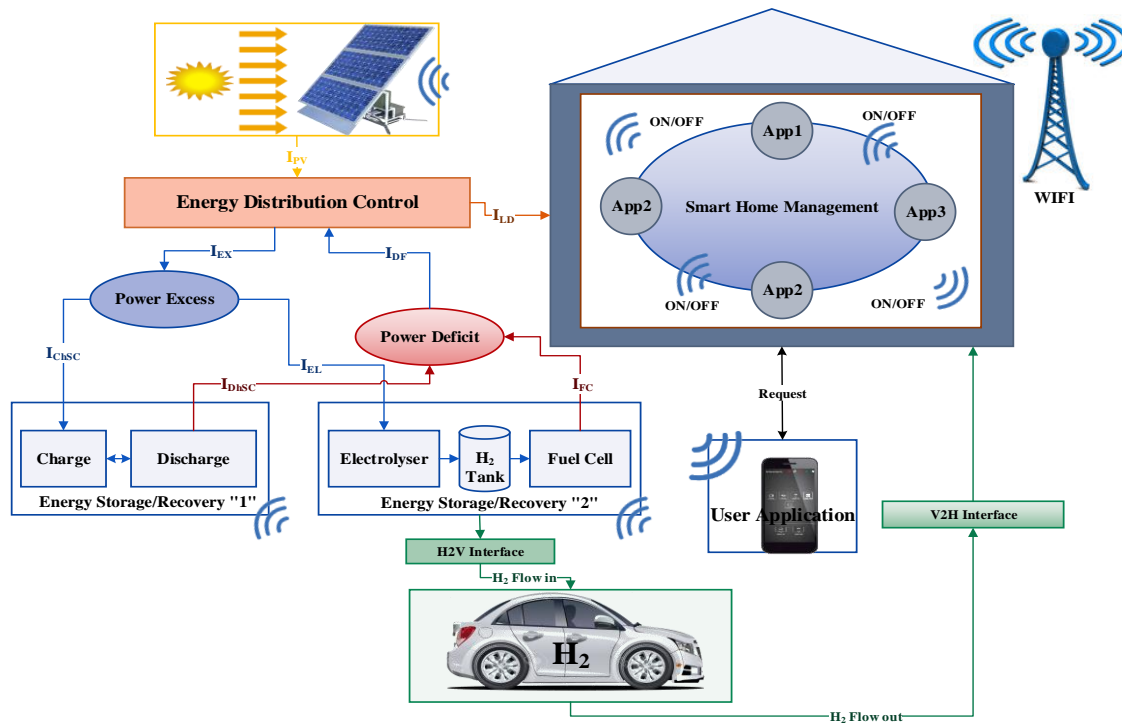


Fig. 1. Design of the Proposed Autonomous Hybrid System.

### III. SMART MANAGEMENT APPROACH

The reliability and the effectiveness of smart home management system are verified by its ability to manage quickly and intelligibly complex occurred constraints and fluctuations. Indeed, performance improvement of the studied system relies on the integration of a smart energy management approaches considering various criteria as:

- Energy distribution flows.
- Fuel flow generation and transfer.
- Energy consumption rates.
- Component state control and secure.

To study system reactions in front of happened events, two main parts can be highlighted:

- Excess power production management to protect storage devices against overcharge and full storage. This can be achieved by developing a smart approach control considering flow transfer from Home to Vehicle “H2V” (Fig. 2).
- Deficit power management to secure backup devices against massive fuel consumption and the deep discharge. Indeed, a smart approach control relying on fuel transfer from Vehicle to Home “V2H” is considered to compensate lacks (Fig. 3).

Thus, several control parameters must be highlighted to accomplish effective management processes as home energy consumption/production, fuel storage/use and charging/discharging of electrical device.

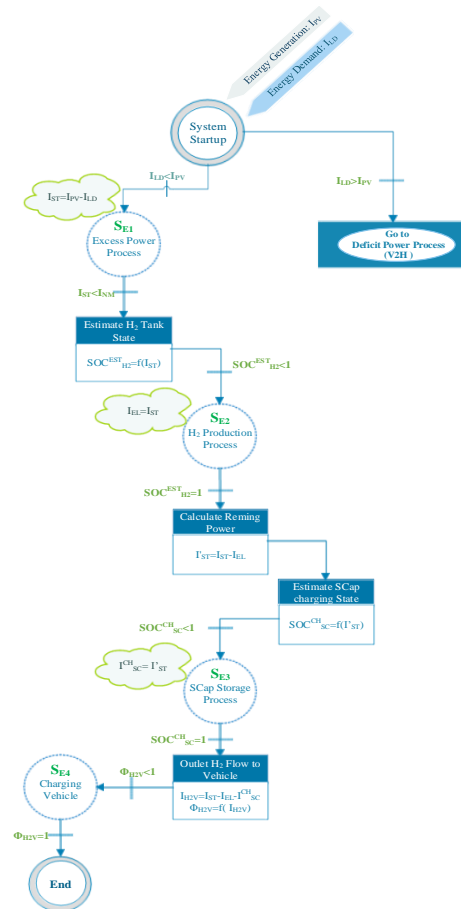


Fig. 2. Home-to Vehicle Energy Distribution Process.

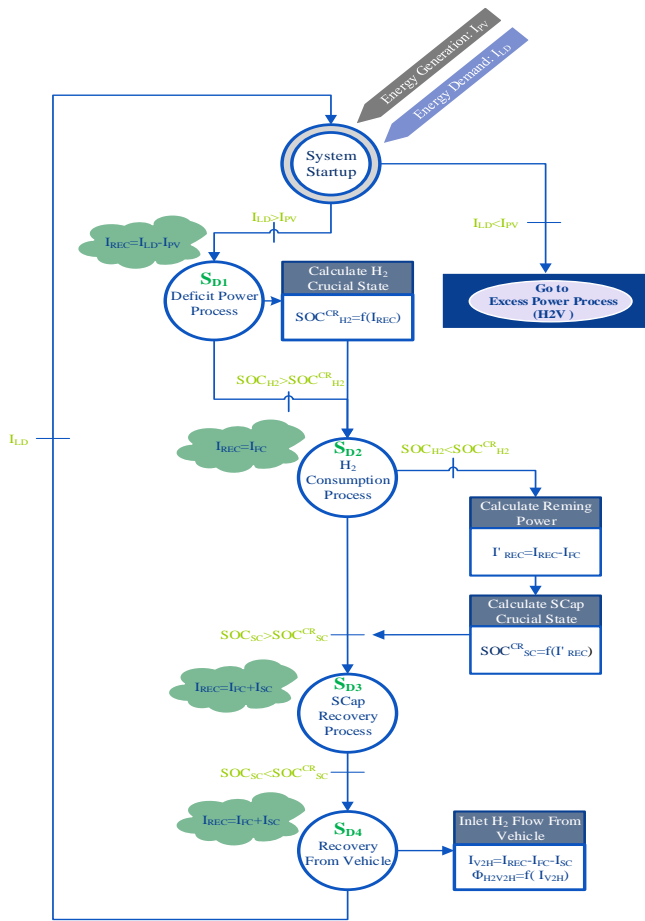


Fig. 3. Vehicle-to-Home Energy Distribution Process.

#### IV. FINDINGS AND RESULTS

##### A. Home to Vehicle

The obtained results have been carried out under the Matlab/Simulink environment to evaluate system performance and demonstrate its reliability against unforeseen events. In fact, experimental consumption profiles are restored to describe the electricity supplied to meet the required energy requirements for domestic devices in order to complete the simulation procedure. Solar energy is considered the main source to meet a continuous energy demand, according to the results obtained. The load profile is also comparable with the load on an intelligent home in the audiovisual environment. Solar energy is controlled by energy demand to determine the system status (excess/deficit) in comparison to energy consumption. The current profile also deals with the house's energy consumption for a period of (24 hours). Fig. 4 illustrates the balance of energy production and consumption. As seen, the system is located within different periods of excess, which will analyze and study the system reaction by referring to them (Fig. 5). The proposed strategy prove an efficient coordination between home and vehicle "H2V". The excess power generation is used to protect storage devices against overload and full storage. Thus, Fig. 6 shows the estimated relative hydrogen volumes and supercapacitor charging capacity respectively. Under satisfied conditions, ( $I_{EX} > I_{EN}$  and  $SOC_{H2} < SOC_{Max}$ ), the system permits the

chemical storage ( $H_2$  gas) process by sending an activation key to Electrolysis device. The system uses also the Super-Capacitor to manage crucial storage states caused by either full  $H_2$  tank or unsatisfied electrolysis operation condition. In addition, the possible fuel amounts production and the amounts to be delivered by the  $H_2V$  system are depicted in Fig. 7. As noticed, once the house is over-energy marked, the surplus is transformed to bring the car. In this case, the car is fed by the house.

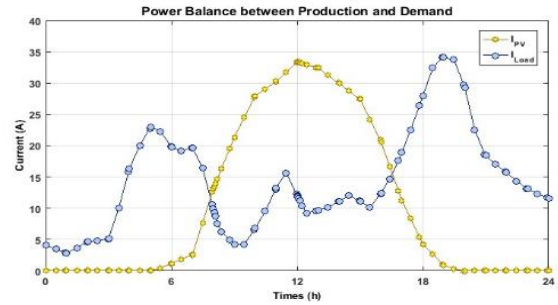


Fig. 4. Power Balance between Consumption and Production.

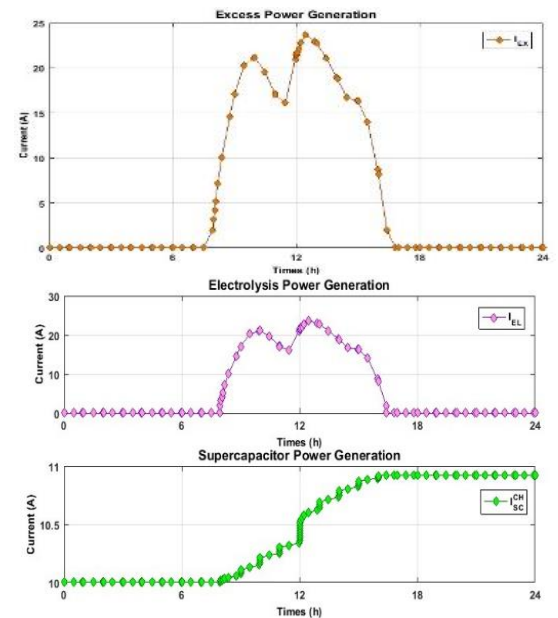


Fig. 5. Excess Power Generation for Storage Devices.

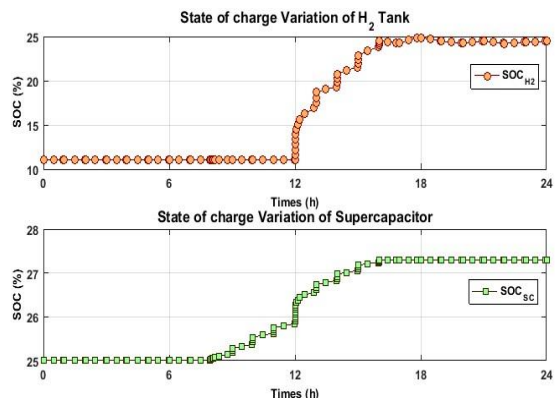


Fig. 6. Hydrogen and Super-Capacitor State of Charge Variations Over 24 hours.

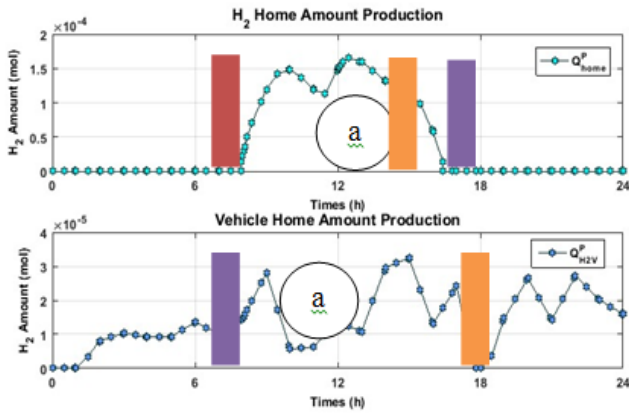


Fig. 7. Home-Vehicle Energy Variations.

### B. Vehicle to Home

Due to the lack of hydrogen ( $SOC_{H_2}=0$ ), the fuel cell cannot be launched to meet energy demand for the first time in deficits. The system uses SCap to make up for the need. The fuel cell is activated during the second period (from 12h) to meet the requirements. Because of full hydrogen consumption and SCap discharge, it seems that the fuel cell and the SCap are located under their critical states (see Fig. 8).

The total amount of  $H_2$  fuel will be converted into electricity and then injected into a network to compensate for its problem of incapacity. When the system is complaining for a new deficit, it provides the  $H_2$  needed to correct the power shortage due to the inability of the Fuel Cell. Fig. 9 is used to describe hydrogen tank amount fluctuation phenomenon during deficit periods. We can therefore note that the Super-Capacitor was used in the deficit power case and when the storage tank is empty, which means that the fuel cell cannot supply the required energy. As a result, the charge status of the Super-capacitor, used in its discharge mode, decreases (50%) from its original level. While in other cases, only  $H_2$  phenomena are underlined in gas production and consumption.

To compensate for deficiencies, the transfer of fuel from the vehicle to the "V2H" home is considered (see Fig.10).

The vehicle provides the necessary energy to the house when the tank is empty and the Super-Capacitor is unable to correct the fluctuation.

### C. Discussion

Based on the scientific literature resources that deal with smart home technology, we noticed the originality of our work as it not only develops an intelligent control strategy but also it treats the possibility of integrating hydrogen vehicles as means to compensate the deficit on the one hand and to ensure the secure energy storage on the other hand. Thus, the two studied techniques H2V and V2H are in fact a challenge for the development of smart home systems. In addition, this work investigates the communication between system elements to improve its performance especially its response time to be face any unwanted event. But it remains to implement these strategies on embedded target board and improve them by the integration of other techniques that serve to optimize certain system equipment.

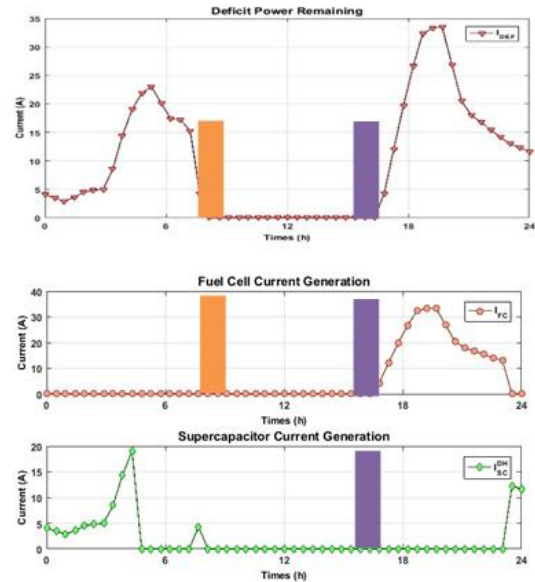


Fig. 8. Fuel Cell and Super-Capacitor Energy Variations Over Deficit Power.

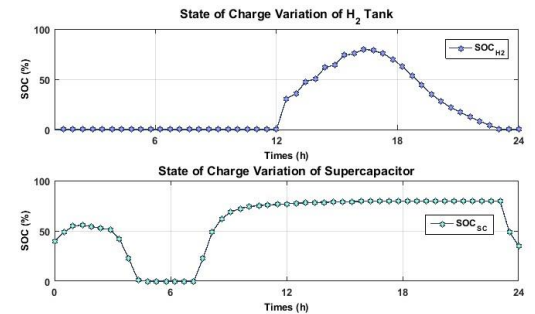


Fig. 9. Hydrogen Tank and Super-Capacitor State of Charge Variations.

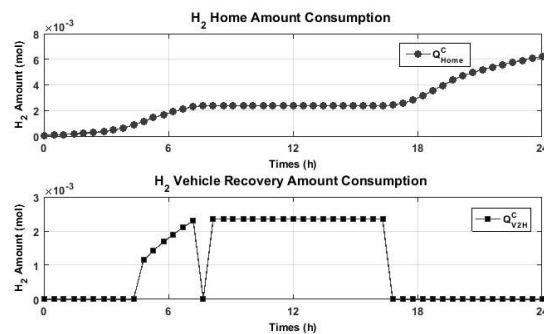


Fig. 10. Home-Vehicle Energy Variations.

## V. CONCLUSION

An intelligent energy management approach is presented and described to manage the energy flows and to ensure power distribution. The proposed system is then made to test its performance with a Matlab / Simulink prototype. The obtained results show that the system is capable of handling changes and their effect on the operation of equipment.

As a future, we tend to develop the whole system based on vehicle charges by produced hydrogen (**H2V/V2H**) with an energy storage component (excess power case).



### ACKNOWLEDGMENT

The author would like to thank the Deanship of Scientific Research (DSR), King Abdulaziz University, and Jeddah, who supported this work under grant No. (G: 665-611-1439). The authors, therefore, gratefully acknowledge the DSR for their technical and financial support.

### REFERENCES

[1] X. Su, P. Wolfs and M. Masoum, "Comprehensive optimal photovoltaic inverter control strategy in unbalanced three-phase four-wire low voltage distribution networks", IET Generation, Transmission & Distribution, vol. 8, no. 11, pp. 1848-1859, 2014. Available: 10.1049/iet-gtd.2013.0841.

[2] R. Liao and N. Yang, "Evaluation of voltage imbalance on low-voltage distribution networks considering delta-connected distribution transformers with a symmetrical NGS", IET Generation, Transmission & Distribution, 2017. Available: 10.1049/iet-gtd.2017.0631.

[3] S. Zalzar, M. Shafiyi, A. Yousefi-Talouki and M. Ghazizadeh, "A smart charging algorithm for integration of EVs in providing primary reserve as manageable demand-side resources", International Transactions on Electrical Energy Systems, vol. 27, no. 4, p. e2283, 2016.

[4] K. Sudheer, K. Aravind kumar and P. Prasanna, "Fuzzy and PI Control of Hybrid Fuel Cell/Battery Distributed Generation Systems", International Journal of Modeling and Optimization, pp. 95-100, 2011. Available: 10.7763/ijmo.2011.v1.17.

[5] H. Fathabadi, "Novel standalone hybrid solar/wind/fuel cell/battery power generation system", Energy, vol. 140, pp. 454-465, 2017. Available: 10.1016/j.energy.2017.08.098.

[6] P. S, "Hybrid Power Generation by Using Solar and Wind Energy Hybrid Power Generation Applicable To Future Electric Vehicle", International Journal of Emerging Trends in Science and Technology, vol. 4, no. 11, 2017. Available: 10.18535/ijetst/v4i11.01.

[7] B. Sami, N. Sihem, S. Gherairi and C. Adnane, "A Multi-Agent System for Smart Energy Management Devoted to Vehicle Applications: Realistic Dynamic Hybrid Electric System using Hydrogen as a Fuel", Energies, vol. 12, no. 3, p. 474, 2019. Available: 10.3390/en12030474.

[8] B. Sami, N. Sihem and Z. Bassam, "Design and implementation of an intelligent home energy management system: A realistic autonomous hybrid system using energy storage", International Journal of Hydrogen Energy, vol. 43, no. 42, pp. 19352-19365, 2018. Available: 10.1016/j.ijhydene.2018.09.001.

[9] A. Haddad, M. Ramadan, M. Khaled, H. Ramadan and M. Becherif, "Study of hybrid energy system coupling fuel cell, solar thermal system and photovoltaic cell", International Journal of Hydrogen Energy, 2018. Available: 10.1016/j.ijhydene.2018.06.019.

[10] S. Sami, "Dynamic Modeling, and Simulation of Hybrid Solar Photovoltaic, and PEMFC Fuel Cell Power System", RA Journal of Applied Research, vol. 4, no. 5, 2018. Available: 10.31142/rajar/v4i5.02.

[11] S. Lim and G. Li, "An Integrated Home Energy Management System", Ponte International Scientific Research Journal, vol. 73, no. 12, 2017. Available: 10.21506/j.ponte.2017.12.53.

[12] E. Park, B. Hwang, K. Ko and D. Kim, "Consumer Acceptance Analysis of the Home Energy Management System", Sustainability, vol. 9, no. 12, p. 2351, 2017.

[13] R. Hemmati, "Technical and economic analysis of home energy management system incorporating small-scale wind turbine and battery energy storage system", Journal of Cleaner Production, vol. 159, pp. 106-118, 2017. Available: 10.1016/j.jclepro.2017.04.174.

[14] R. S. and M. V., "HEM algorithm based smart controller for home power management system", Energy and Buildings, vol. 131, pp. 184-192, 2016. Available: 10.1016/j.enbuild.2016.09.026.

[15] B. Rao, F. Kupzog and M. Kozek, "Phase Balancing Home Energy Management System Using Model Predictive Control", Energies, vol. 11, no. 12, p. 3323, 2018. Available: 10.3390/en11123323.

[16] S. Pirbhulal et al., "A Novel Secure IoT-Based Smart Home Automation System Using a Wireless Sensor Network", Sensors, vol. 17, no. 12, p. 69, 2016. Available: 10.3390/s17010069.

[17] B. S.S. Tejesh and S. Neeraja, "A Smart Home Automation system using IoT and Open Source Hardware", International Journal of Engineering & Technology, vol. 7, no. 27, p. 428, 2018. Available: 10.14419/ijet.v7i2.7.10856.

[18] R. Lakshmi, P. Karthika, A. Rajalakshmi and M. Sathya, "Smart-Home Automation Using IoT-Based Sensing and Monitoring Platform", International Journal of Scientific Research in Computer Science, Engineering and Information Technology, pp. 409-413, 2019. Available: 10.32628/cseit195190.

[19] J. Kim, "HEMS (home energy management system) base on the IoT smart home", Contemporary Engineering Sciences, vol. 9, pp. 21-28, 2016. Available: 10.12988/ces.2016.512316.

[20] S. Pirbhulal et al., "A Novel Secure IoT-Based Smart Home Automation System Using a Wireless Sensor Network", Sensors, vol. 17, no. 12, p. 69, 2016. Available: 10.3390/s17010069.

[21] A. Eslami and T. Ghanbari, "New mathematical model from system standpoint to analyse and mitigate PV leakage current of large PV strings/arrays", IET Generation, Transmission & Distribution, vol. 13, no. 4, pp. 543-552, 2019. Available: 10.1049/iet-gtd.2018.5030.

[22] H. Lee, K. Kim and Y. Kim, "Wireless Sensor Network-Based 3D Home Control System for Smart Home Environment", International Journal of Smart Home, vol. 10, no. 1, pp. 159-168, 2016. Available: 10.14257/ijsh.2016.10.1.16.

[23] F. Tian, X. Long and W. Liao, "Design of Smart home System Based on Basic Radio Frequency Wireless Sensor Network", International Journal of Online Engineering (iJOE), vol. 14, no. 04, p. 126, 2018. Available: 10.3991/ijoe.v14i04.8389.

[24] Y. Devrim and K. Pehlivanoglu, "Design of a hybrid photovoltaic-electrolyzer-PEM fuel cell system for developing solar model", physica status solidi (c), vol. 12, no. 9-11, pp. 1256-1261, 2015. Available: 10.1002/pssc.201510091.

[25] T. Li, H. Liu and D. Ding, "Predictive energy management of fuel cell supercapacitor hybrid construction equipment", Energy, vol. 149, pp. 718-729, 2018. Available: 10.1016/j.energy.2018.02.101.

[26] H. Mehrjerdi, "Off-grid solar powered charging station for electric and hydrogen vehicles including fuel cell and hydrogen storage", International Journal of Hydrogen Energy, vol. 44, no. 23, pp. 11574-11583, 2019. Available: 10.1016/j.ijhydene.2019.03.158.

[27] Y. Devrim and L. Bilir, "Performance investigation of a wind turbine-solar photovoltaic panels-fuel cell hybrid system installed at Incek region-Ankara, Turkey", Energy Conversion and Management, vol. 126, pp. 759-766, 2016. Available: 10.1016/j.enconman.2016.08.062.

### Nomenclature

|                |   |
|----------------|---|
| $I_{GEN}$      | : PV generated current (A)                        |
| $I_{DEM}$      | : Load consumption current (A)                    |
| $I_{AP}$       | : Appliance consumption current (A)               |
| $Q_P$          | : H <sub>2</sub> produced amount (mol)            |
| $SOC_{SC}$     | : Supercapacitor state of charge                  |
| $I_{SC}$       | : Supercapacitor current (A)                      |
| $I_{SCmax}$    | : Supercapacitor maximum current (A)              |
| $P_{st}$       | : Tank pressure (bar)                             |
| $T_{st}$       | : Tank temperature (°C)                           |
| $V_{st}$       | : Tank volume (l)                                 |
| $SOC_{H_2}$    | : H <sub>2</sub> tank state of charge             |
| $SOC_{H_2min}$ | : H <sub>2</sub> tank state of charge min         |
| $Q^S$          | : H <sub>2</sub> tank Stored amount (mol)         |
| $Q^S_{max}$    | : H <sub>2</sub> tank maximum stored amount (mol) |
| $N_{EL}$       | : Electrolyze cell numbers                        |
| $SOC^{EST}$    | : Estimated H <sub>2</sub> tank state of charge   |
| $SOC^{CH}$     | : Estimated Supercapacitor state of charge        |
| $I_{ST}$       | : Estimated excess generated current (A)          |
| $I_{SC}^{CH}$  | : Supercapacitor charging current (A)             |
| $Q_{H_2V}$     | : Vehicle fuel delivery (mol)                     |
| $Q^P$          | : H <sub>2</sub> needed amount (mol)              |
| $Q_{VEH}$      | : Vehicle fuel reserve (mol)                      |
| $F$            | : Faraday constant                                |
| $SOC_{H_2max}$ | : H <sub>2</sub> tank state of charge max         |

# Evaluation of the Performance of the University Information Systems: Case of Moroccan Universities

Ayoub Gacim<sup>1</sup>, Hicham Drissi<sup>2</sup>, Abdelwahed Namir<sup>3</sup>

Laboratory of Information Technology and Modeling

Hassan II University, Faculty of Sciences Ben M'SIK, Casablanca, Morocco<sup>1,3</sup>

Laboratory of Research and Prospects in Finance and Management

Hassan II University, National School of business and Management Casablanca, Morocco<sup>2</sup>

**Abstract**—The purpose of this paper is to develop a conceptual model of university information systems performance measurement. To do this resorted to the choice of 3E-3P model. This model proposes a development under the spectrum of the systemic approach. The objective is to provide a tool to decision-makers in order to understand the dynamics of performance measurement. The model is based on a logic of decomposition of the global performance into three partial performances. The measurement is carried out at each pillar individually using a multi-criteria approach (MACBETH), and subsequently the consolidation of the three partial performances is carried out with the same multicriteria logic.

**Keywords**—Component; information system; performance; multicriteria modeling; university

## I. INTRODUCTION

The evaluation of performance in the current administrative context is unanimously recognized as an essential factor in steering administrations. To measure this performance, decision-makers have to use performance indicators. Regarding the definition of the indicators, it is possible to make a distinction in the literature between the standards and the usual methods of piloting by indicators. In the first case finds repositories like ITIL, COBIT, Their goal is primarily to provide a structure and tools tailored to professionals from a particular sector. The repositories are based on a benchmark principle of the best practices encountered on the possible widest range of companies. Repositories are often used in practice because they provide the elements to be measured and allow quick apprehension of performance system. The conventional indicators provided are useful and it is interesting to use some of them. However, as soon as it is a question of a particular case they are not sufficient and the decision-maker must find how to enrich his performance measure. In the case of usual methods of piloting by indicators can differentiate between sectorized methods from optimization methods. In most cases the indicators target an element or a type of system elements. One of the weaknesses of these approaches seems to us to be the absence of an overall indicator providing a visibility across the system. The multicriteria aspect and the interactions between the criteria are often not taken into account. In addition, the detail they provide, particularly in the definition of indicators not allowing an adequate adaptation to the particular case of the decision-maker. The question

becomes, then, how, beyond the indicators used, the decision-maker can apprehend the performance as a whole. This article will be organized in four sections: (i) explanation and discussion of the problem, its nature and its difficulties, (ii) presentation and comparative study of the multicriteria methods available on the literature; (iii) construction and presentation of the model; and (iv) analysis and interpretation of results; and the article will be closed with a conclusion and perspective.

## II. PROBLEMATIC

You cannot approach the performance of an organization without integrating the dimension of its IS and especially when it comes to service activities such as academic universities.

Several works try to include the intelligent dimension into the information system [1] like the trends in other fields [2] [3] but they don't integrate the efficiency of information system in the evaluation of the global performance [4] [5]. In addition, universities ranking is limited to the research dimension [6] which is easier to measure and evaluate, when they should be improving the information system to get better performance.

In this case the Information System is more than a driving factor, it is a successful information system which improves development, cost, innovation, and network in universities, and as a consequence it leads to obtain a competitive advantage [7]. It is in this context that the notion of "global performance" appears. This multidimensional concept makes it possible to go from a financial representation of the performance to more global approaches including several dimensions. Numerous examples justify this finding, notably the use of the commercial margin in the evaluation of economic performance; ROI (return on investment) in the evaluation of the return on invested capital; Turnover rate in the assessment of social and human performance; The 360 ° method: as a tool allowing managers to be informed about the perception that their professional entourage have of the effectiveness of their behavior in contributing to their mission. This analysis, which focuses on the assessment of the contribution of information systems to the performance of Moroccan universities, is surrounded by the heterogeneous nature of performance criteria. Have found it essential to use a multi-faceted and multi-criteria decision support tool to converge and align selected criteria. To further enhance Campbell's assumption of

coverage of all criteria and to respond to cost optimization logic; total control of operations; and the constraint of time, it is considered appropriate to synthesize this reflection on three aspects of performance evaluation in this case: Economy, Efficiency, Efficiency.

### III. POSITIONING THE SEARCH

This approach is then interpretative-constructivist. Interpretative in the sense that it uses the arrangement between two modeling approaches, as well as a field investigation for the determination of IS performance criteria in Moroccan universities. Subsequently a tree modeling of these performance criteria according to the above model 3E-3P presented, these on one hand. On the other hand, the constructivist aspect of this work stands out in mathematical modeling, MACBETH [8] in essence and the results will be explained below. To provide a tool for reconstructing the reality of measuring the overall performance of IS in Moroccan universities. Modeling proposal is to explain the overall performance in three areas (technical, professional and process). Subsequently articulate these with the contributions and knowledge of the literature on the overall performance of IS.

### IV. CHOICE OF THE MULTICRITERIA METHOD

The ambition stemming from mathematical modeling can be summed up in two essential points. First, propose a suitable multicriteria model and examine its empirical validity. Then check the overall performance of the IS in the Moroccan university. Thus, several models and theories were founded in the object. The table below summarizes the existing methods and their properties [9].

Following a bibliographic (Table I and Fig. 1) study and a comparison between the different multicriteria methods opted for the two methods AHP and Macbeth. They have properties like the simple operating principle; the mathematical consistency and the binary comparison principle that makes the evaluation work practical. Final choice will focus on the Macbeth method given the accessibility of the software. It facilitates the translation of the decision-makers perception and his appreciation of the performance in order to elicit his reasoning model.

#### A. Figures and Tables

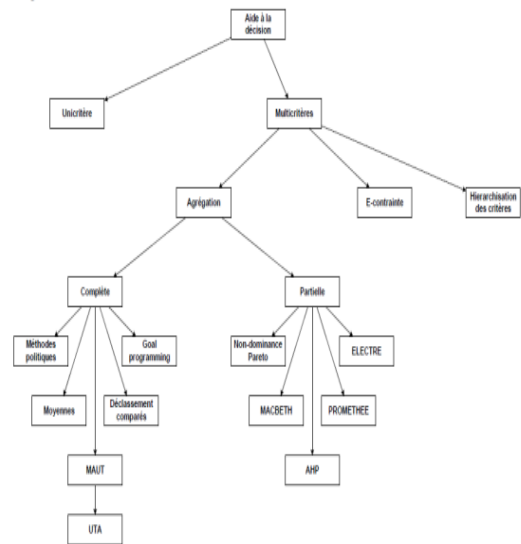


Fig. 1. Categorization of Decision Support Methods.

TABLE I. MULTICRITERIA METHOD COMPARAISON

| Method                        | Author                                 | Consistency   | Criteria               | Software          |
|-------------------------------|--|---|------------------------|-------------------|
| AHP                           | SAATY<br>SCHÄRLIG<br>TKINDT<br>BILLAUT | Analytic hierarchy process relies on the hierarchical structure of the problem consisting of goal levels, criteria. And alternatives. For more details on multicriteria decisions [10]  | Tangible or Intangible | EXPERT CHOICE     |
| MACBETH                       | BANA E COSTA ET<br>VANSNIK             | An approach to measure attractiveness through a category-based evaluation technique [8]   | Tangible or Intangible | M-MACBETH         |
| TOPIS                         | HWANG AND<br>YOON                      | A multi-attribute decision-making technique (MADM) in which alternatives are ranked according to their distance between the ideal and negative ideal solution [11]  | Tangible               | TOPSIS SOLVER     |
| THE STUDY OF<br>NON DOMINANCE | BARICHARD<br>COLLETTE SIARRY           | Consists of dismissing dominated solutions. We say that a solution S1 dominates a solution S2 in the sense of n criteria if the performance of S1 is at least equal to the performance of S2 on the n criteria and strictly superior on one criterion. [12] | Tangible               |                   |
| PROMETHEE                     | BRANS<br>MARESCAL                      | Preference Ranking Organisation Method for Enrichment Evaluations: the principle is to use the flow of classification. That is to say the power of an action compared to others [13]  | Tangible or Intangible | PROMCALC          |
| MAUT Methods                  | FISHBURN<br>KEENEY<br>DYER             | Multi-Attribute Utility Theory : it seeks to define a utility function that summarizes all criteria [14]  | Tangible               | LOGICAL DECISIONS |
| ELECTRE                       | ROY                                    | Elimination and choice translating reality and its variants which consists of constituting a core of action that outclasses the others. The core is the set of actions that are not outperformed by any   | Tangible or Intangible | ELECTRE IS        |

## V. CONSTRUCTION OF THE PERFORMANCE MEASUREMENT MODEL

The approach taken at the level of performance measurement as explained above is based on a multi-criteria concept in order to take into account the different factors influencing performance. Also, the logic of decomposition of the notion of global performance into components must be taken into account in order to facilitate the notion of measurement. But there remains the problem of consolidation of the partial measures carried out. Hence the adoption of a

hierarchical concept that makes it possible both to perform partial. In [15] and [16], authors make measurements separately and at the same time allow an aggregation of the components of the performance into a single global dimension. The overall performance structure is composed of three pillars (3P) essential to know Processes, professionals and the technical platform [17]. Each pillar consists of a set of criteria that respect the representatively of the triplet (3E), economy, efficiency and effectiveness [18]. The tree structure then becomes of the following form: (Fig. 2).

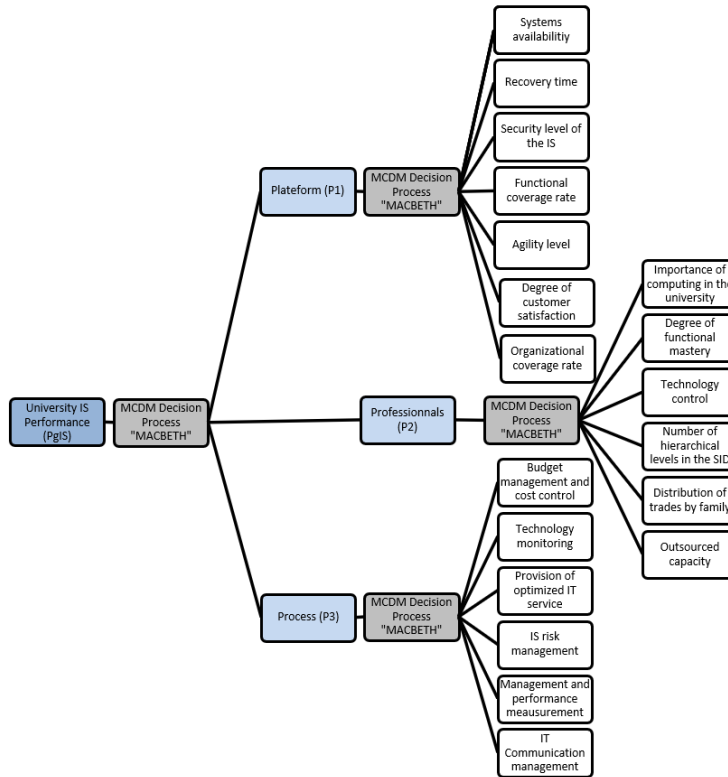


Fig. 2. Tree of the Performance Measurement Model.

## VI. OPERATION OF THE MEASUREMENT MODEL (BASIC PRINCIPLE)

The overall performance and the three pillars are evaluated on the basis of a P1 to P5 scale. P5 is the highest performance value and P1 is the lowest performance value. The measurement tool used in this approach as previously stated is the MACBETH multicriteria tool. The choice was justified and discussed in the section (comparative study between MC methods ...). View the many benefits it presents in this case. The measurement principle is based on an aggregation of the three partial components of the performance into a global measure [19]. It is the same for measuring the performance of each component based on its criteria [8]. It is a sequential iterative process that allows dissociated and individually realized evaluations but at the same time that will take into consideration each other to contribute to the overall judgment [20].

## VII. ANALYSIS AND INTERPRETATION

After engagement of the evaluation process with the help of experts using the M-MACBETH software, obtained the results of the partial evaluations and then injected them to re-evaluate the overall judgment that allowed us to obtain the final value of the overall performance. Below is a summary of the results obtained through the study of the performance of the two universities chosen by teamwork.

1) *Case number 1: Hassan the first university:* The result obtained after measuring the performance of the first pillar (P1: .....). Based on its criteria (Fig. 3).

To extract from the summary shows that the performance of the first pillar is at level 2/5. The tendency of evolution is towards level 3/5. The result obtained after measuring the performance of the second pillar (P2: .....). Based on its criteria (Fig. 4).

| Options        | Global | N1     | N2     | N3     | N4     | N5     | N6     | N7     |
|----------------|--------|--------|--------|--------|--------|--------|--------|--------|
| [ toutes sup ] | 100.00 | 100.00 | 100.00 | 100.00 | 100.00 | 100.00 | 100.00 | 100.00 |
| op 2           | 82.67  | 100.00 | 90.00  | 76.92  | 35.00  | 100.00 | 100.00 | 100.00 |
| op 3           | 73.49  | 70.59  | 70.00  | 46.16  | 100.00 | 70.59  | 81.25  | 85.00  |
| op 1           | 45.96  | 0.00   | 100.00 | 100.00 | 0.00   | 88.24  | 62.50  | 70.00  |
| op 4           | 39.78  | 47.06  | 35.00  | 15.38  | 85.00  | 35.29  | 12.50  | 35.00  |
| op 5           | 19.10  | 23.53  | 0.00   | 0.00   | 70.00  | 0.00   | 0.00   | 0.00   |
| [ toutes inf ] | 0.00   | 0.00   | 0.00   | 0.00   | 0.00   | 0.00   | 0.00   | 0.00   |
| Poids :        | 0.2653 | 0.0204 | 0.2245 | 0.1837 | 0.0612 | 0.1429 | 0.1020 |        |

Fig. 3. Measuring the Performance of the First Pillar P1: Technical Platform UHP.

| Options        | Global | N1     | N2     | N3     | N4     | N5     | N6     |
|----------------|--------|--------|--------|--------|--------|--------|--------|
| [ toutes sup ] | 100.00 | 100.00 | 100.00 | 100.00 | 100.00 | 100.00 | 100.00 |
| op 3           | 88.88  | 100.00 | 100.00 | 100.00 | 50.00  | 52.63  | 86.67  |
| op 4           | 62.87  | 23.53  | 76.47  | 76.47  | 25.00  | 100.00 | 100.00 |
| op 2           | 54.75  | 88.24  | 23.53  | 52.94  | 75.00  | 26.32  | 73.33  |
| op 1           | 38.57  | 64.71  | 0.00   | 41.18  | 100.00 | 0.00   | 53.33  |
| op 5           | 20.12  | 0.00   | 47.06  | 0.00   | 0.00   | 78.95  | 0.00   |
| [ toutes inf ] | 0.00   | 0.00   | 0.00   | 0.00   | 0.00   | 0.00   | 0.00   |
| Poids :        | 0.2500 | 0.1945 | 0.3056 | 0.0833 | 0.1389 | 0.0278 |        |

Fig. 4. Measuring the Performance of the Second Pillar P2: the Professionals UHP.

The extract from the summary shows that: the performance of the second pillar is at the level 3/5 with a tendency of evolution towards the level 4/5. The result obtained after measuring the performance of the third pillar (P3: .....). Based on its criteria (Fig. 5).

The extract from the summary shows that/ the performance of the second pillar is at level 2/5 with a tendency of evolution towards level 3/5. The result obtained after measuring the overall performance (PG: .....): From its components (the three pillars, P1, P2, P3) (Fig. 6).

The excerpt of the summary shows that: the overall performance is at the 3/5 level with a trend towards level 2/5.

2) Case number II: IBN ZOHR university: The result obtained after measuring the performance of the first pillar (P1: .....). Based on its criteria (Fig. 7).

| Options        | Global | N1     | N2     | N3     | N4     | N5     | N6     |
|----------------|--------|--------|--------|--------|--------|--------|--------|
| [ toutes sup ] | 100.00 | 100.00 | 100.00 | 100.00 | 100.00 | 100.00 | 100.00 |
| op 2           | 80.14  | 25.00  | 85.71  | 100.00 | 75.00  | 50.00  | 100.00 |
| op 3           | 65.16  | 50.00  | 57.14  | 57.14  | 50.00  | 100.00 | 75.00  |
| op 1           | 52.96  | 0.00   | 100.00 | 85.71  | 100.00 | 0.00   | 50.00  |
| op 4           | 42.33  | 100.00 | 28.57  | 28.57  | 25.00  | 75.00  | 25.00  |
| op 5           | 16.05  | 83.33  | 0.00   | 0.00   | 0.00   | 25.00  | 0.00   |
| [ toutes inf ] | 0.00   | 0.00   | 0.00   | 0.00   | 0.00   | 0.00   | 0.00   |
| Poids :        | 0.1707 | 0.0244 | 0.2195 | 0.1220 | 0.0732 | 0.3902 |        |

Fig. 5. Measuring the Performance of the Third Pillar P3: the Processes UHP.

| Options        | Global | N1     | N2     | N3     |
|----------------|--------|--------|--------|--------|
| [ toutes sup ] | 100.00 | 100.00 | 100.00 | 100.00 |
| op 3           | 85.76  | 81.82  | 100.00 | 76.92  |
| op 2           | 84.41  | 100.00 | 57.14  | 100.00 |
| op 1           | 46.49  | 45.45  | 35.71  | 53.85  |
| op 4           | 46.06  | 36.36  | 71.43  | 30.77  |
| op 5           | 0.00   | 0.00   | 0.00   | 0.00   |
| [ toutes inf ] | 0.00   | 0.00   | 0.00   | 0.00   |
| Poids :        |        | 0.0909 | 0.3636 | 0.5454 |

Fig. 6. Overall Performance Measurement Result of the Three Pillars UHP.

| Options        | Global | N1     | N2     | N3     | N4     | N5     | N6     | N7     |
|----------------|--------|--------|--------|--------|--------|--------|--------|--------|
| [ toutes sup ] | 100.00 | 100.00 | 100.00 | 100.00 | 100.00 | 100.00 | 100.00 | 100.00 |
| op 3           | 93.14  | 92.31  | 70.00  | 100.00 | 100.00 | 100.00 | 81.25  | 85.00  |
| op 2           | 75.25  | 100.00 | 90.00  | 47.06  | 35.00  | 88.24  | 100.00 | 100.00 |
| op 4           | 54.70  | 61.54  | 35.00  | 64.71  | 85.00  | 35.29  | 12.50  | 35.00  |
| op 1           | 30.36  | 0.00   | 100.00 | 35.29  | 0.00   | 70.59  | 62.50  | 70.00  |
| op 5           | 21.02  | 30.77  | 0.00   | 0.00   | 70.00  | 0.00   | 0.00   | 0.00   |
| [ toutes inf ] | 0.00   | 0.00   | 0.00   | 0.00   | 0.00   | 0.00   | 0.00   | 0.00   |
| Poids :        |        | 0.2653 | 0.0204 | 0.2245 | 0.1837 | 0.0612 | 0.1429 | 0.1020 |

Fig. 7. Measuring the Performance of the First Pillar P1: Technical Platform UIZ.

The extract from the summary shows that: the performance of the first pillar is at the level 3/5 with a tendency of evolution towards the level 2/5. The result obtained after measuring the performance of the second pillar (P2: .....). Based on its criteria (Fig. 8).

The extract from the summary shows that: the performance of the second pillar is at the level 3/5 with a tendency of evolution towards the level 2/5. The result obtained after measuring the performance of the third pillar (P3: .....). Based on its criteria (Fig. 9).

The extract from the summary shows that: the performance of the second pillar is at level 2/5 with a tendency of evolution towards level 3/5. The result obtained after measuring the overall performance (PG: .....): From its components (the three pillars, P1, P2, P3) (Fig. 10).

| Options        | Global | N1     | N2     | N3     | N4     | N5     | N6     |
|----------------|--------|--------|--------|--------|--------|--------|--------|
| [ toutes sup ] | 100.00 | 100.00 | 100.00 | 100.00 | 100.00 | 100.00 | 100.00 |
| op 3           | 88.88  | 100.00 | 100.00 | 100.00 | 50.00  | 52.63  | 86.67  |
| op 2           | 77.28  | 88.24  | 23.53  | 126.67 | 75.00  | 26.32  | 73.33  |
| op 4           | 59.87  | 23.53  | 76.47  | 66.67  | 25.00  | 100.00 | 100.00 |
| op 1           | 36.18  | 64.71  | 0.00   | 33.33  | 100.00 | 0.00   | 53.33  |
| op 5           | 20.12  | 0.00   | 47.06  | 0.00   | 0.00   | 78.95  | 0.00   |
| [ toutes inf ] | 0.00   | 0.00   | 0.00   | 0.00   | 0.00   | 0.00   | 0.00   |
| Poids :        | 0.2500 | 0.1945 | 0.3056 | 0.0833 | 0.1389 | 0.0278 |        |

Fig. 8. Measuring the Performance of the Second Pillar P2: the Professionals UIZ.

| Options        | Global | N1     | N2     | N3     | N4     | N5     | N6     |
|----------------|--------|--------|--------|--------|--------|--------|--------|
| op 2           | 106.60 | 180.00 | 85.71  | 100.00 | 75.00  | 50.00  | 100.00 |
| [ toutes sup ] | 100.00 | 100.00 | 100.00 | 100.00 | 100.00 | 100.00 | 100.00 |
| op 3           | 80.52  | 140.00 | 57.14  | 57.14  | 50.00  | 100.00 | 75.00  |
| op 1           | 52.96  | 0.00   | 100.00 | 85.71  | 100.00 | 0.00   | 50.00  |
| op 4           | 42.33  | 100.00 | 28.57  | 28.57  | 25.00  | 75.00  | 25.00  |
| op 5           | 10.36  | 50.00  | 0.00   | 0.00   | 0.00   | 25.00  | 0.00   |
| [ toutes inf ] | 0.00   | 0.00   | 0.00   | 0.00   | 0.00   | 0.00   | 0.00   |
| Poids :        |        | 0.1707 | 0.0244 | 0.2195 | 0.1220 | 0.0732 | 0.3902 |

Fig. 9. Measuring the Performance of the Third Pillar P3: the Processes UIZ.

| Options        | Global | N1     | N2     | N3     |
|----------------|--------|--------|--------|--------|
| [ toutes sup ] | 100.00 | 100.00 | 100.00 | 100.00 |
| op 2           | 90.91  | 100.00 | 75.00  | 100.00 |
| op 3           | 87.83  | 137.50 | 100.00 | 71.43  |
| op 4           | 39.45  | 62.50  | 50.00  | 28.57  |
| op 1           | 34.74  | 25.00  | 25.00  | 42.86  |
| op 5           | 0.00   | 0.00   | 0.00   | 0.00   |
| [ toutes inf ] | 0.00   | 0.00   | 0.00   | 0.00   |
| Poids :        |        | 0.0909 | 0.3636 | 0.5454 |

Fig. 10. Overall Performance Measurement Result of the Three Pillars UIZ.

The extract of the summary shows that: the overall performance is at level 2/5 with a tendency of evolution towards level 3/5.

VIII. SUMMARY OF THE RESULTS

The two tables below (Table II and Table III) are the results of the evaluation work of this case study.

The synthesis mentioned above is the result of the analysis of the data resulting from the multi-criteria modeling object of the mobilization of the MACBETH tool.

The first table represents the summary of all the criteria of Hassan Premier University.

While the second table represents the summary of all the criteria of IBNOZOHR University.

Thus these tables demonstrate the level of performance of each field by generating both the trend and the judgment value following the evaluation of the three main pillars (P1 platform P2 professional P3 process) across all criteria. To visualize and compare the level of the current performance with that planned

consider useful and meaningful the use of the radar graphic representation and this to estimate the trend of the performance.

The graphical representation of the UHP's radar (Fig. 11), observe an upward trend in the overall performance of the information system. The observation shows that this has important long-term evolution prospects.

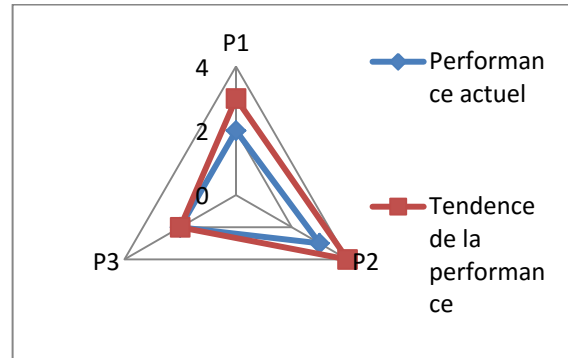


Fig. 11. Representation Current Performance and UHP Trend.

TABLE II. UHP EVALUATION DATA

| Title of the criterion                    | Criteria code | Performance by criterion | Pillars             | Level of performance |                | Trend of performance (Prospective development) |                | GP UHP | Level of performance |                | Trend of performance (Prospective development) |                |
|---|---------------|--------------------------|---------------------|----------------------|----------------|--|----------------|--------|----------------------|----------------|--|----------------|
|   |               |                          |                     | Performance          | Judgment value | Performance                                    | Judgment value |        | Performance          | Judgment value | Performance                                    | Judgment value |
| Systems availability                      | P11           | 2                        | Plateforme (P1)     | 2                    | 82,67          | 3  | 73,49          | GP UHP | 3                    | 85,76          | 2  | 84,41          |
| Recovery time                             | P12           | 1                        |                     |                      |                |  |                |        |                      |                |  |                |
| Security level of the IS                  | P13           | 1                        |                     |                      |                |  |                |        |                      |                |  |                |
| Functional coverage rate                  | P14           | 3                        |                     |                      |                |  |                |        |                      |                |  |                |
| Agility level                             | P15           | 2                        |                     |                      |                |  |                |        |                      |                |  |                |
| Degree of customer satisfaction           | P16           | 2                        |                     |                      |                |  |                |        |                      |                |  |                |
| Organizational coverage rate              | P17           | 2                        | Professionnels (P2) | 3                    | 88,88          | 4  | 62,87          |        | 3                    | 85,76          | 2  | 84,41          |
| Importance of computing in the university | P21           | 3                        |                     |                      |                |  |                |        |                      |                |  |                |
| Degree of functional mastery              | P22           | 3                        |                     |                      |                |  |                |        |                      |                |  |                |
| Technology control                        | P23           | 3                        |                     |                      |                |  |                |        |                      |                |  |                |
| Number of hierarchical levels in the SID  | P24           | 1                        |                     |                      |                |  |                |        |                      |                |  |                |
| Distribution of trades by family          | P25           | 4                        |                     |                      |                |  |                |        |                      |                |  |                |
| Outsourced capacity                       | P26           | 4                        | Processus (P3)      | 2                    | 80,14          | 2  | 65,16          |        | 3                    | 85,76          | 2  | 84,41          |
| Budget management and cost control        | P31           | 4                        |                     |                      |                |  |                |        |                      |                |  |                |
| Technology monitoring                     | P32           | 1                        |                     |                      |                |  |                |        |                      |                |  |                |
| Provision of optimized IT service         | P33           | 2                        |                     |                      |                |  |                |        |                      |                |  |                |
| IS risk management                        | P34           | 1                        |                     |                      |                |  |                |        |                      |                |  |                |
| Management and performance measurement    | P35           | 3                        |                     |                      |                |  |                |        |                      |                |  |                |
| IT Communication management               | P36           | 2                        |                     |                      |                |  |                |        |                      |                |  |                |

TABLE III. UIZ EVALUATION DATA

| Title of the criterion                    | Criteria code | Performance by criterion | Pillars             | Level of performance |                | Trend of performance (Prospective development) |                |               | Level of performance |                | Trend of performance (Prospective development) |                |
|---|---------------|--------------------------|---------------------|----------------------|----------------|--|----------------|---------------|----------------------|----------------|--|----------------|
|   |               |                          |                     | Performance          | Judgment value | Performance                                    | Judgment value |               | Performance          | Judgment value | Performance                                    | Judgment value |
| Systems availability                      | P11           | 2                        | Plateforme (P1)     | 3                    | 93,14          | 2  | 75,25          | <b>GP UIZ</b> |                      |                |  |                |
| Recovery time                             | P12           | 1                        |                     |                      |                |  |                |               |                      |                |  |                |
| Security level of the IS                  | P13           | 3                        |                     |                      |                |  |                |               |                      |                |  |                |
| Functional coverage rate                  | P14           | 3                        |                     |                      |                |  |                |               |                      |                |  |                |
| Agility level                             | P15           | 3                        |                     |                      |                |  |                |               |                      |                |  |                |
| Degree of customer satisfaction           | P16           | 2                        |                     |                      |                |  |                |               |                      |                |  |                |
| Organizational coverage rate              | P17           | 2                        | Professionnels (P2) | 3                    | 88,88          | 2  | 77,28          |               | 2                    | 90,91          | 3  | 87,83          |
| Importance of computing in the university | P21           | 3                        |                     |                      |                |  |                |               |                      |                |  |                |
| Degree of functional mastery              | P22           | 3                        |                     |                      |                |  |                |               |                      |                |  |                |
| Technology control                        | P23           | 3                        |                     |                      |                |  |                |               |                      |                |  |                |
| Number of hierarchical levels in the SID  | P24           | 1                        |                     |                      |                |  |                |               |                      |                |  |                |
| Distribution of trades by family          | P25           | 4                        |                     |                      |                |  |                |               |                      |                |  |                |
| Outsourced capacity                       | P26           | 4                        | Processus (P3)      | 2                    | 106,6          | 3  | 80,52          |               |                      |                |  |                |
| Budget management and cost control        | P31           | 4                        |                     |                      |                |  |                |               |                      |                |  |                |
| Technology monitoring                     | P32           | 1                        |                     |                      |                |  |                |               |                      |                |  |                |
| Provision of optimized IT service         | P33           | 2                        |                     |                      |                |  |                |               |                      |                |  |                |
| IS risk management                        | P34           | 1                        |                     |                      |                |  |                |               |                      |                |  |                |
| Management and performance measurement    | P35           | 3                        |                     |                      |                |  |                |               |                      |                |  |                |
| IT Communication management               | P36           | 2                        |                     |                      |                |  |                |               |                      |                |  |                |

From the analysis of the graphical representation of the radar of the UIZ (Fig. 12), is noted a downward trend in the overall performance of the information system. This observation demonstrates a limitation of evolution and long-term control.

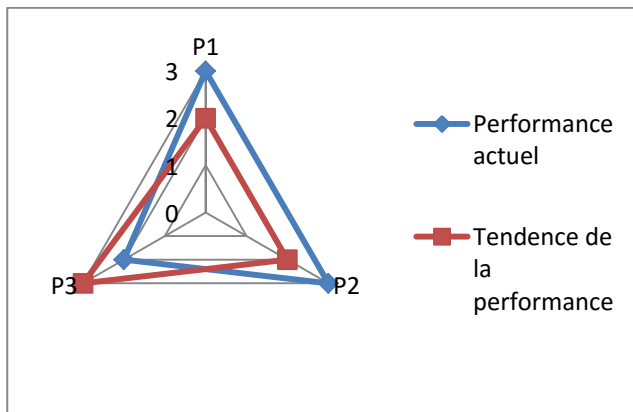


Fig. 12. Representation Current Performance and UIZ Trend.

### IX. CONCLUSION AND PERSPECTIVES

From By way of conclusion, the results obtained show that the management of information systems within the universities in sample is beginning to be structured. But it still lacks efficiency given the results obtained in terms of the mobilization of the means put at their disposal.

Thus results-based management and performance is very embryonic at the level of information systems. Two recommendations seem to us to be crucial: the generalization of multicriteria evaluation in all Moroccan universities; give more importance to the SI function in the organization chart and in the strategic decisions of all university bodies: university councils, school councils, scientific committees. The insufficiencies deciphered by multicriteria model, motivates us to propose research perspectives for more supervision to this problematic. Intend to update the multicriteria evaluation model periodically and permanently on other research projects. The performance indicators recommended at the end of this research work will be proposed in the form of a balanced scorecard in an article that links the SI to management control.

This research shows the importance of the MACBETH multi-criteria approach in elaboration of performance measurement system of Information System University. The tool is based on the comparison of the difference in attractiveness between different alternatives. This comparison is performed by experts. This limitation obligates searchers to choose carefully the experts concerned with prudence and transparent to be able to apply perfectly the multicriteria for the measure of performance. In order to avoid this limitation, an evaluation questionnaire was sent to the manager of the SI as well as the presidents of the universities and to a panel of project managers. Only the answers and information from the interviews with the members of the universities Hassan first of Settat and that of IBNOZOHR in Agadir were sufficiently complete and exhaustive. The totality of the results of the evaluation of the information system cannot be published in detail because of their confidential nature. Only the general features of the multicriteria model have been addressed.

#### REFERENCES

- [1] R. Kresimir, B. G. Marijana, and M. Vlado, "Development of the Intelligent System for the Use of University Information System," *Procedia Engineering*, vol. 69, pp. 402–409, 2014.
- [2] K. Douaioui, M. Fri, C. Mabroukki, and E. A. Semma, "The interaction between industry 4.0 and smart logistics: concepts and perspectives," in *2018 International Colloquium on Logistics and Supply Chain Management (LOGISTIQUA)*, Tangier, 2018, pp. 128–132.
- [3] K. Douaioui, M. Fri, C. Mabrouki, and E. A. Semma, "Smart port: Design and perspectives," in *2018 4th International Conference on Logistics Operations Management (GOL)*, Le Havre, 2018, pp. 1–6.
- [4] S. El Gibari, T. Gómez, and F. Ruiz, "Evaluating university performance using reference point based composite indicators," *Journal of Informetrics*, vol. 12, no. 4, pp. 1235–1250, Nov. 2018.
- [5] X. Zhang and W. Shi, "Research about the university teaching performance evaluation under the data envelopment method," *Cognitive Systems Research*, vol. 56, p. a, Aug. 2019.
- [6] C. Daraio, A. Bonaccorsi, and L. Simar, "Rankings and university performance: A conditional multidimensional approach," *European Journal of Operational Research*, vol. 244, no. 3, pp. 918–930, Aug. 2015.
- [7] Jaf, R., Xinping, X., & Sabr Jaf, S. (2012). The Effect of the Strategic Information Systems (SIS) on the Achievement Competitive Advantage Practical in Samples of Iraqi Banks. *International Conference of Intelligent Systems Design and Engineering Application* (hal. 954 - 959). IEEE.
- [8] Bana e Costa C.A. and J.C. Vansnick. MACBETH: An Interactive Path Towards the Construction of Cardinal Value Functions. *International Transactions in Operational Research*, 1(4):387-500, 1994.
- [9] P. LORINO, « Méthodes et pratiques de la performance, le guide du pilotage », Editions de l'organisation, 1997, p.18.
- [10] Fatimazahra Bentaleb, Charif Mabrouki, Alami Semma. Dry Port Development: A Systematic Review. *J ETA Maritime Sci.* 2015; 3(2): 75-96.
- [11] Keeney R.L. and H. Raiffa. *Decision with Multiple Objectives: Preference and Value Tradeoffs*. Cambridge.
- [12] Parmenter, D., *Measuring Performance In Difficult Times*, Finance & Management, avril 2009, p. 6-11.
- [13] Brans, J. P., Vincke, P., & Mareschal, B. (1986). How to select and how to rank projects: The PROMETHEE method; *European journal of operational research*, 24(2), 228-238.
- [14] Fatimazahra Bentaleb, Charif Mabrouki, Alami Semma. Key Performance Indicators Evaluation and Performance Measurement in Dry Port-Seaport System: A Multi Criteria Approach. *J ETA Maritime Sci.* 2015; 3(2): 97-116.
- [15] Berrah, L., Mauris, G., Vernadat, F., 2004. Information aggregation in industrial performance measurement: rationales, issue and definitions. *International Journal of Production Research*, 42(20), 211-225.
- [16] Berrah, L., Mauris, G., Haurat, A., Foulloy, L., 2000. Global vision and performance indicators for an industrial improvement approach. *Computers in Industry*, 43, 211-225.
- [17] Saaty T.L. *Fundamentals of decision making and priority theory with the Analytic Hierarchy Process*, RWS Publications (1994).
- [18] Roy, B. (1991); The outranking approach and the foundations of ELECTRE methods, *Theory and decision*, 31(1), 49-73.
- [19] Hwang, C. K. Yoon *Multiple attribute decision making: methods and applications* Springer-Verlag, New York (1981).
- [20] Fatimazahra Bentaleb; Charif Mabrouki & Alami Semma (2015) A Multi-Criteria Approach for Risk Assessment of Dry Port-Seaport System, *Supply Chain Forum: An International Journal*, 16:4, 32-49.



# Immuno-Computing-based Neural Learning for Data Classification

Ali Al Bataineh<sup>1</sup>, Devinder Kaur<sup>2</sup>  
EECS Department  
University of Toledo Ohio, US

**Abstract**—The paper proposes two new algorithms based on the artificial immune system of the human body called Clonal Selection Algorithm (CSA) and the modified version of Clonal Selection Algorithm (MCSA), and used them to train the neural network. Conventional Artificial Neural Network training algorithm such as backpropagation has the disadvantage that it can get trapped into the local optima. Consequently, the neural network is usually incapable of obtaining the best solution to the given problem. In the proposed new CSA algorithm, the initial random weights chosen for the neural networks are considered as a foreign body called an antigen. As the human body creates several antibodies in response to fight the antigen, similarly, in CSA algorithm antibodies are created to fight the antigen. Each antibody is evaluated based on its affinity and clones are generated for each antibody. The number of clones depends on the algorithm, in CSA, the number of clones is fixed and in MCSA, number of clones is directly proportional to the affinity of the antibody. Mutation is performed on clones to improve the affinity. The best antibody emerged becomes the antigen for the next round and the process is repeated for several iterations until the best antibody that satisfies the chosen criterion is found. The best antibody is problem specific. For neural network training for data classification, the best antibody represents the set of weights and biases that gives the least error. The efficiency of the algorithm was analyzed using Iris dataset. The prediction accuracy of the algorithms were compared with other nature-inspired algorithms, such as Ant Colony Optimization (ACO), Particle Swarm Optimization (PSO) and standard backpropagation. The performance of MCSA was ahead of other algorithms with an accuracy of 99.33%.

**Keywords**—AIS; CSA; MCSA; ACO; BBNN

## I. INTRODUCTION

Optimization is a process that is widely used in many applications in engineering, for example, optimizing the design of a mechanical part while minimizing the material cost. In computer science, developing algorithms, such as traveling salesman problem, optimize distance while traveling all the cities on an itinerary. In industrial processes such as heat-treat industry, obtaining the desired hardness of the part while minimizing the time through the furnace and lowering the temperature, etc. These are some of the few examples in the engineering domain [1]. The optimization problem regarding artificial neural network is about finding optimal weights and biases of all the neurons in a given neural network architecture designed for specific problem to be addressed. In the traditional back propagation method, the error gradient with respect to the input is propagated backward in the neural network and in the process adjusts the weights connecting the layers of the neural

network. However, the drawback of backpropagation is that it is prone to get stuck into local optima and is computationally intensive [2].

Recently a great deal of interest is emerging in looking towards nature to solve optimization problems. Many nature inspired algorithms such as genetic algorithm, swarm based algorithms such as PSO and other algorithms inspired by the group dynamics of animals working together such as Grey Wolf Optimizer (GWO), Bee Colony Optimization and Harris Hawk algorithm have been applied for optimization [3].

Several nature-inspired algorithms have been suggested to train the neural network that does not require back propagation. They successive iterations adjust the weights based on the dynamics of the nature-inspired algorithm being used.

In this paper, two new algorithms based on artificial immune system are proposed to train the neural network. The algorithms are Clonal Selection Algorithm (CSA) and Modified Clonal Selection Algorithm (MCSA). These are global optimization algorithms and take a global view of the problem and look at the problem from above to see the complete picture. The performance of both algorithms was compared with other algorithms such as Ant Colony Optimization (ACO), Particle Swarm Optimization (PSO) and backpropagation using the benchmark Iris dataset. The paper is organized as follows. Section II presents an introduction of the Immune System. It gives a brief description of the Immune System. Section III gives details about the Clonal Selection theory and the application areas of the algorithm. Section IV, describes the Iris dataset used for data classification. Section V describes the structure of the neural network used in the work. Section VI describes the implementation of the CSA and MCSA algorithms. It provides the flow diagram of the algorithm and the corresponding explanation of the steps involved. In Section VII, discusses the experiments and results. Section VIII provides conclusions.

## II. INTRODUCTION OF THE IMMUNE SYSTEM

The immune system of our body presents the first line of defense against foreign pathogens that invade our body. It consists of anatomical barriers like mucous membranes and skin, endocytic and phagocytic barriers such as macrophages and physiological barriers such as temperature and pH. It is responsible for identifying the malignant foreign cells entering our body that can cause infections and diseases [4, 5].

The immune system has two components, innate immune system and adaptive/acquired immune system. The innate

immune system is inborn immunity, inherited from the mother and is not adaptive to certain kind of pathogen, but acts against the general classes of pathogens. The immune cells can identify the foreign intruders inside the body as pathogens and kill or destroy [6]. The adaptive immune system possesses special features that help them to understand these co-stimulatory signals to combat the external pathogens. It maintains a stable memory of previously known molecular structures and can adapt to them. The innate system plays a significant role by signaling to the adaptive immune system after a specific pathogen has been eliminated [7].

#### A. Physiology and its Components

Fig. 1 illustrates the significant components of the immune system and their relative positions across the body. The immune system is made of lymphoid organs. Lymphoid organs comprise of primary and secondary organs. The primary lymphoid organs supervise the production, growth, development, and maturation of lymphocytes, which are special kind of white blood cells that carry special receptors to identify specific pathogens like a lock and key arrangement. The secondary lymphoid organs are the sites where the lymphocytes interact with pathogens [8]. There are two main types of lymphocytes called the B-cells and the T-cells or B-lymphocytes and T-lymphocytes. The B-cells are named after bone marrow because they mature there and T cells are named after thymus because they mature in thymus. These cells have receptors on their surface that can recognize specific molecular patterns present on the pathogens. They are also capable of multiplying themselves through a cloning process, and the B-cells are capable of introducing genetic variation during reproduction. Therefore, these cells have their number varied with time and B-cells can have their molecular structure changed as well [9]. The two primary lymphoid organs, bone marrow and thymus, have essential functions in the production and maturation of immune cells. All blood cells are created in the bone marrow and are part of the immune system as B-cells. However, some cells that are produced in the bone marrow but migrate to thymus become T cells. After migrating to the thymus and maturing, they become capable to fight against diseases [10] [11].

#### B. Antigens, Antibody and Affinity

The first step of an immune response is to recognize the presence of pathogen. Some parts of pathogens that can facilitate an adaptive immune response are called antigens. Antigens have surface molecules called epitopes, that allow them to be recognized by immune cells and molecules. Fig. 2 depicts immune cells, in particular, B-cells, that are able to recognize epitopes of a given antigen. B-cells and T-cells play a significant role in adaptive immune system. Development of Clonal Selection Algorithm was inspired by the B-cells of the adaptive immune system. The B-cell receptor is also known as antibody or immunoglobulin. The B-cells are monospecific because a single type of receptor is present on their surface. On the contrary, antigens can present various patterns of epitopes. The immune cells and molecules are of various types. The affinity between antigen and antibody is determined by the degree of recognition between the two, higher the recognition, better the affinity and vice versa.

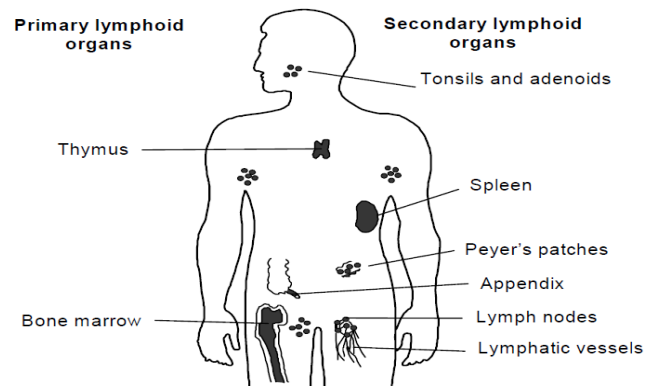


Fig. 1. Physiology of the Immune System [8].

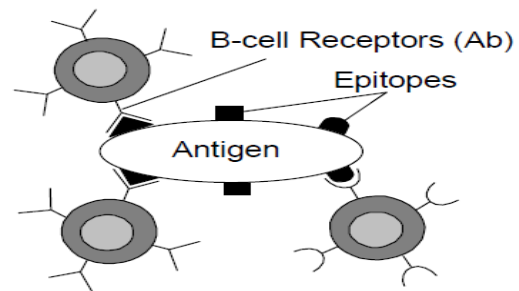


Fig. 2. B-Cells, with their Molecular Receptors Recognizing the Epitopes on Antigens [8].

### III. CLONAL SELECTION ALGORITHM

#### A. Clonal Selection Theory

Australian doctor Frank Macfarlane Burnet proposed the clonal selection theory in 1957 [12]. The scientific theory proposed by Macfarlane forms the basis of modern immunology. This scientific theory models the behavior regarding the response of the immune system to invading pathogen [13]. The immune system is comprised of variety of cells and molecules that remain passive and spring into action only when they encounter a pathogen. After the recognition of pathogen, some cells adhere to the invading antigen. Then the B-cells or T cells stimulate the immune system to reproduce those cells that are capable of identifying the antigen. This process of self-reproduction is called cloning and is asexual in nature. The process of cell division [4] achieves asexual Cellular reproduction. Fig. 3 demonstrates the Clonal Selection process. B cells that have higher affinity to the antigen are chosen to clone themselves, however during the process of cloning some mutation may occur. During the process of mutation, some cloned antibodies (B cells) may become better, that is they develop better receptors to fight the antigen by neutralizing them. The mutated antibody B cells with higher affinity to the antigens become memory cells and antibody plasma cells [8]. This process is also known as clonal expansion and generates cloning cells. During the cloning process, some errors may occur that is called mutation and results in alteration in the structure of the cell. The key features of the clonal selection theory are summarized in the following steps [15]:

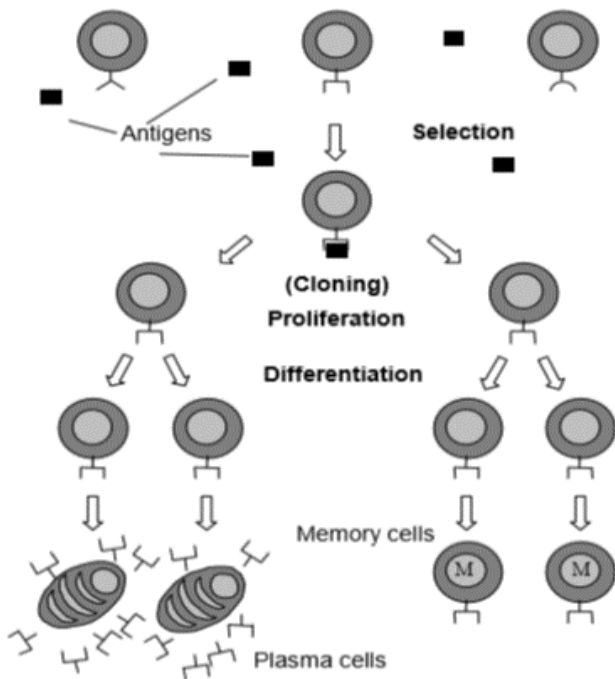


Fig. 3. The Clonal Selection Process [8].

- For a given antigen, generate a random population of different antibodies.
- Keep the antibodies with higher affinity to the antigen and remove the antibodies with lesser affinity to the antigen.
- Clone the antibodies with higher affinity and differentiate them by doing mutation on the clones.

### B. Application Areas of CSA

Several engineering applications have been solved using Clonal Selection Algorithm (CSA). Hart and Timmis [16] studied the contribution of CSA to various domains. Table I summarizes the application areas to which CSA algorithm has been applied. These identified areas have been categorized as clustering/classification, for bioinformatics, computer security using image processing, numerical function optimization in adaptive control applications, anomaly detection to find faults in engineering systems, combinatorial optimization for scheduling, sequencing, and routing, and robotics, learning for web mining.

TABLE I. APPLICATION AREAS OF CSA ALGORITHMS

| Sl. No | Major areas                   | Minor areas      |
|--------|-------------------------------|------------------|
| 1      | Clustering                    | Bio-informatics  |
| 2      | Computer Security             | Image Processing |
| 3      | Numeric Function Optimization | Control          |
| 4      | Anomaly Detection             | Robotics         |
| 5      | Combinatorial Optimization    | Virus Detection  |
| 6      | Learning                      | Web mining       |

1) *Machine learning*: In recent years, machine learning techniques based on immune systems have been used for classification and pattern recognition of DNA.

2) *Robotics*: Clonal Selection Algorithm has been applied to the path planning for mobile robots to simulate some form of self-organizing group behavior [17].

3) *Computer security*: The problem of a system being attacked by virus or hackers has become common these days. Therefore, protecting computers from intruders is one of the biggest challenges nowadays. The immune system based algorithm, like the Clonal Selection Algorithm and negative selection algorithm for the intrusion detection system, have been proposed for this field [18]. Thus, the immune system inspired algorithms are the source of inspiration to combat computer viruses and network intruders.

4) *Optimization*: Immune based algorithms are applied to find the solution for optimization processes. The Clonal Selection Algorithm for optimization starts by defining an objective function. The pattern memorization capabilities for memory cells are used to create a model for pattern recognition. Other features of Clonal Selection Algorithm like self-organization memory, recognition of antigen, adaptation ability, immune response shaping and the ability to get out of local minima helps to achieve optimization [19].

5) *Scheduling*: The job shop scheduling problems have also been addressed by Clonal Selection algorithm. The algorithm helps to generate realistic scheduling solutions efficiently [20].

## IV. IRIS DATASET

Iris dataset is one of the well-known benchmark problems introduced by Ronald Aylmer Fisher to test the new pattern recognition algorithms. The Iris dataset consists of 50 samples each for the three flower species viz. Iris Setosa, Iris Versicolor and Iris Virginica [21]. The dataset consists of four features namely, sepal length, sepal width, petal length, and petal width. The problem is to identify the category of any iris flower based on its four input characteristics of sepal length, sepal width, petal length, petal width [22]. Table II shows an extract from the Iris data set, where a plant with a sepal length of 5.7 can be either a Virginica or a Versicolor. This indicates that each type of the species has no distinguishable length and width ranges, based upon which the classification is done implying that any plant can only be classified by considering all its interrelated features, making the classification more complex. Fig. 4 displays a scatter plot of features of the Iris. In this research, the first 100 samples are used for training and the remaining 50 samples for testing.

TABLE II. EXTRACT FROM THE IRIS DATASET

| Sepal Length | Sepal Width | Petal Length | Petal Length | Species    |
|--------------|-------------|--------------|--------------|------------|
| 4.8          | 3.4         | 1.6          | 0.2          | Setosa     |
| 5.7          | 2.8         | 4.1          | 1.3          | Versicolor |
| 5.7          | 2.5         | 5.0          | 2.0          | Virginica  |

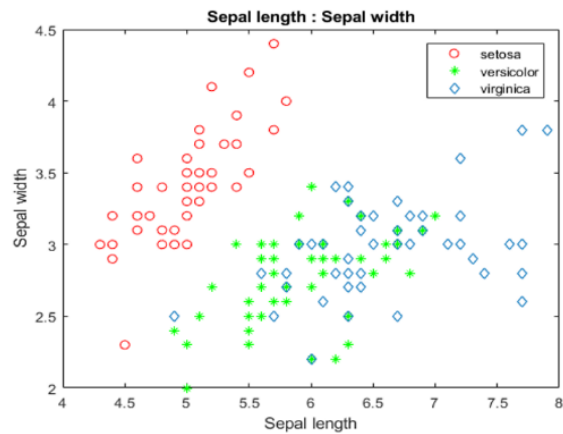
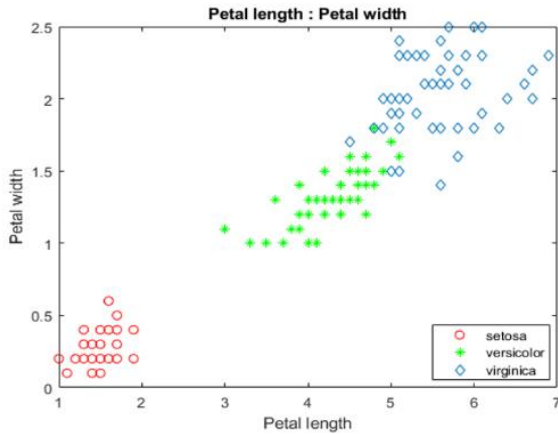


Fig. 4. A Simple Scatter Plot of 4 Features of the Iris Dataset.

### V. ARTIFICIAL NEURAL NETWORK

Artificial Neural Network (ANN) has been successfully used for data classification [23] [24]. The most common algorithm is the back propagation algorithm. This algorithm has two phases: the forward phase and the backward phase. In the forward phase, the outputs for given set of inputs are predicted and in the backward phase gradient of the error is propagated backward and adjusting the weights and the biases in the process. The initial weights and biases are randomly chosen [26] [27]. However, new evolutionary algorithms are emerging that train the weights and biases using evolutionary approach. Genetic algorithms, swarm algorithms and immune system based algorithms come under this category. These algorithms do not have the backward phase and on the contrary, weights are adjusted in every iteration depending on the fitness criterion [25].

In this paper, two neural-network learning algorithms based on the human immune system, namely, Clonal selection Algorithm (CSA) and Modified Clonal Selection Algorithm (MCSA) are proposed to adjust the weights and biases of the neural network.

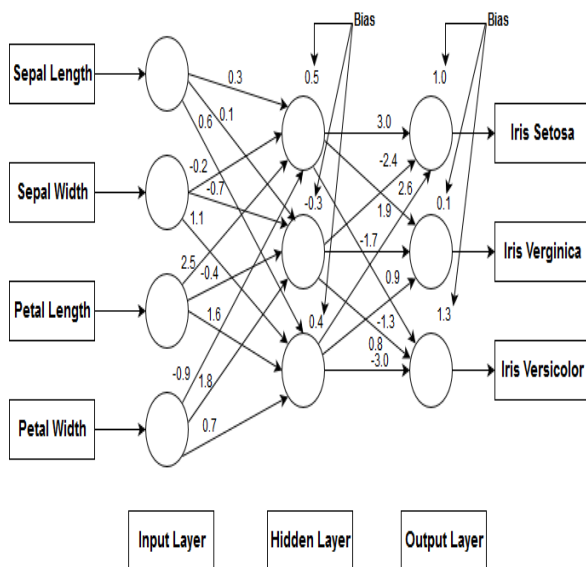


Fig. 5. FFNN Structure for the Iris Data Problem.

Fig. 5 shows the Feed- Forward Neural Network (FFNN) structure for the Iris data classification. The structure of the neural network is determined at the beginning taking into consideration the dimension of the data. Iris data has four inputs namely sepal length, sepal width, petal length and petal width, therefore there are four neurons in the first layer, it has three categories of output, and therefore there are three neurons in the output layer, corresponding to the three Iris species, namely Iris Setosa, Iris Versicolor and Iris Virginica. It has one hidden layer with three neurons. A Neural Network stores the knowledge in the form of weights. The goal is to find optimized sets of weights and biases so that the Iris flowers are correctly classified. The activation function used for the neural network is the sigmoid function. The sigmoid function is mathematically represented by equation (1).

$$Sigmoid(x) = \frac{1}{1+e^{-x}} \tag{1}$$

### VI. IMPLEMENTATION OF CSA AND MCSA

In this section training of the neural network, using CSA and MCSA is described. Table III shows the terminology of Immune system as applied to neural networks. Fig. 6 presents the flowchart for training the neural network to find the weights and biases of the neural network for Iris data classification using CSA. The following steps A thru G describe the complete procedure.

TABLE III. TERMINOLOGY OF IMMUNE SYSTEM APPLIED TO NEURAL NETWORK

| Immune System | Neural Network Model  |
|---------------|---|
| Antigen       | Initial Solution in terms of weights and biases                               |
| Antibody      | Candidate Solution in terms of weight and biases.                             |
| Gene          | Weight or Bias  |
| Affinity      | Fitness value of each antibody to antigen in terms of classification accuracy |
| Cloning       | Creation of multiple copies of antibody                                       |
| Mutation      | Change in one or more genes of antibody                                       |
| Population    | Number of initial antibodies  |
| Generation    | Number of iterations  |

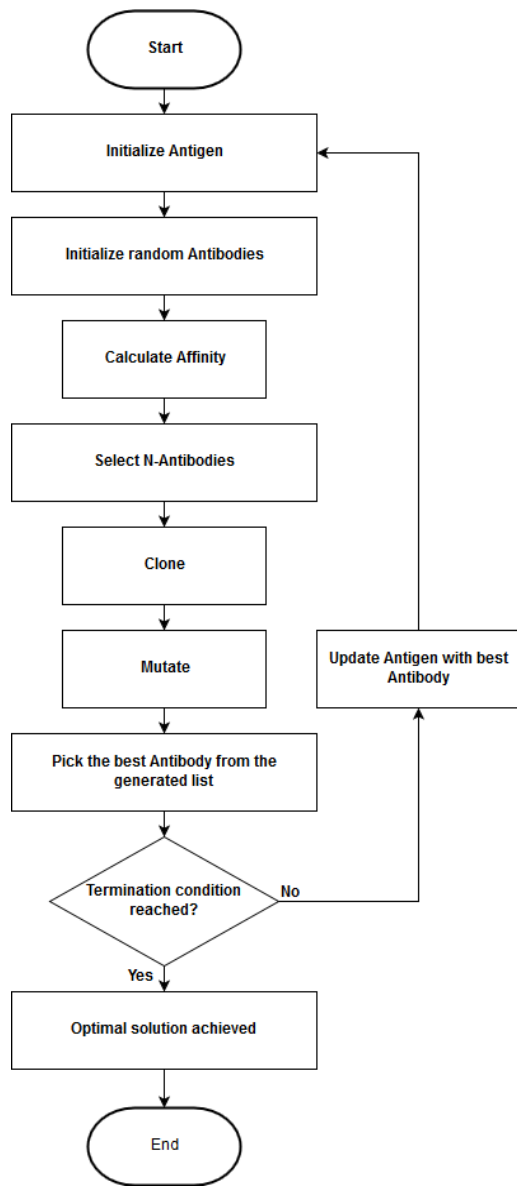


Fig. 6. Flowchart Diagram, Describing Phases of the CSA [3].

### A. Antigen Creation

Antigen refers to a foreign body that attacks the human body such as toxin in the form of virus, bacteria or fungus. In response to the antigen, body creates antibodies and the process of cloning multiplies superior antibodies. Mutation operation is performed on the clones to improve their affinity to overpower and kill the antigen.

Initial antigen for neural network should be in the form of potential solution of weights and biases. Therefore, an array of random weights and biases appropriate to the structure of the neural network is created as antigen.

Fig. 7 shows a sample antigen corresponding to neural network illustrated in Fig. 5. The antigen is an array of 27 individual elements; 20 elements represent the weights of the neural network and the remaining six elements represent the biases of the neurons in the neural network.

### B. Creation of Antibodies

In response to the initial antigen, several antibodies with the same format are created to fight the antigen. For this problem of training the neural network using CSA, 20 antibodies were generated in response to one antigen.

### C. Affinity Calculation

The affinity of each created antibody is calculated according to the objective function of the problem that is being optimized. The objective function for the neural network training is to minimize the error for data classification and that is represented by lowering the mean squared error as described in equation (2). In equation (2),  $n$  represents the number of data points and  $Y_i$  is the original data values and  $f(x_i)$  is the data values predicted by neural network using the weights and biases of the antibody. The lower the mean square error, the higher is the fitness of the antibody. In other words, the CSA attempts to find a set of weights that minimizes the sum of squared errors.

$$MSE = \frac{1}{n} \sum_{i=1}^n (Y_i - f(x_i))^2 \quad (2)$$

Fitness of the antibody is reciprocal of MSE as described in equation (3).

$$Fitness\ of\ Antibody = \frac{1}{MSE} \quad (3)$$

Now, the affinity of antibody to the antigen is calculated as the difference between their fitness as shown in equation (4).

$$Affinity\ of\ Antibody = Antibody_{fitness} - Antigen_{fitness} \quad (4)$$

The antibodies with higher fitness than antigen are considered going forward.

### D. Selection of Antibodies

Five antibodies that have the highest fitness among the 20 antibodies are selected.

### E. Clone the Antibodies

Multiple copies of the selected antibodies are created. CSA creates fixed number of antibodies and MCSA creates clones proportional to the affinity of the antibody.

1) *Cloning for the CSA*: For the CSA algorithm, the number of clones  $N_c$  is fixed to 10 and is the same for all the selected antibodies. Hence, for every iteration 10 clones are generated for each of the 5 selected antibodies.

2) *Cloning for the modified CSA*: For the modified CSA algorithm, the number of clones  $N_c$  for each antibody are proportional to the affinity of antibody. Higher the affinity value, higher is the number of clones  $N_c$ . The number of clones  $N_c$  for MCSA is obtained by equation (5). The maximum number of clones created is 10, hence,  $N_i$  is 10,  $x_{max}$  is the highest affinity and  $x_{min}$  is the lowest affinity value of antibodies during any given iteration.  $x_i$  is the affinity value of  $i$ th antibody. Equation (5) is used to find the number of clones created for antibody with an affinity  $x_i$ .  $Ceil(\cdot)$  is the operator that rounds its argument towards the next higher integer.

|     |      |     |      |     |      |      |     |     |     |     |     |     |      |     |     |      |     |     |      |     |      |     |      |     |     |     |
|-----|------|-----|------|-----|------|------|-----|-----|-----|-----|-----|-----|------|-----|-----|------|-----|-----|------|-----|------|-----|------|-----|-----|-----|
| 0.3 | -0.2 | 2.5 | -0.9 | 0.1 | -0.7 | -0.4 | 1.8 | 0.6 | 1.1 | 1.6 | 0.7 | 0.5 | -0.3 | 0.4 | 3.0 | -2.4 | 2.6 | 1.9 | -1.7 | 0.9 | -1.3 | 0.8 | -3.0 | 1.0 | 0.1 | 1.3 |
|-----|------|-----|------|-----|------|------|-----|-----|-----|-----|-----|-----|------|-----|-----|------|-----|-----|------|-----|------|-----|------|-----|-----|-----|

Fig. 7. A Sample Antigen of the Iris Neural Network.

|     |      |     |      |     |      |      |     |     |     |     |     |     |      |     |     |      |     |     |      |     |      |     |      |     |     |     |
|-----|------|-----|------|-----|------|------|-----|-----|-----|-----|-----|-----|------|-----|-----|------|-----|-----|------|-----|------|-----|------|-----|-----|-----|
| 0.3 | -0.2 | 2.5 | -0.9 | 0.1 | -0.7 | -0.4 | 1.8 | 0.6 | 1.1 | 1.6 | 0.7 | 0.5 | -0.3 | 0.4 | 3.0 | -2.4 | 2.6 | 1.9 | -1.7 | 0.9 | -1.3 | 0.8 | -3.0 | 1.0 | 0.1 | 1.3 |
|-----|------|-----|------|-----|------|------|-----|-----|-----|-----|-----|-----|------|-----|-----|------|-----|-----|------|-----|------|-----|------|-----|-----|-----|

(a)

|     |      |     |     |     |      |      |     |     |     |     |     |     |      |     |     |      |      |     |      |     |      |     |      |     |     |     |
|-----|------|-----|-----|-----|------|------|-----|-----|-----|-----|-----|-----|------|-----|-----|------|------|-----|------|-----|------|-----|------|-----|-----|-----|
| 0.3 | -0.2 | 2.5 | 2.6 | 0.1 | -0.7 | -0.4 | 1.8 | 0.6 | 1.1 | 1.6 | 0.7 | 0.5 | -0.3 | 0.4 | 3.0 | -2.4 | -0.9 | 1.9 | -1.7 | 0.9 | -1.3 | 0.8 | -3.0 | 1.0 | 0.1 | 1.3 |
|-----|------|-----|-----|-----|------|------|-----|-----|-----|-----|-----|-----|------|-----|-----|------|------|-----|------|-----|------|-----|------|-----|-----|-----|

(b)

Fig. 8. Reciprocal Exchange Mutation for the CSA Algorithm. (a) Original Antibody. (b) Antibody after Mutation.

|     |      |     |      |     |      |      |     |     |     |     |     |     |      |     |     |      |     |     |      |     |      |     |      |     |     |     |
|-----|------|-----|------|-----|------|------|-----|-----|-----|-----|-----|-----|------|-----|-----|------|-----|-----|------|-----|------|-----|------|-----|-----|-----|
| 0.3 | -0.2 | 2.5 | -0.9 | 0.1 | -0.7 | -0.4 | 1.8 | 0.6 | 1.1 | 1.6 | 0.7 | 0.5 | -0.3 | 0.4 | 3.0 | -2.4 | 2.6 | 1.9 | -1.7 | 0.9 | -1.3 | 0.8 | -3.0 | 1.0 | 0.1 | 1.3 |
|-----|------|-----|------|-----|------|------|-----|-----|-----|-----|-----|-----|------|-----|-----|------|-----|-----|------|-----|------|-----|------|-----|-----|-----|

(a)

|     |      |     |     |     |      |     |     |     |     |     |     |      |      |     |     |      |      |     |      |     |      |     |      |     |     |     |
|-----|------|-----|-----|-----|------|-----|-----|-----|-----|-----|-----|------|------|-----|-----|------|------|-----|------|-----|------|-----|------|-----|-----|-----|
| 0.3 | -0.2 | 2.5 | 2.6 | 0.1 | -0.7 | 0.5 | 1.8 | 0.6 | 1.1 | 1.6 | 0.7 | -0.4 | -0.3 | 0.4 | 3.0 | -2.4 | -0.9 | 1.9 | -1.7 | 0.1 | -1.3 | 0.8 | -3.0 | 1.0 | 0.9 | 1.3 |
|-----|------|-----|-----|-----|------|-----|-----|-----|-----|-----|-----|------|------|-----|-----|------|------|-----|------|-----|------|-----|------|-----|-----|-----|

(b)

Fig. 9. Reciprocal Exchange Mutation for the Modified CSA Algorithm. (a) Original Antibody. (b) Antibody after Mutation.

$$N_c = \text{ceil} \left( N_i \frac{x_i - x_{\min}}{x_{\max} - x_{\min}} \right) \quad (5)$$

### F. Mutation

The mutation is the process of randomly altering the given chromosome to introduce diversity in the population. Mutation operation enables to achieve global optimization and thus helping to escape from local optimization. In immune system based algorithms, mutation is performed on antibodies with an intent to enhance their ability to better attack the foreign antigen. There are many types of mutation operations such as shift right or left, alter a gene, transpositions, inversion within a random window etc. In this work, the reciprocal exchange mutation is implemented on the cloned antibodies. The best antibody created after cloning and mutation becomes the antigen for the next iteration.

1) *Mutation in CSA*: A single point reciprocal exchange mutation is performed in CSA wherein two random points are selected and the genes are exchanged as shown in Fig. 8.

2) *Mutation in modified CSA*: The modified CSA algorithm uses hypermutation. In hypermutation, the number of mutation points varies inversely proportional to the affinity of antibody. The number of mutation points is low when the affinity of the antibody is high and vice-versa. This is known as affinity maturation. The intent is to preserve the high affinity antibodies without much disturbing them, and to improve the affinity of antibodies which are not that good. The number of mutation points for reciprocal exchange of genes is given by equation (6).

$$M_p = 2 \times ((N_i + 1) - N_c) \quad (6)$$

Where  $M_p$  is the number of mutation points,  $N_c$  is the number of clones, and  $N_i$  is the maximum number of clones allowed which is 10 for this research. Fig. 9 shows a sample reciprocal exchange mutation process for the modified CSA.

### G. Stopping Criteria

The process iterates until the termination condition is reached; that is the antibody according to criterion chosen is

found or the desired number of iterations has been reached, which is chosen as 50 iterations for this research.

## VII. RESULTS AND DISCUSSION

This research compares the classification accuracy of the proposed Clonal Selection algorithms (CSA and MCSA) with standard backpropagation algorithm and swarm based algorithms namely Ant Colony Algorithm (ACO) and Particle Swarm Optimization (PSO). All algorithms find the appropriate sets of weights and biases for neural network of Fig. 5 for the correct data classification with respect to iris data. Fig. 10 shows the comparative performance of the five algorithms in terms of the accuracy of prediction of the three classes of the iris data, viz., Setosa, Versicolor and Virginica. All the five algorithms predict class 1 i.e. Setosa with an accuracy of 100% but not class 2 and 3. Fig. 11 shows the comparison of the classification accuracy of all the five algorithms. The accuracy obtained by the CSA is 96.67 and for the MCSA 99.333. Table IV gives the overall accuracy and accuracy for each class of the Iris flower for all the five algorithms. It establishes that modified Clonal Selection Algorithm is best at accurate data classification.

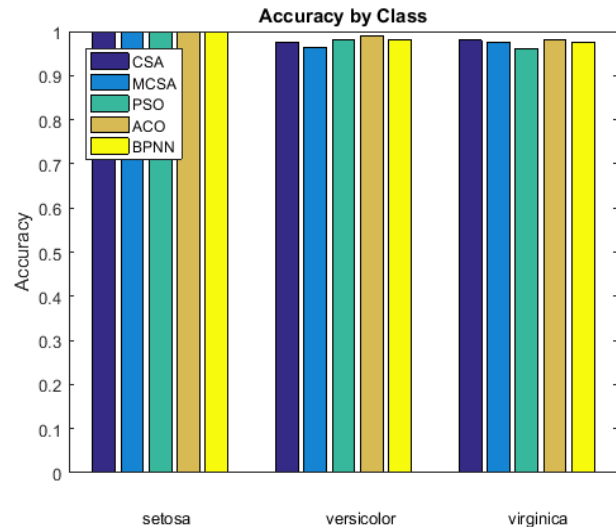


Fig. 10. Accuracy by Class.

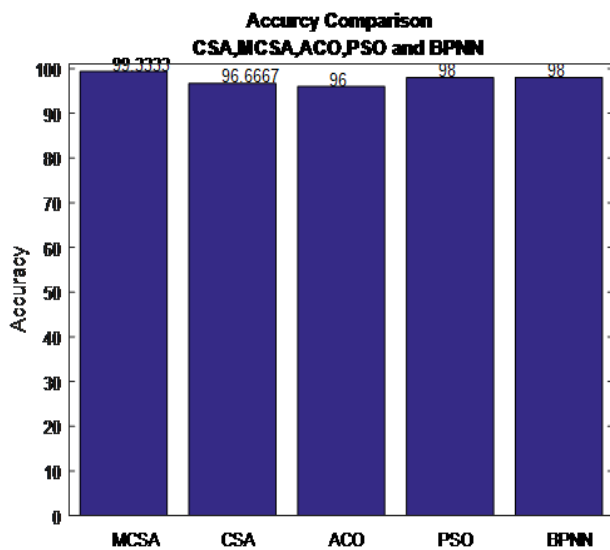


Fig. 11. Classification Accuracy for MCSA, CSA, ACO, PSO and BPNN.

TABLE IV. OVERALL ACCURACY AND ACCURACY OF EACH CLASS

|      | Accuracy | Accuracy by Class |         |         |
|------|----------|-------------------|---------|---------|
|      |          | Class 1           | Class 2 | Class 3 |
| BPNN | 98.00    | 1                 | 0.97    | 0.98    |
| ACO  | 96.00    | 1                 | 0.96    | 0.94    |
| PSO  | 98.00    | 1                 | 0.97    | 0.98    |
| CSA  | 96.67    | 1                 | 0.95    | 0.97    |
| MCSA | 99.33    | 1                 | 0.98    | 0.99    |

### VIII. CONCLUSION

In this paper, two neural-network training algorithms based on CSA and MCSA were proposed to optimize the weights and biases of the network for accurate Iris data classification. The algorithms will work for any dataset. However, the architecture of the neural network will have to be redesigned taking into consideration the dimensions of the data. The structure of antigen and anti-bodies will need to conform to match the architecture of neural network. The accuracy obtained by the CSA is 96.67% and for the MCSA 99.33. Thus, MCSA is a better performing algorithm.

#### REFERENCES

- [1] A. S. DeBruyne and Kaur, D. (2016) Harris's Hawk Multi-Objective Optimizer for Reference Point Problems, in Proceedings of the International Conference on Artificial Intelligence (ICAI), pp. 287.
- [2] Rumelhart, D.E., Hinton, G.E., and Williams, R.J. (1985), Learning internal representations by error propagation.
- [3] Bhandare, A.A. and Kaur, B.D. (2017) Comparative Analysis of Swarm Intelligence Techniques for Data Classification.
- [4] Elgert, K.D. (2009) Immunology: understanding the immune system, John Wiley & Sons.
- [5] Brownlee, J. (2011) Clever algorithms: nature-inspired programming recipes, Jason Brownlee.
- [6] J. D. Capra, C. A. Janeway, P. Travers, and M. Walport, Immunobiology: the immune system in health and disease. Garland Publishing, 1999.

- [7] C. A. Janeway, P. Travers, M. Walport, and M. J. Shlomchik, "Immunobiology: the immune system in health and disease," 2005.
- [8] L. N. De Castro, Fundamentals of natural computing: basic concepts, algorithms, and applications. Chapman and Hall/CRC, 2006.
- [9] Isha Muthreja and Devinder Kaur, "A Comparative Analysis of Immune System Inspired Algorithms for Traveling Salesman Problem" proceedings of the International Conference on Artificial Intelligence ICAI\_2018, World Congress in Computer Science, Computer Engineering and Applied Computing, ISBN: 1-60132-480-4, pp. 164-170, CSREA Press,
- [10] Z.-H. Hu, Y.-S. Ding, X.-K. Yu, W.-B. Zhang, and Q. Yan, "A hybrid neural network and immune algorithm approach for fit garment design," Textile Research Journal, vol. 79, no. 14, pp. 1319-1330, 2009.
- [11] J. Timmis, A. Hone, T. Stibor, and E. Clark, "Theoretical advances in artificial immune systems," Theoretical Computer Science, vol. 403, no. 1, pp. 11-32, 2008.
- [12] F. M. Burnet et al., "A modification of jerne's theory of antibody production using the concept of clonal selection.," Australian J. Sci., vol. 20, no. 3, pp. 67-9, 1957.
- [13] K. Rajewsky, "Clonal selection and learning in the antibody system," Nature, vol. 381, no. 6585, p. 751, 1996.
- [14] M. Cohn, N. A. Mitchison, W. E. Paul, A. M. Silverstein, D. W. Talmage, and M. Weigert, "Reflections on the clonal-selection theory," Nature Reviews Immunology, vol. 7, no. 10, p. 823, 2007.
- [15] L. N. De Castro and F. J. Von Zuben, "The clonal selection algorithm with engineering applications," in Proceedings of GECCO, vol. 2000, pp. 36-39, 2000.
- [16] E. Hart and J. Timmis, "Application areas of ais: The past, the present and the future," Applied soft computing, vol.8, no.1, pp. 191-201, 2008.
- [17] Y. Li, Z. H. Song, and L. Zhao, "Path planning for mobile robot with clonal selection algorithm," in Applied Mechanics and Materials, vol. 256, pp. 2943-2946, Trans Tech Publ, 2013.
- [18] K. Parthasarathy, "Clonal selection method for immunity-based intrusion detection system," Location: <http://web. umr. deu/tauritzd/courses/cs447/project/>, also available from SMG, 2003.
- [19] A. Y. HATATA, M. G. OSMAN, and M. M. ALADL, "A review of the clonal selection algorithm as an optimization method," Leonardo Journal of Sciences, vol. 16, no. 30, pp. 1-14, 2017.
- [20] X. Shui, X. Zuo, C. Chen, and A. E. Smith, "A clonal selection algorithm for urban bus vehicle scheduling," Applied Soft Computing, vol. 36, pp. 36-44, 2015.
- [21] D. Dheeru and E. Karra Taniskidou, "UCI machine learning repository," 2017.
- [22] D. Kaur and P. Nelapati, "Performance enhancement of data classification using selectively cloned genetic algorithm for neural network," International Journal of Computational Intelligence Systems, vol. 3, no. 6, pp. 723-732, 2010.
- [23] Al Bataineh, A., Kaur, D., & Jarrah, A. (2018, July). Enhancing the Parallelization of Backpropagation Neural Network Algorithm for Implementation on FPGA Platform. In NAECON 2018-IEEE National Aerospace and Electronics Conference (pp. 192-196). IEEE.
- [24] Al Bataineh, A., & Kaur, D. (2018, July). A Comparative Study of Different Curve Fitting Algorithms in Artificial Neural Network using Housing Dataset. In NAECON 2018-IEEE National Aerospace and Electronics Conference (pp. 174-178). IEEE.
- [25] Ali Al Bataineh, "A Comparative Analysis of Nonlinear Machine Learning Algorithms for Breast Cancer Detection," International Journal of Machine Learning and Computing vol. 9, no. 3, pp. 248-254, 2019.
- [26] S. Zhang, H. Wang, L. Liu, C. Du, and J. Lu, "Optimization of neural network based on genetic algorithm and bp," in Cloud Computing and Internet of Things (CCIOT), 2014 International Conference on, pp. 203-207, IEEE, 2014.
- [27] M. I. Velazco and C. Lyra, "Optimization with neural networks trained by evolutionary algorithms," in Neural Networks, 2002. IJCNN'02. Proceedings of the 2002 International Joint Conference on, vol. 2, pp. 1516-1521, IEEE, 2002.

# Predictive Method for Service Composition in Heterogeneous Environments within Client Requirements

Saleh M. Altowaijri<sup>1</sup>

Department of Information Systems  
Faculty of Computing and Information Technology  
Northern Border University, Rafha 91911, Kingdom of Saudi Arabia

**Abstract**—Cloud computing is a new delivery model for Information Technology services. Many actors and parameters play an important role in provisioning of dynamically elastic and virtualized resources at the levels of infrastructures, platforms, and softwares. Now-a-days, many cloud services are competing and present often similar offers. From the customer side, it is not always easy to select a suitable service according to customer requirements and cloud services scoring. In a real-world scenario, this is more complicated since service scoring may change over time. Besides this, it interferes with many parameters such as hardware, network infrastructure, customer demand, etc. To tackle this issue, this research work presents a novel approach for the prediction of the future score of any service in order to satisfy user requirements when executing service composition in cloud environments. This approach deals with regression techniques in order to predict the expected future offer of service based on sampling service's history as well as user expectations.

**Keywords**—Workflow; robust regression; prediction; cloud computing

## I. INTRODUCTION

The technological evolution of software applications has gone through different architectural styles starting from trivial single-station programs reaching distributed applications augmented with more and more complex structures. These applications are developed in a component-based architecture; the latter represents independent software structures that communicate through interfaces within the same application or through components for distributed applications.

In this context, when companies are accessible over external networks and the components of one are developed and/or used in others, the adoption of distributed workflow of software components becomes crucial [1]. However, this kind of solution, even though using distributed workflows, relies on layers of proprietary infrastructure marked with a strong and sustainable link between offered functionalities and customers. It is noted that built applications based on this approach have become mostly obsolete.

The component-based architecture, in its earlier versions, was incompatible with the openness of the Internet infrastructure. This situation has become more complicated when combined with the globalization of the use of Internet. In

fact, the distributed workflow should integrate more component-based applications, web services (seen as heterogeneous components) developed and published by different providers [2].

Now-a-days, web services are marked with a continuous growth in term of offers (provided services) and demands (requested services). Thus, the adoption of a reference architecture allowing the information exchange organization between service clients and service providers becomes a necessity. As result, it is essential to model any distributed workflow by an arrangement of executable offered services. In this case, the arrangement is represented by a four-step web process: development, publication, composition and execution [1]. In this specific context, the composition phase has a highly important role.

The field of services have still been the subject of many researches including, among others, the study and use of the service's concept [3], [4] (composition, orchestration, selection of services, semantic service composition) and service oriented architectures (SOA) (service oriented application design methods, distributed execution control mechanisms, quality of offered services and the security of services, etc. [5]). Particularly, the formulation of user needs is among the most controversial research topics [6], [7], [8]. In fact, a major importance has been given to users, service clients, who are struggling to formalize their increasingly complex needs in an unambiguous way. Faced with the complexity of needs, adopting a basic and composite formal representation will allow customers to capture their specification in a better and more accurate fashion. Thus, it is requested that service composition migrates to variable and dynamic process geared towards meeting client's goals/intentions. This is more accentuated in heterogeneous execution environments such as Cloud Computing [9].

Faced with the heterogeneity of environments, it becomes necessary to seek as much information as possible in order to succeed in modeling the future behavior of these environments. This will help in predicting client satisfaction and therefore selecting more eligible services. In this context, this paper proposes a predictive approach for selecting the adequate schedule of service composition based on customer requirements as well as providers offers that vary over time.



In this paper, the interest is to focus on satisfying customer intentions and demands over an SOA architecture and more particularly when it comes to composite services running on heterogeneous platforms, such as Cloud Computing environments. Therefore, the objective here attempts to answer the following questions: How to customize the selection of the adequate service composition in order to predict, anticipate and look ahead to any possible change in the environments' characteristics?

This paper is organized as follows. The next section presents the concept of service composition. Section 3 presents the regression-based models focusing mainly on the linear and ridge regressions. In Section 4, the approach to predict the suitable service composition over time matching customer requirements is presented. The obtained results are presented and discussed in Section 5. Finally, Section 6 presents the conclusions and future work of the paper.

## II. ABOUT SERVICE COMPOSITION MODELS

Several models are used to represent service compositions, such as state/transition diagrams [10], activity diagrams and Petri nets [11] or automata [12]. Most of the current works focus primarily on the expression of services through the features they offer. On the other hand, the expression of services in terms that are understandable by the end-user or customers, and even more by a manager, remains an unresolved problem. In this paper, it is believed that the existing formalisms based on activities, states and automata are not the most suitable to capture pertinent information to client. The problem is therefore to find the right matching between software services offered by providers and the requirement of customers.

In this same context, it is noticed that the description of services is essentially captured by some characteristics (networks, hardware and software) generally related to the quality of services required by the client [1] and other scoring measurements. Quality of Service (QoS) defines the ability of services to communicate with external systems in a satisfactory manner.

Several works have focused exclusively on QoS at the network characteristics level [13], [14] while others have focused exclusively on the description of executable services [2, 1]. Therefore, it is important to consider the QoS associated with all the means involved to meet the expectations of the customer.

The objective is to assign the most appropriate service offer to the client. Moreover, ordinary composition models are service-oriented and neglect the role of the environment as well as the customer requirements. From a practical perspective, the service offers may vary over time. In order to ensure a better QoS in terms of satisfying users' intentions and requirements, it is desirable that the system should be able to predict this variation over time. "Predictions", also known as "estimations" or "forecasts", consist in proposing to score a variable in the future, according to a tolerable margin of error, and based on the previous experience of this same variable [15]. There are a few studies [13] focused on the modeling of the composition by integrating the prediction.

The main objective of this paper is to consider the notion of QoS estimation and thereby predict the degree of customer satisfaction based on sampling measurements of the previous experience. It is believed that, such problem has not been resolved in previous research work related to service composition and/or prediction techniques.

## III. REGRESSION-BASED METHODS

In statistics, a classical problem is to process data modelled by a series of observations  $x_1, x_2, \dots, x_n$  corresponding to the realization of some random variables  $X_1, X_2, \dots, X_n$ . And, it is interesting to find a theoretical distribution of the vector  $(X_k)_{1 \leq k \leq n}$  reflecting the properties of the observations  $(x_k)_{1 \leq k \leq n}$ .

Concretely, the  $x_k$  values are well known. For example, the value of  $x_k$  may reflect the lifespan of a car engine numbered k. Knowing the law underlying an engine lifespan helps the manufacturer to improve the manufacture of engines. It is possible to estimate some indicators related to  $x_k$ , such as the average life of an engine which would be a typical estimation problem with confidence intervals. Then it is important to investigate the validity of the estimation in a context of a test problem. There are several methods for estimating data. In what follows, some of these methods are presented focusing particularly on the regression problems. The general purpose of the regression is to best explain a variable y (the response) as a function of other variables x (vector of explanatory variables, or regressors, or factors).

### A. Simple Linear Regression

The data are presented by n pairs of observations; they are in the form of Table I.

If the estimation of the relationship between the two variables y and  $x_1$  is linear, this implies that the variation of one variable is proportional to the other. By considering that one variable explains the other variable, their relation can be put in the form of a linear model:  $y_i = \beta_0 + \beta_1 x_{1i} + u_i$ ,  $1 \leq i \leq n$  with  $u_i$  an error term,  $\beta_0$  and  $\beta_1$  some constants; in particular  $\beta_1$  represents the increase of y by response to a unit increase of  $x_1$ .

Generally,  $\beta_0$  and  $\beta_1$  are estimated by the "least squares" method which consists in making minimum the sum of the squares of the error terms:

$$S(\beta_0, \beta_1) = \sum_{i=1}^n u_i^2 = \sum_{i=1}^n (y_i - \beta_0 - \beta_1 x_{1i})^2$$

TABLE I. SIMPLE LINEAR REGRESSION : PRESENTATION OF THE DATA WITH 2 VARIABLES

| observation number | y     | $x_1$    |
|--------------------|-------|----------|
| 1                  | $y_1$ | $x_{11}$ |
| 2                  | $y_2$ | $x_{12}$ |
| 3                  | $y_3$ | $x_{13}$ |
|                    |       |          |
|                    |       |          |
| n                  | $y_n$ | $x_{1n}$ |

TABLE II. MULTIPLE LINEAR REGRESSION : P-VARIABLE BASED DATA

| observation number | y              | x <sub>1</sub>  | x <sub>2</sub>  |  | x <sub>p</sub>  |
|--------------------|----------------|-----------------|-----------------|--|-----------------|
| 1                  | y <sub>1</sub> | x <sub>11</sub> | x <sub>21</sub> |  | x <sub>p1</sub> |
| 2                  | y <sub>2</sub> | x <sub>12</sub> | x <sub>22</sub> |  | x <sub>p2</sub> |
| 3                  | y <sub>3</sub> | x <sub>13</sub> | x <sub>23</sub> |  | x <sub>p3</sub> |
| n                  | y <sub>n</sub> | x <sub>1n</sub> | x <sub>2n</sub> |  | x <sub>pn</sub> |

B. Multiple Linear Regression

Multiple linear regression extends the previously single x<sub>1</sub> regressor by p regressors denoted x<sub>1</sub>, x<sub>2</sub>, ..., x<sub>p</sub>. The data are in the form of n sets of observations of the dependent variable y and p regressors; this set is shown schematically in Table II:

The regression between y and x<sub>1</sub>, x<sub>2</sub>, ..., x<sub>p</sub> is written as follows:

$$y_i = \beta_0 + \beta_1 x_{1i} + \beta_2 x_{2i} + \dots + \beta_p x_{pi} + u_i, \quad 1 \leq i \leq n$$

The constants  $\beta_0, \beta_1, \dots, \beta_p$  are called the partial regression coefficients of the model. The least squares method is used to minimize the sum of squares of residues:

$$S(\beta_0, \beta_1, \dots, \beta_p) = \sum_{i=1}^n u_i^2$$

$$= \sum_{i=1}^n (y_i - \beta_0 - \beta_1 x_{1i} - \beta_2 x_{2i} - \dots - \beta_p x_{pi})^2$$

C. Ridge Regression

In statistics, nonlinear regression is a form of regression in which the observation data is modeled by a nonlinear combination of model parameters and depends on one or more independent variables. The data are adjusted by a method of successive approximations. In what follows one important nonlinear regression method is presented: Ridge regression.

Ridge Regression is a variant of Multiple Linear Regression that aims to overcome the obstacle of collinearity between explanatory variables. It achieves this result by renouncing the Least Squares method for estimating model parameters. In doing so, it introduces a bias on the parameter estimates. This slight disadvantage is covered by the reduction of parameter variance, and even by the reduction of their Mean Quadratic Error (MQE). This is an illustration of the fact that a biased but low variance estimator may be more efficient than an unbiased but high variance estimator. Ridge regression imposes a penalty on the size of the coefficients of  $\beta_i$ . Indeed, the  $\beta_i$  are taking large values inducing a large variance. By limiting the size of the coefficients, it is estimated to gain in terms of prediction error. For this purpose, the ridge regression minimizes the sum of the residual squares to which is added a term dependent on the norm of the coefficient vector:

$$\hat{\beta}^{ridge} = \arg \min_{\beta \in R^{p+1}} \{RSS(\beta) + \lambda \|\beta_i\|_2^2\}, \quad RSS(\beta) = \|\mathbf{y} - \mathbf{1}_n \beta_0 - \mathbf{X}\beta\|_2^2$$

Theorem: [15] suppose that X is centered and reduced. The  $\hat{\beta}^{ridge}$  solution of the problem is given by:

$$\hat{\beta}^{ridge}_i = S_\lambda^{-1} X^T \tilde{y}, \quad \hat{\beta}^{ridge}_0 = \underline{y} = \frac{1}{n} \sum_{i=1}^n y_i$$

where

$$S_\lambda = X^T X + \lambda I_p \text{ and } \tilde{y} \triangleq y - \underline{y} \mathbf{1}_n$$

D. Gradient Boosting

Gradient boosting is a machine learning technique that consists in aggregating classifiers (called weak prediction models typically based on decision trees) developed sequentially on a learning sample whose weights of individuals are corrected progressively. Classifiers are weighted according to their performance.

IV. PREDICTIVE APPROACH FOR SERVICE COMPOSITION

The following functions/notations are proposed

- **c(b,p)** is the preferred/required value by the customer for the characteristic **p** satisfying a requirement **b**
- **m(b,p,i,t)** the measurement of the characteristic **p** satisfying a requirement **b** offered by the supplier **i** at the instant **t**

The main idea of our approach is summarized in Fig. 1.

As shown above, gathered information can be divided into two groups of data:

- Static data which are described by the customer requirements. these requirements are defined by c(b,p) and naturally maintain the same value for a long period of time.
- Dynamic data which corresponds to measurements given by m(b,p,i,t) at a certain sampling rate. if it is considered that the current measurement of m is captured at t<sub>0</sub>, then the previous measurements are considered at t<sub>0-1</sub>, t<sub>0-2</sub>, t<sub>0-3</sub>, etc. while the future measurements are considered at t<sub>0+1</sub>, t<sub>0+2</sub>, t<sub>0+3</sub>, etc.

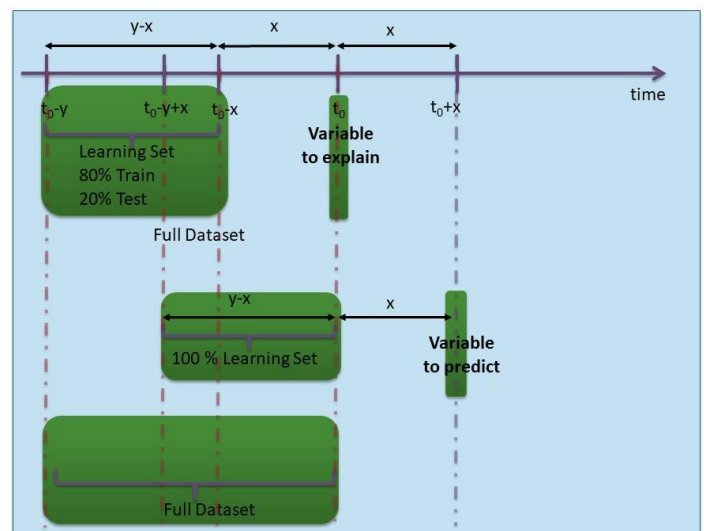


Fig. 1. Two Passes Regression Approach for Service Quality Prediction.

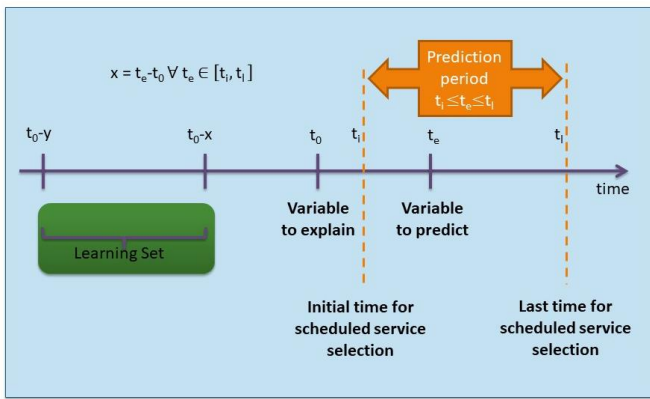


Fig. 2. Adaptation of the Prediction Model to a Scheduled Service Selection.

To seek accurate prediction results,  $t_0$  is estimated by considering for example dynamic data in the instants  $t_{0-10}, t_{0-9}, t_{0-8}, t_{0-7}, t_{0-6}, t_{0-5}, t_{0-4}$  in the learning phase. This phase will ensure that the model will learn based on last measurements of the service offer and considering the customer expectations. In the prediction phase, the model will be feed by some shifted measurements; say for example, the instants  $t_{0-6}, t_{0-5}, t_{0-4}, t_{0-3}, t_{0-2}, t_{0-1}, t_0$  to predict  $t_{0+3}$ . This concept is summarized in Fig. 2. It is noticed that the size of the window is decided by the expert depending on the available data and their variance in time.

The prediction adopting this approach is estimated to be more accurate and meet with client requirement. This is especially true if an efficient regression method is used to predict the future variable. The next section presents the results of the implementation of this approach.

### V. RESULTS AND INTERPRETATION

Data is considered as presented in Table X. Two phases are distinguished. The learning phase deals with  $c, t_{0-10}, t_{0-09}, t_{0-08}, t_{0-07}, t_{0-06}, t_{0-05}, t_{0-04}$  variables, in order to predict  $t_0$ . Data is split into 80% for learning and the remaining 20% for testing the accuracy of the results.

In the prediction phase, the model is fitted by  $c, t_{0-06}, t_{0-05}, t_{0-04}, t_{0-03}, t_{0-02}, t_{0-01}$  and  $t_0$  in order to predict  $t_{0+3}$  as illustrated in Table III.

Our approach is implemented using python 3.7.3 and the development environment Spyder 3.3.3. The library sklearn is mainly used for implementing the regressors models. In what follows the curves with square lines of the training variables to explain  $t_0$  are illustrated in Fig. 3, 4, 5 and 6.

Mainly, three different regression methods are applied: Gradient boost, Ridge and Linear.

The following indicators to measure the accuracy of the predicted results are used.

- Mean Absolute Error (MAE)

$$MAE = \frac{1}{n} \sum |y - \hat{y}|$$

- Mean Absolute Percentage Error (MAPE)

$$MAPE = \frac{100\%}{n} \sum \left| \frac{y - \hat{y}}{y} \right|$$

- Mean Percentage Error (MPE)

$$MPE = \frac{100\%}{n} \sum \left( \frac{y - \hat{y}}{y} \right)$$

- Mean Squared Error (MSE)

$$MSE = \frac{1}{n} \sum (y - \hat{y})^2$$

- Root Mean Squared Error (RMSE)

$$RMSE = \sqrt{\frac{1}{n} \sum (y - \hat{y})^2}$$

TABLE III. PREDICTION VARIABLES AND PHASES

|                     |            | Comment             |                     |
|---------------------|------------|---------------------|---------------------|
| Variables           |            | Training phase      | Prediction phase    |
| $c(b,p)$            | $c$        | regressor variables | regressor variable  |
| $m(b,p,i,t_{0-10})$ | $t_{0-10}$ |                     | X                   |
| $m(b,p,i,t_{0-09})$ | $t_{0-09}$ |                     | X                   |
| $m(b,p,i,t_{0-08})$ | $t_{0-08}$ |                     | X                   |
| $m(b,p,i,t_{0-07})$ | $t_{0-07}$ |                     | X                   |
| $m(b,p,i,t_{0-06})$ | $t_{0-06}$ |                     | regressor variables |
| $m(b,p,i,t_{0-05})$ | $t_{0-05}$ |                     |                     |
| $m(b,p,i,t_{0-04})$ | $t_{0-04}$ |                     |                     |
| $m(b,p,i,t_{0-03})$ | $t_{0-03}$ |                     |                     |
| $m(b,p,i,t_{0-02})$ | $t_{0-02}$ |                     | X                   |
| $m(b,p,i,t_{0-01})$ | $t_{0-01}$ | X                   |                     |
| $m(b,p,i,t_0)$      | $t_0$      | predicted variable  |                     |
| $m(b,p,i,t_{0+3})$  | $t_{0+3}$  |                     | predicted variable  |

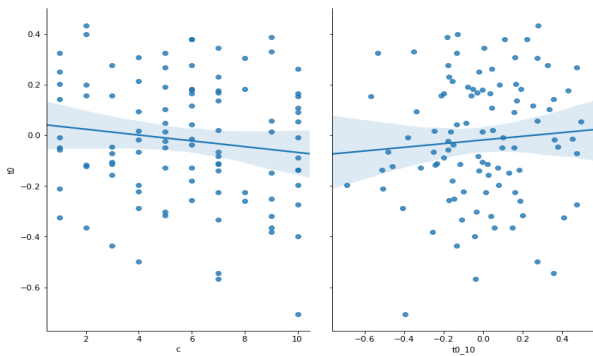


Fig. 3.  $t_0$  Explained by  $c$  and  $t_{0_{10}}$ .

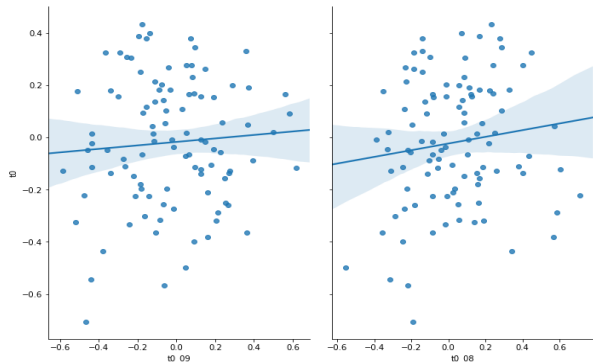


Fig. 4.  $t_0$  Explained by  $t_{0_{09}}$  and  $t_{0_{08}}$ .

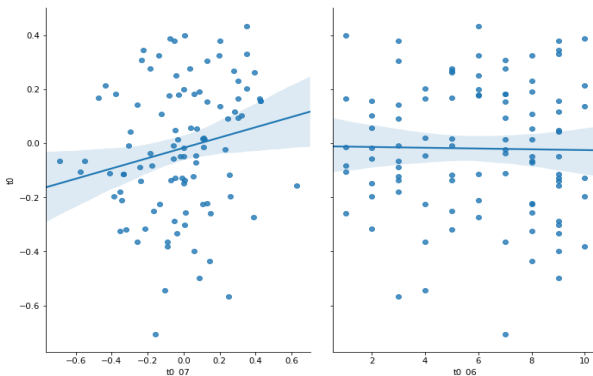


Fig. 5.  $t_0$  Explained by  $t_{0_{07}}$  and  $t_{0_{06}}$ .

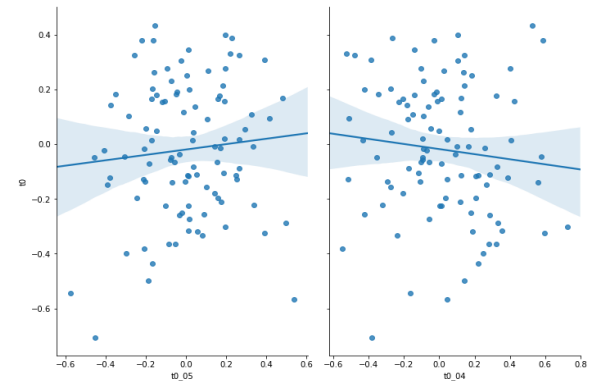


Fig. 6.  $t_0$  Explained by  $t_{0_{05}}$  and  $t_{0_{04}}$ .

### A. Linear Regression

In what follows, Table IV summarizes the related error indicators.

TABLE IV. GRADIENT BOOSTING REGRESSOR PERFORMANCE

|             |               |
|-------------|---------------|
| <b>MAE</b>  | 0.2523649668  |
| <b>MAPE</b> | 2.7418724410  |
| <b>MPE</b>  | -0.0067128932 |
| <b>MSE</b>  | 0.0937286533  |
| <b>RMSE</b> | 0.3061513568  |

In what follows the curves are illustrated in Fig. 7, 8, 9 and 10 to explain  $t_{0+3}$  with the different data variables.

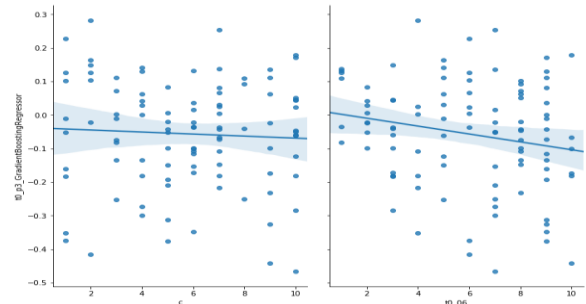


Fig. 7.  $t_{0+3}$  (Predicted by Gradient Boost Regressor) Explained by  $c$  and  $t_{0_{06}}$ .

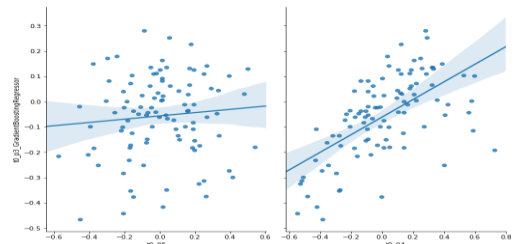


Fig. 8.  $t_{0+3}$  (Predicted by Gradient Boost Regressor) Explained by  $t_{0_{05}}$  and  $t_{0_{04}}$ .

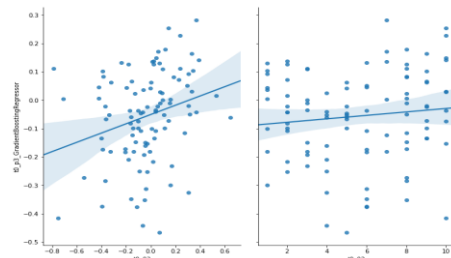


Fig. 9.  $t_{0+3}$  (Predicted by Gradient Boost Regressor) Explained by  $t_{0_{03}}$  and  $t_{0_{02}}$ .

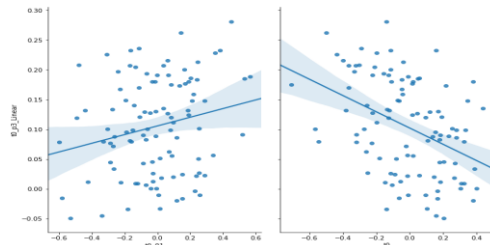


Fig. 10.  $t_{0+3}$  (Predicted by Gradient Boost Regressor) Explained by  $t_{0_{01}}$  and  $t_0$ .

**B. Ridge Regression**

The related error indicators are summarized in Table V.

TABLE V. RIDGE REGRESSION PERFORMANCE MEASUREMENTS

|             |              |
|-------------|--------------|
| <b>MAE</b>  | 0.2178260161 |
| <b>MAPE</b> | 1.1485854694 |
| <b>MPE</b>  | 0.5720847218 |
| <b>MSE</b>  | 0.0713895360 |
| <b>RMSE</b> | 0.2671882034 |

In what follows, the curves with square lines of the training variables are illustrated in Fig. 11, 12, 13 and 14 to explain  $t_{0+3}$  with the different data variables.

**C. Linear Regression**

In Table VI, the related error indicators are summarized.

TABLE VI. LINEAR REGRESSION PERFORMANCE MEASUREMENTS

|             |              |
|-------------|--------------|
| <b>MAE</b>  | 0.2149517136 |
| <b>MAPE</b> | 1.1767757992 |
| <b>MPE</b>  | 0.5045521139 |
| <b>MSE</b>  | 0.0698653593 |
| <b>RMSE</b> | 0.2643205617 |

The following figures illustrate the curves with square lines of the training variables in Fig. 15, 16, 17 and 18 to explain  $t_{0+3}$  with the different data variables.

Table VII illustrates a resume of the error estimator for the three applied regression methods.

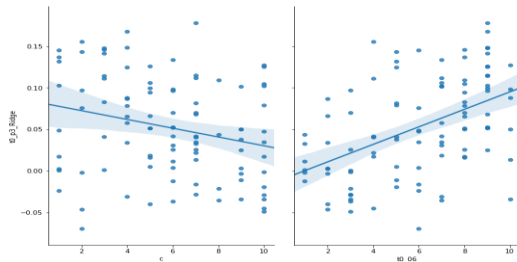


Fig. 11.  $t_{0+3}$  (Predicted by Ridge Regression) Explained by  $c$  and  $t_{0.06}$ .

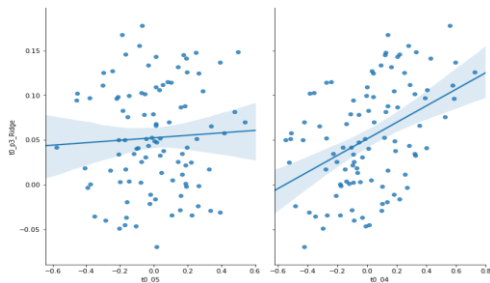


Fig. 12.  $t_{0+3}$  (Predicted by Ridge Regression) Explained by  $t_{0.05}$  and  $t_{0.04}$ .

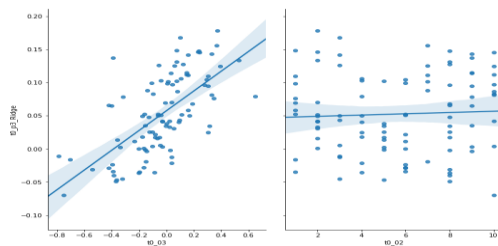


Fig. 13.  $t_{0+3}$  (Predicted By Ridge Regression) Explained by  $t_{0.03}$  and  $t_{0.02}$ .

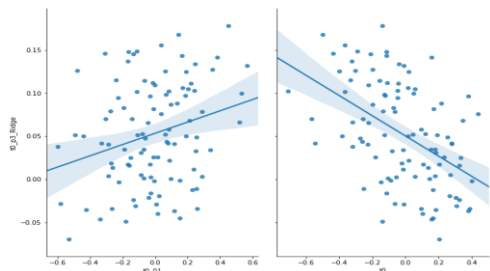


Fig. 14.  $t_{0+3}$  (Predicted by Ridge Regression) Explained by  $t_{0.01}$  and  $t_0$ .

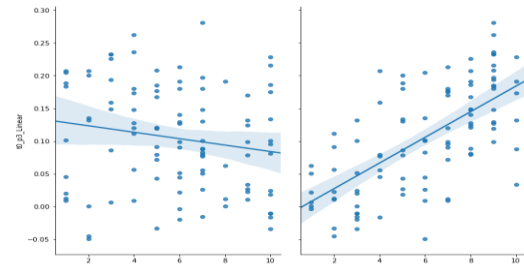


Fig. 15.  $t_{0+3}$  (Predicted by Linear Regression) Explained by  $c$  and  $t_{0.07}$ .

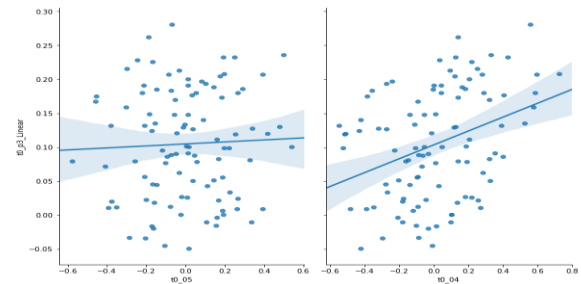


Fig. 16.  $t_{0+3}$  (Predicted by Linear Regression) Explained by  $t_{0.05}$  and  $t_{0.04}$ .

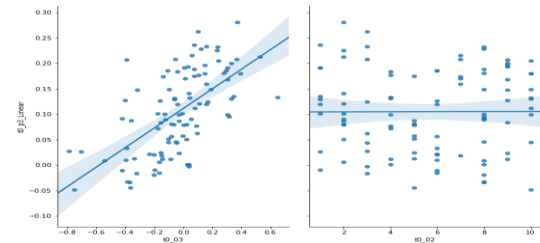


Fig. 17.  $t_{0+3}$  (Predicted by Linear Regression) Explained by  $t_{0.03}$  and  $t_{0.02}$ .

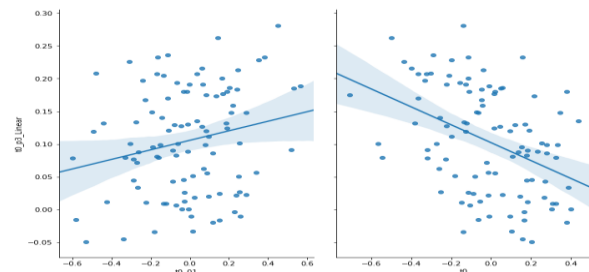


Fig. 18.  $t_{0+3}$  (Predicted by Linear Regression) Explained by  $t_{0.01}$  and  $t_0$ .

TABLE VII. PERFORMANCE MEASUREMENTS

|      | Gradient Boost | Ridge  | Linear |
|------|----------------|--------|--------|
| MAE  | 0.2524         | 0.2178 | 0.2150 |
| MAPE | 2.7419         | 1.1486 | 1.1768 |
| MPE  | -0.0067        | 0.5721 | 0.5046 |
| MSE  | 0.0937         | 0.0714 | 0.0699 |
| RMSE | 0.3062         | 0.2672 | 0.2643 |

In this particular context, the linear and ridge regression presented similar results. Mainly, the ridge regression present better results regarding noisy input data. Therefore, it is believed that ridge regression present in better results when some part of the data is missed or noisy.

## VI. CONCLUSION AND PERSPECTIVES

This paper focused on the composition of remote services required by a customer. One fundamental problem is how to select in each intermediate step the most adequate service according to the client requirements expressed in a numeric form. Besides, service offers are measured periodically in a form of global score since service behavior may change over time. However, the future score of a given service cannot be available before its actual measurement. This future score will help the client to select the most convenient service. Thus, a regressive predictive approach is proposed to predict the future score of a service based on the past measurements and the client experience. This approach differentiates between the data variables of the learning phase and the data variables of the prediction phase. A perspective of this work is to focus on the size of the widow related to learning and predicting phases in accordance with data variance over time. This will aim to decide about the most adequate size of data columns in learning phase to seek more accurate prediction results. Moreover, this will be enhanced by a real case-study result.

## ACKNOWLEDGMENT

The author gratefully acknowledges the approval and the support of this research from the Deanship of Scientific Research study by the grant no CIT-2018-3-9-F-7953, Northern Border University, Arar 91431, KSA.

## REFERENCES

[1] Gil, Y., Gonzalez-Calero, P. A., Kim, J., Moody, J., & Ratnakar, V. (2011). A semantic framework for automatic generation of computational workflows using distributed data and component catalogues. *Journal of Experimental & Theoretical Artificial Intelligence*, 23(4), 389-467.

[2] A. Alkamari. Composition de services web par appariement de signatures. Technical report, MONTRÉAL,, 2008.

[3] Kurniawan, K., Ekaputra, F. J., & Aryan, P. R. (2018, October). Semantic Service Description and Compositions: A Systematic Literature Review. In 2018 2nd International Conference on Informatics and Computational Sciences (ICICoS) (pp. 1-6). IEEE.

[4] Rao, J., & Su, X. (2004, July). A survey of automated web service composition methods. In *International Workshop on Semantic Web Services and Web Process Composition* (pp. 43-54). Springer, Berlin, Heidelberg.

[5] Chung, F. I., & Lo, C. L. (2018). Service-Oriented Architecture Application in Long-Term Care Institution: A Case Study on an Information System Project Based on the Whole Person Concept in Taiwan. *International Journal of Computing Sciences Research*, 1(3), 17-37.

[6] Amina Bourouis, Kais Klai, Nejib Ben Hadj-Alouane and Yamen El Touati "On the Verification of Opacity in Web Services and their Composition". *IEEE Transactions on Services Computing*, vol.PP, no.99, pp.1-1 doi: 10.1109/TSC.2016.2605090. <http://ieeexplore.ieee.org/document/7558131/>

[7] Mahmud, R., Kotagiri, R., & Buyya, R. (2018). Fog computing: A taxonomy, survey and future directions. In *Internet of everything* (pp. 103-130). Springer, Singapore.

[8] Messaoud, W. B., Ghedira, K., & Halima, Y. B. (2016). Towards behavioral web service discovery approach: State of the art. *Procedia Computer Science*, 96, 1049-1058.

[9] Ben Halima, Y., Jamoussi, Y., Ben Ghezala, H., & Tata, S. (2012, June). Prediction of cloud environment characteristics to satisfy user requirements in service compositions. In *Proceedings of the 2012 IEEE 21st International Workshop on Enabling Technologies: Infrastructure for Collaborative Enterprises* (pp. 84-91). IEEE Computer Society.

[10] M. Mecella B. Pernici. Building flexible and cooperative applications based on eservices. Technical report, roma, italy, 2002.

[11] Ngu A. H. Benatallah B. M. Dumas, Q Z. Sheng. Declarative composition and peer topeer provisioning of dynamic web services. page 297 308, San Jose, California USA,, 2002. 18th international Conference on Data Engineering (ICDE 2002), IEEE Computer Society.

[12] M. Lenzerini M. Mecella Berardi D. D. Calvanese, G. De Giacomo. Automatic composition of e-eservices that export their behavior. Trento, Italy 2003. *Proceedings of the 1st International Conference on Service Oriented Computing (ICSOC'03)*,.

[13] Azween B Abdullah Mohamad Izuddin B Nordin and Mahamat Issa Hassan. Goal based cloud broker for medical informatics application : A proposed goal based request and selection strategy. Department of Computer and Information Sciences Universiti Teknologi PETRONAS Bandar Seri Iskandar, 31750 Tronoh, Perak, Malaysia, 2011 *International Conference on Telecommunication Technology and Applications Proc .of CSIT vol.5 (2011) (2011) IACSIT Press, Singapore, 2011*

[14] Niraj Tolia Gunho Lee. Topology aware resource allocation for data intensive workloads. *ACM 978.1.4503.0195*, 2010.

[15] Bernard Delyon. Régression. Technical report, 2019.5

# Spectral Classification of a Set of Hyperspectral Images using the Convolutional Neural Network, in a Single Training

Abdelali Zbakh<sup>1</sup>, Zoubida Alaoui Mdaghri<sup>2</sup>, Abdelillah Benyoussef<sup>3</sup>, Abdellah El Kenz<sup>4</sup>, Mourad El Yadari<sup>5</sup>  
Lab: LaMCSaI, University Mohammed V, Faculty of Sciences Rabat, Morocco<sup>1,2,3,4</sup>  
Moulay Ismail University of Meknes, Morocco<sup>5</sup>

**Abstract**—Hyperspectral imagery has seen a great evolution in recent years. Consequently, several fields (medical, agriculture, geosciences) need to make the automatic classification of these hyperspectral images with a high rate and in an acceptable time. The state-of-the-art presents several classification algorithms based on the Convolutional Neural Network (CNN) and each algorithm is training on a part of an image and then performs the prediction on the rest. This article proposes a new Fast Spectral classification algorithm based on CNN, and which allows to build a composite image from multiple hyperspectral images, then trains the model only once on the composite image. After training, the model can predict each image separately. To test the validity of the proposed algorithm, two free hyperspectral images are taken, and the training time obtained by the proposed model on the composite image is better than the time obtained from the model of the state-of-the-art.

**Keywords**—Classification; spectral; Convolutional Neural Network (CNN); deep learning; hyperspectral data; neural network

## I. INTRODUCTION

Remote sensing makes it possible to identify objects remotely, without physical or chemical contact. Among the most used applications are hyperspectral images (HSI) captured by satellites or aircrafts. The captured HSI are then used in different domains and for different purposes: Geology (Detection of oil, water, ...), Agricultural (presence of diseases in plants and knowledge of plant species in a particular area).

A classic RGB image is an image represented by three layers or bands: Red, Green, and Blue while the hyperspectral image is represented by hundreds of bands. A hyperspectral image is represented by a data cube of two spatial dimensions (X and Y) and a spectral dimension Z. Each pixel corresponds to a spectrum of wavelength, generally corresponding to the visible and near-infrared domains (400 to 2500nm).

Among the methods that allow users to make the data of the HSI usable, and to extract the maximum of useful information, there is the classification.

Classification is an operation that divides a set of individuals into several classes, and each class groups together individuals who share the same similarity. There are two families of classification algorithms: Unsupervised classification (USVC) and Supervised classification (SVC).

In the USVC, we have unclassified elements and unknown classes, and we try to group the elements that have a certain similarity between them to construct a set of classes.

In the SVC, the classes are known in advance and we have examples on each class and we try to assign new elements to these classes. Examples of SVC algorithms: Naïve Bayes [1], Support Vector Machine (SVM), Deep learning [2] (Convolutional Neural Network (CNN), Recurrent Neural Network (RNN), Long Short Term Memory (LSTM),)

In recent years, the domain of SVC and especially deep learning has undergone a great evolution. In addition, the classification of hyperspectral images by supervised algorithms [3], gave accuracy better than USVC algorithms.

This paper study a deep learning classification algorithm called convolutional neural network (CNN) to classify the content of a set of hyperspectral images using a single training. The classification object is to group in each class the pixels that have a certain similarity (common properties): water, vegetation, sand.

The rest of the paper is organized as follows: in Section 2, we will explain the classification by the convolutional neural network (CNN). In Section 3, we will describe our classification proposal. Section 4 contains the experimentation of the proposed model on several data sets. And we end in Section 5 with a conclusion and perspectives.

## II. CONVOLUTIONAL NEURAL NETWORK

This section describes the CNN [4], the most popular supervised deep learning network, and who has shown its power of extracting features in computer vision applications.

### A. CNN Standard Opérations

The convolutional neural network (CNN or ConvNet) is a particular and important type of neural network feed-forward (information spreads from layer to layer, without turning back possible). It is inspired by the biological processes that occur in the visual cortex in the brain of living beings. The CNN models are built on the same model as the multilayer perceptrons of which we find: an input layer, several intermediate hidden layers (depending on the depth of the model) and an output layer. CNN is used to solve several computer vision problems in artificial intelligence, for

example: Self driving cars, video processing, and image classification. The basic operations in a standard CNN network are:

- Convolution operation: The convolution operation is the basic operation in building a CNN network. It allows to slide, step by step, a window named kernel on the whole image, and for each step, we multiply the pixels of the kernel by the pixels of the region on which it slides. Then we take the sum of the result (see Fig. 1).
- Max-Pooling operation: The Max-pooling operation allows to slide, step by step, a window, generously of size 2x2, on the whole image, and takes at each step, the maximum value of the window. It is an optional operation in the design of the network, and in general, in classical CNN's architectures, it is put after each convolution operation, and which aims to reduce the number of samples or neurons. If the size of the window is large, we risk losing the information of the image (see Fig. 2).
- Activation Functions: These are correction functions, which play an important role in deep learning algorithms. The activation function takes in input an  $x$  value and returns the output  $f(x)$ . Activation functions are usually used after each convolution operation. The famous activations functions are: Identity ( $f(x)=x$ ), Binary Step ( $f(x)=0$  if  $x<0$ ; else  $f(x)=1$ ), Logistic or sigmoid ( $f(x)=\frac{1}{1+e^{-x}}$ ), Tanh ( $f(x)=\tanh(x)$ ) and Rectified Linear Unit (ReLU) ( $f(x)=0$  if  $x<0$ ; else  $f(x)=x$ ).
- Dropout: The dropout operation, allows to randomly disable outputs of some neurons with a definite probability (0.5 for example). And this to simulate the real functionality of neurons, which can in an iteration of the learning phase, be inactive. Stalling speeds up learning
- Fully connected (FC): After several Convolution and Max-Pooling operations, come these operations to connect all the neurons of the previous layer (whatever the type), with the neurons of the next layer. It is not necessary to have a number of FCs, but there are often two consecutive layers as final layers in the network.

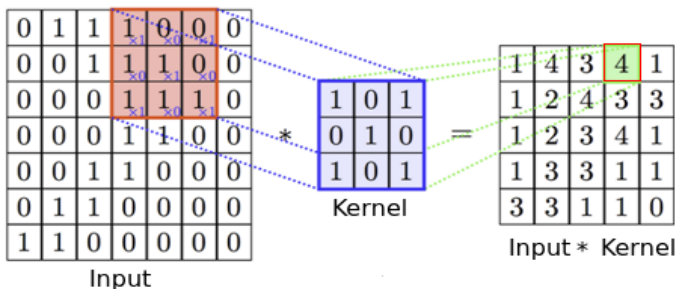


Fig. 1. Description of the Convolution Operation.

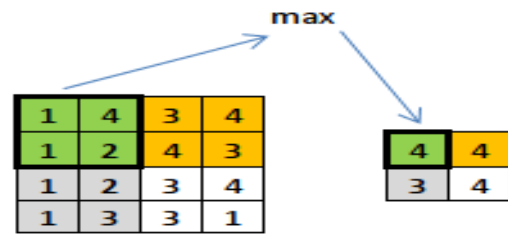


Fig. 2. Description of the Max-Pooling Operation.

### B. Related Work

The first CNN classification model named LeNet-5 [5] was proposed by LeCun et al in 1998 to classify hand-written numbers. The model is composed of 7 layers (without counting the input layer). Other models of classification are appeared and which contains variety of number of layers: AlexNet [6] in 2012 with 9 layers, ZFNet [6] in 2013 with 8 layers, GoogleNet [7] in 2014 with 22 layers, VGGNet [6] in 2014 with 19 layers and ResNet [6] in 2015 with up to 269 layers.

In the classification of HSI using CNN, we find: spectral classification models [11, 9], 2D spatial classification models [9], 3D spatial classification models [10, 9] and Hybrid models [9].

Most of these classification models deals with Overall Accuracy (OA) performance and these OA are almost equal. Some work has focused on the speed of learning, which is a crucial criterion for choosing a model when working on two models of close accuracy. Among these work, we can mention:

- In [11], the authors proposed a CNN classification algorithm based on the spectral characteristics of HSI, and which contains 5 layers. The results (Accuracy, Training Time and Testing Time) are compared with LeNet-5, DNN and RBF-SVM.
- In [12], the authors propose a model of classification CNN, which is based on two channels: the first channel 1D to extract the spectral characteristics and the second channel 2D to extract the spatial characteristics. The results of the two canals are combined by the Softmax classifier. The training time of the model is compared with other model of the state-of-the-art (SSDCNN [13], SSDL [14]).
- In [3], the authors propose a 3D classification model of 5 layers, which uses at the same time the spectral and spatial characteristics of the image. The model is implemented using graphics processing units (GPUs) [9]. The results (Accuracy and training time) are compared with the classic MLP model and a CNN model of the state-of-the-art.

### III. ARCHITECTURE OF THE PROPOSED MODEL

The classification algorithms of the hyperspectral images of the state-of-the-art [12-15-16], function according to the following principle:



Objective: classify the pixels of a hyperspectral image X, according to a certain number of class denoted C.

- Step 1: Divide the image X into two groups of data: X\_train, to train the model and X\_test to validate the model. Then create a classification model based on the parameters of image X (number of rows, number of columns and the number of spectral bands).
- Step 2: Train the created model on the X\_train data, and record the time taken in this step denoted t\_train.
- Step 3: Test the validity of the created model on X\_test data.
- Step 4: Make the classification of the whole image X with the created model, and record the time spent in this step denoted t\_pred. We note that training time is much greater than the prediction time.
- Step 5: Visualize the result.

Although this classification principle is used in almost all CNN based HSI classification algorithms, it has several flaws: among which, if we want to classify two new images Y and Z, we must repeat the same steps from 1 to 5 for the image Y and also for the image Z.

This classical method of classification takes a lot of time [10, 15], caused by the repetition of the training step for each image, and especially when working with a large number of images.

In this paper, we will propose an algorithm for spectral classifying an image hyperspectral composed of several HSI, based on the CNN, and using a single training.

The proposed classification algorithm proceeds as follows:

Objective: Classify the pixels of a hyperspectral image X1 according to a certain number of classes denoted C1.

- Step 1: Take k hyperspectral images of different sizes: X1 (H1, W1, N1, C1), X2 (H2, W2, N2, C2),...,Xk (Hk, Wk, Nk, Ck), with Hi, Wi, Ni, Ci represents the height, the width, the number of spectral bands, and the number of classes for the image i (respectively).
- Step 2: Choose the minimum number of bands between the k images:  $N = \min (N1, N2, \dots, Nk)$ .
- Step 3: Apply the dimensionality reduction algorithm PCA, on each image i that has a number of bands  $Ni > N$
- Step 4: Vertically, concatenate the images obtained, to have a single image X of the following characteristics:
  - the number of pixels:  $m = \sum_{i=1}^k (Hi \cdot Wi)$
  - the number of bands :  $N = \min (N1, N2, \dots, Nk)$
  - the number of classes:  $C = \sum_{i=1}^k (Ci)$
- Step 5: Divide the image X into two groups of data: X\_train for the training and X\_test for validating the prediction. Then create a spectral classification model based on the parameters of image X.

- Step 6: Train the created model on the X\_train data, and we note the time taken in this step denoted t\_train.
- Step 7: Test the validity of the created model on on X\_test data.
- Step 8: Now, we can use the trained model to make the prediction on each image Xi: X1, X2,..., Xk separately, and we note the time in this step, denoted t\_pred.
- Step 9: Visualize the classified image Xi.

#### A. Dimensionality reduction with PCA

The first step of the proposed algorithm is to take images of different sizes, each image Xi of size (Hi, Wi, Ni), will be converted towards the matrix format noted Mi, of size (number of lines Li = Hi x Wi and number of columns Ni). Each column j ( $1 \leq j \leq Ni$ ) of the matrix Mi contains the pixels of the image Xi for the wavelength j and each line k ( $1 \leq k \leq Li$ ) of the image Mi represents the values of a pixel k of Xi for all the wavelengths (see Fig. 3).

In step 2 and 3, we calculate the minimum of bands between the hyperspectral images that we will use:  $N = \min (N1, N2, \dots, Nk)$ , with k the number of images. The PCA reduction algorithm [17] is then applied to each image Mi, and the reduced images are concatenated to obtain the image M. For example, in Fig. 4, there is an illustration of the algorithm on k = 2 images: Pavia University and Salinas.

In the next part, we will propose a CNN spectral classification algorithm, inspired by paper [11] and which will be used for the classification of separate images (like the state-of-the-art) and also to test the proposed algorithm.

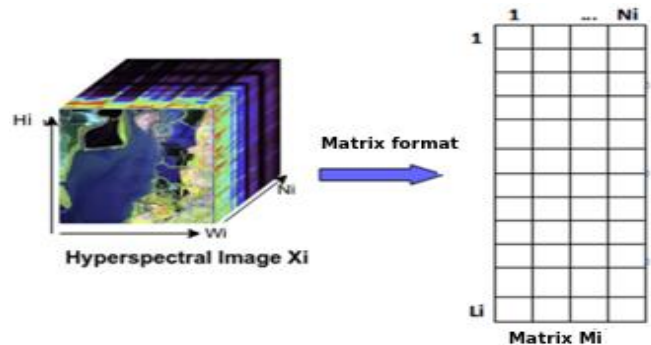


Fig. 3. Matrix Representation of the Hyperspectral Image Xi.

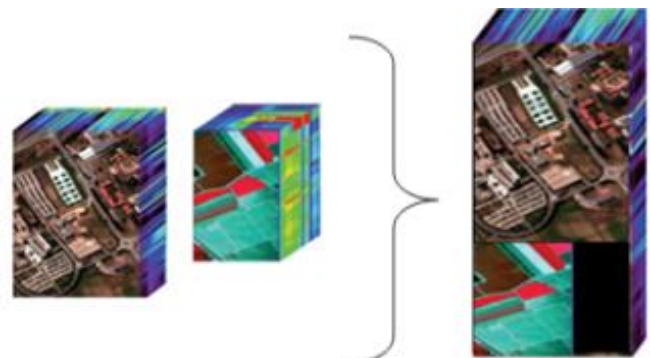


Fig. 4. Reducing the Dimensionality of Images and Concatenation to Obtain a Single Image M.

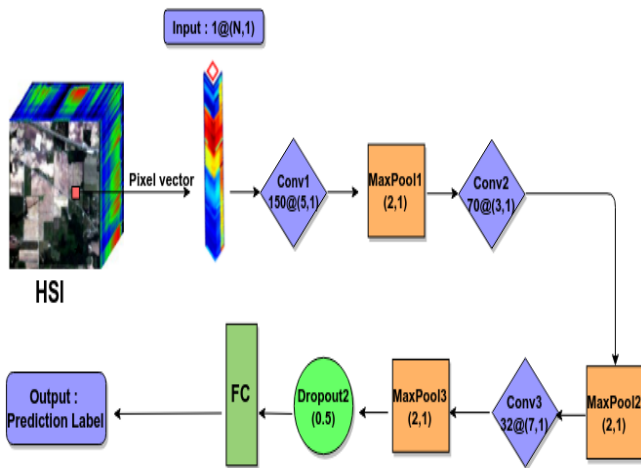


Fig. 5. Architecture of the Proposed CNN Classification Model.

### B. Classification with the Spectral CNN

To classify the pixels of an HSI, we will propose a model composed of 10 layers: Input layer, 3 convolution layers, 3 Max-Pooling layers, a Dropout layer, a Fully Connected Layer and Output layer, with the following configuration (see Fig. 5).

The model takes as input a pixel vector of size N (number of bands), we apply on the pixel vector, various operations: convolution, Max-Pooling, Dropout and Fully Connected Layer according to the following parameters (Table I).

TABLE I. PARAMETERS OF THE PROPOSED MODEL

|                   | Conv1      | Conv2      | Conv3      |
|-------------------|------------|------------|------------|
| Number of filters | 150        | 70         | 32         |
| Kernel size       | 5 x 1      | 3 x 1      | 7 x 1      |
|                   | Max-Pool 1 | Max-Pool 2 | Max-Pool 3 |
| Kernel size       | 2 x 1      | 2 x 1      | 2 x 1      |

## IV. EXPERIMENTAL AND COMPUTATIONAL DETAILS

### A. DataSets

To classify the hyperspectral images using the proposed algorithm, we used two free datasets: Pavia University, and Salinas. For the two datasets, we took 70% pixels for training the model and 30% to test the classification model.

Pavia data: There are two types of Pavia data: Pavia Center and Pavia University. In this experiment, we use the corrected Pavia University [8], which depicts the scene of Pavia, northern Italy captured by the ROSIS (Reflective Optics System Imaging Spectrometer) sensor in 2001. The scene has a spatial dimension of 610 x 340 pixels with 103 bands of spectral reflectance in the wave range 0.43 to 0.86  $\mu\text{m}$ . The scene contains 9 classes.

Salinas scene: The second dataset [8], is captured by the AVIRIS sensor on the Salinas-California valley, we find in this scene 512 x 217 pixels with 224 bands and which contains 16 classes. In this scene, 20 bands were deleted: (108-112; 154-167; 224) which represent water absorption bands.

### B. Details and Results

First, we will begin by applying the proposed classification model on the two images and we note for each image, the accuracy (OA) and the time done in the training phase. Then we will build a single image from the 2 datasets as described in Section 3. And we will apply the classification model on this composite image, and note the accuracy and the training time.

Experiments are performed on a computer equipped with an Intel® Core™ processor i7-2820QM CPU @ 2.30GHz x 8, 16 GB Ram. The classification model is implemented in Python language using the deep learning library named: Keras. The following table (Table II) contains the values of the experiment:

From the paper [11], we took the accuracy (OA) and the training time of the model on the two images: PaviaU and Salinas. Then, two values were calculated: the average accuracy (OA\_avg), and the total training time (T) of the model on the two images:

- $T = \text{Training time(PaviaU)} + \text{Training time (Salinas)}$
- $OA\_avg = (\text{OA(PaviaU)} + \text{OA(Salinas)}) / 2$

To test the efficiency and the speed of the proposed model, we made two experimentations: First, we trained the proposed model until obtaining the accuracy of the paper [11], and we noted the training time performed on each image: PaviaU and Salinas. The total training time obtained on the two images of the proposed model (695.82 s) is much smaller than the total time taken for training the model of paper [11] (3600 s). Secondly, we trained our model until we obtained the training time of paper [11], and we noted the accuracy on each image: PaviaU and Salinas. The average accuracy of the proposed model (94.71%) is better than the average accuracy of the paper [11] (92.58%).

We note that the proposed algorithm, in comparison with the algorithm of paper [11], gives a better accuracy on the two images, in a less time of training. The following graph (see Fig. 6), gives the evolution of the accuracy, as a function of training time for the proposed algorithm.

Since, the proposed model is competitive with the state-of-the-art classification model; we will use it to validate our approach to classify one image composed of several images, using a single training. Table III contains the accuracy value, the training time of the proposed algorithm on a single composite image and the OA\_avg, the total of training time when the model was applied to the separate images

TABLE II. EXPERIMENTATION OF THE PROPOSED MODEL ON SEVERAL IMAGES

|                    | Pavia U     |               | Salinas      |               | OA_avg (%)   | T (s)         |
|--------------------|-------------|---------------|--------------|---------------|--------------|---------------|
|                    | OA (%)      | Time (s)      | OA (%)       | Time (s)      |              |               |
| [11]               | 92.56       | 420           | 92.60        | 3180          | 92.58        | 3600          |
| Proposed model (1) | 92.59       | <b>117.34</b> | 92.8         | <b>578.48</b> | 92.69        | <b>695.82</b> |
| Proposed model (2) | <b>94.2</b> | 408.3         | <b>95.21</b> | 3176.07       | <b>94.71</b> | 3584.37       |

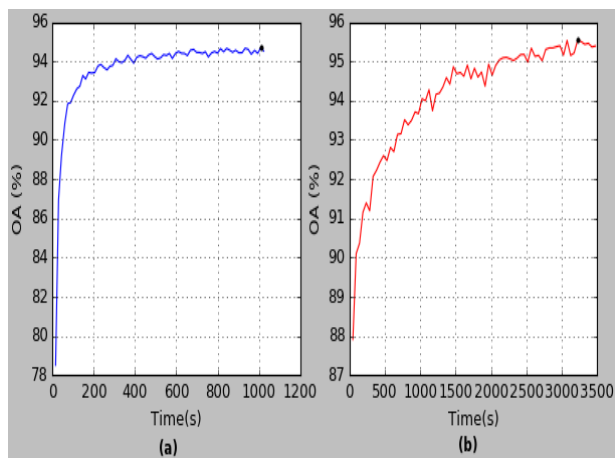


Fig. 6. The Accuracy According to the Training Time for Pavia University (a) and Salinas (b).

According to Table III, we note that the application of the proposed classification model on a single image composed of several HSI, gives a better accuracy value than applying the model on separate images and in a much less training time (see Fig. 7). The visual results of prediction are shown in Fig. 8.

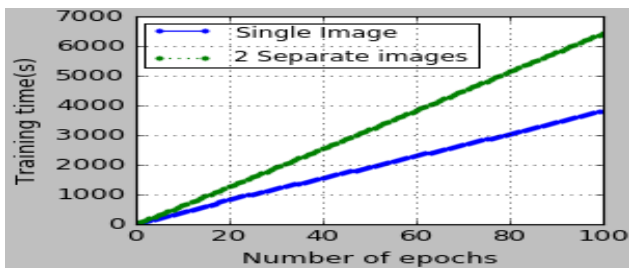


Fig. 7. The Variation of Training Time of the Proposed Model, on the Separate Images and on a Single Composed Image According to the Number of Epochs.

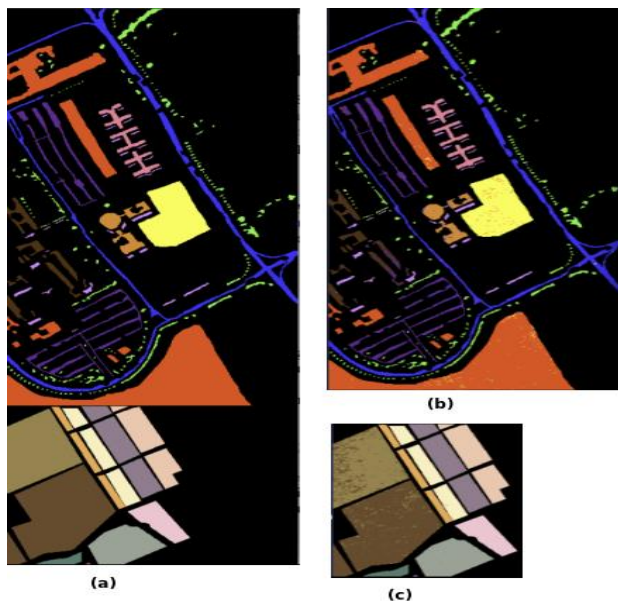


Fig. 8. RGB Composition Maps of Groundtruth for the Composite Image (a), Classification Results from the Proposed Model for : the Pavia U (b), Salinas (c).

TABLE III. EXPERIMENTATION OF THE PROPOSED MODEL ON A SINGLE IMAGE, COMPOSED OF 2 HSI

|                | Proposed model on :<br>Two separate HSI |          | Proposed model on:<br>A single image, composed of 2 HSI |                  |
|----------------|---|----------|---|------------------|
|                | OA_avg                                  | T        | OA  | Training time    |
| <b>Test: 1</b> | 92.69 %                                 | 695.82 s | 92.76 %   | <b>573.8 s</b>   |
| <b>Test: 2</b> | 94.71 %                                 | 3584.37s | 94.75 %   | <b>2869.41 s</b> |

## V. CONCLUSIONS AND FUTURE WORK

In this paper, a new Fast classification model of a hyperspectral image composed of several HSI, using a single training has been proposed. The results of the comparison of the proposed algorithm with a state-of-the-art model [11] and even with the application of this algorithm on several HSI using multiple training, shows the speed and at the same time the performance of the proposed algorithm.

In the next work, we will increase the number of HSI that compose the image to be classified, and then we will create a CNN 3D spatial classification model that will be implemented in a distributed parallel environment.

## REFERENCES

- [1] Lutz M, Biernat E. "Data science: fondamentaux et études de cas: Machine learning avec Python et R". Editions Eyrolles; Oct 2015.
- [2] Razzak, M. I., Naz, S., & Zaib, A.. Deep learning for medical image processing: Overview, challenges and the future. In Classification in BioApps (pp. 323-350). Springer, Cham.2018.
- [3] Paoletti, M. E., Haut, J. M., Plaza, J., & Plaza, A. A new deep convolutional neural network for fast hyperspectral image classification. ISPRS journal of photogrammetry and remote sensing, 145, 120-147. 2018.
- [4] Zhong, Z., Li, J., Ma, L., Jiang, H., & Zhao, H. Deep residual networks for hyperspectral image classification. In 2017 IEEE International Geoscience and Remote Sensing Symposium (IGARSS) (pp. 1824-1827). IEEE. 2017.
- [5] LeCun, Y., Bottou, L., Bengio, Y., & Haffner, P. Gradient-based learning applied to document recognition. Proceedings of the IEEE, 86(11), 2278-2324. 1998.
- [6] Luo, L., Liu, M., Nelson, J., Ceze, L., Phanishayee, A., & Krishnamurthy, A. Motivating in-network aggregation for distributed deep neural network training. In Workshop on Approximate Computing Across the Stack. 2017.
- [7] Szegedy, C., Liu, W., Jia, Y., Sermanet, P., Reed, S., Anguelov, D., ... & Rabinovich, A. Going deeper with convolutions. In Proceedings of the IEEE conference on computer vision and pattern recognition (pp. 1-9). 2015.
- [8] [Online]. Available: [www.ehu.eu/ccwintco/uploads/e/e3/Pavia.mat](http://www.ehu.eu/ccwintco/uploads/e/e3/Pavia.mat); [www.ehu.eu/ccwintco/uploads/f/f1/Salinas.mat](http://www.ehu.eu/ccwintco/uploads/f/f1/Salinas.mat) [Accessed: 01-May-2019].
- [9] Chen, Y., Jiang, H., Li, C., Jia, X., & Ghamisi, P). Deep feature extraction and classification of hyperspectral images based on convolutional neural networks. IEEE Transactions on Geoscience and Remote Sensing, 54(10), 6232-6251. 2016.
- [10] Mei, S., Yuan, X., Ji, J., Zhang, Y., Wan, S., & Du, Q. Hyperspectral image spatial super-resolution via 3D full convolutional neural network. Remote Sensing, 9(11), 1139. 2017.
- [11] Hu, W., Huang, Y., Wei, L., Zhang, F., & Li, H. Deep convolutional neural networks for hyperspectral image classification. Journal of Sensors, 2015.
- [12] Zhang, H., Li, Y., Zhang, Y., & Shen, Q. Spectral-spatial classification of hyperspectral imagery using a dual-channel convolutional neural network. Remote sensing letters, 8(5), 438-447. 2017.

- [13] Yue, J., Zhao, W., Mao, S., & Liu, H. Spectral-spatial classification of hyperspectral images using deep convolutional neural networks. *Remote Sensing Letters*, 6(6), 468-477. 2015.
- [14] Yue, J., Mao, S., & Li, M. A deep learning framework for hyperspectral image classification using spatial pyramid pooling. *Remote Sensing Letters*, 7(9), 875-884. 2016.
- [15] Lee, H., & Kwon, H. Going deeper with contextual CNN for hyperspectral image classification. *IEEE Transactions on Image Processing*, 26(10), 4843-4855. 2017.
- [16] Yang, J., Zhao, Y. Q., & Chan, J. C. W. Learning and transferring deep joint spectral-spatial features for hyperspectral classification. *IEEE Transactions on Geoscience and Remote Sensing*, 55(8), 4729-4742. 2017.
- [17] Zbakh, A., Mdaghri, Z. A., El Yadari, M., Benyoussef, A., & El Kenz, A. Proposition of a Parallel and Distributed Algorithm for the Dimensionality Reduction with Apache Spark. In *Proceedings of the Mediterranean Symposium on Smart City Applications* (pp. 490-501). Springer, Cham. 2017.

# Optical Recognition of Isolated Machine Printed Sindhi Characters using Fourier Descriptors

Nasreen Nizamani<sup>1</sup>, Mujtaba Shaikh<sup>2</sup>, Jawed Unar<sup>3</sup>, Ehsan Ali<sup>4</sup>, Ghulam Mustafa Bhutto<sup>5</sup>, Abdul Rafay<sup>6</sup>

Department of Electronic Engineering, QUEST, Nawabshah, Pakistan<sup>1,2,4,5,6</sup>  
Information Technology QUEST, Nawabshah, Pakistan<sup>3</sup>

**Abstract**—The scale invariance characteristics play an essential role in pattern recognition applications, for example in computer vision, OCR (Optical Character Recognition), electronic publication, etc. In this paper, the shape based feature extraction techniques are used in terms of invariant properties and the region based FD (Fourier Descriptors) have been used for the recognition of isolated printed Sindhi characters. There are 56 isolated characters in Sindhi language than can be categorized to 20 different classes considering the shape of the base of each character. In this work, the dataset contains 4704 images of isolated printed Sindhi characters. The simulation result shows that the proposed method is a capable discriminating algorithm of Similar Sindhi characters and can easily extract the scale invariant features.

**Keywords**—Features extraction; Sindhi optical character recognition; Fourier Descriptors; machine printed Sindhi characters

## I. INTRODUCTION

The Optical character recognition (OCR) is a potential field of computer vision and pattern recognition. The OCR is an electronic conversion of the photographed or scanned images of printed or typewritten text into computer-readable text. The OCR can develop the interface between human and machines in several applications; for example, the office automation, business, cheque verification and data entry [1]. Usually, a typical OCR system comprises of different modules that carry out the recognition procedure. These modules are: (i) *Image acquisition module* – reads the gray scale or color images, (ii) *pre-processing* – this module carries out different operations (binarization and segmentation) operations on the input image, (iii) *Feature extraction* – this module extracts the complicated features from the input image, (iv) *Recognition / classification*: this module performs the recognition / classification task, and (v) *post-processing*. In OCR field, the feature extraction for characters plays an essential role in system. Different methods for recognition of different languages for instance Latin, Chinese and Arabic documents have been proposed in [2,3]. However, the recognition of Sindhi character is still demanding. The main challenges in Sindhi text are Perso-Arabic script having more characters dots and variation of placement and orientation of dots, four dotted characters, a large set of character recognition, the same base shape with variation in number, placement and orientation of dots [4]. In Sindhi text the individual Sindhi characters are rarely used however without individual characters the most of the times sentence has not a complete

sense/meaning. Sindhi isolated characters like ڄ and ڳ, however, without these isolated characters the sentence is incomplete. The Sindhi alphabets have 52 common characters as shown in Fig. 1. In the Arabic script, the base shape “ب” is used only for three characters, “ب”, “ت”, and “ث” whereas, in the Sindhi script the same base shape is used for 9 characters, پ, ڀ, ڄ, ڳ, ڙ, ڻ, ں, ڻ, ڻ. Thus, an Arabic OCR may be able to recognize only three characters for this particular base shape, as well as their changing character forms, Whereas, a Sindhi OCR needs to be able of recognize nine different characters for the same base shape as given in Table I. The few characters like “ت” and “ڻ”, “ڻ” and “ڻ” are more complex because they have the same base shape, only the difference to recognize is the dots orientation in each character. The similar problem is with other shape like “ج” and “ڇ”.

The rotation, size scale (RST) invariant feature extraction methods are described [5, 6]. The Projection transformation process is more proficient because few regular arithmetic operations are performed, and this method is called transformation ring projection (TRP) method [5], and this approach transforms two dimensional (2-D) patterns into one-dimensional (1-D) patterns. This approach has a low recognition rate for similar characters [14]. For that reason, it is difficult to develop an efficient RST invariant feature extraction method. The Fourier descriptors based methods are applied on closed boundary shape of an object [11], which may be hard to get especially in Sindhi characters that usually are separated from each other. These characters have multiple radicals and dots (i.e. ڄ, ڳ, ڙ, etc). The FD don't extract global information, it is due to the fact that, the inter-relationship between the contour components is considered [12]. For this reason, the FD is no more suitable for recognizing such characters. In this paper, another approach called "Sector Projection Fourier Descriptor" (SP-FD) is proposed. The SPFD is exploring the distributed regional pixel of characters using the sector projection. In the Sindhi script fonts, one of the main features is the orientation of dots. These proposed approaches have been applied on all Sindhi characters set, isolated, and characters with different scale and fonts.

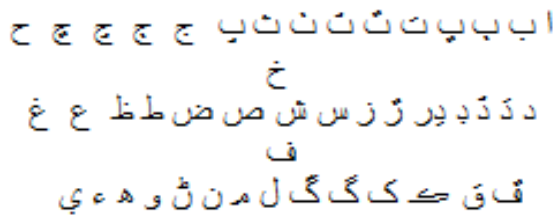


Fig. 1. Common Sindhi Characters.

TABLE. I. COMPARISON OF SINDHI CHARACTERS WITH ARABIC AND PERSIAN CHARACTERS

| Sindhi Characters             | Persian Characters | Arabic Characters |
|-------------------------------|--------------------|-------------------|
| ا ب پ ت ث ٹ پ ج ج ج ح         | ب پ ت ث            | ب ت ث             |
| خ د ذ ڈ یر ژ رس ش ص ض ط ظ ع غ | ح ج ج خ            | ح ج خ             |
| ف ق ک گ گ ل م ن ٹ و ہ ء ی     | د ذ                | ذ                 |
|                               | ر ز ژ              | ر ز               |
|                               | ف ق                | ف ق               |
|                               | ک گ                | ک                 |
|                               | م                  | م                 |
|                               | ن                  | ن                 |
|                               | ء                  | ء                 |

This paper is organized as follows: Section 2 describes the data preparation procedure. Section 3 explains the pre-processing technique followed by feature computation with FD and invariant characteristics. Accordingly, Section 4 presents the comparative analysis of SP-FD (Sector Projection Fourier Descriptors) with invariant feature extraction methods. Finally, Section 5 concludes the article.

## II. DATA PREPERATION

The Sindhi characters contain different shapes for instance; curves, arcs, loops, junctions and lines. The isolated Sindhi characters with different scales and different fonts have been employed in this study. During the data preparation process, the original input images are prepared by manually typing the characters in Microsoft Word. The input images have been prepared in 7 different fonts and 12 different sizes. Then, the prepared are saved as ".BMP" files. All fifty six characters have been used in this study. As a result, fifty six files with seven different fonts (MB Khursheed, MB Lateefi, MB Kufi, AS Basit, MB Supreen Shabir Kumbhar Bahij Nassim and Bahij The Sans Arabic Extra Bold) have been created Subsequently, 12 different font sizes (10, 16, 20, 24, 28, 32, 36, 40, 44, 48, 56 & 72) have been used during dataset creation. The entire dataset consists of 4704 samples in total, as:

$$\text{Total Samples} = 56 \times 7 \times 12 = 4704.$$

These 4704 samples will yield experimental characters for all Sindhi characters consisting of different shapes, fonts and sizes. The succeeding section of the article explains the feature extraction technique used for the computation of intricate features from the input images. These features are then used for character recognition.

## III. FEATURE EXTRACTION

A compact numerical representation of an object is commonly referred to as a feature vector. Contextually, the process of finding out all these unique patterns from an object of interest is known as feature extraction. In the character recognition system, the feature extraction is the most important step. For a recognition process, selection of discriminant features is an important factor. Our goal is to find a set of features that can define the shape of the underlying character as precisely and uniquely as possible [7]. There are many feature extraction techniques exists. These techniques can be categorized into the structural features, statistical feature and the global transformation methods [8, 9]. Generally, the techniques based on Fourier Descriptors are more efficient feature extraction tool used in majority of the digital image processing applications. It represents the boundary of the object by applying Fourier transform (FT) on a (character) shape that is derived from shape boundary coordinates. This is a one dimensional function and is referred to as the shape signature [10, 11]. The Fourier Descriptors are invariant under Rotation, Scale and Translation (RST) and are computationally efficient. The discrete FT is given by:

$$a_m = \frac{1}{M} \sum_{k=0}^{M-1} A(k) \exp\left(-\frac{j2\pi mk}{M}\right), m = 0, 1, \dots, M-1 \quad (1)$$

Fourier coefficients  $a_m$  are chosen, the normalized magnitudes of  $a_n$  are used as features to describe the shape. A variety of FD methods depend on the closed boundary of an object's shape. However, in case of Sindhi characters; this boundary information is difficult to achieve. This is due to the fact that these characters have multiple dots and multiples radicals which are isolated from one another. For example, the Sindhi character 'پ' has five boundaries that are disconnected from each other. Another example is character 'ڄ', which has three boundaries and all the boundaries are also disconnected from each other. Fig. 2 displays both the exemplary characters.

In order to compute the shape boundary, the proposed algorithm consists of the following steps:

### Algorithm

Input: Single Sindhi character binary image

Output:

### Feature Vector

- (1) Find the center of mass of binary image, and set the center of mass at the origin and find the radius.
- (2) Find the particular projection of shape signature by using ring projection function.
- (3) To Calculate FD: Apply FT on  $v(\varphi)$  and obtain the coefficients.

$$v(\varphi) = \int_0^R \delta(\rho, \varphi) d\rho, \varphi \in [0, 2\pi]$$

- (4) The magnitude of each coefficient is calculated and selected to obtain the feature vector.
- (5) To measure dissimilarity between two dissimilar feature values, the Camberra distance method has been used.



Fig. 2. Five and Three Disconnected Closed Boundaries.

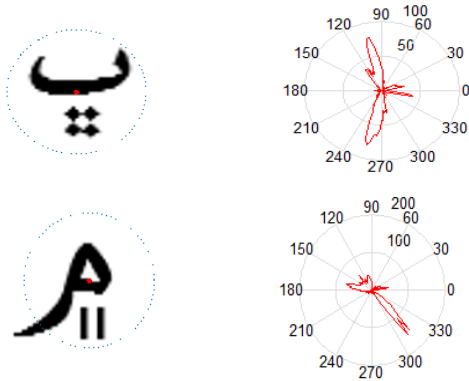


Fig. 3. Sector Projection of Two Sindhi Characters in Polar Space.

In this work, the proposed SP-FD for a particular projection, following the ring projection that can overcome the problem such as one dimensional FD method. The centre of mass  $(x_c, y_c)$  is calculated by setting the centre of mass at origin. Next, the maximum radius of the circle covering the character is obtained. The ring feature extraction function in terms of binary image character  $f(x, y)$  is then defined as:

$$\delta(\rho, \varphi) = \begin{cases} 1, & \text{if } g(\rho, \varphi) \in R \\ 0, & \text{Otherwise} \end{cases} \quad (2)$$

Where  $g(\rho, \varphi)$  represents polar form of binary image  $f(x, y)$ ,  $R$  is the region of character's image. Then the original image will be translated at origin. Afterwards, all the pixels (counted at a particular angle  $\varphi$ ) of image character are projected onto the series of radius denoted by  $v(\varphi)$ . The operation of continuous sector projection can be defined as:

$$v(\varphi) = \int_0^R \delta(\rho, \varphi) d\rho, \varphi \in [0, 2\pi] \quad (3)$$

The discrete form of Equation (3) is:

$$v(\varphi_t) = \sum_{k=0}^n \delta(\rho_k, \varphi_t) \quad (4)$$

Where  $n$  represents number of samples in the radial direction,  $\rho_k = k\varphi_r$ . Fig. 3 illustrates the sector projection for Sindhi characters 'پ' and 'م'.

After applying the Fourier transform on sector projection function, the Fourier coefficients are calculated as follows:

$$f(k) = \int_0^{2\pi} v(\varphi) \exp(-2\pi i k \varphi) d\varphi \quad (5)$$

Thus, the discretized form is:

$$f_k = \sum_{k=0}^{K-1} v\left(\frac{2k\pi}{K}\right) \exp\left(\frac{4\pi^2 k i}{K}\right) \quad (6)$$

Where  $K = 2\pi/\Delta\varphi$ ,  $\Delta\varphi$  is angular step. To obtain the FDs, the normalized coefficients magnitudes  $|f_k|$  are calculated to form a FD feature vector.

#### IV. SINDHI CHARACTER RECOGNITION

Basically, the Sindhi isolated letters are built from 52 main alphabets. Each character may have different shape and differ from other characters in terms of the position of dots. The dots can be above, below, or inside the main shape of the character. In the first step, we classify the Sindhi characters according to their basic shapes. As a result, the procedure yields 56 main (isolated) forms for 52 Sindhi characters. Table II exposes 20 shapes and 20 classes. The total number of classes is 20 as given in Table III.

The characters classification is based on SP-FD and Transformation Ring Projection (TRP) feature vectors by means of statistical analysis. In order to measure the similarity and dissimilarity amongst feature vectors, the Camberra distance can be applied (as explained in Section 4). In the second step, we have enhanced the number of classes up to 56 classes, denoted by  $A_i$ ,  $i=1, 2, \dots, 56$ . The relationship of two classes is  $C_i$  and  $A_i$  as shown in Table III. In this step we have used all the characters having similar shape and their respective dot position separately to find the class of characters.

TABLE II. THE 20 DIFFERENT CLASSIFICATION OF SINDHI CHARACTERS

| Class number | Basic shape of Sindhi character elimination of dots | Class number | Basic shape of Sindhi character elimination of dots |
|--------------|---|--------------|---|
| C_01         | ا   | C_11         | و   |
| C_02         | ب   | C_12         | ڪ   |
| C_03         | ح   | C_13         |   |
| C_04         | د   | C_14         | گ   |
| C_05         | ر   | C_15         | ل   |
| C_06         | س   | C_16         | م   |
| C_07         | ص   | C_17         | ن   |
| C_08         | ط   | C_18         | و   |
| C_09         | ع   | C_19         |   |
| C_10         | ف   | C_20         | ي   |

TABLE. III. THE RELATIONSHIP BETWEEN C AND A

| Class C <sub>i</sub> | Sub-Class A <sub>i</sub>                             | Class C <sub>i</sub> | Sub-Class A <sub>i</sub> |
|----------------------|--|----------------------|--------------------------|
| C1                   | {A1, A56, A43}                                       | C11                  | A37                      |
| C2                   | {A2, A3, A4, A5, A6, A7, A8, A9, A10, A46, A47, A59} | C12                  | A38                      |
| C3                   | {A11, A12, A13, A14, A15, A16, A17}                  | C13                  | A39                      |
| C4                   | {A18, A19, A20, A21, A22, A23}                       | C14                  | A40, A41, A42            |
| C5                   | {A24, A25, A26}                                      | C15                  | A43                      |
| C6                   | {A27, A28}   | C16                  | A44, A45                 |
| C7                   | A29, A30   | C17                  | A46, A47                 |
| C8                   | A31, A32   | C18                  | A48                      |
| C9                   | A33, A34   | C19                  | A49                      |
| C10                  | A35, A36   | C20                  | A55                      |

### V. EXPERIMENTAL RESULTS

In Sindhi language, there are 52 main characters and depending on the position of each character in a word, it may have different shapes. Fig. 4 represents the different shapes of the same character.



Fig. 4. Different Shape of Sindhi Character.

As aforementioned, in this work only the isolated shape of each character is considered.

Similarity Measurement: The similarity is measured for two characters A<sub>i</sub> and A<sub>j</sub>, the corresponding FD feature vector are represented as  $v^i = [v_1^i, v_2^i, \dots, v_n^i]^T$  and  $v^j = [v_1^j, v_2^j, \dots, v_n^j]^T$  respectively. For the statistical analysis, the dissimilarity is measured using Camberra distance [13].

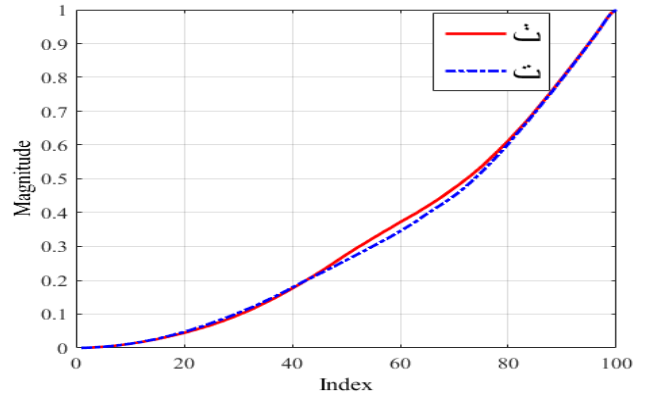
$$dissim(A_i, A_j) = \sum_{k=1}^n \frac{|v_k^i - v_k^j|}{v_k^i + v_k^j} \quad (7)$$

Fig.5 (a) depicts the feature extraction of two Sindhi characters ‘پ’ and ‘ت’ using TRP method. These two characters possess the same shape whereas the only difference is in the position of dots. The red and blue lines display the feature values for character ‘پ’ and ‘ت’ respectively. It is evident that there exists a small difference in numeric value of

feature vectors making discrimination between two characters. for a 100 dimensional vector to represent RST-invariant features 95% similarity is achieved. Therefore, it shows 5% confidence of the classifier to declare the difference between two characters. Fig. 5(b) exhibits the SP-FD features extracted for the two similar characters. Contrary to the previous methods, the similarity measurement boosts the confidence to declare that these two characters are much different. This enhanced confidence level is achieved by considering 29 feature values only. Therefore, a much better observation is presented using SP-FD features.

#### A. Scaling Invariance

In this case, we present the experiments performed on a scaled single Sindhi character. By scaling the character *s* times, the testing set T= {(4), (6), (8) and (10)} as shown in Fig. 6(a). The SP-FD feature vector for each entry in is shown in Fig. 6(b). It shows that the similarity among Sindhi character ‘پ’ at four different scales. The similarity achieved for character ‘پ’ is from 85-95%. These testing characters belong to the same class, and it can be said that, the method of SP-FD is verified. Fig. 6(c) illustrates the sector projection of Sindhi character ‘پ’.



(a) TRP feature extracted for Sindhi characters ‘پ’ and ‘ت’.

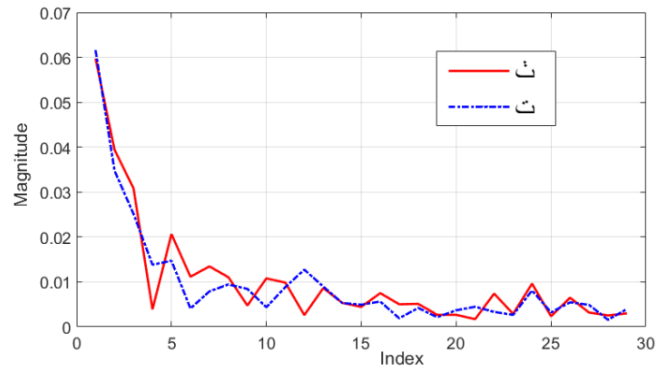
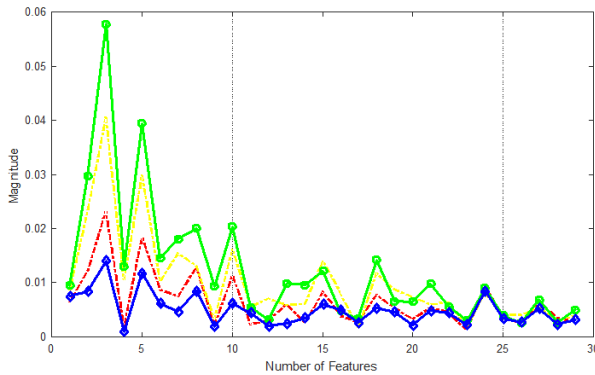


Fig. 5. (b) The Feature Extracted for Sindhi Characters ‘پ’ and ‘ت’ using Sector Projection Fourier Descriptors.





(a) Testing Sample of Sindhi Character 'پ'.



(b) The Similarity Measured using SP-FD Algorithm from Testing Samples of Sindhi Characters 'پ'.

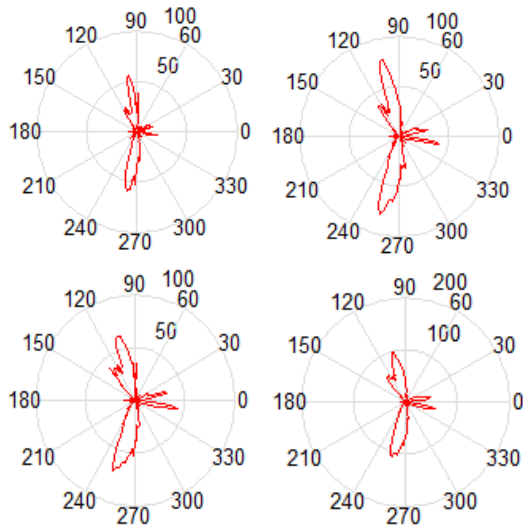


Fig. 6. (c) Projection of Four Testing Samples for پ.

## VI. CONCLUSION

This paper presents an isolated machine printed Sindhi character recognition system. This study proposes SP-FD technique for computation of scale invariant features from Sindhi characters containing different sizes and shapes. This work also presents a comparative analysis of the proposed techniques with other techniques such as RST-invariant feature extraction methods and TRP invariant feature extraction methods. The statistical analysis clearly shows that the proposed technique outperforms other techniques proposed in the available literature. The MATLAB script only extracts the feature vector of a single image. The dissimilarity between different images can be computed by using many existing distance measurement, e.g. l-2, l-1 norm or other norms.

Furthermore, the experimental results also confirm that the SP-FD feature extraction method can produce better results in Sindhi character recognition. In future, we aim to further investigate the accuracy of the proposed feature extraction method using supervised machine learning techniques such as support vector machines (SVM) and artificial neural networks (ANNs).

## ACKNOWLEDGMENT

The authors are thankful Prof. Dr. Ahsan Ahmad Ursani, Department of Biomedical Engineering, Mehran University of Engineering & Technology, Jamshoro, Pakistan for his kind guidance.

## REFERENCES

- [1] Impedovo, S., Ottaviano, L., and Occhinegro, S., "Optical Character Recognition: A Survey", International Journal of Pattern Recognition and Artificial Intelligence, [DOI:org/10.1142/S0218001491000041], Volume 5, No. 1, pp. 1-24, June, 1991.
- [2] Trier, Ø. D., Jain, A.K., and Taxt, T., "Feature Extraction Methods for Character Recognition: A survey", Pattern Recognition, Volume 29, No. 4, pp. 641-662, [DOI: org/10.1016/0031-3203 (95)00118-2], 1996.
- [3] Broumandnia, A., and Shanbehzadeh, J., "Fast Zernike Wavelet Moments for Farsi Character Recognition", Image and Vision Computing, Volume 25, No. 5, pp. 717-726, [DOI: org/10.1016/j.imavis.2006.05.014], 2007.
- [4] Hakro, D.N., Ismaili, I.A., Talib, A.Z., and Mojal, G.N., "Issues and Challenges in Sindhi OCR", Sindh University Research Journal (Science Series), Volume 2, No. 46. pp. 143-152, Jamshoro, Pakistan, 2014.
- [5] Abdel Raouf, A.M., "Offline Printed Arabic Character Recognition", Ph.D. Thesis, School of Computer Science, University of Nottingham, UK, 2012.
- [6] Yang, M., Kpalma, K., and Ronsin, J., "Shape-Based Invariant Feature Extraction for Object Recognition", Advances in Reasoning-Based Image Processing Intelligent Systems, pp. 255-314, [DOI: 10.1007/978-3-642-24693-7\_9], 2012.
- [7] Shaffie, A.M., and Elkobrosy, G.A., "A Fast Recognition System for Isolated Printed Character Using Center of Gravity and Principal Axis", Applied Mathematics, Volume 4, No. 9, pp. 1313-1319, [DOI: 10.4236/am.2013.49177], 2013.
- [8] Kumar, G., and Bhatia, P.K., "A Detailed Review of Feature Extraction in Image Processing Systems", IEEE 4<sup>th</sup> International Conference on Advanced Computing & Communication Technologies, pp. 5-12, [DOI: 10.1109/ACCT.2014.74], Rohtak, India, 2014.
- [9] Taha, S., Babiker, Y., and Abbas, M., "Optical Character Recognition of Arabic Printed Text", IEEE Student Conference on Research and Development, pp. 235-240, [DOI: 10.1109/SCOREd.2012.6518645], Pulau Pinang, Malaysia, 2012.
- [10] Zhang, D., and Lu, G., "A Comparative Study of Fourier Descriptors for Shape Representation and Retrieval", Proceedings of 5<sup>th</sup> Asian Conference on Computer Vision, pp.646-651, [DOI: 10.1.1.73.5993], Springer, Melbourne, Australia, 2002.
- [11] El-ghazal, A., Basir, O., and Belkasim, S., "Farthest Point Distance: A New Shape Signature for Fourier Descriptors", Signal Processing: Image Communication, Volume 24, No. 7, pp. 572-586, [DOI: org/10.1016/j.image.2009.04.001], 2009.
- [12] El-ghazal, A., Basir, O., and Belkasim, S., "Invariant Curvature-Based Fourier Shape Descriptors", Journal of Visual Communication and Image Representation, Volume 23, No. 4, pp. 622-633 [DOI: org/10.1016/j.jvcir.2012.01.011], 2012.
- [13] Johnson, R.A., and Wichern, D.W., "Applied Multivariate Statistical Analysis", New Jersey: Prentice-Hall, 2014.
- [14] Dong, L., Wang, J., Li, Y., & Tang, Y. Y. (2013, June). Sector projection fourier descriptor for chinese character recognition. IEEE International Conference on Cybernetics (CYBCO) pp. 162-167, 2013.

# Junction Point Detection and Identification of Broken Character in Touching Arabic Handwritten Text using Overlapping Set Theory

Inam Ullah<sup>1</sup>, Mohd Sanusi Azmi<sup>2</sup>, Mohamad Ishak Desa<sup>3</sup>  
Faculty of Information Technology and Communication  
Universiti Teknikal Malaysia (UTeM)  
Melaka, Malaysia

**Abstract**—Touching characters are formed when two or more characters share the same space with each other. Therefore, segmentation of these touching character is very challenging research topic especially for handwritten Arabic degraded documents. This is one of the key issue in recognition of the handwritten Arabic text. In order to make the recognition system more effective segmentation of these touching handwritten Arabic characters is considered to be very important research area. In this research, a new method is proposed, which is used to identify the junction or common point of Arabic touching word image by applying overlapping or intersection set theory operation, which will help to trace the correct boundary of the touching characters, identify the broken characters and also segmented these touching handwritten text in an efficient way. The proposed method has been evaluated on Arabic touching handwritten characters taken from handwritten datasets. The results show the efficiency of the proposed method. The proposed method is applicable to both degraded handwritten documents and printed documents.

**Keywords**—Touching characters; segmentation and recognition; overlapping set theory; junction point; broken character

## I. INTRODUCTION

Recognition of handwritten characters, which is challenging problem in the field of pattern recognition [1]. Mostly characters segmentation techniques are used to recognize these segmented text and it is considered very important step for recognition because incorrect segmentation effects the recognition [2][3]. Almost everywhere in the world, Libraries and National archives have huge volume of historical and degraded documents in the form of books. These valuable materials need proper attention in conversion to machine readable format [4]. Although, researchers are busy in solving the problems of these documents in order to provide them in meaningful form for further studies, researches and projects. Some of the work done in this regard is only by scanning of these documents, which is not sufficient to store these information in image format [5]. It requires more research work to convert these historical handwritten and degraded documents into machine understandable format. Therefore, it is still considering as an open and important research area. The big problem facing by researchers is by not following the standard rules of writing in these documents especially in Arabic handwritten documents. Which are facing

a lot of difficulties because of nature and style of Arabic language characters, where characters are connected and direction of writing is from right to left. There is no upper or lowercase letters both in printed and handwritten Arabic writing [6][7].

Arabic language consists of 28 characters and every individual character has a fixed shape. As, in Arabic writing characters are connected with each other to form words, these connections change the shape of the characters i.e. shape of isolated character is different than character in middle and end of the word [8]. In Arabic handwriting, normally the writers don't follow the standard writing rules, means the writer is free to write according to his well, situation etc. so there are great possibilities in writing a document that characters may touch, overlap and not properly written and produce broken character. So, in presence of these problems conversion of handwritten text to electronic form is not fully succeeded and problem becomes more serious, when dealing with touching Arabic handwritten words because still there is a gap between human and machine abilities in reading handwriting text under noisy conditions especially for touching and broken Arabic manuscripts. These challenging situation i.e. Connected/touching components complicate the segmentation and recognition process because of unavailability of databases [9] and also some characters are combine with each other in such a way that it forms ligatures [10].

The rest of the paper is organized as follows. Section II covers possible touching character types in the Arabic handwritten documents. Section III describes the related works. Algorithm details are in Section IV. Experimental results are reported in Section V. Conclusion and future work is discussed in Section VI.

## II. TOUCHING CHARACTERS AND ITS TYPES

As Arabic writing, characters are connected with each other. It creates a challenges situation by comparing with other languages such as English. Therefore, general writing style [11] and some of the touching and overlapping of characters are shown in Fig. 1, Fig. 2 and Fig. 3 [12].

In Arabic handwritten documents, there are four overlapping/touching types as shown in Table I.

Some of the touching characters are highlighted in Fig. 4 [14].

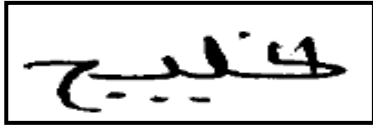


Fig. 1. Overlapping of Characters with Touching.

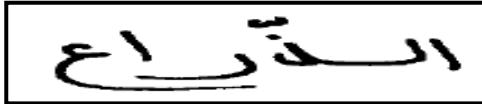


Fig. 2. Overlapping without Touching.

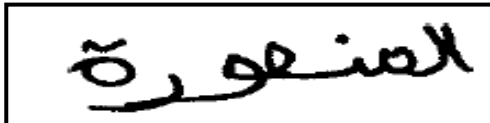


Fig. 3. Touching by Mistake.

Based on Fig. 4 and Table I, some of the possible touching structures are shown in Fig. 5.

TABLE I. TOUCHING TYPES IN ARABIC HANDWRITING [13]

| Type | Letters   | Sample |
|------|---|--------|
| A    | Top: [ر, ز, س, ش, ص, ض, ن, ق, و, ي, ا]<br>Bottom: [ا, ط, ظ, ك, ل] |        |
| B    | Top: [ر, ز, م, و]<br>Bottom: [ص, ض, ة]                            |        |
| C    | Top: [ج, ح, خ, ع, غ]<br>Bottom: [ا, ط, ظ, ك, ل]                   |        |
| D    | Top: [ج, ح, خ, ع, غ]<br>Bottom: [ة]                               |        |



Fig. 4. Touching Character in Arabic Handwriting.

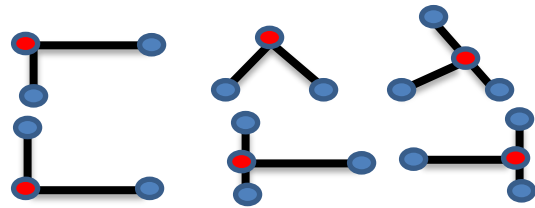


Fig. 5. Possible Touching Structure.

Where ● represents end-points, ● Junction point and — Boundary of character.

### III. RELATED WORK

By exploring the published literature related to junction point detection, there is a lack of research work for handwritten and printed Arabic characters but number of methods proposed for other languages such as Chinese, English and junction point detection for general images. Some of the methods are discussed below.

In [15] proposed method is for stroke extraction of handwritten Chinese characters. In proposed method first of all character image is converted to binary image. Then apply thinning algorithm to converted binary image. Next is to find endpoints and fork point of the skeleton image and then these points are checked with the original image of handwritten Chinese character. Main objectives of this proposed method is to increased segmentation and recognition ratio.

In [16], proposed a junction detection method, which is used for solving the problem of segmentation of touching characters i.e. two touching character string. This proposed method is used only for uppercase printed English Alphabets and this method is applicable to only single touching not working for multiple touching.

Some of the limitations of this proposed method are:

- 1) Segmentation of English Uppercase character.
- 2) Used for selected printed characters.
- 3) Used for segmentation of single touching.
- 4) Not working for multiple touching and handwritten characters.

In [17] Junction based approach for solving the problem of touching remote sensing images. New formula also include minimization criteria for the total weighted distance is proposed. This will detect junction point accurately. Authors claim that its results are much better than popular junction detection detector such as Forstner, JUDOCA (Junction Detection Operator based on circumferential Anchor) and CPDA.

In [18] Junction based approach for solving the problem of touching Chinese characters. The main drawback of this method it is only used for identification not segmentation. In Arabic language characters are connected with each other's thus form sub words in the same word. Here in this work i.e. identification of junction point only collect information around this point and ignore the whole shape of a character. This is very important step in recognition or writer identification.

In [19] Junction based approach for solving the problem of touching Handwritten Devanagari Character Recognition. Finding the junction point where chain code moves in more than one direction in 8-connected neighborhood or in other word a point which have more than two neighboring pixel. The main drawback with this method is can't apply to Arabic language because characters are connected with each for form word or piece of word.

In [20] authors have proposed an improved skeletonization method. This method is basically the combination of straight and curves lines. Its main purpose to improve the junction point detection and topological error near the junction point. This method is only applied for architectural drawings and not for handwritten character images.

#### IV. PROPOSED METHOD

In this section is discussed the proposed method of finding the junction point and identification of broken character in touching handwritten Arabic character images [21]. The outline of the proposed method is shown in Fig. 6.

**Stage-1:** First stage of the model is Image preprocessing. As the proposed method is working on binary images. Thus first step is to convert the input image into binary by applying standard Otsu's method. Binary image is that type of image in which each pixel has two possible values 0 and 1, in other word, this image has two colors background and foreground. Next step is to apply thinning algorithm This Thinning operation is also called skeletonization. This is a morphological operation used to remove selected foreground pixels from binary image. Its main objective is to preserve the important information and make it easy for further processing. Therefore, the output of thinning process is a binary image of only one-pixel width lines. Preprocessing step is shown in Fig. 7.

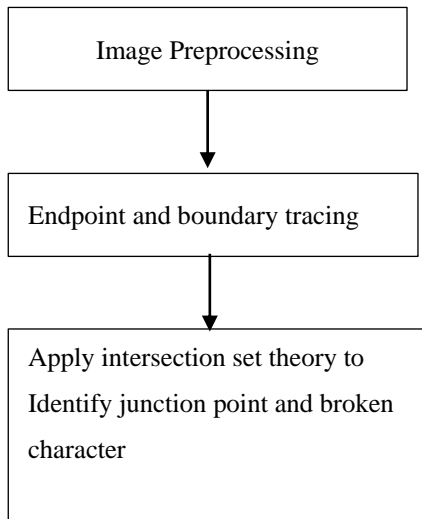


Fig. 6. Proposed Method Stages.

**Stage-2:** In this stage, Endpoints are those points which have only one neighboring point and which is located at the end of character boundary. In Fig. 8 have touching character image. Fig. 8(a) have four endpoints  $E_1, E_2, E_3$  and  $E_4$ . While tracing boundary between endpoints gets two sets  $E_1E_2$  and  $E_3E_4$ .

$$\text{Set A } E_1E_2 = \{(x_1, y_1), (x_2, y_2), \dots, (x_n, y_n)\}$$

$$\text{Set B } E_2E_4 = \{(x_1, y_1), (x_2, y_2), \dots, (x_n, y_n)\}$$

In Fig. 8(b) there are six endpoints  $E_1, E_2, E_3, E_4, E_5, E_6$  and three sets  $E_1E_3, E_2E_5, E_4E_6$ .



Fig. 7. Binary and Thinned Image.

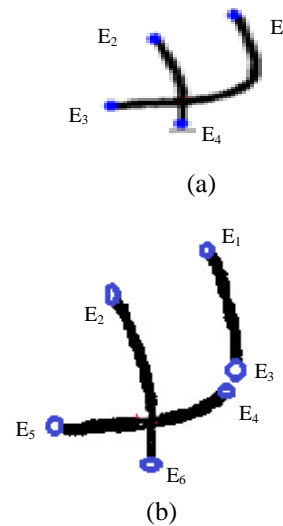


Fig. 8. Touching Character Image.

$$\text{Set A } E_1E_3 = \{(x_1, y_1), (x_2, y_2), \dots, (x_n, y_n)\}$$

$$\text{Set B } E_2E_5 = \{(x_1, y_1), (x_2, y_2), \dots, (x_n, y_n)\}$$

$$\text{Set C } E_4E_6 = \{(x_1, y_1), (x_2, y_2), \dots, (x_n, y_n)\}$$

**Stage-3:** This stage is to apply intersection set theory on sets in Stage-2. By applying intersection set theory on Set A and Set B shown in Fig. 9.

In Fig. 10 both sets have a common element and that is common or touching point. Apply set theory for Set A, Set B and Set C

While in Fig. 11, Set B and Set C have common element that is the Junction point. Set A has no common element that identify that character is broken.

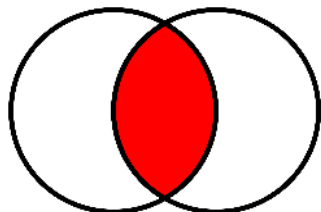
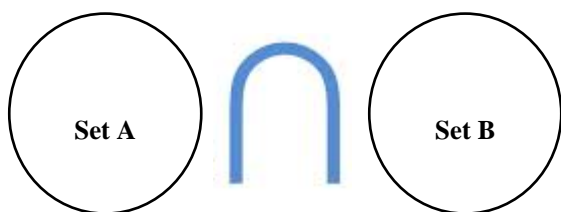


Fig. 9. Overlapping Set Theory.

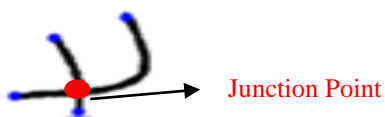


Fig. 10. Junction Point.



Fig. 11. Identification of Broken Character.

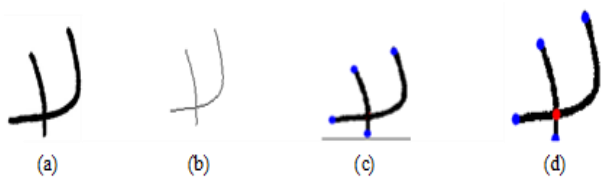


Fig. 12. Output Touching Image with end and Touching Point.

Fig. 12(a), (b), (c) and (d) shows input image, Thinned Image, Endpoints and Junction point.

### V. RESULTS AND DISCUSSION

The proposed method is for finding junction point and to identify the broken characters but due to lack of research and standardized datasets for testing proposed method, especially for touching characters. Data are collected from different available dataset are shown in Table II and did some manual work to make the touching types more complex shown in Fig. 13.

Total number of sample collected 360 touching Arabic handwritten words according to four different type of touching characters shown in Table I. For each type equal numbers of 90 touching characters were selected. Proposed methods were tested on collected data. In Table III describes the result of each touching type.

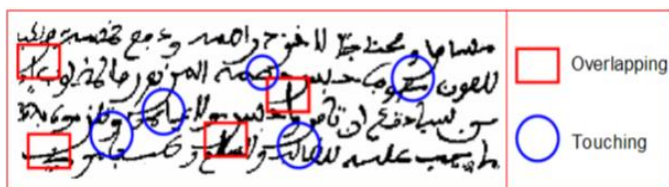


Fig. 13. Manual Touching Collected Data Sample.

TABLE II. COLLECTED DATASETS

| Dataset                | Size  | Purpose                  |
|------------------------|---|--------------------------|
| IFN/ENIT               | 26459 Tunisian City Name                        | Offline handwritten Text |
| CEDAR Arabic Dataset   | 100 pages of text, each comprises 150-200 words | Offline handwritten Text |
| AHDB                   |   | Offline handwritten Text |
| Arabic-Handwritten 1.0 | 5000 handwritten pages                          | Offline handwritten Text |

TABLE III. RESULTS OF FINDING COMMON POINT

| Touching Type | Sample | Correctly Identify Common point | Percentage (%) |
|---------------|--------|---------------------------------|----------------|
| A             | 90     | 88                              | 97.7%          |
| B             | 90     | 86                              | 95.55%         |
| C             | 90     | 80                              | 88.8%          |
| D             | 90     | 82                              | 91.11%         |

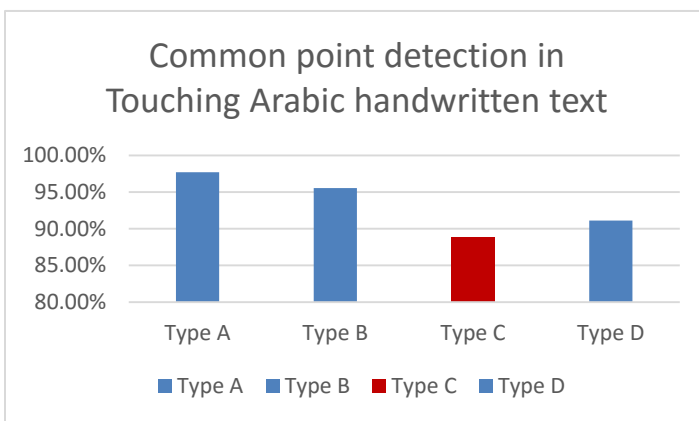


Fig. 14. Analysis of Method.

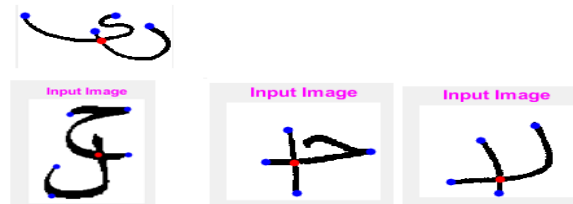


Fig. 15. Sample Output.

The weighted mean of these results is equal to 93.3%, 6.6% rate error because of variety and complexity of Arabic Language. Fig. 14 shows graph of the Table III.

Some of the sample results are given in Fig. 15.

## VI. CONCLUSION

Broken and touching of character images of handwritten exists especially in ancient documents due to the quality of scanning. Thus by exploring the literature for our research we found that broken and touching characters extensively happen in English, Number and Arabic handwritten historical materials. Thus to identify junction point and broken character, proposed new method for finding junction point between the touching characters. This method is based on handwritten Arabic calligraphy where touching of character is most likely occurred. The proposed method is used intersection set theory. This method is not only useful in junction point but also identify the broken character as well. In future this can be applied to others regional languages Urdu, Farsi and many others, which are similar to Arabic language and this method can also be applied to multiple touching characters

## ACKNOWLEDGMENT

The authors would like to thank Ministry of Education for funding this study through the following grant FRGS/1/2017/ICT02/FTMK-CACT/F00345. We would also like to extend our thanks to Universiti Teknikal Malaysia Melaka and Faculty of Information Technology and Communication for providing excellent research facilities.

## REFERENCES

- [1] G. A. Farulla, N. Murru, and R. Rossini, "A fuzzy approach to segment touching characters," *Expert Syst. Appl.*, vol. 88, pp. 1–13, 2017.
- [2] A. Yamamah and D. Branch, "Cursive Multilingual Characters Recognition Based on Hard Geometric Features Amjad Rehman 1 2," 2012.
- [3] S. Zhao, Z. Chi, P. Shi, and H. Yan, "Two-stage segmentation of unconstrained handwritten Chinese characters," *Pattern Recognit.*, vol. 36, no. 1, pp. 145–156, 2003.
- [4] T. Saba and A. Rehman, "Character Segmentation in Overlapped Script using Benchmark Database," pp. 140–143.
- [5] N. Aouadi, S. Amiri, and A. K. Echi, "Segmentation of Connected Components in Arabic Handwritten Documents," *Procedia Technol.*, vol. 10, pp. 738–746, 2014.
- [6] A. P. Giotis, G. Sfikas, B. Gatos, and C. Nikou, "A survey of document image word spotting techniques," *Pattern Recognit.*, vol. 68, pp. 310–332, 2017.
- [7] Y. M. Alginahi, "A survey on Arabic character segmentation," *Int. J. Doc. Anal. Recognit.*, vol. 16, no. 2, pp. 105–126, 2013.
- [8] F. Khan, A. Bouridane, F. Khelifi, R. Almotaeryi, and S. Almaadeed, "Efficient segmentation of sub-words within handwritten arabic words," *Proc. - 2014 Int. Conf. Control. Decis. Inf. Technol. CoDIT 2014*, no. i, pp. 684–689, 2014.
- [9] J. H. Alkhateeb, "A Database for Arabic Handwritten Character Recognition," *Procedia Comput. Sci.*, vol. 65, no. Iccmit, pp. 556–561, 2015.
- [10] Y. Osman, "Segmentation algorithm for Arabic handwritten text based on contour analysis," *Proc. - 2013 Int. Conf. Comput. Electr. Electron. Eng. 'Research Makes a Differ. ICCEEE 2013*, pp. 447–452, 2013.
- [11] T. Sari, L. Souici, and M. Sellami, "Off-line handwritten Arabic character segmentation algorithm: ACSA," *Proc. - Int. Work. Front. Handwrit. Recognition, IWFHR*, no. May 2014, pp. 452–457, 2002.
- [12] A. Lawgali, "A Survey on Arabic Character Recognition," *Int. J. Signal Process. Image Process. Pattern Recognit.*, vol. 8, no. 2, pp. 401–426, 2015.
- [13] N. Ouwayed and A. Belaïd, "Separation of overlapping and touching lines within handwritten arabic documents," *Lect. Notes Comput. Sci. (including Subser. Lect. Notes Artif. Intell. Lect. Notes Bioinformatics)*, vol. 5702 LNCS, pp. 237–244, 2009.
- [14] B. Al-Badr and S. A. Mahmoud, "Survey and bibliography of Arabic optical text recognition," *Signal Processing*, vol. 41, no. 1, pp. 49–77, 1995.
- [15] K. Liu, Y. S. Huang, and C. Y. Suen, "Identification of fork points on the skeletons of handwritten chinese characters," *IEEE Trans. Pattern Anal. Mach. Intell.*, vol. 21, no. 10, pp. 1095–1100, 1999.
- [16] U. K. S. Jayarathna, "A Junction Based Segmentation Algorithm for Offline Handwritten Connected Character Segmentation," 2006.
- [17] J. Zhang, T. Luo, G. Gao, and L. Lian, "Junction Point Detection Algorithm for SAR Image," *Int. J. Antennas Propag.*, vol. 2013, no. 3, pp. 1–9, 2013.
- [18] S. He, M. Wiering, and L. Schomaker, "Junction detection in handwritten documents and its application to writer identification," *Pattern Recognit.*, vol. 48, no. 12, pp. 4036–4048, 2015.
- [19] Arora, S. et al. (2008) 'Combining multiple feature extraction techniques for Handwritten Devnagari Character recognition', IEEE Region 10 Colloquium and 3rd International Conference on Industrial and Information Systems, ICIIS 2008. doi: 10.1109/ICIINFS.2008.4798415
- [20] Hilaire, Xavier & Tombre, Karl. (2001). Improving the Accuracy of Skeleton-Based Vectorization. 273-288. 10.1007/3-540-45868-9\_24.
- [21] Inam Ullah and Azmi, M. S. (2019) 'Segmentation of Touching Arabic Characters in Handwritten Documents by Overlapping Set Theory and Contour Tracing', (IJACSA) International Journal of Advanced Computer Science and Applications, 10(5), pp. 155–160.

# Implementation of Machine Learning Model to Predict Heart Failure Disease

Fahd Saleh Alotaibi<sup>1</sup>

Information Systems Department  
Faculty of Computing and Information Technology  
King Abdulaziz University, Jeddah, Saudi Arabia

**Abstract**—In the current era, Heart Failure (HF) is one of the common diseases that can lead to dangerous situation. Every year almost 26 million of patients are affecting with this kind of disease. From the heart consultant and surgeon's point of view, it is complex to predict the heart failure on right time. Fortunately, classification and predicting models are there, which can aid the medical field and can illustrates how to use the medical data in an efficient way. This paper aims to improve the HF prediction accuracy using UCI heart disease dataset. For this, multiple machine learning approaches used to understand the data and predict the HF chances in a medical database. Furthermore, the results and comparative study showed that, the current work improved the previous accuracy score in predicting heart disease. The integration of the machine learning model presented in this study with medical information systems would be useful to predict the HF or any other disease using the live data collected from patients.

**Keywords**—Machine learning model; medical data; heart failure diagnoses

## I. INTRODUCTION

The main cause of heart stroke is due to blockage in arteries. It has many other names such as cardiovascular disease and arterial hypertension [1]. Approximately, there are almost 26 million people around the world affecting with heart disease [2]. The worry point is, this ratio is expected to increase rapidly in coming years, if precautions are not taken efficiently [3]. Apart from making life style healthy and diet control, the right time diagnosing and comprehensive analysis are other essential factors, which can ultimately save the lives [4]. Therefore, this paper has taken a small step towards saving the lives of HF patients and describes a way to improve the performance of diagnosing the patients on the bases of their medical history.

Most of the time patients goes for several tests, which can overburden them with extra physical activities, time, and for sure additional financial charges [5]. As previous studies suggested the common reasons behind heart disease can be unhealthy food, tobacco, excessive sugar, overweight or extra body fat [3], [6]. Whereas the common symptoms can be pain in arms and chest [7]. Noticeably, these reasons are independent from each other; proper analysis on this kind of dataset can improve the process of diagnosing and can assist the heart surgeons as well. Previously, different researches used number of techniques to improve the HF diagnosis process such as Extreme Learning Machine [8], heart disease classification [9], and machine learning classifiers [1].

Therefore, this research attempts to improve the performance of the classifiers by doing experiments using multiple machine-learning models to make better use of the dataset collected from different medical databases.

The paper is further divided into the following sub-sections: the next section describes a comprehensive overview on the use of machine learning models for predicting the heart disease. Section III explains the data overview, number of attributes and description of each attribute. Section IV shows the data preprocessing steps applied in this study. Furthermore, Sections V, VI and VII present the experiment design, implementation, and performances of the classifiers respectively. Finally, in Section VIII the study has been concluded.

## II. MACHINE LEARNING CLASSIFIERS FOR HEART DISEASE PREDICTION

The identification of heart disease in a patient is complex and requires various details, laboratory tests, and equipment [10]. This research is not for replacing the traditional approach use for diagnosing and predicting the chances of heart failure, rather the study attempted to support this process using advanced technologies such as Machine Learning (ML). The ML is not a new technique and has been used several times for different applications.

A cloud based decision support system proposed by [11] in order to helps the heart consultants during diagnosis process. This system used machine-learning methods for predicting the heart disease. The system was proposed to provide the assistance in affordable way, where the system have the capacity to integrate with existing system. In that research clustering method used for categorizing the dataset based on particular groups in unsupervised manner. The author in [12] used an approach by implementing multiple clustering algorithms on heart disease dataset to understand the optimal solution, which can maximize the prediction accuracy ratio. ML approaches proved to be an effective in predicting the heart disease using historical data is further proved in a research conducted using Naïve Bayes, Decision Tree, support vector model and other models [13]. The results indicated that the support vector machine provided the optimal results between other implemented approaches.

Bashir *et al.*, (2019) attempted to improve the performance of heart disease prediction using feature selection approach. Different models such as Naïve Bayes, Random Forest and

other used in the experiment implemented using Rapid Miner tool. The output indicated the high accuracy measured due to feature selection approach [7]. Furthermore, the Extreme Learning Machine techniques using feedforward neural network applied on Cleveland data based on 300 patients, suggested 80% accuracy in forecasting the heart disease in a patient [8]. In another research, the neural network applied using multi-layer perceptron, which also known as supervised learning. The system was proposed to determine the potential heart disease risk in a patient, using patient's historical data [5]. HF ratio using preserved ejection fraction is another work presented using multiple factors like strain rate, hypertensive situation, and velocity, where overall accuracy computed was more than 80% [14].

The main idea behind this discussion is to put stress on how helpful machine learning approaches are to predict the heart disease using medical data. This research is also emphasizing onto overcome the vulnerable situation and proposed a computerized system, so that heart consultants cannot miss any information due to improper reading and understanding of the data. Such a situation described in a research, that most of the heart diseases would not always detect just by doing ECG (a kind of test for diagnosing the working capability of a heart) [15]. Therefore, this kind of research overwhelmed those situations where doctors are puzzled and left behind some evidences. To support them, computerized medical system [16]–[19] with full of functionalities are there, which specially built to assist healthcare industry for the sake of patient's time, money, and most importantly to help the surgeons to save the patient's life. A kind of system proposed by [1] using ML approach for predicting the heart failure using heart sound reports. The study shown another proof that machine learning methods can applied on life saving system such as heart failure detection.

Moreover, a review report presented in a study [20] that described the importance of classification models and further explained the details of the models already implemented in the healthcare industry. The paper highlighted that there are many researches attempted data mining techniques successfully on medical cases. In the same way, another comparative study shown the performances of the multiple classifiers applied on two different tools; Matlab and Weka. Overall, the accuracy of the decision tree, Linear SVM and other models was recorded between 52% to 67.7%, although the accuracy were considerably low [9]. As per the researches discussed above, still different kind of models are providing variation in the prediction score. Thus, the dimensionality reduction and feature engineering can improve the process of data selection, which ultimately can improve the accuracy estimation [21].

TABLE. I. THE ACCURACY MEASURED IN PREVIOUS WORK

| Techniques          | [UCI, Rapid Miner, 2019] [7] | [UCI, Matlab, 2017] [9] | [UCI, Weka, 2017] [9] |
|---------------------|------------------------------|-------------------------|-----------------------|
| Decision Tree       | 82.22%                       | 60.9%                   | 67.7%                 |
| Logistic Regression | 82.56%                       | 65.3%                   | 67.3%                 |
| Random Forest       | 84.17%                       | X                       | X                     |
| Naïve Bayes         | 84.24%                       | X                       | X                     |
| SVM                 | 84.85%                       | 67%                     | 63.9%                 |

In conclusion, the clear research gap found in the previous researches is that, the measured accuracy is not up to the mark. Somewhere, the common machine learning approaches has not used as shown in Table I. Therefore, this section described the comprehensive overview on the previous work accompanied to predict the heart disease in a patient using ML approaches. The idea of this study is to improve the previous work using the selected dataset and ML models, as described in the next section. The performance of each model is discussed in the result section. Although, the models and dataset selected in this research are based on the previous work. The most commonly ML approaches found and used in this study are; Decision Tree, Naïve Bayes, Random Forest, Support Vector Machine, and Logistic Regression. This study used the dataset collected from Kaggle, the data set originally published on UCI data repository for machine learning. Previously, the experiments attempted for predicting the heart disease, the details and accuracy measured is shown in Table I. Finally, in the result section the comparative study is presented to understand the performance of the classifiers in this study and in the previous work.

### III. DATA OVERVIEW

The dataset used in this research is collected from Kaggle platform, the dataset is also known as Heart Disease Dataset [22]. Altogether, the data was the combination of four different database, but only Cleveland data used in this experiment. It is an open dataset, having number of attributes, but for this experiment only fourteen attributes selected as described and suggested by different scholars that selected 14 attributes are most useful to predict the heart disease in a patient [7], [23]. In addition, the database file contains the record of 303 patients. The complete description of each attribute and the number of values for each attribute is shown in the Table II below:



TABLE. II. DATA OVERVIEW AND ATTRIBUTES DESCRIPTION

| S.No. | Attribute Description   | Distinct Values                                |
|-------|---|--|
| 1     | <b>Age</b> - The first attribute is defining the age of the person. [Minimum Age: 29, Maximum Age: 77]  | Multiple values between 29 and 77              |
| 2     | <b>Sex</b> - The attribute number two describes the gender of a person. ["0" means Female and "1" means Male]   | 0, 1   |
| 3     | <b>CP</b> - The third attribute is defining the level of chest pain (CP) a patient suffering from, when reached to the hospital. There are four kind of distinct values defined for this attribute, where each value is describing a level of chest pain.   | 0, 1, 2, 3                                     |
| 4     | <b>RestBP</b> - The next attribute describes about the blood pressure (BP) figure for the patient while admitted to the hospital. [Minimum BP: 94, Maximum BP: 200]   | Multiple values between 94 and 200             |
| 5     | <b>Chol</b> - This column is showing the cholesterol level recorded while admitting the patient in the hospital. [Minimum Chol: 126, Maximum Chol: 564]   | Multiple values between 126 and 564            |
| 6     | <b>FBS</b> - The next attribute is describing the fasting blood sugar level in the patient. It has binary classified values. The values are depending on, if the patient has more than 120mg/dl sugar = 1, if not = 0.  | 0,1  |
| 7     | <b>RestECG</b> - This parameter is showing the result of ECG from 0 to 2. Where each value is showing the severity of the pain.   | 0, 1, 2  |
| 8     | <b>HeartBeat</b> - The maximum value of heartbeat counted at the time of admission [Minimum: 71, Maximum: 202]  | Multiple values between 71 and 202             |
| 9     | <b>Exang</b> - This parameter was used to understand about, does exercise induce angina or not. If yes, the value will be "1", and "0" for not.   | 0, 1   |
| 10    | <b>OldPeak</b> - The next attribute is defining the patient's depression status. It is assigned as different real number values falls between 0 and 6.2.  | Multiple real number values between 0 and 6.2. |
| 11    | <b>Slope</b> - The condition of the patient during peak exercise. This value defined into three segments [Upsloping, Flat, Down sloping]  | 1, 2, 3  |
| 12    | <b>CA</b> : This attribute is showing status of fluoroscopy. It is showing that how many vessels are colored.   | 0, 1, 2, 3                                     |
| 13    | <b>Thal</b> - This parameter is another kind of test required for the patient having chest pain or breathing difficulty. Four kind of values showing the result of Thallium test.   | 0, 1, 2, 3                                     |
| 14    | <b>Target</b> - This is the last column in the dataset. This Target column is also known as Class column or Label column. As this column describes the number of categories, (classes) defined in the data file. As per the dataset taken in this experiment. There are two different types of classes (0,1), where "0" means there is no chances of Heart Failure, whereas "1" imply that there are strong chances of heart failure in a patient. The value "0" and "1" is based on the other 13 parameters described in this dataset above. | 0, 1   |

#### IV. DATA PREPROCESSING

Data preprocessing is an essential step use to clean the data and make it useful for any experiment associated with machine learning or data mining [24]. In this study, multiple preprocessing steps applied on the selected dataset. Firstly, the size of the dataset was found not enough for the implementation of machine learning approaches. As described by [25] the size of the dataset for machine learning implementation may create biasness and would also effect on the results generated through machine learning models. Therefore, for each attribute using minimum and maximum values, the random number generation technique applied to generate random values for each column [26]. This helped us to enhance the capacity of the data, which has created the positive impact on the performance of the classifier as can be seen in the results section. In conclusion, the data have increased the volume by three times.

Secondly, using rapid miner, data cleaning step applied to find out missing values and noisy data values. The data has some missing values which has been imputed using K Nearest Neighbor (KNN) method. As KNN method is proved to be a useful method for missing data imputation [27]. In addition, the outlier detection methods used to estimate the noise in the data. The data has not found noisy values and no outlier detected in the dataset. The outlier detection applied using rapid miner's operator with distances method [28]. In order to check the other discrepancies in the dataset, data discretization, transformation and binning techniques were applied as well.

The next step was to transform the data values into appropriate data type. In this study, multiple models were applied to check the performance of the prediction accuracy. Therefore, it was essential to convert the data type of some attributes as per the required format based on the model specification. Mainly, the experiment design built using binary classification, which is the process of categorizing the dataset according to predefined classes, which has been widely used in applying machine learning algorithms [29]. Hence, the same binary classification was used in the given dataset, where the binary classification provided the better way to show the performance accuracy of the selected classifier in this study.

Most of the attributes were nominal in the selected dataset i.e. Slope, CA, Thal, and CP. For example, Thal attribute is describing the value of the Thallium test based on the four predefined values (0, 1, 2, 3). In the same way, CP was another independent attribute in the dataset, which highlighting the condition of the chest pain using (0, 1, 2, 3) in the patient at the time of admitting in the hospital, where the "0" means normal and "3" means the worst condition. The Target column in the dataset that also known as class attribute has two types of predefined classes known as "0" and "1". This attribute represent the overall condition of the patients using other independent variables. Whereas the value "0" means that patient does not have chances of heart failure, and "1" means that patient has high probability of heart failure. For example, using a value of all independent variables, if a patient has high blood pressure, sugar and contain high values

in Thallium test can have chances of heart failure and vice versa.

## V. THE EXPERIMENT PREPARATION

This research used five different models to predict the heart disease using collected dataset. The performance of each classifier and comparison with previous work is presented in the next section. After successful implementation of the data preprocessing step, in this section discussed about the selected models, their descriptions and overall methodology used for the experiment. The work presented in this study was a sequel of the research presented by [7], which used the same dataset and implementation tool. That research reduced the number of attributes to 14. The number of records they used for the experiment were 300. The 5-fold cross-validation technique was applied to improve the accuracy and reduce the chances of duplication in record selection. Overall, the experiment computed the accuracy from 82% to 85%.

In this work, the target was to improve the accuracy of the model; therefore different amendment was done in the experiment design. For example, data expansion, 10-fold cross validation, execution of all model at the same time to understand the actual differences in the accuracy measurement. Following are the procedural steps of designed methodology applied in this research.

### Algorithm: Predicting Heart Failure Disease

```
Step 1: Selection of dataset/Data Preprocessing
{
    Data overview
    Detect and remove outliers
    Detect and impute missing data
    Data enhancement using random number generators
    Applying suitable normalization techniques
}
Step 2: Model Selection
{
    Understanding data value (classes)
    Machine learning model selection
}
Step 3: Model Implementation using Rapid Miner
{
    Import Data
    Implementing all models together using Rapid Miner
}
Step 4: Performance Measurement
{
    Calculate Accuracy using "Performance" operator
    Analyzing the result through Confusion Matrix
}
Step 5: Result Comparison
{
    Comparing the accuracy among all models
    Comparing the result with previous work
    Calculate final output
}
```

As discussed above that five machine learning models used for predicting the heart disease in a patient and to analyze up to optimal performance among all. The short description of each model explained in this section.

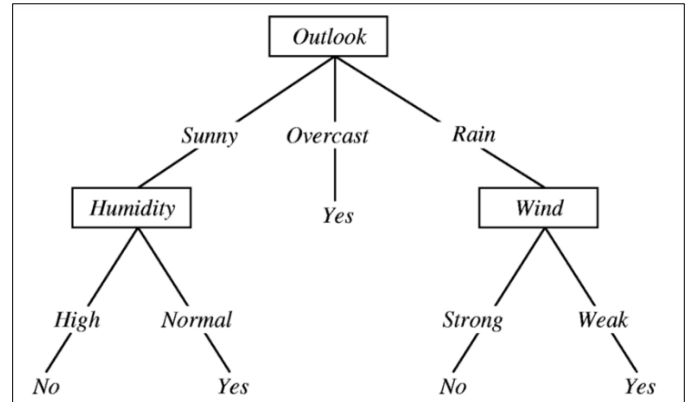


Fig. 1. A Decision Tree Example [31].

### A. Decision Tree

It's a tree like classification model, which built a structure consisting of branches and nodes on the bases of evidence collected for each attributes during model learning phase [30]. The decision tree's branches and nodes connect according to the number of entities described in the dataset. The forwarding process uses the number of values dedicated for each attribute. Furthermore, following the rules describe on each branch and node it reached to the decision for each transaction. Finally, according to the decision node the class label will be assigned to the record. This procedure is iterative and repeat till each transaction got a class category. Therefore, this algorithm converts the attributes into a branches and nodes, and select one of the attributes as decision node, which also known as class label. The class label in rapid miner can select while importing the dataset. A decision tree example is shown in Fig. 1.

### B. Naïve Bayes

The next classifier used in this study is known as Naïve Bayes. It is also a supervised learning classification model, which classify the data by computing the probability of independent variables. After calculating the probability of each class, the high probability class do assign for the complete transaction [7]. Naïve Bayes is a common approach used to predict classes for different types of dataset such as educational data mining [32] and medical data mining [18]. This model also useful for classifying different kind of dataset like sentiment analysis [33] and virus detection [34]. It works by using the values for independent variables and predict a pre-defined class for each record. It measures the probability of A given that B as shown in following equation. Then working on finding out the distinct class for each attributes, in this scenario all other variables are not dependent on each other [18]. Naïve Bayes uses the following equation for measuring the probability:

$$P\left(\frac{A}{B}\right) = \frac{P\left(\frac{B}{A}\right)P(A)}{P(B)} \quad [34]$$

### C. Random Forest

Random forest is the next model selected and implemented in this research. As this model is from classification family, therefore it is also known as supervised learning algorithm. During the learning phase, this model first generates multiple random trees called a forest [35]. For example, a dataset contains “x” number of attributes, it first selects some feature randomly known as “y”. Using all features; (i.e. “y”), it produces nodes using best rift method. Furthermore, the algorithm will work for creating a complete forest by repeating the previous steps. Then during the prediction process, the algorithm tries to combine the trees using estimated outcome and voting procedure [36]. The purpose of merging the random trees through voting in a forest is to opt out the highest forecasted tree, which can enhance the prediction accuracy for future data.

### D. Logistic Regression

Logistic regression is another kind of classification model, which learn and predict the parameters in the given dataset using regression analysis [7]. The learning and prediction processes are based on measuring the probability of binary classification. Logistic regression model requires class variable that should be binary classified. Likewise, in this dataset the “target” column has the two type of binary numbers, “0” for the patient who has no chances of heart failure, and “1” for the patients who has predicted as heart failure patients. On the other side, the independent variables can be of binary classified, nominal or polynomial types [37]. The equation of logistic regression is as follows:

$$\text{Logit}(p) = \ln\left(\frac{p}{1-p}\right) = \frac{\text{prob. of presence of characteristics}}{\text{prob. of absence of characteristics}} \quad [37]$$

### E. SVM

The final machine learning algorithm used in this research is known as support vector machine. This is also called a supervised machine learning model where the classes in the dataset should be pre-defined [7]. It works by categorizing the objects in the given dataset according to the predefined classes. It classify the transactions by assigning one or more classes to maximize the performance in accuracy [38]. Previously, SVM has implemented on medical data application to predict the accurate class for the heart disease patient [39]. Another model proposed by [40] to predict a class using attribute extraction method.

## VI. IMPLEMENTATION

This research used five machine learning models, using predictive approach to forecast the chances of heart failure in a patient admitted in the hospitals. Therefore, as described above the dataset taken from Kaggle having patients’ records, which have been collected from multiple locations. The dataset has a list of 14 attributes, which collectively used for diagnosing the heart disease in a patient. For experiment execution, the Rapid Miner tool used in this study. Rapid Miner, is an open source software, which provides a wide range of pre-programmed operators for numerous tasks related to machine learning, data mining, statistical and others [41].

The proposed algorithm as presented in previous section, this study used five ML models; Naïve Bayes, Decision Tree, Random Forest, Logistic Regression, and SVM. At the first step of implementation, the training dataset used to learn the ML model. For this, the dataset was imported using “Read\_CSV” operator in Rapid Miner. Furthermore, to connect the dataset with ML models, it was copied five times. To avoid similar values selection during model learning and testing phase, 10-fold Cross Validation operator was used. It helps to divide the data into  $k$  equal subsets and to give a chance for each subset to be a part of training and testing phase. The working of cross validation operator considers as an efficient, as it repeats the learning phase  $k$  times, where every time the testing data selection is different from previous. Finally, it repeats the experiment  $k$  times and uses the average results. The cross validation is widely used operator for learning and testing purpose. It provides the data selection in four different ways; liner sampling, shuffled sampling, stratified sampling, and automatic [42]. Whereas, the stratified sampling is used in this study. The experiment execution in rapid miner is shown in Fig. 2.

As shown in Fig. 2, the model name is representing on each cross-validation operator. This operator computes the statistical analysis and model performance of a learning and testing phase. The cross-validation operator is also called a nested operator, which have two types of sub-processes; training sub-process and testing sub-process. The training sub-process is used to handle the training session by learning the model through given dataset and model, while testing sub-process is used to validate the model and estimate the performance of the model, which also known as model accuracy. For clear understanding about sub-processes, the validation operator’s for Naïve Bayes is shown in Fig. 3, while the remaining operators used the same strategy. To maintain the experiment quality and to know the exact accuracy, all models connected with the same dataset and executed at the same time.

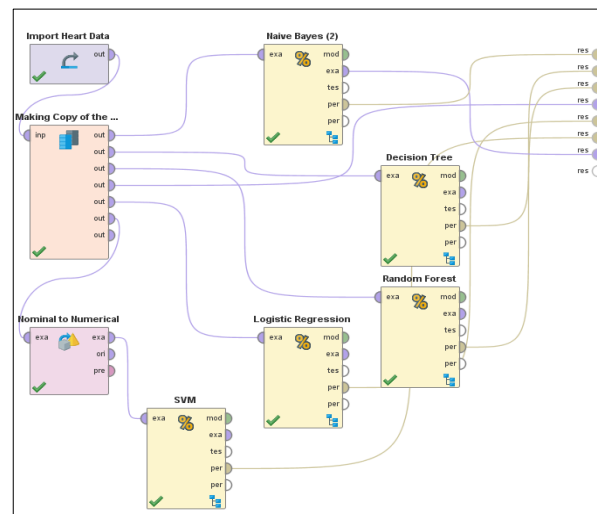


Fig. 2. The Process of Model Implementation in Rapid Miner.

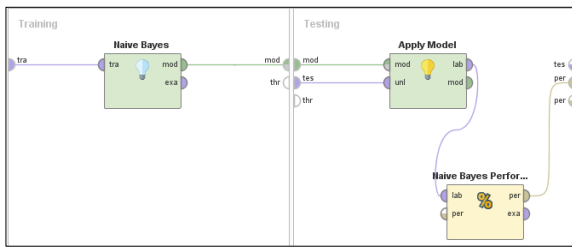


Fig. 3. Training and Testing Sub-Processes.

### VII. DISCUSSION ON MODEL PERFORMANCES AND COMPARISONS

The model performance in the form of confusion matrix is displayed in Table III. A confusion matrix is a table used for describing the performance of a classifier that executed on given test data where the “True” values are considered known data values. In this table, the True Class (1) means the known values for the class category (1); the patients having chances of heart failure. On the other side, True Class (0) denotes the known values for class category (0); the patients showing healthy sign. In the same way, the rows values illustrating the prediction computed for both classes. Accordingly, based on the True values and predicted values, the class precision and class recall values computed and presented in the table. The class recall and class precision values are helpful to identify the overall accuracy of the classifier. As per the displayed values in the table, the precision and recall values for decision tree classifier are maximum, while Naïve Bayes computed minimum among all.

There were total 1013 number of patient’s record in the given dataset. For example, the first classifier Naïve Bayes is showing that 434 patients were known in the dataset as heart failure patient and predicted correctly under the class category (1). However, 57 records were initially belonging to heart failure patients but predicted wrongly under the category (0); non-heart failure patient. In the same way, originally total 522 patients were non-heart failure patients and 450 were predicted correctly and 72 estimations recorded as wrong. Overall, the Naïve Bayes classifier performance was the lowest and the performance of Decision Tree classifier computed highest, among all classifier.

Table IV presented the comparison of the experiment’s results conducted in this study with the previous work. Overall, every classifier has shown good performance in this study as compare to the previous work. According to the table, the accuracy of the decision tree model was the highest between all models, while the performance of the Naïve Bayes has shown the lowest accuracy in this study. The best two model in our experiment are known as SVM and decision tree. Every model significantly enhanced the performances in previous work and shown the satisfactory enhancement, which is greater than 85%.

In comparison with the previous work illustrated in the third column of Table IV, the research applied the experiment using five algorithms [7]. That research used the same dataset (UCI) with feature selection approach. The accuracy of our model has improved the performance of the classifiers. For example, Naïve Bayes accuracy increased 3%, Logistic

Regression and Random Forest enhanced 5%, Decision Tree improved the accuracy ratio 11%, and lastly the SVM machine learning classifier increased 8%. However, in previous work, the study also used the same platform, which is Rapid Miner. But accuracy performance augmented in our work might be because of using 10-fold cross validation, while the previous work used 5-fold cross validation approach. More iteration during the learning phase can help to generate more accurate results. Another possible reason behind the positive enrichment in the accuracy is the size of the dataset, which has been amplified in this study as discussed in data overview section. It highlights that the large size of the dataset can create positive impact on classifier accuracy as it enhances the learning process.

TABLE III. MODEL PERFORMANCES THROUGH CONFUSION MATRIX

| Naïve Bayes         | True (1) | True (0) | Class Precision |
|---------------------|----------|----------|-----------------|
| Prediction (1)      | 434      | 72       | 85.77%          |
| Prediction (0)      | 57       | 450      | 88.76%          |
| Class Recall        | 88.39%   | 86.21%   |                 |
| Decision Tree       | True (1) | True (0) | Class Precision |
| Prediction (1)      | 458      | 36       | 92.71%          |
| Prediction (0)      | 33       | 486      | 93.64%          |
| Class Recall        | 93.28%   | 93.10%   |                 |
| Random Forest       | True (1) | True (0) | Class Precision |
| Prediction (1)      | 436      | 55       | 88.80%          |
| Prediction (0)      | 55       | 467      | 89.46%          |
| Class Recall        | 88.80%   | 89.46%   |                 |
| Logistic Regression | True (1) | True (0) | Class Precision |
| Prediction (1)      | 435      | 72       | 85.80%          |
| Prediction (0)      | 56       | 450      | 88.93%          |
| Class Recall        | 88.59%   | 86.21%   |                 |
| SVM                 | True (1) | True (0) | Class Precision |
| Prediction (1)      | 475      | 62       | 88.45%          |
| Prediction (0)      | 16       | 460      | 96.64%          |
| Class Recall        | 96.74%   | 88.12%   |                 |

TABLE IV. PERFORMANCE COMPARISON WITH PREVIOUS STUDIES

| Technique           | This Study | [UCI, Rapid Miner, 2019] [7] | [UCI, Matlab, 2017] [9] | [UCI, Weka, 2017] [9] |
|---------------------|------------|------------------------------|-------------------------|-----------------------|
| Decision Tree       | 93.19%     | 82.22%                       | 60.9%                   | 67.7%                 |
| Logistic Regression | 87.36%     | 82.56%                       | 65.3%                   | 67.3%                 |
| Random Forest       | 89.14%     | 84.17%                       | X                       | X                     |
| Naïve Bayes         | 87.27%     | 84.24%                       | X                       | X                     |
| SVM                 | 92.30%     | 84.85%                       | 67%                     | 63.9%                 |

Table IV, column number four and five are related to the another research conducted for predicting and classifying the heart disease patient's records [9]. They used the same dataset "UCI", whereas the main idea of that research was to do the experiment in two different platform; i.e. Matlab and Weka, and then compare the results from both perspectives. Decision tree, logistic regression and SVM were the similar models used in both researches. Altogether, it is evident from the above table that in our study, the decision tree classifier has increased the accuracy more than 30% from the previous work. In the same way, logistic regression and SVM also outperform and were computed the better score than previous work. It illustrates that the performance of the Rapid miner has shown better accuracy and performance of the classifiers.

### VIII. CONCLUSION AND FUTURE WORK

The ratio of heart failure patients has been increasing every day. To overcome this dangerous situation and deteriorate the chances of heart failure disease, there is a need of a system that can generate rules or classify the data using machine learning approaches. Therefore, this research discussed, proposed and implemented a machine learning model by combining five different algorithms. Rapid miner is the tool used in this research, which computed the high accuracy than Matlab and Weka tool. In comparison with the previous researches, this study has shown significant improvement and high accuracy than previous work. As far as UCI dataset concerns, the dataset needs to be amplified. As the main limitation in this work is the small size of the dataset. The dataset has limited number of patient's records; therefore, the dataset was augmented using appropriate techniques. In future, the results indicated that the system can be useful and helpful for the doctors and heart surgeons for timely diagnoses the chances of heart attack in a patient.

#### REFERENCES

- [1] M. Gjoreski, A. Gradišek, M. Gams, M. Simjanoska, A. Peterlin, and G. Poglajen, "Chronic heart failure detection from heart sounds using a stack of machine-learning classifiers," in Proceedings - 2017 13th International Conference on Intelligent Environments, IE 2017, 2017, pp. 14–19.
- [2] G. Savarese and L. Lund, "Global Public Health Burden of Heart Failure," *Card. Fail. Rev.*, vol. 3, no. 1, 2017.
- [3] E. J. Benjamin, P. Muntner, and et al. Alonso, Alvaro, "Heart Disease and Stroke Statistics—2019 Update: A Report From the American Heart Association," *Circulation*, vol. 139, no. 10, 2019.
- [4] M. Ramaraj and T. A. Selvadoss, "A Comparative Study of CN2 Rule and SVM Algorithm and Prediction of Heart Disease Datasets Using Clustering Algorithms," *Netw. Complex Syst.*, vol. 3, no. 10, pp. 1–6, 2013.
- [5] A. Gavhane, G. Kokkula, I. Pandya, and P. K. Devadkar, "Prediction of Heart Disease Using Machine Learning," in Proceedings of the 2nd International Conference on Electronics, Communication and Aerospace Technology, ICECA 2018, 2018, pp. 1275–1278.
- [6] H. Murthy and M. Meenakshi, "Dimensionality reduction using neuro-genetic approach for early prediction of coronary heart disease," in International Conference on Circuits, Communication, Control and Computing (I4C), 2014, pp. 329–332.
- [7] S. Bashir, Z. S. Khan, F. H. Khan, A. Anjum, and K. Bashir, "Improving Heart Disease Prediction Using Feature Selection Approaches," in 16th International Bhurban Conference on Applied Sciences and Technology (IBCAST), 2019, pp. 619–623.
- [8] S. Ismaeel, A. Miri, and D. Chourishi, "Using the Extreme Learning Machine (ELM) technique for heart disease diagnosis," in 2015 IEEE Canada International Humanitarian Technology Conference, IHTC 2015, 2015, pp. 1–3.
- [9] S. Ekiz and P. Erdogmus, "Comparative study of heart disease classification," in 2017 Electric Electronics, Computer Science, Biomedical Engineerings' Meeting, EBBT 2017, 2017, pp. 1–4.
- [10] K. Chen, A. Mudvari, F. G. G. Barrera, L. Cheng, and T. Ning, "Heart Murmurs Clustering Using Machine Learning," in 2018 14th IEEE International Conference on Signal Processing (ICSP), 2018, pp. 94–98.
- [11] E. Maini, B. Venkateswarlu, and A. Gupta, "Applying Machine Learning Algorithms to Develop a Universal Cardiovascular Disease Prediction System," in International Conference on Intelligent Data Communication Technologies and Internet of Things, 2018, pp. 627–632.
- [12] S. Kodati, R. Vivekanandam, and G. Ravi, "Comparative Analysis of Clustering Algorithms with Heart Disease Datasets Using Data Mining Weka Tool," in Soft Computing and Signal Processing, Singapore: Springer, 2019, pp. 111–117.
- [13] K. Deepika and S. Seema, "Predictive analytics to prevent and control chronic diseases," in 2016 2nd International Conference on Applied and Theoretical Computing and Communication Technology (iCATecT), 2016.
- [14] M. Tabassian et al., "Diagnosis of Heart Failure With Preserved Ejection Fraction: Machine Learning of Spatiotemporal Variations in Left Ventricular Deformation," *J. Am. Soc. Echocardiogr.*, vol. 31, no. 12, pp. 1272–1284, 2018.
- [15] T. R. Reed, N. E. Reed, and P. Fritzon, "Heart sound analysis for symptom detection and computer-aided diagnosis," *Simul. Model. Pract. Theory*, vol. 12, no. 2, pp. 129–146, 2004.
- [16] P. Amnarayan et al., "Measuring the Impact of Diagnostic Decision Support on the Quality of Clinical Decision Making: Development of a Reliable and Valid Composite Score," *J. Am. Med. Informatics Assoc.*, vol. 10, no. 6, pp. 563–572, 2003.
- [17] C.-S. Lee and M.-H. Wang, "A fuzzy expert system for diabetes decision support application.," *IEEE Trans. Syst. MAN, Cybern. B Cybern.*, vol. 41, no. 1, pp. 139–153, 2011.
- [18] C. B. Rjeily, G. Badr, E. Hassani, A. H., and E. Andres, "Medical Data Mining for Heart Diseases and the Future of Sequential Mining in Medical Field," in Machine Learning Paradigms, 2019, pp. 71–99.
- [19] K. Shameer, K. W. Johnson, B. S. Glicksberg, J. T. Dudley, and P. P. Sengupta, "Machine learning in cardiovascular medicine: are we there yet?," *Heart*, vol. 104, no. 14, pp. 1156–1164, 2018.
- [20] D. Tomar and S. Agarwal, "A survey on Data Mining approaches for Healthcare," *Int. J. Bio-Science Bio-Technology*, vol. 5, no. 5, pp. 241–266, 2013.
- [21] V. V. Ramalingam, A. Dandapath, and M. Karthik Raja, "Heart disease prediction using machine learning techniques: a survey," *Int. J. Eng. Technol.*, vol. 7, no. 2.8, pp. 684–687, 2018.
- [22] UCI, "Heart Disease Data Set." [Online]. Available: <https://www.kaggle.com/ronitf/heart-disease-uci>. [Accessed: 20-Apr-2019].
- [23] S. A. Tiwaskar, R. Gosavi, R. Dubey, S. Jadhav, and K. Iyer, "Comparison of Prediction Models for Heart Failure Risk: A Clinical Perspective," in Fourth International Conference on Computing Communication Control and Automation (IC3CAA), 2019, pp. 1–6.
- [24] F. Al-Mudimigh, A. S., Ullah, Z., & Saleem, "A framework of an automated data mining systems using ERP model.," *Int. J. Comput. Electr. Eng.*, vol. 1, no. 5, 2009.
- [25] A. L'Heureux, K. Grolinger, H. El Yamany, and M. Capretz, "Machine Learning with Big Data: Challenges and Approaches," *IEEE Access*, 2017.
- [26] D. DiCarlo, "Random Number Generation: Types and Techniques," 2012.
- [27] R. Pan, T. Yang, J. Cao, K. Lu, and Z. Zhang, "Missing data imputation by K nearest neighbours based on grey relational structure and mutual information," *Appl. Intell.*, vol. 43, no. 3, 2015.
- [28] R. Miner, "Outlier Detection Using Rapid Miner." [Online]. Available: [https://docs.rapidminer.com/latest/studio/operators/cleansing/outliers/detect\\_outlier\\_distances.html](https://docs.rapidminer.com/latest/studio/operators/cleansing/outliers/detect_outlier_distances.html). [Accessed: 20-Apr-2019].

- [29] R. Kumari and S. K. Srivastava, "Machine Learning: A Review on Binary Classification," *Int. J. Comput. Appl.*, vol. 160, no. 7, 2017.
- [30] R. S, P. Raj H. R., A. C, and V. K, "Medical data mining and analysis for heart disease dataset using classification techniques," in *National Conference on Challenges in Research & Technology in the Coming Decades National Conference on Challenges in Research & Technology in the Coming Decades (CRT 2013)*, 2013, pp. 1.09-1.09.
- [31] J. Shubham, "Decision Trees in Machine Learning," *Medium*, 2018.
- [32] F. Razaque, N. Soomro, S. Ahmed, S. Soomro, J. A. Samo, and H. Dharejo, "Using Naïve Bayes Algorithm to Students' bachelor Academic Performances Analysis," in *Engineering Technologies and Applied Sciences (ICETAS), 2017 4th IEEE International Conference*, 2017, pp. 1-5.
- [33] L. Dey, S. Chakraborty, A. Biswas, B. Bose, and S. Tiwari, "Sentiment analysis of review datasets using naive bayes and k-nn classifier," *arXiv Prepr. arXiv*, vol. 16, no. 10, 2016.
- [34] O. Qasim and K. Al-Saedi, "Malware Detection using Data Mining Naïve Bayesian Classification Technique with Worm Dataset," *Int. J. Adv. Res. Comput. Commun. Eng.*, vol. 6, no. 11, pp. 211-213, 2017.
- [35] N. Donges, "The Random Forest Algorithm," *Towards Data Science*, 2018.
- [36] S. S. Bashar, M. S. Miah, A. H. M. Z. Karim, A. Al Mahmud, and Z. Hasan, "A Machine Learning Approach for Heart Rate Estimation from PPG Signal using Random Forest Regression Algorithm," in *2019 International Conference on Electrical, Computer and Communication Engineering (ECCE)*, 2019, pp. 1-5.
- [37] H. DW Jr, L. S, and S. RX, *Applied Logistic Regression*, 3rd ed. New Jersey: John Wiley & Sons, 2013.
- [38] V. Vapnik, *Statistical Learning Theory*. New York: Wiley, 1998.
- [39] P. Tabesh, G. Lim, S. Khator, and C. Dacso, "A support vector machine approach for predicting heart conditions," in *Proceedings of the 2010 Industrial Engineering Research Conference*, 2010, p. 5.
- [40] K. M, S. F, Z. Z, and P. N, "Predicting MOOC dropout over weeks using machine learning methods," in *Proceedings of the EMNLP 2014 Workshop on Analysis of Large Scale Social Interaction in MOOCs*, *aclweb.org*, 2014, pp. 60-65.
- [41] R. M. Team, "Rapid Miner." [Online]. Available: <https://rapidminer.com/>.
- [42] Rapid Miner, "Cross Validation Operator." [Online]. Available: [https://docs.rapidminer.com/latest/studio/operators/validation/cross\\_validation.html](https://docs.rapidminer.com/latest/studio/operators/validation/cross_validation.html). [Accessed: 01-Apr-2019].

# Hyperparameter Optimization in Convolutional Neural Network using Genetic Algorithms

Nurshazlyn Mohd Aszemi<sup>1</sup>, P.D.D Dominic<sup>2</sup>

Department of Computer and Information Sciences, Universiti Teknologi Petronas, Seri Iskandar, Perak, Malaysia

**Abstract**—Optimizing hyperparameters in Convolutional Neural Network (CNN) is a tedious problem for many researchers and practitioners. To get hyperparameters with better performance, experts are required to configure a set of hyperparameter choices manually. The best results of this manual configuration are thereafter modeled and implemented in CNN. However, different datasets require different model or combination of hyperparameters, which can be cumbersome and tedious. To address this, several works have been proposed such as grid search which is limited to low dimensional space, and tails which use random selection. Also, optimization methods such as evolutionary algorithms and Bayesian have been tested on MNIST datasets, which is less costly and require fewer hyperparameters than CIFAR-10 datasets. In this paper, the authors investigate the hyperparameter search methods on CIFAR-10 datasets. During the investigation with various optimization methods, performances in terms of accuracy are tested and recorded. Although there is no significant difference between propose approach and the state-of-the-art on CIFAR-10 datasets, however, the actual potency lies in the hybridization of genetic algorithms with local search method in optimizing both network structures and network training which is yet to be reported to the best of author knowledge.

**Keywords**—Hyperparameter; convolutional neural network; CNN; genetic algorithm; GA; random search; optimization

## I. INTRODUCTION

Human are capable of recognizing things both environment and object within a second. This recognition skills are trained since human are young. Similarly, if the computers are able to recognize or classifying object and environment by looking for low-level features such as edges and curves, then it can build more abstract concepts of what it recognizes through a series of convolutional layers. Hence, image recognition and classification in the neural network are called Convolutional Neural Network (CNN).

Building CNN requires a set of configurations which is external to the data and manually tune by the machine learning researcher. The variable of the network structure and the network trained of CNN are known as hyperparameters [1]. Finding a set of hyperparameters that gives an accurate model in a reasonable time is also part of the hyperparameter optimization problem [2]. Hyperparameter optimization is a problem that identifies a good model of hyperparameter [3] or a problem of optimizing a loss function over a graph-structured configuration space [4]. Testing all the possible set model of hyperparameter can become computationally expensive [5].

Therefore, the need for an automated and structured way of searching is increasing, and hyperparameter space, in general, is substantial.

Numerous works have been done in optimizing the hyperparameters [3], [6]–[8]. Other optimization methods that have been applied using evolutionary algorithms (EAs) as mentioned in [5]. Bochinski et al [5] defines hyperparameters as the configuration of the network structure which will lead to an optimization problem in finding the optimal configuration of the CNN. Others who have applied evolutionary algorithms are [9] and [10]. However, [11] claims that none of the approaches consider the impact of setting up the hyperparameter which in assumptions that: (1) Hyperparameter setting does not matter, however, selecting among default implementations is sufficient and (2) hyperparameter value may have a significant impact on performance and should always be optimized.

Very less research has been done to validate these assumptions since the optimization of hyperparameter is theoretically and practically significant [11]. Due to these flaws, the idea of automating hyperparameter search is getting attention in machine learning [12]. This means that most common optimization has been done using the random search [3] and a combination of grid search and manual search [13]. Ozaki [14] claim that most people do not have sufficient computing resources and are unwilling to adjust the hyperparameters that use difficult optimization method. Author acknowledge that there is some research that applies genetic algorithms such as [15], [16] on tuning the hyperparameters of the network and the structure of the system [17] and [18]. However, the work aims to hybridize genetic algorithms with local search method in optimizing the CNN hyperparameters that both are of network structures and network trained which is not studied in these prior works.

To the best of author knowledge, there are no approaches that hybridized genetic algorithms with local search method in optimizing both network structures and training algorithms in CNN. As a start, a trial of an experiment on a random search method will be conducted to testify the performance as per said in [3]. The objectives of this work are twofold: (1) to investigate the hyperparameter search method on CIFAR-10 datasets and (2) to perform benchmarking on CIFAR-10 datasets with the state-of-the-art accuracy.

The remainder of this paper is organized as follows. In Section II, the related work in the area of CNNs and GA is provided. Section III presents the background and Section IV

lay out the experimental setup. Experimental results are discussed in Sections V and VI. Finally, the paper is concluded, and future work is recommended in Section VII.

## II. RELATED WORK

In this section, the related works are presented and discussed as follows.

### A. Search Optimization Method

Grid search method is a trial and error method for every hyperparameter setting on the specific range of values. The advantage of using a grid search is that it can be easily parallelized [3]. Researchers and practitioners will specify the boundary and steps between values of hyperparameters which will form a grid of configurations [19]. However, if one fails, the rest of the jobs will fail accordingly. In usual cases, machine learner will use a limited grid and then extend which will make the grid more efficient to configure the best while continually searching for the new grid [19]. Four hyperparameters will become impractical as the number of functions to evaluate will increase with adding parameter; this is due to the limitation on dimensionality [20].

Random search method samples the hyperparameter space 'randomly'. Based on [3], the random search has more benefits than grid search regarding the application which can still use even the cluster of the computer fail. It allows practitioners to change the 'resolution' on the go and it is feasible to add new trials to the set or even ignore the fail test. Simultaneously, the random search method can stop any time, and it will form a complete experiment it can be carried out synchronously [21]. Furthermore, a new trial can be added to the experiment without jeopardizing if more computers become available [22].

Another latest development in hyperparameter tuning is using Bayesian optimization. It uses distribution over functions which is known as Gaussian Process. To train using Gaussian Process; fitting it to given data is essential as it will generate function closely to observe data. In Bayesian optimization, the Gaussian process will optimize the expected improvement and surrogate the model which is the probability of the new trial and will improve the current best observation. The highest expected improvement will be used next, and expected improvement can be calculated at any point in the search space. Widespread implementation of Bayesian optimization includes spearmin that uses Gaussian process [23]. However, Bergstra et al. [3] claim that the method of Bayesian optimization is limited; as it works on high dimensional hyperparameter and it became very computationally expensive. Therefore, it has poor performance.

### B. Genetic Algorithm Optimization

The difference between genetic algorithms and evolutionary algorithms is that the genetic algorithms rely on the binary representation of individuals (an individual is a string of bits) due to which the mutation and crossover are easy to be implemented. Such operations produce candidate values that are outside of allowing searching space. In contrast, the evolutionary algorithms rely on customized data structures and

need appropriately craft mutation and crossover which this will heavily dependents on the problem at hand [24]. The author in [25] has been mentioned that Genetic algorithms can be used when there is no information about gradient function at evaluated points. It can achieve good results when there is several local minima or maxima. Unlike any other search method, the function is not determined in a single place but simultaneously in different areas. They can be carried out in several processors since the calculations of the function on all points of a population are independent of each other [26]. Furthermore, they can be parallelized with little effort which makes many paths to the optimum processed in parallel. In [25], it has been mentioned that genetic algorithm has advantages over local methods as they do not remain trapped in suboptimal local maximum or minimum.

## III. FOUNDATION

### A. Hyperparameters Optimization

The optimization of hyperparameter can be simplified as how many function evaluations will perform on every optimization to select the best hyperparameter in that model. Besides, optimization can be explained in a simple manner which "given a function that accepts inputs and returns a numerical output, how can it efficiently find the inputs, or parameters, that maximize the function's output?" [27]. Hence, upon tuning or optimizing the hyperparameter, author will take input as a function to the hyperparameter model and the output as the measurement on the model performance. Consequently, the hyperparameter optimization problem setup can be formally defined as [2]:

- $\mathcal{A}$  machine learning algorithm  $\lambda$  is a mapping  $\mathcal{A}_\lambda$
- $\mathcal{D} \rightarrow \mathcal{M}$  where  $\mathcal{D}$  is the set of all datasets and  $\mathcal{M}$  is the space of all models
- $\lambda \in \Lambda$  is the chosen hyperparameter configuration with  $\Lambda = \Lambda_1 \times \dots \times \Lambda_p$  being the  $p$ -dimensional hyperparameter space.
- The learning algorithm estimates a model  $M_\lambda \in \mathcal{M}$  that minimizes a regularized loss function  $\mathcal{L}$  (e.g. misclassification rate):

$$\mathcal{A}_\lambda(\mathcal{D}^{(train)}) := \arg \min_{\mathcal{M}_\lambda \in \mathcal{M}} \mathcal{L}(\mathcal{M}_\lambda, \mathcal{D}^{(train)}) + \mathcal{R}(\mathcal{M}_\lambda, \lambda) \quad (1)$$

The task of hyperparameter optimization is to find the optimal hyperparameter configuration  $\lambda$  using a validation set,

$$\lambda^* := \arg \min_{\lambda \in \Lambda} \mathcal{L} \left( \frac{\mathcal{A}_\lambda(\mathcal{D}^{(train)})}{\mathcal{D}^{(valid)}} \right) \quad (2)$$

The  $\mathcal{F}$  will be the miscalculation rate or error rate. The hyperparameter space all possible values that are usually defined as acceptable bounds for each hyperparameter and the number of the hyperparameter is the dimension of the function [28].

Referring to [29], optimizing the hyperparameter require knowledge on the relationship between the settings and the model performance. It will first run a trial to collect performance on several configurations and then will make an



inference which will decide what configuration will be applied next. The purpose of optimizing is to minimize the number of trials on hyperparameter while finding the optimum model [29]. Hence, author can consider the process as sequential and not parallel.

### B. Convolutional Neural Network

Convolutional neural network gain advantages over inputs that consist of images which neurons are arranged in 3 dimensions of width, height, and depth [30]. For examples, CIFAR-10 datasets have volume dimensions of 32x32x3 (width, height, depth). Fig. 1 describes the visualization between a regular three-layer neural network with CNN. A regular 3-layer neural network consists of input – hidden layer 1 – hidden layer 2 – output layer. CNN arrange the neurons into three dimensions of width, height, and depth. Each layer will transform the 3D input to 3D output volume of neuron activations. Hence, the red input layer holds the image, the dimensions of the image will be width and height, and the depth will be the three RGB (red, green and blue) channels.

CNN architectures build in three main types of sequence layers: Convolutional Layer, Pooling Layer, and Fully-Connected Layer. A simple CNN for CIFAR-10 datasets can have the architecture of [INPUT-CONV-RELU-POOL-FC]. As per describe [30].

- INPUT will hold on the raw pixel value of images.
- CONV will compute the output of the neurons.
- RELU stands for Rectified Linear Unit is an activation function that converts all negative pixel values to 0.
- POOL will pass over sections of the image and pool them into the highest value in the section.
- FC (fully-connected) layer will calculate the class scores such as 10 categories in CIFAR-10, and finally, each neuron will be connected to all number in the previous volume.

However, not all layers are in the same sequence as [INPUT-CONV-RELU-POOL-FC]. Some layers have CONV/FC and do not need RELU/POOL. Others require CONV/FC/POOL but not RELU and vice versa. Fig. 2 shows the example of CNN architecture from small VGG Net [31]. The 3D volumes are sliced into rows as it is manageable to see the architecture. For examples, the input can be taken as raw images of the car that eventually will break down into sequences of convolutional layers that will compute and produce the output into their classes. The last layer holds the score of each class which is labeled. The architecture shown is a tiny VGG Net [31]. There are several CNN architectures that have name in image classifications world such as LeNet [32], AlexNet [33], GoogLeNet [34], VGGNet [31] and ResNet [35]. More information about their architectures and state-of-the-art accuracy can be found in their respective papers.

Defining the model architectures can be difficult as there are numerous design choices made available. Author do not know what the optimal model architecture it should be for a given model immediately. Hence, this paper would like to

explore a range of possibilities. An actual machine learner will ask the machine to perform this exploration and configure the optimal model architecture automatically. The variable in the configuration can be called hyperparameters which it is external to the model, and the value cannot be estimated from the data. Hyperparameters can be divided into two types:

a) Hyperparameter that determines the network structure such as:

- *Kernel Size* –the size of the filter.
- *Kernel Type*–values of the actual filter (e.g., edge detection, sharpen).
- *Stride*–the rate at which the kernel pass over the input image.
- *Padding*–add layers of 0s to make sure the kernel pass over the edge of the image.
- *Hidden layer*–layers between input and output layers.
- *Activation functions*–allow the model to learn nonlinear prediction boundaries.

b) Hyperparameter that determines the network trained such as:

- *Learning rate*–regulates on the update of the weight at the end of each batch.
- *Momentum*–regulates the value to let the previous update influence the current weight update.
- *A number of epochs*–the iterations of the entire training dataset to the network during training.
- *Batch size*–the number of patterns shown to the network before the weights are updated.

Models can have more than 10 hyperparameters and finding the best combination can be view as the search problem. Hence, the right choice of hyperparameter values can affect the performance of the model.

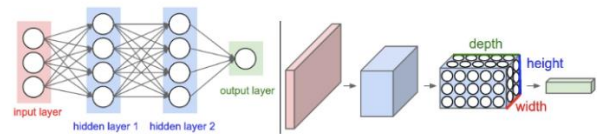


Fig. 1. A regular 3-Layer Neural Network vs. CNNs [30].



Fig. 2. Small VGGNet Architectures [30].

#### IV. EXPERIMENTAL SETUP

CIFAR10 will be used as datasets [31] as it is a subset of the 80-million tiny image database. There are 50,000 images for training, and 10,000 images for testing. All of them are  $32 \times 32$  RGB images. CIFAR10 contains 10 basic categories, and both training and testing data are uniformly distributed over these categories. To avoid using the testing data, 10,000 images have been left from the training set for validation. This will protect from getting overfitting.

Searching for the best combination of hyperparameters requires computational resources. Fortunately, Nvidia Tesla K80 is a supercomputer that is used as a computing platform in this research. It can dramatically lower data center costs by delivering exceptional performance with fewer and more powerful servers. TensorFlow is a framework that will be used in representing computations as graphs, allows easier computation and analysis of these models and utilizing multi-dimensional arrays called Tensors and by computing these graphs in sessions. TensorFlow will implement Keras as the backend to allow for easy and fast prototyping through user friendliness, modularity, and extensibility. It supports the convolutional neural networks as well running smoothly in CPU and GPU.

To test the understanding on search method, experiments were performed on CIFAR-10 datasets using random search method. In the first experiments, the model only had two convolutional layers as is trained on CPU. The height, width, channels and outputs are fixed which is  $32 \times 32 \times 3$  with output of 10. 24 iterations within epoch will run on accuracy check. The maximum number of epochs was 500 with 4 rounds of early stopping. The model then is trained with the hyperparameter configurations based Table I and Table II. Note that the range values randomly. Then, the hyperparameter evaluations are being stored in training logs. The results were being evaluated with two other experiments that will run on GPU. Additional hyperparameters might be added to improve the accuracy, and then the selected hyperparameter configuration will be compared with the state-of-the-art accuracy on CIFAR-10 datasets.

Table I below highlights the hyperparameters considered in this study. Each of the hyperparameters is labeled with shorter and easier name (abbreviation). Also, ranges are indicated within square brackets. The following table presents the network trained hyperparameters.

TABLE I. NETWORK STRUCTURE HYPERPARAMETERS

| Hyperparameter    | Abbreviation | Range                    |
|-------------------|--------------|--------------------------|
| Number of Filters | Filters_1    | [16, 32, 64, 96]         |
| Kernel Size       | Ksize_1      | [3, 4, 5]                |
| Number of Filters | Filters_2    | [48, 64, 96, 128]        |
| Kernel Size       | Ksize_2      | [3, 4, 5]                |
| Number of Filters | Filter_3     | [64, 96, 128]            |
| Kernel Size       | Ksize_3      | [3, 4, 5]                |
| Hidden Layer      | full_hidden1 | [60, 100, 125]           |
| Hidden Layer      | full_hidden2 | [60, 100, 125]           |
| Activation        | activation   | ['relu', 'lrelu', 'elu'] |

TABLE II. NETWORK TRAINED HYPERPARAMETERS

| Hyperparameter | Abbreviation   | Range                           |
|----------------|----------------|---------------------------------|
| Learning rate  | learning_rates | [0.001, 0.003, 0.01, 0.03]      |
| Batch Size     | batch_sizes    | [32, 64, 128, 256]              |
| Momentum       | momentum       | [0.9, 0.95, 0.99]               |
| Optimizer      | optimizer      | ['Adam', 'rmsprop', 'Nesterov'] |

In Table II above, the four-network trained hyperparameters are listed alongside their abbreviations. These abbreviations will be constantly used as reference to any of the above-listed hyperparameters.

##### A. Results on Small CNNs on CPU

The accuracy only reached at **60.85%** and takes **5 days** to run on **CPU**. Hence, the hyperparameter space were minimized by only performing optimization on network structure, learning rate, and batch size. Overall, small CNNs contain 9 network hyperparameters, 2 network trained hyperparameters and 2 layer hyperparameters resulting total of  $9 + 2 + 2 \times 2 = 15$  configurable hyperparameters. The possible combinations of hyperparameters are 15,116,544. Based on the results, training accuracy did not reach satisfaction level and overfitting is not an issue. However, the learning rates were not congregating as shown in Fig. 3. Hence, this will be eliminated on further search experiments. Architecture with more features in fully connected layers perform better. Next experiments, the third convolutional layer are added. Few selections of activation functions and optimization algorithms are included and run on GPU.

##### B. Results on Small CNNs on GPU

In second experiments, activation functions were added and optimization algorithms along with momentum for batch normalization. The border pixels [0, 1, 2] were removed. Third convolutional layers were added and running **3 days** on **GPU**. Based on the results, the accuracy was increased from **60.85%** to **71.17%** and appears the model had difficulty on converging. Overall, small CNNs contain 9 network hyperparameters, 4 networks trained hyperparameters and 3-layer resulting in a total of  $9 + 4 + 3 \times 3 = 22$  configurable hyperparameters.

In Fig. 3 below, the accuracy on fail learning rate were tested by 0.01 and 0.03. The numerical representation of these results is presented in Appendix 1. Subsequently, the accuracy was also tested on small CNN on GPU as depicted in Fig. 4 below. Please refer to Appendix 2 for detailed results.

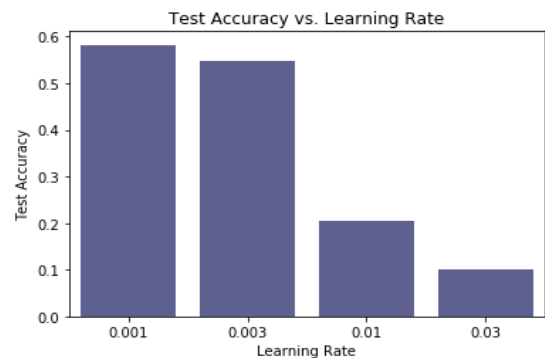


Fig. 3. Test Accuracy on Fail Learning Rate by 0.01 and 0.03.

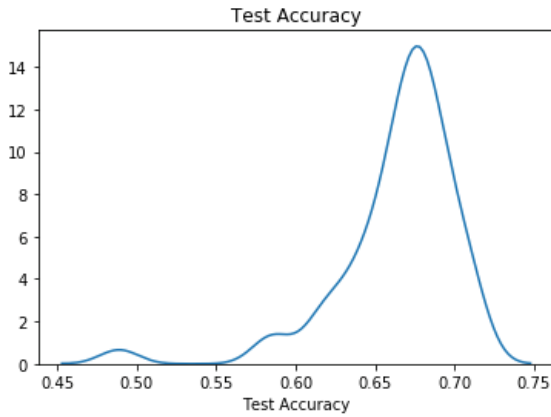


Fig. 4. Test Accuracy of Small CNNs on GPU.

### C. Benchmarks on CIFAR-10 Datasets

In final experiments, hyperparameters that tended to underperform were eliminated. Fig. 4 shows the distribution of test accuracy appears to be models that had difficulty converging. The stride of first CNN layer are reduce from 2 to 1 and patch reduction to 0. The possible combinations of hyperparameters were reduced from **15,116,544** to **3,072**. The increasing number in hyperparameter to learn results in increasing training time. Hence, the hyperparameter setting was sampled accordingly as in Table III. Fig. 5 illustrates the test accuracy in finding the optimum hyperparameter that fits the CNNs model with additional third convolutional layers. ‘relu’ or ‘lrelu’ offer performing better than ‘elu’, with ‘relu’ dominating on activation functions. The Adam optimizer algorithm are better than ‘Nesterov Accelerated Gradient’ or ‘RMSProp’ in this case. Batch size of 32 gives inconsistent results. A batch size of 64 can achieve good results and is more reliable. However, while other CNNs have had success with this approach, there is no benefit from the current architecture.

In the first convolutional layer, number of filters are increased and gives an improvement performance. Interestingly, the next two layers are not performing well with more filters. Perhaps because of overfitting. A 4x4 kernel gives slightly an average performance. In the second experiments, a batch size of 64 and the “lrelu” activation function looks promising. Hence, these were both fixed and with more features in 1<sup>st</sup> conv layers are helping gaining better performance. The stride is reduced from 2 to 1 in the final experiments. Signs of overfitting are shown. Thus, regularization is applied which is the dropout layers and running on **2 days on GPU**. Based on the results, it achieved **80.62% accuracy** which then compared with the state-of-the-art on CIFAR-10 datasets without interfering with the data (data augmentation).

This put the results on the bottom of the leaderboard for cifar-10 in Table IV, which is satisfying and the purpose of this study, was to investigate hyperparameter search on CIFAR-10 datasets [36].

### D. Random Search and Genetic Algorithm

In [41], random search generates randomly individual solutions at any point of search space via calculating and

comparing the value of each solution while genetic algorithms (GA) mimic the natural evolutions process. In the search space, GA works with populations of solutions which each generation is subjected to selection, crossover and mutation operations. This will help GA in obtaining the newly improved generations of the solutions. However, the questions arise as can genetic algorithm become the random search. The author in [41] stated that GA does not have the potential to become a purely random search alone. Conversely, Yahya et al. [42] considered genetic algorithms as “Guided Random Search Algorithms”. The randomness of the algorithms can be controlled and become guided search as GA takes inspirations from the evolution concepts such as survival of the fittest, crossover, mutation and selections. Moreover, the degree of randomness of algorithms can be determined by setting the values of its control parameters, and through it, the algorithms can be purely random search algorithms or deterministic algorithms [42].

The following figures depict the results obtained from the experiments. Starting from Fig. 5 to Fig. 7, accuracy is tested on activation function, optimizer, and batch size.

It can be observed from Fig. 5 that ‘relu’ or ‘lrelu’ offer performing better than ‘elu’, with ‘relu’ dominating on activation functions. The raw results are shown in Appendix 2.

On the other hand, Adam optimizer algorithm is better than ‘Nesterov Accelerated Gradient’ or ‘RMSProp’ in this case, please see Appendix 2.

TABLE III. NETWORK STRUCTURE HYPERPARAMETERS

| Hyperparameter    | Abbreviation  | Range                         |
|-------------------|---------------|-------------------------------|
| Learning rate     | learning_rate | [0.001, 0.003, 0.002, 0.0015] |
| Batch Size        | batch_size    | [64]                          |
| Momentum          | momentum      | [0.9, 0.95, 0.99]             |
| Optimizer         | optimizer     | ['adam']                      |
| Number of Filters | filters1      | [64, 96]                      |
| Kernal Size       | ksize1        | [4, 5]                        |
| Number of Filters | filters2      | [96, 128]                     |
| Kernal Size       | ksize2        | [4, 5]                        |
| Number of Filters | filter3       | [96, 128]                     |
| Kernal Size       | ksize3        | [4, 5]                        |
| Hidden Layer      | full_hidd1    | [100, 125]                    |
| Hidden Layer      | full_hidd2    | [100, 125]                    |
| Activation        | activation    | ['lrelu']                     |

TABLE IV. ACCURACY ON CIFAR-10 WITHOUT DATA AUGMENTATION

| Network   | CIFAR-10 (%) |
|---|--------------|
| ALL-CNN [37]  | 92.00        |
| Deeply-supervised [38]                                | 90.22        |
| Network in Network [39]                               | 89.60        |
| Maxout [40]   | 88.32        |
| <b>3Conv + 2FC + Dropout + stride 1 on all layers</b> | <b>80.62</b> |

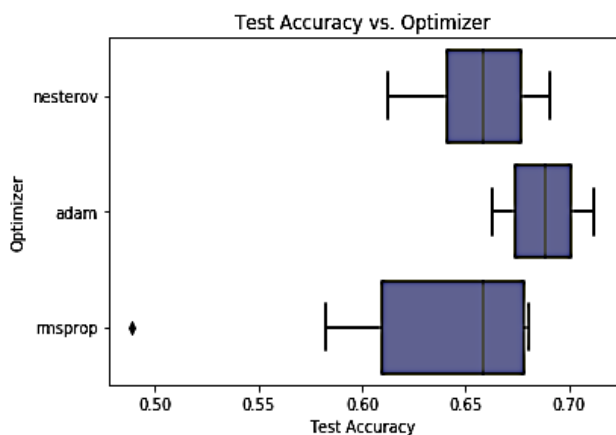


Fig. 5. Accuracy vs Optimizer.

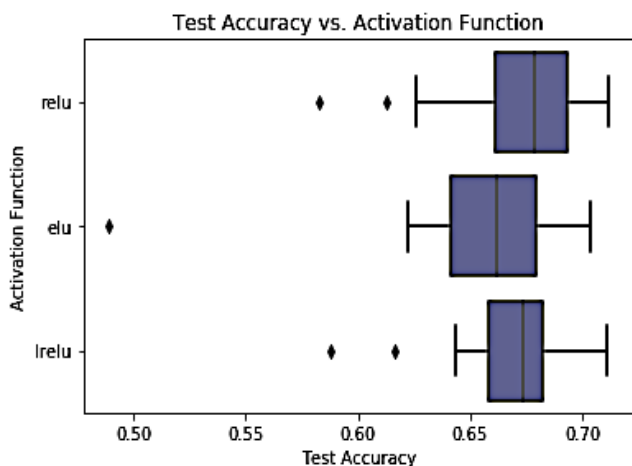


Fig. 6. Accuracy vs Activation Function.

On batch size, results shows that batch size 32 have higher median performance. Although this seems to be good achievement, a higher batch size (64) is capable of achieving

better and reliable results. Next, the results of the optimised network structure hyperparameters are presented. Appendix 2 shows the results in a tabular form.

In Fig. 8 Optimizing the network structure using random search for filters seems to improve performance at first convolutional layer. However, as number of layers increase, the performance begins to decline significantly. Although the exact reasons that have caused the drastic decline might be inconclusive at this stage, author attributed it to the possible overfitting. This is nonetheless subject to debate through more detailed experiments. Please refer to appendix 2 for raw results of filters after being optimized by random search. In Fig. 9 below however, the situation shows better results.

Alternatively, optimizing the network structure using random search for kernel performs better on 4x4 kernel. However, a similar situation with filters is observed in kernel too (Fig. 9). Kernel 1x1, 2x2 and 3x3 performed below average respectively. Yet, slightly better performance is noticed on the rest of the kernels. For better understanding of the results resented in Fig. 9, raw data of the results are as shown in Appendix 2.

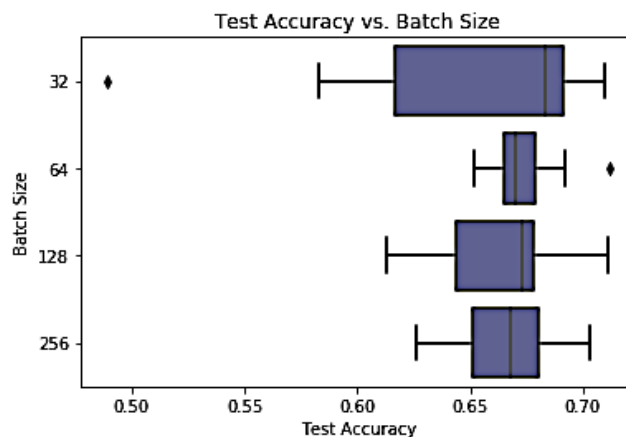


Fig. 7. Accuracy vs Batch Size.

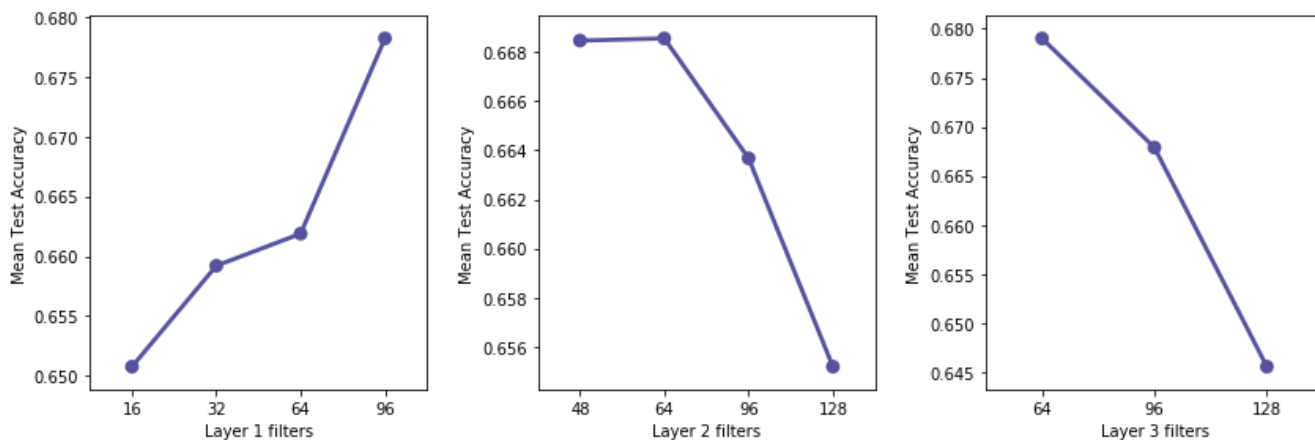


Fig. 8. Network Structure Hyperparameters after being Optimized by Random Search (Filters).

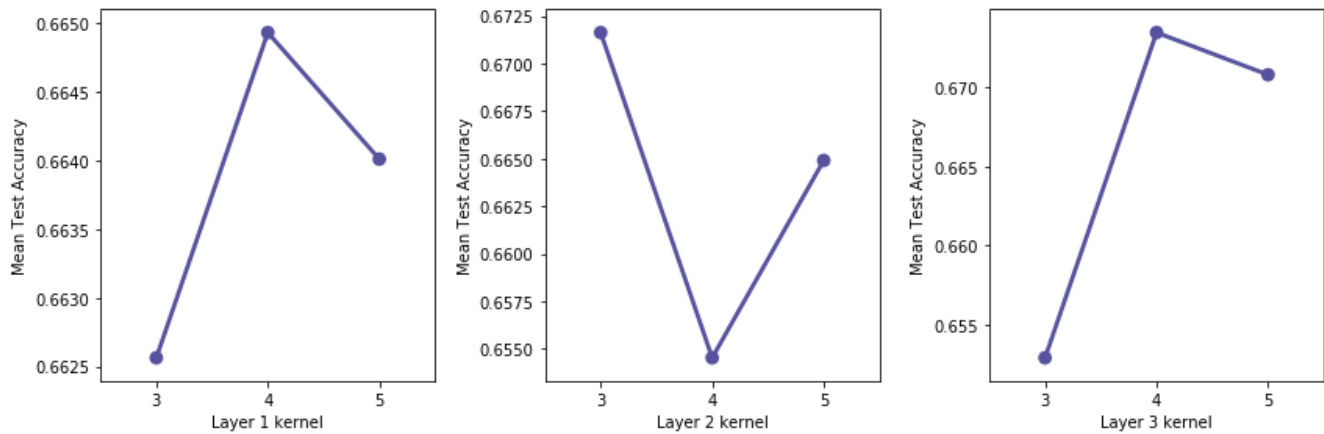


Fig. 9. Network Structure Hyperparameters after being Optimized by Random Search (Kernel).

### E. Computational Considerations

Computing random search on CPU is computational costly as it took around 5 days with limited 3GB memory. Running on GPU accelerate the computing process into 2 days while eliminating the huge hyperparameter combinations. Moreover, constructing CNNs architectures can consume a lot of memory. Modern GPU is equipped on limited of 3/4/6GB memory with the best GPUs of 12GB memory [30]. To avoid this, three sources of memory need to keep track on:

- **Activations:** The raw number of activations can consume a lot. Running CNNs only at test time can reduce this by storing the currents activations at any layer and discards the previous activations.
- **Parameters:** These are the number that holds the network parameters, step cache for optimization such as momentum, ‘Adagrad’ or ‘RMSprop’. The memory store needs to be multiplied by a factor of 3 or so.
- **Miscellaneous:** Every CNN as to maintain the miscellaneous such as image data batches, etc.

Calculate the amount of memory by taking the right estimate of the total number values of activations, parameters, misc. and multiply by 4 to get a raw number of bytes. And then divided by 1024 multiple times to get in KB, MB and finally GB. Another way to make the network fit is to decrease the batch size as the most memory was consumed by activations [30].

### V. CONCLUSIONS AND FUTURE WORK

Author presented a genetic algorithm method on optimizing the convolutional neural network hyperparameter. For this purpose, author first investigate the hyperparameter search method focusing on image classification of CIFAR-10 datasets. Random search method was to choose on running the trial of experiments. The small CNNs on CPU showed that learning rates with range of 0.01 and above are not giving good performance on the models. Performing grid search will waste a lot of time with the mention learning rates. Millions combination of hyperparameter will make Grid search seems impractical. Random search allows some hyperparameter

values to be selected by process of elimination or selection. The random search did not achieve state-of-the-art accuracy by 90% above. However, it satisfies enough to quality over par around 80% on the leaderboard of CIFAR-10 [36].

In the future, genetic algorithms (GA) will be used as an optimization search method with tested CNNs architectures. Combining search methods such as grid search, manual search, random search and local search with a global search like GA will be implement for further research. However, running GA as hyperparameter search space is computationally cost. Hence, running on multiple GPU are taken into considerations by the author. Given enough time, more optimization method such as Bayesian can be investigated like random search on this paper.

### ACKNOWLEDGMENT

The author would like to thank High-Performance Cloud Computing Centre (HPC<sup>3</sup>) and Universiti Teknologi PETRONAS for supporting this study.

### REFERENCES

- [1] L. Xie and A. Yuille, “Genetic CNN,” in Proceedings of the IEEE International Conference on Computer Vision, 2017, vol. 2017-October, pp. 1388–1397.
- [2] M. Wistuba, N. Schilling, and L. Schmidt-Thieme, “Hyperparameter optimization machines,” in Proceedings - 3rd IEEE International Conference on Data Science and Advanced Analytics, DSAA 2016, 2016.
- [3] J. Bergstra, J. B. Ca, and Y. B. Ca, “Random Search for Hyper-Parameter Optimization Yoshua Bengio,” 2012.
- [4] R. Bardenet, M. Brendel, B. Kégl, and M. Sebag, “Collaborative hyperparameter tuning,” Proc. 30th Int. Conf. Mach. Learn., 2013.
- [5] E. Bochinski, T. Senst, and T. Sikora, “Hyperparameter Optimization For Convolutional Neural Network Committees Based on Evolutionary Algorithms,” I2017 IEEE Int. Conf. Image Process., pp. 3924–3928, 2017.
- [6] J. Snoek, H. Larochelle, and R. P. Adams, “Practical Bayesian Optimization of Machine Learning Algorithms,” Jun. 2012.
- [7] T. Domhan, J. T. Springenberg, and F. Hutter, “Speeding up automatic hyperparameter optimization of deep neural networks by extrapolation of learning curves,” in IJCAI International Joint Conference on Artificial Intelligence, 2015.
- [8] K. Eggenberger, M. Feurer, and F. Hutter, “Towards an empirical foundation for assessing bayesian optimization of hyperparameters,” NIPS, BayesOpt Work., pp. 1–5, 2013.

- [9] C. Gagn, "DEAP: Evolutionary Algorithms Made Easy," *J. Mach. Learn. Res.*, vol. 13, pp. 2171–2175, 2012.
- [10] A. Klein, S. Falkner, S. Bartels, P. Hennig, and F. Hutter, "Fast Bayesian Optimization of Machine Learning Hyperparameters on Large Datasets," in *Proceedings - 20th International Conference on Artificial Intelligence and Statistics (AISTATS) 2017*, 2017.
- [11] S. Sanders and C. Giraud-Carrier, "Informing the use of hyperparameter optimization through metalearning," in *Proceedings - IEEE International Conference on Data Mining, ICDM, 2017*, vol. 2017-November, pp. 1051–1056.
- [12] M. Claesen and B. De Moor, "Hyperparameter Search in Machine Learning," 2015.
- [13] P. LeCun, Yann; Bottou, L.;Bengio, Y.;Haffner, "Lecun-01a," *Proc. IEEE*, vol. 86, no. 11, pp. 2278–2324, 1998.
- [14] Y. Ozaki, M. Yano, and M. Onishi, "IPSI Transactions on Computer Vision and Applications Effective hyperparameter optimization using Nelder-Mead method in deep learning," *IPSI Trans. Comput. Vis. Appl.*, vol. 9, 2017.
- [15] L. Xie and A. Yuille, "Genetic CNN," in *Proceedings of the IEEE International Conference on Computer Vision, 2017*.
- [16] H. Pérez-Espinoso, H. Avila-George, J. Rodriguez-Jacobo, H. A. Cruz-Mendoza, J. Martínez-Miranda, and I. Espinosa-Curiel, "Tuning the Parameters of a Convolutional Artificial Neural Network by Using Covering Arrays," *Res. Comput. Sci.*, vol. 121, no. 2016, pp. 69–81, 2016.
- [17] X. Yao and Y. Liu, "A new evolutionary system for evolving artificial neural networks.," *IEEE Trans. Neural Netw.*, vol. 8, no. 3, pp. 694–713, 1997.
- [18] F. Hutter, H. H. Hoos, and K. Leyton-Brown, "Sequential model-based optimization for general algorithm configuration," in *Lecture Notes in Computer Science (including subseries Lecture Notes in Artificial Intelligence and Lecture Notes in Bioinformatics)*, 2011, vol. 6683 LNCS, pp. 507–523.
- [19] L. Li and A. Talwalkar, "Random Search and Reproducibility for Neural Architecture Search," *ArXiv*, 2019.
- [20] I. Dewancker, M. McCourt, and S. Clark, "Bayesian Optimization for Machine Learning: A Practical Guidebook," *Prepr. ArXiv*, 2016.
- [21] J. Bergstra, R. Bardenet, Y. Bengio, and B. Kégl, "Algorithms for Hyperparameter Optimization."
- [22] J. Bergstra, D. L. K. Yamins, and D. D. Cox, "Making a Science of Model Search: Hyperparameter Optimization in Hundreds of Dimensions for Vision Architectures," *Icml*, pp. 115–123, 2013.
- [23] J. Snoek et al., "Scalable Bayesian Optimization Using Deep Neural Networks," Feb. 2015.
- [24] R. Chiong and O. K. Beng, "A Comparison between Genetic Algorithms and Evolutionary Programming based on Cutting Stock Problem," *Eng. Letters*, vol. 14, no. 1, 2007.
- [25] R. Rojas, *Neural Networks: A Systematic Introduction*. Springer-Verlag, 1996.
- [26] H. M. uhlenbein GMD Schloss Birlinghoven D- and S. Augustin, "Asynchronous parallel search by the parallel genetic algorithm."
- [27] Q. V Le, J. Ngiam, A. Coates, A. Lahiri, B. Prochnow, and A. Y. Ng, "On Optimization Methods for Deep Learning," *Proc. 28th Int. Conf. Int. Conf. Mach. Learn.*, pp. 265–272, 2011.
- [28] M. Wistuba, N. Schilling, and L. Schmidt-Thieme, "Learning hyperparameter optimization initializations," in *Proceedings of the 2015 IEEE International Conference on Data Science and Advanced Analytics, DSAA 2015*, 2015.
- [29] E. Hazan, A. Klivans, and Y. Yuan, "Hyperparameter Optimization: A Spectral Approach," *ICLR*, Jun. 2018.
- [30] A. Karpathy, "CS231n Convolutional Neural Networks for Visual Recognition," *Stanford Education*.
- [31] G. Krizhevsky, A., Nair, V., & Hinton, "The CIFAR-10 dataset," 2014. [Online]. Available: online: <http://www.cs.toronto.edu/kriz/cifar.htm>.
- [32] Y. Lecun, L. Eon Bottou, Y. Bengio, and P. H. Abstract, "Gradient-Based Learning Applied to Document Recognition."
- [33] A. Krizhevsky, I. Sutskever, and G. E. Hinton, "ImageNet Classification with Deep Convolutional Neural Networks," *Adv. Neural Inf. Process. Syst.*, pp. 1097–1105, 2012.
- [34] C. Szegedy et al., "Going Deeper with Convolutions," Sep. 2014.
- [35] K. He, X. Zhang, S. Ren, and J. Sun, "Deep Residual Learning for Image Recognition," Dec. 2015.
- [36] R. Benenson, "Classification datasets results," 2016.
- [37] J. T. Springenberg, A. Dosovitskiy, T. Brox, and M. Riedmiller, "Striving for Simplicity: The All Convolutional Net," 2014.
- [38] C.-Y. Lee, S. Xie, P. Gallagher, Z. Zhang, and Z. Tu, "Deeply-Supervised Nets," Sep. 2014.
- [39] M. Lin, Q. Chen, and S. Yan, "Network In Network," Dec. 2013.
- [40] I. J. Goodfellow, D. Warde-Farley, M. Mirza, A. Courville, and Y. Bengio, "Maxout Networks," 2013.
- [41] A. Aab et al., "De Mauro, 41 J.R.T. de Mello Neto, 35 I. De Mitri, 31, 32, 36," *J.R. Hörandel*, vol. 56, p. 24, 2017.
- [42] A. A. Yahya, R. Mahmud, and A. R. Ramli, "Dynamic Bayesian networks and variable length genetic algorithm for designing cue-based model for dialogue act recognition," *Comput. Speech Lang.*, vol. 24, no. 2, pp. 190–218, Apr. 2010.

APPENDICES

APPENDIX 1 (NUMERICAL RESULTS OF ACCURACY ON FAIL LEARNING RATE BY 0.01 AND 0.03)

To get the best accuracy in the test sets, the experiment was performed in three rounds. Up to 60.85% was achieved in the first round (using 2 convolutional, 2 fully connected). In this first round are equipped with two convolutional layers. This was progressively increased to 3 in the subsequent rounds as shown in Appendix 2 and 3. The training of this model was done on CPU; thereby limiting the number of convolutional. This results maps with Fig. 3.

```
In [2]: import pandas as pd  
hyperparam_df = pd.read_csv('./log/model_hyperparam_1.csv')  
hyperparam_df.sort_values(by = ['best_acc'], ascending = False)
```

```
Out[2]:
```

|    | batch_size | best_acc | best_loss | filters_1 | filters_2 | full_hidd_1 | full_hidd_2 | ksize_1 | ksize_2 | learning_rate | no_epochs |
|----|------------|----------|-----------|-----------|-----------|-------------|-------------|---------|---------|---------------|-----------|
| 6  | 256.0      | 0.6085   | 1.124841  | 64.0      | 96.0      | 125.0       | 125.0       | 5.0     | 5.0     | 0.001         | 18.0      |
| 5  | 128.0      | 0.6002   | 1.142996  | 32.0      | 64.0      | 100.0       | 125.0       | 3.0     | 5.0     | 0.001         | 20.0      |
| 0  | 32.0       | 0.5978   | 1.147990  | 32.0      | 96.0      | 100.0       | 80.0        | 3.0     | 4.0     | 0.001         | 19.0      |
| 25 | 64.0       | 0.5903   | 1.196584  | 64.0      | 96.0      | 100.0       | 125.0       | 3.0     | 3.0     | 0.001         | 23.0      |
| 3  | 256.0      | 0.5806   | 1.192041  | 32.0      | 48.0      | 60.0        | 125.0       | 3.0     | 3.0     | 0.001         | 24.0      |
| 2  | 32.0       | 0.5749   | 1.211263  | 16.0      | 32.0      | 60.0        | 100.0       | 5.0     | 4.0     | 0.003         | 35.0      |
| 10 | 64.0       | 0.5735   | 1.226173  | 32.0      | 96.0      | 60.0        | 100.0       | 3.0     | 3.0     | 0.001         | 20.0      |
| 18 | 64.0       | 0.5606   | 1.266603  | 32.0      | 64.0      | 60.0        | 100.0       | 5.0     | 4.0     | 0.003         | 21.0      |
| 12 | 256.0      | 0.5598   | 1.247521  | 8.0       | 32.0      | 125.0       | 80.0        | 5.0     | 3.0     | 0.003         | 30.0      |
| 26 | 64.0       | 0.5589   | 1.245890  | 32.0      | 48.0      | 125.0       | 80.0        | 4.0     | 5.0     | 0.003         | 18.0      |
| 4  | 128.0      | 0.5307   | 1.304451  | 8.0       | 96.0      | 125.0       | 100.0       | 4.0     | 4.0     | 0.003         | 23.0      |
| 24 | 128.0      | 0.5296   | 1.316891  | 8.0       | 64.0      | 100.0       | 125.0       | 3.0     | 4.0     | 0.003         | 18.0      |
| 16 | 32.0       | 0.5266   | 1.396713  | 16.0      | 64.0      | 60.0        | 80.0        | 5.0     | 4.0     | 0.003         | 28.0      |
| 21 | 256.0      | 0.5261   | 1.326381  | 8.0       | 48.0      | 125.0       | 125.0       | 4.0     | 4.0     | 0.001         | 20.0      |
| 8  | 128.0      | 0.4189   | 1.511615  | 16.0      | 96.0      | 125.0       | 80.0        | 4.0     | 4.0     | 0.010         | 20.0      |
| 28 | 64.0       | 0.4175   | 1.584211  | 16.0      | 32.0      | 125.0       | 80.0        | 3.0     | 3.0     | 0.010         | 32.0      |
| 22 | 64.0       | 0.1001   | 2.302906  | 8.0       | 64.0      | 100.0       | 125.0       | 3.0     | 5.0     | 0.010         | 14.0      |
| 15 | 32.0       | 0.1000   | 2.303990  | 16.0      | 32.0      | 125.0       | 80.0        | 4.0     | 3.0     | 0.030         | 12.0      |
| 17 | 256.0      | 0.1000   | 2.302994  | 8.0       | 64.0      | 125.0       | 80.0        | 3.0     | 4.0     | 0.030         | 12.0      |
| 1  | 32.0       | 0.1000   | 2.302861  | 32.0      | 64.0      | 60.0        | 125.0       | 4.0     | 3.0     | 0.010         | 23.0      |
| 19 | 256.0      | 0.1000   | 2.303015  | 32.0      | 48.0      | 60.0        | 125.0       | 4.0     | 4.0     | 0.030         | 13.0      |
| 20 | 128.0      | 0.1000   | 2.303385  | 64.0      | 96.0      | 60.0        | 100.0       | 3.0     | 4.0     | 0.030         | 12.0      |
| 13 | 128.0      | 0.1000   | 2.302733  | 8.0       | 48.0      | 100.0       | 80.0        | 4.0     | 4.0     | 0.010         | 12.0      |
| 23 | 32.0       | 0.1000   | 2.303946  | 8.0       | 32.0      | 60.0        | 100.0       | 3.0     | 4.0     | 0.030         | 12.0      |
| 11 | 32.0       | 0.1000   | 2.303967  | 16.0      | 96.0      | 125.0       | 80.0        | 3.0     | 3.0     | 0.030         | 12.0      |
| 9  | 32.0       | 0.1000   | 2.303927  | 8.0       | 32.0      | 125.0       | 125.0       | 3.0     | 3.0     | 0.030         | 12.0      |
| 7  | 32.0       | 0.1000   | 2.303434  | 32.0      | 96.0      | 60.0        | 80.0        | 5.0     | 5.0     | 0.030         | 13.0      |
| 27 | 128.0      | 0.1000   | 2.302751  | 8.0       | 96.0      | 60.0        | 125.0       | 4.0     | 5.0     | 0.010         | 12.0      |
| 14 | 32.0       | 0.1000   | 2.303959  | 8.0       | 96.0      | 100.0       | 125.0       | 3.0     | 3.0     | 0.030         | 12.0      |

APPENDIX 2 (NUMERICAL REPRESENTATION OF THE RESULTS PRESENTED FROM FIG. 4 – FIG. 9)

In the second round of the experiments, up to 71.17% was achieved using 3 convolutional fully connected layers. This experiment was conducted to test the accuracy of small CNNs on GPU. Also, accuracy was tested against activation function (RELU, LRELU or ELU), optimizer (Adam, RMSProp or Nesterov Adam) as well as batch size. In addition, random search was used to optimise network structure hyperparameters for both filters and kernel.

Table of results

```
In [115]: hyperparam_df = pd.read_csv('./log/model_hyperparam_2.csv')
hyperparam_df.sort_values(by = ['best_acc'], ascending = False)
```

```
Out[115]:
```

| activation | batch_size | best_acc | best_loss | best_train_acc | best_train_loss | filters1 | filters2 | filters3 | full_hidd1 | full_hidd2 | ksize1 | ksize2 | ksize3 | learning_rate |
|------------|------------|----------|-----------|----------------|-----------------|----------|----------|----------|------------|------------|--------|--------|--------|---------------|
| relu       | 64         | 0.7117   | 0.919377  | 0.754637       | 0.711197        | 96       | 96       | 64       | 100        | 125        | 3      | 5      | 3      | 0.0020        |
| lrelu      | 128        | 0.7109   | 0.906563  | 0.758348       | 0.701145        | 32       | 64       | 64       | 125        | 80         | 5      | 3      | 5      | 0.0020        |
| relu       | 128        | 0.7093   | 0.897427  | 0.743490       | 0.734613        | 96       | 128      | 96       | 100        | 100        | 5      | 3      | 4      | 0.0020        |
| relu       | 32         | 0.7093   | 0.873374  | 0.722251       | 0.805403        | 96       | 64       | 64       | 60         | 80         | 5      | 4      | 4      | 0.0030        |
| elu        | 256        | 0.7033   | 0.910308  | 0.734158       | 0.771317        | 96       | 48       | 128      | 100        | 125        | 5      | 5      | 4      | 0.0015        |
| relu       | 128        | 0.7008   | 1.032702  | 0.755814       | 0.708703        | 96       | 96       | 128      | 60         | 125        | 5      | 5      | 5      | 0.0030        |
| relu       | 32         | 0.6966   | 0.940112  | 0.704069       | 0.840530        | 64       | 48       | 64       | 125        | 125        | 4      | 5      | 5      | 0.0030        |
| lrelu      | 32         | 0.6947   | 0.906030  | 0.692000       | 0.867232        | 96       | 48       | 96       | 60         | 80         | 3      | 5      | 3      | 0.0020        |
| relu       | 64         | 0.6923   | 0.946625  | 0.724659       | 0.792448        | 16       | 64       | 128      | 100        | 125        | 5      | 5      | 5      | 0.0030        |
| lrelu      | 32         | 0.6911   | 0.905265  | 0.746788       | 0.762321        | 32       | 128      | 128      | 100        | 125        | 4      | 5      | 5      | 0.0015        |
| relu       | 128        | 0.6898   | 0.896807  | 0.708308       | 0.837255        | 64       | 48       | 64       | 60         | 100        | 3      | 3      | 5      | 0.0010        |
| elu        | 32         | 0.6891   | 0.934515  | 0.723434       | 0.806494        | 32       | 64       | 64       | 125        | 80         | 3      | 4      | 5      | 0.0030        |
| elu        | 32         | 0.6870   | 0.904974  | 0.698303       | 0.855170        | 32       | 48       | 96       | 60         | 125        | 4      | 4      | 3      | 0.0010        |
| lrelu      | 32         | 0.6831   | 0.923607  | 0.696061       | 0.872021        | 96       | 64       | 64       | 100        | 125        | 4      | 5      | 3      | 0.0010        |
| lrelu      | 256        | 0.6810   | 0.904818  | 0.669038       | 0.952634        | 64       | 128      | 128      | 100        | 80         | 5      | 3      | 4      | 0.0020        |
| relu       | 64         | 0.6806   | 0.998204  | 0.728308       | 0.783186        | 96       | 64       | 64       | 100        | 125        | 5      | 3      | 4      | 0.0020        |
| elu        | 32         | 0.6806   | 0.928317  | 0.682667       | 0.900012        | 32       | 64       | 96       | 125        | 80         | 4      | 4      | 3      | 0.0030        |
| relu       | 256        | 0.6802   | 1.084211  | 0.721635       | 0.786616        | 64       | 128      | 64       | 125        | 100        | 3      | 3      | 4      | 0.0020        |

APPENDIX 3

In third and final round of the experiments, up to 80.62% was achieved using 3 convolutional layers, This shows that increase in parameters learning, increase the training time. Accordingly, only 5 hyperparameter were sampled and values of hyperparameter that are not performing well will be eliminated.

Table of results

```
In [4]: hyperparam_df = pd.read_csv('./log/model_hyperparam_3.csv')
hyperparam_df.sort_values(by = ['best_acc'], ascending = False)
```

```
Out[4]:
```

| activation | batch_size | best_acc | best_loss | best_train_acc | best_train_loss | filters1 | filters2 | filters3 | full_hidd1 | full_hidd2 | ksize1 | ksize2 | ksize3 | learning_rate |
|------------|------------|----------|-----------|----------------|-----------------|----------|----------|----------|------------|------------|--------|--------|--------|---------------|
| lrelu      | 64         | 0.8062   | 0.579502  | 0.736910       | 0.751420        | 96       | 128      | 128      | 125        | 100        | 4      | 5      | 5      | 0.0030        |
| lrelu      | 64         | 0.8048   | 0.587198  | 0.761165       | 0.673304        | 96       | 96       | 128      | 125        | 125        | 4      | 5      | 5      | 0.0010        |
| lrelu      | 64         | 0.7894   | 0.622922  | 0.721077       | 0.797818        | 64       | 128      | 128      | 100        | 100        | 5      | 5      | 5      | 0.0030        |
| lrelu      | 64         | 0.7799   | 0.632761  | 0.714930       | 0.794581        | 64       | 96       | 96       | 125        | 100        | 4      | 5      | 5      | 0.0010        |
| lrelu      | 64         | 0.7750   | 0.649881  | 0.697231       | 0.850535        | 64       | 96       | 128      | 100        | 125        | 5      | 4      | 5      | 0.0015        |



# New Method of Faults Diagnostic based on Neuro-Dynamic Sliding Mode for Flat Nonlinear Systems

O.Dhaou<sup>1</sup>, L.Sidhom<sup>2</sup>, A.Abelkrim<sup>3</sup>

Research Laboratory L.A.R.A in Automatic control, National Engineering School of Tunis  
University of Tunis El Manar BP 37, Le Belvédère, 1002<sup>1,2,3</sup>  
National Engineering School of Carthage ENICarthage  
University of Carthage 45, Street of Entrepreneurs, Charguia II, 2035, Tunis, Tunisia<sup>1,3</sup>

**Abstract**—This paper addresses the problem of simultaneous actuator, process and sensor Fault Detection and Isolation (FDI) for nonlinear system having flatness properties with the presence of disturbances and which are operating in closed-loop. In particular, the nonlinear system is corrupted with additive actuator, process or sensor faults with simultaneous occurrence. In this case, the residual signals might be sensitive to all of these faults that can appear in the system. The proposed FDI method is based on both input and parameter estimators that are designed in parallel. With the flatness property of such system, the design of these two estimators requires information on the measured outputs and their successive derivatives. To estimate these last one, a new scheme of the 2nd-order dynamic sliding mode differentiator is proposed. Residuals are next defined as the difference between the estimated and expected behavior. In order to isolate the faults, dynamic neural networks technique is employed. Besides, comparative study between this new differentiator and the well-known 2nd-order Levant's differentiator is provided to show the pros and cons of the proposed FDI method. This latter is validated by the simulation results and is carried out on a three tank system.

**Keywords**—Flat system; fault detection and isolation; inputs/parameters estimator; higher order sliding mode differentiator; dynamic neural network

## I. INTRODUCTION

Recently, FDI problem has received a great deal of attention especially for systems for which the faults occurrence can lead to irreparable damages. Moreover, the FDI problem is addressed in many applications and is important in safety critical systems such as energy domain [1], chemical domains [2] and industry machines [3]. In the literature, FDI methods can be classified in two approaches: process history based methods and model-based ones. A thorough review of such FDI methods can be viewed via the following papers: [1] [2] [3]. The first approach does not need any knowledge of the process mathematical model. This can be a main interest over the second category of FDI approach. In fact conventional methods of such FDI approach for sensors or actuators can basically be defined by the hardware redundancy. However, its main disadvantage is that it requires knowledge of a large amount of data. Moreover, this method cannot deal with the effects caused by measurement noises. Actually, it cannot proceed in the real time case.

For this approach, there are different methods. In [4] the authors present an FDI method to supervise the aircraft gas turbine engine actuator and sensors. This method uses only the system input/output data. Then, it does not require any prior knowledge of the linear model of the system. It has given satisfactory results, but the problem is with regarding the robustness and accuracy of the fault estimation especially in the practical case.

Other methods have been used FDI for nonlinear systems based on Neural Networks (NN) and there are many research results about this subject. However, the limit of the NN method concerns the updating rate of learning weights especially in facing of sudden faults. To overcome this problem, many solutions are proposed as in [3]. In this latter, the Weightless Neural Networks (WNN) based on random access memory devices method is investigated to carry out the detection and identification per fault groups. Even though satisfactory results obtained by this method without residual generation, the proposed of the training and testing method is very complicated and its implementation is also complex. In general way, the methods of this first approach have many disadvantages, such as the complexity of the structure and the need for many learning and tuning parameters that require in-depth analysis and studies to obtain the optimal selection of the structure. In addition, these methods require a large amount of data for proper training of the adjustable parameters available.

The model-based approaches are defined by the analytical redundancy FDI methods. Much kind of methods have been developed for the case of nonlinear systems [5], [6]. In [5], the problem of sensor faults detection for Unmanned Aerial Vehicle (UAV) system is studied. This method is based on NN observer to detect the presence of faults and the weighting parameters which are updated using kalman filter. This method gives efficient results only for sensors faults in the UAV systems. On the other hand, actuator faults may cause significant impact problem in the UAV control system. That's why, other researchers have proposed a fault detection and isolation method in sensor and actuator faults occurring UAV system [6].

However, there is a major disadvantage to such method that is likely going to lead to false results because it uses

simple model for observer's design which is far from reality. Thereby, there are methods based on sliding mode technique which have been strongly used especially in the presence of uncertainties and matched perturbations on the system model. Then, sliding mode observers or differentiators based techniques have been widely considered in FDI methods. For example, in [7], the proposed method is based on multi-models to solve the fault detection and isolation problem for a certain class of nonlinear system. The derivatives of the system's output are calculated by the well-known HOSM Levant's differentiator [8] and the system states are estimated using the HOSM multiple observers. The equivalent output injection of the HOSM multiple observers is used to detect the presence of faults in the system. This method is able to be detected and isolated simple and multiple faults but it has a great drawback consisting in the difficulty implementation especially for the rather complicated systems.

In addition, the result of this method depends on the quality of the derivative signals. In practice, the differentiation operation must provide a best compromise between accuracy and the noise rejection. As well known, the sliding mode differentiator has a major benefit which is known by the simplicity in real-time implementation. But, it presents a main drawback concerning the adjustment of its gains. Indeed, these tuning gains require information of the Lipschitz constant of the derivative signals. So, in the practice case, it is hard to obtain beforehand exact information about the value of this constant. To solve this problem, different new schemes of sliding mode differentiators have been proposed in the literature, let us mention some examples [9], [10], [11].

In this paper, we have investigated a novel model-based fault Diagnosis strategy for a particular class of nonlinear systems called flat ones [12]. The proposed method offers a fast performance in on-line closed loop operation and ensures robustness with respect to additive measurement and plant noises. For our research work, the considered flatness property of the model system leads to estimate the successive derivatives using some differentiation scheme. The outputs of this scheme are used to design both inputs and parameters estimators. For this aim, a High Order Sliding Mode Differentiator with Dynamic Gains (SMDDG) defined in [13] is employed to detect faults. Furthermore, we consider a simultaneous occurrence of actuator, process or sensor faults. Thus, the obtained analytic residual signals might be sensitive to all of these faults which make fault isolation very difficult. That's why, the isolation procedure is formulated here as a pattern recognition problem using a Dynamic Neural Networks (DNN) on the residual signals. Comparing with FDI methods in the existing literature, the main contributions of this paper are:

1) A new scheme of adaptive higher order sliding mode differentiator is used to define a new FDI method [13]. Where this algorithm offers a full segregation between the actual faults and measurement noises, which keeps the false alarms rate at a very low level compared to other proposed adaptive differentiators.

2) The fault isolation is realized using an Adaptive Neural Network. In this step, the approach can easily distinguish

between the three types of faults that can occur in the system, even though they appeared simultaneously.

3) A comparative study with the well-known Levant's differentiator is proposed to show the performance of the proposed approach.

This paper is organized as follows. The problem is formulated in Section 2. In Section 3 the proposed FDI method is explained. The system application is presented in the next section. The simulations cases are given in Section 5 to discuss the results and to show the effectiveness of the proposed method with different fault scenarios.

## II. PROBLEM FORMULATION

Consider the following form of the nonlinear system:

$$\begin{cases} \dot{x} = f(t, x, \theta, F_{x,\theta}) + g(x, F_u)u \\ y = h(t, x, F_y) + \eta \end{cases} \quad (1)$$

Where  $f$  and  $h$  are nonlinear functions;  $x = (x_1, \dots, x_n)$   $u = (u_1, \dots, u_m)$  and  $y = (y_1, \dots, y_p)$  are the state, the input and the output vectors system respectively.  $\theta = (\theta_1, \dots, \theta_r)$  is a finite set of unknown parameters which can be a combination of the system's physical parameters.  $\eta$  is a sensor noise considered here by noises on the outputs system.  $F_{x,\theta}, F_u, F_y$  are finite set of process, actuators and sensor faults variables respectively. The non-linear systems present unknown parameters of additional faults that can appear at the sensors, actuators or process. Based on Fliess' work [12], for this class of system defined in (1), its input and state vectors can be characterized by a set of variables called flat outputs and their finite number of its successive derivatives. According to [12], the system (1) presents a flatness property if it can be described by the following equations:

$$\begin{cases} u_i = \varphi_{1j} \left( L_f^0 y_1, L_f^1 y_1, \dots, L_f^k y_1, \dots, L_f^0 y_m, L_f^1 y_m, \dots, L_f^k y_m \right); \\ x_j = \varphi_{2j} \left( L_f^0 y_1, L_f^1 y_1, \dots, L_f^k y_1, \dots, L_f^0 y_m, L_f^1 y_m, \dots, L_f^k y_m \right); \end{cases} \quad (2)$$

Where  $\varphi_{1j}$  and  $\varphi_{2j}$  are two nonlinear functions.

$j = \{1, \dots, n\}$  and  $k = \{1, \dots, q\}$ ,  $k$  is the differentiation order where  $q$  is the flatness order,  $m$  is the input number and  $L_f h(\cdot)$  is the Lie derivative defined by  $\frac{\partial h}{\partial x} f(\cdot)$ .

Then, considering the flat nonlinear system (2), the aims of this paper are: firstly, detect the presence of faults taking into account of sensor noises. Then, isolate possible acts of faults on the system (actuator, sensor or process). In order to obtain these goals and basing on the flatness property of the system, a generic residual signal is obtained as follows:

$$r_i = F_i \left( t, [u]_e, [\theta]_e, y, [\dot{y}]_e, \dots, [y^{(k)}]_e \right) \quad (3)$$

Where  $y = (y_1, \dots, y_q)$  is the flat output vector,  $u = (u_1, \dots, u_m)$  is the input vector and  $\theta = (\theta_1, \dots, \theta_r)$  is the parameter vector.

$[u]_e$  and  $[\theta]_e$  are the estimated input and parameter vectors.  $[y^{(k)}]_e$  is the estimated derivatives outputs vector.

Note that the obtained residual expression (3) contains information about any type faults which can affect the system. This residual dealt with two issues. The first one is the choice of the differentiation algorithm where it plays a crucial role having good quality of the estimated signal and consequently the capability of accurate fault detection. The second issue concerns the fault isolation. Indeed, for the residual given by (3), it is difficult to dissociate the different types of fault, besides; this problem becomes more important with the presence of other disturbances. To solve these issues, the proposed FDI method is described in the following section.

### III. PROPOSED FDI METHOD

To explain the proposed FDI method, Fig. 1 is presented. Fig. 1 is defined by three blocks: control loop, fault detection and isolation blocks. The FDI procedure is based on residual generation signal  $r_i$  which is defined by input  $[u_i]_e$ , parameter  $[\theta_r]_e$  estimated vectors respectively and also the flat output vector with their successive derivatives  $[y^{(k)}]_e$ . Fig. 1 is illustrated for the case where two flat outputs are present in the system which explains the use of second order differentiator.

But the proposed approach may well be used in the general case where the system presents  $q$  flat outputs. As it is explained above, the choice of the differentiation algorithm is very delicate to give a good quality of the derivatives estimations especially with noisy signal. In the literature, there are different differentiators that have been proposed such as

[9] [10] [11]. For instance, there are a HOSM differentiators proposed by Levant in [8]. In this paper, a new scheme of HOSM Levant's differentiator is employed. It is defined by the higher order Sliding Mode Differentiator with Dynamic Gains (SMDDG) proposed in [13]. As already indicated, the studied system presents only two flat outputs which limit the order of the differentiation to two. In the following, we start by exposing the sliding mode algorithms.

#### A. Abbreviations Differentiation Algorithms

Define abbreviations and acronyms the first time they are used in the text, even after they have been defined in the abstract.

Considering the input function to differentiate as follows

$$y(t) = y_0(t) + \xi(t) \quad (4)$$

Where  $y_0(t)$  is an unknown base signal where the  $(\partial+1)^{th}$  derivative is bounded by a positive Lipschitz constant  $C$  and  $\xi(t)$  is a noise which has only a known upper limit such that  $|\xi(t)| < \varepsilon$ . Where  $\varepsilon$  very much less than 1 and  $|y(t) - y_0(t)| \leq \varepsilon$ .

1) HOSM differentiator: The dynamic equations of the second order differentiator proposed by Levant are as follows:

$$\begin{cases} \dot{z}_0 = \delta_0 \\ \delta_0 = -\lambda_0 |z_0 - y|^{\frac{2}{3}} \text{sign}(z_0 - y) + z_1 \\ \dot{z}_1 = \delta_1 \\ \delta_1 = -\lambda_1 |z_1 - \delta_0|^{\frac{1}{2}} \text{sign}(z_1 - \delta_0) + z_1 \\ \dot{z}_2 = -\lambda_2 \text{sign}(z_1 - \delta_0) \end{cases} \quad (5)$$

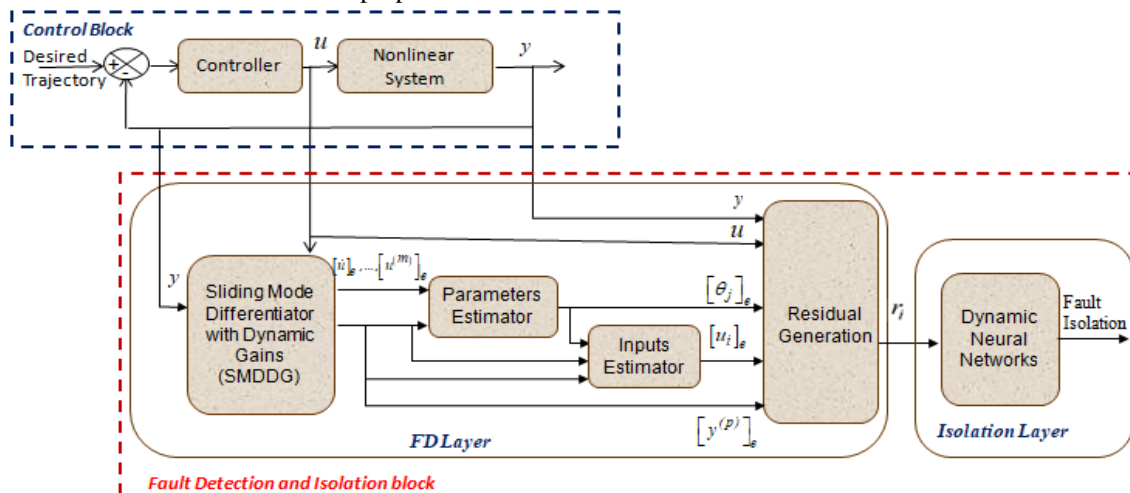


Fig. 1. Block Scheme of Proposed FDI Method.

Note that  $s_0 = z_0 - y(t)$ ,  $s_1 = z_1 - \delta_0$  are the two sliding surfaces of the differentiator which define the derivatives estimation errors. Theoretically and after a convergence time, we have two outputs:  $\delta_0 = \dot{y}(t)$ ,  $s_1 = \ddot{y}(t)$ . In [11] the authors give the inequalities that are established in finite time, for a positive constant  $\mu_i$  depending exclusively on the differentiator parameters:

$$\left\{ |z_i - y_0^{(i)}(t)| \leq \mu_i C^{\frac{i}{\sigma+1}} \varepsilon^{\left(\frac{\sigma-i+1}{\sigma+1}\right)}, \quad i = 0, \dots, \sigma \right. \quad (6)$$

From (6) it can be deduced that the precision is degraded with the increase of the derivative order.

2) *SMDDG differentiator*: The advantage of this new scheme is that its gains are adjusted in real time regardless of the input signal. Considering the input signal defined by (4) and under the same assumption on the noise signal, the second order differentiator with dynamic gains is described by (7):

$$\begin{cases} \dot{z}_0 = \delta_0 \\ \delta_0 = -\hat{\lambda}_0 |s_0|^{\frac{2}{3}} \text{sign}(s_0) - K_0 s_0 + z_1 \\ \dot{z}_1 = \delta_1 \\ \delta_1 = -\hat{\lambda}_1 |s_1|^{\frac{1}{2}} \text{sign}(s_1) - \hat{\lambda}_2 \int_0^t \text{sign}(s_1) dt - K_1 s_1 \end{cases} \quad (7)$$

Where  $K_0, K_1$  are positive convergences gains and  $\hat{\lambda}_0, \hat{\lambda}_1, \hat{\lambda}_2$  are positive dynamic gains of the algorithm computed in real time and depending on the sliding surfaces  $s_0, s_1$ . The dynamic equations are defined by (8).

$$\begin{cases} \dot{\hat{\lambda}}_0 = \left[ |s_0|^{\frac{2}{3}} \text{sign}(s_0) \right] s_0, \quad \hat{\lambda}_0(0) \geq 0 \text{ and } \dot{\hat{\lambda}}_0 > 0 \quad \forall t > 0 \\ \dot{\hat{\lambda}}_1 = \left[ |s_1|^{\frac{1}{2}} \text{sign}(s_1) \right] s_1, \quad \hat{\lambda}_1(0) \geq 0 \text{ and } \dot{\hat{\lambda}}_1 > 0 \quad \forall t > 0 \\ \dot{\hat{\lambda}}_2 = s_1 \int_0^t \text{sign}(s_1) dt \end{cases} \quad (8)$$

With Equations (8), the trajectories of the system (7) converge towards the point  $s_0 = s_1 = 0$  under the assumption that existed unknown positive constants  $\lambda_0^*$  and  $\lambda_1^*$  defined by (9):

Assumption:

$$\begin{cases} \dot{y} = -\lambda_0^* |s_0|^{\frac{2}{3}} \text{sign}(s_0) + z_1 \\ \ddot{y} = -\lambda_1^* |s_1|^{\frac{1}{2}} \text{sign}(s_1) - \lambda_2^* \int_0^t \text{sign}(s_1) dt \end{cases} \quad (9)$$

In the absence of noise, the convergence time of this differentiation algorithm becomes so fast if the tuning of the convergence gains values is high. However, in the case of noisy signals, there is a trade-off between the convergence time and the reduction of the noise amplification. Indeed, the linear terms added on the dynamics equation of the algorithm represent a solution to have more smoothing outputs. Then, in this case, it is necessary not to choose a high value for  $K_i$ ,  $i \in \{0,1\}$ . For more details see [13].

### B. Parameters and Inputs Estimation

Started by the proposed parameter estimator, for this fact, we assume that the system parameters  $\theta^T = [\theta_1, \theta_2, \dots, \theta_r]$  satisfy some identifiability conditions in order to be obtained only from measured data. For this aim the observability test is obtained by rank test condition based on the calculation of the space spanned by gradients of the Lie derivatives of the output functions of the system.

$$\text{rank}(J_0) = \text{rank} \left( \left[ \frac{\partial}{\partial x_{j_1}} L_f^k y_{i_1} \right] \right) = n; \quad (10)$$

With  $j_1 = \{1, 2, \dots, n\}$ ;  $k = \{1, 2, \dots, n-1\}$ ;  $i_1 = \{1, 2, \dots, p\}$

Where  $L_f h(\cdot)$  is the Lie derivative defined by  $\frac{\partial h}{\partial x} f(\cdot)$  and  $J_0$  is the Jacobian matrix.

If  $\text{rank}(J_0) = n$ , so the system is observable. Therefore, by considering parameters as state variables  $P$  and have derivatives are equal to zero  $\dot{P} = 0$ . So, for the described system the parameter identifiability can be treated as a particular case of the observability problem. The rank test of the following matrix is then used to determine the parameters to be identified.

$$\text{rank}(J_1) = \text{rank} \left( \left[ \frac{\partial}{\partial P_{j_2}} L_f^k y_{i_1} \right] \right) = n; \quad (11)$$

$j_2 = \{1, 2, \dots, q\}$ ;  $k = \{1, 2, \dots, n-1\}$ ;  $i_1 = \{1, 2, \dots, p\}$ .

Suppose that the parameters to be identified  $\theta^T = [\theta_1, \theta_2, \dots, \theta_r]$  satisfy the identifiability condition, the estimation of the parameters  $[\theta_\lambda]_e$  could be written by (12)

$$[\theta_\lambda]_e = \phi_\lambda \left( t, [y]_e, [\dot{y}]_e, \dots, [y^{(p)}]_e, u, [\dot{u}]_e, \dots, [u^{(m)}]_e \right) \quad (12)$$

with  $\lambda = \{1, 2, \dots, r\}$

Where  $r$  is the parameters number.

For the input estimator, the estimation of the system's inputs is based on the flatness expression presented in equation (2) and the estimated parameters defined by (12). When including the equations (12) and (2), a relation between the parameter estimations and the system's outputs and their derivatives is defined as follows:

$$[u_i]_e = \gamma\left(t, [y], [\dot{y}]_e, \dots, [y^{(k)}]_e, [\theta_1]_e, \dots, [\theta_r]_e\right)$$

with  $i = \{1, 2, \dots, m\}$

(13)

Where  $\gamma$  is a nonlinear function,  $[y], [\dot{y}]_e, \dots, [y^{(k)}]_e$  are the output and their derivatives estimation given using the SMDDG differentiator and  $[\theta_1]_e, \dots, [\theta_r]_e$  are the parameter estimations.

After the estimation of the system's inputs, a comparison between the estimated inputs  $u_e$  and their nominal values  $u_n$  is performed. The residual signal is then defined as:

$$r_i = u_n - u_e$$
(14)

with  $i = \{1, 2, \dots, m\}$

(15)

Where  $\Gamma_i$  is a nonlinear function.

The residual signal  $r_i$  converge to zero in fault free case meaning that the input estimated  $[u]_e$  is equal to the nominal system input  $[u]_n$ . Besides,  $r_i$  makes a deviation in the presence of any anomaly in the system. Note that the residual vector has the same size of the input vector  $i = \{1, 2, \dots, m\}$  since it is a result of the difference between the nominal and the estimated inputs vector.

$$r_i = \begin{cases} 0 & [u]_e = [u]_n \\ \neq 0 & [u]_e \neq [u]_n \end{cases}$$
(16)

### C. Fault isolation with Neural Network

After the fault has been detected by the proposed FD method, it is necessary to obtain information about it in order to isolate faults. Indeed, it is important to determine which component is faulty in the system and also identify the successive and simultaneous fault cases. This problem is solved by using a Dynamic Neural Network algorithm (DNN). This algorithm is implemented by feed-forward technique explained in Fig. 2. DNN is an adaptive NN with multiple hidden layers of neurons used to model complex non-linear systems. The training consists in giving the proper output according to the corresponding input patterns. For our case, this algorithm is based on the learning method for the residual signal  $r = (r_1, r_2, \dots, r_m)$  obtained by the comparison between the nominal inputs  $(u_1, u_2, \dots, u_m)$  and the estimated ones  $(u_{1e}, u_{2e}, \dots, u_{me})$ .

The DNN's output  $d_i$  is trained to present "0" in the fault free case of the system and "1" in case of fault.

Considering the on-line use, the network training is performed for all possible fault scenarios with using a sliding

window  $T_{sw}$  where  $T_{sw} = 10T_e$  for the residual signal with a step of  $1ms$ . So, the signal is transformed into a matrix  $P$  as follows:

$$P = \begin{bmatrix} r_i(0) & r_i(T_e) & \dots & r_i(9T_e) \\ r_i(T_e) & r_i(2T_e) & \dots & r_i(10T_e) \\ \vdots & \vdots & \ddots & \vdots \\ r_i(\Delta t - 9T_e) & r_i(\Delta t - 8T_e) & \dots & r_i(\Delta t) \end{bmatrix}$$

In order to enable the neural network to learn the imposed input-output pattern, the network weights are adjusted by a specific algorithm called back propagation algorithm which is used in [10]. The main purpose is to bring the network function as close as possible to a given function. So, the learning problem consists to find better weight combinations.

However, the function is not given explicitly but implicitly through some examples. Consider a feed-forward network with  $m$  input and output. This network can have no fixed number of hidden units and can exhibit any desired feed-forward connection pattern. A training set  $\{(r_1, d_1), \dots, (r_i, dp_{NN})\}$  is given and consists of  $p_{NN}$  ordered pairs of  $m$  and  $p_{NN}$  dimensional input and output patterns vectors. The primitive functions of the networks are considered continuous and differentiable. The initial weights are considered as random numbers. In general, when the input  $r_i$  is presented to the network, it produces an output  $t_i$  different to from the desired  $d_i$ . The aim is to make  $t_i$  and  $d_i$  identical by using a learning algorithm. So, it is necessary to minimize the error function of the network, this error is defined by (17).

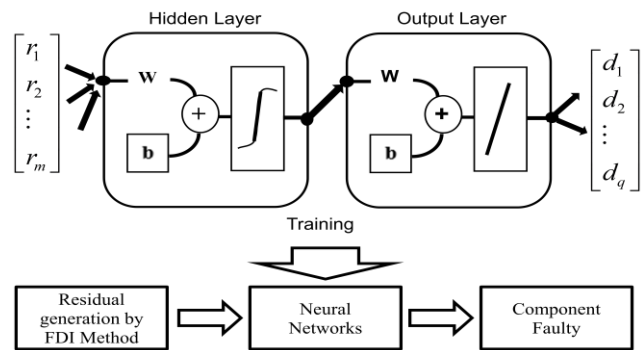


Fig. 2. Neural Network Pattern and Fault Isolation.

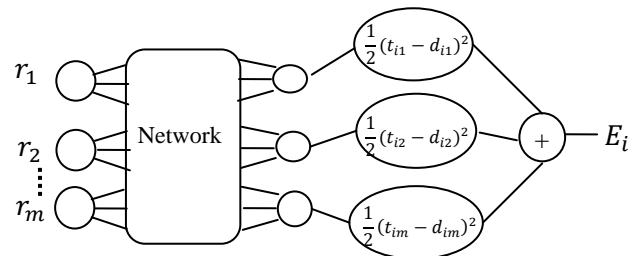


Fig. 3. Network for the Computation of the Error Function.

$$E = \frac{1}{2} \sum_{i=1}^{pNV} \|t_i - d_i\|^2 \quad (17)$$

After minimizing this error function, new unknown input patterns will be presented to the network and meanwhile it's interpolate. In order to obtain a local minimum of the error function, a back-propagation algorithm is used. Based on this algorithm, the network is initialized with random weight. After that we correct the initial weight by calculation of the gradient of the error function. Fig. 3 shows the computation technique of the error function by using the back-propagation technique. The minimization process consists at the first on extending the network to computes automatically the error function.

All the  $j$  output units of the networks evaluate the function  $\frac{1}{2}(t_{ij} - d_{ij})^2$ . The addition of the  $m$  outputs nodes gives  $E_i$  as a result. The same network extension has to be built for each pattern  $d_i$ . All quadratic errors are added in one sum unit  $E_1 + \dots + E_p$  to define the error function  $E$ . Then, the error for a given training set is calculated. In order to make the quadratic error  $E$  as low as possible, the weights are the only parameter that can be modified in the network. We now have w network capable of calculating the total error for given training set.  $E$  is calculated by the extended network exclusively through composition of the node functions, it is a continuous and differentiable function of the weights  $w_1, w_2, \dots, w_l$  in the network. We can thus minimize  $E$  by using an iterative process of gradient descent, for which we need to calculate the gradient.

$$\nabla E = \left( \frac{\partial E}{\partial w_1}, \frac{\partial E}{\partial w_2}, \dots, \frac{\partial E}{\partial w_l} \right).$$

Each weight is updated

$$\text{using the increment } \Delta w_i = -\gamma \frac{\partial E}{\partial w_i} \quad \text{for } i = 1, \dots, l.$$

Where  $\gamma$  represents a learning constant, i.e, a proportionality parameters which defines the step length of each iteration in the negative gradient direction. With this extension of the original network the whole learning problem now reduces to the question of calculating the gradient of a network function with respect to its weights. Once we have a method to compute this gradient, we can adjust the network weights iteratively. In this way we expect to find a minimum of the error function, where  $\nabla E = 0$ .

#### IV. APPLICATION TO THE THREE-TANK-SYSTEM

In order to validate the proposed FDI method, the chosen study system is the three-tank-system shown in Fig. 4. This system consists of three cylindrical tanks with identical section  $S$ . The three tanks are interconnected by two cylindrical pipes of section  $S_p$  and the outflow coefficients of tank 1 and tank 2 are  $q_{31}$  and  $q_{32}$  respectively. The liquid flows from the tank 3, with a valve of section  $S_p$  which supplies the two pumps  $P_1$  and  $P_2$  collected in the tank  $R_0$ .

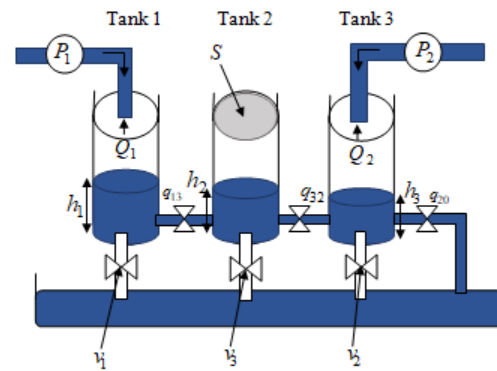


Fig. 4. Three-Tank System.

The two pumps are collected by DC motors, supply the tanks 1 and 2 with flow rates  $Q_1$  and  $Q_2$ . The water levels in the three tanks are noted by  $h_1, h_2$  and  $h_3$  respectively and verify the following inequality:  $h_1(t) > h_3(t) > h_2(t)$ . The three tanks are connected with the tank  $R_0$  by three valves  $v_1, v_2$  and  $v_3$  where their sections are flexible to simulate various failures such as more or less significant leaks on each tank.

The nominal behavior of this system is defined by:

- The valves  $v_1, v_2$  and  $v_3$  must be closed in order to have no leakage rates;
- The fluid is supposed to be perfect. Its characteristics are considered unchanged. So the parameters such as the coefficients of viscosity supposed to be known, certain and have a constant average value;
- The aging and the environment effects on the system's parameters are not considered.

Using the mass balance this system can be presented as follows

$$\begin{cases} S \frac{dh_1}{dt} = Q_1 - q_{13} \\ S \frac{dh_2}{dt} = Q_2 + q_{32} - q_{20} \\ S \frac{dh_3}{dt} = q_{13} - q_{32} \end{cases} \quad (18)$$

$q_{ij}; i, j = \{1, 2, 3\} \forall i \neq j$  represent the flow of water flowing from the tank  $i$  to  $j$ . The expression of the flow is given by:  $q_{ij} = \theta_i \cdot S_p \cdot \text{sign}(h_i - h_j) \cdot \sqrt{2g|h_i - h_j|}$  where  $q_{20}$  represent the outflow that can be expressed by  $q_{20} = \theta_2 \cdot S_p \cdot \sqrt{2g|h_2|}$ . For the next, the following notations are considered to facilitate the model exploitation:

$$x = (x_1, x_2, x_3)^T = (h_1, h_2, h_3)^T \text{ and } u = (u_1, u_2)^T = (Q_1, Q_2)^T .$$

Then the full nonlinear system model is given by

$$\begin{cases} \dot{x}_1 = -\frac{q_{13}}{S}\sqrt{x_1-x_3} + \frac{1}{S}u_1, \\ \dot{x}_2 = \frac{q_{32}}{S}\sqrt{x_3-x_2} - \frac{q_{20}}{S}\sqrt{x_2} + \frac{1}{S}u_2, \\ \dot{x}_3 = -\frac{q_{13}}{S}\sqrt{x_1-x_3} + \frac{q_{32}}{S}\sqrt{x_3-x_2}, \\ \begin{cases} y_1 = x_2, \\ y_2 = x_3, \end{cases} \end{cases} \quad (19)$$

This system has two flat outputs defined by  $y_1$  and  $y_2$ , see equations (20) and (21).

$$\begin{cases} x_1 = y_1 \\ x_2 = y_2 - \left( \frac{q_{13}\sqrt{y_1-y_2} - S\dot{y}_2}{q_{32}} \right)^2 \\ x_3 = y_2 \\ \begin{cases} u_1 = S\dot{y}_1 + q_{13}\sqrt{y_1-y_2}, \\ u_2 = -\frac{2S(q_{13}\sqrt{y_1-y_2} - S\dot{y}_2)}{q_{32}} \\ \quad \times \left( \frac{q_{13}(\dot{y}_1 - \dot{y}_2)}{2\sqrt{y_1-y_2}} - S\ddot{y}_2 \right) \\ \quad - q_{13}\sqrt{y_1-y_2} \\ \quad + q_{20}\sqrt{y_2 - \left( \frac{q_{13}\sqrt{y_1-y_2} - S\dot{y}_2}{q_{32}} \right)^2} \end{cases} \end{cases} \quad (20)$$

According to (20), the second input  $u_1$  is expressed in terms of these two flat outputs and their successive derivatives but its expression is still complex compared to the first input  $u_1$ .

For the parameter estimation of the system, it is necessary to test the identifiability of the latter. So, to obtain information about system's parameters it is necessary to calculate the Jacobean matrix of Lie-derivatives (21):

$$J_I = \begin{bmatrix} \frac{\partial}{\partial P_1} L_f y_1 & \frac{\partial}{\partial P_2} L_f y_1 & \frac{\partial}{\partial P_3} L_f y_1 \\ \frac{\partial}{\partial P_1} L_f y_2 & \frac{\partial}{\partial P_2} L_f y_2 & \frac{\partial}{\partial P_3} L_f y_2 \\ \frac{\partial}{\partial P_1} L_f y_3 & \frac{\partial}{\partial P_2} L_f y_3 & \frac{\partial}{\partial P_3} L_f y_3 \end{bmatrix} \quad (21)$$

$$\text{Where } \frac{\partial}{\partial P_2} L_f y_1 = \frac{\partial}{\partial P_3} L_f y_1 = \frac{\partial}{\partial P_1} L_f y_2 = \frac{\partial}{\partial P_2} L_f y_3 = 0$$

$$\text{and } \det(J_I) = -\frac{\partial}{\partial P_2} L_f y_2 \cdot \frac{\partial}{\partial P_1} L_f y_1 \cdot \frac{\partial}{\partial P_3} L_f y_3 \neq 0; \text{ for } x_1 > x_3 > x_2.$$

So, the rank of the matrix (21) is 3 and also  $n=3$ . Therefore, the system's parameters are identifiable. Then, the observability of the system is justified. Based on equation (19) it can be concluded that the parameter estimation as follows

$$\begin{cases} [\theta_1]_e = \frac{-S[\dot{y}_1]_e + u_1}{S_p \text{sign}(y_1 - y_3) \sqrt{2g|y_1 - y_3|}} \\ [\theta_2]_e = \frac{-S([\dot{y}_1]_e + [\dot{y}_2]_e + [\dot{y}_3]_e) - (u_1 + u_2)}{S_p \text{sign}(y_2) \sqrt{2g|y_2|}} \\ [\theta_3]_e = \frac{-S([\dot{y}_1]_e + [\dot{y}_3]_e) + u_1}{S_p \text{sign}(y_3 - y_2) \sqrt{2g|y_3 - y_2|}} \end{cases} \quad (22)$$

For the input estimator, it is easy to obtain the estimation of the system's inputs using (20) and (22):

$$\begin{cases} [u_1]_e = S[\dot{y}_1]_e + q_{13}\sqrt{y_1-y_2}, \\ [u_2]_e = -\frac{2S(q_{13}\sqrt{y_1-y_2} - S[\dot{y}_2]_e)}{q_{32}} \\ \quad \times \left( \frac{q_{13}([\dot{y}_1]_e - [\dot{y}_2]_e)}{2\sqrt{y_1-y_2}} - S[\ddot{y}_2]_e \right) \\ \quad - q_{13}\sqrt{y_1-y_2} \\ \quad + q_{20}\sqrt{y_2 - \left( \frac{q_{13}\sqrt{y_1-y_2} - S[\dot{y}_2]_e}{q_{32}} \right)^2} \end{cases} \quad (23)$$

The residual expression is given by (24)

$$\begin{cases} r_1 = [u_1]_e - u_1 \\ r_2 = [u_2]_e - u_2 \end{cases} \quad (24)$$

In the following paragraph simulation results of the proposed method are presented.

## V. SIMULATION RESULTS

For the estimation tests, the Matlab SIMULINK is used with sampling period  $T_e = 10^{-3} s$  and in the presence of a Gaussian white noise with noise power equal to 0.01. The known nominal parameters of the system are: the gravity constant  $g = 9.81 m.s^{-2}$ , the tank section  $S = 0.0154 m$

and the pipes section  $S_p = 5.10^{-5} m$ . The nominal values of the viscosity coefficient of the system are:  $\theta_1 = 0.5$ ,  $\theta_2 = 0.675$ ,  $\theta_3 = 0.5$ . For the SMDDG,  $K_0 = 150$  and  $K_1 = 100$  are considered and the dynamic gains initialized to zero. The simulations are achieved under operating conditions that allow the full rank condition for parameter identifiability. To satisfy this condition, the operating conditions are chosen as with operating condition  $x_1 > x_3 > x_2$ .

To prove the effectiveness of the proposed method, various fault scenarios are defined and summarized in Table I. The first one consists on simple actuator fault first one consists on simple actuator fault  $f_{act1}$  which appeared in the first input  $u_1$  of the system. The second scenario is a simple process fault  $f_{proc1}$  that occurs on the first parameter of the system  $\theta_1$ . For scenario 3, three faults are generated. Two faults appear successively at the first, then the second actuator,  $f_{act1}$  and  $f_{act2}$  respectively and another one appears on the output sensor. The last scenario considers the case of simultaneous process faults that arise on the system,  $f_{proc1}$  and  $f_{proc2}$  respectively.

For our studied system, the process faults are generally consisting on leakage faults. However the actuator faults can be defined by a reduction in control effectiveness.

An evaluation with known method in literature will be performed.

#### A. Analysis and Validation of the Fault Detection Schemes

Before presenting the simulation results, it is important to specify the types of faults that are applied. Table II summarizes the forms of the various faults. Here, the actuator fault is a positive intermittent signal, the process faults are an intermittent negative signal and the fault sensors is a step signal.

The effectiveness of the proposed FDI method Fig. 1 presented in the comparison results between the using of the SMDDG Differentiator (7) and the case when we used the Second Order Sliding Mode Differentiator (5).

1) *Simple Actuator fault detection: Scenario 1:* In this case, an intermittent fault  $f_{act1}$  is introduced in the first actuator at  $20ms$ . The simulation results are shown in Fig. 5. Based on equation (23), Fig. 5(a) shows the first and the second input estimation  $[u_1]_e$  and  $[u_2]_e$  respectively. This figure represents the curves given by using the SMDDG and HOSM compared by the nominal input values with any faults.

Remark that the red signal obtained by the SMDDG presents a positive peak which appeared at  $t = 20ms$  and a negative one appeared at  $t = 25ms$ .

This explains that despite of the noise presence, it is well possible to detect an intermittent fault occurring on the first input  $u_1$ .

First output estimation is provided by the SMDDG. However, with the HOSM differentiator fault detection is much more difficult since the failure is almost lost in the noise.

Consequently, only a very small variation appeared in both input and output of the estimated signal at the interval time  $t \in [20 \ 25]ms$ . In Fig. 5(c) it is clear to see that, the first residual given by the SMDDG can introduce the appearance of actuator fault on  $u_1$ . Since this residual is considered as DNN inputs so learning is better than the residual signal obtained using the HOSM.

2) *Simple process fault: scenario 2:* The second scenario represents a case of an intermittent fault  $f_{proc2}$  introduced in the second parameter of the system at  $30ms$ . Fig. 6(a) and Fig. 6(b) represents the first and the second inputs and their estimations by using the SMDDG and the HOSM differentiator. These figures show that a fault occurred at  $t = 30ms$ .

TABLE I. SIMULATION SCENARIOS

| Fault Types and its magnitude    | Actuator 1<br>$f_{act1} = 0.6$ | Actuator 2<br>$f_{act2} = 0.4$ | Process 1<br>$f_{proc1} = -0.5$ | Process 2<br>$f_{proc2} = -0.3$ | Sensor 1<br>$f_{sen1} = 0.01$ |
|----------------------------------|--------------------------------|--------------------------------|---------------------------------|---------------------------------|-------------------------------|
| <i>Fault appearance interval</i> | $[20, 25]ms$                   | $[25, 30]ms$                   | $[20, 28]ms$                    | $[30, 36]ms$                    | $t = 30ms$                    |
| <i>Scenario 1</i>                | ✓                              |                                |                                 |                                 |                               |
| <i>Scenario 2</i>                |                                |                                |                                 | ✓                               |                               |
| <i>Scenario 3</i>                | ✓                              | ✓                              |                                 |                                 | ✓                             |
| <i>Scenario 4</i>                | ✓                              |                                | ✓                               | ✓                               |                               |



TABLE II. FAULT MODEL

| Fault Types    | Model |
|----------------|-------|
| Actuator Fault |       |
| Process Fault  |       |
| Sensor Fault   |       |

In the same time, a perturbation is showed in the second parameter  $[\theta_2]_e$  estimated by using the equation (22).

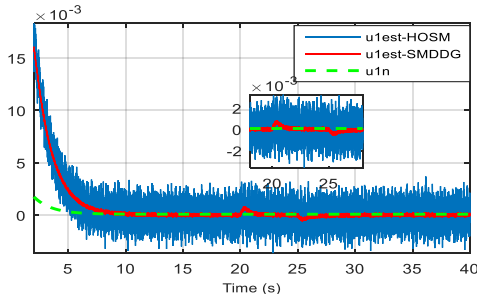
With the SMDDG differentiator, the occurrence of fault is clearly shown compared it to the case of using the HOSM differentiator algorithm. The occurrence of the fault only in the second estimated input explained by its expression in equation (23), where the first input estimation is independent of the second parameter of the system. This difference shows the performance of our differentiator compared to the HOSM differentiator which presents more noise amplification. In

Fig. 6(e) of the residual signal  $r_2$  the fault starts with a negative peak and ends with a positive one.

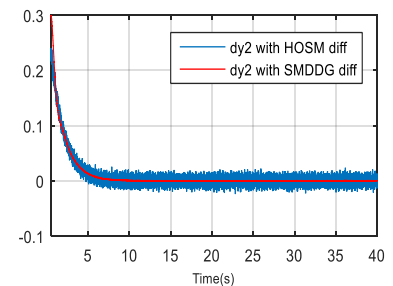
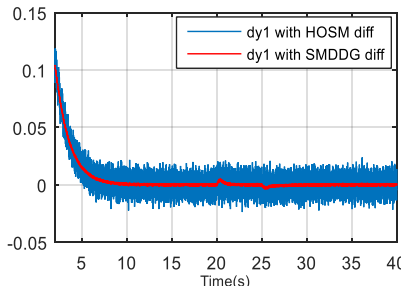
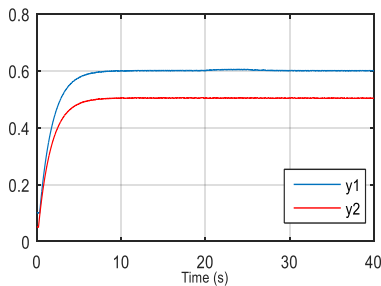
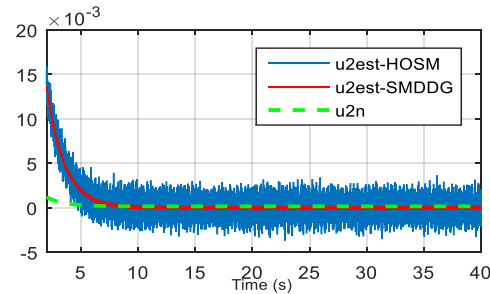
This explains the presence of process fault, because the process defect is described by a leak so the residual, which is the difference between  $[u_2]_e$  and  $u_2$ , gives a decay to the residual curve.

3) *Successive actuator faults detection case scenario 3:* In the practical case of non-linear systems, not only simple faults can appear, but many faults can occur in the same time or/and in a successive way. In this case, successive faults are tested. A fault  $f_{act2}$  is introduced in actuator 2 at 25ms. In the same way, successive faults,  $f_{act1}$  in actuator 1 at 20ms and  $f_{sen1}$  in sensor 1 at 30ms have been simulated. Fig. 7 shows the simulation results of this case.

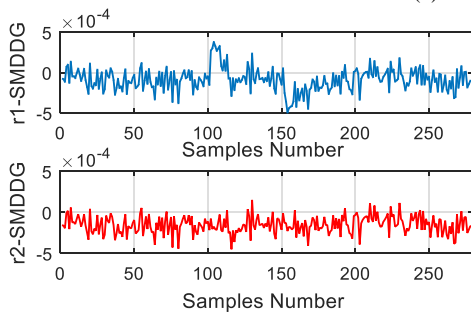
Thanks to the flatness properties, the system presents a strong relation between all parameters; inputs, outputs, there derivatives and even all the parameters of system itself shown in equation (22) and (23). Basing on Fig. 7 and with using the SMDDG, we remark the presence of fault in the output derivatives, Fig. 7(a) and also in the input estimation, Fig. 7(c).



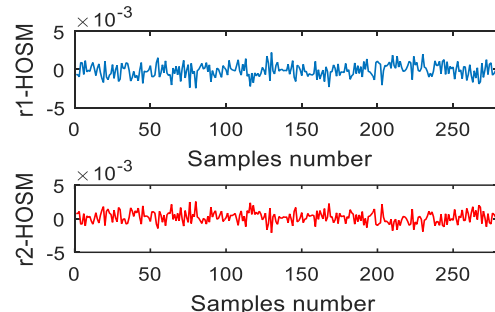
(a). First and second inputs estimation using HOSM and SMDDG.



(b). Outputs and its derivative estimations.



(c). First residual signal with SMDDG



(d). First residual signal with HOSM.

Fig. 5. First Scenario: Simple Actuator Fault.

But for the results that are given by using the HOSM differentiator, a small disturbance is shown, see Fig. 7(d) due to the presence of chattering on the estimated signals. For the residual signals given in Fig. 7(e), the actuator fault is shown like in the previous example and the sensor fault is presented by a high positive magnitude peak.

4) *Simultaneous fault detection case scenario 4*: Now, the scenario considering simultaneous faults is presented. The faults present in this case are: an actuator and a two process faults respectively  $f_{act1} = 0.6$ ,  $f_{proc1} = -0.5$ , and  $f_{proc2} = -0.3$ . The  $f_{act1}$  and  $f_{proc1}$  appeared in the same time on the first input and also a fault in the second parameter

systems  $f_{proc2}$  appeared in next time. The first and the second inputs estimations are shown in Fig. 8(a). The curve of the estimated parameter  $\theta_2$  shows the presence of two faults. The first one caused by  $f_{proc1}$  and the second one by  $f_{proc2} = -0.3$ . This proves the difficulty of the isolation step.

In Fig. 8(d) which corresponds to the residual signals; it is clear that in the case where the SMDDG differentiator is used, faults are visible more clearly than the using of HOSM differentiator. Finally, the proposed simulation results show the effectiveness of the proposed technique in detecting faults compared to the well-known Levant's differentiator.

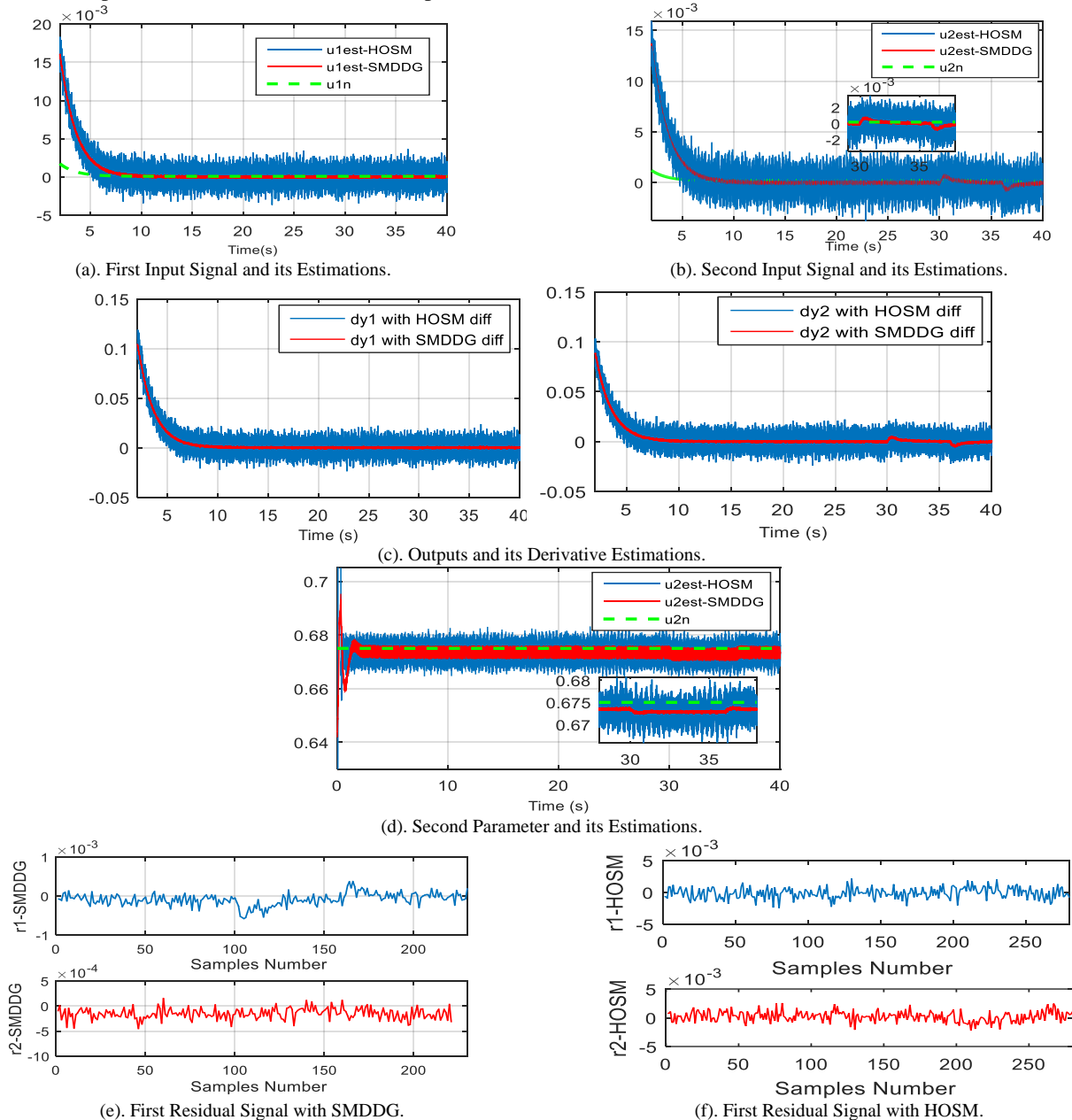


Fig. 6. Second Scenario Simple Process Fault.

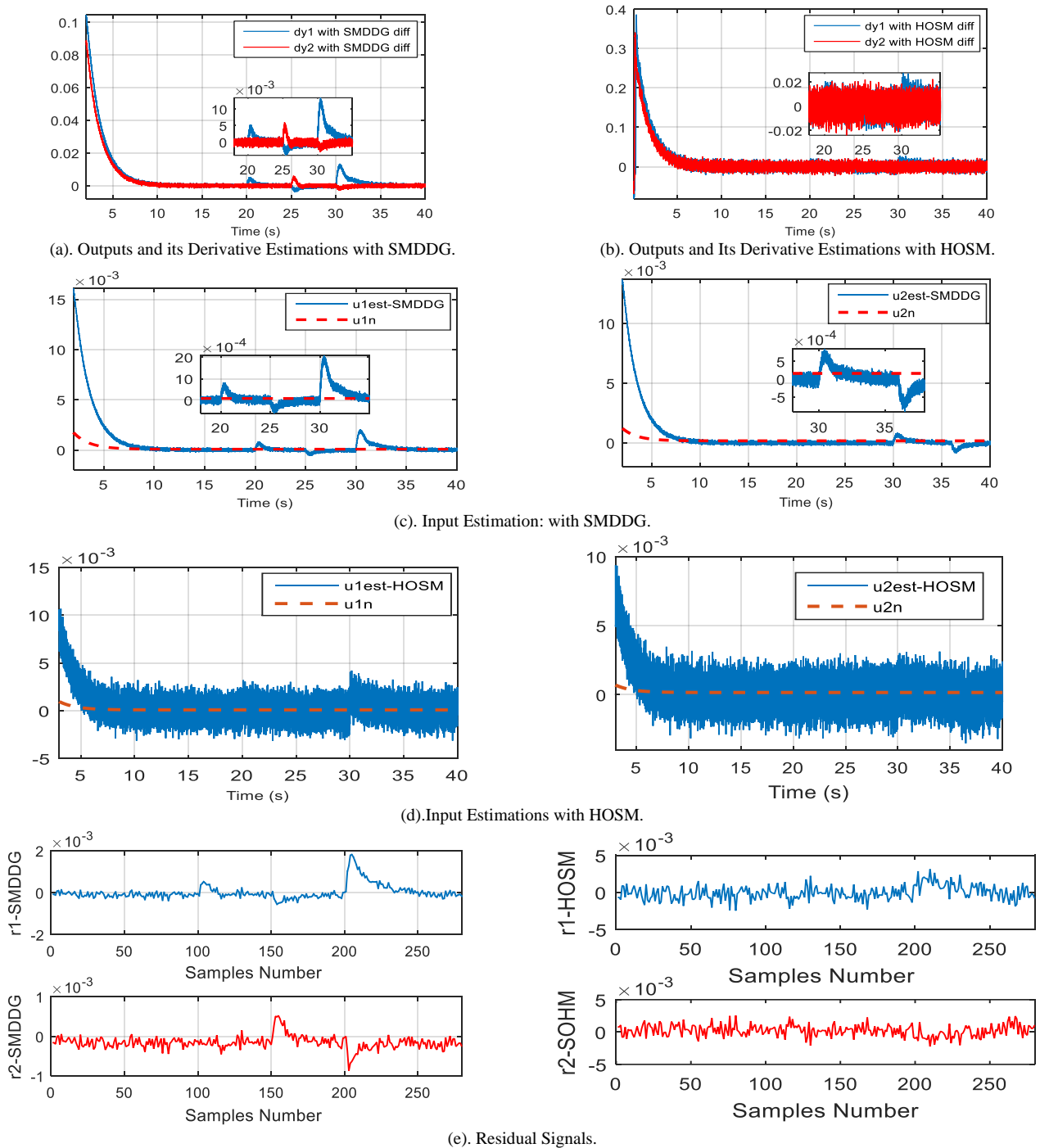


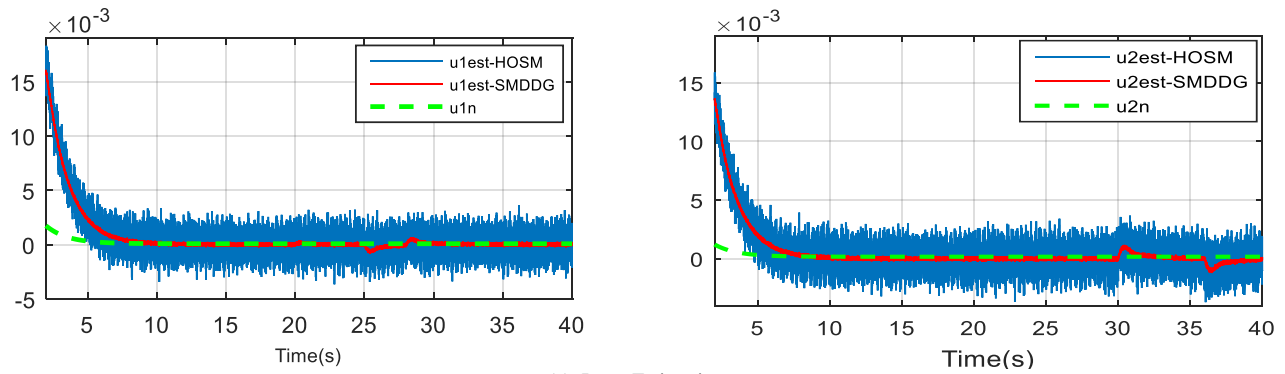
Fig. 7. Third Scenario: Case of Successive Faults.

### B. Fault Isolation

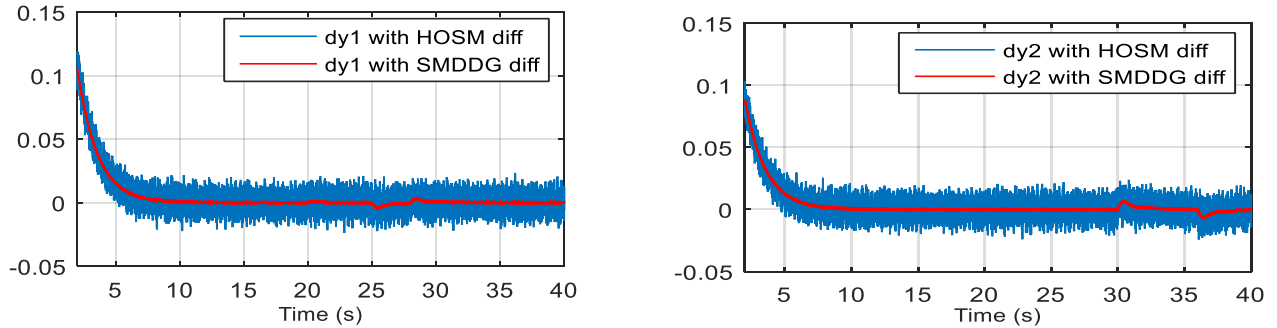
After the detection fault, the fault type is identified by the use of the DNN. The results of the four scenarios are summarized in Tables III and IV.

The first table shows the results in the case of using the SMDDG differentiator. With this last one, the fault kinds are clearly identified in all of the simulation scenarios. For example, in the case of successive actuator faults, we remark that the table presents the value 1 in the box of the first and the

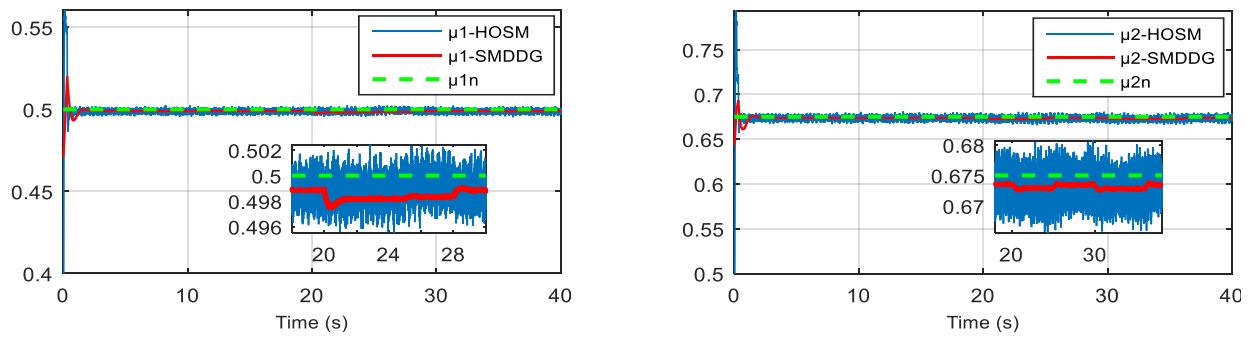
second actuators and also in the box of the first. Table II represents the results of the isolation fault by the DNN in the case of using the HOSM differentiator. In this table, some faulty alarm is presented. For example, in the case of scenario4, where the first actuator fault and the first process fault occurs simultaneously and a fault occurs in the second process, the value 1 is present in the first and the second actuator, in the first process and in the first sensor. Also, in the scenario3, it shows the presence of fault in the second process and the first sensor, which represents a faulty alarm.



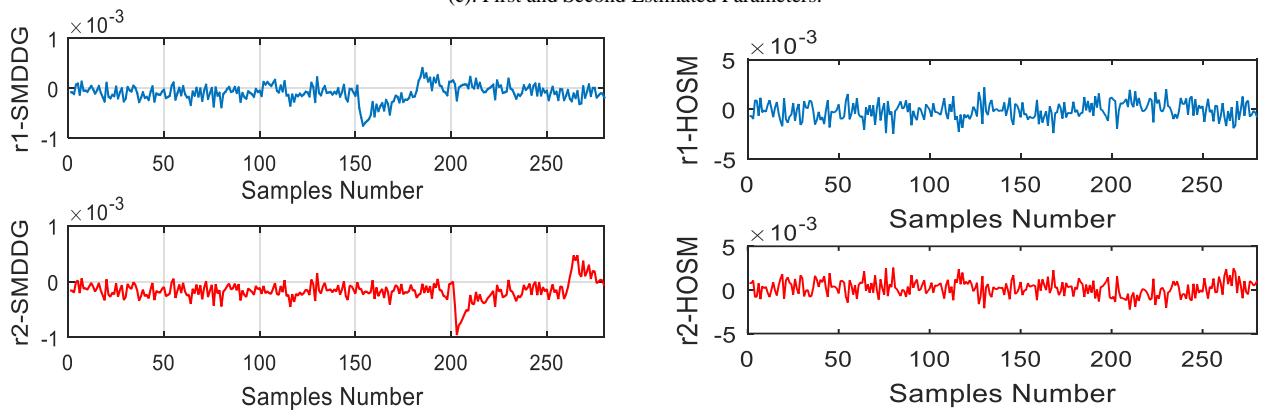
(a). Input Estimations.



(b). Outputs and its Derivative Estimations.



(c). First and Second Estimated Parameters.



(d). Residual Signals.

Fig. 8. Ford Scenario Case of Simultaneous Faults.

TABLE III. NEURAL NETWORK RESULTS: SMDDG CASE

| Residual |       | $f_{act1}$ | $f_{act2}$ | $f_{proc1}$ | $f_{proc2}$ | $f_{sen1}$ | $f_{sen2}$ |
|----------|-------|------------|------------|-------------|-------------|------------|------------|
| S1       | $r_1$ | 1          | 0          | 0           | 0           | 0          | 0          |
|          | $r_2$ | 0          | 0          | 0           | 0           | 0          | 0          |
| S2       | $r_1$ | 0          | 0          | 0           | 0           | 0          | 0          |
|          | $r_2$ | 0          | 0          | 0           | 1           | 0          | 0          |
| S3       | $r_1$ | 1          | 0          | 0           | 0           | 1          | 0          |
|          | $r_2$ | 0          | 1          | 0           | 0           | 0          | 0          |
| S4       | $r_1$ | 1          | 0          | 1           | 0           | 0          | 0          |
|          | $r_2$ | 0          | 0          | 0           | 0           | 1          | 0          |

TABLE IV. NEURAL NETWORK RESULTS: HOSM CASE

| Residual |       | $f_{act1}$ | $f_{act2}$ | $f_{proc1}$ | $f_{proc2}$ | $f_{sen1}$ | $f_{sen2}$ |
|----------|-------|------------|------------|-------------|-------------|------------|------------|
| S1       | $r_1$ | 1          | 0          | 0           | 0           | 1          | 0          |
|          | $r_2$ | 0          | 1          | 0           | 0           | 0          | 0          |
| S2       | $r_1$ | 1          | 0          | 1           | 0           | 0          | 0          |
|          | $r_2$ | 0          | 0          | 1           | 1           | 0          | 0          |
| S3       | $r_1$ | 1          | 0          | 0           | 1           | 1          | 0          |
|          | $r_2$ | 0          | 1          | 0           | 1           | 0          | 1          |
| S4       | $r_1$ | 1          | 0          | 1           | 0           | 0          | 0          |
|          | $r_2$ | 0          | 1          | 0           | 0           | 1          | 0          |

## VI. CONCLUSION

In this paper, a new FDI method is proposed to solve the fault detection and isolation problem in particular class of nonlinear system having the flatness property. This property gives a generic residual signal which is obtained by the difference between the input estimation and the nominal one. The residual signals are ready to be sensitive to all types of fault that can appear in the system which makes the identifiability of the fault very difficult. The effectiveness of the proposed fault detection method is given by the using of the SMDDG differentiator which gives satisfactory results in comparison with results obtained by the Levant's HOSM differentiator. After the fault detection, the isolation phase is done by the use of DNN pattern with back propagation. Many

scenarios are tested to improve the effectiveness of the proposed method which contains an actuator, process or sensor fault. These faults are presented in different situation; simple, successive and simultaneous cases.

Several future works can be considered as a perspective. The first is to apply this approach in the practical case and the second is to extend this approach to be applied on other types of nonlinear systems.

## REFERENCES

- [1] Seogpil, Cho, Zhen et al, "Model based fault detection, fault isolation and fault tolerant control of a blade pitch system in floating wind turbine", Renewable Energy Journal, 2018.
- [2] H. Shahnazari, P. Mhaskar "Actuator and sensor fault detection and isolation for nonlinear systems subject to uncertainty", International Journal Robust Nonlinear Control, 2017.
- [3] José Carlos M. Oliveira, Karen V. Pontes, Isabel Sartori, Marcelo Embiruçu, "Fault Detection and Diagnosis in dynamic systems using Weightless Neural Networks", Expert Systems With Applications, 2017.
- [4] E. Naderi, K. Khorasani, "Data-driven fault detection, isolation and estimation of aircraft gas turbine engine actuator and sensors", Mechanical Systems and Signal Processing, 2018.
- [5] P. Aboutaleb, A. Abbaspour, P. Forouzaneshad, A. Sargolzaei "A Novel Sensor Fault Detection in an Unmanned Quadrotor Based on Adaptive Neural Observer" "Intell Robot Syst Journal", 2017.
- [6] A. Abbaspour, P. Aboutaleb, Kang K.Yen, A. Sargolzaei, "Neural adaptive observer-based sensor and actuator fault detection in nonlinear systems: Application in UAV", ISA Transactions, 2017.
- [7] H. Rios, J. Davila, L. Fridman and C. Edwards, "Fault Detection and Isolation for Nonlinear System via HOSM Multiple-Observer", International Journal of Robust and Nonlinear Control, 2012.
- [8] A. Levant, "Robust exact differentiation via sliding mode technique", Automatica, vol.34, 1998.
- [9] Tiago Roux Oliveira, Victor Hugo Pereira Rodrigues, Antonio Estrada, Leonid Fridman, "Output-feedback variable gain super-twisting algorithm for arbitrary relative degree systems", International Journal of Control, 2043-2059, 2018.
- [10] Hussein Obeid, Leonid Fridman, Salah Laghrouche, Mohamed Harmouche and Mohammad Ali Golkani, "Adaptation of Levant's Differentiator Based on Barrier Function", International Journal of Control, 2017.
- [11] Carlos Vazquez, Stanislav Aranovskiy, Leonid B. Fridovich, Leonid Fridman "Time-Varying Gain Differentiator: A Mobile Hydraulic System Case Study", IEEE Transactions on Control Systems Technology, 1063-6536, 2016.
- [12] Fliess, M., Levine, J., Martin, P. and Rouchon, P. Sur les systèmes non linéaires différentiellement plats, Comptes rendus de l'Académie des sciences, Srie I: Mathématiques 315(5): 619-624, 1992.
- [13] L. Sidhom, M. Smaoui, X. Brun and E. Bideaux, « Robust Estimator Design for Control of Electropneumatic System », IETE Journal of Research, Vol. 7, No.5, pp. 689-701, September 2018.

# Big Data Technology-Enabled Analytical Solution for Quality Assessment of Higher Education Systems

Samiya Khan<sup>1</sup>, Mansaf Alam<sup>4</sup>  
Department of Computer Science  
Jamia Millia Islamia  
New Delhi  
India

Xiufeng Liu<sup>2</sup>  
DTU Management  
Technical University of Denmark  
Lyngby  
Denmark

Kashish Ara Shakil<sup>3</sup>  
College of Computer and  
Information Sciences, Princess Nora  
Bint AbdulRahman University  
Saudi Arabia

**Abstract**—Educational Intelligence is a broad area of big data analytical applications that make use of big data technologies for implementation of solutions for education and research. This paper demonstrates the designing, development and deployment of an educational intelligence application for real-world scenarios. Firstly, a quality assessment framework for higher education systems that evaluate institutions on the basis of performance of outgoing students was proposed. Secondly, big data enabled technological setup was used for its implementation. Literature was surveyed to evaluate existing quality frameworks. Most existing quality assessment systems take into account the dimensions related to inputs, processes and outputs, but they tend to ignore the perspective that assesses the institution on the basis of outcome of the educational process. This paper demonstrates the use of outcome perspective to compute quality metrics and create visual analytics. In order to implement and test the framework, R programming language and a cloud based big data technology that is Google, BigQuery were used.

**Keywords**—Education big data; educational intelligence; educational technology; higher education; quality education

## I. INTRODUCTION

The concept of educational intelligence [1] was introduced as an umbrella term for all analytical solutions created for education and research sectors. A range of applications have been proposed in recent times, ranging from applications for improving the operational efficiency of educational and research institutes, to specific predictive analytical applications for foretelling student dropout rates and prescriptive analytical solutions to improve the quality of education. It is important to note that a majority of the proposed solutions have not been prototyped or implemented. Firstly, this paper proposes an outcome-based quality assessment framework for higher education systems. Secondly, it demonstrates the implementation of an educational intelligence solution with the help of base technologies used for big data storage and processing.

Higher education is the backbone of the education system of any country. Effective management and quality assessment of the higher education system is not just important, but it is also necessary. However, the concept of quality in higher education has found varied definitions and descriptions in literature. The most recent and widely accepted definition of quality describes it as conformance of standards and meeting the set objectives. Besides this, there are many other definitions

that incorporate the perspectives of different stakeholders like students, organization and parents, in addition to others. However, none of the dimensions covers the outcome perspective of the education system. The proposed framework evaluates quality from this perspective.

The key process involved in higher education systems is the process of imparting education or the education process. The outcome of this process is determined by the performance of students after passing out of the course concerned, which is assessed using the information about the university or company that student joins after course completion. Quality score is computed using this information and analytics are generated on the basis of the cumulative study of these quality scores.

The analytical framework proposed in this paper can be used for evaluating the performance of an educational organization on the basis of the cumulative quality scores' analysis of the students who pass out in a year. Moreover, predictive analysis can also be generated to monitor progress and make interventions as and when required, to maintain quality of the educational organizations and system, at large.

There are several ways in which such a quality metric may be relevant. Most quality metrics assume that the responsibility of an educational institution for a student's performance is restricted to the time that the student concerned spends while he or she is enrolled in the institution. However, the responsibility of the student's performance on his or her alma mater extends beyond this timeframe. This is perhaps the reason why organizations take pride in their alumni networks and achievers who hail from their institutes. Therefore, a quality evaluation basis that assesses the organization's performance on the basis of student performance after he or she completes the course is considerable.

Inclusion of this quality dimension to the assessment framework will bring the attention of organizations to this aspect. Quality assurance in this regard shall boost postgraduate and research enrollments, promoting higher and advanced studies. Besides this, such an assessment will also drive educational institutions to groom students for prospective future degrees or jobs, bridging the gap that usually exists between these transitions. In entirety, this quality dimension will bring educational organizations a step closer to fulfilling their purpose, meeting institutional vision and conforming to standards in the outcomes context.

In countries like India, which boast of 34,211 thousand enrollments<sup>1</sup> for the academic year 2014-15 in higher education, the amount of data collected is immense. This data is high in volume, contains images and textual data for variety and is generated on a yearly basis. Moreover, the use of data mining and machine learning in educational analytics [2] makes big data technologies a relevant solution for educational analytics [3]. When projected in the global domain, education data is certainly a ‘big’ data set.

Owing to the volume, variety and velocity of data generated by the education system, education data can easily be termed as a class of big data called ‘big education data’. Some of the information that is recorded as part of this system includes profile of teachers, students and operational data. Therefore, big data technologies can be used to develop educational intelligence solutions. In line with this, the case study done for implementing the proposed framework and providing a proof of concept makes use of Google BigQuery [4] and R programming language [5] to generate analytics.

The motivation behind this paper is to propose a simple technological framework that makes use of base technologies for development of educational intelligence applications. Therefore, this paper demonstrates the designing, development and deployment of an educational intelligence application. The contributions of this paper include the following: (1) proposes an outcome-based quality assessment framework for higher education systems (2) implements an educational intelligence application that use the proposed framework with the help of base technologies (3) deploys the educational intelligence application on cloud for use.

The rest of the paper has been organized in the following manner: Section II provides insights on related work for educational intelligence applications, their viability for higher education systems and the concept of quality and its definition in the higher education context. Section III provides details about the proposed framework. Section IV and Section V describe how big data analytics solutions can be used for handling big data generated by higher education systems and provides a case study of how this framework can be implemented using cloud-based big data technology, BigQuery, and R programming. Lastly, the paper concludes in Section VI and Section VII providing insights on scope for improvements and future work.

## II. RELATED WORK

The applicability of big data technologies [6], implemented using cloud-based infrastructures, to real-world, data-intensive scenarios has given rise to many sub-research areas. Big data has particularly found applications in healthcare [7], geospatial analytics [8] and business intelligence [9], in addition to many others. Education data is a form of big data and can make use of big data technologies for generating valuable analytics for an educational organization [10]. González-Martínez et al. [11] investigated the use of cloud computing in education, citing it as one of the key new-age technologies to have found applications in education.

IBM’s big data model defines five big data characteristics [12], namely, volume, velocity, variety, veracity and value. Evidently, data collected at the student level is ‘big’ in ‘volume’, both on a per-year basis as well as over-the-years. Student profiles include textual and image data like scanned copy of the student’s photograph and signature. The different types of data included in the collection makes up for the ‘variety’ characteristic of big data. Moreover, this data is generated on a yearly basis, accounting for ‘velocity’ of data.

Student data used for processing is manually entered. As a result, the probability of error and associated uncertainty are rather high, which makes veracity a significant characteristic in the education system context. Lastly, educational intelligence solutions [1] can be used for improving the operational efficiency of the system and support administrative processes with improved decision-making, adding value to the data and analytical solutions that it can produce. Educational data mining [13] has also been used for predicting student performance [14], which is one of the typical scenarios that can be converted into a big data case study.

For the purpose of feasibility evaluation of educational intelligence solutions for real world education systems, the Indian higher education system has been considered. The numbers of universities and institutions that can utilize educational intelligence solutions have been given in Table I, with a breakdown of the different types of organizations that it entails. This analysis can be projected to the global scenario to conclude that the education data set is indeed ‘big’. Besides this, the total number of students pursuing different courses in the Indian higher education system has been detailed in Table II.

TABLE I. NUMBER OF HIGHER EDUCATION INSTITUTIONS BY TYPE 2014-15<sup>1</sup>

| Level                   | Type                                     | Total |
|-------------------------|--|-------|
| University              | Central University                       | 43    |
|                         | State Public University                  | 316   |
|                         | Deemed University                        | 122   |
|                         | State Private University                 | 181   |
|                         | Central Open University                  | 1     |
|                         | State Open University                    | 13    |
|                         | Institution of National Importance       | 75    |
|                         | State Private Open University            | 1     |
|                         | Institutions Under State Legislature Act | 5     |
|                         | Others                                   | 3     |
|                         | Total                                    | 760   |
| College                 |  | 38498 |
| Standalone Institutions | Diploma Level Technical                  | 3845  |
|                         | PGDM                                     | 431   |
|                         | Diploma Level Nursing                    | 3114  |
|                         | Diploma Level Teacher Training           | 4730  |
|                         | Institute Under Ministries               | 156   |
|                         | Total                                    | 12276 |

<sup>1</sup> <http://mhrd.gov.in/statist>

TABLE. II. LEVEL-WISE ENROLMENT IN SCHOOL & HIGHER EDUCATION 2014-15<sup>1</sup>

| Level                  | Total (in thousand) |
|------------------------|---------------------|
| Ph.D.                  | 118                 |
| M. Phil.               | 33                  |
| Postgraduate           | 3853                |
| Undergraduate          | 27172               |
| PG Diploma             | 215                 |
| Diploma                | 2508                |
| Certificate            | 170                 |
| Integrated             | 142                 |
| Higher Education Total | 34211               |

The numbers of institutions that can utilize such solutions are high. This makes educational intelligence solutions commercially viable. Moreover, cloud-based big data technologies are deemed most appropriate for developing analytical solutions for education and research [15]. The integration of the analytics derived from such solutions can be integrated with insights to get value-based solutions [16].

The standard meaning of quality is a measurement of standard or excellence. In higher education, the concept of quality emerged in early 1980s and was derived from its commercial counterparts [17]. However, academic quality was considered an abstract term in those days. The traditional concept of quality [18] was inferred from the fact that world-class universities like Harvard and Oxford were considered benchmarks and no further dissection on the dimensions of quality was done.

Green [18] gave an extensive analysis of the literature that defines the term quality and categorized them into the following five approaches:

1) Conforming to standards in terms of the educational

process and outcomes

2) Befitting the purpose: This is a contradictory definition as most scholars feel that if the institution meets standards, it fits its purpose, which may not always be the case.

3) Ability to meet set institutional goals and having a clear vision.

4) Meeting the needs of the customer or student: It is important to state here that the student can be considered a product, customer or both by the higher education institution. While the student is paying for getting education, which makes him or her the customer, it is the student's performance that will determine the quality of the institute, making him also the product.

5) The traditional concept defines quality as strive for excellence.

Recent definitions of quality have added dimensions like ethics and moral values [19] and accountability and accreditation [20] to the core system. Owlia and Aspinwall [21] gave a conceptual framework for measuring quality on the basis of dimensions that take student and administrative perspectives into account. It caters for dimensions from a service-oriented point of view. Another perspective that needs to be taken into account while defining quality is that of the stakeholders. In the higher education context, academics' and students are the main internal stakeholders, in addition to other stakeholders like the state, society, employers, parents and professional associations. Student's perspective on quality [22] is considered extremely important.

Related studies that cover higher education service quality dimensions include Parsuraman [23], Gronroos [24], Lehtinen and Lehtinen [25], Carney [26], Athiyaman [27], Lee et al. [28], Hadikoemoro [29], O'Neill and Palmer [30], Sahney et al. [31], Brooks [32] and Teeroovengadam et al. [33]. A comparison of the dimensions proposed by each of these works and the perspective they cover has been provided in Table III.

TABLE. III. COMPARISON OF QUALITY ASSESSMENT FRAMEWORKS FOR HIGHER EDUCATION SYSTEMS

| Research Work                       | Brief Description  | Dimensions Considered   | Perspective Covered  |
|-------------------------------------|--|---|--|
| Parsuraman [23] and Parsuraman [34] | Parsuraman [23] proposed 10 dimensions, which were later classified into five categories by Parsuraman [34]. Among the identified dimensions, empathy was considered least important while reliability was placed highest on the list. | The categories and corresponding dimensions for them are as follows - <ul style="list-style-type: none"> <li>Tangibles - This category includes dimensions like equipment, physical facilities and appearance of personnel.</li> <li>Reliability - This category includes the ability of staff to provide the service accurately and consistently.</li> <li>Responsiveness - This category includes the ability of staff to respond to demands of students and help them.</li> <li>Assurance - This category includes dimensions like knowledge of employees and their ability to communicate trust and confidence.</li> <li>Empathy - This category includes dimensions like the ability of staff to give individual attention and care for students.</li> </ul> | Takes into account only the student perspective and considers student as a customer. |
| Gronroos [24]                       | Identified six criteria for classifying perceived service quality as good.   | The identified criteria are as follows - <ul style="list-style-type: none"> <li>Skill and Professionalism - This criterion includes knowledge of staff and their ability to solve problems in a professional manner.</li> <li>Flexibility and Access - This criterion includes dimensions like the ability of staff to adjust to the needs of students and their availability in times of need.</li> <li>Behaviour and Attitude - This criterion includes dimensions like friendliness and genuine care for the needs of the student on part of the staff.</li> <li>Reputation and Credibility - This criterion assesses the brand value of the institute by evaluating the perceived credibility and reputation of</li> </ul>                                    | Takes into account only the student perspective and considers student as a customer. |



|                            |  |   |  |
|----------------------------|--|---|--|
|                            |  | <p>the same.</p> <ul style="list-style-type: none"> <li>• Recovery - This criterion evaluates the ability of an institute to recover from an issue or problem.</li> </ul>   |  |
| Lehtinen and Lehtinen [25] | Classified quality dimensions in three categories namely interactive quality, physical quality and corporate quality.  | <p>The dimensions included under each category are similar to those specified by Gronroos [13]. The categories are as follows -</p> <ul style="list-style-type: none"> <li>• Interactive quality - The quality dimensions, which are associated with the interaction between the institution and student are included under this category</li> <li>• Physical quality - The quality dimensions included under this category are measured regardless of the opinion of the student.</li> <li>• Corporate quality - The quality dimensions associated with the reputation and branding of the institute are included under this category. These dimensions take both the customer or student's perspective as well as the institution's perspective into account.</li> </ul>                | Takes into account the student perspective and considers student as a customer. However, this framework also considers dimensions that are independent of student perspective and can be seen as administrative perspective.   |
| Carney [26]                | Proposed a comprehensive set of attributes for studying the image of a college.  | <p>The variables identified relevant to the context include -</p> <ul style="list-style-type: none"> <li>• Student qualities</li> <li>• Student qualification</li> <li>• Quality of instruction</li> <li>• Faculty-student interaction</li> <li>• Academic reputation</li> <li>• Variety of courses run by the college</li> <li>• Career preparation</li> <li>• Class size</li> <li>• Student Activities</li> <li>• Athletic programs</li> <li>• Facilities and equipment</li> <li>• Community service</li> <li>• Physical appearance of the campus</li> <li>• Location</li> <li>• Friendly nature of staff</li> <li>• On-campus residence</li> <li>• Religious atmosphere</li> <li>• Caring atmosphere</li> <li>• Financial aid</li> <li>• Safety in campus</li> </ul>                   | Takes into account the student and administrative perspective. Moreover, dimensions like student qualification and career preparation hint towards the impact of education on the outcome of the educational process, but there is no clear dimension catering to the outcome perspective. |
| Owlia and Aspinwall [21]   | Gave a conceptual framework.   | <p>The six dimensions identified by this framework comprise of the following -</p> <ul style="list-style-type: none"> <li>• Tangibles which include infrastructure, ease of access and supporting infrastructure and facilities</li> <li>• Competence which includes student-staff ratio and quality of staff along with their ability to communicate effectively with students</li> <li>• Attitude which includes guidance and willingness to help</li> <li>• Content which includes curriculum, cross-disciplinarily of knowledge and relevance of courses for future jobs</li> <li>• Delivery which includes effective communication, student feedback and providing encouragement to students</li> <li>• Reliability which includes matching goals and handling complaints</li> </ul> | Takes into account the student and administrative perspectives.  |
| Athiyaman [27]             | Proposed a framework containing eight characteristics for evaluating the services provided by a university.  | <p>The characteristics include -</p> <ul style="list-style-type: none"> <li>• Availability of staff for solving students' problems</li> <li>• Teaching skills of staff and their ability to teach the students well</li> <li>• Computing facilities</li> <li>• Class size</li> <li>• Library facilities</li> <li>• Recreational facilities</li> <li>• Student workload</li> <li>• Difficulty level of course content</li> </ul>   | Takes into account the student perspective.  |
| Lee et al. [28]            | This research work explained that there are two variables that can determine and predict the overall satisfaction level of the student with respect to the provided service. | <p>The two variables include -</p> <ul style="list-style-type: none"> <li>• Overall impression of educational quality</li> <li>• Overall impression of school</li> </ul>  | Takes into account the student perspective.  |
| Hadikoemoro                | This research work identified  | The identified dimensions are as follows:   | Takes into account the   |

|                            |   |  |   |
|----------------------------|---|--|---|
| [29]                       | 35 service-quality items based on interviews conducted for two groups and identified five dimensions.   | <ul style="list-style-type: none"> <li>Academic Services - This dimension includes completeness of the infrastructure and facilities and accurate and dependable delivery of services.</li> <li>Attentiveness and Readiness - This dimension assesses the ability of the university to help students and be promptly available for any consultation</li> <li>Fair and Impartial - This dimension includes the discipline maintenance on the campus and the ability of the institution authorities to implement a democratic campus regulation.</li> <li>Tangible - This dimension includes equipment, facilities and the physical appearance of the campus.</li> <li>General Attitude - The ability to handle students falls under this dimension of this framework.</li> </ul>  | student and administrative perspectives.  |
| O'Neill and Palmer [30]    | This research assessed the importance of dimensions for quality assessment based on student perceptions and it was found that process was the most important dimension. However, the analysis is exploratory and thus, a further analysis is required to establish the results.   | <p>The dimensions used by this research work are as follows:</p> <ul style="list-style-type: none"> <li>Process - This dimension includes factors that assess the ability of staff to solve student's problems, their accessibility and availability and their ability to deal with students. Basically, the factors included in this dimension assess the quality of the process.</li> <li>Empathy - The ability of employees to understand student needs and the amount of attention they are able to pay each student are assessed under this dimension.</li> <li>Tangible - The facilities, equipment and physical appearance of the institution are assessed under this dimension.</li> </ul>   | Takes the students' perspective into account.   |
| Sahney et al. [31]         | The proposed framework emphasised on the need to identify design requirements of the system in addition to customer requirements for assessing quality. Moreover, it also focussed on measuring quality by comparing the perceptions of students with regard to the design requirements and expectations from the system.   | <p>The factors identified by the framework include:</p> <ul style="list-style-type: none"> <li>Competence of the system - This factor refers to the infrastructure, faculty expertise and availability of skilled teaching and support staff.</li> <li>Attitude of the staff - This factor refers to the attention they pay towards maintaining a healthy environment and remain accessible to students for consultation</li> <li>Content - This factor refers to the course curriculum and future needs of the students from the course. Besides this flexibility of the course to adjust to interdisciplinary knowledge is also considered as part of this factor.</li> <li>Delivery of content - This factor refers to the ability of staff to manage classroom and deliver content in a manner that makes the students feel at ease and comfortable.</li> <li>Reliability - This factor includes dimensions like the clarity of course objectives, rules and regulations and guidelines of the institute.</li> </ul> | Takes into account the student and administrative perspectives.   |
| Brooks [32]                | This research work emphasised on the inclusion of university activities for measurement of quality and gave a criterion for quality assessment.   | <p>The dimensions included in the proposed criteria are as follows:</p> <ul style="list-style-type: none"> <li>Reputation</li> <li>Faculty research productivity</li> <li>Student educational experiences and outcomes - This dimension is further divided into program characteristics, program effectiveness and student outcome.</li> </ul>   | This framework takes into account the administrative perspective. However, there is a minor deviation and indication towards a third perspective called the outcome perspective. The student outcome dimension assesses the learning and career outcome of the student. This dimension covers the score and grades obtained by the student in the examination to assess the outcome of the process. |
| Teeroovengadam et al. [33] | Gave a factor/measurement model that was based on qualitative analysis of collected data, in addition to survey of existing literature. The hierarchical model proposed for measurement of service quality for higher educational institutions. This framework is also considered an extension of Owlia and Aspinwall [21]. | <p>The primary identified dimensions were as follows:</p> <ul style="list-style-type: none"> <li>Administrative quality - This dimension has two sub-dimensions namely administrative processes and attitude and behaviours of administrative staff.</li> <li>Physical environment quality - This dimension has three sub-dimensions namely general infrastructure, learning setting and support infrastructure.</li> <li>Core educational quality - This dimension has four sub-dimensions namely pedagogy, competency, curriculum and attitude and behaviour.</li> <li>Support facilities Quality</li> <li>Transformative Quality</li> </ul>   | Takes into account only the student perspective and considers student as a customer.  |

### III. PROPOSED QUALITY FRAMEWORK

While most of the existing frameworks considered student's perspective and/or administrative perspective for defining quality dimensions, only Carney [26] and Brooks [32] hinted on the use of outcome perspective for measuring quality. Telford and Masson [35] emphasized on the importance of considering dimensions related to educational process as a key facet for measuring quality. With that said, computing the outcome of the educational process is one of the key measures for evaluating the education process.

In view of the definition of quality for higher education given in the previous section, it can be understood that a student is not just the customer of the system; he or she is also the product. Besides this, imparting education is a process and the performance of student in real-world scenario after the completion of the course, is the 'outcome' of the process. The proposed framework measures quality by computing quality scores for every student who passes out of a university in a given academic year. This score is calculated using the ranking of the organization that a student joins after passing out.

These scores are cumulatively analyzed to assess the average quality for the organization. Moreover, a year-wise analysis can provide trends and predictions in this regard. The content dimension of quality, which includes 'relevance of courses for future jobs' given by Owlia and Aspinwall [21], 'career preparation' by Carney [26], 'student outcome' by Brooks [32] and 'career prospect' objective mentioned by Teeroovengadam et al. [33] are quantitatively evaluated using the quality score. Consequently, quality monitoring can be performed using quantitative analytics.

#### A. Higher Education System Inputs and Outputs

Higher education system can be broken into three academic categories namely, undergraduate, postgraduate and research. The progress pathway of a student from one academic category to the next is shown in Fig. 1. A student admitted to undergraduate courses in a university, upon completion, may either choose to join a postgraduate course in the same or another university, take up a job or not pursue anything at all.

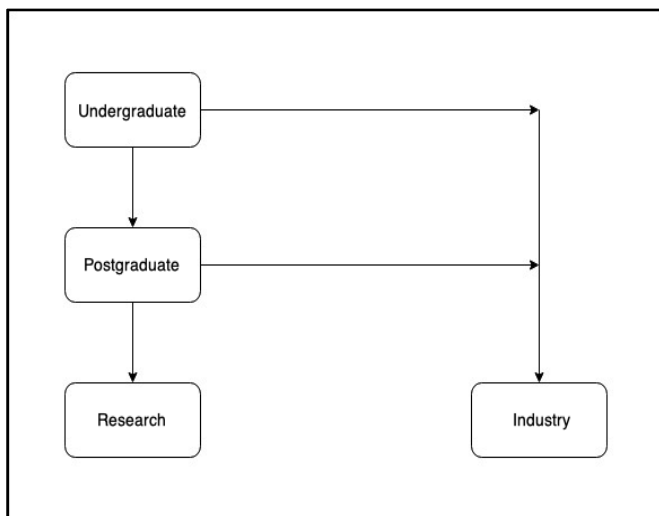


Fig. 1. Breakdown of Higher Education System.

Similarly, a postgraduate student may choose to take up a job, pursue research in the same or a different university or not pursue anything at all. Evidently, there are two transitional states. The first state of transition (Transition 1) is when a student completes an undergraduate course and takes up either a postgraduate course or joins industry. However, the state when a postgraduate student completes a course can be considered the second state of transition (Transition 2). This transition diagram forms the basis of the proposed quality assessment framework.

From Fig. 1, three academic categories of students can be formulated, including Students Pursuing Higher Education (SPHE), Students Opting For Jobs (SOFJ) and Students With No Data Available (SWNDA). SPHE includes the students who choose to pursue a postgraduate degree after undergraduate degree or research after postgraduate degree. SOFJ includes the students who opt for on-campus placements or get an off-campus placement in the following academic year. Therefore, all students who are able to find an industry position within one year after graduation are considered under this academic category.

The last academic category, SWNDA, includes the students who do not fall into the other two academic categories. Since, this is a yearly analysis, any student who finds an off-campus placement after one year, chooses self-employment or does nothing at all for the first year after graduation, is considered under this academic category. It is important to mention that this academic category is added for comprehensiveness. However, for the sake of simplicity, the quality score for this academic category of students is taken as zero.

Understandably, self-employment is a special case scenario. However, even if the student takes up self-employment within the first year of leaving the university or institution, there is no parameter to judge the success of his or her venture in a given time period. Therefore, a more detailed framework is required for calculating the quality score for the self-employment.

#### B. Quality Score (QS) - Metric for Quality Assessment

This paper proposes a metric termed as 'quality score', which shall be calculated at student level on the basis of the transition outcome of the student from one state to another. The quality scores for students enrolled to a university are calculated year-wise on a scale of 1 to 10 and used for further analytics. Quality score calculations for SPHE and SOFJ academic categories of students will be provided in the following sections.

As mentioned previously, students, upon completion of their undergraduate or postgraduate degrees, are expected to pursue higher education or opt for campus placements. University or institute rankings are provided by Government organizations and private ranking agencies on a yearly basis.

In order to ensure and maintain authenticity of the base data used for analysis, the ranking provided by Government agencies is recommended for SPHE. Moreover, a student may move to a university in the same country or may opt to study abroad. In order to accommodate this case, the data for world university ranking must be taken for score calculation if the

student is taking admission abroad, otherwise country-wise ranking can be applied in the other case to accommodate for maximum universities.

In order to calculate QS for every student, the rank of the university in which the student is taking up a postgraduate degree or pursuing research and the maximum rank assigned by the ranking to any university are required as inputs. If the university in which the student is taking up postgraduate degree or research is not ranked in the list, the value zero is assigned to quality score for that student.

The value of QS for a SPHE student with a known university rank is calculated by performing linear scaling. The formula used for linear scaling<sup>2</sup> are given in equations (1), (2) and (3).

$$rate = \frac{scaled_{max} - scaled_{min}}{input_{max} - input_{min}} \quad (1)$$

$$offset = scaled_{min} - (input_{min} * rate) \quad (2)$$

$$ouput = (input * rate) + offset \quad (3)$$

The derivation of the formula for QS calculation in this scenario is given below. The value of variables used in equations (1), (2) and (3) are as follows:

$$input = rank$$

$$output = QS_{SPHE}$$

$$input_{min} = rank_{max}$$

$$input_{max} = 1$$

$$scaled_{min} = 1$$

$$scaled_{max} = 10$$

Substituting these values in equations (1), (2) and (3):

$$rate = \frac{(10-1)}{1-rank_{max}}$$

$$rate = \frac{9}{1-rank_{max}} \quad (4)$$

$$offset = 1 - (rank_{max} * rate) \quad (5)$$

$$QS_{SPHE} = (rank * rate) + offset \quad (6)$$

A description of the variables used in the described formula is given in Table IV.

Placement data like company ranking and package offered can be cumulatively used as base data for the students who opt for campus placed jobs. The company rankings can be taken from survey results of credible private agencies like Economic Times<sup>3</sup>, which have created surveys with the objective to create top recruiters list. Data for package offered by companies to individual students is available with the university and can be directly used for analysis.

Given the fact that the best student performer in this academic category is the one who gets placed in a company with the highest ranking and gets the highest package. On the

other hand, the worst performer is the one who gets placed in an unranked company at the lowest package. In order to compute the total quality score for SOFJ, QS calculated on the basis of industry rankings is added to QS calculated on the basis of relative package score.

A description of the variables used in the described formula is given in Table V.

TABLE IV. VARIABLES USED FOR SPHE QUALITY SCORE CALCULATION

| Variable                    | Description   |
|-----------------------------|---|
| <i>input</i>                | The input value that needs to be scaled                                       |
| <i>output</i>               | The scaled value  |
| <i>input<sub>min</sub></i>  | The minimum value of the input scale  |
| <i>input<sub>max</sub></i>  | The maximum value of the input scale  |
| <i>scaled<sub>min</sub></i> | The minimum value of the output scale   |
| <i>scaled<sub>max</sub></i> | The maximum value of the output scale   |
| <i>rate</i>                 | The rate of scaling   |
| <i>offset</i>               | The offset that needs to be applied for scaling                               |
| <i>rank</i>                 | The university rank for the concerned SPHE student                            |
| <i>rank<sub>max</sub></i>   | The maximum rank assigned to a university in the University Ranking data used |
| <i>QS<sub>SPHE</sub></i>    | Quality Score for SPHE of the concerned student                               |

TABLE V. VARIABLES USED FOR SOFJ QUALITY SCORE CALCULATION

| Variable                           | Description  |
|------------------------------------|--|
| <i>input</i>                       | The input value that needs to be scaled                                  |
| <i>output</i>                      | The scaled value   |
| <i>input<sub>min</sub></i>         | The minimum value of the input scale                                     |
| <i>input<sub>max</sub></i>         | The maximum value of the input scale                                     |
| <i>scaled<sub>min</sub></i>        | The minimum value of the output scale                                    |
| <i>scaled<sub>max</sub></i>        | The maximum value of the output scale                                    |
| <i>rate</i>                        | The rate of scaling  |
| <i>offset</i>                      | The offset that needs to be applied for scaling                          |
| <i>industry_rank</i>               | The company rank for the concerned SOFJ student                          |
| <i>industry_rank<sub>max</sub></i> | The maximum rank assigned to a company in the Company Ranking data used  |
| <i>QS<sub>IR</sub></i>             | Quality Score for SOFJ of the concerned student based on company ranking |
| <i>package<sub>min</sub></i>       | The minimum package that has been offered to any SOFJ student            |
| <i>package<sub>max</sub></i>       | The maximum package that has been offered to any SOFJ student            |
| <i>package</i>                     | Package offered to the concerned SOFJ student                            |
| <i>QS<sub>PO</sub></i>             | Quality Score for SOFJ of the concerned student based on package offered |
| <i>QS<sub>SOFJ</sub></i>           | Cumulative Quality Score for SOFJ of the concerned student               |

<sup>2</sup> [https://www.courses.psu.edu/e\\_met/e\\_met430\\_jar14/pid/ioscal.html](https://www.courses.psu.edu/e_met/e_met430_jar14/pid/ioscal.html)

<sup>3</sup> <http://economicstimes.indiatimes.com/>

Quality score computed on the basis of industry ranking ( $QS_{IR}$ ) makes use of the same concept as used by  $QS_{SPHE}$ . If the company in which the student is taking a campus placement is not ranked in the list, the value zero is assigned to for  $QS_{IR}$  of that student. In order to accommodate this case, the value of  $QS_{IR}$  is calculated on a scale of 1 to 5. The value of  $QS_{IR}$  can be calculated using the equations (1), (2) and (3) with the following parametric values:

$$\begin{aligned} input &= industry\_rank \\ output &= QS_{IR} \\ input_{min} &= industry\_rank_{max} \\ input_{max} &= 1 \\ scaled_{min} &= 1 \\ scaled_{max} &= 5 \end{aligned}$$

Substituting these values in equations (1), (2) and (3),

$$\begin{aligned} rate &= \frac{(5-1)}{1-industry\_rank_{max}} \\ rate &= \frac{4}{1-industry\_rank_{max}} \end{aligned} \quad (7)$$

$$offset = 1 - (industry\_rank_{max} * rate) \quad (8)$$

$$QS_{IR} = (industry\_rank * rate) + offset \quad (9)$$

Scaling of package offered to students opting for campus-placed jobs on a scale of 1 to 5 also requires linear scaling. Therefore, equations (1), (2) and (3) are used with the following parameters:

$$\begin{aligned} input &= package \\ output &= QS_{PO} \\ input_{min} &= package_{min} \\ input_{max} &= package_{max} \\ scaled_{min} &= 0 \\ scaled_{max} &= 5 \end{aligned}$$

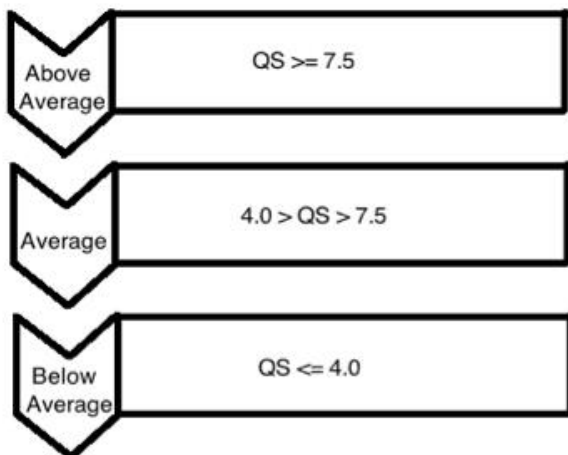


Fig. 2. QS-based Quality Framework.

Substituting these values in equations (1), (2) and (3),

$$\begin{aligned} rate &= \frac{(5-0)}{package_{max}-package_{min}} \\ rate &= \frac{5}{package_{max}-package_{min}} \end{aligned} \quad (10)$$

$$offset = -(package_{min} * rate) \quad (11)$$

$$QS_{PO} = (package * rate) + offset \quad (12)$$

Quality score for SOFJ ( $QS_{SPHE}$ ) is determined using the following equation:

$$QS_{SOFJ} = QS_{IR} + QS_{PO} \quad (13)$$

### C. Quality Score (QS) – Based Analytics

Once quality score is determined for the students passing out of an institute or university at the end of a specific academic year, these values can be used to generate varied types of analytics and graphical interpretations. In order to use QS for decision-making and organizational efficiency management, students need to be divided into three QS categories Fig. 2 illustrates the framework that can be used for student categorization.

On the basis of this categorization, average QS for each category can be determined. Moreover, graphical illustrations like pie charts indicating the share of ‘Above Average’, ‘Average’ and ‘Below Average’ to indicate organization performance for a specific year can be created. Besides this, analytics that use data generated over the years can be used to create line charts for indicating the performance patterns of the organization in all the three categories. These analytics can be used to assess the performance of an institute or organization for an academic year as well as over the years. Cumulatively, these visualizations can be used for performance assessment and comparison.

## IV. METHODOLOGY AND IMPLEMENTATION

The proposed framework utilizes student data profiles to compute quality score per student and use the computed values for advanced analytics. Profiles of students passing out each year are scanned for computing quality scores and quality score data per year is stored for generating time-based analytics.

In order to implement and test the proposed framework, Google BigQuery<sup>4</sup> and R<sup>5</sup> are used as base technologies. A web-based application was developed using shiny package<sup>6</sup> available for R. The backend programming for computation of quality score and creation of visualizations like pie charts and line charts was performed using R programming language.

Dummy data set has been used for testing and validating the framework. The data set used for computation was stored in Google BigQuery, which is a cloud-based big data-warehousing technology. The schema for the three tables used for the implementation of this framework has been shown in Table VI, Table VII and Table VIII.

<sup>4</sup> <https://cloud.google.com/bigquery/>

<sup>5</sup> <https://www.r-project.org/about.html>

<sup>6</sup> <https://cran.r-project.org/web/packages/shiny/index.html>

There are a plethora of big data technologies and tools [36] available in the form of commercial as well as open-source solutions. The choice of these technologies was made because of the cost-effective nature of Google BigQuery and the simplicity of R language for developing analytical visualizations. Moreover, the availability of BigQuery API allows easy integration of Google BigQuery with R programming environment. This is also one of the reasons for this selection.

TABLE. VI. TABLE SCHEMA FOR STUDENT DATA TABLE

| Field Name   | Data Type | Description   |
|--------------|-----------|---|
| course       | STRING    | Course to which the student is enrolled                                 |
| eyear        | INTEGER   | Year of enrolment   |
| code         | STRING    | Code of course to which the student is enrolled                         |
| Id           | INTEGER   | Student ID  |
| Gender       | STRING    | Gender  |
| Region       | STRING    | Region to which the student belongs                                     |
| He           | STRING    | Highest education   |
| Imd          | STRING    | IMD Band  |
| Age          | STRING    | Age Bracket to which the student belongs                                |
| prev_attempt | STRING    | Number of previous attempts taken                                       |
| Credit       | STRING    | Credits studied   |
| Disability   | STRING    | Whether suffering from a disability                                     |
| final_result | STRING    | Final result (Pass or Fail or Withdrawn)                                |
| Univ         | STRING    | University to which student has taken admission after course completion |
| Comp         | STRING    | Company that the student has joined after course completion             |
| Package      | FLOAT     | Package offered   |
| univ_f       | STRING    | Whether joined a university after course completion (Y/N)               |
| comp_f       | STRING    | Whether joined a company after course completion (Y/N)                  |
| q_score      | FLOAT     | Quality score (assigned to zero for initialization)                     |

The developed tool is named “Quality Management Tool for Higher Education Systems”. The user interface of the web application is shown in Fig. 3. It is important to mention that the application uses server-side authentication. Therefore, in order to make the application work, the user will have to provide the JSON file with authentication token, which can be downloaded from the user’s Google BigQuery Account. The application was firstly deployed on the local server and tested. Consequently, it was deployed on the Shiny server and tested. This application is available on Shiny Server, at <https://qmhes.shinyapps.io/qmhes/>.

TABLE. VII. TABLE SCHEMA FOR UNIVERSITY RANK TABLE

| Field Name | Data Type | Description                      |
|------------|-----------|----------------------------------|
| univ_code  | STRING    | University code                  |
| univ_name  | STRING    | Name of the university           |
| univ_city  | STRING    | City of location                 |
| univ_state | STRING    | State of location                |
| univ_score | FLOAT     | Score                            |
| univ_rank  | INTEGER   | Rank                             |
| uryear     | INTEGER   | Year in which rank was generated |

TABLE. VIII. TABLE SCHEMA FOR COMPANY RANK TABLE

| Field Name     | Data Type | Description                       |
|----------------|-----------|-----------------------------------|
| comp_name      | STRING    | Name of the company               |
| comp_sector    | STRING    | Sector of operation               |
| comp_subsector | STRING    | Sub-sector of operation           |
| comp_area      | STRING    | Area/Continent of operation       |
| comp_country   | STRING    | Country of operation              |
| comp_para1     | FLOAT     | Financial parameter               |
| comp_para2     | FLOAT     | Financial parameter               |
| comp_para3     | FLOAT     | Financial parameter               |
| comp_para4     | FLOAT     | Financial parameter               |
| comp_rank      | INTEGER   | Rank                              |
| Cryear         | INTEGER   | Year for which rank was generated |

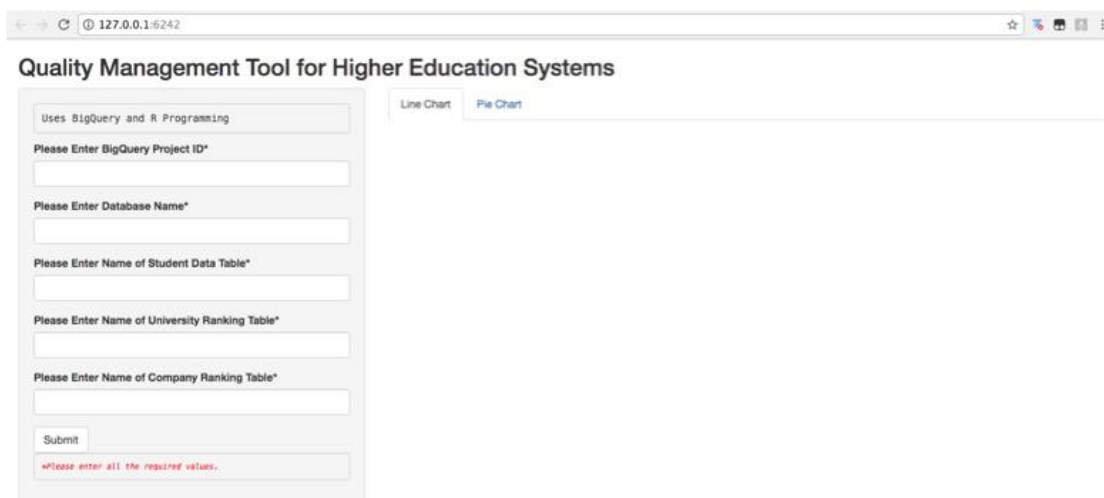


Fig. 3. User Interface of ‘Quality Management Tool for Higher Education Systems’.

V. EVALUATION

The dataset used for testing the implementation of this framework contains dummy data for students, university rankings and company rankings for the years 2013 and 2014. Quality score for every student is calculated on the basis of whether the student joins a research degree or gets a job in a company. The rank of the university determines the quality score of students joining a university.

On the other hand, company ranking and package offered determine the quality score of students joining a company. The package offered to a student is the annual compensation that a company is willing to offer the student upon joining. The computation of quality score for the data set used has been illustrated in Fig. 4 and Fig. 5.

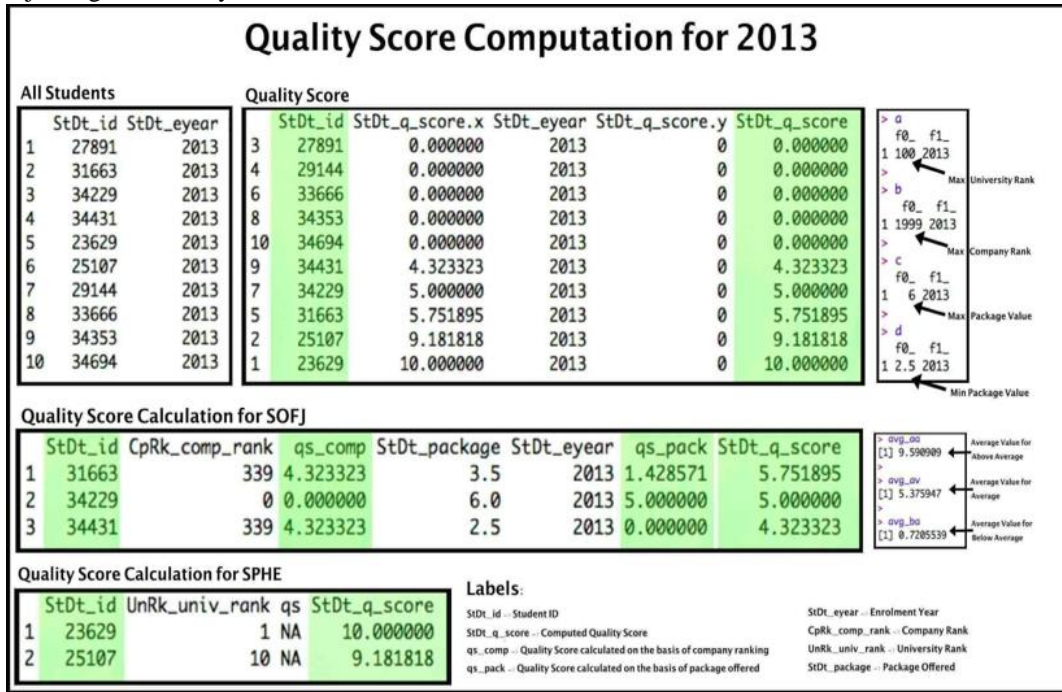


Fig. 4. Computation of Quality Scores for Students enrolled in the Year 2013.

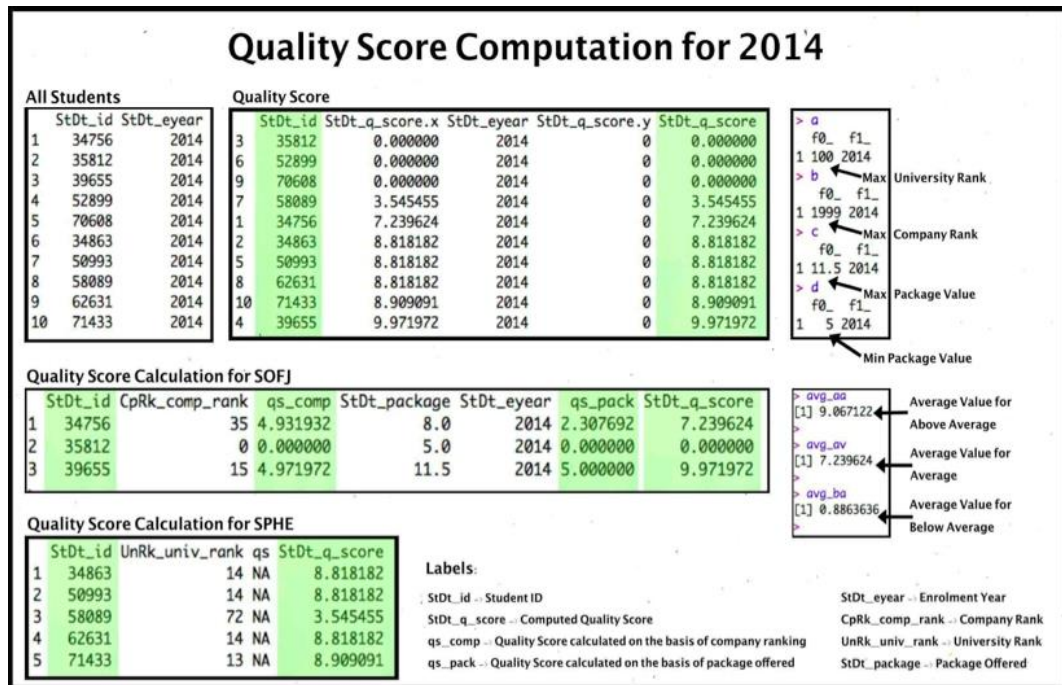
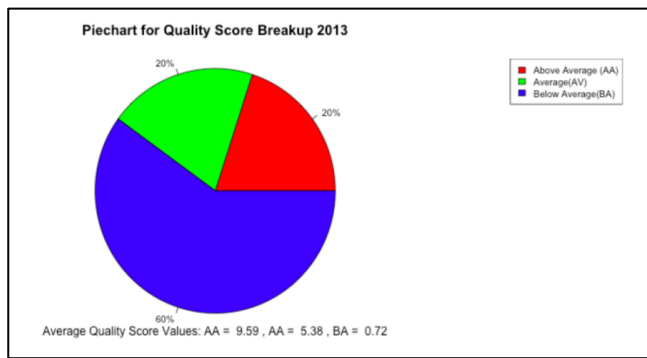
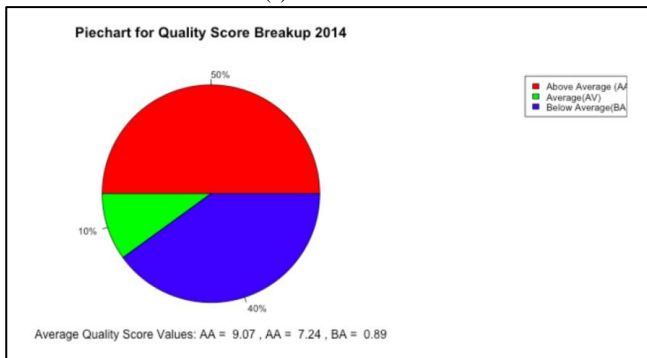


Fig. 5. Computation of Quality Scores for Students enrolled in the Year 2014.



(a) Year – 2013



(b) Year - 2014

Fig. 6. PieChart Generated for Different Years

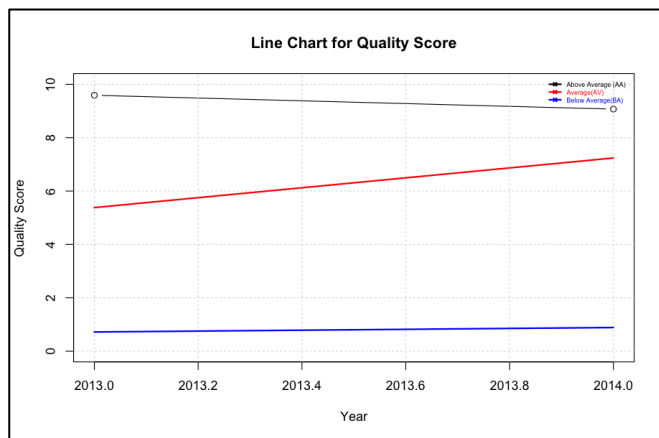


Fig. 7. Line Chart Generated.

On the basis of the quality scores generated for every student passing out of the university during one academic year, average quality scores are calculated. These average values are used to generate line charts for demonstrating trends of quality score values for an educational organization. On the other hand, the numbers of students falling under specific QS categories are used to generate piecharts for specific years. The analytics–pie charts and line chart – created using quality score data computed for the dataset used are shown in Fig. 6(a), Fig. 6(b) and Fig. 7. The inputs required to generate the line chart include project’s BigQuery Project ID, name of the database (inside the BigQuery project) and names for tables containing data related to students, university rankings and company rankings. In order to generate year-specific pie charts, an addition field of year also needs to be filled.

## VI. DISCUSSION

Data about students, who get jobs through off-campus placement immediately after the degree or after taking a gap year, is usually not available. Moreover, data collection related to students who opt for self-employment is also limited. However, off-campus placements within one year of course completion are only considered because the framework generates yearly analysis. This limits the capabilities of the proposed analytical framework by restricting the amount and diversity of data available for analysis. A more robust data collection at the organization level or alumni association levels can be a significant step towards a more efficient outcome-based analysis in the educational context. Moreover, self-employment is not accounted for in the given framework.

This paper is an exploratory study, which encompasses several limitations. The QS is based on the institutions and companies’ rankings, so the proposed framework assesses the quality of Higher Education Institutions (HEIs) based on rankings. The base dataset of rankings used for QS calculation is and must be taken from credible sources like Government agencies and reputed private organizations. This can be a controversial way to “measure” organizations’ quality. The computation of the QS assumes that the type of companies they enroll in after graduation measures the ‘quality’ of the graduates. So, best students will have a job in higher rank companies. But this may not always be true. A graduate may find a job in an excellent company on the basis of references and not because he or she is a high quality student. Looking at such limitations of using the proposed indexes for quality assessment, the use of these indexes along with other quality metrics is recommended for a more comprehensive evaluation.

Therefore, this study intends to contribute to the discussion on the possibilities of enlarging QA schemes to make them able to include outcome perspective along with both the customer and product perspectives. Usually the frameworks include dimensions related to inputs, processes and outputs, but tend to overlook the outcomes, that is what happens after the students graduate and leave institutions. The innovativeness of the proposed concept lies in adding a new dimension to QA schemes and implementing the same using big data technologies. This study demonstrates how big data technologies can be used to develop educational intelligence applications.

## VII. CONCLUSION

The next generation of analytical solutions for education and research are drifting towards educational intelligence. Big data technologies are put to use for storage and analysis of big education data. An educational intelligence application for quality assessment of higher education systems has been designed, implemented and deployed in this paper.

Existing quality frameworks proposed for higher education cover many dimensions of quality including content and delivery. However, most of these frameworks consider education as a service and evaluate quality from a service-oriented perspective. Other systems consider students a product and evaluate quality from the product perspective. However,



student is also the ‘outcome’ of the educational process and this dimension is unexplored.

The proposed framework uses this unexplored dimension of quality. In view of the fact that the students’ performances after graduating are the outcomes produced by higher education institutions, an outcome-based analysis of this transition data can give useful insights into the quality of education provided by the university. Moreover, analytics of this nature can be helpful in decision-making and administrative planning for the educational institutions, contributing to quality improvement.

The framework is implemented in the form of a web-based application, using big data technology, Google BigQuery, and R programming. It is tested using a synthetic data set to demonstrate how quality scores are calculated. With the help of the generated quality scores, analytical visualizations like piecharts and line charts are generated.

### VIII. FUTURE WORK

It is important to mention that the data available for analysis is limited to students who take up a postgraduate course/research degree or campus placement after the completion of their respective courses.

Future research work shall include designing a comprehensive data collection framework and exploration of other variables that may affect and govern outcomes analysis other than transitions from one degree to the next level. Academic categories like self-employed students can also be explored to extend the framework and make it more comprehensive. Therefore, computation parameters for quality score can be improved in future work.

Besides this, the use of other cloud-based technologies for building a big data architecture [37] for comprehensive quality assessment of higher education systems is also planned for future to improve the performance and usability of the educational intelligence application.

### IX. AVAILABILITY OF DATA AND MATERIALS

Quality Management Tool for Higher Education Systems (QMHEs) is available as an open source project in GitHub (<https://github.com/samiyakhan13/qmhes-1>). Synthetic dataset was used to test the application. An electronic version of data will be made available and shared with interested researchers under an agreement for data access (contact: [samiyashaukat@yahoo.com](mailto:samiyashaukat@yahoo.com)).

#### REFERENCES

- [1] S. Khan, K. A. Shakil, and M. Alam. “Educational intelligence: applying cloud-based big data analytics to the Indian education sector” in 2016 2nd international conference on contemporary computing and informatics (IC3I), IEEE, 2016, pp. 29-34.
- [2] E. Salwana, S. Hamid, and N. Mohd Yasin. "Student Academic Streaming Using Clustering Technique." Malaysian Journal of Computer Science, Vol. 30, No. 4, 2017, pp. 286-299.
- [3] B. Williamson. “The hidden architecture of higher education: building a big data infrastructure for the ‘smarter university’”. International Journal of Educational Technology in Higher Education. Vol. 15, No. 1, 2018, pp. 12.
- [4] K. Sato. “An inside look at Google BigQuery”. White paper, 2012. Available from: <https://cloud.google.com/files/BigQueryTechnicalWP.pdf>.
- [5] S. B. Siewert. “Big data in the cloud. Data velocity, volume, variety, veracity”, 2013, pp. 4-21.
- [6] A. Valdez, G. Cortes, S. Castaneda, L. Vazquez, A. Zarate, Y. Salas and G. H. Atondo, “Big Data Strategy” International Journal of Advanced Computer Science and Applications (IJACSA), 10(4), 2019. <http://dx.doi.org/10.14569/IJACSA.2019.0100434>
- [7] H. Ehtesham, R. Safdari, and S. Tahmasebian. “Big Data in Health: New Challenges and New Solutions in Data Management (A Lifecycle Review)”. Indian Journal of Science and Technology. Vol. 10, No. 13, 2017.
- [8] S. Khan, K. A. Shakil, and M. Alam. “Cloud-based big data analytics—a survey of current research and future directions”. In Big Data Analytics. Springer, Singapore, 2018, pp. 595-604.
- [9] G. D. Puri, and D. Haritha. “Survey big data analytics, applications and privacy concerns”. Indian Journal of Science and Technology. Vol. 9, 2016, pp. 1-8.
- [10] B. Daniel. “Big Data and analytics in higher education: Opportunities and challenges”. British journal of educational technology. Vol. 46, No. 5, 2015, pp. 904-20.
- [11] J. A. González-Martínez, M. L. Bote-Lorenzo, E. Gómez-Sánchez, and R. Cano-Parra. “Cloud computing and education: A state-of-the-art survey”. Computers & Education. Vol. 1, No. 80, 2015, pp. 132-51.
- [12] M. D. Assunção, R. N. Calheiros, S. Bianchi, M. A. Netto, and R. Buyya. “Big Data computing and clouds: Trends and future directions”. Journal of Parallel and Distributed Computing, Vol. 1, No. 79, 2015, pp. 3-15.
- [13] L. C. Liñán, and A. A. Pérez. “Educational Data Mining and Learning Analytics: differences, similarities, and time evolution”. International Journal of Educational Technology in Higher Education, Vol. 12, No. 3, 2015, pp. 98-112.
- [14] R. Asif, A. Merceron, S. A. Ali, and N. G. Haider. “Analyzing undergraduate students' performance using educational data mining”. Computers & Education. Vol. 1, No. 113, 2017, pp. 177-94.
- [15] S. Khan, X. Liu, K. A. Shakil, and M. Alam. “A survey on scholarly data: From big data perspective”. Information Processing & Management. Vol. 53, No. 4, 2017, pp. 923-44.
- [16] M. K. Saggi, S. Jain. “A survey towards an integration of big data analytics to big insights for value-creation”. Information Processing & Management. Vol. 54, No. 5, 2018, pp. 758-90.
- [17] J. Newton. “Views from below: academics coping with quality”. Quality in higher education. Vol. 8, No. 1, 2002, pp. 39-61.
- [18] D. Green. “What Is Quality in Higher Education?” Taylor & Francis, 1900 Frost Road, Bristol, PA 19007-1598; 1994.
- [19] A. Prisacariu, and M. Shah. “Defining the quality of higher education around ethics and moral values”. Quality in Higher education. Vol. 22, No. 2, 2016, pp. 152-66.
- [20] A. Y. Hou. “Quality Assurance in Asian Higher Education: Challenges and Prospects” in The Palgrave Handbook of Asia Pacific Higher Education. Palgrave Macmillan, New York. 2016, pp. 381-392.
- [21] M. S. Owlia, and E. M. Aspinwall. “A framework for the dimensions of quality in higher education”. Quality Assurance in Education. Vol. 4, No. 2, 1996, pp. 12-20.
- [22] N. Elassy. “The concepts of quality, quality assurance and quality enhancement”. Quality Assurance in Education. Vol. 23, No. 3, 2015, pp. 250-61.
- [23] A. Parasuraman, V. A. Zeithaml, and L. L. Berry. “A conceptual model of service quality and its implications for future research”. Journal of marketing. Vol. 49, No. 4, 1985, pp. 41-50.
- [24] C. Gronroos. “Service quality: The six criteria of good perceived service”. Review of business. Vol. 9, No. 3, 1988, pp. 10.
- [25] U. Lehtinen, and J. R. Lehtinen. “Two approaches to service quality dimensions”. Service Industries Journal. Vol. 11, No. 3, 1991, pp. 287-303.

- [26] R. Carney. "Building an Image" in Proceedings Symposium for the Marketing of Higher Education, New Orleans, Louisiana: American Marketing Association. 1994.
- [27] A. Athiyaman. "Linking student satisfaction and service quality perceptions: the case of university education". *European journal of marketing*. Vol. 31, No. 7, 1997, pp. 528-40.
- [28] H. Lee, Y. Lee, and D. Yoo. "The determinants of perceived service quality and its relationship with satisfaction. *Journal of services marketing*". Vol. 14, No. 3, 2000, pp. 217-31.
- [29] S. Hadikoemoro. "A comparison of public and private university students' expectations and perceptions of service quality in Jakarta, Indonesia".
- [30] M. A. O'Neill, and A. Palmer. "Importance-performance analysis: a useful tool for directing continuous quality improvement in higher education". *Quality assurance in education*. Vol. 12, No. 1, 2004, pp. 39-52.
- [31] S. Sahney, D. K. Banwet, and S. Karunes. "Customer requirement constructs: the premise for TQM in education: a comparative study of select engineering and management institutions in the Indian context". *International Journal of Productivity and Performance Management*. Vol. 53, No. 6, 2004, pp. 499-520.
- [32] R. Brooks. "Measuring university quality". *The Review of Higher Education*, 2005. Vol. 29, No. 1, 2005, pp. 1-21.
- [33] V. Teeroovengadum, T. J. Kamalanabhan, and A. K. Seebaluck. "Measuring service quality in higher education: Development of a hierarchical model (HESQUAL)". *Quality Assurance in Education*. Vol. 24, No. 2, 2016, pp. 244-58.
- [34] A. Parasuraman A, L. L. Berry, and V. A. Zeithaml. "Understanding customer expectations of service". *Sloan management review*. Vol. 32, No. 3, 1991, pp. 39-48.
- [35] R. Telford, and R. Masson. "The congruence of quality values in higher education". *Quality assurance in education*. Vol. 13, No. 2, 2005, pp. 107-19.
- [36] S. Khan, K. A. Shakil, and M. Alam. "Big Data Computing Using Cloud-Based Technologies: Challenges and Future Perspectives" in *Networks of the Future Chapman and Hall/CRC*, 2017, pp. 393-414.
- [37] F. Azzedin and M. Ghaleb, "Towards an Architecture for Handling Big Data in Oil and Gas Industries: Service-Oriented Approach" *International Journal of Advanced Computer Science and Applications (IJACSA)*, 10(2), 2019. <http://dx.doi.org/10.14569/IJACSA.2019.010026>.

# A Novel Network user Behaviors and Profile Testing based on Anomaly Detection Techniques

Muhammad Tahir\*<sup>1</sup>, Mingchu Li\*<sup>2</sup>, Xiao Zheng<sup>3</sup>, Anil Carie<sup>4</sup>, Xing Jin<sup>5</sup>, Muhammad Azhar<sup>6</sup>, Naeem Ayoub<sup>7</sup>  
Atif Wagan<sup>8</sup>, Muhammad Aamir<sup>9</sup>, Liaquat Ali Jamali<sup>10</sup>, Muhammad Asif Imran<sup>11</sup>, Zahid Hussain Hullo<sup>12</sup>

School of Software Technology, Dalian University of Technology, Dalian, 116620, China<sup>1, 2, 3, 4, 5</sup>

Key Laboratory for Ubiquitous Network and Service Software of Liaoning Province, Dalian, 116020, China<sup>1, 2, 3, 4, 5</sup>

College of Computer Science, Shenzhen University, Shenzhen, 518060, Guangdong, China<sup>6</sup>

Department of Mathematics & Computer Science, University of Southern Denmark

Cam-pusvej 55, DK-5230 Odense M, Denmark<sup>7</sup>

School of Computer Science and Engineering, Nanjing University of Science and Technology, Nanjing, 210094, China<sup>8</sup>

College of Computer Science, Sichuan University, Chengdu, 610065, China<sup>9</sup>

College of Software Engineering, Nankai University, Jinnan District, Tianjin, 300350, China<sup>10</sup>

School of Chemical Engineering, Dalian University of Technology, Dalian, 116024, China<sup>11</sup>

School of Mechanical Engineering, Dalian University of Technology, Dalian, 116024, China<sup>12</sup>

**Abstract**—The proliferation of smart devices and computer networks has led to a huge rise in internet traffic and network attacks that necessitate efficient network traffic monitoring. There have been many attempts to address these issues; however, agile detecting solutions are needed. This research work deals with the problem of malware infections or detection is one of the most challenging tasks in modern computer security. In recent years, anomaly detection has been the first detection approach followed by results from other classifiers. Anomaly detection methods are typically designed to new model normal user behaviors and then seek for deviations from this model. However, anomaly detection techniques may suffer from a variety of problems, including missing validations for verification and a large number of false positives. This work proposes and describes a new profile-based method for identifying anomalous changes in network user behaviors. Profiles describe user behaviors from different perspectives using different flags. Each profile is composed of information about what the user has done over a period of time. The symptoms extracted in the profile cover a wide range of user actions and try to analyze different actions. Compared to other symptom anomaly detectors, the profiles offer a higher level of user experience. It is assumed that it is possible to look for anomalies using high-level symptoms while producing less false positives while effectively finding real attacks. Also, the problem of obtaining truly tagged data for training anomaly detection algorithms has been addressed in this work. It has been designed and created datasets that contain real normal user actions while the user is infected with real malware. These datasets were used to train and evaluate anomaly detection algorithms. Among the investigated algorithms for example, local outlier factor (LOF) and one class support vector machine (SVM). The results show that the proposed anomaly-based and profile-based algorithm causes very few false positives and relatively high true positive detection. The two main contributions of this work are a new approaches based on network anomaly detection and datasets containing a combination of genuine malware and actual user traffic. Finally, the future directions will focus on applying the proposed approaches for protecting the internet of things (IOT) devices.

**Keywords**—Network user behaviors; profile testing; anomaly detection techniques; datasets; anomaly detection algorithms; machine learning

## I. MOTIVATION AND INTRODUCTION

Nowadays, detecting intruders and malware infections [1], in local networks is one of the most difficult and highest studied challenges in modern computer security. From the huge amount of detection methods proposed, a large majority used static rules or reputation methods for performing the detection; until more modern behavioral techniques were introduced. Although very useful, these static techniques were not enough to detect the majority of attacks and malware. In particular, it is believed that the more important limitations of the current techniques are that first, the detections are done per connection and not per user, second, the classifiers are trained and tested on “only normal” and “only infected” datasets and third, the types of attacks and infections evolve and make classifiers quickly less useful. Apart from the more traditional signature-based intrusion detection system (IDS), such as snort [2] and bro [3], there has been extensive research on behavioral detection methods during the last decade. From these new methods, the most used is anomaly detection techniques (ADTs) due to its easy implementation and understandability. Anomaly-based IDS detect anomalies by assuming that more than half the data is normal and then searching for some deviation from that normality. The main benefits of ADTs are its ability to detect previously unknown attacks and the identification of non-malicious problems within the network, such as corporate policy violation. Despite its extensive use, ADTs suffers from several issues that undermine its usefulness. First, it is hard to verify the results, leading to attacks being mixed with normal connections. Second, the anomalies found are not necessarily malicious, generating a high rate of false positives. Third, the nature of the network changes over time, making the original normal model obsolete and prone to more errors. Fourth, ADTs methods usually work with packets, making the methods a little less stable. The amount of errors

generated by these issues tends to be so large that researchers give the output of ADTs to other algorithms to improve the detection. In consequence, ADTs models tend to need constant maintenance and supervision even to achieve acceptable results. Shown below in the 2nd row of Fig. 1, is available from different sources in a multitude of forms.

To improve the current situation, it is proposed that a ADTs method that focuses on the high-level changes in the behavior of a user. The proposed anomaly detection method is analyzing time-fixed user profiles and how they change with regard to the past traffic of the same user. Each profile is composed of a set of features based on the flows received and sent during a time-window. Fig. 2 shows diverse data sources out of the box (i.e., packet, NetFlow, logs, files, 3<sup>rd</sup>-party alerts and threat feeds).

It is hypothesized that it is possible to detect the infected users and to have a small number of false positives by focusing on the high-level behavior in time. The detection approach consists of monitoring a user's computer, and it is collected flows during a fixed time-window. With the data collected in that time-window, profile is created for that user. The profile describes user's behavior during this time-window. With the data obtained during the time-window of each profile, twelve features are computed. These references are featured as profile features (for more details see Section III.C).

The features of a profile cover a wide range of possible changes in traffic to have enough representations of the behavior of the users. For example, one of the features analyzes the number of flows for all the transmission control protocol (TCP) connections from a host, and another feature describes the number of packets for all the TCP connections aggregated by destination ports. If a user is infected with a malware which

tries to connect to a large number of different computers, this last feature will show a very distinctive pattern for the number of packets on each destination port. As another example, if malware steals personal information of a user the features of the profile might show a higher volume of packets sent from the user's computer.

The profiles generated for each time-window may allow us to detect these changes and variances and generate alarms that may prevent the actions of an infected computer.

To be able to detect changes in the behavior of users it is needed to define a baseline of their behaviors. Set of profiles are collected which covers different time intervals such as: working hours, night activity, weekends, etc. Within each profile, each feature describes the user's behavior from a different perspective. Fig. 3, showing data sources in a variety of detection vectors in order to detect the different attacks and stages.

Each perspective contributes a different type of information to the algorithm, and therefore obtaining detections for different behaviors. Each feature of individually is evaluated with the same feature in past profiles.

The initial phase of in anomaly detection method consists in preprocessing the collected data and preparing it for the algorithm. Dimensionality reduction technique is applied to the features of a profile. Each feature has to have the same dimensionality. Then the features of a profile are normalized. Data normalization might significantly improve the performance of anomaly detection algorithms [4]. The normalization is done for each feature individually with respect to the same feature in other profiles.



Fig. 1. Showing the Stages between Malware Infections and Data Losses as well as the Data Sources Needed for Analytics to Accurately Detect the Attack Stage.



Fig. 2. Showing the Comprehensive Subset of Data Sources to Build a Risk of Network user behaviors Profiling for Each Entity.

| Type                      | Examples  | Detection Vectors  |
|---------------------------|---|--|
| Network activity          | Firewall logs<br>IDS/IPS logs<br>Web Proxy logs<br>Email logs<br>Network traffic<br>Network flows | Lateral movement<br>Abnormal resource access<br>Browser exploits<br>Malware activity<br>Suspicious file downloads<br>Command and control activity<br>Beaconing |
| Remote access activity    | VPN logs  | Credential theft, password sharing   |
| Identity                  | AD logs<br>DHCP logs  | Credential violations<br>Account takeover<br>Privilege escalations   |
| Infrastructure            | DNS logs  | Command and control activity<br>Tunneling<br>Exfiltration  |
| 3rd party alerts          | FireEye alerts<br>WildFire alerts   | Incorporate alerts into user risk profiles   |
| Threat intelligence feeds | Commercial & STIX feeds   | Perform historical impact assessment   |
| Logs                      | File integrity monitoring logs  | Suspicious file activity<br>USB, cloud based file exfiltration   |

Fig. 3. Showing the Variety of different Detection Vectors and there Examples.

After the preprocessing phase, the anomaly is trained to detect algorithms (see in Section III.E) by using the normal behavior of a user. An anomaly detection model is created for each feature of a profile, based on all the data of that feature across all the normal profiles of the user. Each profile has twelve different features. Therefore, each feature has its unique normality model.

Once the twelve normal models were trained, it is possible to evaluate the performance of the algorithms using new unseen profiles. The new unseen profiles contain both normal data and normal plus attack data, and they were generated in the same way as the training profiles used to create the normal models. The anomaly detection algorithms, trained in the normal profiles, are used to evaluate the unseen profiles and assign a label to each feature in these profiles. Each feature has a label, and all these labels are used to generate the final label of the profile.

After assigning the labels, the detection method uses majority voting to get the final decisions regarding a profile. If six out of twelve of the final labels assigned by the anomaly detection algorithms classify the profile as anomalous, then the final label of the profile is anomalous.

One of the most important drawbacks of using anomaly detection algorithms is the lack of verified and trusted data. Therefore, the datasets consist of normal profiles and anomalous profiles. A normal profile is a profile which was created before the computer was infected and an anomalous profile is a profile which was created after the infection of the computer. A clean virtual machine is used to create a packet capture for both datasets. The creation of the datasets involved several steps. The first step is to imitate a normal user doing standard things (e.g., checking emails). After some time, the machine is infected with a malware while at the same time it is capable to continue to perform normal actions.

To evaluate the performance of the algorithm it's necessary to have ground-truth labels. It has been assigned the normal label (label = 1) to all the profiles that are created before the infection of the virtual machine. The anomaly label (label = -1) has also been assigned to all the profiles that are created after the infection of the virtual machine. The reason to assign the anomaly labels in this way is the assumption that everything after an infection is worth detecting, and that malware produces changes in the behavior observed in the network. In fact, not all the attacks are anomalies, but this assumption helps us better evaluate our algorithm.

The datasets and labels are used during the experiments to evaluate our hypothesis and proposed approach. Each experiment uses one normal dataset for creating the normal model and one mixed dataset of normal plus attacks for evaluating and testing the performance of the model. Each dataset is split into three parts: train, validation, and test. The train set contains only normal profiles created before the infection. This set is used to create a model of normal network user behavior. The validation set and the test set contains a mix of normal profiles and anomalous profiles.

From all the anomaly detection algorithms that are available, those are selected and reported by the community as

better for this problem. The algorithm that is used in this research work has different parameters that can be adjusted to improve detection. The adjustment of these parameters is done based on the performance metrics computed on the validation set. The validation results allow us to select the best models. The model selection is described in Section III.G and later computes the final performance metrics on the test set.

The evaluation of the algorithms is done in two ways: per individual feature and for the whole profile. First, each feature gives a label for the profile from the point of view of this feature. Then the results are combined using the majority voting to get the final decision for the profile. Having a result per feature allows us to evaluate features individually and learn which ones contribute the most to the detection of the anomalous behavior produced by malware. The analysis of the performance of individual features might also help us better understand how malware communicates.

The analysis of the results is also done by analyzing individual features and then analyzing the result of the majority voting. The analysis of the results shows that most experiments achieved a very low false positive rate (FPR) for individual features in the experiments. FPR does not exceed 0.01 in three out of four experiments for all features. When majority voting is used to produce the final label, the FPR was 0.0 in all experiments. The highest achieved true positive rate (TPR) was 0.44. Although it may seem low, this is the final result among all tested profiles with the FPR 0.0. It means that the algorithm will detect one out of three anomalous profiles with 99.9% approximately success, while at the same time it will not detect a normal profile as an anomalous.

The major highlights and the gap of this study are as follows:

- 1) Analyze the state-of-the-art methods for detecting malicious behaviors with special attention to anomaly detection techniques.
- 2) Propose and implement anomaly detection method to detect changes in computer network user behavior analysis. Infected computers change their behavior, this testing method would help to detect them securely.
- 3) Experimentally evaluate the proposed solution on datasets from cognitive threat analytics (CTA), developed by Cisco Systems, Inc., is a cloud-based software-as-a-service product designed to detect infections on client machines.
- 4) Analyze results of the implemented system and propose further improvements and applications of the solution in network security.
- 5) Finally, the proposed method which is novel in that it analyze features individually across probability distribution of time-window. Results are promising and show that the high-level analysis may provide a good improvement over the current ADTs and the proposed algorithm achieved a low FPR and reasonably high TPR.

In this paper, the remaining sections are explained as follows: Section 2 introduces related work and state-of-the-art in the area of anomaly detection for network security. Section 3 creates a new anomaly detection methodology and facing the

malware infections of computers in networks. Section 4, describe the functional requirements of the dataset used for training and testing in the domain are investigated by using machine learning algorithms and get the final results. Section 5, experimental results of an anomaly detection method is designed and a good dataset generated for training and testing in the hypothesis by running experiments. Section 6, analysis the final results. Section 7, concludes this study along with possible future directions defined in Section 8.

## II. RELATED WORK AND STATE-OF-THE-ART

In this section, related work and state-of-the-art is discussed in the area of anomaly detection for network security. There is much research that has been done in the field of anomaly detection in general and its application to the network security domain in particular. There are multiple survey papers of algorithms for anomaly detection. Chandola et al. [5] reviewed different types of anomalies, the different fields where anomaly detection is used, challenges of anomaly detection and algorithms that could be used for anomaly detection. The paper [6], mentioned that one of the main challenges of applying anomaly detection in the field of network security is that the nature of anomalies keeps changing with time and intruders try to adapt to evade detection.

A central premise of anomaly detection for security was defined by Patcha et al. [7] as that intrusive activity is a subset of anomalous activity. He mentioned that activities in a network could be split into four categories:

- Intrusive but not anomalous—the source of false negatives.
- Not intrusive but anomalous—the source of false positive.
- Not intrusive and not anomalous—true negatives.
- Intrusive and anomalous—true positives.

Among the systems that use flows for anomaly detection is Minnesota intrusion detection system (MINDS) [8] proposal. The system extracts the following features: source and destination IP addresses, source and destination ports, protocol, flags, number of bytes and number of packets. MINDS compute the anomaly score for each IP flow individually. As an anomaly detection algorithm, the creators of MINDS used local outlier factor [9]. One of the main differences between MINDS and it is proposed that the search for anomalies closer to the actions of the user, and not to the network. Anomalies are studied time, from several aggregations of the type of flows.

The methodology used in MINDS was used by Ertoz et al. [10] to develop an agent-based system to detect anomalies in networks by using multiple correlated anomaly detection techniques. Hubballi, N. et al. [11] used NetFlow data and built a trust model to reduce the number of false positive alarms. They combined the output of each agent to build a trust model. Each agent used not only past observations but also anomaly assessments obtained by other agents.

The algorithms that can be used for anomaly detection are varied and include any algorithm that can differentiate between

distributions of data. This is the case of one class SVM that has been used for anomaly detection by Zhang et al. [12], used one class SVM to detect anomalies. They evaluated their approach on the dataset Knowledge discovery data mining KDDCUP99 which was created in 1999. The algorithm showed very promising results compared to other methods. Authors mentioned the problem of obtaining a good dataset with labels to evaluate the anomaly detection methods.

Xu et al. [13] also used NetFlow to analyze the traffic. Their system created a cluster for each internet protocol IP in the current time-window. Clustering was based on the source IP (srcIP). For each cluster, the system computed the normalized entropy of source port (scrPort), destination port (destPort) and destination IP (destIP) and used it as a feature vector to represent clusters. Then the system applied behavior classification scheme to classify each sample in its behavioral class.

All the features in this paper use the state field from IP flows to specify if the connection was established or not established. Mahoney et al. [14] also inspected TCP flags but based on individual packets. The proposed NETAD algorithm built nine models to identify anomalies in nine subsets of packets. Packets were split into subsets based on TCP flag in the packet and on the port. The algorithm achieved 66 detections out of 185 with only 20 false alarms.

One of the examples of creating normal traffic profiles is fire-sight tool [15] from Cisco. This tool allowed a user to specify a sliding time-window length and traffic profile would be created during this window. After the profile was created, the tool allowed detecting abnormal network traffic by comparing it to the profile. To detect abnormal traffic user should define correlation rules which would be triggered ones the traffic deviates from the normal profile.

Another example of profiling a user was presented by G. Pannell et al. [16]. The user profiles was created using multiple characteristics such as the number of running applications, key-stroke analysis, websites viewed, application performance and the number of windows. Each characteristic was modeled separately, and then the evaluation results were combined using a weighting algorithm to produce the final decision. The results showed that combining results was producing a lower FPR than individual characteristics.

The features used for detecting anomalies in this paper were a subset of features created by Benevento, F., et al. [17], and Wagner, Claudia et al [18], both authors of different papers defined a lot of different features to identify users in the social networks even if they would connect from a different place. Subset of features is selected which describes outgoing traffic from a computer of a user since it is wanted to detect the infection of the computer.

## III. METHODOLOGY

In this section, the complete methodology is described step by step. The assumption of the approach is that after an infection the behavior of a host is changing, and the proposed algorithm have to be able to detect these changes.

To create a new anomaly detection method it is necessary to define what should be detected and why. The definition of anomaly depends on the goal of the system, the data available and the conditions of execution. In this paper, it is wanted to detect when a computer is infected by malware while it's still acting normally in the network. The focus is the malware infections of computers in networks. The data available are network packets, but it is decided to use NetFlow to process all the information quickly and to preserve the privacy of users. In consequence, the method is also evaluating if the use of NetFlow may be enough for a good anomaly detection method. The constraints of the method are that detections should be reported as soon as possible and that the number of false positives should be minimized. The proposed method analyzes anomalies in the behavior of the computers from a high-level perspective. This perspective is the actions of the user as they are reflected in flows in the network. Every time a user interacts with a computer, packets are sent via the network. These packets are grouped into flows according to their protocol. These flows are further grouped in this idea in specific new features, such as the number of flows sent to each destination port. These features are a higher level perspective of the actions in the network. To obtain a detection as soon as possible the traffic of each computer is separated in time-windows of five minutes. These time-windows allow the method to run quickly, to capture enough traffic to model behavior, but not to be too big to process. The decision taken by the anomaly detection method is per time-window.

#### A. NetFlows

NetFlow [19] is a data structure developed by Cisco Systems that allow to capture and aggregate information about network traffic each packet which is forwarded through a router or a switch is examined for a set of IP packet attributes. Another way to generate NetFlow is to use a monitoring software such as ARGUS tool to generate them directly from network traffic. Usually, packets are identified by the following attributes.

- IP source address
- IP destination address
- Source port
- Destination port
- Layer 3 protocol type
- Class of Service
- Router or switch interface

After the examination, all packets are grouped based on the attributes described in the list. Constructing anomaly detection methods using NetFlow data has been a subject of research in many works, such as [20-22]. NetFlow data are easy to generate. It can be generated flows from traffic captures or obtain it directly from a router. Also, NetFlow data preserves the anonymity of the users, because it does not contain the content of packets.

The flows in experiments were generated from the packet capture ".PCAP file", using the "Argus tool" [23]. One of the

reasons of using the Argus is the option to generate bi-directional flows. Bi-directional flows contain information about packets sent in both directions. Argus can generate additional fields to the ones that used for flow creation.

The flag field in flows contains two parts separated by an underscore. These are the TCP flags used in the packets in the flow. In the state field generated by Argus, the letters to the left of the underscore character are the TCP flags used in the packets going from the source to the destination. The letters to the right of the underscore character are the TCP flags used in the packets going from the destination to the source.

#### B. Established and not Established Connections

It is determined if a flow between two computers is established or not by the flag field. An established TCP connection is the one which completed a three-way handshake [24]. For example, these are the flags of an established connection flag: SRPA\_FSPA. The Argus state field summarizes the TCP flags used in the packets. In flow state there are the following TCP flags:

- S—synchronization bit (SYN)
- R—reset bit (RES)
- P—push bit
- A—acknowledgment bit (ACK)
- F—final bit (FIN)

These packets could have been sent in any order. An example state of a not established TCP connection is S. It means that the source IP address initiated a connection with SYN flag and did not get any response. For the UDP protocol Argus uses flags such as CON and REQ which are set by Argus. CON flag is set in case of an established UDP connection. REQ flag is set if a client tried to establish a connection but a server did not send anything in response.

#### C. Profiling to Identify Network user behaviors

A profiling is a high-level representation of user behaviors in a network. To create a profile, it is collected network traffic over a predefined time-window. Currently, the creation of the profile only includes the IP protocol version 4 (IPv4) not (IPv6), and the TCP and UDP protocols. Other protocols are not included such as ICMP because they are by far the minority of the packets.

Each feature is constructed in the following way: First, the purpose of the feature is decided; for example, to capture the variations in the destination ports, according to the flows used by the computer being analyzed when the connection is successful. Second, a subset of all the flows in the current time-window is selected according to the previous criteria. In the example, only the established flows are selected. Third, the subset of flows is separated into two groups, one for the TCP protocol and one for the UDP protocol. This separation is done because the purpose of applications using the TCP and UDP protocols is very different and should not be mixed in a single feature. Fourth, the desired field is extracted for all the flows. So far there are two groups of data, one has all the destination ports for established TCP connections, and the other has all the

destination ports for established UDP connections. Fifth, the extracted data is used to create a histogram of the number of flows per destination port. After these steps there are two features, both having a list of values that represents a probability distribution in a time-window. The first feature Client Destination would be called and Port Number of Flows TCP are Established and the second feature Client Destination Port Number of Flows UDP Established.

It is represented features in a profile as vectors of real numbers  $f_k = (x_1, x_2, \dots, x_{65535})$ , where  $x_i$  is a value for  $i$ -th port and 65, 535 is the maximum amount of ports available. A profile contains the following set of features:

- Client Destination Port Total Bytes UDP Established–distribution of a total number of bytes over ports for established UDP connections.
- Client Destination Port Number Of Flows TCP Established–distribution of a total number of flows over ports for established TCP connections.
- Client Destination Port Number Of Flows UDP Not Established–distribution of a total number of flows over ports for not established UDP connections.
- Client Destination Port Total Packets TCP Established–distribution of a total number of packets over ports for established TCP connections.
- Client Destination Port Number Of Flows UDP Established–distribution of a total number of flows over ports for established UDP connections.
- Client Destination Port Total Packets TCP Not Established–distribution of a total number of packets over ports for not established TCP connections.
- Client Destination Port Total Bytes UDP Not Established–distribution of a total number of bytes over ports for not established UDP connections.
- Client Destination Port Total Bytes TCP Established–distribution of a total number of bytes over ports for established TCP connections.
- Client Destination Port Total Packets UDP Not Established–distribution of a total number of packets over ports for not established UDP connections.
- Client Destination Port Number Of Flows TCP Not Established–distribution of a total number of flows over ports for not established TCP connections.
- Client Destination Port Total Bytes TCP Not Established–distribution of a total number of bytes over ports for not established TCP connections.
- Client Destination Port Total Packets UDP Established–distribution of a total number of packets over ports for established UDP connections.

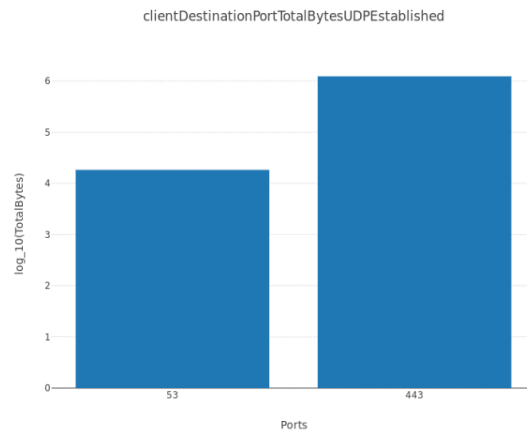
Those features are referenced as "profile features". The profile features describe the behavior of a user from different perspectives.

Fig. 4(a) shows a feature "Client Destination Port Total Bytes UDP Established" of a normal profile and Fig. 4(b) shows the same feature of an anomalous profile. A logarithmic scale is used for the y-axis to allow a large range to be displayed without small values being compressed down into the bottom of the graph.

#### D. Host behavior using Profiles

In the previous section, the complete content of a unique profiling was described, including its twelve features. These profiles are the basic unit of analysis of the anomaly detection method, and together they are part of the complete behaviors of the hosting user. This section first describes how the profiles are used to build the behaviors of a user, and then it describes which is the behavioral analysis method used by anomaly detection techniques.

The behavior of a user is defined by all the actions and decisions taken by the user in a certain period. Their actions are transformed into packets and flows, which are then captured in the already described features of a profiling. This allows each profile to describe the behavior of a user from twelve different points of view, each capturing a different perspective. As time goes by and the user generates more network traffic, and many profiles are generated.



(a) Shows an Example of Histogram for the Feature ‘Client Destination Port Total Bytes UDP Established’ for a Normal Profile. It can be seen that the Amount of Ports is Small.

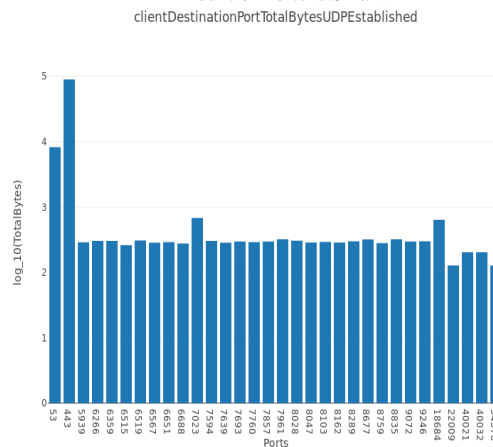


Fig. 4. (b) Shows an Example Histogram for the Same Feature but for an Anomalous Profile (an Attack was being Done). It can be seen a Large Number of Ports used.



The behavior of the user is then defined by all these profiles and their features. However, each feature describes the same data differently and therefore it does not make much sense to compare each feature with each other. Instead, it is proposed to compare each feature in the profile, with the same feature in the rest of the profiles for this user. The idea is that anomalies will arise when the same feature is analyzed in the concatenation of profiles. Fig. 5 shows the idea of searching for anomalies on the same feature on successive profiling.

Each feature in the profile corresponds to some measurement of data per port. Interpreted as a histogram, each feature is defined in the space of 65, 535 dimensions. Working with such a large space has two main limitations. First, data in the histogram are sparse, since most of the ports are never used. Second, the algorithms that analyze this data will have to deal with an increased, and probably unnecessary, complexity. Therefore, a reduction in the dimension of the space of each feature is necessary.

*a) Dimensionality Reduction of the Feature Space:* After normal profiles are collected, features are aggregated by type of data it measures over all profiles, and these are arranged into matrices  $P_i$  ( $i$  is a feature number). The matrix  $P_i$  is a sparse matrix, and it has dimensionality  $n \times 65, 535$ , where  $n$  is the number of profiles these have been collected and  $[0 - 65535]$  is the range of ports. Such number of dimensions might cause a problem with scalability and with the performance of anomaly detection algorithms. To improve the scalability and performance the number of dimensions of the data are needed to be reduced.

A common dimensionality reduction approach is a principal component analysis (PCA). It is a well-known dimensionality reduction technique [25]. PCA was successfully used in [26] to reduce the number of dimensions in features derived from web logs.

PCA derives a reduced set of the most significant uncorrelated features (principal components) that are linear combinations of the original set of features [27]. The new principal components are vectors in the direction of the largest variance of the dataset.

Given  $m$  features, PCA selects  $d < m$  principal components which define a new  $k$ -dimensional space based on normal profiles. There are two ways of specifying  $d$ : one can either set  $d$  to a fixed number or specify a percentage of variance to preserve, and  $d$  will be computed based on this percentage. In that case, the PCA algorithm was configured to preserve 99.9% of variance. It has been observed that dimensions to  $d = 8$  could be reduced in some cases and due to a high percentage of preserved variance the much information had not been lost.

However, after some experimentation, it is realized that there had been a problem with using PCA in the approach. The problem was that an infected computer used ports which were not commonly used by a normal computer. Because ports were not used by the normal computer, the matrix  $P_i$  always had 0 values in the columns corresponding to these ports. PCA was not using these columns when learning how to transform  $P_i$  to  $P'i$  in a new basis.

When the transformation learned was applied on the normal profiles to an anomalous profile in which an anomaly was reflected in columns which were not used in creation of the new basis, the information about the anomaly has lost.

Because of this problem it has been decided against using PCA in the said approach. Due to a problem of unseen ports, a different method of dimensionality reduction is applied.

*b) Anomaly Detection Methodology:* Each profile feature is represented by a vector of real numbers. It is proposed to use the Euclidean distance to compare a profile feature along with other profiles. Fig. 6 below shows the training process of the proposed approach. During the training, the normal profiles are used which are collected at different time intervals. The collected profiles cover the time when a user is active and when the user is idle. Providing a model with different types of the behavior of the user, allows the model to better generalize the network user behaviors.

The dimensionality reduction does not require training, and it is the same for each profile feature. Therefore it is applied during profile creation. The profile features are grouped based on the information they capture. After features have been grouped the profile feature is centered and scaled so all components of individual profile features will have 0 mean and unit variance. The original mean value and standard deviation of components are saved for future because they are required to center and scale new profiles. "Standard-Scaler" is used from python library "sklearn-Preprocessing" for this task.

Then profile features are used as an input to the anomaly detection technique algorithm to train models. The ADTs algorithm is applied to each group of features and for each group it learns a model. After the training phase there are the following models:

- Twelve pairs of parameters ( $[\mu, \sigma]$ ) for scaling and centering of features.
- Twelve models to classify profile by individual features.

Fig. 7 below depicts the inference phase of the proposed algorithm. The algorithm uses the models created during the training phase. The scaling and centering is applied to individual profile features of a testing profile. The scaled features are used as an input to the trained models. Each model produces one of two labels: 1 if the model considers the testing profile normal according to this feature or -1 if it considers the testing profile anomaly according to this feature.

Each output of the models contributes equally to the final decision. If six out of twelve models classify the profile as normal, the final label will be 1. Otherwise, the profile is labeled with -1.

#### *E. Anomaly Detection Algorithms*

The previous sections described how the flows are processed and how the features are created to obtain a suitable set of data to work on. This section describes all the anomaly detection algorithms selected and tested in order to find the best one. Among all the possible options, the following algorithms were selected:

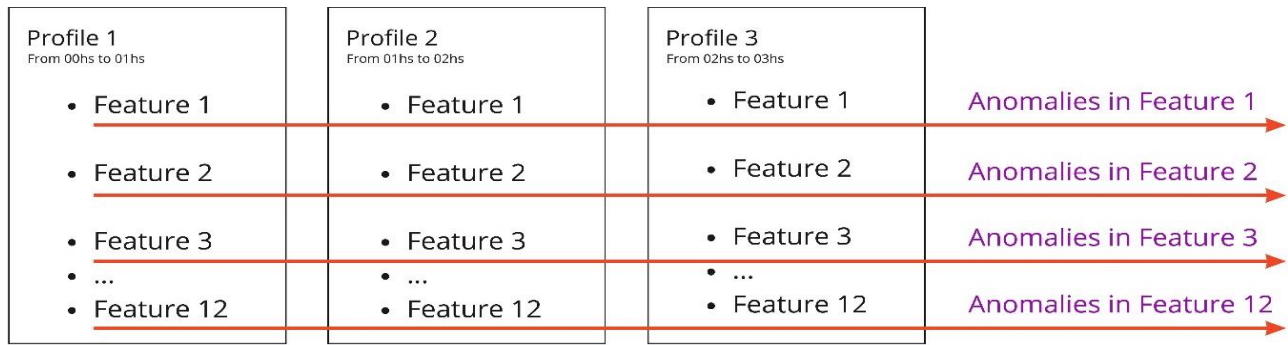


Fig. 5. Design of the Anomaly Detection Techniques. Instead of Comparing Each Feature with Each other, the Method Searches for Anomalies on the Same Feature on Successive Profiling.

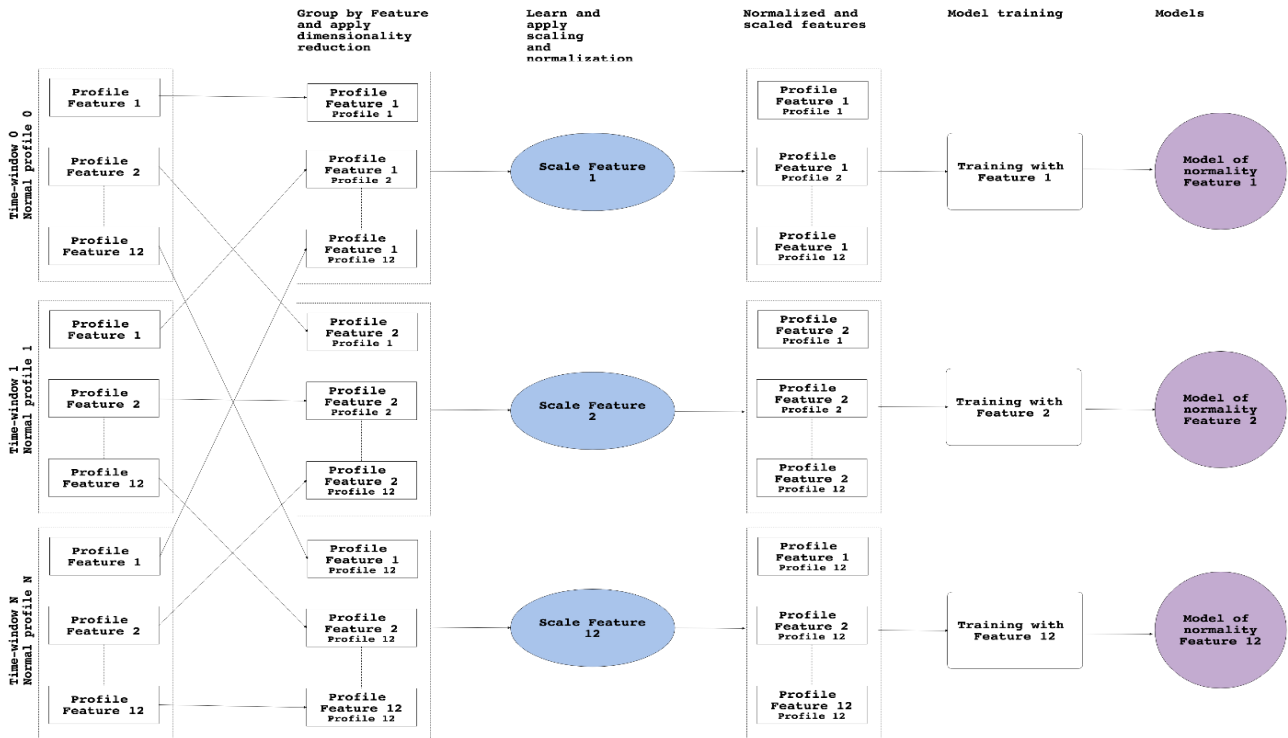


Fig. 6. The Diagram Shows the Training Process of the Proposed Approach. the Training uses  $N$  Collected Normal Profiles. there are Twelve Pairs of Parameters  $(\mu, \Sigma)$  for Scaling and Centering of Features and Twelve Models after the Training.

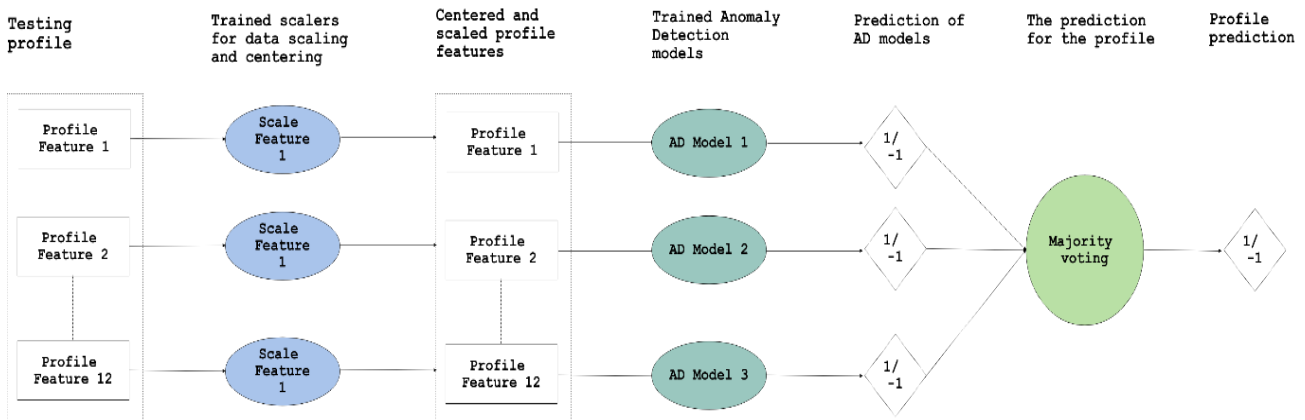


Fig. 7. The Diagram Shows the Inference Process of the Proposed Approach. there is One Profile which is Classified. Each Profile Feature is Scaled and Centered to the Same Scale as in Training Profile Features. Trained Models are used to Give Predictions for Each Feature and then Apply the Majority Voting to Get the Final Prediction for the Profile.

- 1) Local Outlier Factor (LOF) uses collected normal profiles to compute an anomaly score of a new profile.
  - 2) One Class SVM [28]—outputs a boundary around normal data.
  - 3) Isolation Forest [29]—method based on random forest, outputs a model of normal data.
- The following subsections describe the details of how each of these algorithms works:

a) *Local Outlier Factor (LOF) Algorithm:* The LOF algorithm assigns an anomaly score to each data point based on the idea of density. The LOF measures how density around a point differs from the density of its neighbors. It detects outliers in data on regions with different densities.

Fig. 8 shows two clusters  $C_1$ ,  $C_2$  and two additional  $O_1$  and  $O_2$  notations reflects the facts that the complexity is linear to the number of hostnames. It can be seen that the  $C_2$  cluster is much denser than the  $C_1$ .

According to Hawkins' [30], both points ( $O_1$  and  $O_2$ ) are outliers. However, it can be shown that there does not exist any distance-based detector that can mark  $O_2$  and not mark all points in the  $C_1$  cluster.

This example shows that distance-based methods have a problem if there are regions with different densities in the data. The LOF algorithm presented in solves this problem by assigning a value to each object which represents its anomaly score.

This example shows that the distance based methods have a problem if there are regions with different densities in data. The LOF algorithm presented in solves this problem by assigning a value to each object which shows the degree of it being an anomaly.

To use the LOF algorithm, authors in [31], define several notions:  $E$ -neighborhood and  $k$ -distance.

Let  $p$  be an object from a database  $D$ , let  $E$  be a distance value, let  $k$  be a natural number and let  $d$  be a distance metric on  $D$ . Then:

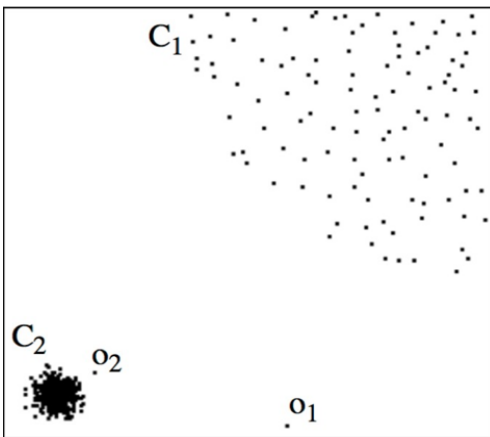


Fig. 8. Shows an Example Situation when there are Clusters with different Density. It is a Demonstration of the Advantage that LOF have over other Distance based Algorithms. This Example is Taken from LOF: Identifying Density-based Local Outliers [9].

Definition 1,

( $E$ -neighborhood)

The  $E$ -neighborhood are the objects  $x$  with  $d(p, x) \leq E : N_E(p) = \{x \in D | d(p, x) \leq E\}$

Definition 2,

( $k$ -distance)

The  $k$ -distance of  $p$  is the distance  $d(p, o)$  between  $p$  and an object  $o \in D$ , such that it holds at least for  $k$  objects  $o' \in D$  it holds that  $d(p, o') \leq d(p, o)$  and for at most  $k - 1$  objects  $o' \in D$  it holds that  $d(p, o') \leq d(p, o)$

Definition 3:

(reachability distance of object  $p$  with regard to object  $o$ )

Let  $k \in \mathbb{N}$ . The reachability distance of object  $p$  with respect to object  $o$  is defined as

$$reach-dist = \max\{k\text{-distance}(o), d(p, o)\}$$

In other words, all objects that belong to the  $k$ -neighborhood of an object  $p$  are considered to be equally distant from the object  $p$ .

The next equation is the equation of local reachability density. It is an inverse of the average reachability of the object  $p$  from its neighbors.

$$lrd(p) = \frac{1}{\frac{\sum_{o \in N_k(p)} reach-dist_k(p, o)}{|N_k(p)|}} \quad (1)$$

The LOF is computed by comparing with local reachability distances of the neighbors:

$$LOF_k(p) = \frac{\sum_{o \in N_k(p)} lrd(o)}{|N_k(p)|} \quad (2)$$

For any object which is inside a cluster, the LOF will be around 1. It does not depend on the density of a cluster, and it will be the same for objects inside cluster  $C_1$  and objects inside  $C_2$  [32], as is depicted in above (Fig. 8).

The main drawback of the LOF algorithm is its time complexity. Computation of the LOF has the complexity  $O(n^2)$ , because it requires computing pairwise distances between all data point.

b) *One Class SVM Algorithm:* One class SVM is an algorithm that identifies regions of space by their support vectors, of which there are far fewer than data points. The one class SVM algorithm solves the following optimization problem to compute the support vectors:

$$\min_{w \in F, \xi \in R, \rho \in R} \frac{1}{2} w^2 + \frac{1}{mv} \sum_{i=1}^m \xi_i - \rho \quad (3)$$

subject to

$$w \cdot \Phi(x_i) \geq \rho - \xi_i \quad \forall i = 1, \dots, m$$

$$\xi_i \geq 0 \quad \forall i = 1, \dots, m$$

Where  $\Phi : R^n \rightarrow F$  is a nonlinear mapping from data space  $R^n$  to feature space  $F$ ,  $\xi_i$  is a slack variable one for every data

sample,  $\rho$  is a distance from the hyper-plane to the origin in feature space, and  $\nu$  is the expected fraction of data samples outside the estimated support. The one class SVM algorithm depends on the choice of two parameters:  $\nu$  and  $\sigma$ . The parameter  $\nu$  controls the sensitivity of the model. More precisely it controls the ratio of outliers in the data. The parameter  $\sigma$  controls the number of support vectors. The lower value of  $\sigma$  leads to "remembering" the training dataset and the model over-fits the larger value leads to oversimplifying dependencies in the dataset, in other words, it leads to high bias.

The other important decision one has to make when training a one class SVM model is a choice of kernel. The general advice is to use a radial basis function kernel (RBF kernel) [33] because usually, it performs better on different datasets. It has been experimented with different kernels, and the RBF kernel was showing the best results. RBF kernel adds one more parameter which can be adjusted to change the performance of the one class SVM algorithm. The parameter  $\gamma$  controls how far the influence of a single training example reaches. The smaller value of  $\gamma$  means that a single example influences other examples far away and the larger value means its influence is shorter.

c) *Isolation Forest*: Isolation Forest is a model-based approach to detect anomalies. In the context of isolation forest "isolation" means "separating an instance from the rest of the instances". The algorithm constructs trees which isolate every single instance of data. Because anomalies are different, they will be isolated faster by the algorithm, which means they will be closer to the root of a tree. To achieve this, isolation forest takes advantage of two properties of anomalies:

- They are in the minority.
- Attribute-values of anomalies significantly differ from normal samples an example of isolation can be seen in Fig. 9(a), (b).

The authors of the paper has define the path length of a point  $x$  as the number of edges and the point of traverses until it terminates in the end node.

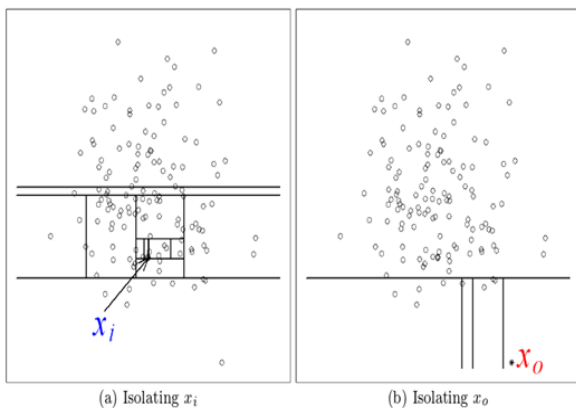


Fig. 9. (a). Shows the Isolation of a Normal Data Sample. (b) Shows the Isolation of an Anomalous Data Sample. Image is Taken from Isolation Forest [29].

There are two stages of anomaly detection with isolation forest. The first stage is a training stage. In this stage, the trees are constructed recursively until all instances are isolated or the specified tree height is reached. The theory behind growing the trees up to some height is that the utmost interest has been shown in points which have a shorter than average path distance. There is no need to grow the trees until each point is isolated. The second stage is the evaluation. The anomaly score of a sample is based on the average path length from root to its termination node.

#### F. Training and Validation

Cross-validation [34], is going to be used which is a common technique to estimate a test error of a model. Dataset is split and hold out a small subset of data to test the model performance and to make sure that the model does not just memorize the dataset. It is ensured that the model does not have a high FPR and also that it detects anomalies. The model is also prevented from overfitting. It means that a model is trained too much and it is fitted too close to the train set. The main sign of overfitting is that a model has the very low error on the train set, but a much higher error on a validation set. The data is split into three sets: train, validation, and test. The train set consists of normal profiles only. The validation and test sets consist of normal and anomalous profiles. All anomalous profiles are taken randomly to select half of them and to insert them into validation set. The other half is inserted into the test set. The split is the following:

- Train set—70% of normal data.
- Validation set—15% of normal data and 50% of anomalous profiles.
- Test set—15% of normal data and the other 50% of anomalous profiles.

As it has been mentioned before the data are scaled and normalized to have 0 mean and unit variance. To avoid information leak from the training data to test data, it has been learnt a mean value and variance for scaling and centering only on train data, and then scaling is applied to validation and test data. The information leak might lead to test error underestimating the actual error.

#### G. Model Selection

In Section III.E, it has been described the algorithms that has been tried for anomaly detection. LOF and one class SVM have both hyper-parameters that can be tuned to improve the performance. When search has been made for the optimal set of parameters for our model, a grid of search is conducted over a range of possible parameter values. If a hyper-parameter is restricted to some range of values we use that range. If a hyper-parameter is not restricted selection of some reasonable size and search inside it have been done.

The evaluation of a network anomaly detection algorithm is a very important step in showing the advantages and efficiency of the proposed method. The main challenge is to acquire labeled data to measure the performance of the model.

To select a model the following criteria is used:

- 1) Find a set, A, of models with the lowest False Positive Rate FPR.
- 2) Select a model slowest with the highest True Positive Rate TPR from the set A.
- 3) Find a set of models B with the FPR less than 0.01.
- 4) Select a model  $S_{threshold}$  with the highest TPR from the set B.
- 5) Select the final model with the highest FPR by comparing FPR of  $S_{slowest}$  &  $S_{threshold}$ .

The FPR metric is very important in anomaly detection. If a model has FPR around 0.05 in a small network with 10 computers and 5 minutes profiles, it will generate 144 false reports daily. Since each report should be checked manually by a system administrator, it would consume many resources.

It has been tried to find model parameters which will have a good trade-off between FPR and TPR. The goal is to maximize TPR while at the same time keeping the FPR below 0.01 or 1%.

#### IV. MACHINE LEARNING DATASETS

The characteristics of the dataset used for training and testing a machine learning algorithm [35] are very important for the results obtained. In fact, the dataset is so important that it completely define if the algorithm works or not, it defines its performance and its generalization power. It does not make much sense to talk about if an algorithm is good or bad without discussing the dataset used.

The dataset used in this research work was created from scratch to fulfill the requirements. In particular, it was very important to have a dataset of real malicious activities [36,37] at the same time that the normal user is also using the computer. This was achieved through a large process of configurations and infections. The setup to create the datasets consisted of a Windows 10 virtual machine running on Virtual-Box. The traffic was captured by Virtual-Box in a “.pcap file”. After the capture was finished, the pcap file was processed with the Argus tool to obtain bidirectional flows.

To work with an anomaly detection algorithm, it's necessary to have a dataset which contains two main parts: normal user activity, and a mix of normal activity and malicious activity. The normal user activity is used for creating a model of normal traffic. Later on, the models are evaluated using the mix of normal traffic and malicious traffic [38].

To generate normal activity, multiple accounts in different services such as Facebook, Gmail, Dropbox, and Twitter are created [39]. All these accounts were used to generate real normal traffic, where the user creates and writes in new documents, chat with friends and synchronizes data in the cloud [40]. There is also normal activity such as visiting websites, searching for information and downloading files, including executable files. In all type of datasets the normal activities lasted several hours, up to several days.

After the normal activity was done, the computer was infected with some malware while the user keeps doing normal actions. This mixed traffic was kept for several hours also.

During all the experiments all the activities done by the normal user were logged and stored. This log was later used for labeling the profiles with normal and anomalous labels [41].

#### A. Ground-Truth Labels Process

In this section, labeling process has been described. For the evaluation of the performance, it is needed to have ground-truth labels. The captures of network traffic [42] are split into two parts: before and after an infection. When profiles are created from the flows it is known that if it belongs to pre or post-infection part.

The normal label (label = 1) is assigned to all profiles which are created before the infection of the virtual machine run on web based adaptive data-driven networks (DDN) management and cooperative network communities [43]. A virtual machine before each capture is created which ensures that it is clean and does not contain any malicious software. The anomaly label (label = -1) is put to all profiles which are created after the infection of the virtual machine. The reason of assigning the anomaly labels this way is the assumption that everything after an infection worth detecting and that malware produces changes in behavior. It is known that not all the attacks are anomalies, but this assumption helps us better evaluate the algorithm.

#### V. EXPERIMENTAL RESULTS

With the help of anomaly detection techniques, method designed and a good dataset generated it was possible to train and test the hypothesis by running experiments. There were five experiments in total, each one verifying a different algorithm with a different dataset. The goal of these experiments was to verifying if the hypothesis was true. Else if hypothesis was not true then it is possible to detect the infected users and to have a small number of false positives by focusing on the high-level behaviors in time. The side effect verification was to see if the method was capable of generalizing to malware which it has not seen during the training.

All the experiments in point were evaluated in two ways. First, labeling to each feature individually was used to trained models. Then second way is to use a voting mechanism to decide if the analyzed profile was anomalous or not. The voting is described in Section III.D.b.

A summary of the experiments follows:

- The first experiment uses one-class SVM trained on the normal part of the first dataset and validated on the mixed part of the first dataset.
- The second experiment uses one-class SVM trained on the normal part of the second dataset and verification on the mixed part of the second dataset (and the mixed part of the third dataset).
- The third experiment uses LOF trained on the normal part of the first dataset and validated on the mixed part of the first dataset.
- The fourth experiment uses LOF trained on the normal part of the second dataset and validated on the mixed part of the second dataset.

- The fifth experiment uses Isolation Forest trained on the normal part of the first dataset and validated on the mixed part of the first dataset.

All the experiments were run in docker container using Ubuntu 16.04, Python 3.6 and the following versions of libraries: “pandas: 0.20.3”, “numpy: 1.13.1” and “scikit-learn: 0.19.0”.

A. The First Experiment

In the first experiment, one class SVM algorithm is used, as it was described in Section III.E.b. this algorithm was trained with the normal part of the first dataset in Section IV, and it was validated on the mixed part of the same first dataset. The SVM algorithm used the Euclidean distance and the RBF kernel function. To train the SVM a grid search over the following parameters is used:

- *Gamma* parameter for RBF kernel: values in range  $[10^{-9}, 10^3]$  with step  $10^2$ .

*Nu* parameter for lower bound of fraction of support vectors: values in range [0.01, 0.99] with step 0.01, depicted in Fig. 10.

The training of the algorithm was performed by splitting the normal part of the first dataset into three sets: train, validation and test. This was done using the `train_test_split` function from the python library `sklearn` [44-46]. To make the data split repeatable, we specify that the random seed is 42. The mixed part of the first dataset (that contains both normal and malicious traffic) was split into two sets: validation and test. Both were generated by randomly selecting half of the profiles in that dataset.

With the sets of data defined a model for each of the twelve features in a profile (see in Section III.C) is trained. After that all models have been trained, the best model is selected by using the validation set. The best model was selected for each feature (see in Section III.G).

The first analysis of these results is done according to each feature. Fig. 11 and Table I below shows that one class SVM

achieved low FPR for each feature. It does not exceed 0.01 in any case, and for eight of the features, it is 0.0. The algorithm also has 1.0 TPR for five features. All of these five features are TCP features. It means that the malware actively uses TCP protocol to communicate and this is very anomalous compared with the normal user.

The interesting observation is that the feature `Client_DestinationPort_NumberOfFlows_TCP_Established` has 0.0 TPR.

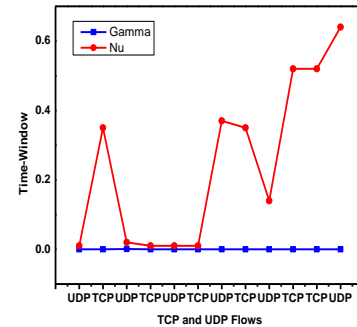


Fig. 10. Shows the Winning Parameters for One Class SVM Model in the First Experiment.

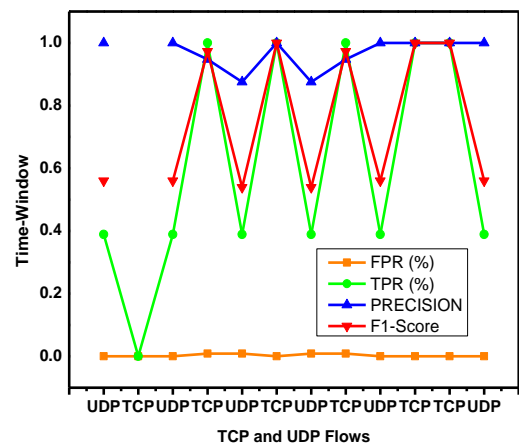


Fig. 11. Shows the Validation Results for Each of the Twelve Features, Present in below Table I.

TABLE I. VALIDATION RESULTS FOR THE FIRST EXPERIMENT. ONE CLASS SVM ALGORITHM TRAINED ON THE NORMAL PART OF FIRST DATASET AND TESTED ON THE MIXED PART OF THE FIRST DATASET. THE VALIDATION SET CONSISTS OF SOME NORMAL PROFILES AND SOME MALICIOUS PROFILES

| Twelve Features Name  | FPR%  | TPR%  | Precision | F1-Score |
|---|-------|-------|-----------|----------|
| 1. Client_DestinationPort_TotalBytes_UDP_Established        | 0.0   | 0.389 | 1.0       | 0.560    |
| 2. Client_DestinationPort_NumberOfFlows_TCP_Established     | 0.0   | 0.0   | ---       | ---      |
| 3. Client_DestinationPort_NumberOfFlows_UDP_NotEstablished  | 0.0   | 0.389 | 1.0       | 0.560    |
| 4. Client_DestinationPort_TotalPackets_TCP_Established      | 0.009 | 1.0   | 0.947     | 0.973    |
| 5. Client_DestinationPort_NumberOfFlows_UDP_Established     | 0.009 | 0.389 | 0.875     | 0.539    |
| 6. Client_DestinationPort_TotalPackets_TCP_NotEstablished   | 0.0   | 1.0   | 1.0       | 1.0      |
| 7. Client_DestinationPort_TotalBytes_UDP_NotEstablished     | 0.009 | 0.389 | 0.875     | 0.539    |
| 8. Client_DestinationPort_TotalBytes_TCP_Established        | 0.009 | 1.0   | 0.947     | 0.973    |
| 9. Client_DestinationPort_TotalPackets_UDP_NotEstablished   | 0.0   | 0.389 | 1.0       | 0.560    |
| 10. Client_DestinationPort_NumberOfFlows_TCP_NotEstablished | 0.0   | 1.0   | 1.0       | 1.0      |
| 11. Client_DestinationPort_TotalBytes_TCP_NotEstablished    | 0.0   | 1.0   | 1.0       | 1.0      |
| 12. Client_DestinationPort_TotalPackets_UDP_Established     | 0.0   | 0.389 | 1.0       | 0.560    |

After running the validation using grid search on the parameters, the best model is selected by using the methodology explained in Section III.G. The winning parameters for these one class SVM models were discussed below:

After the winner parameters were selected during the validation phase, it can be tested the model for its generalization power using the test set Fig. 12 below shows the results on the test set. The results are very similar to the validation set results, which means that there is a good generalization. This test set contains the same malware that was used in the validation set. After testing the one class SVM using our first method of evaluation, the evaluation of the results is done by applying a majority voting mechanism on the output generated for each feature to decide if the profile was anomalous or not. As in the previous testing, it has been tested the majority voting model on the test set from the first dataset. Our approach to a majority voting is described in Section III.D.b. Therefore, the results are shown below in Table II.

Table II shows that the majority votes among the models produces a good result on the test set. The TPR of 0.444 or 44% may seem low, but this is the final result for all the profiles in time, with a 0 FPR and a 100% precision. These results mean that on average the one anomaly will be detected out of three with probability 99.9%. It also means that if it is used the five-minute time-windows to create profiles, it can raise the alarm after first 15 minutes after a malware becomes active. Considering that the evaluation is per profile, it is believe that these results are very good in this area.

**B. The Second Experiment**

In the second experiment, the one class SVM is used, as it was described in (section III.E.b). this algorithm was trained with the normal part of the second dataset in (section IV.), and it was validated on the mixed part of that same dataset. The SVM algorithm used the Euclidean distance and the RBF kernel function.

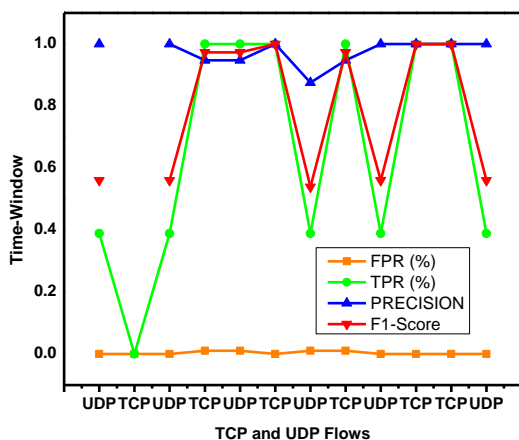


Fig. 12. Shows the Results on the Test Set Experiment, the Results are very Similar to the Validation Set Results, Dipict in (Fig. 11 above) which means that there is Good Generalization.

TABLE II. TEST RESULTS FOR THE FIRST EXPERIMENT USING MAJORITY VOTING. THE MAJORITY VOTING TO THE TWELVE RESULTS ON EACH PROFILE IS APPLIED TO GET THE FINAL DECISION ABOUT A PROFILE. THE TEST SET FOR THE FIRST DATASET WAS USED FOR THE TESTING. THE TEST SET CONTAINS NORMAL PROFILES AND PROFILES CREATED DURING THE INFECTION WITH THE MALWARE

| Feature Name    | FPR% | TPR%  | Precision | F1-Score |
|-----------------|------|-------|-----------|----------|
| Majority voting | 0.0  | 0.444 | 1.0       | 0.615    |

To train the SVM model a grid search over the following parameters is used:

- Gamma parameter for RBF kernel: values in range  $[10^{-9}, 10^3]$  with step  $10^2$ .
- Nu parameter for lower bound of fraction of support vectors: values in range [0.01, 0.99] with step 0.01.

The training of the algorithm was performed by splitting the normal part of the dataset into three sets: train, validation and test. This was done using the train\_test\_split function from the python library sklearn. To make the data split repeatable, it is specified that the random seed is 42. The mixed part of the second dataset (that contains both normal and malicious traffic) was split into two halves: the first half was added to the validation set and the second half was added to the test set. Both were generated by randomly selecting half of the profiles in that dataset.

With the sets of data defined a model is trained for each of the twelve features in a profile (see in Section III.C). After having trained all models, the best model is selected by using the validation set. The best model was selected for each feature (see in Section III.G). After the validation is finished the winner model is selected.

The first analysis of the results is done with regard to each feature, Fig. 13, shows that the models achieved low FPR for each feature. It does not exceed 0.01 in any case, and for seven of the features, it is 0.0. However, TPR is lower than in the first experiment. This might be caused by the nature in which this malware communicates. The mixed capture of the second dataset was generated using [47]. Dark-VNC virtual network computing is used to silently control the computer of a victim, and it does not generate much additional traffic.

This is an example of how the anomaly detection technique might help better understand the communication details of malware. By analyzing results, the analyst could very fast see which protocols are used by malware, if it generates many connections and sends much information. The winning parameters for the best one class SVM models were discussed below:

After the winner parameters were selected during the validation phase, it can be tested the model for its generalization power using the test set. See Fig. 14 and Table III below shows the results on the test set. This test set contains the same malware that was used in the validation set.

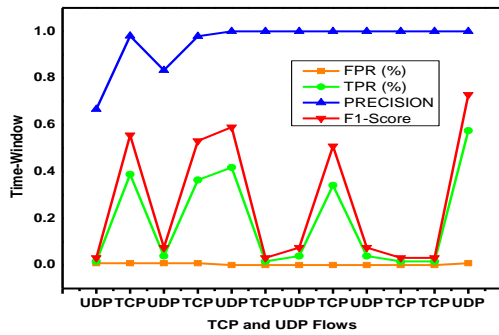


Fig. 13. Shows the Results that Model Achieved Low FPR for Each Feature.

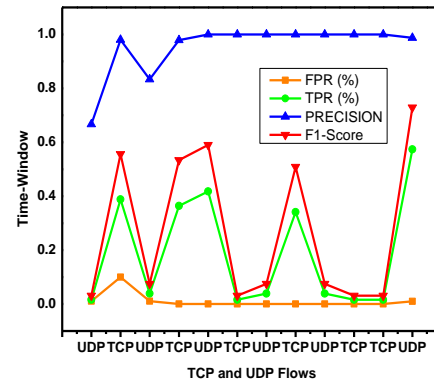


Fig. 15. Shows the Results Obtained for the Mixed Capture from the Third Dataset using the Models Trained on the Second Dataset.

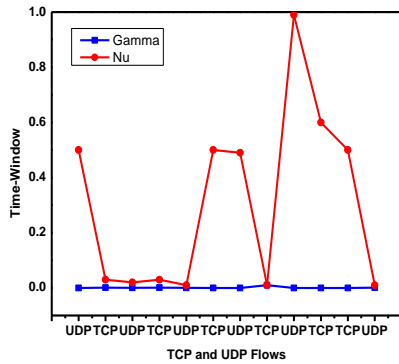


Fig. 14. Shows the Results on the Test Set, this Test Set Contains the same Malware that was used in the Validation Set, Present in Table III.

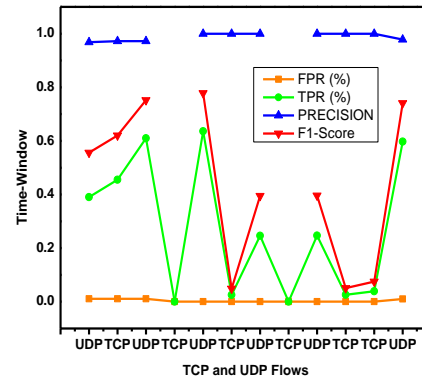


Fig. 16. Shows the Results of different Features Contributing to the Detection of different Types of Infected Malware.

TABLE III. THE WINNING PARAMETERS FOR ONE CLASS SVM MODELS IN THE SECOND EXPERIMENT. THESE PARAMETERS WERE OBTAINED USING THE VALIDATION SET OF THE SECOND DATASET

| Features Name   | $\Gamma$  | $\nu$ |
|---|-----------|-------|
| Client_DestinationPort_TotalBytes_UDP_Established       | $10^{-9}$ | 0.50  |
| Client_DestinationPort_NumberOfFlows_TCP_Established    | $10^{-3}$ | 0.03  |
| Client_DestinationPort_NumberOfFlows_UDP_NotEstablished | $10^{-4}$ | 0.02  |
| Client_DestinationPort_TotalPackets_TCP_Established     | $10^{-3}$ | 0.03  |
| Client_DestinationPort_NumberOfFlows_UDP_Established    | $10^{-4}$ | 0.01  |
| Client_DestinationPort_TotalPackets_TCP_NotEstablished  | $10^{-9}$ | 0.50  |
| Client_DestinationPort_TotalBytes_UDP_NotEstablished    | $10^{-8}$ | 0.49  |
| Client_DestinationPort_TotalBytes_TCP_Established       | $10^{-2}$ | 0.01  |
| Client_DestinationPort_TotalPackets_UDP_NotEstablished  | $10^{-9}$ | 0.99  |
| Client_DestinationPort_NumberOfFlows_TCP_NotEstablished | $10^{-7}$ | 0.60  |
| Client_DestinationPort_TotalBytes_TCP_NotEstablished    | $10^{-9}$ | 0.50  |
| Client_DestinationPort_TotalPackets_UDP_Established     | $10^{-3}$ | 0.01  |

It is wanted to test the generalization power of the models even further, and the mixed capture is used from the third dataset in Section IV to test the performance of the models. Since the mixed capture from the third dataset contains traffic from a different type of malware and it was not used during the selection process of models, this evaluation could be a good estimate for the real error. See Fig. 15 below contains the results obtained for the mixed capture from the third dataset using the models trained on the second dataset:

These results are first analyzed per each feature. Fig. 16 below shows that different features contribute to the detection of different types of malware.

For example, on the one hand, the feature Client\_DestinationPort\_NumberOfFlows\_UDP\_NotEstablished contributes a lot to the detection of Simba malware and on the other hand the same feature does not contribute to the detection.

After testing the one class SVM using the first method of evaluation, it is now evaluated the results of applying a majority voting mechanism on the output generated for each feature to decide if the profile was anomalous or not. As in the previous testing, the majority voting model is tested on the test set from the second dataset. The approach to a majority voting is described in Section III.D.b and the results are shown in above Table II.

Table IV below shows that the majority voting among the models produces FPR of 0.0. However, the TPR is very low, which could be explained by the difficulty of detecting this particular malware. In the future it is wanted to experiment with approaches other than majority voting, for example, neural network will be trained to summarize the outputs of the twelve models into one final result.

Majority of voting to classify the profiles was generated during the infection with the Simba malware in the third dataset. The results are shown in below Table V.



TABLE IV. THE SECOND EXPERIMENT. THE MAJORITY VOTING IS APPLIED TO THE TWELVE RESULTS TO GET THE FINAL DECISION ABOUT A PROFILE. THE RESULTS ARE SHOWN ON THE TEST SET FOR THE SECOND DATASET AND THE FIRST MALICIOUS PART. THE TEST SET CONTAINS NORMAL PROFILES AND PROFILES CREATED DURING THE INFECTION WITH THE FIRST MALWARE

| Feature Name    | FPR% | TPR%  | Precision | F1-Score |
|-----------------|------|-------|-----------|----------|
| Majority voting | 0.0  | 0.031 | 1.0       | 0.060    |

TABLE V. THE SECOND EXPERIMENT THAT IS APPLIED MAJORITY VOTING TO THE TWELVE RESULTS TO GET THE FINAL DECISION ABOUT A PROFILE. THE RESULTS ARE SHOWN ON THE TEST SET FOR THE SECOND DATASET AND THE SECOND MALICIOUS PART. THE TEST SET CONTAINS NORMAL PROFILES AND PROFILES CREATED DURING THE INFECTION WITH THE SECOND MALWARE

| Feature Name    | FPR% | TPR%  | Precision | F1-Score |
|-----------------|------|-------|-----------|----------|
| Majority voting | 0.0  | 0.233 | 1.0       | 0.378    |

The TPR of 0.233 or 23% is lower than in the first experiment. However, this result means that the algorithm will detect one anomalous profile out of five with probability 99.9%. If we use five minutes time-windows to create profiles, the alarm will be raised during the first 25 minutes after a malware becomes active.

### C. The Third Experiment

In the third experiment, the use of the LOF algorithm has been done, as it was described in Section III.E.a. This algorithm was trained with the normal part of the first dataset see in Section IV and it was validated on the mixed part of that same first dataset. The LOF algorithm used the Euclidean distance to compute density estimation.

To train the LOF, a grid search over the following parameters is used:

- *k* parameter for number of neighbors: values in range [1 -10] with a step 1.
- *Contam* parameter for contamination rate (the ratio of anomalies): values in range [0.01, 0.1] with a step approximately 0.002.

The training of the algorithm was performed by splitting the normal part of the dataset into three sets: train, validation and test. This was done using the `train_test_split` function from the python library `sklearn`. To make the data split repeatable, it is specified that the random seed is 42. The mixed part of the first dataset (that contains both normal and malicious traffic) was split into two halves: the first half was added to the validation set and the second half was added to the test set. Both were generated by randomly selecting half of the profiles in that dataset. With these sets of data defined the model has been trained a model for each of the twelve features in a profile (see in Section III.C); after that all trained models, select the best model by using the validation set. The best model was selected for each feature (see in Section III.G).

After the validation is finished the winner model is selected. The first analysis of these results is done according to each feature. Fig. 17 below shows that LOF achieved low FPR for each feature. It exceeds 0.01 only for one profile and only by 0.001, and for other eleven of the features, it is 0.0. The algorithm also has 1.0 TPR for three features. All of these three features are TCP features. It means that the malware actively

uses TCP protocol to communicate and this is very anomalous compared with the normal user.

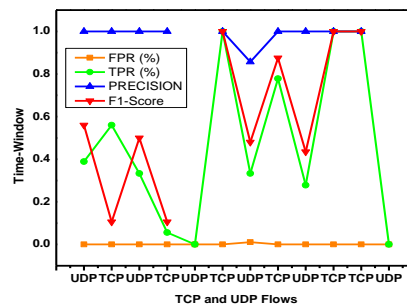


Fig. 17. Shows the Results of LOF Algorithm Achieved Low FPR for each Feature.

After running the validation using grid search on the parameters, the best model is selected by using the methodology explained in Section III.G. The winning parameters for these LOF models are shown in Fig. 18 and Table VI.

After the winner parameters were selected during the validation phase, it can be tested the model for its generalization power using the test set given in Fig. 19 shows the results on the test set. The results for TPR are similar to the results obtained on the validation set, but the FPR is slightly higher for nine profile features. This test set contains the same malware that was used in the validation set.

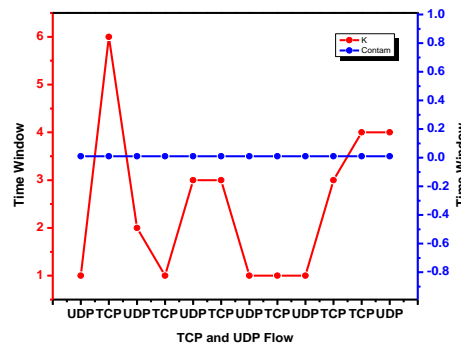


Fig. 18. Shows the Winning Parameters of LOF Model in the Third Experiment, Present in Table VI.

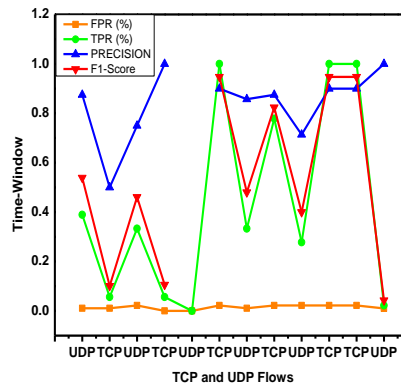


Fig. 19. Shows Results on the Test Set for the First Dataset, the Test Set Contains Normal Profiles and Profiles Created During the Infection with the Malware.

TABLE. VI. THE WINNING PARAMETERS FOR LOF MODELS IN THE THIRD EXPERIMENT. THESE RESULTS WERE OBTAINED USING THE VALIDATION SET OF THE FIRST DATASET

| Features Name   | k | Contam |
|---|---|--------|
| Client_DestinationPort_TotalBytes_UDP_Established       | 1 | 0.01   |
| Client_DestinationPort_NumberOfFlows_TCP_Established    | 6 | 0.01   |
| Client_DestinationPort_NumberOfFlows_UDP_NotEstablished | 2 | 0.01   |
| Client_DestinationPort_TotalPackets_TCP_Established     | 1 | 0.01   |
| Client_DestinationPort_NumberOfFlows_UDP_Established    | 3 | 0.01   |
| Client_DestinationPort_TotalPackets_TCP_NotEstablished  | 3 | 0.01   |
| Client_DestinationPort_TotalBytes_UDP_NotEstablished    | 1 | 0.01   |
| Client_DestinationPort_TotalBytes_TCP_Established       | 1 | 0.01   |
| Client_DestinationPort_TotalPackets_UDP_NotEstablished  | 1 | 0.01   |
| Client_DestinationPort_NumberOfFlows_TCP_NotEstablished | 3 | 0.01   |
| Client_DestinationPort_TotalBytes_TCP_NotEstablished    | 4 | 0.01   |
| Client_DestinationPort_TotalPackets_UDP_Established     | 4 | 0.01   |

TABLE. VII. THE THIRD EXPERIMENT WHICH IS APPLIED MAJORITY VOTING TO THE TWELVE RESULTS TO GET THE FINAL DECISION ABOUT A PROFILE. IS SHOWN IN RESULTS ON THE TEST SET FOR THE FIRST DATASET. THE TEST SET CONTAINS NORMAL PROFILES AND PROFILES CREATED DURING THE INFECTION WITH THE MALWARE

| Feature Name    | FPR% | TPR%  | Precision | F1-Score |
|-----------------|------|-------|-----------|----------|
| Majority voting | 0.0  | 0.333 | 1.0       | 0.496    |

After testing the LOF using the first method of evaluation, it is now evaluated the results of applying a majority voting mechanism on the output generated for each feature to decide if the profile was anomalous or not. As in the previous testing, the majority voting model is tested on the test set from the first dataset. The approach to a majority voting is described in Section III.D.b. The results are shown in below Table VII.

The above Table II shows that the majority voting among the models produces a good result on the test set. The TPR of 0.333 or 33.3% may seem low, but this is the final result for all the profiles in time, with a 0 FPR and a 100% precision. These results mean that on average it will be detected one anomaly out of three with probability 99.9%. It also means that if the five-minute time-windows is used to create profiles, it can raise the alarm during the first 15 minutes after a malware becomes active. Considering that the evaluation is per profile, it is believed that these results are very good in the area.

D. The Fourth Experiment

The first analysis of the results is done with regard to each feature. Fig. 20 below shows that the models achieved low FPR for each feature. It does not exceed 0.01 in any case, and for seven of the features, it is 0.0. However, TPR is lower than in the first experiment. This might be caused by the nature in which this malware communicates. The mixed capture of the second dataset was generated using Dark-VNC malware.

Dark virtual network computing (Dark-VNC) is used to silently control the computer of a victim, and it does not generate much additional traffic.

After running the validation using grid search on the parameters, which are selected the best model using the methodology explained in Section III.G. The winning parameters for these LOF models are shown in Fig. 21 and Table VIII.

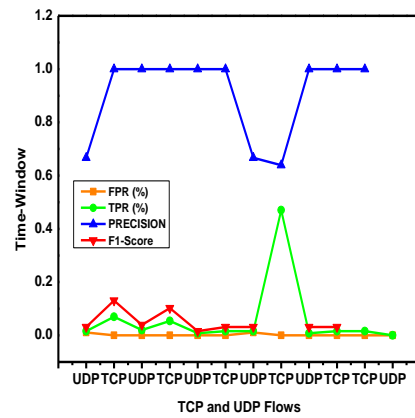


Fig. 20. Shows that the Models Achieved Low FPR for each Feature it doesn't Exceed 0.01 Score in any Case, and for Seven of the Feature, it Takes 0.0 Score.

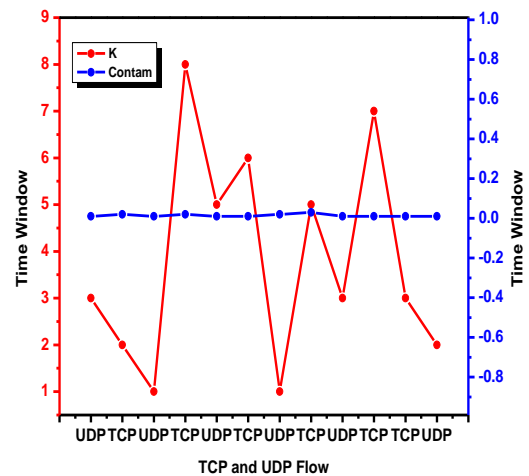


Fig. 21. Results Shows the Wining Parameters for LOF Model in Fourth Experiment, Present in Table VIII.

TABLE. VIII. THE WINNING PARAMETERS FOR LOF MODELS IN THE FOURTH EXPERIMENT THESE RESULTS WERE OBTAINED USING THE VALIDATION SET OF THE SECOND DATASET

| Feature Name  | K | Contam |
|---|---|--------|
| Client_DestinationPort_TotalBytes_UDP_Established       | 3 | 0.01   |
| Client_DestinationPort_NumberOfFlows_TCP_Established    | 2 | 0.02   |
| Client_DestinationPort_NumberOfFlows_UDP_NotEstablished | 1 | 0.01   |
| Client_DestinationPort_TotalPackets_TCP_Established     | 8 | 0.02   |
| Client_DestinationPort_NumberOfFlows_UDP_Established    | 5 | 0.01   |
| Client_DestinationPort_TotalPackets_TCP_NotEstablished  | 6 | 0.01   |
| Client_DestinationPort_TotalBytes_UDP_NotEstablished    | 1 | 0.02   |
| Client_DestinationPort_TotalBytes_TCP_Established       | 5 | 0.03   |
| Client_DestinationPort_TotalPackets_UDP_NotEstablished  | 3 | 0.01   |
| Client_DestinationPort_NumberOfFlows_TCP_NotEstablished | 7 | 0.01   |
| Client_DestinationPort_TotalBytes_TCP_NotEstablished    | 3 | 0.01   |
| Client_DestinationPort_TotalPackets_UDP_Established     | 2 | 0.01   |

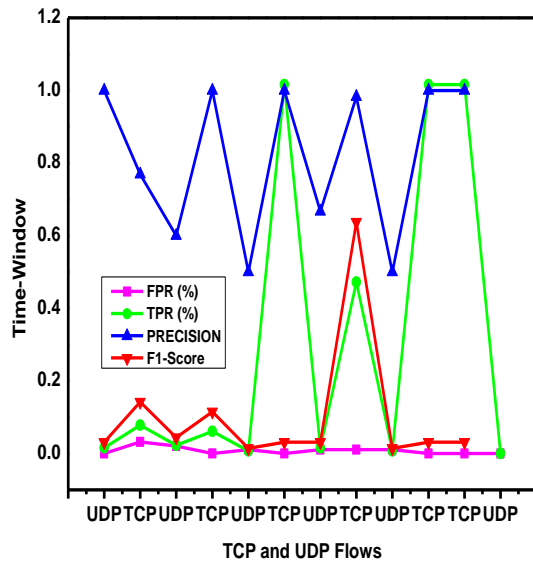


Fig. 22. The Results Shows that the TPR is Similar to the Results Obtained on the Validation Set, but the FPR is Slightly Higher for Five Profile Features.

After the winner parameters were selected during the validation phase, it can be tested the model for its generalization power using the test set. Fig. 22 shows the results on the test set. The results for TPR are similar to the results obtained on the validation set, but the FPR is slightly higher for five profile features. This test set contains the same malware that was used in the validation set.

It is wanted to test the generalization power of the models even further, and it is used the mixed capture from the third dataset (Section IV) to test the performance of the models. Since this mixed capture contains traffic from a different type of malware and it was not used in the during the selection process of models, this evaluation could be a good estimate for the real error. Fig. 23 contains the results obtained for the mixed capture from the third dataset using the models trained on the second dataset:

After testing the LOF using the first method of evaluation, it is now evaluated the results of applying a majority voting mechanism on the output generated for each feature to decide if the profile was anomalous or not. As in the previous testing, It is also apply majority voting to classify the profiles which were generated during the infection with the Simba malware in the third dataset. The results are shown in Table IX, as in the second experiment results of the majority, voting are not satisfactory, and it is going to address this problem in the future work.

E. The Fifth Experiment

In this experiment, it has been tried to use isolation forest on our data. The results were surprising because it was not able to train a model with any true positive detection. The isolation forest is shown to out-perform many algorithms including LOF and one class SVM [48, 49].

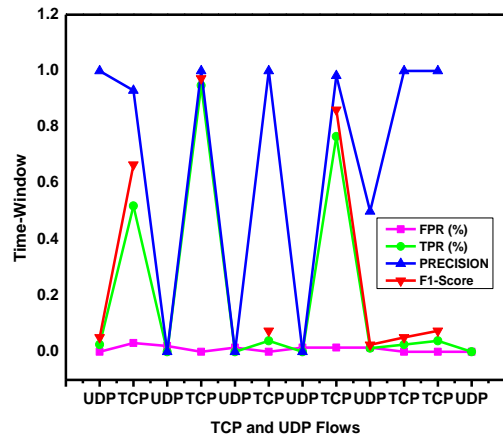


Fig. 23. Contains the Results Obtained for the Mixed Capture from the Third Dataset using the Models Trained on the Second Dataset.

TABLE IX. THE FOURTH EXPERIMENT WHICH IS APPLIED MAJORITY VOTING TO THE TWELVE RESULTS TO GET THE FINAL DECISION ABOUT A PROFILE. RESULTS ARE SHOWN ON THE TEST SET FOR THE THIRD DATASET. THE TEST SET CONTAINS NORMAL PROFILES AND PROFILES CREATED DURING THE INFECTION WITH SIMBA MALWARE

| Feature Name    | FPR% | TPR% | Precision | F1-Score |
|-----------------|------|------|-----------|----------|
| Majority voting | 0.0  | 0.0  | ---       | ---      |

TABLE X. THE FIFTH EXPERIMENT WHICH IS APPLIED MAJORITY VOTING TO THE TWELVE RESULTS TO GET THE FINAL DECISION ABOUT A PROFILE. RESULTS ARE SHOWN ON THE TEST SET FOR THE SECOND DATASET. THE TEST SET CONTAINS NORMAL PROFILES AND PROFILES CREATED DURING THE INFECTION WITH DARKVNC MALWARE.

| Feature Name    | FPR% | TPR% | Precision | F1-Score |
|-----------------|------|------|-----------|----------|
| Majority voting | 0.0  | 0.0  | ---       | ---      |

It could be caused by the nature of anomalies in the dataset. As it is described in Section III.C, each feature of a profile is represented by a vector. When it is detected anomalies among one feature of a profile, it means that it is detected anomalous vectors.

Anomalies in the datasets are reflected in vector components which are irrelevant during the training. They are irrelevant because normal data have only 0 values in these components and these components do not contribute to model training, the final results are shown in Table X.

When it is run interference on a testing profile, the model does not use these components to isolate the profile faster.

As a result, the profile is labeled as normal by the model. Another reason for the poor results could be a mistake in the way it has been trained the isolation forest model. It will be investigated more closely this issue in the future.

VI. ANALYSIS OF RESULTS

The experiments proposed in our analysis try to find how the anomaly detection algorithms may work in a realistic setup where a normal user is infected at the same time that they continue to work. In this sense, this is new computer network testing work in the security area that publishes results using a mixed dataset of real normal actions and real malware actions.

Our experiments were designed, so they were trained with real users and tested with real malware. They were also designed to detect if a profile is anomalous and not the IP address of a user. Finally, the time-window of the profiles is five minutes, which also may affect the algorithm if changed.

Using the one class SVM, it was possible to obtain a good TPR of 44% with 0% FPR. Since these results are per five-minute profile, it means that the algorithm will, out of three anomalous profiles, detect one with 100% probability (or 2 out of 5). It also means that there will be a detection at most every 15 minutes. Moreover, these results are based on a majority voting mechanism, which is not considered to be the best way of improving the results.

In particular, there are some individual features that may have better results under specific circumstances. In the first experiment, six out of twelve features reach 100% TPR with 0% FPR. In the case of the Local Outlier Factor algorithm, the results are very similar, with an average of 33% TPR detection and 0% FPR using majority voting. This means that LOF can also detect one profile correctly out of three anomalous profiles with 100% probability. The detection time is similar to one-class SVM: one anomalous profile every 15 minutes. If the detection of profiles is not done with majority voting, then LOF can reach 77.8% TPR with 2% FPR by using the feature called `Client_DestinationPort_TotalBytes_TCPEstablished`.

LOF also had very good results on the third experiment that used the first dataset. In this case the algorithm can have a 100% TPR, but only at the expense of a 2% FPR. The good part was that these results were obtained with three different features:

`client_DestinationPort_NumberOfFlows_TCP_NotEstablished`  
`client_DestinationPort_TotalBytes_TCP_NotEstablished`,  
`client_DestinationPort_TotalPackets_TCP_NotEstablished`.

The LOF algorithm also had good results on the fourth experiment, which used the second dataset. In this case, the algorithm achieved 47.2% TPR with a 1.1% FPR.

These results were obtained also with the feature `Client_DestinationPort_TotalBytes_TCP_Established`.

In the fourth experiment, with LOF on the third dataset, the algorithm obtained a very good 94.8% TPR with 0% FPR with the feature `client_DestinationPort_TotalPackets_TCP_Established`.

## VII. CONCLUSIONS

The detection of attacks and malware using anomaly detection techniques is a very well-known topic in the area of artificial intelligence and machine learning. This study proposes a new perspective on the problem by analyzing the behavioral features of users in the network and by applying a high-level detection on features in time. By using a completely novel dataset and known anomaly detection methods, promising results can be obtained.

To the best of our knowledge, this research work presented the new anomaly detection method where users were profiled using their network traffic to create behavioral features, and these features were analyzed from different perspectives. The

presented anomaly detection method was based on high-level view of the global network traffic by generating behavioral profiles of the activity of the users inside fixed time-windows. The new profiles of the users were compared to the past profiles to classify them as anomalous or normal. Our approach is different from other anomaly detection algorithms because the model user behavior by combining detailed features that describe all actions of the user from different perspectives.

It is classified profiles by comparing each feature with the same feature in other past profiles. The decision on whether there was an anomaly or not was taken for each feature and then the final label of the profile was decided by majority of voting. The anomalies along with each feature were found using well known algorithm local outlier factor (LOF) and one class Support Vector Machine (one class-SVM).

To evaluate our approach it is needed the data from real normal users and the data from real network traffic infection. The produced datasets were unique because they contain real malware activities at the same time that the real normal user was using the computer. The datasets were made open to the public and feature research.

The datasets were used to test and evaluate how our approach would detect different types of malware. The multiple experiments show that our approach could help in reducing the number of false positive alarms while at the same time being effective in detecting true anomalies. In multiple experiments, it is possible to detect one out of three anomalous profiles with 99% success, and it had 0% false alarms.

Even though the results are satisfactory, there is much research to be done. One of the problems which want to be worked in the future is to solve how to combine twelve different results in order to get the final decision. It would like to be to experiment with training another model which would accept the output of the twelve models described in this work and give the final decision. If it is provided enough data during the training, it may be possible that such a model could help find some non-oblivious relationship between data.

Also, our approach lacks the very important process of updating the model of normal behavior in order to adopt to new network traffic. Since the behavior of user might change with time by time, it is needed to find a way how to keep our models up-to-date. For this, it is needed to create large datasets which would cover an extended period in different situations.

## VIII. FUTURE DIRECTIONS

A very promising research direction it may be worked on the usage of anomaly detection methods in to the Internet of Things (IOT) devices and scheduling based on mobile edge computing [50,51] such as: IP cameras, thermostats, printers mobile users, mobile devices and multiple base stations etc. The number of attacks on IOT devices is growing as well as the amount of malware designed to target these IOT devices. Our approach could be useful in protecting IOT devices because the traffic from these devices is far more stable than a human computer, and therefore it changes less diversity, and the results from an anomaly detection method may be easier to obtain.

#### ACKNOWLEDGMENT

This paper is supported by National Natural Science Foundation (NSFC) of China under grant numbers 61572095, 61877007 and 61802097. Conflicts of Interest: The authors declare no conflict of interest.

#### REFERENCES

- [1] Xiao, F., Lin, Z., Sun, Y. and Ma, Y., 2019. Malware Detection Based on Deep Learning of Behavior Graphs. *Mathematical Problems in Engineering*, 2019.
- [2] Pandey, S.K., 2019. Design and performance analysis of various feature selection methods for anomaly-based techniques in intrusion detection system. *Security and Privacy*, 2(1), p.e56.
- [3] Koning, R., Buraglio, N., de Laat, C. and Grosso, P., 2018. CoreFlow: Enriching Bro security events using network traffic monitoring data. *Future Generation Computer Systems*, 79, pp.235-242.
- [4] Wang, W., Zhang, X., Gombault, S. and Knapskog, S.J., 2009, December. Attribute normalization in network intrusion detection. In *2009 10th International Symposium on Pervasive Systems, Algorithms, and Networks* (pp. 448-453). IEEE.
- [5] Chandola, Varun, Arindam Banerjee, and Vipin Kumar. "Anomaly detection: A survey." *ACM computing surveys (CSUR)* 41, no. 3 (2009): 15.
- [6] Tahir, M., Li, M., Ayoub, N. and Aamir, M., 2019. Efficacy Improvement of Anomaly Detection by using Intelligence Sharing Scheme. *Applied Sciences*, 9(3), p.364.
- [7] Patcha, A. and Park, J.M., 2007. An overview of anomaly detection techniques: Existing solutions and latest technological trends. *Computer networks*, 51(12), pp.3448-3470.
- [8] Ertoz, L., Eilertson, E., Lazarevic, A., Tan, P.N., Kumar, V., Srivastava, J. and Dokas, P., 2004. Minds-minnesota intrusion detection system. *Next generation data mining*, pp.199-218.
- [9] Breunig, M.M., Kriegel, H.P., Ng, R.T. and Sander, J., 2000, May. LOF: identifying density-based local outliers. In *ACM sigmod record* (Vol. 29, No. 2, pp. 93-104). ACM.
- [10] Ertoz, L., Lazarevic, A., Eilertson, E., Tan, P.N., Dokas, P., Kumar, V. and Srivastava, J., 2003, July. Protecting against cyber threats in networked information systems. In *Battlespace Digitization and Network-Centric Systems III* (Vol. 5101, pp. 51-57). International Society for Optics and Photonics.
- [11] Hubballi, N. and Suryanarayanan, V., 2014. False alarm minimization techniques in signature-based intrusion detection systems: A survey. *Computer Communications*, 49, pp.1-17.
- [12] Zhang, M., Xu, B. and Gong, J., 2015, December. An anomaly detection model based on one-class svm to detect network intrusions. In *2015 11th International Conference on Mobile Ad-hoc and Sensor Networks (MSN)* (pp. 102-107). IEEE.
- [13] Xu, K., Zhang, Z.L. and Bhattacharyya, S., 2005. Reducing Unwanted Traffic in a Backbone Network. *SRUTI*, 5, pp.9-15.
- [14] Mahoney, M.V., 2003, March. Network traffic anomaly detection based on packet bytes. In *Proceedings of the 2003 ACM symposium on Applied computing* (pp. 346-350). ACM.
- [15] Siraj, S., Gupta, A. and Badgajar, R., 2012. Network simulation tools survey. *International Journal of Advanced Research in Computer and Communication Engineering*, 1(4), pp.199-206.
- [16] Pannell, G. and Ashman, H., 2010. Anomaly detection over user profiles for intrusion detection.
- [17] Benevenuto, F., Rodrigues, T., Cha, M. and Almeida, V., 2009, November. Characterizing user behavior in online social networks. In *Proceedings of the 9th ACM SIGCOMM conference on Internet measurement* (pp. 49-62). ACM.
- [18] Wagner, C., Mitter, S., Körner, C. and Strohmaier, M., 2012, April. When Social Bots Attack: Modeling Susceptibility of Users in Online Social Networks. In *# MSM* (pp. 41-48).
- [19] NetFlow, C.I., 2006. Introduction to cisco ios netflow a technical overview. White Paper, Last updated: February. (accessed on 19 May 2019).
- [20] Botros, S.M., Diep, T.A. and Izenson, M.D., Visa International Service Association, 2013. Synthesis of anomalous data to create artificial feature sets and use of same in computer network intrusion detection systems. U.S. Patent 8,527,776.
- [21] Veres, G. and Loop, S., Exinda Networks Pty Ltd, 2019. Method and system for triggering augmented data collection on a network based on traffic patterns. U.S. Patent Application 10/193,808.
- [22] Chandrasekaran, B., Srinivas, A. and Zafer, M., NYANSA Inc, 2019. System and method for using real-time packet data to detect and manage network issues. U.S. Patent Application 10/230,609.
- [23] Moustafa, N., Hu, J. and Slay, J., 2019. A holistic review of Network Anomaly Detection Systems: A comprehensive survey. *Journal of Network and Computer Applications*, 128, pp.33-55.
- [24] Postel, J., 1981. Transmission control protocol (No. RFC 793).
- [25] Pearson, K., 1901. Principal components analysis. *The London, Edinburgh, and Dublin Philosophical Magazine and Journal of Science*, 6(2), p.559.
- [26] Sipola, T., Juvonen, A. and Lehtonen, J., 2012. Dimensionality reduction framework for detecting anomalies from network logs. *Engineering Intelligent Systems*, 20(1/2).
- [27] Huang, T., Sethu, H. and Kandasamy, N., 2016. A new approach to dimensionality reduction for anomaly detection in data traffic. *IEEE Transactions on Network and Service Management*, 13(3), pp.651-665.
- [28] Dreiseitl, S., Osl, M., Scheibböck, C. and Binder, M., 2010. Outlier detection with one-class SVMs: an application to melanoma prognosis. In *AMIA Annual Symposium Proceedings* (Vol. 2010, p. 172). American Medical Informatics Association.
- [29] Liu, F.T., Ting, K.M. and Zhou, Z.H., 2008, December. Isolation forest. In *2008 Eighth IEEE International Conference on Data Mining* (pp. 413-422). IEEE.
- [30] Hawkins, D.M., 1980. Identification of outliers (Vol. 11). London: Chapman and Hall.
- [31] Breunig, M.M., Kriegel, H.P., Ng, R.T. and Sander, J., 1999, September. Optics-of: Identifying local outliers. In *European Conference on Principles of Data Mining and Knowledge Discovery* (pp. 262-270). Springer, Berlin, Heidelberg.
- [32] Han, J., Pei, J. and Kamber, M., 2011. *Data mining: concepts and techniques*. Elsevier.
- [33] Singla, M.H.S.C.S. and Shen, Y., Kernel Selection and Dimensionality Reduction in SVM Classification of Autism Spectrum Disorders.
- [34] James, G., Witten, D., Hastie, T. and Tibshirani, R., 2013. An introduction to statistical learning (Vol. 112, p. 18). New York: springer.
- [35] Haria, S., 2019. The growth of the hide and seek botnet. *Network Security*, 2019(3), pp.14-17.
- [36] Xiong, H., Malhotra, P., Stefan, D., Wu, C. and Yao, D., 2009, December. User-assisted host-based detection of outbound malware traffic. In *International Conference on Information and Communications Security* (pp. 293-307). Springer, Berlin, Heidelberg.
- [37] Cabaj, K., Gawkowski, P., Grochowski, K. and Osojca, D., 2015. Network activity analysis of CryptoWall ransomware. *Przegląd Elektrotechniczny*, 91(11), pp.201-204.
- [38] Ken, F.Y. and Harang, R.E., 2017, October. Machine learning in malware traffic classifications. In *MILCOM 2017-2017 IEEE Military Communications Conference (MILCOM)* (pp. 6-10). IEEE.
- [39] Awad, Y., Nassar, M. and Safa, H., 2018, May. Modeling Malware as a Language. In *2018 IEEE International Conference on Communications (ICC)* (pp. 1-6). IEEE.
- [40] Smith, Z.M., 2016. Building an Adaptive Cyber Strategy. Air Command and Staff College, Air University Maxwell Air Force base united States.
- [41] Fu, Y., 2017. using botnet technologies to counteract network traffic analysis.
- [42] Tahir, M., Li, M., Ayoub, N., Shehzaib, U. and Wagan, A., 2018. A Novel DDoS Floods Detection and Testing Approaches for Network Traffic based on Linux Techniques. *Int. J. Adv. Comput. Sci. Appl.*, 9, pp.341-357.
- [43] Tahir, M., Li, M., Shaikh, A.A. and Aamir, M., 2017. The Novelty of A-Web based Adaptive Data-Driven Networks (DDN) Management &

- Cooperative Communities on the Internet Technology. *Int. J. Adv. Comput. Sci. Appl*, 8, pp.16-24.
- [44] Bergstra, J., Yamins, D. and Cox, D.D., 2013. Hyperopt: A python library for optimizing the hyperparameters of machine learning algorithms. In *Proceedings of the 12th Python in science conference* (pp. 13-20).
- [45] Komer, B., Bergstra, J. and Eliasmith, C., 2014. Hyperopt-sklearn: automatic hyperparameter configuration for scikit-learn. In *ICML workshop on AutoML* (pp. 2825-2830).
- [46] Raschka, S., 2015. *Python machine learning*. Packt Publishing Ltd.
- [47] Damshenas, Mohsen, et al. "A survey on malware propagation, analysis, and detection." *International Journal of Cyber-Security and Digital Forensics*, vol. 2, no. 4, 2013, p. 10+. Academic OneFile, (Accessed 19 May 2019).
- [48] Liu, F.T., Ting, K.M. and Zhou, Z.H., 2010, September. On detecting clustered anomalies using SCiForest. In *Joint European Conference on Machine Learning and Knowledge Discovery in Databases* (pp. 274-290). Springer, Berlin, Heidelberg.
- [49] Emmott, A., Das, S., Dietterich, T., Fern, A. and Wong, W.K., 2015. A meta-analysis of the anomaly detection problem. arXiv preprint arXiv:1503.01158.
- [50] Naeem, M.R., Khan, M.U., Shaikh, M.T., Altaf, M., Rana, S.M. and Iqbal, M.M., 2016. Smart Network Communication Using Secure And Smart Internet of things and Fog Computing. *Science International*, 28(4).
- [51] Zheng, X., Li, M., Tahir, M., Chen, Y. and Alam, M., 2019. Stochastic Computation Offloading and Scheduling Based on Mobile Edge Computing. *IEEE Access*.

# Experimental Analysis of Color Image Scrambling in the Spatial Domain and Transform Domain

R. Rama Kishore<sup>1</sup>, Sunesh<sup>2</sup>

USICT, Guru Gobind Singh Indraprastha University, New Delhi, India<sup>1,2</sup>

Research scholar and Department of information Technology, MSIT, New Delhi, India<sup>2</sup>

**Abstract**—This paper proposes two image-scrambling algorithms based on self-generated keys. First color image scrambling method works in the spatial domain, and second, works in the transform domain. The proposed methods cull the R, G, and B plane from the color image and scramble each plane separately by utilizing the self-generated keys. The keenness of security of proposed methods is the keys or parameters used in the scrambling process. The exploratory outcomes show that both proposed image scrambling technique performs well in terms of Number of pixel change rate (NPCR), Normalized correlation (NC), Entropy, and time consumed in encoding and decoding. The adequacy of the proposed framework has demonstrated on a data set of five images. In furtherance, the present paper gives a comparative performance analysis between proposed image scrambling methods of spatial domain and transform domain. The proposed paper also tosses some light on the scrambling work reported in the literature.

**Keywords**—Color image scrambling; pixel position modification; spatial domain; Red Green Blue (RGB); transform domain

## I. INTRODUCTION

With the fast advancement of computer network technology, a large amount of image data had transmitted, quickly and safely over the system that raises different security concerns. For handling the security concern, initially, image encryption had drawn the attention. However, Image encryption is not the same as the content encryption because of some inborn highlights, for example, mass information limit and the great relationship among pixels. In this way, standard cryptographic procedures (DES, IDE, and RSA) are never appropriate for image encryption. Therefore, image scrambling comes out as a vital tool to deal with security concerns. Image scrambling is a technique that realigns all the pixels in an image to various positions to permuted an original image into a new image that is non-recognizable in appearance, confused, and unsystematic.

In literature, The researchers performed scrambling by deploying different concepts like chaos system Fibonacci series, Fibonacci p-code, ASCII code, M-succession, Random number generation, Random shuffling, perfect shuffling, R prime shuffle, and Sudoku puzzle. Many researchers implemented mainly the concept of chaos. The concept of chaos in image scrambling to achieve diffusion and confusion between image pixels in different ways [1]–[10]. Chaotic system map has many unique properties that classify into two

types, namely, 1-D and 2-D. The 1-D chaotic map guide contains a logistic map, Sine map, and tent map. The 2-D chaotic map consists of Arnold, Henon map, and Lorenz system. Background section throws light on the work reported in history.

The Image scrambling methods can be categorized by different ways like based on methodology, based on the domain, based on the type of image. The image scrambling classification is represented by Fig. 1.

Mainly, Image scrambling process uses two types of methodology to accomplish scrambling. One is position shuffling, and other is pixel value modification. The realignment of the pixels is known as pixel position shuffling. Pixel value modification modifies the value of a pixel to achieve image scrambling. Sometimes, the researcher performed pixel value modification alongside pixel position shuffling to improve security. Based on the domain, Image scrambling is classified into two types, termed as spatial domain and transform domain. Image Scrambling in the spatial domain performs scrambling directly on pixels or pixel coordinate. On the other hand, Transform domain scheme performs scrambling by modulating coefficients of the image in the frequency or transform domain [11], [12]. Based on the image type, Image scrambling may be partitioned into two types like grayscale image, color image. In the history, researchers majorly presented various image-scrambling algorithms in the spatial domain for grayscale images in comparison to the transform domain.

In the case of color image scrambling, few researchers reported scrambling algorithm either in the spatial domain or in transform domain. In the last few years, some color image scrambling algorithms in transform domain has been reported. The reported methods carry good efficiency but increased complexity. So, the present paper proposes two color image scrambling methods, one is in spatial domain and second is in transform domain that maintains the efficiency as well as complexity. Both the color image scrambling methods utilizes the concept of self-generated keys. The keys or parameters engaged in scrambling process establish the security of proposed method. Two keys or parameters are adopted by color image scrambling methods. One is self-generated keys that perform scrambling process and second parameter or key controls the complexity of the proposed algorithm. The value of the second parameter may vary; it may be increased or decreased depending upon the requirement.

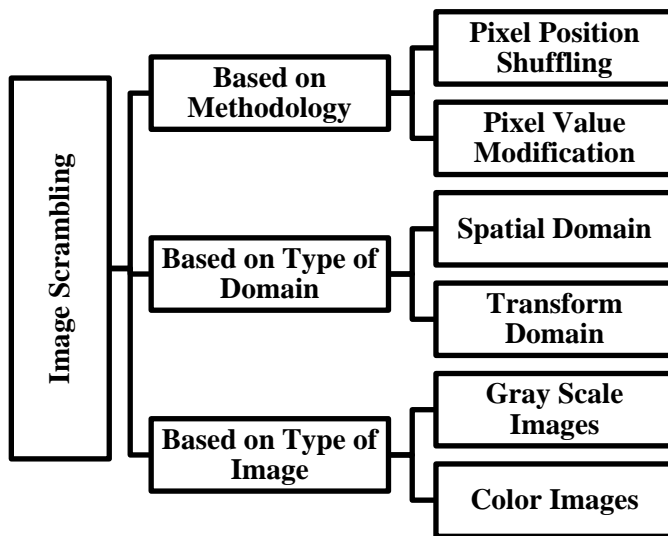


Fig. 1. Classification of Digital Image Scrambling.

Whatever remains of the present paper is sorted out as pursues: Section 2 audits the image scrambling methods reported in the literature. Section 3 presents the proposed color image scrambling in the spatial domain. The proposed color image scrambling algorithm in the transform domain is represented by section 4. Section 5 illustrates the experimental analysis of both proposed methods. Section 6 discusses the Comparative analysis between both the proposed methods. Finally, Section 7 and Section 8 represent finishing comments and future scope respectively.

## II. RELATED WORK

The related work section reviews the work related to image scrambling reported in the literature. Majorly the concept of chaos system was exploited to attain diffusion and confusion between image pixels by different ways [1], [2], [13], [3]–[10].

Chaos-based image scrambling can be cultivated by rearranging pixel positions of the image [1], [2], [6], [9]. In this, Yu et al. proposed an image scrambling system that incorporates S-DES with Logistic map [1]. Here, image scrambling exploits the Sensitivity of initial value and randomness trait of the chaotic map that makes a system with larger key quantities. The idea of simplified DES structure makes computing speed quicker. Though, Dong et al. [2] detailed another image scrambling technique which joins the concept of chaos theory with sorting transformation to improve the initial sensitivity of chaotic map. The strong irregularity trait of sorting information makes scrambling effective and secure. Prasad et al. [14] also presented an encryption scheme in which scrambling is achieved by exploiting randomness of chaos map (henon). Dong et al. proposed a color image scrambling that utilizes the inherent features of a chaotic sequence to transform pixel coordinates of RGB image. In 2014, deacons et al. [9] presented a color image encryption method by employing a chaotic map along with the knight's moving rule that transposes pixel between the RGB components. Numerous researchers likewise accomplished chaos-based image scrambling by changing

pixel value with position shuffling [5]–[7], [9], [10], [12], [13]. Yangling [3] proposed a scrambling algorithm dependent on chaos sequence and mirror mapping. The author employs the randomness, initial value, and parameter sensitivity traits and generates sequences of real values. Pixel value change is accomplished by playing out an Ex-OR operation between every pixel and real-valued chaotic sequence. Ye[6] exhibited another chaos and bit map based image encryption technique by exploiting pseudo-random property, system parameter, and sensitive dependence on initial conditions and un-periodicity of Chaos map. Position encryption is performed by chaos, and gray value alteration is performed by pixel bit.

Zang et al. [5] reported a bit plane scrambling algorithm with multiple chaotic systems. Arnold and logistic map both are deployed to rearrange the places of pixels in bit-plane. Along with position shuffling, the gray values of the image is also modified. Liu et al. [7] presented space bit plane operation SBPO and chaotic sequence based image encryption scheme, which simultaneously changes the pixel value besides with pixel positions. Based on a chaotic sequence, Author picks every eight pixels from the different segments of the image and form a group. SBPO is performed on each group and build eight pixels with different value. Liu [8] also proposed another image scrambling scheme based on the spatial bit-level map and chaotic sequence that rearranges the image pixels in to1-D logistic chaotic sequences and each pixel in the sequence is decomposed into k bits for forming a 2-D matrix. The pixel values are modified by applying a spatial bit map on the 2-D matrix. Wang et al. [10] proposed a digital image scrambling algorithm based on chaotic sequence and decomposition and recombination of pixel values. Through decomposition and recombination of pixels, the algorithm scrambles pixel positions and changes pixel values. Liehuang et al. [13]proposed a new cat chaotic mapping based digital image scrambling method for digital image watermarking. The concept of Cat chaotic mapping is utilized to disorder the pixel coordinates of the digital image. Pixel value modification is achieved by performing XOR operation between the certain pixel value of the disordered image and chaotic value.

Sang et al. [15] also reported a block scrambling scheme that by utilizing Arnold and logistic map both. Logistic map generates the sequence, and this sequence is further applied to different Arnold transformed blocks. Xiong et al. [12] proposed a new kind of scrambling transform named local negative base transform (LNBT). The proposed scrambling transform can shuffle the 2-D image with a good enough scrambling performance. Aside from chaos system, the other imperative ideas are used to accomplish encryption of pictures like the Fibonacci series, Fibonacci p-code, ASCII code, M-sequence, Random number generation, Random shuffling, perfect shuffling, R prime shuffle and Sudoku puzzle [11], [16]–[25]. In 2004, J. Zou et al. [19] proposed another digital image-scrambling plan with the idea of Fibonacci numbers that makes implementation straightforward with the low computational expense. In 2008, Yicong Zhou et al. [11] presented two image scrambling algorithms by using the idea of Fibonacci p-code that encodes grayscale and a color picture in spatial and transforms domain (DCT). On account of color



images, YCbCr color space is utilized, and each color segment is extracted at that point, and scrambling is performed on each color segment independently. In this proposed algorithm,  $p$  is taken as a security key to perform scrambling. The proposed technique is a lossless plan that can be utilized for real-life applications. In 2007, Guodong Ye et al. [20] introduced a simple double image scrambling algorithm by exploiting the concept of ASCII code that implements position and pixel value encoding both. In this method, traditional mathematics knowledge is combined with a binary number of computer languages. Decoding of the image is done only when precise keys are known.

Yang Zou et al. [24] presented a Sudoku puzzle based novel image scrambling image algorithm that scrambles the original image both at the pixel and bit level by giving good security. This algorithm uses the property of  $N \times N$  Sudoku puzzle in which every number from 1 to  $N$  appear only once and maintains the one to one relationship between two Sudoku puzzle. These two Sudoku puzzles are exploited to delineate the original image to a scrambled one. In 2014, H.B. Kekre et al. [26] presented a digital image scrambling method by using qualities of related prime shuffle to give high security. The proposed algorithm is actualized on a block level by partitioning a picture into various blocks. Different  $R$ . prime number is used to shuffle row and column of the block. Combination of all  $r$ -prime numbers used in block level scrambling is used as a security key to decode the key. Kekre et al. [23] presented an analysis of perfect shuffling characteristics like the downsampling effect, the number of iteration required to get back the original image.

In 2008, [27] proposed a new image scrambling method based on parametric  $M$ -sequence.  $M$ -sequences are generated by utilizing a series of shift registers that makes decoding of images difficult without knowing the keys. In 2015, M.M. Aziz et al. [21] reported a simple image scrambling algorithm for grayscale images by utilizing traits of random number generation. In this scrambling is achieved by shuffling pixel position without modifying pixel value. In furtherance, Waghulde et al. also throw light on image scrambling methods based on  $r$ -prime shuffle, Arnold transformation, and random number generation [28]. In 2008, S.Z. Qin et al. [22] presented a random shuffling based scrambling algorithm that can perform scrambling on the non-equilateral image. The proposed method utilizes the concept of random shuffling to accomplish scrambling by shifting the pixel position of the image.

By inspiring from the above scrambling method, the present paper proposes two secure and efficient color image scrambling methods. One performs in the spatial domain and second performs in the transform domain. Section3 and section4 represent both algorithms, respectively.

### III. PROPOSED COLOR IMAGE SCRAMBLING METHOD IN SPATIAL DOMAIN

In this section, the first color image scrambling method that works in the spatial domain is presented. The proposed image scrambling methods contains two algorithms; one is the scrambling algorithm, and the other is unscrambling algorithm in the spatial domain.

#### A. Scrambling Algorithm in Spatial Domain

Step1. Input: Read color image of size  $M \times N$ .

Step2. Keys:  $S_f$ ,  $X(i)$ ,  $Y(j)$ .

Step3. Split the input color image into three planes, namely  $R$ ,  $G$ , and  $B$ .

Step4. Convert each plane into 1-D vector separately. Size of each plane should be equal to  $M \times N$ .

Step5. Keys are generating by using the following rule:

a)  $S_f = (M \times N) / 2$ ;

b) The key  $X(i)$  is generated by utilizing the mentioned below lines

For  $i = S_f : K$

$X(i) = X(S_f + i)$ ;

c) The key  $Y(j)$  is generated by utilizing the mentioned below lines

For  $j = S_f : 1$

$Y(j) = X(S_f - j)$ ;

In this,  $i$  and  $j$  refer to the elements.

Step6. These keys are utilized to obtain  $P(i)$  and  $Q(j)$  sequence, which storing values of  $X$  and  $Y$ , respectively.

Step7. Sequence  $P$  and  $Q$  are applied on each component  $R$ ,  $G$ , and  $B$  separately. Sequence  $P$  and  $Q$  extracts the corresponding Pixel coordinates. The value of  $S_f$  is also stored for performing scrambling.

Step8. The process of scrambling is performed by forming a new 1-D vector named as a shuffled vector. The value at  $S_f$  pixel coordinate is kept at the first position of the shuffled vector. Then, the extracted  $P$  sequence is put up at even locations of the shuffled vector, and the value of the extracted  $Q$  sequence is stored at odd positions of the shuffled vector. This entire process is applied to each Component  $R$ ,  $G$ , and  $B$  Separately and repeated  $Z$  times.  $Z$  is key or parameter which varies depending upon requirements and controls the efficiency and security of the proposed method.

Step9. Generate scrambled  $R$ ,  $G$ , and  $B$  component and concatenate  $R$ ,  $G$ , and  $B$  component together.

Step10. Produce the scrambled color Image.

#### B. Unscrambling Algorithm in Spatial Domain

The proposed color image unscrambling method retrieves the original image from the scrambled image and follows the reverse steps of scrambling. The unscrambling algorithm in the spatial domain is below in the form steps:

Step1. Read the scrambled image

Step2. Split the scrambled image into three planes  $R$ ,  $G$ , and  $B$ .

Step3. Generate three keys, as described in the scrambling algorithm.

Step4. Generate  $P$  and  $Q$  sequences corresponding to each plane  $R$ ,  $G$ , and  $B$ .

Step5. Perform the reverse shuffling for each R, G, and B component. Moreover, repeat the entire shuffling process two times to attain original R, G, and B component.

Step6. Concatenate the extracted R, G, and B plane and generate the original color image.

#### IV. PROPOSED COLOR IMAGE SCRAMBLING METHOD IN TRANSFORM DOMAIN

This section presents the second color image-scrambling method, which performs in the transform domain. In this method, host image is pre-processed by transforming an original color image in discrete cosine transform (DCT) frequencies. Here, section A describes the scrambling process of algorithm in transform domain. On other hand, section B presents the unscrambling process of the proposed method.

##### A. Scrambling Algorithm in Transform Domain

Step1. Input: Read color image I of size M x N.

Step2. Keys:  $Sf_D$ ,  $X_D(i)$ ,  $Y_D(j)$ .

Step3. Partition the input image I into three planes, namely R, G, and B.

Step4. Divide each plane R, G, B into the non-overlapping blocks of size 8x8 and then transform into the discrete transform frequencies.

Step4. Convert the transformed  $R_T$ ,  $G_T$ ,  $B_T$  planes into 1-D vectors. Size of each transformed plane should be equal to M x N.

Step5. Keys are constructed by using the below-mentioned rules:

a)  $Sf_D = (M \times N) / 2$ ;

b) The key  $X_D(i)$  is generated by utilizing the mentioned below lines

For  $i = Sf_D : K$

$X_D(i) = X(Sf_D + i)$ ;

c) The key  $Y_D(j)$  is generated by utilizing the mentioned below lines

For  $j = Sf_D : 1$

$Y_D(j) = X(Sf_D - j)$ ;

In this, i and j refer to the elements.

Step6. Procure the sequence  $P_D(i)$  and  $Q_D(j)$  by utilizing the values of  $Sf_D$ ,  $X_D(i)$ ,  $Y_D(j)$  keys.

Step7. Apply Sequence  $P_D$  and  $Q_D$  to transformed planes  $R_T$ ,  $G_T$ , and  $B_T$ . Sequence  $P_D$  and  $Q_D$  extracts the corresponding Pixel coordinates. The value of  $Sf_D$  is also stored for performing scrambling.

Step8. The process of scrambling is performed by forming a new 1-D vector named as a shuffled vector. The value at  $Sf_D$  pixel coordinate is kept at the first position of the shuffled vector. Then, the extracted  $P_D$  sequence is put up at even locations of the shuffled vector, and the value of the extracted  $Q_D$  sequence is stored at odd positions of the shuffled vector. This entire process is applied to  $R_T$ ,  $G_T$ , and  $B_T$  planes and repeated  $Z_t$  times. The key  $Z_t$  controls the security, complexity of the proposed method.

Step9. Generate scrambled R, G, and B planes and concatenate R, G, and B planes together to produce the scrambled image.

Step10. Display the scrambled image.

##### B. Unscrambling Algorithm in Transform Domain

The color image unscrambling algorithm just follows the reverse steps of the scrambling algorithm. The proposed unscrambling algorithm is explained in the mentioned below steps:

Step1. Read the scrambled image

Step2. Split the scrambled image into three planes R, G, and B.

Step3. Divide each plane R, G, and B into blocks and apply transform on each plane.

Step4. Generate three keys as described in the scrambling algorithm.

Step5. Generate the  $P_D$  and  $Q_D$  sequences by utilizing the keys.

Step6. Perform the reverse shuffling on the transformed  $R_T$ ,  $G_T$ , and  $B_T$  planes. Moreover, repeat the entire shuffling process  $Z_t$  times to attain original R, G and B planes.

Step7. Concatenate the extracted R, G, and B planes and produce the original color image.

Step8. Display the unscrambled image.


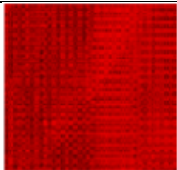
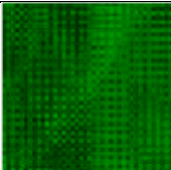
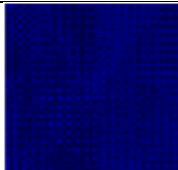



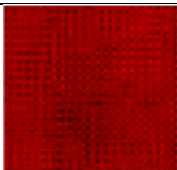
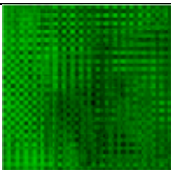
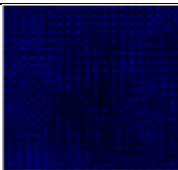
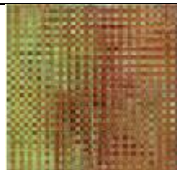


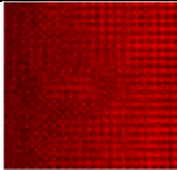
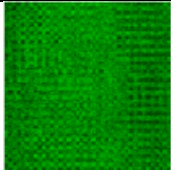
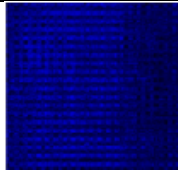



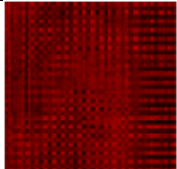
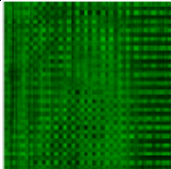
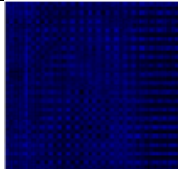



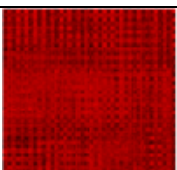
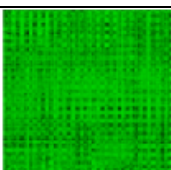
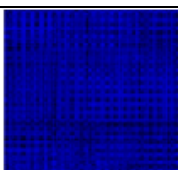


#### V. EXPERIMENTAL RESULT ANALYSIS

The performance of presented algorithms is demonstrated through five different measures such as Bit Error Rate (BER), Number of Pixels Change Rate (NPCR), Entropy, Normalized correlation (NC) and Time consumed in scrambling and unscrambling. Both, the proposed scrambling algorithms are implemented on five images, namely; Lena, Peppers, Baboon, Tiger, and House. Experiments were conducted on MATLAB 2015, a platform with core i5 processor, 4GB RAM. The experimental result section consists of two subsections. The first subsection represents the performance analysis of the proposed scrambling method in the spatial domain. The performance analysis of the second proposed scrambling method in transform domain is illustrated by subsection B.

##### A. Performance Analysis of Proposed Scrambling Method in Spatial Domain

Initially, the proposed image scrambling method in the spatial domain is evaluated in the form of visual quality, NPCR, BER, Entropy, and NC. The objective of visual scrutinize is to accentuate the visual similarities between the original image and its scrambled image. Table I shows the visual analysis of the proposed image scrambling method in the spatial domain. Table I exhibits original image, scrambled planes (red, green and blue), scrambled and unscrambled looks of Lena, Peppers, Baboon, Tiger and House images respectively. By inferring the Table I, it is concluded that there is no perceptual analogy between scrambled and original image.

TABLE. I. VISUALIZATION OF ORIGINAL, SCRAMBLED PLANES, SCRAMBLED IMAGE AND UNSCRAMBLED IMAGE OF PROPOSED METHOD IN SPATIAL DOMAIN ON LENA, PEPPERS, BABOON, TIGER AND HOUSE IMAGE.

| Original Image   | Scrambled Plane   |   |  | Scrambled Image   | Unscrambled Image   |
|--|---|---|--|---|---|
|  | Red Plane   | Green Plane   | Blue Plane   |   |   |
| <br>Lena    |    |    |    |    |    |
| <br>Peppers |    |    |    |    |    |
| <br>Baboon  |    |    |    |    |    |
| <br>Tiger  |   |   |   |   |   |
| <br>House |  |  |  |  |  |

Apart from visual quality analysis, the proposed scrambling method has assessed on some other qualitative parameters that are narrated in Table II and Table III. Table II demonstrates the Number of Pixels Change Rate (NPCR), Bit Error Rate (BER) and Entropy for images Lena, Peppers, Baboon, Tiger, and House.

The parameter NPCR unfolds the strength of image scrambling scheme. Baboon image attains the 99.449 value for NPCR. The proposed watermarking method uses the concept of position shuffling so, the value of UACI indicator comes zero. The proposed method also attains high entropy value in the spatial domain.

For the proposed color image-scrambling scheme, the correlation has been inspected in the two ways. One is on the individual planes (Red, Blue and Green), and other is on the entire image. In both cases, the proposed image scrambling method achieves a high correlation between the original image and the unscrambled image.

Table III delineates the normalized cross-correlation of the red plane, blue plane and green plane of the image individually and combined (all planes) image for Lena, Peppers, Baboon, Tiger, and House images. Time taken in the process of scrambling and unscrambling is also guarded, and Table III depicts the time taken during the scrambling and unscrambling process in seconds.

TABLE. II. NPCR, BER, ENTROPY VALUES OF THE PROPOSED METHOD IN SPATIAL DOMAIN ON LENA, PEPPERS, BABOON, TIGER AND HOUSE

| Image   | NPCR    | BER | Entropy |
|---------|---------|-----|---------|
| Lena    | 99.2443 | 0   | 7.7749  |
| Peppers | 99.3315 | 0   | 7.756   |
| Baboon  | 99.449  | 0   | 7.7624  |
| Tiger   | 99.3993 | 0   | 7.7159  |
| House   | 99.2704 | 0   | 7.4858  |

TABLE III. NC AND TIME CONSUMED IN SCRAMBLING AND UNSCRAMBLING PROCESS OF PROPOSED METHOD IN SPATIAL DOMAIN ON LENA, PEPPERS, BABOON, TIGER AND HOUSE IMAGE

| Image   | NCR | NCG | NCB | NC | Time hold for scrambling and unscrambling (in Sec) |
|---------|-----|-----|-----|----|--|
| Lena    | 1   | 1   | 1   | 1  | 2.26   |
| Peppers | 1   | 1   | 1   | 1  | 2.23   |
| Baboon  | 1   | 1   | 1   | 1  | 2.35   |
| Tiger   | 1   | 1   | 1   | 1  | 2.38   |
| House   | 1   | 1   | 1   | 1  | 2.28   |

The complexity of the proposed can be estimated by looking on the time hold for scrambling and unscrambling. It may be inferred from Table II, Table III, and Table IV that

proposed scrambling method in spatial domain performs excellently on all the performance evaluation parameters.

*B. Performance Analysis of Proposed Method in Transform Domain*

After analyzing the performance of the proposed method in the spatial domain, the second proposed image-scrambling scheme in the transform domain is examined. In the transform domain, proposed method substantiated on visual quality, Number of Pixels Change Rate (NPCR), Bit Error Rate (BER), Entropy, and Normalized correlation. Table IV illustrates the visual quality of the original image, scrambled red plane, scrambled green plane, and scrambled blue plane, scrambled and unscrambled form Lena, Peppers, Baboon, Tiger, and House images. From Table IV, it may be derived that there is no perceptual similarity between the original and unscrambled image in the transform domain.

TABLE IV. VISUALIZATION OF ORIGINAL, SCRAMBLED PLANES, SCRAMBLED IMAGE AND UNSCRAMBLD IMAGE OF THE PROPOSED METHOD IN TRANSFORM DOMAIN ON LENA, PEPPERS, BABOON, TIGER AND HOUSE IMAGE.


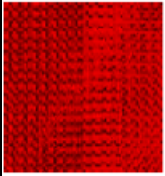
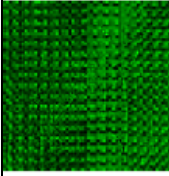
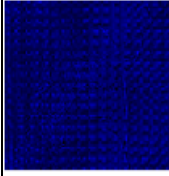



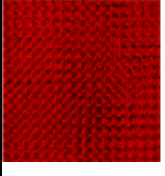
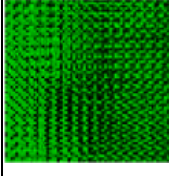
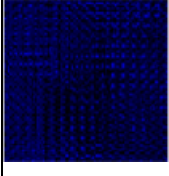
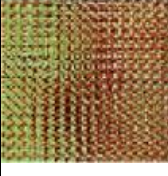


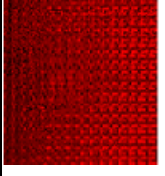
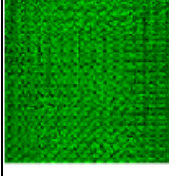
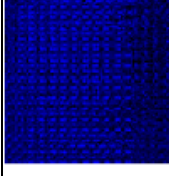



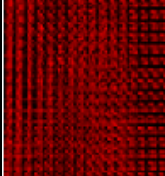
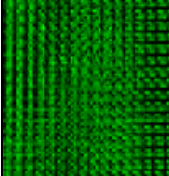
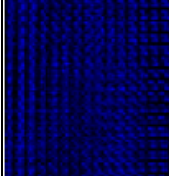



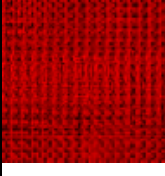
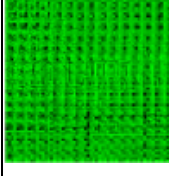
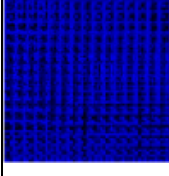


| Original Image   | Scrambled Plane   |   |   | Scrambled Image   | Unscrambled Image   |
|--|---|---|---|---|---|
|  | Red Plane   | Green Plane   | Blue Plane  |   |   |
| <br>Lena     |   |   |   |   |   |
| <br>Peppers |  |  |  |  |  |
| <br>Baboon  |  |  |  |  |  |
| <br>Tiger   |  |  |  |  |  |
| <br>House   |  |  |  |  |  |

TABLE V. NPCR, BER, ENTROPY VALUES OF THE PROPOSED METHOD IN THE TRANSFORM DOMAIN ON LENA, PEPPERS, BABOON, TIGER AND HOUSE

| Image   | NPCR    | BER  | Entropy |
|---------|---------|------|---------|
| Lena    | 99.1665 | 0.14 | 7.78    |
| Peppers | 99.1041 | 0.23 | 7.79    |
| Baboon  | 99.2845 | 0.35 | 7.71    |
| Tiger   | 99.3458 | 0.29 | 7.69    |
| House   | 99.1922 | 0.27 | 7.64    |

TABLE VI. NC AND TIME CONSUMED IN SCRAMBLING AND UNSCRAMBLING PROCESS OF THE PROPOSED METHOD IN TRANSFORM DOMAIN ON LENA, PEPPERS, BABOON, TIGER AND HOUSE IMAGE

| Image   | NCR    | NCG    | NCB    | NC     | Time hold in scrambling and unscrambling in Sec |
|---------|--------|--------|--------|--------|---|
| Lena    | 0.9998 | 0.9995 | 1      | 0.9998 | 39.82   |
| Peppers | 1      | 0.9991 | 0.9986 | 0.9992 | 32.69   |
| Baboon  | 0.9993 | 0.9998 | 0.9987 | 0.9993 | 48.89   |
| Tiger   | 0.9996 | 0.9995 | 0.9992 | 0.9994 | 32.50   |
| House   | 0.9998 | 0.9997 | 0.9994 | 0.9996 | 39.76   |

The other performance evaluation indicators Number of Pixels Change Rate (NPCR), Bit Error Rate (BER), and Entropy are demonstrated in Table V. Table VI manifested that proposed color image scrambling method possesses good NPCR and excellent entropy value on all the test images.

In the transform domain, the proposed scheme is also executed for Normalized correlation and found values very close to 1. This again proves that the proposed scheme has good correlation value between the original image and unscrambled image. Table VI delineates the normalized cross-correlation of combined image and the all the three planes of image(R, G and B) individually, and the combined image for Lena, Peppers, Baboon, Tiger, and House. Table VI also depicts the time taken during the scrambling and unscrambling process in seconds.

From Table IV, Table V, and Table VI, it may be concluded that the second proposed color image scrambling method in the transform domain performs well enough on all the evaluation parameters.

## VI. COMPARATIVE ANALYSIS AND DISCUSSIONS

This section compares the performance of both, proposed color image scrambling methods through four different parameters like visual quality, NPCR, Entropy and NC.

### A. Visual Quality Analyses

Table I and Table IV illustrate the visual quality of the proposed color image scrambling scheme in spatial and transform domain, respectively. It can be deduced from Table I and Table IV that proposed color image scrambling algorithms have no perceptual similarity between the original image and scrambled image, and possess good visual quality in spatial as well as in transform domain on all tested images. From this fact, it may conclude that the proposed color image-scrambling algorithm has good visual quality.

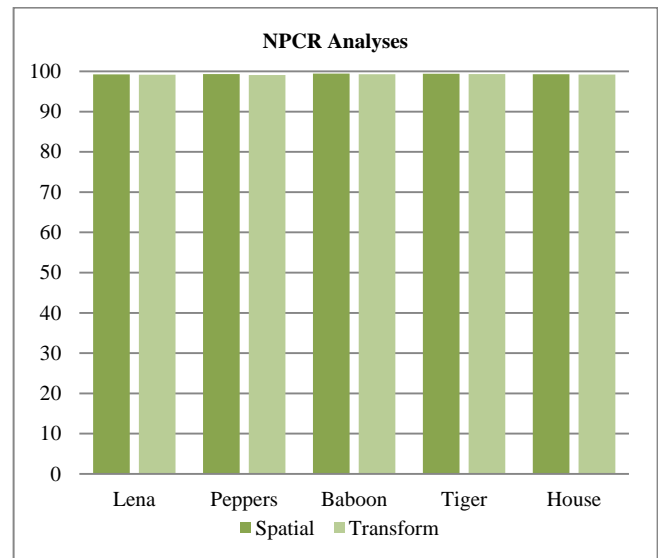


Fig. 2. Comparative Analyses of NPCR in Spatial and Transform domain on Lena, Peppers, Baboon, Tiger, and House Images.

### B. NPCR Analyses

NPCR defines Number of Pixels Change Rate that determines the strength of the image scrambling algorithm. Fig. 2 exemplifies the comparative NPCR analyses of the proposed method for the spatial and the transform domain on Lena, Peppers, Baboon, Tiger, and House images. From Fig. 2, it can identify that the proposed scrambling method has comparable NPCR values for both domains. Comparatively, proposed color image scrambling method attains better value in the spatial domain in comparison to the transform domain. However, it cannot be denied that the proposed scheme has acceptable values for transform domain beyond any doubt. The spatial and transform domain both possess the value of NPCR very close to 100 that is the ideal value. After this comparative analysis, it may conclude that the proposed color image scrambling method has good NPCR.

### C. Entropy Analyses

Entropy measures the degree of randomness. Table II and Table V depict the entropy value in spatial and transform domain for the proposed color image scrambling scheme separately. The entropy values are approximate 7.7 for all the tested images in spatial and transform domain that is very close to the highest entropy value can attain by an image. Fig. 3 demonstrates the comparative analyses of entropy measure in spatial and transform domain. From Fig. 3, it can be noticed that the proposed image-scrambling scheme have comparable entropy values for both domains on all tested images. From this comparative entropy analyses, it may be articulated that the proposed color image scrambling method has excellent entropy.

### D. NC Analyses

In this, NC defines the correlation between the original image and the unscrambled image. The value of the correlation between the original and the unscrambled image should be high. The value of NC ranges from 0 to 1. Fig. 4 demonstrates the comparative analyses of NC between spatial

and transform domain on Lena, Peppers, Baboon, Tiger, and House Images. The value of NC for spatial domain on all tested images are 1 and transform domain acquires NC approximated 0.999. The NC value attained by the transform domain is close to 1. Therefore, it can derive that the proposed method has comparable results in terms of NC for both domains as illustrated in Fig. 3. From Fig. 3, it can conclude that the proposed color image method accomplishes excellent results in terms of NC.

From the above discussions, it can be analyzed that the proposed color image scrambling method has good visual quality, NPCR, Entropy and NC Values in both domains on all the tested images.

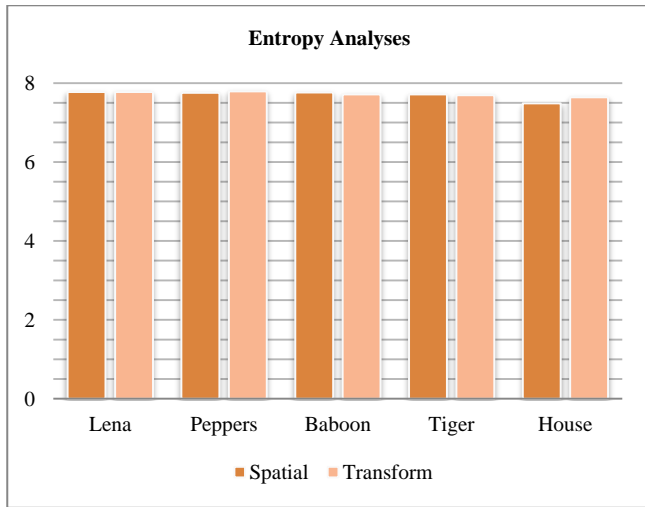


Fig. 3. Comparative Analyses of Entropy in Spatial and Transform Domain on Lena, Peppers, Baboon, Tiger, and House Images.

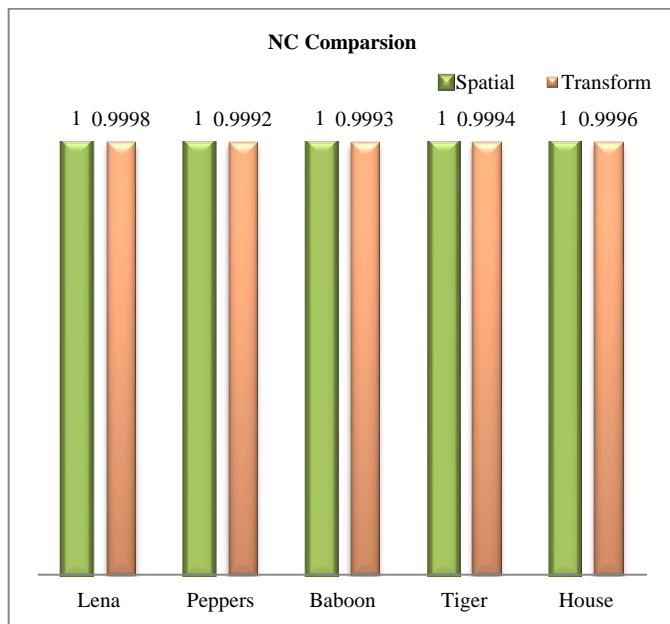


Fig. 4. Comparative Analyses of NC in Spatial and Transform Domain on Lena, Peppers, Baboon, Tiger, and House Images.

## VII. CONCLUSION AND FUTURE SCOPE

The present paper investigates the work associated with digital image scrambling. With this, an effort is put forward in the form of two proposed color image scrambling algorithms that are secure and efficient. The efficiency of the proposed image scrambling method is tested by performing various experiments, as discussed in the experimental results analysis section. The proposed method in the spatial domain is performing excellently in terms of visual quality, NPCR, Entropy, and NC. Whereas in the transform domain, the proposed image scrambling scheme carries excellent results in the form of entropy and performing good in terms of visual quality, NPCR, and NC. In other words, both the proposed color image scrambling algorithms work effectively in their domains.

## VIII. FUTURE SCOPE

Performance of proposed color image scrambling method in the transform domain can be enhanced by optimizing the scrambling process.

### REFERENCES

- [1] Y. Yu, J. Zhang, H. E. Ren, G. S. Xu, and X. Y. Luo, "Chaotic image scrambling algorithm based on S-DES," in *Journal of Physics: Conference Series*, 2006, vol. 48, no. 1, p. 349.
- [2] L. I. U. Xiangdong, Z. Junxing, Z. Jinhai, and H. Xiqin, "Image scrambling algorithm based on chaos theory and sorting transformation," *IJCSNS Int. J. Comput. Sci. Netw. Secur.*, vol. 8, no. 1, pp. 64–68, 2008.
- [3] W. Yanling, "Image scrambling method based on chaotic sequences and mapping," in *Education Technology and Computer Science, 2009. ETCS'09. First International Workshop on*, 2009, vol. 3, pp. 453–457.
- [4] G. Ye, "Image scrambling encryption algorithm of pixel bit based on chaos map," *Pattern Recognit. Lett.*, vol. 31, no. 5, pp. 347–354, 2010.
- [5] H. Zhang and R. Cai, "Image encryption algorithm based on bit-plane scrambling and multiple chaotic systems combination," in *Intelligent Computing and Integrated Systems (ICISS), 2010 International Conference On*, 2010, pp. 113–117.
- [6] M. Prasad and K. L. Sudha, "Chaos image encryption using pixel shuffling with henon map," *Dimension*, vol. 1, p. 50625, 2011.
- [7] R. Liu and X. Tian, "A space-bit-plane scrambling algorithm for image based on chaos," *J. Multimed.*, vol. 6, no. 5, pp. 458–466, 2011.
- [8] R. Liu, "A New Chaotic Image Scrambling Scheme Based on Spatial Bit-Level Map," in *Applied Mechanics and Materials*, 2012, vol. 220, pp. 2589–2594.
- [9] A.-V. Diaconu, A. Costea, and M.-A. Costea, "Color image scrambling technique based on transposition of pixels between RGB channels using Knight's moving rules and digital chaotic map," *Math. Probl. Eng.*, vol. 2014, 2014.
- [10] D. Wang, C.-C. Chang, Y. Liu, G. Song, and Y. Liu, "Digital image scrambling algorithm based on chaotic sequence and decomposition and recombination of pixel values," *Int. J. Netw. Secur.*, vol. 17, no. 3, pp. 322–327, 2015.
- [11] Y. Zhou, S. Agaian, V. M. Joyner, and K. Panetta, "Two Fibonacci p-code based image scrambling algorithms," in *Image Processing: Algorithms and Systems VI*, 2008, vol. 6812, p. 681215.
- [12] G. Xiong, S. Zheng, J. Wang, Z. Cai, and D. Qi, "Local Negative Base Transform and Image Scrambling," *Math. Probl. Eng.*, vol. 2018, 2018.
- [13] L. L. L. H. Zhu Liehuang Li Wenzhuo, "A Novel Image Scrambling Algorithm for Digital Watermarking Based on Chaotic Sequences," *IJCSNS Int. J. Comput. Sci. Netw. Secur.*, vol. 6, no. 8, pp. 125–130, 2006.

- [14] L. Shou-Dong and X. Hui, "A New Color Digital Image Scrambling Algorithm Based on Chaotic Sequence," in *Computer Science & Service System (CSSS)*, 2012 International Conference on, 2012, pp. 922–925.
- [15] Z. Shang, H. Ren, and J. Zhang, "A block location scrambling algorithm of digital image based on Arnold transformation," in *Young Computer Scientists*, 2008. ICYCS 2008. The 9th International Conference for, 2008, pp. 2942–2947.
- [16] J. Chen, Z. Zhu, C. Fu, L. Zhang, and H. Yu, "Analysis and improvement of a double-image encryption scheme using pixel scrambling technique in gyrator domains," *Opt. Lasers Eng.*, vol. 66, pp. 1–9, 2015.
- [17] H. B. Kekre, T. Sarode, P. N. Halarakar, and D. Mazumder, "Comparative Performance of Image Scrambling in Transform Domain using Sinusoidal Transforms," *Int. J. Image Process.*, vol. 8, no. 2, p. 49, 2014.
- [18] J. Chen, Z. Zhu, Z. Liu, C. Fu, L. Zhang, and H. Yu, "A novel double-image encryption scheme based on cross-image pixel scrambling in gyrator domains," *Opt. Express*, vol. 22, no. 6, pp. 7349–7361, 2014.
- [19] J. Zou, R. K. Ward, and D. Qi, "A new digital image scrambling method based on Fibonacci numbers," in *Circuits and Systems*, 2004. ISCAS'04. Proceedings of the 2004 International Symposium on, 2004, vol. 3, pp. III--965.
- [20] G. Ye, X. Huang, and C. Zhu, "Image encryption algorithm of double scrambling based on ASCII code of matrix element," in *Computational Intelligence and Security*, 2007 International Conference on, 2007, pp. 843–847.
- [21] M. M. Aziz and D. R. Ahmed, "Simple Image Scrambling Algorithm Based on Random Numbers Generation," *Int. J.*, vol. 5, no. 9, 2015.
- [22] S. Liping, Q. Zheng, L. Bo, Q. Jun, and L. Huan, "Image scrambling algorithm based on random shuffling strategy," in *Industrial Electronics and Applications*, 2008. ICIEA 2008. 3rd IEEE Conference on, 2008, pp. 2278–2283.
- [23] H. B. Kekre, T. Sarode, and P. N. Halarakar, "Study of Perfect Shuffle for Image Scrambling," *Int. J. Sci. Res. Publ.*, vol. 227.
- [24] Y. Zou, X. Tian, S. Xia, and Y. Song, "A novel image scrambling algorithm based on Sudoku puzzle," in *Image and Signal Processing (CISP)*, 2011 4th International Congress on, 2011, vol. 2, pp. 737–740.
- [25] P. Praveenkumar, R. Amirtharajan, K. Thenmozhi, and J. B. B. Rayappan, "Triple chaotic image scrambling on RGB--a random image encryption approach," *Secur. Commun. Networks*, vol. 8, no. 18, pp. 3335–3345, 2015.
- [26] H. B. Kekre, T. Sarode, and P. Halarakar, "Image Scrambling Using R-Prime Shuffle on Image and Image Blocks," *Int. J. Adv. Res. Comput. Commun. Eng.*, vol. 3, no. 2, 2014.
- [27] Y. Zhou, K. Panetta, and S. Agaian, "An image scrambling algorithm using parameter bases M-sequences," in *Machine Learning and Cybernetics*, 2008 International Conference on, 2008, vol. 7, pp. 3695–3698.
- [28] D. P. M. M. Dhananjay Santosh Waghulde, "A review on digital image scrambling encryption techniques," *Int. J. Res. Appl. Sci. Eng. Technol.*, vol. 5, 2017.

# Hijaiyah Letter Interactive Learning for Mild Mental Retardation Children using Gillingham Method and Augmented Reality

Irawan Afrianto<sup>1</sup>, Agung Faishal Faris<sup>2</sup>, Sufa Atin<sup>3</sup>  
Departement of Informatics Engineering  
Universitas Komputer Indonesia  
Bandung, Indonesia

**Abstract**—Assistive technology for children with special needs is a problem that is interesting to study. Collaboration between methods and latest technology can be used as a learning aid for them. Learning of Hijaiyah letters is the first step to being able to read the Holy Qur'an. Mentally retarded children have IQs below the average normal child, so their learning process is slower and requires special methods. This study aims to develop an application by using the Gillingham and augmented reality methods to help mentally retarded children recognize Hijaiyah letters. The Gillingham method uses a visual, auditory, kinesthetic, and tactile (VAKT) approach, that can be used to facilitate mentally retarded children. While augmented reality is used to develop more interesting and interactive applications. Based on the results of research and testing, it can be concluded that the learning application that was built can improve children's memory and understanding of Hijaiyah letters, The results of the pretest and posttest testing, showed an increase of 12% for children who were difficult to receive learning material and 6% for children who are classified as easy to receive learning material.

**Keywords**—Hijaiyah; intercative learning; mild retarded child; Gillingham; VAKT; augmented reality

## I. INTRODUCTION

Children with mental retardation are children with limited conditions of development. The ability to learn is different from other normal children. Certain assistive methods and technologies are needed to support the teaching of children with special needs. This needs to combine the ability of special schools that handle mentally disabled children with assistive technology that can be used in learning [1].

The method that is widely used in helping children with special needs in letter recognition is the gillingham method. This method uses a multisensory mechanism to provide learning stimuli in the form of sounds, images and flavors to adapt the letters [2]. The Gillingham method is oriented to sound and letter links. Each letter is taught using a multisensory approach. Multisensory approaches used are visual, auditory, kinesthetic, and tactile (VAKT) [3]. Studies related to the VAKT approach have been carried out for children with special needs, such as the application of VAKT to deaf children [4], the application of VAKT to autistic children [5], and the implementation of VAKT in mentally disabled children [6].

The assistive technology used in helping children with special needs such as mental retardation is the development of hardware and software tailored to the abilities possessed by these children [7]. Other assistive technologies center on varied sound processing and displays [8], while other researchers reveal the use of assistive technologies that are self-management tools that are beneficial for mentally disabled people in completing their daily activities [9]. The mobile application is one of the potential solutions for the development of learning for children with special needs, this is shown in research on the use of palmtops for mentally disabled people [10], the MARBEL mobile application for letter recognition learning for mild mental retardation sufferers [11] and android-based motorbike games for mentally disabled children [12]. Due to the limitations of integensia in mentally disabled children, learning models that are more adaptive to their abilities are needed. The interactive learning model is a learning model that can stimulate many activities for mentally disabled children [13]. This learning model can appear in the form of game-based learning for mentally disabled people developed with the help of computers [14] to produce games for mentally disabled children. Other studies use interactive technology and MAS platform games to help improve learning for deaf children [15]. Educational games for caring for mentally disabled children have also been developed and used to train children's motor skills and can be used by teachers as one of the learning media. [16]. Mobile applications and Augmented reality become a potential in the development of learning [17]. Augmented Augmented reality moves to become one of the technologies that has the ability to be used as the basis for developing learning applications for children [18]. The application of augmented reality can also provide flexibility in giving learning strategies [19], and is able to increase student learning motivation [20] and for children with special needs [21]. Augmented reality can also be used as a therapeutic medium for mentally disabled patients [22]. Other studies [23] show that augmented reality can help autistic patients and mentally disabled children to navigate to find a particular location / place.

The use of the VAKT method in this study aims to improve the ability of mildly retarded children in Hijaiyah letter learning. This study also aims to map the VAKT method to technology that allows for the development of interactive multimedia learning media by utilizing augmented reality



technology, with the hope that the application developed can stimulate the visual, auditory, kinesthetic, and tactile senses of mildly retarded children so that they can easier to recognize and learn the letters Hijaiyah. In this study, the application will be tested on 2 groups of mild mentally retarded children to find out the changes in the ability of these children in Hijaiyah letter learning after using the application.

## II. RESEARCH METHOD

The research method used in this research is divided into 4 stages, namely:

- The researcher collects the initial data according to the needs with a literature study in the form of journals and books related to the research that will be conducted. After the data is sufficient to support the research, the researcher will prepare the tools and materials needed for the next stage.
- At the planning stage, researchers make modeling applications that want to be made. The modeling started with system description, system architecture, functional analysis of application until application interfaces design.
- At the development stage, researchers will develop a model that has been made previously in the form of a program that is ready to be tested.
- The last stage is implementation and testing, the researcher implements the application on the appropriate device and tests how feasible the program has been made to be applied to mild mentally retarded children.

## III. RESULT AND DISCUSSION

This section describes the analysis of the current learning conditions, the application architecture developed, mapping the Gillingham method with the VAKT approach to the application developed, system modeling, design and testing of application built.

### A. Analysis of Current Learning Conditions

From observations and interviews conducted by researchers, it was concluded that the current learning conditions still use conventional methods, namely teachers teaching students using ordinary teaching equipment and textbooks. Current procedures for teaching activities can be seen in Fig. 1 and 2.

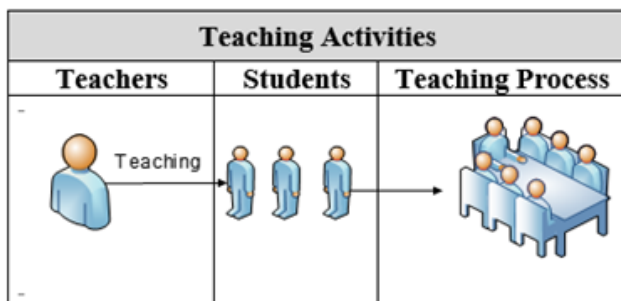


Fig. 1. Current Teaching Activity.

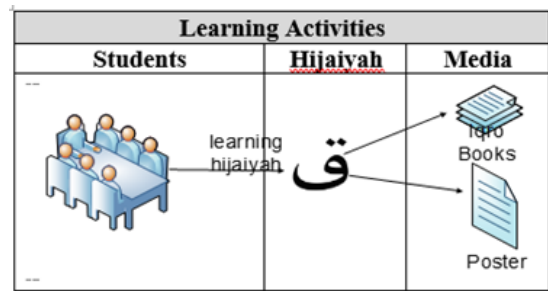


Fig. 2. Current Learning Hijaiyah Activity.

### B. Description of the Application

The interactive learning Hijaiyah is a mobile-based application that is specifically for mild mentally retarded children learning Hijaiyah letters, with a structured and oriented method on sound and letter links. Where each letter is studied multisensory, starting from the sound, tracing the letters and copying letters. This learning method is called the Gillingham method. The VAKT Approach In this application is by introducing the Hijaiyah letters visually, with the help of sounds and images and thickening the letter points (movements) that have been taught. Each letter must be completed in order to proceed to the next letter. This application is made by using specific learning principles for mentally retarded children such as repetition and directed and gradual system flow. Augmented reality with marker frames is used to attract children to learn in more interesting ways. The application description that will be built can be seen in Fig. 3.

### C. Analysis of System Architecture

The system architecture is an overview of the application to provide the initial model of the application to be built [24] [25]. The system architecture that is built consists of several components of learning material presented with several modalities. The modalities used are visual (vision), auditory (hearing), kinesthetic (movement), and tactile (touch). The four are known as VAKT. System architecture in the development of this application introduces and teaches Hijaiyah letters to train children's memory with VAKT modalities- he Gillingham method, which is shown in Fig. 4.

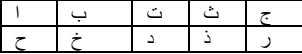
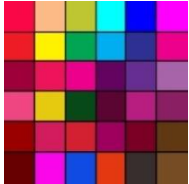




The next step is to synchronize the Gillingham - VAKT method into the application that was built. Table I explains how the mapping of the Gillingham-VAKT method to the application was built.

### D. Analysis of Learning Outcomes

The application that is built has a feature to store learning data in the form of student report cards. Student report cards will show the level of success of students in learning the material contained in the application. The student report card shows the number of correct answers and how many times the student is doing repetitions. Fig. 5 shows the student report card model in the application.

The learning results obtained by students are the values from the guessing feature and writing the letters Hijaiyah. Table II explains the calculations for the assessment of answers.

TABLE I. IMPLEMENTATION GILLINGHAM METHOD ON APPLICATION

| Gillingham  | Application  |
|---|--|
| <b>Visual</b><br>(Learning by seeing)<br>Here, which plays an important role is the senses or vision (visual). This type of student gate of knowledge is the eye, because the only senses that are active and dominant in him are the eyes or vision.   | 1. Showing letters in a structured and focused on one-on-one letter<br>   |
|   | 2. Attractive Colors<br>  |
|   | 3. Animation for ways of writing letter<br>   |
| <b>Auditory</b><br>(Learning by listening)<br>Auditory type students rely on their learning success through their ears (hearing aids), for that teachers should pay attention to their students to their hearing aids. Students who have auditory learning styles can learn faster by using verbal discussion and listening to what the teacher says. | 4. Audio that appears at each stage of learning that explains and teaches by repeating each letter.<br>5. Audio that shows how to use the application<br>  |
|   | 6. Audio encourage and motivate children to study harder   |
| <b>Kinesthetic</b><br>(Learning By Means of Physical Movement)<br>Students who have kinesthetic learning styles how to learn always respond to every lesson received with physical movement. He also prefers the lessons given in the form of games because basically he cannot sit and stay long while studying.                                     | 7. Application of learning by inviting users to participate interact during the learning takes place to make the application more interactive.<br>8. In game card magic users need to use the phone in order to scan the card. The learning process is to train movements and memory of children.<br> |
|   | 9. The process of learning is presented with a smartphone and all of the learning process presented by touching the screen smartphone<br>10. At this stage of learning to write letters the user must browse and thicken dots that form the letter Hijaiyah<br>                                       |

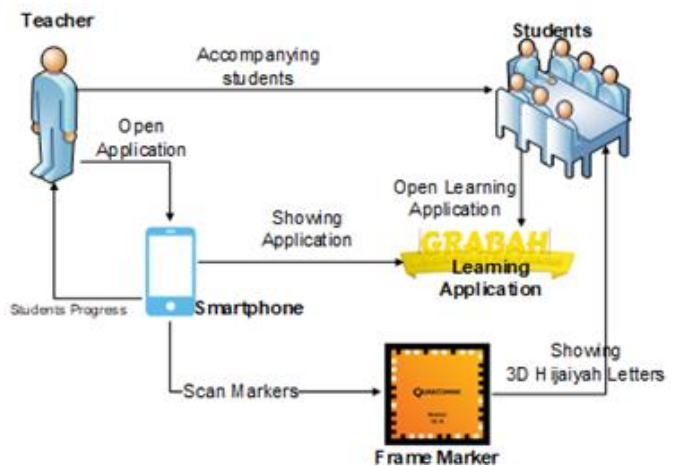


Fig. 3. Description of Application.

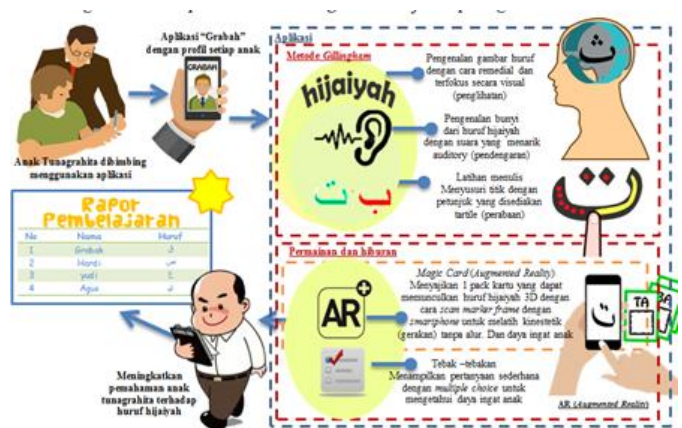


Fig. 4. System Architecture.

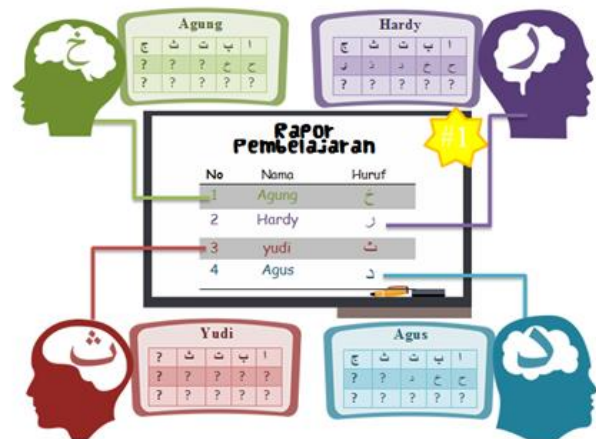


Fig. 5. Student Report Cards.

TABLE II. LEARNING SCORING

| Stages of Learning   | Number of Correct Answers  | System Action                                    |
|----------------------|----------------------------|--|
| Quiz Multiple choice | Answer correctly two times | Continue to the stage of learning write Hijaiyah |
| Write Hijaiyah       | Answer wrong 3 times       | Repeating steps of learning to write Hijaiyah    |

Wrong answers are limited to three times. Checkpoints are obtained from up to Hijaiyah letters that are open or understood and stored in student reports. In the report feature there will be a value in the form of numbers and last letters of the Hijaiyah that have been studied by each student.

E. Analysis of Augmented Reality

Augmented Reality is a real-time direct or indirect view of a physical real-world environment that has been enhanced/augmented by adding virtual computer-generated information to it. Its aims at simplifying the user's life by bringing virtual information not only to his immediate surroundings but also to any indirect view of the real-world environment [26]. The application built on Android, which has a feature to scan markers of Hijaiyah letters to produce an output in the form of a 3D object from the letters of the Hijaiyah. The flow of application of augmented reality in the application that was built, can be seen in Fig. 6.

Augmented reality developed in this application uses marker-based methods. The markers used are in the form of a collection of Hijaiyah letters card as shown in Fig. 7 and poster of the Hijaiyah letters in Fig. 8.

The markers will be scanned by the application to produce a 3D form of the letter Hijaiyah. The 3D model that appears is made tilting 130 degrees to adjust the user's eye. In Fig. 9, a 3D model is displayed that will appear from the scanned marker card.

The 3D model will also appear when the Hijaiyah letter poster is scanned using a built-in application. The 3D model that appears on the line aligns with the marker adjusting the user's eye point of view. Fig. 10 illustrates the appearance of a 3D model that will appear from the poster marker.

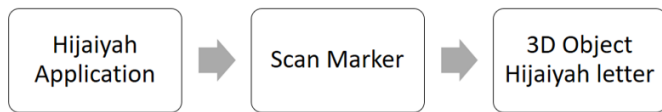


Fig. 6. Implementation of Augmented Reality.

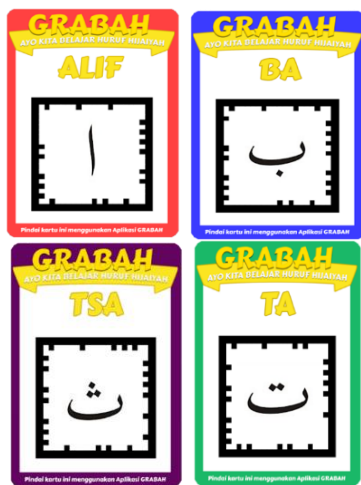


Fig. 7. Hijaiyah Letters Card Marker.

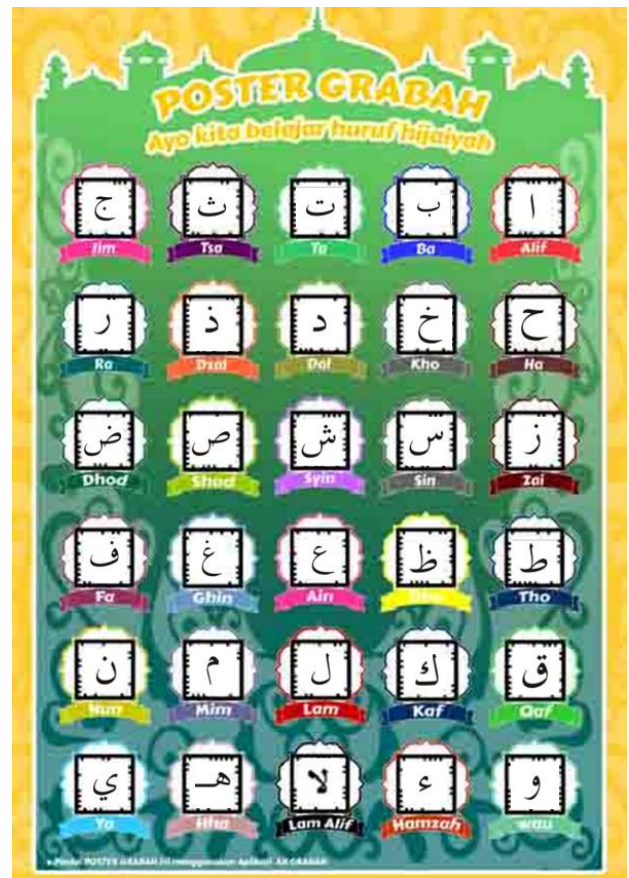


Fig. 8. Hijaiyah Letters Poster Marker.

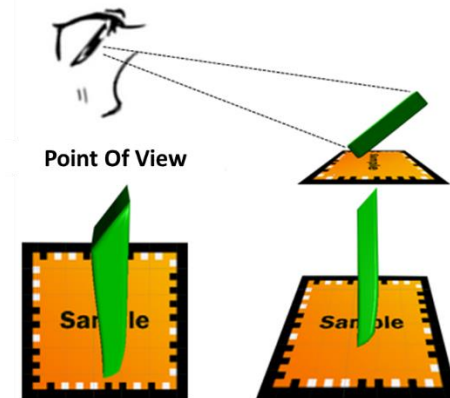


Fig. 9. 3D Model Display Card Hijaiyah Augmented Reality.

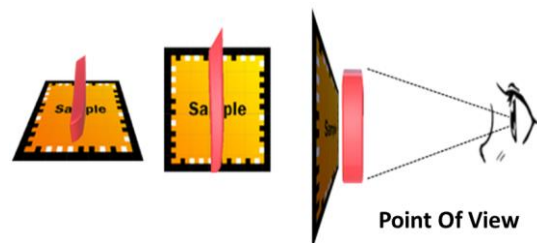


Fig. 10. 3D Model Display Poster Hijaiyah Augmented Reality.

F. Data Store Analysis

Data storage in this application uses PlayerPrefs. PlayerPrefs is a database contained in the Unity application that can be used to store various kinds of data. In this application, PlayerPrefs is used to store application user data, such as student names, letters that have been studied, and scores obtained by each student. Data storage workflow can be seen in Fig. 11.

G. Application Modeling

Modeling application used to facilitate the functional description that will be included in the application [27]. Application modeling is built using a use case diagram to explain the functional requirements contained in the application. Fig. 12 shows the use case diagram of the application that was built, as well as the description of each functional which can be seen in Table III.

H. Animation Design

Animation is a motion picture that is formed from a set of objects (images) arranged regularly following the flow of motion that has been determined based on time [28]. The animation design applied in this application is to illustrate the animation of application characters as seen in Fig. 13, and animation for Hijaiyah letter movements in the application.

Animation in Hijaiyah letters is done by using the Tracking Point method where dots placed above the Hijaiyah letters are useful as a guide for writing Hijaiyah letters, as seen in Fig. 14.



Fig. 11. PlayerPrefs Data Storage.

TABLE III. USE CASE DEFINITIONS

| No | Use Case Name                 | Description   |
|----|-------------------------------|---|
| 1  | Pengaturan                    | The functionality is to go see the profile settings, look about and see the learning report.  |
| 2  | Membuat Profil                | A functionality to create user application with a new profile   |
| 3  | Menghapus Profil              | A functionality to delete a profile that was made before  |
| 4  | Memilih Profil                | A functionality for to determine which profile is active  |
| 5  | Melihat Profil                | A functionality for anyone to see the profile name or an existing child   |
| 6  | Melihat tentang               | Is the functionality to view information about the application maker  |
| 7  | Melihat laporan               | Is the functionality to see the extent to which the child has been studying Hijaiyah  |
| 8  | Pembelajaran huruf            | Functionality is to introduce the Hijaiyah  |
| 9  | Memilih huruf                 | Hijaiyah functionality is to choose which one will be studied. Could continue from last Hijaiyah learned or repeat Hijaiyah has been learned. |
| 10 | Memilih tahap pembelajaran    | A functionality to choose from where the checkpoint will repeat. From each checkpoint consists of 5 letters Hijaiyah.                         |
| 11 | Hentikan sejenak pembelajaran | A pause functionality for learning and there is a menu to get to the home page and the music setting.   |
| 12 | Menampilkan AR huruf          | Is the functionality to display the augmented reality feature or magic playing cards.   |

The tracking point method is used to animate Hijaiyah letters to show how to write the correct Hijaiyah letters. One example of the animation of Hijaiyah letters can be seen in Fig. 15.

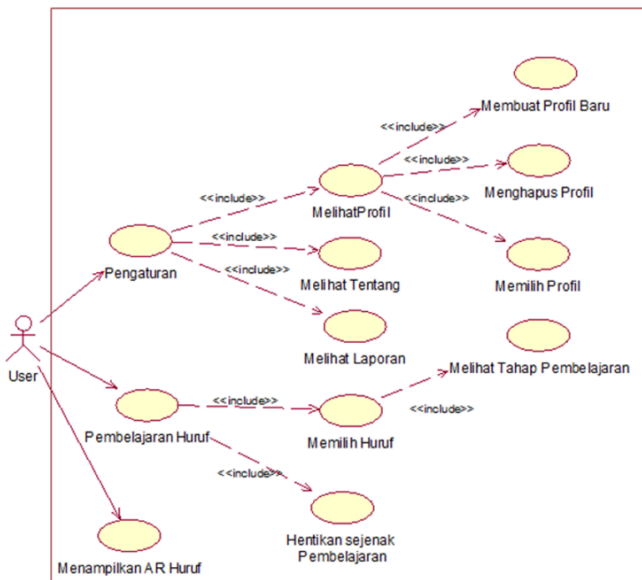


Fig. 12. Use Case Diagram Application.



Fig. 13. Illustration of Character in Application.



Fig. 14. Hijaiyah Letters Tracking Point Design.

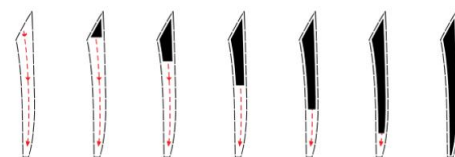


Fig. 15. Animated Hijaiyah Letters.

TABLE IV. MAPPING POINTS HIJAIYAH LETTERS

| Hijaiyah Letter | Number of Points | Position (x,y,z)  |
|-----------------|------------------|---|
| Alif<br>ا       | 10 points        | point[0] position(-8,229,0);<br>point[1] position(-3,190,0);<br>point[2] position(-1,150,0);<br>point[3] position (2,103,0);<br>point[4] position(5,63,0);<br>point[5] position(6,17,0);<br>point[6] position(7,-29,0);<br>point[7] position(6,-73,0);<br>point[8] position(4,-115,0);<br>point[9] position(1,-160,0);  |
| Ba<br>ب         | 13 points        | point[0] position(164,143,0);<br>point[1] position(183,100,0);<br>point[2] position(180,54,0);<br>point[3] position(150,24,0);<br>point[4] position(95,6,0);<br>point[5] position(29,-4,0);<br>point[6] position(-30,-8,0);<br>point[7] position(-83,-7,0);<br>point[8] position(-138,4,0);<br>point[9] position(-181,34,0);<br>point[10] position(-193,84,0);<br>point[11] position(-185,124,0);<br>point[12] position(10,-144,0);   |
| Ta<br>ت         | 13 points        | point[0] position(162,138,0);<br>point[1] position(186,84,0);<br>point[2] position(167,34,0);<br>point[3] position(117,9,0);<br>point[4] position(59,-5,0);<br>point[5] position(0,-12,0);<br>point[6] position(-59,-14,0);<br>point[7] position(-115, -8,0);<br>point[8] position(-163, 9,0);<br>point[9] position(-192,51,0);<br>point[10] position(-188,116,0);<br>point[11] position(48,188,0);<br>point[12] position(-37,189,0); |

With the tracking point method used, each Hijaiyah letter is mapped into points which later become a marker for the animation movement on the letter. Examples of mapping these points can be seen in Table IV.

### 1. Implementation and Testing

The final result of this study is an interactive learning application for mild mentally retarded children where the design application uses the VAKT approach and augmented reality. Some application interface can be seen in Fig. 16, 17, 18 and 19.



Fig. 16. Application Opening Interface.



Fig. 17. Hijaiyah Letter Introduction.

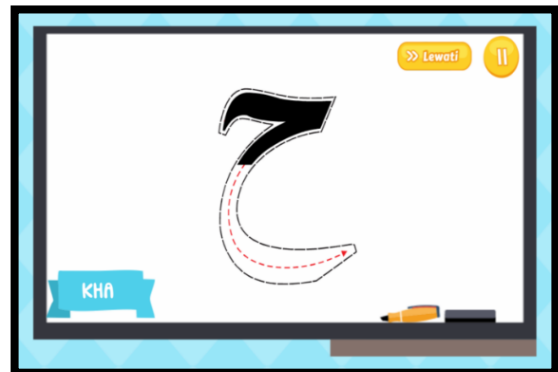


Fig. 18. Drawing Hijaiyah Letter.



Fig. 19. Game the Correct Letters.

Application testing is conducted in two ways, namely, testing the accuracy of the marker used, and testing the ability of students using the application. The results obtained from the marker-augmented reality test concluded that from 30 markers of Hijaiyah letters in the form of cards and posters, 100% of the markers can be scanned and produce 3D objects Hijaiyah letters. Testing students' abilities, using the pretest and posttest method. The pretest method is used to measure students' abilities before using the application, while the posttest method is used after students use the application. Application testing is carried out on 20 students divided into two groups, namely, students who have difficulty concentrating and students who are easy to concentrate. The results of the pretest and posttest tests on students who have difficulty concentrating can be seen in Fig. 20(a), while the results of testing for students who are easy to concentrate can be seen in Fig. 20(b).

IV. CONCLUSIONS

Based on the results of the implementation and testing carried out, it can be concluded that the Gillingham method with the VAKT approach and augmented reality can be developed into an interactive learning application that is able to improve the ability of students with mild mental disabilities. This is indicated by an increase in capacity of 12% for students who have difficulty concentrating and an increase of 6% for students who are easy to concentrate on the material and learning Hijaiyah letters.

For further work, it is necessary to consider other technologies in developing the application in the future, mapping the VAKT method that is more varied in order to produce more diverse learning variations that are in accordance with the ability of children with mild retardation.

ACKNOWLEDGMENT

Our thanks to the Caringin Bandung Special School (SLB) dan UNIKOM, which became a partner in this research, became a place for data searching, discussion, implementation and testing of application.

REFERENCES

- [1] M. L. Wehmeyer, 1999, "Assistive technology and students with mental retardation: utilization and barriers", *Journal of Special Education Technology*, 14(1), pp.48-58, 1999.
- [2] A. Gillingham and B.W. Stillman, *The gillingham manual*. Cambridge, MA: Educators. 1997.
- [3] S. Suhatli, "Meningkatkan kemampuan menulis kata melalui metode gillingham bagi anak kesulitan belajar kelas ii di sd negeri 05 kapalo koto", *Jurnal Penelitian Pendidikan Khusus*, 4(3). 2017.
- [4] V.O. Julita, "Efektivitas metode vakt untuk meningkatkan hafalan surah al-kausar bagi anak tunarungu (penelitian single subject research di kelas v slb luak nan bungsu kota payakumbuh)", *Jurnal Penelitian Pendidikan Khusus*, 4(3). 2017.
- [5] R. Afriliya, "Penggunaan metode visual auditori kinestetik taktil (vakt) terhadap pemahaman kosa kata anak autisme", *Jurnal Pendidikan Khusus*, 7(1). 2015.
- [6] D. Kumilasari, M. Iswari, and G. Sumekar, "Meningkatkan kemampuan menulis huruf vokal (a, i, u, e, o) melalui metode vakt bagi anak tunagrahita sedang di slb talawi sawahlunto", *Jurnal Penelitian Pendidikan Khusus*, 6(1). 2017.
- [7] E.A. Draffan, D.G. Evans, and P. Blenkhorn, "Use of assistive technology by students with dyslexia in post-secondary education", *Disability and Rehabilitation: Assistive Technology*, 2(2), pp.105-116. 2007.
- [8] K.M. Wilkinson and S. Hennig, "The state of research and practice in augmentative and alternative communication for children with developmental/intellectual disabilities", *Mental retardation and developmental disabilities research reviews*, 13(1), pp.58-69. 2007.
- [9] L.C. Mechling, "Assistive technology as a self-management tool for prompting students with intellectual disabilities to initiate and complete daily tasks: A literature review", *Education and Training in Developmental Disabilities*, 42(3), p.252. 2007.
- [10] S.E Stock, D.K. Davies and M.L Wehmeyer, "Evaluation of an application for making palmtop computers accessible to individuals with intellectual disabilities", *Journal of Intellectual and Developmental Disability*, 31(1), pp.39-46. 2006.
- [11] F.A Nurholis and N. Azizah, "Pengaruh mobile application marbel huruf terhadap kemampuan mengenal huruf anak tunagrahita ringan kelas ii di slb negeri wonogiri", *JPK (Jurnal Pendidikan Khusus)*, 13(2), pp.41-56. 2017.
- [12] M.R. Wibisono and Y. Findawati, "Game Motorik Untuk Pendidikan Anak Berkebutuhan Khusus (Tuna Grahita) Berbasis Android", *Informatika*, 1 (6), pp.20-29. 2010.

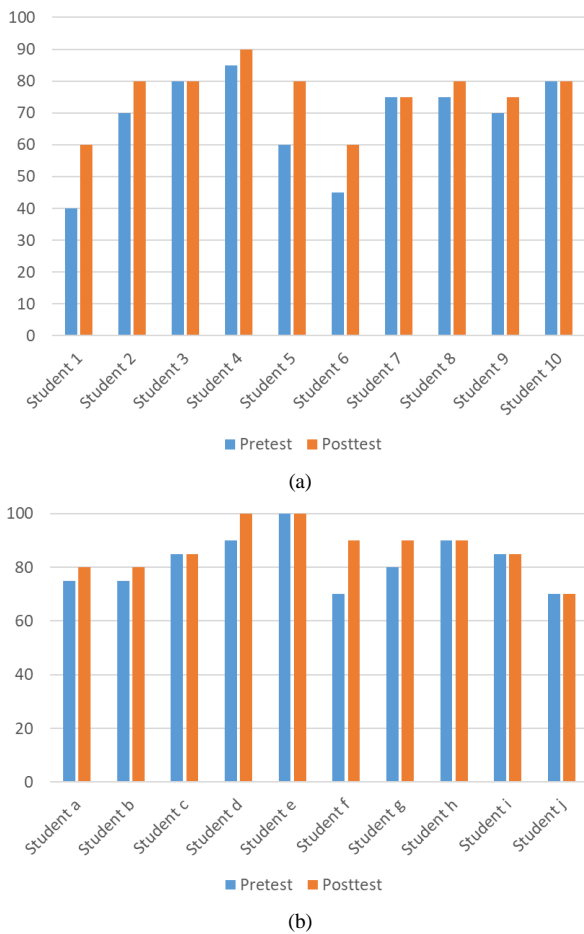


Fig. 20. Pretest and Posttest Results.

From the results of these tests, the average is calculated to determine changes in students' abilities before and after using the application, shown in Table V.

The results of the research conducted gave results of improvement in both test groups of mild mentally retarded children. Children who have difficulty concentrating have increased by 12%, while for children who are easy to concentrate, there is a 6% increase in Hijaiyah letter learning. Likewise with the results of previous studies that by using multisensory-VAKT methods, there is an increase in the learning of children with special needs, in the study [29] the reading ability of kindergarten students increased by 14%, in the other study the reading ability of elementary students with dyslexia increased in the number of word recognition, reading time, and the number of words read per minute [30], and the development of the ability to recognize flat waking in children with cerebral palsy increased with a percentage of 66.6% [31].

TABLE V. RESULTS AFTER USING THE APPLICATION

| Children Group           | Pretest Average | Posttest Average | Increase Score | Percentage (%) |
|--------------------------|-----------------|------------------|----------------|----------------|
| Difficulty concentrating | 680/10 = 68     | 760/10 = 76      | 8              | 12%            |
| Easy concentrating       | 820/10 = 82     | 870/10 = 87      | 5              | 6%             |

- [13] S. Syahrudin, M.S Saleh., and A. Rizal, "Peningkatan koordinasi mata tangan melalui model pembelajaran berbasis bermain bagi anak tuna grahita", In Seminar Nasional Lembaga Penelitian UNM (Vol. 2, No. 1). 2017.
- [14] C.S. Lanyi and D.J. Brown, "Design of serious games for students with intellectual disability", *IHCI*, 10, pp.44-54. 2010.
- [15] R. Colomo-Palacios, F. Paniagua-Martín, Á. García-Crespo and B. Ruiz-Mezcua, "Technology enhanced learning for people with intellectual disabilities and cerebral paralysis: The MAS platform", In International Conference on Technology Enhanced Learning (pp. 11-17). Springer, Berlin, Heidelberg. 2010.
- [16] F.Y. Al Irsyadi, S.L. Sholihah and E. Sudarmilah, "Game edukasi merawat diri untuk anak tunagrahita tingkat sekolah dasar berbasis kinect xbox 360", *Simetris: Jurnal Teknik Mesin, Elektro dan Ilmu Komputer*, 7(2), pp.693-700. 2016.
- [17] E. FitzGerald, R. Ferguson, A. Adams, M., Gaved, Y. Mor and R., Thomas, "Augmented reality and mobile learning: the state of the art", *International Journal of Mobile and Blended Learning (IJMBL)*, 5(4), pp.43-58. 2013.
- [18] D. Incarean, M.B. Alia, N.D.A. Halim and M.H.A. Rahman, "Mobile augmented reality: the potential for education", *Procedia-social and behavioral sciences*, 103, pp.657-664. 2013.
- [19] P.Y. Chao and G.D. Chen, "Augmenting paper-based learning with mobile phones", *Interacting with Computers*, 21(3), pp.173-185. 2009.
- [20] Á. Di Serio, M.B. Ibáñez., and C.D. Kloos, "Impact of an augmented reality system on students' motivation for a visual art course", *Computers & Education*, 68, pp.586-596. 2013.
- [21] C.Y. Lin, H.C. Chai, J.Y. Wang, C.J. Chen, Y.H. Liu, C.W. Chen, C.W. Lin and Y.M., Huang, "Augmented reality in educational activities for children with disabilities", *Displays*, 42, pp.51-54. 2016.
- [22] A.G.D. Correa, I.K. Ficheman, M. do Nascimento and R. de Deus Lopes, "Computer assisted music therapy: A case study of an augmented reality musical system for children with cerebral palsy rehabilitation", In 2009 Ninth IEEE International Conference on Advanced Learning Technologies (pp. 218-220). IEEE. 2009.
- [23] D. McMahon, D.F. Cihak, and R.Wright, "Augmented reality as a navigation tool to employment opportunities for postsecondary education students with intellectual disabilities and autism", *Journal of Research on Technology in Education*, 47(3), pp.157-172. 2015.
- [24] I. Afrianto, L. Warlina, S. Atin and A. Heryandi, "Framework of journal aggregator in indonesia", In International Conference on Business, Economic, Social Science and Humanities (ICOBEST 2018). Atlantis Press. November, 2018.
- [25] A. Finandhita., and I. Afrianto,"Development of e-diploma system model with digital signature authentication", In IOP Conference Series: Materials Science and Engineering (Vol. 407, No. 1, p. 012109). IOP Publishing. August, 2018.
- [26] J. Carmigniani, B. Furht, M. Anisetti, P. Ceravolo, E. Damiani and M. Ivkovic, "Augmented reality technologies, systems and applications. Multimedia tools and applications", 51(1), pp.341-377. 2011.
- [27] I. Afrianto, and S. Atin, "The Journal Aggregator System Concept Using User Centered Design (UCD) Approach", *International Journal of New Media Technology*, 5(2), pp.71-75. 2018.
- [28] K. Fujisawa, T. Inoue, Y. Yamana, and H. Hayashi, "The effect of animation on learning action symbols by individuals with intellectual disabilities", *Augmentative and Alternative Communication*, 27(1), pp.53-60. 2011.
- [29] A.C. Dewi and S. Aryanti, "Meningkatkan kemampuan membaca permulaan melalui metode multisensori pada kelompok b tk ygws semarang", *Media Penelitian Pendidikan: Jurnal Penelitian dalam Bidang Pendidikan dan Pengajaran*, 11(1). 2017.
- [30] M.D. Komalasari, "Efektivitas metode multisensori dalam meningkatkan kemampuan membaca pada peserta didik disleksia di sekolah dasar", *Jurnal Elementary School*, 4(1), pp.14-19. 2017.
- [31] N. Sutisna and A. Rahmawati, "Pengaruh metode vakt terhadap peningkatan kemampuan mengenal bangun datar pada anak cerebral palsy", *Pedagogia*, 16(2), pp.168-179. 2018.

# Causal Impact Analysis on Android Market

Hadiqa AmanUllah<sup>1</sup>, Mishal Fatima<sup>2</sup>, Umair Muneer<sup>3</sup>, Sadaf Ilyas<sup>4</sup>, Rana Abdul Rehman<sup>5</sup>, Ibraheem Afzal<sup>6</sup>

Department of Computer Science, University of Lahore, Gujrat, Pakistan

**Abstract**—Google play store contains a large repository of apps for android users. Play store has two billion active users that have two million apps to download and use. App developers are competing to get a higher success rate and increase user satisfaction but little information is known to developers for succeeding in the android market. This paper presents a comprehensive analytical study on Google play store apps ratings, installs and reviews. This study focuses on the evaluation of the parameters required for the success of an app in different categories. For this purpose data of 10k apps and its reviews are analyzed using exploratory data analysis. This study focuses on finding a correlation between higher ratings, no of installs, reviews with app info like its category, size, and price. We are also going to analyze user reviews to get useful insights. The evaluation shows that personalization, productivity and games categories are performing very well in the android market both in terms of ratings and installs. Most high rated apps are sized below 40MB and priced below 30\$, except game apps that are performing well even if they are bulky. Common customer complaints are functional errors and issues like infrequent updates, excessive ads, limited functionality and high purchase price.

**Keywords**—Android; Google; statistics; mobile applications; data visualization

## I. INTRODUCTION

Google Play Store is a digital service run and developed by Google. The android market serves as a digital store, providing a wide range of apps for education, entertainment, business, lifestyle, food and health etc. In 2017, on Twitter, Google announces that Android devices have more than two million active users monthly. Available numbers of apps on the Google Play Store exceeds 2.6 million in 2018 [1]. According to the analytics of Nielson, United States users stay more active on android apps instead of the web on an average of 56 minutes per day [2]. Android users can install both free and paid apps from the Google Play Store.

Due to high competition in the Android market, a lot of research has been triggered in this field. Despite having millions of users of android applications, aggregated information about these applications is still not well known. Specifically about succeeding in the android market, the impact of developer's actions on app familiarity, pricing of apps and achieving membership in top app lists [3]. There are a number of questions that still do not have a clear answer [22]. How different characteristics lead to an app success? What is the success determinant of an app, its rating or no of installs? What app features to choose from before development? Which apps category has more potential for new developers? In which category high-quality apps are needed? What are the common good and bad reviews?

Recent studies on demand, supply and value creation in mobile app markets suggests that demand factors mainly include app rank, popularity, quality updates and fermium strategy while supply is triggered by features such as marginal cost, file size, app portfolio diversity [25].

To answer all these questions, in this study, we are going to analyze Google Play Store apps ratings and reviews to evaluate the parameters required for the success of an app in different categories. Analyze the android market and get useful insights by using data of 10k play store apps. By finding a correlation between Google Play Store apps ratings, no of installs and user reviews with app size, price and category to evaluate the parameters required for the success of an app in different categories.

The paper is organized into the following sections: Section II briefly discusses the background research on this problem. Section III highlights data and methodology chosen for our analysis. Section IV describes the evaluation of each parameter and Section V concludes this paper.

## II. LITERATURE REVIEW

Google apps have many characteristics than that of web services. With the increase in the use of the smartphone, there is extreme spread in use of Google apps. Affordability and flexibility of smartphone devices is the central reason for the exceptional growth of the Android market in recent years [4]. No of downloads, ratings and satisfaction tends to be higher for blockbuster apps [5]. In a study conducted on prime ranking elements for mobile apps, shows that probability of an app success influenced by its app size, release date, number of languages it supports and popularity of its category [21].

A major source of feedback to developers is the star rating in the Google app store. Ratings computed using the Amazon rating system aggregates the lifetime rating of an app into one rating that is presented on the app store. It is not vibrant enough to grab the diversity of user satisfaction due to the evolution of apps and does not encourage developers to refine their apps with time [7]. In a recent study, an automated system is recommended that can facilitate developers to understand user text reviews and to improve their app features for better user experience [6].

The apps release strategy is an important aspect of app success. Skilled developers believe that user response is influenced by the app release strategy [8]. Price, release date, release content details are salient factors for app rating according to a causal analysis study conducted on the release of popular apps from Google Play and Windows Phone Store for 52 weeks [9].



After the successful release of an app, another step is the need for updates to emerge apps over time. Research has shown that updating apps more often, lead to a high rank of apps [10]. In comparison to Google Play, updates have a higher impact on downloads in iTunes, mainly for the reason that Google Play Store lack quality control due to which developers release both high and low-quality updates without worrying about the quality of update [11]. According to another study, for an update to have more effect on rating developers should focus on the declaration of features instead of bug fixing [12].

Apps are generally divided into two categories, free of cost and paid apps. To make paid apps gain familiarity developers offer a free trial version of their apps. Freemium strategy is positively correlated to high sales volume and revenue of the paid version of their apps [2] [14]. Optimal price of a commercial app can be improved with augmenting users by offering free trials [15]. A study was conducted on user purchase intention and concluded that purchase intention is influenced by app rating, currency value and free alternatives to paid apps [16].

User reviews are a very rich data source for understanding user reported issues to improve the quality of apps and get higher ratings [17]. According to a study, reviews and ratings are not static, developers response to reviews can lead to the constructive outcome on the rating of the app [19]. User feedback can be interpreted using different approaches, one such approach is CRISTAL proposed by Fabio Palomba et al. According to them, developers who update their apps rendering user feedback rewarded with higher ratings [13]. Due to noisy app reviews, direct parsing is mostly ineffective and inflexible to a large number of reviews. To overcome this issue, phrase-based extraction (PUMA) system is proposed, an automated technique which can extract user opinions from app reviews [20]. Most common complaints among user reviews are functional errors, requests for additional features and app crashes [18].

### III. PROCEDURE

This study contains both quantitative and qualitative data. The approach used in this paper is exploratory data analysis. Data for different variables are aggregated and visualized to understand the properties of the Google Play Store. EDA assists us to understand characteristics that can be effective to capture the Android market.

All this work is done in python Jupyter Notebook. Datasets are handled with the help of the Pandas library. Statistical analysis is performed using the NumPy library, and then data is visualized using Matplotlib and Seaborn library to get useful insights from data. In this paper, the correlation between ratings, no of installs and no of reviews are evaluated w.r.t. app size, price and category. To do analysis on user reviews, word clouds are built to get the top frequency words for different sentiments. Upon the frequency of these words, reviews are manually studied to get information about the common good and bad reviews.

#### A. Data

Proposed Sample has data about 10840 apps and contains and 64296 users review. The sample is taken as a dataset from

kaggle.com [27]. It has two files. The 1st file contains parameters about apps info as mentioned in Table I:

2nd file contains parameters about user reviews and sentiments analysis as mentioned in Table II:

#### B. Preprocessing

Original Records were 10841, after removing duplicate and noisy data 9658 records remained. Further, convert app "Size" to MB, remove '+', ',' from "Installs", create classes for "Content Rating" (Everyone, 10+, 13+, 17+, 18+), Convert data types of all columns:

#### C. Statistical Description

Stats are calculated about each numerical and descriptive parameter in data. Statistics for variables in App Info file is presented in Table III and Table IV.

TABLE I. APP INFO

| Name           | Depiction   |
|----------------|---|
| App            | App name  |
| Category       | App category name   |
| Rating         | User rating in the range of [1,5]                                 |
| Reviews        | Quantity of user reviews  |
| Size           | Size of the app   |
| Installs       | Number of user downloads or installs                              |
| Type           | Paid or Free  |
| Price          | App price   |
| Content Rating | Age group the app is targeted on                                  |
| Genres         | Apart from the main category an app can belong to multiple genres |
| Last Updated   | Last time the app was updated                                     |
| Current Ver    | Latest version of the app   |
| Android Ver    | Minimum required Android version                                  |

TABLE II. APP REVIEWS

| Name                   | Depiction                             |
|------------------------|---------------------------------------|
| App                    | App name                              |
| Translated Review      | Translated user feedback              |
| Sentiment              | Feedback sentiment analysis           |
| Sentiment Polarity     | Feedback Sentiment polarity score     |
| Sentiment Subjectivity | Feedback Sentiment subjectivity score |

TABLE III. APP INFO: NUMERICAL DATA STATISTICS

|       | Rating | Reviews  | Size | Installs  | Price |
|-------|--------|----------|------|-----------|-------|
| Count | 8196   | 9658     | 8432 | 9658      | 9658  |
| Mean  | 4.2    | 216615   | 20.4 | 7778312   | 1.1   |
| Std   | 0.5    | 1831413  | 21.8 | 53761004  | 16.9  |
| Min   | 1      | 0        | 0    | 0         | 0     |
| 25%   | 4      | 25       | 4.6  | 1000      | 0     |
| 50%   | 4.3    | 967      | 12   | 100000    | 0     |
| 75%   | 4.5    | 29408    | 28   | 1000000   | 0     |
| Max   | 5      | 78158306 | 100  | 100000000 | 400   |

TABLE IV. APP INFO: DESCRIPTIVE DATA STATISTICS

|                | Count | Unique | Top                | Freq |
|----------------|-------|--------|--------------------|------|
| App            | 9658  | 9658   |                    |      |
| Category       | 9658  | 33     | FAMILY             | 1831 |
| Type           | 9658  | 2      | Free               | 8902 |
| Content Rating | 9658  | 6      | Everyone           | 7903 |
| Genres         | 9658  | 118    | Tools              | 826  |
| Last Updated   | 9658  | 1377   | 3 Aug, 2018        | 252  |
| Current Ver    | 9650  | 2817   | Varies with device | 1054 |
| Android Ver    | 9656  | 33     | 4.1 and up         | 2202 |

TABLE V. APP REVIEWS: NUMERICAL DATA STATISTICS

|       | Sentiment_Polarity | Sentiment_Subjectivity |
|-------|--------------------|------------------------|
| Count | 37427              | 37427                  |
| Mean  | 0.0                | 0.0                    |
| Std   | 0.0                | 0.0                    |
| Min   | -1.0               | 0.0                    |
| 25%   | 0.0                | 0.0                    |
| 50%   | 0.0                | 1.0                    |
| 75%   | 0.0                | 1.0                    |
| Max   | 1.0                | 1.0                    |

TABLE VI. APP REVIEWS: DESCRIPTIVE DATA STATISTICS

|        | App        | Translated_Review | Sentiment |
|--------|------------|-------------------|-----------|
| Count  | 37427      | 37427             | 37427     |
| Unique | 865        | 27994             | 3         |
| Top    | Bowmasters | Good              | Positive  |
| Freq   | 312        | 247               | 23998     |

Statistics for parameters in App Reviews file is presented in Table V and Table VI.

#### IV. EVALUATION

The success of an app can be measured by its rating, no of installs and reviews. In this paper, success parameters are evaluated according to their distribution in different categories. 33 categories are found in the data. Average no. of apps in each category is 292.

The top five categories contain the most active apps in the market are Family, Game, Tools, Business and Medical.

The family contains 19% of apps available in our data. The bottom five categories containing the least apps are Arts & Design, Events, Parenting, Comics and Beauty as visible in Fig. 1.

##### A. Rating

According to word-of-mouth literature, for open platforms like Google Play Store rating is an important success factor [23]. Rating is measured as the star rating, ranging from 1 to 5. Naive users use this rating system to perceive app satisfaction

[7]. Generally, most of the apps are performing well with an average rating of 4.17. Rating pattern across each category is shown in Fig. 2.

To get useful insights, in this paper only those categories are considered in which no. of apps are more than 292. Categories are filtered that has more than average no. of apps.



Fig. 1. No of Apps in each Category.



Fig. 2. Rating Pattern in each Category.

Upon drilling down, we found out that the Personalization category has the highest average rating i.e. 4.33, 4% apps in our data belong to Personalization, distribution of rating in Personalization can be visualized in Fig. 4. The family category is on 5th position and Tools is on 11th position, so Apps in Tools needed more attention from developers as highlights in Fig. 3.

**B. Installs**

No. of Installs is considered to measure the success of an app. In this data no. of installs range from 0 to 1 billion. No. of installs are grouped and their frequency and percentage is obtainable in Table VII. Average installs are 7778312. Only a few apps have more than 100 million installs and they are free apps as shown in Fig. 5.

If more no. of installs is considered as success criteria then results are very different across categories w.r.t. ratings. Average installs are very good across the Communication category. Fig. 6 shows that Productivity is also performing better than many high rating categories.

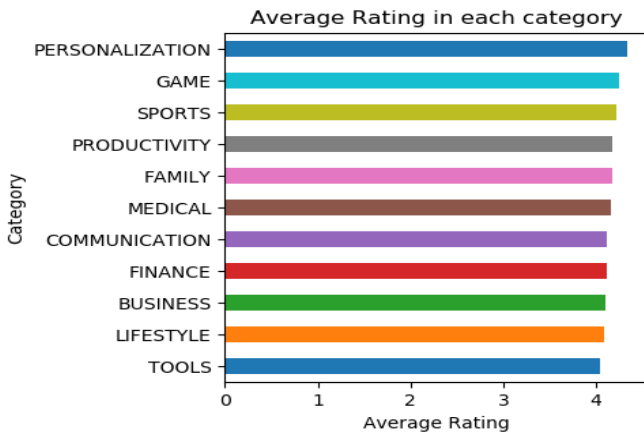


Fig. 3. Average Rating in each Category where no of Apps ≥ 292.

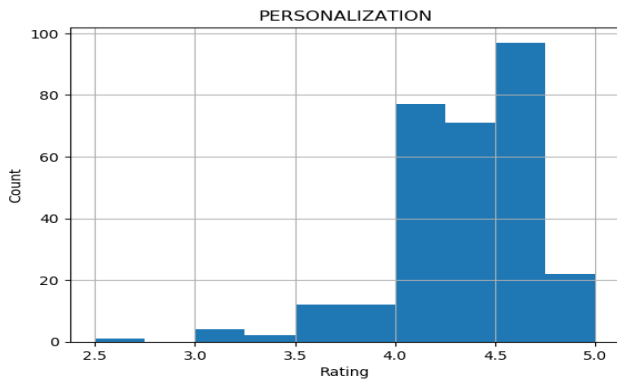


Fig. 4. Distribution of Rating Across Personalization Category.

TABLE VII. INSTALLS STATISTICS

| Installs                      | Count | Percent |
|-------------------------------|-------|---------|
| $I > 0 \ \& \ I \leq 10e8$    | 9614  | 99.5%   |
| $I > 10e8 \ \& \ I \leq 50e8$ | 24    | 0.25%   |
| $I > 50e8 \ \& \ I \leq 10e9$ | 20    | 0.21%   |

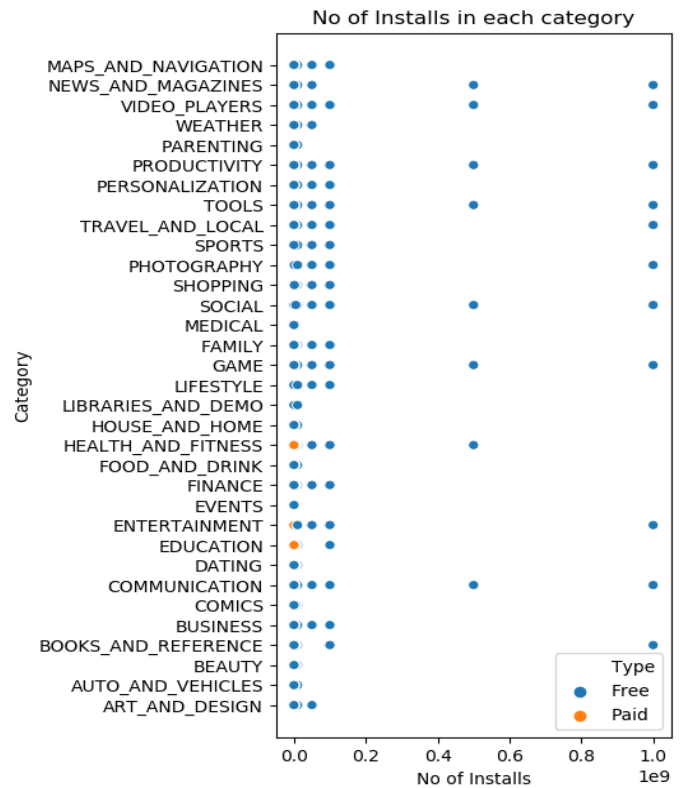


Fig. 5. No of Installs Pattern in each Category.

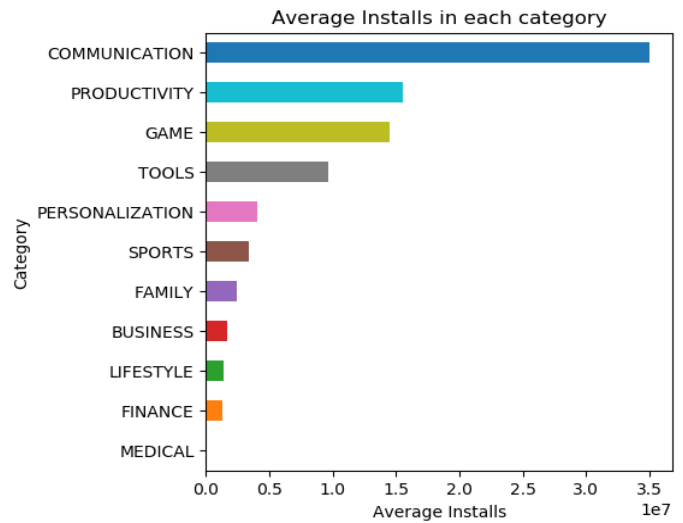


Fig. 6. Average Installs in each Category where no of Apps ≥ 292.

By plotting ratings versus installs, we can see that high rated apps have more installs. Fig. 7 indicates that users tend to install apps that have good reviews and high ratings.

**C. Price**

To prevent consumer negative attitude specialists must develop specific strategies for pricing; failure on pricing will result in the customer losing interest in other app features [26]. There are two types of apps: Free and Paid. Frequency of each type is presented in Table VIII. Frequency distribution for paid apps is obtainable in Table IX.

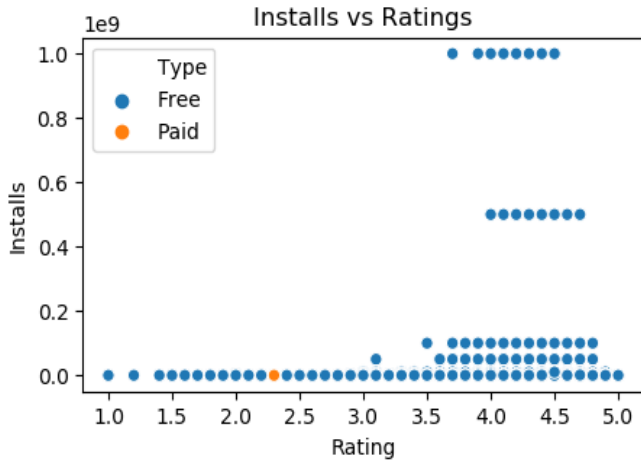


Fig. 7. Correlation between Installs and Ratings.

TABLE VIII. PRICE STATISTICS

| Type | Count | Percent |
|------|-------|---------|
| Free | 8902  | 92%     |
| Paid | 756   | 8%      |

TABLE IX. PAID APPS STATISTICS

| Paid           | Count | Percent |
|----------------|-------|---------|
| P>0 & P<=50    | 733   | 97%     |
| P>50 & P<=350  | 7     | 1%      |
| P>350 & P<=400 | 16    | 2%      |

In Fig. 8, we can see that average Price for Finance, LifeStyle and Medical is fairly high while in rating they stand on 8<sup>th</sup>, 10<sup>th</sup> and 6<sup>th</sup> position respectively. Interestingly, Game apps are reasonably priced below ~20\$.

To understand the impact of price on rating and no. of installs, we plotted price w.r.t. rating and installs in Fig. 9 and Fig. 10, and found out that apps with high price do not deliver high ratings or more installs. Most of the top rated apps are priced between ~1\$ to ~30\$.

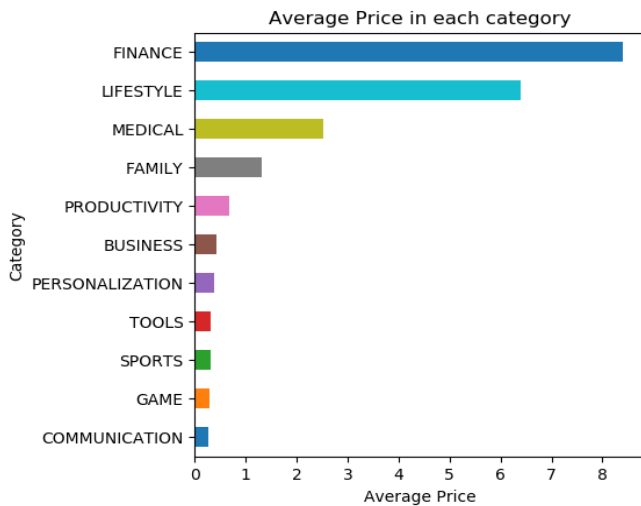


Fig. 8. Average Price in each Category where no of Apps  $\geq$  292.

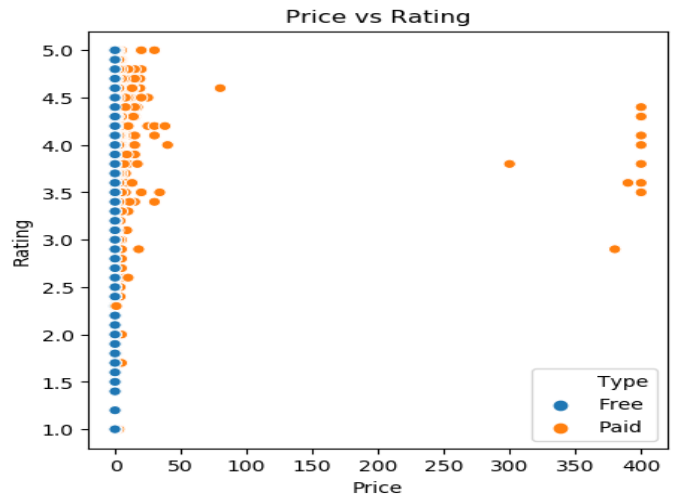


Fig. 9. Correlation between Price and Rating.

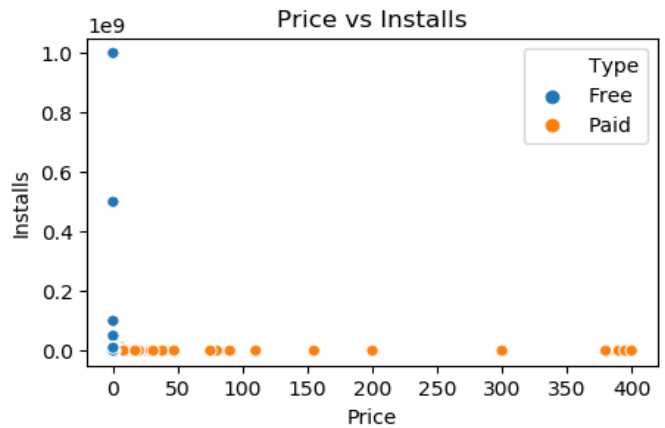


Fig. 10. Correlation between Price and Installs.

#### D. Size

Despite the known fact that app size increases with app functionality, it can also bound users to install apps with greater size due to limited storage capacity [24]. Apps average size is 20 MB and has a range of up to 100 MB. Frequency distribution of app size is given in Table X.

After plotting size and rating in Fig. 11, paid apps appeared to be bulkier relative to free apps. Apps with greater size have low ratings. User likes light and less expensive apps and rates them higher because most of the top-rated apps are neither too heavy nor too light, ranging between ~2MB to ~40MB.

TABLE X. SIZE STATISTICS

| Size          | Count | Percent |
|---------------|-------|---------|
| S>0 & S<=20   | 5465  | 57%     |
| S>20 & S<=40  | 1660  | 17%     |
| S>40 & S<=60  | 707   | 7%      |
| S>60 & S<=80  | 328   | 3%      |
| S>80 & S<=100 | 272   | 3%      |
| nan           | 1226  | 13%     |

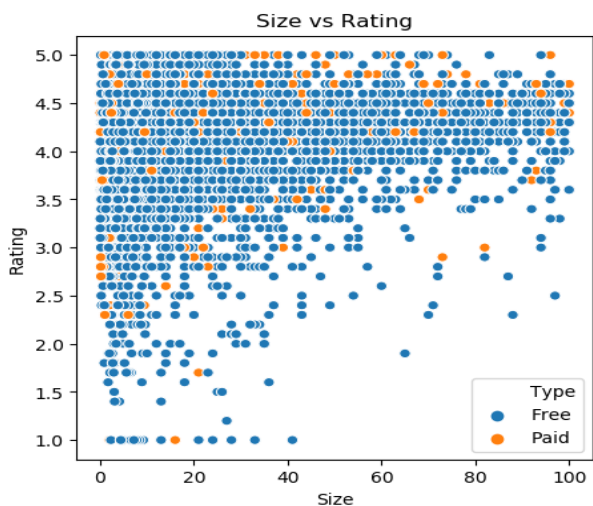


Fig. 11. Correlation between Size and Rating.

Upon drilling down to categories as visualized in Fig. 12 we find out that, average size is higher for Game and Family but these bulky apps are fairly high rated which means that they are bulky for a purpose. To provide better and interactive features in Games developers can enhance its Size. But higher size limits the audience with users that have more space in their smartphones. It's a tradeoff that developers need to balance, for selecting the size of an app, developers should consider its category and respective audience.

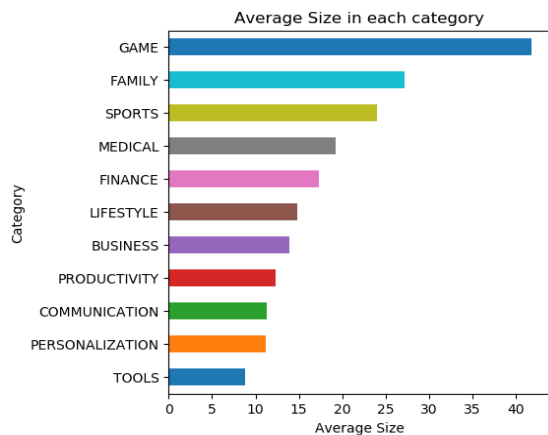


Fig. 12. Average Size in each Category where no of Apps  $\geq 292$ .

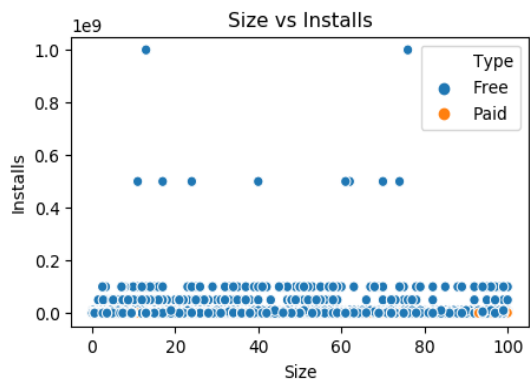


Fig. 13. Correlation between Size and Installs.

No. of Installs is higher for low to medium size apps as plotted in Fig. 13.

E. No. of Reviews

No. of reviews ranges up to 800 million. Average reviews are about 0.2 million. No of reviews are grouped and their grouped frequency is presented in Table XI. No of reviews for Social is at the top as visible in scatter plot of reviews in each category in Fig. 14.

If we compare the average no of reviews for categories in which apps is more than 292, we can see in Fig. 15 that Communication has high average no. of reviews and no. of installs.

F. Reviews

Reviews file has 37,427 translated reviews of 865 unique apps and their calculated sentiment analysis. Sentiment categories and their statistics are presented in Table XII. Sentiment analysis is an automated process of understanding the opinion of a person about a particular subject. Sentiment analysis provides information about polarity and subjectivity. Sentiment count is highlighted in Fig. 16.

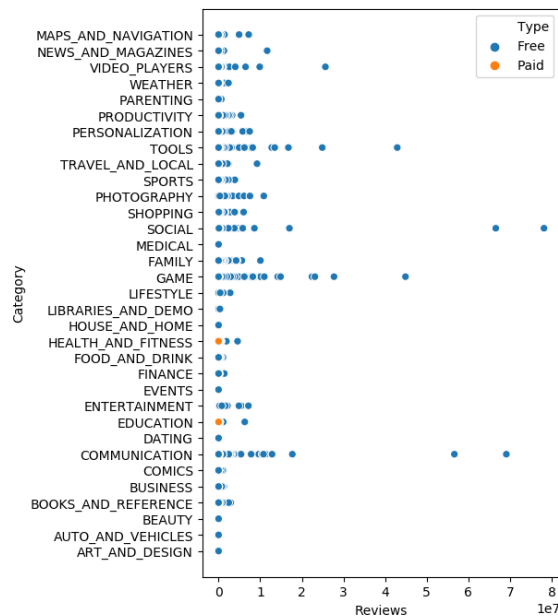


Fig. 14. Reviews Pattern in Each Category.

TABLE XI. REVIEWS STATISTICS

| No. of Reviews                | Count | Percent |
|-------------------------------|-------|---------|
| $R > 0 \ \& \ R \leq 10e7$    | 9628  | 99.7%   |
| $R > 10e7 \ \& \ R \leq 50e7$ | 26    | 0.3%    |
| $R > 50e7 \ \& \ R \leq 80e7$ | 4     | 0.04%   |

TABLE XII. SENTIMENT STATISTICS

| Sentiment | Count | Percent |
|-----------|-------|---------|
| Positive  | 23998 | 64%     |
| Negative  | 8271  | 22%     |
| Neutral   | 5158  | 14%     |

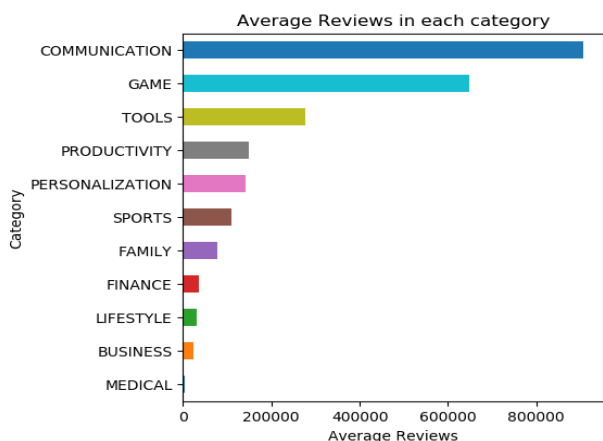


Fig. 15. Average Reviews in each Category where no of Apps  $\geq 292$ .

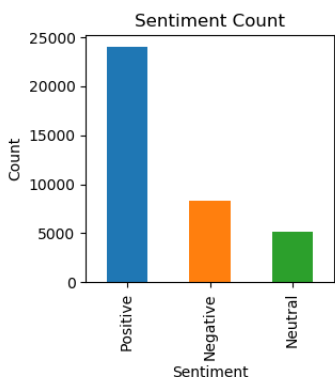


Fig. 16. Sentiment Count for Positive, Negative and Neutral.

The polarity of sentiment lies between -1 to 1, where 1 means positive and -1 means negative. Frequency distribution for sentiment polarity is given in Table XIII. In this data, the polarity of most reviews lies in the range of [-0.25, 0.5] as can be seen in polarity distribution in Fig. 17.

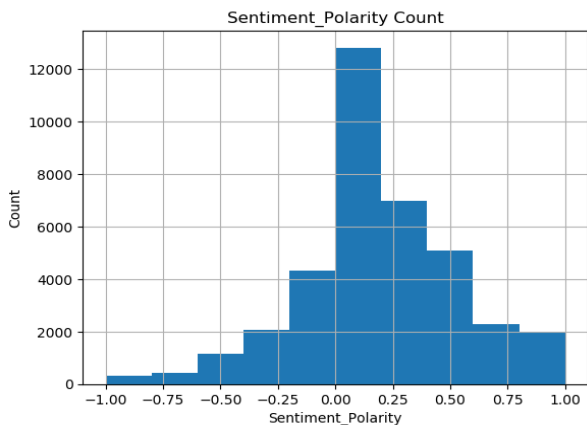


Fig. 17. Distribution of Sentiment Polarity.

TABLE XIII. SENTIMENT POLARITY STATISTICS

| Sentiment Polarity | Count | Percent |
|--------------------|-------|---------|
| SP>-1 & SP<=0      | 13429 | 36%     |
| SP>0 & SP<=1       | 23998 | 64%     |

Subjectivity lies in the range of [0, 1] representing 0 as an objective view or factual information and 1 as a subjective view. Frequency distribution for sentiment subjectivity is given in Table XIV. The subjectivity of most reviews lies in the range of [0.4, 0.8] as plotted in subjectivity distribution in Fig. 18.

Word cloud for top words in reviews is provided in Fig. 19. The most common words in reviews are game, good, app, time, and great.

TABLE XIV. SENTIMENT SUBJECTIVITY STATISTICS

| Sentiment Subjectivity | Count | Percent |
|------------------------|-------|---------|
| SS>0 & SS<=0.5         | 18151 | 48%     |
| SS>0.5 & SS<=1         | 19276 | 52%     |

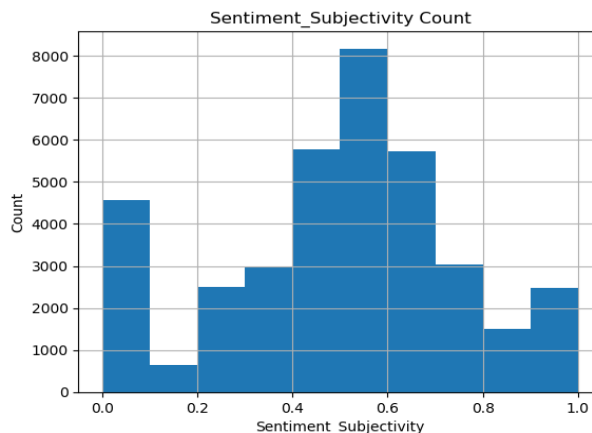


Fig. 18. Distribution of Sentiment Subjectivity.



Fig. 19. Word Cloud for Top 50 Words in Reviews.



Fig. 20. Word Cloud for Top 50 Words in Reviews with Positive Sentiment.

Word cloud for top words with positive sentiment in reviews is provided in Fig. 20. Top words for positive sentiment are great, good, time, love and game.

Customers mostly use simple and short response in positive reviews. Common positive reviews are:

- Great app, good app, killing time.
- Satisfying its purpose like Health apps keep people motivated to be healthy or regulate weight, Education helps in coaching, providing info and easy sharing in Communication apps.
- Appreciating updates.
- Backup and synchronization facilities help to retain the history of user profiles.
- Fewer ads.
- Useful reminders.

Word cloud for top words with neutral sentiment in reviews is plotted in Fig. 21. Most common words for neutral sentiment are work, app, need, phone and time.

Word cloud for top words with negative sentiment in reviews can be visualized in Fig. 22. Common words for negative sentiments are game, app, even, time and make.



Fig. 21. Word Cloud for Top 50 Words in Reviews with Neutral Sentiment.



Fig. 22. Word Cloud for Top 50 Words in Reviews with Negative Sentiment.

Negative reviews are commonly about the Game category and mostly highlight functional errors. Common complaints are:

- Functional errors like slow loading, hanging or freezing apps, utilizing too much memory and synchronization issues, frequently crashing apps.
- No updates and repairs.
- Excessive ads.
- High price with limited functionality
- Needs high bandwidth internet connection for the app to run properly.
- Forced purchases during games.
- Useless notifications.
- Poor navigation, buttons and links not working properly.
- Too much simple and dull apps.

V. CONCLUSION

High ratings and no. of installs are two success parameters considered in this study. After evaluation, we found out that free apps are performing better than paid apps. To get higher ratings, Personalization, Game and Sports are preferable categories with apps size ranging between 2MB to 40MB and priced below 30\$. Exceptionally, bulky apps belonging to games are also getting higher ratings.

To get increased no of installs, Communication, Productivity and Games are preferable. Most of the blockbuster apps with increased installs has high ratings. This sample contains the largest proportion of Family Apps but they are not performing well either in terms of ratings nor installs.

No. of reviews increased with the increase in installs. Users tend to write a review either he is extremely satisfied or dissatisfied. Reviews, ratings and installs show that most of the users are satisfied with apps available on Google play store. Good reviews mostly contain short and simple words and highlight app usability, updates, history retainment and limited ads. User complaints are more elaborate and cover functional errors about the delayed response, frequent crashes, and issues like infrequent updates, excessive ads, limited functionality and high purchase price.

Sports, Tools and Medical categories have quite a potential for developers to work on.

REFERENCES

[1] "Google Play Store: number of apps 2018 | Statista", Statista, 2019. [Online]. Available: <https://www.statista.com/statistics/266210/number-of-available-applications-in-the-google-play-store/>. [Accessed: 28- Apr-2019].

[2] Liu, Charles Z., Yoris A. Au, and Hoon Seok Choi. "An empirical study of the freemium strategy for mobile apps: Evidence from the google play market." (2012)

- [3] Viennot, Nicolas, Edward Garcia, and Jason Nieh. "A measurement study of google play." In ACM SIGMETRICS Performance Evaluation Review, vol. 42, no. 1, pp. 221-233. ACM, 2014.
- [4] Allix, Kevin, Tegawendé F. Bissyandé, Jacques Klein, and Yves Le Traon. "Androzo: Collecting millions of android apps for the research community." In 2016 IEEE/ACM 13th Working Conference on Mining Software Repositories (MSR), pp. 468-471. IEEE, 2016.
- [5] Zhong, Nan, and Florian Michahelles. "Google play is not a long tail market: an empirical analysis of app adoption on the Google play app market." In Proceedings of the 28th Annual ACM Symposium on Applied Computing, pp. 499-504. ACM, 2013.
- [6] Guzman, Emitza, and Walid Maalej. "How do users like this feature? a fine grained sentiment analysis of app reviews." In 2014 IEEE 22nd international requirements engineering conference (RE), pp. 153-162. IEEE, 2014.
- [7] Ruiz, Israel J. Mojica, Meiyappan Nagappan, Bram Adams, Thorsten Berger, Steffen Dienst, and Ahmed E. Hassan. "Examining the rating system used in mobile-app stores." IEEE Software 33, no. 6 (2016): 86-92.
- [8] Nayebi, Maleknaz, Bram Adams, and Guenther Ruhe. "Release Practices for Mobile Apps--What do Users and Developers Think?." In 2016 IEEE 23rd international conference on software analysis, evolution, and reengineering (saner), vol. 1, pp. 552-562. IEEE, 2016.
- [9] Martin, William. "Causal impact for app store analysis." In Proceedings of the 38th International Conference on Software Engineering Companion, pp. 659-661. ACM, 2016.
- [10] McIlroy, S., Ali, N. and Hassan, A. (2015). Fresh apps: an empirical study of frequently-updated mobile apps in the Google play store. Empirical Software Engineering, 21(3), pp.1346-1370.
- [11] Comino, Stefano, Fabio M. Manenti, and Franco Mariuzzo. "Updates management in mobile applications. iTunes vs Google Play." (2016).
- [12] Martin, William, Federica Sarro, and Mark Harman. "Causal impact analysis applied to app releases in Google Play and Windows Phone Store." RN 15.07 (2015).
- [13] Palomba, Fabio, Mario Linares-Vásquez, Gabriele Bavota, Rocco Oliveto, Massimiliano Di Penta, Denys Poshyvanyk, and Andrea De Lucia. "Crowdsourcing user reviews to support the evolution of mobile apps." Journal of Systems and Software 137 (2018): 143-162.
- [14] Lee, Gunwoong, and T. S. Raghu. "Product Portfolio and Mobile Apps Success: Evidence from App Store Market." In AMCIS. 2011.
- [15] Cheng, Hsing Kenneth, and Qian Candy Tang. "Free trial or no free trial: Optimal software product design with network effects." European Journal of Operational Research 205, no. 2 (2010): 437-447.
- [16] Hsu, Chin-Lung, and Judy Chuan-Chuan Lin. "What drives purchase intention for paid mobile apps?—An expectation confirmation model with perceived value." Electronic Commerce Research and Applications 14, no. 1 (2015): 46-57.
- [17] Khalid, Hammad, Emad Shihab, Meiyappan Nagappan, and Ahmed E. Hassan. "What do mobile app users complain about?." IEEE Software 32, no. 3 (2015): 70-77.
- [18] Khalid, Hammad. "On identifying user complaints of iOS apps." In Proceedings of the 2013 International Conference on Software Engineering, pp. 1474-1476. IEEE Press, 2013.
- [19] Hassan, Safwat, Chakkrit Tantithamthavorn, Cor-Paul Bezemer, and Ahmed E. Hassan. "Studying the dialogue between users and developers of free apps in the google play store." Empirical Software Engineering 23, no. 3 (2018): 1275-1312.
- [20] Vu, Phong Minh, Hung Viet Pham, and Tung Thanh Nguyen. "Phrase-based extraction of user opinions in mobile app reviews." In Proceedings of the 31st IEEE/ACM International Conference on Automated Software Engineering, pp. 726-731. ACM, 2016.
- [21] Picoto, Winnie Ng, Ricardo Duarte, and Inês Pinto. "Uncovering top-ranking factors for mobile apps through a multimethod approach." Journal of Business Research (2019).
- [22] Wang, Shujun. "Determinants of mobile apps downloads: A systematic literature review." In The European Conference on Information Systems Management, pp. 353-360. Academic Conferences International Limited, 2017.
- [23] Song, Chihoon, Kyungdo Park, and Byung Cho Kim. "Impact of Online Reviews on Mobile App Sales: Open Versus Closed Platform Comparison." In PACIS, p. 12. 2013.
- [24] Dibia, Victor, and Christian Wagner. "Success within app distribution platforms: The contribution of app diversity and app cohesivity." In 2015 48th Hawaii International Conference on System Sciences, pp. 4304-4313. IEEE, 2015.
- [25] He, Xiaoyun. "Understanding the mobile app markets: demand, supply, and value creation." (2018).
- [26] Wan, Jinlin, Ling Zhao, Yaobin Lu, and Sumeet Gupta. "Evaluating app bundling strategy for selling mobile apps: an ambivalent perspective." Information Technology & People 30, no. 1 (2017): 2-23.
- [27] "Google Play Store Apps". 2019. Kaggle.Com. <https://www.kaggle.com/lava18/google-play-store-apps/activity>.



# Emotion Detection in Text using Nested Long Short-Term Memory

Daniel Haryadi<sup>1</sup>, Gede Putra Kusuma<sup>2</sup>

Computer Science Department, BINUS Graduate Program, Master of Computer Science  
Bina Nusantara University, Jakarta, Indonesia, 11480

**Abstract**—Humans have the power to feel different types of emotions because human life is filled with many emotions. Human's emotion can be reflected through reading or writing a text. In recent years, studies on emotion detection through text has been developed. Most of the study is using a machine learning technique. In this paper, we classified 7 emotions such as anger, fear, joy, love, sadness, surprise, and thankfulness using deep learning technique that is Long Short-Term Memory (LSTM) and Nested Long Short-Term Memory (Nested LSTM). We have compared our results with Support Vector Machine (SVM). We have trained each model with 980,549 training data and tested with 144,160 testing data. Our experiments showed that Nested LSTM and LSTM give better performance than SVM to detect emotions in text. Nested LSTM gets the best accuracy of 99.167%, while LSTM gets the best performance in term of average precision at 99.22%, average recall at 98.86%, and f1-score at 99.04%.

**Keywords**—Sentiment analysis; emotion detection; text mining; nested LSTM; machine learning

## I. INTRODUCTION

According to Liu, sentiment analysis is a field of study that analyzes opinions, sentiments, evaluations, judgments, behaviors, and emotions towards an entity such as products, services, organizations, individuals, issues, events, topics, and attributes [1]. Sentiment analysis analyzes each word or phrase and determines the orientation of the polarity of its sentiments, whether it is positive and negative [2]. Sentiment analysis is closely related to emotion detection. In computer science, text categorization in emotional states is known as sentiment analysis or emotion detection [3]. Text can trigger emotions when someone who reads the text and also can reflect or express the emotional state of the person who wrote it [4]. Humans have the power to feel different types of emotions because human life is filled with many emotions. Happy (joy), fear, anger, and sadness are some of the emotional states that can be found in everyday life [3].

Using a machine learning technique, we could use a computer to learn emotion from the text. In machine learning, computers are not taught to solve a problem by using a set of rules that have been programmed, but by making a model that can evaluate an example so it can predict a sentiment or emotion [5]. Part of machine learning is deep learning, which is also part of artificial intelligence [5]. Deep learning uses deep neural networks to study input data that can be a good representation, which can then perform a specific task [5]. Also, sentiment analysis (positive or negative) using deep learning has been showed to have a better accuracy compared

to the traditional machine learning such as Naïve Bayes (NB) and SVM in [6].

Many studies about emotional detection have been carried out. Many of them are using machine learning techniques. One example of the study of emotional detection in texts conducted in Indonesia in 2012. In this study, emotions are grouped into 6 types, namely excitement, sadness, fear, anger, disgust, and surprise. It uses the methods of NB and K-Nearest Neighbors (KNN) [7]. In addition, there was also a study on evaluating traditional machine learning methods such as NB, SVM, KNN, and J48 for emotion detection in 2016 [8]. However, these studies do not use deep learning methods.

One of the methods of deep learning is LSTM. A study conducted in 2018 shows LSTM can be used to carry out sentiment analysis for classifying sentiment into positive and negative sentiments [9]. LSTM itself has various kinds of architectures such as Nested LSTM, Bi-LSTM, Gated Recurrent Unit (GRU), and Backpropagation Through Time (BPTT). The latest variant found in 2018 is Nested LSTM. Nested LSTM is claimed to be superior to stacking LSTM layers or commonly called Stacked LSTM [10]. Therefore, we are interested in examining the emotion detection found in the text by using deep learning, especially Nested LSTM.

## II. RELATED WORKS

Before working on our research, we have reviewed some works that have been done related to our research. Summary of related works on emotion detection or emotion classification is shown in Table I.

In recent years, various methods of emotional detection have been proposed. In 2012, there was a study using the Multinomial Naïve Bayes (MNB) method and the classification of LIBLINEAR for emotion classification [11]. In this study, the effect of increasing datasets on the classification of MNB and LIBLINEAR was evaluated. They found out that increasing datasets could improve accuracy. The MNB reached 61.15% accuracy and LIBNEAR achieved 61.63% accuracy. Still, in the same year, an emotional detection study was also conducted by comparing the NB method with KNN [7]. In this study, KNN obtained better accuracy at 71.26% than NB at 58.01% for the classification task.

In 2014, a study was conducted using the KNN, PMI, and PMI-IR as classifiers [12]. KNN classifier is used to measure semantic and keyword similarities. When the KNN classifier fails to classify, then the PMI or PMI-IR classifier will be used

to classify again. In 2015, a study showed that emotion detection could be determined by proposing the Maximum Vector and Entropy Machine Support algorithm [13].

TABLE. I. SUMMARY OF RELATED WORKS

| No | Year of research | Title   | Classification  | Method / Algorithm  | Reported Accuracy |
|----|------------------|---|---|---|-------------------|
| 1  | 2012 [11]        | Harnessing Twitter 'Big Data' for Automatic Emotion Identification                                    | Joy, sadness, anger, love, fear, thankfulness, surprise       | Multinomial Naïve Bayes (MNB) dan LIBLINEAR   | 61.63%            |
| 2  | 2012 [7]         | Classification of Emotions in Indonesian Texts Using K-NN Method                                      | Anger, fear, sadness, joy, disgust, shame                     | Naïve Bayes dan K-Nearest Neighbor  | 71.26%            |
| 3  | 2014 [12]        | Emotion Recognition from Text Based on Automatically Generated Rules                                  | Happiness, sadness, surprise, disgust, anger, fear            | KNN classifier, Point Mutual Information (PMI) classifier, and Point Mutual Information with Information Retrieval (PMI-IR) | -                 |
| 4  | 2015 [13]        | Emotion Detection from Punjabi Text using Hybrid Support Vector Machine and Maximum Entropy Algorithm | joy, surprise, anger, love, fear, sadness, disgust            | Support vector machine and maximum entropy.   | -                 |
| 5  | 2016 [14]        | Evaluation of Classification Methods for Indonesian Text Emotion Detection                            | Anger, disgust, fear, joy, sadness, and surprise.             | Naïve Bayes, J48, K-Nearest Neighbor, Support Vector Machine Minimal Optimization (SVM-SMO)                                 | 85.5%             |
| 6  | 2017 [15]        | Detecting Emotion from Text and Emoticon  | 25 emotion such as sad, hurt, happy, angry, confused, advice. | matching keyword analysis, keyword negation analysis, gathering proverbs, emoticon, simplify the word, dan exclamatory word | 80%               |
| 7  | 2017 [16]        | EmoTxt: A Toolkit for Emotion Recognition from Text   | Love, joy, anger, sadness, surprise, fear                     | Support Vector Machine  | -                 |

In 2016, an evaluation of several classification methods for emotional detection in the text was carried out [14]. In the study, evaluations were carried out on the NB, J48, KNN, and SVM-SMO methods. Experiments were conducted using Indonesian texts, which consist of 1000 sentences containing 6 classifications, namely anger, disgust, fear, joy, sadness, and surprise. Preprocessing was done using tokenization, case normalization, stop word removal, stemming. The Term Frequency-Inverse Document Frequency (TF-IDF) was used to extract features. From the results of the study, it can be seen that the SVM-SMO has the highest accuracy compared to the other methods. The results show that the accuracy of NB, J48, KNN, and SVM-SMO are 80.2%, 80.8%, 68.1%, and 85.5% respectively.

Emotion detection study was also carried out in 2017 using keyword analysis matching method, keyword negation analysis, collection of proverbs, emoticons, short forms of words, and exclamations [15]. This study achieved 80% accuracy in classifying 25 emotions. Still, in the same year, a toolkit named EmoTxt was proposed to classify emotions. EmoTxt was developed using the SVM method [16].

From the review on related works, it can be concluded that SVM is a method that produces the best level of accuracy and has been successfully implemented. Thus, we chose SVM as a benchmark method. However, the achieved accuracy has not been satisfactory. Therefore, a deep learning approach is proposed in this work, since deep learning has been shown to be superior to the traditional machine learning methods.

One of the deep learning models is LSTM. The LSTM has been proven to be able to classify both positive and negative sentiments. Besides LSTM, there are also variants of LSTM. One of them is Nested LSTM, which is claimed to have better accuracy than LSTM in making predictions on the character-level prediction of Chinese poetry generation [10]. Therefore, in this study, LSTM and Nested LSTM are examined whether the methods can be used to make better predictions on emotion detection. The classification tasks are not only on positive and negative sentiments, but on multiple emotions classification, namely anger, fear, joy, love, sadness, surprise, and thankfulness.

### III. RESEARCH METHOD

#### A. Dataset

Lots of people expressed their feeling on Twitter. That is the reason Twitter has many resources for opinion or idea about what people feel or think. On the previous study on big data for emotion identification, this work has successfully retrieved more than 2 million tweets on the Twitter site as their dataset in 2012 [11]. Unfortunately, not all of the data can be retrieved because of the Twitter privacy policy. They can share only the tweet id and classification. By utilizing Twitter API, we retrieve the text by tweet id. We have successfully retrieved 980,549 training data and 144,160 testing data. Table II shows the distribution of dataset, which is used in this experiment. Meanwhile, Table III shows some examples of the dataset. This table shows the sample text and the classification category that text belongs to.

TABLE. II. DATASET FOR EXPERIMENT

|              | Training Data | Testing data | Total     |
|--------------|---------------|--------------|-----------|
| Anger        | 214,324       | 31,459       | 245,783   |
| Fear         | 52,763        | 7,992        | 60,755    |
| Joy          | 282,861       | 41,783       | 324,644   |
| Love         | 121,830       | 17,812       | 139,642   |
| Sadness      | 242,840       | 35,434       | 278,274   |
| Surprise     | 9,739         | 1,452        | 11,191    |
| Thankfulness | 56,192        | 8,228        | 64,420    |
| Total        | 980,549       | 144,160      | 1,124,709 |

TABLE. III. SOME EXAMPLES OF THE DATASET

| No | Tweet   | Classification |
|----|---|----------------|
| 1  | adam levinne is my #love #sohot   | Love           |
| 2  | Aaliyahs Christmas is almost done ;) #Excitement  | Joy            |
| 3  | I think I miss my boyfriend.. :( #lonely  | Sadness        |
| 4  | Two big parcels from Francais just arrived courtesy the nicest mailman in the world. #thankful                      | Thankfulness   |
| 5  | @NathanTheWanted Please could you wish me good luck with my prelims? :D It would honestly mean so much! #nervous xx | Fear           |
| 6  | She's not here again #surprise  | Surprise       |
| 7  | It doesn't really make sense that the Big EAST now has 4 teams from way WEST. #desperation                          | Sadness        |

B. Preprocessing

To be able to detect emotion, there are steps need to be done. The first step is preprocessing. Fig. 1 shows the illustration of the preprocessing for the LSTM and Nested LSTM. Preprocessing carried out in this study is eliminating punctuations and changing words into all lowercase letters. The punctuations such as [! " # \$ % & ' ( \* ) + , - . / \ : ; < = > ? @ \ ^ \_ { } | ~ ] are excluded. Then, each word in the sentence is represented by an integer, where the integer is unique for each different word. Then, the addition of padding "0" in the beginning so that each sentence has the same length. When that step is done, the integer will be an input for the neural network. In this preprocessing stage, we also calculate the unique number of words in the training data and the highest number of words in one sentence. There are unique words in the training data and the highest number of words in one sentence is 41 words. These parameters will be used later in the processing layer.

On the other hand, the benchmark method of SVM needs a feature extraction to be able to do the classification. We use TF-IDF as features for the SVM. However, for LSTM and Nested LSTM, we did not use it because a deep neural network does not need a feature extraction method. In this experiment, we use TfidfVectorizer from the Sklearn library to implement preprocessing and convert the text into TFIDF weight.

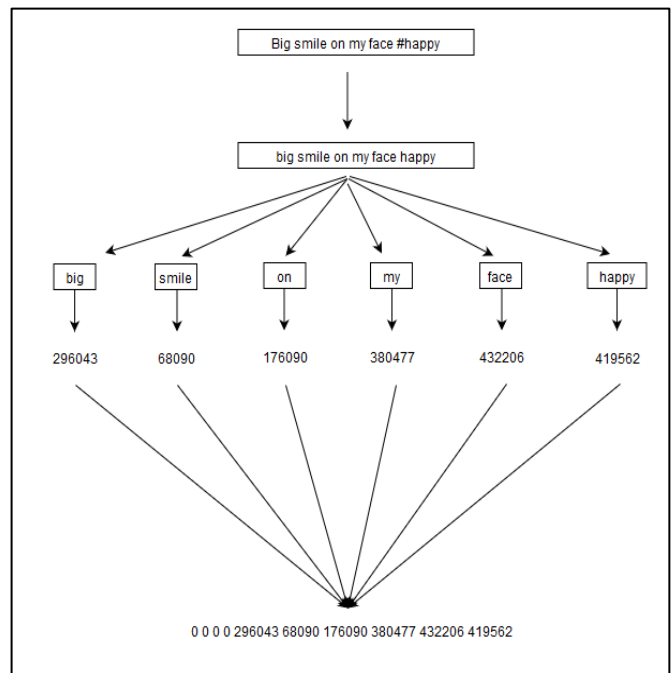


Fig. 1. Preprocessing for LSTM and Nested LSTM.

C. Emotion Classification

Fig. 2 shows an illustration of LSTM modeling using the Keras library. The followings are the specifications of the parameters used in conducting training:

a) Embedding layer

- Input dimension = 502,882 (number of unique words)
- Output dimension = 50 (size of embedding vector)
- Input length = 41

b) LSTM layer

- Units = 50
- Dropout = 0.2

c) Output layer

- Units = 7
- Activation = SoftMax

The embedding layer requires some parameters as its input. In the preprocessing step, we have calculated the highest number of words in one sentence that is 41 words. We put that value as the input length parameter for the embedding layer. That means there are 41 times steps of word embedding. The embedding layer only has one neuron. Every word that passed into this neuron will be transformed into a real-valued vector of length 50 (output dimension). Once the network has been trained, we can get the weights of the embedding layer, which in this case will be of size (502882, 50). It means that every word has one real-valued vector of length 50. The embedding process is implemented based on the word2vec embedding method of Mikolov *et al.* [17].

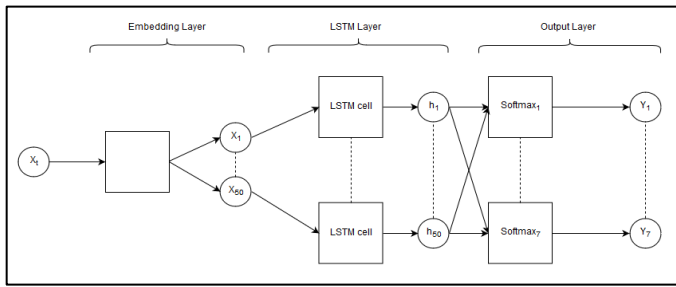


Fig. 2. Processing Layers of LSTM Model.

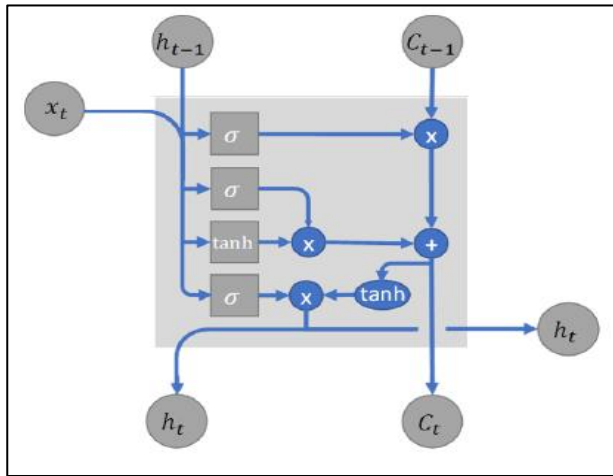


Fig. 3. LSTM Cell [9].

In this experiment, we set the LSTM cell to 50. Each LSTM cell will produce an output vector that is connected to the output layer. The LSTM cell can be seen in Fig. 3. Each LSTM cell consists of 4 gates that process each vector input. At the end of the process, each cell will produce an output that will be used for the output layer.

The first step of LSTM in Fig. 4(A) is a forget gate layer, which has sigmoid activation function that gives an output of 0 or 1. 0 means “let nothing through” and 1 “remember anything”. Next, Fig. 4(B) is to decide which information will be stored. The sigmoid layer (input gate layer) to decide which value will be updated and the tanh layer is creating new candidate values between  $-1$  and  $1$ . Next step, Fig. 4(C), the old cell state is multiplied by output from forget gate, to forget the things that are not needed anymore, and the new information is added to the cell state. The final step in Fig. 4(D) is to decide the output. First, we run a sigmoid layer that decides what parts of the cell state we are going to output. Then, we put the cell state through tanh (to push the values to be between  $-1$  and  $1$ ) and multiply it by the output of the sigmoid gate, so that we only output the parts we decided to [18] [9].

At the output layer, there are 7 neurons where each of these neurons has SoftMax activation to produce values for each classification. The prediction will be based on the highest output value. In the training phase, we use Adam optimizer with a learning rate of 0.00001.

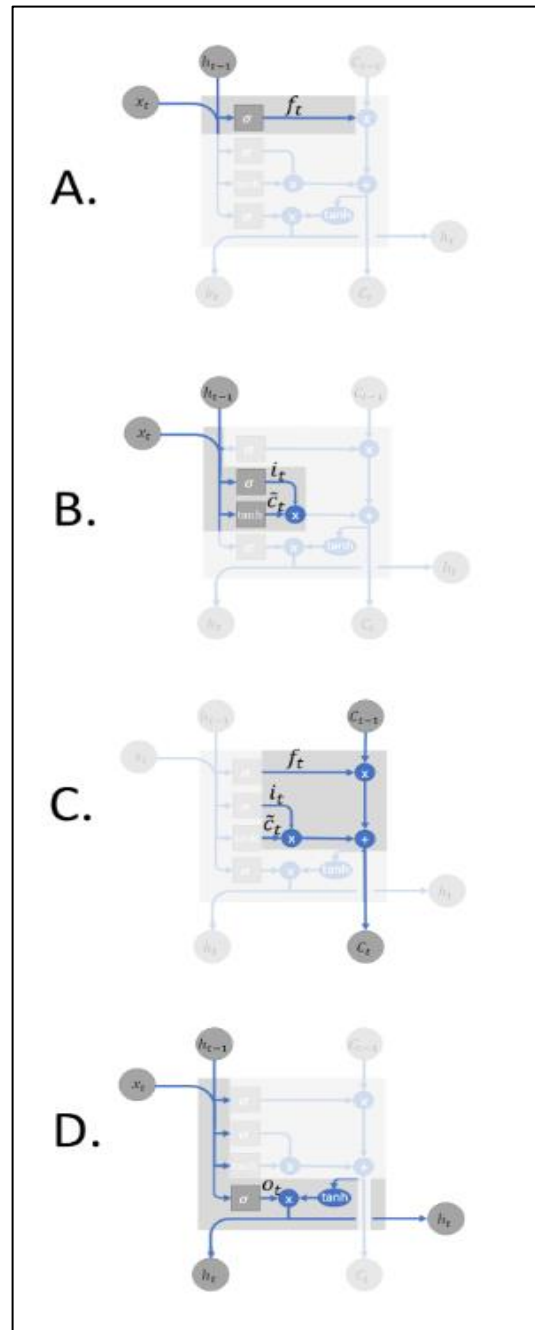


Fig. 4. LSTM Steps [9].

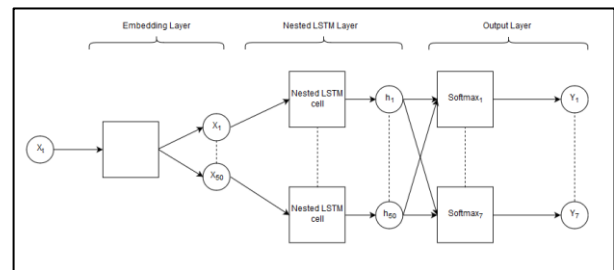


Fig. 5. Preprocessing Layers of Nested LSTM Model.

We also replaced the LSTM layer into Nested LSTM Layer in the experiments. Fig. 5 is an illustration of Nested LSTM modeling. The model consists of several layers, including:

- a) *Embedding Layer*
  - *Input dimension*=502,882 (number of unique word)
  - *Output dimension*=50 (size of embedding vector)
  - *Input length*=41
- b) *Nested LSTM Layer*
  - *Units*=50
  - *Dropout*=0.2
  - *Depth*=2
- c) *Output Layer*
  - *Units*=7
  - *Activation* = SoftMax

The Nested LSTM is similar to the LSTM. The only difference between with LSTM and Nested LSTM is the second layer. Fig. 6 shows nested LSTM cell with depth = 2.

The Nested LSTM is a simple extension of LSTM. Instead of creating stacked LSTM, Nested LSTM created another LSTM via nesting. They called it inner LSTM. The inner memory cells of Nested LSTM form an internal memory, which is only accessible to other computational elements via the outer memory cells, implementing a form of temporal hierarchy. Inner LSTM gets the input from outer LSTM. Nested LSTM replaces the addition operation in Fig. 4(C) on LSTM steps to compute  $c_t$  in LSTM with a concatenation to be an input for inner LSTM [10].

As a comparison to the LSTM and Nested LSTM, we also train SVM with the same training data. To create the SVM model with large scale data, we use SGDClassifier [19] from Scikit-learn library [20], which is a linear classifier of SVM. All parameter used is default parameters, except for the *random\_state* parameter that is set to 0. After all models are created, the models are then tested using the testing data.

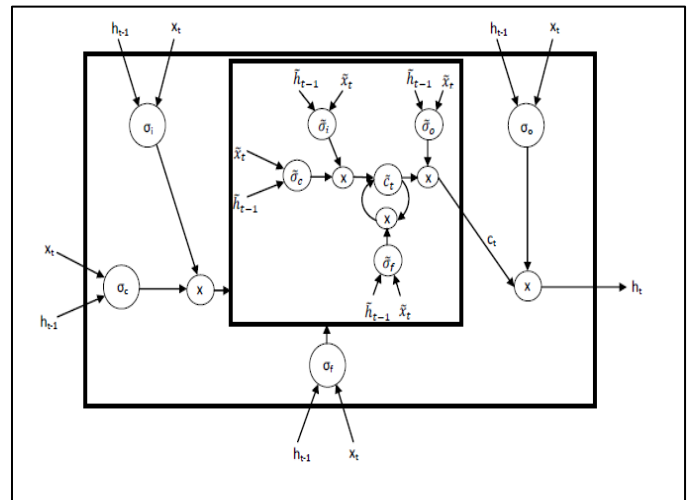


Fig. 6. Nested LSTM Cell [10].

#### IV. EXPERIMENT AND RESULT

##### A. Experiment

During training LSTM and Nested LSTM model, we recorded every epoch of the model as a checkpoint to get accuracy and loss progress. We set the maximum number of the epoch at 50. The accuracy and loss outputs of the LSTM and Nested LSTM from the checkpoints are recorded.

Fig. 7 shows the accuracy and loss outputs of LSTM during the training phase. The loss value is decreased and the accuracy is increased at every epoch of the LSTM model training. The blue line (top) shows the accuracy and the orange line (bottom) shows the loss value. At the end of 50 epoch, the training reaches an accuracy of 100% and a loss value of 0.2%.

Fig. 8 shows the accuracy and loss outputs of Nested LSTM during the training phase. The loss value is also decreased and the accuracy is also increased at every epoch of the Nested LSTM model training. The yellow line (top) shows the accuracy and the blue line (bottom) shows the loss value. At the end of 50 epoch, the Nested LSTM training reaches an accuracy of 99.9% and a loss of 0.3%.

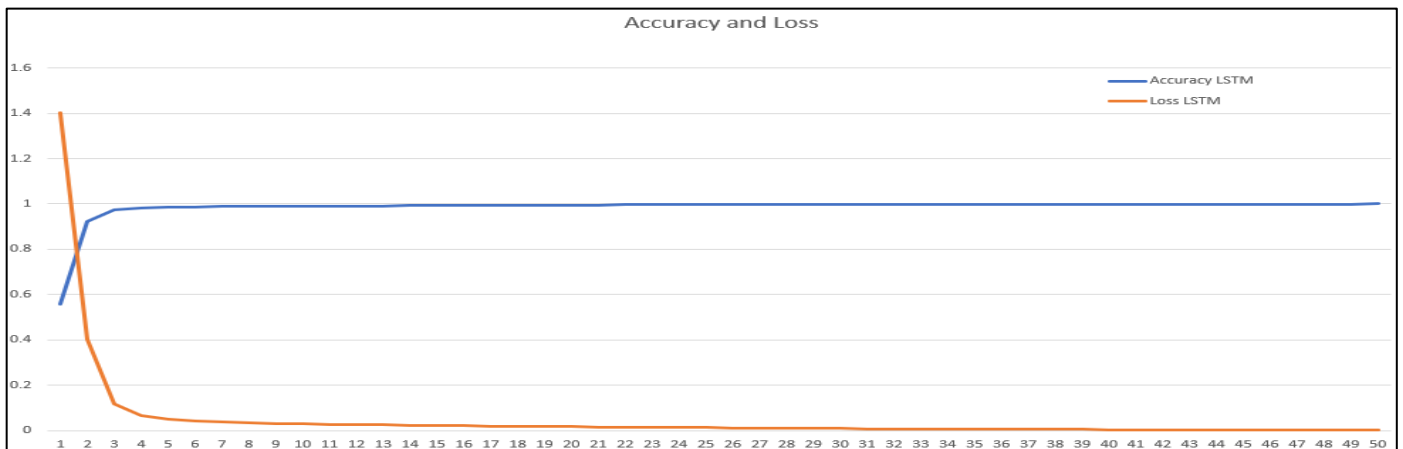


Fig. 7. Accuracy and Loss Outputs of LSTM During Training.

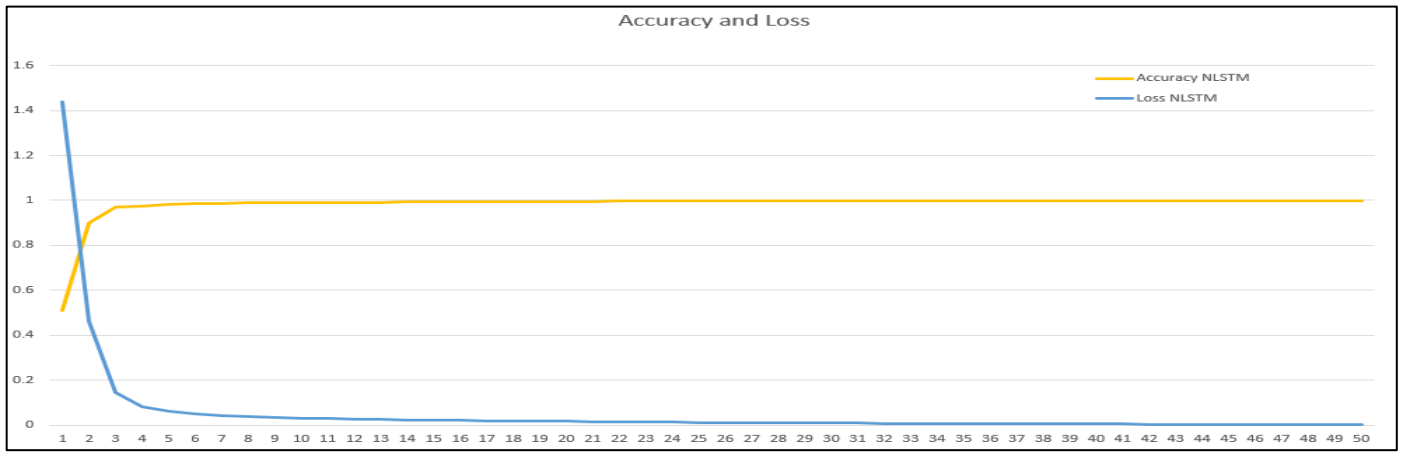


Fig. 8. Accuracy and Loss Outputs of Nested LSTM During Training.

**B. Testing Result**

Table IV shows a confusion matrix for the LSTM method. In this table, A is for Anger; B is for Fear; C is for Joy; D is for Love; E is for sadness; F is for surprise, and G is for thankfulness. The LSTM model is tested using 144.160 testing data. The LSTM achieves an overall accuracy of 99.154%.

Table V shows the precision, recall, and f1-score for the LSTM method. The performances of the LSTM method on each class and its average performances are calculated based on the confusion matrix. The LSTM method yields an average precision of 99.22% and an average recall of 98.86%, and therefore an average f1-score of 99.04%.

Table VI shows a confusion matrix for the Nested LSTM method. The Nested LSTM model is also tested using 144.160 testing data. The Nested LSTM achieves an overall accuracy of 99.167%.

TABLE IV. CONFUSION MATRIX FOR LSTM

|        |   | Predicted |      |       |       |       |      |      |
|--------|---|-----------|------|-------|-------|-------|------|------|
|        |   | A         | B    | C     | D     | E     | F    | G    |
| Actual | A | 31247     | 12   | 62    | 21    | 107   | 0    | 10   |
|        | B | 29        | 7870 | 54    | 8     | 29    | 0    | 2    |
|        | C | 79        | 28   | 41539 | 56    | 61    | 1    | 19   |
|        | D | 27        | 11   | 54    | 17680 | 32    | 0    | 8    |
|        | E | 183       | 31   | 125   | 44    | 35032 | 2    | 17   |
|        | F | 9         | 3    | 7     | 7     | 9     | 1416 | 1    |
|        | G | 7         | 7    | 33    | 10    | 14    | 0    | 8157 |

TABLE V. PRECISION, RECALL, AND F1-SCORE OF LSTM

| Class          | Precision     | Recall        | F1-Score      |
|----------------|---------------|---------------|---------------|
| Anger          | 98.94%        | 99.33%        | 99.13%        |
| Fear           | 98.84%        | 98.47%        | 98.66%        |
| Joy            | 99.20%        | 99.42%        | 99.31%        |
| Love           | 99.18%        | 99.26%        | 99.22%        |
| Sadness        | 99.29%        | 98.87%        | 99.08%        |
| Surprise       | 99.79%        | 97.52%        | 98.64%        |
| Thankfulness   | 99.31%        | 99.14%        | 99.22%        |
| <b>Average</b> | <b>99.22%</b> | <b>98.86%</b> | <b>99.04%</b> |

TABLE VI. CONFUSION MATRIX FOR NESTED LSTM

|        |   | Predicted |      |       |       |       |      |      |
|--------|---|-----------|------|-------|-------|-------|------|------|
|        |   | A         | B    | C     | D     | E     | F    | G    |
| Actual | A | 31206     | 22   | 76    | 16    | 133   | 1    | 5    |
|        | B | 20        | 7855 | 66    | 12    | 37    | 1    | 1    |
|        | C | 38        | 23   | 41587 | 45    | 76    | 5    | 9    |
|        | D | 21        | 6    | 74    | 17672 | 32    | 1    | 6    |
|        | E | 118       | 49   | 148   | 44    | 35072 | 1    | 2    |
|        | F | 6         | 5    | 13    | 0     | 12    | 1416 | 0    |
|        | G | 11        | 5    | 31    | 15    | 15    | 0    | 8151 |

Table VII shows the precision, recall, and f1-score for the Nested LSTM method. The performances of the Nested LSTM method on each class and its average performances are calculated based on the confusion matrix. The Nested LSTM method achieves an average precision of 99.21% and an average recall of 98.83%, and therefore an average f1-score of 99.02%. Meanwhile, Table VIII shows a confusion matrix for the SVM method. The SVM model is also tested using 144.160 testing data. The SVM achieves an overall accuracy of 98.679%. Thus, the SVM model yields the lowest accuracy compared to the LSTM and Nested LSTM models.

Table IX shows the precision, recall, and f1-score for the SVM method. The performances of the SVM method on each class and its average performances are calculated based on the confusion matrix. The SVM method achieves an average precision of 98.53% and an average recall of 98.22%, and therefore an average f1-score of 98.37%. Its performances are lower than the LSTM and Nested LSTM methods.

Comparison of accuracy, precision, recall, and f1-score from all three models can be seen in Table X. Nested LSTM produces the best accuracy of 99.167% among the three methods, even though the difference in accuracy is not significantly different from the LSTM. But on average, LSTM obtained precision, recall, and f1-scores that are better than the Nested LSTM. The Nested LSTM and LSTM get better scores, in terms of accuracy, precision, recall, and f1-score, compared to the SVM.

TABLE. VII. PRECISION, RECALL AND F1-SCORE OF NESTED LSTM

| Class          | Precision     | Recall        | F1-Score      |
|----------------|---------------|---------------|---------------|
| Anger          | 99.32%        | 99.20%        | 99.26%        |
| Fear           | 98.62%        | 98.29%        | 98.45%        |
| Joy            | 99.03%        | 99.53%        | 99.28%        |
| Love           | 99.26%        | 99.21%        | 99.24%        |
| Sadness        | 99.14%        | 98.98%        | 99.06%        |
| Surprise       | 99.37%        | 97.52%        | 98.44%        |
| Thankfulness   | 99.72%        | 99.06%        | 99.39%        |
| <b>Average</b> | <b>99.21%</b> | <b>98.83%</b> | <b>99.02%</b> |

TABLE. VIII. CONFUSION MATRIX FOR SVM

|        |   | Predicted |      |       |       |       |      |      |
|--------|---|-----------|------|-------|-------|-------|------|------|
|        |   | A         | B    | C     | D     | E     | F    | G    |
| Actual | A | 31325     | 7    | 16    | 7     | 51    | 1    | 0    |
|        | B | 4         | 7874 | 17    | 5     | 18    | 1    | 0    |
|        | C | 21        | 40   | 41211 | 315   | 134   | 12   | 15   |
|        | D | 52        | 40   | 386   | 17330 | 288   | 14   | 29   |
|        | E | 47        | 28   | 57    | 43    | 34919 | 3    | 5    |
|        | F | 2         | 3    | 24    | 5     | 8     | 1419 | 1    |
|        | G | 8         | 0    | 72    | 107   | 16    | 2    | 8178 |

TABLE. IX. PRECISION, RECALL AND F1-SCORE OF SVM

| Class          | Precision     | Recall        | F1-Score      |
|----------------|---------------|---------------|---------------|
| Anger          | 99.57%        | 99.74%        | 99.66%        |
| Fear           | 98.52%        | 99.43%        | 98.98%        |
| Joy            | 98.63%        | 98.71%        | 98.67%        |
| Love           | 97.29%        | 95.54%        | 96.41%        |
| Sadness        | 98.55%        | 99.48%        | 99.01%        |
| Surprise       | 97.73%        | 97.06%        | 97.39%        |
| Thankfulness   | 99.39%        | 97.55%        | 98.46%        |
| <b>Average</b> | <b>98.53%</b> | <b>98.22%</b> | <b>98.37%</b> |

TABLE. X. SUMMARY OF PERFORMANCE RESULTS

| Model       | Accuracy       | Precision     | Recall        | F1-score      |
|-------------|----------------|---------------|---------------|---------------|
| LSTM        | 99.154%        | <b>99.22%</b> | <b>98.86%</b> | <b>99.04%</b> |
| Nested LSTM | <b>99.167%</b> | 99.21%        | 98.83%        | 99.02%        |
| SVM         | 98.679%        | 98.53%        | 98.22%        | 98.37%        |

## V. CONCLUSION

In this paper, we presented our study on emotion detection from text. Based on the discussion and evaluation carried out in the previous section, LSTM, Nested LSTM, and SVM methods can be used for multi-classes emotion detection. Nested LSTM has the best accuracy among the three methods with the accuracy of 99.167%. This accuracy is not significantly different from the LSTM, which gets an accuracy of 99.154%. LSTM has better average performances in terms of precision, recall, and f1-score, at 99.22%, 98.86%, and 99.04% respectively. In future works, we plan to employ and evaluate other more sophisticated deep learning models to find out the best method for emotion detections tested in a more challenging dataset.

## REFERENCES

- [1] Liu, Sentiment Analysis and Opinion Mining, San Rafael: Morgan & Claypool, 2012.
- [2] H. Rahmath P, "Opinion Mining and Sentiment Analysis - Challenges and Applications," International Journal of Application or Innovation in Engineering & Management, vol. 3, no. 5, pp. 401-403, May 2014.
- [3] J. Kaur and R. J. Saini, "Emotion Detection and Sentiment Analysis in Text Corpus: A Differential Study with Informal and Formal Writing Styles," International Journal of Computer Applications, vol. 101, pp. 1-9, 09 2014.
- [4] S. M. Kim, "Recognising Emotions and Sentiments in Text," University of Sydney, Sydney, 2011.
- [5] N. Buduma, Fundamentals of Deep Learning, Sebastopol: O'Reilly Media, Inc, 2017.
- [6] P. Singhal and P. Bhattacharyya, "Sentiment Analysis and Deep Learning: A Survey," 2016.
- [7] Arifin and K. E. Purnama, "Classification of Emotion in Indonesian Texts Using K-NN methods," International Journal of Information and Electronics Engineering, pp. 899-903, 2012.
- [8] J. Riany, M. Fajar and M. P. Lukman, "Penerapan Deep Sentiment Analysis penerapan Deep Sentiment Analysis," Jurnal Sisfo, vol. 06, pp. 147-156, 2016.
- [9] F. Miedema, "Sentiment Analysis with Long Short-Term Memory networks," 2018.
- [10] J. R. A. Moniz and D. Krueger, "Nested LSTMs," Computing Research Repository, vol. 1801.10308, 2018.
- [11] W. Wang, I. Chen, K. Thirunarayan and A. P. Sheth, "Harnessing Twitter "Big Data" for Automatic Emotion Identification," Proceedings of the 2012 ASE/IEEE International Conference on Social Computing and 2012 ASE/IEEE International Conference on Privacy, Security, Risk and Trust, pp. 587--592, 2012.
- [12] S. Shaheen, W. El-Hajj , H. Hajj and S. Elbassuoni, "Emotion Recognition from Text Based on Automatically Generated Rules," IEEE International Conference on Data Mining Workshops, pp. 383-392, 2015.
- [13] E. U. Jain and A. Sandu, "Emotion Detection from Punjabi Text using Hybrid Support Vector Machine and Maximum Entropy Algorithm," International Journal of Advanced Research in Computer and Communication Engineering, vol. 4, no. 11, 2015.
- [14] Muljono, N. A. S. Winarsih and C. Supriyanto, "Evaluation of Classification Methods for Indonesian Text Emotion Detection," International Seminar on Application for Technology of Information and Communication, pp. 130-133, 2016.
- [15] R. Rahman, T. Islam and M. H. Ahmed, "Detecting Emotion from Text and Emoticon," London Journal of Research in Computer Science and Technology, vol. 17, no. 3, 2017.
- [16] F. Calefato, F. Lanubile and N. Novielli, "EmoTxt: A Toolkit for Emotion Recognition from Text," 2017 Seventh International Conference on Affective Computing and Intelligent Interaction Workshops and Demos, 2017.
- [17] T. Mikolov, I. Sutskever, K. Chen, G. Corrado and J. Dean, "Distributed Representations of Words and Phrases and Their Compositionality," in Proceedings of the 26th International Conference on Neural Information Processing Systems - Volume 2, Lake Tahoe, Nevada, 2013.
- [18] C. Olah, "Understanding LSTM Networks," 27 August 2015. [Online]. Available: <https://colah.github.io/posts/2015-08-Understanding-LSTMs/>. [Accessed 5 May 2019].
- [19] L. Bottou, "Large-Scale Machine Learning with Stochastic Gradient Descent," Proc. of COMPSTAT, pp. 177-186, 2010.
- [20] P. Fabian, G. Varoquaux, A. Gramfort, V. Michel, B. Thirion, O. Grisel, M. Blondel, P. Prettenhofer, R. Weiss, V. Dubourg, J. Vanderplas, A. Passos, D. Cournapeau, M. Brucher, M. Perrot and É. Duchesnay, "Scikit-learn: Machine Learning in Python," Journal of Machine Learning Research, pp. 2825-2830, 2011.

# Dynamic Matrix Control DMC using the Tuning Procedure based on First Order Plus Dead Time for Infant-Incubator

J. El Hadj Ali<sup>1</sup>, E. Feki, A. Mami<sup>2</sup>

University of Tunis El Manar, Faculty of Science  
UR17ES11 LAPER, 2092 Tunis, Tunisia

**Abstract**—The concept of Model Predictive Control (MPC) is considered as one of the most important controlling strategies. It is used in several fields, such as petrochemical, oil refinery, fertilizer and chemical plants. It is also well spread among the clinicians and in the biomedical fields. In this context, our paper aims to investigate the thermal conditions inside the infant incubator for premature babies. In this study, we propose the Dynamic Matrix Control (DMC) as a control strategy. The most particularity of this strategy is applicable to the Multi-input Multi-output (MIMO) systems. It aims to compare different coupled transfer functions achieved by two identification methods in previous work. Also, a simulation of the air temperature and humidity is achieved inside the unit care. In this work, we focus on the tuning controlling parameters because it is considered as a key step in the successful performance of (DMC). Then, to obtain the (DMC), we have used an analytic tool, which is the Process Reaction Curve (PRC), for higher order transfers function because it needs a lot of work for this purpose. It should be approximated as a low order transfer function with time delay, which is achieved by using the First Order Plus Dead Time (FOPDT) of processing models. Finally, the result of the comparison of the infant-incubator is provided to show an optimal and good performance of the thermal behavior of our propos methodology and prove that a good identification ensures a better performance.

**Keywords**—*Infant-incubator; DMC; MPC; higher-order; FOPDT; PRC and MIMO*

## I. INTRODUCTION

It is well-known that the period from 1970 to 1980 witnessed the appearance of the first generation of Model Predictive Control (MPC). One of the most popular MPC technologies called Dynamic Matrix Control (DMC) was developed by a crew of engineers from the Shell Oil company lead up by Culter and Remarker [1, 2]. Also, in 1980, Prett and Gillette [3] presented an application of DMC. Since the existence of the first generation of MPC, this latter has a large effect on the image of the industrial applications.

The DMC is a linear control technique which uses the First Order Plus Dead Time (FOPDT) model. The advantage of this method has already been established and has been found to work correctly for a long period of time DMC is used in the majority of industrial applications, where its biggest particularity lies in the MIMO systems. Besides, the use of the model response to a unit step change is needed to predict the

future response of the dependent parameters and formulates a sequence of control actions for all independent variables. The series of control action is chosen to minimize the error of the process over the time horizon. Also, it is applicable to multivariable processes as long as they are asymptotically stable and without integrators (Prada, Serrano, & Vega, A comparative study of GPC and DMC controllers, 1994) [4]. DMC is used in the implementation of Single-input Single-output (SISO) and MIMO systems, but in this study, focuses only on the multivariable case, particularly two decoupled inputs and two outputs (the temperature and the humidity inside the unit care of the infant incubator).

Over the years the technology witnessed a development in all fields, especially in the biomedical field. Until today, the infant-incubator for the preterm babies is considered as one of the important issues in the neonatal field. The incubators have been designed to achieve a helpful and appropriate hygrothermal environment for the newborn babies. In this context, a neonatal incubator requires agreeable conditions to establish a good range of temperature and humidity also a minimum waste energy. In general the closed incubator structure is depicted with four walls made of one layer of Plexiglas Fig. 1. In addition, all infant incubators perform in the same manner. The fan is used to circulate warm air over a heating element and a water container through two small ports. Also, the majority of the incubator system has a passive humidification system. But in this case, the heater is replaced by a dimmer to permit external control as it is an infinitely variable control.

The essential objective of this study is to develop a mathematical model of the infant incubator and obtain a good tuning of the control strategy to ameliorate the performance of the control inside this device for coupling temperature and humidity and prove that the identification and the tuning play a radical way in the final response.

The outlines of this paper start with a brief introduction. Then, Section 2 presents the related works of the infant incubators over the past years. The dynamic matrix control modeling for MIMO case is described in Section 3. As for Section 4, it highlights the validation of the tuning strategy of the two methods and discusses the simulation results. Then, Section 5 is dedicated to a comparative study of both methods. Finally, the concluding remarks and future works are presented in Section 6.



## II. RELATED WORKS

Over the past few decades, the problem of preterm infants and congenital patients has been addressed as a very important issue. For this reason, many studies in the literature have focused on controlling the relative temperature and humidity of an infant incubator with several strategies of control due to demands to improve the performance of the intensive care unit. Despite all the research and developments in this context, there is still little focus on the incubators controller with the predictive controls, which is the interest of this study.

The predictive control strategy was first brought into use in 2006, within the study of Gustavo H. C. Oliveira which is based on the identification of the Laguerre function [5]. Then, the same researchers proposed a hybrid predictive control for mixed logical and dynamical models [6].

In 2010, the authors of this paper developed a robust predictive control strategy for multivariable systems with multiple delays and input constrains [7].

In [8], the same authors developed an application of Indirect Adaptive Generalized Predictive Control compared with ON-OFF and PID controller. In the same year, they designed a new active system which is able to generate the control of humidity and carried out a comparative study between GA-PID and GA-MPC [9].

In 2014, the authors developed a theoretical model for the thermal behavior (air temperature and relative humidity) which was controlled by decoupling the generalized predictive controller (DGPC) in order to achieve optimal thermal conditions [10].

In [11], in this study, they have designed the Simulink model using Generalized Predictive Control (GPC) as compared with PID control with and without newborn inside the infant incubator.

## III. DYNAMIC MATRIX CONTROL MATHEMATICAL MODELING

### A. Dynamic Matrix Control Mathematical Modeling

The Since the appearance of DMC in the literature, researches have detailed the derivation of the MIMO-DMC control law [12, 13], Prett and Gracia [14], it can be considered as an extension of the SISO case dealt with in the previous works [1, 2, 17]. The former researchers were deeply reviewing the mathematical formulation and the tuning parameters of DMC [15]. For the sake of this paper, only a short study and a recap of DMC will be presented below.

In our case, considering a system of two inputs, two outputs TITO (2 × 2), we then obtain the output from the step response coefficients, as follows [16, 17]:

Where  $u_i(k)$  and  $\Delta u_i(k)$  are considered as the  $i^{\text{th}}$  input besides its variation in sample time  $k$  as  $u_i(k) - u_i(k - 1)$ . In addition, the step response coefficients at sample time  $i$  are  $a_i$ ,  $b_i$ ,  $c_i$  and  $d_i$ . Also, the sample time  $N$  at each step response reaches its steady state.

$$\begin{cases} y_1(k) = \sum_{i=1}^N a_i \Delta u_1(k-i) + a_{N+1} u_1(k-N-1) \\ \quad + \sum_{i=1}^N b_i \Delta u_2(k-i) + b_{N+1} u_2(k-N-1) + d_1(k) \\ y_2(k) = \sum_{i=1}^N c_i \Delta u_1(k-i) + c_{N+1} u_1(k-N-1) \\ \quad + \sum_{i=1}^N d_i \Delta u_2(k-i) + d_{N+1} u_2(k-N-1) + d_2(k) \end{cases} \quad (1)$$

The appearance of any difference or change between the manipulated output (measuring system) and the predicted output among the above model is presented by equation (2):

$$\begin{cases} d_1(k) = y_1^{meas}(k) - y_1^{model}(k) \\ d_2(k) = y_2^{meas}(k) - y_2^{model}(k) \end{cases} \quad (2)$$

Where  $y^{meas}$  and  $y^{model}$  are the measured output and the output of the model respectively. These errors refer to the mismatch between the model/system and external disturbances (noises). In addition,  $P$  is known as the future predictions of the system output established on a control horizon  $M$ . They are described on the following matrix-vector form which yields the following:

$$S_f = \begin{array}{c|ccc|ccc} \begin{matrix} a_1 & 0 & \dots & 0 \\ a_2 & a_1 & \dots & 0 \\ \vdots & \vdots & \vdots & \vdots \\ a_M & a_{M-1} & \dots & a_1 \\ \vdots & \vdots & \vdots & \vdots \\ a_p & a_{p-1} & \dots & a_{p-M+1} \end{matrix} & \begin{matrix} b_1 & 0 & \dots & 0 \\ b_2 & b_1 & \dots & 0 \\ \vdots & \vdots & \vdots & \vdots \\ b_M & b_{M-1} & \dots & b_1 \\ \vdots & \vdots & \vdots & \vdots \\ b_p & b_{p-1} & \dots & b_{p-M+1} \end{matrix} \\ \hline \begin{matrix} c_1 & 0 & \dots & 0 \\ c_2 & c_1 & \dots & 0 \\ \vdots & \vdots & \vdots & \vdots \\ c_M & c_{M-1} & \dots & c_1 \\ \vdots & \vdots & \vdots & \vdots \\ c_p & c_{p-1} & \dots & c_{p-M+1} \end{matrix} & \begin{matrix} d_1 & 0 & \dots & 0 \\ d_1 & d_1 & \dots & 0 \\ \vdots & \vdots & \vdots & \vdots \\ d_1 & d_1 & \dots & d_1 \\ \vdots & \vdots & \vdots & \vdots \\ d_p & d_{p-1} & \dots & d_{p-M+1} \end{matrix} \end{array} \quad (3)$$

For the case of the multi variable (TITO) the Dynamic matrix process is achieved by the coefficients of the four step response models from the plant. It is represented by the dimension as  $(2P \times 2M)$ .

The move suppression weight which is known as  $\gamma$  is used to form the diagonal matrix which is represented by  $\Gamma$  and given by:

$$\Gamma = \text{diag}(\underbrace{\gamma_1, \dots, \gamma_2, \dots, \gamma_n}_{\text{Length } P}) \quad (4)$$

Where  $n$  is the number of the manipulated variables and  $(nP \times nP)$  is the dimension of the move suppression matrix. The diagonal matrix is formed by using the control variable weights ( $\lambda$ ) which is depicted by the following equation:

$$\Lambda = \text{diag}(\underbrace{\lambda_1, \dots, \lambda_2, \dots, \lambda_n}_{\text{Length } M}) \quad (5)$$

The dimension of the control variable weight matrix is  $(nM \times nM)$ .

The previous expression equation (5) can be rewritten with a matrix vector as follows equation (6):

$$y^{lin} = S_f \Delta u + y^{past} + d \quad (6)$$

Where P and M are the prediction and control (moving) horizons, respectively; and  $y^{past}$  indicates the effects of the past inputs on the predicted outputs in the future. Also, the matrix A, which is named a dynamic matrix of the process, depends on the step response coefficients.

Likewise,  $\Delta u$  which is the control moves is calculated according to the solution to the optimization problem of the Two input Two output, in this case, such that:

$$\text{Min}_{\Delta u} (y^{sp} - y^{lin})^T \Gamma^T \Gamma (y^{sp} - y^{lin}) + \Delta u^T \Lambda^T \Lambda \Delta u$$

Where

$y^{sp}$ : is the desired output trajectory,

$\Gamma$ : is the weighting matrices on the prediction error, and,

$\Lambda$ : is the control effort.

Under the unconstrained minimization, the optimal input is determined as follows:

$$\Delta u = \underbrace{(S_f^T \Gamma^T \Gamma S_f + \Lambda^T \Lambda)^{-1} S_f^T \Gamma^T \Gamma}_{K} (y^{sp} - y^{past} - d) \quad (8)$$

Error vector  $\bar{e}$

Generally, the first line of the  $\Delta u$  is applied to the system. This procedure is performed in each sampling interval.

### B. Role of the Tuning Parameters of Multi-Input Multi-Output of Dynamic Matrix Control

The design of the DMC controller enables the adjustment of the prediction horizon and control horizon, which presents an optimal control action for the process. For that reason, the tuning parameters of the DMC along with the control horizon M, prediction horizon P and sample time T can provide a superior performance of controlling the humidity and temperature in the unit care of newborn babies. In this paper, user-friendly tuning strategy is developed and defined based on an algorithm that will calculate the above-mentioned parameters for an unconstrained MIMO system [18, 19]. Dougherty and Cooper (2003) [20] proposed some guidelines in order to use the MIMO-DMC. These guidelines are summarized in the next 7 steps [21, 22]:

- **Step1**

Approximate the process dynamics of the controller output to measure the process variable pairs of the integrating sub processes with FOPDT models, as follows:

$$\frac{y_j(s)}{u_i(s)} = \frac{K_{p_{ij}}^* e^{-\theta_{p_{ij}} s}}{\tau_{p_{ij}} s + 1} \quad \text{for } (i=1,2, \dots, S; j=1,2, \dots, R)$$

- **Step2**

Select the sample time as close as possible to

$$T = 0.1 \tau_{ij} \quad \text{or} \quad T = 0.5 \theta_{ij},$$

Whichever is smaller ( $i=1,2, \dots, S; j=1,2, \dots, R$ )

- **Step3**

Compute the prediction horizon P and the model horizon, N, as the process settling time in samples (rounded to the next integer), such that:

$$P = N = \text{Max} \left( \frac{5 \tau_{ij}}{T} + k_{ij} \right)$$

where

$$k_{ij} = \left( \frac{\theta_{ij}}{T} + 1 \right) \quad (i=1,2, \dots, S; j=1,2, \dots, R)$$

- **Step4**

Select the control horizon M as an integer (usually between 1 to 6).

- **Step5**

Select the controlled variable weights  $\gamma_j^2$  to scale the measurements to similar magnitudes.

- **Step6**

Compute the move suppression coefficients,  $\lambda_j^2$ , as follows:

$$\lambda_j^2 = \frac{M}{500} \sum_{i=1}^R \left[ \gamma_j^2 K_{ij}^2 \left( P - k_{ij} - \frac{3 \tau_{ij}}{2 T} + 2 - \frac{(M-1)}{2} \right) \right]$$

- **Step7**

Implement DMC using the traditional step response matrix of the actual process and the initial values of the parameters computed in steps 1 to 6.

## IV. TUNING STRATEGY VALIDATION FOR MULTIVARIABLE PROCESS AND DISCUSSION

Fig. 1 presents the real photo of the infant incubator, the isolette® Dräger 8000C which is used in this experiment. In this system, the set point is defined as 37°C and the input energy varies between 0-100%, i.e. equivalent to 0 and 400 Watt. An ultrasonic nebulizer, which is an instrument for converting a liquid into a fine spray, is also used. As for the humidifier power, it varies between 0-150 watts. This system is able to increase the humidity by 80% [12].

### A. Case1: Dynamic Matrix Control for Ident Toolbox

The tuning strategy is provided and validated in this paper to control the temperature and the humidity of the infant-incubator. Besides the transfer function of this process, it is also extracted from previous works [23]. It is a system of (2x2) of the coupled system and third order system, as illustrated in the Fig. 2.



Fig. 1. The Real Photo of the Infant Incubator Dräger 8000 C.

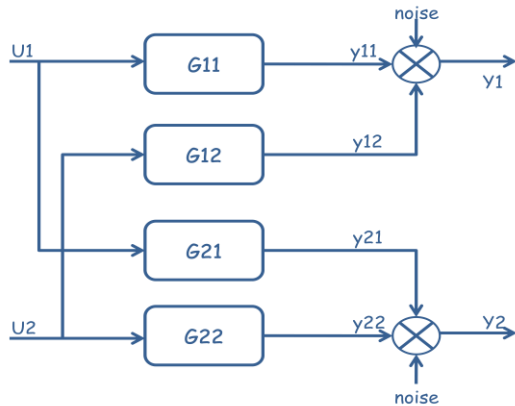


Fig. 2. Two-Input Two-Output Processes.

The transfer function matrix can be written with a sample time  $T_s=20$ , as follows:

$$G(z) = \begin{bmatrix} G_{11}(z) & G_{12}(z) \\ G_{21}(z) & G_{22}(z) \end{bmatrix} = \begin{bmatrix} z^{-d_{11}} \frac{B_{11}(z^{-1})}{A_{11}(z^{-1})} & z^{-d_{12}} \frac{B_{12}(z^{-1})}{A_{12}(z^{-1})} \\ z^{-d_{21}} \frac{B_{21}(z^{-1})}{A_{21}(z^{-1})} & z^{-d_{22}} \frac{B_{22}(z^{-1})}{A_{22}(z^{-1})} \end{bmatrix} \quad (9)$$

Each transfer function of the system is detailed in the following expression:

$$\begin{cases} G_{11}(z) = z^{-d_{11}} \frac{B_{11}(z)}{A_{11}(z)} = z^{-10} \frac{0.0005875z^{-1} + 0.0005941z^{-2}}{1 - 0.3464z^{-1} + 0.6463z^{-2}} \\ G_{12}(z) = z^{-d_{12}} \frac{B_{12}(z)}{A_{12}(z)} = 0 \\ G_{21}(z) = z^{-d_{21}} \frac{B_{21}(z)}{A_{21}(z)} = z^{-32} \frac{0.000137z^{-1} - 4.193e-05z^{-2}}{1 - 0.2832z^{-1} + 0.7133z^{-2}} \\ G_{22}(z) = z^{-d_{22}} \frac{B_{22}(z)}{A_{22}(z)} = z^{-3} \frac{0.00203z^{-1} - 0.00088z^{-2}}{1 - 0.5091z^{-1} + 0.4262z^{-2}} \end{cases} \quad (10)$$

Also, all these functions can be rewritten as a continuous form and it is obvious that the model order is increased to handle real negative poles, as illustrated in equation (11):

$$\begin{cases} G_{11}(s) = \exp(-200*s) \frac{3.423e-05s^2 - 4.204e-07s + 9.026e-07}{s^3 + 0.04343s^2 + 0.02515s + 5.577e-06} \\ G_{12}(s) = 0 \\ G_{21}(s) = \exp(-640*s) \frac{3.569e-06s^2 + 1.281e-06s + 6.924e-08}{s^3 + 0.03368s^2 + 0.02496s + 2.542e-06} \\ G_{22}(s) = \exp(-60*s) \frac{0.0001034s^2 + 8.64e-06s + 2.707e-06}{s^3 + 0.083s^2 + 0.02649s + 6.019e-05} \end{cases} \quad (11)$$

The First Order Plus Dead Time (FOPDT) models are used to represent the behavior of numerous processes for the reason that some responses of such models like step or pulse inputs can propose an interesting and excellent approximation for the actual responses of many systems and sub-systems in many applications. Anyhow, the theoretical development of many system identification algorithms is available in the literature [25, 26].

Hence, this system is modeled according the Process Reaction Curve known as (PRC). It is identified by performing in an open loop step test of the process and finding model parameters for the initial step. A typical process reaction curve is generated using the following method [24-26]:

- 1) Find  $\Delta y$  from step response.
- 2) Find  $\Delta u$  from step response.
- 3) Calculate  $k_p = \frac{\Delta y}{\Delta u}$ .
- 4) Find the apparent dead time  $\theta_p$ , from step response.
- 5) Find  $(0.632 \times \Delta y)$  from step response.
- 6) Find  $t_{0.632}$  for  $y(t_{0.632}) = 0.632 \times \Delta y$  from step response.
- 7) Calculate  $\tau_p = t_{0.632} - \theta_p$ .

As a result, of this method, it is obvious that the process reaction curve obtained from the real time model and its approximation is as shown below.

Table I below summarizes the values of each parameter which are taken from the fitting curve and computed by the above method of approximation FOPDTs whose transfer function is given by  $G_{ij}^{approx}$ .

TABLE I. APPROXIMATION COMPUTED VALUES AS FOPDT

|            | $\Delta y$ | $\Delta u$ | $k_p$  | $\theta_p$ | $y(t_{0.632})$ | $\tau_p$ | $G_{ij}^{approx}$                   |
|------------|------------|------------|--------|------------|----------------|----------|-------------------------------------|
| <b>G11</b> | 0.162      | 1          | 0.162  | 201        | 0.1023         | 4711     | $\frac{0.162e^{-201s}}{4510s + 1}$  |
| <b>G21</b> | -          | -          | -      | -          | -              | -        | 0                                   |
| <b>G21</b> | 0.0272     | 1          | 0.0272 | 605        | 0.0172         | 9845     | $\frac{0.0272e^{-605s}}{9845s + 1}$ |
| <b>G22</b> | 0.045      | 1          | 0.045  | 60         | 0.02844        | 440      | $\frac{0.045e^{-60s}}{440s + 1}$    |

Fig. 3, Fig. 4 and Fig. 5 shows the different step responses of the continuous third order functions and their approximations First Order Plus Dead Times of this system which is the infant incubator in open loop. Two curves which are very close to each other are obtained; this is why have been zoomed on the figures to distinguish between the two curves.

As a result of those steps the multivariable system of infant incubator with two inputs and two outputs can be represented as follows:

$$\begin{bmatrix} y_1(s) \\ y_2(s) \end{bmatrix} = \begin{bmatrix} G_{11}^{approx} & G_{12}^{approx} \\ G_{21}^{approx} & G_{22}^{approx} \end{bmatrix} \begin{bmatrix} u_1(s) \\ u_2(s) \end{bmatrix} = \begin{bmatrix} \frac{0.162e^{-201s}}{4510s+1} & 0 \\ 0.0272e^{-605s} & \frac{0.045e^{-60s}}{9845s+1} \end{bmatrix} \begin{bmatrix} u_1(s) \\ u_2(s) \end{bmatrix} \quad (12)$$

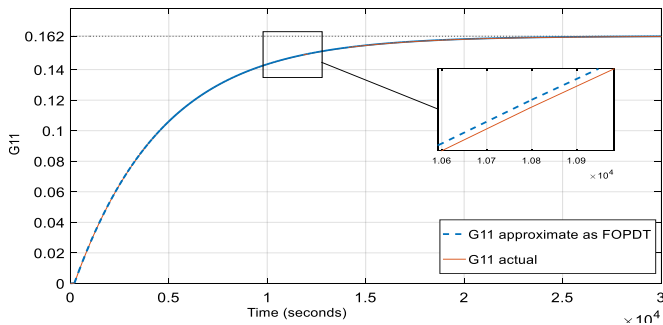


Fig. 3. Comparison of the Open Loop of Step Response between  $G_{11actual}(s)$  and  $G_{11FOPDT}(s)$ .

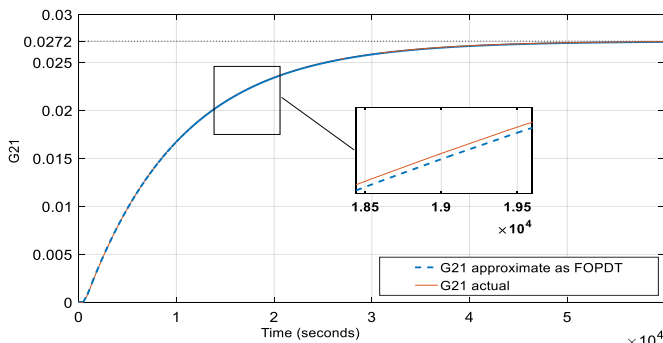


Fig. 4. Comparison of the Open Loop of Step Response between  $G_{21actual}(s)$  and  $G_{21FOPDT}(s)$ .

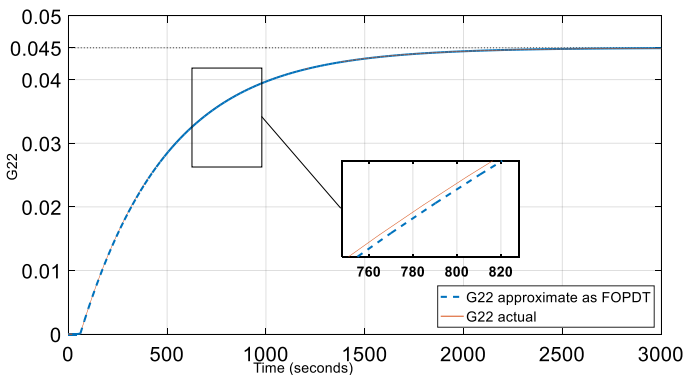


Fig. 5. Comparison of the Open Loop of Step Response between  $G_{22actual}(s)$  and  $G_{22FOPDT}(s)$ .

In equation (12)  $y_1(s)$  and  $y_2(s)$  are the process responses and  $u_1(s)$  and  $u_2(s)$  are the inputs functions. Then, the transfer functions  $G_{11}^{approx}$ ,  $G_{12}^{approx}$ ,  $G_{21}^{approx}$  and  $G_{22}^{approx}$  are taken from Table I. The obtained environmental conditions have been investigated to understand the dynamic relation between the temperature and humidity inside the infant incubator.

To realize the process of testing, the regulation is affected in order to tune the Dynamic Matrix Control. The control horizon of fixed for both temperature and humidity such that  $N_{cu1}=N_{cu2}=6$ . Concerning the prediction horizon, it is kept to be equal to the maximum lengths of the model which are  $N_{py1}=1437$  and  $N_{py2}=2725$ . The other parameters are summarized in the Table II. Several changes are made for each figure to prove the varying effect on the tuning of the DMC controller.

TABLE II. TUNING PARAMETERS OF DMC FOR SIMULATION OF INFANT-INCUBATOR

| Case | Error weight |            | Control weight |             | Figure |
|------|--------------|------------|----------------|-------------|--------|
|      | $\alpha_1$   | $\alpha_2$ | $\lambda_1$    | $\lambda_2$ |        |
| 11   | 6.2          | 1          | 0.035          | 0.052       | Fig. 6 |
| 21   | 6.2          | 5          | 0.035          | 0.052       |        |
| 31   | 6.2          | 10         | 0.035          | 0.052       |        |
| 41   | 6.2          | 20         | 0.035          | 0.052       |        |
| 51   | 6.2          | 30         | 0.035          | 0.052       |        |
| 12   | 10.2         | 5          | 0.035          | 0.052       | Fig. 7 |
| 22   | 8.2          | 5          | 0.035          | 0.052       |        |
| 32   | 6.2          | 5          | 0.035          | 0.052       |        |
| 42   | 10.2         | 5          | 0.035          | 0.052       |        |
| 52   | 0.2          | 5          | 0.035          | 0.052       |        |
| 13   | 6.2          | 5          | 0.2            | 0.052       | Fig. 8 |
| 23   | 6.2          | 5          | 0.07           | 0.052       |        |
| 33   | 6.2          | 5          | 0.05           | 0.052       |        |
| 43   | 6.2          | 5          | 0.035          | 0.052       |        |
| 53   | 6.2          | 5          | 0.01           | 0.052       |        |
| 14   | 6.2          | 5          | 0.035          | 0.12        | Fig. 9 |
| 24   | 6.2          | 5          | 0.035          | 0.07        |        |
| 34   | 6.2          | 5          | 0.035          | 0.052       |        |
| 44   | 6.2          | 5          | 0.035          | 0.03        |        |
| 54   | 6.2          | 5          | 0.035          | 0.01        |        |

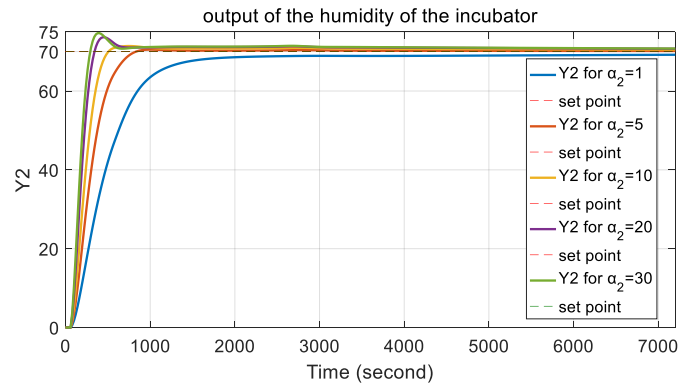


Fig. 6. The Effect of the Error Weight ( $\alpha_2$ ) on the Humidity.

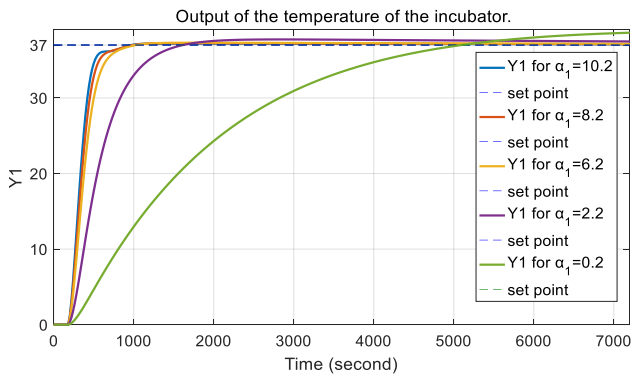


Fig. 7. The Effect of the Control Weight ( $\alpha_1$ ) on the Temperature.

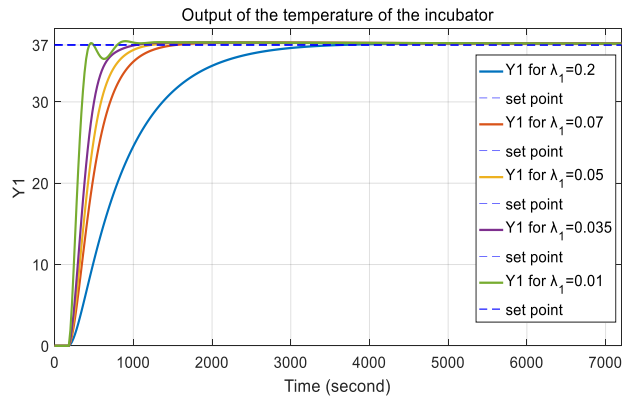


Fig. 8. The Effect of the Control Weight ( $\lambda_1$ ) on the Temperature.

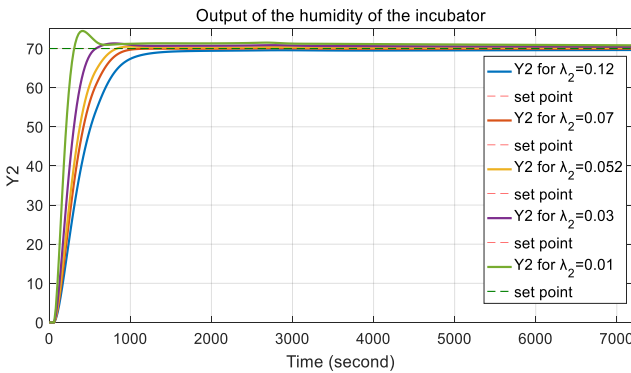


Fig. 9. The Effect of the Control Weight ( $\lambda_2$ ) on the Humidity.

The effect of the tuning parameters of the infant incubator is illustrated in Fig. 6 through 9 which demonstrate several trials created to tune the Dynamic Matrix Control arranged to achieve the most perfect desirable set of tuning parameters listed in the Table II.

In this paper, spotlighting the effect of the role of the weighting tuning parameters  $\alpha_i$  and  $\lambda_i$  which are, the error weight vector and the weight of control move vector, respectively.

Proceeding the trails from the small value of the error weight  $\alpha_2$  that varies from 1 to 30. The other parameters starting from case 11 to case 51 are fixed and correspond to Fig. 6, as illustrated in Table II. It is noted that raising the possibility of error makes the responses of the humidity rapid.

Fig. 7 corresponds to the tuning effect of  $\alpha_2$  which varies from 10.2 to 0.2. The other fixed values from case 12 to 52 are maintained, as provided in Table II. It is figure out, that the decrease in the error obliges the response of the temperature to be faster in controlling the temperature inside the infant incubator.

Then, Fig. 8 illustrates the tuning effect of the control weight  $\lambda_1$  which varies from 0.2 to 0.01. As for the other parameters, they are also fixed. Fig. 8 also shows the result of the change in this parameter, so it is clear that dropping these parameters drive the system to be quick, but with an overshoot equal to 0.8118.

Finally, Fig. 9 presents the effect of the tuning control weight  $\lambda_2$  on the humidity which varies from 0.12 to 0.01, the other values starting from case 14 to 54 are fixed, as it is shown in Table II. As the graph demonstrates, when this weight of controlling vector raises, the response of the system is damaged, which makes the response sluggish.

**B. Case2: Dynamic Matrix Control for Hito Identification Hidden**

In this part, will focus on the implementation of DMC that was identified by Hito Identification (Herramienta Integrada para Total Optimizacion, Integrated Tool for Total Optimisation) is a software tool oriented to implement MPC control called Hidden toolbox [23] which are a functions are extracted from the previous work. The transfer function of the infant incubator by this software tool under Matlab/environment [23] can be written with a sample time  $T_s=20$  (second), as follows:

$$\begin{cases} G_{11}^{hidden}(z) = z^{-d_{11}} \frac{B_{11}(z)}{A_{11}(z)} = z^{-10} \frac{-0.00010265z^{-1} + 0.00014208z^{-2}}{1 - 1.944z^{-1} + 0.9441z^{-2}} \\ G_{12}^{hidden}(z) = z^{-d_{12}} \frac{B_{12}(z)}{A_{12}(z)} = 0 \\ G_{21}^{hidden}(z) = z^{-d_{21}} \frac{B_{21}(z)}{A_{21}(z)} = z^{-32} \frac{0.0001286z^{-1} - 0.00011951z^{-2}}{1 - 1.9776z^{-1} + 0.977651z^{-2}} \\ G_{22}^{hidden}(z) = z^{-d_{22}} \frac{B_{22}(z)}{A_{22}(z)} = z^{-3} \frac{0.0055284z^{-1} - 0.003159z^{-2}}{1 - 1.06023z^{-1} + 0.34497z^{-2}} \end{cases} \quad (13)$$

Besides, it can to be transformed as a continuous form as follows:

$$\begin{cases} G_{11}^{hidden}(s) = \exp(-200*s) \frac{-6.306e-06s + 1.014e-07}{s^2 + 0.002876s + 2.573e-07} \\ G_{12}^{hidden}(s) = 0 \\ G_{21}^{hidden}(s) = \exp(-640*s) \frac{6.272e-06s + 2.288e-08}{s^2 + 0.00113s + 1.264e-07} \\ G_{22}^{hidden}(s) = \exp(-60*s) \frac{0.0003638s + 1.001e-05}{s^2 + 0.05321s + 0.001203} \end{cases} \quad (14)$$

Table III below exhibits all the parameters of each response by using the same approximation as method First Order Plus Dead Times as the previous section in paragraph A to obtain the responses of the approximate functions of the system  $G_{ij}^{approx}$ .

Fig. 10 to Fig. 12 represents the various step responses of the continuous third order function and their approximations FOPDTs of this system modeling by Hidden identification toolbox under Matlab/environment [23].

TABLE III. APPROXIMATION COMPUTED VALUES OF AS FOPDT

|                   | $\Delta y$ | $\frac{\Delta}{u}$ | $k_p$      | $\theta_p$ | $y(t_{0.632})$ | $\tau_p$  | $G_{ij}^{approx}$                 |
|-------------------|------------|--------------------|------------|------------|----------------|-----------|-----------------------------------|
| $G_{11}^{hidden}$ | 0.394      | 1                  | 0.         | 52<br>0    | 0.249          | 1090<br>0 | $\frac{0.394e^{-520s}}{10900s+1}$ |
| $G_{12}^{hidden}$ | -          | -                  | -          | -          | -              | -         | 0                                 |
| $G_{21}^{hidden}$ | 0.182      | 1                  | 0.182      | 97<br>6    | 0.115          | 8424      | $\frac{0.182e^{-976s}}{8424s+1}$  |
| $G_{22}^{hidden}$ | 0.008<br>3 | 1                  | 0.008<br>3 | 60         | 0.00525        | 19        | $\frac{0.00832e^{-60s}}{19s+1}$   |

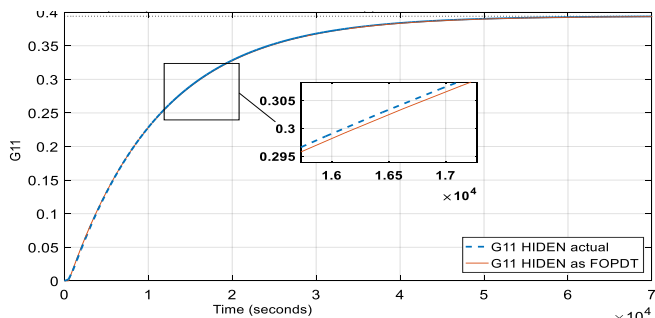


Fig. 10. Comparison of the Open Loop of Step Response between  $G_{11}^{HIDDEN}$  (s) and  $G_{11}^{HIDDEN}$  (s).

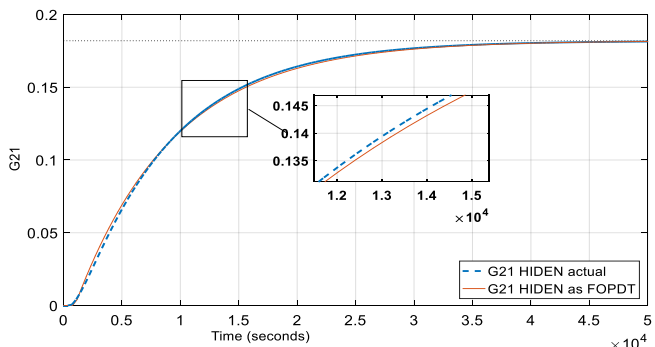


Fig. 11. Comparison of the Open Loop of Step Response between  $G_{21}^{HIDDEN}$  (s) and  $G_{21}^{HIDDEN}$  (s).

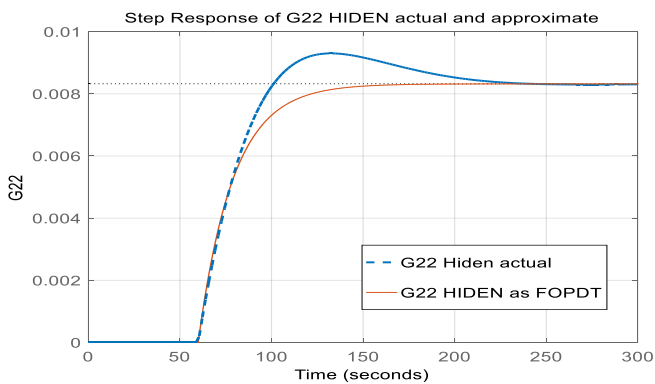


Fig. 12. Comparison of the Open Loop of Step Response between  $G_{22}^{HIDDEN}$  (s) and  $G_{22}^{HIDDEN}$  (s).

Table IV contains the parameters of tuning for the DMC controller.

To realize the process of testing, the regulation is affected in order to tune the Dynamic Matrix Control. The control horizon is fixed for both temperature and humidity to be equal to  $N_{cu1}=N_{cu2}=6$ . The prediction horizon is chosen to be equal to the maximum lengths of the model, namely  $N_{py1}=1437$  and  $N_{py2}=2725$ . The other parameters are summarized in Table IV. Several changes are caused for each figure to prove the varying effect on the tuning of the DMC controller.

TABLE IV. TUNING PARAMETERS OF DMC FOR SIMULATION OF INFANT-INCUBATOR

| Case | Error weight |             | Control weight |               | Figure  |
|------|--------------|-------------|----------------|---------------|---------|
|      | $\alpha_1$   | $\alpha_2$  | $\lambda_1$    | $\lambda_2$   |         |
| 11   | 25           | <b>10</b>   | 0.3            | 0             | Fig. 13 |
| 21   | 25           | <b>5</b>    | 0.3            | 0             |         |
| 31   | 25           | <b>0.9</b>  | 0.3            | 0             |         |
| 41   | 25           | <b>0.5</b>  | 0.3            | 0             |         |
| 51   | 25           | <b>0.05</b> | 0.3            | 0             |         |
| 12   | <b>5</b>     | 2           | 0.3            | 0             | Fig. 14 |
| 22   | <b>15</b>    | 2           | 0.3            | 0             |         |
| 32   | <b>25</b>    | 2           | 0.3            | 0             |         |
| 42   | <b>35</b>    | 2           | 0.3            | 0             |         |
| 52   | <b>45</b>    | 2           | 0.3            | 0             | Fig. 15 |
| 13   | 25           | 2           | <b>0.09</b>    | 0             |         |
| 23   | 25           | 2           | <b>0.3</b>     | 0             |         |
| 33   | 25           | 2           | <b>0.8</b>     | 0             |         |
| 43   | 25           | 2           | <b>1.5</b>     | 0             |         |
| 53   | 25           | 2           | <b>2.5</b>     | 0             | Fig. 16 |
| 14   | 25           | 2           | 0.3            | <b>0</b>      |         |
| 24   | 25           | 2           | 0.3            | <b>0.0001</b> |         |
| 34   | 25           | 2           | 0.3            | <b>0.0009</b> |         |
| 44   | 25           | 2           | 0.3            | <b>0.01</b>   |         |
| 54   | 25           | 2           | 0.3            | <b>0.1</b>    |         |

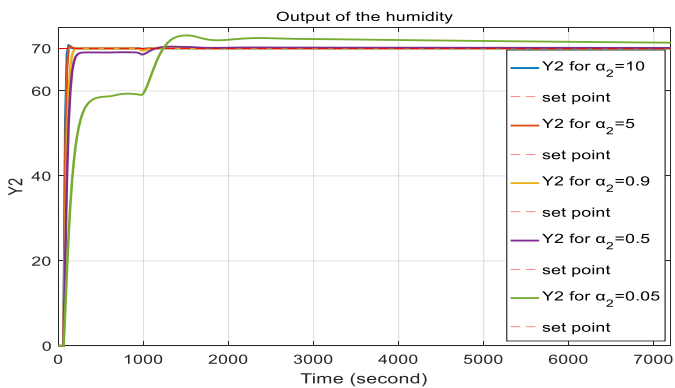


Fig. 13. The Effect of the Control Weight ( $\alpha_2$ ) on the Humidity.

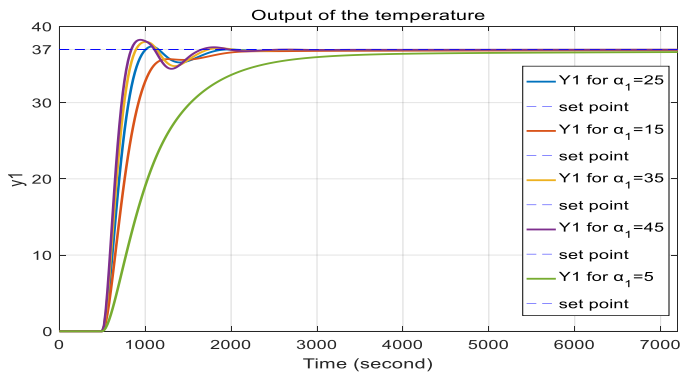


Fig. 14. The Effect of the Control Weight ( $\alpha_1$ ) on the Temperature.

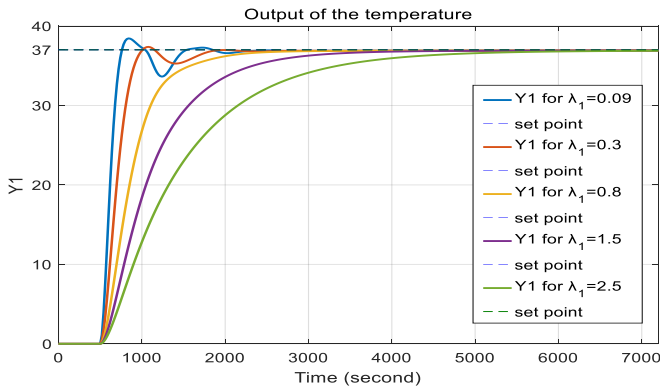


Fig. 15. The Effect of the Smoothing Factor ( $\lambda_1$ ) on the Temperature.

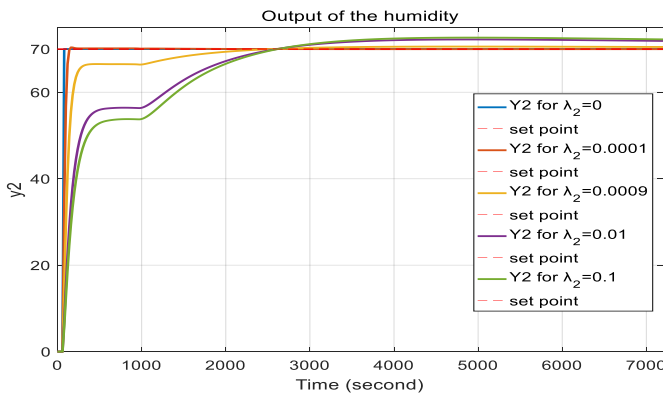


Fig. 16. The Effect of the Smoothing Factor ( $\lambda_1$ ) on the Humidity.

The effect of the tuning parameters of the infant incubator is demonstrated in Fig. 13 through 16 which demonstrate the various trials that made it tune the Dynamic Matrix Control arranged to achieve a good set of tuning parameters. These several values are listed in Table IV.

In this part, will be concentrate as the previous part on the effect of the role of the weighting tuning parameters which account for the error weight vector and the weight of control move vector known as  $\alpha_i$  and  $\lambda_i$ , respectively.

The trails begin from an enormous value of the error weight  $\alpha_2$  that varies from 10 to 0.05. The other parameters starting from case 11 to case 51 are still fixed as it is illustrated in Table IV and correspond to Fig. 13. As

previously, noted, the diminution of the error makes the responses of the humidity more unstable and less rapid and lazy.

Fig. 14 coincides with the tuning effect of  $\alpha_2$  varying from 25 to 54. The other values from case 12 to 52 are settled, as shown in Table IV. It is very noticeable that the reduction in the error obliges the response of the temperature to be faster in controlling the temperature inside the infant incubator. But with this gain in the speed of the peak time, it is very clear that there is an overshoot and undershoot which are penalizing the system.

Fig. 15 depicts the tuning effect of the control weight  $\lambda_1$  which fluctuates from 0.09 to 2.5 while the other parameters are fixed. The figure shows the result of the change in this parameter, where it is obvious that dropping these parameters drive the system to be very slow and achieve stability after an interval of time.

Finally, Fig. 16 corresponds to the effect of the tuning control weight  $\lambda_2$  on the humidity which varies from 0 to 0.1 while the other values from case 14 to 54 are fixed as it is presented in Table IV. As previously noticed from the graph, when we increase this weight of controlling vector, the response of the system is penalized and becomes sluggish and lazy.

## V. COMPARATIVE STUDY AND DISCUSSION

From the curve of the response step which is implemented by Matlab/environment, it is possible to realize different parameters. But, we will only focus on the overshoot and the rise time which is cited in Table V.

Besides, Ziegler-Nichols [27-29] is the researcher who suggested the trial and error method based on sustained oscillations. To obtain the criteria of the curves (response process), there are many methods used to compare the difference between those responses. However, the most popular one is the Integral of the Absolute Error (IAE) which is written as follows:

$$IAE = \int_0^{\infty} |e(t)|.dt \quad (15)$$

The second method is the Integral of the Square Error (ISE) which is expressed as follows:

$$ISE = \int_0^{\infty} e^2(t).dt \quad (16)$$

With  $e(t)$  is the difference or deviation (error) between the response and the desired set point.

The main goal of the control of the infant incubator application is to maintain the humidity and the temperature at the desired value. Furthermore, the sample time is set to be equal to 20 sec. Hence, the parameters of the DMC controller are taken from both Table II and Table IV and given in Table V. Choosing the best performance and smoothest control signal of the output response of both methods for the sake of comparison.

TABLE V. THE PERFORMANCE COMPARISON OF DMC OF THE INDEX OF THE INCUBATOR

| Output response | Ident toolbox |          | Hidden toolbox |           |
|-----------------|---------------|----------|----------------|-----------|
|                 | T(°C)         | H (%)    | T(°C)          | H (%)     |
| Overshoot(s)    | 0.3872        | 0.4937   | 0              | 1.2503e-6 |
| Rise Time(s)    | 17.35         | 21.0045  | 15.847         | 0.8       |
| IAE             | 818.3214      | 1.18e+3  | 887.9422       | 280       |
| ISE             | 2.2337e+4     | 5.557e+4 | 2.1783e+4      | 2.1791e+4 |

In this paper, the result is obtained by comparing the time domain specifications and the performance of the index criteria IAE and ISE of both methods which were illustrated in the previous paragraph. In addition, we remove (taken) the peak overshoot and the rise time from the time specifications. The controller which has less error, a minimum rise time and a peak overshoot is reckoned as the best controller. While comparing the time specifications, it is noted that the second method proves a minimum overshoot and less rise time compared to the first method. Moreover, for the criteria index, it is clear the presence of a satisfactory performance of the temperature response, yet an improved performance of the humidity response. Depending on the result of the system that is illustrated in the table below, it is very obvious that the second method of Hidden identification shows an amelioration of the responses of the humidity and the temperature.

Finally, the limitation of this study is presented because it is focus only on the mathematical model of the infant incubator which can be used for the simulation in computer for the infant incubator.

## VI. CONCLUSION AND FUTURE WORK

Different tools and software have been used in this work. The identification is performed on Matlab thanks to two toolbox methods, namely, the ident toolbox and HIDENT. In this paper, all the results of simulation implemented by the Matlab environment with the Dynamic Matrix Control (DMC) controller indicate that the use of this controller leads to good performance. The comparative study made between the two identification tools of the same system allows us to conclude that the identification has a huge effect on the final result that is able to ameliorate the performance, which is an important advantage. In addition, the choice of Dynamic Matrix Control as a controller is due to the ease and efficiency of this strategy. The future work may concern the parameters optimization of the infant incubator with intelligent methods, such as the Particle Swarm Optimization (PSO) and Genetic Algorithm (GA).

### REFERENCES

[1] C. R. Cutler, "Dynamic matrix control: an optimal multivariable control algorithm with constraints," Ph.D. Dissertation, University of Houston, TX, 1983.  
[2] J. L. Marchetti, A. Duncan, and D. E. Seborg. "Predictive control based on discrete convolution models," *Industrial & Engineering Chemistry Process Design and Development* vol. 22( 3), 1983. pp. 488-495.

[3] D. M. Prett and R. D. Gillette, "Optimization and constrained multivariable control of a catalytic cracking unit," *Joint automatic control conference*. No. 17. 1980.  
[4] C. Prada, J. Serrano, P. Vega and M.A. Píera, "A comparative study of GPC and DMC controllers," in *Advances in Model Based Predictive Control* (D. W. Clarke, Ed.). Oxford University Press, 1994, pp. 38–52.  
[5] G. H.C. Oliveira, M. F. Amorim, and C. Pacholok. "A real-time predictive scheme for controlling hygrothermal conditions of neonate incubators," In *Proc. of the IFAC Symposium on Modelling and Control of Biomedical Systems*, Reims/France, 2006.  
[6] G. H.C. Oliveira and Luis. H. Ushijima, "A Hybrid Predictive Control Scheme for Hygrothermal Process," *Proceedings of the 17th World Congress, The International Federation of Automatic Control*, Seoul, Korea, July, 2008, pp. 6-11,  
[7] M. U. Cavalcante, B. C. Torrico, O. da Mota Almeida, A. P. de Souza Brag and F. L. M da Costa Filho, "Filtered model-based predictive control applied to the temperature and humidity control of a neonatal incubator," *2010 9th IEEE/IAS International Conference on Industry Applications-INDUSCON 2010*. IEEE, 2010.  
[8] M. A. Zermani, E. Feki, A. Mami, "Application of Adaptive Predictive Control to a Newborn Incubator," *American J. of Engineering and Applied Sciences*, vol. 4(2), 2011, pp. 235-243.  
[9] M. A. Zermani, E. Feki and A. Mami, "Application of Genetic Algorithms in identification and control of a new system humidification inside a newborn incubator," *International Conference on Communications, Computing and Control Applications*, 2011, pp. 1-6.  
[10] M. A. Zermani, E. Feki and A. Mami, "Building simulation model of infant-incubator system with decoupling predictive control," *IRBM 35*, 2014, pp. 189-201.  
[11] E. Feki, M. A. Zermani and A. Mami, "GPC temperature control of simulation model infant-incubator and practice with arduino board," *IJACSA* vol. 8(6), 2017.  
[12] C. Ionescu, "Automatic tuning of MPC from step response approximation with FODT and closed loop sensitivity (internal report) ," Ghent University, Belgium, 2017.  
[13] Q. Bi, W. Cai, L. Lee, Q. G. Wang, C. Hang and Y. Zhang, "Robust identification of first-order plus dead-time model from step response," *Control Engineering Practice*, vol. 7(1) , 1999, pp. 71-77.  
[14] D. M. Prett and C. E. García, "Fundamental process control: Butterworths series in chemical engineering," Butterworth-Heinemann. 2013.  
[15] R. Shridhar, and J. C. Douglas. "A tuning strategy for unconstrained SISO model predictive control," *Industrial & Engineering Chemistry Research* vol. 36(3), 1997, pp. 729-746.  
[16] B. W. Bequette, "Process control: modeling, design, and simulation," Prentice Hall Professional, 2003.  
[17] J. S. Qin and T. A. Badgwell, "An Overview of Industrial Model Predictive Control Technology," *Preprints, Proc. Chem. Process Cont. Conf., CPC V*; Tahoe City, California, 1996.  
[18] G. M. de Almeida, et al. "Optimal tuning parameters of the dynamic matrix predictive controller with ant colony optimization," *2014 11th IEEE/IAS International Conference on Industry Applications*. IEEE, 2014.  
[19] P. Bagheri and A. Khaki-Sedigh, "Tuning of dynamic matrix controller for FOPDT models using analysis of variance," *IFAC Proceedings* Vol. 44(1), 2011, pp. 12319-12324.  
[20] D. Dougherty and J. C. Douglas, "Tuning guidelines of a dynamic matrix controller for integrating (non-self-regulating) processes," *Industrial & engineering chemistry research* vol. 42(8), 2003, pp. 1739-1752.  
[21] T. Klopot, P. Skupin, M. Metzger and P. Grelewicz, "Tuning strategy for dynamic matrix control with reduced horizons," *ISA transactions*, vol. 76, 2018, pp. 145-154.



- [22] D. M. Prett and R. D. Gillette, "Optimization and constrained multivariable control of a catalytic cracking unit," In Proceedings of the joint automatic control conference, 1980.
- [23] J. El Hadj Ali, E. Feki, M. A. Zermani, C. de Prada and A. Mami. "Incubator system identification of humidity and temperature: Comparison between two identification environments," 2018 9<sup>th</sup> International Renewable Energy Congress (IREC). IEEE, 2018, pp. 1-6.
- [24] L. M. Kunene, "Autotuning Predictive Control for Industrial Applications," 2017.
- [25] K. Burn, and C. Chris., "Curve fitting software for first order plus dead time (FOPDT) model parameter estimation using step or pulse response data: a tutorial,".
- [26] H-P. Huang, and J-C. Jeng., "Process reaction curve and relay methods identification and pid tuning," PID Control. Springer, London, 2005, pp 297-337.
- [27] K. Krishnan, and G. Karpagam. "Comparison of PID controller tuning techniques for a FOPDT system," International Journal of Current Engineering and Technology Vol. 4(4) 2667-2670. 2014.
- [28] A. Bemporad, M. Morari, and N. Lawrence Ricker. "Model Predictive Control Toolbox User's Guide." The mathworks. 2010.
- [29] K. M. Hussain, R. A. R. Zepherin and M. S. Kumar, "Comparison of tuning methods of PID controllers for FOPTD system," International journal of innovative research in electrical, electronics, instrumentation and control engineering vol. 2(3), 2014, pp. 1177-1180.

# Dense Hand-CNN: A Novel CNN Architecture based on Later Fusion of Neural and Wavelet Features for Identity Recognition

Elaraby A. Elgallad<sup>1</sup>  
Deanship of Information Technology  
Tabuk University, KSA

Wael Ouarda<sup>2</sup>, Adel M. Alimi<sup>3</sup>  
Research Groups in Intelligent Machines  
ENIS, BP 1173, Sfax, 3038, Tunisia<sup>2,3</sup>

**Abstract**—Biometric recognition or biometrics has emerged as the best solution for criminal identification and access control applications where resources or information need to be protected from unauthorized access. Biometric traits such as fingerprint, face, palmprint, iris, and hand-geometry have been well explored; and matured approaches are available in order to perform personal identification. The work emphasizes the opportunities for obtaining texture information from a palmprint on the basis of such descriptors as Curvelet, Wavelet, Wave Atom, SIFT, Gabor, LBP, and AlexNet. The key contribution is the application of mode voting method for accurate identification of a person at the fusion decision level. The proposed approach was tested in a number of experiments at the CASIA and IITD palmprint databases. The testing yielded positive results supporting the utilization of the described voting technique for human recognition purposes.

**Keywords**—Deep learning; fusion; palmprint; squeezeNet; voting

## I. INTRODUCTION

Biometrics is an authentication method that uses human characteristics to identify a person. Based on the traits, biometric can be divided into two broad types as in [1]: physical and behavioral. Physical biometric is a biometric system that evaluates the physical characteristic of a human body to recognize a person, such as fingerprint, face, retina, etc. On the other hand, behavioral characteristic analyzes the human behavioral traits, such as gait, signature, keystroke, etc. Behavioral biometric is less secured than physical biometric because people can change their behavior anytime they want. For example, people can adjust their signature, keystroke, or walking pattern easily. Today, multimodal biometric systems, which incorporate more than one biometric, with appropriate security measures are acknowledged as more robust and more accurate than unimodal biometrics, because even when the score of one biometric recognition is poor due to environmental conditions, the final outcome can be positive because the score from another biometric recognition is considered.

In the recent years, the computer vision has been increasingly dominated by deep learning, which has proven to have notable capacities to achieve top scores across various tasks and contests. ImageNet stands out as the most recognized among such contests. The ImageNet competition

tasks researchers with creating a model that most accurately classifies the given images in the dataset. Back in 2012, a paper from the University of Toronto was published [2]. The paper proposed to use a deep Convolutional Neural Network (CNN) for the task of image classification. It was relatively simple compared to those that are being used today. The main contributions that came from this paper were using a deep for large scale image classification. This was made possible because of the large amounts of labelled data from ImageNet, as well as training the model using parallel computations on two GPUs. They used ReLU for the non-linearity activation functions, finding that they performed better and decreased training time relative to the tanh function. The techniques of data augmentation that consisted of image translations, horizontal reflections, and mean subtraction are used. These techniques are very widely used today for many computers. Their proposed style of having successive convolution and pooling layers, followed by fully-connected layers at the end is still the basis of many state-of-the-art networks today. Basically, AlexNet set the bar, providing the baseline and default techniques of using CNNs for computer vision tasks.

The VGGNet paper came out in 2014, Simonyan and Zisserman [3], their main idea was that you didn't really need any fancy tricks to get high accuracy. Just a deep network with lots of small 3x3 convolutions and non-linearities will do the trick. They use of only 3x3 sized filters instead of the 11x11 used in AlexNet. The GoogleNet architecture [4] was the first to really address the issue of computational resources along with multi-scale processing.

Through the use of 1x1 convolutions before each 3x3 and 5x5, the inception module reduces the number of feature maps passed through each layer, thus reducing computations and memory consumption. GoogleNet introduces a new idea that CNN layers didn't always have to be stacked up sequentially. The authors of the paper showed that you can also increase network width for better performance and not just depth. Since its initial publication in 2015, ResNets have created major improvements in accuracy in many computer vision tasks [5].

The main contribution of residual learning in ResNet architecture is to show that a naive stacking of layers to make the network very deep won't always help and can actually make things worse. To address the above issue, they introduce residual learning with skip-connections. The idea is that by

using an additive skip connection as a shortcut, deep layers have direct access to features from previous layers. This allows feature information to more easily be propagated through the network. It also helps with training as the gradients can also more efficiently be back-propagated.

At the same time, the development of DenseNets significantly expanded the perspective of shortcut connections [6]. The above networks implement comprehensive cross-layer feed-forward pathway connections. Such an arrangement made it possible to outperform ResNets, as it enables each respective layer to employ as inputs the entire range of feature maps from prior layers, whereas the emerging maps serve as inputs for subsequent layers. To this end, DenseNets are associated with an ability to mitigate the vanishing gradient issue coupled with significant reductions in the parameter numbers, incentives for repeat feature use, and enhanced feature propagation. Moreover, a relatively small convolutional neural network (CNN) titled SqueezeNet designed by authors in [7]. They proved to require fifty times fewer parameters to produce a level of accuracy equal to that of AlexNet. On top of such an accomplishment, this CNN can be reduced to 0.5MB. This size is 510 times smaller than that of AlexNet. Correspondingly, such compressed architecture has a number of advantages, as it is applicable for less bandwidth, uses less inter-server communication in the course of training, and has more feasibility for implementation on field-programmable gate arrays (FPGAs), as well as other limited memory hardware.

The paper emphasizes the opportunities for obtaining texture information from a palmprint on the basis of such descriptors as Curvelet [8], Wavelet [9], Wave Atom [10], SIFT [1], Gabor [11], LBP [12], and AlexNet [7]. The key contribution is the application of mode voting method for accurate identification of a person at the fusion decision level. The experiments on IITD and CASIA databases have presented the efficiency of the proposed approach.

This paper is designed as follows. Section 2 describes the related works of palmprint recognition are obtainable and examined. In Section 3, we describe the methodology of the proposed approach. Section 4 explains the experiments and results of the suggested method. Section 5 assesses the results and feeds the conclusion.

## II. RELATED WORK

Palmprint is emerging as alternative hand-based biometrics with user friendliness, flexibility in adapting the environment, and power of discrimination. The uniqueness and stability of palmprints make them a powerful source for ensuring sound criminal identification and access control. Research has reported progress in overcoming the limitations of wavelet analysis and synthesis by the application of composite dual-tree complex transforms coupled with Fourier transform for the purpose of extracting texture features for Support Vector Machine (SVM) detector.

Han [13] calculated seven detailed lines shapes from palmprint with three fingers using the low frequency data obtained from wavelets. This new feature vector is reduced its dimensionality using PCA. Optimum positive Boolean

function and Global learning vector quantization are used to construct the final decision.

Mu, Ruan and Shen [14] claimed a new approach to palmprint representation, which encompasses differentiation of a palmprint into separate areas of equal size. Discriminative local binary patterns statistic (DLBPS) are then utilized to identify the palmprint texture characteristics by the means of examining the distribution of patterns.

Zeng and Huang [15] solve the problem of linked features which generated because of using PalmCode for distinctive palms. In order to remove this correlation, they used PalmCodes and phase data that obtained from Gabor filters. The phase data is merged to obtain the Fusion Code using a fusion rule.

Conversely, hybrid approaches take the global and local features into consideration, which is arguably to be potentially the best approach. The author in [16] adopted such an approach to detect palmprint features from an image through the combined efforts of Discrete Cosine Transform (DCT) and Discrete Wavelet Transform (DWT). The use of Euclidean distance as a matching metric resulted in improved recognition outcomes as opposed to those produced by a separate implementation of DCT or DWT.

The author in [17] applied Hough transform for an extraction of distinct fingerprint features. This study will consider implementing Dempster-Shafer evidence theory and Bayesian fusion technique [18], majority rule [19], weighted majority algorithm [20], behavior-knowledge space method [21] and disjunction ("AND") vs conjunction ("OR") models [22] for fusion at the decision level.

The texture features extracted using Gabor filters have often performed well for recognition tasks including iris, face, and fingerprint. In the case of palmprint recognition, it has been shown to outperform line based and appearance-based approaches. Several techniques have been proposed for palmprint identification based on binary encoding of quantized Gabor features, including the use of subspace methods to reduce dimension. These approaches have gained popularity due to its efficient and compact representations, which are more suitable for online applications as in [23], [24], and [25].

One study of palmprint recognition [9] established the productivity of wavelet transforms in generating a successful 90% mid-level reference. Another study, Misar and Gharpure [26] described the features of palmprint images post extraction through the utilization of wavelet coefficients.

This study will involve an exception of the target palm area from the palm image based on the palm geometry, whereby the palm will need to be present in any direction opposite to the camera.

Wave Atom has advantage of compression above the other transforms [27]. In [28], the Wave Atom and the bidirectional 2D principal component analysis (B2DPCA) are applied to the cropped image to decrease the feature vectors dimension and they use the Extreme Learning Machine (ELM) as a classifier.

In [8], a comparison between Curvelet transform, Gabor filter, discrete cosine-transform and wavelet is performed which retrieves capabilities of Curvelet transform superior than all of other transforms in this study. For palmprint recognition, authors in [29] firstly implemented digital curvelet transform and the recognition rate of the experiment was up to 95.25%. In [30], the Support Vector Machine (SVM) as a classifier for the curvelet decomposed features of palm-print, the recognition accuracy became 98.5%. In [31], the second frequency band of curvelet coefficients is used to represent the palmprint image. The recognition accuracy of the experiments was up to 99.9%.

Furthermore, researchers Chen and Moon [32] effectively extracted palmprint features using Scale Invariant Feature Transformation (SIFT) descriptions and fusion based on Symbolic Aggregate Approximation (SAX). Zhao, Bu and Wu [33] fused competitive coding and SIFT to enhance palmprint verification.

In their turn in [34], they proposed a new verification system on a basis of palmprint and hand shape fusion screened through SIFT. Such an adjustment improved the effectiveness of SIFT in extracting the features that are invariant to scaling and image rotation across various applications such as object identification and video tracking. The experiments revealed promising matching score findings in the aspect of fusing palmprint and handshape features using the IIT Delhi Touchless Palmprint Database [35].

Reference [36] applied the sparse representation of SIFT to implement a touchless method for palmprint identification by extracting the left and right palms' print features. The SVM probability distribution detector was used to produce the rank level fusion in finalizing a personal identification.

Several studies yielded competitive palmprint identification findings on the bases of REGim Sfax Tunisia (REST) hand database [36] and CASIA Palmprint Database [1]. In particular, they developed a bimodal identification approach using SIFT descriptors for obtaining hand shape and palmprint features. The researchers applied a local sparse representation technique to examine images with high discrimination. Additionally, they implemented a cascade fusion at decision and feature levels to reach a notable 99.57% rate of identification, which is among the best related outcomes reported in research literature.

Local Binary Pattern (LBP) is one of the simple techniques to extract an identification feature in use across different computer applications [37]. Researchers in [38] utilized boosted LBP for purposes of palmprint identification. Under this method, scalable sub-sections in the LBP based histograms serve to depict the scanned palmprint features. However, the resulting texture is distorted and involves vague multidirectional ridges and lines. Later in [39], LBP shaped the basis for feature extraction in an enhanced identification approach grounded in the directional shifts of gradient operator. Finally, the above method was further improved in the aspects of speed and precision (Promila and Laxmi [12]).

Deep learning is a well-known machine learning subsegment, which addresses algorithms in the field of

artificial neural networks modeling the neurobiological behavior of the human brain.

The author in [40] utilized CNN to classify handwriting digits using the method of backward error propagation. They accomplished notable progress as indicated by 150,000 testing images, 1.2 million training, and 50,000 validations. In the ImageNet Large Scale Visual Recognition Challenge (ILSVRC) contest from 2015, authors in [2] were able to train a comprehensive CNN capable of categorizing nearly 1.2 million images in high resolution under one thousand distinct categories. This expert achieved impressive 17% and 37.5% scores on the top-five and top-one fault rates in the test phase effectively surpassing the earlier records. Correspondingly, his AlexNet encompasses five convolutional layers, sixty million factors, and 650,000 neurons. Three of the above are full-scale layers with no less than 1000-way SoftMax, whereas the other two are supported by ordinary max pooling layers. Some important suggestions were made to increase the training speed by the means of improving the convolution process with regard to graphics processing unit (GPU) and non-saturate neurons. Moreover, the problem of overfitting in the three connected layers was addressed by a very progressive regularization method of "dropout." As a result, the modified version of AlexNet produced the 15.3% winning score on the top-five fault rate as compared to 26.2% from its closest competitor in the ILSVRC-2012.

Another massive-scale classification of images using a comprehensive 19-weight-layers convolutional network was performed by Simonyan and Zisserman [3]. The experiment indicated the usefulness of illustration depth in enhancing the accuracy of categorization. Overall, the utilized models proved to have high generalizability across different sets of data and tasks, whereby they were capable of outperforming some more sophisticated recognition systems. Furthermore, a substantial deep convolutional architecture with 22 layers entitled GoogleNet [4] was designed in 2015. Its chief distinctive characteristic is the improved process of inside-network computing resources utilization. GoogleNet was also expanded in width and depth at no significant extra costs from the computational budget. The quality optimization was achieved through multi-scale processing intuitions and the Hebbian principle.

In this regard, the steady increase in network depth prompted the development of deep residual learning methodology [5] for training facilitation. In contrast to approaching layers as targeting non-referenced functions, under this framework, they are re-conceptualized to learn residual functions with an emphasis on the input domains. The resulting residual architectures are both deeper and less complex contributing to the increased accuracy and ease of optimization. In the Dense Convolutional Network or DenseNet designed by authors [6] in 2017, all layers are cross-connected in a feed forward pathway. Some significant advantages of such an architecture include a marked reduction in the parameter numbers, enhanced feature propagation, mitigation of the vanishing gradient issue, and incentive for repeat feature use. To this end, a small ImageNet-based CNN entitled Squeezenet [7] proved to require fifty times fewer parameters to accomplish the same level of accuracy than

AlexNet. With the use of compression techniques, it can be reduced to up to 510 size of AlexNet, which is equal to 0.5 MB.

Deep learning has been effectively utilized across diverse biometric domains as a breakthrough method in computer-based image processing. Highly satisfactory outcomes have been particularly linked to palmprint recognition. The author in [41] used a three-step process in implementing the above technique for palmprints within a deep confidence architecture. They first developed top-to-down training with no supervision to instruct the selected samples. The researchers further identified optimum parameters to amend the system for an improved performance. Finally, they employed deep learning models to examine the test samples. In the outcome, the deep learning approach proved to be associated with advanced recognition scores for palmprints as

compared with the traditional techniques, including LBP and principal component analysis (PCA).

Minaee and Wang [42] designed a convolutional scattering transform/network for purposes of palmprint recognition through multi-layer representations. The network runs on default wavelet transforms. Its initial layer targets the relevant features for processing through SIFT description, whereas the higher layers extract contents of increased frequency inaccessible for descriptors. PCA contributes to the process of recognition by adjusting its computational complexity. It is specifically used to reduce scattering feature dimensionality following an extraction. Finally, recognition is ensured by two distinct classifiers, including a minimum distance classifier and a multi-class SVM. The described procedure yielded 99.95% to 100% accurate recognitions upon its testing at a recognized palmprint database.

TABLE I. COMPARISON BETWEEN PALMPRINT BIOMETRIC SYSTEMS IN THE RELATED WORK [46]

| Ref. | Database  | Features Classification  | Features Extraction                                    | RR  |
|------|---|--|--|---|
| [13] | Grabbed from a CCD camera                         | GLVQ approach  | Wavelet  | FRR = 1.6%, FAR = 36.3%   |
| [29] | PolyU   | Euclidian distance classifier                                    | Digital Curvelet Transform                             | 95.25   |
| [47] | PolyU Palmprint Database                          | SVM  | Dual-tree complex wavelet transforms                   | 97  |
| [38] | UST-HK palmprint database                         | Chi square distances   | Boosting Local Binary Pattern                          | Equal Error Rate = 2%   |
| [32] | PolyU   | Symbolic Aggregate approximation                                 | SIFT   | Equal Error Rate = 0.37%  |
| [39] | palm print tracking in dynamic environment        | Chi square and PNN   | Sobel and LBP  | PNN: EER=0.74%<br>Chi: EER=1.52%  |
| [30] | PolyU   | SVM  | Digital Curvelet Transform                             | 98.5  |
| [14] | Fujitsu fi-60F high speed flatbed scanner is used | Nearest neighbor (NN) classifier based on the Euclidean distance | Discriminative local binary patterns statistic (DLBPS) | 98  |
| [15] | PolyU Palmprint Database                          | Euclidean distance and the nearest neighbor classifier           | Gabor features   | 100   |
| [9]  | Hong Kong Polytechnic University 2D_3D Database   | Mean square error  | Wavelets   | 93  |
| [12] | PolyU   | Chi-square test and Pearson correlation test                     | LBP  | 99.22   |
| [33] | IITD  | Competitive code algorithm                                       | SIFT   | Equal Error Rate = 0.49%  |
| [16] | IITD, PolyU                                       | Euclidean Distance   | DWT - DCT  | 94.44, 95.65  |
| [34] | IITD  | Matching Score   | SIFT   | Palmprint = 94.05<br>Hand shape + Palmprint = 97.82   |
| [24] | CASIA IITD  | Euclidean Distance   | 2D Gabor filter  | 90.76<br>91.4   |
| [41] | Beijing Jiao Tong University                      | DBN  | DBN  | 90.63   |
| [26] | IITD  | Neural Network   | Discrete Wavelet Transform                             | 75.6  |
| [31] | PolyU   | Nearest neighbor method  | Digital Curvelet Transform                             | 99.9  |
| [36] | IITD  | Matching score   | SIFT and Gabor   | Palmprint = 91.08 Hand shape + Fingers + Palmprint = 98.04  |
| [1]  | IITD Bosphorus                                    | SVM  | SIFT sparse representation                             | IITD: Palmprint = 96.73<br>Hand shape + Palmprint = 99.57<br>Bosphorus: Palmprint = 94.95<br>Hand shape + Palmprint = 97.61 |
| [42] | PolyU   | Minimum distance SVM   | Scattering Features + PCA                              | 99.95<br>100  |
| [43] | PolyU   | Softmax  | CNN-F architecture                                     | 100   |
| [45] | IITD 11k  | SVM  | CNN-features + LBP                                     | IITD: CNN Fea. = 90<br>CNN Fea. + LBP = 94.8<br>11k: CNN Fea. = 94.8<br>CNN Fea. + LBP = 96                                 |

A deep CNN was also employed in a project implemented by authors in [43] to extract palmprint features. Because of its capacity to combine features across all levels, the CNN has been marked for its outstanding performance with respect the processing of images, speech, and video. The researchers specifically applied the CNN-F model to identify and verify convolutional features across different architecture layers. The resulting findings on the basis of PolyU palmprint database yielded 0.25% and 100% with respect to verification accuracy and identification score respectively evidencing the reliability and effectiveness of CNN in the aspect of palmprint recognition. Another block approach entitled “Squeeze-and-Excitation” (SE) was introduced in [44] to provide explicit inter-channel modeling for purposes of improving the flexibility of channeled feature reactions. The researchers found that Squeeze-and-Excitation Networks (SENet) developed through a combination of blocks had high generalizability across a wide variety of sets of channeling data. Finally, the extensive dataset of hand images containing empirical evidence for biometric and gender identification suggested by Afifi [45] contributed to the sound CNN training in the aspect of biometric identification. The trained system proved effective in extracting features to yield a range of SVM classifiers.

Table I summarizes the unimodal system palmprint methods, proposed in the literature.

### III. METHODOLOGY

Two systems are used in this paper; the block diagram of the first system is shown in Fig. 1. Whereas the second system shown in Fig. 2. The segmented palmprint (ROI) palmprint of CASIA [48] and IITD databases [35] are used for the two systems. IITD database consists of 230 subjects, about 10 images for each, left and right with size 150x150 pixels in grayscale. CASIA database contains 240 subjects, around 10 images for each subject classified left and right with size 192x192 pixels. Images are resized to 227x227 pixel and converted to RGB to extract features for CNN.

#### A. Features Extraction

In the initial setting, the project uses a variety of feature representations extracted from the same person using such texture-based techniques as Curvelet, Wavelet, Wave Atom, SIFT, Gabor, LBP, and AlexNet. Such an undertaking shapes a new methodology for improving the matching process accuracy in palmprint recognition.

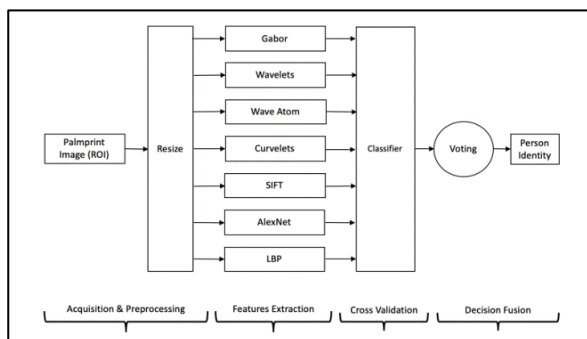


Fig. 1. System 1: Human Identification using Texture based Descriptors for Palmprint Images (Elgallad et al., 2017).

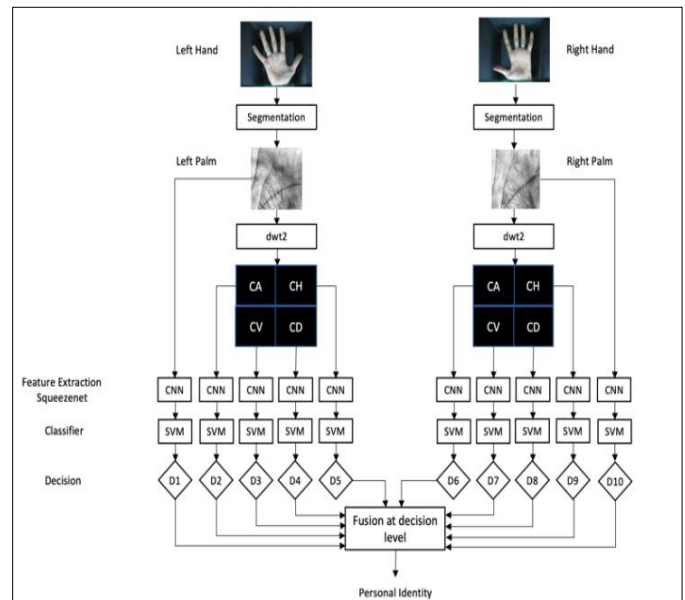


Fig. 2. System 2: Dense Hand-CNN: CNN Architecture based on Later Fusion of Neural and Wavelet Features.

Wave-packet transforms such as Gabor function, wavelets, wave atoms and curvelet are used in this system. 2D wave packets is denoted as  $\varphi_{\mu}(\chi_1, \chi_2)$ . The main parameters for wave packet architectures which are used as indicator are  $\alpha$  and  $\beta$ . If ( $\alpha = 1$ ), this indicates that multiscale decomposition is used. While ( $\alpha = 0$ ) indicates that it is not. Base elements may be either local or weakly directional.  $\beta$  parameter is used to index the base element. When ( $\beta = 1$ ), it is extended and entirely directional when ( $\beta = 0$ ) [8]. When ( $\alpha = 1, \beta = 1/2$ ), this match Curvelet. Wavelets match ( $\alpha = \beta = 1$ ), and the Gabor transform is match to ( $\alpha = \beta = 0$ ). Wave atoms are described as the point  $\alpha = \beta = 1/2$ .

Using (1) to extract Gabor features from the resized image (64x64 pixels):

$$G(x, y, \theta, u, \sigma) = \frac{1}{2\pi\sigma^2} \exp\left\{-\frac{x^2 + y^2}{2\sigma^2}\right\} \quad (1)$$

The features vector is constructed by merging the mean squared energy and mean amplitude matrices. Two factors are examined to get the best possible features, wavelet scales' number and filter orientations' number.

Haar wavelet filter is used to perform Single-level wavelet transform. The resized input image (64x64 pixels) is used to obtain the approximation coefficients matrix using (2a, 2b):

$$w(a, b_1, b_2) = \frac{1}{a} \int_{-\infty}^{+\infty} \int_{-\infty}^{+\infty} I(x, y) \psi\left(\frac{x-b_1}{a}, \frac{y-b_2}{a}\right) dx dy \quad (2a)$$

$$\psi_H(x, y) = \begin{cases} 1, 0 \leq x < \frac{1}{2}, 0 \leq y < 1; \\ -1, \frac{1}{2} \leq x < 1, -1 < y \leq 0; \\ 0, \text{else} \end{cases} \quad (2b)$$

Partitioning of the frequency in parabolic scaling with a single defined oscillation direction and real-valued frame forms the basis of the forward 2D wave atom transform extended by mirror. As described in (3), the wave atom transform is utilized to extract a cell array comprising the related coefficients from the input image with adjusted size of 64x64.

$$|\varphi_\mu(\omega)| \leq C_M \cdot 2^{-j} (1 + 2^{-j} |\omega - \omega_\mu|)^{-M} + C_M \cdot 2^{-j} (1 + 2^{-j} |\omega + \omega_\mu|)^{-M}$$

and

$$|\varphi_\mu(x)| \leq C_M \cdot 2^{-j} (1 + 2^{-j} |x - x_\mu|)^{-M} \text{ for all } M > 0,$$

where

$$x_\mu = 2^{-j} n \quad \omega_\mu = \pi 2^{-j} m \quad C_1 2^j \leq \max_{i=1,2} |m_i| \leq C_2 2^j \quad (3)$$

where C1 and C2 > 0, and will be indirect by the details of the execution.

In DWT, multi-stage filter banks with high-pass (HP) and lowpass (LP) filters are used to perform a series of dilations. detail coefficients are obtained after the HP filters while the approximate coefficients are obtained after the LP filter [26]. Furthermore, the two-dimensional setting involves three distinct classes of detail coefficients situated across diagonal, horizontal, and vertical pathways. To this end, the detail coefficients are represented by the respective subbases LH<sub>j</sub>; HL<sub>j</sub>, and HH<sub>j</sub>; j = 1; 2;...; J, whereby the most coarse or the largest decomposition scale is denoted as J and j identifies the scale. The multilevel wavelet decomposition is depicted at the third level under Fig. 3.

To extract the curvelet coefficients, Fast Discrete Curvelet Transform via wedge wrap is used for 128x128 input images as in (4a,4b):

$$c_{j,\ell,b} = \int \hat{f}(\omega) U_{j,\theta_\ell}(\omega) e^{ib \cdot \omega} d\omega, \quad (4a)$$

where  $U_{j,\theta_\ell}$  is a real wedge frame value that expanded to measure j and by the shearing process, parabolic restricted to angles close to  $\theta_\ell$ . The value of b in (4a) should be evaluated to discrete curvelet factors which are still a fitted structure:

$$f(x) = \sum_{i,\ell,k} \langle f, \varphi_{j,\ell,k} \rangle \varphi_{j,\ell,k}(x), \quad (\text{conv. in } L^2). \quad (4b)$$

Constant local feature arguments are extracted using the Scale Invariant Feature Transform [1]. To select key locations in scale space, local smallest and highest values of a variance of Gaussian function are used by Comparing each pixel to its neighbors as in (5), (7):

$$L(x, y, \sigma) = G(x, y, \sigma) * I(x, y) \quad (5)$$

where the scale space is L(x, y, σ), I(x, y) is the input image, and G(x, y, σ) is defined as:

$$G(x, y, \sigma) = \frac{1}{2\pi\sigma^2} e^{-(x^2+y^2)/2\sigma^2} \quad (6)$$

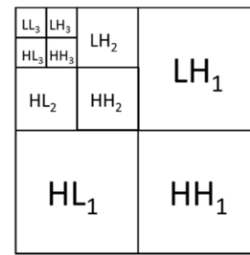


Fig. 3. Level 3 Wavelet Decomposition [49].

which is a variable scale function, and the Gaussian difference scale space is defined as:

$$\begin{aligned} D(x, y, \sigma) &= (G(x, y, k\sigma) - G(x, y, \sigma)) * I(x, y) \\ &= L(x, y, k\sigma) - L(x, y, \sigma) \end{aligned} \quad (7)$$

When extreme points locations are detected, the key points that are invariant to affine transformations and unaffected to noise must be used.

As in (8), (9), to compute the direction, a neighborhood is determined around the key point to find its descriptor using gradient magnitude  $m(x,y)$  and the scale.  $\theta(x,y)$  is the orientation of the key point.

$$m(x, y) = \sqrt{(L(x+1, y) - L(x-1, y))^2 + (L(x, y+1) - L(x, y-1))^2} \quad (8)$$

$$\theta(x, y) = \tan^{-1} \left( \frac{L(x, y+1) - L(x, y-1)}{L(x+1, y) - L(x-1, y)} \right) \quad (9)$$

AlexNet is utilized as a CNN for purposes of extracting learned image features. The corresponding architecture encompasses a combined activity of two layer types, including the three connected layers and the initial five convolutional layers. As seen in Fig. 4, a 1000-way softmax delivers distributions beyond 1000 class labels serving as the output of the mentioned connected layers [2].

The palmprint identification perspective involves discriminative LBP features [38]. Upon the detection of the dominant pixel in the representation, the pattern code is matched against neighbors to produce the needed calculation as per (10).

$$LBP_{P,R} = \sum_{p=1}^P s(g_p - g_c) 2^{p-1} \quad (10)$$

where

$$s(x) = \begin{cases} 1, & x \geq 0 \\ 0, & x < 0 \end{cases}$$

The second setting employs such feature extraction instruments as SqueezeNet and discrete wavelet transform. The former is an architecture with default training based on the ImageNet database sample comprising over one million of images. The model can thus categorize images across 1000 respective object categories. There are three key techniques used in SqueezeNet to design CNN systems [7]. Firstly, 3x3 filters need to be replaced by 1x1 filters, as the latter have nine times fewer parameters. Secondly, squeeze layers should be applied to achieve a drop in the number of input channels.

Thirdly, the sample should be downed late in the system to ensure significant maps of activation for convolution layers.

### B. Cross Validation

Originally introduced by Vapnik [50], the SVM is utilized as a cross-validation classifier in the mentioned settings. SVM belongs to the class of Maximum Margin Classifiers (MMC) and is linked to Structural Risk Minimization (SRM). It serves as an input vector to the space of the upper dimension featuring the top separating hyperplane. The project particularly involves a multi-class linear SVM to account for the 230 of its subjects or classes [1].

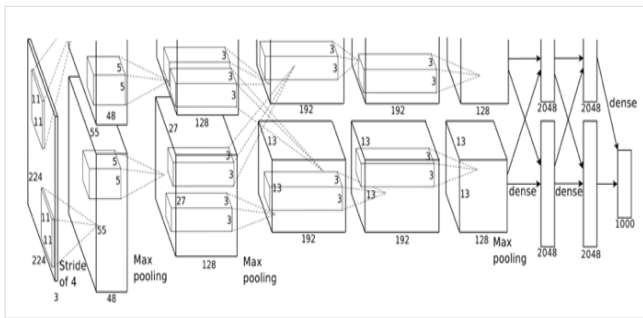


Fig. 4. AlexNet Convolutional Neural Network Architecture [2].

The training data set and its labels is  $(x_n, y_n), n=1, \dots, N, x_n \in \mathbb{R}^D, t_n \in \{-1, +1\}$ , SVMs learning includes the subsequent controlled optimization:

$$\begin{aligned} \min_{w, \xi_n} &= \frac{1}{2} w^T w + C \sum_{n=1}^N \xi_n \\ \text{s. t.} & w^T x_n t_n \geq 1 - \xi_n \quad \forall n \\ & \xi_n \geq 0 \quad \forall n \end{aligned} \quad (11)$$

where  $\xi_n$  are the slack variables,  $w$  is the vector of coefficients, and  $C$  is the capacity constant.

The unconstrained optimization problem in (11) that is recognized as the primal form problem of L1-SVM:

$$\min_w = \frac{1}{2} w^T w + C \sum_{n=1}^N \max(1 - w^T x_n t_n, 0) \quad (12)$$

Meanwhile L1-SVM is not differentiable, the L2-SVM is used to minimize the squared hinge loss as in (12):

$$\min_w = \frac{1}{2} w^T w + C \sum_{n=1}^N \max(1 - w^T x_n t_n, 0)^2 \quad (13)$$

The class label of a test data  $x$  is:

$$\arg_t \max(w^T x) t \quad (14)$$

Multiclass SVM uses one-vs-rest approach to represent the output of the  $k$ -th SVM.

$$a_k(x) = w^T x \quad (15)$$

the forecast class is

$$\arg_k \max a_k(x) \quad (16)$$

### C. Score Fusion

Among the greatest information fusion system challenges is the problem of determining the needed type of data for consolidation under the fusion module. Multiple fusion

strategies are available across all four levels. The discussed settings in [51] involve the match score level fusion as representative of the principal fusion level in biometrics.

The match score identifies similarities between the default biometric feature and the input vectors. In its turn, the match score level fusion is accomplished to make an outcome recognition decision upon the consolidation of output match scores based on the relevant biometric matches [51]. There were many approaches that are used in fusion at decision level such as: Majority Voting and Weighted Majority Voting. In our proposed systems, we introduced a novel approach in decision level technique, the Mode Voting Technique (MVT).

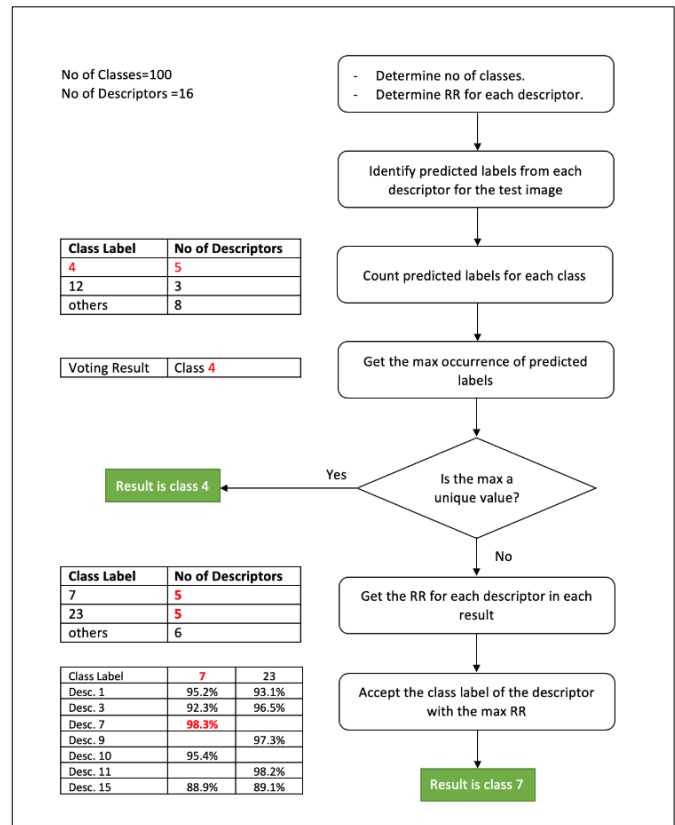


Fig. 5. Flowchart of Mode Voting Technique (MVT).

### D. Mode Voting Technique

Mode Voting Technique (MVT) is a novel voting technique that is consolidating information at the decision level. This method utilizes the standard class label values that are retrieved from the predicted label array obtained through the SVM discriminate classifier.

Fig. 5 explains the flowchart of MVT with illustrated example.

The mode voting technique uses the most common class label values obtained from the predicted label array that was extracted from SVM classifier. In order to identify human, the mode voting technique is implemented to find the most frequent non-repeated scores in the predicted label array  $X$ .

$$Z = \text{mode}(X_{k,i}) \quad (17)$$



where  $Z$  is the class label of the test image,  $k$  is the index of the test image, and  $i$  is the index of the descriptor.

#### IV. EXPERIMENTAL RESULTS

In the proposed systems, two sets of databases are which are CASIA Palmprint Database and Delhi Touchless Palmprint Database IIT version 1.0. CASIA Palmprint database contains 2400 palmprint images for 240 subjects from left and right palms in size 192x192 pixels for the segmented palmprint ROI. The images are 8 bit gray-level JPEG files. IITD database basically contains hand images saved in format of bitmap and contains both of left-right hands images for 230 persons in size 150x150 pixels. The age varied between 14 and 56 years old. The segmented and normalized of palmprint regions are available. For CNN feature extraction, the images are improved to RGB and resized to 227x227 pixels. In both systems, SVM classifier is used.

In the first system, the Gabor features are 120. The recognition rate is 70.29% with IITD, and 87.46% with CASIA.

The Wavelets features are 1024. The recognition rate is 80.94% with IITD, and 92.46% with CASIA.

In wave atom, the output array is obtained and organized to get 1120 elements. The recognition rate is 77.32% with IITD, and 92.39% with CASIA.

In Fast Discrete Curvelet Transform, features are 121. The recognition rate is 79.57% with IITD, and 91.16% with CASIA.

In Scale Invariant Feature Transform, 1024 features are extracted from 150x150 images. The recognition rate is 96.96% with IITD, and 98.91% with CASIA.

AlexNet convolutional neural network is used to extract 4096 features from the last fully-connected layer. The recognition rate is 93.91% with IITD, and 98.55% with CASIA.

LBP output the histogram of 64x64 input images. The output array has 256 features. The recognition rate is 66.81% with IITD, and 82.54% with CASIA.

Table II illustrates the results of the used seven descriptors for both databases. The fusion at decision level using mode voting technique, which depends on each descriptor's predicted label array, achieved a recognition rate equals to 99.57% with IITD database, with processing time for each image 1.88 sec. With CASIA database, the recognition rate is 100%, with 2.36 sec processing time for each image.

Fig. 6 shows CMC Curves of system1, probability of detecting the correct identity within the top K ranks for the descriptors.

The main objective of the second system is to reduce the processing time for each image and maintain the high recognition rate obtained from the first system.

TABLE II. RESULTS OF THE FIRST SYSTEM

| Descriptor        | Features | IITD         | CASIA       |
|-------------------|----------|--------------|-------------|
| Gabor             | 120      | 70.29        | 87.46       |
| Wavelets          | 1024     | 80.94        | 92.46       |
| WaveAtoms         | 1120     | 77.32        | 92.39       |
| Curvelet          | 121      | 79.57        | 91.16       |
| SIFT              | 1024     | 96.96        | 98.91       |
| AlexNet           | 4096     | 93.91        | 98.55       |
| LBP               | 256      | 66.81        | 82.54       |
| <b>Voting</b>     |          | <b>99.57</b> | <b>100</b>  |
| <b>Time / Sec</b> |          | <b>1.88</b>  | <b>2.36</b> |

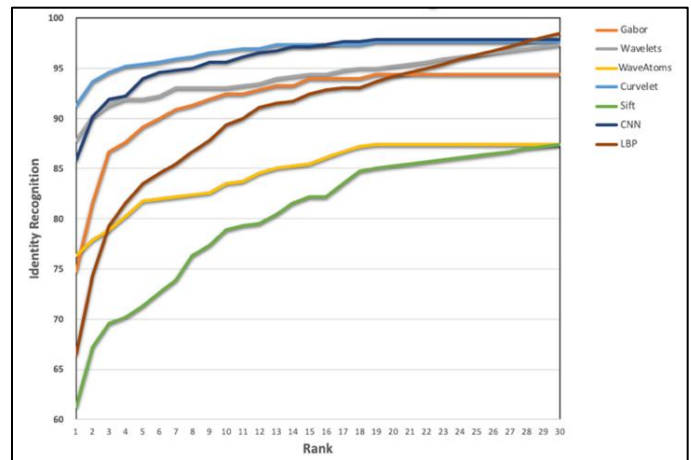


Fig. 6. CMC Curves: Probability of Detecting the Correct Identity within the top K Ranks.

SqueezeNet has 50x fewer parameters compared with AlexNet. It has a model compression technique which can compress SqueezeNet to less than 0.5MB (510 smaller than AlexNet). Due to these advantages, it's used as a feature extractor in the second system.

The left and right palm for each subject is used. The features are obtained from Squeezenet for the palm images, and the single-level 2-D discrete wavelet transform (DWT) of the images using the Haar wavelet filter. The DWT yields the approximation coefficients matrix  $cA$  with the detail coefficients matrices  $cH$  (horizontal),  $cV$  (vertical), and  $cD$  (diagonal).

The predicted label arrays obtained from SVM as a classifier for the obtained features are fused using mode voting technique. The recognition rate equals to 100% with IITD database, with processing time for each image 0.74 sec. With CASIA database, the recognition rate is 99.6%, with 0.67 sec processing time for each image.

Table III illustrates the detailed result of the second system.

TABLE III. RESULTS OF THE SECOND SYSTEM

| Descriptor | IITD  |      |       |      | CASIA |      |       |      |
|------------|-------|------|-------|------|-------|------|-------|------|
|            | L     |      | R     |      | L     |      | R     |      |
|            | RR    | t/s  | RR    | t/s  | RR    | t/s  | RR    | t/s  |
| SqueezeNet | 96.96 | 0.06 | 97.61 | 0.07 | 97.92 | 0.09 | 96.25 | 0.07 |
| CA         | 88.70 | 0.06 | 89.57 | 0.07 | 92.92 | 0.07 | 90.42 | 0.06 |
| CH         | 87.83 | 0.07 | 90.00 | 0.07 | 64.79 | 0.06 | 46.46 | 0.06 |
| CV         | 93.91 | 0.07 | 94.13 | 0.07 | 87.08 | 0.06 | 82.71 | 0.06 |
| CD         | 62.46 | 0.09 | 53.91 | 0.09 | 5.00  | 0.07 | 5.42  | 0.07 |
| Voting %   | 100   |      |       |      | 99.6  |      |       |      |
| Time/sec.  | 0.74  |      |       |      | 0.67  |      |       |      |

### V. DISCUSSION

The results show that the fusion at decision level promises an outstanding recognition rate regardless of low recognition rate of some descriptors and filters. The mode voting technique positions top of the list of SVM classifiers used for each descriptor.

Table IV displays the performance of the proposed palmprint recognition systems vs. current systems in the related work that use IITD and CASIA databases.

A significant issue in this comparison table is the processing time that is explained in Table V. in System1, the processing time for an image of IITD database is 1.88s, while in CASIA is 2.36s. In the second system, the process time is 0.74s in IITD, and 0.67 in CASIA database.

TABLE IV. PERFORMANCE COMPARISON OF PROPOSED PALMPRINT RECOGNITION SYSTEM VS. EXISTING SYSTEMS USING IITD AND CASIA DATABASES

|                    | System1       |       | System2          |              |
|--------------------|---------------|-------|------------------|--------------|
| Palmprint Database | IITD          | CASIA | IITD             | CASIA        |
| Hand               | Left          | Left  | Left & Right     | Left & Right |
| No of Subjects     | 230           | 230   | 230              | 240          |
| Feature extraction | 7 descriptors |       | SqueezeNet & dwt |              |
| Classifier         | SVM           |       | SVM              |              |
| Result by Fusion   | 99.57         | 100   | 100              | 99.6         |
| Time/image in sec. | 1.88          | 2.36  | 0.74             | 0.67         |

TABLE V. PROCESSING TIME COMPARISON

| Ref.                     | Features Extractor         | Features Classifier        | Database              | RR(%)   |
|--------------------------|----------------------------|----------------------------|-----------------------|---|
| [33]                     | SIFT                       | competitive code algorithm | IITD                  | Equal Error Rate = 0.49%  |
| [16]                     | DWT - DCT                  | Euclidean Distance         | IITD, PolyU           | 94.44, 95.65  |
| [34]                     | SIFT                       | Matching Score             | IITD                  | Palmprint = 94.05<br>Hand shape + Palmprint = 97.82   |
| [24]                     | 2D Gabor filter            | Euclidean Distance         | CASIA<br>IIT Delhi    | 90.76<br>91.4   |
| [26]                     | Discrete Wavelet Transform | Neural Network             | IITD                  | 75.6  |
| [36]                     | SIFT and Gabor             | Matching score             | IITD                  | Palmprint = 91.08<br>Hand shape + Fingers + Palmprint = 98.04   |
| [1]                      | SIFT sparse representation | SVM                        | IITD<br>Bosphorus     | IITD: Palmprint = 96.73<br>Hand shape + Palmprint = 99.57<br>Bosphorus: Palmprint = 94.95<br>Hand shape + Palmprint = 97.61 |
| [45]                     | CNN-features+LBP           | SVM                        | IITD<br>11k           | IITD: CNN Fea. = 90<br>CNN Fea. + LBP = 94.8<br>11k: CNN Fea. = 94.8<br>CNN Fea. + LBP = 96                                 |
| <b>Proposed system 1</b> | <b>7 Descriptors</b>       | <b>SVM</b>                 | <b>IITD<br/>CAISA</b> | <b>99.57<br/>100</b>  |
| <b>Proposed system 2</b> | <b>SqueezeNet +dwt</b>     | <b>SVM</b>                 | <b>IITD<br/>CAISA</b> | <b>100<br/>99.6</b>   |

## VII. CONCLUSION

This work statements two palmprint recognition systems depending on the mode voting technique, and compares the performance of the systems for image processing time. The novelty comes from using mode voting technique at decision level. Our experimental results demonstrate the effectiveness of the suggested systems.

The selection of SqueezeNet and DWT in the second system depends on the result of the first system. As Alexnet achieved high recognition rate, we looking forward to deep learning especially for SqueezeNet due to its advantage. Also, for DWT, the four filters are used, compared with one filter in the first system, to increase the number of predicted label arrays that are needed for mode voting technique.

For future work, MVT can be tested on other experiments in [52:56] to enhance the result and ensure the quality of MVT.

### REFERENCES

- [1] N. Charfi, H. Trichili, A.M. Alimi and B. Solaiman, "Bimodal biometric system for hand shape and palmprint recognition based on SIFT sparse representation". *Multimedia Tools and Applications*, 2016, pp.1-26.
- [2] A. Krizhevsky, I. Sutskever and G.E. Hinton, "ImageNet classification with deep convolutional neural networks", In *Advances in neural information processing systems*, 2012, pp. 1097-1105.
- [3] K. Simonyan and A. Zisserman, "Very deep convolutional networks for large-scale image recognition", 2014, arXiv preprint arXiv:1409.1556.
- [4] C. Szegedy, W. Liu, Y. Jia, P. Sermanet, S. Reed, D. Anguelov, D. Erhan, V. Vanhoucke and A. Rabinovich, "Going deeper with convolutions", In *Proceedings of the IEEE conference on computer vision and pattern recognition*, 2015, pp. 1-9.
- [5] K. He, X. Zhang, S. Ren and J. Sun, "Deep residual learning for image recognition", In *Proceedings of the IEEE conference on computer vision and pattern recognition*, 2016, pp. 770-778.
- [6] G. Huang, Z. Liu, L. Van Der Maaten and K.Q. Weinberger, "Densely Connected Convolutional Networks", In *CVPR*, 2017, Vol. 1, No. 2, p. 3.
- [7] F.N. Iandola, S. Han, M.W. Moskewicz, K. Ashraf, W.J. Dally and K. Keutzer, "Squeezenet: Alexnet-level accuracy with 50x fewer parameters and < 0.5 mb model size", arXiv preprint arXiv:1602.07360, 2016.
- [8] I.J. Sumana, M.M. Islam, D. Zhang and G. Lu, "Content based image retrieval using curvelet transform", In *Proceedings of 2008 International Workshop on Multimedia Signal Processing*, pp. 11-16.
- [9] H. Kekre, B. Tanuja, K. Sarode and A.A. Tirodkar, "A study of the efficacy of using Wavelet Transforms for Palm Print Recognition", *International Conference on Computing, Communication and Applications*, Dindigul, Tamilnadu, 2012, pp. 1-6.
- [10] Demanet and Ying, "Wave atoms and sparsity of oscillatory patterns", Elsevier, 2007, pp. 368-387.
- [11] W. Ouarda, H. Trichili, A.M. Alimi and B. Solaiman, "Face recognition based on geometric features using Support Vector Machines", *Soft Computing and Pattern Recognition (SoCPar)*, 6th International Conference of, Tunis, 2014, pp. 89-95.
- [12] Promila and V. Laxmi, "Palmprint Matching Using LBP", *International Conference on Computing Sciences*, Phagwara, 2012, pp. 110-115. doi: 10.1109/ICCS.2012.55.
- [13] C.C. Han, "A hand-based personal authentication using a coarse-to-fine strategy", *Image and Vision Computing*, 2004, 22 (11) 909-918.
- [14] M. Mu, Q. Ruan and Y. Shen, "Palmprint Recognition Based on Discriminative Local Binary Patterns Statistic Feature", *International Conference on Signal Acquisition and Processing*, Bangalore, 2010, pp. 193-197.
- [15] Z. Zeng and P. Huang, "Palmprint recognition using Gabor feature-based two-directional two-dimensional linear discriminant analysis", *International Conference on Electronic & Mechanical Engineering and Information Technology*, Harbin, Heilongjiang, China, 2011, pp.191-1921.
- [16] V. Varshney, R. Gupta and P. Singh, "Hybrid DWT-DCT based method for palm-print recognition", *IEEE International Symposium on Signal Processing and Information Technology (ISSPIT)*, Noida, 2014, pp. 000007-000012.
- [17] A.K. Jain, S. Prabhakar and S. Chen, "Combining Multiple Matchers for a High Security Fingerprint Verification System", *Pattern Recognition Letters*, 1999, 20(11-13): 1371-1379.
- [18] L. Xu, A. Krzyzak and C.Y. Suen, "Methods for Combining Multiple Classifiers and their Applications to Handwriting Recognition. *IEEE Transactions on Systems, Man, and Cybernetics*, 1992, 22(3): pp.418-435.
- [19] L. Lam and C.Y. Suen, "Application of Majority Voting to Pattern Recognition: An Analysis of its Behavior and Performance", *IEEE Transactions on Systems, Man, and Cybernetics, Part A: Systems and Humans*, 1997, 27(5):553-568.
- [20] L.I. Kuncheva "Combining Pattern Classifiers-Methods and Algorithms", Wiley, 2004.
- [21] Y.S. Huang and C.Y. Suen, "Method of Combining Multiple Experts for the Recognition of Unconstrained Handwritten Numerals", *IEEE Transactions on Pattern Analysis and Machine Intelligence*, 1995, 17(1):90-94.
- [22] J. Daugman, "Combining Multiple Biometrics", 2000, Available: <http://www.cl.cam.ac.uk/users/jgd1000/combine/combine.html>. [Accessed 15 May 2017].
- [23] I. Fogel and D. Sagi, "Gabor filters as texture discriminator". *Biol. Cybern.* 1989, 61, 103-113.
- [24] G. Jaswal, R. Nath and A. Kaul, "Texture based palm Print recognition using 2-D Gabor filter and sub space approaches", *International Conference on Signal Processing, Computing and Control (ISPC)*, Wagnaghat, 2015, pp. 344-349.
- [25] A. Teuner, O. Pichler and B.J. Hosticka, "Unsupervised texture segmentation of images using tuned matched Gabor filters", *IEEE Trans. Image Process*, 1995, 4 (6), 863-870.
- [26] M. Misar and D. Gharpure, "Extraction of feature vector based on wavelet coefficients for a palm print based biometric identification system", *2nd International Symposium on Physics and Technology of Sensors (ISPTS)*, Pune, 2015, pp. 113-119.
- [27] Z. Haddad, A. Beghdadi, A. Serir and A. Mokraoui, "A new fingerprint image compression based on wave atoms transform". *IEEE International Symposium on Signal Processing and Information Technology (ISSPIT)*, Ajman, 2009, pp. 89-94.
- [28] A.A. Mohammed, Q.M. Jonathan Wu and M.A. Sid-Ahmed, "Application of Wave Atoms Decomposition and Extreme Learning Machine for Fingerprint Classification", In: A. Campilho and M. Kamel (eds) *Image Analysis and Recognition. ICIAR 2010. Lecture Notes in Computer Science*, vol 6112. Springer, Berlin, Heidelberg, 2010.
- [29] K. Dong, G. Feng and D. Hu, "Digital curvelet transform for palmprint recognition, *Advances in Biometric Person Authentication*", Springer Berlin Heidelberg, 2005, pp. 639-645.
- [30] X. Xu, D. Zhang, X. Zhang and Y. Cao, "Palmprint Recognition Based on Discrete Curvelet Transform and Support Vector Machine", *Journal of Infrared and Millimeter Waves*, 2009, vol. 28, no. 6, pp. 456-460.
- [31] F. Liu, L. Zhou, Z.M. Lu and T. Nie, "Palmprint Feature Extraction Based on Curvelet Transform", *Journal of Information Hiding and Multimedia Signal Processing*, 2015, 6(1), pp.131-139.
- [32] J. Chen and Y. Moon, "Using SIFT features in palmprint authentication", *19th International Conference on Pattern Recognition*, 2008, pp. 1-4.
- [33] Q. Zhao, W. Bu and X. Wu, "SIFT-based image alignment for contactless palmprint verification", in: *Proceedings of International Conference on Biometrics*, 2013, pp. 16.
- [34] N. Charfi, H. Trichili, A.M. Alimi and B. Solaiman, "Bimodal biometric system based on SIFT descriptors of hand images". *IEEE International Conference on Systems, Man, and Cybernetics (SMC)*, San Diego, CA, 2014, 2014, pp. 4141-4145.
- [35] IIT Delhi Touchless Palmprint Database version 1.0, [http://web.iitd.ac.in/~ajaykr/Database\\_Palm.htm](http://web.iitd.ac.in/~ajaykr/Database_Palm.htm). [Accessed 10 October 2018].

- [36] N. Charfi, H. Trichili, A.M. Alimi and B. Solaiman, "Personal recognition system using hand modality based on local features". 11th International Conference on Information Assurance and Security (IAS), Marrakech, 2015, pp. 13-18.
- [37] T. Ojala, M. Pietikainen and D. Harwood, "A comparative study of texture measures with classification based on feature distribution", *Pattern Recognition*, 1996, 29:51-59.
- [38] X. Wang, H. Gong, H. Zhang and Z. Zhuang, "Palmpoint Identification using Boosting Local Binary Pattern. *Pattern Recognition*", 18th International Conference on Pattern Recognition (ICPR'06), Hong Kong, 2006, pp. 503-506.
- [39] G.K.O. Michael, T. Connie and A.B.J. Teoh, "Touch-less palm print biometrics: Novel design and implementation", *Image and Vision Computing*, 2008, 26(12), pp.1551-1560.
- [40] Y. LeCun, B. Boser and JS. Denker, "Backpropagation applied to handwritten zip code recognition", *Neural Comput* 1(4):541-551, 1989.
- [41] D. Zhao, X. Pan, X. Luo and X. Gao, "Palmpoint recognition based on deep learning", In: *International Conference on Wireless, Mobile and Multi-Media*, 2015, pp. 214-217.
- [42] S. Minaee and Y. Wang, "Palmpoint recognition using deep scattering convolutional network", arXiv preprint arXiv:1603.09027, 2016.
- [43] Q. Sun, J. Zhang, A. Yang and Q. Zhang, "Palmpoint recognition with deep convolutional features", In *Chinese Conference on Image and Graphics Technologies*, Springer, Singapore, 2017, pp. 12-19.
- [44] J. Hu, L. Shen and G. Sun, "Squeeze-and-excitation networks", arXiv preprint arXiv:1709.01507, 7, 2017.
- [45] M. Afifi, "11K Hands: Gender recognition and biometric identification using a large dataset of hand images." arXiv preprint arXiv:1711.04322, 2017.
- [46] E.A. Elgallad, N.A. Charfi, W. Ouarda and M. Alimi, "Human identity recognition using sparse auto encoder for texture information representation in palmpoint images based on voting technique". *Sudan Conference on Computer Science and Information Technology (SCCSIT)*, Elnihood, Sudan, 2017, pp. 1-8.
- [47] G.Y. Chen, T.D. Bui and A. Krzyzak, "Palmpoint classification using dual-tree complex wavelets", in: *Proceeding of International Conference on Image Processing*, 2006, pp. 2645-2648.
- [48] CASIA Palmpoint Database, <http://biometrics.idealtest.org/>. [Accessed 10 October 2018].
- [49] L. Lei, C. Wang and X. Liu, "Discrete Wavelet Transform Decomposition level determination exploiting sparseness measurement", *International Journal of Electrical, Computer, Energetic, Electronic and Communication Engineering*, 2013, 7,1182-1185.
- [50] V. Vapnik, "The Nature of Statistical Learning Theory". NY: Springer-Verlag, 1995.
- [51] A.A. Ross, K. Nandakumar and A. Jain, "Handbook of multibiometrics (Vol. 6)", Springer Science & Business Media, 2006, pp.73-82.
- [52] W. Ouarda, H. Trichili, A. M. Alimi and B. Solaiman, "Towards A Novel Biometric System For Smart Riding Club.", *Journal of Information Assurance & Security* . 2016, Vol. 11 Issue 4, p201-213.
- [53] W. Ouarda, H. Trichili, A. M. Alimi and B. Solaiman, "Bag of face recognition systems based on holistic approaches", 15th International Conference on Intelligent Systems Design and Applications (ISDA), Marrakech, 2015, pp. 201-206. doi: 10.1109/ISDA.2015.7489225.
- [54] I. Jarraya, W. Ouarda and A.M. Alimi, "Deep neural network features for horses identity recognition using multiview horses' face pattern", *Proc. SPIE* 10341, Ninth International Conference on Machine Vision (ICMV 2016), 103410B (17 March 2017); doi: 10.1117/12.2269064.
- [55] S. M. Eragi, W. Ouarda and A. M. Alimi, "Human identity recognition based on facial images: Via supervised autoencoder features representation," *Sudan Conference on Computer Science and Information Technology (SCCSIT)*, Elnihood, 2017, pp. 1-6. doi: 10.1109/SCCSIT.2017.8293056.
- [56] K. Larbi, W. Ouarda, H. Drira, B. Ben-Amor and C. Ben-Amar, "DeepColorFASD: Face Anti Spoofing Solution Using a Multi Channeled Color Spaces CNN", *IEEE International Conference on Systems, Man, and Cybernetics (SMC)*, Miyazaki, Japan, 2018, pp. 4011-4016. doi: 10.1109/SMC.2018.0068.

# Detection of Suspicious of Diabetic Feet using Thermal Image

Brian Meneses-Claudio<sup>1</sup>, Witman Alvarado-Díaz<sup>2</sup>, Fiorella Flores-Medina<sup>3</sup>

Natalia I. Vargas-Cuentas<sup>4</sup>, Avid Roman-Gonzalez<sup>5</sup>

Senior Member, IEEE<sup>5</sup>

Image Processing Research Laboratory (INTI-Lab)<sup>1, 2, 3, 4, 5</sup>

Universidad de Ciencias y Humanidades, Lima, Perú

**Abstract**—Diabetic foot is a chronic disease that occurs due to increased glucose levels, in addition to being the result of poorly controlled diabetes. In this case, the affected foot increases in temperature, because it contains accumulated blood. According to the Alianza para el Sivataje del Pie diabético en el Perú reported that currently has been increasing the cases of diabetic foot being 8% of the Peruvian population suffering from diabetic foot. Many research papers mention that the temperature difference of both feet has to be minimal due to the homogeneous distribution of the body, but when the temperature of the feet is higher than 2.2 ° C degrees with respect to the other foot, it is an indicative of diabetic foot. That is why the thermal evaluation of feet with suspected diabetic foot was raised in this research to prevent future damage or even amputation of the foot; first a thermal image of both feet is captured using the FLIR ONE Pro thermal camera following a temperature range protocol, then the images are processed in the MATLAB software in order to obtain the zones where the variations are greater or equal 2.2 degrees of temperature and finally superimpose it on the foot with higher temperature to determine the area where the highest temperature was detected. It was obtained as results, that patients with diabetic foot do not have sensitivity in both feet, which will indicate us as a result and in addition to the difference in temperature between both feet which is a possible diabetic foot.

**Keywords**—Diabetic foot; thermal images; image processing; Roberts method; heat map

## I. INTRODUCTION

Diabetic foot is considered a chronic disease, this is caused by the increase of glucose (sugar) levels in the blood [1]. This increase is due to the absence of insulin secretion, insulin is secreted by the pancreas that helps control glucose, meaning that if there is no insulin, and glucose stays in the blood for a long time causing serious problems in the blood health.

According to the National Institute of Diabetes and Digestive and Kidney Diseases (NIH) and the Alianza para el Sivataje del Pie diabético en el Perú indicate that around the world every 20 seconds a limb is amputated and most of these cases are due to the diabetes, because it is a silent disease and currently in Peru affects 8% of the Peruvian population. In 25% of patients with diabetic foot, it can start as a callus or a small wound that does not heal because of diabetes, therefore, it causes an infection that is happening inside [2].

The diabetic foot is an alteration to the nerves and indicated by hyperglycemia (high sugar) [1], in which with or without coexistence of ischemia, produces injury and / or ulceration of the foot called diabetic foot. In addition, it is also considered hereditary because in case the patient has relatives with diabetics and diabetic foot means that he or she is prone to suffer from the same evils; that is why doctors always identify these risks, recommend care and prevention of sugars.

The causes of diabetic foot injuries are peripheral neuropathy which is the loss of sensation in the foot, means that you do not feel any pain, in order to not perceive the injuries that can be caused internally and the vasculopathy that is known as the lack of blood flow [3], this is due to the constant increase in blood glucose causes some small blood vessels that irrigate the foot to narrow causing the oxygen and essential nutrients not reach complete to the foot, by conclusion, due to the decrease in blood supply, makes the wounds take longer to heal and be of high risk when infected [4].

In [5], a comparative map was proposed between patients with and without diabetic foot using infrared thermography, 479 subjects were taken of whom 277 people had diabetic foot with a mean age of 63.41 years, having as a result the difference of different areas of the soles of the feet bilaterally, also reached the conclusion that the use of infrared thermography is important as an evaluation method for the risk of diabetic foot, thus giving diagnosis and prevention in areas where Higher temperature index is identified.

In [6], they indicate that used the FLIR ONE to capture images of the soles of the feet to identify diabetic foot on the basis of a temperature difference of 0.987 and 0.0981, and after they processed the images, they clinically proved that the results obtained were from patients with diabetic foot. In this case, in this research work they want to have thermal cameras in the health centers for the verification and validation of diabetic foot in an instantaneous way and thus diagnoses about the care that these patients should have.

The main objective of the research work is the detection of suspicions of diabetic foot using thermal images to prevent future amputations because it is a disease that has as a consequence harsh repercussion. This detection is due to the processing of images where we will show if the patient has a

temperature difference greater than 2.2 °C [7], which is considered as an abnormal temperature variation between both feet.

Thermography is the study of the variation of temperature, that is, it identifies exact temperatures of a body and objective without the need of physical contact, just by pointing with the thermography analyzer equipment, it has as purpose the study of said signals for the detection of evils [8] where temperature is an important and / or decisive factor. The equipment makes use of thermography can be modified based on the temperature range to be measured, one of the best known are the FLUKE or FLIR ONE Pro [9], equipment, due to its compatibility with the Android and IOS systems. Currently, there are thermal cameras that connect to Smartphone and are used in various areas of research.

The thermal images show the thermal composition of a body or objective, in addition to identifying in which areas there is a higher temperature, also, the thermal cameras have software in which the images can be processed to provide accurate data of the pixels of the image [10]. These thermal images have many applications being one of the most necessary in the field of medicine because the temperature variation of the human body is a key to the development of the same and the detection of diseases or internal sutures.

The following research work is structured as follows: In section II, the development of the processing of thermal images of the possible diabetic foot will be presented. In Section III, the results will show the thermal image of the feet and the image of the warmer foot with the superimposed heat map indicating the temperature zones greater than 2.2° C. In Section IV, we present the discussions of the research work and finally in Section V, the conclusions, as well as the future work that is to be achieved with the research work.

## II. METHODOLOGY

In this part, each part of the segmentation of the thermal image is developed for the detection of suspicions of diabetic foot, which consist of the acquisition of the image, processing of the image and finally the results that correspond to the segmented image superimposed on the real image. The stages of the system are shown in Fig. 1 where the processes of the thermal image will be subjected are indicated.

### A. Image Acquisition

For our research, it requires a camera capable of capturing thermal images, for this reason, it uses the FLIR ONE Pro thermal camera, which is compatible with Android and IOS mobile devices. In addition, it has its own application for mobile devices and software to process the thermal images stored in the device that is connected. This device has two lenses as shown in Fig. 2, the upper lens captures digital images and the lower lens captures the thermal images that will be stored in the mobile device that is connected. In this case, an Android mobile device was used then a C to Micro USB connector was required because the thermal camera has a C connector from factory.

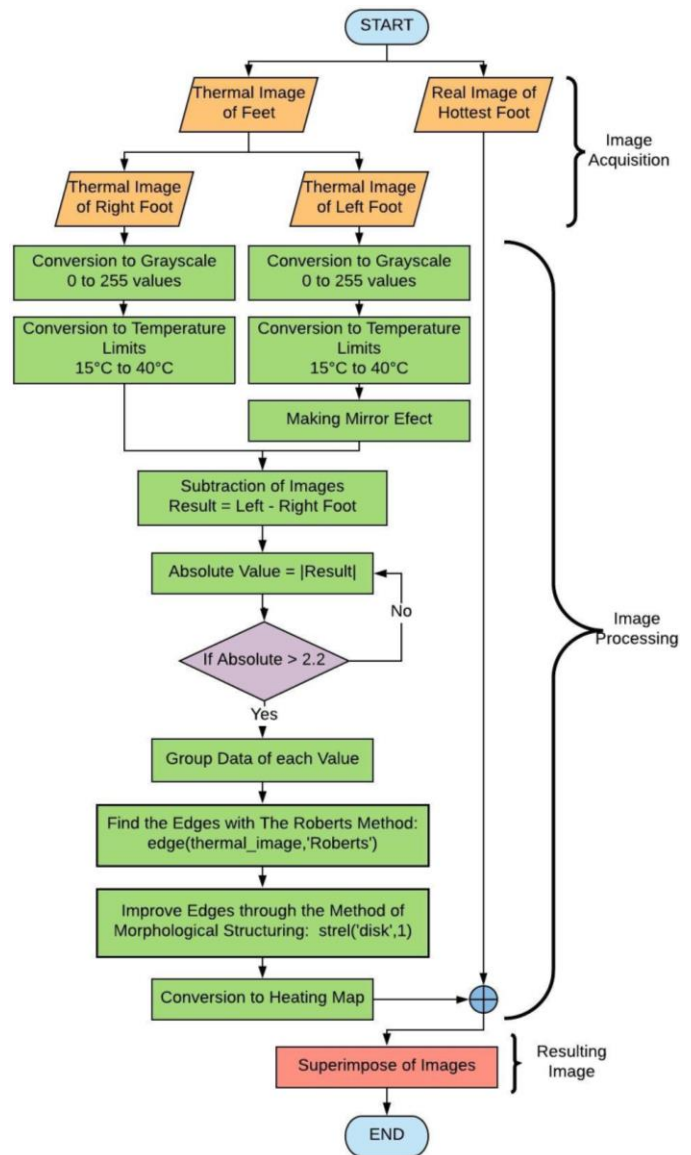


Fig. 1. Diagram of Flow for the Detection of Suspected Diabetic Foot.



Fig. 2. FLIR ONE Pro Thermal Camera and Type C to Micro USB Connector Adapter.

TABLE I. CHARACTERISTICS OF THE FLIR ONE PRO

| FLIR ONE Pro       |                          |
|--------------------|--------------------------|
| Temperature Range  | -20 °C – 400 °C          |
| Compatibility      | IOS y Android devices    |
| Distance           | 1.8 meters               |
| Weight             | 36.5 g.                  |
| Dimensions         | 68 x 34 x 14 millimeters |
| Thermal Resolution | 160 x 120                |
| Operating Time     | 1 hour                   |

The thermal camera has characteristics in which its images and operation are governed; these characteristics are shown in Table I.

The FLIR ONE Pro thermal camera is an electronic device whose main function is to capture images in temperature ranges, in its principles, it was used to identify faults in industrial equipment and improve repair time, at present, they are used in several fields in which one of the requested is to medicine due to the variation of temperature as detection of internal and / or pathological evils; as in this case, detection of suspicion of diabetic foot.

### B. Image Processing

The images obtained are processed to identify the points where the highest temperature variation indexes are observed as shown in Fig. 3, where we observe the real image, then the thermal image, the subtraction of both images identifying the heat zones, and finally superimposed on the foot with higher temperature.

The MATLAB Software reads the images using FLIR ONE Pro, each thermal image is composed of pixels in 3 dimensions because it is in RGB form, so, it will convert this image to gray scale. It has to take into account, that they are 2 foot and it must process both for this, the software makes a weighted sum taking the values of each pixel of the image of each dimension and multiplying with a normed value as shown below:

$$0.2989 * R + 0.5870 * G + 0.114 * B \quad (1)$$

After converting both feet to gray scale that is within the range of 0 – 255 in two dimensions, we have to convert it to a temperature scale.

To convert gray scale images to a temperature scale, we have to map the image and therefore using the following formula:

$$\text{Map} = ((\text{Pixel\_Image} - \text{FromLow}) * (\text{ToHigh} - \text{ToLow}) / (\text{FromHigh} - \text{FromLow})) + \text{ToLow} \quad (2)$$

Where:

- FromLow y FromHigh = 0 y 255 (Gray Scale)
- ToLow y ToHigh = Temperature Range to which we will convert the image.

Replacing formula 2, we will put the values to which we want the image, as shown in the following formula:

$$\text{output1} = ((\text{Pixel\_Image} - 0) * (40 - 15) / (255 - 0)) + 15$$

We do the following process for both images to obtain them in temperature range, then it applies Mirror method to the coldest foot so it is in the same position as the warmer foot, we do this process because the MATLAB software will proceed with the subtraction of each pixel, thus identifying the hottest areas. For the subtraction of the images we use a simple subtraction.

$$\text{Subtraction} = \text{Thermal\_After} - \text{Thermal\_Before} \quad (3)$$

According to [4], they explain that the temperatures of both feet can have a minimum temperature range of up to 1.4° C but when the temperature difference is greater than 2.2° C, also when is resting for more than 20 minutes, it is an indicative of diabetic feet [7]. That is why after obtaining the subtraction of both images, it sectorizes the pixels where there is a difference greater than 2.2° C, as shown in Fig. 1, in the flow diagram.

It is indicated that when the pixel meets the aforementioned value, the data will be grouped and will show only the points that exceed the value of 2.2° C.

After obtaining the zones with the highest temperature, it will identify the edges, for this case, the Roberts Method was used because it is the only method of edge detection of morphologically modified images, meaning that they do not have a specific shape. Roberts' method uses a filter that focuses on each pixel through the following formula:

$$\frac{df}{dx} = f(x + 1, y) - f(x, y) \quad (4)$$

$$\frac{df}{dy} = f(x, y + 1) - f(x, y)$$

Where to locate the pixel (x, y) that is in gray scale within the range of 0 to 255, if the areas have a constant intensity, will turn them into 0.

After obtaining the edges, as it knows that the image does not have a specific shape, in the same way the edges will be distorted, therefore, a filter was used to improve the segmentation called Morphological Structure Method as shown below:

$$\delta_B(X) = X \oplus B = \{x | X \cap B_x \neq \emptyset\} \quad (5)$$

Where it is indicated that X will travel through the whole image, when it passes through B, it will give the information of the data of the neighbors of that pixel, converting it to the maximum value of the environment of that neighborhood defined by the element of the structure. The values that are around each pixel are called neighborhood. Then when the pixel has a neighborhood of values different from it, it will take the maximum value of that neighborhood.

Finally, all the images obtained as the edges, the image of the subtraction of the thermal images and the real image will be superimposed, to obtain the image with the zones where there is a temperature difference of 2.2° C being an indicative of suspicions of diabetic foot, as shown in Fig. 3(d).

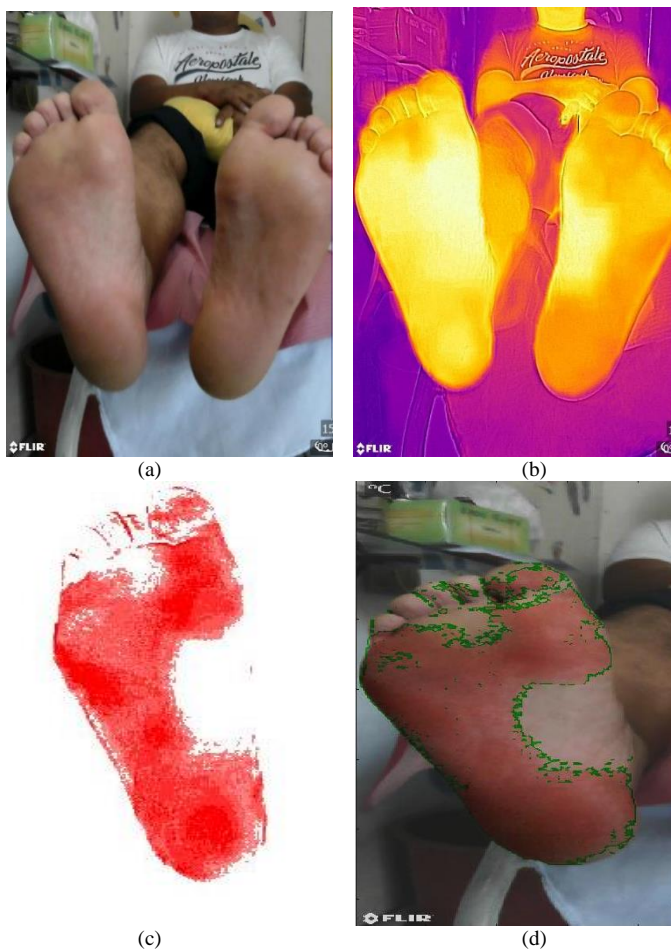


Fig. 3. (a) Real Image. (b) Thermal Image. (c) Subtraction of Thermal Images in Heat Map. (d) Superimpose of Possible Diabetic Foot Images.

### III. RESULTS

The thermal images were acquired in a Podiatric Center and following an image capture protocol [11] because all the images are required to have the same characteristics and also the same processing. In Table II, the protocols we follow to obtain the thermal images are indicated:

In Fig. 4, the reader can see the results of many patients that could present diabetic feet. As the objective was focus, this is study is a prevent study to detect suspicious of diabetic feet using thermal images so it has a major percentage that those results could be diabetic feet. This study had 15 people where it sectorized the cases with more temperature differences following the protocol showed in the Table II.

TABLE II. CHARACTERISTICS OF THERMAL IMAGES

| Thermal Images                  |                    |
|---------------------------------|--------------------|
| Distance                        | 30 cm              |
| Temperature Range               | 15 °C – 40 °C      |
| Connected Device                | Huawei P20         |
| Place where the image was taken | Feet Floor (Soles) |
| Rest Time Before Study          | 20 minutes.        |

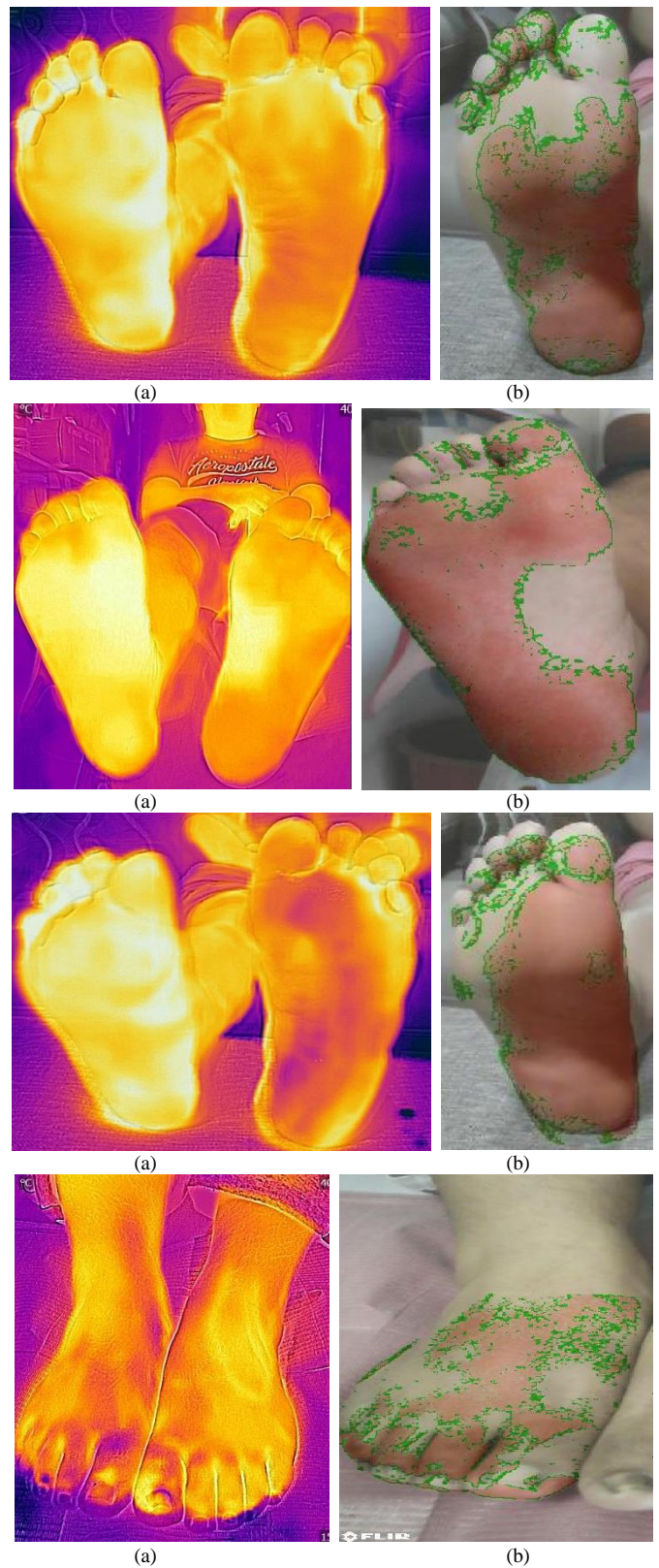


Fig. 4. (a) Thermal Images of the Feet. (b) The Superposition of the Zone with a Temperature Greater than 2.2 °C on the Real Image.



#### IV. DISCUSSION

The research work confirms the use of thermal images for the detection of suspicion of diabetic foot due to the variation of temperature in the feet.

For the image processing, the real image and the thermal image were required because at the end of the process it was necessary to superimpose the segmented area of the suspicion of diabetic foot to the real image.

Many patients are alarmed when identifying that they have diabetic foot; that is why we indicate that this research work is a preliminary work to detect suspicions of diabetic foot, because there are many factors being food one of the most relevant.

This study is for the prevention of the diabetic feet, we are not considering the clinic historical so this is study has more variable to take into consideration.

#### V. CONCLUSIONS

It is concluded that a possible diabetic foot can be detected through thermal images in an efficient and fast way because it only requires capturing the images and then the software will segment it automatically obtaining the area where is the possibility of having a case of diabetic foot.

It is concluded that the podiatry center provides relevant information for the thermal image processing and that it complements the protocol with the rest period to regularize the internal temperature of the patients' feet.

As work in the future, it is necessary to detect diabetic foot in short time so that patients follow a healing process, besides that externally it is not possible to identify if a foot is diabetic that is why through thermal imaging you can know if you have signs or suspicious of diabetic foot.

#### REFERENCES

- [1] Uçkay, J. Aragón-Sánchez, D. Lew, and B. A. Lipsky, "Diabetic foot infections: what have we learned in the last 30 years?," *Int. J. Infect. Dis.*, vol. 40, pp. 81–91, Nov. 2015.
- [2] S. Seclén, "Diabetes Mellitus en el Perú: hacia dónde vamos," *Rev. Medica Hered.*, vol. 26, no. 1, pp. 3–4, 2015.
- [3] Y. García García, E. Hernández Lao, A. Hernández Soublet, J. A. Barnés Domínguez, and Z. Durán Balmaseda, "Therapeutic education on diabetes for patients with first amputation caused by diabetic foot," *Rev. Cuba. Angiol. y Cirugía Vasc.*, vol. 17, no. 1, pp. 0–0, 2000.
- [4] J. Federico, R. Cruz, E. Bonilla Huerta, R. Cocolletzi, and J. Crispín Hernández Hernández, "Advances in the Development of a Thermographic Image Classifier of Diabetic Foot Plant Based on Backpropagation Neural Network," 2016.
- [5] Á. Astasio-Picado, E. Escamilla Martínez, and B. Gómez-Martín, "Mapa térmico comparativo del pie entre pacientes con y sin diabetes mediante el uso de termografía infrarroja," *Enfermería Clínica*, Jan. 2019.
- [6] R. F. M. van Doremalen, J. J. van Netten, J. G. van Baal, M. M. R. Vollenbroek-Hutten, and F. van der Heijden, "Validation of low-cost smartphone-based thermal camera for diabetic foot assessment," *Diabetes Res. Clin. Pract.*, vol. 149, pp. 132–139, Mar. 2019.
- [7] C. Liu, J. J. van Netten, J. G. van Baal, S. A. Bus, and F. van der Heijden, "Automatic detection of diabetic foot complications with infrared thermography by asymmetric analysis," *J. Biomed. Opt.*, vol. 20, no. 2, p. 026003, Feb. 2015.
- [8] R. Vardasca, L. Vaz, C. Magalhães, A. Seixas, and J. Mendes, "Towards the Diabetic Foot Ulcers Classification with Infrared Thermal Images."
- [9] V. Sagan et al., "UAV-Based High Resolution Thermal Imaging for Vegetation Monitoring, and Plant Phenotyping Using ICI 8640 P, FLIR Vue Pro R 640, and thermoMap Cameras," *Remote Sens.*, vol. 11, no. 3, p. 330, Feb. 2019.
- [10] A. J. Singer, P. Relan, L. Beto, L. Jones-Koliski, S. Sandoval, and R. A. F. Clark, "Infrared Thermal Imaging Has the Potential to Reduce Unnecessary Surgery and Delays to Necessary Surgery in Burn Patients," *J. Burn Care Res.*, vol. 37, no. 6, pp. 350–355, Nov. 2016.
- [11] B. Meneses-Claudio, W. Alvarado-Díaz, and A. Roman-Gonzalez, "Detection of Suspicions of Varicose Veins in the Legs using Thermal Imaging," 2019.

# Blind Image Quality Evaluation of Stitched Image using Novel Hybrid Warping Technique

Sanjay T. Gandhe<sup>1</sup>, Omkar S. Vaidya<sup>2</sup>

Department of Electronics & Telecommunication Engg.  
Sandip Institute of Technology & Research Centre Nashik, India  
Savitribai Phule Pune University, Pune, India

**Abstract**—Image stitching is collection of sequential images captured at fixed camera center having considerable amount of overlap and produces aesthetically pleasing seamless panoramic view. But, practically it is very difficult to obtain clean and pristine stitched panoramic image of particular scene as such images are apparently distorted. In this paper, a novel Hybrid Warping technique is used that combine two global warps and one local warp and helps to refine image alignment stage. Our proposed method optimizes Homography Screening to rectify problem of perspective distortion and Edge Strength Similarity approach to quantify structural irregularities. The Blind Image Quality Evaluation models such as Blind Image Quality Index (BIQI), Blind/Reference-less Image Spatial QUality Evaluator (BRISQUE) and BLind Image Integrity Notator using DCT Statistics (BLIINDS-II) are employed to measure objective quality of stitched image. The experimental results showed that blind image quality score of proposed method is significantly better than latest existing methods.

**Keywords**—Blind image quality evaluation; hybrid warping; image stitching; panoramic image

## I. INTRODUCTION

Now-a-days image stitching technology is available readily in advanced digital cameras and smart phone devices. Also with launch of several commercial image stitching software, user can obtain panoramic view which has great demand in photogrammetry, medical surgery, underwater survey, UAV imagery etc. But, results obtained in above cases face one of the issues like structural misalignments, colour differences, motion blur and noticeable seams. To overcome above issues, most of the researchers have used geometric transformation, image warping algorithms and image compositing techniques.

The proposed work is focused on accurate alignment of two overlapping images using novel Hybrid Warping technique. On other side, many warping models such as APAP [1], SPHP [2], ELA [3], AANAP [4] etc. produces stitched image with distinctive objects. To access the stitched image quality, standard reference image plays an important role. If pristine reference image is available and quality of distorted image is compared against it, such type of model is known as full reference image quality (FR IQA) model. In case of image stitching application, the resulting image of above mentioned warping models are apparently distorted and hence standard reference images are unavailable. Therefore, blind image quality evaluation (i.e. no-reference image quality model) is introduced which does not require reference image to measure objective quality of stitched image. The score obtained from

blind image quality models address the issues like severity of perceptual distortion, loss of visual information due to blurring and loss of resolution due to limited depth of field.

In this paper, the growth of successive image stitching algorithm is surveyed in Section II. Section III described novel hybrid image warping technique for image stitching in detail. Section IV covered different blind image quality models with mathematical representations. The parameter setting of proposed method and comparative analysis with other image stitching method is given in Section V. At last, conclusion is drawn in Section VI.

## II. REVIEW OF RELATED WORK

In order to obtain seamless panoramic image stitching result, considerable efforts have been taken by many researchers in last few decades which are reviewed below:

Richard Szeliski described common pipeline of image stitching which are image alignment techniques, 2-D motion models, 3-D transformations and image blending algorithms in [5]. Brown reviewed important distinction, feature spaces, similarity metrics and search strategies used in image registration [6]. Chen laid down fundamental idea behind image stitching in [7] and evaluated combinations of image registration and merging methods. The detection and description of keypoint features from images is key step in image stitching. Authors in [8]-[14] proposed several feature extraction techniques and demonstrated comparative analysis by keeping in view of proper image registration. Fischler and Bolles introduced statistically robust fitting model named RANSAC in [15] which finds correct feature matches (i.e. inliers) between two images with overlap. However in case of multi-structure data, probability of hitting all inliers is main challenge. To achieve this issue, authors in [16] used multi-guided sampling algorithm to accelerate hypothesis generation and require less CPU time as compared to RANSAC.

To align two images of planar scene and preserve projective nature of registered image, 8 parameters  $3 \times 3$  homography matrix is useful. But, if images are acquired from different viewpoint and transformed other than rotation, then alone homography transformation is not sufficient to align the images [6], [17].

Authors in [18] used two homographies; one for distant plane (i.e. objects far away from camera) and another for ground plane (i.e. objects closer to camera) to register pair of images. If in case of arbitrary scenes (i.e. background and

This work is financially supported by Savitribai Phule Pune University, India under Research Mentorship Program Scheme (18TEC001416).

foreground plane is unable to separate), then stitching is unsuccessful. Wen-Yan Lin et al. used 6 parameters affine transformation matrix. In [19], smoothness is employed to extrapolate non-overlapping region and produced protrusion free stitched image. But, due to limited degree of freedom distortions occurred in non-overlapping regions of stitched image.

In [1], the source image is divided into mesh which consists of group of pixels. From each mesh, central positioned coordinate is warped using global homography. This produces projective warp that fits in overlapping region to obtain accurate alignment. This approach is called as Moving Direct Linear Transform (MDLT). This method accurately aligns objects in overlapping region but produces excessive enlargement in non-overlapping region in source image.

To resolve above issue, authors constructed shape preserving projective warps (SPHP) in [2]. Here, from pair of images global homography is estimated and then u-v coordinates are derived. The projective warp is divided into two half spaces; on one half space similarity transformation used for extrapolation and on other half space projective transformation is performed for alignment purpose. Still, problem of parallax is unresolved with this. This method is more meaningful if combined with APAP method.

To alleviate the problem of parallax, researcher proposed elastic local alignment (ELA) model and Bayesian feature refinement model in [4]. This method has better computational complexities as compared with above mentioned methods. In case of severe occlusion, this method gives undesired results.

As per as objective quality of stitched image is concerned, very few research attention is paid to blind image quality assessment of panoramic view. Recently, Suiyi Ling et al. proposed no reference convolutional sparse coding using trained kernel capture distortion in local region of stitched image [20].

### III. NOVEL HYBRID IMAGE WARPING TECHNIQUE

The mathematical representation of proposed Hybrid Warping model is submitted in our previous work [21]. In overlapping area of two images, the moving direct linear transform warp is employed while differentiating local Homography (i.e. smoothed) is achieved by computing weights in non-overlapping region. Finally global similarity transformation is applied to entire image to have regular perspective panoramic scene. The dataflow of proposed work is shown in Fig. 1.

The main contribution of our research work is as follows:

The term gamma ( $\gamma$ ) is offset parameter and its value is in range 0 and 0.1. If the value of  $\gamma = 0$ , then stitched image has wavy effects because of its fixed nature in Gaussian Weighting. Also, if value is kept 1, then warp loses its flexibility. Similarly, the scale parameter ( $\sigma$ ) value depends on image size to get better stitched results. Therefore, the value of  $\gamma$  is optimized in range of 0 to 1 and that of  $\sigma$  is from 8.5 to 12. To minimize perspective distortion, calculation of average weights [a, b, c, d] is carried out with respect to previous grid

value and assigned it to similarity transformation and local moving DLT warp.

Another approach is Homography Screening in which homographies are filtered depending on its sum of distances between four corner values (i.e.  $C_i$  and  $\bar{C}_i$ ). From image initially four corner points  $C_i$  are obtained and by its respective homography its corresponding four corner points  $\bar{C}_i$  are calculated. According to eq. (1) best fitting similarity transformation ( $H_s$ ) is computed.

$$H_s = \arg \min_{H_s} \sum_{C_i} \| H_s C_i - \bar{C}_i \|^2 \tag{1}$$

The sum of distances between  $C_i$  and  $\bar{C}_i$  are normalized and if this value is more than specified threshold value (i.e. 0.001), then such homographies are discarded.

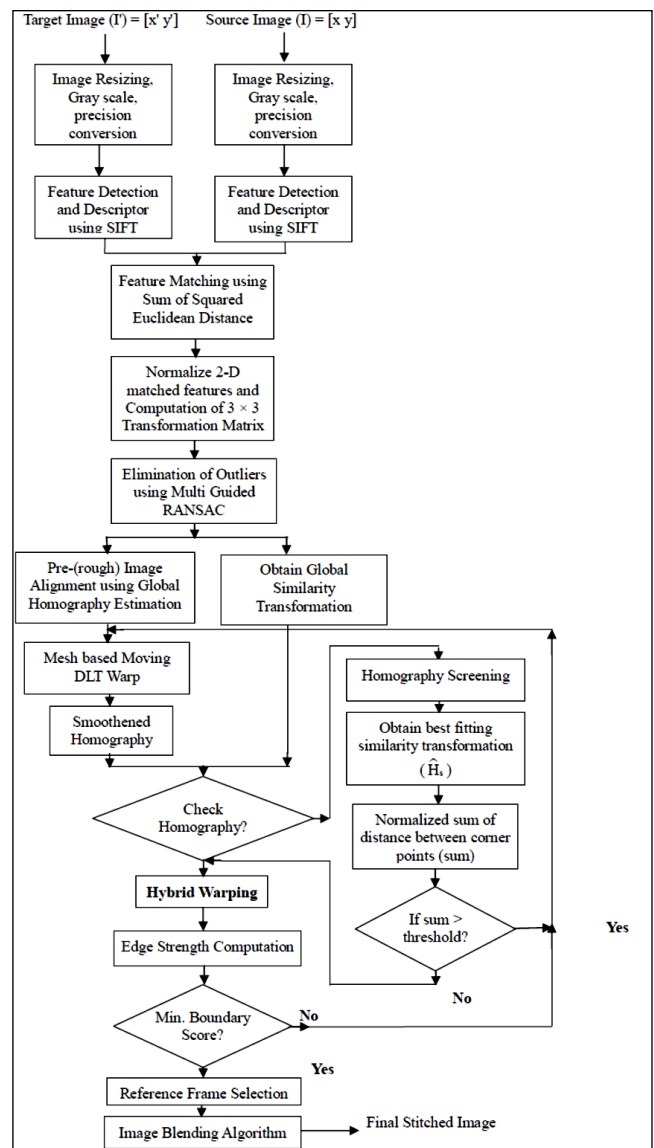


Fig. 1. Data Flow of Proposed Method.

One more approach is investigated in this paper based on edge structural similarity (ESSIM) to determine the boundaries in stitched image. From this, total boundary score is calculated. The minimum score value indicates less misalignment error in stitched image.

Our proposed technique is very efficient in terms of geometric realism as it passes through three improving stages viz. Hybrid Warping, Homography Screening and canny edge detection (for estimating least boundary score). To obtain planar perspective scene, rectilinear reference frame is chosen. Then to conceal colour inconsistencies and visible seams, image blending technique is employed over final warped image. Finally, image quality assessment is carried out using blind image quality evaluation models on stitched image.

#### IV. BLIND IMAGE QUALITY MODELS

There are mainly three approaches of Blind Image Quality models viz. (a) Distortion Specific, (b) Feature Extraction with Learning, (c) Natural scene statistics (NSS). The distortion specific approach determines the amount of distortion in image and estimates the score accordingly. In second approach, features are extracted from image and sort distorted image with undistorted one using trained learning mechanism. The NSS model determines statistical behaviour of natural image and quantifies the introduction of distortion based on distance measure or direction calculation. The use of above approaches is discussed in some of well-known blind image quality models as follows.

##### A. Blind Image Quality Index (BIQI)

Moorthy and Bovik proposed a two stage framework named BIQI in [22]. In first stage, image features are computed using wavelet transform. After that the presence of distortion (such as blur, additive white Gaussian noise, JPEG, JPEG2K and fast fading) is judged and classified using support vector machine. The probability of each distortion ( $P_i$ ) is calculated using multi class radial basis function. In second stage, to obtain image quality of image ( $q_i$ ) towards these distortions, support vector regression is used. Finally, the BIQI score is given in eq. (2):

$$BIQI = \sum_{i=1}^5 P_i q_i \quad (2)$$

Where,  $P_i = \{i=1, \dots, 5\}$  and  $q_i = \{i=1, \dots, 5\}$

The BIQI score is in range of 0 to 100, where lower value indicates best quality and higher value indicates poor quality.

##### B. Blind/Refereneceless Image Spatial Quality Evaluator (BRISQUE)

Furthermore, Mittal et al. developed spatial domain, opinion aware (OA), distortion aware (DA) NSS based model named BRISQUE in [23]. It is transform free (i.e. do not require mapping of data from one form to other especially DCT or wavelet). It is. The development of BRISQUE model is given below:

Consider Image I (m, n), where m and n are spatial co-ordinate indicate image height and width respectively. The local non-linear operation is applied to image is given in eq. (3)

$$\hat{I}(m, n) = \frac{I(m, n) - \mu(m, n)}{\sigma(m, n) + C} \quad (3)$$

Where,  $\mu(i, j)$  is local mean and  $\sigma(i, j)$  is local variance (highlight object boundaries and high contrast).

$$\mu(m, n) = \sum_{k=-K}^K \sum_{l=-L}^L \omega_{k,l} I_{k,l}(m, n) \quad (4)$$

$$\sigma(m, n) = \sqrt{\sum_{k=-K}^K \sum_{l=-L}^L \omega_{k,l} (I_{k,l}(m, n) - \mu(m, n))^2} \quad (5)$$

$\omega = \{\omega_{k,l} | k = -3, \dots, 3, l = -3, \dots, 3\}$  is Gaussian weighting function. K and L are standard deviations.

The presence of distortion is judged by finding the mean subtracted contrast normalized (MSCN) coefficients. To observe the changes in coefficient, generalized Gaussian distribution (GGD) with zero mean is used. It is given in eq. (6).

$$f(x; \alpha, \sigma^2) = \frac{\alpha}{2\beta\Gamma(1/\alpha)} \exp\left(-\left(\frac{|x|}{\beta}\right)^\alpha\right) \quad (6)$$

Where,  $\beta = \sigma \sqrt{\frac{\Gamma(1/\alpha)}{\Gamma(3/\alpha)}}$  is scale parameter and  $\Gamma(\cdot)$  is gamma function.

From GGD, the shape factor ( $\alpha$ ) and variance ( $\sigma^2$ ) are computed to obtain feature set and such feature sets are helpful to quantify the distortion in image. The distribution of MSCN coefficient is homogeneous in case of clean distortion-free image and thus neighborhood of MSCN coefficient is modeled along four dimensions like vertical, horizontal, two diagonals. At last all extracted features are mapped into quality score with the help of support vector machine regressor (SVR). The quality score is computed in range of 0 and 100; lower value indicates good quality and higher value is poor in terms of image quality.

##### C. Blind Image Integrity Notator using DCT Statistics (BLIINDS-II)

Saad and Bovik introduced a model which extracts features like contrast, structural information, sharpness and orientation anisotropies with the help of discrete cosine transform [24]. To obtain image contrast, 2-D DCT is applied to local patch of  $17 \times 17$  size. The final value is averaged from all patches prior to normalization. From the non-DC DCT frequency coefficient, the structural information is retrieved. It is observed the peak values especially at zero position (i.e. magnitude of coefficient on X-axis) on histogram in case of distorted images. To find the degree of peak values of histogram, kurtosis is used which is given in eq. (7).

$$\kappa(x) = \frac{E(x - \mu)^4}{\sigma^4} \quad (7)$$

Where,  $\mu$  is mean of  $\chi$  while  $\sigma$  is standard deviation.

The value of kurtosis is considered as lowest 10th percentile of obtained values. To evaluate scene's directional information due to degradation process, then it is necessary to calculate orientation anisotropy. Such features are measured using Renyi entropy. Firstly, 1-D DCT patch is considered and along four orientations (i.e.  $\theta = 0^\circ, 45^\circ, 90^\circ, 135^\circ$ ) DCT image patches are computed. The normalized DCT coefficient with local patch is given in eq. (8).

$$P_\theta[n, k] = \frac{P_\theta[n, k]^2}{\sum_k P_\theta[n, k]^2} \quad (8)$$

Where, n is spatial index and k is frequency DCT coefficient. The Renyi entropy of eq. (8) is given in eq. (9).

$$R_\theta[n] = -\frac{1}{2} \log \left( \sum_k P_\theta[n, k]^3 \right) \quad (9)$$

Collectively for every image patch average per orientation is given by  $E[R_\theta]$ . The value of anisotropy is maximum of variance across four orientation is given by  $\text{var}(E[R_\theta])$ .

After calculating all features, the quality score is determined using prediction model viz. multivariate Gaussian and multivariate Laplacian distribution. The BLIINDS-II score is in range 0 to 100 and lower value indicates good quality and higher value means degraded quality.

### V. EXPERIMENTATION

To validate the effectiveness of proposed method, the experiment is implemented on Intel Processor (Corei3) having 4 GB physical memory and 2 GHz CPU speed. The evaluation is performed in MATLAB 2017a combined with Computer Vision toolbox. To assess the blind image quality metrics, the standard image dataset is used especially for image stitching application and compared our results with As Projective As Possible (APAP), Adaptive As Natural As Possible (AANAP), Shape Preserving Half Projective (SPHP) and Elastic Local Alignment (ELA) methods.

There are different image sizes used from  $240 \times 320$  to  $898 \times 1197$  pixels. From pair of input image, initially features are extracted using Scale Invariant Feature Transform (SIFT) and matched such keypoints using SIFT descriptor. The computations of dense features are possible with the help of open source portable library named VLFeat [25] which is suitable for speed optimization. After extraction, keypoint matching between two images is done based on squared Euclidean distance. The default threshold is set to 1.5. To obtain fundamental matrix and estimate homography matched position keypoints are normalized. The multi-guided RANdom SAMple Consensus (RANSAC) fits the maximum number of inliers by comparing threshold value of 0.1. Further in mesh based MDLT warping, the grid size is kept as  $100 \times 100$  cells.

For fair comparison, blind image quality models are employed on output stitched images of APAP, AANAP, SPHP, ELA and our proposed method.

### A. Quantitative Comparison

The quality score obtained by blind image quality models such as BIQI, BRISQUE and BLIINDS-II is depicted in Table I.

TABLE I. COMPARISON AMONG STATE-OF-THE-ART STITCHING METHODS BASED ON BLIND IMAGE QUALITY EVALUATION SCORE

| Image Datasets | Blind Image Quality Parameters | Image Stitching Methods |       |             |              |              |
|----------------|--------------------------------|-------------------------|-------|-------------|--------------|--------------|
|                |                                | APAP                    | SPHP  | ELA         | AANAP        | Ours         |
| Temple         | BIQI                           | 21.45                   | 31.47 | 39.65       | 22.82        | <b>10.64</b> |
|                | BRISQUE                        | 46.13                   | 48.59 | 60          | 53.59        | <b>41.83</b> |
|                | BLIINDS-II                     | 18                      | 8.5   | 21          | 16.5         | <b>7</b>     |
| Railtracks     | BIQI                           | 28.98                   | 33    | 27.58       | 24.59        | <b>12.98</b> |
|                | BRISQUE                        | 43.81                   | 48.59 | 63.59       | 53.49        | <b>40.19</b> |
|                | BLIINDS-II                     | 18                      | 25.5  | 11.5        | 17           | <b>8.5</b>   |
| Rooftops       | BIQI                           | 26.47                   | 22.84 | <b>2.12</b> | 27.57        | 15.11        |
|                | BRISQUE                        | 62.7                    | 48.59 | 33          | <b>30.13</b> | 31.61        |
|                | BLIINDS-II                     | 20.5                    | 40.5  | 15.5        | 13.5         | <b>0.7</b>   |
| Garden         | BIQI                           | 21.53                   | 31.82 | 31.88       | 16.14        | <b>7.52</b>  |
|                | BRISQUE                        | <b>13.18</b>            | 48.59 | 56          | <b>13.18</b> | 35.49        |
|                | BLIINDS-II                     | 15                      | 18    | 10          | 14.5         | <b>1.5</b>   |
| Apartment      | BIQI                           | 18.47                   | 29.36 | 47.37       | 17.62        | <b>8.7</b>   |
|                | BRISQUE                        | 20.05                   | 49    | 63.59       | 35.63        | <b>18.35</b> |
|                | BLIINDS-II                     | 12                      | 20.5  | 6.5         | 4            | <b>0.5</b>   |
| Chess-Girl     | BIQI                           | 24.37                   | 33.28 | 36.35       | 23.8         | <b>11.54</b> |
|                | BRISQUE                        | 20.38                   | 48    | 57          | 47.31        | <b>7.82</b>  |
|                | BLIINDS-II                     | 12                      | 8.5   | 9.5         | 7.5          | <b>0.75</b>  |
| Coach          | BIQI                           | 31.43                   | 48.62 | 41.41       | 22.52        | <b>13.6</b>  |
|                | BRISQUE                        | 22.59                   | 44    | 62          | 33.21        | <b>18.55</b> |
|                | BLIINDS-II                     | 9                       | 24.5  | 7.5         | 3            | <b>0.55</b>  |

Table I illustrate that the blind image quality assessment parameters in our proposed method give excellent result as compared with other methods for all datasets. The lower values of parameters indicate reduced content of distortion in stitched panoramic image.

The lower quality score of BIQI infers that image has lower Gaussian blur as well as less JPEG2K and JPEG compression level. For temple dataset, in case of APAP, ELA and SPHP method stitched image shows significant blur. The lower value of BRISQUE gives close relation between statistical features of stitched image to natural scene statistics. In our proposed system, BRISQUE score is lowest (except Garden and Rooftops) among all stitching methods and thus such results are highly correlated with human perception. This is due to noticeable remaining black (or white) pixels as compared with total number of pixels in stitched image of Garden and Rooftops dataset. The BLIINDS-II score exhibit most of behavior of human visual systems i.e. perceptual distortion,

visually sensitive structural anomalies and edge impairments (especially around aligned part of stitched image). The value of BLINDS-II score is obtained in all dataset is lowest in our proposed method, this itself speak about quality of stitched image.

### B. Qualitative Comparison

Consider the target and source image of temple dataset as shown in Fig. 2(a) and (b) respectively.

Image stitching using APAP method is shown in Fig. 3. The part in red colour rectangle box showed structural misalignment and green colour rectangle box shows slant shape of building structures.

Fig. 4 shows stitched output using AANAP method. The image is highly blurred in overlapping region due to homography linearization. Also, parallax is observed in overlapping region and is highlighted by red colour rectangle box.

The stitched image using SPHP method is shown in Fig. 5. After stitching, source image is rotated and perspective nature is lost. The rectangle red box indicates severe parallax error (roof of temple) and local misalignments (ground plane).

The image stitching obtained by ELA method is shown in Fig. 6. The common structural mistakes like curved alignment of paver block and roof of temple are corrected in this method. However, the non-overlapping part is highly extrapolated like APAP. The ghosting effect is observed around the person standing on road. The temple object and buildings are not parallel with each other.

Fig. 7 shows image stitching using our proposed method. The yellow colour rectangle boxes show that accurate alignment without any parallax error and ghosting artifact. The motion blur is eliminated in overlapping part. The stitched output images shown in Fig. 3 to Fig. 7 are best viewed on computer screen.



Fig. 2. (a) Target Image, (b) Source Image.



Fig. 3. Image Stitching using APAP Method.



Fig. 4. Image Stitching using AANAP Method.

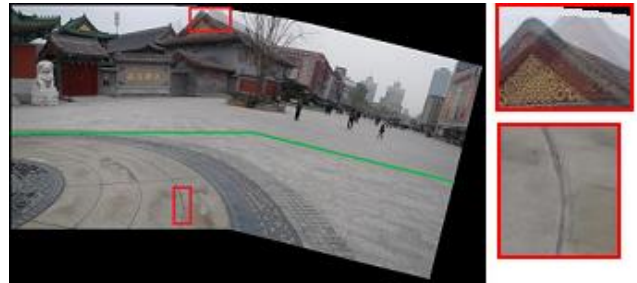


Fig. 5. Image Stitching using SPHP Method.



Fig. 6. Image Stitching using ELA Method.

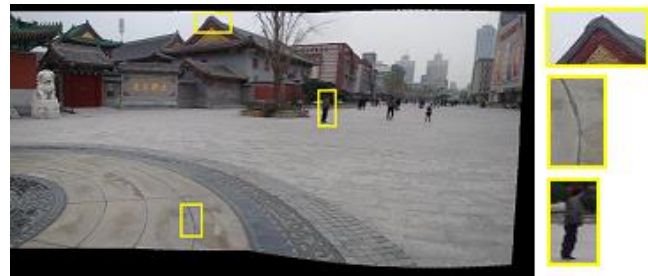


Fig. 7. Image Stitching using our Proposed Method.

## VI. CONCLUSION

A novel hybrid image stitching approach is presented in this paper. In order to obtain natural distortion-free panoramic view, an idea of homography screening and edge strength similarity measure is executed while warping the images. Later, the concept and mathematical representations of blind image quality models is explained. The quantitative analysis evidenced that our proposed method performed well among state-of-the-art stitching methods. From qualitative analysis, it is verified that stitched result produced using proposed method is free from parallax, motion blur, structural misalignment and colour inconsistencies. In future, the full reference image quality assessment will be investigated only in overlapping regions of stitched image.

#### ACKNOWLEDGMENT

This research work is financially supported by Savitribai Phule Pune University (SPPU), India through Assistance by SPPU for Project-based Innovative Research (ASPIRE) under Research Mentorship Program Scheme (18TEC001416) which is supervised by Internal Quality Assurance Cell (IQAC), SPPU, Pune, India.

#### REFERENCES

- [1] Julio Zaragoza, Tat-Jun Chin, Quoc-Huy Tran, Michael S. Brown and David Suter, "As-Projective-As-Possible Image Stitching with Moving DLT", IEEE Transactions on Pattern Analysis And Machine Intelligence, Vol. 36, No. 7, pp. 1285 – 1298, July 2014. DOI: 10.1109/TPAMI.2013.247.
- [2] Che Han Chang, Yoichi Sato and Yung Yu Chuang, "Shape preserving half projective warps for Image Stitching", IEEE Conference on Computer Vision and Pattern Recognition (CVPR), pp. 3254-3261, 23-28 June 2014, Columbus, USA. DOI: 10.1109/CVPR.2014.422.
- [3] Jing Li, Zhengming Wang, Shiming Lai, Yongping Zhai and Maojun Zhang, "Parallax-Tolerant Image Stitching Based on Robust Elastic Warping", IEEE Transactions on Multimedia, Vol. 20, No. 7, pp. 1672-1687, July 2018. DOI: 10.1109/TMM.2017.2777461.
- [4] Chung-Ching Lin, Sharathchandra U. Pankanti, Karthikeyan Natesan Ramamurthy and Aleksandr Y. Aravkin, "Adaptive As-Natural-As-Possible Image Stitching", IEEE Conference on Computer Vision and Pattern Recognition (CVPR), pp. 1155-1163, 7-12 June 2015, Boston, USA. DOI: 10.1109/CVPR.2015.7298719.
- [5] Richard Szeliski, "Image Alignment and Stitching: A Tutorial", Foundations and Trends in Computer Graphics and Vision Journal, Vol. 2, No. 1, pp. 1-104, January 2006. DOI: 10.1561/06000000009.
- [6] Lisa Brown, "A Survey of Image Registration Technique", ACM Computing Surveys (SCUR), Vol. 24, No. 4, pp. 325-376, December 1992. DOI: 10.1145/146370.146374.
- [7] Chia-Yen Chen, "Image Stitching - Comparisons and New Techniques", Computer Science Department, CITR, The University of Auckland, New Zealand, October 1998.
- [8] David G. Lowe, "Distinctive Image Features from Scale-Invariant Keypoints", International Journal of Computer Vision (IJCV), Vol. 60, No. 2, pp. 91-110, November 2004. DOI: 10.1023/B:VISI.0000029664.99615.94.
- [9] Herbert Bay, Tinne Tuytelaars, and Luc Van Gool, "SURF: Speeded Up Robust Features", European Conference on Computer Vision (ECCV), pp. 410-417, 7-13 May 2016, Austria. DOI: 10.1007/11744023.
- [10] Yan Ke and Rahul Sukthankar, "PCA-SIFT: A More Distinctive Representation for Local Image Descriptors", IEEE Conference on Computer Vision and Pattern Recognition (CVPR), pp. 506-513, 27 June - 2 July, 2004, Washington, USA. DOI: 10.1109/CVPR.2004.1315206.
- [11] Jian Wu, Zhiming Cui, Victor S. Sheng, Pengpeng Zhao, Dongliang Su and Shengrong Gong, "A Comparative Study of SIFT and its Variants", Measurement Science Review, Vol. 13, No. 3, pp. 122-131, June 2013. DOI: 10.2478/msr-2013-0021.
- [12] Omkar S. Vaidya, Dr. S. T. Gandhe and Pooja B. Sonawane, "Performance Analysis of KLT, Harris and SIFT Feature Detector for Image Stitching", International Journal of Electrical and Electronics Engineers (IJEEE), Vol. 8, No. 1, pp. 536-544, January-June 2016.
- [13] M. Hassaballah, Aly Amin Abdelmgeid and Hammam A. Alshazly, "Image Features Detection, Description and Matching", Image Feature Detectors and Descriptors Foundations and Applications, Springer International Publishing, pp.11-45, Switzerland 2016. DOI: 10.1007/978-3-319-28854-3\_2.
- [14] Omkar S. Vaidya and Dr. Sanjay T. Gandhe, "The Study of Preprocessing and Postprocessing Techniques of Image Stitching", IEEE International Conference On Advances in Communication and Computing Technology (ICACCT), pp. 431-435, 8-9 February 2018, AVCOE, Sangamner, India. DOI: 10.1109/ICACCT.2018.8529642.
- [15] Martin A. Fischler and Robert C. Bolles, "Random Sample Consensus: A Paradigm for Model Fitting with Applications to Image Analysis and Automated Cartography", Communications of the ACM, Vol. 24, No. 6, pp. 381-395, June 1981. DOI: 10.1145/358669.358692.
- [16] Tat-Jun Chin, Jin Yu, and David Suter, "Accelerated Hypothesis Generation for Multi-Structure Robust Fitting", European Conference on Computer Vision (ECCV), pp. 533-546, 5-11 September, 2010, Greece. DOI: 10.1007/978-3-642-15555-0\_39.
- [17] Richard Hartley and Andrew Zisserman, "Multiple View Geometry in Computer Vision", Second Edition, Cambridge University Press, 2003. DOI: 10.1017/CBO9780511811685.
- [18] Junhong Gao, Seon Joo Kim and Michael S. Brown, "Constructing Image Panoramas using Dual-Homography Warping", IEEE Conference on Computer Vision and Pattern Recognition (CVPR), pp. 49-56, 20-25 June 2011, Colorado Springs, USA. DOI: 10.1109/CVPR.2011.5995433.
- [19] Wen-Yan Lin, Siying Liu, Yasuyuki Matsushita, Tian-Tsong Ng and Loong-Fah Cheong, "Smoothly varying affine stitching," IEEE Conference on Computer Vision and Pattern Recognition (CVPR), pp. 345-352, 20-25 June 2011, Colorado Springs, USA. DOI: 10.1109/CVPR.2011.5995314.
- [20] Suiyi Ling, Gene Cheung and Patrick Le Callet, "No-Reference Quality Assessment for Stitched Panoramic Images using Convolutional Sparse Coding and Compound Feature Selection", IEEE International Conference on Multimedia and EXPO (ICME), pp. 1-6, 23-27 July, 2018, San Diego, USA. DOI: 10.1109/ICME.2018.8486545.
- [21] Omkar S. Vaidya and Dr. Sanjay T. Gandhe, "Improvement in Image Alignment using Hybrid Warping Technique for Image Stitching", International Journal of Engineering Research and Technology (IJERT), Vol. 12, No. 3, pp. 350-356, March 2019.
- [22] Anush Krishna Moorthy and Alan Conrad Bovik, "A Two-Step Framework for Constructing Blind Image Quality Indices", IEEE Signal Processing Letters, Vol. 17, No. 5, pp. 513-516, May 2010. DOI: 10.1109/LSP.2010.2043888.
- [23] Anish Mittal, Anush Krishna Moorthy, and Alan Conrad Bovik, "No-Reference Image Quality Assessment in the Spatial Domain", IEEE Transactions on Image Processing, Vol. 21, No. 12, pp. 4695-4708, December 2012. DOI: 10.1109/TIP.2012.2214050.
- [24] Michele A. Saad, Alan C. Bovik and Christophe Charrier, "Blind Image Quality Assessment: A Natural Scene Statistics Approach in the DCT Domain", IEEE Transactions on Image Processing, Vol. 21, No. 8, pp. 3339-3352, August 2012. DOI: 10.1109/TIP.2012.2191563.
- [25] Andrea Vedaldi and Brian Fulkerson, "VLFeat - An open and portable library of computer vision algorithms", International Conference on Multimedia, pp. 1469-1472, 25-29 October 2010, Italy. DOI: 10.1145/1873951.1874249.

# Bio-inspired Think-and-Share Optimization for Big Data Provenance in Wireless Sensor Networks

Adel Alkhalil<sup>1</sup>, Rabie Ramadan<sup>2</sup>, Aakash Ahmad<sup>3</sup>  
College of Computer Science and Engineering  
University of Ha'il  
Saudi Arabia

**Abstract**—Big data systems are being increasingly adopted by the enterprises exploiting big data applications to manage data-driven process, practices, and systems in an enterprise wide context. Specifically, big data systems and their underlying applications empower enterprises with analytical decision making (e.g., recommender/decision support systems) to optimize organizational productivity, competitiveness, and growth. Despite these benefits, big data applications face some challenges that include but not limited to security and privacy, authenticity, and reliability of critical data that may result in propagation of false information across systems. Data provenance as an approach and enabling mechanism (to identify the origin, manage the creation, and track the propagation of information etc.) can be a solution to above mentioned challenges for data management in an enterprise context. Data provenance solution(s) can help stakeholders and enterprises to assess the quality of data along with authenticity, reliability, and trust of information on the basis of identity, reproducibility and integrity of data. Considering the wide spread adoption of big data applications and the needs for data provenance, this paper focuses on (i) analyzing state-of-the-art for holistic presentation of provenance in big-data applications (ii) proposing a bio-inspired approach with underlying algorithm that exploits human thinking approach to support data provenance in Wireless Sensor Networks (WSNs). The proposed ‘Think-and-Share Optimization’ (TaSO) algorithms modularizes and automates data provenance in WSNs that are deployed and operated in enterprises. Evaluation of TaSO algorithm demonstrates its efficiency in terms of connectivity, closeness to the sink node, coverage, and execution time. The proposed research contextualizes bio-inspired computation to enable and optimize data provenance in WSNs. Future research aims to exploit machine learning techniques (with underlying algorithms) to automate data provenance for big data systems in networked environments.

**Keywords**—Big data systems; data provenance; fuzzy logic; bio-inspired computing

## I. INTRODUCTION

Traditionally, the provenance of an object or data includes information about the ownership, source, transformation and evolution of data or object during their life span [1]. The term data provenance, as per the Encyclopedia of Database Systems, formally refers to ‘a record trail that accounts for the origin of a piece of data (in a database, document or repository) together with an explanation of how and why it got to the present place [33].

Provenance of data have been proven as a useful technique—optimizing visibility and transparency of the data—to enhance traceability of errors back to their root cause(s) during data analytics and processing [34]. In big data systems, provenance information enhances the data trustworthiness (identification of data sources) and support data compliance (policies for data processing), to ensure accountability and compliance [2]. In data-centric systems and applications, preserving the security and privacy of data are of central importance to avoid the exploitation or misuse of critical data [25, 35]. Critical data or specifically security critical data can be diverse that can range from personal information of users [35] to security features of systems such as access control usage control decisions and data forensics [25].

The characteristics of big-data systems such as size and magnitude of data, distributed users, and heterogeneous platforms poses some serious challenges to data provenance. Further, big-data applications are usually dynamic and heterogeneous by nature. They involve many components provided by various vendors which must be integrated together to develop and operate the system. Therefore, tracing the provenance of an object in big data including the collection of evidences and data from various sources to determine the causes and effects is very difficult [3]. Many of big-data applications rely on Wireless Sensor Networks (WSN) for their common activities to process and transmit data among applications [7]. A WSN consists of many small and low-cost sensor nodes. The nodes in WSNs have different limitations such as energy, processing capabilities, small communication range, small sensing range, and storage capabilities. These characteristics make the data transmitted across WSNs exposed to various threats. This signifies the need for a mechanism that can enhance the reliability of data collected from WSNs by assessing their trustworthiness. This paper addresses the challenge of node trust in WSNs that transmit large amount of data in an enterprise context. The primary question to be answered by this research is: How nodes that process, generate, and consume large size of data in WSNs can be trusted to maintain the integrity of data?

This paper reviews the current situation with regards to big-data provenance. It focuses on how to apply data provenance in WSNs and gain nodes trust with minimum memory usage and reduced packets size. This paper also proposes a solution to the aforementioned problems by applying data provenance in WSN systems. Data provenance



can help support data integrity, ultimately enhancing data security in networked systems [34] to improve the security. However, enhanced security measures need high computation and storage resources that represent the challenge for big data systems. The proposed contributions of this research are:

- Exploiting bio-inspired approach to support data provenance in WSNs in the context of enterprise scale systems.
- Developing a novel algorithm named Think and Share Optimizations (TaSO) that modularizes and automates nodes' selection process inspired from human collaboration in education.

We have evaluated the proposed solution and its underlying algorithms based on test-case strategy. Results of the evaluation demonstrate algorithmic efficiency in terms of connectivity, closeness to the sink node, coverage, and execution time.

The paper is structured as follows: Section 2 provides an overview of big data provenance. Section 3 summarizes the state-of-the-art with a holistic presentation of provenance in big data applications. Section 4 discusses our proposed solution for data provenance in WSNs. Section 5 presents the bio-inspired algorithm as a modular solution for data provenance in WSNs. Section 6 presents the experimental results of evaluation. Section 7 presents some threats to the validity of proposed solution with conclusions and dimensions of future work.

## II. BACKGROUND AND RELATED WORK ON BIG-DATA PROVENANCE

Data provenance is a well-known research area within database and data mining. It considers the problem of identifying the origin, the creation, as well as the propagation processes of data [4]. It may be defined as the process of detecting the lineage and the derivation of data and data objects [5]. The execution environment of transformation such as the library versions, operating systems, and the nodes responsible for executing the transformation may also be considered as provenance data [3].

Data provenance is an essential component in various areas such as: database management systems, workflow management systems, distributed systems, and debugging ICT systems [4]. In the case of security violations, a system administrator should be able to identify the origination of the error, in addition to its causes and impacts [6].

In the literature (see for example [3, 5, and 7]), a number of advantages for applying provenance data can be obtained from different resources in several areas including:

- *Business Domain.* Data provenance can provide stakeholders an integrated vision of valuable historical data from multiple sources.
- *Data Quality.* Data provenance can be utilized to assess the reliability and trust of data.
- *Audit Trail.* It can be used to trace audit trails for error detections and debugging.

- *Reusability and Reproducibility.* It can be used to verify, compare, and repeat results.
- *Informational.* The provenance meta-data can be used to query data for discovering and browsing historical data.
- *Benchmarking.* It can be used to identify and analyze performance, compute performance metrics, and test the ability to exploit commonalities in data and processing.

Being an important area for data quality and authenticity, the application of data provenance has received an increasing attention in research [8]. It is a well-known topic in the fields of database management systems, workflow management systems, and distributed systems communities [9, 10]. However, applying data provenance in big data is a fairly new trend that involves continuing development for provenance-aware systems. Therefore, most of the existing studies on data provenance in big-data applications are exploratory [2, 3, 4, 5, and 7], descriptive [11], or case-based research [12]. For example, studies from [13], [14], and [15] focus on the general conceptualization and definition of data provenance, as well as its importance, challenges, and applications. Further, many previous studies explored the business benefits, such as [16, 17]. The problem of security and privacy encountered in provenance management also received an increasing attention [2, 18, 19].

Although big data provenance has been increasingly gaining attention, it is still in an early stage of maturity. Majority of the existing research on big data provenance focused on the application of data provenance on big data [3], exploring the challenges of capturing, analyzing, visualizing big data provenance, and identifying future research directions. Further, a number of studies are focused on capturing and modeling provenance, visualizing [20], and mining provenance data [13]. Despite the fact that those works provided a considerable contribution to the advancement of data provenance utilization onto big data, the size, heterogeneity, complexity, and overhead computation and storage remain significant challenges.

This section highlights some of the contributions in big-data provenance. In [4] the author highlighted the problem of collecting and analyzing provenance in big data. The study reviewed a number of studies in this area in an attempt to present the state-of-the-art. This was followed by the provision of an overview of 14 research issues and challenges of provenance within big data in which the author highlighted potential future research directions. Similarly, Glavic [3] highlighted the need for provenance in big data. The author argued that without provenance information, it is impossible for a user to understand the relevance of data, estimate its quality, investigate unexpected or inaccurate results, and define meaningful access control policies. Glavic then examined how Big Data bench-marking could benefit from provenance information. Simmhan et al. [7] created a taxonomy of data provenance techniques, and applied a classification to existing studies in the area. It aimed to help in building scientific and business management systems in order to understand the designs of existing provenance systems. The taxonomy is focused on categorizing provenance studies based on their intentions, contexts, provenance storage and propagation.

### III. RELATED WORK ON DATA PROVENANCE APPLICATIONS

A number of studies focused on data provenance utilization within a specific context of big-data applications. This section explores some of the recent applications of data provenance including social media, E-science, cloud computing.

#### A. Social Media

In the today's ubiquitous influence of social-media's contents and activities, information credibility has increasingly become a major issue [13]. Correspondingly, the identification of false information and rumors circulation in social-media environments attracted a considerable recent research and interests [20]. A number of studies attempted to address the lack of information credibility in social media through data provenance. Although information diffusion in social media networks has received an increasing attention [21], there is limited works on the reverse process of information diffusion, information provenance [22].

In [13] the author developed a web-based tool for collecting a number of attributes of interest associated with a social-media user. It provides a technique to effectively combine different attributes from different social-media sites into a single user profile. The tool was evaluated using different types of Twitter and Facebook users. In the case of further provenance attributes are needed, the tool offers best possible URL (Uniform Resource Locator) to help for further findings. Although, the contribution of this work provides helpful user-profile metadata, it lacks other essential provenance information including paths and sources. The study in [23] considered seeking the provenance of information for a few known recipients. To achieve this there is a need to find the provenance paths first. Therefore, the study attempted first to explain propagation processes from the sources to the P-nodes. It also includes information of the nodes responsible for retransmitting information through intermediaries. In [24] a method was developed that integrate provenance data on two levels; a low-level through information cascades, and a high-level through similarity-based clustering.

#### B. Cloud Computing

Cloud computing is still at an early level of maturity and it is still evolving in which provenance is yet to be fully implemented. A recent attention has been devoted to this aspect. They explored the challenges of implementing provenance in the cloud environment as in [25 and 26]. In [25] the authors highlighted the challenge of collecting and merging provenance information from a dynamic environment in which resources are independence; for example, different domains (scientific, business, database), different platforms (windows, Linux), and various applications. Further, computation and storage overhead also presents another challenge [26]. In [27] a framework named CloudProv was developed. It aimed to integrate, model and monitor data provenance in cloud computing environments. CloudProv was based on a method that allows users to model the collected provenance information to continuously obtain and monitor such information to be utilized for real-time applications. Oruta [28] developed a privacy-preserving auditing

mechanism. It supports data sharing in untrusted cloud environments. The proposed mechanism makes use of homomorphism authenticators that allows third parties auditors to check the integrity of the shared data from a certain user group, without the need for accessing all data.

#### C. E-Science

Provenance in e-Science is studied comprehensively see for example [7, 29, 30]. The research in e-Science provenance has focused on the process of capturing, modeling, and storing provenance information. It uses provenance for various purposes within the scientific domains. Publications and Digital Object Identifiers (DOIs) are common examples of provenance [7]. The Geographic information system (GIS) standards advise that metadata about the quality elements of a dataset should include a description of its lineage. This can help users to decide if the dataset meets their requirements [2].

#### D. Provenance in Wireless Sensor Networks

Typically, all nodes have sensing, limited data processing, and communicating capabilities. Unlike wired computer networks, the nodes of WSNs are often resource-tightened and deployed in an unprotected environment [31]. Further, communications in WSNs depend upon multi-hop wireless signal relays. These unique characteristics make data transmitted across WSNs exposed to threats. Therefore, there is a need for a mechanism that can enhance the reliability of the data collected from WSNs by assessing their trustworthiness. Provenance is a mechanism of trust and reputation evaluation which can enhance the security of networks [32]. Network information is crucial for seeking provenance information [1]. There are two main approaches: First, the use of available information to search the provenance directly. It is suitable in cases that all recipients are known for particular information. The second approach is to detect the flow of information propagation from origins to all known recipients. It can be suitable in cases of small number of recipients [1].

### IV. WSN MODEL AND PROBLEM STATEMENT

WSNs consist of a set of nodes  $S$  forming a connected network that can be represented by a graph  $G(V, E)$ , where  $V$  is the nodes and  $E$  are the links in the graph.  $E$  represents the connectivity of each node, communication range  $s_r$ , in the graph  $G$ . In addition, a node might be able to sense its surroundings with a sensing range  $s_s$ . the sensing model in this context is considered as a binary model where any target falls within the sensing range of a node will be detected (1) and otherwise the node will report undetected (0). A node could work on one of two modes sensing or routing. During the sensing mode, a node is responsible for sensing the environment and sending its findings to its neighbor towards a sink node. In this case, the node is considered as a source node in the network. The sink node is considered as one of the powerful nodes that could handle the received messages from all of the source nodes. The second mode of a node is the routing mode where a node works only as a router that forwards the received nodes from its neighbors.

We assume a WSN with a set of source nodes  $S$  distributed in the networks and another set of routing nodes  $S_r$ . Nodes,

either sources or routers; have different limitations such as energy, processing capabilities, small communication range, small sensing range, and storage capabilities. At the same time, they are usually deployed in unattended areas in which it is exposed to multiple threats such as packet injection or node capturing. Therefore, data provenance is a must especially for critical WSNs such as the ones used for battle field or healthcare monitoring. However, it is not appropriate that nodes keep track of each and every packet with accumulated route, especially in a large scale WSN. Thus, the focus of this paper is on how to apply data provenance in such networks and gain nodes trust with minimum memory usage and reduced packets size.

The second problem that this paper handles is the nodes trust. As stated before, nodes in a WSN is prone to failure as well as attacks; so, the question is how nodes in such network can be trusted? We consider three parameters that could help in nodes trust which are nodes availability, nodes neighbors' opinion, and node's drop rate. Although these parameters could form a satisfying trust model for a sensor node, this information could be uncertain. Therefore, another issue that needs to be considered is the parameters uncertainty.

### V. DATA PROVENANCE SOLUTION APPROACH

In this section, we show how data provenance problem in WSN could be solved. The solution considers limited node resources in terms of energy, memory, and communication range. In addition, we propose a trust model based on fuzzy logic considering the previously mentioned parameters: nodes availability, nodes neighbors' opinion, and node's drop rate.

The data provenance problem in WSNs is transferred into an optimization problem where instead of keeping all nodes busy with data provenance, some of these nodes will be selected as data provenance nodes (DP). For a node to be a DP node, it has to satisfy the following conditions:

- 1) Closed to a source node  $s \in S_s$
- 2) Each Source  $s \in S_s$  is covered by at least one provenance node.
- 3) Has enough energy to handle the data provenance requirements.
- 4) Has enough memory to handle the data provenance requirements.
- 5) Trusted node in terms of availability, neighbors' votes, and Message Drop Rate (MDR).
- 6) The DP nodes have to be connected to each other.

These conditions show that finding DPs in this case is a hard problem where optimal solutions might not be able to find nodes using these constraints. Therefore, greedy algorithms could be the best solution. In the following subsections, our proposal for node trust and the proposed node selection solutions are described.

#### A. Fuzzy based Trust Model

Looking at the nodes properties and their role in WSNs, there are some parameters that can be used to trust a node. For instance, non-availability, neighbors voting, and message drop rate. These parameters do not have to be captured during the

initialization phase; however, in the subsequent phases, these parameters are captured for trust evaluation.

The non-availability parameter means how much time a node is turned off compared to the total time that it supposed to be on. Neighbor's vote is another parameter that it is used to evaluate nodes' trust. One more parameter is used for nodes trust which is message drop rate which could be computed by the sink node.

A fuzzy logic controller is used to handle nodes trust. The trust will be computed for all of the nodes during the setup phase with rough estimate; however, in the following rounds, the trust becomes more realistic due to the actual operation of the nodes. The input membership functions are based on three linguistic variables as shown in Fig. 1(a), (b), and (c). Linguistic variables are assumed to be low, medium, and high. The output membership function with two linguistic variables, trusted and not trusted, is presented in Fig. 2.

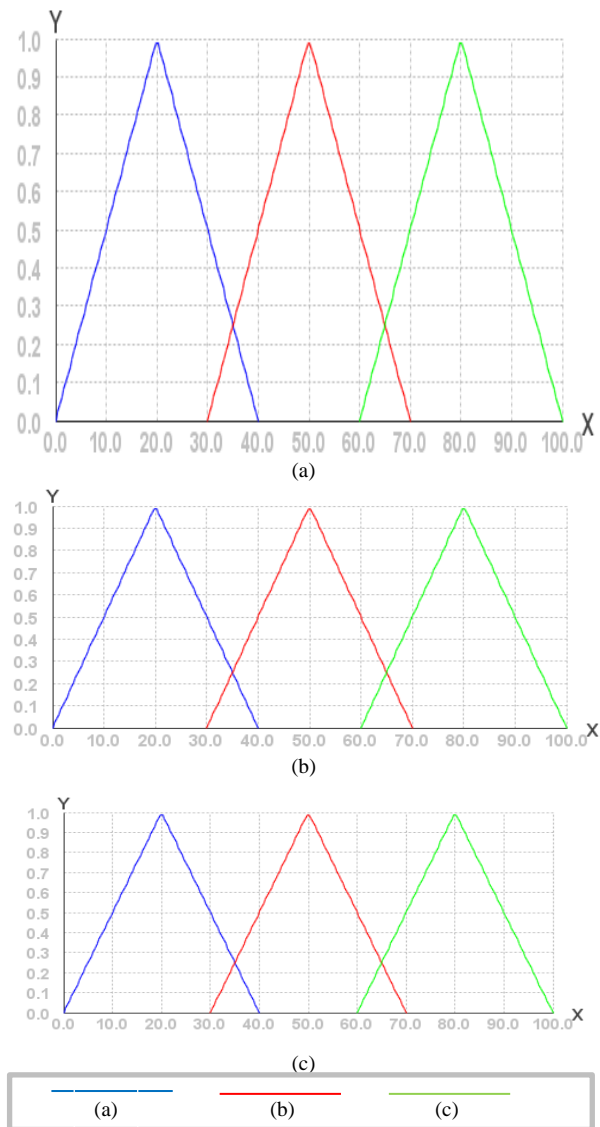


Fig. 1. Fuzzy Input Linguistics, (a) Availability ,(b) Neighbors Votes ,(c) Message Drop Rate.

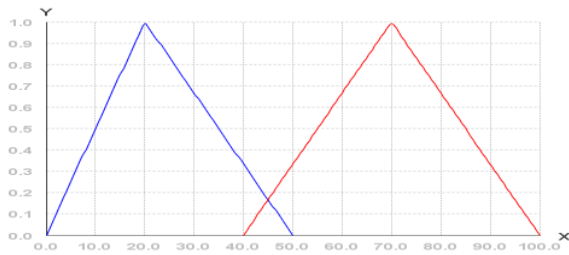


Fig. 2. Fuzzy Output Linguistics.

### B. Think-and-Share Optimization (TaSO) Algorithm

In the following, we now present the algorithm as a modular solution for data provenance. The algorithm is presented in terms of the required inputs, outputs and processing steps along with the description of the algorithm and its underlying steps. TaSO algorithm consists of four different phases which are *Think*, *Pair*, *Share*, and *Evaluate* as detailed below.

**Phase 1. Think Phase:** represents the initial phase in which the system generates initial solutions for the problems under consideration.

**Phase 2. Pair Phase:** focuses on generating some agents and solutions (from Phase 1) are assigned/distributed to the individual agents. Each of the generated agents aims to find the optimal solution from the set of solutions that have been assigned to it. The agents can work iteratively until the most optimal solution is found.

**Phase 3. Share Phase:** represents a phase where the agents share the optimal solutions with each others to proceed for building the final solution. During the share phase, the algorithm may jump back to the Paring Phase (Phase 2) for some rounds.

**Phase 4. Evaluation Phase:** is the terminal phase that aims to evaluate the best possible solution. **From a technical perspective**, the most optimal solution(s) is passed to the Think phase (Phase 1) to assess, evaluate, and select the optimal solution that have been shared by the agents.

The TaSO could be summarized in steps as follows:

#### TaSO Algorithm:

##### Input

problem description,  
number of internal Iterations (I),  
number of external Iterations (E),  
[required performance],  
icounter = 0, xcounter=0 , n, m

**Phase 1 - Think:** the thinker generates n random solutions, S1, S2, ....., Sn.

##### Pair:

1. Generate m agents A1,....., Am
2. Divide the n solutions on the m agents
3. Evaluate the solutions
4. Generate new solutions based on the old ones

5. icounter ++;
6. if (icounter < I) go to step 3

##### Phase 2 - Share:

1. xcounter++
2. Agents share their best solutions to each other
3. Agents evaluate their current solutions
4. Agents remove solutions with minimum performance
5. if (xcounter < E) go to Pair step 3

##### Phase 3 - Evaluation:

1. Agents return their best solutions to the thinker
2. The thinker evaluates the returned solutions and selects the best solution(s) as final solution to the problem.
3. Terminate

---

Given a set of nodes, some of them are source nodes, deployed in a specified area. Regarding to our problem, some random solutions are initially generated; at the same time, a set of agents are generated to work on the solutions. Agents try to find the best solutions and pass them to the main agent. Solutions are evaluated based on the following criteria:

- Closeness the sink node in terms of number of hops. To simplify the computation, we assume that the max number of hop is equal to (n-1) where n is the number of nodes in the network, considering the network is a linear network.
- Percentage of covered source nodes out of the total number of source nodes.
- For energy, the node has to have more than 50% of the max energy.
- For memory, the node has to have enough memory for at least half of the nodes IDs.
- The node is trusted as output of the fuzzy logic controller.
- Connectivity percentage is measured by the percentage of the selected nodes out of the total number of selected provenance nodes.

#### VI. EVALUATION AND EXPERIMENTAL RESULTS

In this section, we will test the think and share algorithm compared to Brute Force algorithm for solving the data provenance in WSNs [35]. Comparison criteria involve running time, coverage to the source node, closeness to the sink node, and connectivity percentage. The simulation is built using java program running in Intel Core i7 with 8GB RAM. The deployment area is assumed to be a square of 2000 m X 2000 m. 100 nodes are initially deployed in this area with 100 m communication range. 20 nodes are considered source nodes and they are randomly distributed in the deployment area. The number of internal and external iterations of TaSO are 100 and 10, respectively. Agents may use crossover and mutation techniques to find alternatives to the solution they have. The used mutation is 25% of the solution length and the crossover technique is to cross 50% of the solution. The following are the test cases for the TaSO algorithm.

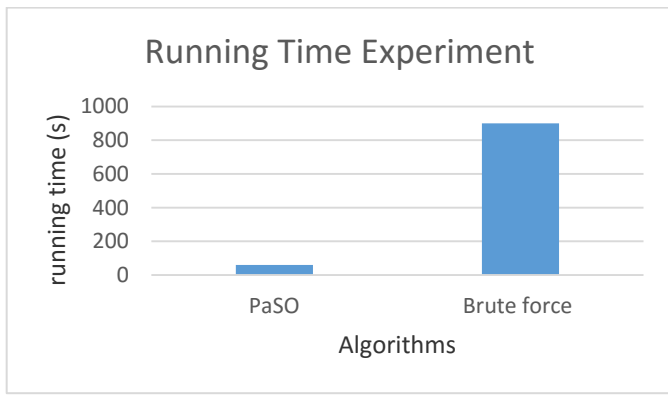


Fig. 3. Running Time Comparison.

A. Running Time Comparison

In this test case, a set of 10 experiments are averages to compare the running time of the TaSO with the Brute force algorithm. As can be seen in Fig. 3, although the number of iterations is 1000 iterations, the difference in time between TaSO and the Brute force trying every combination is very large. In addition, 100 nodes in WSNs are considered as a small network; therefore, it is expected that Brute force running time for large scale network to be huge.

B. Coverage to the Source Node

In this subsection, the coverage percentage of the source nodes from the selected provenance node is examined. As can be seen in Fig. 4, TaSO is covering only 70% of the source nodes; however, with increasing the number of iterations, this percentage has been increased to reach 85% which is good percentage for a greedy algorithm.

C. Closeness to the Sink Node

Here, 10 experiments are averaged showing the average distance of all of the selected provenance nodes to the sink node. The sink node in this case is located at point (0, 0) which is the left top corner of the deployment area. As shown in Fig. 5, compared to the Brute force algorithm, TaSO still satisfying almost 90% of what Brute force algorithm is gaining.

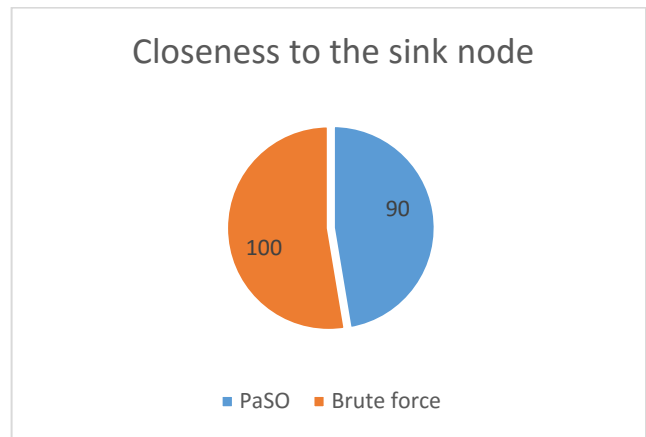


Fig. 5. Closeness to the Sink Node.

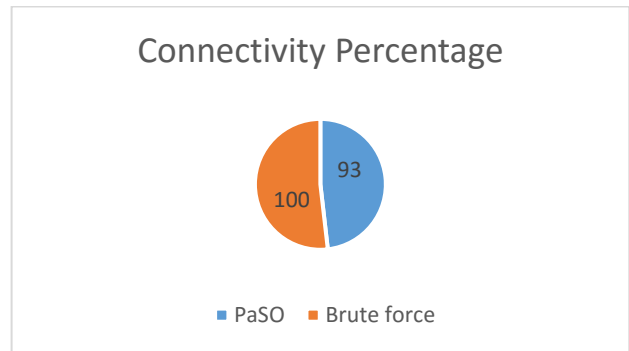


Fig. 6. Connectivity Percentage.

D. Connectivity Percentage

The connectivity percentage, in this context, means the degree of connectivity between the selected provenance nodes out of 100%. This percentage will have a great impact on the connectivity of the overall network. The average of the connectivity percentage, as shown in Fig. 6, of TaSO turns to be 93% with a drop of 7% of the elected nodes with 2200 iterations.

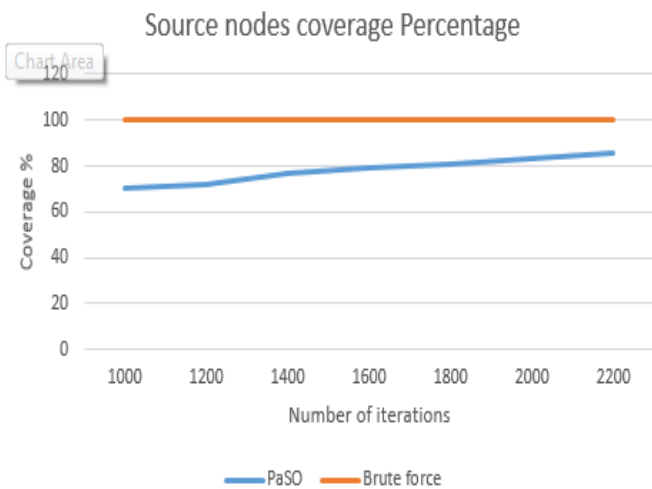


Fig. 4. Source Node Coverage Percentage.

VII. CONCLUSIONS AND FUTURE RESEARCH

We now conclude the paper with a discussion of the potential threats to the validity of research and possible dimensions of the futuristic research. In this paper, we present a bio-inspired technique and it's under think and share optimization algorithm for big data provenance in the context of WSNs. In addition, major applications of data provenance are stated. One of the important examples of big data provenance with many restrictions on the used devices such as memory, storage, and processing capabilities is WSNs. Therefore, this paper focused on the problem of selecting the best nodes to serve as data provenance. Different parameters are considered during the selection process including the connectivity of the selected nodes, within the range of a source node, nodes memory, nodes energy, and trust. The paper proposed a novel algorithm (TaSO) for the nodes' selection process that inspired from human collaboration in education. Moreover, we proposed a technique to solve the node's trust using fuzzy logic with three membership functions which are availability, neighbors' votes, and

message drop rate. The initial results show that the algorithm is efficient in terms of connectivity, closeness to the sink node, coverage, and running time.

7) *Potential threats to the validity*: Validity threats refer to cases or scenarios in terms of assumptions or constraints that represent some limitations for the proposed solutions. For example, in the proposed solution, limited number of trials for experimental results and validations can be considered as a potential threat. This means that based on more trials with divers case studies and inputs different results may be obtained. If such threats are not highlighted and addressed (as part of extension of future work), they can pose some limitations to proposed solution(s). We have identified following two types of threats:

a) *Threat I–Availability of Diverse Data Set for Evaluation*: In the proposed solution, we have performed experimental analysis based on comparatively limited amount of available data. Our proposed Futuristic research is also focused on incorporating more data for further validations of the solution. The primary challenge is the acquisition of more data from different systems to measure the quality attributes such as scalability and performance of the systems when new data is provided.

b) *Threat II–Data Provenance in an Industrial Context*: The second threat is about the applicability and customization of the solution in the context of industry scale data provenance. With an emergence of the Internet of Things (IoTs) and their role in industrial IoTs, can be a significant challenge for data management and provenance. The primary challenge is about the customization and scalability of the proposed solution at industry scale. The proposed algorithm will require appropriate parameterization (for customization) and user intervention (human decision support) for the to develop a solution that can address data provenance issues in larger and practical systems.

8) *Dimensions of futuristic research*: As part of the future research, we aim to extend the proposed bio-inspired algorithm with applied machine learning approach. The incorporation of machine learning and intelligence can optimize the algorithm (as part of autonomic computing) for efficient data provenance in networked and cyber-physical systems. We are currently in process for analyzing the existing challenges and solution for machine learning in the context of big data provenance. The ultimate solution can be built as an extension to the previous solution with specific focus on provenance intelligence in large, data-intensive systems.

#### ACKNOWLEDGMENT

This research is funded by the University of Ha'il through the Deanship of Scientific Research under the grant number 'BA- 1513'.

#### REFERENCES

- [1] Taxidou, Io, Sven Lieber, Peter M. Fischer, Tom De Nies, and Ruben Verborgh. "Web-scale provenance reconstruction of implicit information diffusion on social media." *Distributed and Parallel Databases* 36, no. 1 (2018): 47-79.
- [2] Pasquier, Thomas, Jatinder Singh, Julia Powles, David Evers, Margo Seltzer, and Jean Bacon. "Data provenance to audit compliance with privacy policy in the Internet of Things." *Personal and Ubiquitous Computing* 22, no. 2 (2018): 333-344.
- [3] Hu, Die, Dan Feng, Yulai Xie, Gongming Xu, Xinrui Gu, and Darrell Long. "Efficient Provenance Management via Clustering and Hybrid Storage in Big Data Environments." *IEEE Transactions on Big Data* (2019).Cuzzocrea, A., "Big Data Provenance: State-Of-The-Art Analysis and Emerging Research Challenges," In *EDBT/ICDT Workshops*, 2016.
- [4] Cuzzocrea, A., "Provenance Research Issues and Challenges in the Big Data Era," In *Computer Software and Applications Conference (COMPSAC)*, 2015 IEEE 39th Annual, Vol. 3, pp. 684-686.
- [5] Abbadi, Imad M., and John Lyle. "Challenges for Provenance in Cloud Computing." In *TaPP*. 2011.
- [6] Simmhan, Y.L., Plale, B. and Gannon, D., "A survey of data provenance in e-science," *ACM Sigmod Record*, 34(3), 2005, pp.31-36.
- [7] Zeng, Yu, Xing Zhang, Rizwan Akhtar, and Changda Wang. "A Blockchain-Based Scheme for Secure Data Provenance in Wireless Sensor Networks." In *2018 14th International Conference on Mobile Ad-Hoc and Sensor Networks (MSN)*, pp. 13-18. IEEE, 2019.
- [8] Crawl, D., Wang, J., and Altintas, I., "Provenance for mapreduce-based data-intensive workflows," In *WORKS'11, Proceedings of the 6th Workshop on Workflows in Support of Large-Scale Science*, co-located with , SC11, Seattle, WA, USA, 2011, pp. 21–30.
- [9] Bhardwaj, V., & Johari, R., "Big data analysis: Issues and challenges," *International Conference on Electrical, Electronics, Signals, Communication and Optimization (EESCO)*, 2015 pp. 1-6
- [10] Arshad, B., "NeuroProv-A visualisation system to enhance the utility of provenance Data for neuroimaging analysis" (Doctoral dissertation, University of the West of England), 2015.
- [11] Hammad, R. and Wu, C., "Provenance as a service: A data-centric approach for real-time monitoring." In *2014 IEEE International Congress on Big Data*, Anchorage, AK, USA, 2014, pp. 258–265.
- [12] Gundecha, P., Ranganath, S., Feng, Z., & Liu, H., "A tool for collecting provenance data in social media," In *Proceedings of the 19th ACM SIGKDD international conference on Knowledge discovery and data mining*, ACM, 2013, pp. 1462-1465.
- [13] Chen, P., & Plale, B. A., "Big data provenance analysis and visualization," *International Symposium on Cluster, Cloud and Grid Computing (CCGrid)*, 15th IEEE/ACM, 2015 (pp. 797-800).
- [14] Liu, Y. and Xu, S., "Detecting rumors through modeling information propagation networks in a social media environment," *IEEE Transactions on Computational Social Systems*, 3(2), pp.46-62, 2016.
- [15] Bertino, E., Ghinita, G., Kantarcioglu, M., Nguyen, D., Park, J., Sandhu, R., & Xu, S., "A roadmap for privacy-enhanced secure data provenance," *Journal of Intelligent Information Systems*, 43(3), 481-501, 2014.
- [16] Karvounarakis, G., Ives, Z. G., & Tannen, V., "Querying data provenance," In *Proceedings of the 2010 ACM SIGMOD International Conference on Management of data ACM*, 2010, pp. 951-962.
- [17] McDaniel, P., Butler, K., McLaughlin, S., Sion, R., Zadok, E., Winslett, M. (2010). In *2nd USENIX workshop on the theory and practice of provenance*.
- [18] Lyle, J., & Martin, A., In *2nd USENIX workshop on the theory and practice of provenance*, 2010.
- [19] Qazvinian, V., Rosengren, E., Radev, D.R. and Mei, Q., "Rumor has it: Identifying misinformation in microblogs." In *Proceedings of the Conference on Empirical Methods in Natural Language Processing*, Association for Computational Linguistics, 2011, pp. 1589-1599.
- [20] Taxidou, I., De Nies, T., Verborgh, R., Fischer, P.M., Mannens, E. and Van de Walle, R., "Modeling information diffusion in social media as provenance with W3C PROV," In *Proceedings of the 24th International Conference on World Wide Web*, ACM, 2015, pp. 819-824.
- [21] De Nies, T., Taxidou, I., Dimou, A., Verborgh, R., Fischer, P.M., Mannens, E. and Van de Walle, R., "Towards multi-level provenance reconstruction of information diffusion on social media," In *Proceedings*

- of the 24th ACM International on Conference on Information and Knowledge Management ACM, 2015, pp. 1823-1826.
- [22] Gundecha, P., Ranganath, S., Feng, Z. and Liu, H., "A tool for collecting provenance data in social media," In Proceedings of the 19th ACM SIGKDD international conference on Knowledge discovery and data mining, ACM, 2013, pp. 1462-1465.
- [23] De Nies, Tom, et al, "Towards multi-level provenance reconstruction of information diffusion on social media," Proceedings of the 24th ACM International on Conference on Information and Knowledge Management, ACM, 2015.
- [24] Katilu, Victoria M., Virginia NL Franqueira, and Olga Angelopoulou, "Challenges of Data Provenance for Cloud Forensic Investigations." Availability, Reliability and Security (ARES), 2015 10th International Conference on. IEEE, 2015.
- [25] Muhammad Imran and Helmut Hlavacs, "Provenance Framework for the Cloud Infrastructure: Why and How?" International Journal on Advances in Intelligent Systems, vol 6 no 1 & 2, 2013.
- [26] Hammad, R. and Wu, C., "Provenance as a service: A data-centric approach for real-time monitoring," In 2014 IEEE International Congress on Big Data, Anchorage, AK, USA, 2014, pp. 258–265.
- [27] Wang, B., and Li, H., Oruta, "Privacy-preserving public auditing for shared data in the cloud," IEEE T. Cloud Computing, 2014, 2(1):43–56.
- [28] Davidson, S. B. and J. Freire, "Provenance and scientific workflows: challenges and opportunities," In Proceedings of the ACM SIGMOD International Conference on Management of Data, SIGMOD 2008, Vancouver, BC, Canada, 10-12, 2008, pp. 1345–1350.
- [29] Muniswamy-Reddy, K., Macko, P., and Seltzer, M. I., "Provenance for the cloud," In USENIX Conference on File and Storage Technologies, 2010, (FAST), volume 10, pp. 15–14.
- [30] Wang, Changda, Wenyi Zheng, and Elisa Bertino. "Provenance for Wireless Sensor Networks: A Survey," Data Science and Engineering 1.3, 2016, pp. 189-200.
- [31] Priyanka, 2M.Devika, 2016, "A Survey of provenance management in wireless sensor network," nt. Journal of Engineering Research and Applications www.ijera.com ISSN: 2248-9622, Vol. 6, Issue 1, (Part - 5) 2016, pp.91-93.
- [32] Liu, L. (2009). Encyclopedia of database systems (Vol. 6). M. T. Özsu (Ed.). New York, NY, USA:: Springer.
- [33] Spiekermann, R., Jolly, B., Herzig, A., Burleigh, T., & Medycky-Scott, D. (2019). Implementations of fine-grained automated data provenance to support transparent environmental modelling. Environmental Modelling & Software.
- [34] Sajjad, Maryam, Aakash Ahmad Abbasi, Asad Malik, Ahmed B. Altamimi, and Ibrahim Mohammed Alseadoon. "Classification and mapping of adaptive security for mobile computing." IEEE Transactions on Emerging Topics in Computing , 2018.
- [35] A. Shadi, M. B. Yassein. A Resource-efficient Encryption Algorithm for Multimedia Big Data. In Multimedia Tools and Applications vol. 76, no. 21, pp: 22703-22724, 2017.

# Fragile Watermarking based on Linear Cellular Automata using Manhattan Distances for 2D Vector Map

Saleh Al-Ardhi\*<sup>1</sup>, Vijey Thayanathan\*<sup>2</sup>, Abdullah Basuhail<sup>3</sup>  
Faculty of Computing and Information Technology (FCIT)  
King Abdulaziz University, Jeddah, Saudi Arabia

**Abstract**—There has been a growing demand for publishing maps in secure digital format, since this ensures the integrity of data. This had lead us to put forward a method of detecting and locating modification data that is extremely accurate and simultaneously guarantees that the exact original content is recovered. More precisely, this method relies on a fragile watermarking algorithm that is developed in accordance with a frequency manner and, for every spatial feature, it can embed hidden data in 2D vector maps. The current paper proposes a frequency data-hiding scheme, which will be examined in accordance with Linear Cellular Automata Transform using Manhattan distances. Various invertible integer mappings are applied in order to find out the Manhattan distances from coordinates. To begin with, the original map is transformed into LCA, after which the watermark insertion process is carried out to transform the coefficient of the transformation result frequency into LSB. Lastly, a watermarked map is created by applying the inverse LCA transform, meaning that a LCA-transformed map is produced. Findings indicate that the suggested method is effective since in terms of invisibility and the capacity to allow for modifications. The methods also allow the detection of modification data, the addition and removal of some features, and enable the exact original content from the 2D vector map to be included.

**Keyword**—Reversible watermarking; fragile watermarking; linear cellular automata; Manhattan distances; vector map

## I. INTRODUCTION

The digital map is very a very accurate, automated procedure, which is highly beneficial. It also has lossless scaling in comparison to paper maps [1]. Other advantages of it include easy storage and simple distribution, as well as easy data manipulation. It generates a higher need for map producers to ensure that publication maps are subject to high security services as a means of protecting the integrity of the map. It also requires distortions resulting from these security services to be eliminated from the map. Fragile watermarking is deemed to be a highly effective technique for carrying out authentication and integrity for vector map verification. In comparison to conventional methods (such as digital signatures), fragile watermarking allows for both the detection and locate of any modifications made to the original content.

The integrity of the data refers to the authenticity of the data, that is, whether the data has been manipulated with a common or malicious data processing. A digital watermarking technology is used to embed hidden information in a digital map in order to indicate the author of the content [2-7], and

authenticate the integrity of the content [8-12]. To remove the distortions introduced by authentication and tamper detection ability, fragile watermarking for digital maps can be included in frequency watermarking [13]. The watermark in frequency watermarking is different from the space domain present in transform-domain embedding methods, since the watermark is not inserted by adapting the vertices' coordinates, but rather by changing their transform coefficients. Fragile watermarks are typically applied to safeguard integrity and authenticity of data content. When this is modified, the watermark becomes damaged, and jeopardizes the data integrity, meaning it cannot be ensured that the data is authentic A fragile watermark thus takes advantage of reversible watermarking techniques in order to insert the authentication data. And this not only enables the location of malicious attacks, but allows for the original content to be recovered [14]. In the present research paper, we will propose a reversible method for conducting fragile watermarking in vector maps. The proposed technique will be developed in accordance with Linear Cellular Automata Transform [15], with Manhattan Distances being employed. This is a new approach that is yet to be used for the first time in research. The Manhattan distances used here will be those between the adjacent vertices, and they will be applied to cover data, with the aim of creating a distance- based scheme [16] that can allow for the coordinates in which the watermark is embedded to be located. Linear Cellular Automata Transform will be used to enhance the ability and invisibility of the final, resulting maps. This suggested method will be able to accurately locate and detect any features that have been tampered with once data has been manipulated. It will also be possible to recover the original vector map in its exact form by extracting the hidden data in cases when there has been no attack.

The purpose of this research is to create a successful method to ensure that the integrity of geospatial data can be protected in a more effective and efficient manner than is currently possible and then has been proposed by previous research into the topic. The research results are expected to heighten confidence in the development of digital maps created in computerized environments. In order to enhance content authentication in vector maps, the present research paper puts forward a new and innovative approach to vector map watermarking. This method will rely on the LCA transformation algorithm. It is important to note that the cellular automata transform (CAT) algorithm has been used frequently in the past in cases of multimedia watermarking [17-18], however there is yet to be any research that has used



vector maps as the embedded media. The primary advantages of our new approach are that there is a high degree of reversibility and invisibility, as well as low computational complexity, and insertion outcomes [19] that are of advanced quality. Another key point here, is that the approach proposed in the current paper provides various features that enable and promote data origin authentication, primarily resulting from the scrambling technique [20]. What's more, as the approach can only be used on a single transform plane, it is very unique in comparison to current frequency domain watermarking methods. Additionally, it provides multi-frequency domains that can allow for successful DW. The rest of the paper will be organized in the following way: Section 2 will focus on exploring Linear Cellular Automata. Section 3 will discuss the reversible fragile watermarking scheme that is used in our technique in great depth. Section 4 is where we will present the experimental findings and algorithm analysis. Finally, section five will present summarized conclusions.

## II. LINEAR CELLULAR AUTOMATA

Linear cellular Automata Transform can be described as an important algorithm that is applied to represent a certain dynamic given in a discrete time and a frequency domain. Cells are organized to create a regular lattice structure, and it is imperative that each of these cells possesses a finite number of states. As a whole, LCAT is applied as a means of working out the discrete transformation in a fast and efficient manner, and can often be useful in lowering the number of complexities. In general, the following equation can be used to explain the LCAT formulation (1) [21].

$$(C^{t+1})^T = M_n \cdot (C^t)^T \pmod{2} \tag{1}$$

When  $M_n$  indicates the following local transition matrix, if  $n = 5k$ , then:

$$M_n = \begin{pmatrix} 1 & 1 & 1 & 0 & 0 & \dots & \dots & \dots & 0 & 0 & 0 \\ 1 & 1 & 1 & 1 & 0 & \dots & \dots & \dots & 0 & 0 & 0 \\ 1 & 1 & 1 & 1 & 1 & \dots & \dots & \dots & 0 & 0 & 0 \\ 0 & 1 & 1 & 1 & 1 & \dots & \dots & \dots & 0 & 0 & 0 \\ 0 & 0 & 1 & 1 & 1 & \dots & \dots & \dots & 0 & 0 & 0 \\ & & & & \dots & & & & & & \\ & & & & \dots & & & & & & \\ 0 & 0 & 0 & 0 & 0 & \dots & \dots & \dots & 1 & 1 & 1 \\ 0 & 0 & 0 & 0 & 0 & \dots & \dots & \dots & 1 & 1 & 1 \\ 0 & 0 & 0 & 0 & 0 & \dots & \dots & \dots & 1 & 1 & 1 \end{pmatrix}$$

If we use  $M_n$  to represent the transition matrix for the cellular automaton  $An$ . As previously stated, the matrix is an  $n$ th order and is pentadiagonal in nature. This matrix has non-zero coefficients that equate to 1. In cases where  $M_n$  is representative of the pentadiagonal matrices,  $(C^t)^T$  is representative of the linear matrix that is made up of a number of random parts. However, it is important to point out that the inverse formulation for LCAT is expressed using the following equation (2).

$$(C^t)^T = M_n^{-1} \cdot (C^{t+1})^T \pmod{2} \tag{2}$$

The formula for the transition matrix of the inverse cellular automaton of  $An$  is as follows: if  $n = 5k$  then:

$$M_n^{-1} = \begin{pmatrix} M_5^{-1} & B & B & \dots & B \\ B^T & M_5^{-1} & B & \ddots & \vdots \\ B^T & A^T & \ddots & \ddots & \vdots \\ \vdots & \ddots & \ddots & M_5^{-1} & B \\ B^T & \dots & B^T & B^T & M_5^{-1} \end{pmatrix}$$

Where

$$M_5^{-1} \begin{pmatrix} 0 & 0 & 1 & 1 & 0 \\ 0 & 0 & 0 & 1 & 1 \\ 1 & 0 & 1 & 0 & 1 \\ 1 & 1 & 0 & 0 & 0 \\ 0 & 1 & 1 & 0 & 0 \end{pmatrix} \pmod{2}, B = \begin{pmatrix} 0 & 0 & 1 & 1 & 0 \\ 0 & 0 & 0 & 1 & 1 \\ 0 & 0 & 1 & 0 & 1 \\ 0 & 0 & 0 & 0 & 0 \\ 0 & 0 & 0 & 0 & 0 \end{pmatrix}$$

The size of the transition matrix starts from 5 elements as defined in the following equation (3):

$$|M_n| \pmod{2} = \begin{cases} 1, & \text{if } n = 5k \text{ or } n = 5k + 1, \text{ with } k \in N \\ 0, & \text{otherwise} \end{cases} \tag{3}$$

### A. Linear Cellular Automata Transform

In order to improve the copyright protection performance features of vector maps, the present research paper suggests that fragile digital watermarking domain transformation is used to serve as proof of copyright, and this watermarking is achieved through LCAT data transformation algorithm. The CAT algorithm is commonly employed throughout the multimedia watermarking field [22,23], but has never been inserted into a vector map in embedded media form before. In the current paper, the watermark is inserted as a form of copyright indicator that is visible on the vector map and this is achieved by using a transformation domain on the vertices' coordinates. The procedure for inserting the watermark is a process in which the coefficient of the transformation result frequency has to be implemented into the vector map data. The map coordinates have to be adapted into a Linear Cellular Automata Transform (LCAT) in order to transform the vector map into a domain frequency signal. The key principle underpinning the process is that the coordinate  $v_{x1}$  on the original map is transformable by applying LCAT. The following equation can be used to explain the LCAT(4):

$$T(M) = \sum_{n=0}^{N-1} M_n \cdot v_{x1} \pmod{2} \tag{4}$$

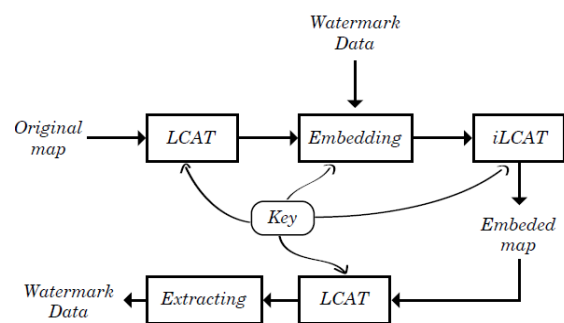


Fig. 1. The Flow Chart of the Linear Cellular Automata Transform Algorithm.

$T(M)$  represents the domain transformation of the original map, whilst  $v_{x1}$  represents the digital media value of the original map. Furthermore,  $N$  represents the number of

vertices that must be modified into a frequency domain.  $M_n$  is the transition matrix of Linear cellular automaton.

The key principle of the method is that the  $v_{x1}'$  coordinate of the original map can be modified using the LCAT, after which the encrypted watermark can be implemented. The following formula explains this method of embedding the watermark (5):

$$v_{x1}'' = v_{x1}' + \alpha W \quad (5)$$

$\alpha$  here represents the embedding parameter, with  $W$  the  $n$  representing the watermark bit. As can be seen in the watermark (5) formulation previously outlined, the higher the  $\alpha$ , the greater the changes will be on the vector map file. However, the strength of the watermark resistance will be much greater. The  $\alpha$  value used in the present research will be as high as 3 bit, which is very much an acceptable level for vector map changes. This value also shows a high level of resistance. The numerous stages of the linear cellular automata transform algorithm can be seen in Fig. 1.

In the meantime, the inverse formula for LCAT can be seen in the following equation (6):

$$iT(M) = \sum_{n=0}^{N-1} M_n^{-1} \cdot v_{x1}'' \pmod{2} \quad (6)$$

$iT(M)$  represents the inverse domain transformation value for the original map, whilst  $v_{x1}''$  represents the original map's transform digital media value.

### III. PROPOSED WATERMARKING SCHEME

Throughout section three, the proposed watermarking method will be introduced in two primary stages. Firstly, we will discuss the method used to insert watermarks into the vector MAP for every spatial feature (see Fig. 2). Secondly, we will discuss the method used to extract the watermarks and for the recovery of the original vector map (see Fig. 3).

#### A. Watermark Embedded Procedure

A polyline feature refers to a structured group of vertices that come together to create a single or multiple line segments. This happens in such a way that precisely two segments will share the endpoint of every segment (otherwise known as a vertex)  $v(x, y)$ . When the endpoints are the same, then a polyline will be closed (this is known as a polygon). As a whole, the coordinates of D vector map vertices are in the form of floating-point numbers

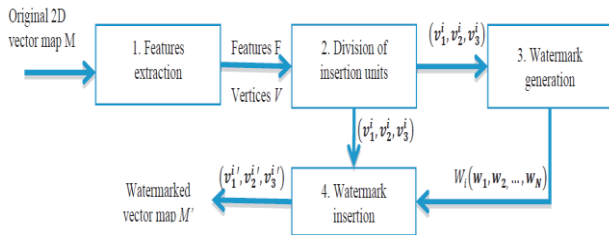


Fig. 2. Watermark Insertion Procedure.

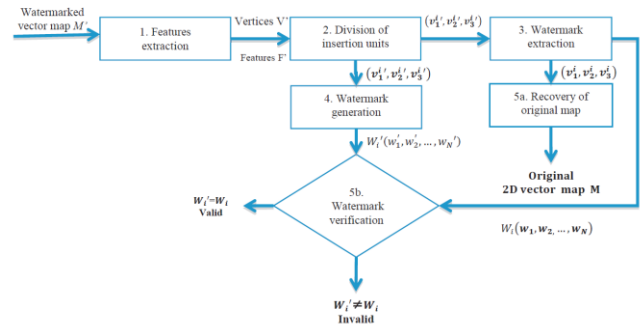


Fig. 3. Watermark Verification Procedure.

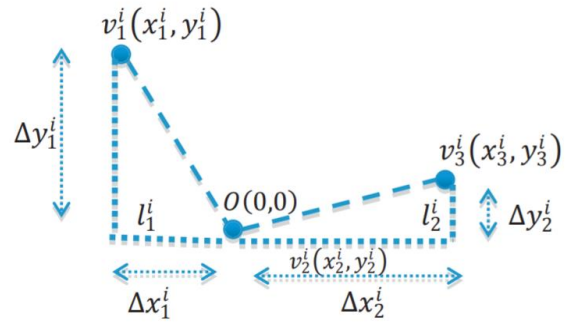


Fig. 4. An Insertion unit.

If we allow  $d_{max}$  to serve as the maximum number of digits following the decimal point,  $(x, y)$  can represent the original coordinates. In order to allow for the restoration of the original coordinates  $(x, y)$ , equation (1) can be used to extract the integer coordinates  $(xi, yi)$ .

$$(x^i, y^i) = \lfloor (x, y) \times 10^d \rfloor, d \leq d_{max} \quad (7)$$

The three consecutive vertices for every feature can be grouped as an insertion unit. The structure of an insertion unit can be seen in Fig. 4. The following formula represents  $N$  units in  $F$ :

$$(v_1^i, v_2^i, v_3^i) \{ (x_1^i, y_1^i), (x_2^i, y_2^i), (x_3^i, y_3^i) \},$$

$$i \in \{1, 2, \dots, N\}.$$

The following formula shows the relative coordinates  $(\Delta x, \Delta y)$  for every insertion unit, with  $v_2^i$  serves as the center point  $O(0,0)$ , resulting from equation (8).

$$\begin{cases} \Delta x_1^i = x_1^i - x_2^i & \Delta x_2^i = x_3^i - x_2^i \\ \Delta y_1^i = y_1^i - y_2^i & \Delta y_2^i = y_3^i - y_2^i \end{cases} \quad (8)$$

$$\begin{cases} l_1^i = |\Delta x_1^i| + |\Delta y_1^i| \\ l_2^i = |\Delta x_2^i| + |\Delta y_2^i| \end{cases} \begin{cases} r_1^i = \left\lfloor \frac{|\Delta x_1^i| - |\Delta y_1^i|}{2} \right\rfloor \\ r_2^i = \left\lfloor \frac{|\Delta x_2^i| - |\Delta y_2^i|}{2} \right\rfloor \end{cases} \quad (9)$$

As demonstrated in both Fig. 4 and equation (9), the Manhattan distances  $l_1^i$  and  $l_2^i$  refer to the distances between the center point and the two nearest neighbouring vertices, respectively. Moreover,  $r$  represents the integer mean

difference value, and this will not be impacted by modifications at all during the embedding process. In a given pair, the following formula shown in equation (10) can be applied to work out the difference (di) and integer-mean (mi) of the two Manhattan distances.

$$\begin{cases} d^i = l_1^i - l_2^i \\ m^i = \left\lfloor \frac{l_1^i + l_2^i}{2} \right\rfloor \end{cases} \quad (10)$$

The primary purpose of calculating the Manhattan distances is to allow for the location of the implemented watermark bits to be detected through the modification of the difference di (see equation (5) and Fig. 5).

$$w_k \in W(k = 1, 2, \dots, NW)$$

This is based on the premise that the insertion unit fulfills the two conditions required of embedded data. W represents the embedded data, and may be in the form of cryptographic hash value for the host vector map, the purpose of which is to verify the integrity of data or to highlight any secret data.

1) The coordinates acquired by working out the difference di between the vertex points are subsequently converted into LCAT.

2) The method presented in [20] can be employed in order to encrypt the factors relating to W\* and to identify any patterns in data  $W^* = \{w_i^* \mid w_i^* \in \{0, 1\}, i = 0, 1, \dots, l - 1\}$ .

3) If one is to assume that there is a double floating-point number in the form of a 16-digit coordinate value, and that this is inserted in decimal fraction format, and if W\* is embedded into the two final successive digits, then they will have relatively little impact on accuracy. Precision. What's more, the embedded value is not in line with the w\_i\* instead lying somewhere between 0 to 99. If D is presumed to be the integer resulting from the two digits, then the following formula is to be applied:

$$W^* = \begin{cases} \text{if } w_i^* \text{ is } 0 \text{ then } D \leq 50 \text{ and saved at the positions;} \\ w_i^* = 1, \text{ otherwise} \end{cases} \quad (11)$$

4) When the iLCAT is used after the watermark has been embedded, the frequency domain vector map can be restored to the original form.

5) The third and fourth steps can be repeated K number of times in high capacity situations, with blind watermarking and LCAT able to be employed as a means of extract the watermark.

To enable, secret communication, two criteria must be fulfilled in the proposed method:

Criterion 1. To guarantee the ability to recover the original 2D vector map, each watermarked vertice has to remain in the same region as the original vertices. To clarify, this means that the relative coordinates of original vertices (Δx, Δy) have to possess the exact same numbers as the corresponding watermarked vertices (Δx', Δy').

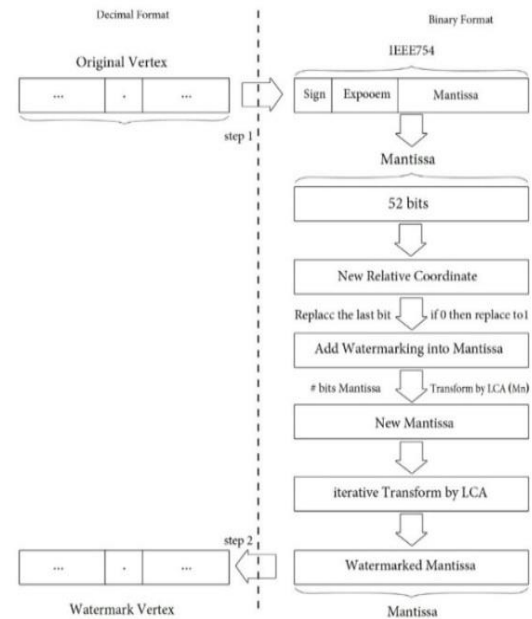


Fig. 5. The Binary Transform Process for Cover Data.

Condition 2. In order to guarantee the high quality of the watermarked 2D vector map, it is crucial to restrict as much as possible the distortion causing by the embedding process. This must be restricted by the map's precision tolerance [15]. Euclidean distances can be employed here to work out the extent of the distortions (Eq. (12)).

$$\sqrt{(x_1^{i'} - x_1^i)^2} , \sqrt{(x_3^{i'} - x_3^i)^2} \leq \tau \quad (12)$$

If the embedding of wk is complete, then the modified Manhattan distances l\_1^{i'} and l\_2^{i'} can be acquired from the d' and mi by using equation (13). Subsequently, the vertices coordinate of the watermarked unit (v\_1^{i'}, v\_2^{i'}, v\_3^{i'}) may be worked out using the formula: l\_1^{i'} and l\_2^{i'} and by subsequently employing equations (14) (15). This is chosen based on the values of Δx\_1^i and Δy\_1^i

$$\begin{cases} l_1^{i'} = m_i + \left\lfloor \frac{d_i^{i'} + 1}{2} \right\rfloor \\ l_2^{i'} = m_i - \left\lfloor \frac{d_i^{i'}}{2} \right\rfloor \end{cases} \quad (13)$$

$$\begin{cases} x \\ y \end{cases} \Delta x_1^{i'} = \begin{cases} r_1^i + \left\lfloor \frac{l_1^{i'} + 1}{2} \right\rfloor, \text{ if } \Delta x_1^i \geq 0 \\ -r_1^i - \left\lfloor \frac{l_1^{i'} + 1}{2} \right\rfloor, \text{ if } \Delta x_1^i < 0 \end{cases} \Delta x_1^i \begin{cases} r_1^i + \left\lfloor \frac{l_1^{i'} + 1}{2} \right\rfloor, \text{ if } \Delta x_2^i \geq 0 \\ -r_1^i - \left\lfloor \frac{l_1^{i'} + 1}{2} \right\rfloor, \text{ if } \Delta x_2^i < 0 \end{cases} \quad (14)$$

$$\begin{cases} x_1^{i'} = x_2^i + \Delta x_1^{i'} \\ y_1^{i'} = y_2^i + \Delta y_1^{i'} \end{cases} \begin{cases} x_1^{i'} = x_2^i + \Delta x_2^{i'} \\ y_1^{i'} = y_2^i + \Delta y_2^{i'} \end{cases} \quad (15)$$

### B. Watermark Verification Procedure

There are three fundamental processes underpinning the watermark verification procedure. These are the extraction of watermarks, the verification of such watermarks, and recovering of the original map. When the watermarked vector map has been obtained M', the following formula can be used to extract the watermark:

1) The watermark can be extracted from the watermarked map  $M'$  into  $\{F_1', F_2', F_D'\}$  feature groups. These groups are in the form of integers. In every group  $F_i'$ , three consecutive vertices must be separated to form a watermarked insertion unit.

$$(v_1^{i'}, v_2^{i'}, v_3^{i'}) \{(x_1^{i'}, y_1^{i'}), (x_2^{i'}, y_2^{i'}), (x_3^{i'}, y_3^{i'})\}, i \{1, 2, \dots, N\}$$

2) For each of the watermarked unit insertions, steps two to six outlined below must be carried out.

3) Work out the units' Manhattan distances  $l_1^{i'}$  and  $l_2^{i'}$  by employing equations (13) and (14).

4) Use equation 15 to work out the difference  $'$  and the integer – mean  $mi$  of  $l_1^{i'}$  and  $l_2^{i'}$ .

5) After acquiring a set of coordinates for every feature, this is then to be transformed into an LCAT form.

6) To extract the embedded watermark location and watermark bits, equation (16) must be employed.

$$W^* = \begin{cases} \text{if } D \leq 50 \text{ then } w_i^* \text{ is } 0 \\ w_i^* = 1, \text{ otherwise} \end{cases} \quad (16)$$

1) Private key  $K$  must be used here to extract the initial embedded watermark pattern  $W$ . To do this, the inverse watermark pattern must be used.

Once the outlined process is complete, then the original difference  $di$  for each unit will be obtained. When collaborating these with the integer- mean  $mi$ , it is then possible to work out the original coordinates of each unit by applying equations (13) to (15). To work out the watermark  $W'$  through the given method, the process above must be used. A group  $F_i$  is considered to be authentic when two watermarks  $W$  and  $W'$  are equal. The watermark is considered tampered, and thus unauthentic, if they are not equal

#### IV. RESULTS AND ANALYSIS

In the proposed method, the shape file format (.shp) of Environmental Systems Research Institute, Inc. (ESRI) is used. A simple shape file (.shp) vector map of “King Salman road map in Riyadh city” is the original map used to explore and test our proposed method. The map used to be a vector map, and has thirty polyline features and 130 vertices. Given the identical nature of geometric data structures of both polygon and polyline features, the findings of the polyline features will be presented in detail. Experiments have been carried out on computer using the software CPU 2.3 GHz, 16GB RAM, Win 10 Professional, QGIS Version 3.0, python language. When attempting to hide data, the secret bits corresponding to each transform coordinate carried  $\alpha$  in  $LSB$ ,  $Mn$  is  $matrix\ size\ equal = 35$  and  $T = 1$  represent iterative embedding.

It is worth noting that the proposed scheme was implemented to vector maps. Furthermore, in this case, the map employed represents the Riyadh Development Authority. Additionally, to serve as the watermark, an image was utilized (see Fig. 6). During the first test, we attempted to verify the quality of our proposed watermarking technique. To assess the subjective quality of the embedded vector map, comparisons were between the watermarked map and its original vector map

counterpart. By adhering to Fig. 7(a) and 7(b), it is evident that the watermarked vector map is invisible.

We made effective use of the root mean square error (RMSE) to work out the objective quality of the watermarked vector map using equation (17).

$$RMSE = \sqrt{\frac{\sum_{i=0}^N \sum_{j=0}^N \frac{|I(i,j) - U(i,j)|^2}{|I(i,j)|^2}}{N}} \quad (17)$$

On both the original map ( $M$ ) and the watermarked map ( $M'$ ),  $V_M$  and  $V_{M'}$  are the corresponding vertices, with  $N$  representing the total vertices. The RMSE of watermarked vector map in our experiment is  $1.973 \times 10^{-10}$ . As has been previously discussed, when exploring the watermark embedding procedure in Section 3.1, the features of the 2D map play a major role in influencing the quality of the map. To improve invisibility as much as possible, it is important to choose the original vector map that has the highest correlation.

Fig. 4 presents the correlation between insertion distortion created from the Euclidean distances and the quality of the watermarked vector map worked out through RMSEs. To enhance the quality of watermarked vector map, it is crucial to minimize distortion. This is done by raising the map's precision tolerance. This results in a reduction of the total number of insertion units, and thus lowers the watermark's ability to be embedded.

Fig. 7 shows the findings of the experiment. The vector map presented in Fig. 7(a) has been subjected to the proposed watermarking scheme. To assess the subjective quality of the embedded vector, a human visual system (HVS) was employed. Through this, comparisons were made between the original vector maps and their watermarked counterparts. As shown in Fig. 7(a) and 7(b), there is a high level of invisibility in the watermarked vector maps. Fig. 7(c) shows the subset of the watermarked vector map and how this overlaps the original vector map, which allows for the differences between the two maps to be seen. Such variations indicate changes to the position of coordinates for original map features caused during the insertion process. It is possible to recover the original map so long as there have been no modifications to the watermarked map and the two watermarks must be identical.



Fig. 6. Example of Watermark.

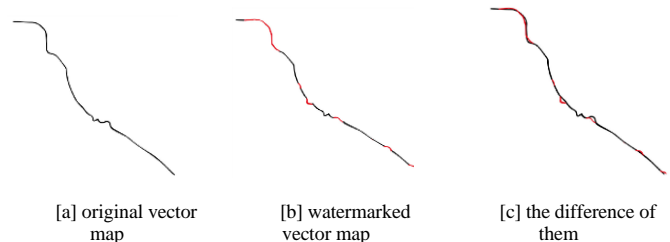


Fig. 7. Watermark Imperceptibility Proof.

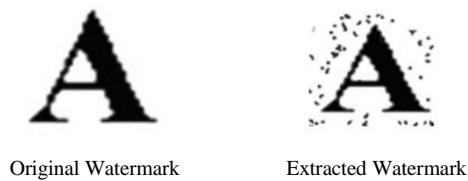


Fig. 8. Well Extracted Watermark.

The capacity of the suggested scheme to identify tampering and to localize these was revealed in the second test. Modifications were made to certain areas (such as the coordinates of vertices, the addition of vertices and removal of some vertices). Fig. 7(a) shows the vector map following the process of watermark embedding. It has been modified by employing QGIS. One such modification that was made here is the removal of some features. Subsequently, we assessed the integrity of the manipulated vector maps through the watermark verification procedure. Fig. 8 shows the output of the watermark verification process. The dashed line shows the exact point where tampering occurred.

## V. CONCLUSIONS

The proposed scheme of reversible fragile watermarking relies on the implementation of Manhattan distances using certain features as computation units. The watermark can then be inserted into the 2D vector map. Not only is the process beneficial in clarifying the map's integrity, but it can also precisely detect any modifications to map features. What's more, the embedding of watermark information accounts for the map's error tolerance. There is still a high level of practical value in the map following watermark insertion. When data must be very accurate, it is possible to recover the original vector map by conducting integrity verification. The findings of the experiments indicate that it is possible to accurately recover the original vector map following the extraction of watermark, so long as there have been no modifications made to the data. In terms of invisibility, the findings of the test case show that the quality of the relevant data cover is a crucial factor in improving the method's performance. Cover data that is highly correlated could lead to high capacity and invisibility. In future, we will investigate the scheme in more depth and examine how the scheme can be applied to point features. We will also investigate methods of improving the scheme's capacity through the iterative embedding on highly correlated data set.

## REFERENCES

[1] K.-T. Chang, Introduction to geographic information systems, McGraw-Hill, 2012. Li, W. Zhou, B. Lin, and Y. Chen, Copyright protection for GIS vector data production, Proceedings of SPIE, 2008, vol. 7143, p. 71432X–71432X–9.

[2] A. Li, Y. Chen, B. Lin, W. Zhou, and G. Lü, "Review on Copyright Marking Techniques of GIS Vector Data," in 2008 International Conference on Intelligent Information Hiding and Multimedia Signal Processing, 2008, pp. 989–993.

[3] Kim J, Won S, Zeng W, Park S (2011) Copyright protection of vector map using digital watermarking in the spatial domain. In: 7th international conference on digital content, multimedia technology and its applications, pp 154–159 67.

[4] Kitamura I, Kanai S, Kishinami T (2001) Copyright protection of vector map using digital watermarking method based on discrete fourier transform. In: International symposium on geoscience and remote sensing, vol 3, pp 1191–1193.

[5] A. Li, B. Lin, Y. Chen, and G. Lü, "Study on copyright authentication of GIS vector data based on Zero-watermarking," The International Archives of the Photogrammetry, Remote Sensing and Spatial Information Sciences., vol. XXXVIII Pa, pp. 1783–1786, 2008.

[6] S. Tao, X. Dehe, L. Chengming, and S. Jianguo, "Watermarking Gis Data For Digital Map Copyright Protection," ICC, pp. 1–9, 2009.

[7] L. Zheng and F. You, "A Fragile Digital Watermark Used to Verify the Integrity of Vector Map," in E-Business and Information System Security, 2009. EBISS'09. International Conference on, 2009, pp. 1–4.

[8] N. Wang and C. Men, "Reversible fragile watermarking for 2-D vector map authentication with localization," Computer-Aided Design, Nov. 2011.

[9] X. Wang, C. Shao, X. Xu, and X. Niu, "Reversible Data-Hiding Scheme for 2-D Vector Maps Based on Difference Expansion," IEEE Transactions on Information Forensics and Security, vol. 2, no. 3, pp. 311–320, Sep. 2007.

[10] Neyman S, Sitohang B, C ahyono F (2013) An improvement technique of fragile watermarking to assurance the data integrity on vector maps. In: International conference on computer, control, informatics and its applications, pp 179–184 107.

[11] Zheng L, Li Y, Feng L, Liu H (2010) Research and implementation of fragile watermark for vector graphics. In: 2nd international conference on computer engineering and technology, vol 1, pp 522– 52.

[12] Wang Q , Zhu C (2012) Fragile watermarking algorithm for vector geographic data exactau then citation. J Geom Sci Technol

[13] eng F, Guo RS, Li CT, Long M (2010) A semi-fragile watermarking algorithm for authenticating 2d cad engineering graphics based on log-polar transformation. Comput Aided Des 42(12):1207–1216

[14] AL-ardhi S , Thayananthan V, Basuhail A (2020) Copyright Protection and Content Authentication Based on Linear Cellular Automata Watermarking for 2D Vector Maps. In: Arai K., Kapoor S. (eds) Advances in Computer Vision. CVC 2019. Advances in Intelligent Systems and Computing, vol 943. Springer, Cham.

[15] Neyman SN, Sitohang B, Sutisna S (2013) Reversible fragile watermarking based on difference expansion using manhattan distances for 2d vector map. Procedia Technol 11:614–620.

[16] R. Shiba, S. Kang and Y. Aoki: An image watermarking technique using cellular automata transform. In TENCON 2004 IEEE Region 10 Conference (2004), pp. 303–306.

[17] A. Dalhoum et al.: Digital image scrambling using 2D cellular automata. IEEE Multimedia, 2012.

[18] R. Shiba, S. Kang and Y. Aoki, "An Image Watermarking Technique using CAT", 2004 IEEE region 10 Conference, Vol.1, pp.303-306, 2004.

[19] N, Zhang H, Men C (2014) A high capacity reversible data hiding method for 2D vector maps based on virtual coordinates. Comput Aided Des 47:108–117.

[20] A. Marti and G. Rodri: Reversibility of linear cellular automata. Applied Mathematics and Computation 217 (21) (2011), 8360–8366.

[21] S. Wolfram, Theory and Applications of Cellular Automata, World Scientific Publishing Company, Singapore, 1986.

[22] S. Wolfram, Cryptography with Cellular Automata, Springer- Verlag, Beilin, 1986.

# A Watermarking System Architecture using the Cellular Automata Transform for 2D Vector Map

Saleh AL-ardhi<sup>\*1</sup>, Vijey Thayanathan<sup>\*2</sup>, Abdullah Basuhail<sup>\*3</sup>  
Faculty of Computing and Information Technology (FCIT)  
King Abdulaziz University  
Jeddah, Saudi Arabia

**Abstract**—Technological advancement, paired with the emergence of increasingly open and sophisticated communication systems, has contributed to the growing complexity of copyright protection and ownership identification for digital content. The technique of digital watermarking has been receiving attention in the literature as a way to address these complexities. Digital watermarking involves covertly embedding a marker in a piece of digital data (e.g., a vector map, database, or audio, image, or video data) such that the marker cannot be edited, does not interfere with the quality or size of the data, and can be extracted accurately even under the deterioration of the watermarked data (e.g., as a consequence of malicious activity). The purpose of this paper is to describe a watermarking system architecture that can be applied to a 2D vector map. The proposed scheme involves embedding the watermark into the frequency domain, namely, the linear cellular automata transform (LCAT) algorithm. To evaluate the performance of the proposed scheme, the algorithm was applied to vector maps from the Riyadh Development Authority. The results indicate that the watermarking system architecture described here is efficient in terms of its computational complexity, reversibility, fidelity, and robustness against well-known attacks.

**Keywords**—Digital watermarking; spatial database; 2d vector map; linear cellular automata transform

## I. INTRODUCTION

Although digital technologies have yielded numerous benefits, the unlawful use of data through piracy, counterfeiting, and copyright infringement remains a fundamental challenge. Until recently, the schemes proposed for mitigating these challenges have largely been inefficient and ineffective [1, 2]. One of the principal reasons for this relates to the fact that with suitable software, it is possible to deform, copy, and modify digitally-stored data in a relatively straightforward way.

To date, the most efficient and effective solution to this challenge is referred to as digital watermarking [3]. As a result of the technique's robustness in protecting digital copyrights, as well as other applications such as source tracking, authentication, and fraud and tamper detection, many researchers have started to investigate the topic. At its heart, digital watermarking involves inserting a marker (also known as the "hidden information", "payload", or "watermark") into a piece of digital data that is amenable to watermarking (also known as a "host signal" or a "cover work"). The types of cover work are varied, ranging from images, audio and videos to vector maps and databases; while the types of watermark

range from images and pieces of identification text to secret messages [4-6].

Diverse constraints are necessary for a watermarking system to function effectively. Foremost among these constraints is the requirement for the payload to be (a) undetectable and (b) resistant to replacement or removal. Another critical constraint is that the quality and size of the cover work must not be affected by the insertion of the payload. Furthermore, it is essential for the payload to remain extractable even in situations where the quality of the cover work has degraded. Lastly, the existence or non-existence of the payload must only be perceptible to the party with relevant permissions to access it (e.g., the holder of a private key).

This paper is concerned with presenting an efficient and effective digital watermarking architecture for concealing a payload within a spatial database. The proposed scheme was designed to apply especially to 2D vector maps. The scheme involves the provision of frequency domain information, where the insertion of the payload into the cover work relies on the linear cellular automata transform (LCAT) algorithm. Specifically, the coordinate is separated into the least significant digit (LSD) [7] and the most significant digit (MSD) [8] planes, where the LSD is typically found in the LSD. Given that the human eye cannot detect minor alterations in the LSD planes of 2D vector maps, the payload was concealed in the LSD zones. Additionally, the robustness of the proposed scheme in terms of its security was reinforced by utilising both a public and a private key [9].

## II. DIGITAL WATERMARKING

### A. Definitions and Concepts

Despite the steganography dimensions of digital watermarking [10], the finality of each is distinct, and the procedures associated with each are distinguished by their roles. That is to say, steganography is concerned with the transmission of a secret message from a sender to a receiver, while digital watermarking architectures are concerned with embedding invisible payloads into cover work without undermining its quality or increasing its size.

As previously noted, digital watermarking is the best-known way to solve the problem of copyright protection for digital content. The aim of the technique is to embed an invisible and non-temporary mark in a piece of digital data that is amenable to watermarking (also known as a "host signal" or a "cover work"). The watermark must not be detectable by any

party other than the data owner, and it should be resistant to all malicious attempts to extract it. When a digital watermarking process satisfies these key constraints, it can be considered robust.

Permission information relevant to the cover work is typically contained in the payload. As noted in the introduction section, document authentication applications can benefit from digital watermarking because these schemes allow data owners to confirm the integrity of the cover work [11-13]. Furthermore, a payload can be used to determine which entity is the owner of the document [14-16]. In terms of what the payload consists of when it is used for document owner identification purposes, it can be a distinctive code that specifies the author or the original purveyor of the document.

Robust digital watermarking schemes that can be deployed in real-world settings are characterised by the following characteristics: firstly, the invisibility of the payload to the human eye and, furthermore, the ability of payload insertion not to degrade or undermine the quality of the cover work; secondly, specificity (also known as unambiguity), which means that the payload must be retrievable by the detection system, and that it must provide a clear indication of the cover work owner; and finally, the resistance of the payload against common attacks (e.g., attempts to remove the payload) must be high, and any removal of the payload should undermine the cover work's quality.

### B. Watermarking System Process

The embedding component and the recovery component are the fundamental elements of any digital watermarking system. The inputs to the embedding component are the watermark itself ( $w$ ) and the cover work ( $c$ ), as well as any required keys and the original map. Significantly, the embedding process in a digital watermarking system involves the utilisation of a private key. In view of this, the private key is also critical for the watermark detection component. An overview of the watermark embedding component is presented in Fig. 1, the output of which is the watermarked map.

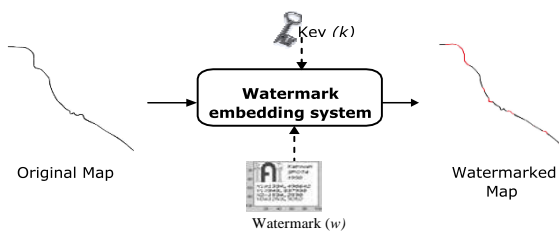


Fig. 1. Watermark Embedding Process.

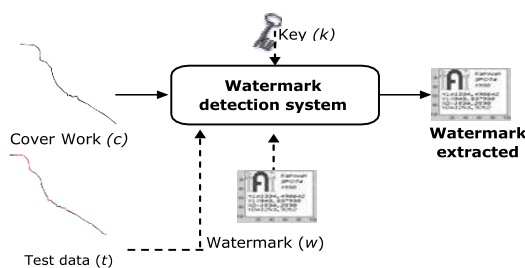


Fig. 2. Watermark Detection Process.

The recovery component of a digital watermark embedding system removes the payload from the cover work, and its inputs are the following: firstly, the test data ( $t$ ), which could be distorted; secondly, the private key; thirdly, the watermark ( $w$ ); and finally, the cover work ( $c$ ). In the event that  $t$  was not subjected to malicious removal attempts, then the output of the watermark removal component is the extracted watermark or an indication of its presence [3], which characterises the mark presence probability. Alternatively, if  $t$  was subjected to attacks by an adversary, then nothing is outputted from the watermark removal component. An overview of watermark removal component is presented in Fig. 2.

### C. Watermarking Techniques

Traditional digital watermarking techniques are non-complex and lack robustness, but the degree to which these techniques are complex, sophisticated, and robust has increased in recent years. The classification of a digital watermarking technique is typically based on the associated domain, where the principal domains are the following: firstly, the space domain; and secondly, the transform domain. In view of this, the two main groups of digital watermarking techniques are space domain approaches and transform domain approaches. Nevertheless, it is worth noting that some researchers differentiate between digital watermarking techniques based on the nature of the system's watermark embedding component. From this perspective, the techniques can be viewed as either additive (where the payload is added to the features of the cover work) or subtractive (where coefficients of the cover work are replaced to embed the digital watermark).

- **Space-domain approaches:** Space domain approaches to digital watermarking involve shifting a map's vertices inside a predetermined tolerance range, and then employing suitable embedding strategies (see the following subsection). In this case, the embedding space can be represented using polar coordinates [17], blocks [18], topological relations [19], or Cartesian coordinates [7] (see Fig. 3).
- **Transform-domain approaches:** Compared to space domain approaches, their transform domain counterparts greatly advance the degree to which the digital watermarking system is robust and resistant to malicious activities [5]. The embedding component of a digital watermarking system that is based on a transform domain approach first applies a transformation on the cover work. As shown in Fig. 4, this is achieved using the discrete cosine transform (DCT), discrete wavelet transform (DWT), discrete Fourier transform, or fast Fourier transform (FFT) [20-22]. Following this, the watermark insertion phase begins, which is achieved by changing coefficients within the cover work to produce a transformed, watermarked version of the cover work. The final phase, which involves applying the reverse transformation to the output of the second phase, yields a watermarked version of the cover work. An overview of the watermarking process for transform domain approaches is presented in Fig. 5.

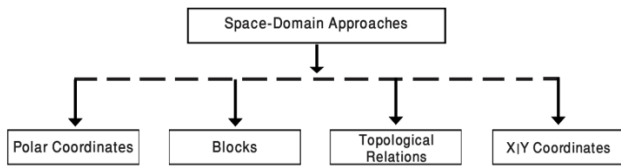


Fig. 3. The Classification Space-Domain Approach.

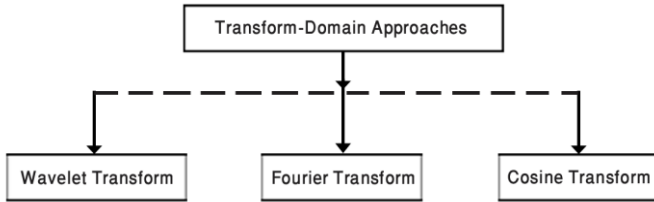


Fig. 4. The Classification Transform-Domain Approach

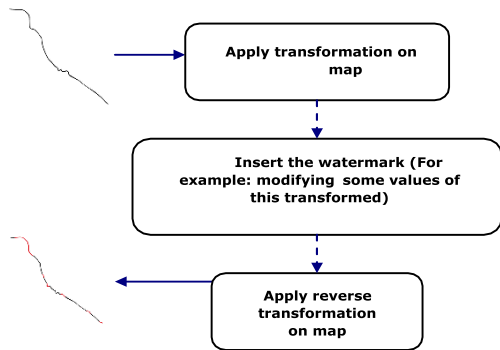


Fig. 5. General Watermarking Process in Frequency Domain.

### III. LINEAR CELLULAR AUTOMATA

The linear cellular automata transform (LCAT) algorithm is employed to represent a dynamical in a frequency domain and a discrete time domain. The cellular automata are configured into regular lattice structures, each of which possesses a set of states that is limited in size. Generally speaking, LCAT is employed for rapid and efficient calculations of the discrete transformation, and one of the fundamental strengths of the algorithm relates to the fact that it can reduce complexity. LCAT can be expressed as shown in equation (1) [23].

$$(C^{t+1})^T = M_n \cdot (C^t)^T \pmod{2} \tag{1}$$

where,  $M_n$ , letting  $n = 5k$ , is the local transition matrix given below.

$$M_n = \begin{pmatrix} 1 & 1 & 1 & 0 & 0 & \dots & \dots & \dots & 0 & 0 & 0 \\ 1 & 1 & 1 & 1 & 0 & \dots & \dots & \dots & 0 & 0 & 0 \\ 1 & 1 & 1 & 1 & 1 & \dots & \dots & \dots & 0 & 0 & 0 \\ 0 & 1 & 1 & 1 & 1 & \dots & \dots & \dots & 0 & 0 & 0 \\ 0 & 0 & 1 & 1 & 1 & \dots & \dots & \dots & 0 & 0 & 0 \\ & & & & \dots & & & & & & \\ & & & & \dots & & & & & & \\ 0 & 0 & 0 & 0 & 0 & \dots & \dots & \dots & 1 & 1 & 1 \\ 0 & 0 & 0 & 0 & 0 & \dots & \dots & \dots & 1 & 1 & 1 \\ 0 & 0 & 0 & 0 & 0 & \dots & \dots & \dots & 1 & 1 & 1 \end{pmatrix}$$

Suppose that  $M_n$  is the transition matrix of  $An$ , a cellular automaton. Hence,  $M_n$  can be described as an  $n$ th order pentadiagonal, matrix for which the non-zero coefficients are 1. Where,  $M_n$  denotes the pentadiagonal matrices and  $(C^t)^T$  is the transposition of a linear matrix containing varying random bits. Equation (2) states the inverse formulation of LCAT.

$$(C^t)^T = M_n^{-1} \cdot (C^{t+1})^T \pmod{2} \tag{2}$$

$M_n^{-1}$ , the transition matrix for the inverse cellular automaton of  $An$ , letting  $n = 5k$ , can be expressed as follows:

$$M_n^{-1} = \begin{pmatrix} M_5^{-1} & B & B & \dots & B \\ B^T & M_5^{-1} & B & \dots & \vdots \\ B^T & A^T & \dots & \dots & \vdots \\ \vdots & \dots & \dots & M_5^{-1} & B \\ B^T & \dots & B^T & B^T & M_5^{-1} \end{pmatrix}$$

where

$$M_5^{-1} = \begin{pmatrix} 0 & 0 & 1 & 1 & 0 \\ 0 & 0 & 0 & 1 & 1 \\ 1 & 0 & 1 & 0 & 1 \\ 1 & 1 & 0 & 0 & 0 \\ 0 & 1 & 1 & 0 & 0 \end{pmatrix} \pmod{2}, B = \begin{pmatrix} 0 & 0 & 1 & 1 & 0 \\ 0 & 0 & 0 & 1 & 1 \\ 0 & 0 & 1 & 0 & 1 \\ 0 & 0 & 0 & 0 & 0 \\ 0 & 0 & 0 & 0 & 0 \end{pmatrix}$$

As specified in equation (3), the transition matrix's size begins at 5 elements.

$$|M_n| \pmod{2} = \begin{cases} 1, & \text{if } n = 5k \text{ or } n = 5k + 1, \text{ with } k \in N \\ 0, & \text{otherwise} \end{cases} \tag{3}$$

#### A. Linear cellular Automata Transform

The need exists for new techniques that can be used to apply digital watermarks to vector maps in a robust, attack-resistant, and efficient way, thereby promoting copyright protection performance. Therefore, this study proposes a novel digital watermarking domain transformation that can serve as proof of copyright on vector maps, which relies on the linear cellular automata transform (LCAT) algorithm. Although LCAT is widely-used in the field of digital watermarking for multimedia cover work [24, 25], it has not been previously applied to vector maps as the inserted media. For this study, the digital watermark serves as a copyright marker on the vector map, and it is applied on the transformation domain for the coordinate of the vertices. As for the process of embedding the watermark, this is used for the coefficient of the transformation result frequency of the vector map data. The modification of the vector map coordinate into an LCAT takes place in this study in order to facilitate the transformation of the vector map into a domain frequency signal. The key concept to note for the proposed scheme is that  $v_{x1}$ , the coordinate of the host map, can be transformed using LCAT. Regarding the formulation of LCAT, this is given in equation (4) (see Fig. 6).

$$T(M) = \sum_{n=0}^{N-1} M_n \cdot v_{x1} \pmod{2} \tag{4}$$

where  $T(M)$  represents the host map's domain transformation value,  $v_{x1}$  represents the host map's digital media value,  $N$  refers to the total number of vertices that will be modified to become a frequency domain, and  $M_n$  is the linear cellular automaton's transition matrix.



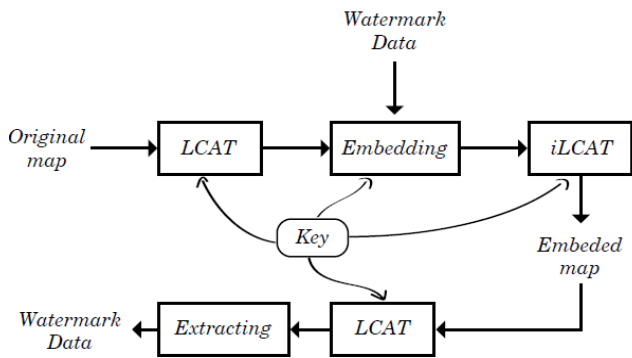


Fig. 6. The Flow Chart of the Linear Cellular Automata Transform Algorithm.

The key concept is that  $v_{x1}'$ , the coordinate of the host map, is transformed using LCAT, after which the encrypted watermark bit is inserted into the cover work. Equation (5) describes the watermark insertion technique associated with the proposed scheme.

$$v_{x1}'' = v_{x1}' + \alpha W \quad (5)$$

where  $W$  denotes the watermark bit and  $\alpha$  represents the embedding parameter. A noteworthy feature of equation (5) is that a directly proportional relationship exists between the size of  $\alpha$  and the extent of the modifications that will take place to the vector map file. However, the fact should not be overlooked that larger  $\alpha$  values are associated with higher watermark resistance. In the proposed scheme, a 3-bit  $\alpha$  value is employed, which confers satisfactory resistance and, moreover, vector map alterations that are within acceptable limits. A flow chart for LCAT is given below.

The inverse formulation of LCAT is stated in equation (6).

$$iT(M) = \sum_{n=0}^{N-1} M_n^{-1} \cdot v_{x1}'' \pmod{2} \quad (6)$$

where  $iT(M)$  represents the value of the host map's inversion domain transformation and  $v_{x1}''$  denotes the host map's transform digital media value.

#### IV. OUR CONTRIBUTION

The proposed digital watermarking architecture is robust and appropriate for copyright protection, when a public key is used to Encrypt (three parts, namely a vector map, the size of LCA transition matrix ( $Mn$ ) and a watermark that scrambles the elements) and when a private key is used to decrypt. The proposed scheme relies on the linear cellular automata transform (LCAT) algorithm, and it operates in the frequency domain. Additionally, the proposed scheme does not depend on a previous knowledge of the cover work. This scheme is resistant to all Vertex insertion attacks, including Vertex deletion (50%) and Vertex modification (50%), and it does not fall under geometric attacks, namely, translation, scaling, and rotation

##### A. Proposed Architecture

As shown in Fig. 7, the architecture of the proposed digital watermarking system is separated into the following three

modules: firstly, the vector map base and watermark set comprise the containing information system; secondly, the user interface is an online interface, meaning that users can straightforwardly interact with the spatial database, download existing vector maps, and consult existing vector maps; and thirdly, the watermarking system itself, which constitutes the critical component of the system, and which contains both the embedding unit and extraction unit. It should be noted that the watermarking system in this architecture contains another unit, namely, the evaluation unit, the purpose of which is to verify the watermarking process and evaluate system quality. This is achieved by following up on the output of the watermarking stage. The database owner controls the evaluation unit. For the remainder of this paper, the discussion centres around the third module of the system architecture.

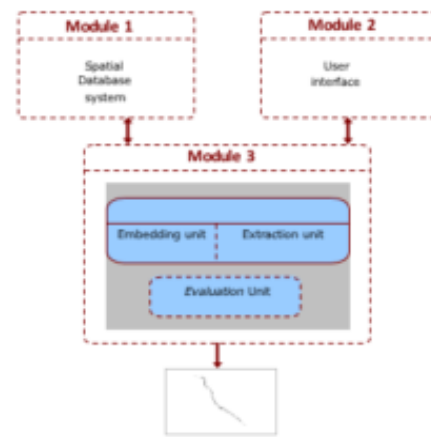


Fig. 7. Proposed Architecture.

#### V. WATERMARKING TECHNIQUE

##### A. Embedding Scheme

The embedding unit of the proposed scheme involves the insertion of the watermark into the details (maps). Noteworthy, one of the fundamental strengths of LCAT is the way in which it guarantees the invisibility of the payload. Additionally, given that minor changes in low frequency do not register on the human visual system, the scheme embeds the digital watermark in the low frequency zones of the decomposed map. Keys were employed for the embedding and recovery phases to increase the degree to which the scheme was robust.

Fig. 8 provides an overview of the process used to embed the payload into the cover work. The steps involved in each stage of the embedding unit's algorithm are the following:

- 1) To serve as  $M$ 's vector map, choose a pair of reference vertices  $v_{f1}$  and  $v_{f2}$ , where  $1 \leq v_{f1}, v_{f2} \leq n$ . This promotes the security of the embedding process.
- 2) Calculate the number of vertices in  $M$ , the map file, where the length ( $N$ ) is subsequently changed into a domain frequency without the references.

- 3) Transform the coordinates collected from the vertex point using LCAT.
- 4) Employ the approach described in [23] for the purpose of encrypting the factors of  $W^*$ , and derive the data sequence  $W^* = \{w_i^* \mid w_i^* \in \{0, 1\}, i = 0, 1, \dots, l-1\}$ .
- 5) Posit a double floating-point number as a 16-digit coordinate value in a decimal fraction format, and then insert  $W^*$  into the final two digits. The final two digits are chosen due to the fact that these have an extremely limited impact on the scheme's precision.

It is worth noting that the inserted value does not match  $w_i^*$ , and it falls in the 0-99 range. Thus, supposing that  $D$  is the integer created by the final digits, it is possible to state the following:

$$W^* = \begin{cases} \text{if } w_i^* \text{ is } 0 \text{ then } D \leq 50 \text{ and saved at the positions;} \\ w_i^* = 1, \text{ otherwise} \end{cases} \quad (7)$$

- 6) Once the watermark has been embedded in the cover work, the inverse formulation of LCAT (iLCAT) is used to restore the frequency domain vector map to its original shape file.
- 7) Repeat the fifth and sixth stages of the algorithm  $K$  times under high-capacity situations and blind watermarking, and use CAT to extract the watermark.

### B. Detecting Scheme

The procedure followed to embed and extract the digital watermark are comparable, but one is the reverse of the other. The three stages of the extraction procedure are the embedding procedure's results, which are the following: firstly,  $v_{f1}$  and  $v_{f2}$  (i.e., the reference vertices); secondly,  $M_n$  (i.e., the fixed-size LCA transition matrix); and finally, the watermarked vector map (see Fig. 9). A detailed overview of the seven steps involved in the extraction procedure is given below.

- 1) Under the control of the private key, select the reference vertices  $v_{f1}$  and  $v_{f2}$ , where  $1 \leq v_{f1}, v_{f2} \leq n$ , which apply to  $M$ 's vector map.
- 2) Calculate the number of vertices in  $M$  and the length ( $N$ ) that will subsequently undergo transformation to produce a domain frequency without the reference vertices.
- 3) Having collected every feature's set of coordinates, transform into a LCAT transform.
- 4) Use equation (8) to extract the embedded watermark location, as well as the watermark bits.

$$W^* = \begin{cases} \text{if } D \leq 50 \text{ then } w_i^* \text{ is } 0 \\ w_i^* = 1, \text{ otherwise} \end{cases} \quad (8)$$

- 5) If necessary, apply the third and fourth steps again.
- 6) Undertake the extraction of the originally embedded watermark  $W$  using the private key, which can be achieved by inverting the watermark pattern.
- 7) Rebuild the watermark pattern to obtain the watermark.

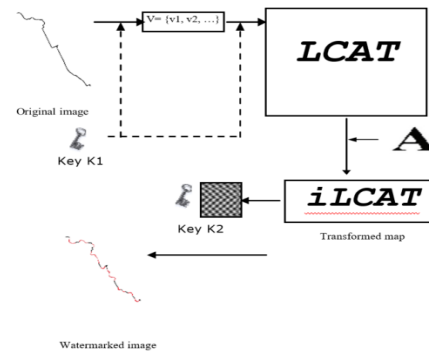


Fig. 8. Embedding Scheme.

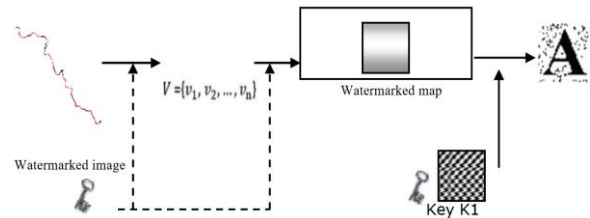


Fig. 9. Detecting Scheme.

### C. Evaluation Scheme

The purpose of the evaluation unit is to assess the digital watermarking procedure's quality based on specific indicators. These indicators are listed below, and the purpose of Section VI of this study is to provide an account of the proposed scheme's performance in relation to each indicator (see Fig. 10).

- 1) Fidelity: Map quality following watermark insertion into the cover work.
- 2) Robustness: The degree to which the watermarked map is likely to fall under common attacks.
- 3) Capacity: Watermark coverage.
- 4) Complexity: The procedure's computational complexity.
- 5) Security: The degree to which the watermarked zones within the map are secure.
- 6) Reversibility: An indication of whether a reversibility technique exists that can restore the initial cover work following the extraction of the watermark data.

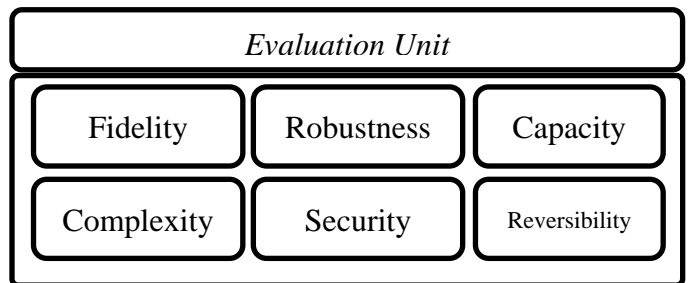


Fig. 10. The Proposed Evaluation Module Watermarked Vector Map Scheme.

## VI. RESULTS

The researchers' personal computer was used to conduct the performance evaluation, for which the specifications were as follows: CPU 2.3 GHz, 16GB RAM, Windows 10 Professional, QGIS Version 3.0, Python, and MATLAB. For the data concealing operations, the secret bits associated with every transform coordinate conveyed  $\alpha$  in *LSB*,  $Mn$  with a matrix size of 30, and  $T = 1$ , which indicates iterative embedding. To create the tests, the initial cover work was modified through watermark insertion, and then a range of attacks were levelled against the watermarked vector map (see Fig.11). Following this, the RSME between the watermarked and original maps was computed; the NC between the extracted mark and the original mark was conducted; and finally, the mark was extracted to gauge the level of resistance against attacks.

As indicated in Table I, the proposed scheme was characterised by a high level of resistance against all of the common attacks. In particular, these attacks included Vertex insertion, Vertex deletion (50%), Vertex modification (50%), and the same geometric attacks (namely, rotation, scaling, and translation).

It is worth noting that the proposed scheme was implemented to vector maps. Furthermore, in this case, the map employed represents the Riyadh Development Authority. Additionally, to serve as the watermark, an image was utilised (see Fig. 12). Most importantly, the results of the performance evaluation for the proposed scheme were satisfactory, as shown in Fig. 13 and 14. In particular, Fig. 13 shows that the differences in distance values between the original vector map and the watermarked vector map were not substantial, while Fig. 14 provides an illustration of a well-extracted digital watermark.

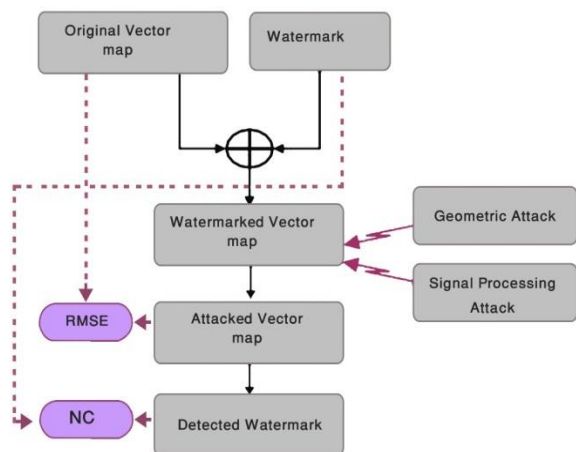


Fig. 11. Test Process.



Fig. 12. Example of Watermark.

Further to the results presented in Fig.13, it is clear that the distance values for the vector maps were lower than 0.1 mm, which is critical because this is indicative of the reversibility of the procedure. In other words, the procedure can be considered reversible and, moreover, as having the ability to meet the precision needs of most applications, under a situation where the disparities between the coordinates of the watermarked and original coordinates are not substantial. To improve watermarked vector map's quality, it is necessary to lower distortion by elevating the map's permissible precision tolerance. This is because it lowers the overall number of insertion units, thus lowering the watermark bits' capacity.

The purpose of the evaluation unit was to assess the watermarking system's quality based on the evaluation criteria specified in Section V. D. These evaluation criteria are as follows: namely, fidelity, robustness, capacity, complexity, security, and reversibility. The results of the analysis of each of these evaluation criteria are given in Table II.

TABLE I. RESULTS OF RESISTANCE FACING DIFFERENT ATTACK

| Deformations                 | RMSE between watermarked map and original one (dB) | NC between extracted mark and original one (dB) |
|------------------------------|--|---|
| Vertex insertion (50%)       | 0.79   | 0.76  |
| Vertex deletion ((50%)       | 0.80   | 0.76  |
| Vertex modification (50%)    | 0.82   | 0.78  |
| Rotation ( $\rho=60^\circ$ ) | 0.94   | 0.92  |
| Scaling ( $\zeta = 0.5$ )    | 0.90   | 0.89  |
| Translation (4.2 , 5.6)      | 0.91   | 0.90  |

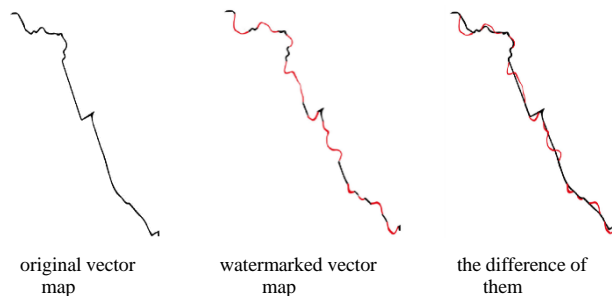


Fig. 13. Watermark Imperceptivity Proof.

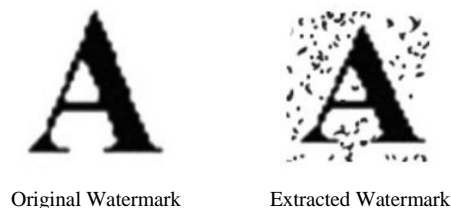


Fig. 14. Well Extracted Watermark.

TABLE. II. PARAMETERS ANALYSIS OF LCAT

| Parameters Analysis      |      |
|--------------------------|------|
| Evaluation Metrics       | LCAT |
| Invisibility             | High |
| Capacity                 | High |
| Reversibly               | High |
| Computational Complexity | Low  |
| Security                 | High |
| Geometrical Attacks      | 83%  |

## VII. CONCLUSION

This study proposed a technique for 2D vector map watermarking using the linear cellular automata transform (LCAT) algorithm. The algorithm is an example of a blind marking algorithm, and it represents a significant contribution in terms of its possible applications in areas such as copyright protection and digital content authentication. Although the performance evaluation yielded positive results, particularly in terms of robustness against attacks, it is important to recognise that the increasingly sophisticated nature of adversaries means that the proposed scheme may not resist every type of attack. That is to say, while the proposed scheme is the product of years of research and expertise in the field of digital watermarking, attackers themselves, as well as the toolkits they have access to, are progressing at the same time. Thus, the authors foresee that the proposed scheme will hold benefits for applications in copyright protection and authentication, but further research should be conducted to devise new methods, and to identify the robustness of the proposed scheme under a broader range of novel and sophisticated attacks.

## REFERENCES

- [1] Abbas TA, Jawad MJ (2013) Digital vector map watermarking: applications, techniques and attacks Oriental. J Comput Sci Technol 6(3):333–339
- [2] Abubahia, A & Cocca, M 2017, 'Advancements in GIS map copyright protection schemes - a critical review', Multimedia Tools and Applications, vol. 76, no. 10, pp. 12205–12231. <https://doi.org/10.1007/s11042-016-3441-z>.
- [3] Abbas T, Jawad M, Sudirman S (2013) Robust watermarking of digital vector maps for copyright protection. In: 14th annual postgraduate symposium on the convergence of telecommunications, networking and broadcasting. 978-1-902560-27-4. Liverpool.
- [4] R. Shiba, S. Kang and Y. Aoki: An image watermarking technique using cellular automata transform. In TENCON 2004 IEEE Region 10 Conference (2004), pp. 303–306.
- [5] Adwan, A. A. Awwad et al., A novel watermarking scheme based on two dimensional cellular automata, Proc. of the 2011 International Conference on Computers and Computing, pp.88-94, 2011
- [6] Blind audio watermarking technique based on two dimensional cellular automata.
- [7] AL-ardhi S , Thayananthan V, Basuhail A (2020) Copyright Protection and Content Authentication Based on Linear Cellular Automata Watermarking for 2D Vector Maps. In: Arai K., Kapoor S. (eds) Advances in Computer Vision. CVC 2019. Advances in Intelligent Systems and Computing, vol 943. Springer, Cham.
- [8] Lafaye J, B'eguec J, Gross-Amblard D, Ruas A (2007) Geographical database watermarking by polygon elongation. Tech. rep., HAL.
- [9] N, Zhang H, Men C (2014) A high capacity reversible data hiding method for 2D vector maps based on virtual coordinates. Comput Aided Des 47:108–117.
- [10] Schyndel, R.G., Tirkel, A.Z., Osborne, C.F.: A Digital Watermark. In: ICIP 1994. Proceedings of IEEE International Conference on Image Processing, Austin, USA, vol. 2, pp. 86–90. IEEE, Los Alamitos (1994).
- [11] Min LQ, Zhu XZ, Li Q (2012) A robust blind watermarking of vector map. In: Zhang T (ed) Instrumentation, measurement, circuits and systems, advances in intelligent and soft computing, vol 127. Springer, Berlin, pp 51–59.
- [12] Wang X, Huang D, Zhang Z (2012) A robust zero-watermarking algorithm for vector digital maps based on statistical characteristics. J Softw 7(10):2349–2356.
- [13] Xun W, Hai L, Hujun B (2004) A robust watermarking algorithm for vector digital mapping. J Comput Aided Des Comput Graph 1377–1381.
- [14] Niu XM, Shao CY, Wang XT (2007) Gis watermarking: hiding data in 2d vector maps. In: Pan JS, Huang HC, Jain L, Fang WC (eds) Intelligent multimedia data hiding, studies in computational intelligence, vol 58. Springer, Berlin, pp 123–155.
- [15] Wang N, Men C (2012) Reversible fragile watermarking for 2-d vector map authentication with occlusion. Comput Aided Des 44(4):320–330.
- [16] Wang N, Men C (2013) Reversible fragile watermarking for locating tampered blocks in 2d vector maps. Multimedia Tools Appl 67(3):709–739.
- [17] Mouhamed M, Rashad AM, ella Hassanien A (2012) Blind 2d vector data watermarking approach using random table and polar coordinates. In: 2nd international conference on uncertainty reasoning and knowledge engineering, pp 67–70.
- [18] Li A, Lin BX, Chen Y, Lu G (2008) Study on copyright authentication of gis vector data based on zero-watermarking. Int Arch Photogramm Remote Sens Spat Inf Sci 37:1783–178.
- [19] Cao L, Men C, Li X (2010) Iterative embedding-based reversible watermarking for 2d-vector maps. In: 17th IEEE international conference on image processing, pp 3685–3688.
- [20] B Liang, J Rong, C Wang. A Vector Maps Watermarking Algorithm Based On DCT Domain. ISPRS Congr. 2010; XXXVIII(3).
- [21] Ling Y, Lin CF, Zhang ZY (2012) A zero-watermarking algorithm for digital map based on dwt domain. In: He X, Hua E, Lin Y, Liu X (eds) Computer, informatics, cybernetics and applications, LNEE, vol 107. Springer, Netherlands, pp 513–521.
- [22] Neyman SN, Pradnyana INP, Sitohang B (2014) A new copyright protection for vector map using fft based watermarking. TELKOMNIKA Telecommunication, Computing, Electron Control 12(2):367– 37.
- [23] Marti and G. Rodri: Reversibility of linear cellular automata. Applied Mathematics and Computation 217 (21) (2011), 8360–8366
- [24] S. Wolfram, Theory and Applications of Cellular Automata, World Scientific Publishing Company, Singapore, 1986.
- [25] S. Wolfram, Cryptography with Cellular Automata, Springer- Verlag, Beilin, 1986.

# Electromyography Signal Acquisition and Analysis System for Finger Movement Classification

Alvarado-Díaz Witman<sup>1</sup>, Meneses-Claudio Brian<sup>2</sup>, Roman-Gonzalez Avid<sup>3</sup>

Image Processing Research Laboratory (INTI-Lab)  
Universidad de Ciencias y Humanidades Lima, Peru

**Abstract**—Electromyography (EMG) is very important to capture muscle activity. Although many jobs establish data acquisition system, however, it is also essential to demonstrate that these data are reliable. In this sense, one proposes a design and implementation of a data acquisition system with the Myoware device and the ATmega329P microcontroller. One also proved its reliability by classifying the movement of the fingers of the hand, with the help of the algorithm k-Nearest Neighbors (KNN) and the application of Classification Learner code of Matlab. The results show a success rate of 99.1%.

**Keywords**—EMG; muscles; disability; classification learner; Myoware

## I. INTRODUCTION

In the national report of the socio-demographic profile<sup>1</sup>, carried out by the Statistics and Informatics National Institute (INEI for its Spanish name), it mentions that in Peru 10.4% of the population suffers from some disability. From this population, 15.1% cannot move or walk. Under this problem, it is necessary to facilitate the taking of samples of the signals that occur during the movement, to build robotic systems that perform the actions that disabled people require.

Wyoware [1] was used to obtain data, which is an electro-diagnostic system to evaluate and record the electrical activity produced by the skeletal muscles. These sensors are used in prostheses, robotics, and much more. The Wyoware detects the electrical activity of the muscles, then convert them into a variable voltage that can be read on the analog input pin of any microcontroller, in our case the ATmega328P microcontroller.

The Wyoware device is an individual device which reduces the ability to pick up signals from different parts at the same time. This reason is why a basic system of securing 4 Wyoware is created, which will represent four channels of data acquisition. A sampling algorithm is also developed in Python, and another one for signal processing in Matlab focused on people partially amputated from the upper limbs.

In [2] an eight-channel, low-cost hardware system is developed focused on the acquisition of EMG data which validates using it for the classification of the signals, obtaining an 80% effectiveness.

In [3] an EMG data transmission system is developed wirelessly through FM antennas (modulated frequency), they have a two-channel system, one of which acquires EMG data and the other captures the data of the signals produced by the

carotid, in order to help regulate the proper flow of blood to the brain in war pilots.

In [4] a shield for Arduino one is developed, to acquire data of ECG, EMG, and EOG, which can be used together, which allows obtaining different types of signals.

In [5], a system is developed to read data from an Arduino board from Python, which allows extracting the characteristic curves of the signals.

In [6] they create a 5-channel system based on operational amplifiers, a signal acquisition system is proposed, from which nine characteristics have been extracted in the time domain and 7 in the frequency domain; which are classified with different algorithms achieving a precision that goes from 57.69% to 99.92%.

In [7] there is a summary of other works related to prostheses and EMG, advances in upper limb prosthesis technology, Adam's Hand electronics are described, a transradial myoelectric prosthesis does not say that the mechanism can act 15 degrees of freedom with a single motor. A bracelet with sensors and an Arduino system are used to obtain myoelectric signals.

In [8] a wireless four-channel EMG acquisition system with high precision, low latency is designed, they mention us that the sEMG (superficial electromyogram) characterizes the functional state of the human nerves and muscles to a certain degree; they allow to predict the force, to recognize the movements, as well as to diagnose muscular disorders.

Section II presents the methodology that has been followed for the research work. In Section III, one finds the preliminary results obtained. Finally, in Section IV, one presents the discussions and conclusions for this research work.

## II. METHODOLOGY

For the present work, the methodology to follow is outlined in the block diagram shown in Fig. 1.

### A. Wyoware

The Wyoware is a system that detects the electrical activity of the muscles, but it is complicated when it is positioned around the arm, therefore a fastening system was built; for this purpose, a 3D base was designed, in which the electrodes could be placed as you can see in Fig. 2. The slots have been placed on the sides in the edge which a strap will pass, so it could ensure that the electrodes are kept in a fixed position.

<sup>1</sup> INEI, "Perfil Sociodemográfico, Informe Nacional," 2017. [Online]. Available: [http://censo2017.inei.gob.pe/publicaciones\\_especiales/](http://censo2017.inei.gob.pe/publicaciones_especiales/). [Accessed: 27-May-2019].

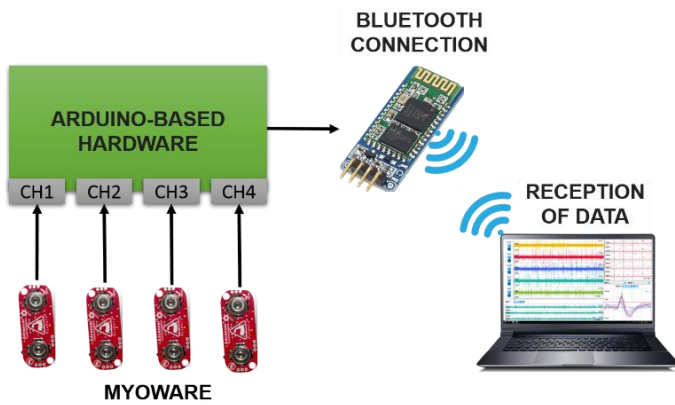


Fig. 1. Work Scheme

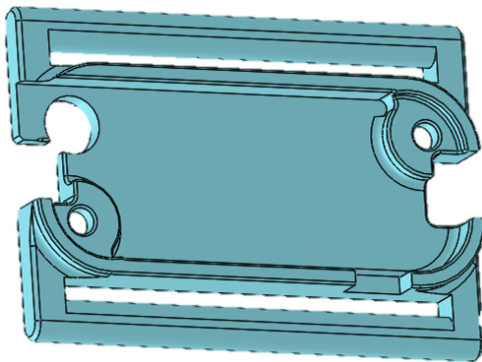


Fig. 2. Myoware Support.

This design, besides being able to be used on the arms, can be used on the legs, and other parts of the body where you want to study the signals of the muscles which represents an extra feature of the design.

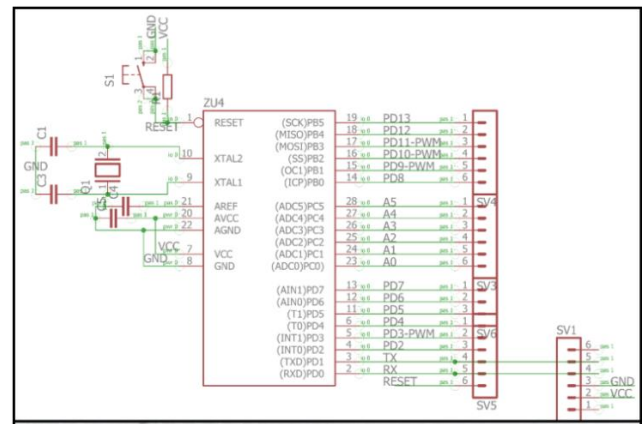
The Myoware has three main connections, of which 2 correspond to the power supply of the system with 5 volts and the last one is where the signals are sent in analog form, which can be acquired by microcontrollers.

### B. Hardware Design and Implementation

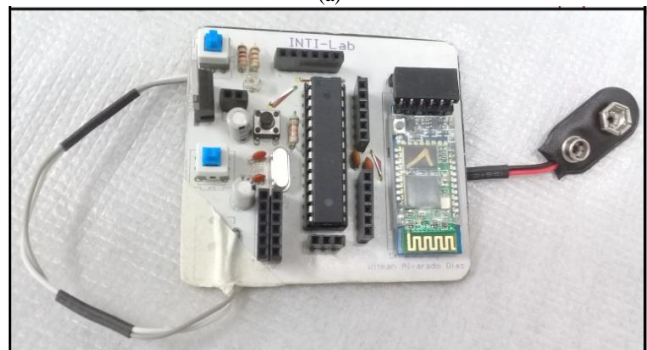
It is necessary to design an electronic system which allows us to capture the signals sent by the Myoware, based on the ATmega328P microcontroller, which is chosen by the ease with which it can be programmed based on Arduino one for recording in the microcontroller, the same bootloader that uses Arduino one, with this, the microcontroller can be programmed with greater ease.

In Fig. 3(a), the reader can see the basic connection diagram for the operation of the ATmega328P microcontroller, to this design, it added a power supply which provides continuous 5v to all the electronic devices; in the lower right part of Fig. 3, you can see the connection for the Bluetooth module HC-05. In Fig. 3(b), you can see the electronic system already finished, which has all the necessary connections for the operation of the system.

Additionally, in order to hold the electronic board created, a support was designed and printed in 3D, which you can see in Fig. 4.



(a)



(b)

Fig. 3. (a) Connection Scheme. (b) Electronic Board Completed.

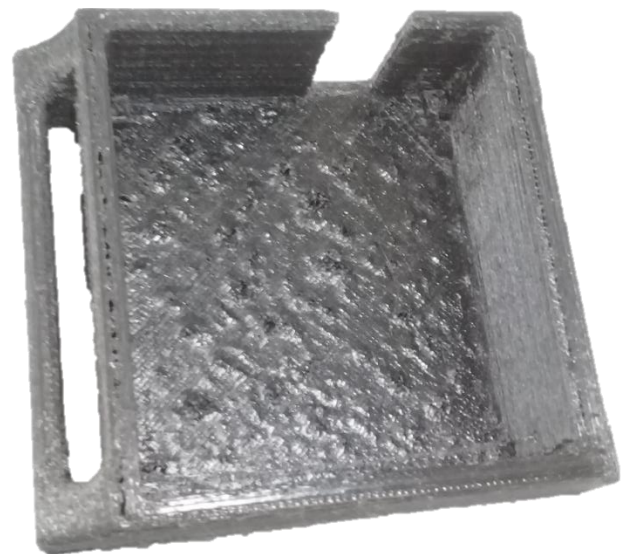


Fig. 4. Support for the Electronic Board.



Fig. 5. Bluetooth Adapter.

### C. Bluetooth Communication

The Bluetooth connection as mentioned above is done through the HC-05 module and a Bluetooth adapter for the PC as USB type (Fig. 5), which is linked and connected to the HC-05 by a serial port in our case "COM4".

Once the data transmission devices are linked, the transmission of data corresponding to the readings of the Myoware starts; to verify that there is communication, you can use the PuTTY tool which opens the corresponding port in serial mode, and shows us the receiving data, you can see that the communication is correct; in order to save the data to be processed later, a data reception system is developed.

### D. Data Reception System

The data reception system is divided into three: Arduino, Python and Matlab:

1) *Arduino*: Arduino<sup>2</sup> is an open source electronic platform based on easy-to-use hardware and software. They have the ability to read analog and digital inputs. It can control the card what to do by sending a set of codes based on the programming language "Wiring" through a user interface based on "Processing".

This project is based on the Arduino one, which has 6 analog signal inputs, of which it uses 4 to read the data sent by the Myoware, the scheme of the implemented code can be seen in Fig. 6; in which you can see the Bluetooth connection, which is done through the serial port on pins 2 and 3 of the ATmega328P microcontroller which correspond to the reception and transmission of data respectively.

It sets a data transmission speed to 38400 baud which allows us to have an approximate sampling frequency of 333 Hz.

The sending of data and reading of the analog pins is done by means of the command "Serial.print (analogRead (A1))"; the data is sent by comma separating the values of each data channel, which are received in the same way by Python.

2) *Python*: Python<sup>3</sup> is a programming language oriented to object, interpreted and interactive; combines remarkable efficiency with clear syntax. It has different modules, classes, exceptions, dynamic high-level data and dynamic writing.

In our case, it used Python as an extension language for Matlab, creating a layer code to provide Matlab with an easy way the data corresponding to the muscle signals obtained by the Myoware.

The code used in Python is graphed in Fig. 7; in the code the user enters the amount of data to be obtained in our case 3996 corresponding to approximately 12 seconds of sample at a frequency of 333Hz. You must verify in which serial port the bluetooth connection was made and configure the port in Python to be able to read data.

The data is saved in .txt format. A file is created and opened in which the received data is written line by line until the required amount of data is completed, after the file is saved;

This process must be repeated according to the number of samples required.

3) *Matlab*: Matlab<sup>4</sup> is a software that combines a desktop environment for iterative analysis and design processes with a programming language that expresses matrix mathematics.

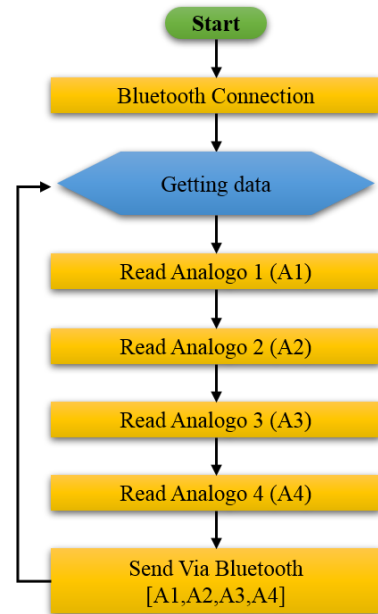


Fig. 6. Diagram of the Programming in the ATmega328p Microcontroller.

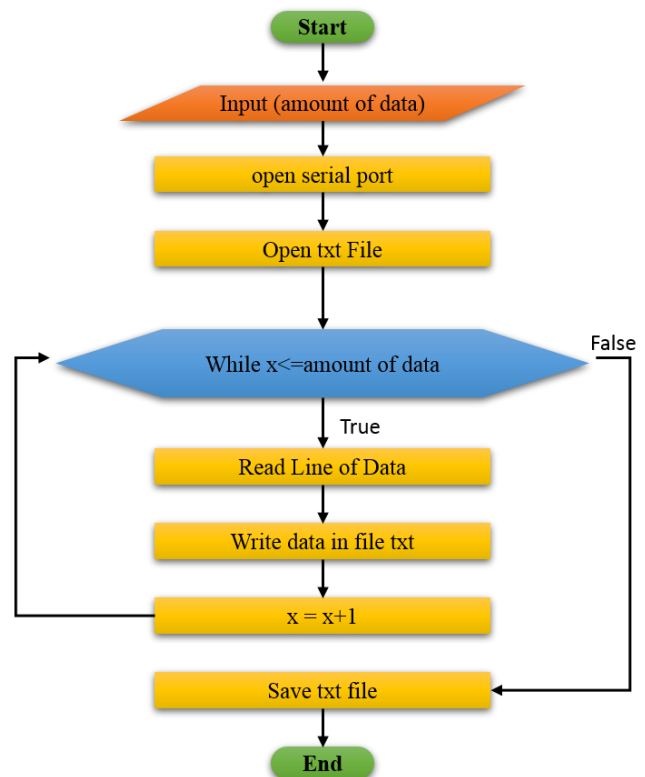


Fig. 7. Diagram of Programming in Python.

<sup>2</sup> Arduino, "Arduino." [Online]. Available: <https://www.arduino.cc/en/Guide/Introduction#>.

<sup>3</sup> Python, "The Python Wiki." [Online]. Available: <https://wiki.python.org/moin/FrontPage>.

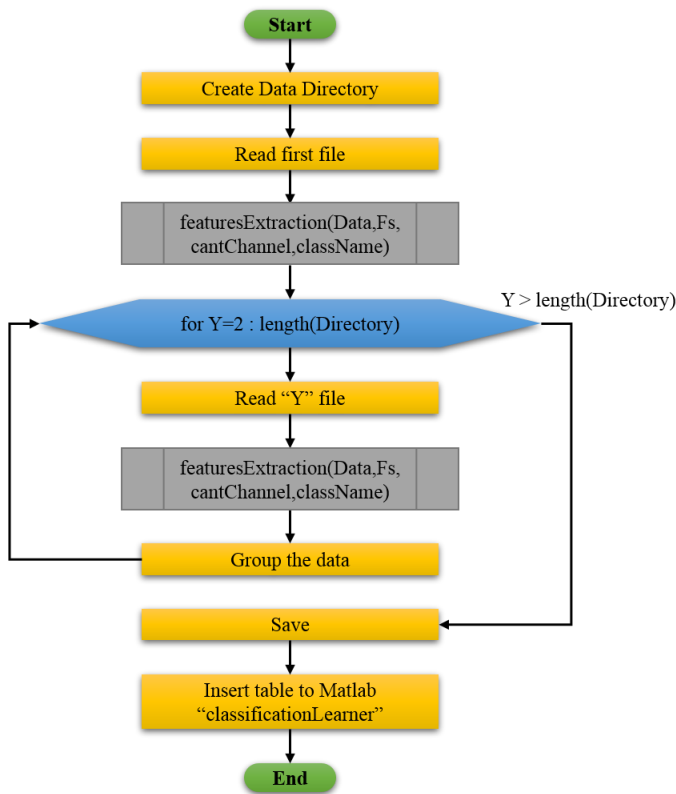


Fig. 8. Main Diagram of the Programming in Matlab.

It use Matlab to process and classify the data obtained using its Classification Learner application, it must extract the characteristics of the signals, for which we apply the algorithm of Fig. 8; which creates a directory with all the files generated by Python, reads the first file and extracts its characteristics, then enters a loop, which reads each of the available files, and then extracts the characteristics of the data, finally groups and save the results, which will be used for classification in the Classification Learner application, where you must manually enter the data table and choose the algorithm to classify.

There is a function (featuresExtraction) that extracts the characteristics, which has input parameters that are:

- Data: It is the data matrix read from the text files in our case is a matrix of 4x3996 data.
- Fs: It is the sampling frequency in our case 333Hz.
- cantChannel: It is the amount of data channels; our system is working with 4 data channels.
- className: Is the name of the class to which the data belongs, we will have 5 classes that correspond to the names of the fingers of the hand little finger, ring finger, middle finger, index finger and thumb in our case.

The mentioned parameters enter a function whose work diagram can be seen in Fig. 9.

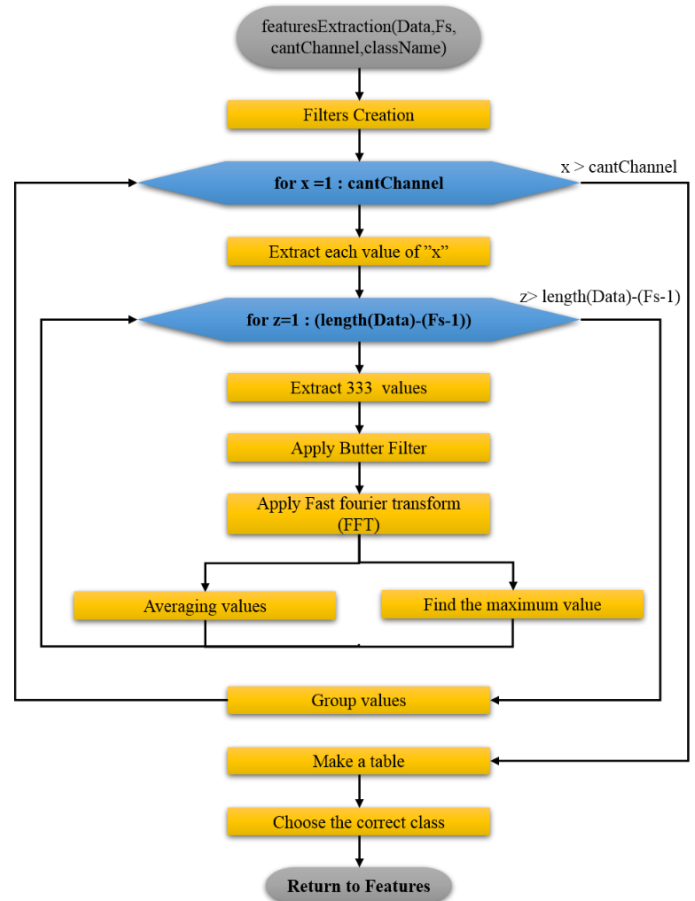


Fig. 9. Diagram of the Programming of the Features Extraction Function.

Taking into account that work will be carried out with amplitude signals between 0 to 10 mV and a frequency of 10 to 100Hz [2], [8], [9] and [10], the necessary filters are created for this purpose. Subsequently, each data channel is extracted, to then apply the filters and find the fast Fourier transform at intervals of 333 values which correspond to the sampling frequency, the intervals where it is applied are from the first data to the data 333, from the second data to 334, from third to 335, and so on, up to the full length of the data; then averaged and found the maximum value, thus obtaining the characteristics we need to classify, finally the values are grouped and converted to a data table by adding the class which they belong. With these operations, two feature vectors are generated for each channel.

### III. RESULTS

The implementation of the system can be seen in Fig. 10(a), in which you can see all the connections made for its operation. In Fig. 10(b), the reader can see the placement of the system in the forearm from where it could obtain signals corresponding to the movement of the fingers of the hand.

In order to demonstrate the functioning of the system, samples of the movement of the fingers of the hand were taken, placing our development in the muscles of the forearm as in Fig. 10(b); samples are taken with an amount of data equivalent to 12 seconds with a sampling frequency of 333Hz;

<sup>4</sup> "Matlab." [Online]. Available: <https://es.mathworks.com/products/matlab.html>.



sampling is done as follows: the first 3 seconds no movement is made after that, 6 seconds of movement in a finger is done applying force, finally the last 3 seconds no movement is made; It should be mentioned that samples are taken from a healthy person with a soft ball in the hand where the test is performed. A total of 71 samples are taken, which are processed according to the aforementioned algorithms and then classified.

In Fig. 11(a), the reader can see the signals obtained, following the aforementioned procedure. The thumb is corresponding to channels 1, 2, 3 and 4; in Fig. 11(b), the reader can observe the characteristics of the first channel; this type of signals is obtained for each data channel, which correspond to the peaks and averages respectively; in these signals, you can see that there are clear differences between one and the other, which will improve the efficiency of the classifier.

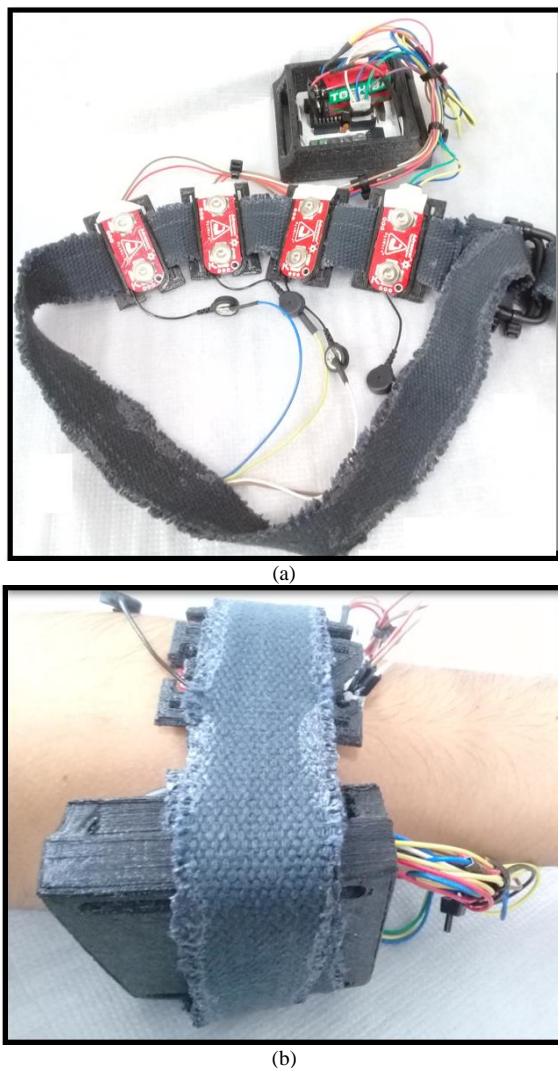


Fig. 10. (a) System Implemented.(b) Placement of the System in the Forearm.

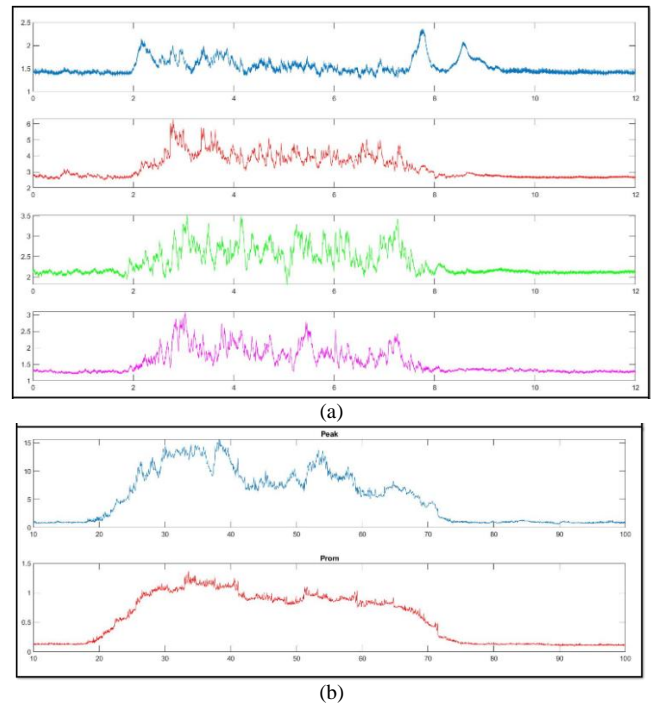


Fig. 11. (a) Raw Signals in Each Data Channel. (b) Signals of the Characteristics of the Channel 1 Data.

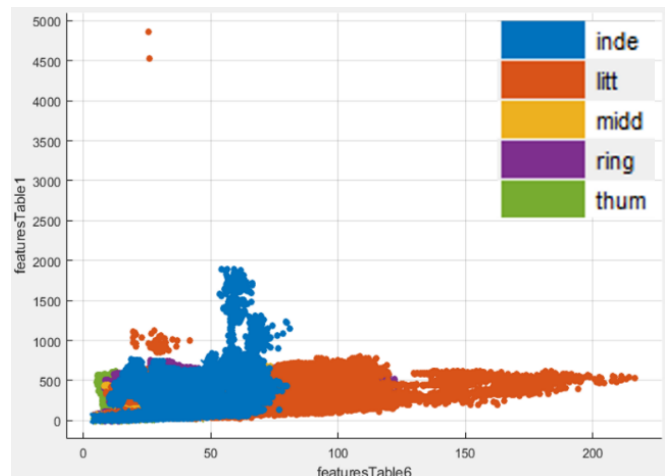


Fig. 12. Characteristics Plotted in the Classification Learner Application.

The characteristics obtained were introduced in the Classification Learner application, which can be seen in Fig. 12, which shows the graph of the characteristics of the 5 categories entered.

After entering the characteristics, the data classification algorithm is chosen, in our case, it chooses k-Nearest Neighbors (KNN) which generates a certain rate of 99.1% and also generates a confusion matrix, which the reader can see in the Fig. 13, which the performance of the chosen algorithm is evaluated.

| True class | Predicted class |       |       |       |       |
|------------|-----------------|-------|-------|-------|-------|
|            | inde            | litt  | midd  | ring  | thum  |
| inde       | 54213           | 28    | 346   | 55    | 318   |
| litt       | 24              | 51143 | 39    | 54    | 36    |
| midd       | 329             | 18    | 50686 | 81    | 182   |
| ring       | 57              | 54    | 78    | 54719 | 52    |
| thum       | 355             | 49    | 145   | 46    | 47037 |

Fig. 13. Confusion Matrix Generated by the Classification Learner Application.

#### IV. DISCUSSION

In the research work [2], it used 8 data channels and got an efficiency of 80%. In the research work [6], it used 5 data channels, and a variable efficiency was obtained between 57.69% and 99.92%. In [11], the average efficiency of 54% was achieved by testing multiple configurations of samples and data processing. In [12] the error rate is 7% by classifying 14 kinds of finger signals. In [13] an average efficiency of 70% was obtained, making the classification of 52 classes of movements with different classification algorithms. In [14], the effectiveness of 60% was obtained for the creation of a database, testing different classifiers.

#### V. CONCLUSIONS

In conclusion, the classification of EMG signals has been achieved. On this work, with 4 data channels have reached a percentage of correct answers of 99.1%, which shows that our system is reliable and optimal for obtaining EMG signal data in future jobs.

#### REFERENCES

- [1] K. Hartman, "Getting Started with MyoWare Muscle Sensor," 2018.
- [2] S. Pancholi and R. Agarwal, "Development of low cost EMG data acquisition system for arm activities recognition," 2016 Int. Conf. Adv. Comput. Commun. Informatics, ICACCI 2016, pp. 2465–2469, 2016.
- [3] D. Bansal, M. Khan, and A. K. Salhan, "Wireless transmission of EMG signal and analysis of its correlation with simultaneously acquired carotid pulse wave using dual channel system," 2nd Int. Conf. eHealth, Telemedicine, Soc. Med. eTELEMED 2010, Incl. MLMB 2010; BUSMMed 2010, pp. 125–129, 2010.
- [4] K. K. M. Rahman, M. M. Subashini, M. Nasor, and A. Tawfik, "Development of bio-shields for Arduino Uno," 2018 Adv. Sci. Eng. Technol. Int. Conf. ASET 2018, pp. 1–5, 2018.
- [5] E. Machado, "Sistema de adquisición de datos con Python y Arduino," ISSN 2448-623X Sist., no. October 2017, 2018.
- [6] S. Pancholi and A. M. Joshi, "Portable EMG Data Acquisition Module for Upper Limb Prosthesis Application," IEEE Sens. J., vol. 18, no. 8, pp. 3436–3443, 2018.
- [7] F. Gaetani, G. A. Zappatore, P. Visconti, and P. Primiceri, "Design of an Arduino-based platform interfaced by Bluetooth low energy with Myo armband for controlling an under-actuated transradial prosthesis," ICICDT 2018 - Int. Conf. IC Des. Technol. Proc., pp. 185–188, 2018.
- [8] R. Zhou, Q. Luo, X. Feng, and C. Li, "Design of a wireless multi-channel surface EMG signal acquisition system," 2017 3rd IEEE Int. Conf. Comput. Commun. ICC 2017, vol. 2018-Janua, pp. 279–283, 2018.
- [9] M. Tariquzzaman, F. Khanam, M. H. A. Sohag, and M. Ahmad, "Design and implementation of a low cost multichannel rectified EMG acquisition system," 19th Int. Conf. Comput. Inf. Technol. ICCIT 2016, pp. 261–265, 2017.
- [10] H. Ghapanchizadeh, S. A. Ahmad, and A. J. Ishak, "Developing multichannel surface EMG acquisition system by using instrument opamp INA2141," pp. 258–263, 2014.
- [11] S. Pizzolato, L. Tagliapietra, M. Cognolato, M. Reggiani, H. Müller, and M. Atzori, "Comparison of six electromyography acquisition setups on hand movement classification tasks," PLoS One, vol. 12, no. 10, pp. 1–17, 2017.
- [12] R. N. Khushaba, S. Kodagoda, D. Liu, and G. Dissanayake, "Muscle computer interfaces for driver distraction reduction," Comput. Methods Programs Biomed., vol. 110, no. 2, pp. 137–149, 2013.
- [13] M. Atzori et al., "A Benchmark Database for Myoelectric Movement Classification," Trans. Neural Syst. Rehabil. Eng., 2013.
- [14] A. Gijssberts, M. Atzori, C. Castellini, H. Müller, and B. Caputo, "Movement error rate for evaluation of machine learning methods for sEMG-based hand movement classification," IEEE Trans. Neural Syst. Rehabil. Eng., vol. 22, no. 4, pp. 735–744, 2014.

# Blood Vessels Segmentation in Retinal Fundus Image using Hybrid Method of Frangi Filter, Otsu Thresholding and Morphology

Wiharto<sup>1</sup>, YS. Palgunadi<sup>2</sup>

Department of Informatics, Universitas Sebelas Maret  
Jl. Ir. Sutami, No. 36A, Surakarta Indonesia

**Abstract**—Diagnosis of computer-based retinopathic hypertension is done by analyzing of retinal images. The analysis is carried out through various stages, one of which is blood vessel segmentation in retinal images. Vascular segmentation of the retina is a complex problem. This is caused by non-uniform lighting, contrast variations and the presence of abnormalities due to disease. This makes segmentation not successful if it only relies on one method. The aims of this study to segment blood vessels in retinal images. The method used is divided into three stages, namely preprocessing, segmentation and testing. The first stage, preprocessing, is to improve image quality with the CLAHE method and the median filter on the green channel image. The second stage, segmenting using a number of methods, namely, frangi filter, 2D-convolution filtering, median filtering, otsu's thresholding, morphology operation, and background subtraction. The last step is testing the system using the DRIVE and STARE dataset. The test results obtained sensitivity 91.187% performance parameters, 86.896% specificity, and area under the curve (AUC) 89.041%. Referring to the performance produced, the proposed model can be used as an alternative for blood vessel segmentation of retinal images.

**Keywords**—Segmentation; morphology; frangi filter; retinal; blood vessels

## I. INTRODUCTION

Diagnosis of hypertensive retinopathy can be done by analyzing the retina of the eye. Analysis of the retina of the eye can be done using the image processing approach. The analysis was carried out to identify changes in retinal blood vessel patterns. Recognizing the pattern of blood vessels, a segmentation process is needed, which is to separate the blood vessels of the retina from the background. Segmentation results will clarify the pattern of retinal blood growth. The process of retinal image segmentation can be done using a number of existing segmentation methods. The segmentation method in image processing is divided into 4 classes, namely edge detection, thresholding-based, region-based and clustering-based [1]. Blood vessel segmentation in the retina is relatively difficult because the retinal image produced by the fundus camera has non-uniform lighting and contrast variations [2]. Another thing that causes difficulty in the process of segmentation is the presence of a disease so that an abnormality will emerge which may be similar to a blood vessel or other sign. This condition makes segmentation not only using one method but a combination of a number of methods.

A number of studies have segmented retinal blood vessels by various methods. Sabaz & Atila [3] have segmented the retinal blood vessels by using a frangi filter. Frangi filter is a Hessian matrix based filter. The study succeeded in segmenting blood vessels, with the results of testing using the DRIVE dataset obtained 97.6% sensitivity, 72.6% specificity, and 86.04% accuracy. The resulting performance parameters have a high difference between sensitivity and specificity, so the AUC value is low. The performance of the study was relatively lower for specificity parameters if compared with the research conducted by Manikis et al. [4], which both used the hessian matrix-based segmentation method. The performance of the study was 74.14%, the specificity was 96.69% and the accuracy was 93.71%, but the performance was also not balanced between the performance parameters of sensitivity and specificity, which resulted in a low AUC value.

The segmentation of blood vessel based on Hessian matrix has also been done previously, namely by Ortiz et al. [5] and Ortiz et al. [6]. Both studies combined hessian matrix and Gabor filters for segmentation, except that in both studies they did not measure the performance of the segmentation method used, but focused more on determining venous arterial ratios. The study of frangi filter was also used in the research of Oloumi & Dhara [7]. The study not only uses frangi filtering, but also Gabor filters and a number of other methods. The segmentation method tested is a frangi filter, multiscale filter, gamma corrected green component, matched filter, and adaptive thresholding. The results of testing a number of methods, both single and hybrid, showed the highest specificity of 99.0%, but the sensitivity was very low at 12.8% and the accuracy was only 87.8%. This shows the ability of a number of methods combined with frangi filters has not been able to increase sensitivity. This condition makes the system unable to provide a balanced performance between sensitivity and specificity parameters, so the AUC value also becomes low.

The latest study was conducted by Khan et al. [8], which combines the frangi filter with the Vessel location map (VLM). The resulting performance, for parameter sensitivity was 73.0%, specificity was 97.93% and accuracy was 95.8%. The study was similar to that of Shahid & Taj [2], which is a combination of the frangi filter with VLM. The results of these studies provide relatively the same performance. Similar research was also carried out by Nugroho et al. [9]. The research of Nugroho et al. [9] has proposed a segmentation

method that combines frangi filters with morphological reconstruction. Tests performed using the DRIVE dataset show sensitivity of 72.13%, specificity of 96.65% and accuracy of 94.5%. The combination of frangi filter method with VLM, or frangi filter with morphology, has not been able to suppress differences in sensitivity performance parameters with specificity so that the AUC performance parameters produced are not optimal.

A number of studies on blood vessel segmentation using the frangi filter show that the frangi filter has not been able to work optimally when not combined with other methods. This is also supported in research conducted by Jothi & Jayaram [10] [10]. The study concluded that the use of frangi filters with 3D hessian matrix has a fast computational process, but does not guarantee high accuracy in detecting blood vessels. Another thing is that the performance produced on the frangi-based filter segmentation that has been carried out has higher specificity performance parameters than sensitivity, but with a big difference. A number of studies with such performance are carried out by [2], [4], [9], [11]–[17]. Another study is that sensitivity performance parameters are higher than specificity, but with high differences as well, as done by [3], [18]. The large difference between the two parameters makes the AUC parameter low.

Referring to a number of studies that have been conducted, this study proposes a combination of the frangi filter with a number of methods with the aim of improving performance. The performance improvement is indicated by the sensitivity and specificity being balanced so that the AUC value is better. The system model proposed in this study is segmentation using the hybrid method. The method consists of a frangi filter, 2D-convolution filter, FIR filter, otsu's thresholding, and morphology image. System performance is measured using sensitivity, specificity and AUC parameters.

## II. RESEARCH METHODS

Research on the retinal blood vessel segmentation in the fundus image uses a combination of a number of methods. A combination of a number of methods with the aim of providing a balanced performance between sensitivity and specificity, so that the AUC value becomes higher. The proposed method is divided into 3 main processes, namely preprocessing, segmentation and performance analysis. Complete the proposed method as shown in Fig. 1. This study uses two datasets for testing, namely DRIVE [19] and STARE [20], which can be obtained by online.

### A. Preprocessing

Preprocessing aims to improve the quality of retinal images. Preprocessing consists of three stages, first doing the process of separating retinal images into three channels, red, green and blue. The three channels are green channels which have the best quality, so the green channel is used for the next process. Second, improve the quality of retinal images using Contrast-limited adaptive histogram equalization (CLAHE) [21]. CLAHE is used to distribute color contrast. Third, to eliminate the amount of noise that appears, it is done using the median filter [22].

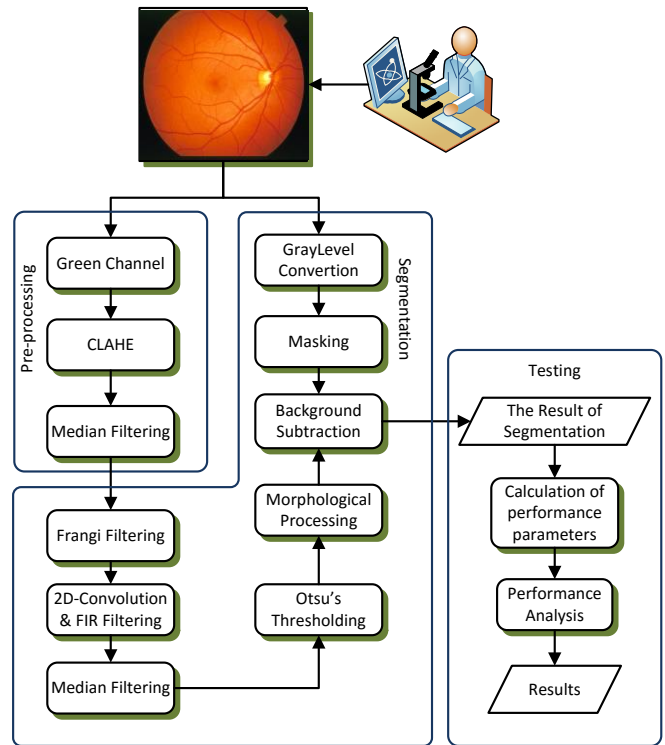


Fig. 1. Proposed Method.

### B. Frangi Filter

The segmentation stages are a number of methods used, including the Frangi filter. Frangi filter serves to detect and improve the quality of blood vessels in retinal images. The retinal blood vessels have a wide diameter, the frangi filter will give the output of each pixel which has the maximum response when it detects blood vessels in the retina. The process of detecting frangi filter blood vessels using a hessian matrix kernel [3].

The Hessian matrix kernel in the frangi filter functions to analyze a function with more than one variable that is maximum or minimum under certain conditions. If a function is  $f(x,y,z)$ , the Hessian matrix can be formulated as shown in equation (1). The Hessian matrix shown in equation (1) is a Hessian matrix for functions of 3-dimensional [3].

$$Hf(x,y,z) = \begin{bmatrix} \frac{\partial^2 f}{\partial x^2} & \frac{\partial^2 f}{\partial x \partial y} & \frac{\partial^2 f}{\partial x \partial z} \\ \frac{\partial^2 f}{\partial y \partial x} & \frac{\partial^2 f}{\partial y^2} & \frac{\partial^2 f}{\partial y \partial z} \\ \frac{\partial^2 f}{\partial z \partial x} & \frac{\partial^2 f}{\partial z \partial y} & \frac{\partial^2 f}{\partial z^2} \end{bmatrix} \quad (1)$$

In the case of retinal images, it is enough to use 2 dimensions, namely  $f(x,y)$ , so that the Hessian matrix is as shown in equation (2) [23].

$$Hf(x,y) = \begin{bmatrix} \frac{\partial^2 f}{\partial x^2} & \frac{\partial^2 f}{\partial x \partial y} \\ \frac{\partial^2 f}{\partial y \partial x} & \frac{\partial^2 f}{\partial y^2} \end{bmatrix} \quad (2)$$

In this study  $f(x,y)$  is a function with a Gaussian distribution. The Gaussian function for 2D can be shown in equation (3). The Hessian matrix is made using derivatives of equation (3).

$$F(x,y) = \frac{1}{2\pi\sigma^2} e^{-[(x-x_0)^2+(y-y_0)^2]/(2\sigma^2)} \quad (3)$$

The eigenvalue transformation in the Hessian matrix is used to obtain eigenvalues  $\lambda_1$  and  $\lambda_2$ , while  $\sigma$  is used to describe the scale of blood vessel repair. The filter response will be optimal if the scale  $\sigma$  corresponds to the size of the blood vessel so that if the value of  $\sigma$  is not correct it will reduce the performance of the frangi filter in detecting blood vessels. Frangi equation for finding the optimal retinal blood vessels, for two-dimensional images expressed in equations (4) [18].

$$V_f(s) = \begin{cases} 0 & \text{if } \lambda_2 > 0 \\ \exp(-\frac{R_B}{\beta^2})(1 - \exp(-\frac{S^2}{2c^2})) & \text{otherwise} \end{cases} \quad (4)$$

The  $\beta$  and  $c$  parameters in equation (4) are sensitivity parameters. The parameter value  $R_B$  in equation (4) can be calculated by equation (5), while for the  $S$  parameter it is calculated using equation (6) [18].

$$R_B = \frac{|\lambda_1|}{|\lambda_2|} \quad (5)$$

$$S = \sqrt{\lambda_1^2 + \lambda_2^2} \quad (6)$$

### C. Convolution Filtering

Convolution filtering is a 2D filter that is greatly influenced by the type of kernel it uses. In general, the convolution process can be shown in equation (7).

$$G(x,y) = \sum_{s=-a}^a \sum_{t=-b}^b w(s,t)f(x-s,y-t) \quad (7)$$

where  $g(x,y)$  is the convolution output,  $f(x,y)$  is the original image, while  $w(s,t)$  is the kernel used in the filter. The values of the parameters  $s$  and  $t$  are in the range of values  $-a \leq s \leq a$  and  $-b \leq t \leq b$ . To improve the quality of blood vessels, the convolution filter is also integrated with a 2D FIR filter, with its type filter Circular averaging filter.

### D. Otsu's Thresholding

The optimal threshold is the thresholding which results in the smallest possible segmentation error. The method that can be used to obtain optimal thresholding results is with Otsu [24]. Otsu thresholding has several advantages compared to other methods, namely computational speed and good capabilities when combined with other methods for performance improvement, and stable performance [25]. Otsu thresholding will automatically choose the optimal thresholding of the image, working on the assumption that the pixel of an image has two classes or a bimodal histogram. The Otsu method searches thoroughly by minimizing variance in the class [26]. The variance equation for each class is shown in equation (8).

$$\sigma_w^2(t) = q_1(t)\sigma_1^2(t) + q_2(t)\sigma_2^2(t) \quad (8)$$

Where 1 and 2 show two classes, background, and foreground. The probability for each class and its variance can be calculated by equations (9-11).

$$q_1(t) = \sum_{i=1}^t P(i) \quad (9)$$

$$q_2(t) = \sum_{i=t+1}^K P(i) \quad (10)$$

$$\sigma_1^2(t) = \sum_{i=1}^t [i - \mu_1(t)]^2 \frac{P(i)}{q_1(t)} \quad (11)$$

where  $\mu_1(t)$  and  $\mu_2(t)$  are the means of the class, which can be calculated by the equation (12-13).

$$\mu_1(t) = \sum_{i=1}^t \frac{iP(i)}{q_1(t)} \quad (12)$$

$$\mu_2(t) = \sum_{i=t+1}^K \frac{iP(i)}{q_2(t)} \quad (13)$$

Where the pixel value is in range of 0 to  $K$ . Referring to Fig. 1, the use of the Otsu's method for thresholding is carried out after the frangi filtering process, which is then carried out by the morphology image process. In this study, the threshold value generated uses the Otsu method on a scale of 0-1.

### E. Morphology Processing

Morphology is an operation to change the shape structure contained in the image. Morphology operations involve two two-dimensional matrices. The first is a matrix of images that will be subject to morphology operations, while the second is the kernel matrix. This study uses three operations, namely closing, diagonal fill and Bridges unconnected pixels.

The closing operation is carried out using the mathematical model shown in equation (14). Referring to this equation, the closing operation is carried out by performing a dilation operation first and then followed by erosion operations [27].

$$A \cdot B = (A \oplus B) \ominus B \quad (14)$$

Diagonal fill operation is an operation to eliminate the 8-connectivity background. The next operation Bridges unconnected pixels is bridging non-connected pixels, that is, specifying pixels worth 0 to 1 if they have two non-zero neighbors that are not connected. The binary morphology image operation aims to improve the quality of the output image of the Otsu thresholding, namely by reducing non-blood vessel pixels.

### F. Performance Analysis

The performance of this research is measured by referring to the confusion matrix, as shown in Table I. The parameters used are sensitivity, specificity, accuracy, and area under the curve. These parameters can be shown in a formula in equations (15-17). Testing is done using two datasets, namely DRIVE and STARE. The each of dataset consists of 20 unsegmented images and 20 manually segmented images.

$$\text{Sensitivity} = \frac{TP}{TP+FN} \quad (15)$$

$$\text{Specificity} = \frac{TN}{TN+FP} \quad (16)$$

$$\text{AUC} = \frac{\text{Sensitivity}+\text{Specificity}}{2} \quad [28] \quad (17)$$

TABLE I. CONFUSION MATRIX

| Actual Class | Predictive Class    |                     |
|--------------|---------------------|---------------------|
|              | Positive            | Negative            |
| Positive     | TP (True Positive)  | FN (False Negative) |
| Negative     | FP (False Positive) | TN (True Negative)  |

The model proposed in this study was implemented using Matlab R2014 software. The making and testing of the system are done by using a computer with Intel (R) Core (TM) i3-5005U CPU @ 2.00GHz 2.00 GHz, Memory 4.00GB, and using a 64-bit operating system.

### III. RESULTS AND DISCUSSION

#### A. Results

Research carried out using the method as shown in Fig. 1 produced a number of outputs. First, the output for each process in preprocessing, as shown in Fig. 2. Fig. 2 is the test result using the DRIVE dataset. In Fig. 2(a) is the retinal image of the CLAHE process output and median filtering. Fig. 2(b) is the frangi filtering output and the final output of the segmentation method. The same test results using the STARE dataset, are shown in Fig. 3(a) and Fig. 3(b).

The next system output is the result of the proposed system performance measurement. Performance measurement is done by using two datasets, namely DRIVE and STARE. Performance parameters are measured by reference to equations (15-17), namely sensitivity, specificity, and AUC. The data used amounted to 20 retinal images, the results of segmentation using the proposed model were compared with the results of segmentation done manually by experts available in both datasets. Test results from 20 available retinal image data can be shown in Table II.

#### B. Discussion

The testing of the segmentation model proposed using the DRIVE and STARE datasets are able to provide performance as shown in Table II. Table II shows that for the DRIVE dataset it has a sensitivity that is greater than the specificity. This condition shows the system's average ability to detect pixels as blood vessels lower than the system's ability to detect pixels as background. In general, when referring to the AUC performance parameters indicate that the system is in a good category, that is, the AUC value is in the range of 80%-90% [29]. For the STARE dataset, the performance is relatively lower, because the characteristics of the STARE dataset between the background and blood vessels are finer than the DRIVE dataset, but the AUC value is still in the range of 80%-90%.

The differences of the performance parameter sensitivity with relatively small specificity, when compared with a number of previous studies. Referring to Table III, the average difference between the two parameters is 23%. The proposed system model is able to reduce sensitivity differences and specificity reaching 4.291%. Sensitivity parameters in the proposed system, one of which is caused by the lack of accuracy in determining the combination of frangi filter parameter values, namely  $c$  and  $\beta$  in equation (4). Incorrect combinations cause the values of the two parameters to be

mutually opposite, or give a value that is not optimal. The performance generated in Table II is obtained by conducting a number of experiments, the combination of parameters  $c$  and  $\beta$ , which is done manually. The results of a number of experiments obtained the best performance in the parameter value  $c = 106.580$  and  $\beta = 0.1058$ . The choice of the best combination of  $c$  and  $\beta$  values, it can be possible to develop using a number of computational intelligence algorithms, so that optimal performance will be obtained. Computational intelligence algorithms that can be used such as genetic algorithms, particle swarm optimization, and ant colony optimization.

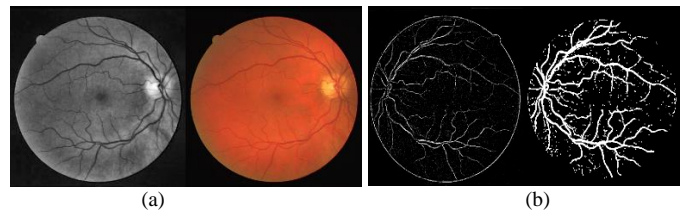


Fig. 2. Output System for DRIVE Dataset.

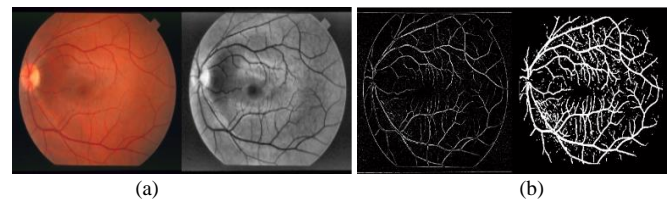


Fig. 3. Output System for STARE Dataset.

TABLE II. TESTING RESULTS USING DATASET

| No          | DRIVE         |               |               | STARE         |               |               |
|-------------|---------------|---------------|---------------|---------------|---------------|---------------|
|             | SEN           | SPE           | AUC           | SEN           | SPE           | AUC           |
| 1           | 88.649        | 92.714        | 90.681        | 89.651        | 84.393        | 87.022        |
| 2           | 91.823        | 90.216        | 91.019        | 91.943        | 79.152        | 85.547        |
| 3           | 89.839        | 86.331        | 88.085        | 86.145        | 87.844        | 86.994        |
| 4           | 93.012        | 85.979        | 89.495        | 98.865        | 42.726        | 70.796        |
| 5           | 93.824        | 84.013        | 88.918        | 86.914        | 92.068        | 89.491        |
| 6           | 93.023        | 82.239        | 87.631        | 88.904        | 82.065        | 85.485        |
| 7           | 92.422        | 84.721        | 88.571        | 85.025        | 92.139        | 88.582        |
| 8           | 93.582        | 80.260        | 86.921        | 87.465        | 91.941        | 89.703        |
| 9           | 94.450        | 82.215        | 88.332        | 88.914        | 93.385        | 91.149        |
| 10          | 92.022        | 85.583        | 88.803        | 90.874        | 83.557        | 87.216        |
| 11          | 89.141        | 86.249        | 87.695        | 85.832        | 95.664        | 90.748        |
| 12          | 89.547        | 88.150        | 88.849        | 90.680        | 91.524        | 91.102        |
| 13          | 90.580        | 85.201        | 87.891        | 90.303        | 85.932        | 88.118        |
| 14          | 89.934        | 90.734        | 90.334        | 89.996        | 90.794        | 90.395        |
| 15          | 88.409        | 90.040        | 89.224        | 87.798        | 88.191        | 87.995        |
| 16          | 90.139        | 89.463        | 89.801        | 95.311        | 76.284        | 85.797        |
| 17          | 91.049        | 85.129        | 88.089        | 87.049        | 93.018        | 90.033        |
| 18          | 89.413        | 89.321        | 89.367        | 97.386        | 56.280        | 76.833        |
| 19          | 90.279        | 90.822        | 90.551        | 97.551        | 47.418        | 72.484        |
| 20          | 92.603        | 88.535        | 90.569        | 97.107        | 54.945        | 76.026        |
| <b>Mean</b> | <b>91.187</b> | <b>86.896</b> | <b>89.041</b> | <b>90.686</b> | <b>80.466</b> | <b>85.576</b> |

TABLE III. COMPARISON WITH PREVIOUS RESEARCH

| Author                    | SEN           | SPE           | SEN-SPE      | AUC           |
|---------------------------|---------------|---------------|--------------|---------------|
| Aguirre-Ramos et al. [11] | 72.960        | 96.870        | 23.910       | 84.915        |
| Akhavan et al. [30]       | 72.520        | 97.330        | 24.810       | 84.925        |
| Ali et.al. [31]           | 78.180        | 96.880        | 18.700       | 87.530        |
| Chakraborti et al. [12]   | 72.050        | 95.790        | 23.740       | 83.920        |
| Dash & Bhoi [15]          | 71.900        | 97.600        | 25.700       | 84.750        |
| Frangi et al. [18]        | 91.370        | 65.370        | 26.000       | 78.370        |
| Jebaseeli et.al [32]      | 70.040        | 99.800        | 29.760       | 84.920        |
| Khan et al. [33]          | 74.620        | 98.010        | 23.390       | 86.315        |
| Manikis et al. [4]        | 74.140        | 96.690        | 22.550       | 85.415        |
| Memari et al. [14]        | 76.100        | 98.100        | 22.000       | 87.100        |
| Nugroho et al. [9]        | 72.130        | 96.650        | 24.520       | 84.390        |
| Oloumi et al. [7]         | 87.600        | 91.800        | 4.200        | 89.700        |
| Sabaz et al.[3]           | 97.600        | 72.600        | 25.000       | 85.100        |
| Shah et al. [13]          | 72.050        | 98.140        | 26.090       | 85.095        |
| Shahid & Taj [2]          | 73.000        | 97.930        | 24.930       | 85.000        |
| Zhao et al. [34]          | 73.540        | 97.890        | 24.350       | 85.715        |
| Our proposed              | <b>91.187</b> | <b>86.896</b> | <b>4.291</b> | <b>89.041</b> |

The performance of the proposed hybrid segmentation model, when referring to the AUC parameter shows better capabilities than a number of studies that have been carried out, as shown in Table III. The proposed model has relatively the same performance compared to the model proposed by Oloumi et al. [7]. Unfortunately, the study which done by Oloumi et al. [7] used a combination of a number of methods which were relatively more numerous. The combined method is Multiscale Gabor filter, Frangi filter, gamma corrected green component, matched filter and line operator, with a fixed threshold. This means that good performance in the study of Oloumi et al. [7] must be supported by so many methods with high computation so that it also has a high complexity in its implementation and longer computation time.

The next comparison with the research conducted by Khan et al. [33] and Shahid & Taj [2]. Both of these studies use a method that combines the frangi filter in segmentation. In this study, it produced almost the same performance, namely, AUC 86.315% and 85.00% for the DRIVE dataset. This performance is still lower compared to the proposed system. The same thing happened in a study conducted by Sabaz et al. [3], even parameter of specificity is lower when compared to the proposed segmentation model. Research by Sabaz et al. [3] has advantages in sensitivity parameters which can reach 97.6%, but besides AUC the value of accuracy is also lower compared to the proposed system.

#### IV. CONCLUSIONS

The segmentation model using a hybrid frangi filter, otsu's thresholding and morphology image are able to provide performance with an AUC parameter value of 89.041%. or included in the good category. The proposed system specificity value, if seen the difference with the sensitivity parameter is not too high, which is only 4.291%. This value is smaller than a number of studies that have been conducted. The model proposed, referring to the AUC value, can be an

alternative method in segmenting retinal blood vessels. The performance of the proposed segmentation model can still increase when the values of the  $c$  and  $\beta$  parameters on the frangi filter are optimal values. Further research, in determining the parameter values can take advantage of a number of optimization algorithms, such as particle swarm optimization.

#### ACKNOWLEDGMENT

We would like to thank the Sebelas Maret University Indonesia. which has provided research grants of fundamentals with funding PNPB UNS. by contract number: 516/UN27.21/PP/2019. The authors thank the anonymous referees for their constructive suggestions and comments which helped in the improvement of the presentation of the manuscript.

#### REFERENCES

- [1] S. Samaddar and D. A. R. Reddy, "Comparative Study Of Image Segmentation Techniques On Chronic Kidney Diseases," *Int. J. Pure Appl. Math.*, vol. 118, no. 14, pp. 235–239, 2018.
- [2] M. Shahid and I. A. Taj, "Retracted: Robust Retinal Vessel Segmentation using Vessel's Location Map and Frangi Enhancement Filter," *IET Image Process.*, vol. 12, no. 4, pp. 494–501, Apr. 2018.
- [3] F. Sabaz and U. Atila, "Roi Detection And Vessel Segmentation In Retinal Image," *ISPRS - Int. Arch. Photogramm. Remote Sens. Spat. Inf. Sci.*, vol. XLII-4/W6, pp. 85–89, Nov. 2017.
- [4] G. C. Manikis et al., "An image analysis framework for the early assessment of hypertensive retinopathy signs," in *The 3rd International Conference on E-Health and Bioengineering - EHB, Iași, Romania*, 2011, pp. 1–6.
- [5] D. Ortiz et al., "Support system for the preventive diagnosis of Hypertensive Retinopathy," in *32nd Annual International Conference of the IEEE EMBS, Buenos Aires, Argentina*, 2010, pp. 5649–5652.
- [6] D. Ortiz et al., "System Development for Measuring the Arterious Venous Rate (AVR) for the Diagnosis of Hypertensive Retinopathy," in *Andean Region International Conference, Cuenca, Ecuador*, 2012, pp. 53–56.
- [7] F. Oloumi, A. K. Dhara, R. M. Rangayyan, and S. Mukhopadhyay, "Detection of Blood Vessels in Retinal Fundus Images," *Comput. Sci. J. Mold.*, vol. 22, no. 2, pp. 155–185, 2014.
- [8] K. B. Khan, Amir. A. Khaliq, A. Jalil, and M. Shahid, "A robust technique based on VLM and Frangi filter for retinal vessel extraction and denoising," *PLOS ONE*, vol. 13, no. 2, p. e0192203, Feb. 2018.
- [9] H. A. Nugroho, R. A. Aras, T. Lestari, and I. Ardiyanto, "Retinal vessel segmentation based on Frangi filter and morphological reconstruction," in *2017 International Conference on Control, Electronics, Renewable Energy and Communications (ICCREC), Yogyakarta*, 2017, pp. 181–184.
- [10] A. Jothi and S. Jayaram, "Blood Vessel Detection in Fundus Images Using Frangi Filter Technique," in *Smart Innovations in Communication and Computational Sciences*, vol. 670, B. K. Panigrahi, M. C. Trivedi, K. K. Mishra, S. Tiwari, and P. K. Singh, Eds. Singapore: Springer Singapore, 2019, pp. 49–57.
- [11] H. Aguirre-Ramos, J. G. Avina-Cervantes, I. Cruz-Aceves, J. Ruiz-Pinales, and S. Ledesma, "Blood vessel segmentation in retinal fundus images using Gabor filters, fractional derivatives, and Expectation Maximization," *Appl. Math. Comput.*, vol. 339, pp. 568–587, Dec. 2018.
- [12] T. Chakraborti, D. K. Jha, A. S. Chowdhury, and X. Jiang, "A self-adaptive matched filter for retinal blood vessel detection," *Mach. Vis. Appl.*, vol. 26, no. 1, pp. 55–68, Jan. 2015.
- [13] S. A. A. Shah, T. B. Tang, I. Faye, and A. Laude, "Blood vessel segmentation in color fundus images based on regional and Hessian features," *Graefes Arch. Clin. Exp. Ophthalmol.*, vol. 255, no. 8, pp. 1525–1533, Aug. 2017.

- [14] N. Memari, A. R. Ramli, M. I. B. Saripan, S. Mashohor, and M. Moghbel, "Retinal Blood Vessel Segmentation by Using Matched Filtering and Fuzzy C-means Clustering with Integrated Level Set Method for Diabetic Retinopathy Assessment," *J. Med. Biol. Eng.*, Nov. 2018.
- [15] J. Dash and N. Bhoi, "A thresholding based technique to extract retinal blood vessels from fundus images," *Future Comput. Inform. J.*, vol. 2, no. 2, pp. 103–109, Dec. 2017.
- [16] K. B. Khan, Amir. A. Khaliq, A. Jalil, and M. Shahid, "A robust technique based on VLM and Frangi filter for retinal vessel extraction and denoising," *PLOS ONE*, vol. 13, no. 2, p. e0192203, Feb. 2018.
- [17] C. Zhu et al., "Retinal vessel segmentation in colour fundus images using Extreme Learning Machine," *Comput. Med. Imaging Graph.*, vol. 55, pp. 68–77, Jan. 2017.
- [18] A. F. Frangi, W. J. Niessen, K. L. Vincken, and M. A. Viergever, "Multiscale vessel enhancement filtering," in *Medical Image Computing and Computer-Assisted Intervention — MICCAI'98*, vol. 1496, W. M. Wells, A. Colchester, and S. Delp, Eds. Berlin, Heidelberg: Springer Berlin Heidelberg, 1998, pp. 130–137.
- [19] J. Staal, M. D. Abramoff, M. Niemeijer, M. A. Viergever, and B. van Ginneken, "Ridge-Based Vessel Segmentation in Color Images of the Retina," *IEEE Trans. Med. Imaging*, vol. 23, no. 4, pp. 501–509, Apr. 2004.
- [20] A. D. Hoover, V. Kouznetsova, and M. Goldbaum, "Locating blood vessels in retinal images by piecewise threshold probing of a matched filter response," *IEEE Trans. Med. Imaging*, vol. 19, no. 3, pp. 203–210, Mar. 2000.
- [21] J. Ma, X. Fan, S. X. Yang, X. Zhang, and X. Zhu, "Contrast Limited Adaptive Histogram Equalization-Based Fusion in YIQ and HSI Color Spaces for Underwater Image Enhancement," *Int. J. Pattern Recognit. Artif. Intell.*, vol. 32, no. 7, 2018.
- [22] K. Noronha, K. T. Navya, and K. P. Nayak, "Support system for the automated detection of hypertensive retinopathy using fundus images," in *International Conference on Electronic Design and Signal Processing (ICEDSP)*, Manipal, India, 2012, pp. 7–11.
- [23] P. T. H. Truc, Md. A. U. Khan, Y.-K. Lee, S. Lee, and T.-S. Kim, "Vessel enhancement filter using directional filter bank," *Comput. Vis. Image Underst.*, vol. 113, no. 1, pp. 101–112, 2009.
- [24] N. Otsu, "A Threshold Selection Method from Gray-Level Histograms," *IEEE Trans. Syst. Man Cybern.*, vol. 9, no. 1, pp. 62–66, Jan. 1979.
- [25] W.-X. Kang, Q.-Q. Yang, and R.-P. Liang, "The Comparative Research on Image Segmentation Algorithms," in *2009 First International Workshop on Education Technology and Computer Science*, Wuhan, Hubei, China, 2009, pp. 703–707.
- [26] M. A. Ansari and S. K. Mahraj, "A Robust Method for Identification of Paper Currency Using Otsu's Thresholding," presented at the 2018 International Conference on Smart Computing and Electronic Enterprise (ICSCEE), Shah Alam, Malaysia, 2018, pp. 1–5.
- [27] F. Y. Shih, *Image Processing and Mathematical Morphology Fundamentals and Applications*. Boca Raton: CRC Press, 2009.
- [28] E. Ramentol, Y. Caballero, R. Bello, and F. Herrera, "SMOTE-RSB \*: a hybrid preprocessing approach based on oversampling and undersampling for high imbalanced data-sets using SMOTE and rough sets theory," *Knowl. Inf. Syst.*, vol. 33, no. 2, pp. 245–265, Nov. 2012.
- [29] F. Gorunescu, *Data Mining Concepts, Models and Techniques*, Intelligent Systems Reference Library. Berlin, Heidelberg: Springer, 2011.
- [30] R. Akhavan and K. Faez, "A Novel Retinal Blood Vessel Segmentation Algorithm using Fuzzy segmentation," *Int. J. Electr. Comput. Eng. IJECE*, vol. 4, no. 4, pp. 561–572, 2014.
- [31] A. Ali, W. M. D. Wan Zaki, and A. Hussain, "Retinal blood vessel segmentation from retinal image using B-COSFIRE and adaptive thresholding," *Indones. J. Electr. Eng. Comput. Sci.*, vol. 13, no. 3, pp. 1199–1207, Mar. 2019.
- [32] T. J. Jebaseeli, C. A. D. Durai, and J. D. Peter, "Segmentation of retinal blood vessels from ophthalmologic Diabetic Retinopathy images," *Comput. Electr. Eng.*, vol. 73, pp. 245–258, Jan. 2019.
- [33] K. BahadarKhan, A. A. Khaliq, and M. Shahid, "A Morphological Hessian Based Approach for Retinal Blood Vessels Segmentation and Denoising Using Region Based Otsu Thresholding," *PLOS ONE*, vol. 11, no. 7, p. e0158996, Jul. 2016.
- [34] Y. Qian Zhao, X. Hong Wang, X. Fang Wang, and F. Y. Shih, "Retinal vessels segmentation based on level set and region growing," *Pattern Recognit.*, vol. 47, no. 7, pp. 2437–2446, Jul. 2014.



# A New Image Inpainting Approach based on Criminisi Algorithm

Nouho Ouattara<sup>1</sup>, Georges Laussane Loum<sup>2</sup>, Ghislain Koffi Pandry<sup>3</sup>, Armand Kodjo Atiampo<sup>4</sup>

Laboratoire de Recherche en Informatique et Télécommunication/UMRI EEA  
Institut National Polytechnique Felix-Houphouët Boigny  
Yamoussoukro, Côte d'Ivoire

**Abstract**—In patch-based inpainting methods, the order of filling the areas to be restored is very important. This filling order is defined by a priority function that integrates two parameters: confidence term and data term. The priority, as initially defined, is negatively affected by the mutual influence of confidence and data terms. In addition, the rapid decrease to zero of confidence term leads the numerical instability of algorithms. Finally, the data term depends only on the central pixel of the patch, without taking into account the influence of neighboring pixels. Our aim in this paper is to propose an algorithm to solve the problems mentioned above. This algorithm is based on a new definition of the priority function, a calculation of the average data term obtained from the elementary data terms in a patch and an update of the confidence term slowing its decrease and avoiding convergence to zero. We evaluated our method by comparing it with algorithms in the literature. The results show that our method provides better results both visually and in terms of the Peak Signal-to-Noise Ratio (PSNR) and Structural SIMilarity index (SSIM).

**Keywords**—Image inpainting; Criminisi algorithm; priority function; data term; confidence term; identity function

## I. INTRODUCTION

Problems related to image degradation are numerous and occur in several areas. In the case of medical imaging, especially endoscopic imaging, some highlights may appear as white areas and this is often embarrassing when interpreting the scene [1]-[4]. This is similar to the search for white objects in a foliage. Here, the highlights are sometimes confused with the white objects being sought.

For the correcting of the above-mentioned problems, the technique of digital image inpainting is generally used. Image inpainting is intended to fill in missing parts of an image or to remove information that disturbs the interpretation of a scene. There are mainly two categories of inpainting methods: those based on diffusion processes and those based on exemplars [5]-[7].

Diffusion-based methods [8]-[11] simulate how human proceeds to fill a missing part in an image. These methods use the pixels of the known region neighboring the region to be restored to determine the structure and content of the diffusion. This reconstruction is done iteratively, from near to near, the outside to the inside of the unknown area. Masnou et al. [8] were the first to propose a diffusion-based inpainting model. Their disocclusion model is based on level lines. Subsequently, Bertalmio et al. [9] described a model based on

partial difference equations (PDEs) called the Bertalmio-Sapiro-Caselles-Bellester model (BSCB). Chan and Shen [10] developed a model by minimizing total variation (TV) using the Euler-Lagrange equation. In addition, in order to take into account geometric curves, they proposed the Curvature Diffusion model (CCD). The main limitation of diffusion-based inpainting methods is the size of the area to be restored. These methods provide good results for small areas. However, for large areas, they produce a blurred effect in painted areas and thus reduce the quality of the restoration.

To solve this problem, exemplar-based methods have been proposed [12]-[18]. These methods are based on repeating patterns in an image. Efros and Leung [19] were the first to present a model based on image statistics and similarity between different image regions. Criminisi et al. [12] have revolutionized inpainting methods based on pattern repetition by integrating textural and structural information. Their algorithm preserves textures and linear structures and provides better results than geometric methods for large areas.

However, for reasons of inconsistencies in restoration due to the parameters related to the Criminisi algorithm, several studies have been conducted to improve it.

Criminisi et al. proposed in their approach a priority function to define the filling order of the area to be reconstituted. This priority function is based on the multiplication of two terms, confidence and data. Work has been done to show the influence that each term can have on the other based on the product [13], [14]. Indeed, when one of the two terms tends to zero, the product with the second term gives a result of very low value. This can negatively affect the filling order and therefore the quality of the restoration. Thus, some researchers have proposed several methods to solve the problem related to the calculation of the priority function [20]-[24]. Chi et al. [20] proposed to raise the confidence term to a power of 3 in order to increase the importance of the data term. Their goal is to improve texture details to increase the accuracy of the restoration. A commonly used approach is to replace the multiplication with a weighted sum to avoid the influence of one term on the other [13]-[15].

Another major problem of Criminisi algorithm is the rapid convergence of the confidence term to zero when it is updated. Indeed, to favor pixels that have never been filled or that have been earlier, the value of the confidence term of the filled pixels is lower than those that allowed it to be updated. This convergence to zero can lead to poor restoration of large areas.

Nan and Xi [13] then used a logistics function to update the confidence term for large areas. When the area to be restored contains less than 1500 pixels, the update proposed by [12] is used. Otherwise, they use the derivative of the logistics function. Unfortunately, the principle of reducing the value of the confidence term is not always respected. There is generally an increase in the value of the confidence term rather than a decrease in large areas. Yuheng and Hao [25] proposed redefining the confidence term to avoid its convergence to zero by combining Manhattan's distance with that proposed in the Criminisi algorithm.

Improvements in the priority function were also made to the data term. Hou [15] proposed a new approach of Criminisi algorithm by providing sequential structural optimization. He defined a new data term and used the Sobel gradient instead of the one used in Criminisi algorithm to strengthen the repair of highly structural regions. Wu and Ruan [26] exploited the TV diffuse model while Xi et al. [27] used entropy as a data term. Yin and Chang [28] have improved the data term by introducing isophote curvature information.

In order to avoid the problem of the multiplication of confidence and data terms in calculating the priority of [12], we propose to use their weighted sum. We also propose a new approach of confidence term update based on two linear functions to avoid convergence to zero. The first is lower than the identity function up to a defined threshold value. Its role is to promote patches that have never been filled. The second function is close to a constant. It allows to bring closer to the threshold, all the update values that are lower than it. Finally, to take into account all the structural information in a patch to be reconstructed, the value of the data term of each boundary pixel is calculated and their average value is retained as the value of the data term of this patch.

The rest of this paper is structured as follows. Section 2 is devoted to a detailed review of the Criminisi algorithm. In Section 3, we present our approach. Section 4 presents our results and a comparative analysis with those of the methods in the literature. Our work ends with a conclusion that leads to perspectives.

## II. CRIMINISI ALGORITHM

The Criminisi algorithm is an algorithm capable of restoring linear structures and texture simultaneously. It is suitable for repairing large damaged surfaces. It assumes that an image to be restored consists of three parts. The first part is the known region ( $\Phi$ ), the second is the unknown region ( $\Omega$ ) and the third is the border separating the two regions ( $\delta\Omega$ ). This principle is illustrated in Fig. 1.

To fill the unknown area, some elements must be defined. The  $\delta\Omega$  border is made up of a set of pixels. A pixel of this boundary is designated by  $p$ .  $\psi_p$  is a patch to be reconstituted centered on the pixel  $p$ . It is also called the target block. This patch contains a known part and an unknown part that will be rebuilt. The gradient  $\nabla I_p^\perp$  represents the intensity and direction of the illumination line and  $n_p$  is the normal unit vector at the contour  $\delta\Omega$  at point  $p$ . The gradient  $\nabla I_p^\perp$  is defined by (1).

$$\nabla I_p^\perp = \frac{(-I_y(p), I_x(p))}{\sqrt{[I_x(p)]^2 + [I_y(p)]^2}} \quad (1)$$

The Criminisi algorithm is described in four steps.

### A. Step 1: Calculate the Priorities of Each Patch Along the $\delta\Omega$ Border and Select the Patch with the Highest Priority

The priority is used to define the filling order and the highest value determines the patch to be filled. The priority is calculated as follows (2):

$$P(p) = C(p)D(p) \quad (2)$$

where  $C(p)$  and  $D(p)$  are respectively the confidence term and the data term. These terms are defined as follows (3) and (4):

$$C(p) = \frac{\sum_{q \in \Psi_p \cap \Phi} C(q)}{|\Psi_p|} \quad (3)$$

$$D(p) = \frac{|\nabla I_p^\perp \cdot n_p|}{\alpha} \quad (4)$$

$|\Psi_p|$  represents the total number of pixels in the patch  $\psi_p$  and  $\alpha$  is a normalization coefficient. The value of  $\alpha$  is  $256 \times 3$  for an 8-bit RGB image.

The confidence term must follow the initial conditions defined in (5):

$$C(q) = \begin{cases} 0 & \text{if } q \in \Omega \\ 1 & \text{if } q \in \Phi \end{cases} \quad (5)$$

The selected patch is obtained from (6):

$$\Psi_{\hat{p}} = \text{Arg max}_{\Psi_p} P(p) \quad (6)$$

### B. Step 2: Determination of the Best Filling Patch

The search for the best patch corresponding to the patch to be filled is carried out in the known region. The selected patch is obtained by comparing the known part of the patch to be inpainted with its correspondent in the filling patch. This comparison is made through the sum of squared differences (SSD). The SSD is defined by (7):

$$d(\Psi_p, \Psi_q) = \sum_{i=1}^m \sum_{j=1}^m [(p_{ij}^R - q_{ij}^R)^2 + (p_{ij}^G - q_{ij}^G)^2 + (p_{ij}^B - q_{ij}^B)^2] \quad (7)$$

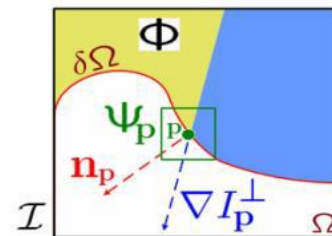


Fig. 1. Basic Principle of Criminisi Algorithm.

where  $p_{ij}^R$ ,  $p_{ij}^G$  and  $p_{ij}^B$  are the RGB color channel values of the pixels of the patch to be filled and  $q_{ij}^R$ ,  $q_{ij}^G$  and  $q_{ij}^B$  are those of the current patch.  $m$  is the number of known pixels in the  $\psi_p$  patch to be restored. The selected patch is the one with a minimum  $d(\psi_p, \psi_q)$  value. Its equation is as follows (8):

$$\Psi_{\hat{q}} = \text{Arg max}_{\Psi_q \in \Phi} d(\Psi_{\hat{p}}, \Psi_q) \quad (8)$$

The filling process is illustrated in Fig. 2.

In Fig. 2(a),  $\psi_q$  is selected as the patch similar to  $\psi_p$ . Thus, in Fig. 2(b), its content is used to fill in the unknown part of  $\psi_p$ . The inpainting result is perceived in Fig. 2(c).

### C. Step 3: Update of the Confidence Term

When a patch is filled with the pixel values of the best corresponding patch, the pixels of this patch initially belonging to the unknown part of the image, will have a new value of the confidence term. This value is that of the central pixel of the patch calculated from (3). The expression of the confidence term update is defined as follows (9):

$$C(q) = C(\hat{p}) \quad \forall q \in \Psi_{\hat{p}} \cap \Omega \quad (9)$$

### D. Step 4: Repeat Steps 1 to 3 until the Area to be Inpainted is Completely Filled

## III. PROPOSED METHOD

### A. Improvement of the Priority Function and Data Term

Several authors have shown that the priority function proposed in the Criminisi algorithm using the product of confidence and data terms, negatively influences the filling order and therefore, the result of the restoration. Thus, an alternative that has addressed the problem of the multiplication of confidence and data terms is the use of the weighted sum. Until now, the calculation of the filling priority has been based on the central pixel of the patch to be restored.

However, a patch can be defined as a sub-image contained in the entire image  $I$ . In this case, a patch to be inpainted  $\psi_p$  contains three parts: a known part  $\psi_p \cap \Phi$ ; an unknown part  $\psi_p \cap \Omega$ ; and a set of boundary pixels  $\psi_p \cap \delta\Omega$ . Fig. 3 shows an image in which a patch to be inpainted is defined.

In Fig. 3, the red line in the black contour ellipse represents all the boundary pixels of the patch to be filled  $\psi_p$ . Thus, we believe that each pixel of this boundary can provide information about the data term.

In our approach, we propose a new priority function based on all the pixels of  $\psi_p \cap \delta\Omega$  and not only on the central pixel of the patch. This function also exploits the advantages of the weighted sum of the confidence and data terms. Its formula is defined by (10):

$$P(p) = \alpha C(p) + \beta \bar{D}(p) \quad (10)$$

with

$$\alpha + \beta = 1 \quad (11)$$

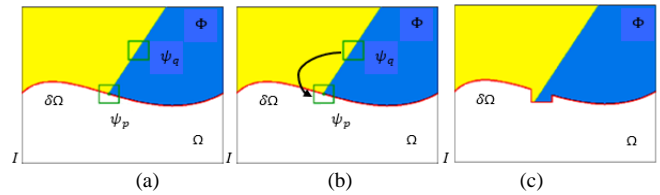


Fig. 2. Patch Filling Process.

where the term  $\bar{D}(p)$  is the average value of the data terms defined for each pixel of the border between known and unknown regions in the patch  $\psi_p$ . It is obtained from (12):

$$\bar{D}(p) = \frac{\sum_{p \in \delta\Omega \cap \Psi_p} D(p)}{|\delta\Omega \cap \Psi_p|} \quad (12)$$

### B. Proposition to update the Confidence Term

1) *Motivation and general description of our method:* In order to favor patches that have never been filled or patches that have been filled earlier, Criminisi et al. proposed to reduce the value of the updated confidence term of the newly filled pixels compared to the confidence term values of the known pixels. As a result, after several filling levels, the values of the updated confidence terms decrease to zero. Their convergence is a limitation to their algorithm. This has been the subject of studies by several researchers who have tried to solve this problem [12],[23].

To address the problem of convergence of confidence terms to zero, we propose to slow the decrease of its update. Slowing down the decrease of the confidence term does not guarantee non-convergence to zero. Thus, we define a threshold value from which we will increase the  $C(\hat{p})$  value of the obtained confidence term.

Indeed, after a filling, the value of the confidence term of the patch to be filled  $C(\hat{p})$  can be either lower or higher than the initial minimum value of the confidence terms. In the case where this value is higher than the initial minimum, the update value of the confidence term must decrease but remain higher than the initial minimum. Otherwise, the updated confidence term must increase while remaining below the initial minimum. This double adjustment makes it possible to guarantee the decrease in confidence terms and to avoid convergence to zero. Fig. 4 illustrates our model of confidence term update.

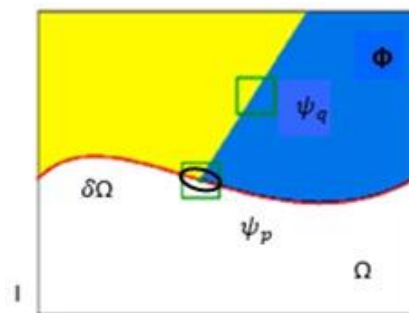


Fig. 3. Representation of a Patch to be Inpainted.

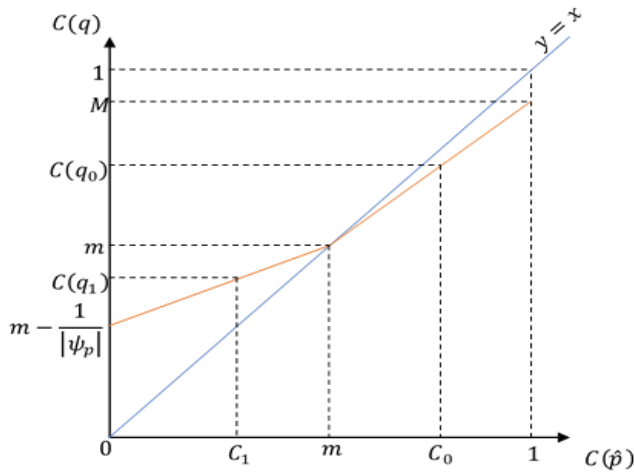


Fig. 4. Evolution of the Confidence Term update  $C(q)$ .

The blue line represents the identity function as well as the update of the Criminisi confidence term. The two segments in red are a representation of our update of the confidence term.  $M$  and  $m$  are respectively the maximum and minimum values of the confidence term of the  $\delta\Omega$  border pixels in the initial image. The number  $\frac{1}{|\Psi_p|}$  is a very small value to control the convergence of the updated confidence term  $C(q)$  when the value of the confidence term of the reconstituted patch is less than  $m$ .  $q$  is a pixel of the initially unknown area of the patch that has just been filled.  $C_0$  and  $C_1$  are values of the confidence terms of the patches filled in  $C(\hat{p})$ .  $C(q_0)$  and  $C(q_1)$  are their updated correspondents  $C(q)$  respectively. We can see that  $C(q_0)$  is less than  $C_0$  and  $C(q_1)$  more than  $C_1$ .

2) Steps of the algorithm of the confidence term update  $C(q)$

- Calculation of the confidence terms of the patches to be reconstituted (confidence term of the central pixel) at initialization:  $C_0(p)$ ;
- Search for the minimum and maximum of the initial  $C(p)$ :  $m = \min(C_0(p))$  and  $M = \max(C_0(p))$ ;
- Search for two linear functions to simulate the evolution of confidence terms:

When the confidence term of the filled patch  $C(\hat{p})$  is between  $\min(C_0(p))$  and  $\max(C_0(p))$ , the function must respect the constraint of reducing the value of the confidence term and the constraint of non-convergence to zero. To do this, we propose an increasing line that is below the first bisector ( $y=x$ ) and cuts the first bisector in  $\min(C_0(p))$ . This requires that the updated values  $C(q)$  be between  $\min(C_0(p))$  and  $\max(C_0(p))$ . Thus, the linear function is defined from (13):

$$C(q) = \alpha C(\hat{p}) + \beta$$

(13) with the following condition:

$$C(q) = \begin{cases} \max(C_0(p)) & \text{if } C(\hat{p})=1 \\ \min(C_0(p)) & \text{if } C(\hat{p})=\min(C_0(p)) \end{cases} \quad (14)$$

thus:

$$\alpha = \frac{\max(C_0(p)) - \min(C_0(p))}{1 - \min(C_0(p))} \quad (15)$$

and

$$\beta = \frac{\min(C_0(p)) [1 - \max(C_0(p))]}{1 - \min(C_0(p))} \quad (16)$$

In a patch whose elementary confidence terms  $C(p)$  have values close to  $\min(C_0(p))$ , it is possible to obtain a confidence term of the patch to be reconstituted  $C(\hat{p}) < \min(C_0(p))$ . Thus, the second function must be increasing. It must converge towards  $\min(C_0(p))$  and its graphical representation must be above the first bisector. Its growth must be slow. We define this function by a linear function verifying the conditions (17) and (18):

$$C(q) = \min(C_0(p)) - \frac{1}{|\Psi_p|}, \quad \text{if } C(\hat{p}) = 0 \quad (17)$$

$$C(q) = \min(C_0(p)), \quad \text{if } C(\hat{p}) = \min(C_0(p)) \quad (18)$$

The linear function thus obtained is as follows (19):

$$C(q) = \frac{1}{|\Psi_p| \min(C_0(p))} C(\hat{p}) + \min(C_0(p)) - \frac{1}{|\Psi_p|} \quad (19)$$

#### IV. EXPERIMENTAL RESULTS AND DISCUSSIONS

##### A. Choice of Parameters

This section focuses on the choice of weighting coefficients for confidence and data terms and patch size. These choices are made concurrently. The experiments were carried out on a set of 256x256 colour images.

To better characterize the texture present in our images, we varied the window from 5x5 to 11x11 in increments of 2. The variations in the weighting coefficient of the confidence term  $\alpha$  were studied by varying it from 0.1 in the range 0.1 to 0.9. Thus, for a given image, we obtain 36 images of which we must select the best one. This allows to choose both the best patch size and the best coefficients  $\alpha$  and  $\beta$  for the confidence and data terms respectively. Fig. 5 illustrates this experience.

The performance of the algorithms was evaluated using the Peak Signal-to-Noise Ratio (PSNR) and the Structural SIMilarity (SSIM). For an original image  $I_0$  and the reconstructed image  $I_r$ , these two metrics are defined in (20) and (22).

$$PSNR = 10 \cdot \log_{10} \left( \frac{d^2}{MSE} \right) \quad (20)$$

where  $d$  is the dynamics of the original image and MSE is the Mean Square Error. This error is obtained by (21):

$$MSE = \frac{1}{mn} \sum_{i=0}^{m-1} \sum_{j=0}^{n-1} (I_0(i, j) - I_r(i, j))^2 \quad (21)$$

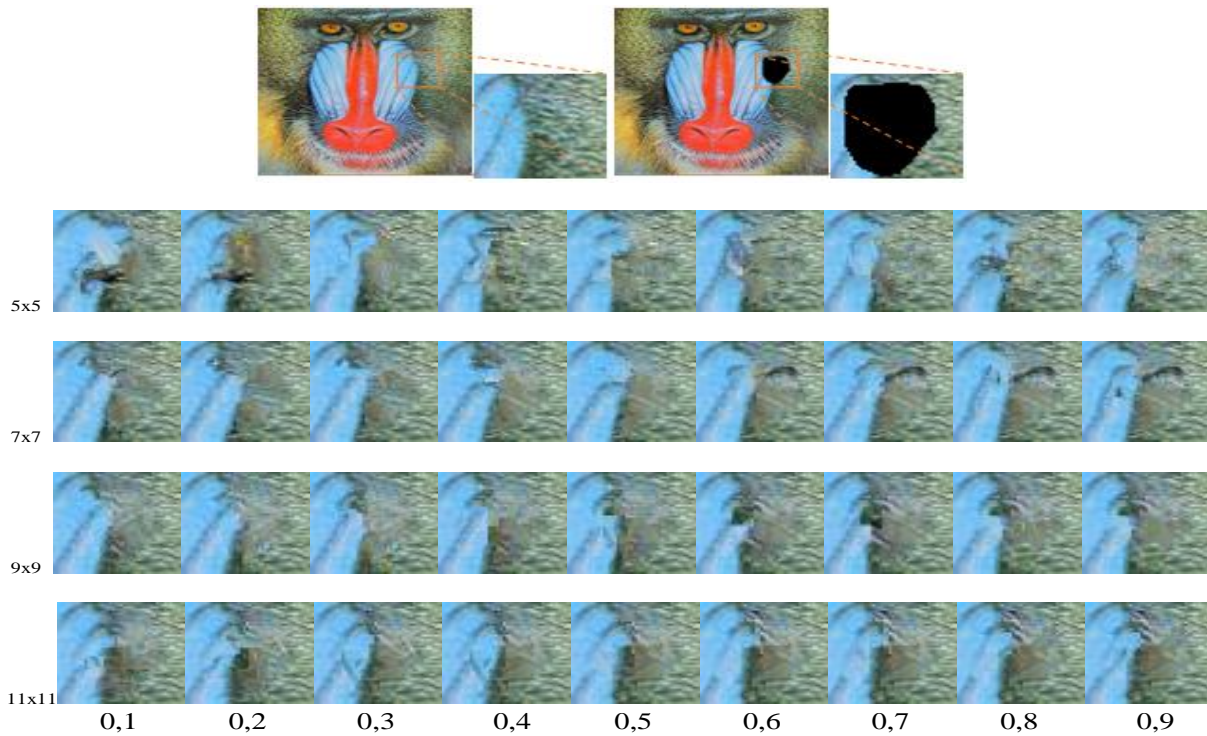


Fig. 5. Images Results of the Baboon Image Inpainting for different Patch Sizes and different Coefficients  $\alpha$  of the Confidence Term.

with  $m$  and  $n$  denoting the number of rows and columns of the images  $I_0$  and  $I_r$ .

$$SSIM(x, y) = \frac{(2\mu_x\mu_y + c_1)(2\sigma_x\sigma_y + c_2)(2cov_{xy} + c_3)}{(\mu_x^2 + \mu_y^2 + c_1)(\sigma_x^2 + \sigma_y^2 + c_2)(\sigma_x\sigma_y + c_3)} \quad (22)$$

with

- $x$  and  $y$  the original  $I_0$  and restored  $I_r$  images respectively;
- $\mu_x, \mu_y$  the respective averages of the images  $x$  and  $y$  ;
- $\sigma_x^2, \sigma_y^2$  their variance;
- $cov_{xy}$  the covariance of  $x$  and  $y$  ;
- $C_1, C_2$  and  $C_3$  the division stabilization variables when the denominator is very low.

The PSNR is used to measure the reconstitution consistency between the restored image and the original image. The SSIM allows to evaluate the visual quality of restoration by comparing the restored image and the original image.

These results show that it is difficult to define the best patch size and coefficient of the confidence term. However, the 9x9 and 11x11 size patches seem to produce the best results. For these patch sizes, coefficients 0.1 to 0.5 give better results. Starting from the observation that the visual aspect alone does not allow us to choose our parameters, we used PSNR and SSIM for the quantitative evaluation. The results are collected in Tables I and II.

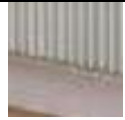

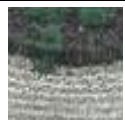
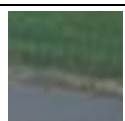
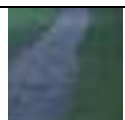
TABLE. I. BABOON IMAGE PSNR RESULTS FOR DIFFERENT PATCH SIZES AND VARIABLE COEFFICIENTS

| $\alpha$ | 5 x 5   | 7 x 7   | 9 x 9         | 11 x 11 |
|----------|---------|---------|---------------|---------|
| 0,1      | 32,6694 | 35,9045 | 36,215        | 35,8816 |
| 0,2      | 34,2809 | 35,3802 | 36,0053       | 35,5391 |
| 0,3      | 36,2197 | 35,8309 | <b>36,919</b> | 36,2681 |
| 0,4      | 34,913  | 36,2447 | 36,8832       | 36,2214 |
| 0,5      | 34,932  | 35,8147 | 36,3861       | 35,7203 |
| 0,6      | 35,3008 | 35,3759 | 34,6359       | 35,0639 |
| 0,7      | 35,7355 | 35,2724 | 35,3292       | 35,2091 |
| 0,8      | 34,1555 | 35,1694 | 35,6763       | 35,1676 |
| 0,9      | 34,3502 | 35,3179 | 35,6818       | 35,3486 |

TABLE. II. BABOON IMAGE SSIM RESULTS FOR DIFFERENT PATCH SIZES AND VARIABLE COEFFICIENTS

| $\alpha$ | 5 x 5  | 7 x 7  | 9 x 9        | 11 x 11 |
|----------|--------|--------|--------------|---------|
| 0,1      | 0,9909 | 0,9923 | <b>0,993</b> | 0,9916  |
| 0,2      | 0,9903 | 0,9922 | 0,9928       | 0,9917  |
| 0,3      | 0,9929 | 0,9923 | 0,9926       | 0,9926  |
| 0,4      | 0,9911 | 0,9922 | 0,9926       | 0,9922  |
| 0,5      | 0,9917 | 0,9926 | 0,9923       | 0,9914  |
| 0,6      | 0,9913 | 0,9921 | 0,991        | 0,9909  |
| 0,7      | 0,9916 | 0,9922 | 0,9912       | 0,991   |
| 0,8      | 0,9912 | 0,9921 | 0,9917       | 0,9909  |
| 0,9      | 0,9916 | 0,9922 | 0,9917       | 0,9911  |

TABLE III. BEST RESULTS F PSNR AND SSIM FOR DIFFERENT IMAGES AND DIFFERENT PATCH SIZES

|   |      | 5x5     | 7x7            | 9x9           | 11x11          |
|---|------|---------|----------------|---------------|----------------|
|  | PSNR | 45,3101 | 45,5046        | 45,918        | <b>46,3161</b> |
|   | SSIM | 0,997   | 0,9973         | <b>0,9974</b> | 0,9973         |
|  | PSNR | 36,2197 | 35,9045        | <b>36,919</b> | 36,2681        |
|   | SSIM | 0,9929  | 0,9926         | <b>0,9930</b> | 0,9926         |
|  | PSNR | 33,4775 | 32,2674        | 33,9514       | <b>34,2936</b> |
|   | SSIM | 0,9809  | 0,981          | <b>0,9818</b> | 0,9808         |
|  | PSNR | 47,4129 | <b>47,6068</b> | 47,5378       | 47,1245        |
|   | SSIM | 0,9972  | <b>0,9975</b>  | 0,9973        | 0,9972         |
|  | PSNR | 41,7133 | <b>44,2778</b> | 43,4745       | 43,764         |
|   | SSIM | 0,9969  | <b>0,9981</b>  | 0,9978        | 0,9975         |

In the PSNR table, the best result is obtained from the coefficient  $\alpha = 0.3$  and the size of the patch  $9 \times 9$ . On the other hand, in the SSIM, the resulting image by applying the coefficient  $\alpha = 0.1$  and the patch size  $9 \times 9$  give the best result. This study was carried out on a set of images with different textures and structures. The best results of PSNR and SSIM for the different patch sizes are summarized in Table III.

This table shows that the best results, for images with more structure, are obtained from  $9 \times 9$  patch sizes. This is perceptible through the three images at the top of Table III. For images containing more homogeneous areas, the  $7 \times 7$  size provides the best results (see the two images at the bottom of Table III).

Thus, for the choice of the  $\alpha$  coefficient, we have classified our set of images into two categories according to their textural and structural characteristics. We applied  $9 \times 9$  size patches to six images containing textured, structured and homogeneous areas. We used  $7 \times 7$  size patches of five other images containing areas that tended to be homogeneous. We varied the  $\alpha$  coefficient from 0.1 to 0.9 and presented the results in Fig. 6 and 7. Fig. 6(a) and 7(a) represent the PSNR results obtained by applying  $7 \times 7$  and  $9 \times 9$  patches respectively according to the structural information of the images. The SSIM ones are represented by Fig. 6(b) and 7(b).

Through the results of the PSNR and SSIM, the choice of the best coefficient remains difficult. However, the 0.5 coefficient seems to be close to the best for  $7 \times 7$  size patches and 0.4 for  $9 \times 9$  size patches. Thus, we opt for the choice of  $\alpha = 0.5$  and the  $7 \times 7$  size patch when the area to be restored has fewer textures and structures. Otherwise, we choose  $\alpha = 0.4$

and the patch size  $9 \times 9$ . This imposes the values of 0.5 and 0.6 for  $\beta$  respectively (11).

### B. Results and Evaluations

In practice, it is difficult to quantitatively evaluate the result of image restoration using an inpainting method. Indeed, to perform the quantitative evaluation, it is necessary to know the original image that has not been damaged in order to determine the similarity with the restored image. Thus, our experiments will be carried out in two phases. The first concerns a set of images for which the information in the background of the area to be reconstructed is unknown. Fig. 8 and 9 illustrate this experience. In these cases, it is a subject of object removal. The evaluation is visual and therefore subjective. For an objective evaluation, we carried out the second phase of our experiments. We have selected other images in which we have inserted a task to remove. Fig. 10 to 17 present the results of this experiment. In Fig. 10 to 12, we also represented the evolution curves of the confidence terms and priority functions according to the number of iterations to show the influence of the product and the weighted sum on the evolution of the priority function. These curves also show the influence of the evolution of the confidence term on the shape of the priority function. We used the PSNR and SSIM to conduct the quantitative evaluation.

Table IV represents the comparative results of our algorithm with those of Criminisi and Nan.

### C. Discussions

Fig. 8(c) to 8(e) are the inpainting results of the Criminisi, Nan and our algorithm respectively. The sections framed in red show the discussion areas of the three methods. We can see reconstruction defects at the bottom of the roof. In the Criminisi and Nan results, the defects are reflected in the appearance of certain plants on the roof. In our results, we can see a better reconstitution of the roof. The reconstruction of the shoreline seems to be of good quality for both our method and Nan's method, unlike Criminisi's result. In Fig. 9, we see a big difference in the background restoration. Our method seems to better reconstruct the information in the background of the removed tree. In the Criminisi and Nan results, however, there are abnormal earth blocks in the background of the tree.

The graphs obtained in Fig. 10(f), 11(f) and 12(f) show the rapid decrease in the confidence term proposed by Criminisi. This decrease, combined with the use of the product of the confidence and data terms, justifies the near-zero values of the priority function observed in Fig. 10(g), 11(g) and 12(g). This makes it difficult to determine the priority patch. Similarly, at the level of the algorithm proposed by Nan, the values of the confidence term are almost constant per interval or increase per place. This is due to the shape of an inverted parabola of the curve of the update confidence term. In the case where the values of the confidence term are constant, only the data term influences the priority function. This causes the observed oscillations around the same value of the priority function. This can have a negative impact on the reconstitution of textures.

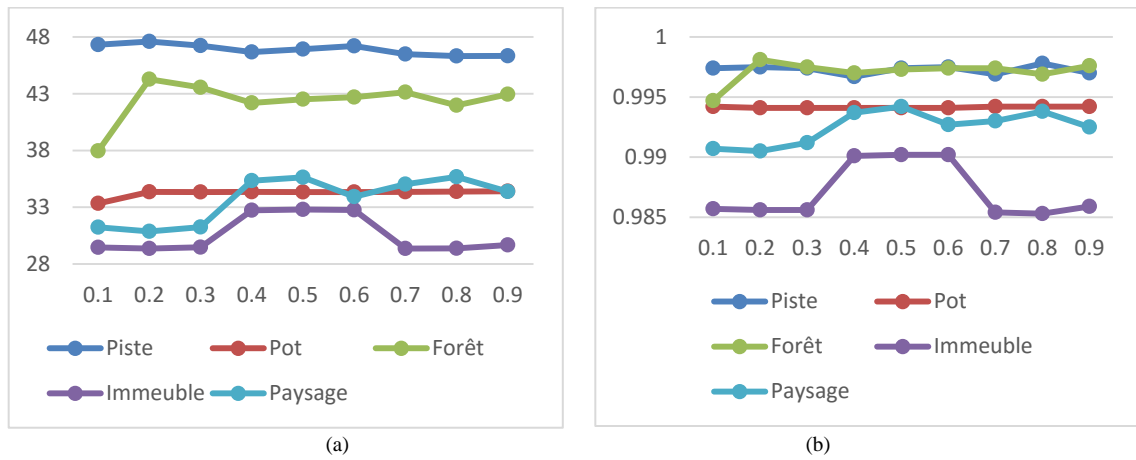


Fig. 6. Representation of PSNR and SSIM for different Coefficients  $\alpha$  for 7x7 size Patches. (a) PSNR Graphs; (b) SSIM Graphs.

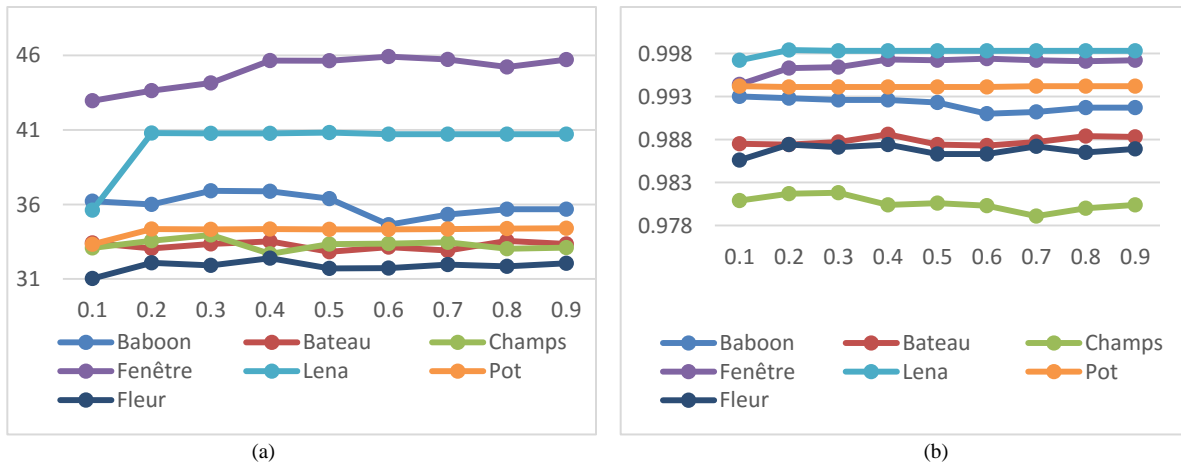


Fig. 7. Representation of PSNR and SSIM for different Coefficients  $\alpha$  for 9x9 Size Patches. (a) PSNR Graphs; (b) SSIM Graphs.

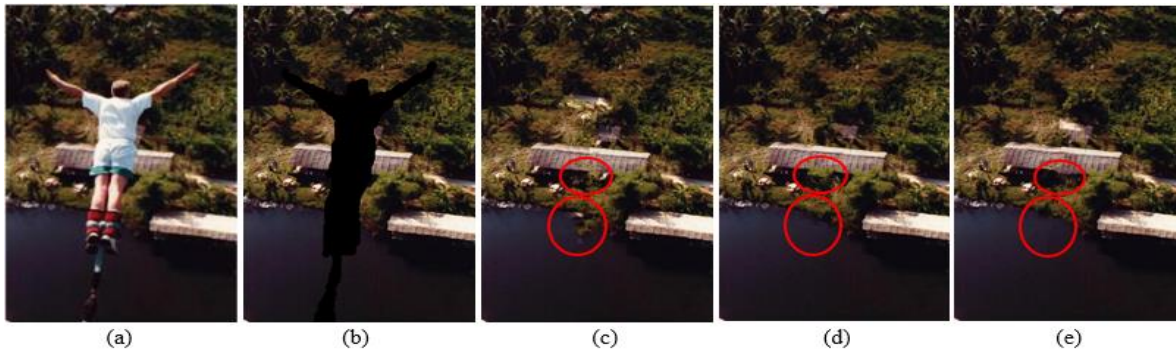


Fig. 8. Inpainting Result of "Bungee". (a) Original Image; (b) Masked Image; (c) Criminisi Result; (d) Nan Result; (e) our Result.

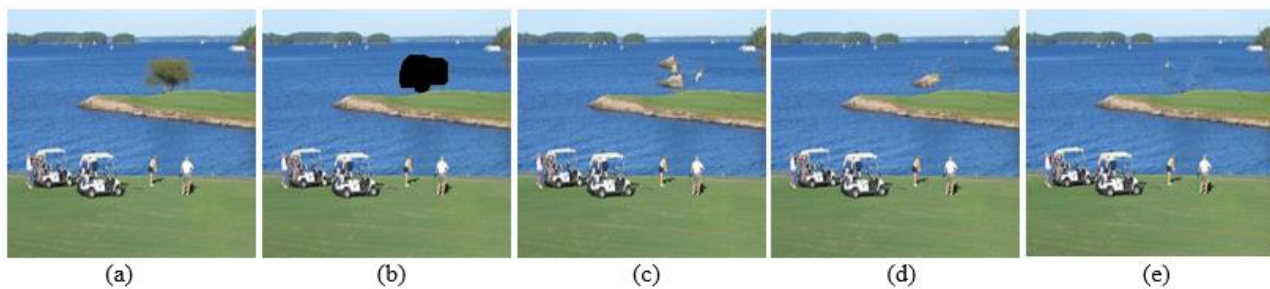


Fig. 9. Inpainting Result of "Island". (a) Original Image; (b) Masked Image; (c) Criminisi Result; (d) Nan Result; (e) Our Result.

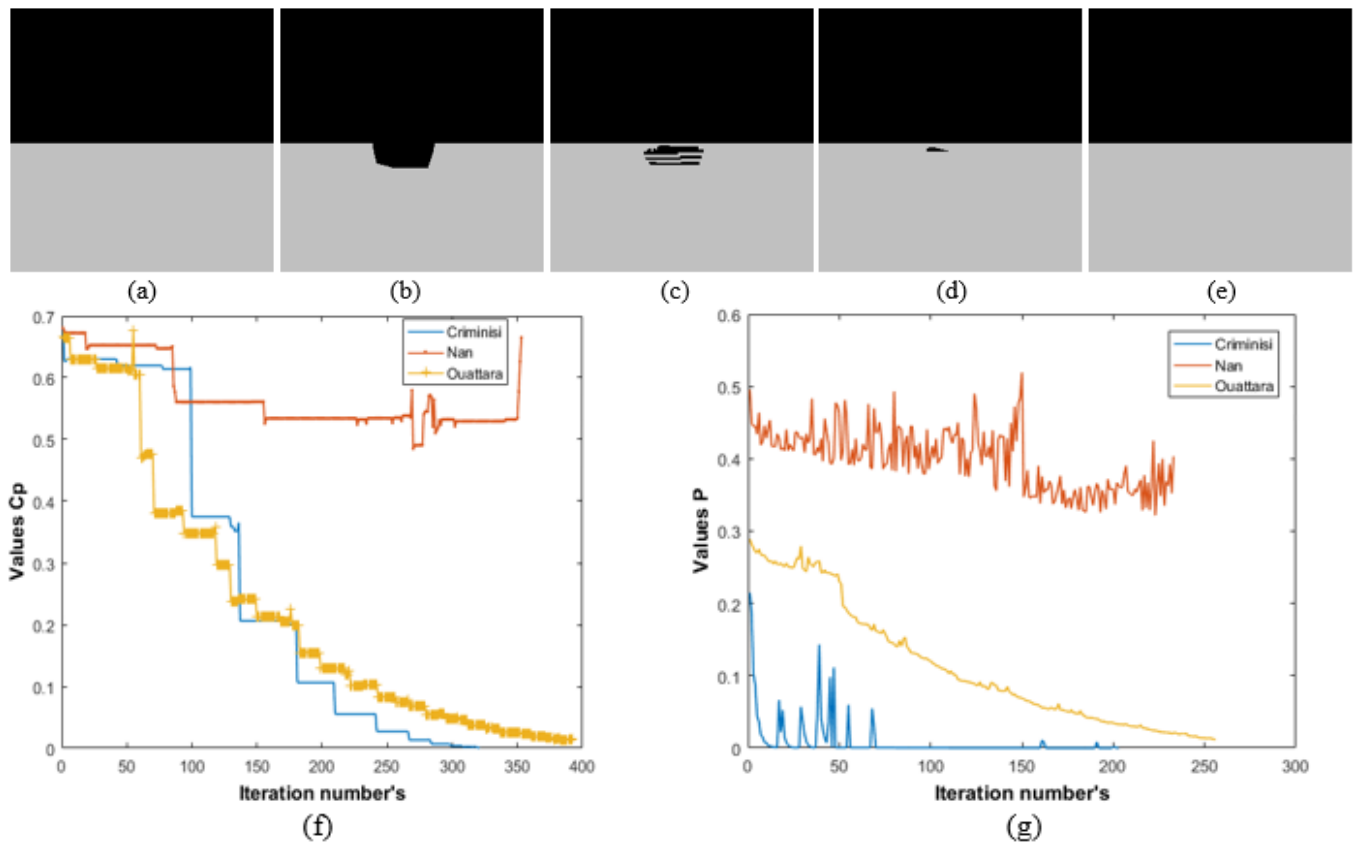


Fig. 10. Synthesis Image Inpainting Results. (a) Original Image; (b) Masked Image; (c) Criminisi Result; (d) Nan Result; (e) Our Result; (f) C(p) Values; (g) P(p) Values.

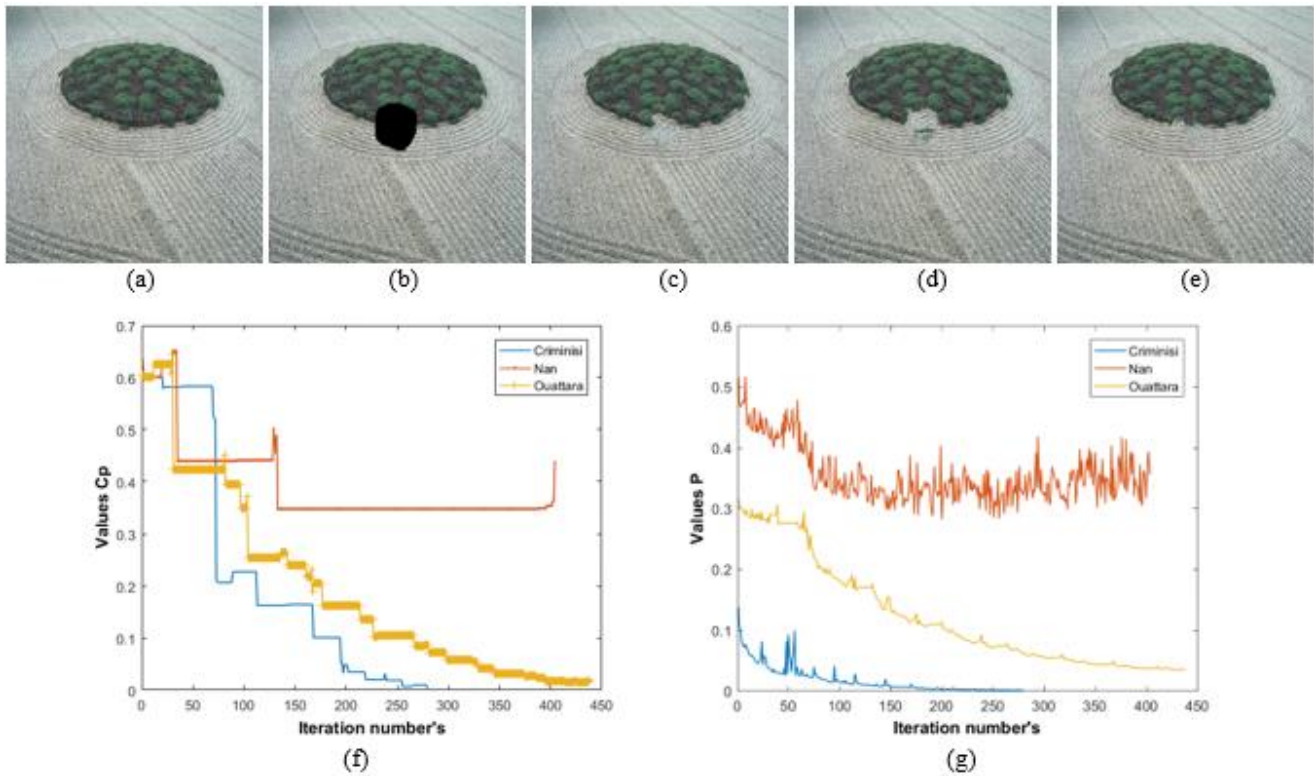


Fig. 11. Inpainting Result of "Nursery Garden". (a) Original Image; (b) Masked Image; (c) Criminisi Result; (d) Nan Result; (e) Our Result; (f) C(p) Values; (g) P(p) Values.



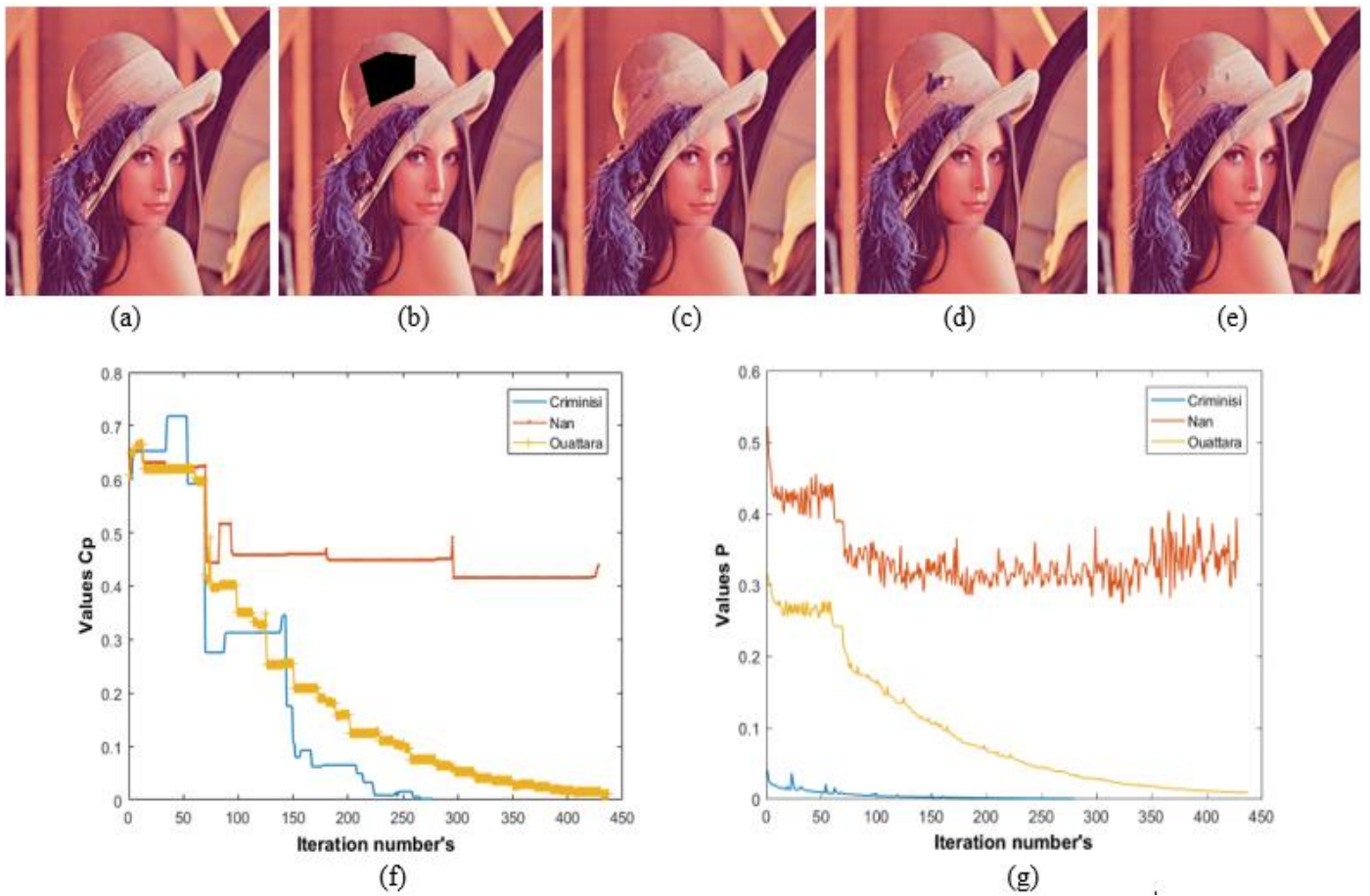


Fig. 12. Inpainting Result of “Lena”. (a) Original Image; (b) Masked Image; (c) Criminisi Result; (d) Nan Result; (e) Our Result; (f) C(p) Values; (g) P(p) Values.

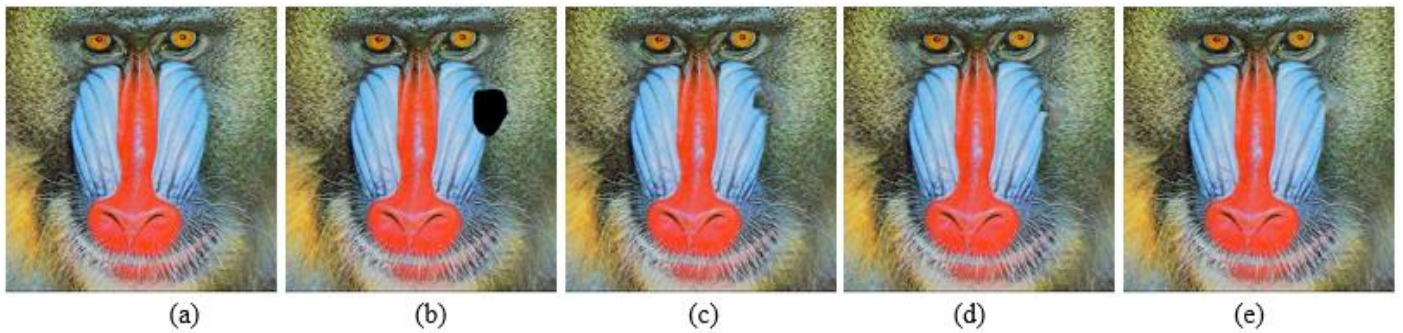


Fig. 13. Inpainting Result of “Baboon”. (a) Original Image; (b) Masked Image; (c) Criminisi Result; (d) Nan Result; (e) Our Result.



Fig. 14. Inpainting Result of “Shang Dynasty Bronze Cooking Tripod”. (a) Original Image; (b) Masked Image; (c) Criminisi Result; (d) Nan Result; (e) Our Result.



Fig. 15. Inpainting Result of “Radiator”. (a) Original Image; (b) Masked Image; (c) Criminisi Result; (d) Nan Result; (e) Our Result.

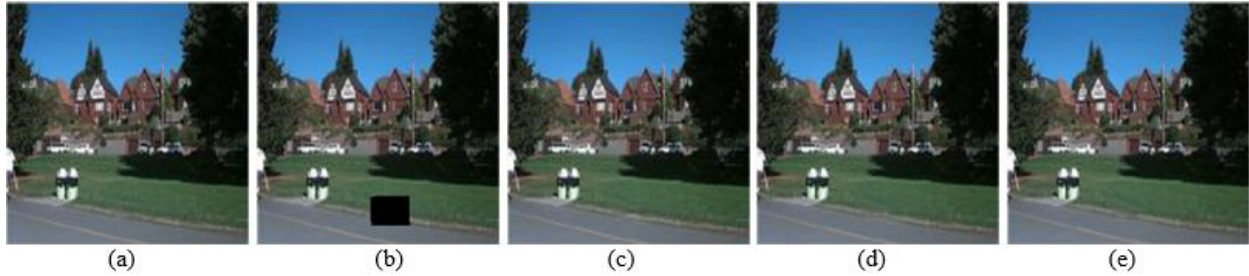


Fig. 16. Inpainting Result of “Runway”. (a) Original Image; (b) Masked Image; (c) Criminisi Result; (d) Nan Result; (e) Our Result.



Fig. 17. Inpainting Result of “Forest”. (a) Original Image; (b) Masked Image; (c) Criminisi Result; (d) Nan Result; (e) Our Result.

TABLE IV. PSNR AND SSIM RESULTS

|                                     |      | Criminisi | Nan           | Ours           |
|-------------------------------------|------|-----------|---------------|----------------|
| Nursery garden                      | PSNR | 30,6118   | 27,9657       | <b>32,6820</b> |
|                                     | SSIM | 0,9796    | 0,9785        | <b>0,9804</b>  |
| Synthesis                           | PSNR | 25,0545   | 42,1786       | $\infty$       |
|                                     | SSIM | 0,9838    | 0,9983        | <b>1,000</b>   |
| Baboon                              | PSNR | 31,9447   | 35,5832       | <b>36,8832</b> |
|                                     | SSIM | 0,9877    | 0,9918        | <b>0,9926</b>  |
| Boat                                | PSNR | 33,2237   | 31,5973       | <b>33,5203</b> |
|                                     | SSIM | 0,9867    | 0,9854        | <b>0,9886</b>  |
| Radiator                            | PSNR | 43,1780   | 43,2911       | <b>45,6559</b> |
|                                     | SSIM | 0,9952    | 0,9963        | <b>0,9973</b>  |
| Shang Dynasty bronze cooking tripod | PSNR | 29,4801   | 28,0416       | <b>34,347</b>  |
|                                     | SSIM | 0,9728    | 0,9756        | <b>0,9941</b>  |
| Runway                              | PSNR | 44,7967   | 46,6525       | <b>46,9254</b> |
|                                     | SSIM | 0,9961    | 0,9969        | <b>0,9975</b>  |
| Flower                              | PSNR | 30,0323   | 31,9666       | <b>32,3962</b> |
|                                     | SSIM | 0,9858    | <b>0,9880</b> | 0,9874         |
| Forest                              | PSNR | 43,7404   | 42,0271       | <b>44,2778</b> |
|                                     | SSIM | 0,9975    | 0,9962        | <b>0,9981</b>  |
| Building                            | PSNR | 31,0260   | 31,4830       | <b>32,7926</b> |
|                                     | SSIM | 0,9891    | 0,9889        | <b>0,9902</b>  |
| Landscape                           | PSNR | 32,5483   | 33,9106       | <b>35,6248</b> |
|                                     | SSIM | 0,9880    | 0,9925        | <b>0,9942</b>  |

The curves obtained from our algorithm effectively show a slower decrease in the confidence term than the Criminisi one and their non-convergence at zero. Also, this same decrease can be observed in the curves of the priority function.

From Table IV, we can see that our method provides better results than the Criminisi and Nan algorithms. Indeed, the higher the PSNR and SSIM are, the better the result of inpainting is. The difference between the quality of our inpainting results and those of other methods is visible in Fig. 10 to 17.

## V. CONCLUSION

In this work, we proposed an improvement of the inpainting algorithms based on the exemplar. We proposed a new priority function based on the weighted sum of its component terms and a new approach to calculating the data term. Our data term takes into account all the structural information of the patch and not the structural information related only to the central pixel of the patch. We have redefined the function of confidence term update to slow down its decrease and avoid its convergence towards zero. Our method generally gives better results than the literature. This is noticeable both visually and in relation to PSNR and SSIM.

We also carried out a study to select the patch size and coefficients of confidence and data terms based on the structural information of the area to be reconstructed. This study made it possible to establish a correspondence between the chosen size and the different coefficients. This correspondence is based on the structural information surrounding the area to be restored. However, this field remains open and can be improved. Thus, in our future work, we will deepen the search for the best coefficients of confidence and data terms with respect to patch size and structural information.

## REFERENCES

- [1] Y. Gao et al., 'Dynamic Searching and Classification for Highlight Removal on Endoscopic Image', *Procedia Computer Science*, vol. 107, pp. 762–767, 2017.
- [2] S. M. Alsaleh, A. I. Avilés, P. Sobrevilla, A. Casals, and J. K. Hahn, 'Automatic and robust single-camera specular highlight removal in cardiac images', 2015 37th Annual International Conference of the IEEE Engineering in Medicine & Biology Society (EMBC), pp. 675–678, 2015.
- [3] S. M. Alsaleh, A. I. Aviles, P. Sobrevilla, A. Casals, and J. K. Hahn, 'Adaptive segmentation and mask-specific Sobolev inpainting of specular highlights for endoscopic images', in 2016 38th Annual International Conference of the IEEE Engineering in Medicine and Biology Society (EMBC), 2016, pp. 1196–1199.
- [4] S. M. Alsaleh, A. I. Aviles, P. Sobrevilla, A. Casals, and J. Hahn, 'Towards robust specular detection and inpainting in cardiac images', in *Proc. SPIE, 9786, Medical Imaging 2016: Image-Guided Procedures, Robotic Interventions, and Modeling*, p. 97861Q.
- [5] C. Guillemot and O. Le Meur, 'Image Inpainting : Overview and Recent Advances', *IEEE Signal Processing Magazine*, vol. 31, no. 1, pp. 127–144, Jan. 2014.
- [6] O. Le Meur and C. Guillemot, 'Super-Resolution-Based Inpainting', in *Computer Vision – ECCV 2012*, vol. 7577, A. Fitzgibbon, S. Lazebnik, P. Perona, Y. Sato, and C. Schmid, Eds. Berlin, Heidelberg: Springer Berlin Heidelberg, 2012, pp. 554–567.
- [7] J. Zeng, X. Fu, L. Leng, and C. Wang, 'Image Inpainting Algorithm Based on Saliency Map and Gray Entropy', *Arabian Journal for Science and Engineering*, vol. 44, no. 4, pp. 3549–3558, Apr. 2019.
- [8] S. Masnou and J.-M. Morel, 'Level lines based disocclusion', in *Proceedings 1998 International Conference on Image Processing. ICIP98 (Cat. No.98CB36269)*, Chicago, IL, USA, 1998, vol. 3, pp. 259–263.
- [9] Bertalmio, G. Sapiro, V. Caselles, and C. Ballester, 'Image inpainting', in *Proceedings of the 27th annual conference on Computer graphics and interactive techniques*, 2000, pp. 417–424.
- [10] J. Shen and T. F. Chan, 'Mathematical Models for Local Nontexture Inpaintings', *SIAM Journal on Applied Mathematics*, vol. 62, no. 3, pp. 1019–1043, Jan. 2002.
- [11] D. Tschumperlé, 'Fast Anisotropic Smoothing of Multi-Valued Images using Curvature-Preserving PDE's', *Int J Comput Vision*, vol. 68, no. 1, pp. 65–82, Jun. 2006.
- [12] A. Criminisi, P. Perez, and K. Toyama, 'Region Filling and Object Removal by Exemplar-Based Image Inpainting', *IEEE Transactions on Image Processing*, vol. 13, no. 9, pp. 1200–1212, Sep. 2004.
- [13] A. Nan and X. Xi, 'An improved Criminisi algorithm based on a new priority function and updating confidence', in 2014 7th International Conference on Biomedical Engineering and Informatics, Dalian, China, 2014, pp. 885–889.
- [14] P. Yuan, X. Gong, S. Cao, J. Y. Guo, C. Y. Wang and H. M. Zou, 'A Modified Exemplar based Inpainting Algorithm', *CRSSC-CWI-CGRc*, 2010.
- [15] Z. Hou, 'Criminisi Image Concealment Algorithm Based on Priority Function and Blocking Matching Principle', *Revista Tecnica De La Facultad De Ingenieria Universidad Del Zulia*, vol. 39, no. 9, pp. 203–209, Dec. 2016.
- [16] P. Buysens, M. Daisy, D. Tschumperle, and O. Lezoray, 'Exemplar-based Inpainting: Technical Review and new Heuristics for better Geometric Reconstructions', *IEEE Transactions on Image Processing*, vol. 24, no. 6, pp. 1809–1824, Mar. 2015.
- [17] Q. Zhang and J. Lin, 'Exemplar-Based Image Inpainting Using Color Distribution Analysis', *Journal of Information Science and Engineering*, vol. 28, no. 4, pp. 641–654, 2012.
- [18] H. Ying, L. Kai, and Y. Ming, 'An Improved Image Inpainting Algorithm Based on Image Segmentation', *Procedia Computer Science*, vol. 107, pp. 796–801, Jan. 2017.
- [19] A. A. Efros and T. K. Leung, 'Texture synthesis by non-parametric sampling', in *Proceedings of the Seventh IEEE International Conference on Computer Vision, Kerkyra, Greece, 1999*, pp. 1033–1038 vol.2.
- [20] Y. Chi, N. He, and Q. Zhang, 'A Fast Image Restoration Method Based on an Improved Criminisi Algorithm', *Journal of Computers*, vol. 12, no. 6, p. 11, 2017.
- [21] A. Li, Y. Li, W. Niu, and T. Wang, 'An improved criminisi algorithm-based image repair algorithm', in 2015 8th International Congress on Image & Signal Processing (CISP), Shenyang, China, 2015, pp. 263–267.
- [22] L.-J. Deng, T.-Z. Huang, and X.-L. Zhao, 'Exemplar-Based Image Inpainting Using a Modified Priority Definition', *PLOS ONE*, vol. 10, no. 10, p. e0141199, Oct. 2015.
- [23] D. Lei, J. Dai-Hong, D. Bin, and J. K. Hahn, 'Improved Digital Image Restoration Algorithm Based on Criminisi', *Journal of Digital Information Management*, vol. 14, no. 5, p. 9, 2016.
- [24] G. Ma, 'Inpainting technology in art pictures based on edge and texture feature', *Journal of Interdisciplinary Mathematics*, vol. 21, no. 5, pp. 1199–1203, Jul. 2018.
- [25] S. Yuheng and Y. Hao, 'Image Inpainting Based on a Novel Criminisi Algorithm', arXiv:1808.04121 [cs], Aug. 2018.
- [26] J. Y. Wu and Q. Q. Ruan, 'Object Removal By Cross Isophotes - Exemplar-based Inpainting,' *The 18th International Conference on Pattern Recognition*, vol. 3, pp. 810–813, 2006.
- [27] X. Xi, F. Wang, and Y. Liu, 'Improved Criminisi Algorithm Based on a New Priority Function with the Gray Entropy', in 2013 Ninth International Conference on Computational Intelligence and Security, 2013, pp. 214–218.
- [28] L. Yin and C. Chang, 'An effective exemplar-based image inpainting method', in 2012 IEEE 14th International Conference on Communication Technology, 2012, pp. 739–743.

# Improving Knowledge Sharing in Distributed Software Development

Sara Waheed<sup>1</sup>, Bushra Hamid<sup>2</sup>, NZ Jhanjhi<sup>3</sup>, Mamoona Humayun<sup>4</sup>, Nazir A Malik<sup>5</sup>  
Department of Information Technology, PMAS Arid Agriculture University, Rawalpindi, Pakistan<sup>1,2</sup>  
School of Computing & IT (SoCIT), Taylor's University, Subang Jaya, Selangor, Malaysia<sup>3</sup>  
College of Computer and Information Science (CCIS), Jouf University Al-Jouf, Saudi Arabia<sup>4</sup>  
Department of Computer Science, Bahria University, Islamabad, Pakistan<sup>5</sup>

**Abstract**—Distributed Software Development has become an established software development paradigm that provides several advantages but it presents significant challenges to share and understand the knowledge required for developing software. Organizations are expected to implement appropriate practices to address knowledge management. From the existing studies, it is been analyzed that there were problems of collaboration between distributed team members which effects knowledge sharing. Documentation problem (such as missing, poor and outdated documents) and knowledge vaporization (as much of the conversation and communication is done via chat and retrieving it later is a great headache) is a major challenge in Distributed Software Development in knowledge sharing. Our main objective is to improve knowledge sharing between distributed team members and prevent knowledge vaporization and reduced documentation problem that will help in improving software development process in a distributed environment. To eliminate these challenges we proposed a framework which deals with documentation and knowledge vaporization problems and evaluated it through industrial case study and evaluate the framework performance in real-life context where actually the problem arises, we conducted the interviews and analyzed the data using thematic analysis and SUS questioner we came to the conclusion on team members response that they are satisfied with our proposed solution and it improved their knowledge sharing process. Our intention was to improve the knowledge process with our proposed solution and the evaluation showed that we resolved these problems.

**Keywords**—Distributed software development; knowledge sharing; knowledge management

## I. INTRODUCTION

From few decades' creation maintenances and development of software become advanced from being centralized (at one location) to being dispersed at several locations [1], in distributed development teams are scattered geographically at multiple sites while working on the same product this concept is known as Distributed Software Development (DSD). Multiple sites include a different location such as different cities in the same country or it may be scattered along with the globe. DSD offers numerous benefits such as intense resource pool, reduction in cost, less resource consumption, variety of different skills and expertise around the world and continuous working around the clock. These benefits overall increase the quality of the software products [29]. Along with the several advantages of DSD, it brings numerous challenges that are

geographically distributed teams may encounter such as product quality compromise due to team dispersion, Coordination, Communication and Collaboration challenges, lack of face to face communication leads to non-trust worthy behavior [2] and not sharing required knowledge. Many techniques support DSD approach and literature presented numerous ways to tackle these challenges but still, there is a need of enhancement in some areas such as knowledge management many existing techniques address knowledge sharing but it lacks to some extent.

Knowledge management is considered to be the most required resource of an organization [1]. Knowledge can be explained as "Knowledge, while made up of data and information, can be thought of as much greater understanding of a situation, relationships, causal phenomena, and the theories and rules (explicit and implicit both) that underlie a given domain or problem" [30]. Knowledge management is considered to be a very vast field, it provides ways to share knowledge and aids in increasing mutual understanding solves collaboration and coordination challenges [3]. In an organization lots of knowledge resides in different software processes, activates, organizational assets and methodologies, environment, knowledge reside in team members mind. It is very important to share and transfer the knowledge to deliver the product to the customer which he/she requested knowledge is needed to be managed shared and transferred from the beginning to the end of SDLC (software development life cycle) [4].

When the teams are geographically distributed they need to share knowledge in explicit form for that documentation plays an important role but in distributed development, there is a lack of proper documentation [5], [6]. Most of the organization in these days are using agile approaches which does not support many docsumentation [7], [8] and they also focus on sharing tacit knowledge there is a lack of creating and maintaining explicit knowledge much of the product knowledge remains in source code, test files, documentation remains outdated as regard to the project the dispersed team members need proper documentation for understanding the product knowledge incomplete and abstract documents are not enough for effective knowledge sharing from the literature documentation problems (such as poor, missing and outdated documentation) is identified [5], [6], [9]. Also agile and distributed development often clashes due to their distant nature.

Alongside documentation problem another issue is knowledge vaporization local team members and remote team members need to communicate to work together on the same project much of the knowledge is existing in electronic media such as during chat retrieving this knowledge is not easy because it's not easily accessible at one place [7], [8], [10]. So our main focus is to reduce these issues to facilitate knowledge sharing in distributed development. In this paper, our main objective is to improve knowledge sharing between distributed team members and prevent documentation problem and knowledge vaporization it will help in improving Software Development Process in a distributed environment and help to get more advantages of DSD. Therefore our study aimed to explore the following research questions:

RQ1: What are the existing knowledge exchange/sharing mitigation strategies in distributed development?

RQ2: What are the knowledge exchange/sharing issues and challenges in distributed software development?

RQ3: Does the proposed solution overcome the knowledge vaporization and documentation problem in distributed software development?

In the next sections we will present a literature review and then we will propose our solution and we will present its evaluation and results followed by limitation, future work and conclusion of the study.

## II. LITERATURE REVIEW

In DSD multiple sites are involved in the development of a certain product, DSD does not necessarily require multiple number of organization, there can be one organization with different branches that can be located in different cities either in one country or in different countries when the organizations are from around the globe there is a time zone difference as well as cultural diversity arises because one organization share the same culture where as multiple organizations do not share the same culture, traditions and languages. So DSD provides versatility in team members. In DSD the situation becomes more problematic when the multiple team members from different culture, language, time zone, and geographical locations works at the same project [1], [2] communications and collaboration among team members become a challenge and knowledge sharing in this scenario seems totally impossible.

In our research, our main focus is on knowledge sharing when the teams are geographically distributed. The knowledge management process includes knowledge creation, knowledge store and retrieval, knowledge sharing and knowledge application. Knowledge is categorized into two different levels explicit knowledge and tacit knowledge. The Explicit type of knowledge is in countable form like a written document, books, any material which is in physical form, explicit knowledge is easy to transfer, whereas tacit knowledge is the knowledge resides in peoples mind, they can include skills, thoughts, ideas, perceptions, values, and faiths so it is very hard to share this type of knowledge [1], [11]. Knowledge sharing is the process to transfer the knowledge of source to the

destination. The source and destination can be anything like individual groups within the same company or different companies where the team members are scattered [12]. Knowledge sharing is very essential for project success and for teams to work together. And it is one of the key domain being affected by the DSD. As the base of developing software relies on sharing knowledge, and whose success factor is wholly based on practical sharing of knowledge around software developers of distributed teams. The most complicated phase is to share both explicit and tacit knowledge among the geographically distributed teams. In study [13], [14], knowledge sharing is considered to be the essential process of knowledge management. In DSD vendors usually have the knowledge and technical expertise of a project, while the clients hold the requisite and application domain knowledge. If the clients and vendors are unable to share the product knowledge, the clients may not suitably supply requirements related to business and products domain so in the absence of knowledge understating of the vendors without proper domain knowledge causes negative effect on product development and they cannot effectively and efficiently use their skills and technical expertise to build the product effectively [15].

The use of approaches in Agile and importance on tacit communication may perhaps negatively affect creating and maintaining knowledge which is explicit [16], [17]. According to studies [5], [17] describes much of the project knowledge remained scattered in test cases and source code, documents are not synced with the required and updated information which is the reason for misunderstanding between distributed teams who are looking for accurate knowledge. These studies [5], [6], [16], [17], [18], [19], [20], [21] shed light on the effect of the absence of proper and consistent documentation on knowledge sharing in a distributed environment. Abstract requirement description was not sufficient for offshore teams it's another reason for causing misunderstanding [21], [22]. Study [21] Identified that requirements are written informally on personal notebooks and whiteboards; this method found considered improper and forbid knowledge transfer properly because it was difficult for teams in offshore to make social relations with the users in business [21]. Also most of the companies in today's era are using agile methodology for software development, agile focuses more on short iteration and source code and less attention is paid to documents [7], [8], whereas in DSD where teams are geographically distributed they need to share the knowledge on a daily basis for that they use synchronous and asynchronous means for communication. Most of the communication is done via chats, emails, video conferencing there is major issue of knowledge vaporization because in many informal chats some important conversations happen which becomes difficult to remember at the time of need or when we want to retrieve it. Knowledge vaporization is a major challenge because much of the knowledge is available in unstructured electronic media retrieving this knowledge is not easy because it's not easily accessible and a time consuming process [7], [8], [20], [23], [24], [25]. There are some knowledge sharing challenges and their mitigation strategies are identified from the literature and its answers RQ1 and RQ2 [6], [9] and presented in Table I.

TABLE. I. KNOWLEDGE SHARING CHALLENGES AND APPROACHES

| Knowledge Sharing challenges in Distributed Software Development   | Knowledge Sharing Approaches in Distributed Software Development   |
|--|--|
| Ch1: Knowledge sharing expenditure<br>Ch2: Workers turnover rate<br>Ch3: Lower priority recognition to sharing knowledge activities<br>Ch4: Structural hierarchy<br>Ch5: Ambiguous characterization of roles and responsibilities<br>Ch6: Problems in documentation<br>Ch7: The difference of contextual settings<br>Ch8: Variation in educational and technical expertise<br>Ch9: Social impediments, contextual and social impediments<br>Ch10: Technological and Organizational impediments<br>Ch11: Knowledge vaporization<br>Ch12: Flaws in retaining group awareness<br>Ch13: Technology and cultural impediments<br>Ch14: Knowledge storing issue<br>Ch15: Lack of knowledge awareness mechanisms<br>Ch16: Communication barriers due to distance | AP1: Bonus and motivation<br>AP2: Short term collocation<br>AP3: Flexible communication structure<br>AP4: Understandable work-structure<br>AP5: Combined work between sites<br>AP6: The documentation problem<br>AP7: Confirming common understanding between sites<br>AP8: The usage of boundary spanning roles<br>AP9: Forming virtual communities of practice<br>AP10: Continuous knowledge transfer process in the organizations<br>AP11: Knowledge sharing in agile virtual teams<br>AP12: Providing groupware<br>AP13: Success model for knowledge management<br>AP14: Efficient storage of knowledge<br>AP15: Novel Expertise and solutions<br>AP16: Raising team qualification and expertise |

### III. PROPOSED FRAMEWORK

The framework is presented in Fig. 1. In our research we provide a solution for poor, missing, outdated documentation problem and knowledge vaporization in dispersed teams. Our framework deals with poor documentation problem by creating documents artefacts (product specification, design specification, development handbook, etc.), missing documentation is facilitated by identifying related documents of the projects, outdated documentation facilitated by the syncing mechanism so that every team member have the latest document at their workstation, knowledge vaporization is facilitated by tagging mechanism following are the main phases of framework.

#### A. Actors Layer

Actor's layer characterizes the arrangement of the distributed teams and interactions. In DSD there are onshore and offshore companies working together on a product, developers and managers act as the main actors for sharing the artefacts. These artefacts are linked with the actors as there is a client or vendor team working in site A and their offshore vendor team working at site B. So the developers and managers at site A use their own product specification and design specification artefacts and share them because they are collocated and they do not need to share with the vendor team at site B, Then the managers at site A prepare product specification and design specification artefacts for vendor team developers and managers at site B which is specifically prepared for them and shared between developer and managers at site B and manager of site A. Information architecture and development handbook artefacts shared between remote location's developers and manager.

#### B. Artefacts Layer

To deal with the poor documentation artefact based knowledge sharing technique will resolve the problem of poor documentation. Software Engineering is typically assisted by a

broad diversity of artefacts that documents numerous knowledge types concerning to the software product being created or maintained. Software documentation plays a very vital role in sharing of knowledge especially when the teams are geographically distributed and there is no way of face to face interaction opportunity so in this case, the teams rely heavily on documentation to develop a common understanding about the product being developed. As agile practices are becoming famous and adopted by many firms agile practices promote and focuses on creating executables artefacts such as source code rather than producing artefact that documents the knowledge about requirements, architecture and design decisions. We classified the artefacts as architectural information specification document, product specification document, and design specification document and development standards handbook. Summary of these documents is given in Table II.

TABLE. II. AN OVERVIEW OF DOCUMENT TYPES

| Document Artefacts                              | Description  |
|---|--|
| Architecture Information Specification Document | Contains snapshots drawings and sketches of flow of information with relevant reviews and comments. Represents user interface, business processes and business domain knowledge. |
| Product Specification Document                  | Contains business logics and functional requirements of the product.   |
| Design specification Document                   | Contains design's detailed solution e.g. data models reports, formats, field mapping, structures of database etc   |
| Development Standard Handbook                   | Contains architectural information and solutions, quality checks, naming conventions, coding standards, database design rules, tools configurations, repository configurations.  |

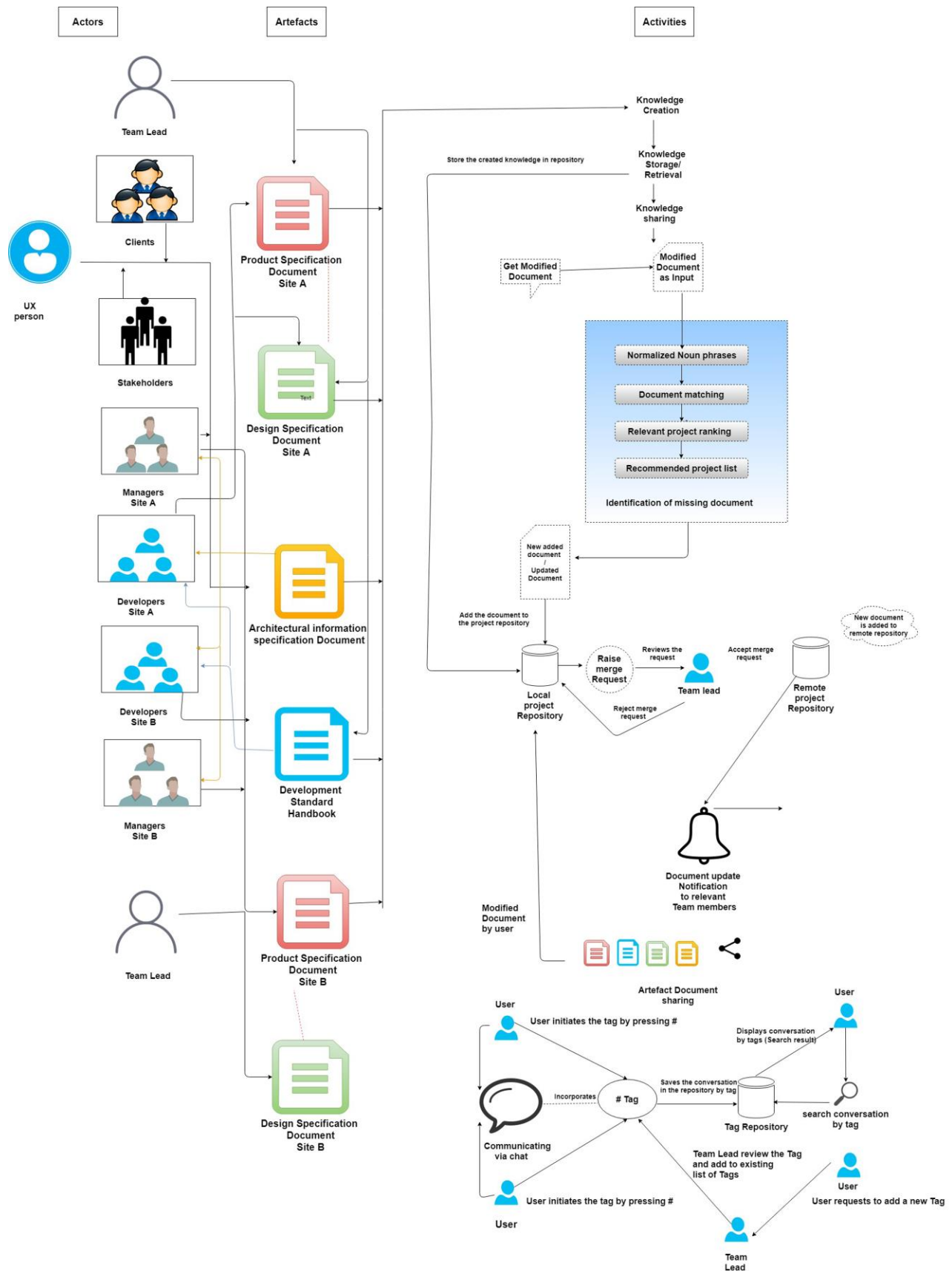


Fig. 1. Proposed Framework

### C. Activity Layer

- **Knowledge Management Process:** Knowledge management process include knowledge creation, retrieval, sharing and knowledge application. Our main focus is on knowledge sharing process because the development style we choose is not central it is distributed the teams are geographically scattered at different locations they need to share the extensive amount of knowledge to develop a software product.
- **Identification of missing documents:** There is a possibility that some team member create document in a untracked directory and forgot to upload it so our framework will provide a mechanism to resolve this issue it identifies the relevant document and notifies the team member about the relevant document which may be needed for the desired project following are the steps:

1) *Normalized noun phases:* Noun phases will be used in the documentation as a feature for matching to a relevant project The noun phrases are annotated and normalized by applying a variety of Natural Language Processing (NLP) techniques to mine the input text and generates all relevant annotations, including sentence boundaries, tokenization, part-of-speech tags, and phrase chunking. Noun phrases are extracted based on a relatively simple pattern of part-of-speech (POS) tag sequences.

2) *Document matching:* The Okapi BM25 algorithm is used frequently for matching it is a technique of information retrieval. The matching document is ranked conferring to their relevance to a given document. The input will be a document which is recently modified in the system this modified document will be considered the document as input and the output contains the ranked project which mostly matches with the software project along with the scores which were based on the input document text. We converted the document text into normalizing noun phase's annotations for the matching algorithm.

3) *Relevant project ranking:* The Okapi BM25 can be described as below: Given an input text Q, containing noun phrases  $q_1, q_2, \dots, q_n$ , the BM25 score of a paper D is: Where,  $f(q_1, d)$  is  $q_1$ 's frequency in

$$\text{score}(D, Q) = \sum_{i=1}^n \text{IDF} \cdot \frac{f(q_i, D) \cdot (k_1 + 1)}{f(q_i, D) + k_1 \cdot (1 - b + b \cdot \frac{|D|}{\text{avgdl}})}$$

Document D,  $|D|$  is the length of document D in noun phrases, and  $\text{avgdl}$  is the weighted document length in the project. The parameters  $k_1$  and  $b$  allow for adapting the algorithm to different use cases. In our case, used 1.5 for  $k_1$ , 0.6 for  $b$  and measured 68 for  $\text{avgdl}$  as the average document length The frequent term like "a", "this", "an", "the text" etc. may appear in every document they are not important terms to eliminate these highly occurred terms in the document Inverse document frequency formula is used to extract non frequent terms because they are important in our case. We use IDF

described below for extracting non-frequent terms Formula of Inverse document frequency is:

$$\text{IDF}(Q_i) = \log \frac{N - n(q_i) + 0.5}{n(q_i) + 0.5}$$

Where 'N' is the entire number of documents of the project and  $n(q_i)$  is the number of documents having  $q_i$  (noun phases) after this we get a ranked document list with a BM25 score for each document that already exists in the project repository the top document in the list is the document most related to the input document

4) *Recommended project list:* The next step is to use recommended project ranking algorithm which interprets the scores of the individual document to scores for projects. Keep all projects documents with the maximum BM25's score of the ranked documents and extract the similarity of the input document score with the existing project documents score, calculate the average BM25 score of each project by averaging the score of all documents in the project formula is:

$$\text{score}(F, Q) = \frac{\sum_{i=1}^{N_F} \text{score}(D_i, Q)}{N_p}$$

we take the average to be precise for project size. The user will get the recommended project on the basis of the matched document.

- **Document Sync:** When the document is changed by any team member it will be synced in all those team members PC's who are the relevant users a notification will be generated to let the team members know that some latest document is uploaded and they should get those update. In our case, we are using Git [26] for document versioning control and for the remote repository. When the document is matched and copied/moved to the project documentation repository. The person who is adding the document in the local repository must have to push the branch (containing the newly added document/ or updated document) to the remote repository and raise a merge request for the master branch. The responsible person (team lead) review the merge request and either accepts or rejects the request to merge the branch in the master branch if the request is accepted and user branch is merged into the master branch and the master branch got updated.
- **Document update notification:** A notification is generated when the relevant documents got updated and synced so team members will be aware of any changes made to the documents.
- **Conversation storage and retrieval by using Tagging mechanism:** To deal with knowledge vaporization can be solved with the help of tagging mechanism. The remote teams rely heavily on textual media for interaction as IM chat reduces the communication gap caused by linguistic differences. To deal with knowledge vaporization these chats interactions can be stored and retrieved later by using the tagging mechanism. There is a list of tags already available



created by some responsible and experienced team members. The user cannot add or delete the tag. The tags are added by meeting by experienced members when they think there is a need of adding or removing a tag or a meta tag. So tags are maintained by the admin panel. There are meta tags all the tags are related to this meta-tag, for example a meta tag can be #code and #javaTricks can a be tag related to the meta tag, meta tag can be explained as parent tag and each parent tag has some child tags which come under parent tag. The advantage of using Meta tag or parent tag is when the team member wants to retrieve some topic but was not able to remember the exact tag he/she can search for the parent tag initially and child tags are listed any child tag can be selected and search can be initiated. The main reason for using tagging is to restore knowledge at later times, as in distributed development teams are located at remote locations and working together on the same project. They rely heavily on using IM tools where some important knowledge existed in the team member's conversation these conversation parts can be stored by tags and these conversation act as an important reviser of knowledge. User can search the conversation via tag and gain the required knowledge when needed also if the user does not initiate the tag using # but uses the tag in the conversation the conversation will be stored because of the automatic tagging mechanism.

#### IV. EVALUATION AND RESULTS

The evaluation of our framework was done via a case study and it answers our RQ3. It includes case study results and expert review through interviews. This section also represents the research findings and their discussion.

##### A. Case Study

To answer RQ3 we have taken a case study of DSD based Software Company. Our research topic is focusing on DSD so we selected a company which is distributed in nature. It is located in Islamabad, Karachi, Lahore, Rawalpindi and its head quarter is in Karachi. The company started in 2001 and is set out to redefine Pakistan computing industry. They offers a complete range of technology services such as business applications, Managed services, and IT infrastructure and solutions. Our case study evaluation mainly focuses on to improve knowledge sharing process with the help of our proposed framework the case study used to evaluate the proposed framework's impact on knowledge sharing. In software engineering, the cases are contemporary phenomena in software engineering in real life setting. We considered development teams who are major source of knowledge sharing and where there was a need to retrieve the knowledge and the knowledge vaporization issue emerge from here also the company we selected is distributed in nature so they face documentation problem such as poor, missing and outdated documents and knowledge loss due to knowledge vaporization because the teams use chat tools for daily communication.

Our case study is a single case study and embedded in design as we had three units of analysis first unit of analysis is

documentation problem and second unit of analysis is the knowledge vaporization problem in distributed teams third and the final unit of analysis is the overall case itself which is knowledge sharing in distributed environments For data collection set of semi-structured interviews were conducted one prior to explaining the framework and one after describing framework and a tool support is provided to aid the framework and its work flow was described to the team members. At the initial stage interview question were consisted of how they are currently exchanging the knowledge and how they are documenting and dealing with knowledge vaporization problem and after two weeks another interview was conducted when the framework and tool workflow was explained and used by the development team the interview question consisted of how the framework helps them mitigate knowledge sharing challenges is there any improvement in documentation and knowledge vaporization problem. After data collection, next phase was data analysis we analyze the interview data by using qualitative data analysis method called thematic analysis.

After reviewing the interview data we performed coding on that data. Coding was performed by extracting data chunks pointing to the point where the employees describe the proposed framework impact on their work, during an exchange of knowledge via conversation and document creation and sharing. We also coded scattered quotations referring to the needs and motivation behind knowledge sharing certain practices and associated challenges. The code resulted in evolving themes in data collected. Knowledge sharing practices of team members, the extent of knowledge shared. Impact of our framework on their knowledge sharing activities, etc.

##### B. Framework Tool Support (Blueprint)

We provide a prototype to support our framework and its activities these are four document artefacts (as described in Table II). We used Git as a remote repository to store the documents so that the dispersed team members can access them easily. When the main branch such as master is updated Git does not notify the user that the new/updated content is added but our system will alert the user as shown in Fig. 2 when the master branch got updated by any team member and the user can pull the changes in by simply clicking the notification bar. Sometimes the user creates documents in another directory which is not tracking by Git such as he/she writes a document in some folder and forgets to add this on project repository our system will identify the document which is modified in the system and will match with the documents of project documentation repository a notification will be generated shown in Fig. 3 that this document is related to that specific project click on it to copy that document in the specified project in the remote repository. Team members can share the documents via our tool.

For tagging mechanism, the system had a pre-loaded list of tags added by team leads during sprint meeting. Users can initiate the tag using # pre-loaded list of tags will be displayed then the user can select the relevant tag and continue chatting this conversation will be stored. Tags needs to be used only when the user thinks that the discussion needs to be saved that may be needed later via search feature we can search the tags,

auto complete list will be displayed to the user in the search bar user can select the tag and search against that tag and the related conversation will be displayed to the user including sender name, date time and the conversation main interface is shown in Fig. 4.

### C. Case Study Results and Discussion

Our case study findings answers RQ3, we evaluated the interviews data and coded the data using Nvivo12 tool. We first created a mind map for our themes as shown in Fig. 5 and then we identified several themes in our data based on coding. The identified themes are “documentation problem”, “knowledge vaporization issue”, “reduced knowledge vaporization problem”, “improved documentation”, “improved knowledge sharing”, “framework correctness”. This theme helped us to understand what knowledge sharing problems they had and how they deal with it and what impact does our framework had on the company’s knowledge sharing process Thematic analysis response is shown in Fig. 6.

By analyzing the data we had identified current knowledge sharing techniques in the company the team members use IM tools such as Slack and Email for communicating and sharing of knowledge, for video conferencing they use skype. The company faced documentation problem before presenting our framework our analysis revealed they face problems in documentation such as missing, poor and outdated documents. “We normally come across situations like file or documents placed somewhere in directories but we forget where we put them in the first place. Sometimes we face document inconsistency and redundancy because of no document management tool” the team leads described “There is a document management system missing in our company. As the company is ISO certified so detailed documentation is mandatory but an automated document management system is missing because of which we only manage documents manually, send them by emails and the manager store them in repository manually.” They had outdated documents because there was no mechanism to update the document periodically the developers explained “we have to review old and new docs to maintain consistency in documents and we have to cross check our documents multiple times which is time taking also we had to maintain directories and need to make sure manually that everything is up to date and it wastes a lot of our energy.” The company once used the Wiki as a repository but it did not resolve their issue of outdated documents. Manager told us “there are some outdated documents which we do not update once they are made. They just stay in the repository Still, the documents go missing.” one of their developers told us “We use to face the problems like missing outdated and redundant documents (in few cases). Sometimes, it’s hard to find the related document, as one couldn’t recall the document name exactly and every document has some issues which need to be addressed. I review it several times.”

Knowledge vaporization also existed in the company because they relied heavily on IM tools and sending/receiving emails there is a high tendency of misplacing a relevant document and when they need to recall some knowledge they need to manually search the old conversation which is a time-consuming process couple of developers told us “yes this is a

huge problem for us as there is no mechanism to retrieve knowledge that is once shared in chats. we have to share it again on chat messengers, as in the free version of slack chats gets deleted when message limits to reached to 10000, we either copy important points to notepad or we have to re-share them.”, “We do face vaporization of knowledge I use to save the chats in notepad, we normally save important chats to notepad for future reference.” Upon analyzing the data most of team members showed interest in some kind of mechanism to store and retrieve the knowledge to avoid knowledge vaporization problem. The team members of the company used our framework for two weeks and also they use scrum as an agile methodology their sprint consists of two weeks so they used our framework in their sprint session. The team members gives feedback of our proposed framework regard to documentation problem they described “it helps in reducing the time to find any document that is already stored somewhere in my system’s hard disk by its document matching mechanism and it helps in updating the documents and it keeps track of every document and suggest the matching documents to save us from reinventing the wheel It seems useful if it is strictly followed by company. Otherwise, it will never give them desired results.”, “it helps to reduce the redundancy of documentation by introducing documents type documents are always well managed and we can search them easily afterwards keeping documents randomly made them messy”, “managing documents in categories make them more organized these document types are most common document types which are needed most of the times. So it’s worthy to use”. For knowledge vaporization, the team member’s gives feedback after using the framework with a provided tool they described “it become easy to search the relevant knowledge using tags. shared knowledge can be retrieved from the tags which is very helpful for us”, they said “somehow it solves the problem, but there will be some issues for non-technical person I think”, “tags search mechanism is good to find desired shared knowledge it pretty much solves the problem by offering quick retrieval of knowledge by introducing tagging mechanism by using it we don’t have to save chats in notepad”, “It has allowed us to focus on development related problems. The tagging mechanism is a good facility. It’s just like tagging on Facebook which make it easy to see only the tagged comment from millions of comments.”, “I think so. Knowledge shared by my seniors/supervisor when stored in the form of tags make them more understandable and categorized, and to the extent that you get everything written down instead of verbal or informal communication.” We asked the team members about any improvements they suggest so we can enhance the solution we asked about proposed framework number of activates what they think about it and what would they suggest if something did redundantly or missing in the framework they described “The proposed solution seems perfect when used among technical people by technical it means IT professionals., its document matching mechanism and tags search have solved many of our problems and it has increased our project development pace”, “I think so knowledge vaporization is an important problem especially for those team who needs to work with other team members located at a remote location.” The framework provides a centralized solution solving many of the small problems. we asked them if anything is missing?

They described “it seems good with current features. But can be improved for version controls (Git tracks the commits of users and it can be used further).”, “This framework can be improved by adding individual chat along with group chats and I think we should be able to create different teams for different projects in chats. Although searching can be made stronger by providing more and more options that would be an extra feature and not a missing thing.”, “I think Information Architecture (IA) and Product Description (PD) will overlap at some point and the features provided are good and not redundant. Each one of them is important in their own.”, The team lead identified “if someone keeps changing a file in GIT repository, everyone will be pissed off from notifications with too much complex scenarios and iterations, I think this will lead to some redundancy on its own. Following improvements would be plus e.g. Adding more Document types, dealing with

larger documents involving multiple tags search shared knowledge efficiently, Integration with other applications e.g. servers containing files and wikis There is always a place for further improvement the framework provides good options under one roof.” In terms of usability of our tool blueprint, we obtained a SUS score of 83.6 (std =13.8), suggesting a high usability perception on the knowledge sharing tool. However, Fig. 7 presents this result using a curved grading scale [27], where we observed that around 9% of the participants perceived the knowledge sharing tool as having low usability (C and D grades on Fig. 7). The SUS [28] result suggests that participants perceived the knowledge sharing tool as highly usable. Which is further strengthn its importance for knowledge management as well [31-33] as explained by the authors.

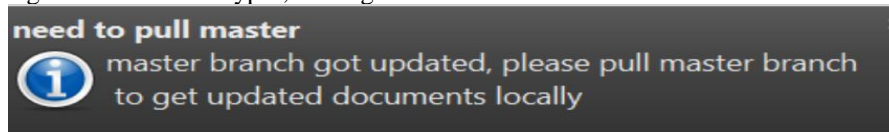


Fig. 2. Master Branch update Notification.

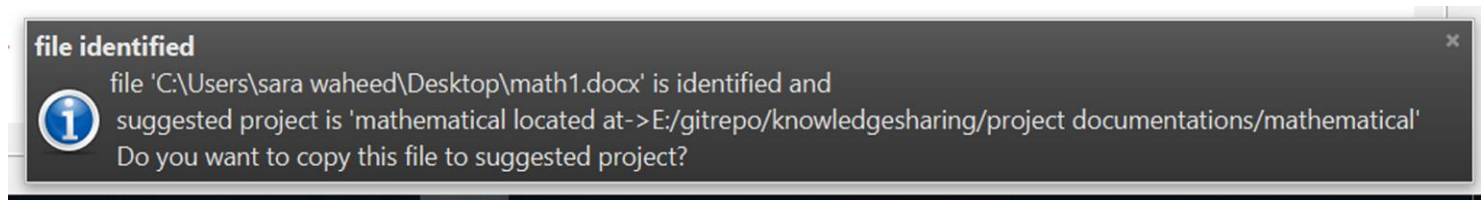


Fig. 3. File Identification Notification.

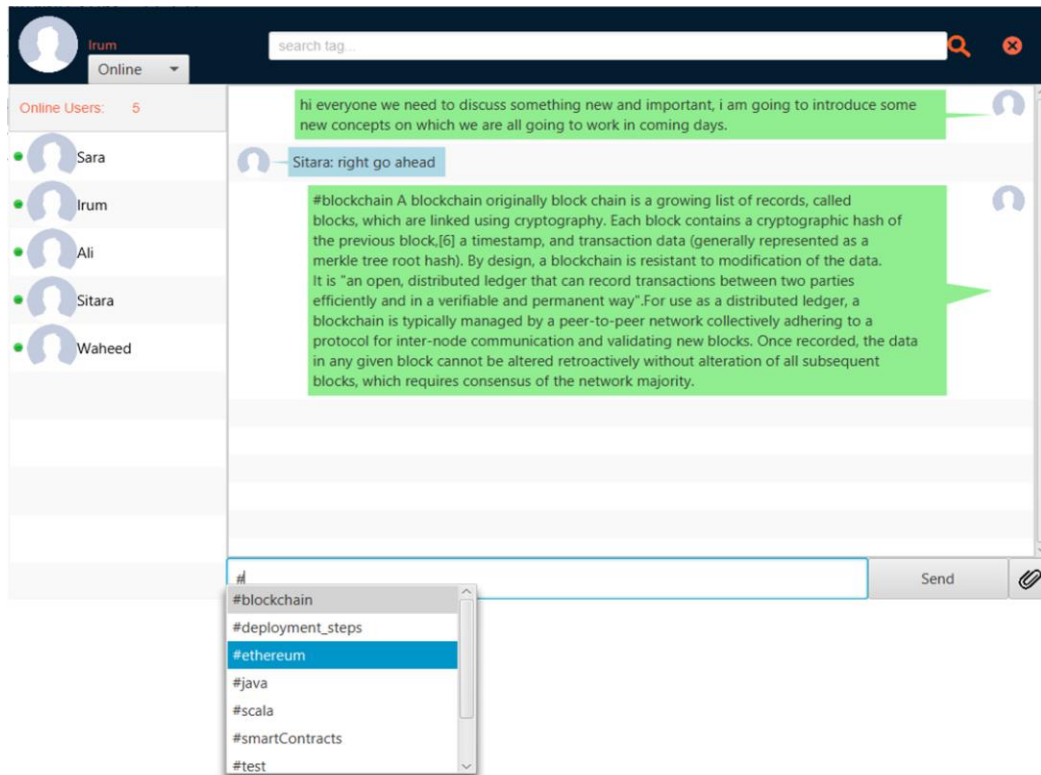


Fig. 4. Tool Support.

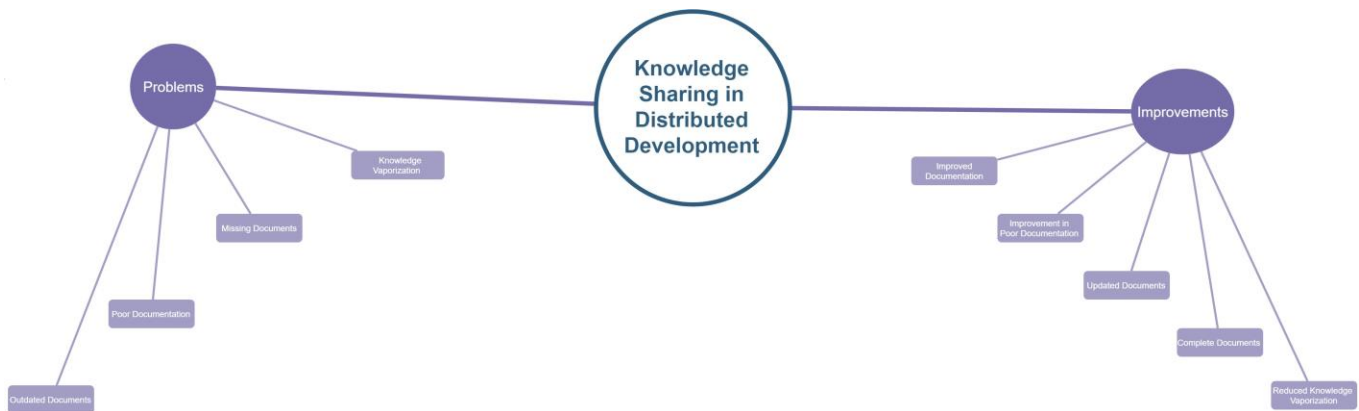


Fig. 5. Mind Map.

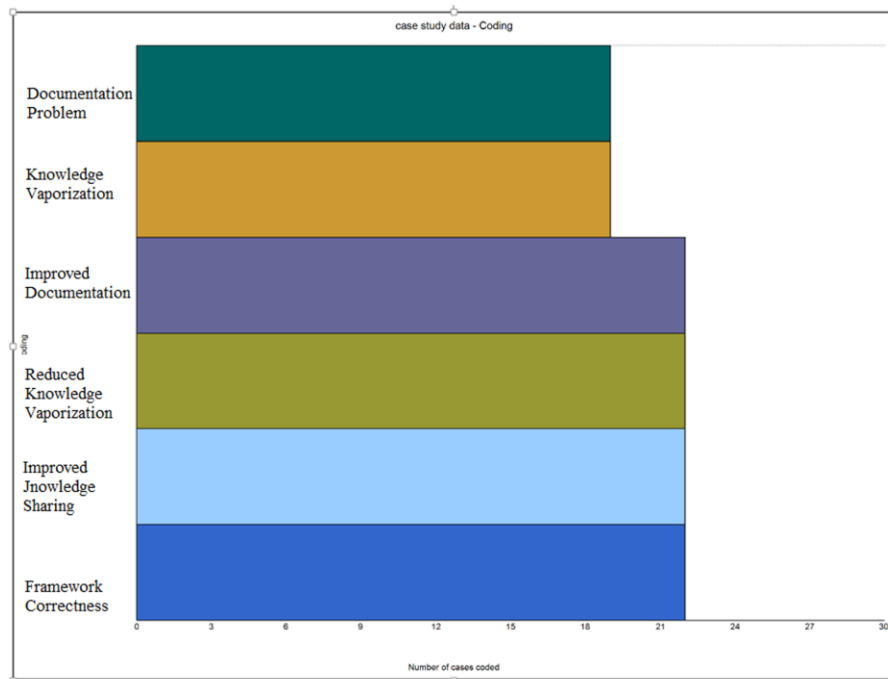


Fig. 6. Interview Resopnses.

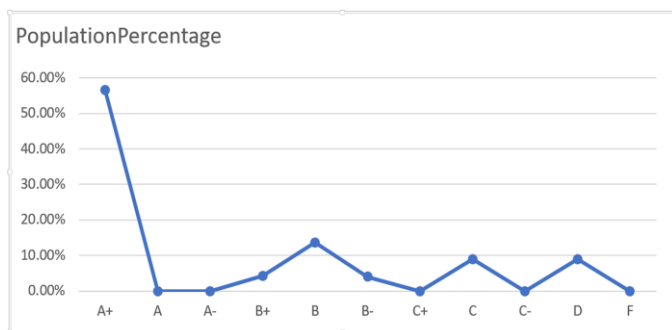


Fig. 7. SUS Result.

## V. LIMITATION AND FUTURE WORK

The proposed solution is evaluated via case study and it showed the positive results in improving knowledge sharing process but we evaluated our solution in a single context results

may differ in other context because our solution is for distributed eniornments and as a future work there is always a possibility to improve the current solution to make it more suitable for distributed teams and they can share knowledge easily multi tags can be added for advanced search, documents can be tagged to make it more organized and searchable.

## VI. CONCLUSION

In this research work, we focused on knowledge sharing which is an important phase of knowledge management the knowledge sharing process is itself complex in nature and it involves people, Knowledge sharing process becomes more critical when the development teams are dispersed around the globe. We identified several problems in knowledge sharing process when the teams are distributed geographically among all the challenges we identified documentation problem such as missing, poor and outdated documents and knowledge vaporization problem as much of the conversation and

communication is done via chat and emails and retrieving them later is a great headache. To eliminate these challenges we proposed a framework which deals with documentation problem and knowledge vaporization. We evaluated our framework by case study to evaluate frameworks performance in the real-life context, where actually the problem arises we conducted the interviews before and after describing our framework and came to the conclusion on team members response that they are satisfied with our proposed solution and it improved their knowledge sharing process. They indicated documentation improvement by having well managed, updated and complete documents and they also indicated reduced knowledge vaporization problem they used the tags in their daily conversation and retrieve these tags when required it produces less vaporization of knowledge. All these improvements positively increased knowledge sharing process which leads to fast product development and information flow in global software projects.

#### REFERENCES

- [1] L. H. Wong and R. M. Davison, "Knowledge sharing in a global logistics provider: An action research project," *Information & Management*, vol. 55, no. 5, pp. 547-557, 2018.
- [2] B. Afsar, A. Shahjehan, S. I. Shah, and A. Wajid, "The mediating role of transformational leadership in the relationship between cultural intelligence and employee voice behavior: A case of hotel employees," *International Journal of Intercultural Relations*, vol. 69, pp. 66-75, 2019.
- [3] D. Hislop, R. Bosua, and R. Helms, *Knowledge management in organizations: A critical introduction*. Oxford University Press, 2018.
- [4] I. Rus, M. Lindvall, and S. Sinha, "Knowledge management in software engineering," *IEEE software*, vol. 19, no. 3, pp. 26-38, 2002.
- [5] M. Zahedi and M. A. Babar, "Knowledge sharing for common understanding of technical specifications through artifactual culture," in *Proceedings of the 18th International Conference on Evaluation and Assessment in Software Engineering*. ACM, 2014, p. 11.
- [6] R. Anwar, M. Rehman, K. S. Wang, and M. A. Hashmani, "Systematic Literature Review of Knowledge Sharing Barriers and Facilitators in Global Software Development Organizations Using Concept Maps," *IEEE Access*, 2019.
- [7] G. Borrego, A. L. Moran, and R. Palacio, "Preliminary evaluation of a tag-based knowledge condensation tool in agile and distributed teams," in *Global Software Engineering (ICGSE), 2017 IEEE 12th International Conference on*. IEEE, 2017, pp. 51-55.
- [8] G. Borrego, A. L. Morán, R. R. Palacio, A. Vizcaíno, and F. O. García, "Towards a reduction in architectural knowledge vaporization during agile global software development," *Information and Software Technology*, 2019.
- [9] M. Zahedi, M. Shahin, and M. A. Babar, "A systematic review of knowledge sharing challenges and practices in global software development," *International Journal of Information Management*, vol. 36, no. 6, pp. 995-1019, 2016.
- [10] G. Borrego, "Condensing architectural knowledge from unstructured textual media in agile gsd teams," in *Global Software Engineering Workshops (ICGSEW), 2016 IEEE 11th International Conference on*. IEEE, 2016, pp. 69-72.
- [11] H. Saint-Onge, "Tacit knowledge the key to the strategic alignment of intellectual capital," *Planning Review*, vol. 24, no. 2, pp. 10-16, 1996.
- [12] E. D. Darr and T. R. Kurtzberg, "An investigation of partner similarity dimensions on knowledge transfer," *Organizational behavior and human decision processes*, vol. 82, no. 1, pp. 28-44, 2000.
- [13] C. Wei Choo and R. Correa Drummond de Alvarenga Neto, "Beyond the ba: managing enabling contexts in knowledge organizations," *Journal of Knowledge Management*, vol. 14, no. 4, pp. 592-610, 2010.
- [14] V. Santos, A. Goldman, and C. R. De Souza, "Fostering effective inter-team knowledge sharing in agile software development," *Empirical Software Engineering*, vol. 20, no. 4, pp. 1006-1051, 2015.
- [15] C. Ebert and J. De Man, "Effectively utilizing project, product and process knowledge," *Information and Software Technology*, vol. 50, no. 6, pp. 579-594, 2008.
- [16] S. Sarker, D. Nicholson, and K. D. Joshi, "Knowledge transfer in virtual systems development teams: An exploratory study of four key enablers," *IEEE transactions on professional communication*, vol. 48, no. 2, pp. 201-218, 2005.
- [17] K. Stapel and K. Schneider, "Managing knowledge on communication and information flow in global software projects," *Expert Systems*, vol. 31, no. 3, pp. 234-252, 2014.
- [18] A. Boden, G. Avram, L. Bannon, and V. Wulf, "Knowledge sharing practices and the impact of cultural factors: reflections on two case studies of offshoring in sme," *Journal of software: Evolution and Process*, vol. 24, no. 2, pp. 139-152, 2012.
- [19] M. Bugajska, "Piloting knowledge transfer in it/is outsourcing relationship towards sustainable knowledge transfer process: Learnings from swiss financial institution," *AMCIS 2007 Proceedings*, p. 177, 2007.
- [20] A. L. Chua and S. L. Pan, "Knowledge transfer and organizational learning in is offshore sourcing," *Omega*, vol. 36, no. 2, pp. 267-281, 2008.
- [21] J. W. Rottman and M. C. Lacity, "A us client's learning from outsourcing it work offshore," in *Information Systems Outsourcing*. Springer, 2009, pp. 443-469.
- [22] A. Boden, B. Nett, and V. Wulf, "Operational and strategic learning in global software development," *IEEE software*, vol. 27, no. 6, pp. 58-65, 2010.
- [23] J. Bosch, "Software architecture: The next step," in *European Workshop on Software Architecture*. Springer, 2004, pp. 194-199.
- [24] B. Kristjansson, R. Helms, and S. Brinkkemper, "Integration by communication: Knowledge exchange in global outsourcing of product software development," *Expert Systems*, vol. 31, no. 3, pp. 267-281, 2014.
- [25] A. Averbakh, E. Knauss, and O. Liskin, "An experience base with rights management for global software engineering," in *Proceedings of the 11th International Conference on Knowledge Management and Knowledge Technologies*. ACM, 2011, p. 10.
- [26] J. Loeliger and M. McCullough, *Version Control with Git: Powerful tools and techniques for collaborative software development*. O'Reilly Media, Inc., 2012.
- [27] J. Sauro and J. R. Lewis, *Quantifying the user experience: Practical statistics for user research*. Morgan Kaufmann, 2016.
- [28] A. Bangor, P. T. Kortum, and J. T. Miller, "An empirical evaluation of the s usability scale," *Intl. Journal of Human-Computer Interaction*, vol. 24, no. 6, pp. 574-594, 2008.
- [29] D. Damian and D. Moitra, "Guest editors' introduction: Global software development: How far have we come?" *IEEE software*, vol. 23, no. 5, pp. 17-19, 2006.
- [30] R. F. Rich, "Knowledge creation, diffusion, and utilization: Perspectives of the founding editor of knowledge," *Knowledge*, vol. 12, no. 3, pp. 319-337, 1991.
- [31] Abbas, Syed Fakhar, Raja Khaim Shahzad, Mamoona Humayun, NZ. Jhanjhi, and Malak Alamri. "SOA Issues and their Solutions through Knowledge Based Techniques-A Review." *International Journal of Computer Science And Network Security* vol. 19, no. 1, pp.8-21, 2019.
- [32] M Humayun, NZ Jhanjhi, "Exploring The Relationship Between Gsd, Knowledge Management, Trust And Collaboration", *Journal of Engineering Science and Technology*, vol. 14, issue 2, pp 820-843, 2019.
- [33] S. S. A. Bukhari, M. Humayun, S. A. A. Shah and N. Jhanjhi, "Improving Requirement Engineering Process for Web Application Development," 2018 12<sup>th</sup> International Conference on Mathematics, Actuarial Science, Computer Science and Statistics (MACS), Karachi, Pakistan, 2018, pp. 1-5.

# IRPanet: Intelligent Routing Protocol in VANET for Dynamic Route Optimization

Rafi Ullah<sup>1</sup>, Shah Muhammad Emad<sup>2</sup>, Taha Jilani<sup>3</sup>, Waqas Azam<sup>4</sup>, Muhammad Zain uddin<sup>5</sup>

College of Computing and Information Sciences, PAF-KIET Karachi, Pakistan<sup>1, 2, 3, 5</sup>

Solution Architect and Project Manager, 10Pearls, Karachi, Pakistan<sup>4</sup>

**Abstract**—This paper presents novel routing protocol, IRPANET (Intelligent Routing Protocol in VANET) for Vehicular Adhoc Network (VANET). Vehicular Ad Hoc Networks are special class of Mobile Adhoc Network, created by road vehicles installed with wireless gadgets). Since the environment is dynamic due to high mobility and the topology changes are too frequent, no connection or path can be established between nodes. The issues are challenging for the design of an effective and efficient protocol for such a dynamic environment. This problem can be solved using probabilistic, heuristic and even machine learning based approaches incorporated with store and forward mechanism. Here, we proposed a design framework using heuristics and probabilistic approaches composite with the time series techniques for selecting best and optimize path for forwarding packets using open street map (OSM). Our proposed algorithm uses various parameters (Heuristics Based Routing) for calculating optimal path for packets to be sent, such geographical position (GPS installed in every vehicle), velocity / speed of vehicle, priority of the packets, distances (Euclidean, Haversine, Vicinity) between vehicle, direction of vehicle, communication range of the vehicle, free buffer of nodes and network congestion. These networks can be used for medical emergency, security, entertainment and routing purposes (applications of VANET). These parameters while used in collaboration provide us a very strong and admissible heuristics. We have mathematically proved that the proposed technique is efficient for the routing of packets especially in medical emergency situation.

**Keywords**—Intelligent routing protocol; heuristics based routing; applications of VANET; Vehicular Adhoc Network; VANET routing protocol

## I. INTRODUCTION

Mobile ad hoc network usually denoted by MANET can be defined as a network that has many free or autonomous nodes wirelessly connected, composed of mobile devices or mobile objects that can arrange themselves in various ways and operate without strict top-down network administration (infrastructure-less networks and self-configuring networks). These freely movables devices can move in any of the direction specified independently of other nodes, hence results highly complex sceneries such as dynamic topology, autonomous topology, frequent network disconnections, efficient and fast routing of packets and many of the characteristics that make it distinguish from traditional networks. Wireless ad hoc network or ad hoc wireless networks are the alternative terms used for MANET. When

vehicles are used as movable objects in MANET, this special class of MANET is known as Vehicular Adhoc Networks usually known as VANETs [1] [2]. VANET Communication usually take place between vehicle to vehicle or vehicle to roadside unit (like base station, stationary towers etc.) [3]. In VANET the high speed nodes (vehicles having speed generally from 40 km/hr. to 180 km/hr.) can be used as transmitters and receivers. Communication environment is dynamic and it changes constantly with time. Nodes are carrying a lot of battery power with itself along with auto-recharge facility hence it is a favorable condition to perform high computation at node. Smart and efficient “store and forward” mechanism is used to buffer a packet at current node or to pass it to the next node. All discussed characteristics of VANET are mainly connected to single common issue that design of smart and efficient routing protocols.

Applications of VANET can be real time traffic analysis, route decision in case of emergency, entertainment systems, electronic toll collections, parking availability, post-crash notifications; road hazards control notification, remote vehicle personalization or diagnostic, availability of internet connection in some area and many more potential applications.

Proposed technique focuses on the issues of designing efficient and smart routing protocol using heuristics. A lot of work has been observed on mentioned issue, there are many heuristics used in literature for routing, proposed technique tried to merge these parameters and apply probabilistic and heuristic approach for making smart decision for routing in VANET [4] [5] [6]. Every node must broadcast their positions to its neighbor and hence it can maintain local routing information with every node. This information will be used for making routing decisions. Machine learning techniques i.e. probabilistic approaches for predicting behavior of traffic in some geographical location will be incorporated in future.

Paper is organized as follow, Section II describes the literature review, Section III describes characteristics of VANET, Section IV describes pros and cons of some of the protocols proposed in VANET, Section V describes Open Street Map (OSM), Section VI describes proposed methodology (Different components of system, Algorithms and techniques), Section VII describes about the heuristics used in proposed methodology, Section VIII describes Applications of proposed technique, Section IX describes theoretical results obtained, Section X explains the conclusion and future work has been discussed in Section XI.

## II. RELATED WORK

Several protocols has been discussed in [7] based on Geographic position of vehicles named as GR (geographic routing) or position based routing protocol (PBR) and shown these protocols very adequate in VANET due to robustness in dynamic environment. These protocols do not exchange link state information. The pros and cons of each of the GR protocol has been discussed.

Due to problem of connectivity in vehicular network, various parameters such as speed, density, direction and inter-vehicular distance for measurement of connectivity have been discussed in [8].

As there are various challenges in VANET such as high node mobility, changing topology, links breakages, constancy of networks and scalability of network. ANTSC protocol has been proposed that results in improved routing by considering various parameters such as speed differences between vehicles, direction, connectivity level and node distance etc. Proposed protocol in [9] is more scalable, robust and stable than existing one.

In [10] a message passing mechanism has been proposed for vehicular network.

Authors in [11], have a survey study on comparison of various protocols used for routing in vehicular ad-hoc networks. A comparison has been done on the basis on various parameters such as scalability, robustness, quality etc.

Authors in [12] highlighted the problem of designing routing algorithm for Ad-hoc VANET due to dynamic topology. Stimulated Annealing, clustering [13] [14], neural network using radial basis function are used considering many parameters such as velocity, free buffer size, etc. Simulations show the proposed performs outstanding in term of discovery rate and packet delivery rate.

Routing algorithm being a problem of finding shortest path, and that path should be optimized. Many of the optimized algorithms such as Ant Colony Optimization Algorithms, AOMDV, CRLLR, AQRV and T-AOMDV Algorithms are compared with proposed technique known as CRLLR (Clustering Based Reliable Low-latency Routing) in [15]. Parameters used for comparison used in that paper are throughput, Reliability, E2E Latency, Average Energy Consumption and Number of Beacons Messages. Considering these parameters two different experiments were performed.

1) *Experiment A*: The Impact of different relative velocities of vehicles having speed range between 40 km/hour to 120 km/hour over the performance of CRLLR.

2) *Experiment B*: The impact of different of different variety of vehicles on roads ranging from 30 vehicles to 100 vehicles to measure the significance of the proposed technique CRLLR, where it has been observed the average velocity of the vehicles is 60 kilometer per hours.

## III. CHARACTERISTICS OF VANET

Vehicular Ad-hoc Network VANET holds some unique characteristics which make it distinguish from others networks

such as MANET. These characteristics make it difficult and challenging to design VANET applications [16]. Following are the characteristics; one can target one of the characteristic and design routing protocol for that.

### A. High Dynamic Topology

Vehicle moves at high speed up to 120 km/hr., which results different topologies at different time. So the topology is dynamic i.e. it changes with respect to time. Consider two vehicles are moving at the speed of 30m/sec and the radio range between them is 120 m. Then the link between the two vehicles will last  $120/30 = 4$  seconds that is vehicles are connected just for 4 seconds.

### B. Frequent Disconnected Network

There is a chance of network disconnection between nodes i.e. vehicles, due to dynamic topology. One can have connectivity for very small duration i.e. connection period for information exchange may be for a very short interval. For sparse network this problem will be frequent.

### C. Mobility Modeling

Mobility pattern of vehicles (nodes) highly dependent on road structure, speed of vehicles, driver's driving behavior, traffic environment. The geographic location also play vital role in designing routing protocols.

### D. Battery Power and Storage Capacity

As compared to Mobile Ad-hoc NETWORK there is enough computing power [11], battery power and storage. This enables us to work with effective communication and complex routing decisions.

### E. Communication Environment

Environment of communication between vehicles is different in different networks i.e. urban environment and rural environment which can also be classified as sparse network and dense network. In those environments such as villages, cities, etc. [17]. there are building, trees and other objects behaves as obstacles and on highways these obstacles are less or even absent, so design of routing protocols are different according to the environment.

### F. Interaction with on-Board Sensors

GPS plays important role in most of the routing protocols' design. Since the current position and movement of vehicles can be easily sensed by GPS. It will help us to design effective routing protocols.

## IV. EXISTING PROTOCOL PROS AND CONS

Existing routing protocols are broadly classified into three different categories such as Pro-active Routing Protocol, Reactive Routing Protocols and Geo-graphic Routing Protocols. A node contributing in pro-active routing protocol maintains one or many tables representing the entire network topology, these routing tables are updated regularly for up-to date routing information from other nodes. Reactive routing protocol does not keep information of the entire network, it compute route to destination first while geographic routing protocol are based on the geographic locations of nodes [18] [19] [20].

### A. Fisheye State Routing

FishEye State Routing Protocols is a proactive routing protocol (also known as Table driven protocol) as discussed in. Table driven protocols are where every node collects information from neighboring nodes. After collecting information, routing table is calculated. It is based on the link state routing & an improvement of Global State Routing. Mentioned Algorithm has variety of pros and cons [21].

#### Pros:

- FSR exchanges partial update information with their own neighbor only, so reduce consumed bandwidth, hence results reduction in routing overhead.
- Reduce routing overhead.
- Link failure doesn't results changes in routing table.

#### Cons:

- Not performed well for small ad-hoc network.
- Less knowledge about distant nodes.
- Storage complexity and processing overhead is proportional to increase in network size.
- Insufficient information for route establishing.

### B. Ad-Hoc on Demand Distance Vector (ADOV)

ADOV described in [22] stands for Ad-Hoc On Demand Distance Vector routing protocol, a reactive routing protocol which only establish a route when a node requires to send data packets to other nodes. It is capable of unicast and multi-cast routing.

#### Pros:

- An up-to-date path to the destination because destination sequence
- Reduces excessive memory requirements and redundancy.
- AODV responses to the link failure in the Network.
- It can be applied to large scale ad-hoc network.

#### Cons:

- Require more time connection setup & initial communication to establish a route.
- It leads to inconsistency in case of out dated information at intermediate nodes.
- Control overhead will be heavy as there are multiple route reply packets.
- Consuming extra or excess bandwidth due to periodic and frequent beaconing.

### C. Temporally Ordered Routing Protocol (TORA)

Temporally Ordered Routing Protocol uses Directed Acyclic Graph (DAG) concept for broadcasting packets. Here link reversal algorithm is used that creates a DAG (A directed graph that has a topological sorted order, a sequence of the

vertices' such that every edge is directed from earlier to later in the sequence) towards destination, here source node act as a root of the tree.

#### Pros:

- It creates DAG (Direct acyclic graph) upon requirements.
- Intermediate nodes does not rebroadcast the messages, hence reduce network overhead.

#### Cons:

- DSR and AODV performed well as compared to TORA
- TORA is not scalable Routing Technique

### D. Geographic Routing Protocol (DTN)

Geographic routing proposed in [7] is a routing that each node knows its own & neighbor node geographic position by position determining services like GPS. It doesn't maintain any routing table or exchange any link state information with neighbor nodes. Information from GPS device is used for routing decision.

#### Pros:

- Route management and route discovery is not needed
- Scalable routing technique
- Performed very well for high node mobility pattern

#### Cons:

- It is based on GPS, hence it will not work in places where GPS services are not available.

### E. Delay Tolerant Networks

Delay Tolerant Network (DTN) analyzed in [23], another routing technique uses carry and forward strategy in order to reduce frequent disconnection of nodes in the high mobility nodes network. Whenever a node is not in the contact with other node(s), then it store packet for some time on the basis of some defined metric and then on fulfilling some requirements it forward packet(s).

## V. OPEN STREET MAP

Open Street Map, OSM is a map of the world, free to use under an open license. This is off-line version of map. API (Application Programmer Interface) is available in many different languages. OSM provide us details of the location like source to destination path, road types, junction etc. OSM uses A\* Search Algorithm to find shortest path from source to destination. In A\* Search the path is selected on the basis of following evaluation function

$$f(n) = g(n) + h(n) \quad \text{----- (1)}$$

Where g (n) is the cost to next neighbor and h(n) is the heuristic function, cost from neighbor to destination usually calculated by Euclidean distance formula, given by

$$d = \sqrt{(x_2 - x_1)^2 + (y_2 - y_1)^2} \quad \text{----- (2)}$$



Here  $x_2, y_2$  and  $x_1, y_1$  are the latitude and longitude of two points in a path that is road.

## VI. METHODOLOGY

This proposed technique can be used in three different applications. One of the applications of proposed technique is emergency applications of VANET in a high dense urban area as shown in Fig. 1, where there are a lot of junctions and high traffic flow. It is difficult for ambulance or fire brigade ambulance to choose optimize route (typical use case from the situation shown in Fig. 1). The ambulance has to decide an optimize route. One cannot rely on straight forward route decided at start, because the traffic pattern is highly dynamic in urban areas, so it may change in small interval of time. OSM provides details of roads and their type's i.e. highway, motorway, etc. OSM has predefined junctions; junction can be view as a point where more than one road meets. The ambulance starts its journey from source point. It reads the first junction from OSM, then forwarded packet to know about the state of junction. The packet will be transfer to best neighbor among node and so on, at last the nodes available at junction (first node at some predefined radius) will reply broadcast message to all neighbors in its range and all neighbors will reply back to that node and then this node will respond back with traffic status (either yes or no and their speed, their own destinations) back to sender node. Hence it can show real time traffic information over off-line map services like OSM. This node will collect all information from nodes at junctions and will do some processing whether this route is good or not? And this information will be sent back to initial sender i.e. Ambulance. This node will also try to predict the current position of Ambulance using available information.

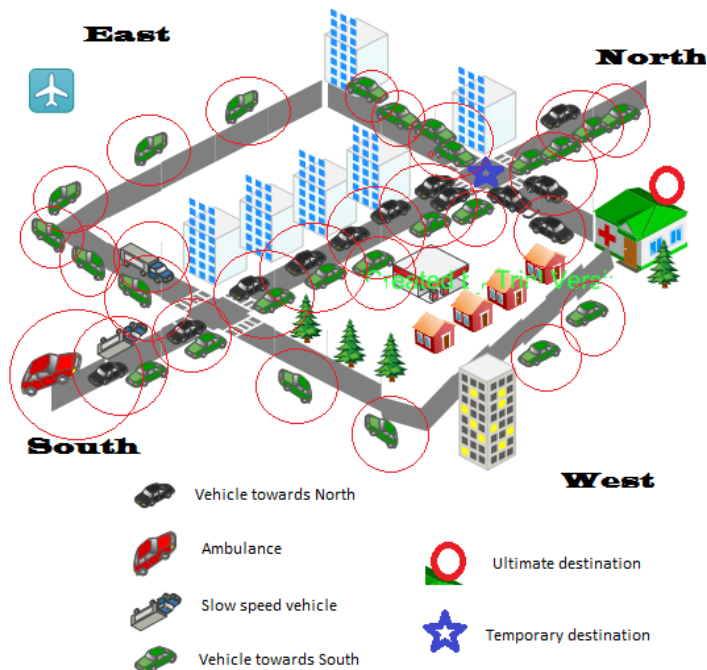


Fig. 1. Urban Area, Range of Vehicle Shown.

## Sender Packet Information

Following information are sent from source to node available near destination.

- 1) Sender\_ID
- 2) Sender\_Geo\_Location (using GPS)
- 3) Speed\_of\_Ambulance
- 4) Direction\_of\_Ambulance
- 5) Destination\_address
- 6) Current\_time\_stamp
- 7) Road\_Status\_value

Where

- Sender\_ID is the Global Identifier of source node; Sender\_Geo\_Location is the position (Latitude and Longitude) by the GPS services of Vehicle.
- Speed\_of\_Ambulance is the current speed of Source Node (Ambulance), which can be read by the speed meter device installed in vehicle.
- Direction\_of\_Ambulance can also be calculated at source node by observing successive GPS positions. Proposed technique considers only four directions North, West, East and South.
- Destination\_address is the Address of Location about which one is interested to know the status; in this case it is the real time traffic situations in urban areas.
- Current\_time\_stamp is the time interval at which source node is sending packet to other node(s).
- Road\_Status\_value is an integer value initially set to zero when sending packet from source node.

Every node (nodes not near junction) that is forwarding this packet just increment this value by 1.

## Intermediate Nodes Operations

All the nodes that are just forwarding the packets with little update in packets are defined Intermediate Nodes. Every node when receives packets it check whether it should broadcast or not by comparing its own current position with destination address in packet.

### Algorithm at Intermediate Nodes:

- 1..... Read destination address from packet
- 2.....Read its own Position
- 3..... Difference = Position\_current – Destination
- 4.....if Difference <= someRange
- 4.1.....CollectInformationFromNodes()
- 5.....else
- 5.1..... Read Road\_Status\_value from packet
- 5.2.....Increment this value by 1

Collect information method is only executed at the node, which is in the range of destination. This method can be scripted as given below:

### First Node near destination

The first encounter node, near destination will broadcast message to all neighbor nodes, and all neighbor nodes near that nodes (radius must be defined) will reply back by giving following information:

- 1) Traffic status (with yes or no, 1 or 0 bit)
- 2) Speed of the vehicle
- 3) Destination of each vehicle

Here, the intruder nodes are not taken into account, which may occurs some nodes can produce false information and may change the content of packet. In this technique no encryption or authentication schemes has been considered. It is considering all nodes to real and authentic nodes. The security aspect of this technique will be considered in future work. The Node processes this information will convert these into insights like the traffic congestion, time to clear, number of vehicles presents at junction, where there can be a possibility of congestion. The node will then create a response packet and send to that node that is Ambulance. The main problem is now what should be location/position of ambulance. Position, distance and location can be calculated by formulas mentioned below:

$$position_{initial} = Location_{source} \quad (3)$$

$$distance_{covered} = Speed_{source} * (time_{current} - time_{source}) \quad (4)$$

$$Location_{current} = Location_{source} + distance_{covered} \quad (5)$$

The intermediate node also known as Helper Node will also calculate where the next possible traffic is jam by calculating usage of roads. Helper node will find all the roads and their usage using the destination of all nodes there at junction.

### Algorithm CollectInformationFromNodes:

Once it is detected that node in the range of destination, it will execute following algorithm's steps

- 1...Broadcast Hello-beacon to all nodes in range
  - 2...Every node at junction send Beacon-Reply
  - 3...Add Length (all nodes that replied) to Road\_Status\_value
  - 4...Find Average Speed of nodes at junction
  - 5...calculateTimeToClear()
  - 6...predictCurrentPositionOfSender()
  - 7...findRoadStatus()
  - 8...createPacket()
  - 9...Send Packet to Original Sender
- Hello-beacon: Contains hello message  
Beacon-Reply: Contains speed, destination address

### Algorithm predictCurrentPositionOfSender:

- 1...speed = Read speed from Sender Packets
- 2...position = Read position from Sender Packets
- 3...direction = Read direction from Sender Packets
- 4...time<sub>sender</sub> = Read time stamp from from Sender Packets
- 5...timeSinceThen = Time<sub>sender</sub> - Time<sub>current</sub>

- 6...Calculate distance covered till packet sent by using speed
- ....equation, distance = speed \* timeSinceThen
- 7 ...position = position + distance (covered in direction)
- 8....return predicted position

### Algorithm findRoadsStatus:

- Static: Dictionary
- 1..... for all nodes at junction
  - 1.1..... road\_id = findRoad(destination)
  - 1.2 .....if road\_id not in Dictionary
  - 1.2.1.....Add road\_id and count = 1
  - 1.3 .....else
  - 1.3.1.....Increase road count by 1
  - 1.4.....return Dictionary

createPacket is the name of function, which implements the computation of creating packets, it do all necessary steps before forwarded by helper node.

### Algorithm createPacket:

Helper Node collects all the information calculated by previous methods and then sends back to Original Sender, in our case it is Ambulance. In this packet it will change source address to junction/location address and the destination address is set to the next predicted address of Original Sender i.e. Ambulance.

Helper node will create a packet having following information:

- 1) Source\_address
- 2) Destination\_address
- 3) Road\_Status\_value
- 4) Congested\_Roads\_informations
- 5) Time\_to\_Clear

### Main Algorithm Mode 1:

- 1...if there are nodes in the range of Ambulance
- 1.1.....Send Request-Beacon to all nodes
- 1.2.....All nodes returns Response-Beacon
- 1.3.....If there are all 0's in Response-Beacon
- 1.3.1.....wait() and go to step 1
- 1.4.....else
- 1.4.1.....packet sent successfully, wait for response
- 2...else
- 2.1.....Keep packet until node appear in range

Request-Beacon: Contains Initial Packets discussed under heading Sender Packet Information (SPI).

Response-Beacon: If value is 1, it means packet is send forwarded and discarded packet in case of value 0.

### Main Algorithm Mode 2:

- 1...if there are nodes in the range of Ambulance
- 1.1.....Send Request-Beacon to all nodes
- 1.2.....All nodes returns Response-Beacon
- 1.3.....if direction is opposite of destination
- 1.3.1.....remove that nodes
- 1.3.2.....Rem\_Nodes are remaining Nodes
- 1.3.3.....Select best node amongst from Rem\_Nodes

- 1.3.4.....Forward packet to that node
  - 1.3.5.....wait() for response
  - 2...else
  - 2.1.....Keep packet until node appear in range
- Request-Beacon: Contains Request Hello Message
- Response-Beacon: Contains following information,
- 1) Speed
  - 2) Direction
  - 3) Buffer size
  - 4) Range
  - 5) GPS Position

## VII. HEURISTICS USED IN METHODOLOGY

In case of more than one available nodes i.e. vehicles which is a most obvious situation in urban dense area, multi-lane roads, it is necessary to pass packet to only node which is best node, to avoid broad-cast overhead. In order to find the best candidate node available, there are certain criteria like speed of vehicle, distance between ambulance and neighbors, distance between nodes and destination, buffer size, range of vehicle which is given below.

$$f(n) = S + R + B + \left(\frac{1}{g(n)+h(n)}\right) \text{---- (6)}$$

Where  $f(n)$  is the cost of node, this value will be used for selecting best node for transmitting packet,  $g(n)$  is the distance between Ambulance and Neighbor,  $h(n)$  is the distance between node and destination,  $S$  is the speed of vehicle (node),  $R$  is the range of the vehicle (node),  $B$  is the size of buffer that vehicle have,  $g(n)$  and  $h(n)$  will be calculated by Euclidean distance formula given in equation (2). Select Node having large  $f(n)$  Value and forwarded packet to that node.

**Logic behind heuristic function:** A node having larger buffer, high speed, large range, node nearest to ambulance and destination is good. High speed vehicle is good to deliver packet early and quick. Long range nodes are good to deliver packet from large distance. High buffer size nodes are good to select to keep packet(s) for long time.

Weighted heuristic function for selecting best node can be used as distance from node to destination and from source (ambulance) has very less impact, so we can assign low weight to this using following equation.

$$f(n) = W_1(S + R + B) + w_2 \left(\frac{1}{g(n)+h(n)}\right) \text{----- (7)}$$

Where  $w_1$  and  $w_2$  are the weights we can assign, but keep in mind that  $w_1+w_2 = 1$ , for example  $w_1 = 0.8$ , then  $w_2 = 0.2$

If  $w_2 = 0$ , and  $w_1 = 1$ , it means you are totally ignoring  $g(n)$  and  $f(n)$ , then equation will look like following

$$f(n) = S + R + B \text{----- (8)}$$

## VIII. OTHER APPLICATIONS

Apart from above discussed technique for specialized purpose, we can also modify this technique for following purposes, like

1) *Entertainment Purpose:* A song in one vehicle listens by another person in vehicle. Or we can even use it to play game between different vehicles over the network.

2) *Emergency Purpose:* Same as case given in this paper, this can be used for Ambulance, School Vans, Fire Fighter Ambulance or in case of emergency like accidents.

3) *Location Analysis:* To know about some fixed entity at some remote location like pizza shop, mall, item order etc. for example ordering something before you arrive at any point.

4) *Real Time Traffic Analysis:* This technique can be modified to analyze real time traffic pattern in some urban area as shown in Fig. 1 above. This will help us to find optimize routes in case of any emergency, accidents, war, or any natural disaster.

## IX. RESULTS

In proposed technique there is no broadcast overhead as only Helper node process information, all other nodes are free from sending broadcasts. Connection establishment is not required so as connection termination. Low processing, i.e. computation is carried out at some intermediate vehicles but not having redundant and waste processing on different nodes. Memory efficient Routing Protocol, i.e. no routing table or information is maintained at intermediate nodes. The proposed technique overcome problem discussed in DTN, that is problem of tracking locations where GPS is not working by using off-line maps such as OSM.

## X. CONCLUSIONS

Efficient routing protocols can be designed using different heuristics like the position, speed, and direction of vehicles. In vehicular networks nodes can be having excess of energy and computation power, so we have to just take care of the delay and packet delivery of networks. Due to high mobility of nodes it was difficult to use a single parameter like speed or position. The use of off-line maps services like OSM, we can design best routing protocols. But still there is a lot of gap or research area to be work on these protocols designs. Store and forwards mechanism uses little bit intelligent approach. We have successfully shown on demand store and forward mechanism. Various applications of VANET has been discussed in this paper. Applications are emergency applications, security applications, entertainment applications and routing applications. Proposed system has not been proven effective by simulation and we are using heuristics which can misguide the routing process. These limitations are will be considered in future work of proposed system.

## XI. FUTURE WORK

Bio-inspired Algorithms and Machine Learning Algorithm can be used predict the pattern of traffic within some urban environment, so that routing decisions can be made properly and efficiently that will be incorporated in proposed technique in future. There is issue of security, any node if change packet content, will destroy whole communication and will leads to unreliable communication and process. A new technique can be designed in future by the name of Geo Encryption Technique, which will be location based encryption and decryption.

REFERENCES

- [1] Jaap, Sven, Marc Bechler, and Lars Wolf. "Evaluation of routing protocols for vehicular ad hoc networks in typical road traffic scenarios." Proc of the 11th EUNICE Open European Summer School on Networked Applications (2005): 584-602.
- [2] Lin, Yun-Wei, Yuh-Shyan Chen, and Sing-Ling Lee. "Routing protocols in vehicular ad hoc networks: A survey and future perspectives." J. Inf. Sci. Eng. 26, no. 3 (2010): 913-932.
- [3] Chekima, Ali, Farrah Wong, and Jamal Ahmad Dargham. "A Study on Vehicular Ad Hoc Networks." In 2015 3rd International Conference on Artificial Intelligence, Modelling and Simulation (AIMS), pp. 422-426. IEEE, 2015.
- [4] Al-Kharasani, Nori, Zuriati Zulkarnain, Shamala Subramaniam, and Zurina Hanapi. "An efficient framework model for optimizing routing performance in VANETs." Sensors 18, no. 2 (2018): 597.
- [5] Masegosa, Antonio D., Enrique Onieva, Pedro Lopez-Garcia, and Eneko Osaba. "Applications of soft computing in intelligent transportation systems." In Soft Computing Based Optimization and Decision Models, pp. 63-81. Springer, Cham, 2018.
- [6] Touluni, Hamza, and Benayad Nsiri. "Cluster-based routing protocol using traffic information." International Journal of High Performance Computing and Networking 11, no. 2 (2018): 108-116.
- [7] Boussoufa-Lahlah, Souaad, Fouzi Semchedine, and Louiza Bouallouche-Medjkoune. "Geographic routing protocols for Vehicular Ad hoc NETWORKS (VANETs): A survey." Vehicular Communications 11 (2018): 20-31.
- [8] Hassan, Ahmed Nazar, Omprakash Kaiwartya, Abdul Hanan Abdullah, Dalya Khalid Sheet, and Ram Shringar Raw. "Inter Vehicle Distance Based Connectivity Aware Routing in Vehicular Adhoc Networks." Wireless Personal Communications 98, no. 1 (2018): 33-54.
- [9] Mehmood, Amjad, Akbar Khanan, Abdul Hakim HM Mohamed, Saeed Mahfooz, Houbing Song, and Salwani Abdullah. "ANTSC: An intelligent Naïve Bayesian probabilistic estimation practice for traffic flow to form stable clustering in VANET." IEEE Access 6 (2017): 4452-4461.
- [10] Singh, Vijander, and G. L. Saini. "Dtn-enabled routing protocols and their potential influence on vehicular ad hoc networks." In Soft Computing: Theories and Applications, pp. 367-375. Springer, Singapore, 2018.
- [11] Kumar, Rakesh, and Mayank Dave. "A comparative study of Various Routing Protocols in VANET." arXiv preprint arXiv:1108.2094 (2011).
- [12] Bagherlou, Hosein, and Ali Ghaffari. "A routing protocol for vehicular ad hoc networks using simulated annealing algorithm and neural networks." The Journal of Supercomputing (2018): 1-25.
- [13] Touluni, Hamza, and Benayad Nsiri. "Cluster-based routing protocol using traffic information." International Journal of High Performance Computing and Networking 11, no. 2 (2018): 108-116.
- [14] Khan, Ammara Anjum, Mehran Abolhasan, and Wei Ni. "An evolutionary game theoretic approach for stable and optimized clustering in vanets." IEEE Transactions on Vehicular Technology 67, no. 5 (2018): 4501-4513.
- [15] Abbas, Fakhar, and Pingzhi Fan. "Clustering-based reliable low-latency routing scheme using ACO method for vehicular networks." Vehicular Communications 12 (2018): 66-74.
- [16] Agarwal, Pallavi. "Technical review on different applications, challenges and security in VANET." Journal of Multimedia Technology & Recent Advancements 4, no. 3 (2018): 21-30.
- [17] Rana, Kamlesh Kumar, Sachin Tripathi, and Ram Shringar Raw. "Analytical Analysis of Improved Directional Location Added Routing Protocol for VANETS." Wireless Personal Communications 98, no. 2 (2018): 2403-2426.
- [18] Paul, Bijan, Md Ibrahim, Md Bikas, and Abu Naser. "Vanet routing protocols: Pros and cons." arXiv preprint arXiv:1204.1201 (2012).
- [19] Singh, Gagan Deep, Ravi Tomar, Hanumat G. Sastry, and Manish Prateek. "A review on VANET routing protocols and wireless standards." In Smart computing and informatics, pp. 329-340. Springer, Singapore, 2018.
- [20] Krishnan, V.G. and Sankar N.R., ICR: information, cluster and route agent based method for efficient routing in VANET. *International Journal of Engineering & Technology* 7(2018), no. 1.9 (pp10-15)
- [21] Pei, Guangyu, Mario Gerla, and Tsu-Wei Chen. "Fisheye state routing: A routing scheme for ad hoc wireless networks." In 2000 IEEE International Conference on Communications. ICC 2000. Global Convergence Through Communications. Conference Record, vol. 1, pp. 70-74. IEEE, 2000.
- [22] Kohli, Sandhaya, Bandanjot Kaur, and Sabina Bindra. "A comparative study of Routing Protocols in VANET." Proceedings of IS CET (2010).
- [23] Raw, Ram Shringar, and Arushi Kadam. "Performance Analysis of DTN Routing Protocol for Vehicular Sensor Networks." In Next-Generation Networks, pp. 229-238. Springer, Singapore, 2018.

# Depth Limitation and Splitting Criteria Optimization on Random Forest for Efficient Human Activity Classification

Syarif Hidayat<sup>1</sup>, Ahmad Ashari<sup>2</sup>, Agfianto Eko Putra<sup>3</sup>

Department of Informatics, Faculty of Industrial Technology, Universitas Islam Indonesia, Yogyakarta, Indonesia  
Department of Computer Science and Electronics, Faculty of Mathematics and Natural Sciences  
Universitas Gadjah Mada, Indonesia, Yogyakarta, Indonesia

**Abstract**—Random Forest (RF) is known as one of the best classifiers in many fields. They are parallelizable, fast to train and to predict, robust to outlier, handle unbalanced data, have low bias, and moderate variance. Apart from these advantages, there are still opportunities to increase RF efficiency. The absence of recommendations regarding the number of trees involved in RF ensembles could make the number of trees very large. This can increase the computational complexity of RF. Recommendations for not pruning the decision tree further aggravates the condition. This research attempts to build an efficient RF ensemble while maintaining its accuracy, especially in problem activity. Data collection is performed using an accelerometer sensor on a smartphone device. The data used in this research are collected from five peoples who perform 11 different activities. Each activity is carried out five times to enrich the data. This study uses two steps to improve the efficiency of the classification of the activity: 1) Optimal splitting criteria for activity classification, 2) Measured pruning to limit the tree depth in RF ensemble. The first method in this study can be applied to determine the splitting criteria that are most suitable for the classification problem of activities using Random Forest. In this case, the decision model built using the Gini Index can produce the highest accuracy. The second method proposed in this research successfully builds less complex pruned-tree without reducing its classification accuracy. The research results showed that the method applied to the Random Forest in this study was able to produce a decision model that was simple but yet accurate to classify activity.

**Keywords**—Activity; accuracy; classification; fall; optimization; random forest

## I. INTRODUCTION

Nowadays, there were researches in the field of activity classification and fall detection due to the development of mobile [1] and wearable device [2]. It promised an important role in improving human life quality. Among its application are healthcare, security, work safety [3], [4]. There were several techniques that could be utilized in the activity classification and fall detection system. Khojasteh et al. use a rule-based system to decrease computational cost [5]. Fall detection could also be solved using threshold-based algorithms [6]–[8]. Meanwhile, others trying to make use of machine learning algorithms to increase the accuracy of fall detection [9]–[11]. Aziz et al. compared the accuracy of the two methods in an

experiment involving ten participants. The outcomes demonstrate that the general performance of falls detection of the five machine learning was superior to the performance of five threshold-based methods. Likewise, the testing of the five machine learning demonstrates Support Vector Machine (SVM) as the best performer notably when sensitivity and specificity measure combined [12]. Indeed, current states of the art in Machine Learning are Random Forest and Support Vector Machine [14]. However, Support Vector Machine is more suitable in the case of two class problem [13]. Furthermore, Support Vector Machine tends to work best in a situation where data are reasonably clean with a few outliers. Random Forest generally outperforms Support Vector Machine in many class cases with many outliers to be expected. Research on fall detection which becomes part of human activity classification research needs to identify several activities. Moreover, the accelerometer data generated from human activity could be very noisy [15]. Hence, Random Forest will likely to be more suitable in this case as it needs to classify several classes.

Random Forest is essentially a group classifier that comprises of several decision trees. Those trees then vote to get the final prediction result. It is one of the best-recognized ensemble methods. It could solve the classification task as well as regression task [16].

As Random Forest consisted of several decision trees, it shares the same traits which are bias, variance and overfitting as if in decision trees. The decision model will produce high accuracy if tested on training data. This is also known as the low bias term. However, when the resulting model is tested on testing data that has never been seen before, the accuracy is low. This is referred to as high variance. Supposedly, a good model must be able to produce high accuracy in both training and testing data. Random Forest will likely result in better model stability as it capable of suppressing variance while maintaining bias.

Random Forest will have best performance if the decision tree produces high accuracy (low bias) from the start. Splitting criterion is one of the most influencing factors in decision tree accuracy [18]. Therefore, this study will investigate the most fitting splitting criteria to produce a classification model with highest accuracy.

Random Forest will build unpruned trees [19]. Unpruned trees will produce a model with high accuracy (low bias). However, this will make the generalization ability low (high variance). This research aim for classification model that produce high accuracy (low bias) while still having high generalization ability. As the trees accuracy seems to be not increased after a certain depth, this research proposes optimal depth limitation as a mean of pruning in Random Forest decision tree.

Therefore this research is answering the question of which splitting criterion will make the most accurate trees (resulting in low bias model) and the optimal depth of the tree to produce highest generalization model.

## II. THEORETICAL FRAMEWORK

### A. Random Forest

Fall activity would be classified using the legacy random forest where a number of decision trees are constructed as sampling data using bootstrap and some randomly selected features. Classification by group of trees in Random Forest work by voting a class after each tree in the group make a classification. Random Forest will choose the class which is supported by most of the trees. Fundamentally, data classification techniques using Random Forest works as follows:

- 1) Assume that the number of the original training data record is A.
- 2) Perform bootstrapping on original data by sampling A into a which are chosen randomly with replacement such as  $a < A$ .
- 3) Perform the bootstrapping for n time to create training data from n trees.
- 4) Given some feature/predictor is B, select of b variable at random such as  $b < B$  for each sub-sample created before.
- 5) Build decision trees for each sub-sample data by splitting a node using the best split on the n predictor.
- 6) Grow tree as large as possible **with no pruning**.
- 7) Make a classification by voting the classification result of n trees. The majority class will be selected as the Random Forest classification result.

The decision trees vote to classify activity. This research tried to understand the effect of decision tree depth and the splitting criterion by performing classification on trees with the depth of 5, 10, 15, and 20.

### B. Splitting Criteria

Decision Tree used several measures for selecting best split based on impurity measures. Decision tree tried to split the nodes on all available predictor and choose the best splitter which able to produce the most similar sub-nodes. This step resulted in sub-nodes with higher homogeneity compared to original nodes. There are three most commonly used measures in decision tree splitting:

- 1) *Information gain (IG)*: Information Gain provides an overview of how much information the feature provides in determining the class. When a feature highly determines a

class, the value of information gain will be maximal. On the other hand, a feature that does not correspond to class determination will likely give no information [20]. IG provides an overview of the relation of the predictor to a class by measuring the reduction in entropy value. Entropy gives an overview of class impurity of several data records. Entropy is a measure of impurity in an arbitrary collection of examples. When the node is less impure, the information to describe it is lesser. On the contrary, the more impure node will likely give more information. Entropy function is expressed by (1).

$$H = \sum_{i=1}^k p_k \log p_k \quad (1)$$

Information Gain is described by (2).

$$\Delta H = H - \frac{m_L}{m} H_L - \frac{m_R}{m} H_R \quad (2)$$

- 2) *Gain ratio*: Information gain has a relatively high bias on high branching features. Gain ration modifies information gain so that bias could be reduced when applied on high branching features. Feature selection is taking into account the number and size of branches [20]. Information gain was normalized by intrinsic information of a split. Intrinsic information could be described as the number of information needed to decide on a node to classify a record. It gives an overview of how much information could be acquired whenever dataset split into i partitions. Intrinsic information could be described by (3).

$$D = \sum_{j=1}^i \frac{|D_j|}{D} \cdot \log_2 \left( \frac{|D_j|}{D} \right) \quad (3)$$

Intrinsic information with higher value resulted make the size of sub-sample that is generated during splitting relatively to be the same. On the other hand, less intrinsic information resulted in few sub-sample that contain most of the data record. Gain ratio will select feature that generates a maximum gain ratio. Gain ratio could be described by (4).

$$\text{Gain Ratio}(F) = \frac{\text{Gain}(F)}{\text{Intrinsic Info}(F)} \quad (4)$$

- 3) *Gini index*: Gini index shows the number of randomly picked data that is incorrectly labeled. It reaches its maximum value on heterogeneous data [21]. Consequently, it gets a minimum value on similar data. Gini Index could be described by (5).

$$\text{Gini} = 1 - \sum_{i=1}^k (p_k)^2 \quad (5)$$

## III. MATERIALS

The research data was obtained through accelerometer sensor readings from 5 respondents. Each respondent performed 11 different activities. Each activity was repeated five times to increase the variety of data. There are seven attribute information on the data recorded. Table I contains an example of one data.

Accelerometer data type in Table I could be explained as follows:

TABLE. I. DATA DESCRIPTION

| Type          | Value                   |
|---------------|-------------------------|
| Sequence Name | A01                     |
| Timestamp     | 633790226053172000      |
| Date          | 27.05.2009 14:03:25:317 |
| X             | 4.373908043             |
| Y             | 1.887959599             |
| Z             | 0.769018948             |
| Activity      | walking                 |

a) *Sequence Name*: It contains person and repetition code. Sensor readings of five respondents are marked with the letters A to E. Repetition activities marked with the number 01 to 05. For example, C05 shows the results of the readings from the third respondent in the fifth repetition.

b) *Timestamp*: Each data is given a timestamp to mark the time of the accelerometer sensor readings.

c) *Date*

d) X shows accelerometer sensor reading on axis X

e) Y shows accelerometer sensor reading on axis Y

f) Z shows accelerometer sensor reading on axis Z

g) *Activity*: There are 11 activities which are 1) walking, 2) falling, 3) sitting, 4) sitting down, 5) lying, 6) lying down, 7) sitting on the ground, 8) on all fours, 9) standing up from sitting on the ground, 10) standing up from sitting, and 11) standing up from lying.

#### IV. METHODOLOGY

This research follows methodology including a) Data pre-processing, b) Feature extraction, c) Splitting-Criteria Optimization, d) Tree-Depth Optimization, and e) Validation.

##### A. Data Pre-Processing

The data used in the study needs to be pre-processed so that it can be in accordance with the context of this study. The length of the data for each activity is different. Thus, the information regarding the minimum data of accelerometer record needed to be able to recognize an activity is necessary. This information will be used as a base reference for what is called the data window. Activities with the minimum record will only be represented by one data while activities with more data lengths than data window will be divided into several data. In this research, fall activities have the minimum data representation. The minimum data for fall activities is 17 data. Thus, all other activities data would be windowed by this number.

##### B. Feature Extraction

There are a number of accelerometer feature. It is important to extract the right features in order to be able to classify activity efficiently. Pannurat et al summarize 36 Accelerometer Feature to detect activities including fall [22]. This research extracts 21 features from the data which are:

1) *Mean ( $\mu$ )*: This feature is informative in classifying static activities such as sitting and lying. This feature is extracted for each axis. Equation (6) used to obtain this feature.

$$\mu = \frac{1}{N} \sum_{i=1}^N x_i \quad (6)$$

where  $x$  = accelerometer data on each axis,  $i$  = the data index, and  $N$  = number of data samples.

2) *Standard deviation ( $\sigma$ )*: This feature is useful for classifying dynamic activities such as walking and running. Equation (7) used to obtain this feature.

$$\sigma = \sqrt{\frac{1}{N} \sum_{i=1}^N (x_i - \mu)^2} \quad (7)$$

3) *Variance ( $\sigma^2$ )*: This feature is calculated to measure the spread between accelerometer data in each axis. Equation (8) used to obtain this feature.

$$\sigma^2 = \frac{1}{N} \sum_{i=1}^N (x_i - \mu)^2 \quad (8)$$

4) *Standard deviation magnitude ( $|\sigma|$ )*: This feature measure the spread between the combination of accelerometer data on all axis. Equation (9) used to obtain this feature.

$$|\sigma| = \sqrt{\sigma_x^2 + \sigma_y^2 + \sigma_z^2} \quad (9)$$

5) *Sum vector magnitude ( $|a|$ )*: This feature is useful for detecting abnormal activities such as falling. However, this feature alone is not enough to detect falls because jumping activity also results in sudden changes. Equation (10) used to obtain this feature.

$$|a| = \sqrt{a_x^2 + a_y^2 + a_z^2} \quad (10)$$

where  $a_x$ ,  $a_y$ , and  $a_z$  denote the accelerometer value on the x, y, and z axis

6) *Standard deviation of sum vector magnitude ( $\sigma_{|a|}$ )*: This feature measures the spread between the sum vector magnitudes values previously calculated. Equation (11) used to obtain this feature.

$$\sigma_{|a|} = \sqrt{\frac{1}{N} \sum_{i=1}^N (|a|_i - \mu_{|a|})^2} \quad (11)$$

7) *Sum vector magnitude on horizontal plane ( $|a|_h$ )*: Instead of counting sum vectors from the entire axis, this feature only observes the sum vector in the horizontal plane between axis x and y. Equation (12) used to obtain this feature.

$$|a|_h = \sqrt{a_x^2 + a_y^2} \quad (12)$$

8) *Sum vector magnitude on vertical plane ( $|a|_v$ )*: This feature only observes the sum vector in the vertical plane between axis x and z. Equation (13) used to obtain this feature.

$$|a|_v = \sqrt{a_x^2 + a_z^2} \quad (13)$$

9) *Standard deviation of sum vector magnitude on horizontal plane ( $\sigma_{|a|_h}$ )*: This feature analyzes the distribution of the data from the previous feature vector sum magnitude. Equation (14) used to obtain this feature.

$$\sigma_{|a|_h} = \sqrt{\frac{1}{N} \sum_{i=1}^N (|a|_{h_i} - \mu_{|a|_h})^2} \quad (14)$$

10) *Energy on axis X ( $E_x$ )*: This feature represents the change of acceleration at each measurement in a single window on the axis X. Equation (15) used to obtain this feature.

$$E_x = \sqrt{\frac{1}{w-1} \sum_{i=1}^{w-1} |x_{i+1} - x_i|} \quad (15)$$

where w is the window size.

11) *Energy on axis Y ( $E_y$ )*: This feature represents the change of acceleration at each measurement in a single window on the axis Y. Equation (16) used to obtain this feature.

$$E_y = \sqrt{\frac{1}{w-1} \sum_{i=1}^{w-1} |y_{i+1} - y_i|} \quad (16)$$

12) *Energy on axis Z ( $E_z$ )*: This feature represents the change of acceleration at each measurement in a single window on the axis Z. Equation (17) used to obtain this feature.

$$E_z = \sqrt{\frac{1}{w-1} \sum_{i=1}^{w-1} |z_{i+1} - z_i|} \quad (17)$$

13) *Energy XY ( $E_{xy}$ )*: This feature represents the change of acceleration at each measurement in a single window on the plane X and Y. Equation (18) used to obtain this feature.

$$E_{xy} = \sqrt{\frac{1}{w-1} \sum_{i=1}^{w-1} \left| \sqrt{x_i^2 + y_i^2} - \sqrt{x_{i+1}^2 + y_{i+1}^2} \right|} \quad (18)$$

14) *Energy YZ ( $E_{yz}$ )*: This feature represents the change of acceleration at each measurement in a single window on the plane Y and Z. Equation (19) used to obtain this feature.

$$E_{yz} = \sqrt{\frac{1}{w-1} \sum_{i=1}^{w-1} \left| \sqrt{y_i^2 + z_i^2} - \sqrt{y_{i+1}^2 + z_{i+1}^2} \right|} \quad (19)$$

15) *Energy XZ ( $E_{xz}$ )*: This feature represents the change of acceleration at each measurement in a single window on the plane X and Z. Equation (20) used to obtain this feature.

$$E_{xz} = \sqrt{\frac{1}{w-1} \sum_{i=1}^{w-1} \left| \sqrt{x_i^2 + z_i^2} - \sqrt{x_{i+1}^2 + z_{i+1}^2} \right|} \quad (20)$$

### C. Splitting Criteria Optimization

This method is used to determine whether splitting criteria have a significant impact on classification performance. If the impact is significant, this study will provide recommendations for splitting the most appropriate criteria to solve the problem of classification of human activity. Splitting Criteria Optimization stages can be illustrated in Fig. 1.

The stages of Splitting Criteria Optimization in Fig. 1 can be explained as follows:

- 1) Build the Random Forest ensemble n times where n is the number of splitting criteria that you want to investigate. This study evaluated three of the most widely used splitting criteria, namely Information Gain, Gain Ratio, and Gini Index.
- 2) Generate decision trees in each forest without pruning. The number of decision trees that are generated is as many attributes as there are. Because this study uses 20 features / attributes, each forest will have 20 decision trees.
- 3) Measure the average accuracy of the decision tree in each Random Forest using Out-Of-Bag data (data that is not used in the training process).
- 4) Compare the results of the accuracy between the three ensembles with the same number of trees.
- 5) Determine splitting criteria that is able to build Random Forest ensemble with the best average accuracy value.

### D. Tree-Depth Optimization

One of the main contributions in this study was the limitation of tree depth with measured pruning techniques. The original Random Forest algorithm does not do pruning. Thus, the decision tree structure becomes very deep and large. Furthermore, it will make the variance even higher. High variance means that the classification model will be very accurate if tested using training data yet will be inaccurate if tested using testing data that is never seen before. This is known as overfitting which is often found in classification algorithms (Kuhn and Johnson, 2013). The pruning technique could make the decision tree in Random Forest ensemble concise. It resulted in a group of small size trees. Thus, the complexity of the decision tree becomes smaller. It will give considerable classification strength even though the data conditions are diverse and have not been recognized before. However, this technique needs to be applied carefully as if it performed improperly will reduce the accuracy of the classification model.

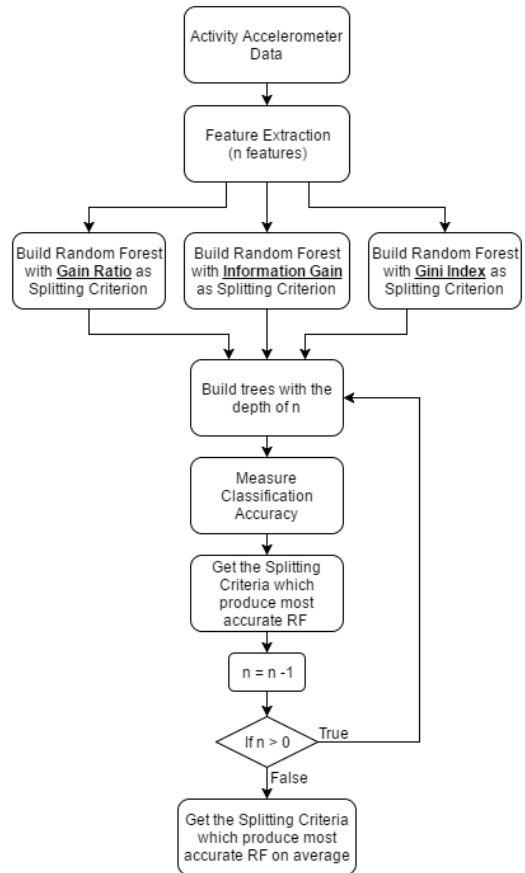


Fig. 1. Splitting Criteria Optimization Method.



This study proposes a measured pruning technique by evaluating the accuracy as a result of tree depth reduction. The steps to get the optimal tree depth are as follows:

- 1) Build Random Forest ensemble without pruning to get maximum accuracy.
- 2) Measure the classification accuracy of the Random Forest classification model.
- 3) Reduce the depth of the tree in Random Forest classification model.
- 4) Repeat the accuracy measurement for the new Random Forest classification model.
- 5) If the accuracy does not changes significantly, go to step 3.
- 6) If the accuracy changes significantly, stop reducing the depth of the tree as the optimum tree depth has been obtained.

The pseudocode used in this study to reach the optimal depth in the Random Forest ensemble is as follows:

```
k = 21
for j=1 to 5
  build trees() with depth of k;
  RF_vote();
  Acc_old = RF_Accuracy();

  Acc_new = 100;
  While Acc_new >= Acc_old
    k = k - 1
    for j=1 to 5
      build trees() with depth of k;
      RF_vote();
      Acc_new = RF_Accuracy();
  return k;
```

In this study the initial depth of tree (k) is 21 because in the worst case scenario, the decision tree will use the entire feature (twenty one features) as leaf nodes to determine the class of a data. Variable i indicates the number of decision trees in Random Forest ensemble. This study only shows results of performance measurement in the ensemble Random Forest classification consisting of 5, 10, 15, and 20 decision tree as the results are significant to each other.

### E. Validation

The performance of the activity classification system needs to be measured correctly to determine the quality of the system being built. The measuring index that is generally used to determine the performance of the classification system is the value of specificity, sensitivity, and accuracy (Han, Kamber et al., 2011). However, this study only uses accuracy as a measure of performance which is calculated using the following formula:

$$Accuracy = \frac{TP+TN}{P+N} \quad (21)$$

where TP = True Positive, TN= True Negative, P = Positive, N = Negative.

This research makes use of 10-Fold Cross-Validation to obtain accuracy value in activity classification as the performance value calculated by the K-fold cross-validation method is less dependent on the data distribution characteristics in the training set and test set. Therefore the resulting performance value can be considered more.

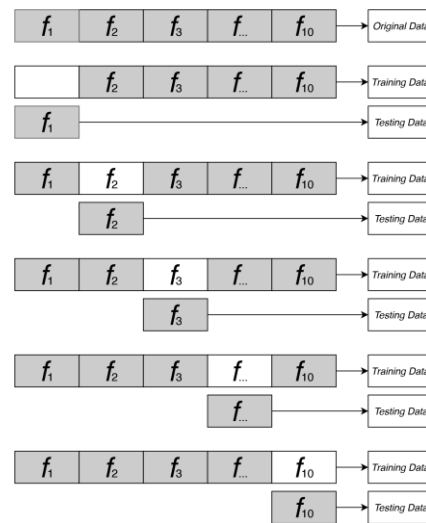


Fig. 2. Ten-Fold Cross-Validation.

The 10-Fold Cross Validation is superior to the usual split method. The number of folds selected, which is ten, also proved to have produced a variance against a relatively small performance. Taking into account the computational complexity required, this method is better than the more expensive methods, such as leave-one-out cross-validation [24]. The fold cross validation method with k = 10 becomes the standard for predicting the performance of algorithms in machine learning. The dataset benchmark test shows that k = 10 represents the number of folds appropriate to obtain the best accuracy estimation [25] (Fig. 2).

## V. EXPERIMENT RESULT

The resulting experiment shows Random Forest Accuracy with the number of trees in each ensemble varies from 5, 10, 15, and 20 trees. On each ensemble, classification accuracy was measured and analyzed towards tree depth to find out the optimum tree depth for activity classification.

### A. Random Forest with 5 Trees

The first experiment tested the accuracy of the Random Forest algorithm when using 5 trees. The results of the research show that initially, Random Forest was able to achieve accuracy up to 87.86% when classifying human activities.

However, the accuracy starts to decrease significantly when the tree depths is 7. Here, Random Forest that uses Information Gain as the splitting criterion is slightly better than one that uses Gini Index and Gain Ratio as the splitting criterion (Fig. 3).

Fig. 3 also shows that Gain Ratio and Gini Index have better ability to retain accuracy on the occasion of tree depth reduction. On the event that tree depth is reduced from 7 to 3, both splitting criteria have better result compared to Information Gain. Classification result in trees with Information gain shows significant accuracy drop to only 67%.

### B. Random Forest with 10 Trees

The second experiment measures the classification accuracy of the Random Forest with 10 trees. Increasing the number of trees involved in Random Forest improved human

activities classification accuracy up to 89.29%. The accuracy starts to decrease significantly when the tree depths is 6. Gini Index exhibits better performance when compared to Gini Index or Information Gain as Random Forest splitting criterion (Fig. 4). We also noticed that additional trees affect the tree depth as the classification accuracy started to decrease at the depth of 6 instead of 7 in the first experiment.

C. Random Forest with 15 Trees

Further increment on the number of Random Forest trees shows that Random Forest with 15 trees could achieve accuracy up to 91.43% when classifying human activities. The accuracy starts to decrease significantly when the tree depths is 5. This finding assures previous assumption that additional trees could reduce the tree depth as the more trees lead to shallower tree depth (Fig. 5).

Gini Index and Gain Ratio exhibit better performance as Random Forest splitting criterion compared to Information Gain. However, Gini Index exhibits better performance on shallow tree depth as it gives better accuracy even at the depth of 3.

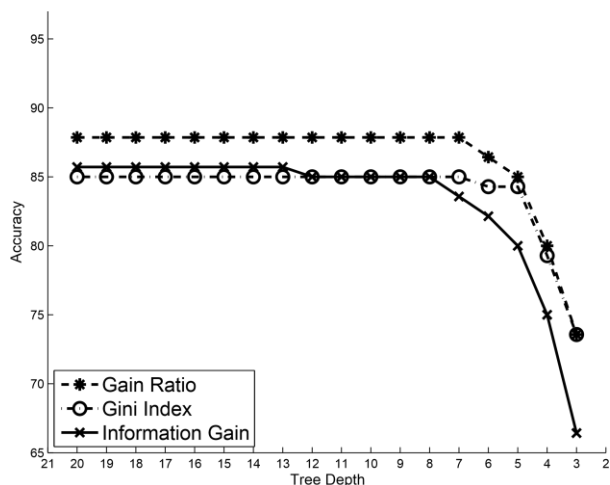


Fig. 3. Splitting Criterion Impact on Random Forest with 5 Trees Activity Classification Accuracy.

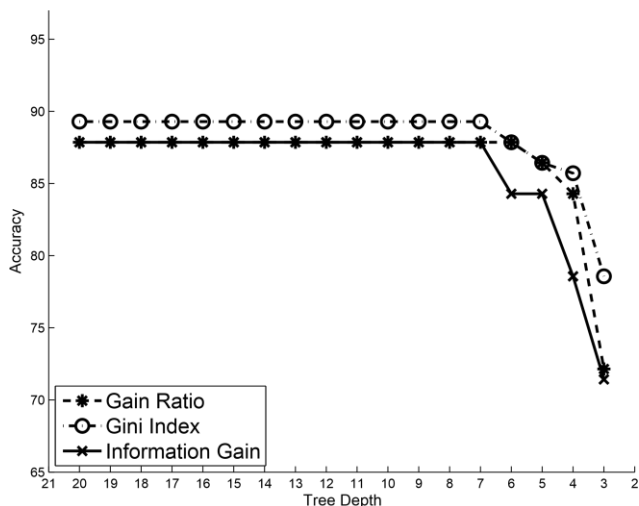


Fig. 4. Splitting Criterion Impact on Random Forest with 10 Trees Activity Classification Accuracy.

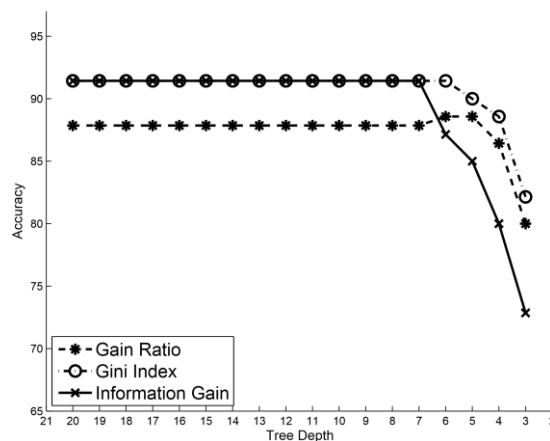


Fig. 5. Splitting Criterion Impact on Random Forest with 15 Trees Activity Classification Accuracy.

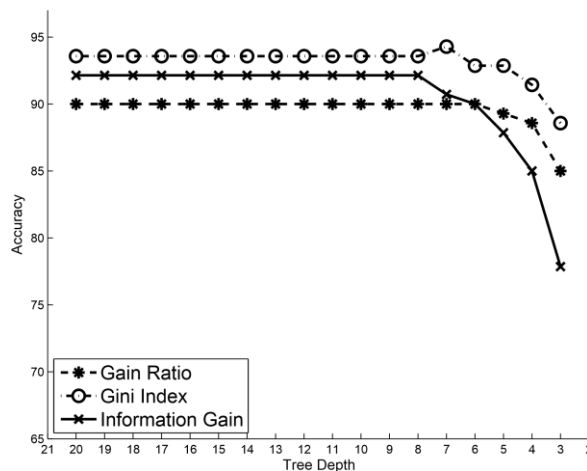


Fig. 6. Splitting Criterion Impact on Random Forest with 20 Trees Activity Classification Accuracy.

D. Random Forest with 20 Trees

The last experiment, Random Forest with 20 trees is able to achieve accuracy up to 93.57% when classifying human activities including falls. The accuracy starts to decrease significantly when the tree depths is 5 (Fig. 6). This result suggests that additional trees on Random Forest Ensemble no longer reduce tree depth.

In this experiment setup, Gini Index clearly gives the best result in contrast to Information Gain or Gain Ratio. This experiment results even further emphasize the previous hypothesis that Gini Index has better performance compared to other splitting criteria as it could retain accuracy in the minimum tree depth.

VI. DISCUSSION

The experiment result indicates that Gini Index generally gives better performance for Activity Classification. When the number of trees in the RF ensemble is small, the three splitting criteria look like they give relatively the same accuracy, but when the number of trees increases, the Gini Index has a significant impact. The only time Gini Index has lower performance compared to other splitting criteria was in the experiment with 5 trees. Above those number, Gini Index

clearly outperforms other splitting criteria. Based on this, it can be concluded that the most optimum splitting criteria for activity classification is Gini Index.

Furthermore, RF decision trees that are built using the Gini Index show the ability to produce better performance in conditions where decision trees depth are less. Fig. 3 shows that that Gini Index has the lowest performance at the beginning (deepest trees). At the end, as the depth of the trees becoming less, it was able to outperform other splitting criteria at the depth of 3. Thus, it can be inferred that Gini Index has the ability to maintain classification accuracy.

The minimum depth to have good accuracy is 5. It could be achieved with 10 trees. By choosing the right splitting criterion, classification accuracy drop could be reduced. As could be seen in Fig. 3, Gini Index splitting criteria relatively could retain accuracy better than other splitting criteria.

There is a trade-off between the number of trees and the depth of the tree. The more trees, the lower the depth of trees needed to achieve the best accuracy. Likewise the opposite, the smaller number of trees, the deeper is the tree in order to achieve the best accuracy. However, this thing only happens before a certain point. The depth of the tree involved in the ensemble could be suppressed until the number of trees is 15. Afterward, additional trees only improved accuracy only. It could not take advantage of lowering the depth of the trees. In another word, additional accuracy after that point would add significant complexity. As an illustration, 10 trees with the depth of 6 will have  $10 \cdot (2^6) = 640$  logic gate while 15 trees with the depth of 5 will only have  $15 \cdot (2^5) = 480$  logic gate. This proves that 15 trees with the depth of 5 are less complex than 10 trees with the depth of 6. Therefore other than Gini Index as splitting criteria and 5 as the most optimum depth in RF ensemble, it could be conclude that the most optimum number of trees in Random Forest ensemble is 15.

## VII. CONCLUSIONS

This research proposed several methods to optimize Random Forest algorithm performance as Human Activity Classifier. Those are the selection of the most optimal splitting criterion and measured pruning to limit the tree depth in RF ensemble in order to find the minimum depth of the tree to get optimum accuracy.

The results of this study indicate that splitting criteria greatly influence the accuracy of the decision models produced by Random Forest. The first method in this study found that Gini Index is the most suitable splitting criteria to construct decision tree models used solve activity classification. Gini Index exhibits the ability to retain classification accuracy on the shallow tree depth. Furthermore, trees that was build using Gini Index has the minimum accuracy reduction upon reduction of the tree depth.

The measured pruning method applied in this research find that the minimum tree depth for activity classifier is 5. Additional depth no longer increases the accuracy yet significantly increases computational complexity. Limiting the depth of the decision tree will reduce the complexity of the algorithm, thereby increasing the efficiency of the decision model.

## VIII. FUTURE WORK

This research was aimed to be preliminary research on efficient fall detection using the accelerometer. There is a trend in the increasing number of cores in the processor. The Random Forest can benefit from this trend by distributing decision trees evenly on each core. Therefore, the use of RF activity classification can be done quicker as it performed in parallel.

This study provides methods to optimize decision tree models constructed with Random Forest algorithm by utilizing the most splitting criteria for certain problem and limiting the trees depth. Other than those two things, the number of trees in the Random Forest ensemble also influences the complexity of the decision model that is built. However, there are no exact numbers to determine the number of trees in the RF ensemble. Therefore, there is still an opportunity to maximize the Random Forest algorithm by compressing the number of RF trees. The next research could address this issue to extend the efficiency of Random Forest.

## ACKNOWLEDGMENT

This research was supported by The Ministry of Research, Technology and Higher Education (Kemenristekdikti) of the Republic of Indonesia (Grant No. 109/SP2H/LT/DRPM/2018).

## REFERENCES

- [1] Hakim, M. S. Huq, S. Shanta, dan B. S. K. K. Ibrahim, "Smartphone Based Data Mining for Fall Detection: Analysis and Design," *Procedia Computer Science*, vol. 105, hlm. 46–51, Jan 2017.
- [2] P. Kumari, L. Mathew, dan P. Syal, "Increasing trend of wearables and multimodal interface for human activity monitoring: A review," *Biosensors and Bioelectronics*, vol. 90, hlm. 298–307, Apr 2017.
- [3] P. Jatesiktat dan W. T. Ang, "An elderly fall detection using a wrist-worn accelerometer and barometer," dalam 2017 39th Annual International Conference of the IEEE Engineering in Medicine and Biology Society (EMBC), 2017, hlm. 125–130.
- [4] M. Daher, A. Diab, M. E. B. E. Najjar, M. A. Khalil, dan F. Charpillat, "Elder Tracking and Fall Detection System Using Smart Tiles," *IEEE Sensors Journal*, vol. 17, no. 2, hlm. 469–479, Jan 2017.
- [5] S. Khojasteh, J. Villar, C. Chira, V. González, dan E. de la Cal, "Improving Fall Detection Using an On-Wrist Wearable Accelerometer," *Sensors*, vol. 18, no. 5, hlm. 1350, Apr 2018.
- [6] A. K. Bourke, J. V. O'Brien, dan G. M. Lyons, "Evaluation of a threshold-based tri-axial accelerometer fall detection algorithm," *Gait & posture*, vol. 26, no. 2, hlm. 194–199, 2007.
- [7] M. Kangas, A. Konttila, I. Winblad, dan T. Jamsa, "Determination of simple thresholds for accelerometry-based parameters for fall detection," dalam 29th Annual International Conference of the IEEE Engineering in Medicine and Biology Society, 2007. EMBS 2007, 2007, hlm. 1367–1370.
- [8] J. Jacob dkk., "A fall detection study on the sensors placement location and a rule-based multi-thresholds algorithm using both accelerometer and gyroscopes," dalam 2011 IEEE International Conference on Fuzzy Systems (FUZZ), 2011, hlm. 666–671.
- [9] T. H. Nguyen, T. P. Pham, C. Q. Ngo, dan T. T. Nguyen, "A SVM Algorithm for Investigation of Tri-Accelerometer Based Falling Data," *American Journal of Signal Processing*, vol. 6, no. 2, hlm. 56–65, 2016.
- [10] B. T. Nukala dkk., "An Efficient and Robust Fall Detection System Using Wireless Gait Analysis Sensor with Artificial Neural Network (ANN) and Support Vector Machine (SVM) Algorithms," *Open Journal of Applied Biosensor*, vol. 3, no. 04, hlm. 29, 2015.
- [11] F. A. J. Parera dan C. Angulo, "Accelerometer Signals Analisis Using Svm And Decision Tree In Daily Activity Identification," *Gerontechnology*, vol. 7, no. 2, hlm. 184, 2008.

- [12] O. Aziz, M. Musngi, E. J. Park, G. Mori, dan S. N. Robinovitch, "A comparison of accuracy of fall detection algorithms (threshold-based vs. machine learning) using waist-mounted tri-axial accelerometer signals from a comprehensive set of falls and non-fall trials," *Med Biol Eng Comput*, hlm. 1–11, Apr 2016.
- [13] M. Kounelakis, M. Zervakis, dan X. Kotsiakis, "Chapter 13 - The Impact of Microarray Technology in Brain Cancer," dalam *Outcome Prediction in Cancer*, A. F. G. Taktak dan A. C. Fisher, Ed. Amsterdam: Elsevier, 2007, hlm. 339–388.
- [14] T. Nef dkk., "Evaluation of Three State-of-the-Art Classifiers for Recognition of Activities of Daily Living from Smart Home Ambient Data," *Sensors (Basel)*, vol. 15, no. 5, hlm. 11725–11740, Mei 2012.
- [15] Q. Li, "Noise Reduction of Accelerometer Signal with Singular Value Decomposition and Savitzky-Golay Filter," *Journal of Information and Computational Science*, vol. 10, no. 15, hlm. 4783–4793, Okt 2013.
- [16] V. Svetnik, A. Liaw, C. Tong, J. C. Culberson, R. P. Sheridan, dan B. P. Feuston, "Random Forest: A Classification and Regression Tool for Compound Classification and QSAR Modeling," *J. Chem. Inf. Comput. Sci.*, vol. 43, no. 6, hlm. 1947–1958, Nov 2003.
- [17] A. Cutler, D. R. Cutler, dan J. R. Stevens, "Random Forests," dalam *Ensemble Machine Learning*, C. Zhang dan Y. Ma, Ed. Boston, MA: Springer US, 2012, hlm. 157–175.
- [18] M. Jaworski, L. Rutkowski, dan M. Pawlak, "Hybrid Splitting Criterion in Decision Trees for Data Stream Mining," dalam *Artificial Intelligence and Soft Computing*, vol. 9693, L. Rutkowski, M. Korytkowski, R. Scherer, R. Tadeusiewicz, L. A. Zadeh, dan J. M. Zurada, Ed. Cham: Springer International Publishing, 2016, hlm. 60–72.
- [19] Leo Breiman, "Random forests," *Machine learning*, vol. 45, no. 1, hlm. 5–32, 2001.
- [20] J. R. Quinlan, "Induction of decision trees," *Machine learning*, vol. 1, no. 1, hlm. 81–106, 1986.
- [21] L. Breiman, *Classification and regression trees*. Routledge, 2017.
- [22] N. Pannurat, S. Thiemjarus, dan E. Nantajeewarawat, "Automatic Fall Monitoring: A Review," *Sensors*, vol. 14, no. 7, hlm. 12900–12936, Jul 2014.
- [23] B. H. Menze dkk., "A comparison of random forest and its Gini importance with standard chemometric methods for the feature selection and classification of spectral data," *BMC Bioinformatics*, vol. 10, no. 1, hlm. 213, 2009.
- [24] R. Kohavi, "A study of cross-validation and bootstrap for accuracy estimation and model selection," dalam *Ijcai*, 1995, vol. 14, hlm. 1137–1145.
- [25] R. Bouman dan J. van Dongen, *Pentaho solutions: business intelligence and data warehousing with Pentaho and MySQL*, 1. Aufl. Indianapolis, Ind: Wiley, 2009.

# The Mathematical Model of Hybrid Schema Matching based on Constraints and Instances Similarity

Edhy Sutanta<sup>1</sup>, Erna Kumalasari Nurnawati<sup>2</sup>, Rosalia Arum Kumalasanti<sup>3</sup>

Department of Informatics Engineering, Institut Sains & Teknologi AKPRIND Yogyakarta Yogyakarta, Indonesia

**Abstract**—Schema matching is a crucial issue in applications that involve multiple databases from heterogeneous sources. Schema matching evolves from a manual process to a semi-automated process to effectively guide users in finding commonalities between schema elements. New models are generally developed using a combination of methods to improve the effectiveness of schema matching results. Our previous research has developed a prototype of hybrid schema matching utilizing a combination of constraints-based method and an instance-based method. The innovation of this paper presents a mathematical formulation of a hybrid schema matching model so it can be run for different cases and becomes the basis of development to improve the effectiveness of output and or efficiency during schema matching process. The developed mathematical model serves to perform the main task in the schema matching process that matches the similarity between attributes, calculates the similarity value of the attribute pair, and specifies the matching attribute pair. Based on the test results, a hybrid schema matching model is more effective than the constraints-based method or instance-based method run individually. The more matching criteria used in the schema matching provide better mapping results. The model developed is limited to schema matching processes in the relational model database.

**Keywords**—Constraint-based; hybrid schema matching model; instance-based; mathematical model

## I. INTRODUCTION

Schema matching is a crucial issue in applications that involve multiple databases from heterogeneous sources, e.g., for query mediation and data warehouse [1]. The problem has emerged since the early 1980s [2]. Technically schema matching is a process of database integration that results in generalization or specialization [3]. The method of database integration generally faces the constraints caused by heterogeneity problems [4]. Database integration solutions consist of 3 levels, namely database, middleware, and applications [5]. The task of schema matching is limited to detecting the similarities and relationships between the elements of two schemas [6]. An example of an integration effort at the database level for a relational database schema is performed on [7] while using ontology is found in [8] and [9]. Integration at the middleware level is developed [10], while integration at the application level through business process integration is among others performed by [11] and [12].

Studies at [13] have at least found 36 schema matching models ever developed before. The schema matching

prototype first appeared on SemInt [14], while the latest is COMA 3.0 [15]. Schema matching evolved from manual to semi-automatic ways. Until the end of the 2002 year, the schema matching model has been still done mainly by using manual methods [16], only a small developed model for the most familiar domain and suitable for applications with different schema languages [17]. The manual approach has disadvantages that are time-consuming, tedious, and impractical when it is applied, which involve many schemas [16]. The manual process is also expensive and error-prone. So, it needed new methods that are semi-automated to reduce manual effort [18]. The goal is to expertly guide users in solving schema matching problems [17]. The issue of schema matching is how to arrange a mapping between two elements of schema or ontology that have in common. The mapping process involves two schemas or ontology, one of which acts as a source and the other as a target. The schema matching model cannot be fully automated because it still encounters conflict problems at the naming level and data abstraction before it can be generalized for database integration [3].

According to [19], schema matching is a work similar to pairing, whereas according to [18], [20], and [21] schema matching is a process for finding the relation between elements in two schemas. The purpose of schema matching is given two schema input and or additional information, then determining the result of mapping the similarity of schema elements entered after verification by a user [22]. Generally, schema matching requires knowledge that is not always available in the schema so that the process cannot be performed automatically and requires user interaction to verify or provide suggestions for the model results [23].

Schema matching models can be developed using one or a combination of methods. The methods of schema matching are classifying in different ways, e.g. [7], [24], and [25] distinguishing into seven categories, i.e., linguistic-based, structure-based, constraint-based, instance-based, rule-based, hybrid, and auxiliary information dictionary, WordNet, or Corpus. In the case of schema matching performed using more than one method, the way of combining is doing using a hybrid or composite. The hybrid model runs several methods simultaneously [26], [27], while the composite runs the ways independently on each schema matched and combines on the result [28]. The term hybrid matcher is synonymous with intra-matcher parallelism, composite matcher equivalent with inter-matcher parallelism, while hybrid schema matching is also known as a mixed strategy [15], [29].

Based on survey results [13], research [7] developed a hybrid schema matching model by combining simultaneously constraints-based method approaches and instance-based methods. The model was tested 36 times and yielded the interval parameter values Precision (P) between 71.43% - 100.00%, Recall I at 75.00% -100.00% intervals, and F-measure (F) at intervals 81.48% -100.00 %. The focus on [7] is to develop a logical model and operational architecture for the hybrid schema matching model. The novelty of this paper is to present a mathematical formulation for the hybrid schema matching model [7], so it can be run for different cases and the basis of development to improve the effectiveness of output and or efficiency of schema matching process. The developed mathematical model serves to perform the primary task in the schema matching process that matches the similarity between attributes, calculates the similarity value of the attribute pair, and specifies the matching attribute pair.

The remainder of this contribution is structured as follows: Section 2 describes the material and method which is already applied in several real-world relational databases. Section 3 discusses the results and discussion of the results of the experiment, and finally, Section 4 contains the conclusion and opportunities for further research.

## II. THE MATERIAL AND METHOD

The process in schema matching requires two types of input, i.e., database pairs to match and user verification of the mapping output generated by the model. In this research, the test data consist of a simulation database and test database. Both were developed using a relational database model. The input database is called DBSource (database matched) and DBTarget (database for matching reference).

The simulation database is prepared specially by the researcher for logical model validity testing. Constraints and instances in the simulation database are arranged to vary in a controlled manner so that when used for testing, it can display possible errors. The simulation database consists of 4 db\_loc1, db\_loc2, db\_loc3, and db\_loc4, each containing the master data of the provincial, district, and sub-district codes used in e-government applications in Indonesia and developed using MySQL. Each of the simulation databases is composed of 3 tables, eight attributes, and 9.953 instances. The test database is the result of a survey that meets the various criteria on aspects of DBMS, application domain, and size, used as many as 30 pieces. Based on the DBMS used, the test database consists of 22 databases developed using MySQL and eight others developed using MS Access. Based on the application domain, it consists of 8 college educational applications, 12 high school academic applications, eight e-government applications, and two e-commerce applications. By size, the most significant test database composed of 204 tables, the largest attribute count is 1,851, the largest instance count is 232,893 items, and the largest capacity is 79,769 Kb while the smallest test database contains 1 table, with 16 attributes, 480 instances, measuring 115 Kb.

The process sequence in our model is:

1) accept DBSource and DBTarget input;

- 2) extracting constraints and instances;
- 3) perform matching and computation of similarity values (SIM) in the attribute pair in DBSource and DBTarget;
- 4) specify the matching attribute pairs;
- 5) displaying the initial result of mapping the similarity of the attribute pair for the DBSource and DBTarget pair;
- 6) receive user verification of the initial finding of mapping the similarity of the attribute pair;
- 7) displaying the final result of mapping the similarity of the attribute pair that has been verified by the user; and calculate and display the values of effectiveness parameters, i.e., P, R, and F.

The output generated by the model includes:

- 1) general information about DBSource and DBTarget, including constraint and instance;
- 2) attribute values (SIM) of each pair of attributes in DBSource and DBTarget;
- 3) initial results mapping the similarity of the attribute pair as an output model;
- 4) the result of the mapping of the similarity of attribute pair which has been verified by the user; and
- 5) the effectiveness parameter values P, R, and F.

The values of Precision (P), Recall (R), and F-measure (F) are calculated using the following formula [30]:

$$P = \frac{TP}{TP+FP} \quad (1)$$

$$R = \frac{TP}{TP+FN} \quad (2)$$

$$F = \frac{2*P*R}{P+R} \quad (3)$$

The TP represents the relevant model output, and the user accepts it. TN is outward of the relevant model, and the user does not accept it. The FP is an outsource of the model that is irrelevant and accepted by the user, and the FN is the outward model that is irrelevant and is not accepted by the user.

Precision reflects the share of real correspondences among all found ones, Recall specifies the share of real correspondences that found, and F-measure represents the harmonic mean of Precision and Recall and is the most common variant of F-measure in Information Retrieval.

Overall this research consists of 7 stages, namely, 1) development of logical model, 2) development of model architecture, 3) development of procedures, 4) development of prototype model, 5) testing the validity of the model using the database simulation, 6) the development of mathematical models, and 7) testing model using the test database. Stage 1-5 has been performed on [7], and the focus of this paper is to present the mathematical model (steps 6) and show the comparison of the effectiveness of the hybrid schema matching model over the constraint-based method and the instance-based method performed separately (stage 7). The matching mechanism and the similarity value calculation of the attribute pair in the hybrid schema matching model shown in Fig. 1.

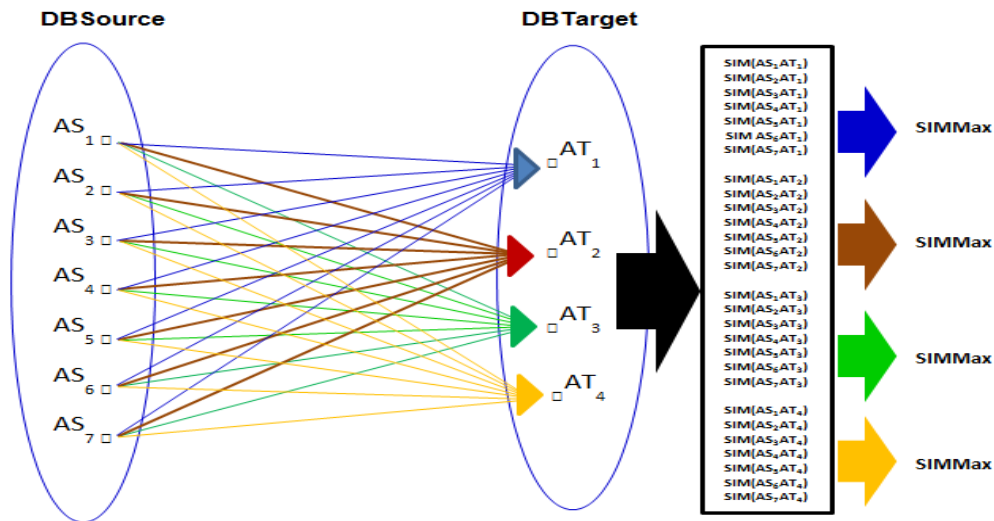


Fig. 1. Matching Mechanism and Computing the Similarity Value.

III. RESULT AND DISCUSSION

A. A Sample of Hybrid Schema Matching

To provide an overview process of the hybrid schema matching model, the following given a simple example of schema matching process for the employee (Table I and Table II) and religion (Table III and Table IV).

Table I to Table IV show the constraints and instances of employee and religion. Each possible attribute pair on employee and religion is then matched and calculated by the value of the similarity to determine the matching pair. Then it is verified to ascertain whether the pair that is declared to be matched by the model strictly matches, or must be revised, or otherwise unpaired. In this example, the calculation of the similarity value of each pair of attributes is based on the assumption that each matching criterion has the same weight so that each value is 0.166. The matching criteria on the constraint are of type, width, nullable, unique, and domain, whereas in an instance the attribute pair is the same if found at least one value of the same value. In each matching process using a specific criterion, if found similarity, then the value of similarity on the criterion is 0.166, otherwise the value of the similarity is 0.000. The attribute pair SIM value calculates by summing the similarity values across all criteria. Based on the SIM attribute pair values, then determined the attribute pair that is declared suitable that has the highest value or 1.00.

TABLE I. THE TABLE STRUCTURE OF EMPLOYEE

| Column        | Type    | Width | Null | Unique | Domain |
|---------------|---------|-------|------|--------|--------|
| employee_id   | char    | 3     | no   | yes    | -      |
| employee_name | varchar | 100   | no   | no     | -      |
| religion_id   | char    | 1     | no   | no     | -      |

TABLE II. THE INSTANCE OF EMPLOYEE

| employee_id | employee_name     | religion_id |
|-------------|-------------------|-------------|
| emp_01      | Edhy Sutanta      | M           |
| emp_02      | Erna Kumalasari N | M           |
| emp_03      | Rosalia Arum K    | C           |

TABLE III. THE TABLE STRUCTURE OF RELIGION

| Column        | Type    | Width | Null | Unique | Domain |
|---------------|---------|-------|------|--------|--------|
| religion_id   | Char    | 1     | no   | yes    | -      |
| religion_name | varchar | 10    | no   | yes    | -      |

TABLE IV. INSTANCE OF RELIGION

| employee_id | religion_name |
|-------------|---------------|
| emp_01      | Moslem        |
| emp_02      | Christian     |

There are three attributes on employee and two attributes in religion, so the matching process will doing six times. The matching pair of attributes is employee\_id in employee and religion\_id in religion, employee\_name in employee and religion\_id in religion, religion\_id in employee and religion\_id in religion, employee\_id in employee and religion\_name in religion, employee\_name in employee and religion\_name in religion. The result obtained three pairs of attributes that are otherwise suitable, is religion\_id in employee match with religion\_id in religion on SIM = 0.664, employee\_id in employee match with religion\_name in religion on SIM = 0.332, and employee\_name in employee match with religion\_name in religion on SIM = 0.332. Then, when verification, only one pair of attributes are found to be suitable is religion\_id in employee match with religion\_id in religion. The effectiveness parameter values obtained are P = 1.00, R = 0.25, and F = 0.40.

B. The Hybrid Schema Matching Logical Test

Testing the validity of the model is done to ensure that the logical model, model architecture, procedures, and prototypes developed are valid logically. Testing is done in 2 ways, manually and using a software of model prototype. The test was conducted 16 times using a combination of 4 databases simulated as source and target. The values of TP, FP, FN, and TN, and P, R, and F in each test using the developed and manually model are the same as the results obtained in the test using the model prototype so that the developed model is

validly valid logically. The end result obtained the average value of P = 94.42%, R = 100.00%, and F = 97.02%.

### C. The Hybrid Schema Matching Logical Test

The description of the mathematical model for our hybrid matching schema is as follows:

$DS = \{RS_1, RS_2, \dots, RS_m\}$ ,  $RS_i$  is a table in DS

$RS_i = (AS_{i1}, AS_{i2}, \dots, AS_{ik_i})$ ,  $1 \leq i \leq n$ , representation of  $RS_i$  as attribute pair

$tS_{ij} = (vS_{i1j}, vS_{i2j}, \dots, vS_{ik_ij})$ ,  $1 \leq j \leq k_i$ , tuple to-j in  $RS_i$

where

$tS_{ij} \in r(RS_i) \subset \text{DOM}(AS_{i1})_x \text{DOM}(AS_{i2})_x \dots \text{DOM}(AS_{ik_i})$

$DT = \{RT_1, RT_2, \dots, RT_n\}$ ,  $RT_i$  is a table in DT

$RT_p = (AT_{p1}, AT_{p2}, \dots, AT_{pr_p})$ ,  $1 \leq p \leq m$ , representation of  $RT_i$  as attribute pair

$tT_{pq} = (vT_{p1q}, vT_{p2q}, \dots, vT_{pr_pq})$ ,  $1 \leq q \leq s_p$ , tuple to-q in  $RT_i$

where

$tT_{pq} \in r(RT_p) \subset \text{DOM}(AT_{p1})_x \text{DOM}(AT_{p2})_x \dots \text{DOM}(AT_{pr_p})$

DS declares the source database to be matched (DBSource). RS is a relation in DS, and AS is an attribute in the RS. tS is a tuple in RS. vS is the data value in tS. M is the relation cache in DS. DT is the reference target database for matching (DBTarget). RT is a relation in the DT, and AT is an attribute in the RT. tT is a tuple in RT. vT is the value of data in tT, and n is a relation count in DT. While a DMATCH is representing the result of schema matching for the pair of DS and DT, where x is a cache attribute in DS, and y is a cache attribute in DT, then;

$DMATCH = \{(AS_1, AT_1, AS_1, AT_2), \dots, (AS_x, AT_y)\}$

The C represents the set of the match criteria;

$C = \{T, W, N, U, D, I\}$

where the T, W, N, U, D, and I represent the type, the width, the nullable, the unique, the domain, and the instance, respectively.

The similarity value for any pair of attributes in the DS and the b attribute in the DT value is calculated as follows:

$$SIMT(AS_a, AT_b) = \begin{cases} 1, T(AS_a) = T(AT_b) \\ 0, \text{others} \end{cases} \quad (4)$$

$$SIMW(AS_a, AT_b) = \begin{cases} 1, W(AS_a) = W(AT_b) \\ 0, \text{others} \end{cases} \quad (5)$$

$$SIMN(AS_a, AT_b) = \begin{cases} 1, N(AS_a) = N(AT_b) \\ 0, \text{others} \end{cases} \quad (6)$$

$$SIMU(AS_a, AT_b) = \begin{cases} 1, U(AS_a) = U(AT_b) \\ 0, \text{others} \end{cases} \quad (7)$$

$$SIMD(AS_a, AT_b) = \begin{cases} 1, D(AS_a) = D(AT_b) \\ 0, \text{others} \end{cases} \quad (8)$$

$$SIMI(AS_a, AT_b) = \begin{cases} 1, \exists I(AS_a) = I(AT_b) \\ 0, \text{others} \end{cases} \quad (9)$$

Where the SIMT is the value of similarity for the T criteria. The SIMI is the value of similarity for I criteria. The SIMW is the value of similarity for W criteria. The SIMN is the value of similarity for N criteria. The SIMU is the value of similarity for U criteria. The SIMD is the value of similarity for D criteria, and the SIMI is the value of similarity for I criteria. In general, the calculation of the similarity value of the attribute pair for any C member is:

$$SIM_c(AS_a, AT_b) = \begin{cases} 1, x(AS_a) = x(AT_b) \\ 0, \text{others} \end{cases} \quad (10)$$

where  $x(A)$ = criteria x for A.

While WI is the weight of the instance, WT is the weight of type, WW is the width weight, WN is the nullable weight, WU is a specific weight, and WD is the domain weight. Thus, the  $AS_a$  and  $AT_b$  pair similarity values are calculated as follows:

$$SIM(AS_a, AT_b) = \sum_{y \in C} SIM_y(AS_a, AT_b) W_y \quad (11)$$

Paired attributes that are otherwise matched by the model, if the  $AT_b$  matched to  $AS_a$  then  $AT_b$  are taken which meets the following conditions:

$$SIM(AS_a, AT_b) = \text{Max}_{z=1}^m SIM(AS_a, AT_z) \quad (12)$$

where

$z = 1, 2, \dots, m$ .

### D. The Hybrid Schema Matching Test Result

A valid hybrid schema matching model, then tested 32 times using a combination of randomly chosen test database pairs, and the results displayed in Table V.

Based on the test results in Table V and Table VI, it is known the highest P-value is 93.04% in the hybrid model, the lowest P-value is 33.28% in the constraint-based method, while the instance-based method is between constraint-based and hybrid. These results show that hybrid models provide the best results from the precision. Compared to the instance-based method, there was an increase of 31.94%, while compared to the constraint-based approach, there was an increase of 59.76%. This condition occurs because the hybrid model matches by involving more criteria (6 criteria at once), compared to the constraint-based method using five criteria or the instance-based method using one criterion. The more criteria applied for matching between attributes, and the results increase the value of the parameter P because the pair declared matched by the model have a higher chance of being accepted by the user as the right pair. These results indicate that the similarity of instances can be the basis for finding the matching attribute pair with an average P of 61.10%. Lowest P occurs in the constraint-based method, which is 33.28%. These results show that, even if the matching attribute pair has the same constraint, the result is still lower than the hybrid model and the instance-based method individually.



Based on the experiments on each model, effectiveness obtained, as shown in Table VI.

The highest R-value is 100.00% that is in the constraint-based method and the instance-based method, and both are equal. The lowest R-value is 99.83%, in the hybrid model. The value of R = 100.00% indicates that all attribute pairs declared matched by the model (in the initial result) are perfectly matched and accepted by the user (TP = N), and the attribute pair stated unmatched by the model (in the initial result) is received by the user (FN = 0).

TABLE V. THE RESULT OF HYBRID SCHEMA MATCHING

| DBSource      | DBTarget         | Test Result (%) |        |        |
|---------------|------------------|-----------------|--------|--------|
|               |                  | P               | R      | F      |
| sipt_admision | sipt_admision    | 89.90           | 100.00 | 94.68  |
| sipt_admision | sipt_academic    | 85.11           | 100.00 | 91.95  |
| sipt_academic | sipt_payroll     | 85.42           | 98.80  | 91.62  |
| sipt_academic | sipt_employee    | 83.08           | 96.43  | 89.26  |
| sipt_academic | sipt_tax_pph     | 91.37           | 99.45  | 95.24  |
| sipt_academic | sipt_workshop    | 82.95           | 100.00 | 90.68  |
| sipt_academic | sipt_library     | 88.46           | 100.00 | 93.88  |
| sipt_academic | sipt_user        | 92.98           | 100.00 | 96.36  |
| egov_dptkp    | license          | 94.64           | 100.00 | 97.25  |
| egov_dptkp    | license_oln      | 88.48           | 100.00 | 93.89  |
| egov_dptkp    | egov_dptbgcpt    | 100.00          | 100.00 | 100.00 |
| egov_dptkp    | quickcount_bgcpt | 94.01           | 100.00 | 96.91  |
| egov_dptkp    | egov_dptbtl      | 100.00          | 100.00 | 100.00 |
| egov_dptkp    | egov_dptkp       | 100.00          | 100.00 | 100.00 |
| egov_dptkdy   | ecomm_rsmitra    | 94.12           | 100.00 | 96.97  |
| egov_dptkdy   | ecomm_motorcred  | 90.55           | 100.00 | 95.04  |
| nuptk         | nuptk            | 99.41           | 100.00 | 99.71  |
| nuptk         | hs_sinisa        | 89.37           | 100.00 | 94.39  |
| nuptk         | hs_sipp          | 93.15           | 100.00 | 96.45  |
| nuptk         | hs_psb           | 98.01           | 100.00 | 99.00  |
| hs_sipp       | hs_sinisa        | 99.69           | 99.97  | 99.83  |
| hs_sipp       | hs_sipp          | 99.35           | 100.00 | 99.68  |
| hs_sipp       | hs_psb           | 93.73           | 100.00 | 96.76  |
| hs_sipp       | hs_grade         | 93.96           | 100.00 | 96.89  |
| hs_sipp       | hsgrade_ol       | 90.45           | 100.00 | 94.99  |
| hs_sipp       | hs_report        | 98.76           | 100.00 | 99.38  |
| hs_sipp       | hs_hspwt         | 94.49           | 99.98  | 97.16  |
| hs_sipp       | hs_forum         | 90.06           | 100.00 | 94.77  |
| hs_sipp       | hs_announcement  | 87.52           | 100.00 | 93.34  |
| hs_sipp       | hs_webinfo       | 98.24           | 100.00 | 99.11  |
| hs_sipp       | hs_osis          | 91.05           | 100.00 | 95.32  |
| hs_sipp       | hs_elearning     | 98.99           | 100.00 | 99.49  |
| Average:      |                  | 93.04           | 99.83  | 96.25  |

TABLE VI. THE RESULT OF HYBRID SCHEMA MATCHING

| Method                                       | Test Result Average (%) |        |       |
|--|-------------------------|--------|-------|
|  | P                       | R      | F     |
| Hybrid (constraint-based and instance-based) | 93.04                   | 99.83  | 96.25 |
| Constraint-based method                      | 33.28                   | 100.00 | 38.60 |
| Instance-based method                        | 61.10                   | 100.00 | 69.87 |

The highest F value is 96.25%, i.e. in the hybrid model, while the lowest is 38.60% in the constraint-based method. Value F = 96.25% indicates that the estimated level of effort required to add FN and eliminate FP has reached the best condition. The value of F in the hybrid model, compared with the instance-based method has increased by 26.38%, and when compared with the constraint-based method, there is an increase of 57.65%. This increase occurs because hybrid models perform matching by involving more criteria that are using six criteria at once, so the attribute pair declared fit by the model has a higher chance of being accepted by the user as a matching pair.

The experimental results in this study indicate that the mathematical model for hybrid schema matching has functioned as expected and provided better effectiveness than the original constraint-based method and instance-based method. The model that we have developed is still likely to be further investigated, at least to improve the effectiveness of output, process efficiency, and modification so that the model can be applied to non-relational databases.

This hybrid schema matching model still contains problems related to the effectiveness of the outcome because the constraint matching criteria and instance are assumed to have equal weight when calculating the similarity values (SIM) of each pair of attributes. Each criterion on the constraint is also considered to have the same weight. These criteria can have different weights in determining the value of similarity (SIM); one of the weighting ideas ever done [31]. The results of the survey at the time of collecting the test database also found the fact that the database designer has the freedom to make the database schema definition, including determining the data size (width) in the string data type. In this test, the string attribute pair is declared the same if it has the same size; it has not yet accommodated the freedom of the database designer.

Another problem is related to process efficiency. The developed model requires repetition of matching steps and simulated (SIM) value calculations on all possible attribute pairs. When schema matching performed on a database pair it involves many foreign keys, the model still encounters efficiency problems in matching and simulated values (SIM) and user verification steps that can only be done manually.

#### IV. CONCLUSIONS

The main contribution of this paper is to present the proposed mathematical model for hybrid schema matching. The model is developed based on a combination of two methods, namely the constraints-based method and an instance-based method. The model has been tested using a relational database, and the results are more effective than the original constraint-based method or instance-based method. Our research further refines the model by adding features to improve output effectiveness and process efficiency. Also, the model developed to run in non-relational database formats.

#### ACKNOWLEDGMENT

The authors would like to thanks the Directorate of Research and Community Service, Directorate General of Research and Development Strengthening at the Ministry of

Research, Technology and Higher Education of the Republic of Indonesia under Fundamental Research Grant Contract No.: 109/SP2H/LT/DRPM/2018.

REFERENCES

- [1] L. A. P. P Leme, M. A. Casanova, K. K. Breitman, and A. L Furtado, "OWL Schema Matching," *Journal of the Brazilian Computer Society*, 16(5), pp. 21-34, April 2010, DOI: 10.1007/s13173-010-0005-3.
- [2] I. F. Cruz, F. P. Antonelli, and C. Stroe, "AgreementMaker: Efficient Matching for Large Real-World Schemas and Ontologies (demo paper)," in *International Conference on Very Large Data Bases (VLDB)*, 2009, DOI: 10.14778/1687553.1687598.
- [3] C. Kavitha, G. S. Sadasivam, and S. N. Shenoy, "Ontology-Based Semantic Integration of Heterogeneous Databases," *European Journal of Scientific Research*, 64(1), pp. 115-122, November 2011.
- [4] S. Hamill, M. Dixon, B. J. Read, and J. R. Kalmus, "Interoperating Database Systems: Issues and Architectures," *Council for the Central Laboratory of The Research Councils, United Kingdom, Technical Report 1997*.
- [5] Ministry of Communication and Information Republic of Indonesia, "SIFONAS Sebagai Tulang Punggung e-Governance (SIFONAS as The Backbone of e-Governance)," 2002.
- [6] P. Martinek, "Schema Matching Methodologies and Runtime Solutions in SOA Based Enterprise Application Integration," *Department of Electronics Technology, Faculty of Electrical Engineering & Informatics, Budapest University of Technology and Economics, Hungary, Ph.D. Thesis, 2009*.
- [7] E. Sutanta, R. Wardoyo, K. Mustofa, and E. Winarko, "A Hybrid Model Schema Matching using Constraint-Based and Instance-Based," *International Journal of Electrical and Computer Engineering (IJECE)*, 6(3), pp.1048-1058, June 2016, DOI: 10.11591/ijece.v6i3.pp 1048-1058.
- [8] H. Alani and S. Saad, "Schema Matching for Large-Scale Data Based on Ontology Clustering Method," *International Journal on Advanced Science, Engineering and Information Technology (IJASEIT)*, 7(5), pp. 1790-1797, 2017, DOI: 10.18517/ijaseit.7.5.2133.
- [9] K. H. Shafa'amri and J. O. Atoum, "A Framework for Improving the Performance of Ontology Matching Techniques in Semantic Web," *International Journal of Advanced Computer Science and Applications (IJACSA)*, 3(1), pp. 8-14, 2012.
- [10] N. H. Azizul, A. M. Zin, and E. Sundararajan, "The Design and Implementation of Middleware for Application Development within Honeybee Computing Environment," *International Journal on Advanced Science, Engineering and Information Technology (IJASEIT)*, 6(6), pp. 937-943, 2016, DOI: 10.18517/ijaseit.6.6.1415.
- [11] D. Sulisworo, Tawar, and U. Ahdiani, "ICT Based Information Flows and Supply Chain in Integrating Academic Business Process," *International Journal on Advanced Science, Engineering and Information Technology (IJASEIT)*, 2(6), pp. 44-48, 2012, DOI: 10.18517/ijaseit.2.6.243.
- [12] M. Mohammadi and Muriati Mukhtar, "Business Process Modelling Languages in Designing Integrated Information Systems for Supply Chain Management," *International Journal on Advanced Science, Engineering and Information Technology (IJASEIT)*, 2(6), pp. 464-467, 2012, DOI: 10.18517/ijaseit.2.6.245.
- [13] E. Sutanta, R. Wardoyo, K. Mustofa, and E. Winarko, "Survey: Models and Prototypes of Schema Matching," *International Journal of Electrical and Computer Engineering (IJECE)*, 6(3), pp. 1011-1022, June 2016, DOI: 10.11591/ijece.v6i3.pp1011-1022.
- [14] W. S. Li and C. Clifton, "Semantic Integration in Heterogeneous Databases Using Neural Networks," in *The 20th International Conference on Very Large Data Bases (VLDB)*, Santiago de Chile, Chile, 1994, pp. 1-12.
- [15] E. Rahm, "Schema Matching and Mapping: Towards Large-Scale Schema and Ontology Matching," in *Data Centric Systems and Applications*, Z. Bellahsene, A. Bonifati, and E. Rahm, Eds. New York, USA: Springer, 2011, pp. 3-27, DOI: 10.1007/978-3-642-16518-4\_1.
- [16] H. H. Do, S. Melnik, and E. Rahm, "Comparison of Schema Matching Evaluations," in *Proceedings of The 2nd International Workshop Web and Databases*, In *Lecture Notes In Computer Science (LNCS) 2593*, Springer-Verlag, Germany, 2002, pp. 221-237, DOI: 10.1007/3-540-36560-5\_17.
- [17] H. H. Do, "Schema Matching and Mapping-Based Data Integration," *Interdisciplinary Center for Bioinformatics and Department of Computer Science, University of Leipzig, Leipzig, Germany, Ph.D. Thesis, 2005*.
- [18] D. Engmann and S. Massmann, "Instance Matching with COMA++," in *Datenbank Systeme in Business, Technologie und Web (BTW Workshop): Model Management and Metadata*, Aachen, Germany, 2007, pp. 28-37, [https://dbs.uni-leipzig.de/file/BTW-Workshop\\_2007\\_EngmannMassmann.pdf](https://dbs.uni-leipzig.de/file/BTW-Workshop_2007_EngmannMassmann.pdf).
- [19] J. Li, J. Tang, Y. Li, and Q. Luo, "RiMOM: A Dynamic Multistrategy Ontology Alignment Framework," *IEEE Transaction Knowledge Data Engineering*, 21(8), pp. 1218-1232, August 2009, DOI: 1109/TKDE .2008.202.
- [20] P. A. Bernstein, B. Harry, P. Sanders, D. Shutt, and J. Zander, "The Microsoft Repository," in *Proceedings of The 23rd International Conference Very Large Data Bases (VLDB)*, Athens, Greece, 1997, pp. 3-12.
- [21] A. Stabenau, G. McVicker, C. Melsopp, G. Proctor, M. Clamp, and E. Birney, "An Overview of ENSEMBL," *Genome Research Journal*, 14(5), pp. 929-933, May 2004, DOI: 10.1101/gr.1860604.
- [22] J. Madhavan, P. A. Bernstein, and E. Rahm, "Generic Schema Matching with CUPID," in *Proceedings of The 27th International Conference on Very Large Data Bases (VLDB)*, Roma, Italy, 2001, pp. 49-58, <http://dl.acm.org/citation.cfm?id=645927.67219>.
- [23] S. Melnik, E. Rahm, and P. Bernstein, "RONDO: A Programming Platform for Generic Model Management," in *Proceedings of The ACM-SIGMOD Conference on Management of Data (SIGMOD)*, San Diego, California, USA, 2003, pp. 193-204, DOI: 10.1145/872757.872782.
- [24] P. A. Bernstein, M. Jayant, and E. Rahm, "Generic Schema Matching, Ten Years Later," in *The 33 International Conference on VLDB Endowment*, Seattle, Washington, 2011, pp. 695-701, [http://www.vldb.org/pvldb/vol4/p695-bernstein\\_madhavan\\_rahm.pdf](http://www.vldb.org/pvldb/vol4/p695-bernstein_madhavan_rahm.pdf).
- [25] A. A. Alwan, A. Nordin, M. Alzeber, and A. Z. Abualkhishik, "A Survey of Schema Matching Research using Database Schemas and Instances," *International Journal of Advanced Computer Science and Applications (IJACSA)*, 8(10), pp. 102-111, 2017.
- [26] S. Bergamaschi, S. Castano, and M. Vincini, "Semantic Integration of Semistructured and Structured Data Sources," *SIGMOD Record*, 28(1), pp. 54-59, March 1999, DOI: 10.1145/309844.309897.
- [27] T. Milo and S. Zohar, "Using Schema Matching to Simplify Heterogeneous Data Translation," in *Proceedings of The 24th International Conference on Very Large Data bases (VLDB)*, New York, USA, 1998, pp.122-133, <http://dl.acm.org/citation.cfm?id=645924.671326>.
- [28] A. H. Doan, P. Domingos, and A. Y. Halevy, "Reconciling Schemas of Disparate Data Sources-A Machine-Learning Approach," in *Proceedings of The ACM SIGMOD International Conference Management of Data*, Santa Barbara, California, 2001, pp. 509-520, DOI: 10.1145/376284.375731.
- [29] A. Gross, M. Hartung, T. Kirsten, and E. Rahm, "On Matching Large Life Science Ontologies in Parallel," in *Proceedings of The 7th International Conference Data Integration in the Life Sciences (DILS)*, Gothenburg, Sweden, 2010, pp. 35-49, <http://dl.acm.org/citation.cfm?id=1884477.1884483>.
- [30] Y. Karasneh, H. Ibrahim, M. Othman, and R. Yaakob, "An Approach for Matching Relational Database Schemas," *Journal of Digital Information Management*, 8(4), pp. 260-269, 2010, <https://dblp.org/rec/bib/journals/jdim/KarasnehIOY10>.
- [31] M. B. Shuaibu, "Determining an Appropriate Weight Attribute in Fraud Call Rate Data Using Case-Based Reasoning," *International Journal on Advanced Science, Engineering and Information Technology (IJASEIT)*, 4(1), pp. 34-36, 2014, DOI: 10.18517/ijaseit.4.1.357.

# The Role of Technical Analysis Indicators over Equity Market (NOMU) with R Programming Language

Mohammed A. Al Ghamdi  
Computer Science Department  
Umm Al Qura University, Makkah City, Saudi Arabia

**Abstract**—The stock market is a potent, fickle and fast-changing domain. Unanticipated market occurrences and unstructured financial information complicate predicting future market responses. A tool that continues to be advantageous when forecasting future market trends in a global aspect is correlation analysis to significant market events. Data analysis can be used for the difficult task of making stock market forecasts in case the stock price rises or fall. A high number of automated exchanges in the stock market are done with advanced prognostic software. Data analysis is centered on the main idea that previously recorded data is used to predict future patterns. This advancement is aimed speculators in pinpointing hidden data in real evidence that would give them some financial foresight when considering their ventures of choice. Data analysis can be applied in order to predict the rises and falls of stocks in the future. This paper aims to critically investigate, develop and judge the different systems that predict and assess future stock trades as these systems have their own various process to foretell the fluctuations in the costs of stocks. Several different technical analysis indicators have been applied in this study including; Chaikin Money Flow (CMF), Stochastic Momentum Index (SMI), Relative Strength Index (RSI), Bollinger Bands (BBands), and Aroon (Aroon) indicator. The experiments have been conducted using R programming language over two companies' real-world datasets obtained for two years from Saudi stock market (NOMU) which is a parallel stock market with lighter listing requirements that serves as an alternative platform for companies to go public in the main market. To the best of our knowledge, this is the first work to be conducted in NOMU stock market.

**Keywords**—Data mining; data analysis; R programming language; Chaikin Money Flow (CMF); Stochastic Momentum Index (SMI); Relative Strength Index (RSI); Bollinger Bands (BBands); Aroon indicator

## I. INTRODUCTION

The equity market which is known popularly as stock market is defined as a platform where stock's trading take place for specific listed companies. The economy has a direct effect on the performance of the stock market. It is a variable system with little defined parameters that making it challenging to accurately explaining them. Speculators have continuously tried to understand how stock prices can be foreseen and forecasted in order to make their sales and

investments on the market. In order to achieve this goal, scientists used strategies of key examination- in which data related to the industry, macroeconomics, and important figures are used to make exchanging rules. Technical analysis methods usually are conducted using stock volume, price, and historical data by several researchers. Techniques used to estimate and extrapolate stock volume, prices and movements are what is referred to as technical analysis.

The supposition that history is repeated and that analyzing historical pricing information to predict upcoming market advances is what this revolves around. Hence it can be expected that profit can be made by making use of existing price trends and tendencies.

The stock market is very erratic and indeterminate. There will be stocks that hardly undergo drops and there will be some that undergo major price hikes, and some will not change very much.

The data used in this paper are the historical prices of two Saudi Arabia Stock Exchange-listed companies in (NOMU) over two years.

Investors support the four ensuing guiding principles:

- When investing in stocks, don't follow the herd.
- Until you understand its composition, do not invest in stock.
- Do not trust the rumors, but first, confirm the facts.
- Determine your personal risk appetite before investing in stock by considering an acceptable risk-reward ratio.

The stock market is a platform that made it easier for individuals as well as companies to trade their stocks at an agreed price of listed companies. Listed companies are defined as the companies that their shares are offered for public trading by stock exchanges. Stock markets are steadily becoming central to national and global economies as they can greatly affect them with the rises and falls of stocks. It is known that a key of countries economic power is their stock markets. There can be one or more stock markets in each region or country depends on the market size, and numbers of companies.

The authorities of the stock market focus on finding financial frauds in the market and investors usually check with investment portfolio management and stock market prices. In order to gain maximum revenue from the market investors should predict the fall and rise of prices so they can invest accordingly.

The most critical point here is to identify potential stock rises and falls so that profits can be earned in a relatively sustainable manner. Stock market data such as price and volume play crucial roles in studying the behavior of the market. The price of the stock market consists of four main prices, i) open price which is determined based on opening auction that is conducted between 9:30 am to 10:00 am, where investors issuing their trade orders, then the fair price for the open price is selected [1], ii) close price which is computed in the same way that open price is calculated but the time is different from 3:00 pm to 3:10 pm [1], iii) high price is the highest trading price during the day, iv) low price is the lowest trading price in the day. Stock market' volume is described as the number shares in specific time. A correct approach to these parameters would allow for substantial investments to be made.

There are two common tools that can be implemented in order to support investors decision in the stock market [2], [6], [3], and [4]. Firstly, fundamental analysis where the focus is on the evaluation process of the intrinsic value of a security [3]. Fundamental analysis is performed based on three main phases known as economy, industry, and company (EIC) and each of which has his own factors and indicators to be analyzed and studied well by investors [4]. Interest rate, inflation rate, and unemployment rate play crucial roles in the development of any national economy [6]. Industries' competitive analysis and life cycle analysis of industry are two factors related to industry analysis [4]. Investors deal with the different factors that have affect for the company performance such as company business concept and financial statement for company [6].

The second aspect helps investors in enhance their decision for investments at stock market are known as technical analysis. Technical analysis is also known as "Charting" as it is based on using charts for the past prices movement in order to forecast the future changes of the proposed prices [5]. The focus in technical analysis is only on analysis the stock price and volume in order to predict the future price change [2]. This is affected by the demand and supply in the stock market, as if the demand is at high level then the price will be higher, and when the supply is at high level the price will be lower. The study in [7] has defined three main premises affect the technical analysis; i) discount and built-in any information affect the price of stock, ii) tendencies is essential in determined prices, and iii) the repeated movements of prices are often.

The strategy of the technical analysis is to employ mathematical calculations in order to detect the stock prices activities during proposed periods of times. Technology can be applied in such matter in order to enhance the behavior of the different of the indicators related to the technical analysis. R is a programming language that has been created by Ross

Ihaka and Robert Gentleman in 1991 in Statistics Department at Auckland University, New Zealand [8]. Then in the announcement of the R language to the public has been made. R is an open source programing language and applied mainly in statistical computing area of research. It is free and also run on all standard computing platform. Added to this the user community of R is highly active, and it has been using by well-known companies such as Microsoft, Google, IBM, and Oracle.

The rest of the paper is organized as follow. Section II discusses the related works and Section III presents the methodology that is applied in this work. The results of experiments and discussion are presented in Section IV while conclusion is stated in Section V.

## II. RELATED WORKS

Many important changes in the environment of financial markets have occurred over the last two decades. The development of powerful facilities for communication and commerce has expanded investors' selection. The provision of stock returns is a significant financial topic that has attracted the attention of researchers for many years. It implies that in the past, basic information available to the public has predictive links with future stock returns. Therefore, several studies have focused on technical analysis and the use of advanced mathematics and science in such area of research.

Investors in stock market usually interrelate with different sources of information in order to maximize their benefit from trading in stocks. Stock market analysis is one of these ways that may support investors in making their decision [9]. Applying forecasting in stock market is considered as challenging task due to the intricacies of the market [10], [11] and [12]. However, forecasting has several different benefits for both sellers and buyers through helping in plan for upcoming events and providing information for allocating resources and determining the foreseen prices in future [13].

Applying forecasting models for stock market may help investors in making their decision through applying ARIMA approach which is beneficial also in stock market studies as in different real-world challenges such as education and health [13]. Several different technical analysis methods are applied in order to study the historical data of stock market for finding the hidden through applying 5 different techniques including; 1) Typical Price (TP), 2) Bollinger Bands (BBands), 3) Relative Strength Index (RSI), 4) Chaikin Money Flow (CMF), and 5) Moving Average (MA) [14]. The data of three Nigerian banks in the stock market has been studied and analyzed by applying data mining tools such as liner regression and moving average approaches [15]. The study confirms also that applying data mining methods over stock market shows beneficial return and help in increasing the investments on stock market.

Three technical indicators including; Stochastics Oscillator (SO), Relative Strength Index (RSI), and Moving Average Convergence-Divergence (MACD) have been applied in order to measure how beneficial to apply the predictive model built by applying these three indicators over chosen workload, and the results shows that SO, and RSI may improve the decision

made by investors comparing with MACD. Auto Regressive Integrated Moving Average (ARIMA) model has been conducted over two datasets achieved from New York Stock Exchange (NYSE) and Nigeria Stock Exchange (NSE) in order to develop an extensive process of building stock price predictive, and the results show that applying such technical indicator could play crucial role in supporting investors decision in stock market [16].

The study in [17] has applied technical analysis methods in order to monitor and forecast the trends of the stock market. The data used for the study was for six months from January to June 2016.

On the basis of research, it has been found that there are limited studies conducted on the Saudi Stock Market alongside technical analysis Hence, the following objects are highlighted:

- To study the efficiency of applying technical indicators over Saudi stock market (NOMU).
- To build predictive model for Saudi stock market by using R programming language.
- To analyze the selected companies with technical indicators.

### III. METHODOLOGY

Technical analysis indicators are grouped within four different categories [17]; 1) Trend indicators, 2) Momentum indicators, 3) Volatility indicators and 4) Volume indicators. Trend indicators are applied to measure the trend's direction and strength to produce average value, where the buy mode is activated when the price moves above the average and sell mode is detected when the price goes below the average value. The speed of price movement can be identified by using the momentum indicators. Volatility indicators detect the prospect points where the direction of the market may change. The total amount of trading occurs within given period of time is represented by Volume indicators.

In this paper, five technical analysis indicators have been applied on the proposed data; i) Chaikin Money Flow (CMF) - Volume indicator, ii) Stochastic Momentum Index indicator (SMI) - Momentum indicator, iii) Relative Strength Index indicator (RSI) - Momentum indicator, iv) Bollinger Bands indicator (BBands)-Volatility indicator, and v) Aroon indicator (Aroon) - Trend indicator.

This work aims to study the impact of the technical analysis indicators over Saudi stock market (NOMU). NOMU market is an alternative stock market where the requirements of the listed companies are lighter compared to the main Saudi market. The main aim of NOMU market is to support the sector of small and medium-sized companies by providing the sector with numerous funding resources in order to rise their revenues and profits. The stock trading in NOMU market opened on Sunday 26<sup>th</sup> February 2017. The experiments in this work have been conducted over two datasets from real-world of two companies listed in NOMU market; 1) Al-Samaani Factory for Metal Industries and, 2) Arab Sea Information System using R language in R-Studio platform. R-Studio is

cost-free and open source, and integrated development environment for R language. Where the user run its R scripts in a user-friendly environment. There are two editions from the R-Studio which is; i) R-Studio Desktop, ii) and R-Studio Server. In the desktop version the written program is run locally like other desktop application, where the server version allow user from accessing to remote Linux server through web browser in order to run the code. R in this work is applied through using TTR package which contains several essential functions that can be used for technical analysis [8].

#### A. Chaikin Money Flow Indicator (CMF)

The Chaikin accumulation distribution (AD) is the intrinsic factor of the Chaikin Money Flow indicator [18]. CMF indicator measures the total amount of money flow volume within selective period called buying and selling pressure. A move into positive zone indicates buying pressure, and selling pressure is indicated when the move occurs into the negative. The CMF indicator is calculated by dividing the total of accumulation distribution (AD) by the total of the volume within specific period ( $n$ ). The formula (1) and (2) can be used to calculate the CFM indicator [18].

$$CMF = \frac{\sum_{i=1}^n AD}{\sum_{i=1}^n Volume} \quad (1)$$

$$AD = Volume * \frac{(close\ price - open\ price)}{(high\ price - low\ price)} \quad (2)$$

In general, the buying pressure is stronger when the indicator value of CMF is more than zero (positive) and selling pressure is stronger when CMF indicator value is less than zero (negative).

#### B. Stochastic Momentum Index Indicator (SMI)

SMI was developed by William Blau based on the stochastic oscillator [20]. The values of SMI indicator has range between (+100) and (-100) [19].

The SMI indicator value is above zero when the closing price is more than midpoint and is below zero when the closing price is less than the midpoint.

Extreme values of SMI (high or low) indicate that overbought or oversold mode is detected. When the SMI rises above (-50), or when it crosses the signal line, a buy signal is generated. SMI is used by investors as a general trend indicator. In general, if SMI value more than (+40) then the bullish trend is detected and if SMA value greater than (-40) a bearish trend is activated. The formula (3), (4) and (5) are applied in order to calculate SMI value.

$$cm = close\ price - \left( \frac{highest\ high\ value + lowest\ low\ value}{2} \right) \quad (3)$$

$$SMI = 100 * \left( \frac{cm}{(highest\ high\ value - lowest\ low\ value)/2} \right) \quad (4)$$

$$Signal = EMA(SMI) \quad (5)$$

#### C. Relative Strength Index Indicator (RSI)

RSI indicator has been developed to measure both the price movements speed and its change as well. The range of the RSI indicator is between 0 to 100. Overbought case is indicated when the value of the RSI indicator above (+70),

and oversold case occurs when RSI indicator value below the value of (30) [21]. In general, overbought state is indicated when the value of the RSI indicator is more the value of 70. On the other side when the value of the indicator is less than 30 the mode of the market is in oversold mode. RSI indicator is calculated by applying the equation (6).

$$RSI = 100 - \left( \frac{100}{1 + \left( \frac{\text{average gain}}{\text{average loss}} \right)} \right) \quad (6)$$

#### D. Bollinger Bands Indicator (BBands)

A simple average moving band is the bases of the Bollinger Bands (BBands) indicator as the standard deviation calculation using SMA methods. This indicator is presented as a three lines group plotted on a figure where the middle band is the average moving of the stock prices, and the upper band is above the middle band in two standard deviations; the low band is below the middle band for two standard variations.

The top and bottom lines (bands) can show the volatility of the market. In other words, the market volatility is high when the space between these two lines are not close. The two bands become close together during when the market is less volatility. BBands is generally used as a guide, indicating potential reversals in trends. If current price breaks through Bollinger's bottom band, a buy signal will be considered. A sell signal is considered if current price breaks through the upper band.

$$\text{Middle Band} = \text{SMA}(\text{price}) \quad (7)$$

$$\begin{aligned} \text{Upper Band} = \\ \text{Middle band} + (\text{Standard Deviation of price} * 2) \end{aligned} \quad (8)$$

$$\begin{aligned} \text{Lower Band} = \\ \text{Middle band} - (\text{Standard Deviation of price} * 2) \end{aligned} \quad (9)$$

#### E. Aroon Indicator

Aroon is an indicator that has been developed in order to specify the status of the market whether it is trending or not. It also shows how strong the trend of the market if it is trending. The indicator tries to connect the price of the market with the time and it is range between 0 to 100. Aroon indicator has two separate indicators; 1) Aroon Up, and 2) Aroon Down, and these two indicators can be computed by using the equations (10) and (11), respectively.

$$\text{Aroon Up Indicator} = \left( \frac{\text{No. of Periods} - \text{No. of Periods since Highest High}}{\text{No. of Periods}} \right) * 100 \quad (10)$$

$$\text{Aroon Down Indicator} = \left( \frac{\text{No. of Periods} - \text{No. of Periods since Lowest Low}}{\text{No. of Periods}} \right) * 100 \quad (11)$$

### IV. EXPERIMENTS, RESULTS AND DISCUSSION

The proposed experiments have been conducted in this work over real-data for two companies (Al-Samaani Factory for Metal Industries Company and Arab Sea Information System Company) listed in the Saudi stock market (NOMU). The dataset was obtained for these two companies from 26<sup>th</sup> February 2017 to 24<sup>th</sup> February 2019. The following sub-sections present the experiments results and discussion.

#### A. Chaikin Money Flow Indicator

CMF indicator was developed by Marc Chaikin. It is a volume-weighted average within specific period of accumulation and distribution as well. In general, when the CMF value is continuous above zero this means that there are buying operations. The sell operation is recommended when the CMF value is continuous below zero.

In R Chaikin Money Flow indicator can be executed by using CFM() function, where the function has three arguments [22]. The first argument is the data object, and, in this case, it contains the high, low, and close prices (HLC), while the second parameter in the function is the volume related to the object data (volume). The last argument is the number of periods that is selected, and it is 2 in this experiment (n).

1) *Al-Samaani factory for metal industries company:* Fig. 1 presents the implementation of the CMF indicator over the first data set which is the data of Al-Samaani Factory for Metal Industries Company. At the beginning periods on this dataset shows that there are continuous buying operations as the CMF value is greater than zero (from 5<sup>th</sup> to 13<sup>th</sup> March 2017). Then the CMF goes down below the value of zero where the sell operations are detected (from 14<sup>th</sup> to 15<sup>th</sup> March).

2) *Arab sea information system company:* The experiments result from applying the CMF indicator over the data set of the Arab sea information system company is shown in Fig. 2. The figure shows that are several different crosses of the zero line within the used dataset. The figure also states that buying operations are active during the period as an example from 7<sup>th</sup> March to 9<sup>th</sup> April 2017. The operation of selling is detected during several times during the experiments (i.e. 6<sup>th</sup> to 18<sup>th</sup> June 2017).

#### B. Stochastic Momentum Index Indicator

SMI computes the distance between the close price of the stock and the median (midpoint) of the low or high prices with range between the values (+100) and (-100). The value of SMI is positive if current close price is more than the median or the low/high range and vice versa. SMI is applied by the traders to detect the oversold or overbought modes in the proposed market. The experiments result from applying the SMI indicator over the used data sets in this work as shown in Fig. 3 and 4.

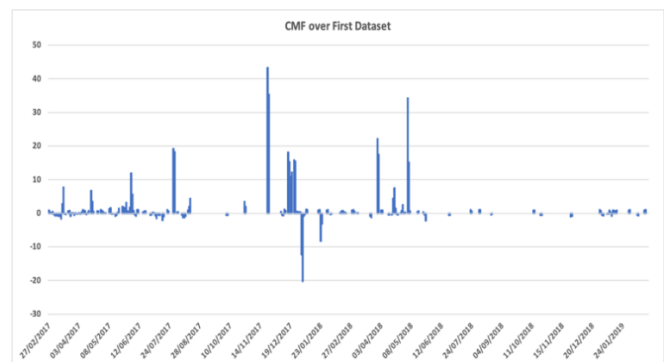


Fig. 1. Chaikin Money Flow Indicator Over First Data Set.

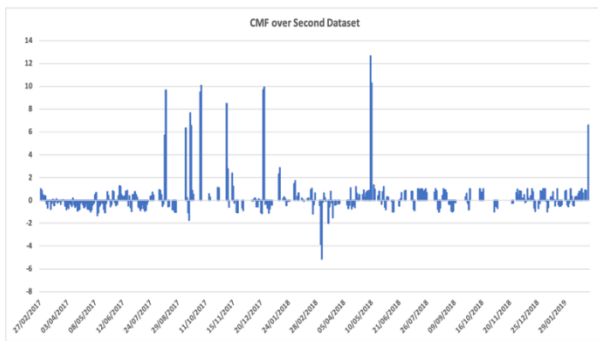


Fig. 2. Chaikin Money Flow Indicator Over Second Data Set.

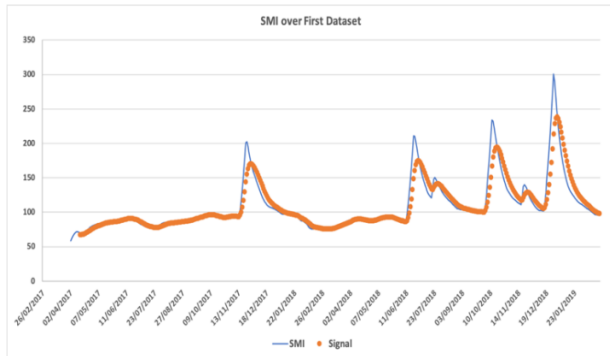


Fig. 3. Stochastic Momentum Index Indicator Over First Data Set.

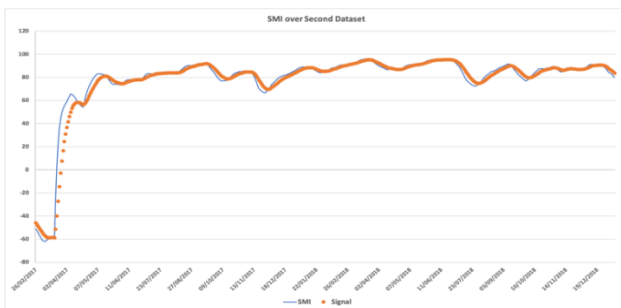


Fig. 4. Stochastic Momentum Index Indicator Over Second Data Set.

The SMI indicator can be applied in R by using SMI() function which is existing in TTR() package [22]. The function has multiple parameters and in this experiment 5 parameters are defined, and the rest left as in default. The first argument in the function is data object which is represented by the high, low, and close prices (HLC). The second parameter is the number of periods that is chosen, and it is 13 in this experiment. The third, fourth, and fifth parameters used in SMI() function are the numbers of periods for initial, number of periods for double smoothing, and numbers of periods for signal line, and they are valued by 13, 2, and 9 respectively.

1) *Al-Samaani factory for metal industries company*: Fig. 3 presents the results from applying the SMI indicator over the first data set. It is clear that the SMI indicator values during these experiments always being over the value of +40 representing that the stocks are overbought. The figure also shows that the signal cross over SMI indicator in different occasions indicating bearish trend (see mid-November 2017, end June 2018, mid-October 2018, and end December 2018).

2) *Arab sea information system company*: The results from applying the SMI indicator over the second dataset are presented in Fig. 4. The stock market of the proposed company was in oversold mode as the value of the SMI was below -40 until the beginning of May 2017. After that the stocks market for the proposed company becomes stable for around three weeks (end of May 2017). Then it is converted to the overbought conditions as the SMI indicator values become more than +40. The bearish trend can be pointed from the figure in some cases where the signal crosses below the signal line; for example, see at the beginning May 2017, end May 2017, beginning April 2017.

### C. Relative Strength Index (RSI) Indicator

RSI was developed by J. Welles Wilder. It is applied in order to measure the change of the price movements and its speed. RSI calculates the ratio of the recent expanding value of the price movements to the absolute price movement itself, and it ranges between 0 and 100.

The mode of the market is indicated as; i) overbought when the value of SMI indicator is more than 70, and ii) oversold if the SMI indicator value is less than 30.

In R programming language the function RSI() is applied to execute the RSI indicator [22]. The function RSI() has several arguments including; 1) the price of the market, in this experiment the close price is selected to represent the price here, 2) the total periods selected to represented the moving averages for the selected price, and 14 periods has been selected in this experiment, and 3) other arguments that applied in specific situation.

1) *Al-Samaani factory for metal industries company*: The results from applying the RSI indicator over the first dataset is presented in Fig. 5. Several overbought modes have been detected in the following periods; i) end of December 2017, ii) end of January 2018, iii) end of December 2018, iv) From 22<sup>nd</sup> January 2019 to 3<sup>rd</sup> February 2019, and v) from 12<sup>th</sup> to 24<sup>th</sup> February 2019.

The modes of oversold have been spotted in different several slots of time; from 10<sup>th</sup> to 23<sup>rd</sup> July 2017, from 9<sup>th</sup> to 13<sup>th</sup> August 2017, from 17<sup>th</sup> to 25<sup>th</sup> October 2017, from 2<sup>nd</sup> to 24<sup>th</sup> July 2018, 12<sup>th</sup> August to 20<sup>th</sup> November 2018.

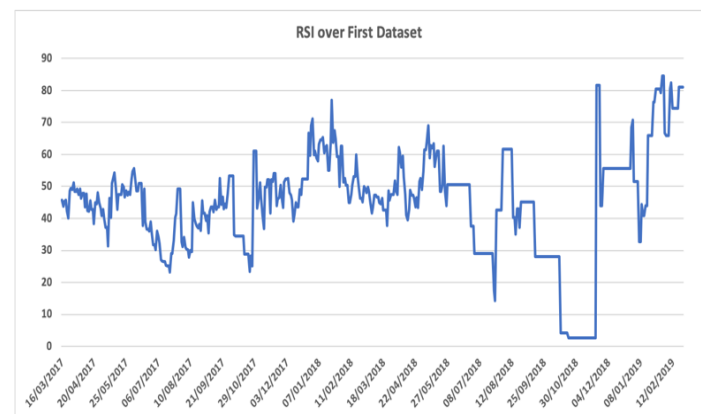


Fig. 5. Relative Strength Index (RSI) Indicator Over First Dataset.

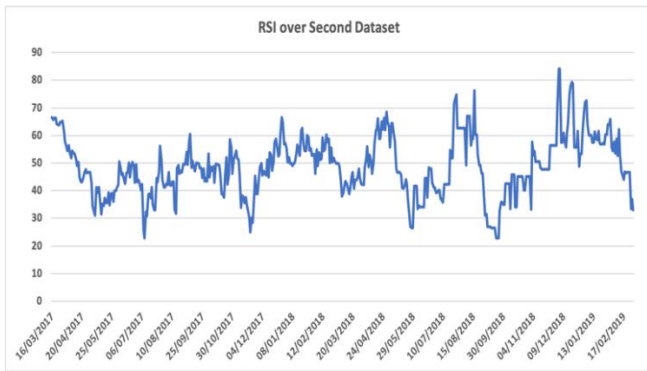


Fig. 6. Relative Strength Index (RSI) Indicator Over Second Dataset.

2) *Arab sea information system company*: Fig. 6 presents the results of conducting the RSI indicator over the second dataset. In Fig. 6 the overbought mode has been pointed in the periods of; 23<sup>rd</sup> to 25<sup>th</sup> July 2018, 16<sup>th</sup> August 2018, 2<sup>nd</sup> to 5<sup>th</sup> December 2018, 16<sup>th</sup> to 19<sup>th</sup> December 2018, 2<sup>nd</sup> to 3<sup>rd</sup> January 2019.

In this dataset the periods of; 9<sup>th</sup> to 10<sup>th</sup> July 2017, 20<sup>th</sup> November 2017, 22<sup>nd</sup> November 2017, 27<sup>th</sup> to 29<sup>th</sup> May 2018, and 9<sup>th</sup> to 20<sup>th</sup> September – have been shown as in oversold conditions.

#### D. Bollinger Bands (BBands) Indicator

BBands indicator is used in order to compute the volatility in the proposed market. It also applied in order to determine the conditions of overbought and oversold of the market. BBands indicator has three moving lines, where the middle band represented by the simple moving average of the price for a specific period. The upper and lower lines are the standard deviations of the target prices and they are able to capture up to 95% of a security's price movement and perfect channel for capturing volatility. It is known that the market is highly volatile when the lower band and upper band close together and vice versa. The obtained results from applying BBands indicators over the used datasets are shown in Fig. 7 and 8 respectively.

BBands in R programming language is executed by applying BBands() function which has several different variables [22]. The first variable is known as data object which represent the data used in this experiment and contains the high, low, and close prices, while the second variable in BBands() function is the selected periods for moving averages for the data, and in this experiment is valued by 20. The third variable in the function is the standard deviations number used in this experiment which is 2 standard deviations.

1) *Al-Samaani factory for metal industries company*: Fig. 7 shows the three lines obtained from applying the BBands indicator over the first dataset that used in this work. It is advised to wait for a stock to close less than the lower BBands to buy it in the following day, and this scenario not happening in this dataset. In 26<sup>th</sup> to 27<sup>th</sup> December 2018 the upper band and lower band are squeezed together, and this means the volatility is low. In such situation it is expected to the figure to move downside or upside.

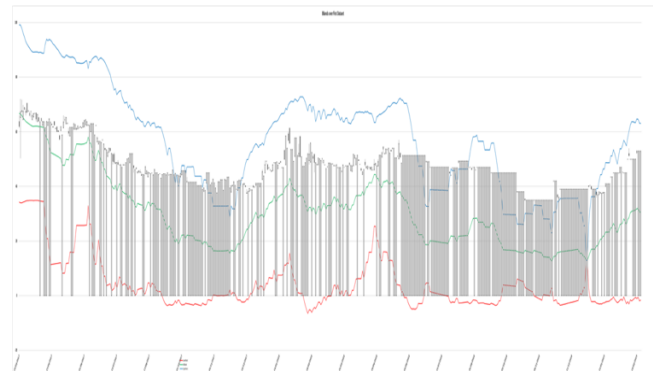


Fig. 7. Bollinger Bands (BBands) Indicator Over First Dataset.

2) *Arab sea information system company*: The results from applying the BBands indicator over the second dataset that used in this work are presented in Fig. 8. The two lines of the BBands (lower band line and upper band line) are squeezed in this dataset also in the period from 1<sup>st</sup> to 5<sup>th</sup> June 2017, and after this squeezed period the stock is go downside. Based on the theory of the indicator which is stated the following; the buy process is advised to be made after the stock to close less than the lower BBands. This scenario happens in the second dataset in the following dates; 18<sup>th</sup> to 19<sup>th</sup> April 2017, and 3<sup>rd</sup> May 2017. The figure shows also that stock is less volatile in March and April.

#### E. Aroon Indicator

The indicator has been developed by Tushar Chande and the aim of this indicator is to be able to detect the start of the new trend in the market. The indicator is represented in percentage form between 0% to 100%. Based on Aroon indicator, the uptrend is expected when the Aroon up line crosses over the Aroon-Down, and the downtrend is expected to be occurred when Aroon-Down crosses over the Aroon-Up. The results of applying Aroon indicator over the two datasets are shown in Fig. 9 and 10.

The Aroon indicator can be applied in R programming language by using aroon() function which is included in the TTR() package [22]. There are two arguments within the function; 1) the data object used in the experiment, and in this case the high and low prices are chosen to represent the data, and 2) the periods that has been used in the calculation of the indicator value, and it is selected in this case as 20.

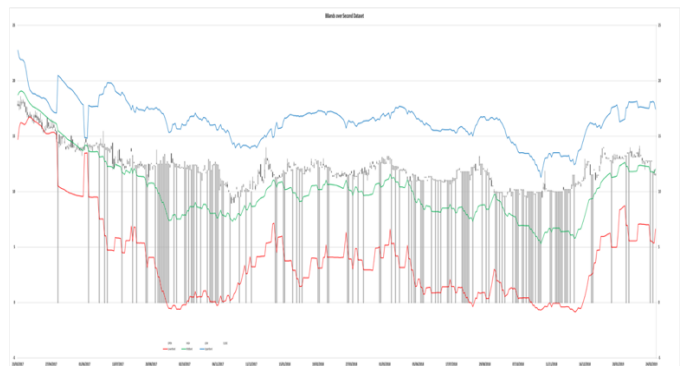


Fig. 8. Bollinger Bands (BBands) Indicator Over Second Dataset.



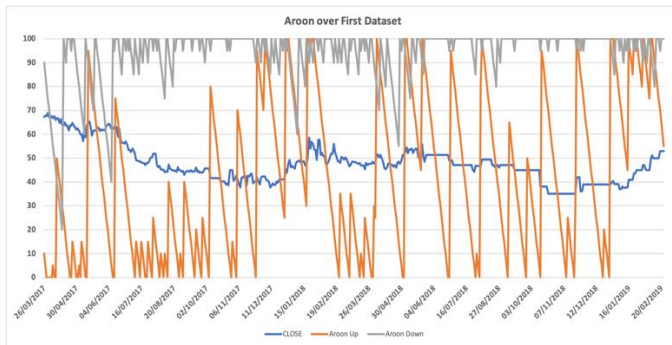


Fig. 9. Aroon Indicator over First Dataset.

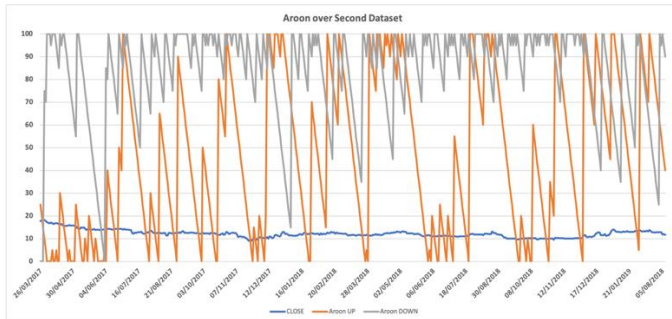


Fig. 10. Aroon Indicator over Second Dataset.

1) *Al-Samaani factory for metal industries company*: When the value of Aroon Up range between 0 to 30 and value of Aroon Down range between 70 to 100, the downtrend is expected of the stock price. This scenario is shown in Fig. 9 as the price of the stock market moves down starting from 26<sup>th</sup> February to 10<sup>th</sup> December 2017 and during this period the Aroon Down reaches 100 and in most cases ranges between 70 to 100, while the value of Aroon Up range was between 0 and 30. The stock market start trending up from 11<sup>th</sup> December 2017 to 31<sup>st</sup> January 2018. The Aroon indicator catches this uptrend as the Aroon Up line crosses over Aroon Down line.

2) *Arab sea information system company*: The Aroon indicator catches the changes occur in the price of the market. This is clear in some cases as shown in Fig. 10 for example the period between beginning of December to end of December 2017 as the price is trending up and the Aroon Up crosses above Aroon Down. The second example as shown in Fig. 10 as the price is trending up when the Aroon Up crosses above Aroon Down in 29<sup>th</sup> March to 2<sup>nd</sup> April 2018.

## V. CONCLUSION AND FUTURE WORK

Five different technical analysis indicators have been identified and analyzed in this study to focus on how these indicators can be used in order to understand the trading in the stock market by using R programming language. Added to this, the study will help the investors in the stock market in the importance of these technical analysis indicators for improving their knowledge and increasing investments returns. The study has been conducted over two real-data

obtained from Saudi stock market (NOMU). The dataset was for two full years starting from 26th February 2017 to 24th February 2019. The future plan is to extend this work by applying the AI technology in predicting the future of the stock market in collaboration with the different technical analysis indicators.

## REFERENCES

- [1] <https://www.tadawul.com.sa>. [Accessed on 20th June 2019].
- [2] R. Isidore. and P. Christie, "Fundamental analysis versus technical analysis-a comparative review", International Journal of Recent Scientific Research, 2018, Vol. 9, Issue, 1 (B), pp. 23009-23013.
- [3] V. Drakopoulou. "A review of fundamental and technical stock analysis technique". Journal of Stock & Forex Trading, 2015, 5(1), 1-8.
- [4] A. Suresh. "A study on fundamental and technical analysis". International Journal of Marketing, Financial Services & Management Research, 2013, 2(5), 44-59.
- [5] A. Lo, H. Mamaysky, and J. Wang. "Foundations of technical analysis: computational algorithms, statistical inference, and empirical implementation". The Journal of Finance, 2000, 55(4), 1705-1765.
- [6] S. Jakpar, M. Tinggi, A. Hisham, and C. Wen, "Fundamental Analysis VS Technical analysis: The Comparison of Two Analysis in Malaysia Stock Market", UNIMAS Review of Accounting and Finance, 2018, Vol. 1 No. 1.
- [7] S. Mitra. "Usefulness of moving average based trading rules in India". International Journal of Business and Management, 2011, 6(7), 199-206.
- [8] <https://www.r-project.org>. [Accessed on 20<sup>th</sup> June 2019].
- [9] Y. Wang and H. Deng, "Expectations, Behavior, and Stock Market Volatility", Emerging Markets Finance & Trade, 2018, 54:3235-3255, DOI: <https://doi.org/10.1080/1540496X.2018.1498331>.
- [10] P. Pai and C. Lin, "A hybrid ARIMA and support vector machines model in stock price forecasting" Omega, 2005, vol. 33, pp. 497-505.
- [11] J. Wang, J. Wang, Z. Zhang, and S.. Guo, "Stock index forecasting based on a hybrid model," Omega, 2012, vol. 40, pp. 758-766.
- [12] L. Wei, "A hybrid model based on ANFIS and adaptive expectation genetic algorithm to forecast TAIEX," Econ. Model., 2013, vol. 33, pp. 893-899.
- [13] A. Atkins, M. Niranjana, and E. Gerding, "Financial news predicts stock market volatility better than close price", The Journal of Finance and Data Science, 2018, Volume 4, Issue 2. Pp 120-137. <https://doi.org/10.1016/j.jfds.2018.02.002>.
- [14] K. Kannan, P. Sekar, M. Sathik and P. Arumugam, "Financial stock market forecast using data mining Techniques", Proceeding of the international MultiConference of Engineers and Computer Scientists 2010, Vol I, IMECS 2010, March 17-19, Hong Kong.
- [15] S. Olaniyi, A. Kayode, and G. Jimoh. "Stock Trend Prediction Using Regression Analysis – A Data Mining Approach". ARPN Journal of Systems and Software, 2011, Volume 1 No. 4.
- [16] A. Adebisi, A. Adewumi, C. Ayo, "Stock price prediction using the ARIMA model", 16th IEEE International Conference on Computer Modelling and Simulation (UKSim), 2014, pp. 106 -112.
- [17] J. Vaiz and M. Ramaswami, "Forecasting Stock Trend Using Technical Indicators with R", International Journal of Computational Intelligence and Informatics, 2016, Vol. 6: No. 3.
- [18] C. Kirkpatrick, and J. Dahlquist, "Technical Analysis: The Complete Resource for Financial Market Technicians" FT Press; 3 edition, 2015.
- [19] F. Labs. "FM Labs Indicator Reference". Retrieved from <http://www.fmlabs.com/reference>. [Accessed on 20<sup>th</sup> June 2019].
- [20] William Blau, "Momentum, Direction, and Divergence", Wiley Trader's Exchange Book, 2008, 1<sup>st</sup> Edition.
- [21] J. Wilder, "New Concepts in Technical Trading Systems", Trend Research, 1978.
- [22] <https://www.rstudio.com/>, [Accessed on 20<sup>th</sup> June 2019]

# A Circular Polarization RFID Tag for Medical Uses

Nada Jebali<sup>1</sup>, Ali Gharsallah<sup>2</sup>

Laboratory for Research on Microwave Electronics, Department of Physics  
Faculty of Sciences, El Manar I, Tunis, Tunisia

**Abstract**—The aim of this paper is to present Radio Frequency Identification (RFID) Tag. The use of this kind of antennas in the medical field has a great importance in making people's life easier and improving the way to get medical information. This article is dedicated to explain the details of the method used to obtain the circular polarization using a shaped cross slot. A simulation study with the SAR values is performed to obtain an idea about the effects of the electromagnetic waves. In this study, a specific diode pin CPINUC5206-HF has been used in order to obtain a high frequency (3 GHz). Two fabrication methods have been adapted: the printed circuit board method (PCB) and metal cutting through laser ablation method (MCTLA). A comparison study between the two methods has been also conducted.

**Keywords**—Radio Frequency Identification (RFID); circular polarization; metal cutting through laser ablation method

## I. INTRODUCTION

RFID is an innovative technology that can be used to identify a person or an object and track tags attached to objects using electromagnetic fields. The RFID antenna uses a radio frequency to read information from a small device called tag which contains information stored electronically [1] and [2]. Compared to bar-code, the RFID system represents many advantages, such as remote communication, high safety and an important mass information processing. That is why this technology has been quickly developed in the few recent years [3] and has become one of the most useful technologies in the medical applications [4, 5, 6]. To be able to monitor his own health status, the patient needs a practical device like the wearable mobile medical monitoring which is increasing quantities in the economic market [7].

As a matter of fact, the use of RFID technology in medical applications can offer patient tracking, safe guarding [8] and even physiological monitoring [9]. According to the advancements in the field, the RFID technology is used whether as a standalone system or in combination with other wireless technologies [10]. Various factors are considered for wearable medical instruments such as, performance, design and the safe use on the human body. Many researchers are also studying the ability to use wearable medical instruments and health-monitoring systems [11]. According to [12] and [13], radio frequency (RF) engineers have developed wearable antennas in many forms, for example wristbands or attachments to clothing. In order to obtain wearable antennas, the radiation pattern reconfigurable antennas, which have many advantages like the ability to adjust beam directions [11] can be used.

According to [14] and [15], there exists a switching technique that helps to adapt the beam directions. For this reason, many switches such as pin diodes and FET switches have been used. Beam-steering techniques are realized by using different structures [11]. The examples [16] and [17] present antenna using double loops and folded dipoles. The presence of beam-reconfigurable antennas in the domain of wearable antennas can help to improve this field especially in the use of communication systems [11].

The present paper depicts the realization of a radiation-pattern reconfigurable antenna to be used in medical applications [2]. According to [11], the performance of the antenna is improved after adding beam-switching skills. This study compares two antennas with the same method to obtain the circular polarization (having an arrow shaped cross slot [1]), yet with two different methods of fabrication, namely the ordinary PCB method and the MCTLA method. In addition, the paper presents the antenna return loss, the directivity and the specific absorption rate (SAR) results. The antenna performance and the specific absorption rate simulation results help to have an idea about whether the electromagnetic waves have a negative effect on the human body [11].

The goal of the present study is to have a CP (circular polarization), which helps to reduce the loss of polarization misalignment between the signals of transmitter and receiver antennas [18]. The polarized antenna is used, in different systems, to reduce the multi-pass effect between the transmitter and receiver antennas.

Also, there exist, the systems of wireless data links and radar [19]. Many techniques and shapes of micro strip antennas such as: log spiral [19], spiral antenna for wide bandwidth [20] and corner truncated ground for narrow band application [21], have been used. The spiral shape and truncate forms of the patch, in these methods, control the current distribution on the surface of the antenna, with the aim of achieving the CP [19-21]. In this study, the reason to obtain a circular polarized patch antenna is to benefit from its various advantages such as: low cost, light weight, ease of integration and compatibility [22].

In the present paper, a proposed RFID TAG is studied and simulated using CST with the aim of converting a linear polarized antenna to circular one.

This study took into consideration that the SAR value shall be acceptable and not exceed the limit value in order to guarantee a safe use in medical field and to ensure an acceptable rate of axial ratio necessary to prove the circular polarization existence.

During this research, two fabrication methods were done and are represented in the following sections: the first is the PCB method which is the most used in antenna manufacturing while the second is the MCTLA which is not well known in this field but it gives a more flexible antenna, more comfortable and more suitable for medical use.

## II. ANTENNA DESIGN

In [11], three proposed antennas have been proposed and presented with different theta angles 30, 90 and 150 degree. Every antenna consists of a monopole and a loop antenna, where the loop is opened at the point of contact with the pole. Two p-i-n diodes have been used as switches in an open circuit [11]. In addition, a pole is loaded on the top of the monopole, which is referred to as top loading [11]. The two main reasons behind the use of the top of the monopole are realizing the antenna miniaturization and controlling the beam direction by changing the angle (30°, 90° and 150°) of the top. Based on the theta angle, both sides of the top-loading poles are bent [11]. The simulation results are acceptable for theta 30 and 150. That's why this study has been conducted using these two angles. Fig. 1 presents the antennas design for theta 30 and 150. There are two states and two switches in case 1, the switch 1 is in the ON state while the switch 2 is in the OFF state, with the voltage measured at 1.2 v. Case 2 is exactly the opposed of case 1, where the switch 1 is in the OFF state and the switch 2 is in the ON state [11].

As a first step of this study, the dimensions of antenna were modified with conservation of the same design. The cases of theta (30) and theta (150) yields acceptable results.

The schematic diagram of the PIN diode connections is shown in Fig. 2. The  $V_c$  is a DC voltage, which is the control voltage of the switch. It is obtained by using a battery of 1.2V and can be valued at +1.2 or -1.2 following the direction of a battery connection. The RF signal  $V_s$  is connected through a DC block to protect the RF measuring device [23]. The antenna consists of a loop and a wire where the loop behaves as a folded dipole and the open wire as a reflector [24]. The use of a reconfigurable antenna can control a beam in the direction where the strength of the signal is stronger or in a direction that can avoid noise sources [25, 26].

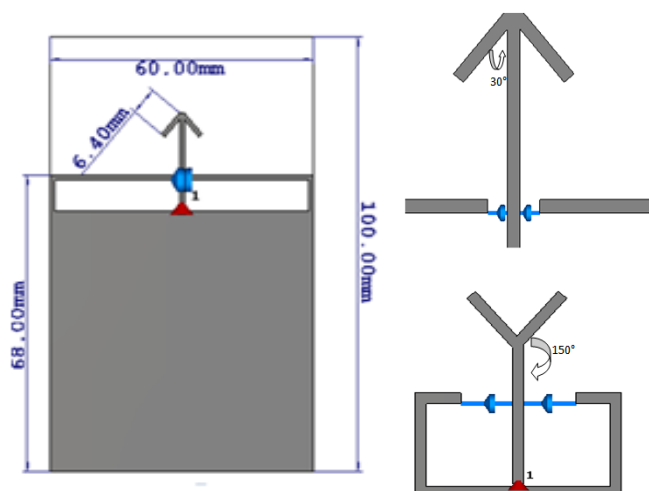


Fig. 1. Geometry of the Linear Polarization Antennas.

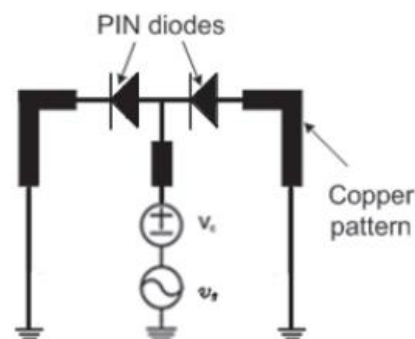


Fig. 2. Schematic Diagram of the PIN Diode [23].

Fig. 3 shows the antenna return loss of the three proposed simulated antennas in the two cases: case 1 and case 2. As shown in Fig. 3, there is a little deviation in the results and there is no big difference between the two cases.

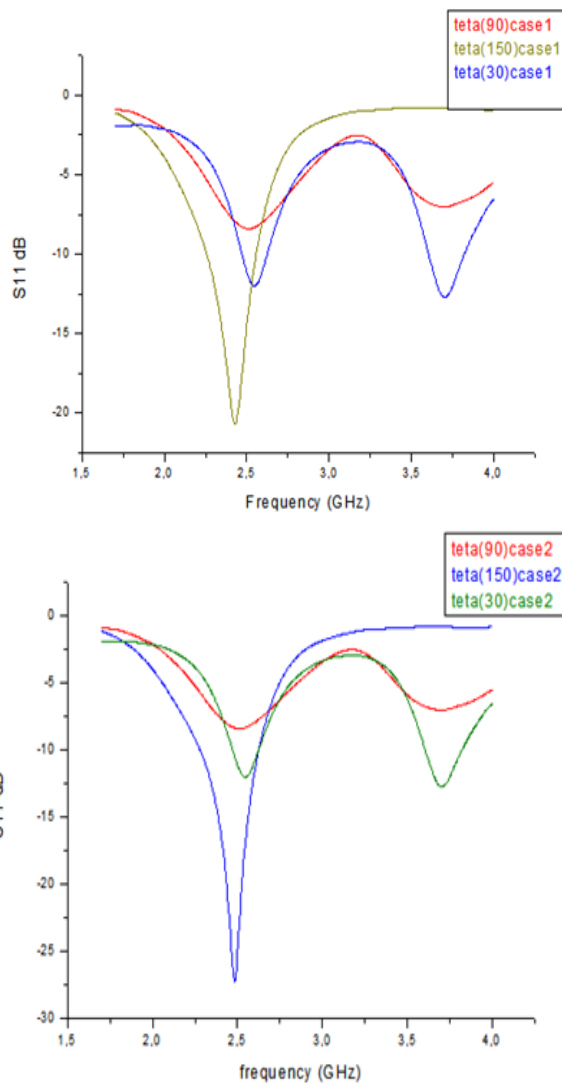


Fig. 3. Simulation's Results of the Proposed Antennas. (a) CASE1 (b) CASE2.

The return loss of the antenna in case1 depend on the theta angle .When the theta angle is equal to 150°, the resonant frequency is valued at 2.47GHz and when the theta angle is 30°, the resonant frequency is measured at 2.53 GHz and 3.7GHz. Fig. 3(b) presents the return loss depending on the theta angle 150° and 30° for case2. In this case, the resonant frequency is 2.5 GHz and 3.68 GHz for the (30°) degree angle and 2.5GHz for the (150°). At the beginning; the study should be based on an antenna with a linear polarization (which is the case here), then circular polarization study is conducted. According to the simulation results, both theta angles of 30° and 150° yields acceptable results.

For the rest of this study, theta angle was fixed at 30° since this value gave the best results.

Fig. 4 reveals that the antenna directivity is measured at 4.47 dBi for a frequency of 2.45 GHz and the energy distribution is located in the plan y. Fig. 4(b) presents the beam main lobe direction which is 149 degrees with a beam width of 52.1 degrees.

Fig. 5 presents the method used following [27] to obtain the circular polarization. The design of the slot is presented in [27].

The antenna is simulated when the theta angle is equal to 30°. From the feed line, the patches are capacitive and coupled. An arrow shaped coupling slot is used here to provide the ground plane. The arrow shaped coupling slot with an angle of 45° is inclined with the upper cross slots [27].

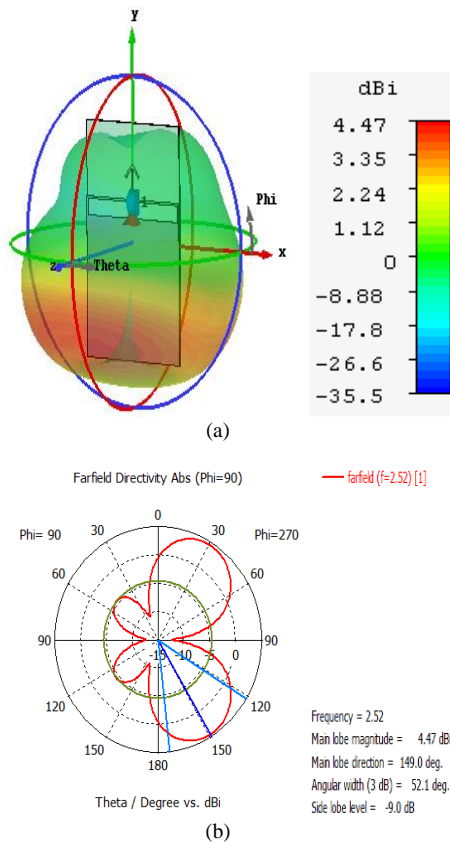


Fig. 4. 2.52 GHz Radiation Pattern (a) 3D Antenna Directivity (b) Polar Slot of the Antenna.

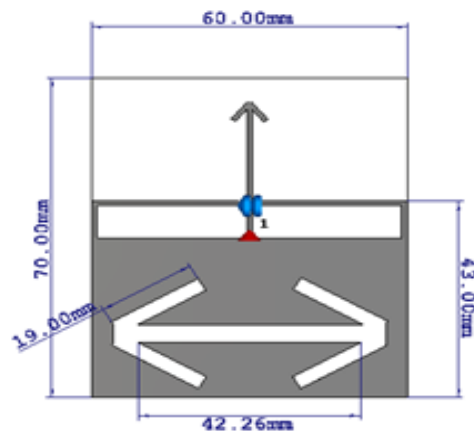


Fig. 5. Geometry of Circularly Polarized Patch Antenna.

The dimensions of the coupling slot are shown in Fig. 5. The coupling slot is selected to be narrow and is etched on the ground plane [28].

Fig. 6 presents the antenna which is fabricated with the PCB method and consists of: the FR-4 substrate. The pin diode CPINUC5206-HF is used as a switch, and a SMA connector is deployed to obtain 50ohm.

In the present study, an antenna is designed with two fabrication techniques the PCB and MCTLA methods [29].

The use of these methods helps to get a flexible antenna which can be useful in the medical field. Fig. 7 presents the fabricated antenna. To design this latter, in this method there are few steps to follow.

The dimensions of a small piece of ceramic covered with the scotch are first fixed. Second, the liquid silicone is mixed with n. Heptan by using two syringes for fifty times as shown in Fig. 9. After that a machine called (Laurell spin-coater) shown in Fig. 8 is used, to distribute the mixture on the ceramic plate.

Then the procedure is repeated for 3 times, and each time with 6 mm of solution. In the end, the metal stainless steel (stainless stell), on which the dimensions of the patch antenna will be fixed using the laser set up machine is added.



Fig. 6. Fabricated Antenna with PCB Method.



Fig. 7. Antenna manufactured using Laser Method.



(a) silicone (b) n Heptan (c) two syringes for the liquid exchange

Fig. 9. The Substrate Liquid Constituted of Silicone with n.Heptan.

### III. RESULTS AND ANALYSIS

#### A. Simulation Results

1) *Pre-incorporation of the human phantom:* The simulated return losses (S11) of the antenna are shown in Fig. 10. A resonant frequency of 3.07 GHz is found with an attenuation of - 23.39 dB and a bandwidth band of 82 MHz.

As shown in Fig. 11(a), the directivity is valued at 4.39 dBi and the energy distribution is localized in the Z+ plan where there is the slit with an arrow form. The beam main lobe direction for the proposed antenna is 10 degrees with a beam width of 94 degrees as shown in Fig. 11(b).

In order to validate the circular polarization of the designed antenna, the axial ratio shall be identified based on a CST simulation. Fig. 12 presents the axial ratio result, which is acceptable in the frequency range between 3.06 GHz and 3.11 GHz (in a frequency band of 41.2 MHz).



Fig. 8. The Laurell Spin-Coater Machine.

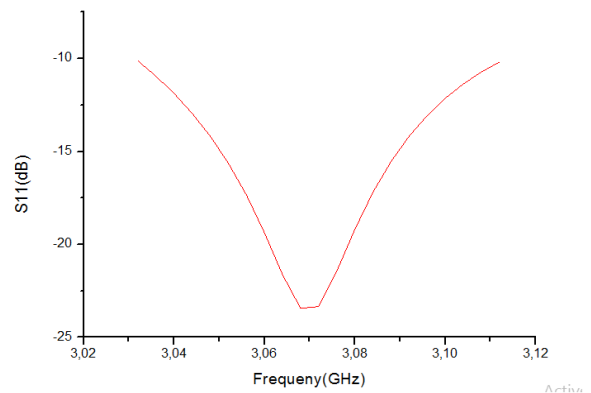


Fig. 10. Reflection Coefficient S11 of the Designed Antenna before Incorporation of the Phantom.

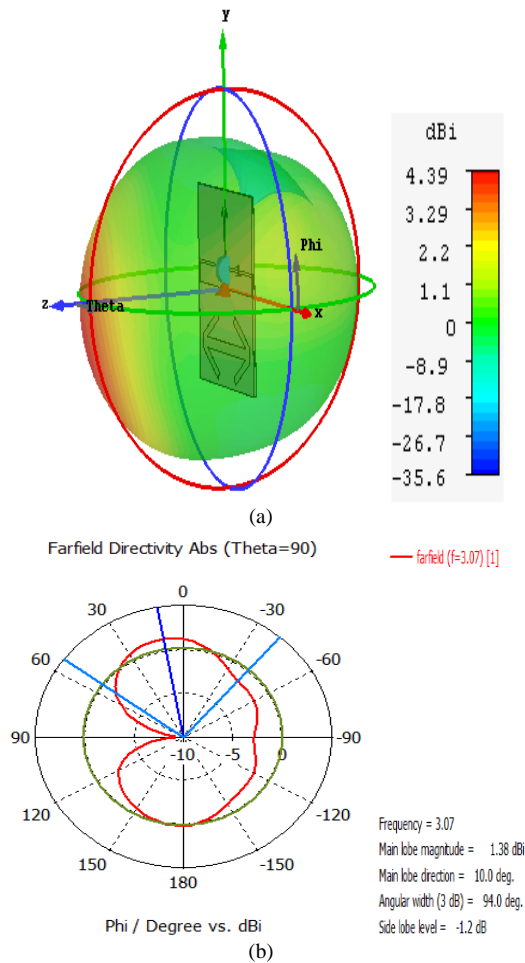


Fig. 11. 3.07 GHz Radiation Pattern (a) 3D Antenna Directivity (b) Polar Slot of the Antenna.

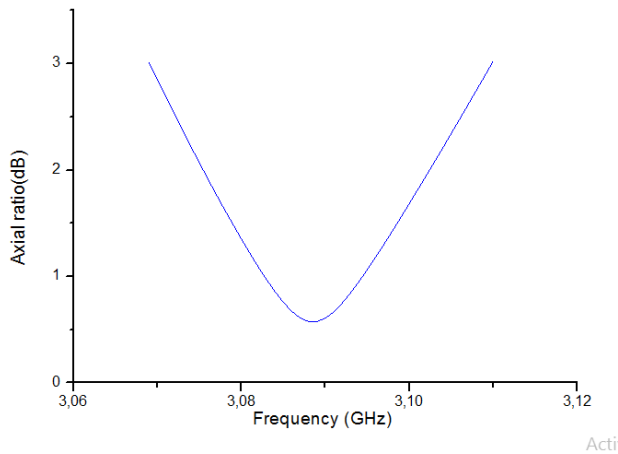


Fig. 12. The Antenna's Axial Ratio before Incorporation of the Phantom.

2) *Post-incorporation of the human phantom:* Fig. 13 presents the constituent of the human phantom. The incorporation of the antenna in the human phantom is done using the CST microwave studio. As shown in Fig. 13, the human phantom consists of: skin of: 2mm ( $\epsilon_r=40, \sigma=1.3$ ) [31], fat of 10mm ( $\epsilon_r=5, \sigma=0.06$ ) [31], muscle of 15mm ( $\epsilon_r=55, \sigma=1.14$ ) [30]. In this case, a pin diode CPINUC5206-

HF is used to get a high frequency (3 GHz), which can help to have an idea about whether this frequency is useful in the medical application. The (Specific Absorption Rate) SAR, which is defined as the rate at which energy is absorbed per mass unit of body tissue [31], can vary from one law to another, the local SAR should not be superior to 2 W/kg in 10g of tissue in the European standard [31].

The antenna resonant frequency is valued at 3.07 GHz with an attenuation of -23.99dB as shown in Fig. 14. In addition, the bandwidth band is measured at 102.3 MHz which is a widened one.

As shown in Fig. 15, an acceptable axial ratio from 3.057 GHz to 3.089 GHz (in a frequency band of 32 MHz) is obtained, which confirms the obtain ability of a circular polarization.

Fig. 16 presents the antenna directivity measured at 5.39 dBi. The above mentioned figure shows also an interesting energy distribution in the position of the slits in the Z+ plan in the two side lobes. Fig.16(b) presents the beam main lobe direction which is valued at 0.847 degree with a beam width of 222.1 degrees.

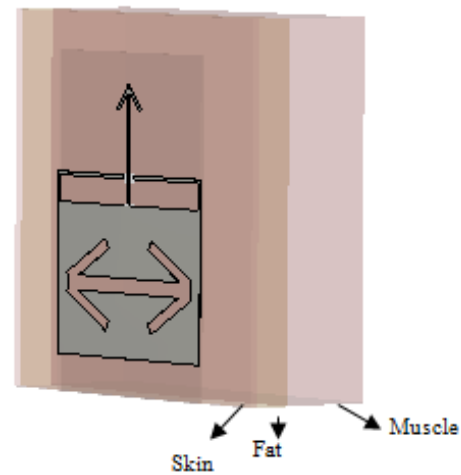


Fig. 13. The Compositions of the Phantom.

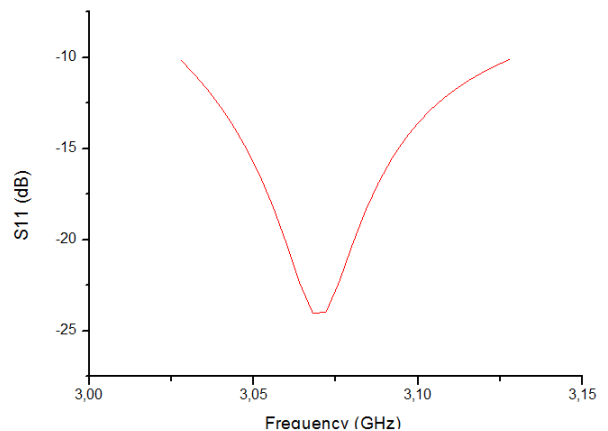


Fig. 14. Reflection Coefficient S11 of the Designed Antenna after Incorporation of the Body Phantom.

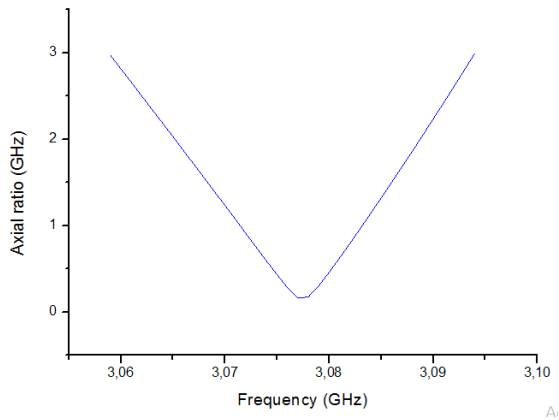


Fig. 15. The Antenna' Axial Ratio after Incorporation in the Phantom.

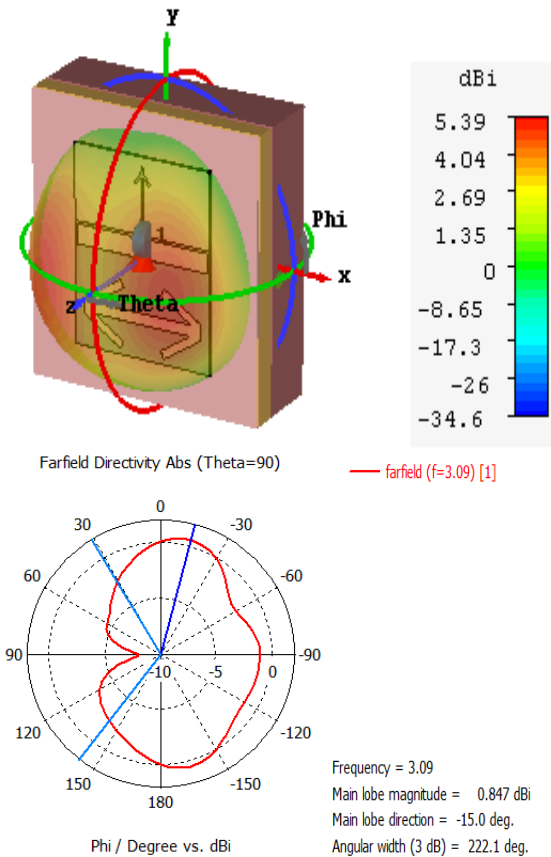


Fig. 16. 3.07 GHz Radiation Pattern (a) 3D Antenna Directivity (b)Polar Slot of the Antenna

As shown in Fig. 17, a value of 1.16 w/kg is obtained in a frequency of 3.07 GHz, which is acceptable according to the European standards.

3) *The comparative study according to simulation results:* Table I compares the simulation results of the initial antenna and the proposed antenna, where an improvement of 30% for the width and 100.9% for the return loss is noted.

Table II presents a comparison between the results before and after implantation, where an increase in the directivity (from 4.39dBi to 5.39dBi ) and in the bandwidth band (from

80 MHz to 102.8 MHz) is noticed, which offers in turn an improvement of 28.25% and 22.77%, respectively.

**B. Realization Results**

1) *The PCB fabrication technique (Printed Circuit Board):* Fig. 18 presents a resonant frequency of 3.1GHz for the fabricated antenna (PCB method), with an attenuation of -15.4 dB.

A small deviation was noted while comparing the PCB fabricated antenna with the simulated one which has a resonant frequency of 3.07 GHz.

This deviation is mainly due to experimental procedure.

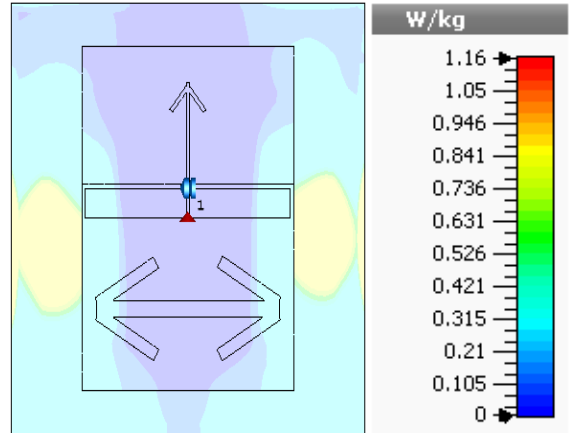


Fig. 17. Antenna's Resulted SAR.

TABLE. I. COMPARISON BETWEEN THE INITIAL ANTENNA AND THE DESIGNED ANTENNA

|                           | Comparison Results |                  |  |
|---------------------------|--------------------|------------------|--|
| Antenna paramaters        | Initial antenna    | Proposed antenna | The improvement of proposed antenna over initial antenna |
| Width                     | 100 mm             | 70mm             | 30%  |
| Return loss (S-parameter) | -11.64             | -23.39           | 100.9%   |
| polarization              | Linear             | Circular         | -  |

TABLE. II. FREQUENCY RESULTS BEFORE AND AFTER INCORPORATION OF THE BODY PHANTOM

|             | The improvement percentage           |                                     |                 |
|-------------|--------------------------------------|-------------------------------------|-----------------|
|             | Before Incorporation of body phantom | After incorporation of body phantom | The improvement |
| Bandwidth   | 82 MHz                               | 102.6 MHz                           | 25.12%          |
| Directivity | 4.39 dBi                             | 5.39 dBi                            | 22.77%          |

IV. CONCLUSION

In this paper, a circular polarization was obtained by inserting an arrow shaped slot to an antenna initially designed with linear polarization. The simulation results were then noted and analyzed and the fabrication of antennas were made using two different methods. A comparison study was later made between simulation results and manufactured antenna's performances in order to assess any potential difference. The latter revealed that the SAR has an acceptable value even with the use of pin diode with a high frequency (3 GHz). The use of the metal cutting through laser ablation method can help to have a flexible antenna, which is suitable for the medical application. The simulation results and the realization ones are almost equal. Finally, the safety of the antenna use is valorized with the SAR value.

Since the obtained results are acceptable and the SAR is within the admissible values, the next step in the research will include the miniaturization of the antenna's dimensions with the use of more flexible substrate in order to ease the use of the antenna and make it effective, comfortable and easy marketed.

REFERENCES

- [1] P.Ken ,S.Arief,Santiko,A.B ,P. Reza ,M.Ali , "Millimeter Wave Antenna for RFID Application " ,International Conference on Radar, Antenna, Microwave, Electronics, and Telecommunications, Jakarta, Indonesia, 23-24 Oct, 2017.
- [2] R.Romi , H.Eka, S.Baihaqi ,S.Mohammad, S.Opim , "RFID Presence Monitoring System as an Input to Measure the Workload of Employee " 4th International Conference on Computer Applications and Information Processing Technology (CAIPT) , Kuta Bali, Indonesia, 8-10 Aug. 2017
- [3] W.Rongwei,X Rensheng, W.Tailei,C. Dong, S.Tao, k.Lei , and Z. Shouzheng "Design of Semi-active RFID Antenna " ,Progress In Electromagnetics Research Symposium, Russia, 22–25 May,2017
- [4] A.M. Wicks,J.K. Visich,and S.Li, "Radio frequency identification Applications in hospital environments," Hospital Topics, vol.84, ,pp.3-8, 2006.
- [5] H.A.NahasandJ.S.Deogun,"Radio frequency identification Applications in smart hospitals,"in Proceedings of the 20th IEEE International Symposium on Computer-Based Medical Systems ,pp.33 7-342, 2007.
- [6] A.Lahtela,"A short overview of the RFID technology in healthcare,"in 4th International Conference on Systems and Networks Communications ,pp.165-169, 2009.
- [7] L.Ting , Y. Yong , "Wearable medical monitoring systems based on wireless networks", IEEE Sensors Journal,vol.16,pp. 8186 - 8199,2016
- [8] Manzari S., Occhiuzzi C., Marrocco G.: 'Feasibility of body-centric systems using passive textile RFID tags', IEEE Antennas Propag. Mag , 54, (4), pp. 49–62 , 2012.
- [9] Wang J., Bolic M.: 'Exploiting dual-antenna diversity for phase cancellation in augmented RFID system'. Int. Conf. on Smart Communications in Network Technologies (SaCoNeT), pp. 1–6 , 2014
- [10] Yoo S.K., Cotton S.L.: 'Improving signal reliability for indoor off-body communications using spatial diversity at the base station'. The 8th European Conf. on Antennas and Propagation (EuCAP 2014) , pp. 857–861, 2014
- [11] C.M.Lee, C.W.Jung , "Radiation-Pattern-Reconfigurable Antenna using monopole-loop for fitbit flex wristband", IEEE Antennas and wireless propagation letters, Vol.14, 2015.
- [12] J. Lee, S. I. Kwak, and S. Lim, "Wrist-wearable zeroth-order resonant antenna for wireless body area network applications," Electron. Lett.,vol. 47, no. 7, pp. 431–433, Mar. 2011
- [13] S. J. Kim, K. Kwon, and J. H. Choi, "Design of a miniaturized high-isolation diversity antenna for wearable WBAN application," J. Electromagn.Eng. Sci., vol. 13, no. 1, pp. 28–33, Mar. 2013

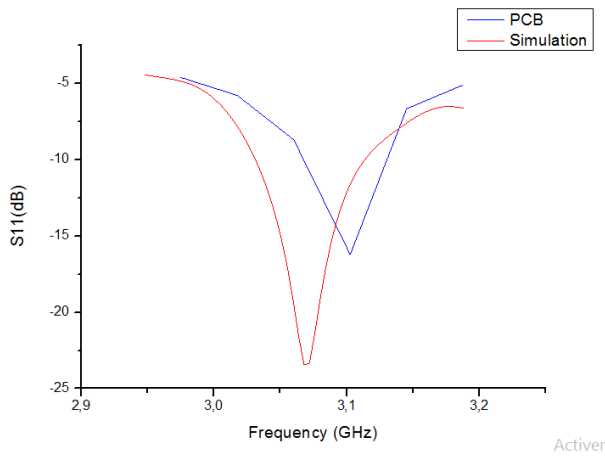


Fig. 18. Reflection Coefficient Comparison between PCB Method and CST Simulation Results.

2) *The Metal Cutting Through Laser Ablation Fabrication Technique (MCTLA)*: Fig. 19 presents a resonant frequency of 3.3 GHz for the designed antenna, with an attenuation of -17.8 dB. Compared to the simulated antenna, we can confirm the similarity in results with a little deviation because of the realization procedure and the difference of the materials used in the manufacture.

3) *Analysis of frequency results*: Table III presents a comparative analysis of the frequency results; where, there is a similarity between the simulation result and the PCB result. But, a small frequency deviation in the laser result is noted, which can be caused by the use of different compositions (the liquid silicon, the n heptan and the metal stainless steel) in the laser.

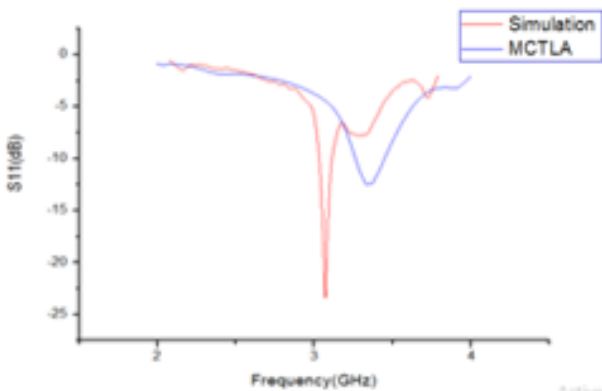


Fig. 19. Reflection Coefficient Comparison between PCB Method and MCTLA Simulation Results.

TABLE. III. THE FREQUENCY COMPARISON

| Frequency Comparison Results |            |             |         |
|------------------------------|------------|-------------|---------|
|                              | Simulation | Realization |         |
|                              |            | PCB         | MCTLA   |
| Frequency                    | 3.07 GHz   | 3.1GHz      | 3.3 GHz |



- [14] W. Kang, K. H. Ko, and K. Kim, "A compact beam reconfigurable antenna for symmetric beam switching," *Prog. Electromagn. Res.*, vol.129, pp. 1–16, 2012.
- [15] W. Kang and K. W. Kim, "A beam pattern-reconfigurable antenna using PIN diodes," in *Proc. Antenna Propag. Soc. Int. Symp.*, Jul. ,vol. 40, no. 23, pp. 1–4, 2010.
- [16] J. Y. Kim, B. J. Lee, and C. W. Jung, "Reconfigurable beam steering antenna using double loops," *Electron. Lett.*, vol. 47, no. 7, pp. 430–431, Mar. 2011.
- [17] S. Lim and H. Ling, "Design of electrically small, pattern reconfigurable Yagi antenna," *Electron. Lett.*, vol.43, no.24, pp. 1326–1327, Nov. 2007.
- [18] Ding, Kang, Tongbin Yu, Qiao Zhang, and Kang Luo. "Dual-band Circularly Polarized Aperture Coupled Annular-ring Microstrip Antenna for GNSS Applications." *Frequenz* 68, no. 1-2 ,pp.19-24,2014
- [19] Jahangiri, Payam, Ramezan Ali Sadeghzadeh, and Ali Pourziad. "Log spiral antenna with CPW feed line for UWB application and circular polarization." *Microwave and Optical Technology Letters* 58, no. 1 ,pp. 17-21,2016.
- [20] Mashaal, O. Ahmad, S. K. A. Rahim, A. Y. Abdulrahman, M. I. Sabran, M. S. A. Rani, and P. S. Hall. "A coplanar waveguide fed two arm Archimedean spiral slot antenna with improved bandwidth." *IEEE Transactions on Antennas and Propagation* 61, no. 2 ,pp. 939-943,2013.
- [21] K. Pedram, J. Nourinia, C. Ghobadi, and M. Karamirad, "A multiband circularly polarized antenna with simple structure for wireless communication system," *Microwave and Optical Technology Letters*, vol. 59, pp. 2290-2297, 2017.
- [22] Zhongbao Wang, Shaojun Fang, Shiqiang Fu and Shouli Jia, "Single-fed broadband circularly polarized stacked patch antenna with horizontally meandered strip for universal UHF RFID applications", *IEEE Transactions on microwave theory and techniques*, vol.59 No. 4, April 2011
- [23] W. Kang and K. W. Kim, "A beam pattern-reconfigurable antenna using PIN diodes," in *Proc. Antenna Propag. Soc. Int. Symp.*, Jul. 2010, vol. 40, no. 23, pp. 1–4.
- [24] Balanis, C.A.: 'Antenna theory: analysis and design' (John Wiley & Sons, Inc., New Jersey, 3rd edn , 2005
- [25] Cummings, N.P. 'Active antenna bandwidth control using reconfigurable antenna elements', Ph.D. dissertation, (Virginia Tech, Blacksburg, Virginia, USA, 2003)
- [26] Kang, W.S., Park, J.A., and Yoon, Y.J.: 'Simple reconfigurable antenna with radiation pattern', *Electron. Lett.*, 2008, 44, (3), pp. 182–183
- [27] A.Maria , V.Vishnupriya, A.John K.K, T.Mathew " Dual band circularly and WiMAX Applications", *IEEE*,2015
- [28] Hua - Ming Chen, Kuo- Yung Chiu, Yi-Fang Lin, " Single-layer circularly polarized patch antenna for RFID reader application" *Antennas & propagation society International symposium*, 2009
- [29] M. Schuettler, S. Stiess, B. V. King, and G. J. Suaning, "Fabrication of implantable microelectrode arrays by laser cutting of silicone rubber and platinum foil," *Journal of neural engineering*, vol. 2, no. 1, S121, <http://stacks.iop.org/1741-2552/2/i=1/a=013>, 2005.
- [30] P. Momenroodaki, Z. Popovic, Antenna ,M. Fallahpour, "Probes for Power Reception from Deep Tissues for Wearable Microwave Thermometry", *IEEE International Symposium on Antennas and Propagation & USNC/URSI National Radio Science Meeting*,2017
- [31] <http://www.emitech.fr/fr/mesure-DAS.asp>

# Passenger and Luggage Weight Monitoring System for Public Transport based on Sensing Technology: A Case of Zambia

Apolinalious Bwalya<sup>1</sup>, Jackson Phiri<sup>2</sup>, Monica M. Kalumbilo<sup>3</sup>, David Zulu<sup>4</sup>  
School of Natural Science, Department of Computer Science, The University of Zambia

**Abstract**—The prevalence of overloading, which is exceeding the maximum load weight, on public buses in Zambia is very rampant because there is currently no system to measure and monitor load weight at bus stations, apart from weighbridges on few selected roads located far away from the loading points. The aim of this study was to design and develop a passenger and luggage weight monitoring system to mitigate the challenge of overloading on public buses. To achieve this, a baseline study was conducted to appreciate the challenges of the current system being used to manage passenger and luggage, i.e., load weight, on public buses. The risk factors considered to contribute to compromised road safety leading to road traffic accidents were also established from all stakeholders as follows: 54 percent human, 39 percent road/environmental, 6 percent vehicle and 1 percent was attributed to other factors. The results were then used as a basis to design and develop a load weight monitoring system (LWMS) based on sensing and other emerging technologies like Load Cells, Wireless Sensor Network (WSN), Internet of Things (IoT), and Cloud Computing concepts to automate the measurement of the load weight, capture and transmit data.

**Keywords**—Overloading; load weight; load cells; emerging technologies

## I. INTRODUCTION

The use of emerging technologies in today's world has greatly improved the way of life, including application in industry and business enterprises to improve organization and business processes. A business process is defined as "a set of logically related tasks and behaviours that organizations develop over time to produce specific business results and the unique manner in which these activities are organized and coordinated" [1]. The Public Transport Sector has also embraced the new era of emerging technologies such as the Wireless Sensor Network (WSN), Internet of Things (IoT), Digital Communication, Cloud Computing, Motion and Weight Sensing, and "big data" analysis [2] which has created a new global potential for less costly "Intelligent Transport Systems (ITS)" to improve road safety and more efficiently manage transport assets.

In 1992 the public transport sector in Zambia was liberalized from state owned to private ownership. This resulted in sharp rise in the number of bus operators and buses. The current public transport sector is largely unregulated though the government through local authorities and various agencies regulate, enforce and superintendent over

bus stations, bus registration and licensing, transport fares, road safety, and axial load control, among others [3].

At bus stations, the loading points, the current system of loading passengers and luggage on public buses is not well defined and is chaotic. The bus crews have no system or means to establish how much *load weight* is to be loaded on the bus within the prescribed maximum *load weight* limits. The only point where the bus weight is measured is at designated weighbridges on few selected roads way off from the loading point. This challenge leads to overloading which in turn leads to compromised road safety, damage to road pavements, damage to vehicle, higher fuel consumption and so on. Since the *load weight* loaded on the buses is not measured, the bus owners or operators also do not have any means to obtain detailed accurate data on how much *load weight* is carried on their buses, apart from relying on number of passenger tickets to calculate expected income and apparently very little or no income from luggage.

Vehicle overloading is a phenomenon resulting from either exceeding the permissible Maximum Axle Load or the Maximum Gross Vehicle Mass (GVM) [4]. Axle load is defined as the weight transmitted onto the road by an axle bearing two tyres or more, while GVM is defined as the net weight of a motor vehicle or trailer together with such weight of goods or passengers or both. The maximum permissible load limits take into account the road design capacity and vehicle tyre ratings among other things [5]. Vehicle overloading results in rapid deterioration of the road pavement infrastructure, leading to high road maintenance costs [6]. A study conducted by the International Road Dynamics Inc., found that 10 percent increase in weight can accelerate pavement damage by over 40 percent [7]. Therefore, the damage caused by overloading rises exponentially with each additional ton of axle load, and this reduces the life of a road substantially. Despite several regulations to deter overloading, enforcement is lacking mainly due to no specific policy and no mechanism of establishing *load weight* loaded on the buses exist at the moment [7].

The Metrology Act for Zambia Metrology Agency in reference to the National Measurement Units states that "a person shall not, without reference to the standard unit of measurement, in relation to any goods and services quote a price or charge; issue or exhibit a price list, invoice or other document; state a quantity in an advertisement, poster or document; or indicate the net quantity of a commodity on a

package”[8]. Alas, at the bus stations, the bus crew load the luggage on the bus and even prescribe charges without any reference to any standard unit of measurement.

The rest of this paper is divided into following sections: Section II comprehensively deals with literature review and related works; Section III discusses the methodology that cover: scope of study, specification of developed system, hardware, system flowcharts and prototype design. Section IV highlights the research results; Section V discusses the result; and Section VI gives the research conclusion and future works.

## II. LITERATURE REVIEW

### A. Introduction

The Roads and Road Traffic Act of Zambia provides guidelines on the prescribed *load weight* limits for public vehicles [9]. The scientific word for how much an object weighs on a scale is “*mass*”. The words “*weight*” and “*mass*” are often used interchangeably, because both are used in everyday language. In many contexts, scales are used to measure weight or mass of an object [10].

Different types of scales are available and can basically be classified as Analog or Digital scale, the latter is of interest for our study. A *Digital scale* is a scale that has electronic devices on it like digital and LCD screens while an *Analog scale* is one with mechanical moving parts. A *Load Cell* is principal component of the Digital or Electronic scale. Accuracy is one of the most important parameter of any scale while calibration is the process of adjusting the scale for accuracy. Factors that can affect the system's weighing accuracy are Load Cell Accuracy, Load Factors, Environmental Forces, Interference with Signal Transmission, and Instrumentation and Control [10].

The use of technology and proliferation of computers and internet has brought enormous changes in the way organizations conduct business. Not only in the business world but also the education sector where the application of ICTs has brought about huge improvements in the education processes like in administration, assessment and management of various stages in education. The application of ICT in business and social life has opened up new possibilities for running and managing organizations as noted by [11]. With the rapid development of processing and storage technologies and success of the internet, computing resources have become cheaper, more powerful and more available than ever before. This technological trend has enabled the realization of a new computing model called cloud computing, in which resources are provided as general utilities that can be leased and released by users through the internet in an on-demand style [12]. The Education sector has also taken advantage of these technological developments so as to improve the management of processes especially in the area of learning, assessment and candidate registration.

### B. ICTs in Public Transport Systems

Transportation is rapidly being changed by new technologies, such as Intelligent Transportation Systems (ITS) which including smart cards, on-board diagnostics and

information systems, and smarter highways, transit, automobiles, logistics systems, and other information systems [13]. The range of options and their impacts will continue to expand as new technologies are introduced over the next decades, and may alter transportation systems in many ways. Adoption of ICTs has a significant influence in public transport systems in term of the mobility of people and goods. ICTs are also a potentially important enabler of change in social and business organizational systems, thus affecting the demand for public transport in spatial and temporal terms. Technological trends will meet the demand for safety, speed and comfort through advances in ICT in the field of telematics. This covers systems for traffic and transport management, travel information and reservations, vehicle guidance, and mobility cards [14]. Over the last few years firms operating in the public transport sector have made significant progress in their adoption of new technologies, particularly those linked to the internet and e-business. Advanced traffic management systems could increase road capacity significantly while improving safety and respecting other objectives such as pedestrian comfort.

Over the longer run, automation could make order of magnitude improvements in safety, capacity, and convenience. To obtain the quality solutions needed in the organization and operation of public transport system, the use of interoperable ICT and Intelligent Transport Systems (ITS) in the transport should be encouraged further as a matter of priority [15].

A specific role for interoperability could be found in the exchange of information between agencies, operators and bus crews. Thus, means of transport synchronize their activities and the transported goods and passengers reach their destination on time and in full transparency of information. Smart technologies such radio frequency identification (RFID) should be introduced to contribute to improved efficiency and security, and provide new quality services for mobility of people and goods [16].

### C. Load Cells

A load cell is a transducer that is used to convert a force into electrical signal. This is indirect conversion which occurs in two stages. Through a mechanical arrangement, the force being sensed deforms a strain gauge. Load Cells are used in several types of measuring instruments such as Laboratory Balances, Industrial and Commercial Scales, Platform Scales, and Weighbridges.

There are many configurations, but the most popular and the focus of our study is the Strain Gauge Load Cell (SGLC). Fig. 1 shows a typical example of SGLC, a double bending load cell element. The SGLC measures strain, and then transfers that force into electric energy which manifests as measurement for interpretation. Measuring strain effects helps preserve the integrity of the unit under pressure as well as protects equipment and people nearby [17].



Fig. 1. Strain Gauge Load Cell [18].

SGLC are attached to structural bearing or support beam of an application that endures stresses and pressures, oftentimes with superglue or some other appropriate adhesive. When strain is put upon the bearing, the material's change in tension exerts force upon the SGLC, which sends an electrical signal through a switching unit. This signal manifests as a measurement of the load, and reveals how much tension is being placed upon the unit. Load cell display unit displays tension forces as well as temperature, voltage to frequency comparisons and other important information about the application. The measurement is calculated by a complex equation based on the reaction of four different measurements of stress and compression [18].

D. Wireless Sensor Networks

A Wireless Sensor Network (WSN) can be defined as a network of devices, denoted as *nodes*, which can cooperatively sense and may control the environment enabling interaction between persons or computers and the surrounding environment, and communicate the information gathered through wireless links [19]. The data is forwarded, possibly via multiple hops, to a *sink* (sometimes denoted as *controller* or *monitor*) that can use it locally or is connected to other networks (e.g., the Internet) through a *gateway*. The nodes can be stationary or moving; can be aware of their location or not; and can be homogeneous or not [20].

Fig. 2 shows a traditional Single-Sink (left part) and Multi-Sink (right part). Most of the scientific papers in the literature deal with such a definition. This single-sink scenario suffers from the lack of scalability: by increasing the number of nodes, the amount of data gathered by the sink increases and once its capacity is reached, the network size cannot be augmented. Moreover, for reasons related to Medium Access Control (MAC) and routing aspects, network performance cannot be considered independent from the network size [21].

E. Cloud Technology [23]

With the spread of broadband internet across the globe, more emphasis has been placed on how to effectively and efficiently utilize and allocate all the available computing, processing and storage capacity available globally. Resource sharing has enabled concepts such as Software as a Service, Platform as a Service and Database as a Service where the end user does not need to worry about the technical requirements of systems, software and the technical specifications of the database but just focuses on service usage. Cloud computing has made it possible for emerging companies to rollout their services at a much faster pace as the cost of data centres is slowly becoming a non-factor with cloud based solutions such as Data Centre as a Service (DCaaS). Cloud computing has brought about novel ideas where a computer is no longer viewed as a standalone entity but can span multiple hardware platforms and multiple geographical locations.

F. Internet of Things

Internet of Things (IoT) is defined as “the system of physical objects or things hooked up with hardware, software, sensors, and system connectivity which empowers these objects to gather and alternate information” [24]. IoT makes

use of different kinds of protocols to work with exclusive objects [25].

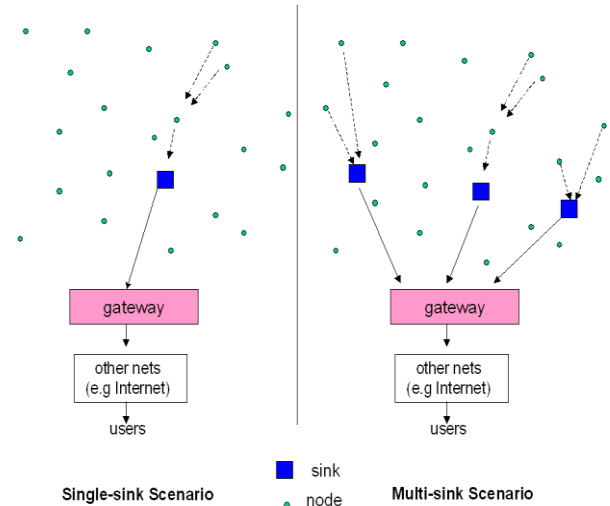


Fig. 2. Left Part: Single-Sink WSN. Right Part: Multi-Sink WSN [21] [22].

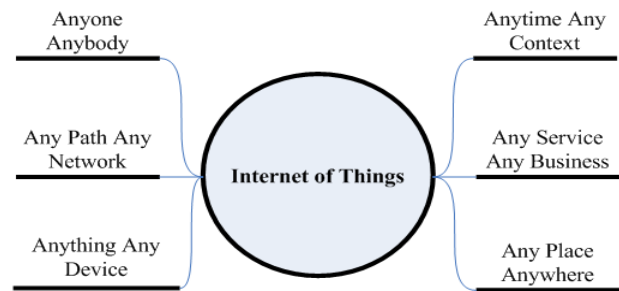


Fig. 3. IoT Definition/Concept [26] [27].

TABLE I. IOT SMART APPLICATIONS AND SERVICES [27]

| No. | Application of Internet of things |  |
|-----|-----------------------------------|--|
|     | Service Domain                    | Services   |
| 1   | Smart Home                        | Entertainment, Internet Access   |
| 2   | Smart Office                      | Secure File Exchange, Internet Access, VPN, B2B  |
| 3   | Smart Retail                      | Customer Privacy, Business Transactions, Business Security, Business Security, B2B, Sales & Logistics Management   |
| 4   | Smart City                        | City Management, Resource Management, Police Network, Fire Department Network, Transportation Management, Disaster Management                                |
| 5   | Smart Agriculture                 | Area Monitoring, Condition Sensing, Fire Alarm, Trespassing  |
| 6   | Smart Energy & Fuel               | Pipeline Monitoring, Tank Monitoring, Power Line Monitoring, Trespassing & Damage Management   |
| 7   | Smart Transportation              | Road Condition Monitoring, Traffic Status Monitoring, Navigation Support, Smart Car support, Traffic Information Support, Intelligent Transport System (ITS) |

IoT also provides networking to connect people, things, applications, and data through the Internet to enable remote control, management, and interactive integrated services [28]. Fig. 3 and Table I shows a summary of the definition or concept of IoT and the numerous applications of IoT among others, respectively.

G. Sensing Technology [29]

Remote sensor networks have traditionally relied on four components, a sensor to collect the data, an aggregator to centralize the collection of data, an uplink network to relay the data and a server to which the data is to be sent. Wireless sensor network can be further broken down into two main components, the remote sensor network and the uplink. The remote sensor network is that part of the network that is composed of the sensors which have energy sources and some kind of personal area network used for localized communication. The network may also comprise a collaboration algorithm which may determine its work mode. The three main work modes that enable collaboration in a wireless sensor network are a star network, a mesh network or a ring network. The remote sensors basically sense, process and send the data either individually or through aggregator.

III. METHODOLOGY

The purpose of the baseline study was to establish the challenges by the public transport system with regard to management of load weight on buses. The method that guided this research was a Mixed Methods Research Methodology which comprises a combination of qualitative and quantitative research types. Descriptive statistics analysis technique was used to analyse the data obtained from the questionnaire. Qualitative data was analyzed by bringing out emerging themes that were categorized and interpreted to form part of the input in the design of proposed system. The use of filter questions in interviews was applied because not all and same questions were asked to the institutions/agencies, bus owners/operators and the bus crew. The use of filter questions is a common method in standardized questionnaire surveys to make the interview more effective and efficient.

This study was confined to Lusaka province of Zambia. It catered eleven (11) institutions/agencies with thirty-six (36) participants; fourteen (14) bus owners/operators; and forty-two (42) bus crew; giving a population sample size of ninety two (92) participants. Non-probability sampling technique was used in this study because of the different specialized knowledge and work experience possessed in the subject area. This approach was preferred as the research required information from different stakeholders; those who were responsible for policy, regulation, enforcement, bus owners/operators, and the bus crew, who include drivers, conductors, inspectors, ticket sellers, and bus loaders. The age of the respondents who participated in this study ranged from 17 to 56 years old with 19.6% female and 80.4 % male. The highest levels of education for the participants ranged from School Certificate to Master’s degree. The current mode of load weight management on public buses in Zambia is as shown in Fig. 4.

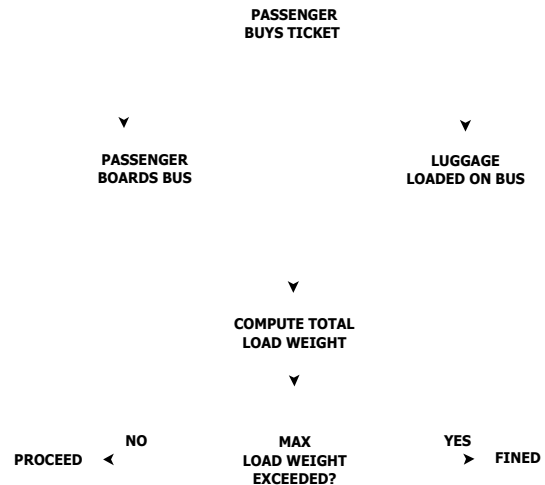


Fig. 4. Current Load Weight Management on Public Bus in Zambia.

A. Proposed Load Weight Monitoring System

Due to none existence of means to measure load weight on public buses, the need to come up with one motivated this study. Therefore, a Load Weight Monitoring System (LWMS) is proposed. The results of the baseline study were used to come up with a conceptual model and design for the LWMS on public buses as shown in Fig. 5.

The system development method used was the Water Fall Model approach and the qualitative data obtained from both the questionnaires and the interviews were used to come up with the system requirements. Currently, the bus seating capacity determines the limit and hence the number of tickets/passengers to loaded on the bus while there is no means to measure the weight of the luggage which is left to the discretion of the bus loaders and crew.

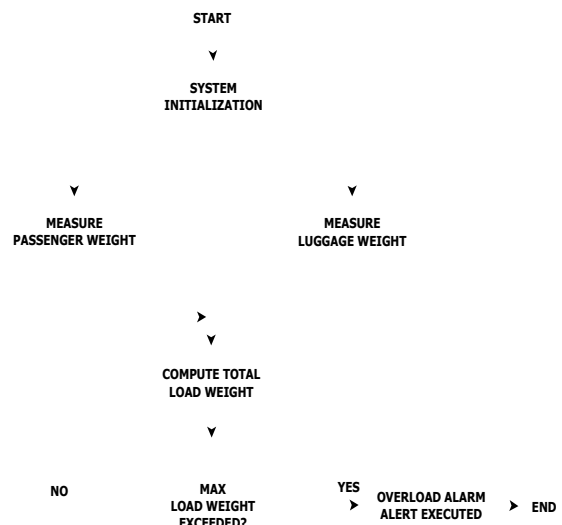


Fig. 5. Flowchart of Proposed LWMS Model.

## B. System Design of LWMS

The LWMS model was developed using of selected software and hardware materials suitable, to achieve the task at hand. Load Cells, Microcontrollers and Sensors were used to measure, monitor and control the weight of the load weight on the bus. A SIM900A GPRS/GSM Shield was used to provide GPRS services and connect to internet. This was essential to enable load weight data to be captured and logged in to the central database server for stored. This information which mainly consisted on the status of the load weight from the model was displayed using web pages created using HyperText Markup Language (HTML), Cascading Style Sheets (CSS) and HyperText Preprocessor (PHP). Through the use of the GPRS/GSM service, the same information in form of Short Messaging System (SMS) was able to be sent to relevant agencies and/or owners/operators.

1) *Load cell*: A load cell is a transducer which converts force into a measurable electrical output. Load cell designs can be distinguished according to the type of output signal generated and the way the detect weight. They various types of load cells include: Hydraulic; Pneumatic; and Strain Gauge Load Cells. For details on load cell, refer to Literature Review in the previous section.

2) *Arduino microcontroller*: Arduino is an open-source electronics platform based on easy to use hardware and software. In its simplest form, an Arduino is a tiny computer that can be programmed to process inputs and outputs going to and from the chip. The Arduino is what is known as a Physical or Embedded Computing platform, which is an interactive system and through the use of hardware and software, it can interact with its environment. The main advantages of using an Arduino include following: Inexpensive; Cross-platform; Simple, Clear Programming Environment; Open Source and Extensible Software and Hardware.

3) *SIM900A GPRS shield*: The GPRS module is a breakout board and minimum system of SIM900A Quad-band/SIM900A and Dual-band GSM/GPRS module. It is capable of communicating with controllers via ATention (AT) commands which are instructions used to control a modem. These instructions help: Get information about the mobile phone; Get basic information about the subscriber; Get the current status of the mobile phone or GPRS/GSM module; Establish a data connection or voice connection to a remote modem; Send or delete an SMS message and obtain notifications of newly received SMS messages; Perform security related tasks such as changing a password; Control the presentation of error messages of AT commands; Get or changes the Configurations of a mobile phone or GPRS/GSM module; and Save the Configurations of a mobile phone or GPRS/GSM module. The module also furthermore supports software power on and reset functions.

4) *Programming environment*: Because the project include a web application to be developed, the use of HTML was essential. HTML which stands for Hypertext Markup Language is a standard markup language for creating web pages and web applications. Through the use of HTML, CSS

(Cascading Style Sheet) and JavaScript was included to make the web application more dynamic and responsive.

PHP is a widely-used open source general-purpose scripting language that is especially suited for web development and can be embedded into HTML. What distinguishes PHP from other server-side scripting languages is that it is simple to use and code written can be executed on the server which then generates the required HTML pages. Further, more configuration of a webserver to process all HTML files using PHP is possible. For the purpose of this project, the latest version of PHP which was PHP 7.0 was used to create the web application necessary for the project.

Firebase is a mobile and web application development platform. It primarily consists of services such as: Firebase Clouding; Firebase Authentication; Real-time Database; and Firebase Hosting. An Arduino IDE platform was used to programme the microcontroller, sensors and shields used to develop the module. The Arduino IDE provided an easy interface to programme the different software programs required run the hardware devices of the model.

## C. System Implementation of LWMS

The design of the LWMS model was split into two main separate modules for implementation purposes:

- **LOADING BAY MODULE**—represents the loading bay of luggage and is also concerned with measuring, monitoring and calculating the weight of luggage placed in the luggage compartment.
- **STEP SENSOR MODULE**—represents a step on the bus and is also concern with measuring, monitoring and calculating the weight of passengers and hand luggage in and out of the bus.

The main technique used in the design was Process Modelling and used the flowcharts for clarity and easy of description of the logic for the entire model. Fig. 5 shows the flowchart for the proposed LWMS model.

1) *Loading bay*: Fig. 6 below shows the flow of the proposed Loading Bay module for the LWMS model. The Loading Bay module was used to measure, monitor and calculate the weight of luggage either in or out of the luggage compartment of the bus. A threshold was set to indicate the maximum allowed luggage weight loaded on the bus. Main components of the Loading Bay module were: Arduino Uno Microcontroller; Load Cell; Liquid Crystal Display (LCD); and Piezo Buzzer.

2) *Step and motion sensors*: Fig. 7 shows the flow chart for the proposed Step Sensor module for LWMS model. The Step Sensor initialization occurs when the system boots, thereafter it remains idle and waits for any motion to be detected. Once motion is detected, code in the Step Sensor determines whether it was a forward motion, that is, a passenger steps into the bus or backward motion, that is, a passenger steps out of the bus. Depending on the type of motion, the load value on the local storage of the Step Sensor, the Arduino storage is updated with a new value for the load weight of the vehicle, this value is then transferred to the

online database. It is the value in the database that the system checks to ensure the vehicle is not exceeding the allowed maximum load weight.

The Step Sensor is crucial in detecting passenger weight and it consists of the following components: Motion Sensors, a GSM module and load cell, all of which are linked through an Arduino Uno Microcontroller development board.

Fig. 8 illustrates diagrammatically the set-up of the Step and Motion Sensors. The Side view shows how the sensors are positioned one after the other, in relation to the position of the load cell while the Top view shows the sideward position of the Sensors in order to detect the forward or backward motion direction. The bus entrance has one of the steps embedded with a load cell under it.

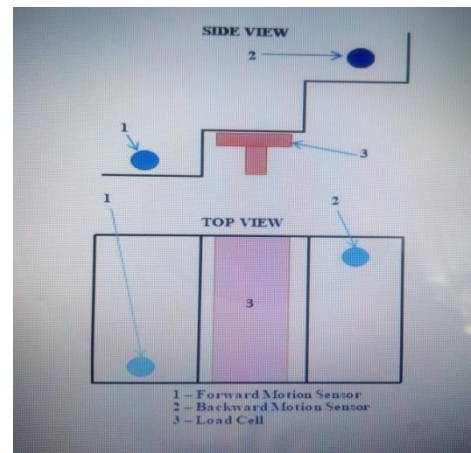


Fig. 8. Step- Motion Sensors Design.

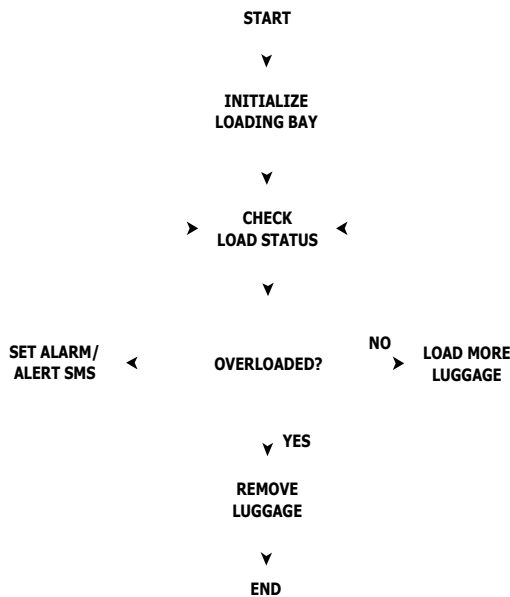


Fig. 6. Flowchart of Proposed Loading Bay.

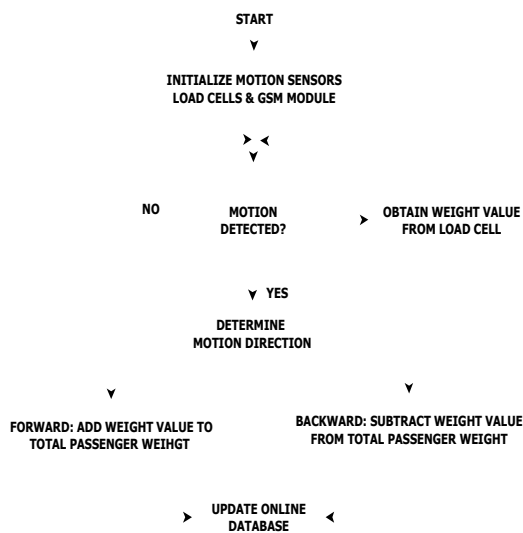


Fig. 7. Flowchart of Proposed Step/Motion Sensor.

The HC-SR501 Passive Infra-Red (PIR) Motion Sensor is compatible with an Arduino Uno Microcontroller. It possess a 110 degrees viewing area, range of 3 to 7 meters, a LHI778 Infrared Sensor that detects light, and a BISS0001 Integrated Circuit which controls how motion is detected.

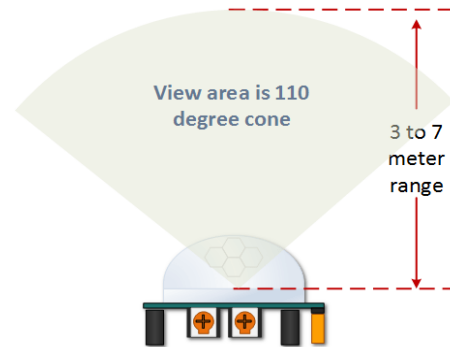


Fig. 9. HC-SR501 Field of View and Range [25].

The HC-SR501's field of view is enhanced by the presence of a spherical Fresnel cap which reflects light inwards towards the infrared sensor [30] as shown in Fig. 9 above. The positioning of the motion sensors is very important; one sensor is placed in front of the other in the step sensor. This is designed in this way so that the order in which the motion sensors are triggered determines the direction of motion of the step and subsequently whether to add or subtract the value of the weight that is detected by the load cell placed underneath the step. Fig. 10 below is the layout of the HC-SR501 motion sensor.

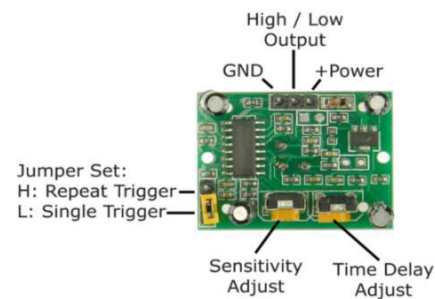


Fig. 10. Layout of HC-SR501 PIR Motion Sensor.

3) *GSM module*: The LWMS model updates the online centralized database through the use of wireless digital communication link, the GSM module. The specification of module used in the model is the TinySine GSM shield which uses the SIM900 module. It can be used to send and receive data, voice calls and SMS messages, hence its suitability for the model. However the speed of the device is slow, which is a great hindrance to updating the database. This makes the use of the Arduino and GSM module inappropriate for commercial deployment of the proposed system but is adequate for demonstration purposes. When the maximum load weight of the bus is exceeded the GSM module sends an SMS to the bus owner/operator and relevant agencies.

IV. RESULTS

The main focus of the study was to appreciate the challenge of passengers and luggage overloading on public buses and then propose a solution, the LWMS, to mitigate overloading.

A. Baseline Study

The results of the baseline study are presented as derived from the analysis of the questionnaire. All key stakeholders confirmed that there was rampant overloading on public buses because of none availability of means to measure luggage and passengers at the bus stations. The research findings confirm that the challenge of overloading, as indicated in Table II, was attributed mainly to luggage at 93 percent while that of passengers was only about 7 percent.

Another interesting revelation from the study was the varying perception from various stakeholders on the most risk factors contributing to road traffic accidents (RTAs) as shown in Table III.

Worth noting is also the overall responses from all stakeholders on the most risk factor that contributes to RTAs as being the human factor at 54 percent compared to the next road/environmental factors at 39 percent as shown in Fig. 11 below. Further analysis of human factors, revealed issues of over speeding, driver fatigue, substance use or drunk driving and use of cell phone while driving. However, there was no direct mention of overloading as a cause of RTA, though acknowledged to rampant and a road safety hazard. Indirect mention of tyre burst as a cause of RTA due to overloading was mentioned.

B. System Implementation of LWMS

The LWMS prototype model was implemented successfully and it was capable of performing the required tasks as specified. The separation of the Loading Bay and Step Sensor modules was done to facilitate easy in design and implementation, and clarity in explanation.

1) *Loading bay module*: Fig. 12 below shows the fully implemented Loading Bay module for the LWMS. The main components include: No.1: Weighing Platform–surface upon which the luggage is placed for measurement; No.2: Load Cell–active component transducer that converts physical

weight into electric signals; and No.3 Base Mounting–firm base that holds and supports the entire device.

2) *Step sensor module*: Fig. 13 shows the fully implemented Step Sensor module for the LWMS. The main components include: No.1: Motion Sensors–shielded to avoid wrong motion detection; No.2: Step Sensor–imbedded with a Load Cell; No.3: Arduino/GSM–module for control and communication; and No. 4: Breadboard–used to inter connections.

TABLE. II. CHALLENGE OF OVERLOADING ON BUSES

|   | CAUSE      | NUMBER | PERCENT |
|---|------------|--------|---------|
| 1 | Luggage    | 86     | 93.4    |
| 2 | Passengers | 06     | 6.6     |
| 3 | TOTAL      | 92     | 100     |

TABLE. III. MOST RISK FACTOR CONTRIBUTING TO RTAS

|   | FACTOR S | INSTITUTION S | OWNER S | CRE W | OVERAL L |
|---|----------|---------------|---------|-------|----------|
| 1 | Human    | 75%           | 29%     | 35%   | 54%      |
| 2 | Road/En  | 19%           | 64%     | 55%   | 39%      |
| 3 | Vehicle  | 03%           | 07%     | 10%   | 06%      |
| 4 | Others   | 03%           | 00%     | 00%   | 01%      |
| 5 | TOTAL    | 100%          | 100%    | 100%  | 100%     |

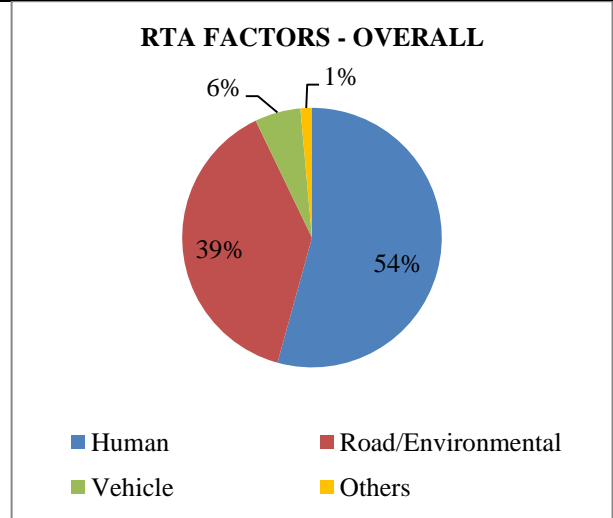


Fig. 11. Factors of RTA–Overall Perception.

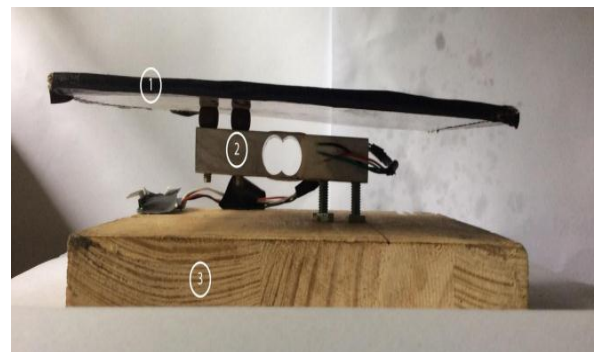


Fig. 12. Loading Bay for the LWMS.



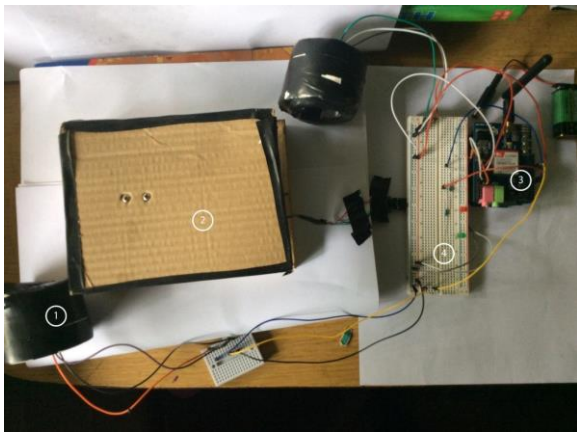


Fig. 13. Step Sensor Component for the LWMS

3) *Web application and mobile app*: This module provides the user interface to enable the user to monitor the current load weight of the bus as the passengers and luggage are loaded, using the Software Component of the system. It was essential for users of the system to have real time information displaying the current status of load weight of the bus at any given time. This is achieved through use of a thin client model in a browser. A user of the system is able to login to the system, using his/her credentials and check the status of the bus through a browser. use of a browser is not very efficient as it is not real time, so the client is able to access his/her bus status through a mobile application. Fig. 14 shows the screenshot of the user's view of the current weight calculated from the prototype model.

The client can view the current weight of the bus through the browser as shown above. Upon reading the Loading Bay and Step values, they are added and then data was sent to online database through the GSM module already described above. The process of transmitting data was successful with the only drawback of the slow speed at which the Arduino uploaded the data. When the maximum load weight is exceeded, an overload alert alarm is excited and an SMS message is sent to the bus owner/operator and relevant agencies using the GSM module which is equipped with a SIM card to connect to Mobile Network Service Provider to report overloading. Fig. 15 shows the screenshot the alert message.

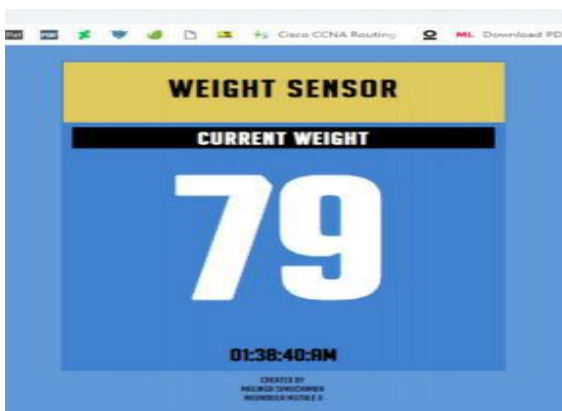


Fig. 14. User View of the Current Weight.



Fig. 15. Screenshot\_2019-01-15-12-43-27.

## V. DISCUSSION

The objectives of the research study were realized; conduct baseline study, propose and design new system, and develop prototype model of new system. A baseline study was conducted in order to establish the challenge of overloading on public buses in Zambia to which all stakeholders positively affirmed its existence and also affirmed need to have an automatic load weight monitoring system to prevent overloading. From results of analysis of the respondents' feedback, it was overwhelming that overloading was real, attributed to over loading of luggage and passengers. While there was currently no mean to measure the weights of both luggage and passengers, the latter was relatively easy to handle because it is limited by the seating capacity of the bus. Accordingly, the number of tickets sold corresponds to the bus seating capacity thereby limiting number of passengers boarding the bus, hence rarely contribute to overloading. On the other hand, the former in current situation is very difficult to manage in establishing the weight of luggage loaded on each bus because apart from passenger luggage, there is also additional unaccompanied luggage carried on the bus for extra income for the crew without the knowledge of the owners/operators.

The baseline findings helped to come up with a solution that is perceived to be much better so as to solve the challenge of overloading on public buses using modern technology to improve efficiency in operation, road safety, reduce infrastructure and vehicle degradation, and many more.

## VI. CONCLUSION

This research study brought out important points on the fact that the challenge of overloading on public buses in Zambia is related to one of the factors that contribute to road traffic accidents, that is, the human factor. Further analysis of human factors revealed that a number of issues ranging from social-economic factors to survival requirements contribute to the crew overload the buses to make extra income without the knowledge of the bus owners/operators and contravening road traffic regulations.

The proposed LWMS would introduce an orderly, logical and accountable system with up-to-date accurate data on the load weight of each bus at any given time using the state-of-art technology. A major contribution of this paper is in explaining the challenge of overloading on public buses which helped to come up with a solution that uses the current technologies to ensure efficiency and road safety in the public road transport system. Many other sectors of the road transport system can also take advantage of the emerging technologies to ensure compliance of maximum load weight limit at the source, for example, at the quarry the trucks carrying construction materials can be weighed at the source also to prevent overloading of the trucks. The results obtained show that in Zambia, there is already a wide use of these ICTs like digital communication system of Public Mobile Network which was easily integrated to be used for data transmission to all other relevant parties. Other ICT infrastructure already in use like the Transport Intelligent System (TIS) and Vehicle Identification (VID) may be easily integrated with the LWMS.

As technology keeps on changing and advancing, it is important that the management and operation of public transport system in Zambia is kept abreast with the world trends like tighter coordination between all agencies in the sector by sharing computer infrastructure resources cloud computing, centralized databases, and so on. The phenomenon of overloading on public buses is multi-sectorial in nature and hence requires consented effort from all stakeholders to combat. These efforts may require policy, legal, social, institutional and infrastructural reforms. As a way forward, employing technology in the management of load weight on buses could be well integrated with other initiatives like the intelligent road management systems. The introduction of Global Positioning System (GPS) on some public buses to monitor speed in dealing with the challenge of over-speeding can also in a similar way be made to incorporate overloading. The use of Weight-In-Motion (WIM) technology in the management load weight of commercial vehicles on the roads as done in developed countries need to be thoroughly studied so that it can also be incorporated in our systems too.

Future works for this prototype model would see it develop to be a full-fledged bus system, one to be used for ticketing of passengers. The addition of a full-fledged user Mobile application would lend to this idea, passengers would be able to book a ticket and also make payments through it. Adding RFID for use with the luggage tracking would improve the security of the system too. Future editions of the system would seek to use better communication technology, possibly through the use of a Wi-Fi module to improve on the speed at which the w values of the weights are uploaded. Furthermore, clients of the system, i.e. bus owners should be given more functionality through a Client App. The option to intervene when the bus is overloaded would be of great benefit, for instance, the option to disable the bus through the app would go a long ways to preventing road infrastructure damage and all other associated risks. Additionally, power to the client would be in form of GPS functionality to the Client App., the ability to monitor the position, speed, and so on of the bus would be an added benefit for the system versatility.

On the overall, the anticipated benefits and associated cost savings of LWMS to reduced overloading relates to operational enhancements, road infrastructure preservation, increased road safety, reduced vehicle damage, congestion, fuel consumption and reduced harmful emissions.

It is recommended that strong collaboration exists between all relevant stakeholders to combat overloading. It is also recommended that this proposal be extended to other heavy commercial vehicles (HCV) with modification to establish load weight at the source, e.g., construction vehicles from the quarry sites, trucks from industrial loading bays, and so on.

#### ACKNOWLEDGMENT

We are grateful to the various institutions/agencies ZMA, ZABS, RTSA, NRFA, RDA, ZACL, ZAMPOST, LIBT, ZCILT, BTOAZ, PPDZ; bus owners/operators, and some all bus crew of LIBT for allowing us to carry out this research and for positive responses, and for providing us with valuable data in pursuit of proposing an automated system of monitoring load weight.

#### REFERENCES

- [1] Laudon, K. C., and Laudon, J. P., "Management Information Systems - Managing the Digital Firm", 13th Global ed., Harlow, Essex: Pearson Education Limited, 2014.
- [2] Milumbe, B., Phiri, J., Kalumbilo M.M., Nyirenda, M., "Developing a Candidate Registration System for Zambia School Examinations using the Cloud Model", International Journal of Advanced Computer Science Applications (IJACSA), Vol. 9, No.7, 2018, pp. 38.
- [3] Richard Iles, "Problems and Characteristics of Public Transport in Developing Countries"Emerald Group Publishing Limited,2005,pp.5-37.
- [4] Hashim, W., Kami, I. A. and Mustaffa, M., 2012. "An Overview of Heavy Vehicles Safety Related to Speed and Mass Limit in Malaysia". Mara, UiTM.
- [5] Zambia, Laws of Zambia. Public Roads Act No. 12 of 2002, Lusaka, Lusaka: Zambian Parliament, 2002.
- [6] Nordengen, P. A. and Naidoo, O. J., 2014. "Evaluation of the Road Transport Management System, a self-regulation initiative in heavy vehicle transport in South Africa". Transport Research Arena, pp. 2-3.
- [7] Karim, M. R., Ibrahim, N. I., Saifuzil, A. A. and Yamanaka, H., 2014. "Effectiveness of Vehicle Weight Enforcement in a Developing Country using Weigh-in-Motion Sorting System considering Vehicle By-pass and Enforcement Capability". International Association of Traffic and Safety Science Research (IATSSR), Issue 37, p. 124-129.
- [8] Zambia, Laws of Zambia. Metrology Act No. 6 of 2017. Lusaka, Lusaka: Zambian Parliament, 2017.
- [9] Zambia, Laws of Zambia. Roads and Road Traffic Act of Zambia, Chapter 464, Part XIV, Sub-Article 245. Lusaka, Lusaka: Zambian Parliament, 1995.
- [10] Russo, F., and Comi, A., "Measurements in Freight Transportation", Journal of Urban Planning and Development, June 2011, Vol. 137, No. 2, pp. 142-152.
- [11] Lucey, T., Management Information Systems, 9th edition, London: BookPower, 2005.
- [12] Avram Olaru, M.G., "Advantages and challenges of adopting cloud computing from an enterprise perspective", Procedia Technology, vol. 12, pp. 529-534, 2014.
- [13] Lawrence E. Decina et al., 2007, "Automated Enforcement: A Compendium of Worldwide Evaluations of Results", U.S. Department of Transportation, National Highway Traffic Safety Administration, Report No. DOT HS 810 763, Washington, DC.
- [14] Nolan, P., Zhang, J. and Liu, C., "The global business revolution, the Cascade Effect, and the Challenge for Firms from Developing Countries", Cambridge Journal of Economics, Vol. 32, No. 1, 2011, pp. 29-47.

- [15] Hamilton, A., Waterson, B., Cherrett, T., Robinson, A. and Snell, I. "The Evolution of Urban Transport: Changing Policy and Technology", *Transportation Planning and Technology*, Vol. 36 No. 1, pp. 24–43, 2013.
- [16] Kittelson and Associates, et al., 2007, TCRP Report 118: Bus Rapid Transit Practitioner's Guide, National Academies Transportation Research Board, U.S. Federal Transit Administration, Washington, DC.
- [17] Ghanvat S.M., Patil H.G., "Shape Optimization of S-Type Load Cell using Finite Element Method" *International Journal of Engineering Innovation and Research (IJEIR)*, Vol. 1, Issue 3, ISSN:2277-5668, 2012.
- [18] James F. Doyle, J.F., and Phillips, J.W., "Manual on Experimental Stress Analysis", Society for Experimental Mechanics, 2010.
- [19] Tubaishat M., Madria S., *Wireless Sensor Networks: An Overview*. IEEE Potentials. 2003; 22:20–30.
- [20] Verdone, R., Dardari, D., Mazzini, G., Conti, A., "Wireless Sensor and Actuator Networks". Elsevier; London, UK: 2008.
- [21] IEEE 802.15.4 Standard, Part 15.4: Wireless Medium Access Control (MAC) and Physical Layer (PHY) Specifications for Low-Rate Wireless Personal Area Networks (LR-WPANs) IEEE; Piscataway, NJ, USA: 2006.
- [22] IEEE Standard 802.15.4, 2015, Revised IEEE Standard 802.15.4 2011, "IEEE Standard for Low-Rate Wireless Networks", pp. 1–709, Apr. 2016.
- [23] Muyunda, T., Phiri, J., "A Web based Inventory Control System using Cloud Architecture and Barcode Technology for Zambia Air Force", *International Journal of Advanced Computer Science and Applications (IJACSA)*, Vol. 8, No. 11, 2017, pp. 134.
- [24] Chihana, S., Phiri, J. and Kunda, D., "An IoT based Warehouse Intrusion Detection (E-Perimeter) and Grain Tracking Model for Food Reserve Agency", *International Journal of Advanced Computer Science and Applications (IJACSA)*, Vol. 9, No. 9, 2018, pp. 214.
- [25] Laxmirajam, E. C., and Kawitkar, D.R.S., "A Survey: IoT based Vehicle Tracking System," *International Journal of Advanced Research in Computer and Communication Engineering*, Vol. 6, No. 5, pp. 791-795, 2017.
- [26] Choudhari, S., Rasal, T., Suryawanshi, S., Mane, M., and Yedge, P.S., "Survey Paper on Internet of Things: IoT", *International Journal of Engineering Science and Computing*, Vol. 7, No. 4, pp. 10564-10567, 2017.
- [27] Bandyopadhyay, D., and Sen, J., "Internet of Things - Applications and Challenges in Technology and Standardization", *Wireless Pers- commum*, 2011.
- [28] Phiri, H. and Phiri, J., "Real Time Sensing and Monitoring of Environmental Conditions in a Chicken House", *ResearchGate*, Conference Paper –May 2018.
- [29] Mulima, C., Phiri, J., "A Remote Sensor Network using Android Things and Cloud Computing for the Food Reserve Agency in Zambia." *International Journal of Advanced Computer Science and Applications (IJACSA)*, Vol. 8, No. 11, 2017, pp. 412.
- [30] Caussignac J.M., Rougier J.C., "Fibre Optic WIM Sensor and Optoelectronic System-Preliminary Tests", *Hermes Science Publications*, Paris, 1999.

# Survey Energy Management Approaches in Data Centres

Bouchra Morchid<sup>1</sup>, Siham Benhadou<sup>2</sup>, Mariam Benhadou<sup>3</sup>, Abdellah Haddout<sup>4</sup>, Hicham Medromi<sup>5</sup>

Engineering Research Laboratory (LRI), System Architecture Team (EAS)<sup>1, 2, 5</sup>

National and High School of Electricity and Mechanic (ENSEM) Hassan II University, Casablanca, Morocco

Research Foundation for Development and Innovation in Science and Engineering<sup>2, 5</sup>

Laboratory of industrial management and energy and technology of plastics and composites<sup>3, 4</sup>

National and High School of Electricity and Mechanic (ENSEM) Hassan II University Casablanca

Morocco Research Foundation for Development and Innovation in Science and Engineering

**Abstract**—Data centers are today the technological backbone for any company. However, the failure to control energy consumption leads to very high operating costs and carbon dioxide emissions. On the other hand, reducing power consumption in data centers can lead to a degradation of application performance and quality of service in terms of SLA Service Level Agreement. It is therefore essential to find a compromise in terms of energy efficiency and resource consumption. This paper highlights the different approaches of energy management, related studies, algorithms used, the advantages and weaknesses of each approach related to server virtualization, consolidation and deconsolidation of virtual machines.

**Keywords**—Data center; power management; virtual machines; physical servers "hosts"; energy efficiency; SLA (Service Level Agreement); PUE (Power Usage Effectiveness); QoS (Quality of Service)

## I. INTRODUCTION

Currently, technological advances and new business models of cloud computing have contributed to the development of data centers in number and size.

This strong growth has not only contributed to an increase in the cost of electricity and enormous energy consumption, but has also generated significant carbon dioxide emissions, thus contributing to the greenhouse effect [1]. Indeed, in addition to the significant amount of electricity consumption for IT resources, it requires such considerable energy resources to cool this infrastructure from the heat dissipated, including servers and storage racks.

Data centers' energy costs are increasing, which requires reducing their energy consumption and improving energy efficiency through the development of efficient management approaches.

The rest of this paper is organized as follows: In Section II, we describe different energy management approaches in Data center. In Section III, we present related studies especially on server virtualization, consolidation and deconsolidation of virtual machines for optimizing energy efficiency in data centers. Section IV describes discussions about some limitations of the related studies. Finally, the conclusion and perspectives of evolution of different approaches are drawn in Section V.

## II. STATE OF THE ART

### A. Context

Each new service to be implemented by companies often requires the acquisition of new equipment. According to many estimates, the level of server utilization is generally less than 20% [2], although a significant part of the energy consumed in the data center is used to power inactive machines [3]. An underutilized server consumes more energy and has a negative impact on energy efficiency due to the non-linear characteristics of server power proportionality at these usage levels [4].

Moreover, the energy consumption of IT resources directly impacts the cooling power required to cool and maintain the ambient temperature of the data center at a predetermined threshold value. Indeed, according to Patel et al. [1], each watt consumed by computer equipment requires an additional power of 0.5 to 1 watt to operate the cooling system.

In [5], an indicator of energy efficiency in data centers "PUE: Power Usage Effectiveness" is the usage efficiency metric, which corresponds to the ratio between the total energy consumed in the data center and the total energy consumed by IT equipment (servers, storage, networks).

From an energy point of view, a data center with a PUE equal to 1 consumes less energy and is most efficient [6].

In this regard, the approaches used to improve energy efficiency in data centers must take into account the various parameters that influence energy efficiency.

### B. The Different Approaches

Several energy management approaches have been discussed to optimize energy efficiency. In [7], these techniques can be divided into static and dynamic: Static energy management and dynamic energy management (see Fig. 1):

*a) Static energy management:* The first approach consists in applying optimization methods when designing hardware components (circuit, logic, architectural system levels) and also software components such as OS, compilers, etc. The low-powered ARM system or atom-based processor servers that have a reduced performance capability and are

more energy efficient can be used as a system device to reduce static energy consumption [1]. In order to optimize the static energy consumption of the data center, it is necessary to avoid oversizing of capacity, however, care must be taken to design a precise dimensioning while taking into account possible evolutions to avoid bottlenecks and respect SLA services.

b) *Dynamic energy management:* The second approach is to apply different methods of power optimization at the hardware and software level to ensure energy efficiency.

- At the hardware level: Dynamic power management (DPM), Dynamic voltage and frequency scaling (DVFS).
- At the software level: Virtualization controls, thermal controls and server heterogeneity controls, etc.

The DPM method consists of reducing or eliminating static server consumption by either disabling the server or switching it to a low-power standby state when it is not used on the basis of the workload.

Workload is a factor used to determine when a server can be disabled or transferred to standby mode or turned off.

This method saves energy on certain types of workloads [8]. However, additional configuration time for the transition of the server from a low-power state (Standby or off) to an operational state or vice versa can negatively affect performance and power consumption. The effectiveness of this method is based on effective workload management to meet SLAs and a rapid transition to and from standby mode.

The DVFS method consists in reducing the number of instructions that a processor can generate over a given time interval. It is about:

- Decrease the frequency and/or voltage of the processor when it is not fully used;
- Increase the processor frequency and/or voltage if performance should be improved.

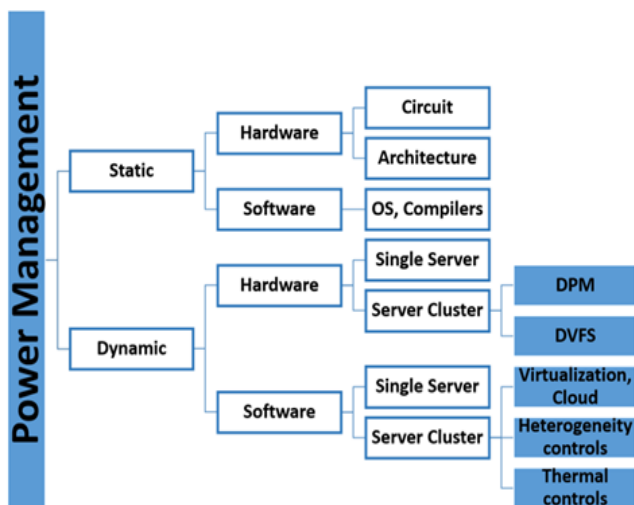


Fig. 1. Energy Management Techniques.

The DVFS method is an efficient way to manage the CPU's power consumption. However, the decrease in frequency and/or voltage has a negative impact on performance, which contributes to the increase in the time required to perform workload tasks. In addition, the increase in frequency and/or voltage contributes to much higher energy consumption.

The method based on the controls of consolidation and deconsolidation of virtual machines consists in consolidating workloads to fewer physical servers and disabling inactive servers or putting them in a low-power state. The advantage of this approach is that it is very appropriate in Cloud Data Centers and contributes to improving energy efficiency through server consolidation and disabling unused servers. Data center location can also be taken into account to migrate virtual machines to servers hosted at low-power data centers. However, this method faces constraints such as:

- A degradation in application performance due to aggressive consolidation;
- The increase in the temperature of the server hosting the virtual machines migrated to it and the creation of thermal hot spots, which also increases the cooling power required to dissipate the additional heat generated.

The method based on thermal controls consists in maintaining the thermal state of IT resources within an acceptable operating range. The increase in IT energy consumption has a direct impact on cooling power. The advantage of this method is that it allows the maintaining of the appropriate thermal profile for all IT resources in the data center, which ensures maximum reliability, longevity and return on investment. However, the dependence (linear and non-linear) between IT and non-IT class must be studied together to ensure that the total energy consumption of the data center is optimized.

The method based on server heterogeneity controls allows the workload to be allocated to the server with the most energy-efficient architecture. This is a technique used for a clustered server architecture.

This technique makes it possible to use the best features of each server to achieve energy efficiency at all levels of use. In addition, the heterogeneity of a server is considered according to the performance of the processor and the power consumption for a range of workloads. In some cases [1], such as an Infrastructure as a service (IaaS) data center, the knowledge of application workloads and the time during which virtual machines are used is unknown, which helps to depend on processor performance.

### III. RELATED STUDIES

In this section we will review some related studies that focus on the use of server virtualization, virtual machine consolidation and deconsolidation approaches to optimize energy efficiency in data centers. It also reviews the different algorithms and techniques used to select virtual machines to migrate, and to select the machines to activate or deactivate.

### A. The Concept of Server Virtualization and Consolidation

Virtualization has become a very common technique in modern IT architectures. This technique allows several virtual machines to coexist on the same physical server to increase its utilization rate (see Fig. 2).

Virtualization provides the following advantages [9]:

- High flexibility in server management, administration and occupancy.
- Allows users and administrators to create, save (control point), copy, share, migrate, read, modify and cancel the execution state of the machine.
- Reduction of costs.
- Reduction of energy costs.
- Reduction of CO2 emissions.

Concerning the consolidation of virtual machines, it is a technique that eliminates the energy consumption of underutilized servers. It consists in migrating virtual machines from an underutilized physical server to another physical server. This technique makes it possible to disable underutilized physical servers or put them in low-power mode, and to increase the utilization rate of the physical server containing the migrated virtual machines.

In addition, the main factors driving the consolidation of virtual machines are the impact on performance and energy consumption. In fact, a massive migration leads to a degradation of performance and additional energy consumption. This is why it is important to study when virtual machines can be consolidated or deconsolidated? To which physical servers should the virtual machine be migrated to, which will ensure energy savings? What is the migration scenario to adopt? What are the migration costs?

### B. pMapper

pMapper is an application mapping framework (see Fig. 3), in a cluster environment of heterogeneous virtualized servers, that dynamically places them on physical hosts in order to minimize energy consumption while respecting performance guarantees and so that the cost/power trade-off is optimized.

The pMapper framework is based on the use of three different managers, with one arbitrator to ensure consistency between the three managers [10]:

**Performance Manager:** It provides an overview of the application in terms of QoS, SLA and performance, and communicates software actions such as virtual machine resizing and/or resting. In the case of heterogeneous platforms, the performance manager has a knowledge base to determine the performance of an application when a virtual machine is migrated from one platform to another.

**Power Manager:** It initiates power management on a hardware layer; it examines current power consumption and can suggest a limitation by applying a technique that adjusts the voltage/frequency dynamically or explicitly limits the processor.

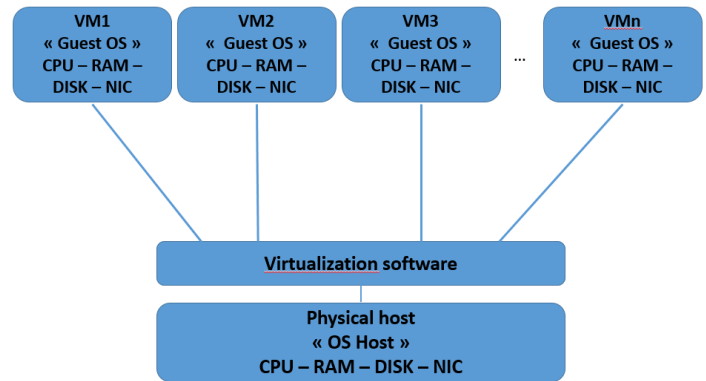


Fig. 2. Virtual Machine Diagram.

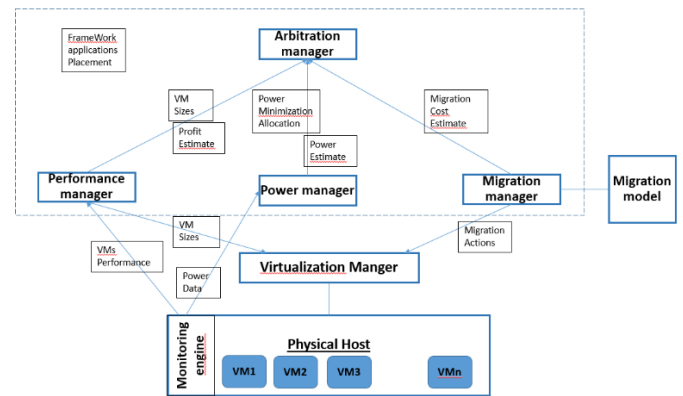


Fig. 3. pMapper Architecture for the Placement of Applications[10].

**Migration Manager:** Executes direct migration of virtual machines to consolidate workload. The migration manager estimates the cost of moving from one location to another and uses the migration model to make the estimate.

**Arbitration Manager:** It explores the configuration space of eligible virtual machine sizes and locations and implements an algorithm to calculate the best virtual machine locations and sizes, based on estimates received from Performance, Power and Migration managers.

This approach uses application placement algorithms to minimize the overall cost of "power and migration" while respecting performance constraints:

- The Min Power Parity (mPP) algorithm: It allows to place virtual machines on all servers in a way that the overall power consumed by all servers is minimized. However, the last configuration is not taken into account by this algorithm, which can lead to large-scale migrations and therefore a high overall cost (power + migration).
- The Min Power Placement with History (mPPH) algorithm: It works in the same way as mPP except that it takes into account the history (the previous placement is also taken into account). The mPPH algorithm tries to minimize migrations by relocating a minimum number of virtual machines, while migrating to the new optimal use of server targets.

- The pMaP algorithm: It is placed at the arbitration manager level to optimize the compromise of power migration. However, when the load is unbalanced to minimize power, pMaP leads to a large number of abandoned requests. The decrease in applications is considered as penalty of placement.
- The pMaP +: It takes into account the penalty and only selects intermediaries with a penalty below a predefined threshold.

The pMaP and mPPH algorithms are the two best performing algorithms, even with an increased number of servers.

The mPP and mPPH dynamic algorithms are capable of saving about 25% power from static virtual machine locations and with balanced load.

In view of the weaknesses of this solution, the effects of migration, in particular on total energy consumption and performance are not taken into account. When the load is unbalanced, a large number of requests are abandoned or delayed by applying the pMaP algorithm.

### C. Kusic's Approach: Limited Anticipation Control (LLC)

The approach adopted consists in minimizing energy costs in a virtualized server cluster environment and under conditions of workload uncertainty, using sequential optimization using limited anticipation control (LLC). The purpose of this control is to minimize energy consumption and SLA contract violations in order to maximize the profits that may be lost while waiting for a virtual machine and its host to be activated, usually between three and four minutes. Pragmatically, revenues can be generated through response times, when they are below a predetermined threshold value, they give rise to a reward for the service provider, but if they exceed this threshold and contribute to violations of the SLA contract, they result in the payment of a penalty by the provider.

So, to meet this objective of profit maximization, the online controller determines the number of physical and virtual machines to allocate to each service for which virtual machines and their hosts are enabled or disabled based on workload demand, as well as the part of the CPU to allocate to each virtual machine.

The LLC approach models the cost of control, i.e. the transition costs from an inactive to an active state when provisioning virtual machines or vice versa from an active to an inactive state. The LLC approach explicitly encodes the risk associated with procurement decision-making, since in an operating environment with a highly variable workload, an aggressive transition of virtual machines can occur and can therefore reduce benefits. Also, the LLC approach uses a hierarchical LLC structure, which breaks down the control problem into a set of smaller sub-problems and is solved cooperatively by several controllers, to achieve faster operation when workload intensity changes very quickly. This decomposition into sub-controllers will allow the main

controller to adapt to these variations and plan resources over short periods of time, generally in the range of 10 seconds to a few minutes.

The Kalman filter is used to estimate the number of future requests, thus allowing to predict the future state of the system and consequently makes reallocations of CPU parts and virtual machine hosting mappings.

This approach has been implemented in a virtualized server cluster environment. The LLC method allows multi-objective optimization "in terms of energy reduction, reduction of SLA contract violations, increase in profits" under explicit operating constraints [2].

In terms of results, the server cluster, managed according to the LLC approach, maintains, on average, 22% of the cost of energy consumption over a 24-hour period compared to a system that operates without dynamic control while meeting QoS objectives.

The controller's execution time is relatively short, which does not pose any constraints in a high-demand operating environment.

Taking into account the notion of risk inherent in procurement decision-making has effects on control performance because a controller who takes this risk factor into account reduces the number of SLA violations by 35% compared to a controller with no risk.

The weaknesses of this approach mean that DVS controls are not taken into account.

This model requires supervised learning for application-specific adjustments, the number of virtual machines contributes more to energy consumption than resource use aspects. On the other hand, due to the complexity of the model, the execution time of the optimization controller reaches 30 minutes, even for 15 nodes, which is not suitable for large real systems.

### D. Migration based on utilization "UMA"

The Migration based on utilization is a technique that consists of migrating virtual machines to stable physical servers in order to effectively reduce migration time and energy consumption (see Fig. 4).

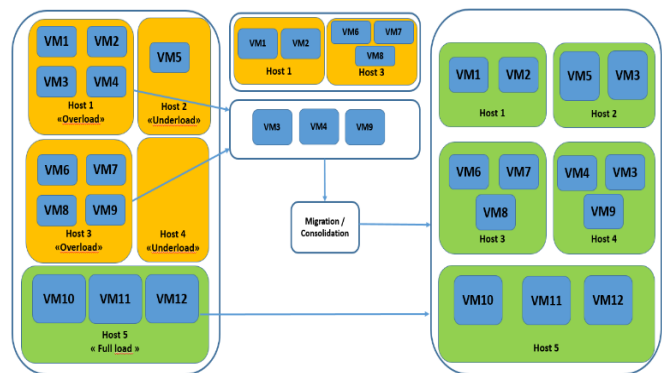


Fig. 4. VM Consolidation Framework based on Utilization [11].

This approach is based on a workload detection module that categorizes hosts into three classes: overloaded, fully loaded and underloaded. The migration probability is calculated for virtual machines hosted at the overloaded hosts and thus queue candidates waiting for migration are identified. Virtual machines hosted at the underloaded host level are consolidated to improve host utilization. No changes are made to the hosts at full load. With this solution, hosts can achieve optimal performance while offering high energy efficiency.

This approach uses Tabu Search to find the optimal solution when some inactive hosts are enabled to host virtual machines to migrate.

This algorithm uses the BFD algorithm first for a pre-migration for all virtual machines. Thus, a mapping table of virtual machines and hosts is created. After that, the virtual machine is optimized using the Tabu Search algorithm. In the Tabu search algorithm, if a possible migration has already occurred in a short period of time, this migration is placed in the tabu list, to avoid that the algorithm considers this possibility several times. Then after a number of iterations, the optimal solution is obtained.

The results of a study are carried out on four available hosts with uses of 50%, 60%, 65% and 0% respectively in a homogeneous environment. Five virtual machines are waiting for migration with MIPS requests for 20%, 20%, 20%, 15%, 15%, 15% and 10% processor utilization. The Tabu list was used, the UMA algorithm can achieve the optimal overall solution to the problem and which allowed a use of 70%, 60%, 65%, and 60% respectively for all hosts, which is closer to the total load [11].

UMA technology reduces about 77.5-82.4% of virtual machine migrations and saves up to 39.3-42.2% in energy consumption compared to MinPower policy "mPP". In terms of the number of active servers, this technique reduces the number of active hosts from 39.2% to 45.7% compared to the MinPower policy "mPP". The resource exploitation rate is between 70% and 90%.

For the SLA violation, the results show that UMA slightly mitigates the SLA violation. Compared to MinPower "mPP", UMA works a little better than the MinPower "mPP" algorithm when the overload threshold is equal to 0.8, and very similar when the overload threshold is equal to 0.9 in terms of SLA violations.

The weaknesses of the UMA technique are:

The power transition of the server state and the costs associated to the transition latency are not taken into account.

The impact of migration, in particular on total energy consumption and performance, is not also taken into account [1].

#### E. Modified Best Fit Decreasing Adjustment Approach "MBFD"

The best modified decreasing adjustment "MBFD" is a technique that consists in placing virtual machines in such a way that the most used virtual machine is migrated to the physical server that provides the lowest power consumption.

The virtual machines are ordered in decreasing order according to CPU usage, and each virtual machine is then assigned to a host that allows a small increase in power consumption using the MBFD algorithm.

In addition, selecting the machine to migrate is an essential step in optimizing the allocation of virtual machines. To this end, selection strategies are applied to determine when and which virtual machines should be selected for migration. This consists of defining two upper and lower CPU usage thresholds for each host and maintaining total CPU usage by all virtual machines between these two thresholds. When a host has CPU usage below the lower usage threshold, all virtual machines must be migrated from this host and put into standby mode. If a host has CPU usage above the upper usage threshold, some virtual machines must be migrated from this host to reduce resource usage and prevent SLA violations. The strategies for selecting virtual machines to be migrated from a host whose CPU usage has exceeded the upper usage threshold are [12]:

- **Minimization of Migration Time (MMT):** The algorithm sorts the list of virtual machines in decreasing order of CPU usage. Then, this algorithm performs several iterations to identify a virtual machine and remove it from the list until the host CPU usage is below the maximum usage threshold. The complexity of the algorithm is proportional to the number of overused hosts and the number of virtual machines allocated to these hosts.
- **Highest Potential Growth (HPG):** This strategy consists of migrating virtual machines with lower CPU usage relative to the usage capacity defined in the virtual machine settings, in order to minimize the potential increase in host usage and avoid SLA violations.
- **Random Choice (RC):** This strategy of random choice (RC) is based on a random selection of a number of virtual machines necessary to reduce the CPU usage of a host that has exceeded the maximum usage threshold.

The MBFD approach reduces energy consumption by 77% compared to the NPA policy and by 53% compared to the DVFS approach with 5.4% of SLA violations.

The weaknesses of this solution are the fact that this work uses different virtual machine migration models, actions to reconfigure reactive virtual machines instead of proactive, and time of transition and consumption to turn servers on and off and vice versa.

#### IV. DISCUSSION

In this paper we have presented different approaches to power management in data centers and related studies including virtualization, consolidation and deconsolidation of virtual machines with some associated algorithms, as well as their advantages and weaknesses.

We find that most approaches use virtual machine placement algorithms to minimize energy costs. In addition, the costs of migrating virtual machines and the impact on performance are not always taken into account and therefore it



is difficult to quantify a net benefit in terms of total energy consumption.

## V. CONCLUSION AND PERSPECTIVES

In this paper we focused on dynamic energy management at the software level by applying virtualization, consolidation and deconsolidation techniques to virtual machines. This technique can lead to the creation of hot spots on the server hosting several virtual machines.

We started by making a comparative study of the different power management approaches within data centers. Then we identified the weaknesses of some approaches in virtualization, consolidation and deconsolidation of virtual machines.

There are still challenges to be addressed in adopting a virtual machine consolidation approach to optimize energy efficiency improvements without impacting performance. It is interesting to note that these approaches studied may include many extensions, the main ones are as follows: Consideration of migration costs, dynamic workload and also the non-IT components (cooling equipment) to avoid the creation of hot spots.

We intend to do a detailed comparative study of the different architectures in terms of virtualization, consolidation and deconsolidation the virtual machines to draw an optimal architecture that aims to optimize the energy efficiency of the data centers while taking into account the aforementioned extensions.

## REFERENCES

- [1] V.K. MohanRaj, R.Shriram, 22 April 2016, Power management in virtualized datacenter – A survey.
- [2] Dara Kusic, Jeffrey O. Kephart, James E. Hanson, Nagarajan Kandasamy, Guofei Jian, September 21, 2008, Power and Performance Management of Virtualized Computing Environments Via Lookahead Control.
- [3] Andrew Krioukov, Prashanth Mohan, Sara Alspaugh, Laura Keys, David Culler, Randy Katz, NapSAC : Design and Implementation of a Power-Proportional Web Cluster, Computer Science Division, University of California, Berkeley.
- [4] Annavaram,M., Wong,D., 2012. KnightShift: scaling the energy proportionality wall through server-level heterogeneity .In : Proceedings of the Annual IEEE /ACM International Symposiumon Micro architecture.pp.119–130.
- [5] Seyed Morteza Nabavinejad, Maziar Goudarzi, Communication-Awareness for Energy-Efficiency in Datacenters Department of Computer Engineering, Energy Aware Systems Lab, Sharif University of Technology, Tehran, Iran, p. 203.
- [6] [6] Fabien Douchet, Juin 2016, Optimisation énergétique de data centers par utilisation de liquides pour le refroidissement des baies informatiques, Thèse / Université de Bretagne-Sud.
- [7] Beloglazov,A. , 2013, Energy-Efficient Management of Virtual Machines in Data Centers for Cloud Computing (Ph.D.Thesis). University of Melbourne.
- [8] Gandhi,A., Kozuch,M., Harchol-Balter,M., 2012, Are sleep states effective in data centers? In: Proceedings of the International Green Computing Conference and Workshops.pp.1–10.
- [9] Ankita Jiyani, 2016, Energy Efficient Techniques In Virtualized Data Center : A Survey, Research Scholar : Computer Science & Engineering Dept. Swami Keshvanad Institute of Technology Jaipur, India, p. 145.
- [10] Akshat Verma, Puneet Ahuja, Anindya Neogi, pMapper : Power and Migration Cost Aware Application Placement in Virtualized Systems, IBM India Research Lab, IIT Delhi.
- [11] Qi Chen, Jianxin Chen, Baoyu Zheng, Jingwu Cui, Yi Qian, 2015, Utilization-based VM Consolidation Scheme for Power Efficiency in Cloud Data Centers.
- [12] Anton Beloglazov, Jemal Abawajy, Rajkumar Buyyaa, 2011, Energy-aware resource allocation heuristics for efficient management of data centers for Cloud computing.

# Comparative Study of Methods that Detect Levels of Lead and its Consequent Toxicity in the Blood

Kevin J. Rodriguez<sup>1</sup>, Alicia Alva<sup>2</sup>, Virginia T. Santos<sup>3</sup>, Avid Roman-Gonzalez<sup>4</sup>  
Image Processing Research Laboratory (INTI-Lab)<sup>1, 2, 4</sup>  
Interdisciplinary Research Center Science and Society (CIICS)<sup>3</sup>  
Universidad de Ciencias y Humanidades, Lima, Perú<sup>1, 2, 3, 4</sup>

**Abstract**—The present work is the study of the different methods used to determine the toxicity produced by the presence of a contaminating metal in the blood. Mainly, the presence of lead in the blood was taken as a reference to focus the work, knowing that metals like Cadmium (Cd) and Mercury (Hg) are also toxic to health and the environment. Although the information is extensive on the methods to be studied and in some cases it is not detailed to define each process, a comparative study of the most relevant and currently used methods can be carried out, taking into account that the choice will be defined according to the main characteristics of each one. Although all agree to be electrochemical processes, there are details to know which method to choose, either by sensitivity, economic or even structural factors, such as having a laboratory for its development. Environmental pollution with toxic elements is very harmful to health, even in small quantities can be very dangerous. These can be present in rivers, soil and even in the air, and these spaces are more than enough to contaminate the human being since these particles adhere in both cases for many years. It is a problem until today and therein lies the importance of the study.

**Keywords**—Blood lead; toxicity; voltammetry; absorption spectroscopy; healthcare

## I. INTRODUCTION

According to the World Health Organization (WHO), lead is included in the list of 10 chemicals that cause serious public health problems, so that the intervention of the Member States is necessary to safeguard the health of workers, children and women of childbearing age. The Institute of Health and Sanitary Evaluation has estimated that, according to the data updated in 2015, exposure to lead was responsible for 494,550 deaths [1] and became the loss of 9.3 million Disability-adjusted life year (DALY), which is understood as a measure of the global disease. The exposure to lead according to the data was responsible for 12.4% of the global burden of intellectual disability, 2.5% of the overall burden of the quality of ischemic heart disease (is the disease caused by arteriosclerosis of the coronary arteries, which are responsible for supplying blood to the heart muscle), and the last 2.4% of the global burden of stroke. In Peru, there are high levels of lead toxicity in some districts of the capital where industrial areas cause greater health effects. Among the materials produced by these factories are chemical products in general,

metal handling, grinding of non-metallic industrial metals, recovery of lead and alloys, which are the main responsible for the environmental impact that have been increasing in recent decades.

International standards admit a maximum level of  $0.5\mu\text{g} / \text{m}^3$  [2], a higher value than this will be a problem to attack. The danger of a toxic element in the blood, being able to detect and, above all, provide a follow-up, is an objective for the future and an analytical method so that the amount of lead that many people's body goes through can be identified and taken into account. They had an experience, but not only for the human being, but for all the species within the habitable ecosystem in which we live. This neurotoxin has a direct relationship with health problems [3], such as learning deficit, reduction of intellectual abilities, damage to the central nervous system, muscle pain, weakening of the bones and, in general, the damage to the immune system and the central nervous system. The high exposure to Pb in pregnant women can cause premature abortions, with an intoxication higher than 10dl / mg, the probability of decreasing fertility increases. Analogously, in men it can cause discomfort in the reproductive organ. One of the damages [4] that can cause in the man is the reduction of the spermatozoa and the decrease of the fertility.

Recent studies in children from 1 to 13 years old developed between March and April 2017 [2] in the district of Callao-Lima resulted in a high proportion of children contaminated with lead. This was because of the construction material of their homes, the consumption of food, toys, state of conservation of the house paint and many other forms that seem to be harmless but they are not. There are several methods of analysis, each of them, the problem and the interest in the evidence. Our interest is, in effect, an economical and practical method for the measurement of this toxic element. The objective of the study is the meaning of the construction of each method and help you to select the most appropriate procedure to achieve a specific objective, since we all have the characteristic of having electronic, physical and chemical engineering as elements of studies and we do it. There is no doubt that with the use of current technology it will be possible to create new and better methods of analysis; although it is difficult to find the description.

## II. ANALYSIS OF DIFFERENT METHODS FOR THE DETERMINATION OF LEAD IN BLOOD

There are several methods to determine the lead in the blood, each one of these data of use. In this part, some of these aspects are mentioned below.

### A. Atomic Absorption Spectrophotometry (AAS)

In this technique, the sample to be analyzed is vaporized and the element of interest is atomized at elevated temperatures. To determine the concentration of the element, the wavelength absorbed by it is measured after being subjected to incident light [5]. This method is one of the most common analytical techniques used to calculate the determination of an analyte [6]. Specifically, it can be said that the atoms that are initially in a fundamental state, go to a state of excitation by absorbing energy, jumping from one level of energy to another level so that they then return to their normal state. This process of jumping energy level and returning to its normal state is known as absorption and emission, with which generate specific wavelength patterns.

1) *Flame Atomic Absorption Spectroscopy (FAAS)*: Its foundation is the absorption of radiation energy by free radical atoms. The process contains several stages, so a hollow cathode light source that can emit a very short wavelength is necessary. This lamp is very much used for this type of experience, since it will be the one that will excite the analyte. Once the light of the lamp hits the analyte, as see in Fig. 1, there will be a decrease in the number of photons, which will then be sent to the monochromator to be able to divide the different wavelengths, which will eventually pass to the detector to convert the photons obtained in an electrical signal [7].

2) *Graphite Furnace Atomic Absorption (GFAAS or ETAAS)*: This is also known as electrothermal atomization. This method is the most sensitive within the Atomic Absorption Spectrophotometry (AAS). The sample is placed inside a graphite tube, as see in Fig. 2, to which a potential difference is applied which allows us to obtain the necessary energy for the atomization [8] that is, the atoms of an element absorb energy heating them and achieving vaporization of the sample becoming free atoms. The graphite tube is aligned with a light from a spectral lamp. The atomic vapor produced by the sample located inside the graphite tube will absorb the light emitted by the spectral lamp. It should be mentioned that a similar result could also be achieved with a continuous source and a high-resolution spectrometer, although the absorbance signal lasts a maximum of 5 seconds and generates a transient peak from which a calibration curve can be constructed [9].

3) *Hydride Generation Atomic Absorption Spectrophotometry (HGAAS)*: Knowing that atomic absorption spectrometry is one of the most common methods that helps us determine the presence of metals in a sample, here we mention one more procedure, called atomic absorption spectrometry, as

see in Fig. 3, with the generation of hydrides or abbreviated as HGAAS. The analyte is passed to a form of gas hydride, which will later go through an atomization process inside a chamber containing argon (Ar). After the atomization process is needed an external stimulus to the resulting analyte, in this case the generator of hydride with which we can measure its absorbance [10].

### B. Voltammetric Methods

This method [11] is based on the pre-concentration of the analyte in the working electrode, after which a potential is applied during which the analyte is withdrawn from the solution. Finally, the response obtained is proportional to the concentration analyzed.

1) *Anodic Stripping Voltammetry (ASV)*: Within the known voltammetric methods, we will begin to talk about ASV, commonly called "STRIPPING", is an electrochemical process that seeks to relate the behavior of a sample in the form of a current signal, applying a potential difference from anode to cathode [12]. This potential difference will cause a change in the sample adhered to the electrodes, as see in Fig. 4, making it oxidize or reduce.

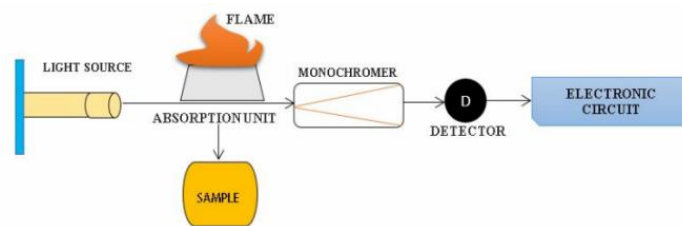


Fig. 1. All the System is Constituted for a Light Source, Absorption unit, Flame, Monochrome, Detector and the Electronic Circuit that will be in Charge of Processing the Information.

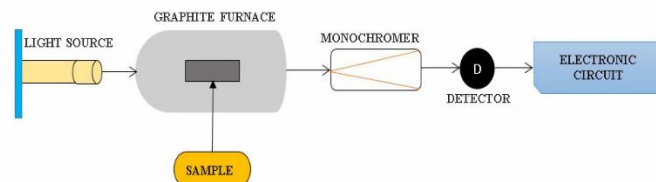


Fig. 2. A Light is Emitted by a Light Source, and this Light Strikes the Atomized Sample the Monochromator Selects the Wavelength of Interest the Detector Measures the Amount of Absorption and the Electronic Circuit Processes the Information.

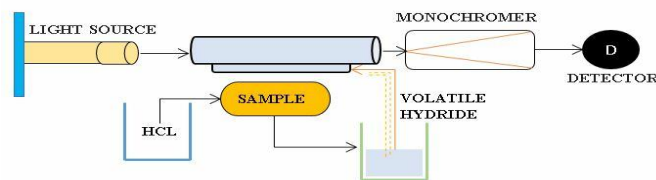


Fig. 3. The Presented Scheme is Composed for a Light Source, a Monochromator, a Detector and a Hydride Generator in other Cases, you can Appreciate an Optic Cell, a Double Beam Instruments and Even a Constant Flame.

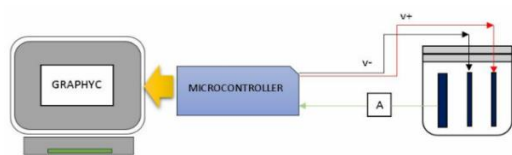


Fig. 4. Block Diagram of the Process, there are Three Electrodes Connected and the Data is Sent to the Microcontroller.

2) *Cathodic Stripping Voltammetry (CSV)*: Within the voltammetric methods, Cathodic Stripping Voltammetry (CVS) [13] can also be found which is mainly applied in the analysis of low levels of analyte or sample and to compounds containing sulfur. Comparing with Anodic Stripping Voltammetry (ASV) in which a potential difference is applied to generate a positive sweep, here the analyte is pre-concentrated in the electrode with a few drops of mercury. In order to carry out the experience, this is based on the measurement of a reductive current response based on the sweep performed in the negative direction, for which a reference potential is previously applied and thus the analyte behavior can be analyzed.

3) *Adsorptive Stripping Voltammetry (AdSV)*: Following with the voltammetric methods, the extraction method is based on the accumulation of ions or compounds to be determined in the working electrode. As well as Anodic Stripping Voltammetry and Cathodic Stripping Voltammetry, [14] we can achieve the accumulation by adsorption of the species in the working electrode, as see in Fig. 5, and that there are compounds that have adsorption properties. It can be carried out on most of the electrodes used in voltammetry for which it is possible to reproduce it throughout the measurement process, assuring a constant surface.

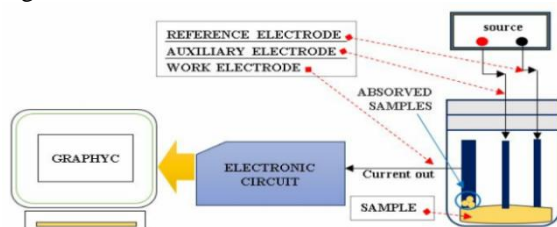


Fig. 5. Basic Scheme of Connection - Adsorptive Stripping Voltammetry (AdSV).

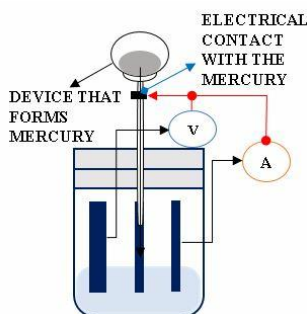


Fig. 6. The Image Shows the Container that Drops Mercury through a Capillary Tube to the Sample the Connections of the Voltmeter and the Ammeter to the Electrodes and to a Point Placed in the Capillary Tube.

### C. Polarography

This electrochemical process is a method derived from voltammetry, which contains characteristics similar to electrolysis, but instead of eliminating an unwanted component of a solution. On the other hand, the polarography [15] keeps the sample, as it was in order to be able to recover it while small currents are applied in less time. Created in 1922 by Jaroslav Heyrovský, polarography is a specific type of measurement found within the linear sweep Voltammetry where the potential of the electrode is altered from the initial potential to the end. The attractiveness of this method is that several properties of the mercury, as seen in Fig. 6, which will fulfill the function of an electrode, are derived. The elegance of this method [16] are the various properties of mercury as an electrode material. Because it is a liquid material, it provides an easy revocability and reproducibility of the surface.

### III. COMPARATIVE STUDY

In the previous comparative table, the main characteristics of each method developed in this work will be mentioned below. This table will serve as a guide to identify what method to use in any future study that you want to do.

As we can see in Table I, Graphite Furnace Atomic Absorption method is more expensive than the aforementioned voltammetric methods, and it is useful for small samples in the  $ug/l$  range. In addition to this, a laboratory with the necessary equipment is important because the sample must be subjected to various processes before being able to analyze the result. Similar to GFAAS, the Flame Atomic Absorption Spectroscopy method requires a laboratory and equipment to carry out the experience. Analyze trace metals. This method, unlike the graphite furnace, can detect larger quantities in the  $mg/l$  range. Hydride Generation Atomic Absorption Spectrophotometry improves the detection of the analyte that is analyzed, in turn, it supports interferences produced in the process, but it needs a stage of generation of hydride and laboratory materials to be able to develop the experience with which it becomes a costly process. Anodic Stripping Voltammetry is an inexpensive process and good sensitivity, used to analyze metals present in a sample. Its operation is easy, precise and portable for the analysis of blood. Cathodic Stripping Voltammetry as well as the ASV is of low cost and good sensitivity. It is worth mentioning that it is not necessary to add reagents to the sample to be analyzed. Adsorptive Stripping Voltammetry is a method with good sensitivity and inexpensive. It can present problems in the current measurements since it is susceptible to the interference of other substances present in the sample, so we must be careful with the substances to analyze.

Finally, the Polarography method is a low cost process and of good precision compared to the CSV or ASV methods. This method is longer and more complex than the aforementioned methods. The attractiveness of this method is that it uses an electrode as the working electrode subjected to drops of mercury (EGM), which makes it essentially different from other voltammetric methods.

TABLE I. COMPARATIVE TABLE OF THE METHODS FOR THE DETERMINATION OF LEAD

| Methods  | Fixed laboratory environment | Portable laboratory environment | Low cost | High cost | Sensitivity with the sample |
|--|------------------------------|---------------------------------|----------|-----------|-----------------------------|
| Flame Atomic Absorption Spectroscopy                   | X                            |                                 |          | X         |                             |
| Graphite Furnace Atomic Absorption                     | X                            |                                 |          | X         |                             |
| Hydride Generation Atomic Absorption Spectrophotometry | X                            |                                 |          | X         | X                           |
| Anodic Stripping Voltammetry                           |                              | X                               | X        |           | X                           |
| Cathodic Stripping Voltammetry                         |                              | X                               | X        |           | X                           |
| Adsorptive Stripping Voltammetry                       |                              | X                               | X        |           | X                           |
| Polarography   |                              | X                               | X        | X         |                             |

#### IV. DISCUSSION

It is mention that all the methods shown in the present work fulfill a common objective which is to determine the concentration of a specific analyte present in a sample. A major difference of some methods over others is the need for a laboratory and expensive equipment. We must take into account the degree of sensitivity that is required, the efficiency and precision that is desired to be able to use the most correct method. Highlighting all the analyzed models, voltammetry since they are possible methods of reproducing and assembling according to the case of study analysis, allowing in its construction process to understand electronics, physics, chemistry and biology, including its practicality of mobilization and low cost.

#### V. CONCLUSIONS

In this research work, we presented the different methods to determine the presence of toxic metal in the blood, we can conclude that in the process of voltammetry, there is the advantage that the electrodes occupy very small surfaces and the applied potential will generate low currents, which will be easy to measure. Finally, in voltammetry, only a small amount of sample is needed, while in the others the sample is converted to another state through vaporization processes, atomization or generation of hydrides.

#### VI. FUTURE WORK

In this work, we present an initial and fundamental comparative study of the most used methods for the detection of heavy metals in the blood. Our future interest is the construction of an electronic device that allows us to take measures on this problem, so that this study allows to understand the variants of each existing model, knowing the advantages and disadvantages to advance towards its manufacture. For our process, the ASV method is the choice to build the device in the short term, the main idea being to detect levels of Pb in the blood, nowadays it is a social problem in many places of Peru.

#### ACKNOWLEDGMENT

We want to thank the Image Processing Research Laboratory (INTI-Lab) and the Universidad de Ciencias y Humanidades (UCH) for their support in this research. Also, to the National Fund for Scientific, Technological and Technological Innovation (FONDECYT), according to the contract "N ° 091-2018-FONDECYT-BM-IADT-AV" for the

financing of this project and the Electronics Laboratory of the UCH for assigning us their facilities and being able to carry out the respective tests.

#### REFERENCES

- [1] World Health Organization, "Questions and answers: international lead poisoning prevention awareness campaign week of action 22-28 october 2017," 2017.
- [2] M. Morales, Juan, MD, MgSc, PHD; Fuentes-Rivera, José, MD, MgSc, PHD; Bax, Vincent, Ing, MgSc; Matta, Hernán H, MD, MgSc, PHD; Delgado-Silva, Carlos Alberto, MD, "Niveles de plomo sanguíneo y factores asociados en niños residentes de un distrito del Callao," AVFT , vol. 37, no. 2, 2018.
- [3] A. Evens et al., "The impact of low-level lead toxicity on school performance among children in the Chicago Public Schools: a population-based retrospective cohort study," Environ. Heal., vol. 14, no. 1, p. 21, Dec. 2015.
- [4] Agency for Toxic Substances and Disease Registry, Toxicological Profile for Lead, Draft for Public Comment. 2019.
- [5] N. P. Cheremisinoff, "Elemental and structural characterization tests," in Polymer Characterization, Elsevier, 1996, pp. 43–81.
- [6] W. Yawar, "Determination of wear metals in lubricating oils by flame atomic absorption spectrophotometry," J. Anal. Chem., vol. 65, no. 5, pp. 489–491, May 2010.
- [7] T. Alasadi, "Flame atomic absorption", Wasit University, Tech.Rep., 140, 2016.
- [8] Paul Riemann Cruz Ausejo and Indira Consuelo Nájera Gálvez, "Evaluación del contenido microbiológico y cuantificación de plomo en pinturas faciales infantiles obtenidas en el Mercado Central de Lima. Setiembre 2015," universidad nacional mayor de san marcos, 2017.
- [9] J. A. Holcombe and D. L. G. Borges, "Graphite Furnace Atomic Absorption Spectrometry," in Encyclopedia of Analytical Chemistry, Chichester, UK: John Wiley & Sons, Ltd, 2010.
- [10] B. Stephen, "Studies of essential and non-essential elements in cereal-based weaning foods for infants commercially available on the ghanaiian market," University of Ghana , 2013.
- [11] P. Worsfold et al., "Voltammetry | Stripping Voltammetry," Encycl. Anal. Sci., pp. 238–257, Jan. 2019.
- [12] M. R. J. and J. B.-O. J Barón-Jaimez, "Anodic stripping voltammetry–ASV for determination of heavy metals," 2nd Int. Meet. Res. Mater. Plasma Technol., 2013.
- [13] E. P. Achterberg, M. Gledhill, and K. Zhu, "Voltammetry—Cathodic Stripping," Ref. Modul. Chem. Mol. Sci. Chem. Eng., Jan. 2018.
- [14] R. Kalvoda, "Adsorptive Stripping Voltammetry in Trace Analysis," in Contemporary Electroanalytical Chemistry, Boston, MA: Springer US, 1990, pp. 403–405.
- [15] Shodhganga, "General principle of polarography," 1980, pp. 27–28.
- [16] S. Al-Amri and B. H. A. Al-Ameri, "Differential Pulse Polarography Procedure for the Estimation of Deferoxamine in Pharmaceuticals Voltammetry View project Analytical chemistry View project," Chem. Sci. Trans., vol. 7, no. 2, pp. 272–281, 2018.

# Smart Smoking Area based on Fuzzy Decision Tree Algorithm

Iswanto<sup>1</sup>, Kunnu Purwanto<sup>2</sup>, Weni Hastuti<sup>3</sup>, Anis Prabowo<sup>4</sup>, Muhamad Yusvin Mustar<sup>5</sup>

Department of Electrical Engineering, Universitas Muhammadiyah Yogyakarta, Yogyakarta, Indonesia<sup>1,2,5</sup>

Department of D3 Nursing, Institut Teknologi Sains dan Kesehatan PKU Muhammadiyah Surakarta, Surakarta, Indonesia<sup>3,4,5</sup>

**Abstract**—Cigarette smoke is very dangerous for both active and passive smokers who smoke inside a room because nicotine from cigarette smoke can stick on the wall or in the furniture and produce carcinogenic substances when reacting with air. The carcinogen chemicals in cigarettes are more dangerous when cigarette smoke is trapped in a limited space. An exhaust fan is usually used in a special room for smokers that serves to remove cigarette smoke without exchanging air in it. A smart smoking room tool specifically for smokers was made to answer the problem. The room used an 'in and out' exhaust fan ventilator. This fan ventilator rotated based on the quantity of carbon monoxide (CO) gas in the room detected by using a smoke sensor. Arduino Uno based on Fuzzy Decision Tree algorithm was used to control of the input voltage level in the fan ventilator. The result showed that by using the tool, the cigarette smoke in the room can be controlled effectively.

**Keywords**—Fuzzy decision tree algorithm; smart smoking room; microcontroller; smoke sensor

## I. INTRODUCTION

This paper is presented systematically starting from introduction which describes the need for a cleaner room free from cigarette smoke, the relevant researches, the aim of the research and the research limitation. The second session presents the method used in this research. The research result is discussed in the third session and the conclusion of the research is written in the fourth session.

Indonesia is the third country in the world with the highest number of smokers after China and India. Smoking in the room will leave nicotine on home furniture and wall. Nicotine reacts with air and produces carcinogenic substances. The carcinogenic chemicals in cigarettes are more dangerous when cigarette smoke is trapped in a limited space. There is usually an exhaust fan to remove cigarette smoke without circulating the air in and out the smoking room. This makes unhealthy conditions. Keeping the room windows open will not solve the problem. Large amount of cigarette smoke actually stays or returns to the room and continues to stay indoor for hours.

Based on the problem, a tool which is a prototype of a smart room specifically for smoking was made. This room used two ventilators namely exhaust fans to circulate the air in and out the room. These ventilators made the air flow in the room replacing the air and out the room to remove the cigarette smoke so that it would reduce the risk of sticking harmful gases that stick to the walls of the room. These fan ventilators rotated based on the quantity of carbon monoxide (CO) gas in the room. The level of carbon monoxide (CO) in

the room will be monitored by the LCD and there was an indicator light as a warning system if the air level in the room reached a dangerous level; controlling the input voltage level of the fan ventilator using Arduino Uno.

Detecting smoke using a microcontroller has been investigated by previous researchers. Smart Home Automation was studied by Islam to control lights, heating water machine, washing machine and doors. The system uses several sensors consisting of flame sensor to detect fire, camera sensor to detect people's movements, DHT11 sensor to detect temperature, and smoke sensor with MQ 3 and MQ135 by using CRIPS algorithm [1]. The fire detection system was examined by Elizalde using temperature sensor, GPS sensor and ionization sensor. Ionization sensor is a sensor that can detect smoke. The three sensors were processed by ATmega328 by using Comparative algorithm sent using the Zigbee and GSM modules [2].

A vehicle accident notification system was investigated by Dias using several sensors processed by Arduino. Those sensors were shock sensor, accelerometer sensor and GPS sensor used for tracking, and smoke sensor and GPS sensor for detecting accidents and providing accident position notifications by using tracking algorithm [3]. Monitoring forest fire was investigated by Fengbo using several sensors including smoke sensor, temperature, humidity, fire, and light sensors connected to CC2530 microcontroller type. The microcontroller was used to process data by using data processing algorithm transferred to the monitoring terminal using Zegbee [4].

A healthy environmental monitoring system for smart cities was examined by Ghosal using a quadrotor. To monitor a healthy environment, several sensors such as LM35 sensor, AM1001 sensor, LDR Sensor, MQ 6 Sensor and MQ135 Sensor connected to Arduino were carried by the quadrotor. The sensors were processed by Arduino ATmega328. The data were then captured by using WiFi [5]. A server space control and monitoring system was investigated by Roihan by using several sensors connected to Wemos microcontroller. The system consisted of Arduino type Wemos, DHT11 sensor to detect humidity and temperature, and MQ2 sensor to detect smoke. The system is equipped with a GSM module so that it can send the data to the internet [6].

A house environmental monitoring system was examined by Mahara Jothi connected with GSM communication. This system consisted of temperature sensor, PIR sensor, ultrasonic sensor, and smoke sensor connected to Arduino. The system

worked remotely for monitoring and control since it was connected to GSM controlled using a mobile phone [7]. A fire extinguisher robot was designed and examined by Bose using a PIC16F876A type microcontroller. This system consisted of fire sensors including gas sensor and temperature sensor connected to a microcontroller. When the amount of smoke or the temperature increases, this system turns on the fire extinguisher pump [8].

Environmental quality monitoring system was examined by Islam using cloud data logging. To detect air quality, this system used a sensor consisting of CO<sub>2</sub>, CO, LPG, Smoke, alcohol, benzene, NH<sub>3</sub>, temperature and pH sensors connected to Arduino Uno. The data from Arduino Uno were processed by using artificial intelligent algorithm and then sent to the cloud server using GPRS [9]. Detection of asthma triggers was investigated by Indulakshmi using the reference air quality index. MQ2 sensor was used in this system to determine the air quality in the environment. MQ2 sensor data were read and processed by the nodeMCU type microcontroller by using comparative algorithm and then transmitted to the network using cloud servers from Adafruit [10].

The alarm system to determine the location of the accident was examined by the Desima using smoke sensor, fire sensor and switches. The smoke sensor uses MQ135 to detect gas carbon dioxide (CO<sub>2</sub>) fumes. The sensors were the Arduino Uno microcontroller inputs then they were processed to be transmitted using the GSM module [11]. The vehicle accident tracking system was investigated by John using alcohol sensor, eye sensor, and smoke sensor. The system used an ATmega328 microcontroller to read the alcohol sensor, eye sensor, pizzo-electric vibration sensor, smoke sensor and tilt sensor. The data processed by the microcontroller were transmitted using a GSM module [12].

Portable systems for transmitting and accounting data were examined by Yordanov. This acquisition data were used for sensor data such as humidity, air pollution gas, dust and smoke. These transmission data send the data using Bluetooth and GPRS or GSM. PIC type microcontrollers were needed to process sensor data [13]. Environmental monitoring in the factory area for employee safety was examined by Kodali. The system used three sensors namely temperature sensor, smoke sensor, and ultrasonic sensor. MTQQ algorithm was applied to Arduino NodeMCU type microcontroller used to process sensor data and sends the data to the internet using Wi Fi [14].

Many previous researchers have conducted researches on smoke sensors. The smoke sensors have been used for smart home systems, fire detection systems, vehicle accident notification systems, forest fire monitoring systems, healthy environmental monitoring systems, fire-fighting robots, asthma trigger detection systems and many others. The methods used by the previous researchers are Comparative algorithm and smart control methods such as MTQQ algorithm, artificial intelligent, and data processing algorithm. The author uses fuzzy decision tree method.

This paper presents MQ2 and MQ7 smoke sensors to make a smart smoking area system. This system uses two exhaust fans to suck in and blow the smoke out the room. The research is limited for a small room.

## II. RESEARCH METHOD

Two methods for a smart smoking area were presented namely block diagram design method and algorithmic method. Fig. 1 shows the smart smoking area design. It can be seen that the system consists of input system, output system and control system. The input system uses smoke sensors to detect cigarette smoke. This input system uses MQ-2 and MQ-7 gas sensors to detect and read carbon monoxide gas as the result of burning cigarettes. The data are processed by the control system using Arduino uno [15]. The output system consists of an exhaust fan for sucking the air, an exhaust fan for blowing the air, and an LCD display [16], [17].

An algorithm fuzzy decision tree [18]–[20] method for a smart smoking area is shown by a flowchart decision tree in Fig. 2. The chart shows that the smoke sensor uses I2C communication. The MQ2 and MQ7 sensor data are processed using fuzzy algorithm by comparing sensor data with set points. When the smoke is above than 200, the red LED light is on and the fan is on. When the smoke is less than 200, the blue LED light is on, and the fan is off.

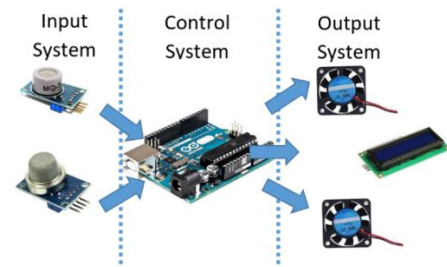


Fig. 1. Block Diagram of a Smart Smoking Area System.

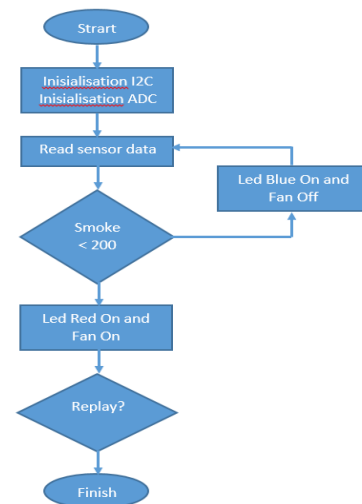


Fig. 2. Flowchart of a Smart Smoking Area.

### III. DISCUSSION

Testing the smart smoking area using Arduino with the MQ7 and MQ2 sensors was carried out on a prototype with size of 38 x 29 x 21. In the prototype, there were MQ7 and MQ2 gas sensors to detect CO gas levels in the box. The prototype was connected to a controller circuit served to adjust the AC in the fan in and fan out.

Fig. 3 shows the smart smoking-room system. The tests on MQ2 and MQ7 sensors were performed by connecting the MQ2 and MQ7 sensors to the Arduino Uno module and to the laptop to upload the program in the Arduino Uno module to check the MQ7 and MQ2 Sensors. The sensor works in accordance to the desired input. Table I is the result of MQ7 gas sensor voltage test at every 5 second increase.

Referring to the table, there is a slight difference in MQ7 gas sensor voltage test in the Arduino IDE monitor series with a measured multi-meter in comparison with an average difference of 0.0081. This proved that the sensor works as it should. There was an error at the time of measurement with an average error of 0.001228641 or 0%.

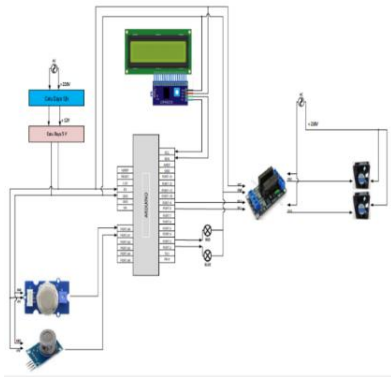


Fig. 3. Smart Smoking Room System.

TABLE I. RESULT OF THE MQ7 GAS SENSOR VOLTAGE TEST

| No      | Time (s) | Monitor series voltage (volt) | Multimeter voltage (volt) | Error (error) | Percentage (%) |
|---------|----------|-------------------------------|---------------------------|---------------|----------------|
| 1       | 5        | 0.69                          | 0.701                     | 0.0006        | 0%             |
| 2       | 10       | 0.7                           | 0.691                     | 0.0006        | 0%             |
| 3       | 15       | 1.06                          | 1.049                     | 0.0010        | 0%             |
| 4       | 20       | 1.22                          | 1.215                     | 0.0011        | 0%             |
| 5       | 25       | 1.3                           | 1.291                     | 0.0012        | 0%             |
| 6       | 30       | 1.33                          | 1.299                     | 0.0012        | 0%             |
| 7       | 35       | 1.36                          | 1.401                     | 0.0013        | 0%             |
| 8       | 40       | 1.55                          | 1.547                     | 0.0015        | 0%             |
| 9       | 45       | 1.56                          | 1.556                     | 0.0015        | 0%             |
| 10      | 50       | 1.88                          | 1.819                     | 0.0017        | 0%             |
| Sum     |          |                               | 0.081                     | 0.0122        | 0%             |
| Average |          |                               | 0.0081                    | 0.0012        | 0%             |

Fig. 4 shows MQ7 sensor voltage test graph. It can be seen in the figure that the ratio between LCD voltage and the multi-meter voltage is getting higher, due to the sensor heating. The hotter the sensor the higher is the voltage. Table II is the result of MQ2 gas sensor voltage test at every 5 second increase.

There is a similarity between the MQ7 gas measurement and the voltage measurement that is the voltage measured by the multi-meter and the voltage measured in the Arduino IDE serial monitor shows a slight difference. This proves that the sensor works as it should. The average error is 0.001279668 or 0%.

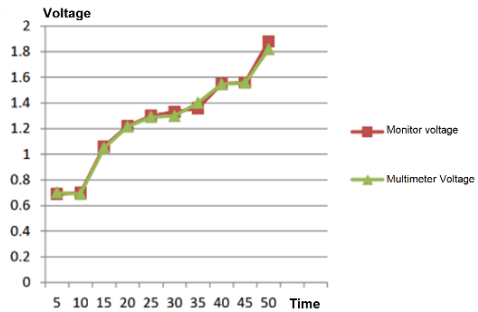


Fig. 4. MQ7 Sensor Voltage Test.

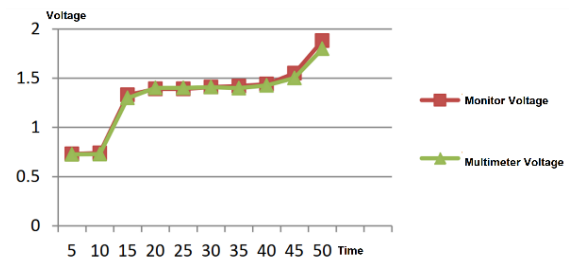


Fig. 5. MQ2 Sensor Voltage Test.

TABLE II. MQ2 GAS SENSOR VOLTAGE TEST SENSOR

| No      | Time (s) | Monitor series voltage (volt) | Multimeter voltage (volt) | Error (error) | Percentage (%) |
|---------|----------|-------------------------------|---------------------------|---------------|----------------|
| 1       | 5        | 0.73                          | 0.726                     | 0.0007        | 0%             |
| 2       | 10       | 0.74                          | 0.729                     | 0.0007        | 0%             |
| 3       | 15       | 1.33                          | 1.299                     | 0.0012        | 0%             |
| 4       | 20       | 1.39                          | 1.401                     | 0.0013        | 0%             |
| 5       | 25       | 1.39                          | 1.401                     | 0.0013        | 0%             |
| 6       | 30       | 1.41                          | 1.409                     | 0.0013        | 0%             |
| 7       | 35       | 1.42                          | 1.399                     | 0.0013        | 0%             |
| 8       | 40       | 1.44                          | 1.427                     | 0.0013        | 0%             |
| 9       | 45       | 1.55                          | 1.502                     | 0.0014        | 0%             |
| 10      | 50       | 1.88                          | 1.798                     | 0.0017        | 0%             |
| Sum     |          |                               |                           | 0.0127        | 0%             |
| Average |          |                               |                           | 0.0012        | 0%             |



Table III is the test on the characteristics of the MQ2 sensor was performed by testing the output voltage when the chimney is closed for 3 minutes 20 seconds as shown in Fig. 5. The figure shows that the tests were carried out every 20 seconds increasing from 20 seconds to 160 seconds using a multi-meter.

The table shows that the voltage decreases every 20 second increase. This proves that the less smoke is in the room, the lower the voltage will be and vice versa.

As illustrated in Fig. 6, it can be seen in the graph that the more smoke in the room, the higher the voltage produced. Afterward, when the fan is active, the smoke will decrease and so will the voltage. Table IV is the test on the characteristics of the MQ7 sensor was performed by testing the output voltage when the chimney is closed for 3 minutes 20 seconds. The tests were carried out every 20 seconds increasing from 20 seconds to 160 seconds using a multi-meter.

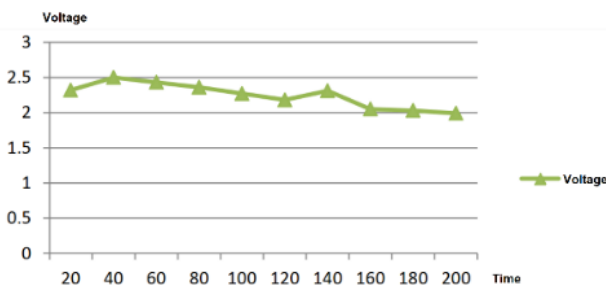


Fig. 6. Results of MQ2 Gas Characteristics Test.

TABLE III. RESULTS OF MQ2 GAS SENSOR CHARACTERISTICS TEST

| No | Time (second) | Voltage (volt) |
|----|---------------|----------------|
| 1. | 20            | 2,32 volt      |
| 2. | 40            | 2,50 volt      |
| 3. | 60            | 2,43 volt      |
| 4. | 80            | 2,36 volt      |
| 5. | 100           | 2,27 volt      |
| 6. | 120           | 2,18 volt      |
| 7. | 140           | 2,31 volt      |
| 8. | 160           | 2,05 volt      |

TABLE IV. RESULTS OF MQ7 GAS SENSOR CHARACTERISTICS TEST

| No | Time (second) | Voltage (volt) |
|----|---------------|----------------|
| 1. | 20            | 2,32 volt      |
| 2. | 40            | 2,50 volt      |
| 3. | 60            | 2,43 volt      |
| 4. | 80            | 2,36 volt      |
| 5. | 100           | 2,46           |
| 6. | 120           | 2,41           |
| 7. | 140           | 2,4            |
| 8. | 160           | 2,35           |

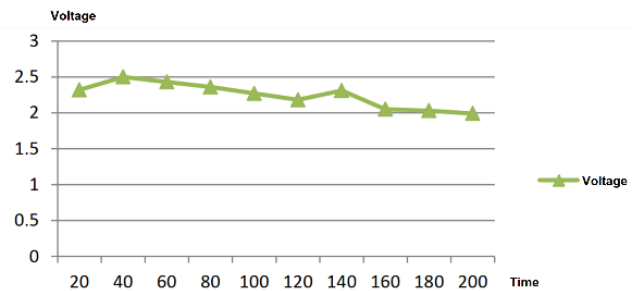


Fig. 7. Results of MQ2 Gas Characteristics Test.

The table shows that the more CO gas content in a room, the higher the voltage. Afterward, when the fan is active the voltage will decrease due to the decrease of the CO gas.

Fig. 7 shows the same characteristic of gas sensor in that the higher voltage is generated from the higher CO gas content in the room. Similar to the previous graph, the greater the gas content in the room, the higher the voltage produced.

#### IV. CONCLUSION

Based on the results of testing and discussion, it can be concluded that a smart smoking area system has been realized. The system can detect cigarette smoke in the room. When the cigarette smoke in the room increases, the DC motor moves the fan to circulate cigarette smoke out and in the room. The room is clean of smoke because the air inside the room is sucked out and the fresh air from outside is sucked in the room. Therefore, the room will always contain fresh air. From the smokers' point of view, this smart smoking room can help them to feel more comfortable because there is no cigarette smoke that causes cough and eyes. It is expected that an algorithm or technology is added for larger smart smoking rooms.

#### REFERENCES

- [1] A. Islam, "Android Application Based Smart Home Automation System Using Internet of Things," in 2018 3rd International Conference for Convergence in Technology (I2CT), 2018, pp. 1-9.
- [2] D. Q. R. Elizalde, R. J. P. Garcia, M. M. S. Mitra, and R. G. Maramba, "Wireless Automated Fire Detection System on Utility Posts Using ATmega328P," in 2018 IEEE 10th International Conference on Humanoid, Nanotechnology, Information Technology, Communication and Control, Environment and Management (HNICEM), 2018, pp. 1-5.
- [3] R. Dias, V. Ghike, J. Johnraj, N. Fernandes, and A. Jadhav, "Vehicle Tracking and Accident Notification System," in 2018 3rd International Conference for Convergence in Technology (I2CT), 2018, pp. 1-4.
- [4] W. Fengbo, L. Xitong, and Z. Huike, "Design and Development of Forest Fire Monitoring Terminal," in 2018 International Conference on Sensor Networks and Signal Processing (SNSP), 2018, pp. 40-44.
- [5] M. Ghosal, A. Bobade, and P. Verma, "A Quadcopter Based Environment Health Monitoring System for Smart Cities," in 2018 2nd International Conference on Trends in Electronics and Informatics (ICOEI), 2018, pp. 1423-1426.
- [6] A. Roihan, F. Sudarto, and T. Cahyo Putro, "Internet of Things on Monitoring and Control System in Server Area," in 2018 International Seminar on Application for Technology of Information and Communication, 2018, pp. 116-120.
- [7] T. Mahara Jothi, A. Periyanyaki, R. Srimathy, M. Vinotha, and G. Gopika, "GSM Based Home Environment Monitoring System," in 2018 2nd International Conference on Trends in Electronics and Informatics (ICOEI), 2018, no. Icoei, pp. 1263-1268.

- [8] J. S. C. Bose, M. Mehrez, A. S. Badawy, W. Ghribi, H. Bangali, and A. Basha, "Development and designing of fire fighter robotics using cyber security," in 2017 2nd International Conference on Anti-Cyber Crimes (ICACC), 2017, pp. 118–122.
- [9] M. S. Islam, "An Intelligent System on Environment Quality Remote Monitoring and Cloud Data Logging Using Internet of Things (IoT)," in 2018 International Conference on Computer, Communication, Chemical, Material and Electronic Engineering (IC4ME2), 2018, pp. 1–4.
- [10] S. Indulakshmi, M. Adithya, A. R. Anirudh, and A. Jawahar, "Design and Development of Prototype Model for Asthma Trigger Detection," in 2018 International Conference on Wireless Communications, Signal Processing and Networking (WiSPNET), 2018, pp. 1–5.
- [11] M. A. Desima, P. Ramli, D. F. Ramdani, and S. Rahman, "Alarm system to detect the location of IOT-based public vehicle accidents," in 2017 International Conference on Computing, Engineering, and Design (ICCED), 2017, pp. 1–5.
- [12] A. John and P. R. Nishanth, "Real time embedded system for accident prevention," in 2017 International conference of Electronics, Communication and Aerospace Technology (ICECA), 2017, pp. 645–648.
- [13] R. Yordanov, R. Miletiev, P. Kapanakov, and E. Lontchev, "Design of a portable system for sensor data acquisition and transmission," in 2017 XXVI International Scientific Conference Electronics (ET), 2017, pp. 1–3.
- [14] R. K. Kodali and A. Valdas, "MQTT based environment monitoring in factories for employee safety," in 2017 3rd International Conference on Applied and Theoretical Computing and Communication Technology (iCATccT), 2017, pp. 152–155.
- [15] K. Purwanto, I. -, T. Khristanto, and M. Yusvin, "Microcontroller-based RFID, GSM and GPS for Motorcycle Security System," *Int. J. Adv. Comput. Sci. Appl.*, vol. 10, no. 3, pp. 447–451, 2019.
- [16] A. N. N. Chamim, M. H. Gustaman, N. M. Raharja, and Iswanto, "Uninterruptable power supply based on switching regulator and modified sine wave," *Int. J. Electr. Comput. Eng.*, vol. 7, no. 3, pp. 1161–1170, 2017.
- [17] A. N. N. Chamim, D. Ahmadi, and Iswanto, "Atmega16 implementation as indicators of maximum speed," *Int. J. Appl. Eng. Res.*, vol. 11, no. 15, pp. 8432–8435, 2016.
- [18] T. P. Tunggal, A. Supriyanto, R. Nur Mukhammad Zaidatur, I. Faishal, I. Pambudi, and T. Iswanto, "Pursuit algorithm for robot trash can based on fuzzy-cell decomposition," *Int. J. Electr. Comput. Eng.*, vol. 6, no. 6, pp. 2863–2869, 2016.
- [19] Iswanto, O. Wahyunggoro, and A. I. Cahyadi, "Path planning based on fuzzy decision trees and potential field," *Int. J. Electr. Comput. Eng.*, vol. 6, no. 1, pp. 212–222, 2016.
- [20] I. Iswanto, O. Wahyunggoro, and A. I. Cahyadi, "Formation Pattern Based on Modified Cell Decomposition Algorithm," *Int. J. Adv. Sci. Eng. Inf. Technol.*, vol. 7, no. 3, p. 829, Jun. 2017.

# A Comprehensive Collaborating Filtering Approach using Extended Matrix Factorization and Autoencoder in Recommender System

Mahamudul Hasan<sup>1</sup>

Department of Computer Science and Engineering  
East West University  
Dhaka, Bangladesh

Falguni Roy<sup>2</sup>

Institute of Information Technology,  
Noakhali Science and Technology University  
Noakhali, Bangladesh

Tasdikul Hasan<sup>3</sup>

Department of Computer Science and Engineering  
East West University  
Dhaka, Bangladesh

Lafifa Jamal<sup>4</sup>

Department of Robotics and Mechatronics Engineering  
University of Dhaka  
Dhaka, Bangladesh

**Abstract**—Recommender system is an approach where users get suggestions based on their previous preferences. Nowadays, people are overwhelmed by the huge amount of information that is being present in any system. Sometimes, it is difficult for a user to find an appropriate item by searching the desired content. Recommender system assists users by providing suggestions of required information or items based on the similar features among the users. Collaborative filtering is one of the most re-known process of recommender system where the recommendation is done by similar users or similar items. Matrix factorization is an approach which can be used to decompose a matrix into two or more matrix to generate features. Again, autoencoder is a deep learning based technique which is used to find hidden features of an object. In this paper, features are calculated using extended matrix factorization and autoencoder and then a new similarity metric has been introduced that can calculate the similarity efficiently between each pair of users. Then, an improvement of the prediction method is introduced to predict the rating accurately by using the proposed similarity measure. In the experimental section, it has been shown that our proposed method outperforms in terms of mean absolute error, precision, recall, f-measures, and average reciprocal hit rank.

**Keywords**—Recommender system; deep learning; autoencoder; matrix factorization; similarity measures

## I. INTRODUCTION

Recommender system is introduced as an assistant for the users to obliterate information overload problem of the internet. It finds the best information for the users by identifying the pattern from the dataset and then recommends it to the users. The real life examples of recommender system can be seen on most of the websites like YouTube, Amazon where it recommends videos or products. In those websites, two users are selected as similar when both follow the same feature pattern. Content-based and collaborative filtering are the two approaches in the field of recommender system [1]. In collaborative filtering, the behavior of the similar users are being analyzed and on the basis of the analysed result, the recommendation has been done to the target users. On the basis of similarity measures' methodology, collaborative

filtering further divided into two category, one is memory-based approach and another one is model-based approach [2]. Again, memory-based collaborative filtering could be sub categorised as user-based approach and item-based approach [3]. In user-based collaborative filtering approach, products are recommended to a user which have been liked by other similar users [4]. On the other hand in item-based collaborative filtering, items are recommended according to the similarity of the products or on the basis of the ratings of the user on a similar product which has been rated previously [5].

Many sites like Amazon, Pandora and Netflix are using recommender system for optimizing performance, making more profit and also for boosting sales [6]. It is not only bringing profit to the sites but also creating public trusts for those sites. Recommender system already has been captured most of the space of computer science. As, it is a multi-disciplinary field so analysis and exploration can be done for this field in the context of information mining, machine learning, human-computer interaction, social statistics, network analysis, distributed and mobile systems, artificial societies, computational trust, etc. Researchers are now exploring how the content information can be used to calculate the recommendations.

User behavior is a very complex function so it would be very difficult to find the similarity between users [7]. In this research, a user-based collaborative filtering approach has been employed with matrix factorization and autoencoder. Matrix factorization can provide better performance in predicting and finding the similarity between users. Again, autoencoder is also a very useful technique for satisfactory recommendation. Combination of this two techniques have been implemented in this paper with good performances. So in this paper, the features for the users have been extracted by using the Autoencoder (AE) [8] and the Extended Matrix Factorization (EMF) [9]. After that, the similarity between the users have been calculated and by using the similarity, a recommendation prediction algorithm have also been proposed to accelerate the performances of the recommender system. Finally, the performance of our system are shown in the result section

to evaluate the final recommender system accuracy.

## II. BACKGROUND STUDY AND RELATED WORKS

In the recommender system, there are many methods which are used to provide better performance and deep learning technique is one of them [10]. Sometimes, it can provide the best solution where others method may fail to do so [11]. It can be used as a solution of multiple problems like, speech recognition, image processing and recognition, natural language processing etc. Few types of deep learning methods are discussed here which are being used in most of the recommender system.

### A. Multilayer Perceptron

Multilayer perceptron (MLP) is a kind of feedforward neural network which has multiple hidden layers. There can be more than linear layers or neurons in the MLP [12]. It is like the basic structure of the neural network when three layers are taken where the input layer is the first layer, the hidden layer is the second layer and the output layer is the last layer. The structure of the MLP is represented in Fig. 1. MLPs can be construed as stacked nonlinear transformation layers and layers can be taken as much as needed for the sake of computation.

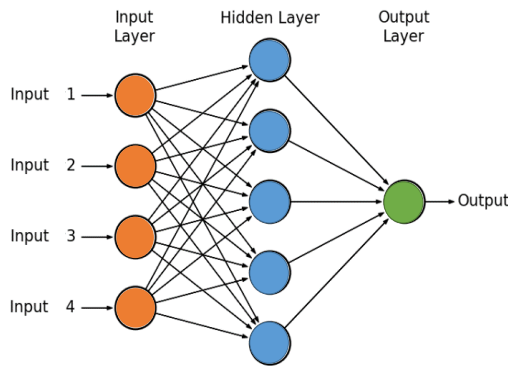


Fig. 1. Multilayer Perceptron.

### B. Convolutional Neural Networks

Mostly convolutional neural networks (CNN) are ideal for image processing. Here, Fig. 2 is an example of convolutional neural network [13]. CNN is normally designed for reduced processing requirements otherwise this it is same as the simple multilayer perceptron. In the hidden layers of the CNN, multiple convolution layers, normalization layers, and pooling layers are utilized [14].

### C. Recurrent Neural Networks

Recurrent neural network (RNN) is designed to recognize the sequential characteristics of the data. They are designed with the loop or they are neural networks with loop and that helps data to preserve it in its memory [15]. They have a specialty that they use the feedback loops to process the data sequences. It can process data into output but the difference is that it can use feedback loops throughout the process unlike other regular feedforward system. These things help RNN to process sequential data. A visual comparison of RNN and traditional feedforward network is shown in Fig. 3.

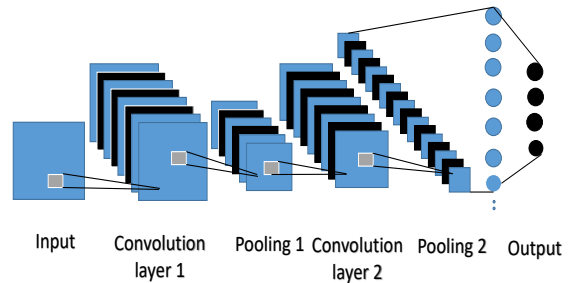


Fig. 2. Convolutional Neural Networks.

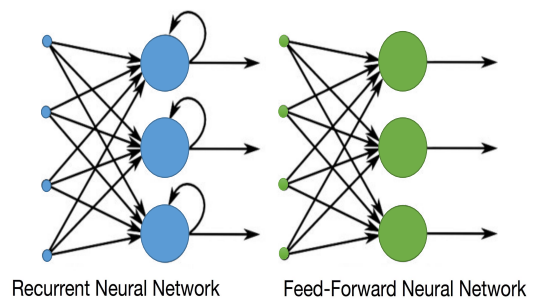


Fig. 3. Comparative Image of RNN and Traditional Feedforward Network.

### D. Restricted Boltzmann Machines

A Restricted Boltzmann Machine (RBM) may be a generative stochastic falsified neural arrangement capable of learning a likelihood of transmission over its set of inputs [16]. Boltzmann Machines (BMs) are a particular type of Markov Random Field (MRF) log-straight. Boltzmann Machines further confine BMs to those without noticeable unmistakable and covered up concealed associations. The energy function  $P(x, y)$  of a RBM is defined as follows:

$$P(x, y) = -a'x - b'y - b'Wu \quad (1)$$

here,  $W$  represents the weights connecting hidden and visible units and  $a, b$  are the offsets of the visible and hidden layers, respectively.

### E. Principal Component Analysis

Simplification of complexity in high dimensional data is done by principal component analysis (PCA). PCA perform its work by transforming data into fewer dimension [17]. PCA is an unsupervised learning and also similar to the clustering method. PCA lowers data by expressing it geometrically on significantly lower dimensions called main components (PCs), with the aim of choosing the best overview of data by using a limited amount of PCs. PCA gets a new set of configurations (or a set of views) so that all the measurements are orthogonal (and therefore linearly independent) and actually ranked

according to the variance between the data. PCA works by measuring the data point covariance matrix and by calculating its eigen vectors and their eigen values.

#### F. Singular Value Decomposition

The singular-value decomposition (SVD) is a factorization of a real or complex matrix [18] and it decomposes a matrix into three other matrices that are shown in equation 2.

$$A = U\Sigma V^T \quad (2)$$

where,  $A$  is an  $m \times n$  matrix,  $U$  is an  $m \times m$  orthogonal matrix,  $S$  is an  $n \times n$  diagonal matrix,  $V$  is an  $n \times n$  orthogonal matrix. By using the complex features of SVD, recommendations are made to the users.

#### G. Collaborative Filtering

Collaborative filtering (CF) is the most popular technique in the field of recommender system. It uses algorithms to find out the similar users or items with similar preferences and characteristics to make a personalized recommendation [19]. User-based CF calculates similarity between each pair of users which is used for recommendation. Again, item-based CF is another similarity based approach where similarities are calculated between items and then similar items are recommended to the users for the purpose of recommendation [20]. Suppose, there are  $m$  users and  $n$  items in a system in which the  $m \times n$  is a matrix that is signified the past behavior of the users. Each cell in the matrix represents the user-item association or interaction. For example, this signifies how user  $u$  prefers item  $m$ . There are two sorts of suppositions, express sentiment and a certain feeling. The preceding one explicitly indicates how a customer rates a item (consider rating an application or a film), although the last one just fills in as an intermediary giving us heuristics about how a customer loves a item (e.g. a number of preferences, clicks, visits) [21]. Express supposition is simpler than testable supposition because we do not have to think about what the number indicates. For example, there may be a tune that is particularly loved by the user, yet he once tunes in to it in view of the fact that he was occupied while tuning in to it. Without express sentiment, it can't be made sure whether the client loathes that thing or not. Notwithstanding, a large portion of the criticism that is gathered from users are understood.

Some collaborative filtering approaches are discussed here.

1) *Clustering Method using Classification Algorithm*: One of the issue of recommender system is the cold start issue which is identified with the existence of new users and items [22]. Recommender system does not have adequate data to make recommendations at the time of new users arrival [23]. This framework uses a technique of three arrangements to make suggestions for new users. Users are called as neighbors with the greatest amount of closeness to new users.

2) *Centroid-based Clustering Method Oriented*: The calculation created for centroid-based grouping is used for personalized recommender systems. This strategy includes two suggestion stages [24]. In the first stage, user's remarks are collected and in the second stage, suggestions for dynamic

users are finished by selecting the best quality groups. This framework solves many issues like cold start problem.

3) *Hierarchical Cluster Method*: For the suggestion, this strategy is used. Various leveled grouping is a technique of research to fabricate group progression [25]. It comprises of two types, agglomerative and disruptive. In this part, individual user profiles move towards similar user profiles and clients are isolated into a few gatherings in terms of closeness.

4) *Deep Semantic Similarity Model*: Deep semantic similarity model (DSSM) represents a broader model of semantic similarity [26]. DSSM, created by the MSR Deep Learning Technology Center, is a profound neural system (DNN) displaying strategy for speaking to content strings (sentences, inquiries, predicates, substance specifics, and so on.) in a consistent semantic space and demonstrating semantic similitude between two content strings [27]. DSSM has wide applications including data recovery and web look positioning, promotion choice/significance, logical substance hunt, and intriguing quality undertakings, question noting, information derivation, picture, and machine interpretation. DSSM can be utilized to create idle semantic models that venture elements of various kinds (e.g., inquiries and archives) into a typical low-dimensional semantic space for an assortment of machine learning assignments, for example, positioning and order. For instance, in web seek positioning, the significance of a report given a question can be promptly figured as the separation between them in that space.

### III. PROPOSED SYSTEM USING EXTENDED MATRIX FACTORIZATION AND AUTOENCODER

Usually, a recommender system's performance depends on the accuracy of similarity determination of users or items and this similarity is identified in an acceptable rate when there exists fairly dense amount of data in the data set. But at the case of new user or item, it is hard to predict the recommendation for that user or item because of the existence of the small amount of correlated data. The problem is considered as the cold start problem. Again, when the data set is sparse or when a new user or item enters in the system, there exists no similarity metrics that can be used. To eliminate these issues, a similarity measure have been proposed here. A flowchart has been displayed in Fig. 4 to depict our proposed recommender system.

#### A. User Similarity Determination by using Extended Matrix Factorization

Matrix factorization (MF) is a newly developed technique for finding parts-based data and linear representations. It has many sub categories with individual specialties but for the proposed system, non-negative matrix factorization (NNMF) has been used with some extension. NNMF is a group of logistic regression and linear algebra methodologies in which a  $T$  matrix is factorized into two  $P$  and  $Q$  matrices with the assumption that there exists no negative elements in all three matrices and an example can be seen from Fig. 5.

Formal consideration is given to extended matrix factorization (EMF) algorithm to solve the problem: extended matrix factorization given the non-negative matrix  $T$ , non-negative matrix factors  $P$  and  $Q$  as the following equations 3:

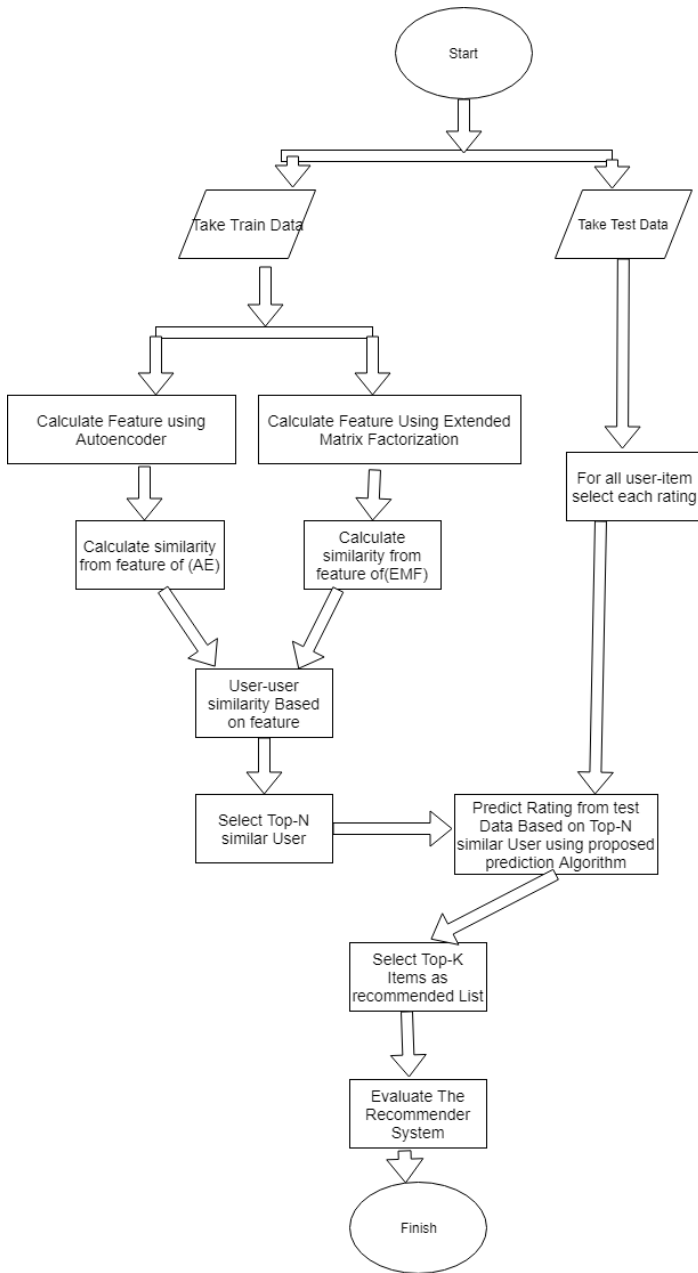


Fig. 4. Flowchart of the Proposed System.

$$T \sim P \times Q \quad (3)$$

In fact, these algorithms are very easy to implement and conversion properties are guaranteed which means continual update regulation iterations are pretty much guaranteed to converge an optimal local matrix factorization. For calculating similarity of the users, a user-item rating matrix has been taken where each column of the matrix denotes a movie and every row determine the system's users. For the calculation of the prediction of the rating of user-movie pair is done by using following equation 4:

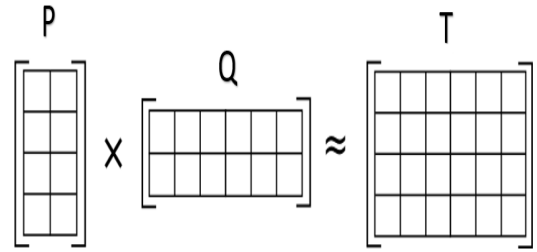


Fig. 5. Matrix Factorization.

$$\hat{X}_{ij} = \sum_{k=1}^k y_{ik} \times z_{kj} \quad (4)$$

After few iterations, it will generate predictions with errors. So get the desired output, the errors must be minimized with some function. So, gradient descent is a good option to minimize the errors and make the prediction more accurate as it helps converge to the minimum error. To calculate the errors, the following equation 5 have been used:

$$f_{ij} = (x_{ij} - \hat{x}_{ij}) = (x_{ij} - \sum_{k=1}^k y_{ik} \times z_{kj}) \quad (5)$$

To reduce the errors as small as possible and actually find the curve of the errors by taking the error gap for each element or value, the successive equations (equation 6 and 7) are used.

$$\frac{\delta}{\delta y_{ik}} = -2(x_{ij} - \hat{x}_{ij})(z_{kj}) = -2f_{ij}z_{kj} \quad (6)$$

$$\frac{\delta}{\delta z_{kj}} = -2(x_{ij} - \hat{x}_{ij})(y_{ik}) = -2f_{ij}y_{ik} \quad (7)$$

By using the learning rate, errors have to be updated. The learning rate determines that how far the gradient should be traveled. If the learning rate is not set properly, it might be set to a rate which does not overshoot the minimum and does not bring any unnecessary complexity. Equation 8 and 9 have been used for the updating of the errors.

$$y'_{ik} = y_{ik} + \alpha \frac{\delta}{\delta y_{ik}} f_{ij} = y_{ik} + 2\alpha f_{ij} z_{kj} \quad (8)$$

$$z'_{kj} = z_{kj} + \alpha \frac{\delta}{\delta z_{kj}} f_{ij} = z_{kj} + 2\alpha f_{ij} y_{ik} \quad (9)$$

At these stage, by subtracting the similarity of users, the difference between each pair of users can be found and after multiplying with  $-1$ , this difference turns into similarity.

$$Similar_{EMF}(u, v) = \sum_{k=1}^K (y_{(u,k)} - y_{(v,k)}) \times (-1) \quad (10)$$

After these calculation, the similarity of user-user can be found by using extended matrix factorization.

$$outL_i^j = \frac{1}{1 + e^{-L_i^j}} \quad (12)$$

### B. User Similarity Determination by using Autoencoder

Autoencoder (AE) is neural network that has the same outputs as the inputs. Its aim is to compress the input and rebuild the output from latent representation. This sort of neural network comprises of two parts, one being encoder and the other being decoder. An encoder is a major part of the neural network which mainly compresses the input into a latent representation. This can be presented with the  $l = f(x)$  encoding function. A decoder is a part meant for the restoration of the input representation of latent space. It can be defined with the function  $r = g(h)$  to decode. As the structure of the autoencoder is like a basic neural network so it gives the freedom to choose as much layers as needed on the basis of the requirement. For the proposed system, the rating has been considered as the input. So, the input layer has ratings as input data and the amount of input data is the same as the total dataset. The second layer contains 100 neurons and act as an encoder. The third layer is the latent feature representation layer which contains 50 neurons and the fourth layer contains 100 neurons also. Finally, the last layer contains the same number of neurons as the input layer. So, this autoencoder contains total five layers. All the layers and neurons are connected to each other. Their weights are also initialized. The main target of this stage is to find similarity between users by using autoencoder like in Fig. 6.

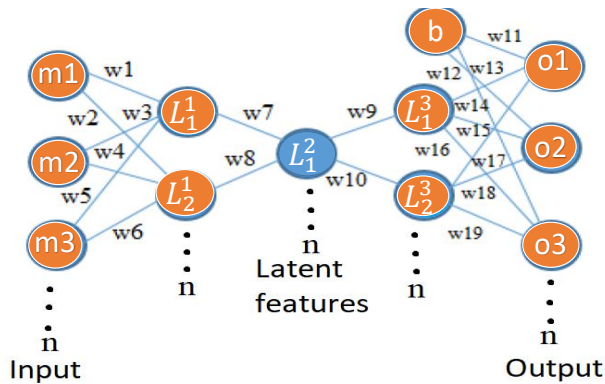


Fig. 6. Autoencoder with Five Layers.

Here,  $m_1, m_2, m_3$  to  $n$  denote the input neurons and synapses are initialized. For the computation value of the every neuron must be calculated. For calculating the neuron's value of the hidden layer, the ensuing equation 11 is used.

$$L_i^j = \sum m_i \times w_i \quad (11)$$

Here,  $L_i^j$  is the hidden layer where  $i$  is identified as the number of neurons and  $j$  is the number of hidden layers. For activation function, sigmoidal function has been used as the outputs of sigmoidal function exits between 0 and 1. After getting the value of  $L$ , it should be passed through the activation function to activate it. So here equation 12 is the activation function equation.

As all the neurons have the same structure and that's why calculation of the neurons till the output layer is the same with some added bias. After the calculation to the output layer, prediction can be found with some errors and to identify the errors following equation 13 has been used:

$$TotalF = \sum (m_i - o_i)^2 \quad (13)$$

At the stage to minimize and updating the errors, backpropagation is used which helps to minimize the errors and update the value of every neuron to make the correct prediction. The calculation of backpropagation for the output layers is as follows:

$$\frac{\delta TotalF}{\delta w_i} = \frac{\delta TotalF}{\delta outo_i} \times \frac{\delta outo_i}{\delta o_i} \times \frac{\delta o_i}{\delta w_i} \quad (14)$$

After backpropagation, errors will be reduced and these errors will help to update the weights and also produce accurate prediction. So, the updating equation:

$$w_i^+ = w_i + \alpha \delta w_i \quad (15)$$

The calculation of the backpropagation is not same for all hidden layers and different from the output layers also because the output of every hidden layer neurons contributes to several output neurons.

$$\frac{\delta TotalF}{\delta w_i} = \frac{\delta TotalF}{\delta outL_i^j} \times \frac{\delta outL_i^j}{\delta L_i^j} \times \frac{\delta L_i^j}{\delta w_i} \quad (16)$$

$$\frac{\delta TotalF}{\delta w_i} = (\delta_i \times w_i) \times outL_i^j \times i \quad (17)$$

$$\delta_i = (x_i - o_i) \times (outo_i) \times (1 - outo_i) \quad (18)$$

For these layers updating equation is the same which has been shown before. At this stage, the latent feature representation can be found at the third layer and after sufficient iterations, the prediction of the rating can be done. Afterward, subtracting the features of each user pair dissimilarity can be identified and multiplying it with  $-1$  user-user similarity is found. After that the similarities between users achieved from autoencoder and extended matrix factorization have been used for the prediction method.

$$Similar_{AE}(u, v) = \sum_{k=1}^K (L_{(u,k)} - L_{(v,k)}) \times (-1) \quad (19)$$

#### IV. PROPOSED PREDICTION METHOD

The prediction method which is described here is similar to the generic recommender system prediction method [28]. User based similarity that is achieved from both EMF and autoencoder, has been taken to make prediction more accurate. It can be called a comprehensive prediction method as two methods have been merged.

$$pred_{u,m} = \bar{r}_u + \frac{\sum_{v \in U} [Sim_{AE}(u,v) \times Sim_{EMF}(u,v) \times (r_{v,m} - \bar{r}_v)]}{\sum_{v \in U} Sim_{AE}(u,v) \times Sim_{EMF}(u,v)} \quad (20)$$

Here,  $\bar{r}_u$  is the average rating of the user  $u$  and  $r_{(v,m)}$  is the actual rating. Here,  $\bar{r}_v$  represents the average rating of the user  $v$ .

---

#### Algorithm 1 Proposed Prediction Function Algorithm.

---

INPUT: User( $u$ ), Item( $m$ ), Rating, Similarity  
 OUTPUT: Predicted Rating

- 1:  $SU \leftarrow 0, TU \leftarrow 0, minRating \leftarrow 1, maxRating \leftarrow 5$
- 2: **for all**  $v \in Users$  **do**
- 3:     **if**  $ratings_{v,m} <> 0$  **then**
- 4:          $SU \leftarrow SU + sim(ae)_{u,v} \times sim(emf)_{u,v} \times (ratings_{v,m} - avgRat_v)$
- 5:          $TU \leftarrow TU + sim(ae)_{u,v} \times sim(emf)_{u,v}$
- 6:     **end if**
- 7: **end for**
- 8:  $userOffset \leftarrow (SU/TU)$
- 9:  $rating_{u,m} \leftarrow userOffset + avgRatings_u$
- 10: **if**  $(rating_{u,m} < minRating)$  **then**
- 11:      $rating_{u,m} \leftarrow minRating$
- 12: **end if**
- 13: **if**  $(rating_{u,m} > maxRating)$  **then**
- 14:      $rating_{u,m} \leftarrow maxRating$
- 15: **end if**
- 16: **if**  $(rating_{u,m} <> 0)$  **then**
- 17:     **Return**  $rating_{u,m}$
- 18: **end if**
- 19: **Return**  $(rating_{u,m})$

---

#### V. PERFORMANCE EVALUATION

Most of the existing recommender system's calculation is focused on the offline predictive accuracy assessment. The benefit of offline evaluation is that it is fast, cost-effective and can be used different data sets and metrics frequently. For our experimental purpose, offline analysis has been focused. The data set has experimented here is the Movielens (ML-1M) dataset. It contains a total user of 6040 and total movies of 3952 with a rating of 1000209 which is shown in Table I. Each user in the data set has been rated at least 20 movies. The density of the user-item matrix 4.1% in Movielens ML-1M data set. The important parameters of the data set are listed in the following Table I which are used in the experimental section.

The most commonly used evaluation methodologies are mean absolute error, precision, recall, f-measures, and average reciprocal hit rank. With regard to the system task, each metric has advantages and disadvantages. A true positive (TP) is an

TABLE I. IMPORTANT PARAMETERS OF THE DATASET.

| Dataset   | Users | Items | Rating |
|-----------|-------|-------|--------|
| Movielens | 6040  | 3952  | 1-5    |

upshot where the system accurately forecasts the positive class. Similarly, a true negative (TN) is an upshot where the system accurately forecasts the negative class. A false positive (FP) is an upshot where the system inaccurately forecasts the positive class. And a false negative (FN) is an upshot where the system inaccurately forecasts the negative class [29].

#### A. Mean Absolute Error

In the group of statistical accuracy metrics, the mean absolute error (MAE) compares the predicted ratings with the actual ratings [29]. MAE takes into consideration in particular the absolute average difference between the predicted rating and the user's actual rating which is shown in equation 21.

$$MAE = \frac{\sum_{i=1}^{m_a} |R_{a,i} - P_{a,i}|}{m_a} \quad (21)$$

However, evidence suggests that when the MAE is reduced, other metrics have shown significant improvement. In the field of recommender system, the good rating should be predicted as good so that good predicted item with good rating can be recommended. Mean absolute error also takes the bad rating into consideration. This shows that for the Top-N recommendations, MAE is not the best evaluation measure.

#### B. Precision

Precision actually defines that how precise a classification model is. When dealing with the classification, precision can be proved as a very useful evaluation measurement. It is the amount of correct positive prediction [30]. The proportion of recommended items which is precision that users in the test set really liked [31]. For better performance, this value should be high.

$$Precision = \frac{TP}{TP + FP} \quad (22)$$

#### C. Recall

The recall is the fraction of the relevant documents that are successfully retrieved [30]. value is well in the training set, which ranks the average percentage of components in the test set. For better performance, this value should be high.

$$Recall = \frac{TP}{TP + FN} \quad (23)$$

#### D. F-measure

Precision and recall are two of the important evaluation measurement and the weighted average of them is f-measure [32]. Good precision and bad recall results in bad recommendation. Again, bad precision and good recall results in bad recommendation as well. So, both effects should be higher for



better recommendation. F-measure value might be higher when both of the value of precision and recall is high is given in equation 24. Both precision and recall are taken into account to calculate the measure where precision is the ratio of right positive results divided by the number of positive outcomes and recall is the number of precise positive results divided by the number of positive outcomes.

$$F_{Measures} = \frac{2 \times Precision \times Recall}{Precision + Recall} \quad (24)$$

### E. Average Reciprocal Hit Rank

The average reciprocal hit rank (ARHR) [33], [34] is a statistical measure of the ranking which offers a list of recommendations sorted by the probability of accuracy. The average reciprocal hit rank can be defined using the equation 25.

$$ARHR = \frac{1}{N} \times \sum_{i=1}^N \frac{1}{rank_i} \quad (25)$$

## VI. EXPERIMENT AND MEASUREMENT

Fig. 7 to 15 shows the results obtained with the data set of movielens 1 – m. From these figures, it has seen that how the proposed method and the quality measures (MAE, precision, recall, f - measures, ARHR) are carried out. Here, the results are generated using top-n neighbors vs precision, top-n neighbors vs recall, top-n neighbors vs f-measures, and top-k recommendation vs average reciprocal hit rank. With the increase of the neighbour size and recommendation significant improvement have been observed.

### A. Top-N Neighbor Vs Evaluation Measures

Mean absolute error, precision, recall, f-measures are utilized to evaluate the collaborative filtering recommender system. From Fig. 7 and 8, it can be seen that the relationship between neighbor size and MAE is inverse that is with the increase of the the neighbor size the mean absolute error will decrease. From Fig. 8, it is observed that the comprehensive approach of both autoencoder and extended matrix factorization (ACCFAERS) outperforms in all circumstances.

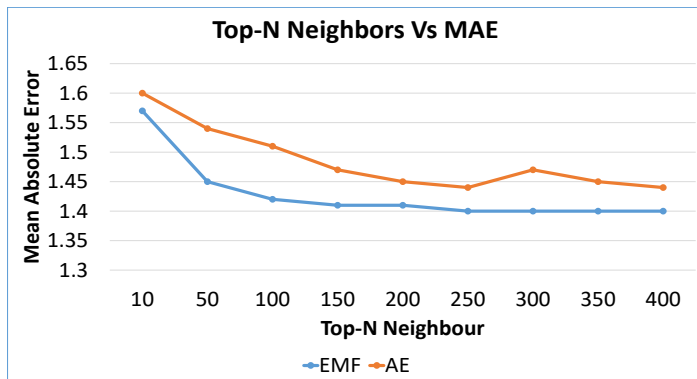


Fig. 7. Top-N Neighbor vs. mean absolute error for AE and EMF.

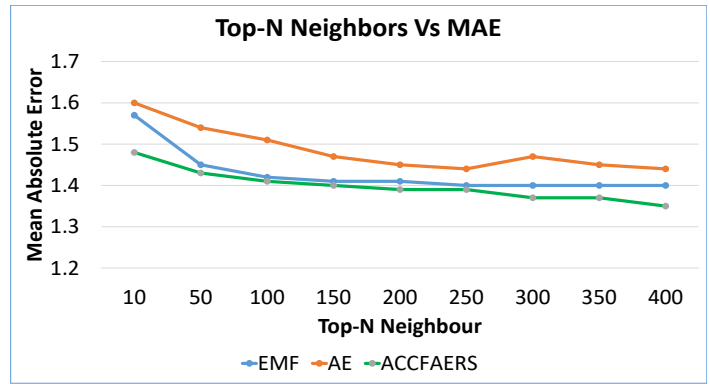


Fig. 8. Top-N Neighbor vs. mean absolute error for Proposed Method.

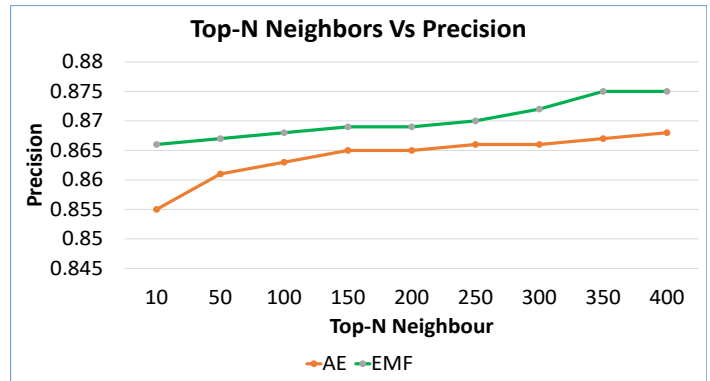


Fig. 9. Top-N Neighbor vs. Precision For AE and EMF.

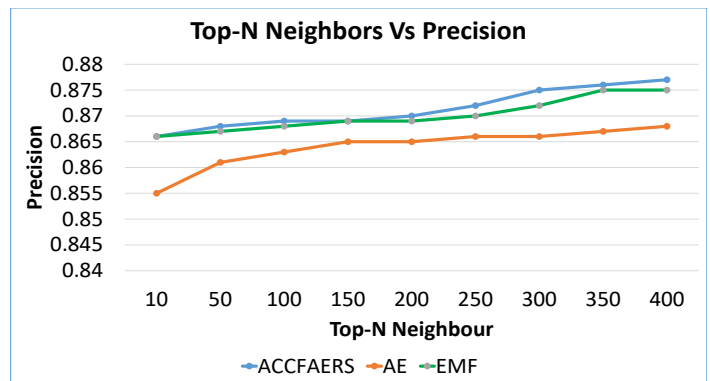


Fig. 10. Top-N Neighbor vs. Precision For Proposed method.

Again from Fig. 9 and 10, it is clear that the precision increases with the increase of neighbor size and the proposed method performs better than other methods.

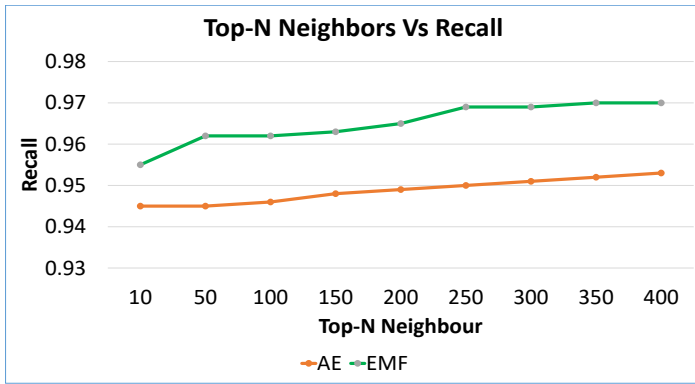


Fig. 11. Top-N Neighbor vs. Recall For AE and EMF.

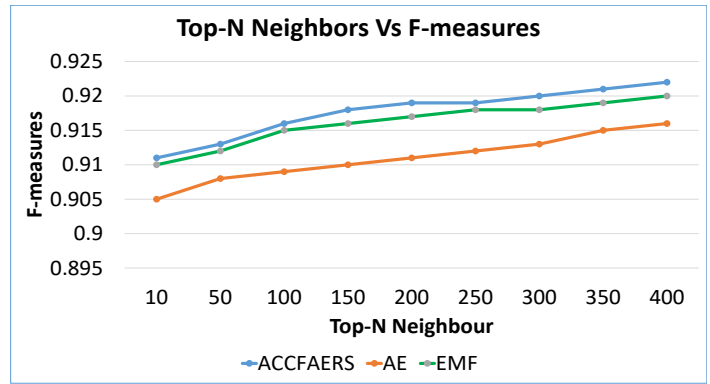


Fig. 14. Top-N Neighbor vs. F-measures For Proposed method.

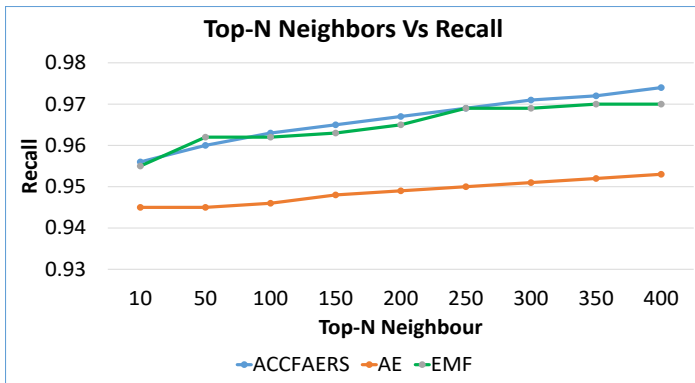


Fig. 12. Top-N Neighbor vs. Recall For Proposed method.

B. TOP-K Recommendation vs. ARHR

Results have been evaluated in this paper using the top-K recommendation versus the average reciprocal hit rank that are utilized on the collaborative filtering recommendation system. In Fig. 15, the result of average reciprocal hit rank have been shown. The more accurate the average reciprocal hit rank result in more accurate list of recommendations.

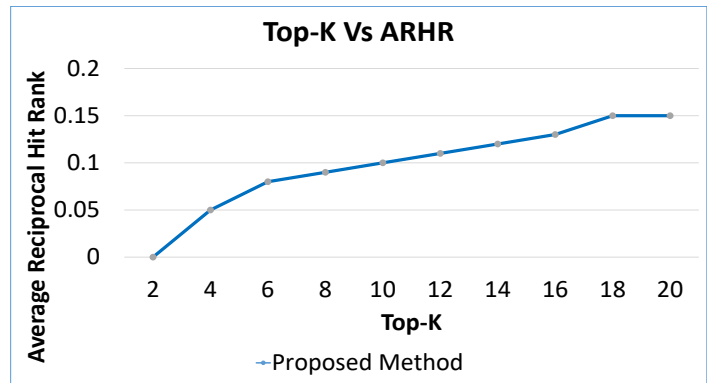


Fig. 15. Top-k Recommendation vs. ARHR.

Finally, Fig. 11, 12, 13, and 14 are used to show that recall and f-measures also increase with the increase of the neighbor size.

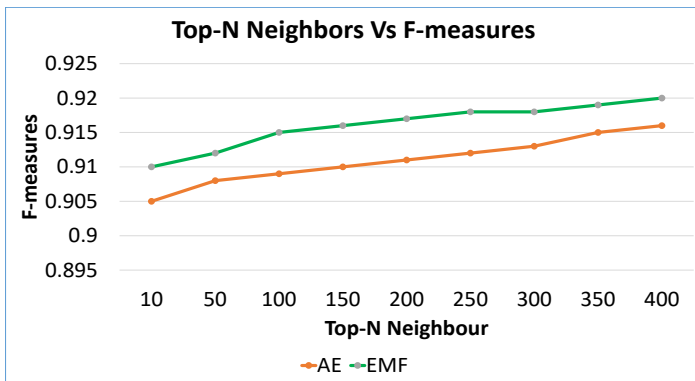


Fig. 13. Top-N Neighbor vs. F-measures For AE and EMF.

It is observed that the comprehensive approach of both autoencoder and extended matrix factorization provide better recommendation and also yield better results in terms of evaluation measures.

VII. CONCLUSION

Deep learning based methods can be called the soul of the recommender system. Performance of the recommender system mostly depends on how much accurate these methods perform. Autoencoder and matrix factorization both performs well in recommender system. They provide good performance individually but the performance of the combination of both methods is better. An approach has also been discussed in this research that how similarity between users can be found using autoencoder and extended matrix factorization for better prediction. Deep learning methods has gone further with the newer tools and techniques. Other methods like convolutional neural network, recurrent neural network, adversarial networks, and the attention based model can be used to improve the recommendation performance.

REFERENCES

- [1] R. Katarya and O. P. Verma, "Effective collaborative movie recommender system using asymmetric user similarity and matrix factorization," in *2016 International Conference on Computing, Communication and Automation (ICCCA)*, pp. 71–75, IEEE, 2016.
- [2] N. Mittal, R. Nayak, M. C. Govil, and K. C. Jain, "Recommender system framework using clustering and collaborative filtering," in *2010 3rd International Conference on Emerging Trends in Engineering and Technology*, pp. 555–558, IEEE, 2010.
- [3] F. Roy, S. M. Sarwar, and M. Hasan, "User similarity computation for collaborative filtering using dynamic implicit trust," in *International Conference on Analysis of Images, Social Networks and Texts*, pp. 224–235, Springer, 2015.
- [4] A. Pujahari and V. Padmanabhan, "Group recommender systems: Combining user-user and item-item collaborative filtering techniques," in *2015 International Conference on Information Technology (ICIT)*, pp. 148–152, IEEE, 2015.
- [5] A. Pal, P. Parhi, and M. Aggarwal, "An improved content based collaborative filtering algorithm for movie recommendations," in *2017 Tenth International Conference on Contemporary Computing (IC3)*, pp. 1–3, IEEE, 2017.
- [6] C. A. Gomez-Uribe and N. Hunt, "The netflix recommender system: Algorithms, business value, and innovation," *ACM Transactions on Management Information Systems (TMIS)*, vol. 6, no. 4, p. 13, 2016.
- [7] J. Lund and Y.-K. Ng, "Movie recommendations using the deep learning approach," in *2018 IEEE International Conference on Information Reuse and Integration (IRI)*, pp. 47–54, IEEE, 2018.
- [8] B. Yi, X. Shen, Z. Zhang, J. Shu, and H. Liu, "Expanded autoencoder recommendation framework and its application in movie recommendation," in *2016 10th International Conference on Software, Knowledge, Information Management & Applications (SKIMA)*, pp. 298–303, IEEE, 2016.
- [9] Q. Lu, D. Yang, T. Chen, W. Zhang, and Y. Yu, "Informative household recommendation with feature-based matrix factorization," in *proceedings of the 2nd Challenge on Context-Aware Movie Recommendation*, pp. 15–22, ACM, 2011.
- [10] D. Li, R. Li, and S. Zhang, "A deep learning image recognition framework accelerator based parallel computing," in *Proceedings of the 2018 2nd International Conference on Deep Learning Technologies*, pp. 16–20, ACM, 2018.
- [11] P. Tzirakis, J. Zhang, and B. W. Schuller, "End-to-end speech emotion recognition using deep neural networks," in *2018 IEEE International Conference on Acoustics, Speech and Signal Processing (ICASSP)*, pp. 5089–5093, IEEE, 2018.
- [12] A. Utku, I. A. DoGru, and M. A. Akcayol, "Permission based android malware detection with multilayer perceptron," in *2018 26th Signal Processing and Communications Applications Conference (SIU)*, pp. 1–4, IEEE, 2018.
- [13] Y. Shen, X. He, J. Gao, L. Deng, and G. Mesnil, "Learning semantic representations using convolutional neural networks for web search," in *Proceedings of the 23rd International Conference on World Wide Web*, pp. 373–374, ACM, 2014.
- [14] T. Guo, J. Dong, H. Li, and Y. Gao, "Simple convolutional neural network on image classification," in *2017 IEEE 2nd International Conference on Big Data Analysis (ICBDA)*, pp. 721–724, IEEE, 2017.
- [15] N. Chowdhury *et al.*, "A comparative analysis of feed-forward neural network & recurrent neural network to detect intrusion," in *2008 International Conference on Electrical and Computer Engineering*, pp. 488–492, IEEE, 2008.
- [16] E. Merindasari, M. R. Widyanto, and T. Basaruddin, "An overview of learning algorithms and inference techniques on restricted boltzmann machines (rbms)," in *Proceedings of the 2nd International Conference on Software Engineering and Information Management*, pp. 16–20, ACM, 2019.
- [17] K. George, "An application of pca to rank problem parts," in *Proceedings of the Second International Conference on Computational Science, Engineering and Information Technology*, pp. 341–345, ACM, 2012.
- [18] D. Novrilianto, H. Murfi, and A. Wibowo, "The singular value decomposition-based anchor word selection method for separable non-negative matrix factorization," in *2017 International Conference on Asian Language Processing (IALP)*, pp. 289–292, IEEE, 2017.
- [19] S. S. Peerzade, "Web service recommendation using pcc based collaborative filtering," in *2017 International Conference on Energy, Communication, Data Analytics and Soft Computing (ICECDS)*, pp. 2920–2924, IEEE, 2017.
- [20] Y. Koren, "Factorization meets the neighborhood: a multifaceted collaborative filtering model," in *Proceedings of the 14th ACM SIGKDD international conference on Knowledge discovery and data mining*, pp. 426–434, ACM, 2008.
- [21] Y. Koren, "Tutorial on recent progress in collaborative filtering," in *RecSys '08 Proceedings of the 2008 ACM conference on Recommender systems*, pp. 333–334, ACM, 2008.
- [22] A. Kyriakopoulou and T. Kalamboukis, "Using clustering to enhance text classification," in *Proceedings of the 30th annual international ACM SIGIR conference on Research and development in information retrieval*, pp. 805–806, ACM, 2007.
- [23] J. Erman, M. Arlitt, and A. Mahanti, "Traffic classification using clustering algorithms," in *Proceedings of the 2006 SIGCOMM workshop on Mining network data*, pp. 281–286, ACM, 2006.
- [24] F. Gullo and A. Tagarelli, "Uncertain centroid based partitioned clustering of uncertain data," *Proceedings of the VLDB Endowment*, vol. 5, no. 7, pp. 610–621, 2012.
- [25] R. Florence, B. Nogueira, and R. Marcacini, "Constrained hierarchical clustering for news events," in *Proceedings of the 21st International Database Engineering & Applications Symposium*, pp. 49–56, ACM, 2017.
- [26] G. Zhao and J. Huang, "DeepSim: deep learning code functional similarity," in *Proceedings of the 2018 26th ACM Joint Meeting on European Software Engineering Conference and Symposium on the Foundations of Software Engineering*, pp. 141–151, ACM, 2018.
- [27] D. Hu, X. Lu, and X. Li, "Multimodal learning via exploring deep semantic similarity," in *Proceedings of the 24th ACM international conference on Multimedia*, pp. 342–346, ACM, 2016.
- [28] M. Hasan, S. Ahmed, M. A. I. Malik, and S. Ahmed, "A comprehensive approach towards user-based collaborative filtering recommender system," in *2016 International Workshop on Computational Intelligence (IWCI)*, pp. 159–164, IEEE, 2016.
- [29] L. Mendo, "Estimation of a probability with guaranteed normalized mean absolute error," *IEEE Communications Letters*, vol. 13, no. 11, pp. 817–819, 2009.
- [30] P. Prashar and T. Choudhury, "Suicide forecast system over linear regression, decision tree, naive bayesian networks and precision recall," in *2018 8th International Conference on Cloud Computing, Data Science & Engineering (Confluence)*, pp. 310–313, IEEE, 2018.
- [31] P. Lingras and C. J. Butz, "Precision and recall in rough support vector machines," in *2007 IEEE International Conference on Granular Computing (GRC 2007)*, pp. 654–654, IEEE, 2007.
- [32] J. Sepulveda and S. Velastin, "F1 score assesment of gaussian mixture background subtraction algorithms using the muhavi dataset," 2015.
- [33] M. A. Najork, H. Zaragoza, and M. J. Taylor, "Hits on the web: How does it compare?," in *Proceedings of the 30th annual international ACM SIGIR conference on Research and development in information retrieval*, pp. 471–478, ACM, 2007.
- [34] D. Xiaomeng and M. Su, "Incorporating consumer browse data: Extended item-based top-k recommendation algorithms," in *In 2013 International Conference on Information Technology and Applications*, pp. 248–253, IEEE, 2013.

# Satellite Image Enhancement using Wavelet-domain based on Singular Value Decomposition

Muhammad Aamir<sup>1\*</sup>, Ziaur Rahman<sup>2</sup>, Yi-Fei Pu<sup>3</sup>  
College of Computer Science,  
Sichuan University, Chengdu, China, 610065

Waheed Ahmed Abro<sup>4</sup>  
School of Computer Science and Engineering,  
Southeast University, Nanjing, China, 210096

Kanza Gulzar<sup>5</sup>  
School of Big Data and Software Engineering  
Chongqing University, Chongqing, 401331, China  
University Institute of Information Technology,  
PMAS Arid University,  
Rawalpindi, 46000, Pakistan

**Abstract**—Improving the quality of satellite images has been considered an essential field of research in remote sensing and computer vision. There are currently numerous techniques and algorithms used to achieve enhanced performance. Different algorithms have been proposed to enhance the quality of satellite images. However, satellite images enhancement is considered a challenging task and may play an integral role in a wide range of applications. Having received significant attention in recent years, this manuscript proposes a methodology to enhance the resolution and contrast of satellite images. To improve the quality of satellite images, in this study, first, the resolution of an image is improved. For resolution enhancement, first, the input image is decomposed into four frequency components ( $LL, LH, HL, and HH$ ) using the stationary wavelet transform (SWT). Second, Singular value matrices (SVMs)  $U_A$  and  $V_A$  which contains high-frequency elements of an input image are obtained using singular value decomposition (SVD). Third, the high-frequency components ( $LH, HL$ ) of an input image are obtained using discrete wavelet transform (DWT) and corrected by SVMs and SWT. Next, the interpolation factor is added and the high-resolution image is obtained using inverse discrete wavelet transform (IDWT). Second, the contrast of the image is optimized. For the contrast enhancement, the image is decomposed using DWT into sub-bands such as ( $LL, LH, HL, and HH$ ). Next, the singular value matrix (SVM) of the  $LL$  sub-band is obtained which contains the illumination information. Then, SVM is modified to enhance the contrast. Finally, the image reconstructed using the IDWT. In this paper, the results from the method above are compared with existing approaches. The proposed method achieves high performance and yields more insightful results over conventional technique.

**Keywords**—Satellite Images; Image Enhancement; Singular Value Decomposition (SVD); Discrete Wavelet Transforms (DWT); Stationary Wavelet Transform (SWT)

## I. INTRODUCTION

In recent years, the demand for visual information is increasing exponentially. It has been observed that visual information such as photos, audios, videos, etc. is one of the fundamental resources of receiving data which plays an integral role in people's lives [1]. Most of the information people receive and work with is visual information, particularly audio and image based. The human brain has the capability of processing visual information efficiently. The more substantial part of the human brain is dedicated to handling visual information. In contrary, the computer systems have not the

ability to interpret, sense and effectively process the visual information. The performance of the visual systems can be influenced by many factors such as viewpoint and perspective, illumination, scale, deformation, and high intraclass variations. While discussing the visual information and their importance in today's life, one cannot ignore the growing demand for the quality images in many applications such as geosciences studies [2], biomedical imaging [3], astronomy [4], geographical information systems [5], surveillance [6], and remote sensing [7]. The usage of quality images is an essential requirement to achieve robust results. Furthermore, many factors such as poor illumination, adverse weather conditions, moving object, poor camera resolutions, etc. can affect the quality of images. These factors can extensively influence the contrast and resolution (dimension) of the images.

Extending the discussion about the quality of the images, in remote sensing, the quality of satellite images is also essential. Satellite images are widely used in many applications including urban planning and management, military planning, population estimation, and disaster monitoring. The resolution (dimension) and contrast of an image considered as one of the most significant quality characteristics in satellite images. The images can be transformed to get high-quality images with high resolution and standard contrast. Therefore, to improve the quality of satellite images, the image enhancement in satellite images has been an aspiration of rigorous research for numerous years. Over the years, many techniques have been proposed to enhance the resolution and contrast of 'poor-quality satellite images. Besides, these algorithms have the great ability to deal with diverse aspects of image quality, such as dark areas, noise, light distortion, texture details, colour, scale, etc. The interpolation is one the most commonly used techniques to image resolution enhancement. The interpolation is a widely adopted method to increase the number of pixels in an image [8], [9], [10]. The most commonly used interpolation techniques are bilinear interpolation, wavelet zero padding [11], bi-cubic interpolation [12] and nearest neighbor interpolation.

Furthermore, the wavelet transform also plays an incredible role to enhance the quality of the image. Many wavelet-based techniques have been developed to increase the dimension of the image. In particular, discrete wavelet transform (DWT), integer wavelet transforms (IWT), and stationary wavelet trans-

form (SWT) are the mostly adopted techniques respectively. Moreover, as we discussed, the contrast is one of the essential quality factors in the satellite images. Besides, in satellite images one the most common problems are their low contrast [13]. Contrast improvement is the pre-processing step in different remote sensing applications, and it is considered one of the most challenging issues [14]. Contrast is determined by the difference in high and low-intensity levels of an object with other objects. The contrast enhancement is necessary to provide better interpret-ability, analysis, representation, diagnosis, and perception of information in the low contrast images [15]. Low contrast image is flat with variations in the brightness and density value such as it is hard to differentiate between their dark and light values. The low contrast of an image could be the result of many reasons such as a low-resolution camera, aliasing due to improper selection of sampling rate or poor illumination.

Moreover, the information in the low contrast images is highly concentrated over a narrow range in some areas. The data may be lost in those areas which are extremely and uniformly concentrated. Therefore, to obtain a high contrast image which represents all the information to provide better input for remote sensing applications is necessary. Over the years, researchers have put lots of efforts in this field and several methods has been presented. Among them, Histogram equalization (HE) is the most popular technique to enhance the contrast of an image. Furthermore, HE is divided into two kinds: global histogram equalization (GHE) and local histogram equalization (LHE). Both of the methods have their advantages and disadvantages. GHE is a simple and more effective method to improve the contrast of the image based on global information. GHE required a less computational cost.

On the other hand, in compare to GHE, LHE is more robust in improving the overall contrast of the image, but it needed a high computational cost. Moreover, both methods change the brightness value of the input image significantly. This change results in some unwanted artefacts, which causes the saturation in uniform areas (very bright and very dark intensities) of the processed image. Furthermore, to avoid these inadequacies, several methods have been developed [16], [17], [18], [19], [20]. On the contrary, to prevent the limitations associated in HE method to enrich the contrast of the image. Singular value decomposition-based techniques have been introduced [14], [21], [22], [23], [24], [25].

In this paper, a combined approach to enhance the quality of the image has been proposed. The method first uses the bi-cubic interpolation to improve the dimension of the low-resolution images based on SVD, SWT, and DWT. Next, the contrast of the high-resolution image is enhanced based on SVD and DWT.

The rest of the paper is organized as follows: Section II discusses the theoretical background of the study, Section III elaborates the proposed methodology in detail, Section IV presents the experimental results and analysis, Section V contains the summary of the paper, and finally Section VI describes the future work.

## II. THEORETICAL BACKGROUND

In recent years, a great deal of effort has been invested in the development of approaches to image enhancement in satellite, aerial and natural images [30][31]. Furthermore, earlier works and initiatives that have been made to enrich the contrast and resolution of the images adequately are briefly examined as follows. Neena et al. [8], proposed a technique for image enhancement. The proposed technique up-scaled the resolution of an input image based on bi-cubic interpolation and stationary wavelet transform (SWT). The proposed model achieved excellent performance over conventional methods but required a high computational cost. Zhang et al. [9], suggested a model which combines two methods of interpolation that rational and fractal models which upscale the input image (low-resolution) to high-resolution image. The proposed method achieves robust performance with smooth edges and less blurring. However, the process produced high complexity. Kang et al. [10], introduced a model, which uses image interpolation based on direct adaption and image restoration. The proposed method adopts the bi-linear and bicubic interpolation filters to reduce the jaggling artefacts in edge regions. The experimental result shows that the method achieved good interpolation efficiency compared to state-of-the-art techniques. Though, the system has some weaknesses. Tinku et al. [11], has proposed an algorithm for image resolution. The technique is based on both non-adaptive and adaptive image interpolation. The process yields robust performance and improves the quality of an image vigorously. Furthermore, Keys et al [12], has developed a method which is based on cubic convolutional interpolation. The proposed method has a robust performance in resampling the discrete data and yields the excellent performance in scaling up the resolution on an image.

Demirel et al. [21][22] have developed the model to contrast enhancement. The method used the singular value decomposition to equalized the processed image. In comparing to HE methods, the proposed methods yield good performance. However, the method performance is not good for the low contrast images as the intensity of Low-contrast image varies in three different types, i.e., low range (dark image), mid-range (grey image), and high range (bright image). The method used in Demirel et al. [21], [22], is based on the scaling of singular value and is not suitable for mid-range (grey image). Since, a correction coefficient is close to "1", which suggests that there is no significant change in a singular matrix. Hence, there is no substantial improvement in the intensity of input images. The method is only suitable for low range intensity (dark) images [8].

Contrary to Demirel et al. findings, the proposed model is ideal for both Low and mid-range intensity images (dark and grey) and carries the ability to enhance the contrast. So, based on this experimental finding, Atta et al. [23], the proposed model presents new insights. The method produces better results for the for mid-range (grey image) intensities value. However, its performance is reduced in comparison to the methods [21], [22] in term of mean, standard deviation, and entropy values.

Based on these findings, the authors are of the view that their experimental approach will provide more meaningful insights into the image quality of the satellite images through low-resolution and low-contrast satellite imaging. The current

study is in comparison to the recent studies and distinguished in its findings.

### III. PROPOSED METHODOLOGY

In this paper, an efficient model is proposed for image enhancement from low resolution and low-contrast satellite imagery. The proposed method comprises two stages, i.e., resolution enhancement and contrast enhancement. In the first stage, the input image is taken to improve dimension by using a DWT method of Fourier transform based on SWT and SVD. Then, the DWT approach is applied to the enhanced resolution image to increase the contrast. The flowchart of the proposed framework is shown in Fig. 1.

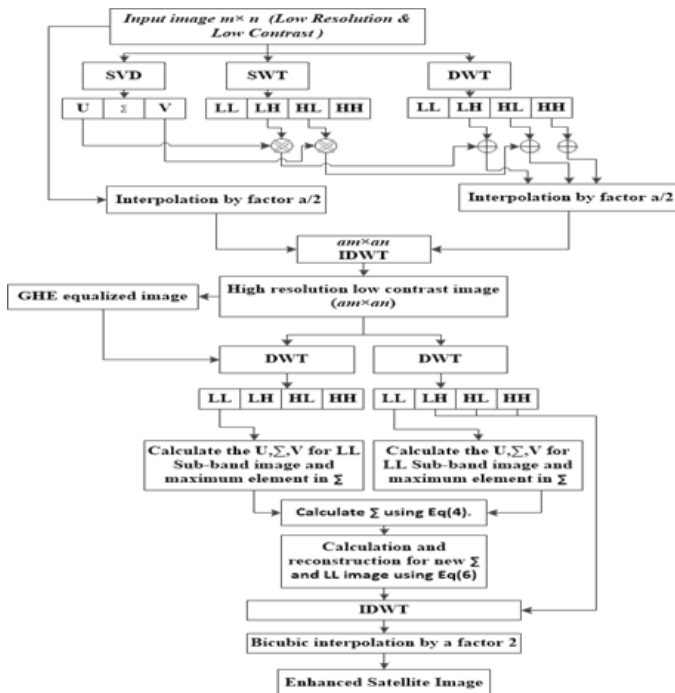


Fig. 1. Proposed method's general flow diagram.

#### A. Image Resolution Enhancement

In satellite images, the resolution is one of the essential features. The resolution of the images can be improved to make the system's overall performance better. In this paper, the resolution of the satellite images is increased using DWT based on SVD and SWT. First, the low-contrast input image  $A$  is decomposed by applying DWT and SWT along the rows and columns of the input image separately. This decomposition results in four different sub-bands, namely, low-low ( $LL$ ), low-high ( $LH$ ), high-low ( $HL$ ), and high-high ( $HH$ ) bands, respectively.

Moreover, the edges are concentrated on  $LH$ ,  $HL$ , and  $HH$  sub-bands which are high-frequency components. Therefore, to obtain the image with high resolution, the high-frequency sub-bands ( $LH$ ,  $HL$ ,  $HH$ ) are corrected. Second, input image has converted to SVD domain to acquire the singular value matrix which is the product of three matrices named an orthogonal matrix  $U_A$ , the transpose of an orthogonal matrix  $V_A$  and a diagonal matrix  $\Sigma_A$ . The singular value matrices  $U_A$

and  $V_A$  contains elements with high-frequency values, and  $\Sigma_A$  contains the illumination information such as intensity of the input image. Third, the coefficients of the orthogonal matrix  $U_A$  along with its transpose matrix  $V_A$  are multiplied with the high-frequency components ( $LH$ ,  $HL$ ) of the input image obtained using SWT. Next, this multiplication result is added to high-frequency components ( $LH$ ,  $HL$ ) obtained using DWT. Then, the bicubic interpolation with a factor of 2 is applied to an input image and estimated coefficients ( $LH$ ,  $HL$ ) along with  $HH$  of DWT. Finally, the interpolated outputs are combined using the inverse discrete wavelet transform (IDWT) to get a high dimensional image.

#### B. Image Contrast Enhancement

Next, the high-resolution, low contrast image  $A$  and its histogram-equalized image  $\hat{A}$  are decomposed by applying 1-D DWT along the horizontal direction (rows) of the image and then the results are decomposed along the vertical direction (columns). The effect of the decomposition is four different kinds of sub-bands namely, low-low ( $LL$ ), low-high ( $LH$ ), high-low ( $HL$ ), and high-high ( $HH$ ) bands, as shown in Fig. 1. As we discussed in the previous section, the edges are concentrated on high-frequency ( $HF$ ) components such as  $LH$ ,  $HL$ , and  $HH$ . Further, any transformation in low-frequency components, such as the  $LL$  sub-band, will not affect the edge information in high-frequency bands since illumination information was concentrated in the  $LL$  sub-band. Second, the  $LL$  sub-band of both input image  $A$  and its histogram-equalized image  $\hat{A}$  are chosen for further processing to improve the contrast of an image.

At this point, the decomposed image has been converted to the SVD domain to obtain the singular value matrix (SVM) which is the product of three matrices, named an orthogonal matrix  $U_A$ , the transpose of an orthogonal matrix  $V_A$ , and a diagonal matrix  $\Sigma_A$ . The SVM contains the illumination information, such as the intensity of the input image. The normalization of the SVM values is attained to change the contrast of the image. The intensity of the input image will only be affected by the modification in the singular values. The  $\Sigma_A$  contains the intensity information of the image. It is one of the leading advantages of using SVD for image equalization [28][29]. Therefore, the SVD of an image, which can be taken as a matrix of size  $N \times N$  can be defined in Eq. (1):

$$A = U_A \sum_A V_A^T \quad (1)$$

Further, the method calculates the ratio of the maximum singular value of the generated normalized matrix, with zero arithmetic mean and unity variance over a normalized image. The mathematical formulation is shown in Eq. (2):

$$\xi = \frac{\max(\sum_{N(\mu=0, \text{var}=1)})}{\max(\sum_A)} \quad (2)$$

Where  $\sum_{N(\mu=0, \text{var}=1)}$  taken as the coefficient, is the SVM of the synthetic intensity matrix and is used to regenerate an equalized image by using Eq. (3):

$$\Xi_{eqA} = U_A(\xi \sum_A)V_A^T \quad (3)$$

Therefore, from the definition of SVD, the SVMs of  $LL$  sub-band images of both  $A$  and  $\hat{A}$  are obtained. Next, the correction coefficient  $c$  is achieved, which is the maximum element in both SVMs and take their ratio using Eq. (4):

$$c = \frac{\max(\sum_{LL_{A'}})}{\max(\sum_{LL_A})} \quad (4)$$

Where  $\sum_{LL_{A'}}$  is the SVM of the  $LL$  sub-band image of the histogram-equalized image  $A$  and  $\sum_{LL_A}$  is the SVM of the  $LL$  sub-band of the input image. Eq. 5(a) and Eq. 5(b) obtain the new sub-band image:

$$\overline{\sum_{LL_A}} = \left(\frac{\xi}{1+\xi}\right)\left(\xi \sum_{LL_A} + \frac{1}{\xi} \sum_{LL_{A'}}\right) \quad (5a)$$

$$L\overline{L}_A = U_{LL_A} \overline{\sum_{LL_A}} V_{LL_A} \quad (5b)$$

Finally, the contrast-enhanced image  $A$  is obtained by applying IDWT on the estimated  $LL$  sub-band  $L\overline{L}_A$  along with high-frequency components  $LH_A$ ,  $HL_A$ , and  $HH_A$  sub-bands:

$$\overline{A} = IDWT(L\overline{L}_A, LH_A, HL_A, HH_A) \quad (6)$$

Additionally, from the achieved results, it is quite clear that the edge components of the HF bands are not disturbed and remain undamaged. The illumination information is the only thing to be manipulated alone to enhance the contrast of an image.

#### IV. RESULTS AND DISCUSSIONS

In order to, check the quality and efficiency of the proposed approach. Most of the experiments were carried out on different satellite images publicly made available to use for a wide variety of remote sensing tasks, such as resolution enhancement, and contrast enhancement. Moreover, all the experiments were conducted adequately in MATLAB 2015a with the following PC specifications: 2.5-GHz CPU, 4 GB of RAM, and Windows 10. Furthermore, to evaluate the performance of the proposed technique. Four  $256 \times 256$  low-contrast with low-resolution satellite images were utilized, as shown in Fig. 2 .

Row (a) was the low resolution and contrast input image. Row (b) contains enhanced images using the proposed approach. Row (c) show enriched images using SWT-IWT methods based on SVD [8]. Row (d) illustrates the result obtained using WZP method [11]. Row (e) depicts the result attained using DWT-SWT methods [27]. Finally, Row (f) displays the image enhancement result achieved using DWT technique [26]. Moreover, the quantitative quality assessment is done to check the suitability of the proposed method. To assess the quality and to compare the performance of the proposed method with existing approaches to image enhancement. The following quality measure criteria were used such as mean square error (MSE), peak-to-signal-noise ratio (PSNR) and entropy.

These measures are the best way to evaluate performance. Mathematically, these measures were defined as:

$$MSE = \sqrt{\frac{\sum_{x=0}^{M-1} \sum_{y=0}^{N-1} [A(x,y) - A'(x,y)]^2}{M \times N}} \quad (7)$$

$$PSNE = 10 \times \log_{10} \left( \frac{R^2}{MSE} \right) \quad (8)$$

$$Entropy = - \sum_{i=0}^n p_i \log_2 p_i \quad (9)$$

Where  $A(x,y)$  is the pixel value of the original image and  $\hat{A}(x,y)$  is the pixel value of the output image  $M$  is the size of the image and  $R$  is the maximum pixel value.

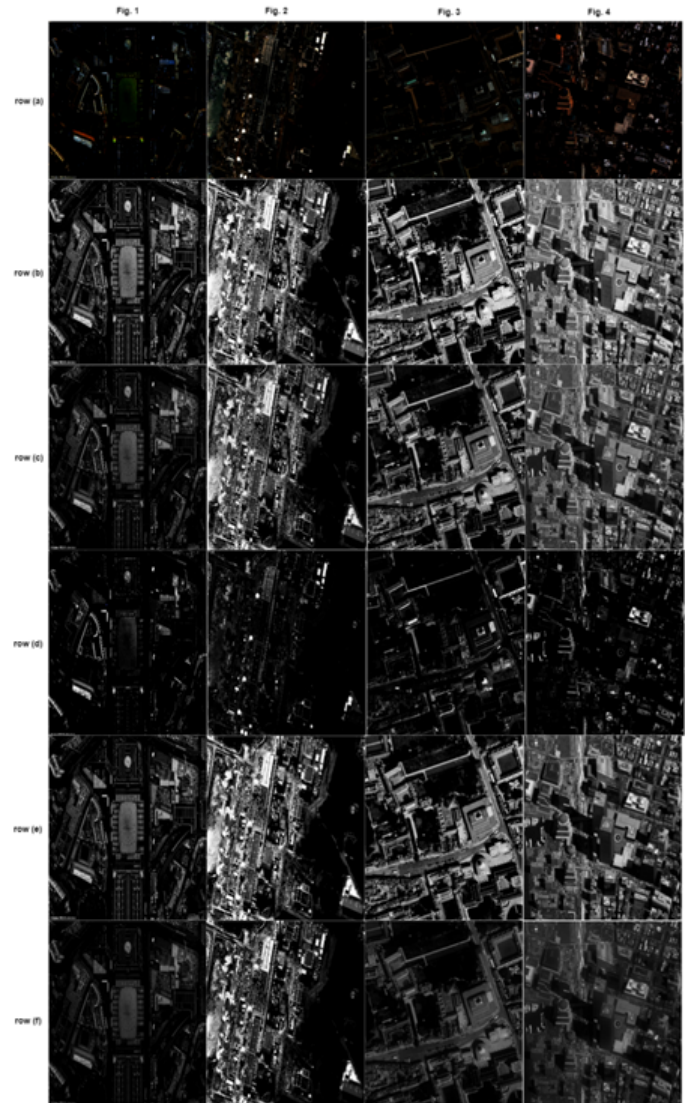


Fig. 2. Row (a) low-quality satellite images; (b) Enhanced images using the proposed approach row; (c) Enriched images using SWT-IWT methods based on SVD;(d) Improved images using WZP method;(e) Image enhancement using DWT-SWT techniques; (f) Image enhancement using DWT method.

TABLE I. QUALITY ASSESSMENT MEASURE: MEAN SQUARE ERROR (MSE).

| Methods            | Fig. 1 | Fig. 2 | Fig. 3 | Fig. 4 | Average MSE |
|--------------------|--------|--------|--------|--------|-------------|
| Tinku et al [11]   | 225.21 | 253.48 | 248.81 | 205.6  | 233.75      |
| Hassan et al [26]  | 98.9   | 113.71 | 109.60 | 101.13 | 105.83      |
| Demirel et al [27] | 222.10 | 251.10 | 241.94 | 199.20 | 228.58      |
| Neena et al [8]    | 27.12  | 41.37  | 31.99  | 35.33  | 33.95       |
| Author's           | 24.33  | 38.93  | 28.61  | 32.36  | 31.05       |

Table I shows the comparison of the quality measure that MSE of the proposed approach with the existing methods. Four different low resolution and contrast satellite images of size  $256 \times 256$  have been taken for the testing purpose. It can be seen, from Table I that the proposed method yielded a noticeable performance. As compared to existing approaches, the proposed method generated less error of 24.33%. Certainty, this is due to the proposed method's image enhancing capability.

TABLE II. QUALITY ASSESSMENT MEASURE: PEAK SIGNAL TO NOISE RATIO (PSNR).

| Methods            | Fig. 1 | Fig. 2 | Fig. 3 | Fig. 4 | Average PSNR |
|--------------------|--------|--------|--------|--------|--------------|
| Tinku et al [11]   | 24.60  | 24.09  | 24.17  | 25.00  | 24.65        |
| Hassan et al [26]  | 28.17  | 27.57  | 27.73  | 28.08  | 27.88        |
| Demirel et al [27] | 24.66  | 24.13  | 24.29  | 25.13  | 24.55        |
| Neena et al [8]    | 33.79  | 31.96  | 33.08  | 32.64  | 32.86        |
| Author's           | 34.26  | 32.22  | 33.56  | 33.03  | 33.26        |

Furthermore, the comparison of the PSNR values of the proposed method produced along with other methods is given in Table II. It can be observed from the table that the recommended method results in a robust PSNR of 33.26 dB, which is the best rate when the input images are low resolution and contrast satellite images. The proposed method dramatically improves the quality of a degraded image to an acceptable ratio which makes the technique a better approach.

TABLE III. ENTROPY: AMOUNT OF INFORMATION.

| Methods            | Fig. 1 | Fig. 2 | Fig. 3 | Fig. 4 | Average Entropy |
|--------------------|--------|--------|--------|--------|-----------------|
| Original Image     | 8.02   | 7.91   | 7.32   | 7.45   | 7.67            |
| Tinku et al [11]   | 7.31   | 6.8    | 6.71   | 7.11   | 6.98            |
| Hassan et al [26]  | 7.03   | 6.89   | 6.23   | 5.66   | 6.45            |
| Demirel et al [27] | 7.82   | 7.51   | 6.69   | 7.18   | 7.3             |
| Neena et al [8]    | 8.3    | 7.79   | 6.99   | 8.05   | 7.78            |
| Author's           | 9.68   | 8.20   | 7.89   | 8.12   | 8.47            |

Moreover, Table III depicts the entropy performance comparison of the proposed approach with extent methods. Furthermore, it can be analyzed from the Table III that the amount of information within an image for the proposed method is higher than prior approaches. As we can see, the proposed method achieved the excellent value of visual information that 8.47, which is considered as the best quality of a well-enhanced image.

## V. CONCLUSIONS

In this paper, a new technique has been proposed to enhance the quality that resolution and contrast of satellite images. For resolution enhancement, the input image has been decomposed into four frequency components ( $LL, LH, HL, HH$ ) using SWT. Next, the SVD is applied to obtain the Singular value matrices  $U_A$  and  $V_A$  contains high-frequency elements. Then, the high-frequency components ( $LH, HL$ ) obtained using DWT are corrected by singular value matrices and SWT. Later the interpolation factor is added. Finally, the high-resolution image is obtained using IDWT. For the contrast enhancement, the proposed system enhances the contrast of high-resolution with low-contrast satellite images using the concept DWT based on SVD. The low-contrast satellite image is decomposed into DWT sub-bands such as ( $LL, LH, HL, and HH$ ). Next, the SVM of the  $LL$  sub-band is obtained which contains the illumination information. Then, SVM is modified to enhance the contrast. Finally, the images reconstructed using the IDWT.

In summary, the result depicts that the proposed technique achieved promising results in PSNR, entropy, and MSE. From the quantitative results, it is cleared that the application of the proposed method is useful and supports the obtained visual results better. Hence, the visual and quantitative results show that wavelet transforms work well to enhance satellite images.

## VI. FUTURE WORK

Moreover, the result obtained is sufficient and meaningful as compared to conventional approaches. Based on the results received, authors believe that the current study could be applied in many applications such as medical image processing, object recognition, surveillance, remote sensing, edge detection, video processing, feature matching, building detection in satellite images, image cropping, object detection and classification, and others. Wherever it is necessary to provide better interpretability, analysis, representation, diagnosis, and perception of information in the images, furthermore, researchers could extend this work for detecting building objects from low-contrast satellite images.

Besides the implications as mentioned above, the authors believe that the present study could be extended for future research to enhance the quality of the satellite images which are darker and less visible and affected due to several factors such as fog or smoke, noise, color distortion, and dense weather. Apart from this, in the future, the application of fractional calculus and deep learning technologies will be introduced to enhance the quality of the images. Our next task is to make the proposed technique applicable for different size and types of images.

## ACKNOWLEDGMENT

This work was supported by the National Natural Science Foundation of China under Grants 61571312, Academic and Technical Leaders Support Foundation of Sichuan province under Grants (2016)183-5, National Key Research and Development Program Foundation of China under Grants 2017YFB0802300.



REFERENCES

- [1] Ayoub, Naeem; Gao, Zhenguo; Chen, Bingcai; Jian, Muwei. 2018. "A Synthetic Fusion Rule for Salient Region Detection under the Framework of DS-Evidence Theory." *Symmetry* 10, no. 6: 183.
- [2] Farahbakhsh, Ehsan, Rohitash Chandra, Hugo KH Olierook, Richard Scalzo, Chris Clark, Steven M. Reddy, and R. Dietmar Muller. "Computer vision-based framework for extracting geological lineaments from optical remote sensing data." arXiv preprint arXiv:1810.02320 (2018).
- [3] Kavanagh DP, Gallagher MT, Kalia N. Tify: A quality-based frame selection tool for improving the output of unstable biomedical imaging. *PLoS one*. 2019 Mar 11;14(3):e0213162.
- [4] Ofek EO. A code for robust astrometric solution of astronomical images. arXiv preprint arXiv:1903.02015. 2019 Mar 5.
- [5] Li X, Anderson B, Li C, Xie F. Landscape Pattern Recognition on Water Quality Protection in an Urbanizing Delta Using Remote Sensing and GIS Techniques. In *Recent Developments in Intelligent Computing, Communication and Devices 2019* (pp. 899-905). Springer, Singapore.
- [6] Ho GT, Tsang YP, Wu CH, Wong WH, Choy KL. A computer vision-based roadside occupation surveillance system for intelligent transport in smart cities. *Sensors*. 2019 Jan;19(8):1796.
- [7] Gao L, Song W, Dai J, Chen Y. Road Extraction from High-Resolution Remote Sensing Imagery Using Refined Deep Residual Convolutional Neural Network. *Remote Sensing*. 2019 Jan;11(5):552.
- [8] Neena, K. A., Aiswriya Raj, and Rajesh Cherian Roy. "Image enhancement based on stationary wavelet transform, integer wavelet transforms and singular value decomposition." *International Journal of Computer Applications* 58, no. 11 (2012).
- [9] Zhang, Yunfeng, Qinglan Fan, Fangxun Bao, Yifang Liu, and Caiming Zhang. "Single-Image Super-Resolution Based on Rational Fractal Interpolation." *IEEE Transactions on Image Processing* 27, no. 8 (2018): 3782-3797.
- [10] Kang, Wonseok, Jaehwan Jeon, Eunsung Lee, Changhun Cho, Junghoon Jung, Taechan Kim, Aggelos K. Katsaggelos, and Joonki Paik. "Real-time super-resolution for digital zooming using finite kernel-based edge orientation estimation and truncated image restoration." In *Image Processing (ICIP), 2013 20th IEEE International Conference on*, pp. 1311-1315. IEEE, 2013.
- [11] Tinku Acharya, Pin-Sing Tsai, "Computational Foundations of Image Interpolation Algorithms", *ACM Ubiquity Vol.8* 2007.
- [12] Keys, Robert. "Cubic convolution interpolation for digital image processing." *IEEE transactions on acoustics, speech, and signal processing* 29, no. 6 (1981): 1153-1160.
- [13] Atta, Randa, and Mohammad Ghanbari. "Low-contrast satellite images enhancement using discrete cosine transform pyramid and singular value decomposition." *IET Image processing* 7, no. 5 (2013): 472-483.
- [14] Aamir, Muhammad, Yi-Fei Pu, Ziaur Rahman, Muhammad Tahir, Hamad Naeem, and Qiang Dai. "A Framework for Automatic Building Detection from Low-Contrast Satellite Images." *Symmetry* 11, no. 1 (2019): 3.
- [15] Rahman, Ziaur, Yi-Fei Pu, Muhammad Aamir, and Farhan Ullah. "A framework for fast automatic image cropping based on deep saliency map detection and gaussian filter." *International Journal of Computers and Applications* (2018): 1-1.
- [16] Kim, Y.-T.: 'Contrast enhancement using brightness preserving bi-histogram equalization', *IEEE Trans. Consum. Electron.*, 1997, 43, (1), pp. 1-8.
- [17] Ibrahim, H., Kong, N.S.P.: 'Brightness preserving dynamic histogram equalization for image contrast enhancement', *IEEE Trans. Consum. Electron.*, 2007, 53, (4), pp. 1752-1758.
- [18] Sun, C.C., Ruan, S.J., Shie, M.C., Pai, T.W.: 'Dynamic contrast enhancement based on histogram specification', *IEEE Trans. Consum. Electron.*, 2005, 51, (4), pp. 1300-1305.
- [19] Aгаian, S.S., Silver, B., Panetta, K.A.: 'Transform coefficient histogram-based image enhancement algorithms using contrast entropy', *IEEE Trans. Image Process.*, 2007, 16, (3), pp. 741-758.
- [20] Arici, T., Dikbas, S., Altunbasak, Y.: 'A histogram modification framework and its application for image contrast enhancement', *IEEE Trans. Image Process.*, 2009, 18, (9), pp. 1921-1935.
- [21] Demirel, H., Anbarjafari, G., Jahromi, M.N.S.: 'Image equalization based on singular value decomposition'. *Proc. 23rd IEEE Int. Symp. Computer and Information Science*, Istanbul, Turkey, October 2008, pp. 1-5.
- [22] Demirel, H., Ozcinar, C., Anbarjafari, G.: 'Satellite image contrast enhancement using discrete wavelet transform and singular value decomposition', *IEEE Geosci. Remote Sens. Lett.*, 2010, 7, (2), pp. 333-337.
- [23] Atta, R., and Abdel-Kader, R.F., 2015, "Brightness preserving based on singular value decomposition for image contrast enhancement," *Optik* 126, pp. 799-803.
- [24] Bhandari, A.K., Kumar, A., Padhy, P.K.: 'Enhancement of low contrast satellite images using discrete cosine transform and singular value decomposition', *World Acad. Sci. Eng. Technol.*, 2011, 55, pp. 35-41.
- [25] Kumar, A., Bhandari, A.K., Padhy, P.: 'Improved normalised difference vegetation index method based on discrete cosine transform and singular value decomposition for satellite image processing', *IET Signal Process.*, 2012, 6, (7), pp. 617-625.
- [26] Hasan Demirel and Gholamreza Anbarjafari, "Discrete Wavelet Transform-Based Satellite Image Resolution Enhancement", *IEEE transactions on geosciences and remote sensing*, June 2011.
- [27] Hasan Demirel and Gholamreza Anbarjafari, "Image Resolution Enhancement by Using Discrete and Stationary Wavelet Decomposition" *IEEE transactions on Image Processing*, VOL. 20, NO. 5, May 2011.
- [28] Lamard, M.; Daccache, W.; Cazuguel, G.; Roux, C.; Cochener, B. Use of a JPEG-2000 Wavelet Compression Scheme for Content-Based Ophthalmologic Retinal Images Retrieval. In *2005 IEEE Engineering in Medicine and Biology 27th Annual Conference*; IEEE, 2005; pp. 4010-4013.
- [29] Demirel, H.; Anbarjafari, G. Satellite Image Resolution Enhancement Using Complex Wavelet Transform *IEEE Geosci. Remote Sens. Lett.* 2010, 7, 123-126, doi:10.1109/LGRS.2009.2028440.
- [30] Dai, Qiang; Pu, Yi-Fei; Rahman, Ziaur; Aamir, Muhammad. 2019. "Fractional-Order Fusion Model for Low-Light Image Enhancement." *Symmetry* 11, no. 4: 574.
- [31] Rahman, Ziaur; Aamir, Muhammad; Pu, Yi-Fei; Ullah, Farhan; Dai, Qiang. 2018. "A Smart System for Low-Light Image Enhancement with Color Constancy and Detail Manipulation in Complex Light Environments." *Symmetry* 10, no. 12: 718.

# Convolutional Neural Networks in Predicting Missing Text in Arabic

Adnan Souiri<sup>1</sup>, Mohamed Alachhab<sup>2</sup>, Badr Eddine Elmohajir<sup>3</sup>  
New Trend Technology Team  
Abdelmalek Essaadi University  
Tetouan, Morocco

Abdelali Zbakh<sup>4</sup>  
LaMCSaI Laboratory, Faculty of Sciences  
Mohamed V University  
Rabat, Morocco

**Abstract**—Missing text prediction is one of the major concerns of Natural Language Processing deep learning community's attention. However, the majority of text prediction related research is performed in other languages but not Arabic. In this paper, we take a first step in training a deep learning language model on Arabic language. Our contribution is the prediction of missing text from text documents while applying Convolutional Neural Networks (CNN) on Arabic Language Models. We have built CNN-based Language Models responding to specific settings in relation with Arabic language. We have prepared our dataset of a large quantity of text documents freely downloaded from Arab World Books, Hindawi foundation, and Shamela datasets. To calculate the accuracy of prediction, we have compared documents with complete text and same documents with missing text. We realized training, validation and test steps at three different stages aiming to increase the performance of prediction. The model had been trained at first stage on documents of the same author, then at the second stage, it had been trained on documents of the same dataset, and finally, at the third stage, the model had been trained on all document confused. Steps of training, validation and test have been repeated many times by changing each time the author, dataset, and the combination author-dataset, respectively. Also we have used the technique of enlarging training data by feeding the CNN-model each time by a larger quantity of text. The model gave a high performance of Arabic text prediction using Convolutional Neural Networks with an accuracy that have reached 97.8% in best case.

**Keywords**—Natural Language Processing; Convolutional Neural Networks; deep learning; Arabic language; text prediction; text generation

## I. INTRODUCTION

Several documents like ancient manuscripts, old handwritings and autographs suffer from problems, such as character degradation, stains and low quality. In such cases, text is often partially or entirely illegible. In other words, we frequently found in such documents a large quantity of missing text that makes these documents not available for exploitation.

In this paper, we address the use of CNN dealing with Arabic Language with the objective of predicting missing text from Arabic documents. The process of prediction is the main challenge raised in this work since it depends on a large scale of elementary operations such as text segmentation, words embedding detection, sense retrieval. The motivation held by text prediction is that it carries on several forms of document exploitation but not limited to semantic analysis, historical period detection of undated manuscripts and writing style analysis. Otherwise, dealing with Arabic put the focus

of some features of this morphologically rich language such as word scheme meaning, writing units (letter, word and sentence), different letter shapes, lack of vowelization and little use of punctuation marks. Our idea is based on Human skill in extracting meanings from either a text or a part of speech that involves in understanding the meaning of a word (a sentence or a part of text) in its context of use. In [1], author explains the principle of learning meanings as follows: "Once the discrimination appears from the child, he heard his parents or his educators utter verbally, and refer to the meaning, he understand so that word is used in that meaning, i.e: the speaker wanted that meaning".

By analogy to this principle, the CNN model presented in this paper takes a text at his inputs, train on it and predicts some text according to its training and its learning process. The use of deep CNN had been motivated by the success of CNN models facing many problems in several areas including script identification [2], text classification [3], text recognition [4] character recognition [5], [6]. The success of CNN models had been attributed to their ability to learn features in an end-to-end fashion from large quantities of data.

In a previous research, [7], we proved the automatic generation of Arabic text using Recurrent Neural Networks (RNN). Hence, while using it as a generative and predictive model, CNN gave more accurate results. In one hand the CNN proposed model had been built responding to some Arabic language features. In the other hand, we have prepared adequate datasets in which to apply the CNN model. We have used more than a hundred forty text files, with more than four millions of words, from novels of known Arabic authors. Data had been freely downloaded, cleaned up and divided into Training data, validation data and test data. Then the CNN-model had been fed up according three stages: unique author data, unique source data, and author-source combination data.

The organisation of this paper is as follows, in section 2 a state of the art concerning the application of CNN-models on Arabic language. In addition, we have mentioned our previous work dealing with neural networks and Arabic language. Section 3 gives an overview about CNN architecture, while Section 4 presents Arabic features on which we have based in this work. In Section 5, we detail our experiments and results. We explicit the process of data preparation, then we give characteristics of the model inputs before to explain the proposed model architecture. We discuss then our results. Finally, Section 6 concludes the research.

## II. RELATED WORK

In the literature, a considerable quantity of work have dealt with CNN application on Arabic language as well as on other languages. In [8], authors propose to auto-encode text a byte-level using CNN with recursive architecture. Experiments had been done on datasets in Arabic, Chinese and English. The motivation was to explore whether it is possible to have scalable and homogeneous text generation at byte-level in a non-sequential fashion through the simple task of auto-encoding. The work showed that non-sequential text generation from a fixed-lengths representation is not only possible, but also achieved much better auto-encoding results than the use of RNN.

In [9], authors have used CNN to address three demographic problem classification (gender, handedness, and the combined gender-and-handedness). The research was carried out on two public handwriting databases IAM and KHATT containing English text and Arabic text respectively. CNN have proven better capabilities to extract relevant handwriting features when compared to using handcrafted ones for the automatic text transcription problem. Authors in [9] have used a unique configuration of CNN with specific parameter values for the three considered demographic problems. Finally, the proposed gender-handedness prediction method remains relatively robust fore more than one alphabet.

Reference [10] have used CNN as a deep learning classifier for Arabic scene text recognition. Authors assume that such an approach is more appropriate in cursive scripts. Thus, their model had been applied to learn patterns of visual images in which Arabic text was written. The experimental results indicate that CNN can improve accuracy on large and variant datasets.

Moreover, the work presented in this paper involves as a continuity to our previous work dealing with Recurrent Neural Networks application on Arabic language, Arabic text segmentation and a study about Arabic datasets and corpora. In [11], we assumed that Arabic scripts has numerous challenges associated. We mention here the variant shape of letters depending on their position in a word, the problem of writing units, the length of sentences due to little use of punctuation marks, the lack of space between sentence components in usual cases, and the lack of vowelization. For these reasons and more others, it involves being harder to segment Arabic script with automated tools. Therefore, by keeping in view these features in Arabic script, we have used our segmentation method proposed in [11] basing on what we hav called writing units. The segmentation method helps in partitioning text into units that will be converted in a next step into vectors (numerical representations) that will serve as input to the CNN model.

In addition, the study of corpora is on the heart of this field of research. Consequently, we had the opportunity to present a study on Arabic corpora in [12]. We have concluded in that work, that the hole majority of Arabic corpora are not free or not available publically. Moreover, a large number of corpora are limited to some specific subjects. The main idea of [12] was the creation of a framework to build freely accessible Arabic corpora that covers a variety of domains. As consequences, working on data preprocessing in this paper was a motivation, mainly to parametrize inputs of the CNN model.

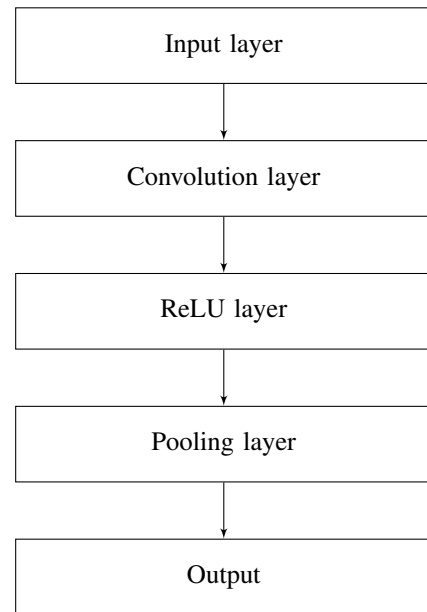


Fig. 1. Typical CNN architecture

From another side, the work presented in [7] had been as ground to the actual work. We have proposed a method to generate Arabic text using RNN, especially Long-Short Term Memory (LSTM). The goal of the paper was to demonstrate the ability of such networks to generate correct Arabic text. The principle was to build a RNN language model adapted to some Arabic criteria and then apply it on Arabic text. Experiments in [7] have shown the ability of LSTM to generate sequences of Arabic characters after a step of training. The generation process had been based on a kind of mimicking the training text. Hence the idea of exploiting those results to predict the missing text proved feasible by further parametrizing the model or rather using CNN architecture.

## III. CONVOLUTIONAL NEURAL NETWORKS

Among the main goals of machine learning system, is data prediction and data generation [13], classification [14], and feature detection [14], [15]. Recently, some deep learning-based models - such as Deep Belief Networks (DBN), RNN and CNN - have been proposed to reach these goals. The processing of these models is based on networks with several layers. It involves a class of models that try to learn multiple levels of data representation, which helps to take advantage of input data such as text, speech and image. Comparing to RNN or DBN, CNN have been found to be a good alternative in text prediction and generation [13], classification [16], [17], and feature detection [14], [15].

CNN are feedforward networks based on combination of input layers, hidden layers (convolution layers, max pooling, drop out) and output layers. Deep CNN-models are powerful in terms of learning hierarchical representation of the data, and extracting the features from raw data. Their powerful is illustrated by the manner on which the layers are connected. The connection between layers requires fewer parameters and reduce memory consumption space. Moreover, the computing efficiency of CNN-models requires fewer operations.

A commonly used CNN-model architecture is presented in Fig. 1. The architecture of a CNN can be detailed as follows: **Input layer.** It serves for feeding the model by raw data to process the network.

**Convolution layers.** Layers within the attributes: Input and Number of filters. The input is a tensor determining quantity of data (number, width, height, and depth). While the number of filters is characterized by width, height and depth. A convolutional operation is carried out by the layer and its result is passed to the next layer.

**Convolution filter.** Small spatial window with width and height smaller than the width and height of the input data.

**Rectified linear unit (ReLU).** An element-wise activation function  $g(z) = \max(0, z)$  which is applied on the input data. It changes its value while preserving its spatial dimensions in output.

**Pooling layers.** They combine the outputs if neuron clusters at a layer into a single neuron in the next layer in order to reduce data dimensions. Pooling compute, in general, a max or an average. Max pooling conserves the maximum value from each cluster of a neuron while average pooling conserves the average value.

**Fully connected layers.** They connect all-to-all, i.e. every neuron in a layer is connected to every neuron in another layer.

#### IV. ARABIC LANGUAGE FEATURES

Arabic is a semitic language spoken by around 400 million native speakers world-wide and used by more than 1.7 billion people daily in their prayers. It is one of the six official languages used in the United Nations Organization [18].

Arabic is written from right to left, in a cursive style, and includes 28 letters. Letters in Arabic can change shapes depending on their position in a word if it is at the starting, the middle or at the end. We find also for some cases different shapes even at the same position. Table I shows an example.

TABLE I. SHAPES OF THE LETTER AIN

| English | Arabic | Position of the letter |
|---------|--------|------------------------|
| Eye     | عين    | starting               |
| The eye | العين  | middle                 |
| Tear    | دمع    | ending                 |
| Street  | شارع   | ending                 |

Letters change their phonetic pronunciation depending to the vowelization mark. Let us consider the word

فهم

It can be interpreted as <understanding>, <he understood>, or <so they>. The lack of vowelization makes the process of understanding depends on the context.

Space separated units in Arabic are not necessarily words, they can be sentences or letters having their own role or meaning. We note here that in Arabic, a writing unit can be a letter, a word or a sentence as shown in the examples below: 1).

2).

كتب

3).

فستكتبونها

with the respective meanings of 1). and 2). books, and 3). then you will write it.

Moreover, we find another feature in Arabic that is words have schemes that influence their meaning consequently. The meaning of a word is got once interpreting its scheme and without having to know the word before. As an illustration, the word

كتب

(he wrote) has the scheme

فعل

refers to the verb in its 3rd singular person form. But the word

كاتب

(author) has the scheme

فاعل

which means that the word refers to someone who is responsible of the act (writing him this example). Similarly the word

مكتوب

(written) has the scheme

مفعول

which means that it refers to the effect of an action. By analogy, words

نطق ناطق منطوق

refer respectively to the action of a verb, the responsible of the act, and the effect of the action, it comes here that the first word means spell (the verb in its 3rd singular person form), the second words means the speller, and the third word is the speech.

Arabic language possesses a list of around four hundred schemes, but in this work we have limited the use of a hundred schemes to feed up the CNN model. Table II shows some of schemes meanings used in this work. With this in mind, the main advantage of teaching the model such language features is increasing the performance of missing text prediction and generation.

#### V. EXPERIMENTS AND RESULTS

##### A. Data Preparation

At the starting of every work dealing with a huge quantity of data, the operation of data preparation remains to be a necessary task to prepare the dataset on which we have worked. We have first freely downloaded several text documents in portable document format (pdf) from three sources on the web: Arab World Book (AWB) [19], Shamela Library (ShL) [20], and Hindawi organisation (HND) [21]. We have collected several text novels and poems of some Arab authors. The global size of our dataset was about 130 MB of text, distributed over 144 text files with more than four millions of words. Table III gives an overview about our dataset.

We mention here that AWB is a cultural club and Arabic bookstore that aims to promote Arab thought [19]. It provides a

TABLE II. SOME OF ARABIC SCHEMES AND THEIR ASSOCIATED MEANING

| Schemes | Transliteration | The associate meaning  |
|---------|-----------------|--|
| فعل     | fa'ala          | Refers to someone who acts. 3rd singular person form   |
| فاعل    | fAil            | The subject. The responsible of such an action   |
| مفعول   | maf'Ol          | The effect of an action  |
| مفعلة   | mifaaala        | A noun of an instrument, a machine   |
| فعلة    | fa'ala          | Something done for one time  |
| استفعل  | istafaaala      | To demand, to request something  |
| مستفعل  | mostaffilon     | The subject, the responsible of such an action which its verb has the scheme:<br>استفعل<br>: |

TABLE III. AN OVERVIEW OF SOME DOCUMENTS USED IN THIS RESEARCH

| Dataset | number of documents | number of words |
|---------|---------------------|-----------------|
| AWB     | 38                  | 1009365         |
| ShL     | 67                  | 2133442         |
| HND     | 39                  | 1082727         |
| Total   | 144                 | 4225534         |

public service for writers and intellectuals, and exploits the vast potential of the Internet to open a window in which the world looks to Arab thought, to identify its creators and thinkers, and to achieve intellectual communication between people of this homeland [19]. The reference [20] is a huge free program that aimed, to be comprehensive for all what the researcher needs of books and research. The library is currently working on a suitable system for receiving files of various text and arranging them in one frame with the possibility of searching. Reference [21] is a non profit foundation that seeks to make a significant impact on the world of knowledge. The foundation is also working to create the largest Arabic library containing the most important books of modern Arab heritage after reproduction, to keep from extinction.

All pdf documents from these sources have been converted to text format using <Free pdf to Text Converter> tool available at [http://www.01.net.com/telecharger/windows/Multimedia/scanner\\_ocr/fiches/115026.html](http://www.01.net.com/telecharger/windows/Multimedia/scanner_ocr/fiches/115026.html). Table IV lists some of these documents we have used in our experiments and their authors respectively. We have assigned an ID for each document to designate it during the Python implementation phase.

TABLE IV. SOME DOCUMENTS AND AUTHORS USED IN THIS RESEARCH

| Document title  | Author name          | ID        |
|-----------------|----------------------|-----------|
| The days        | Taha Hussein         | HND_TH_1  |
| Tear and smile  | Jabran Khalil Jabran | HND_JKJ_7 |
| Homeland        | Mahmoud Darweesh     | HND_MD_1  |
| Diwan           | Maarof Rosafi        | AWB_MR_2  |
| Back wave       | May Ziyada           | AWB_MZ_5  |
| The misers      | Al Jahid             | ShL_JHD_1 |
| Kalila wa dimna | Ibn Almoqafaa        | ShL_MQF_1 |

After an exploration of these text files, it was found that the text must be cleaned up of certain aspects such as the succession of multiple spaces, and the appearance of some undesirable characters like <? > and < square >. This is due to two problems: Arabic character encoding and the

correspondence between Arabic letters encoding and shapes. In one hand, to face the encoding problem, we have chosen utf-8 encoding, and in the other hand, undesirable characters appear while using different writing fonts in different environments, we proceed by unifying fonts of the entire text in one.

Once data are cleaned up, we proceed by the operation of dividing it into three subsets: Training set (TrD), Validation set (VD), and Test set (TsD). The training process is an operation that consists of teaching the CNN model how to write the Arabic text, the categories of words in Arabic, the particularities of Arabic (especially those taken into consideration by our research), morphology, grammar, conjugation, and semantics. That being said, the model learns by browsing a multitude of documents written in Arabic while remembering, among other things, the order of words and the composition of the phrases. At the end of the training operation, the model has enough luggage to be able to generate Arabic text or to predict it. We then proceed with the validation operation, which consists in evaluating the learning of the model by giving it documents already processed but this time with missing text. The model, therefore, must predict the missing text and we compare with the original text and calculate the accuracy of the results. The step of test then comes up by feeding the model by new documents with missing text. These documents have not been treated by the model at all. The CNN-model try to predict text basing on its learning.

AS in the most state of the art of data preparation, TrD took about 70% of data, i.e. 94 document files of the 144. VD and TsD took each one around 15% of data, i.e. 25 document files each. Table V shows the distribution of documents and words per dataset for each sources of our three sources.

TABLE V. DISTRIBUTION OF NUMBER OF DOCUMENTS AND WORDS PER EACH DATASET

| Dataset | TrD |         | VD |        | TsD |        |
|---------|-----|---------|----|--------|-----|--------|
| AWB     | 24  | 762910  | 7  | 178235 | 7   | 158220 |
| ShL     | 45  | 1544197 | 11 | 289077 | 11  | 300168 |
| HND     | 25  | 810873  | 7  | 163448 | 7   | 108406 |
| Total   | 94  | 3117980 | 25 | 630760 | 25  | 566794 |

### B. Inputs of the CNN-Model

In the following, we provide details about our preprocessing strategy for text datasets, prior to feeding

TABLE VI. MATRIX  $M$  ASSOCIATED TO AN EXCERPT FROM DOCUMENT HND\_MD\_1, WITH VARIATION OF  $N = 5$

| $M[i, 4]$ | $M[i, 3]$ | $M[i, 2]$ | $M[i, 1]$ | $M[i, 0]$ |           |
|-----------|-----------|-----------|-----------|-----------|-----------|
| بين       | وطنه      | في        | المرء     | يعيش      | $M[0, j]$ |
| أهله      | بين       | وطنه      | في        | المرء     | $M[1, j]$ |
| و         | أهله      | بين       | وطنه      | في        | $M[2, j]$ |
| أصدقائه   | و         | أهله      | بين       | وطنه      | $M[3, j]$ |

TABLE VII. VECTOR  $Y$  ASSOCIATED TO  $M$  REPRESENTED IN TABLE VI

|         |           |
|---------|-----------|
| أهله    | $Y[0, 0]$ |
| و       | $Y[1, 0]$ |
| أصدقائه | $Y[2, 0]$ |
| .       | $Y[3, 0]$ |

information to the CNN-model. Text already prepared to be as input to the CNN-model had been transformed into numerical codes since CNN architecture needs numerical data at inputs. The transformation had been carried out according to the following steps:

1. Dividing text into writing units (WU) separated by space.
2. Attributing a unique numerical  $ID$  to each WU.
3. For each  $ID$ , we have calculated its binary equivalent code. We have called it Binary Writing Unit Code (BWUC).
4. Creating a dictionary associating BWUC, which are unique, to their respective WU.

Another parametrizing step consists in representing each BWUC in a fixed dimensional vector ( $v$ ) of size  $k$ , where ( $2^k = \text{vocabulary size}$ ). The elements of input feature vector ( $iv$ ) are the associated BWUC of successive WU ( $wu_i$ ) in a text document ( $D$ ), such that:

$$iv = (wu_1, wu_2, wu_3, wu_4, \dots, wu_N)$$

The succession of  $N wu_i$  in a text necessarily generates a unique WU (or with higher accuracy at least, with other WU with lower accuracy) which will improve the prediction process. The  $iv$  is fed into the CNN-model and, at the output, the next WU is given, i.e. a vector ( $v$ ) of  $N$  elements ( $wu_1, wu_2, wu_3, wu_4, \dots, wu_N$ ) leads to the prediction of the next WU which will be  $wu_{N+1}$ .

To reduce document browsing and to gain in terms of execution time, we no longer limited to the use of vectors, but rather we opted for matrices (rows and columns). We have created a matrix  $M$  containing a number  $N$  of BWUCs in its columns.  $N$  is determined depending the performance of the prediction results (we have evaluated  $N = 3, N = 4$ , and  $N = 5$ ).

The order of elements of a row in  $M$  is the same as the

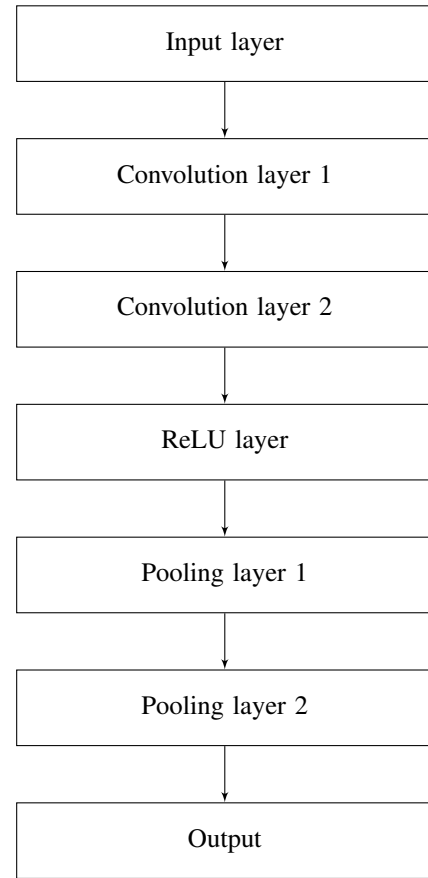


Fig. 2. The proposed CNN-model

appearance of WU in text. The matrix  $M$  associated to the excerpt from text <alwatan> of the document HND\_MD\_1 is illustrated by the Table VI.

The number of rows ( $nr$ ) of  $M$  is determined by:

$$nr = nWU/N$$

where  $nWU$  is the total number of WU in the whole text.

Each row in  $M$  contains  $N$  columns, and each column is an element ( $Mij$ , where  $i$  refers to the  $(i + 1)^{th}$  line and  $j$  refers to the  $(j + 1)^{th}$  column in  $M$ ) referring to a WU. We have adjusted lengths of all WU by completing these lengths by the empty character to have the same length for all WU.

The next step involves to create a column vector  $Y$  containing one element per each row.  $Y$  has the same  $nr$  as  $M$ . The correspondence between  $M$  and  $Y$  is that after each group of elements in a row of  $M$ , we find necessarily the element in the same row of  $Y$ , i.e. after each group of  $N$  WU in the text, we have the WU which is referred by the element in  $Y$ . Table VII shows the vector  $Y$  corresponding to matrix  $M$  presented in Table VI. We created then  $M\_codes$ , an equivalent matrix to  $M$ , and  $Y\_codes$  an equivalent vector to  $Y$ .  $M\_codes$  and  $Y\_codes$  serve as inputs for the CNN-model.  $M\_codes$  and  $Y\_codes$  contain BWUC of WU in text.

C. The Proposed CNN Model

We have implemented our model under Python programming language using Keras API with TensorFlow library as backend. Keras is a high-level neural networks API written with Python. It provides functionalities to deal with deep learning models. TensorFlow is a Python library used for symbolic numerical computations. Symbolic expressions in TensorFlow define computational architectures such as CNN models.

The structure of our CNN is shown in Fig. 2. It consists of an input layer, two convolution layers with ReLU as nonlinear activation function, two max pooling layers, and a fully connected layer. The last one is the output layer.

D. Results and Discussion

Our experiments are based on three essential stages; training, validation and test.

The training, validation and test operations were carried out in three stages according to three different processes in order to analyze and interpret the results of the prediction of the missing text, and also aiming at improving the overall accuracy of this prediction. First we started the training on the documents of a single author, we repeat the process for each author, we validate on documents already treated in training and then we test our results on documents that will be provided to CNN-model for the first time. The second stage is to provide documents from different authors but from the same source, since each of the three sources (AWB, ShL and HND) had its own priorities of classifying documents, choosing documents, choosing topics, putting up topics, and choosing authors obviously. We carry out the same process concerning training, validation and test. And finally, the third stage proves to provide documents in Arabic to the CNN-model without taking into account neither the author nor the data source with the objective of Arabic text prediction. These three stages are detailed below.

1) Stage 1: We proceeded by training the CNN on the documents of the same author. Generally, each author is characterized by his writing style, his method of describing facts or expressing ideas and more other features. These features have been taken into consideration by the model when it predicts the missing text in a document. When the model has to predict a missing text from a document of Mahmoud Darweesh for example, the text is often in relation with the notions of the homeland, the earth, and love, so text of these domains has a higher rate to be predicted rather than text of other domain. However, if dealing with Nabil Farouq’s documents, we find that his writings, as a whole, are in touch with the world of crime and the security of states, so the higher probability of prediction corresponds to text of these domains.

The prediction of missing texts on the processed documents had been carried out on the basis of both a statistical and a probabilistic approach. the model calculate the rate of a WU appearance after N other WU in a text. In the same text, even of the same author, we can find after 5 WU for example the appearance of multiple WU depending on the context. The model calculate then the probability of each WU appearance (PWUA) and predict the missing text according to the higher probability. Table VIII gives an illustration about this concept.

TABLE VIII. PREDICTION PROBABILITY CALCULATING

Table with 7 columns: PWUA, Y, and M (with sub-columns). Rows show prediction probabilities for various terms like 'أهله', 'عائلته', 'أقاربه', 'أصدقائه', and 'other'.

At this experimental stage, results have shown a high level of overall accuracy attending a hundred percent in several cases. Given these results, our interpretation is that the model did learn the author’s writing style to the point where he can correctly predict the missing text of his writings with a widely acceptable error rate. We noticed another aspect of prediction that was not part of our research is that the model can predict even formatting (text in bold, underlined text, text in color). This can be the subject of a future work.

For the test, we propose to our CNN-model documents with missing text, always of the same author, but this time these documents have never been treated by the CNN-model neither at the training stage nor at the validation stage. The model responded satisfactorily as the predicted results reached a maximum of 92.8% as overall accuracy. Results are represented in Table IX.

As first observation, prediction accuracy seems to have proportional relation with the amount of both trained and tested text. Table IX shows that more text amount is higher (in both training step or validation step) more prediction overall accuracy (POA) is higher (in both validation step or test step). This proves that the CNN-model learning is more interesting when the amount of data is more important. So we try next to feed up the CNN-model by a more larger quantity of data and calculate the accuracy.

TABLE IX. PREDICTION OVERALL ACCURACY PER EACH AUTHOR

Table with 6 columns: Author, TrD, ND, VD, POA(%), ND, TsD, POA(%). Rows list authors like Taha Hussein, Jabran Khalil Jabran, Ghassan Kanafani, etc., and a Total row.

2) Stage 2: The second stage took place while keeping in mind that each data source is different from the other. We tried then, in this step, to evaluate the prediction of the missing text belonging to the same data source, without taking into consideration the author of the text, with the purpose of assuming if the prediction is realized by following the same criteria as in the first stage (prediction by domain, writing style, and conservation of formatting).

The model had been fed up by texts from the same source

of any confused author. we did carried out the training, the validation and the test in the same way as for the first stage. The model had been trained on AWB TrD set, provides AWB VD set texts for validation, then had been tested with AWB TsD set texts. The same operations are repeated for texts of ShL apart and texts of HND apart. The prediction results of this stage are described in the Table X where the number of documents used is presented by ND.

TABLE X. PREDICTION OVERALL ACCURACY PER EACH DATA SOURCE

| Dataset   | TrD |    |        | VD |    |        | TsD |    |        |
|-----------|-----|----|--------|----|----|--------|-----|----|--------|
|           | ND  | ND | POA(%) | ND | ND | POA(%) | ND  | ND | POA(%) |
| AWB       | 24  | 7  | 97.3   | 7  | 7  | 94.8   |     |    |        |
| ShL       | 45  | 11 | 98.1   | 11 | 11 | 96.9   |     |    |        |
| HND       | 25  | 7  | 98.4   | 7  | 7  | 95.6   |     |    |        |
| Rate mean | 94  | 25 | 97.93  | 25 | 25 | 95.77  |     |    |        |

Certainly, at this experimental stage we have achieved satisfactory results in terms of POA. It is clear and obvious that POA, at the validation step (98.4 as maximum), is higher than POA calculated at the test step (96.9), since the VD texts have already been processed by the model while the TsD texts are treated by the model for the first time. The POA at this stage is even higher compared to the first stage, knowing that the variant that is discussed at this level is the amount of text provided in each of the two stages. We partially conclude that the amount of text provided during the training and test steps is proportional with the POA calculated at the validation step.

3) Stage 3: The last experimentation process was performed by taking documents of different authors from the three data sources. The aim was to have documents in Arabic and to be able to predict the missing text of these documents. The results of this process are reported in Table XI.

TABLE XI. PREDICTION OVERALL ACCURACY

| Dataset   | TrD | VD | TsD  |    |      |
|-----------|-----|----|------|----|------|
| Rate mean | 94  | 25 | 99.6 | 25 | 97.8 |

At this stage, we have calculated POA by a cumulative method, i.e. we have provided the CNN-model with a quantity of text and we have calculated POA, then we have enlarged the training set (validation set and test set as well) by increasing the amount of text to improve performance. We have done as well by feeding CNN-model by texts and calculating POA until we supply all the text. We experimented with 4 steps of transformations (e.g. one author, one source, combination of authors per source, combination of sources per author) each transformation had been applied twice while enlarging data from first time to the second. Table XII shows the best performance of POA while dealing with data augmentation.

## VI. CONCLUSION

Compared to traditional Machine Learning, CNN is one of best solutions for automatic learning using the raw text data directly. In this work, our CNN-model depends on both words and characters of Arabic language to encode text data, which involves in dealing with large input vectors while using word encoding. We have proposed an Arabic text encoding method that is based on converting  $N$ -gram unique dictionary integer ID number to its equivalent binary value. To be compatible

TABLE XII. BEST PERFORMANCE FOR DATA AUGMENTATION

| Dataset          | Data percentage | $N = 3$ | $N = 4$ | $N = 5$ |
|------------------|-----------------|---------|---------|---------|
| Mahmoud Darweesh | 18.75 %         | 45.9    | 66.8    | 89.4    |
| Taha Hussein     | 22.00 %         | 52.3    | 66.3    | 92.8    |
| Najeeb Mahfod    | 17.36 %         | 50.0    | 63.2    | 87.9    |
| AWB              | 26.39 %         | 64.0    | 76.2    | 94.8    |
| HND              | 27.08 %         | 58.9    | 77.3    | 95.6    |
| ShL              | 45.53 %         | 59.2    | 78.1    | 96.9    |
| AWB + HND        | 53.47 %         | 58.4    | 74.2    | 95.6    |
| HND + ShL        | 72.61 %         | 54.0    | 72.4    | 94.2    |
| ShL + AWB        | 71.92 %         | 59.0    | 75.1    | 95.7    |
| AWB + HND + ShL  | 100 %           | 60.0    | 77.1    | 97.8    |

and efficiency with the encoding method, we have proposed our CNN-based architecture with horizontal and vertical convolutional layers.

The CNN-model initialization requires then adequate weight parametrizing, but in our experiments, we have opted for low level representation of text data to reduce the input feature vector. We have observed that the performance and the accuracy of the model had been influenced by the way we feed up the CNN at inputs.

We have make the deal to challenge the lack of research on Arabic text prediction using CNN. For measure, our models have achieved a competitive accuracy and our results have shown the powerful use of CNN and its ability to predict Arabic missing text using a statistical and probabilistic approach.

Our work has shown limitations on the amount of CNN input data. Indeed, at a number of fifty MB the machine crashes, knowing that we have worked on a CPU. We will adapt our algorithm and our CNN-model to work on a GPU and therefore we can discuss more efficient results.

## REFERENCES

- [1] Ibn Taymiya. Book of Al Iman. Fifth Edition. 1996.
- [2] Wenzhe Shi, Jose Caballero, Ferenc Husz ar, Johannes Totz, Andrew P. Aitken, Rob Bishop, Daniel Rueckert, and Zehan Wang. Real-time single image and video super-resolution using an efficient sub-pixel convolutional neural network. In Proceedings of the IEEE Conference on Computer Vision and Pattern Recognition, pages 1874–1883, 2016.
- [3] WANG, Shasha, JIANG, Liangxiao, et LI, Chaoqun. Adapting naive Bayes tree for text classification. Knowledge and Information Systems, 2015, vol. 44, no 1, p. 77-89.
- [4] WANG, Tao, WU, David J., COATES, Adam. End-to-end text recognition with convolutional neural networks. In : Proceedings of the 21st International Conference on Pattern Recognition (ICPR2012). IEEE, 2012. p. 3304-3308.
- [5] COATES, Adam, CARPENTER, Blake, CASE, Carl, Sanjeev Sathesh, Bipin Suresh, Tao Wang, David J Wu, and Andrew Y Ng. Text Detection and Character Recognition in Scene Images with Unsupervised Feature Learning. In : ICDAR. 2011. p. 440-445.
- [6] SIMARD, Patrice Y., SZELISKI, Richard, BENALOH, Josh. Using character recognition and segmentation to tell computer from humans. In : Seventh International Conference on Document Analysis and Recognition, 2003. Proceedings. IEEE, 2003. p. 418-423.
- [7] SOURI, Adnan, EL MAAZOUZI, Zakaria, AL ACHHAB, Mohammed, ELMOHAJIR, and Badr Eddine. Arabic Text Generation Using Recurrent Neural Networks. In : International Conference on Big Data, Cloud and Applications. Springer, Cham, 2018. p. 523-533.
- [8] ZHANG, Zizhao, XIE, Yuanpu, et YANG, Lin. Photographic text-to-image synthesis with a hierarchically-nested adversarial network. In : Proceedings of the IEEE Conference on Computer Vision and Pattern Recognition. 2018. p. 6199-6208.



- [9] MORERA, Angel, SANCHEZ, Angel, VELEZ, José Francisco. Gender and handedness prediction from offline handwriting using convolutional neural networks. *Complexity*, 2018, vol. 2018.
- [10] AHMED, Saad Bin, MALIK, Zainab, RAZZAK, Muhammad Imran. Sub-sampling Approach for Unconstrained Arabic Scene Text Analysis by Implicit Segmentation based Deep Learning Classifier. *Global Journal of Computer Science and Technology*, 2019.
- [11] SOURI, Adnan, AL ACHHAB, Mohammed, and EL MOHAJIR, Badr Eddine. A proposed approach for Arabic language segmentation. In : 2015 First International Conference on Arabic Computational Linguistics (ACLing). IEEE, 2015. p. 43-48.
- [12] SOURI, Adnan, AL ACHHAB, Mohammed, and EL MOHAJIR, Badr Eddine. A study towards building an Arabic corpus. (2015, October) *Journées Doctorales sur l'Ingénierie de la Langue Arabe. ENSA-Fès*.
- [13] TENSMEYER, Chris and MARTINEZ, Tony. Analysis of convolutional neural networks for document image classification. In : 2017 14th IAPR International Conference on Document Analysis and Recognition (ICDAR). IEEE, 2017. p. 388-393.
- [14] LECUN, Yann, BENGIO, Yoshua, and HINTON, Geoffrey. Deep learning. *nature*, 2015, vol. 521, no 7553, p. 436.
- [15] GIRSHICK, Ross, DONAHUE, Jeff, DARRELL, Trevor. Rich feature hierarchies for accurate object detection and semantic segmentation. In : *Proceedings of the IEEE conference on computer vision and pattern recognition*. 2014. p. 580-587.
- [16] SZEGEDY, Christian, LIU, Wei, JIA, Yangqing. Going deeper with convolutions. In : *Proceedings of the IEEE conference on computer vision and pattern recognition*. 2015. p. 1-9.
- [17] SIMONYAN, Karen et ZISSERMAN, Andrew. Very deep convolutional networks for large-scale image recognition. *arXiv preprint arXiv:1409.1556*, 2014.
- [18] <https://www.un.org/ar/>
- [19] <https://www.arabworldbooks.com/>
- [20] <http://shamela.ws/index.php/main>
- [21] <https://www.hindawi.org/>

# Multi-Modal Biometric: Bi-Directional Empirical Mode Decomposition with Hilbert-Hung Transformation

Gavisiddappa<sup>1</sup>

Channabasaveshwara Institute of Technology  
Gubbi, India  
ORCID 0000-0003-3385-2640

Chandrashekar Mohan Patil<sup>2</sup>

Vidyavardhaka College of Engineering,  
Mysore, India  
ORCID 0000-0002-5220-4799

Shivakumar Mahadevappa<sup>3</sup>

GSSS Institute of Engineering and Technology for Women  
Mysore, India  
ORCID 0000-0003-1247-6009

Pramod KumarS<sup>4</sup>

Kalpataru Institute of Technology  
Tiptur, India  
ORCID 0000-0001-7457-3432

**Abstract**—Biometric systems (BS) helps in reorganization of individual person based on the biological traits like ears, veins, signatures, voices, typing styles, gaits, etc. As, the Uni-modal BS does not give better security and recognition accuracy, the multimodal BS is introduced. In this paper, biological characters like face, finger print and iris are used in the feature level fusion based multimodal BS to overcome those issues. The feature extraction is performed by Bi-directional Empirical Mode Decomposition (BEMD) and Grey Level Co-occurrence Matrix (GLCM) algorithm. Hilbert-Huang transform (HHT) is applied after feature extraction to obtain local features such as local amplitude and phase. The combination of BEMD, HHT and GLCM are used for achieving effective accuracy in the classification process. MMB-BEMD-HHT method is used in Multi-class support vector machine technique (MC-SVM) as a classifier. The false rejection ratio has improved using feature level fusion (FLF) and MC-SVM technique. The performance of MMB-BEMD-HHT method is measured based on the parameters like False Acceptance Ratio (FAR), False Rejection Ratio (FRR), and accuracy and compared it with an existing system. The MMB-BEMD-HHT method gave 96% of accuracy for identifying the biometric traits of individual persons.

**Keywords**—Biometric Systems (BS); multimodal biometrics; bi-directional empirical mode decomposition; Hilbert-Huang transform; Multi-Class Support Vector Machines technique (MC-SVM); 2000 Mathematics Subject Classification: 92C55, 94A08, 92C10

## I. INTRODUCTION

MMBS uses two or more physiological or behavioural characteristics for identification and it is more convenient than traditional authentication techniques. The main objective of the MMBS is to minimize the False Acceptance Rate (FAR), False Rejection Rate (FRR) and Failure To Enroll Rate (FTE) [1], [2]. In different orientations, the directional bank filter involves to extract the palm vein patterns and also the non-vein pixels are identified by assessing the Directional Filtering Magnitude (DFM) [3]. Feature level fusion (FLF) helps to extract the features from fingerprint and face. Then the impact over the matching performance is analysed using the random projection based transformation and proportion weight factor. Then FLF

fuses the off-line signature along with curvelet transform is used for feature extraction [4], [5]. A fused multimodal system like FLF is used over the fingerprint, retina and finger vein to reduce the genuine acceptance rate (GAR) and also the security against spoofing is improved [6]. A chaff point based fuzzy vault extracts the features of face and ear points and the best point is created by selecting the best locations of feature vectors which is found by the particle swarm optimization (PSO) [7]. The fusion over the face and voice modules made by the transformation based fusion algorithm over an ensemble classifier and also the fusion of these behaviour traits are made by Adaptive Neuro Fuzzy Inference System (ANFIS) [8], [9].

The two circular detection detects the iris and then the features of face and iris are combined with support vector machine [10]. Fuzzy vault template is added to enhance the security based on the biometric features of the fingerprint and iris [11]. An adaptive combination of multiple biometric modalities is achieved by using palm print, finger-knuckle print and iris along with PSO is used for optimizing the selection of score level combination, decision threshold and corresponding parameters [12]. Score level fusion occurs over the finger vein, fingerprint, finger shape and finger knuckle print features from the human and it performs based on the triangular norm. Features from the score level fusion may not be compatible and large dimensionality of feature space leads to irrelevant and redundant data [13]. The fuzzy-weighted image quality assessment fuse five types of biometric features such as hand geometry, palm print, palmar knuckle print, palm vein and finger vein. During the fusion, more weights are combined with the images to attain better quality. The vein images are not constant at all times; it changes based on the medical condition [14]. Match score level fusion combines the features of face and signature. Face and signature features are extracted by the Long Term Potential (LTP) and Hidden Markov model (HMM) respectively. Accuracy of the MMBS is not compatible, when the system does not have perfect matching [15]. The existing systems have some limitations like less accuracy, less sensitivity and recall. In order to overcome

that, the MMB-BEMD-HHT method is developed to enhance the accuracy for identifying the individual biometric traits. The major contributions of this research work is stated as follows:

- 1) To improve the accuracy of the image recognition, two different feature extraction techniques are combined here such as HHT and GLCM.
- 2) The FLF is used for fusing the feature vectors of finger print, face and iris. This FLF is pre classification technique which is used before matching and it gives more accurate results when compared to post classification techniques such as score level and decision level fusion. Because the FLF provides the richer information about the extracted feature vectors.
- 3) Then the classification of features performs by placing the hyperplanes among the margins in MC-SVM.

This research work is composed as follows, Section 2 presents an extensive survey of recent papers based on MM-BS. Section 3 briefly described the MM-BS using feature level fusion with MC-SVM based matching. Section 4 describes about an experimental result of a MMB-BEMD-HHT and conventional methods. The conclusion of this research work is given at the end.

## II. LITERATURE SURVEY

Yang et al. [16] presented the cancellable multi-biometric system that comprises of fingerprint and finger vein and it provided the template protection and revocability. Fingerprint and fingerprint vein were extracted by the alignment of free local structures and image based technique respectively. The minutia based fingerprint feature set and image based finger vein feature set were fused by FLF which have three different kinds of fusion options. This method was used to improve the GAR. The multi-biometric system affects by non-linear distortion and the noise which present in the fingerprint image.

Puneet et al. [17] introduced the multi-modal (MM) authentication which depends on the palm-dorsa vein pattern. The fusion which is present in this MM have four types such as multi-algorithm fusion, data fusion, feature fusion and score fusion. The genuine vein patterns were extracted by multi-algorithm fusion and the false vein patterns were cancelled from the extracted vein patterns via fusion. There are three types of features are extracted from the vein pattern such as shape features, minutiae and features of hand boundary shape. Finally, third level of fusion was applied for fusing the minutiae and shape features. These three fusion algorithms were used to improve the accuracy, but this system is unstable because of the elastic nature of the skin.

Xiaojun et al. [18] improved the feature level of MM-BS fusion using a multi-set generalized canonical discriminant projection (MGCDP) method. This MGCDP increased the correlation of intra class features during the minimization of correlation among the class. More than two types of BM features were fused with serial MGCDP (S-MGCDP) and parallel MGCDP (P-MGCDP). This MGCDP was used to improve the recognition rate that has ability to identify the new samples.

Asaari et. al. [19] considered the fusion of finger vein and finger geometry recognition to introduce a multimodal

finger biometrics. The Band Limited Phase Only Correlation (BLPOC) determined the similarity between the finger vein images and the recognition of finger geometry using the width-centroid contour distance (WCCD) combined with centroid contour distance (CCD). The fusion of WCCD and CCD improved the accuracy of finger geometry recognition compared to the single type of feature. If the non-linear distortion is present in finger-vein images, it affects the performance of BLPOC-based finger vein matching [20], [21].

The issue over the non-linear distortion overcome by an ideal high pass filter in MMB-BEMD-HHT method and then the recognition rates improved by using two different feature extraction techniques such as HHT and GLCM. The MMB-BEMD-HHT is clearly explained in Section 3.

## III. MMB-BEMD-HHT METHODOLOGY

Multi-modal BS are high-performance security systems. This research work introduced a new MMB-BEMD-HHT to improve the classification accuracy. This MMB-BEMD-HHT method involves two major process database creation and testing. Fig. 1 shows the MMB-BEMD-HHT method.

### A. MMB-BEMD-HHT Training

The MMB-BEMD-HHT Training section consists of six major steps namely image acquisition, pre-processing, hybrid feature extraction, fusion and database generation. Three different combinations of inputs such as face, iris, and fingerprint are taken for training. The input images are enhanced with the help of Sharpening filter. The enhanced feature values are extracted by the hybrid feature extraction technique (HHT and GLCM), the feature values, and added by the fusion technique i.e. FLF. Finally, the fused vectors of the images are stored in the database and then these features are tested in MCSVM testing for identifying the features of individuals.

1) *Image Acquisition:* In this MMB-BEMD-HHT method, three types of biological characters such as face, iris, and fingerprint are taken to identify the individual's biological characters that are presented in Fig. 2. The face and iris images are captured by digital mobile camera and the fingerprint image is captured from the scanner.

2) *Pre-processing:* A high-pass filter used in this pre-processing for an image enhancement. These filters emphasize fine details in the image and the quality of an image highly degrades when the high frequencies are attenuated or completely removed. The high-frequency components of an image are enhanced that improve the image quality. For example, if the face image is given as an input, then the filter functions for an ideal high pass filter is expressed in Eq. (1):

$$X_F(m, n) = \begin{cases} 0 & \text{if } D(m, n) \leq D_0 \\ 1 & \text{if } D(m, n) > D_0 \end{cases} \quad (1)$$

Where  $D(m, n)$  is the distance between the centre of frequency rectangle and  $X_F(m, n)$  is the enhanced image. Similarly, the iris and fingerprint images are enhanced by this filter and it is expressed as  $X_I(m, n)$  and  $X_{Fp}(m, n)$ , respectively.

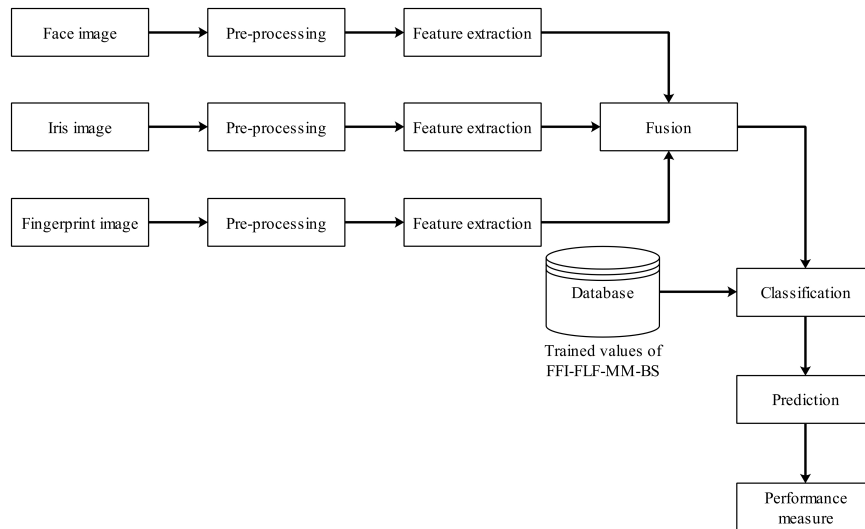


Fig. 1. Block diagram for MMB-BEMD-HHT

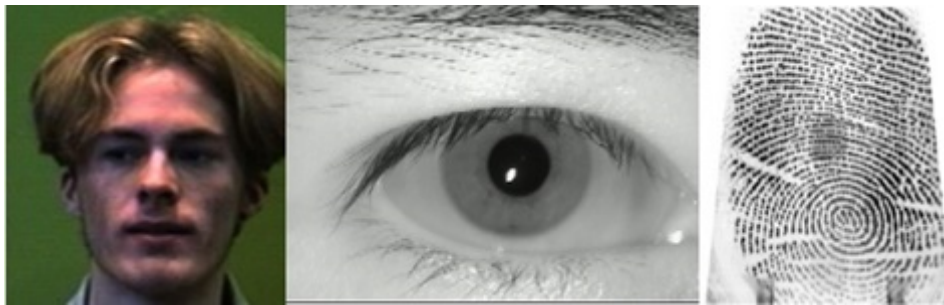


Fig. 2. Image acquisition

3) *Hybrid Feature Extraction Technique:* The pre-processed images are sent to the hybrid feature extraction. The complicated data set can be decomposed into finite and small number of Intrinsic Mode Function (IMF) components that become the basis representing the data. IMF and residues features of the face, iris and fingerprint are extracted by BEMD and then the Hilbert transform is achieved to handle both non stationary non linear values. Here GLCM also used for extracting the statistical texture features from the pre-processed images. Then the features of GLCM are combined with features from HHT by using FLF.

**IMF and residue feature extraction using BEMD:** The features of the face, iris and fingerprint images are extracted by BEMD. The nonlinear and non-stationary data are processed by Empirical Mode Decomposition (EMD). The EMD provides sum of oscillatory functions by decomposing the signal and the oscillatory functions are called as Intrinsic Mode Function (IMF). This IMF satisfies the two conditions which are given below:

- The amount of extreme and the amount of zero crossing of an entire data set are either equal or differ at most by one.
- Local minima define the envelope mean value at any point.

From these two conditions, a meaningful instantaneous frequency is calculated. This EMD decomposes a signal  $(X(t))$  into a set of IMF's by shifting process. This EMD is also used in the decomposition of images or 2D data which is defined as Bi-dimensional EMD.

An image  $X_F(m, n)$  is an enhanced face image and the steps of BEMD feature extraction is given as follows:

- 1) The local minima and maxima of the image  $X(m, n)$  are identified.
- 2) Upper envelope  $(X_{Fup}(m, n))$  and lower envelope  $(X_{Flow}(m, n))$  are obtained by using the cubic spline interpolation between the local minima and maxima.
- 3) The following Eq. (2) is used to calculate the mean of upper and lower envelope.

$$S(m, n) = \frac{X_{Fup}(m, n) + X_{Flow}(m, n)}{2} \quad (2)$$

- 4) The signal  $X_{1F}(m, n)$  is achieved by subtracting the  $S(m, n)$  from  $X_F(m, n)$  and the mathematical expression for  $X_{1F}(m, n)$  is given in Eq. (3).

$$X_{1F}(m, n) = X_F(m, n) - S(m, n) \quad (3)$$

- 5) Then check if  $X_{1F}(m, n)$  accepts the criteria for an IMF. If it is not satisfy means,  $X_F(m, n)$  is replaced by  $X_{1F}(m, n)$  and repeats the process to achieve the IMF.

The first IMF from the BEMD is in Eq. (4).

$$C_{1F}(m, n) = X_{1F}(m, n) \quad (4)$$

Where, the intrinsic mode function is denoted as  $C_{1F}(m, n)$ . The residue ( $r_f$ ) is obtained by subtracting the  $C_{1F}(m, n)$  from  $X_F(m, n)$ , which is shown in Eq. (5).

$$r_f(m, n) = X_F(m, n) - C_{1F}(m, n) \quad (5)$$

Based on the residue value from Eq. (5), the next IMF values are calculated. The shifting process is continued until the final residue becomes constant or it is a function which includes only one maxima or minima from that no more IMF's are obtained. The texture feature of each IMF is denoted by fractal dimensions. Here three IMF's ( $C_{1F}$ ,  $C_{2F}$  and  $C_{3F}$ ) and one residue ( $r_f$ ) value are obtained from an enhanced face image. Similarly, the IMF's and residue from the iris and fingerprint are extracted. The IMF's from the iris and fingerprint are ( $C_{1I}$ ,  $C_{2I}$  and  $C_{3I}$ ) and ( $C_{1Fp}$ ,  $C_{2Fp}$  and  $C_{3Fp}$ ) respectively as well as  $r_i$  is the residue of iris and  $r_{fp}$  is the residue of fingerprint. Then these IMF and residue values of face, iris and fingerprint are given to the input for HHT to extract the local phase and amplitude.

**Hilbert-Huang transform:** The IMF's and residue from the BEMD are given to HHT for achieving the local features such as amplitude and phase. A 2D analytical signals are obtained by using Riesz transform on the 2D IMF's and residue of the BEMD. Riesz transform are family of generations Hilbert - Huang transforms. The generalization of Hilbert transform is the combination of image and its transform is called as monogenic signal. Here, the partial Hilbert transform is performed on the IMF's and residue with respect to a half space which is chosen by introducing a preference direction and it is given in Eq. (6).

For example the first IMF value of Eq. (4) is taken to find the Hilbert transform.

$$H(\vec{C}_{1F}) = j \text{sign}(\vec{C}_{1F}, \vec{d}) \quad (6)$$

where,  $\vec{d}$  is one preference direction. This Hilbert transform missed the isotropy.

Furthermore, the Riesz transform is utilized in the Hilbert transform and a multidimensional generalization of the Hilbert transform. The frequency domain expression of Riesz transformed signal is in Eq. (7).

$$F_R(\vec{C}_{1F}) = \frac{i\vec{C}_{1F}}{C_{1F}} F(\vec{C}_{1F}) = H(\vec{C}_{1F}) F(\vec{C}_{1F}) \quad (7)$$

The sparse representation of Eq. (7) is shown in following Eq. (8).

$$f_{RF1}(\vec{y}) = -\frac{\vec{y}}{2\pi|\vec{y}|^3} \times f_{1F}(\vec{y}) = h(\vec{y}) \times f_{1F}(\vec{y}) \quad (8)$$

The 2D analytical signal is constituted by Riesz transformed signal and the original signal, and this analytical signal is monogenic signal which is in Eq. (9).

$$f_{MF1}(\vec{y}) = f_{1F}(\vec{y}) - (i, j) f_{RF1}(\vec{y}) \quad (9)$$

The above formulation is Eq. (9) 2D analytical signal which is a 3D vector as well as it should used for achieving local features of monogenic signal.

**Phase:** The phase of the 2D analytical signal of first IMF is given in Eq. (10).

$$\text{atan3}(x, y) = \frac{\vec{y}_D}{|\vec{y}_D|} \text{atan} \left( \frac{|\vec{y}_D|}{\langle (0, 0, 1)^T, \vec{y} \rangle} \right) \quad (10)$$

Where the direction of the rotation vector is  $\vec{y}_D = (0, 0, 1)^T \times \vec{y}$ . The phase of monogenic signal is in Eq. (11).

$$\varphi_{1F}(\vec{y}) = \text{atan3}(f_{MF1}(\vec{y})) = \arg(f_{MF1}(\vec{y})) \quad (11)$$

**Amplitude:** The local amplitude of  $f_{MF1}(\vec{y})$  is in Eq. (12)

$$|f_{MF1}(\vec{y})| = \sqrt{f_{MF1}(\vec{y}) \overline{f_{MF1}(\vec{y})}} \quad (12)$$

$$= \sqrt{f_{1F}^2(\vec{y}) + |f_{RF1}(\vec{y})|^2} \quad (13)$$

The following Eq. (14) is reconstructed from Eq. (12).

$$f_{MF1}(\vec{y}) = |f_{MF1}(\vec{y})| \exp(-j, i, 0) \varphi_{1F}(y) \quad (14)$$

The monogenic signal of each IMF allows to calculate local amplitude and local phase. Likewise, the local phase and amplitude is calculated for remaining two IMF and residue values which is denoted as  $\varphi_{1F}, \varphi_{2F}, \varphi_{3F}, \varphi_{4F}$  and  $f_{MF1}, f_{MF2}, f_{MF3}, f_{MF4}$ , respectively. These local phase and amplitude values are combined in one array which is shown in the following Eq. (15) and (16), respectively.

$$\varphi_f = \{\varphi_{1F}, \varphi_{2F}, \varphi_{3F}, \varphi_{4F}\} \quad (15)$$

$$f_{Mf} = \{f_{MF1}, f_{MF2}, f_{MF3}, f_{MF4}\} \quad (16)$$

Similarly the local phase and local amplitude values are calculated for the IMF's and residue of iris and fingerprint. Hence  $\varphi_i$  and  $f_{Mi}$  for iris and  $\varphi_{fp}$  and  $f_{Mfp}$  for fingerprint.

**Grey level co-occurrence matrix:** The images which is enhanced by the ideal high pass filters are given as an input to the GLCM. It is used for extracting the second order statistical texture features and it is introduced by Haralick. GLCM transforms the image into a matrix with respect to the pixels of an original image. The calculation of mutual occurrence of pixel pairs is required and it is calculated for a specific distance oriented at a particular direction. Then the statistical features are extracted for further process. There are different types of features are extracted from the GLCM of pre-processed face image and the expression of features are given in below Eq. (17)-(27).

Auto correlation

$$F1 = \sum_m \sum_n (mn) X_F(m, n) \quad (17)$$

Contrast

$$F2 = \sum_{i=0}^{N_g-1} i^2 \left\{ \sum_{i=1}^{N_g} \sum_{j=1}^{N_g} X_F(m, n) \right\} \quad (18)$$

Correlation

$$F3 = \frac{\sum_i \sum_j (mn) X_F(m, n) - \mu_x \mu_y}{\sigma_x \sigma_y} \quad (19)$$

Energy

$$F4 = \sum_i \sum_j X_F(m, n)^2 \quad (20)$$

Entropy

$$F5 = \sum_i \sum_j X_F(m, n) \log(X_F(m, n)) \quad (21)$$

Homogeneity

$$F6 = \sum_i \sum_j \frac{1}{1+(m-j)^2} X_F(m, n) \quad (22)$$

Sum average

$$F7 = \sum_{m=2}^{2N_g} m X_{F_{x+y}}(m) \quad (23)$$

Sum entropy

$$F8 = - \sum_{i=2}^{2N_g} X_{F_{x+y}}(m) \log(p_{x+y}(m)) \quad (24)$$

Sum variance

$$F9 = \sum_{m=2}^{2N_g} (m-F8)^2 X_{F_{x+y}}(m) \quad (25)$$

Difference variance

$$F10 = \text{variance of } X_{F_{x-y}} \quad (26)$$

Difference entropy

$$F11 = - \sum_{m=0}^{N_g-1} X_{F_{x-y}}(m) \log(X_{F_{x-y}}(m)) \quad (27)$$

where,  $X_F(m, n)$  is the entry of a normalized GLCM,  $N_g$  is the number of distinct grey levels in the quantized image [22].

4) *Feature Level Fusion (FLF)* : FLF receives the feature vectors from the hybrid feature extraction technique and it has the rich information about the biometric features. This FLF performs before matching and performs two levels of fusion. At first, this FLF fuses the features from the HHT with GLCM for face, iris, and fingerprint individually. In second level fusion, the fusion vectors of face, iris, and fingerprint are fused together.

The response time of the feature level fusion is less than the score level fusion. FLF concatenates the extracted features. The dimensionality of the fused feature vector maximizes by the feature set of concatenation. The steps which are performed in the FLF are:

- Normalization of feature vector.
- Fusing the feature vector.

**Normalization of feature vector:** The feature vectors which are extracted from face, iris and fingerprint are incompatible in nature. Because of the variation in its own range and distribution. This problem overcome by normalizing the feature vector.

**Fusing the feature vector:** The final fused vector is achieved by concatenating the feature vector from face, iris and fingerprint. The expression for first level fusion is given in Eq. (28), (29) and (30).

$$f = [\varphi_f, f_{Mf}, F] \quad (28)$$

$$i = [\varphi_i, f_{Mi}, I] \quad (29)$$

$$fp = [\varphi_{fp}, f_{Mfp}, FP] \quad (30)$$

Where  $f$ ,  $i$  and  $fp$  are first level fusion vectors of face, iris and fingerprint respectively. In second level fusion, these features are combined together and the fused vector ( $z_v$ ) is shown in the following Eq. (31).

$$z_v = [f_1, f_2, \dots, f_n, i_1, i_2, \dots, i_n, fp_1, fp_2, \dots, fp_n] \quad (31)$$

Where,  $f_1, f_2, \dots, f_n, i_1, i_2, \dots, i_n$  and  $fp_1, fp_2, \dots, fp_n$  defines the normalized vectors of face, iris and finger print, respectively. These fused vectors are stored in the database and it is used for the identification of individuals.

Furthermore, the extracted features of face, iris and fingerprint are stored into the database. Then it is transferred to the MCSVM for testing.

#### B. MMB-BEMD-HHT Training by MC-SVM

The fused vector data about the face, iris and fingerprint are trained in the MC-SVM classifier. MC-SVM is a pattern classification algorithm which depends on the statistical learning theory [23]. A small classification samples (nonlinear samples) and high dimensional problems overcome by using SVM and it depends on the Structural Risk Minimization (SRM) which reduces the upper bound over the expected risk in contrast. The basic principle behind the SVM is to resolve the classification problems. The basic structure for SVM is shown in Fig. 3.

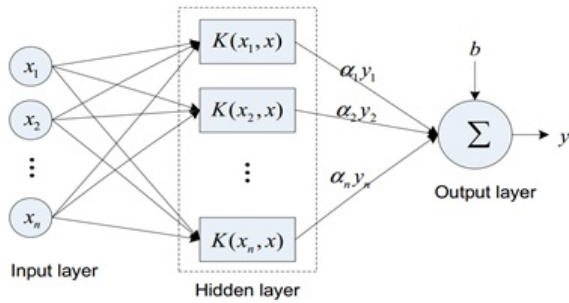


Fig. 3. Structure of SVM

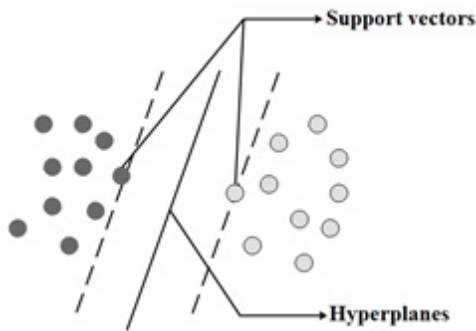


Fig. 4. Linearly separable data with multiple hyper plane.

The SVM is a two class SVM that separate the data into two classes by identifying the hyper plane among the data with maximum margin. There may be multiple numbers of hyper planes present inside the SVM. MMB-BEMD-HHT has to find the optimal hyper plane that separates the data in error free and also increases the margin among the two classes. Fig. 4 and 5 shows the linear separable data with multiple and optimum hyper plane, respectively. Then the nonlinear separable data is shown in Fig. 6.

SVM has a kernel function which performs the separating function and this function use for determining the optimal hyper plane. The kernel function of SVM is an integral part of SVM that divides the input data into two classes involving a less number of support vectors. There are four types of kernel functions that is given below.

- 1) Linear,  $K(z_i, z_j) = z_i^T z_j$
- 2) Polynomial,  $K(z_i, z_j) = (\gamma z_i^T z_j + r)^d, \gamma > 0$
- 3) Radial Basis Function (RBF),

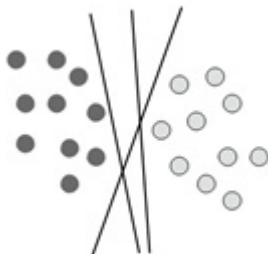


Fig. 5. Linearly separable data with optimum hyper plane.

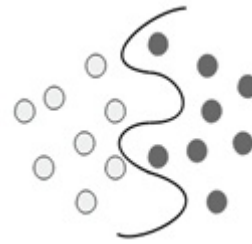


Fig. 6. Nonlinear separable data.

$$K(z_i, z_j) = \exp(-\gamma \|z_i - z_j\|^2), \gamma > 0$$

$$4) \text{ Sigmoid, } K(z_i, z_j) = \tanh(z_i^T z_j + r)$$

Where,  $r, \gamma$  and  $d$  are the kernel parameters. The kernel function is chosen based on the classification problem. From the four kernel functions, the radial basis function (RBF) is chosen because the samples are non-linearly mapped to a high dimensional space. The relation among class labels and the non-linear attributes of class labels are managed by the RBF.

1) *Multi Class Classification of SVM* : SVM is employed for binary class problem. Then the SVM is extended to a multi class SVM. The conversion of SVM to Multi class SVM has two strategies such as one against one strategy and one against rest strategy. One against one strategy use to classify between each pairs and one against rest strategy classifies among each class and all the remaining biometric traits. These two schemes use to create the multiclass SVM. The one against one strategy needs a  $k(k-1)/2$  binary SVMs and one against rest strategy needs a  $k$  binary SVMs to build a  $k$  classifier. Finally, the trained values from the MC-SVM is stored as a database and it is given to the input for testing process.

2) *MMB-BEMD-HHT Testing by MC-SVM*: Image Acquisition is the process of capturing the biological input image. Then the captured input image is enhanced by the high-pass filter. The pre-processed image feature values are extracted by the HHT and GLCM which is similar to feature extraction. Then the feature values are fused by the FLF fusion method that is given in feature level fusion. The fused feature values are given to MC-SVM prediction with the trained features of face, fingerprint and iris that predicts whether the tested image is authenticated or not. This MC-SVM is used for classifying an individual biometric trait.

#### IV. RESULTS AND DISCUSSION

The MMB-BEMD-HHT method was analysed with the help of MATLAB 2017b. This MMB-BEMD-HHT method was developed with the biometric features of face, iris and fingerprint to enhance the security of the desired system. Here, the database for face, iris and fingerprint are MIT CBCL, MMU and Casia V5 respectively [26], [27], [28]. The performance of the MMB-BEMD-HHT was evaluated in terms of FAR, FRR and accuracy.

In MMB-BEMD-HHT method, the particular person is identified by anyone of the biometric feature like face, iris and fingerprint. Total 150 images were used in MMB-BEMD-HHT training and this 150 images comprised of 50 face images, 50



Fig. 7. Pre-processed images of face, iris and fingerprint.



Fig. 8. Feature extracted images of face, iris and fingerprint.

TABLE I. COMPARATIVE ANALYSIS OF MMB-BEMD-HHT

| Parameters      | SIFT-KNN-MM-BS [24] | FLF-FFF-MM-BS [25] | MMB-BEMD-HHT |
|-----------------|---------------------|--------------------|--------------|
| <b>FAR</b>      | 3.75%               | 5%                 | 0.10%        |
| <b>FRR</b>      | 7.5%                | 5%                 | 2.0%         |
| <b>Accuracy</b> | 92.5%               | 95%                | 96%          |

|  |  |   |
|--|--|---|
| 1 <sup>st</sup> Face image BEMD feature values | 1 <sup>st</sup> Iris image BEMD feature values | 1 <sup>st</sup> Fingerprint image minutiae feature values |
|--|--|---|

Fig. 9. Example of fusion structure.

|  |
|--|
| 1 <sup>st</sup> face, 1 <sup>st</sup> iris & 1 <sup>st</sup> fingerprint database value    |
| 2 <sup>nd</sup> face, 2 <sup>nd</sup> iris & 2 <sup>nd</sup> fingerprint database value    |
| 3 <sup>rd</sup> face, 3 <sup>rd</sup> iris & 3 <sup>rd</sup> fingerprint database value    |
| .  |
| .  |
| .  |
| .  |
| 50 <sup>th</sup> face, 50 <sup>th</sup> iris & 50 <sup>th</sup> fingerprint database value |

Fig. 10. Database structure for MMB-BEMD-HHT.

iris images and 50 fingerprint images of 10 persons. Here, the biometric traits of single person have 5 face images, 5 iris images and 5 fingerprint images. Initially, the pre-processing process takes place to enhance the clarity of biometric traits. The pre-processed images of face, iris and fingerprint are shown in Fig. 7. Then the features of pre-processed images

were extracted by HHT and GLCM. The feature extracted images are shown in Fig. 8. After extracting the features, it was stored in the database. Later, these features were tested in MC-SVM for testing. There are 60 images are used in the testing of MMB-BEMD-HHT and these 60 images comprises of 20 face images, 20 iris images and 20 fingerprint images of 10 persons. The pre-processing and feature extraction of MMB-BEMD-HHT testing are similar to the training. Finally, the features of the MMB-BEMD-HHT testing were compared with the trained features of face, iris and fingerprint to identify the features of individuals.

The extracted BEMD features of face, iris and fingerprint were fused by FLF and the example of FLF structure along with face, iris and fingerprint features are shown in Fig. 9. Then these feature values were stored in the database and the database structure is shown in Fig. 10.

The input images used in the MMB-BEMD-HHT training are taken as an input to the testing section. Testing also takes three different biometrics such as face, iris and fingerprint. HHT and GLCM and FLF fusion of testing are similar to the MMB-BEMD-HHT training. Based on the MC-SVM, the similarity between the database images to specific person is identified.

Fig. 11 shows the example of the class allocation for different images in the database. The first and second row represents the pictures and the respective classes of the images.



|          |    |    |    |    |    |    |    |    |    |     |       |     |     |     |     |     |
|----------|----|----|----|----|----|----|----|----|----|-----|-------|-----|-----|-----|-----|-----|
| Pictures | P1 | P2 | P3 | P4 | P5 | P6 | P7 | P8 | P9 | P10 | ----- | P46 | P47 | P48 | P49 | P50 |
| Class    | C1 |    |    |    |    | C2 |    |    |    |     | ----- | C50 |     |     |     |     |

Fig. 11. Class allocating for MMB-BEMD-HHT.

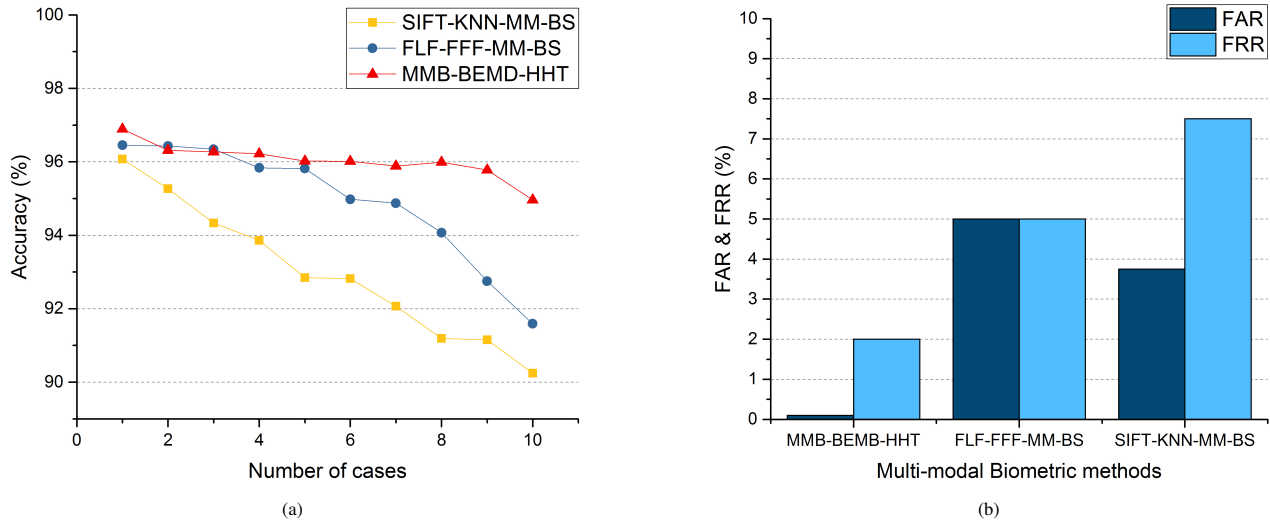


Fig. 12. Comparison of MMB-BEMD-HHT Vs existing methods (a) Accuracy (b) FAR and FRR.

From the classes, the correlated values are discovered to find the true positive (TP), true negative (TN), false positive (FP) and false negative (FN). A true positive is an outcome where the model correctly predicts the positive class. Similarly, a true negative is an outcome where the model correctly predicts the negative class. A false positive is an outcome where the model incorrectly predicts the positive class. And a false negative is an outcome where the model incorrectly predicts the negative class. These values helps to determine the following performance measures like False acceptance ratio (FAR), False Rejection Ratio (FRR) and accuracy using Eq. (32)-(34).

1) *False acceptance ratio (FAR)*: FAR is the measure of the Biometric Security System (BSS) which incorrectly accepts an unauthorized operator. The following Eq. (32) describes the FAR mean.

$$FAR = \frac{FP}{FP + TN} \quad (32)$$

2) *False Rejection Ratio (FRR)*: FRR is the measure of the likelihood which incorrectly reject an access attempt by an authorized user in MM-BS. The expression for FRR is given in the following Eq. (33).

$$FRR = \frac{FP}{TP + FN} \quad (33)$$

3) *Accuracy (A)*: The accuracy of the respective image determine based on the specificity ( $S | p$ ) and sensitivity ( $S_e$ ). Quantity of the image is accurately represented by using the following Eq. (34).

$$A = \frac{TP + TN}{TP + FP + TN + FN} \quad (34)$$

The MMB-BEMD-HHT is compared with two existing methods, which is explained below.

In first method, the image description and feature extraction of face and fingerprint images were performed by Scale Invariant Feature Transform (SIFT) and then the classification of biometric traits were made by K Nearest Neighbour (KNN) classifier. A SIFT algorithm used in this MM-BS was based on the gradient of each pixel. The pixel values which were affected by the noise is eliminated by cascade filtering technique. The removal of noise pixels affects the recognition performance [24]. In second method, the finger knuckle and finger vein were taken in MM-BS. A repeated line tracking method was used to extract the features from the finger knuckle and finger vein. Then these image features are fused by FLF with fractional firefly (FFF) optimization. Here, the layered k-SVM to carry out the recognition [25].

Table I shows the performance analysis of MMB-BEMD-HHT technique. Fig. 12 shows the comparative analysis of the MMB-BEMD-HHT Vs existing methods. Here the accuracy is compared with existing methods, because in real time systems accuracy plays a crucial role in image recognition. From the comparison, conclude that the MMB-BEMD-HHT method gives better performance in terms of accuracy as well the other parameters like FAR, and FRR also improved. By improving the accuracy of the desired system, the authentication of an individual person becomes easy.

## V. CONCLUSION

MMB-BEMD-HHT method is developed based on the three different biometric traits of face, iris and fingerprint to improve the accuracy in finding the individuals. In MMB-BEMD-HHT method, the images of face, iris and fingerprints are enhanced by using the high pass filter. The features of the image is extracted by HHT and GLCM. Then these feature vectors are fused by FLF. MC-SVM is used as the classifier and it verifies the person's identity based on the feature vectors which is stored in the database. The performance of MMB-BEMD-HHT is analysed with an existing technique. The experimental results show that the MMB-BEMD-HHT gives 96% of accuracy, 0.10 % of FAR and 2% of FRR for multimodal biometric recognition. The MMB-BEMD-HHT gives better accuracy of 96% compared to the existing methods. Furthermore, the optimization technique can be used in the feature extraction technique which may improve recognition accuracy. The proposed method is worked on limited dataset, in next phase more datasets with attributes will be considered.

## COMPLIANCE WITH ETHICAL STANDARDS

**Conflict of Interests:** Conflict of Interests: The authors of this paper declare that there is no conflict of interests regarding the publication of this manuscript.

**Ethical Approval:** This article does not contain any studies with human participants or animals performed by any of the authors.

## ACKNOWLEDGMENTS

The authors acknowledge the Massachusetts Institute of Technology, Multimedia University, Malaysia and Chinese Academy of Sciences for critical role in the creation of publicly available database of face, iris and fingerprint respectively, used in this study.

## REFERENCES

- [1] D. J. Ghate and S. B. Patil, "Survey of Biometric , Multimodal Biometric Systems," *International Journal of Science and Research (IJSR)*, vol. 3, no. 11, pp. 2012–2015, 2014.
- [2] A. T. Siddiqui, "An Enhanced Multi-Modal Biometric System for Secure User Identification," *Asian Journal of Technology and Management Research*, vol. 06, no. 01, pp. 2249–892, 2016.
- [3] K. S. Wu, J. C. Lee, T. M. Lo, K. C. Chang, and C. P. Chang, "A secure palm vein recognition system," *Journal of Systems and Software*, vol. 86, no. 11, pp. 2870–2876, 2013. [Online]. Available: <http://dx.doi.org/10.1016/j.jss.2013.06.065>
- [4] W. Yang, S. Wang, J. Hu, G. Zheng, and C. Valli, "A fingerprint and finger-vein based cancelable multi-biometric system," *Pattern Recognition*, vol. 78, pp. 242–251, 2018. [Online]. Available: <https://doi.org/10.1016/j.patcog.2018.01.026>
- [5] M. V. Karki and S. S. Selvi, "Multimodal Biometrics at Feature Level Fusion using Texture Features," *International Journal of Biometrics and Bioinformatics (IJBB)*, vol. 7, no. 1, pp. 58–73, 2013.
- [6] D. Jagadiswary and D. Saraswady, "Biometric Authentication Using Fused Multimodal Biometric," in *Procedia Computer Science*, vol. 85, no. Cms. Elsevier Masson SAS, 2016, pp. 109–116. [Online]. Available: <http://dx.doi.org/10.1016/j.procs.2016.05.187>
- [7] G. Amirthalingam and G. Radhamani, "New chaff point based fuzzy vault for multimodal biometric cryptosystem using particle swarm optimization," *Journal of King Saud University - Computer and Information Sciences*, vol. 28, no. 4, pp. 381–394, 2016. [Online]. Available: <http://dx.doi.org/10.1016/j.jksuci.2014.12.011>
- [8] F. S. Assaad and G. Serpen, "Transformation based Score Fusion Algorithm for Multi-modal Biometric User Authentication through Ensemble Classification," in *Procedia Computer Science*, vol. 61. Elsevier Masson SAS, 2015, pp. 410–415. [Online]. Available: <http://dx.doi.org/10.1016/j.procs.2015.09.175>
- [9] F. Alsaade, "Neuro-fuzzy logic decision in a multimodal biometrics fusion system," *Scientific Journal of King Faisal University*, vol. 11, no. 2, pp. 163–177, 2010.
- [10] Y. G. Kim, K. Y. Shin, E. C. Lee, and K. R. Park, "Multimodal biometric system based on the recognition of face and both irises," *International Journal of Advanced Robotic Systems*, vol. 9, pp. 1–6, 2012.
- [11] M. S. Panag and T.S., "Heterogeneous Multimodal Biometric System with Fuzzy Vault Template Security," *International Journal of Advanced Research in Computer Science and Software Engineering*, vol. 4, no. 9, 2014.
- [12] O. M. Aly and T. A. Mahmoud, "An Adaptive Multimodal Biometrics System using PSO," *International Journal of Advanced Computer Science and Applications*, vol. 4, no. 7, pp. 158–165, 2013.
- [13] J. Peng, A. A. El-Latif, Q. Li, and X. Niu, "Multimodal biometric authentication based on score level fusion of finger biometrics," *Optik*, vol. 125, no. 23, pp. 6891–6897, 2014. [Online]. Available: <http://dx.doi.org/10.1016/j.ijleo.2014.07.027>
- [14] G. K. O. Michael, T. Connie, and A. B. J. Teoh, "A contactless biometric system using multiple hand features," *Journal of Visual Communication and Image Representation*, vol. 23, no. 7, pp. 1068–1084, 2012. [Online]. Available: <http://dx.doi.org/10.1016/j.jvcir.2012.07.004>
- [15] S. T. Krishna Shinde, "Development of Face and Signature Fusion Technology for Biometrics Authentication," *International Journal of Emerging Research in Management & Technology*, vol. 9359, no. 9, pp. 61–65, 2017.
- [16] W. Yang, S. Wang, G. Zheng, and C. Valli, "Impact of feature proportion on matching performance of multi-biometric systems," in *ICT Express*. Elsevier B.V., 2018, pp. 1–5. [Online]. Available: <https://doi.org/10.1016/j.ict.2018.03.001>
- [17] P. Gupta and P. Gupta, "Multi-modal fusion of palm-dorsa vein pattern for accurate personal authentication," *Knowledge-Based Systems*, vol. 81, no. March, pp. 117–130, 2015. [Online]. Available: <http://dx.doi.org/10.1016/j.knosys.2015.03.007>
- [18] M. Xin and J. Xiaojun, "Correlation-based identification approach for multimodal biometric fusion," *Journal of China Universities of Posts and Telecommunications*, vol. 24, no. 4, pp. 34–39–50, 2017. [Online]. Available: [http://dx.doi.org/10.1016/S1005-8885\(17\)60221-8](http://dx.doi.org/10.1016/S1005-8885(17)60221-8)
- [19] M. S. Mohd Asaari, S. A. Suandi, and B. A. Rosdi, "Fusion of Band Limited Phase only Correlation and Width Centroid Contour Distance for finger based biometrics," *Expert Systems with Applications*, vol. 41, no. 7, pp. 3367–3382, 2014. [Online]. Available: <http://dx.doi.org/10.1016/j.eswa.2013.11.033>
- [20] C. M. Patil and S. Patilkulkarni, "An efficient process of recognition of human iris based on contourlet transforms," *Procedia Computer Science*, vol. 2, no. 2009, pp. 121–126, 2010. [Online]. Available: <http://dx.doi.org/10.1016/j.procs.2010.11.015>
- [21] C. M. Patil, "An Efficient Iris Recognition System to Enhance Security Environment for Personal Identification," *International Journal of Communications Networking System*, vol. 2, no. 12, pp. 174–179, 2013.
- [22] L. K. Soh and C. Tsatsoulis, "Texture analysis of sar sea ice imagery using gray level co-occurrence matrices," *IEEE Transactions on Geoscience and Remote Sensing*, vol. 37, no. 2 I, pp. 780–795, 1999.
- [23] P. Sharma and M. Kaur, "Multimodal Classification using Feature Level Fusion and SVM," *International Journal of Computer Applications*, vol. 76, no. 4, pp. 26–32, 2013.
- [24] G. W. Mwaura, P. W. Mwangi, and C. Otieno, "Multimodal Biometric System :- Fusion Of Face And Fingerprint Biometrics At Match Score Fusion Level," *International Journal of Scientific and Technology Research Volume*, vol. 6, no. 04, pp. 41–49, 2017.
- [25] S. Veluchamy and L. Karlmarx, "System for multimodal biometric recognition based on finger knuckle and finger vein using feature-level fusion and k-support vector machine classifier," *IET Biometrics*, vol. 6, no. 3, pp. 232–242, 2017. [Online]. Available: <http://digital-library.theiet.org/content/journals/10.1049/iet-bmt.2016.0112>

- [26] B. Weyrauch, B. Heisele, J. Huang, and V. Blanz, "Component-based face recognition with 3D morphable models," in *IEEE Computer Society Conference on Computer Vision and Pattern Recognition Workshops*, vol. 2004-Jan, no. January, 2004.
- [27] Malaysia Multimedia University. MMU1 iris image database, 2004. [Online]. Available: <http://pesona.mmu.edu.my/ccteo/>
- [28] "Casia iris image database." Institute of Automation, Chinese Academy of Sciences, 2012. [Online]. Available: <http://biometrics.idealtest.org/>

# Heuristics Applied to Mutation Testing in an Impure Functional Programming Language

Juan Gutiérrez-Cárdenas<sup>1</sup>, Hernan Quintana-Cruz<sup>2</sup>, Diego Mego-Fernandez<sup>3</sup>, Serguei Diaz-Baskakov<sup>4</sup>  
Carrera de Ingeniería de Sistemas  
Universidad de Lima

**Abstract**—The task of elaborating accurate test suites for program testing can be an extensive computational work. Mutation testing is not immune to the problem of being a computational and time-consuming task so that it has found relief in the use of heuristic techniques. The use of Genetic Algorithms in mutation testing has proved to be useful for probing test suites, but it has mainly been enclosed only in the field of imperative programming paradigms. Therefore, we decided to test the feasibility of using Genetic Algorithms for performing mutation testing in functional programming environments. We tested our proposal by making a graph representations of four different functional programs and applied a Genetic Algorithm to generate a population of mutant programs. We found that it is possible to obtain a set of mutants that could find flaws in test suites in functional programming languages. Additionally, we encountered that when a source code increases its number of instructions it was simpler for a genetic algorithm to find a mutant that can avoid all of the test cases.

**Keywords**—Mutation testing; heuristics; functional programming

## I. INTRODUCTION

Usually, when a programmer develops a software, it requires that when this code is executed; the obtained answers are correct given the right set of inputs. However, this required performance is sometimes not achieved, due to incorrect answers given when the execution of the program is completed. The main reason for this so-called abnormal behavior of an application is due to the presence of flaws within the code. In a way to perform an extensive search for these flaws is to elaborate a group of tests cases; in which a program should return the correct answers established by them. The elaboration of these tests cases is not a trivial task because it requires a certain level of detail to try to catch a flaw in the program tested. Because of this, it is needed a form to evaluate the quality of these test cases. An important part to consider when developing a test case is that this should detect if a program behaves abnormally when specific inputs are entered. A naive way to perform the quality of a test case would be to cause intentional flaws in a program and to observe if the answer that this faulty program returns is the same as the original program. We usually called this flawed program a mutant. In the case that a mutant and a original program return different outputs when dealing with the same input that is in a test case, we say that test case has killed the mutant. In the opposite case we can say that the mutant has survived. This mutant generation can be performed by using techniques based on heuristics, such as using Genetic Algorithms. We found two things related to the use of heuristics in mutation testing: a) The different methods for mutation generation using Genetic Algorithms

are efficient in terms of searching in an ample solution space and, b) Even though, Heuristics has been used for mutation testing in imperative languages, their use for testing functional programs was scarce. This last characteristic could be due that programs made by using functional paradigms are less prone to flaws, this because of the formal or mathematical aspects of their constructs. We came up with the research question if that strength of the functional paradigm could also be present in impure versions of functional programming languages such as in Scheme. It is worthy of mentioning that an impure functional language is the one that has some imperative within it. With this research question in mind, we wanted to test how well perform mutation testing in functional paradigms. This article is divided in the following sections: In Section II, we made a brief introduction to test, mutation testing and Genetic Algorithms. In Section III, we developed our genetic operators and fitness function; along with a graphical conversion of the code that will be exposed to these genetic operators. In Section IV, we show our results obtained by testing our technique in the implementation of different functional programs, ending with the conclusions of this research work.

## II. BACKGROUND AND RELATED WORK

### A. Software Testing

Now-a-days, software development is an activity that is present in many aspects of the daily routines and activities in which the human being is immersed. Some of these tasks could be reasonably trivial such as processing pictures or processing documents, while others could perform critic tasks as controlling an airplane. This is the main reason why a simple error in the software could affect a considerable number of users and stakeholders. Nevertheless, the software should not contain errors or behave in unexpected ways deviated from their regular tasks. There exists a certain number of factors that could affect the software behavior brought up from their implementation part. The field of software design tries to discover these factors in a structured and detailed process that is oriented to the development of tests. These test could allow us to prove the validity of the implemented software [1].

One way of testing if a program behaves correctly is to prove it by using a technique known as mutation testing. A mutant is program altered that, when exposes to a set of different inputs, we can observe if, by behaving in a different or anomalous way, a set of test cases could detect this defective program. A simple way to understand this technique is shown in Fig. 1.

We can observe in Fig. 1 that we start with the source code of a program that we would like to test. Considering

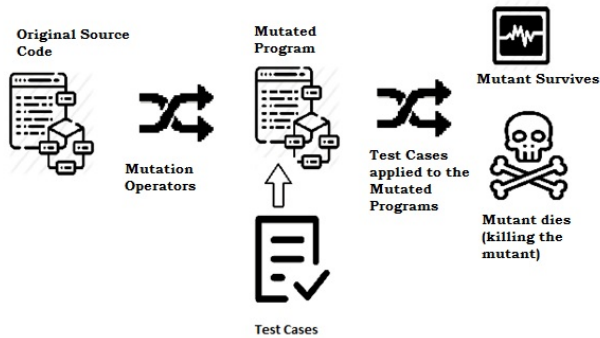


Fig. 1. Relationship between the Mutated programs and the Test Cases

this initial code one can generate modified versions of the same program called mutants. Therefore, a mutant suffers inner modifications of their original code, and after these changes, they are exposed to a set of test cases. The test cases will serve to prove if they are capable of finding errors in this mutated program. This verification process follows the criteria that a test case should be able of detecting anomalous behaviors of a code. If the mutated program, when is exposed to a test case, returns an output different to the one that the original program returns; this would mean that the test case was able to detect this error. Therefore, we can say that the mutant is killed. The problem arises when both, the original and the mutated program, returns the same answer that was given by the test case. In the situation mentioned above, we can say that the mutant survives. The main reason for this behavior is because the test case was unable to detect an unusual mode, and therefore the test cases should be improved. An important issue to mention is that, in the generation of mutants, we should consider generating fully-functioning mutants instead of non-executable ones. An interesting point of view is expressed in the book of Paul Ammann and Jeff Offutt [1], where the authors mention that in the test cases, irrelevant if their manual or automatically generated, they are tested to verify the output of a program. In consequence, if there is an erroneous output, the program should be corrected, and the mutation process is performed in the same fashion as we described before. At this point, we believe that it will be valuable to mention a set of formal definitions that should hold in the process of killing mutants:

**Definition 1:** Given a mutant  $m \in M$  such that  $m$  is a valid mutant and  $m$  is derived from the ground string  $p$ . Then if the  $answer(m) \neq answer(p)$  given a test  $t$ ,  $t$  kills  $m$  if the first condition holds.

**Note:** According to Paul Ammann and Jeff Offutt [1], a ground string is defined as a source code without any alteration.

The authors also mention that a mutant should uphold the following conditions:

- a) **Reachability:** This feature refers that when we test a mutant, the test case should be able to reach until the point where we mutated an instruction.
- b) **Infection:** An infection occurs when a reached mutated

instruction will generate a change in the state of a program. The state of a program, in this scenario, is similar to the concept given in the different paradigms in which a programming language could be enclosed.

c) **Propagation:** Once the mutant is executed, the program could output an erroneous output.

The process of killing mutants is the one that will allow us to determine the effectivity of a test case, for this purpose there exist a metric named the mutation score and it can be defined as follows:

$$mutation\ score = \frac{|deleted\ mutants|}{|non - equivalent\ mutants|} \quad (1)$$

According to equation (1), a perfect metric will hold a value of one, but this theoretical value can be complicated to obtain; so it would be better to work with threshold values.

There exists, also, a special kind of mutants called of equivalent type. An equivalent mutant is the one that returns the same answer as an unmodified program when they are exposed to a set of test cases. In summary, it does not exist a set of test cases that can find differences between the mutated program and the original program [2]. Some authors, such as Budd and Angluin [3], mentions that this is an irresolvable problem; therefore, it does not exist an efficient or at least known-way that could detect a set of mutants that are equivalents. Other authors like Offutt and Pan [4] also mention the problem of the creation of equivalent mutants. These authors followed a restriction-based system considering a variant of the Feasible Path Problem (FTP). The three conditions that a mutant should uphold mentioned by Paul Ammann and Jeff Offutt [1] are also defined by other researchers such as Botacci [5], but with subtle modifications. For example, this author considers that the features that should be present are:

- a) **Reachability.**
- b) **Necessity,** according to these criteria if we compare the original program  $P$  with a mutated line on a mutated program  $M$ , there should exist a difference in the state of execution of a program.
- c) **Sufficiency,** this feature determines that the output of  $P$  and  $M$  should be distinct.

Mutation testing is a vast and evolving area of study, that has changed from simple code modifications to complex ones to examine the strength of our test suites. The reader interested in a complete survey about this subject is encouraged to review the research work of Papadakis, Kintis, Zhang, Jia, and Le Traon [11] In the research work of Le, Amin, Gopinath and Groce [10] is mentioned the fact that mutation testing has been primarily applied to imperative programming. Nevertheless due to the relevance that is having this paradigm in some fields such as Big Data, Data Science and with the inclusion of functional paradigm constructs in imperative languages, the interest of performing mutation testing in functional languages was envisioned as an exciting research field. The authors mentioned previously developed a software tool denominated MuCheck that performed mutation testing in a functional paradigm by using Haskell as the chosen language. It is worthy of mentioning that Haskell belongs to the family of pure functional languages, while in our research, we have considered

Scheme, which is categorized as an impure one. An impure functional language is the one that despite belonging to the functional paradigm; it has some characteristics that are present in other paradigms, such as imperative constructs. The reason for choosing this impure functional language was because Scheme, represented actually by the Racket programming language, has applications in different real-world applications. Furthermore, Racket or Scheme is considered a programming language that it could raise the development of the Language-Oriented Programming (LOP). A LOP language is the one that would allow developers to use a programming language that could help them to design programming languages oriented to suit their needs, so eventually, it fulfills the need of using different programming languages constructs in one host programming language by allowing the programmer to develop their personalized programming language [12]. The reader interested in this particular characteristic can review the following link: <https://beautifulracket.com/>

### B. Genetic Algorithms

The Genetic Algorithms (GAs) are a technique of searching and optimization based on heuristics. These are clear contraposition of other methods based on calculus or in dynamic programming. One of the main reasons for their usage is that they perform appropriately in higher dimensions where the problem known as the curse of dimensionality, could be present. Previous techniques based on non-guided searches or randomly generated have existed before the appearance of the GAs, but with the limitation that they could get stuck in a local optimum [6].

#### Components of a GA and Genetic Operators

In this section, we will describe some components and operators that are commonly used on the GAs. We should consider that the literature about this topic is diverse, but we will focus our work in the research made by Goldberg [6], Mitchell [7] and Sivanandam [8]. Among their principal components are the chromosome, part that allows forming a population; and a fitness function that will select the best individuals by following a set of Genetic Operators. There exist two types of operators that are work jointly with the population and the fitness functions. The operator of Selection allows us to chose a couple of parents for generating a new individual [8]. The techniques for the selection of individuals are diverse, but most of them are centered into probabilistic or stochastic methods. According to Sivanandam [8], there exists what is called a pressure selection, which is a trick that allows one individual to be chosen over another one. Another type of operator is called Reproduction, and according to Holland [9] it is a function that allows forming a new population, considering the selection criteria performed by the fitness function. For reproducing a couple of individuals, they use two functions more. The first one selects randomly two parts of each chromosome to be exchanged with one another in a process called Crossover. After this process and before a new couple of chromosomes are about to be put into the pool of individuals, an operator of mutation can be present. The operation of mutation what it does is to select one portion of each chromosome and randomly, with a very small probability, changes its value one value for another. The importance of this operator is that it will allow, in some cases, to push the

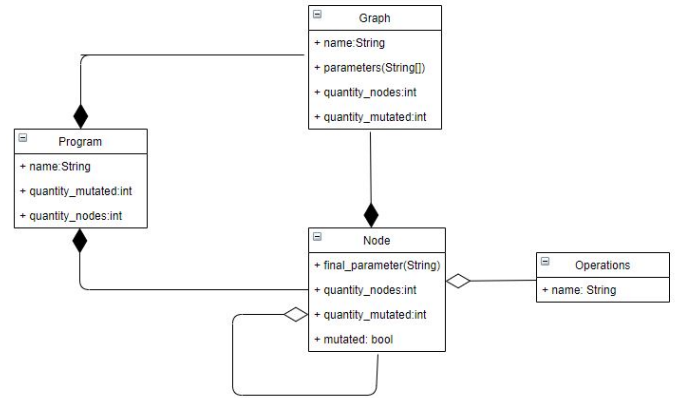


Fig. 2. Relationship between the Mutated programs and the Test Cases

chromosomes to be replaced for subtle modifications of them and to permit a diversification into the search space.

## III. METHODOLOGY

### A. Class Diagram

We have developed a set of classes with the sole goal of parsing our source code. It also helps to define other constituents such as functions and parameters, and operations that would aid in converting our source code into a graph representation. The graph representation would serve then for the mutant generation, which at the end will form part of the population for our genetic Algorithm. Our schemata of classes present the following components:

**Program:** It represents the code analyzed or its mutation. It contains data of type string which stores the name, a list of graphs that represents the defined functions and a list of nodes which corresponds to the called functions.

**Graph:** Represents the definition of a un function. It contains data of type string for storing its name, a list also of type string that contains its parameters and a node that points to the actions to be performed.

**Note:** It can represent a parameter. In the way we program our classes a node can also be a function that is why this class has a list of nodes that represents the parameters of a function. It contains an attribute of type operation and a string data type that stores the name of the parameter in the case that it does not correspond to a function.

**Operation:** Represents the name of the function that is being executed.

In Fig. 2, we can observe the class diagram of our solution.

### B. Algorithms

We have defined the following algorithms for our solution:

```
Algorithm: Parser code for function search.
```

```
if character!= EOF
```

```
while character = \" or character = \\n\"
or character = \)\"
  if scan(character) = EOF
    return
  if character = \\(\\
    scan(character)
    word <- obtain_word(character)
    if word = \\define\"
      graph <- parse_function(character)
      program.funciones.push(graph)
      parse(character, program)
    else
      num <- 0
      character <- \\(\\
      node <- parse_code(character, num)
      node.operation.name <- word
      program.codigo.push(node)
      parse(character, program)
    else if character = \\ ' \"
      num <- 0
      node <- parse_code(character, num)
      node.operation.name <- \\ ' \\
      program.codigo.push(node)
      parse(character, program)
```

Algorithm: Code parser. Adds the parameters or arguments of a function

```
num++
while character = \\ \\ or character = \\n\"
  scan(character)
  if character = \\(\\
    scan(character)
    if character = \\(\\
      node.operation.name <- \\ \\
    else
      node.operation.name <-
        obtain_word(character)
    while character ?= \\)\"
      while character = \\ \\
      or character = \\n\"
        scan(character)
        node.parameters.
          push(parse_code(character, num))
        scan(character)
    else if character = \\ ' \\
      node.operation.name <- \\ ' \\
      scan(character)
      while character = \\ \\ or character= \\n\"
        scan(character)
      if character = \\(\\
        scan(character)
        while character ?= \\)\"
          while character = \\ \\ or
            character = \\n\"
            scan(character)
            node.parameters.push
              (parse_code(character, num))
            scan(character)
        else
          node.parameters_final <-
```

```
        obtain_word(character)
      else
        node.parameters_final <-
          obtain_word(character)
    return node
```

Algorithm: Function parser. Creates a graph and inputs the information of the declared function

```
while character = \\ \\ or character = \\n\"
  scan(character)
  if character = \\(\\
    scan(character)
    graph.name <- obtain_word(character)
    while ( character!= \\)\"
      string <- obtain_word(character)
      graph.parameters.push(string)
      scan(character)
    else
      graph.name <- obtain_word(character)
  num <- 0
  graph.code <- parse_code(character, num)
  graph.nodes_quantity <- num
  return graph
```

For the part of the Genetic operators that we used, we defined the following algorithms:

Algorithm: Obtain word. Returns a string with the posterior word to the character that was input as a parameter.

```
list l
if operation = \\list\" || operation=\\vector\"
|| operation = \\ ' \"
  if operation = \\list\" || operation=\\ ' \\
    l.push_back(\\vector\")
  else
    l.push_back(\\list\")
else if operation = \\car\" || operation=\\cdr\"
  l.push_back(\\car\")
  l.push_back(\\cdr\")
  l.remove(operation)
else if operation = \\+\" || operation = \\-\" ||
operation = \\*\" ||
  operation = \\/\
  l.push_back(\\+\")
  l.push_back(\\-\")
  l.push_back(\\*\")
  l.push_back(\\/\")
  l.remove(operation)
else if operation = \\<\" || operation = \\>\"
|| operation = \\<=\" ||
  operation = \\>=\"
  l.push_back(\\<\")
  l.push_back(\\>\")
  l.push_back(\\<=\")
  l.push_back(\\>=\")
  l.remove(operation)
else if operation = \\and\" || operation = \\or\"
  l.push_back(\\and\")
```

```
l.push_back(\or")
l.remove(operation)
else
return 0
m <- random(l.size)
operation <- l[m]
mutated <- 1
return 1
```

Algorithm: Program crossover. Extracts parts of a program and exchanges them.

```
m <- random(program1.functions.size)
function1 <- program1.functions[m]
function2 <- program2.functions[m]
destination1 <-random(function1.nodes.size)
destination2 <-random(function2.nodes.size)
intercambiar(destination1, destination2)
```

### C. Genetic Operators

Because we worked with the functional paradigm, we chose the following operators or instructions to be exchanged. This process is performed within the mutation step of a program.

1) *Fitness Function*: The Fitness or Adaptation function is the one in charge of selecting the best individuals among a population of entities in a given generation of a GA. We have defined the following items and equations for this section:

$T =$  quantity of tests

$e_n =$  correct answer for the  $n$  test (value of 1 or 0)

$t_n =$  quantity of mutants not detected by test  $n$

$m =$  quantity of mutants

$c_n =$  it counts the results for the  $n$  test, irrelevant if the answer is correct or not

$N_a =$  quantity of nodes in the actual program

$N_i =$  quantity of nodes in the original program

These parts have served to formulate the following equations, that we have preferred to call them criteria:

#### Criteria 1:

$$\sum_{n=1}^T [e_n (1 - \frac{7t_n}{10m})] * 10$$

This equation counts the number of tests that left the mutant undetected. Approximately, 70 percent of the score is given to the test that detected a certain amount of mutants. The highest score is given to the test that picked most of the remaining mutants. The value of 7/10 is for giving more weight to those mutants that evade the tests.

#### Criteria 2:

$$\sum_{n=1}^T (c_n) * \frac{1}{T}$$

It counts the number of answers given by a mutant, irrelevant if these are correct or not.

#### Criteria 3:

$$\left(1 - \frac{|N_a - N_i|}{3N_i}\right)$$

It measures how much has varied the number of nodes of the mutant with regard to the original program. Less variation means a higher score. This criterion is used for neglect programs with a mutation threshold higher than what could be considered an useful mutation.

When we combine the criteria above mentioned we would end up with the following fitness function:

$$\sum_{n=1}^T [e_n (1 - \frac{7t_n}{10m})] * 10 + \sum_{n=1}^T (c_n) * \frac{1}{T} + \left(1 - \frac{|N_a - N_i|}{3N_i}\right)$$

Once that we have defined our algorithms and operators to be used in our Genetic Algorithm we proceed to the implementation of our proposal. We have tested our program with three different types of programs, made under the functional paradigm and using Scheme as a programming tool. The programs tested were a) a sorting function using quicksort, b) a function that solves a quadratic equation, and c) two functions that implement the Prim and Kruskal algorithms for obtaining minimum weighted spanning trees. We will describe the results of our experimentation in the following section.

## IV. RESULTS

At the moment of executing our program with the target source codes; it starts to search for an opening bracket in the source code. If this is found the next instruction is analyzed and if it corresponds to the term define; a graph that represents this function is created along with its corresponding parameters. This procedure is done in two steps: a) we obtain the name or the parameters of a function, and b) we collect the statements or calling to other programs if this is the case. With these, we create a node that stores all the information of a function and is ready to be mutated. It is worthy of mentioning that with the graph obtained from a program, we generate several copies and each of these copies is mutated according to the operators defined in Section 3.3. Each mutated program or mutant is executed with all the tests and, later, a score is assigned by using our fitness function. When we end up with this procedure, we keep 20 percent of the mutants with a higher score, crossing them form generating new individuals. The process mentioned above is repeated until we reached the number of programs that we defined beforehand as the number of individuals in each generation. For all the three programs we have chosen the following parameters:

- Number of mutants or individuals by generation: 100
- Number of tests: 3
- Generations: 80

### A. Quicksort

The original code is the following:

Quicksort: Original source code

```
#lang racket
```

```
(define (partition compare l1)
```

```
(cond
```

```
((null? l1) '())
```

```
((compare (car l1)) (cons (car l1)
```



TABLE I. NUMBER OF TESTS EVADED BY THE QUICKSORT MUTANT

|          | Generation | Altered Nodes | Evaded Tests | Score |
|----------|------------|---------------|--------------|-------|
| Mutant 1 | 1          | 33            | 2            | 21.02 |
| Mutant 2 | 3          | 33            | 2            | 20.51 |
| Mutant 3 | 2          | 33            | 2            | 20.25 |

```
(partition compare (cdr l1)))
(else (partition compare (cdr l1))
)))
```

```
(define (quicksort l1)
  (cond
    ((null? l1) '())
    (else (let ((pivot (car l1)))
            (append (append (quicksort
                             (partition (lambda (x) (<x pivot))
                             l1))
                      (partition (lambda (x) (=x pivot)) l1)
                      (quicksort (partition (lambda (x)
                                             (> x pivot)) l1))))
            )))
```

```
(quicksort (read))
(sleep 5)
```

In Fig. 3, we can observe the number of generations that our GA had to pass for reaching a stable score. In Table I, we can see that we managed only to evade two of the test cases given. In this situation, we can argue that while the original program contains less number of code lines, this would be less likely to obtain a useful mutant program. The mutated code is the following:

Quicksort: Mutated version.

```
(define (partition compare l1 )
  ( cond ( ( null? l1 ) ' ( ) )
    ( ( compare ( car l1 ) ) ( cons(
      car l1 ) ( partition compare
      ( cdr l1 ) ) ) )
    ( else ( partition compare (cdr l1)
      ) ) ) )
```

```
(define (quicksort l1 )
  ( cond ( ( null? l1 ) ' ( ) )
    ( else ( let ((pivot ( car l1)))
            ( append ( append ( quicksort
                             ( partition ( lambda ( x )
                             (>x pivot) ) l1)) --modified line
                      ( partition ( lambda ( x )
                      (= x pivot ) ) l1 ) )
                      ( quicksort ( partition ( lambda ( x )
                      (> x pivot ) ) l1 ) ) ) ) ) ) )
```

```
( quicksort ( read ) )
```

and in Fig. 4 we can observe the graph generated of a mutant version of Quicksort.

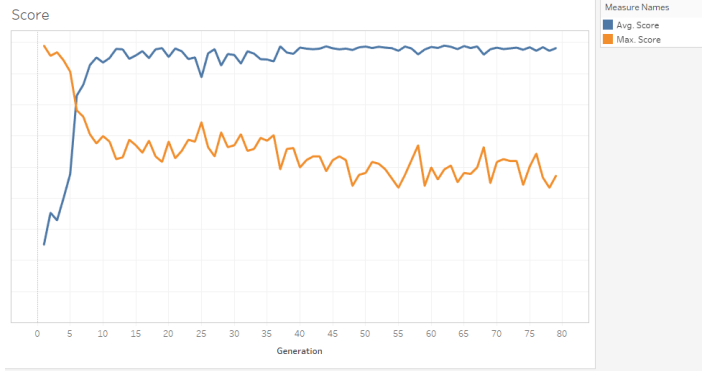


Fig. 3. Number of generations performed by the GA for the Quicksort program

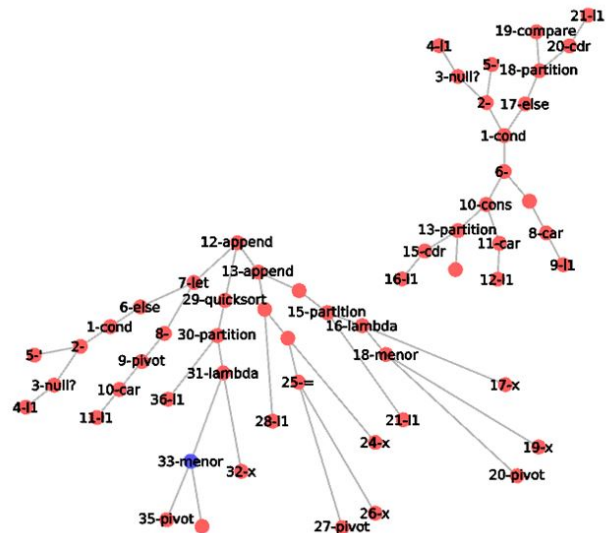


Fig. 4. Generated graph sample of a mutated version of Quicksort

### B. Quadratic Equation

In this example, we tried to generate mutant versions of a quadratic equation solver. We can see in Table II, the different test cases with their corresponding correct outputs that should be returned by each mutated program. The approximate running time for the generation of mutants was roughly 10 hours, and a version of the original program is the following:

```
Quadratic Equation Solver: Original source code.
#lang racket
(define (calc-disc a b c)
  (+ (expt b 2) (* -1 (* 4 a c))))

(define (quad-eq a b c)
  (if (< (calc-disc a b c) 0)
    (begin
      false
    )
    (begin
      (if (= (calc-disc a b c) 0)
        (/ (* -1 b) (* 2 a))
```

TABLE II. INPUTS AND OUTPUTS OF THE THREE DISTINCT TEST CASES TO BE USED IN THE QUADRATIC EQUATION SOLVER.

|        | Test 0              | Test 1      | Test 2               |
|--------|---------------------|-------------|----------------------|
| Input  | 0.5<br>0.5<br>0.125 | 1<br>1<br>9 | 8<br>20<br>2         |
| Output | -0.5                | #f          | -0.10435<br>-2.39564 |

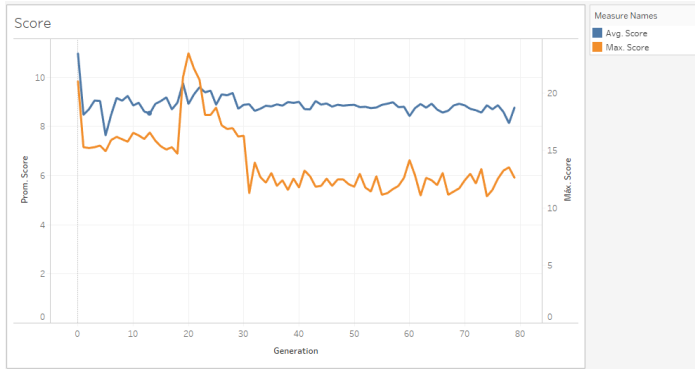


Fig. 5. Scores obtained in each of the generations

```
(values (calc-eq a b (sqrt
(calc-disc a b c)))
(calc-eq a b (* -1 (sqrt
(calc-disc a b c))))
))
```

```
(define (calc-eq a b d)
(/ (+ (* -1 b) d) (* 2 a)))
```

```
(quad-eq (read) (read) (read))
```

In Fig. 5 and Table III, we can observe that the generation in which we obtained a mutant that bypassed the three test cases appeared on generation 19. The presence of this mutant means that the test case was not able to find unusual situations in a flawed version of the program. This implies that the test suit requires improvements or to cover a more considerable amount of probable cases that would allow the mutant to be detected.

TABLE III. NUMBER OF TESTS EVADED BY THE QUADRATIC EQUATION MUTANT SOLVER

|          | Generation | Altered Nodes | Evaded Tests | Score   |
|----------|------------|---------------|--------------|---------|
| Mutant 1 | 20         | 7,19          | 3            | 23.4392 |
| Mutant 2 | 21         | 7,19          | 3            | 22.1092 |
| Mutant 3 | 19         | 7,19          | 3            | 21.3392 |

The source code of the mutant that managed to evade the three test cases is the following:

Quadratic Equation Solver: Mutated Version.

```
#lang racket
(define (calc-disc a b c)
(+ (expt b 2) (* -1 (* 4 a c))))
```

TABLE IV. INPUTS AND OUTPUTS VALUES FOR THE GENERATION OF A TEST SUITE USING THE ALGORITHMS OF PRIM AND KRUSKAL

|        | Test 0  | Test 1   | Test 2  | Test 3   |
|--------|---|--|---|--|
| Input  | ((4 0 1) (4 0 2)<br>(6 0 3) (6 0 4)<br>(2 1 2)(8 2 3)<br>(9 3 4)) | ((75 0 2) (9 0 1)<br>(95 1 2) (19 1 3)<br>(42 1 4) (51 2 3)<br>(31 3 4)) | ((13 0 3) (24 0 1)<br>(22 0 4)(13 0 2)<br>(22 1 2)(13 1 3)<br>(13 1 4) (19 2 3)<br>(14 2 4) (19 3 4)) | ((10 0 1) (10 1 2)<br>(8 1 6) (13 1 7)<br>(8 2 7) (132 8)<br>(10 2 3) (10 3 4)<br>(8 3 8) (10 5 6)<br>(10 6 7) (10 7 8)<br>(10 8 9)) |
| Output | '((0 1)<br>(0 3) (0 4)<br>(1 2) (1 0)<br>(2 1) (3 0)<br>(4 0))    | '((0 1)<br>(1 3) (1 0) (2 3)<br>(3 1)(3 2) (3 4)<br>(4 3))               | '((0 3)(0 2)<br>(1 3) (1 4)<br>(2 0) (3 1)<br>(3 0) (4 1))  | '((0 1) (1 6) (1 0)<br>(2 7) (3 4) (3 8)<br>(4 3) (5 6) (6 1)<br>(6 5) (7 2) (8 9)<br>(8 3) (9 8))                                   |

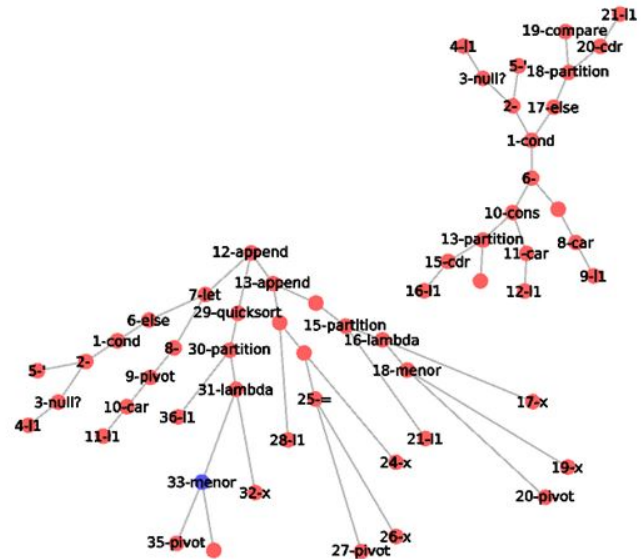


Fig. 6. Scores obtained in each of the generations

```
(define (quad-eq a b c)
(if (< (calc-disc a b c) -1)
(begin false)
(begin
(if (= (calc-disc a b c) 0)
(* -1 b) --missing (* 2 a)
(values (calc-eq a b
(sqrt (calc-disc a b c)))
(calc-eq a b (* -1
(sqrt (calc-disc a b c)))
))))))
```

```
(define (calc-eq a b d) (/ (+ (* -1 b) d) (* 2 a)))
```

```
(quad-eq (read) (read) (read))
```

, and the generated graph of the mutant can be observed in Fig. 6:

### C. Prim and Kruskal

As the latest test for our proposal, we applied our technique for the generation of mutants of two well-known algorithms such as Prim and Kruskal. For these two algorithms, we decided to prove how many tests were evaded from a test suit of four items. We generated approximately 100 mutants, and our GA ran for 80 generations. The average time for obtaining useful mutants was roughly about 20 hours. In Table IV, we can observe the corresponding inputs and the right outputs that should be obtained when executing these algorithms.

TABLE V. DESCRIPTION OF THE MUTANT THAT MANAGED TO AVOID THE THREE TEST CASES FOR THE ALGORITHM OF PRIM

|          | Generation Number | Altered Nodes             | Evaded Tests | Score   |
|----------|-------------------|---------------------------|--------------|---------|
| Mutant 1 | 15                | 9, 10, 11, 12, 13, 21, 25 | 3            | 29.2684 |

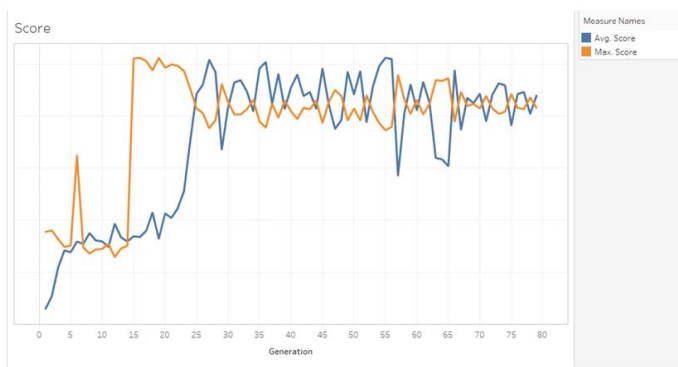


Fig. 7. Scores obtained in each of the generations

In Fig. 7, we can observe the number of generations that had to pass until our GA converged to a stable value for the Prim case. In Table V, we can see the data from a mutant that was not detected by the three cases of the test suite and was found in generation number 15.

The original source of the implementation of the Prim algorithm is the following:

Prim Algorithm source code: Original version.

```
#lang racket
(require graph)

(define grafoP (weighted-graph/undirected null))

(define (mayor valor lista)
  (if (empty? lista)
      valor
      (if (> (car valor) (caar lista))
          (mayor valor (cdr lista))
          (mayor (car lista) (cdr lista)))))

(define (orden x y)
  (if (= (length y) 0)
      x
      (orden (cons (mayor '(-1 -1 -1) y) x)
              (remove (mayor '(-1 -1 -1) y)
                      y))))
```

```
(define ordenar (lambda (lista)
  (orden '() lista)))

(define (agregarVecinos grafoP lista nodo)
  (if (empty? lista)
      '()
      (if (or (= (cadar lista) nodo) (=
        (caddar lista) nodo))
          (if (and (= (cadar lista) nodo)
            (not (has-vertex? grafoP
              (caddar lista))))
              (cons (list (caar lista)
                (caddar lista) nodo)
                  (agregarVecinos grafoP
                    (cdr lista) nodo))
              (if (and (= (caddar lista)
                nodo) (not (has-vertex?
                  grafoP (cadar lista))))
                  (cons (list (caar lista)
                    (cadar lista) nodo)
                      (agregarVecinos grafoP
                        (cdr lista) nodo))
                  (agregarVecinos grafoP
                    (cdr lista)
                    nodo))))))
```

```
(define (prim grafoP nodos temporal nodo
  primero)
  (if (equal? primero #t)
      (let ((aux (remove-duplicates (ordenar
        (agregarVecinos grafoP
          nodos nodo))))))
```

```
(begin
  (add-edge! grafoP (cadar aux)
    (caddar aux) (caar aux))
  (prim grafoP nodos
    (remove-duplicates
      (ordenar
        (append (cdr aux)
          (agregarVecinos grafoP
            nodos (cadar aux))))))
    nodo #f)))
  (if (empty? temporal)
      (get-edges grafoP)
      (let ((aux (remove-duplicates
        (ordenar (append temporal
          (agregarVecinos grafoP nodos
            (cadar temporal))))))
            (if (not (has-vertex? grafoP
              (cadar aux)))
                (begin
                  (add-edge! grafoP (cadar
                    aux) (caddar aux) (caar aux))
                  (prim grafoP nodos (cdr aux)
                    nodo #f))
                (prim grafoP nodos (cdr aux)
                  nodo #f)))))
```

```
(define nodos (read))
```

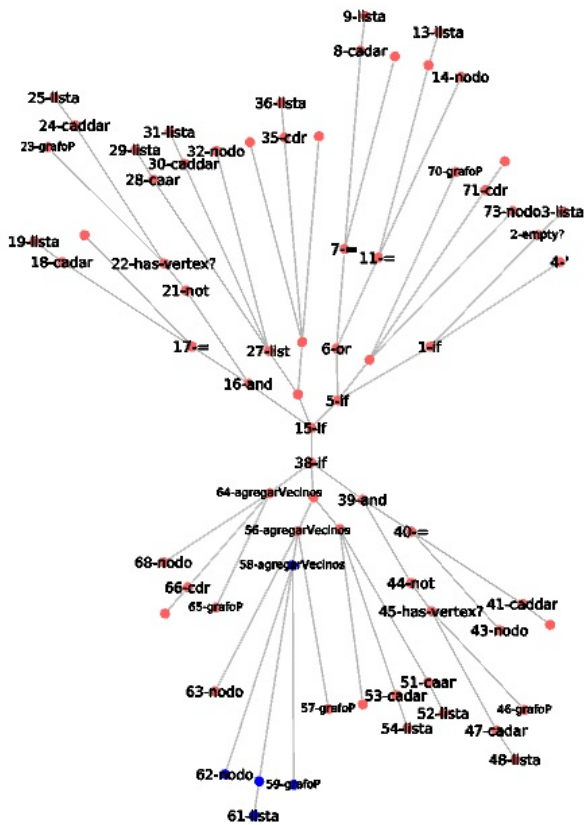


Fig. 8. Graph generated for the mutated version of the Prim algorithm

When we tested an implementation of the Kruskal algorithm we also found a mutant that, with sublet modifications, was able to evade all the test cases defined. The source code of our implementation was:

Kruskal implementation: original source code

```
#lang racket

(define nodos1 (read))

(define grafoK (weighted-graph/undirected
  null))

(define (mayor valor lista)
  (if (empty? lista)
      valor
      (if (> (car valor) (caar lista))
          (mayor valor (cdr lista))
          (mayor (car lista) (cdr lista))
          )))

(define (orden x y)
  (if (= (length y) 0)
      x
      (orden (cons (mayor '(-1 -1 -1) y) x)
              (remove (mayor '(-1 -1 -1) y) y))))

(define ordenar (lambda (lista)
  (orden '() lista)))

(define ciclo (lambda (v1 v2 grafo)
  (if (and (has-vertex? grafo v1)
           (has-vertex? grafo v2))
      (let ((aux1 (get-neighbors grafo v1))
            (aux2 (get-neighbors grafo v2)))
        (if (and (equal? (member v2 aux1) #f)
                 (equal? (member v1 aux2) #f))
            #t
            #f))
      #f))

(define kruskalAux (lambda (grafoK nodos
  funcionCiclo primero)
  (if (equal? primero #t)
      (begin
        (add-edge! grafoK (cadar nodos)
                    (caddar nodos) (caar nodos))
        (kruskalAux grafoK (cdr nodos)
                    funcionCiclo #f))
      (if (empty? nodos)
          (get-edges grafoK)
          (if (equal? (funcionCiclo
                      (cadar nodos)
                      (caddar nodos) grafoK) #f)
              (begin
                (add-edge! grafoK (cadar nodos)
                                    (caddar nodos)
                                    (caar nodos))
                (kruskalAux grafoK (cdr
                                    nodos) funcionCiclo #f))
              ))))
```

```
(prim grafoP nodos '() 0 #t)
```

and a section of the mutated version of the source code with the portions changed commented:

Prim Algorihtm source code: Mutated Version

```
#lang racket
(define grafoP ( weighted-graph/undirected
  null ) )

(define (mayor valor lista ) ( if ( empty?
  lista )
  valor ( if ( > ( car valor ) (caar
  lista ) )
  ( mayor valor ( cdr lista ) )
  ( mayor ( car lista )
  ( cdr lista ) ) ) ) )

(define (orden x y ) ( if ( = ( length y ) 0)
x ( orden
  ( cons ( mayor ' ( -1 -1 -1 ) y ) x)
  ( remove ( mayor ' ( -1 -1 y ) y ) y )
  --modified line ) ) )

(define ordenar ( lambda ( lista )
  ( orden ' ( ) lista ) ) )
```

The generated graph of the mutant can be observed in Fig. 8.

```

(kruskalAux grafoK (cdr
  nodos) funcionCiclo
  #f))))))
(define (kruskal grafoK nodos)
  (kruskalAux grafoK (ordenar nodos)ciclo #t))
(require graph)
(kruskal grafoK nodos1)

```

and the mutated version was the following, notice that we have only included the portion of the source code that was mutated:

Kruskal implementation: Mutated version

#lang racket

```

(define ciclo
  (lambda ( v1 v2 grafo )
    ( if ( and ( has-vertex? grafo v1 ) (
      has-vertex? grafo v2 ) )
      ( let ( ( aux1 ( get-neighbors
        grafo v1 ) )
        (aux2 ( get-neighbors grafo v2)))
        ( if ( or ( equal? --mutated line
          ( member v2 aux1 ) #f )
          ( equal? ( member v1 aux2 ) #f )
          ) #t #f ) ) #f ) ) )
(define (kruskal grafoK nodos ) ( kruskalAux
  grafoK( ordenar nodos ) ciclo grafoK ) )
--mutated line

```

In Fig. 9 we have shown a graph of the mutated version of the implementation of the Kruskal algorithm, while in Table VI, we depict the number of generations that had to pass for our GA to reach a convergence point. Also, we show which nodes were altered and the final score of the mutant obtained.

TABLE VI. DESCRIPTION OF THE MUTANT THAT MANAGED TO AVOID THE THREE TEST CASES FOR THE ALGORITHM OF KRUSKAL

|          | Generation Number | Altered Nodes | Evaded Tests | Score |
|----------|-------------------|---------------|--------------|-------|
| Mutant 1 | 10                | 6,24          | 4            | 38.64 |

We can derive some discussion about the results obtained from the three programs that we tested. In the case of the Quicksort, we could argue that the test set evaluates all the probable paths of the mutated codes. Therefore, and because it does not have so many lines of code that could be mutated, then the tests successfully detect them. For the Quadratic equation code, we found a similar case that when we test the Quicksort one, the limit number of lines of code and the inclusion of a mutated math operator ( $/(2 a)$ ) it did not alter the result when compared to a test. Consequently, we can conclude that compact source codes will be less prone to exhibit a variety of mutations when applied a heuristic technique. For the case of the Prim and Kruskal algorithm, which were form by moderate lines of code, we found subtle modifications present on the mutated codes, that bypassed some test cases on our test suit.

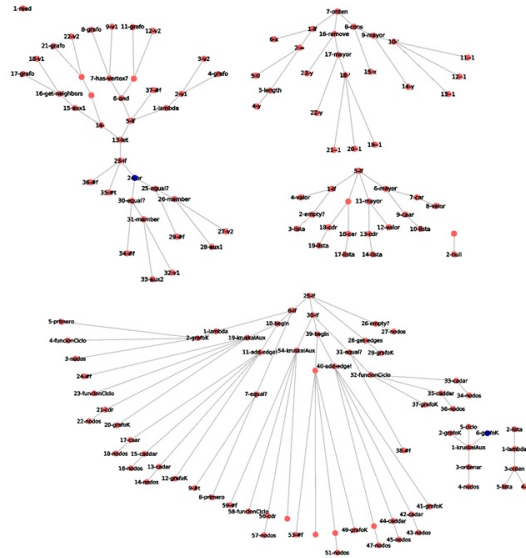


Fig. 9. Graph generated for the mutated version of the Kruskal algorithm

## V. DISCUSSION

Mutation testing techniques have been broadly used for testing a source code based on imperative programming, while research oriented to perform mutation testing on functional paradigms is rarely explored [11] survey). We argue that a primary reason could be that pure functional languages have a rigorous and formal way to develop programs in these environments, making them less prone to flaws due to their mathematical nature. Pure functional languages, such as Haskell, do not endorse some constructs that are present in imperative programming languages, such as side-effects presented by a change of state in a program, but impure functional languages can exhibit these characteristics. Impure functional programming languages, for example, Racket, has increased the interest in new paradigms such as the LOP way of programming that can be used for deploy Domain Specific Languages within a chosen language (eDSL) applications or software that consolidate different programming solutions into a host programming language [12]. Therefore, we believe that even though the LOP paradigm could make more suited and tailored applications developed by programmers, it will be necessary to test these developed programs, and mutation testing joined with heuristics could be a valuable starting point to detect probable flaws in our developed software products based on this new paradigm.

## VI. CONCLUSIONS

We have presented a set of proofs for the implementation or generation of mutants that can be applied for examining test suites, oriented to functional programs by using the Scheme programming language. We were able to determine that as long as the lines of codes increase, the task of generating mutants by using heuristics, the generation of mutants is achievable such that test suites could not detect them. The use of mutation testing employing heuristics, such as Genetic Algorithms, allows the tester to cover a more extensive broad

of possibilities in the generation of mutants that help in detecting flaws into the test suites.

#### REFERENCES

- [1] Paul Ammann and Jeff Offutt. *Introduction to Software Testing*. 1st ed. USA: Cambridge University Press, 2008.
- [2] Konstantinos Adamopoulos, Mark Harman and Robert M. Hierons. *How to Overcome the Equivalent Mutant Problem and Achieve Tailored Selective Mutation Using Co-evolution*. Proceedings of the 2004 Conference on Genetic and Evolutionary Computation GECCO 04, Springer. Seattle, USA, 2004.
- [3] Timothy A. Budd and Dana Angluin. *Two notions of correctness and their relation to testing*. Acta Informatica, vol. 18, pp.31-45, Mar. 1982.
- [4] A. Jefferson Offutt and Jie Pan. *Automatically detecting equivalent mutants and infeasible paths*. Software Testing, Verification and Reliability, vol.7, pp. 165-192, 1997.
- [5] Leonardo Bottaci. *A Genetic Algorithm Fitness Function for Mutation Testing*. SEMINAL: Software engineering using metaheuristic inovative algorithms, workshop, 2001.
- [6] David E. Goldberg. *Genetic Algorithms in Search, Optimization and Machine Learning*. Addison-Wesley Longman Publishing Co., Inc., 1989.
- [7] Melanie Mitchell. *An Introduction to Genetic Algorithms*. Cambridge, MA, USA: MIT Press, 1996.
- [8] S. N Sivanandam and S. N. Deepal. *Introduction to Genetic Algorithms*. Springer Publishing Company, Incorporated, 2007.
- [9] John H. Holland. *Adaptation in Natural and Artificial Systems: An Introductory Analysis with Applications to Biology, Control and Artificial Intelligence*. Cambridge, MA, USA: MIT Press, 1992.
- [10] D. Le, M. Amin Alipour, R. Gopinath, and A. Groce, *MuCheck: an extensible tool for mutation testing of haskell programs*. In Proceedings of the 2014 International Symposium on Software Testing and Analysis (ISSTA 2014). ACM, New York, NY, USA, pp. 429-432, 2014. DOI: <https://doi.org/10.1145/2610384.2628052>
- [11] M. Papadakis, M. Kintis, J. Zhang, Y. Jia, Y. Le Traon, and M. Harman, *Mutation Testing Advances: An Analysis and Survey*. Advances in Computers, 2018.
- [12] M. Felleisen, R. Findler, M. Flatt, S. Krishnamurthi, E. Barzilay, J. McCarthy, and S. Tobin-Hochstadt, *A programmable programming language*. Commun. ACM 61, 3 , pp. 62-71, February 2018. DOI: <https://doi.org/10.1145/3127323>

# Exploiting the Interplay among Products for Efficient Recommendations

Anbarasu Sekar<sup>1</sup>, Sutanu Chakraborti<sup>2</sup>  
Dept. of Computer Science and Engineering  
Indian Institute of Technology Madras  
Chennai, India 600036

**Abstract**—Recommender systems are built with the aim to reduce the cognitive load on the user. An efficient recommender system should ensure that a user spends minimal time in the process. Conversational Case-Based Recommender Systems (CCBR-RSs) depend on the feedback provided by the user to learn about the preferences of the user. Our goal is to use the feedback provided by the user effectively by exploiting the interplay among the products to build an efficient CCBR-RS. In this work, we propose two ways towards achieving that goal. In the first method, we utilize the higher order similarity and trade-off relationship among the products to propagate the evidence obtained through user feedback. In our second method, we utilize the diversity among cases/products along with the similarity and trade-off relationship to make the best use of the feedback provided by the user.

**Keywords**—Preference-based feedback; case-based conversational recommender system; evidence; trade-offs; compromise; diversity

## I. INTRODUCTION

The way product recommendation is handled by a recommender system in most of the on-line websites is very different from how a sales executive would deal with a customer in a store. Though a large amount of data is mined everyday, as rightly mentioned in [5], in some domains where a specific user is expected to buy a product once in a lifetime say for example ‘housing domain’ or ‘a luxury car domain’, collaborative systems fail due to lack of data about the user. In contrast to that, knowledge-based recommender systems like the CCBR-RSs are known to handle cold start conditions [6] with ease and work more like their human counterparts. Case-Based Reasoning Recommender systems (CBR-RSs) uses the notion of similarity among cases to approximate the utility of a product to users. Products are represented as feature value pairs. The user is allowed to express their preference by stating one or more feature values. For example, in a camera domain, the user’s query may be ‘10 MP resolution’. A CBR-RS uses the similarity measure to find all products whose resolution is similar to ‘10 MP’. Sometimes it could be possible that no recommendations are made as the products don’t match the query exactly [3]. The advantage with CBR-RS is that even if there are no cameras with exactly ‘10 MP’ resolution, cameras with resolution similar to ‘10 MP’ will be retrieved. A global similarity measure based on feature level similarity is defined using domain knowledge.

A Single-shot CBR-RS stops with recommending products to a user based on their initial query. If the user is not satisfied with the recommendation she has to give a new

query to the system. A CCBR-RS helps the user navigate the product space. It engages the user in two phases: a) The feedback phase, where the feedback regarding the products recommended to the user is received, and b) The recommendation phase, where the system recommends appropriate products based on the user query/feedback. We will refer to the set of products recommended in the recommendation phase as the Recommendation set (RS). The system learns the preferences of the user incrementally at every interaction with the user and recommends based on the learned preferences. A CCBR-RS aims to reduce the time a user spends on the system by making the interaction with the user effective and reducing the number of interaction cycles. Traditionally CCBR-RSs reported in literature works on modelling the user in a better way to improve the efficiency of the system. Our work tries to achieve the goal by capturing the rich interplay among the products in the domain.

The authors in Evidence-Based Recommendation (EBR) [2] propose a novel view of the feedback provided by the user in CCBR-RSs. A product in the domain needs evidence that it would be preferred by the user before it could be included in RS. The feedback given by the user plays the role of attributing evidence to each product in the domain. We cannot expect the user to give feedback on each product in the domain, so the evidence from feedback provided by the user on a minimal set of products are propagated to the rest of the products in the domain. We extend the idea of evidence propagation to include higher order propagation by posing the evidence propagation as a random surfer model. The work by authors in [14] focuses on bringing out the advantage in utilizing the trade-off relationship among products. They argue that trade-off is the relationship that is particular of the products in the domain and is not with respect to the user query. McSherry in his work [11] brings out the idea of using compromise (the relationship of a product with respect to the user query) in improving the success rate of a CBR-RS. As the second part of our work, we combine the best of both the static trade-off relationship among products and the dynamic compromise relationship between the user query and the products to bring out the idea of utilizing the collective evidence of the RS and build an efficient CCBR-RS in contrast to EBR which deals with evidence of individual products. We evaluate our methods on three datasets and report the results in comparison to the base works.

In the next Section, we introduce the background for our work: This is followed by the related works in Section III. The details of our approach are presented in Section IV. This is followed by the evaluation and results in Section V and we

conclude in Section VI.

## II. BACKGROUND

In this section, we go into the details of the background and set the context for our work before we move on to the related works.

### A. Case Representation and Approximation of Utility

We work in the context where the cases/products are from the same domain. For example a camera domain has only cameras in it. Each product, is represented as a fixed set of features/attributes with values corresponding to each of the features. In domains like motorcycle, the features of the domain can be categorized into More is Better (MIB) and Less is Better (LIB) [12]. For example, the feature 'Mileage' is an MIB feature. Given two motorcycles with similar feature values, people often tend to choose the motorcycle with higher 'mileage'. In contrast, 'price' is an LIB feature. Given two motorcycles with similar feature values, people often tend to choose the motorcycle with lower 'price'. If the query is '5000 \$' motorcycle, then any motorcycle with the price less than or equal to '5000 \$' may be deemed useful to the user. The higher the price above '5000 \$' the lower the utility. Had the query been '100 horse power'(MIB feature), then any motorcycle with more or equal horse power would be deemed useful to the user and lesser the value the less useful it is. The feature values are normalised appropriately such that for an MIB feature the highest value is set to 1 and the lowest value is set to 0; for an LIB feature the highest value is set to 0 and the lowest value is set to 1. The score a product would receive is given in equation below where  $Q_i$  stands for query value of feature  $i$  and  $P_i$  stands for the value of feature  $i$  of product  $P$ .

$$lsim(Q_i, P_i) = \begin{cases} 1, & \text{if } P_i \geq Q_i \\ \frac{P_i}{Q_i}, & \text{otherwise} \end{cases} \quad (1)$$

A global similarity measure based on a Multi-attribute utility theory (MAUT) [7] is used to approximate utility. The similarity of a product to another product is the average of feature level similarities. If  $Q$  is the query and  $P$  is the product then the similarity between them is given in the equation below, where  $lsim$  is as given in (1).

$$sim(Q, P) = \frac{\sum_{i \in Attributes} lsim(Q_i, P_i)}{|Attributes|} \quad (2)$$

Among a pair of products  $A$  and  $B$ , if  $A_x$  is greater than  $B_x$  for an MIB feature  $x$ , then product  $A$  is said to dominate product  $B$  with respect to feature  $x$ . Similarly, for an LIB feature  $y$ , product  $A$  is said to dominate product  $B$  with respect to feature  $y$  if  $A_y$  is less than  $B_y$ .

### B. Preference based Feedback

The feedback provided by the user in each interaction cycle is used to modify the query for the next interaction cycle. User ratings [15], critiquing [4] and preference based feedback [9] are the common ways in which feedback is obtained from the user. Preference-based feedback (PBF) poses a lesser cognitive load on the user compared to the other feedback mechanisms

[16]. In PBF, the user picks one product out of the  $k$  products recommended to her as her product of preference. The PBF is treated as the query in the next interaction cycle. The various ways in which PBF is used is explained in Section III. We restrict our focus to CCBRS with PBF.

### C. Random Surfer Model

In the first part of our work, we use the idea of utilizing higher order relationship among the products to enhance [2]. We solve our problem by posing it as a random surfer model. Assume a hypothetical cyclist Alice who keeps touring with her cycle with no specific destination. In the hypothetical world she lives, all roads are one way, no roads intersect and there is exactly one restaurant at the junction of roads and nowhere else. She keeps travelling on the road and when she encounters a junction of roads, she rests a while in the restaurant and chooses one of the roads randomly and keeps travelling. Occasionally, if she is bored she gets teleported with her bike from a restaurant to some random restaurant and starts touring again. Given a restaurant in her world, what is the probability that she would have visited the restaurant? Let  $N$  be the number of restaurants,  $1-d$  be the probability with which she teleports,  $inNeighbours_I$  of a restaurant  $I$  is the set of restaurants such that for each restaurant  $X$  in the set there is a road from  $X$  to  $I$ .  $outNeighbours_I$  of a restaurant  $I$  is the set of restaurants such that for each restaurant  $X$  in the set there is a road from  $I$  to  $X$ . The probability that restaurant  $I$  would have been visited at time step  $t$  is given in the equation below. At  $t=0$ , the probability that a restaurant is visited is  $1/N$ . The event of the Alice visiting each restaurant can be associated with the flow of evidence to each product in the domain, the details of which we will elaborate in Section IV.

$$p(I; t) = \frac{(1-d)}{N} + d * \sum_{J \in inNeighbours_I} \frac{p(J; t-1)}{|outNeighbours_J|} \quad (3)$$

## III. RELATED WORKS

### A. Modelling User Preferences

More Like This (MLT) [9] is an early approach that uses PBF for query expansion. The PBF in the current interaction cycle becomes the query for the next interaction cycle. In MLT all the feature values of the PBF are assumed to be indicative of the preferences of the user. The authors in [9] assert the fact that every attribute value of the PBF may not be equally desirable to the user and they propose weighted MLT (wMLT) that assigns weights to each of the features. The weight is based on the uniqueness of the feature value. For example, if the motorcycle preferred by the user is 'Air Cooled' but the rest of the motorcycles in the RS are 'Liquid Cooled' we can be more sure about the preference of the user on that feature. The feature weights model the preferences of the user and thus helps with the personalisation of the recommendations. The work by authors in [13] points out the drawback with learning feature weights independent of the other features in the domain. For the example considered above, one might have chosen 'Air Cooled' engine because the motorcycle is the cheapest of the lot. Assigning higher weights



TABLE I. PRODUCTS RECOMMENDED TO USER

|   | price(\$) | mileage (kmpl) | top speed (kmph) |
|---|-----------|----------------|------------------|
| A | 5000      | 10             | 120              |
| B | 5000      | 8              | 150              |
| C | 7000      | 6              | 250              |

to ‘Air Cooled’ engine without considering the cost would not reflect the preferences of the user in an adequate manner. In [13], the authors make an assumption that the utility of PBF is greater than or equal to the utility of each of the rejected products. They use a weighted MAUT based similarity model as given in the equation below to model the utility of a product, where  $w_i$  is the weight given to feature  $i$ .

$$wSim(Q, P) = \frac{\sum_{i \in Attributes} w_i * lsim(Q_i, P_i)}{|Attributes|} \quad (4)$$

Consider the example domain given in Table I. Let us consider an instance where the user is recommended products A, B and C, assume the user preferred A. We make an assumption that the utility of A is greater or equal to the utility of B and the utility of A is greater or equal to the utility of C. The assumptions can be expressed as inequalities. For illustration, the assumption that utility of A is greater than or equal to the utility of B is expressed as an inequality which is given in (5). In practice, the values are normalised and used in the inequalities. The generalised inequality is given in (6). The  $\Delta$ s represent the difference in the values and  $w_i$  represents weight of the feature  $i$ . The sign corresponding to the weights of LIB attributes is negative as shown in the equations. The inequalities are solved for the feature weights. The number of products recommended to the user is usually lesser than the number of attributes in the domain and hence the solutions to the feature weights form a convex region in the feature weights space. We term the region of solutions as the *preference region* of the user. One solution from the *preference region* is picked as the feature weights.

$$-(5000 - 5000) \times w_{price} + (10 - 8) \times w_{mileage} + (120 - 150) \times w_{topspeed} \geq 0 \quad (5)$$

$$-w_{price} \times \Delta_{price} + w_{mileage} \times \Delta_{mileage} + w_{topspeed} \times \Delta_{topspeed} \geq 0 \quad (6)$$

This model is termed Compromise Driven Preference Model (CDPM). In our work, we do not attempt to model the user by using feature weights.

### B. Profiling Products in the Domain

The products preferred by the users themselves are representative of the preferences of the user. The idea of profiling the products even before the recommendation could start is proposed by authors in [1]. They employ a method similar to the one used by authors in [13] to characterize each product in the domain. Their work argues that each product in the domain has prospective buyers. The prospective buyers of the product are modelled in the form of a region of feature weights in the feature weights space. They assume, for every product, their  $k$  most similar products as the competitors of the product. A prospective buyer of a product would assume that the utility of

TABLE II. TRADE-OFF REPRESENTATION AND SIMILARITY BETWEEN TRADE-OFFS

|                        | price(\$)        | mileage (kmpl) | top speed (kmph) |
|------------------------|------------------|----------------|------------------|
| A                      | 5000             | 10             | 120              |
| B                      | 5000             | 8              | 150              |
| C                      | 7000             | 6              | 250              |
| D                      | 7500             | 6              | 275              |
| $T_{AB}$               | 0                | 1              | -1               |
| $T_{AC}$               | 1                | 1              | -1               |
| $T_{BD}$               | 1                | 1              | -1               |
| $tSim(T_{AB}, T_{AC})$ | (0+1+1)/3 = 0.66 |                |                  |

the product of her desire is greater than or equal to the utility of each of its competitors.

Similar to the work by the authors in [13], inequalities are formed and solved for the feature weights. The solution to the inequalities is a region in the feature weights space which the authors term as *dominance region* of the product. In the course of recommendation, the amount of overlap between the *dominance region* of a product and the *preference region* of the user is used to enrich the measure of utility of a product to the given user. The authors show that using the score from the overlap of the regions improve the efficiency of the CCBRRS. This work is based on the predicted preference of the user and hence termed Predicted Preference Region-based Method (PPRM). We do not pre-process our data as in this work. No attempt is made to profile the individual products but the theme that the products themselves are representative of the preferences of the user is prevalent in our work too.

### C. Trade-off based Recommendation

Consider the products from Table I. If the user query is ‘price: 5000 \$’ and ‘top speed: 200 kmph.’ then there is no product in the domain that satisfies all the requirements of the user. If we consider product A, it fails to satisfy the ‘top speed’ requirement but satisfies the ‘price’ requirement. Likewise, product C fails to satisfy ‘price’ but satisfies ‘top speed’. Since we are not aware of the compromise a user would be willing to make, say if we are allowed to show only two products at a time then it is desirable to recommend products A and C instead of products A and B. If products A and B are recommended and if the user is not willing to compromise on ‘price’ then none of the products in the current recommendation cycle satisfies the user. McSherry in [11] proposes to recommend products with varied compromises (this is called Compromise Driven Retrieval (CDR)) to improve the success rate of the recommendation system.

Compromises capture the ability/inability of the products to satisfy the requirements of the user. Even without taking the user query into account, if we compare two products say in our example products A and C, we can notice the distinguishing characteristics of each of the products. The MIB, LIB categorization helps us define the dominance relation between the features of any pair of products. Among the products A and C, A dominates C with respect to the features ‘price’ and ‘mileage’ similarly C dominates A with respect to the feature ‘top speed’. If one has to choose A over C she has to compromise on ‘top speed’ for the gain in other features. This relation among the product pairs is termed trade-offs by authors in [14]. They define a representation for the trade-offs and a measure of similarity for a pair of trade-offs.

Table II shows the representation of the trade-offs  $T_{AB}$ ,  $T_{AC}$  and  $T_{BD}$ . A Trade-off represents the set of features one has to compromise for the gain in another set of features in choosing one product over the other.  $T_{AB}$  represents that if one has to accept A over B she has to compromise on the feature ‘top speed’ for the gain in ‘mileage’. The dominating feature in the product that one would be willing to accept is represented with a ‘1’ and the dominated feature with a ‘-1’, a feature that neither dominates nor is dominated is represented by a ‘0’. The similarity between a pair of trade-offs is proportional to the count of the number of matching symbols in the given pair. If T and S are the trade-offs the match/similarity between the trade-offs is given in the equation below.  $\mathbf{1}()$  is an indicator function that gives a value 1 if the symbols match and 0 otherwise.

$$tSim(T, S) = \frac{\sum_{i \in Attributes} \mathbf{1}(T_i = S_i)}{|Attributes|} \quad (7)$$

The authors in [14] propose several methods, one of which uses the trade-off choices made by the user in each interaction cycle to identify the potential products of interest to the user (MLT with Trade-off Matching **MLT TM**). In our work, we combine the benefits of both the *trade-off* based relationship and the diversity based on *compromise* to achieve better efficiency.

#### D. Evidence-based Recommendation

In the work by authors in [2], the PBF given by the user in every interaction cycle is used to account for the evidence of the products in the domain. In a given interaction cycle, only  $k$  products are shown to the user and the user prefers only one product among them, then how is the evidence propagated to other products in the domain? The similarity and trade-off relation among the products is exploited to propagate the evidence of the products. For example, if Jane says she likes ‘lemon’ better than ‘apple’ it may be the case that she likes ‘orange’ better than ‘apple’ too as both ‘lemon’ and ‘orange’ are citrus fruits. Though the feedback given by Jane is only on ‘lemon’, the similarity relation between ‘lemon’ and ‘orange’ helps us to propagate the feedback on ‘lemon’ to ‘orange’. Here in the given example, ‘lemon’ is the dominant product and ‘apple’ is the dominated product. The dominance relation of PBF on the rest of the products in the RS is propagated based on the hypothesis that *the dominance relation between two pairs of products are similar if they involve similar dominant and dominated products, provided the trade-off relations between the pairs are also similar*. For example, among the products in Table II the user prefers product A over product C. It is highly likely that the user would prefer product B over product D as products A and B are similar (dominating products) and products C and D are similar (dominated products) and the trade-off similarity between  $T_{AC}$  and  $T_{BD}$  is high. We base our work on the idea of EBR and provide significant extensions to the same.

## IV. OUR APPROACH

As discussed previously, the motivation of this work is to explore ideas on how EBR can be effectively used to improve the efficiency of CCB-RSs. We propose two broader themes

in this work. The first idea deals with higher order evidence propagation. The second theme deals with collective evidence of the RS as opposed to the evidence of individual products.

#### A. Higher order Evidence Propagation

In a CCB-RS the preferences of the user should ideally be aggregated across interaction cycles. In methods where the preferences are modelled as feature weights, the weights reflect the aggregated preferences. In EBR, the user given feedback in an interaction cycle ascribes preferences to various degrees to every product in the domain. The evidence for a product is aggregated across interaction cycles by taking all the feedback the user has provided into consideration. Imagine a directed completely connected graph with each product as a node. Each edge represents the action of the user choosing one node (destination) over the other (source). The node preferred by the user is called *dominant* node (destination node) and the node that is preferred over is called *dominated* node (source node). The dominant node and dominated node pair is termed as the dominance relation pair. Each edge is associated with a weight. Consider the nodes A and B. If there is an edge from B to A, the weight of the edge from B to A denotes the probability with which product A would be selected by the user over product B. If we can assign weights to the edges of the graph then we can find higher order dominance relationship among products. Let us term the graph preference graph.

At each interaction cycle, we pose the problem as random surfer model and find the probability that the random surfer would be found at every node in the graph (the probability that Alice would have visited a restaurant). In our work since we assume a strongly connected graph, every node is equally likely to be visited from a given node, but the weights that we assign to the edges plays the role of assigning probabilities that an edge will be traversed by the surfer. We can assume that the roads in Alice’s world are of different widths and Alice chooses a road with probability proportional to the width of the road. The modified formulation is given in the equation below, where the probability that a road from restaurant  $J$  to  $I$  would be taken is represented as  $w_{JI}$ .  $p(I; t)$  is the probability that a node  $I$  is visited at time step  $t$ . We keep finding the probabilities of the nodes for successive iterations in an iterative way. If at a time step, the sum of the changes in the probabilities of the nodes of the graph with respect to the previous time step is below a threshold we stop the iterative process and the nodes/products with the top  $k$  probabilities are recommended to the user. In our set up, the higher the weights of the edges leading to a node from other nodes the higher the probability that the random surfer would visit that node. If a particular product dominates other products to a greater extent then the probability of that product is expected to be high. Based on (3), we have the following formulation:

$$p(I; t) = \frac{(1 - d)}{N} + d * \sum_{J \in inNeighbours_I} \frac{w_{JI} * p(J; t - 1)}{\sum_{L \in outNeighbours_J} w_{JL}} \quad (8)$$

**Assigning edge weights:** In our work we made the weight of an edge depend on three quantities a) the similarity of the destination node to the products already preferred by the user

TABLE III. PRODUCT-PRODUCT SIMILARITY

|   | A   | B   | C   | D   | E   |
|---|-----|-----|-----|-----|-----|
| A | 1.0 | 0.5 | 0.6 | 0.7 | 0.5 |
| B | 0.5 | 1.0 | 0.5 | 0.5 | 0.4 |
| C | 0.6 | 0.5 | 1.0 | 0.7 | 0.9 |
| D | 0.7 | 0.5 | 0.7 | 1.0 | 0.9 |
| E | 0.5 | 0.4 | 0.9 | 0.9 | 1.0 |

in previous interaction cycles; b) the similarity of the source node to the user rejected products; c) the similarity of the trade-off one has to make in choosing the destination node over the source to the trade-offs the user has made in all the previous interaction cycles. We form  $k - 1$  dominance relation pairs by pairing PBF with each of the rejected products in every interaction cycle. Let  $UDR$  (User Dominance Relations) be the set of all the dominance relations that we have aggregated from the user through PBF,  $UPP$  (User Preferred Products) be the set all the PBFs the user has provided and  $URP$  (User Rejected Products) be the set of all products that are dominated by any of the products from  $UPP$ . The edge weights are computed based on (9), where  $w_{SD}$  denotes the weight of the edge from the Source node (S) to Destination node (D),  $R_d$  and  $R_r$  denotes the dominant product and dominated/rejected product respectively in the relation  $R$ . We term our method **HEBR** (Higher-order EBR).

$$w_{SD} = \alpha * \left( \frac{\sum_{M \in UPP} sim(M, D)}{|UPP|} + \frac{\sum_{N \in URP} sim(N, S)}{|URP|} \right) + (1 - \alpha) * \left( \frac{\sum_{R \in UDR} tSim(T_{R_d R_r}, T_{DS})}{|UDR|} \right) \quad (9)$$

**Illustration:** Consider domain where we have 5 products A, B, C, D, and E. Let us assume products A and B are shown to the user and the user has preferred A over B. Now we need to recommend products based on the feedback from the user. Let us construct the preference graph from the data we have. The product-product similarity matrix is given in Table III. The trade-off similarity of every pair of edge with the user made trade-off (A over B) is computed and let us assume it is as given in Table IV. The weights of the edges are computed based on (9). Let  $d = 0.85$ ,  $\alpha = 0.9$  and at  $t = 0$  each product is considered to be equally likely. We need to order the product C, D and E in the domain so that they can be recommended to the user. The scores for the products based on EBR are [0.525, 0.590, 0.455] corresponding to C, D and E. The scores based on HEBR for C, D and E are [0.188, 0.180, 0.194]. HEBR places E in the first place even though products C and D are more similar to the PBF (A) than E is to the PBF. E is highly similar to C and D so the evidence from C and D propagate to E making it highly probable. (We cannot talk just in terms of similarity with PBF alone, but we use it for the sake of clarity.)

**Step by step recommendation process:** The following are the steps in HEBR:

**Step 1:** The preferences of the user are expressed in terms of query Q. Q has one or more values corresponding to the

TABLE IV. TSIM OF PRODUCT-PRODUCT TRADE-OFF WITH TRADE-OFF  $T_{AB}$

|   | A   | B   | C   | D   | E   |
|---|-----|-----|-----|-----|-----|
| A | 0.0 | 0.6 | 0.5 | 0.4 | 0.7 |
| B | 0.4 | 0.0 | 0.7 | 0.6 | 0.5 |
| C | 0.5 | 0.3 | 0.0 | 0.3 | 0.2 |
| D | 0.6 | 0.5 | 0.7 | 0.0 | 0.3 |
| E | 0.3 | 0.5 | 0.8 | 0.7 | 0.0 |

features in the domain.

**Step 2:** Products are ranked based on (2). The top  $k$  ranked products are recommended to the user. The user picks a product as PBF and continues her recommendation process or accepts one of the recommended products.

**Step 3:** PBF is added to the set  $UPP$ . Every product other than PBF in the RS is added to the set  $URP$ .  $k - 1$  pairs corresponding to  $k - 1$  rejected products are matched with the dominant product PBF and are added to the set  $UDR$ .

**Step 4:** A strongly connected graph ‘preference graph’  $G$  with all the products as nodes is constructed and the weights of the edges are assigned based on (9).

**Step 5:** The probability of nodes in the graph  $G$  are updated based on (8) iteratively for several time steps till the sum of the difference in the probabilities of the nodes from one iteration to the next iteration is below a fixed threshold.

**Step 6:** The products with top  $k$  probability values are recommended to the user.

**Step 7:** The user picks her PBF and continues the recommendation process (back to Step 3) or accepts one of the recommended products

## B. Evidence for Successful Recommendation

A successful recommendation depends on the contribution of individual products as well as the collective contribution of the products. In EBR, the RS is filled with products that have higher evidence from the feedback provided by the user. The utility of the RS is approximated by the sum of the evidence scores of all the constituent products. The interaction among the products in the RS is not taken into consideration in this view. The earliest work from the literature that considers the interplay among products in RS is MLT with Adaptive Selection (MLT AS) [10]. The authors categorize the interaction cycles into ‘Refine phase’ and ‘Refocus phase’. In ‘Refine phase’ the products are recommended based on only similarity, in ‘Refocus phase’ diverse products are recommended to the user based on bounded greedy approach [17]. They show that the efficiency of the system can be improved by methodically introducing diversity. Though the similarity of products in the ‘Refocus phase’ is not maximized, the efficiency of the system is expected to improve by taking into account the collective utility of the RS. We base our work on MLT TM.

We explain how MLT TM can be understood in terms of evidence maximization and enrich the method to include the effect of interaction among the products with the help of the compromise criterion.

**MLT TM in the light of EBR:** Consider the example products given in Table II. Products A and B have good fuel efficiency but lose out on power. Irrespective of the user query, just by analysing the products, one can characterize the preferences of the user who would buy each of the products. Similar to the idea used in PPRM, a prospective buyer of a sports motorcycle would prefer ‘top speed’ feature more than the fuel efficiency feature. Instead of using the trade-off relations to learn feature weights, MLT TM uses the features themselves to model a given user and recommend products that would better serve her need. EBR records evidence in the level of products whereas in MLT TM the evidence is aggregated in terms of features. In Table II if products C and B are shown to user and the user prefers product C then the fact that feature ‘top speed’ is preferred over features ‘price’ and ‘mileage’ ( $T_{CB}$ ) is used as evidence for promoting product D because the comparison of D with B also yields the same trade-off ‘top speed’ over ‘mileage’ and ‘price’ ( $T_{DB}$ ). In EBR the dominance relations are used to propagate the evidence. In MLT TM, the trade-offs are used to propagate the evidence among products.

**Evidence of the recommendation set:** Compromises are subjective to the user. McSherry asserts that the compromises a user would be willing to make is not known in advance and is independent of the feature preferences of the user. CDR aims to improve the success of the system by suggesting products that are diverse with respect to the compromises they offer with respect to the user query. We propose a revised utility approximation in MLT TM that accommodates the interaction among the products in terms of compromises they offer to model the effective evidence of the RS in a better manner. We formulate two methods to realize our idea.

**Greedy Evidence Maximization (GEM):** In GEM, products are added incrementally to the RS. There are three criteria for inclusion of a product in the RS. The first criterion is similarity. If a product is more similar to the query then it is more evident that it would satisfy the requirements of the user. The second criterion is trade-off. The user preferred product in a given interaction cycle is compared against the rejected products and the corresponding trade-offs are recorded. The hypothesis in MLT TM is that a product would be useful to the given user if it makes similar trade-offs as the PBF with the user rejected products. The trade-off evidence score is given in (10), where  $C$  is the candidate product that we are evaluating to be included in the RS, Rejected List is the set of products in the RS other than PBF, the user preferred product PBF is represented as  $P$ .

$$tradeE(C, P) = \frac{\sum_{X \in RejectedList} tSim(T_{CX}, T_{PX})}{|RejectedList|} \quad (10)$$

The third criterion is different from the first two criteria. It is based on compromises. We formulate the criterion such that it ensures maximization of the utility of the RS as opposed to individual products. The Compromise Set is the set of features with respect to which the candidate product  $C$  compromises on the PBF/query. It is as given in (11). The compromise distance

in (12) measures the dissimilarity in the compromise sets of a pair of products ( $C_1, C_2$ ) with respect to the query product  $P$ . The compromise evidence  $compE$  measures the utility of  $C$  if it is added to the RS. Since the RS is filled incrementally when there is no product in RS the value of  $compE$  is taken as zero.  $compE$  measures the average dissimilarity in the compromises made by the candidate  $C$  with respect to the rest of the products included in the RS. We want the dissimilarity score to be high so that the products included in the RS have varied compromises with respect to the query. The varied compromise choices provided by the products in RS improves the utility of RS as a whole.

$$CS(C, P) = \{i | i \in Attributes \text{ and } P \text{ dominates } C \text{ with respect to } i\} \quad (11)$$

$$compDist(C_1, C_2, P) = 1 - \frac{CS(C_1, P) \cap CS(C_2, P)}{CS(C_1, P) \cup CS(C_2, P)} \quad (12)$$

$$compE(C, P, RS) = \frac{\sum_{R \in RS} compDist(C, R, P)}{|RS|} \quad (13)$$

Each product in the domain is evaluated based on the combined score of the three criteria as given in (14). The product with the highest  $cScore$  is included in the RS. The products in RS are included in a greedy manner incrementally rather than finding the set of products that maximizes the  $cScore$  of the products in RS.

$$cScore(C, P, RS) = \alpha * sim(P, C) + \beta * tradeE(C, P) + \gamma * compE(C, P, RS) \quad (14)$$

**Greedy Evidence Maximization Bounded (GEMB):** In GEM each product in the domain needs to be evaluated  $k$  times as the products are added incrementally. Instead of evaluating all the products in the domain every time before including a product in RS, in GEMB a) we set a bound  $\mathbf{B}$  b) we sort the products based on similarity and trade-off evidence and evaluate only the top  $\mathbf{B}$  products for inclusion in RS. This provides a good speed-up of the system with some loss in efficiency.

**Step by step recommendation process:** The following are the steps for the two methods:

*Step 1 and 2:* Same as in HEBR

*Step 2a (Only for GEM):* All the products in the domain are selected for further evaluation.

*Step 2b (Only for GEMB):* The products in the domain are sorted based on the sum of  $sim$  and  $tradeE$  scores, the top  $\mathbf{B}$  products are selected for further evaluation.

*Step 3:* The products are evaluated based on  $cScore$  and the product with the highest score is added to the RS.

*Step 4:* While the RS has less than  $k$  products repeat Step 3.

Step 5: The user picks her PBF (PBF becomes the new query) and continues the recommendation process (back to Step 2a or 2b based on the method used) or accepts one of the recommended products

*Handling nominal attributes:* The nominal attributes are treated in the same way in all the methods proposed in this work (HEBR, GEM and GEMB). In the similarity calculation step, we give a value 1 if the attribute value matches, else we give the value 0. In trade-off representation, if both the products have the same attribute values we assign the symbol '0' else we assign '1'. While considering for compromises, if the attribute values are same then we consider it as 'no compromise' else it is assumed to have compromised.

## V. EVALUATION AND RESULTS

We evaluate our methods with the standard evaluation procedure followed in CCB-RSs literature [8]. It is widely used in CCB-RS literature ([8], [9], [13], [1], [14]). We take three real-world datasets namely Camera, PC and Used Cars, each of which has 210, 120 and 956 cases respectively. All the datasets have numeric and nominal attributes. The numeric attributes of our domain are categorized into MIB or LIB features. In Camera domain, among numeric attributes 'price' and 'weight' are categorized as LIB and the rest are categorized as MIB. In Used Cars dataset, the attributes 'price' and 'miles' are categorized as LIB and the others are categorized as MIB. In PC dataset 'price' is the only LIB attribute.

### A. Leave-one-out Evaluation Procedure

We simulate an artificial user. We assume that one of the products in the domain ideally suits all the preferences of the user. The ideal product is removed from the domain (left-out product). We identify a product in the domain that is most similar to the left out product and set it as the 'Target product'. The left-out product is used to generate the initial query for the artificial user. A randomly chosen subset of the attribute values of the left-out product is made as the initial query of the user. We generate three levels of queries namely hard, medium and easy. The level of hardness is based on the number of attribute values included in the initial query. A hard query has only 1 attribute value, a medium query has 3 and an easy query has 5 attribute values of the left-out product.

In feedback phase, if the artificial user encounters the 'Target' product in the RS the recommendation process stops and the number of interaction cycles taken to identify the product of interest is recorded else the product that is most similar to the left-out product is selected from the RS as the PBF. The PBF becomes the query for the next interaction cycle. The product to be left out is selected randomly from the domain and the Target product is fixed, the 3 levels of queries are generated from the left-out product and the recommendation process is simulated using the artificial user. This process is repeated 1000 times in each of the domains used for evaluation. The average number of cycles taken to reach the 'Target' product is calculated separately for each of the levels (hard, medium and easy) of queries. We compare HEBR against EBR

to evaluate the effect of higher-order evidence propagation. The GEM and GEMB methods are compared against MLT TM to evaluate the effect of maximizing the evidence of RS considering the interaction among products. We have also compared our methods against MLT and MLT-AS.

### B. Results

Tables V, VI and VII display the comparison of HEBR against EBR along with MLT and MLT AS. Tables VIII, IX and X display the comparison of GEM and GEMB against EBR along with MLT and MLT AS. The 1000 queries in each query level (hard, medium and easy) are split into 10 partitions of 100 queries per partition and the difference in averages are tested for statistical significance (paired t-test with  $p < 0.05$ ). The results in bold are significantly better than the rest.

TABLE V. EFFICIENCY IN PC DATASET (THE LESSER THE AVERAGE CYCLE LENGTH THE BETTER)

| Query Size | MLT  | MLT AS | EBR         | HEBR        |
|------------|------|--------|-------------|-------------|
| 1          | 8.29 | 6.09   | 4.08        | <b>3.76</b> |
| 3          | 6.14 | 4.22   | <b>3.20</b> | <b>3.28</b> |
| 5          | 3.67 | 2.19   | <b>1.97</b> | 2.31        |

TABLE VI. EFFICIENCY IN CAMERA DATASET (THE LESSER THE AVERAGE CYCLE LENGTH THE BETTER)

| Query Size | MLT   | MLT AS | EBR         | HEBR        |
|------------|-------|--------|-------------|-------------|
| 1          | 11.41 | 6.90   | 5.13        | <b>4.72</b> |
| 3          | 9.54  | 5.89   | <b>4.64</b> | <b>4.51</b> |
| 5          | 6.42  | 4.04   | <b>3.59</b> | 3.83        |

TABLE VII. EFFICIENCY IN CAR DATASET (THE LESSER THE AVERAGE CYCLE LENGTH THE BETTER)

| Query Size | MLT   | MLT AS | EBR         | HEBR        |
|------------|-------|--------|-------------|-------------|
| 1          | 24.42 | 14.32  | 9.28        | <b>7.68</b> |
| 3          | 19.18 | 10.91  | <b>7.55</b> | <b>7.45</b> |
| 5          | 15.12 | 8.08   | <b>5.85</b> | 6.58        |

TABLE VIII. EFFICIENCY IN PC DATASET (THE LESSER THE AVERAGE CYCLE LENGTH THE BETTER)

| Query Size | MLT  | MLT AS | MLT TM | GEM         | GEMB        |
|------------|------|--------|--------|-------------|-------------|
| 1          | 8.29 | 6.09   | 5.50   | <b>4.72</b> | <b>4.20</b> |
| 3          | 6.14 | 4.22   | 3.96   | <b>3.52</b> | 3.31        |
| 5          | 3.67 | 2.19   | 2.19   | <b>1.99</b> | 2.01        |

TABLE IX. EFFICIENCY IN CAMERA DATASET (THE LESSER THE AVERAGE CYCLE LENGTH THE BETTER)

| Query Size | MLT   | MLT AS | MLT TM | GEM         | GEMB        |
|------------|-------|--------|--------|-------------|-------------|
| 1          | 11.41 | 6.90   | 6.28   | <b>4.99</b> | <b>5.00</b> |
| 3          | 9.54  | 5.89   | 5.45   | <b>4.66</b> | <b>4.64</b> |
| 5          | 6.42  | 4.04   | 3.94   | <b>3.41</b> | 3.64        |

TABLE X. EFFICIENCY IN CAR DATASET (THE LESSER THE AVERAGE CYCLE LENGTH THE BETTER)

| Query Size | MLT   | MLT AS | MLT TM | GEM          | GEMB  |
|------------|-------|--------|--------|--------------|-------|
| 1          | 24.42 | 14.32  | 12.14  | <b>10.47</b> | 11.57 |
| 3          | 19.18 | 10.91  | 9.64   | <b>8.15</b>  | 9.26  |
| 5          | 15.12 | 8.08   | 7.53   | <b>6.20</b>  | 7.07  |

### C. Discussion

HEBR performs better than EBR for hard queries in all the three datasets but on easier queries, the higher order evidence propagation degrade the efficiency. The performance of HEBR

<sup>1</sup><http://www.mycbr-project.org/download.html>

on medium level queries seems to be on par with EBR. The number of cycles needed for hard queries is high so with more feedback the efficiency improvement is high, in contrast with lesser feedback the noise from the preference graph dominates the feedback leading to the depreciation in efficiency. For hard queries, HEBR reduces the cycle length by 7.8%, 7.9% and 17% in PC, Camera and Used Car datasets, respectively.

GEM performs better than MLT TM in all the datasets for all the query sizes. The performance of GEMB is found to be statistically better than MLT TM in PC and Camera datasets, in Used Car dataset alone GEMB performs only as good as MLT TM. In Used car dataset alone, though the averages of GEMB seems to be better than MLT TM they are not significantly better. The time GEMB takes for execution is in the order of MLT TM but with better performance. If the execution time is critical then GEMB offers marginally good performance in a significantly lesser time when compared against GEM. GEM outperforms GEMB in most of the cases but takes more time to execute when compared against GEMB. Using GEM the reduction in average cycle length for hard, medium and easy queries in PC dataset is 14%, 11% and 9% respectively, in Camera dataset it is 20%, 14% and 13% and in Used Car dataset the numbers are 13%, 15% and 17%, respectively.

HEBR is expected to perform better than EBR for all query levels but it only performs well in the hard queries. The propagation of noise could be the reason for the same. We cannot expect the users to make informed decisions throughout the recommendation process. HEBR can be extended to account for the noise in the feedback provided by the user. The strength of CBR-RS lies in its ability to explain why a recommendation has been made. Explanations add to the trust of a recommendation system. The work in its current form fails to utilize the explanatory potential of CBR-RS. Our future work would include explanations along with the recommendations made to enhance the value of the recommendation system as a whole.

## VI. CONCLUSION

We have proposed two themes as an extension to the EBR. The first one is propagation of higher order evidence. The second explains MLT TM in the light of EBR and deals with handling the interaction among products in the RS to enhance evidence maximization. The works are compared against the state of art in the area. The results suggest the effectiveness of our approach in improving the efficiency of state-of-the-art.

## REFERENCES

- [1] Anbarasu Sekar, and Sutanu Chakraborti, "Towards Bridging the Gap between Manufacturer and Users to Facilitate Better Recommendation", The Thirty-First International Flairs Conference. 2018.
- [2] Anbarasu Sekar, and Sutanu Chakraborti, "Show me your friends, I'll tell you who you are: Recommending products based on hidden evidence", Accepted in 27th International Conference on Case-Bases Reasoning 2019, to appear in LNAI Springer, 2019.
- [3] Bridge, D., "Product Recommendation Systems: A New Direction", In Proceedings of the Workshop Programme at the Fourth International Conference on Case-Based Reasoning, pages 79-86, Vancouver, BC, Canada, 2001.
- [4] Burke, R. D., K. J. Hammond, and B. C. Young, "The Findme Approach to Assisted Browsing", IEEE Expert, 12(4), 32-40. ISSN 0885-9000. 1997.
- [5] Burke, R., "Knowledge-Based Recommender Systems", In Encyclopedia of Library and Information Systems, 2000. Marcel Dekker, 2000.
- [6] Gediminas Adomavicius, Alexander Tuzhilin, "Toward the Next Generation of Recommender Systems: A Survey of the State-of-the-Art and Possible Extensions", IEEE Transactions on Knowledge and Data Engineering, v.17 n.6, pp.734-749. 2005.
- [7] Keeney, Ralph L., and Howard Raiffa. "Decisions with multiple objectives: preferences and value trade-offs" Cambridge university press, 1993.
- [8] McGinty L. and Smyth B., "Evaluating preference-based feedback in recommender systems", In Artificial Intelligence and Cognitive Science, pp 209-214. Springer 2002.
- [9] McGinty L. and Smyth B., "Comparison-based recommendation", In S. Craw and A. Preece, editors, Advances in Case-Based Reasoning, Proceedings of the 6th European Conference on Case Based Reasoning, ECCBR 2002, pp 575-589, Springer Verlag, 2002.
- [10] Lorraine McGinty and Barry Smyth., "On the role of diversity in conversational recommender systems". In Proceedings of the 5th international conference on Case-based reasoning: Research and Development (ICCBR'03), pp. 276-290, Springer-Verlag, Berlin, Heidelberg, 2003
- [11] McSherry D., "Similarity and Compromise". Case-Based Reasoning Research and Development. Lecture Notes in Computer Science, vol 2689. Springer, Berlin, Heidelberg, 2003.
- [12] McSherry, David., "Coverage-Optimized Retrieval", Proceedings of the Eighteenth International Joint Conference on Artificial Intelligence, pages 1349-1350. Morgan Kaufmann Publishers Inc. 2003.
- [13] Mouli, S. Chandra, and Sutanu Chakraborti. "Making the Most of Preference Feedback by Modeling Feature Dependencies" Proceedings of the 9th ACM Conference on Recommender Systems. ACM, 2015.
- [14] Sekar A., Ganesan D., Chakraborti S., "Why Did Naethan Pick Android over Apple? Exploiting Trade-offs in Learning User Preferences. In: Cox M., Funk P., Begum S. (eds) Case-Based Reasoning Research and Development. ICCBR 2018. Lecture Notes in Computer Science, v. 11156. Springer 2018.
- [15] Smyth, B. and P. Cotter, "Surfing the Digital Wave, Generating Personalised TV Listings using Collaborative, Case-Based Recommendation", In ICCBR '99: Case-Based Reasoning Research and Development, Proceedings of the Third International Conference on Case-Based Reasoning, pages 561-571, Seon Monastery, Germany, July 27-30, 1999. Springer Verlag, 1999.
- [16] Smyth, B., "Case-Based Recommendation", In The Adaptive Web. pp. 342-376, Springer 2007.
- [17] Smyth B. and McClave P., "Similarity vs Diversity", In D. Aha and I. Watson, editors, Proceedings of the International Conference on Case-Based Reasoning, pp 347-361. Springer 2001.

# An Assessment of Open Data Sets Completeness

Abdulrazzak Ali<sup>1</sup>

Fakulti Teknologi Maklumat dan Komunikasi  
Universiti Teknikal Malaysia Melaka  
Hang Tuah Jaya, 76300, Ayer Keroh  
Melaka, Malaysia

Nurul A. Emran<sup>2</sup>

Computational Intelligence Technologies (CIT) Research Group  
Universiti Teknikal Malaysia Melaka  
Hang Tuah Jaya, 76300, Ayer Keroh  
Melaka, Malaysia

Siti A. Asmai<sup>3</sup>

Optimization, Modeling, Analysis,  
Simulation and Scheduling (OptiMASS) Research Group  
Universiti Teknikal Malaysia Melaka  
Hang Tuah Jaya, 76300, Ayer Keroh, Melaka, Malaysia

Amelia R. Ismail<sup>4</sup>

Department of Computer Science, Kulliyah of ICT  
International Islamic University Malaysia  
P.O. Box 10, 50728  
Kuala Lumpur

**Abstract**—The rapid growth of open data sources is driven by free-of-charge contents and ease of accessibility. While it is convenient for public data consumers to use data sets extracted from open data sources, the decision to use these data sets should be based on data sets' quality. Several data quality dimensions such as completeness, accuracy, and timeliness are common requirements to make data fit for use. More importantly, in many cases, high-quality data sets are desirable in ensuring reliable outcomes of reports and analytics. Even though many open data sources provide data quality guidelines, the responsibility to ensure data of high quality requires commitment from data contributors. In this paper, an initial investigation on the quality of open data sets in terms of completeness dimension was conducted. In particular, the results of the missing values in 20 open data sets measurement were extracted from the open data sources. The analysis covered all the missing values representations which are not limited to nulls or blank spaces. The results exhibited a range of missing values ratios that indicated the level of the data sets completeness. The limited coverage of this analysis does not hinder understanding of the current level of data completeness of open data sets. The findings may motivate open data providers to design initiatives that will empower data quality policy and guidelines for data contributors. In addition, this analysis may assist public data users to decide on the acceptability of open data sets by applying the simple methods proposed in this paper or performing data cleaning actions to improve the completeness of the data sets concerned.

**Keywords**—Data completeness; missing values; open data; open data sources; data collection

## I. INTRODUCTION

Data completeness is an essential dimension in data quality like accuracy and timeliness. Data completeness plays a major role to guarantee the completeness of query answers [1], [2] and ensure reliable analysis [3], [4]. In the context of software quality, completeness is also an important attribute that determines the quality of Software Requirement Specification (SRS) [5]. Several types of data completeness exist [6], [7]. Given a data set with a set of attributes, the most common case of data completeness are as follows: (1) all attributes' values are missing for a record (missing record/tuple), (2) some of the values of the attributes are missing for a record (missing values) [7], [8]. The first case represents the total

loss of information where the attributes' values for the whole record are missing. The second case however, represents some level (ratio) of the incompleteness of the attributes of a record. For example, assume that we have a simple data set which is supposed to have ten records of students' information. This dataset consists of 6 attributes, namely, *StudentId*, *Name*, *Sex*, *Level*, *Class*, *Grade* as shown in Table I.

TABLE I. STUDENTS INFORMATION

| No | StudentId | Name  | Sex | Level | Class | Grade |
|----|-----------|-------|-----|-------|-------|-------|
| 1  | B11       | John  | M   | 5     | A     | B     |
| 2  | B12       | Mona  | F   | 4     | A     | A     |
| 3  | B13       | Marta | F   | 4     | C     | B     |
| 4  | B15       | Helen | F   |       | B     |       |
| 5  | B16       | Mark  | M   |       |       |       |
| 6  | B17       |       | F   |       | A     | D     |
| 7  | B18       |       | M   | 4     |       | C     |
| 8  | B19       | Sozan | F   | 5     | B     |       |
| 9  | B20       | Ahmed | M   | 5     | B     | B     |

Table I illustrates a set of student records with the completeness problem. All records are uniquely identified by an identification attribute, *StudentId*. A missing record can be represented by the absence of the student's record with id 'B14' from the data set. Records 4<sup>th</sup> to 8<sup>th</sup> are examples of records with missing values. In this example, missing values are detected through the blank spaces in the table. Missing values are not necessarily represented by nulls or blank spaces as illustrated in Section II-B. Thus, the effort to detect missing values requires a proper understanding of its representation. The ability to detect missing values is the pre-requisite for any missing values effort. In many data-intensive applications, the recoverability of missing values is the key to avoid failure in query answering [1]. The execution of queries on any data set containing missing values may result in unrealistic and high

cost [9], [10], [11].

Missing values recovery becomes more challenging especially in the case where key attributes are surrogate keys (keys that are not real and unnatural like student Id) and the natural candidate keys are missing. Candidate keys are usually useful in recovering the values of other attributes that are missing, based on their functional-dependency property. (The role of functional dependency can also be seen in storage space optimization (refer to [12])).

In the next section, the problem of missing values will be elaborated in terms of the causes and representation aspects. Section III presents the methodology used to conduct the analysis. Section IV consists of the analysis results and discussion. Finally, Section V concludes this paper.

## II. BACKGROUND OF MISSING VALUES PROBLEM

Missing data or missing value can be defined as a value that is not stored or not exist in a dataset [13], [14], [15]. It is either referred as blank, unknown or null (in database world). The problem of missing values is fairly common and can occur at various stages of data processing, ranging from data collection to data storage phase [16]. The presence of a small ratio of missing values can greatly affect the results that can be derived from most databases including electronic medical records [17], [18]. Hence, missing values are a crucial problem in many decision-making systems as precise decision depends on the completeness of the information at hand [19], [20], [21].

The impact of missing values can also be seen in large data sets [22]. Many statistical methods have difficulties in dealing with the missing data especially in assigning an arbitrary value to the missing data. The fact that missing values is a common (but yet unsolved) problem has motivated many researchers in improving the existing system ability to work on incomplete data sets. (See an example of clinical support systems in [23].)

In general, handling the problem of missing values need to follow the following steps [17]:

- 1) Determine the reasons for missing data.
- 2) Determine the representation of the missing value.
- 3) Analysis of the percentage of missing values.
- 4) Determine the proper method for handling missing values.

### A. Reasons of Missing Data

Several studies reported the causes of missing values in databases as follows:

- Lack of data constraints: No restrictions are imposed on the user to enter all data. This leaves some fields missing [24].
- Insufficient users' experience: Low user experience in dealing with data entry systems and lack of knowledge in the correct mechanism of data entry may cause the loss of data. For example, users might leave the date and time fields blank if they are not sure of the format.
- Merge multiple data sources of different schema: Data repositories such as data warehouse (DW) data sets are merged from several sources. Database schema differences among the contributing sources will cause data sets

originated from the source with lack of attributes to be missing values within the merged data sets [2].

- Respondents' answering behavior: In survey data, missing values are often caused by reasons like respondents refuse to answer the survey or they do not understand the questions in the questionnaires [25], [26].
- Error in data collection tools: Research data is also prone to missing values problem due to an error in data collection tool (such as sensors) or human researcher's fault. So, failure software and hardware are significant examples that cause the problem of missing data [2].

Most statistical programs work to remove the missing values automatically from the original data sets. This approach leads to the lack of sufficient data to complete an analysis and thus may give misleading results [27], [28].

Kalkan (2018) stated that although there is a direct correlation between the rate of missing values and the quality of statistical analysis, there is no acceptable proportion of missing values in the data set for the correct statistical conclusion [29], [26]. However, Schafer (1999) argued that the ratio of 5% or less of missing values is inconsequential [30]. Bennett (2001) stated that if the amount of missing values is greater than 10%, the results of the statistical analysis will be biased [31].

### B. Missing Values Representation

Data completeness studies have been conducted since 1970 where missing information in the database community was the crux of the problem. The problem of missing values representation was overcome within the relational tables. Completeness studies on distinguishing the null types are triggered by the desire to ascertain the existence of the completeness problem. If nulls are present in the 'non-existence' case, then the presence is treated as legitimate unlike in the 'unknown' case. In short, while the presence of 'non-existence' nulls shows no completeness problems, the presence of "unknown" nulls shows the contrary [32][21].

The @ symbol [33], ! and 'x', 'y' and 'z' have often represented nulls [34]. ANSI/SPARC interim report listed 14 manifestations of nulls. However, the two common types of null used are the unknown nulls in which the values are missing because of the unknown status, and the non-existence nulls in which the values are missing because the attributes relation are not applicable. For example, if someone is not a vehicle owner in London, the attribute 'vehicle owned' is considered null.

### C. Methods for Handling Missing Values

In literature, several ways are adopted to handle missing values. In a customer database of a shopping centre, for example, some customers' data such as the age data might be missing. This situation can be handled in one of the following ways [8]:

- 1) Ignore records that contain missing values: Records which have the missing values are separated from the analysis [35]. For example, special software for statistical analysis is utilized in the analysis task which will run multiple times and the results are maintained, ignoring the missing



values [36]. In general, ignoring missing values is inefficient unless the record has very little missing values. This method may affect the overall results of the planned analysis if there are many missing values in a large number of records in a dataset.

- 2) Manual completion of missing values: This method can be considered a waste of time and effort [37], [38]. It may also be impossible to be adopted especially in the case of a large amount of data with a large number of missing values. The data sets may be used only if a small number of values are missing [39].
- 3) Use a global or uniform constant to replace missing values: In this case, all the missing values in a field can be replaced by a constant and uniform value or a label such as "unknown", but in this case when performing the analysis and data mining, the exploration programs will believe that this common label has a particularly important meaning. The number of relatively large missing values will indicate a poor analysis[40].
- 4) Use one of the values of central tendency metrics instead of missing values: This method is used to fill the numeric type missing values with the measures of central tendency such as the mean or the arithmetic mean [41]. For example, if we have a customer database of a shopping centre and the missing value is the customer's age, the mean age is used to replace the missing values in the 'Age' box. This method will enhance that value in the database and increase the unwanted repetition of a large number of customers which may affect the results of analysis and exploration.
- 5) Use the most likely value by predicting the missing values: This complex method is acquired through specialized exploration techniques such as the decision tree, aiming to predict missing values by exploring existing and available data of the results of the analysis [42].

Osborne (2013) pointed that, despite obvious distortion that missing values can cause, the number of researchers that deals explicitly with this problem is limited. In a survey conducted with his students in prestigious journals of the American Psychological Association, 38.89% of the authors reported that some data are missing in the data sets that have been used in their articles. Nevertheless, it is uncertain whether the remaining authors (61%) were failed to report their missing data or they completed their data in their articles [22]. In the case where missing values are recovered, the question of whether they effectively deal with the lost data remains unanswered.

In the context of time-series data, researchers in [43] reported that the level of missing values acceptability varies. Some data sets can contain missing values from 5%-50% while others allow up to 80% percent of missing values. As the level of missing values acceptability is high, the results of the analysis drawn from the data sets is incomplete.

Kim *et al.* (2019) estimated that the missing values in the precipitation data of the Korea Meteorological Agency will be up to 16% from year 2015–2016, and about 19% for weather data in 2017 [44]. This estimation drives the Korean government to plan for data imputation strategy as the missing values can affect power generation prediction performance.

### III. METHODOLOGY

In order to understand the problem of missing values in open data sets, 20 data sets were extracted from two open data sources: Center for Intelligent Learning and Intelligent system (UCI Machine Learning Repository) and data.gov.uk. UCI provided over 350 databases that were used for the automated learning of the experimental analysis, while data.gov.uk stores data of the government agencies, public bodies and local authorities in the United Kingdom (UK). The data sets consist of information about the government works, research, applications and services.

The selected data sets cover several domains such as education, healthcare, agriculture, and communities. In this paper, the types of completeness concerning the missing values were analyzed. We measure the ratio of missing values in each data set (on attribute level) and the coverage of affected attributes.

The steps conducted are as follows:

- Download data sets from the open data source: Data sets were downloaded from the UCI and data.gov.uk. Table II shows the details of the selected data sets covered by the analysis. The total number of records for all data sets is around three million records.
- Convert data sets into Excel spreadsheet format: The data sets were originally recorded in several formats, such as a text file (.txt) and Excel file (.Xls, .Csv). The data sets in the text files format (.txt) were converted to Excel format for standardization and processing ease. The data sets are categorized into four categories, namely, Medical, Educational, Security and Miscellaneous.
- Perform missing values detection: In order to detect missing values in the data sets, we refer the representation of missing values presented earlier in Section B. In addition to nulls (or blank cells), symbols "?" and "unknown" are detected for missing values in the data sets under study.
- Measure missing values ratio: To describe the formula used to measure missing values, simple ratio method (refer to [45]) which is usually applied to measure completeness is used. The following are descriptions of the notations:

Suppose that:

$D$  is the data set under measure,

$A$  is the set of attributes in  $D$ , where  $A = \{a_1, a_2, a_3, \dots, a_n\}$ , where  $n$  is the number of attributes,

$R$  is the set of records in  $D$ , where

$R = \{r_1, r_2, r_3, \dots, r_m\}$ ,

$|V_1|$  is the number of values that are supposed to be in  $a_1$ .

$|V'_1|$  is the number of missing values in  $a_1$

As  $|V_1| = |R|$ , the ratio of missing values (in percentage) for  $a_1$  is calculated as:

$$\frac{|V'_1|}{|V_1|} \times 100 = \frac{|V'_1|}{|R|} \times 100 \quad (1)$$

The ratio of missing values for  $D$  is calculated as:

$$\frac{\sum_{a=1}^n |V'_a|}{|R|} \times 100 \quad (2)$$

TABLE II. DATA SETS UNDER STUDY

| No | Type                        | Dataset Name   | Attributes                    | Instances |
|----|-----------------------------|--|-------------------------------|-----------|
| 1  | Medical                     | Arrhythmia   | 279                           | 452       |
| 2  |                             | Diabetes 130-US hospitals  | 55                            | 101767    |
| 3  |                             | Cervical cancer (Risk Factors)   | 36                            | 858       |
| 4  |                             | Details of GPs, GP Practices, Nurses and Pharmacies from Organisation Data Service | 20                            | 85280     |
| 5  |                             | GPS_Details_Nuers_Pharmaces  | 19                            | 85280     |
| 6  |                             | GP Prescribing Data  | 17                            | 473116    |
| 7  |                             | Sickness Absence Rates in the NHS  | 10                            | 85839     |
| 8  |                             | Numbers of Patients Registered at a GP Practice                                    | 9                             | 326328    |
| 9  |                             | Recorded Dementia Diagnoses  | 7                             | 608281    |
| 10 |                             | Educational  | Leeds schools all information | 54        |
| 11 | School Locations            |  | 37                            | 1555      |
| 12 | Schools List                |  | 14                            | 101       |
| 13 | Public libraries in England |  | 7                             | 3079      |
| 14 | Security                    | Communities and Crime normalized Data Set  | 147                           | 2215      |
| 15 |                             | Communities and Crime  | 128                           | 1994      |
| 16 |                             | Street Level Crime Data  | 10                            | 68177     |
| 17 | Miscellaneous               | Plants   | 70                            | 34781     |
| 18 |                             | BasicCompanyData-2017-12-01-part1  | 55                            | 849999    |
| 19 |                             | Indicator data   | 16                            | 33930     |
| 20 |                             | Traffic Commissioners goods and public service vehicle operator licence records    | 13                            | 37097     |

#### IV. RESULTS, ANALYSIS AND DISCUSSIONS

As shown in Table III high ratio of missing values (more than 40%) was found in three data sets. The first data set is ‘Plant’, where this dataset is extracted from the USDA plants database. It contains all plants (species and genera) in the database and the states of the USA and Canada where the plants exist. This dataset exhibits the highest ratio of missing values as compared to other data sets which are about 86.16% of missing values. From 70 attributes, 97% of it consists of missing values.

The second data set is ‘BasicCompanyData’ which consists of the first part of basic company data of live companies registered in the UK. The ratio of missing values for this data sets is also high (51.3%) that affects 74.55 of its attributes.

The third data set is ‘Leeds schools all information’, with 46.75% of missing values involving 70.37% of its attributes.

TABLE III. THE RESULTS OF MISSING VALUES MEASUREMENT

| Type                        | Dataset Name   | Number of Affected Attribute  | Affected Attribute (%) | Missing Values (%) |
|-----------------------------|--|-------------------------------|------------------------|--------------------|
| Medical                     | Arrhythmia   | 5/279                         | 1.79                   | 0.32               |
|                             | Diabetes 130-US hospitals  | 7/55                          | 12.73                  | 3.79               |
|                             | Cervical cancer (Risk Factors)   | 26/36                         | 72.22                  | 11.73              |
|                             | Details of GPs, GP Practices, Nurses and Pharmacies from Organisation Data Service | 11/20                         | 55                     | 14.76              |
|                             | GPS_Details_Nuers_Pharmaces  | 10/19                         | 52.63                  | 14.83              |
|                             | GP Prescribing Data  | 2/17                          | 11.76                  | 0.61               |
|                             | Sickness Absence Rates in the NHS  | 3/10                          | 30                     | 0.39               |
|                             | Numbers of Patients Registered at a GP Practice                                    | 3/9                           | 33.33                  | 11.18              |
|                             | Recorded Dementia Diagnoses  | 1/7                           | 14.29                  | 0.01               |
|                             | Educational  | Leeds schools all information | 38/54                  | 70.37              |
| School Locations            |  | 14/37                         | 37.84                  | 16.46              |
| Schools List                |  | 10/14                         | 71.43                  | 10.04              |
| Public libraries in England |  | 6/7                           | 85.71                  | 3.35               |
| Security                    | Communities and Crime normalized Data Set  | 41/147                        | 27.89                  | 13.7               |
|                             | Communities and Crime  | 97/128                        | 75.78                  | 15.36              |
|                             | Street Level Crime Data  | 5/10                          | 50                     | 5.59               |
| Miscellaneous               | Plants   | 68/70                         | 97.14                  | 86.16              |
|                             | BasicCompanyData-2017-12-01-part1  | 41/55                         | 74.55                  | 51.03              |
|                             | Indicator data   | 2/16                          | 12.5                   | 0.34               |
|                             | Traffic Commissioners goods and public service vehicle operator licence records    | 2/13                          | 15.38                  | 0.03               |

Nine data sets exhibit low ratio in missing values (less than 10%) while other data sets show between 11-20%. Fig. 1 illustrates that the completeness ratio (in percentage) for data sets from ‘Medical’ and ‘Security’ category are considerably high (80% and above).

High ratio of missing values in some data sets may due to several reasons. The merging operation that requires data from several sources (with different database schemas) to be integrated is a common cause of missing values. The immediate consequence of this scenario is attributes that do not originally exist in their contributing source will be populated with nulls.

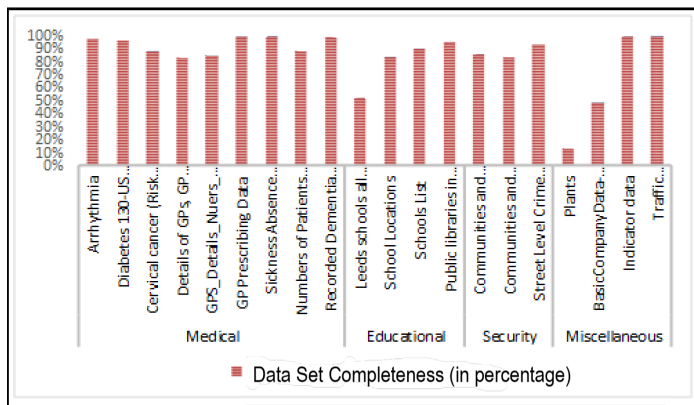


Fig. 1. The ratio of data sets completeness

Secondly, the use of nulls as the default values might be the reason for the missing values in the data sets. For Plants data sets in particular, the missing values might be due to the nature of Plants' species with unknown properties. In this case, missing values are mostly legitimate during data collection.

Another reason of missing values might be caused by lack of enforcement to complete the data sets, which is closely related to data governance and policy.

## V. CONCLUSIONS

In conclusion, we presented the results of assessing data completeness problem in open data sets. The assessment results involving twenty open data sets show varying missing values ratios that perhaps can be explained by the nature of the data set, data collection policy and enforcement (which is set by the contributing sources).

The findings support our hypothesis on the varying completeness of open data sets that may require further action by data consumers and open data source providers. The findings reported in this paper may motivate further research on dealing with missing values involving open data sets.

Even though most statistical methods will easily calculate the presence of missing data, future work could focus on examining the appropriateness of the methods used and investigate the mechanism that may affect the validity of the results.

## ACKNOWLEDGMENT

We would like to thank and acknowledge financial assistance received from the Universiti Teknikal Malaysia Melaka (UTeM) in publishing this work.

## REFERENCES

- [1] W. Nutt, S. Razniewski, and G. Vegliach, "Incomplete Databases : Missing Records and Missing Values," in *In International Conference on Database Systems for Advanced Applications*, vol. 7240. Berlin, Heidelberg: Springer, 2012, pp. 298–310.
- [2] F.-Z. Hannou, B. Amann, and M.-A. Baazizi, "Explaining Query Answer Completeness and Correctness with Minimal Pattern Covers," *VLDB Endowment*, vol. 12, p. 14, 2019.

- [3] N. A. Emran, S. Embury, and P. Missier, "Measuring Population-Based Completeness for Single Nucleotide Polymorphism (SNP) Databases," in *Advanced Approaches to Intelligent Information and Database Systems*, J. Sobocki, V. Boonjing, and S. Chittayasothorn, Eds. Cham: Springer International Publishing, 2014, pp. 173–182.
- [4] N. A. Emran, S. Embury, P. Missier, and A. K. Muda, "Measuring Data Completeness for Microbial Genomics Database," in *In Asian Conference on Intelligent Information and Database Systems*, ser. Lecture Notes in Computer Science. Berlin, Heidelberg: Springer, 2013, pp. 186–195.
- [5] U. Anuar, S. Ahmad, and N. A. Emran, "A Simplified Systematic Literature Review: Improving Software Requirements Specification Quality with Boilerplates," in *9th Malaysian Software Engineering Conference (MySEC)*. IEEE, 2016, pp. 99–105.
- [6] N. A. Emran, S. M. Embury, and P. Missier, "Model-driven component generation for families of completeness," in *QDB/MUD*. Auckland, New Zealand: CTIT workshop proceedings series, 2008, pp. 123–132.
- [7] N. A. Emran, "Data Completeness Measures," in *In Pattern Analysis, Intelligent Security and the Internet of Things*. Cham: Springer International Publishing, 2015, pp. 117–130.
- [8] P. Bhatia, *Data Mining and Data Warehousing: Principles and Practical Techniques*. Cambridge University Press, 2019.
- [9] A. A. Alwan, H. Ibrahim, N. I. Udzir, and F. Sidi, "Estimating Missing Values of Skylines in Incomplete Database," in *In Proceedings of the 2th International Conference on Digital Enterprise and Information Systems*, 2013, pp. 220–229.
- [10] W. Cheng, X. Jin, J. T. Sun, X. Lin, X. Zhang, and W. Wang, "Searching dimension incomplete databases," *IEEE Transactions on Knowledge and Data Engineering*, vol. 26, no. 3, pp. 725–738, 2014.
- [11] J. Cambroner, J. K. Feser, M. J. Smith, and S. Madden, "Query Optimization for Dynamic Imputation," *VLDB Endowment*, vol. 10, no. 11, pp. 1310–1321, 2017.
- [12] N. A. Emran, N. Abdullah, and M. N. M. Isa, "Storage Space Optimisation for Green Data Center," *Procedia Engineering*, vol. 53, pp. 483–490, 2013.
- [13] H. Kang, "The prevention and handling of the missing data," *Korean journal of anesthesiology*, vol. 64, no. 5, pp. 402–406, 2013.
- [14] R. L. Vaishnav and K. M. Patel, "Analysis of Various Techniques to Handling Missing Value in Dataset," *International Journal of Innovative and Emerging Research in Engineering*, vol. 2, no. 2, pp. 191–195, 2015.
- [15] R. V. McCarthy, M. M. McCarthy, W. Ceccucci, and L. Halawi, *Applying Predictive Analytics: Finding Value in Data*. Springer, 2019.
- [16] R. S. Somasundaram and R. Nedunchezian, "Missing Value Imputation using Iterative Refined Mean Substitution," *International Journal of Computer Science Issues (IJCSI)*, vol. 9, no. 4, pp. 306–313, 2012.
- [17] C. Salgado, C. Azevedo, H. Proença, and S. Vieira, "Missing Data," in *Secondary Analysis of Electronic Health Records*. Springer, 2016, ch. Missing Da, pp. 143–162.
- [18] F. Leza and N. Emran, "Data Accessibility Model Using QR Code for Lifetime Healthcare Records," *World Applied Sciences Journal (Innovation Challenges in Multidisciplinary Research & Practice)*, vol. 30, pp. 395–402, 2014.
- [19] J. W. Graham, "Missing Data Analysis: Making It Work in the Real World," *Annual Review of Psychology*, vol. 60, no. 1, pp. 549–576, 2009.
- [20] I. Azimi, T. Pahikkala, A. M. Rahmani, H. Niela-Vilén, A. Axelin, and P. Liljeborg, "Missing data resilient decision-making for healthcare IoT through personalization: A case study on maternal health," *Future Generation Computer Systems*, vol. 96, pp. 297–308, 2019.
- [21] R. J. A. Little and R. B., Donald, *Statistical Analysis with Missing Data*, 2nd ed. Wiley, 2019.
- [22] J. W. Osborne, "Six: Dealing with Missing or Incomplete Data: Debunking the Myth of Emptiness," in *Best Practices in Data Cleaning: A Complete Guide to Everything You Need to Do before and after Collecting Your Data*. SAGE, 2013.
- [23] M. K. Markey, G. D. Tourassi, M. Margolis, and D. M. DeLong, "Impact of missing data in evaluating artificial neural networks trained on complete data," *Computers in Biology and Medicine*, vol. 36, no. 5, pp. 516–525, 2006.

- [24] D. Vucevic and W. Yaddow, *Testing the data warehouse practicum: Assuring data content, data structures and quality*. Trafford Publishing, 2012.
- [25] M. N. Norazian Ramli, A. S. Yahaya, N. A. Ramli, N. F. Yusof, and M. M. Abdullah, "Roles of imputation methods for filling the missing values: A review," *Advances in Environmental Biology*, vol. 7, no. 12, pp. 3861–3869, 2013.
- [26] Ö. K. Kalkan, Y. Kara, and H. Kelecioğlu, "Evaluating Performance of Missing Data Imputation Methods in IRT Analyses," *International Journal of Assessment Tools in Education*, vol. 5, no. 3, pp. 403–416, 2018.
- [27] SPSS, "Missing Data : The Hidden Problem," *Ibm Spss*, pp. 1–8, 2009.
- [28] J. P. Hoffmann, *Principles of Data Management and Presentation*. Univ of California Press, 2017.
- [29] Y. Dong and C. Y. J. Peng, "Principled missing data methods for researchers," *SpringerPlus*, vol. 2, no. 1, pp. 1–17, 2013.
- [30] J. L. Schafer, "Multiple imputation: A primer," *Statistical Methods in Medical Research*, vol. 8, no. 1, pp. 3–15, 1999.
- [31] D. A. Bennett, "How can I deal with missing data in my study?" *Australian and New Zealand Journal of Public Health*, vol. 25, no. 5, pp. 464–469, 2001.
- [32] N. A. Emran, "Definition And Analysis Of Population-Based Data Completeness Measurement," Ph.D. dissertation, University of Manchester, 2011.
- [33] E. Codd, "Understanding relations (installment #7)," *FDT-Bulletin of ACM SIGMOD*, vol. 7, pp. 23–28, 1975.
- [34] I. Tomasz and W. L. Jr., "Incomplete Information in Relational Databases," *Journal of the ACM (JACM)*, vol. 31, no. 4, pp. 761–791, 1984.
- [35] A. Anderson, *Statistics for Big Data For Dummies*. John Wiley & Sons, 2015.
- [36] J. Honaker and G. King, "What to Do about Missing Values in Time-Series Cross-Section Data," *American Journal of Political Science*, vol. 54, no. 2, pp. 561–581, 2010.
- [37] S. Zhang, J. Zhang, X. Zhu, Y. Qin, and C. Zhang, "Missing value imputation based on data clustering," in *In Transactions on computational science*. Berlin, Heidelberg: Springer, 2008, pp. 128–138.
- [38] P. Rahman, C. Hebert, and A. Nandi, "ICARUS: Minimizing Human Effort in Iterative Data Completion," *Proceedings of the VLDB Endowment*, vol. 11, no. 13, pp. 2263–2276, 2018.
- [39] Z. M. Kumar and R. Manjula, "Regression model approach to predict missing values in the Excel sheet databases," *International Journal of Computer Science & Engineering Technology (IJCSET)*, vol. 3, no. 4, pp. 130–135, 2012.
- [40] M. Kantardzic, *Data Mining: Concepts, Models, Methods, and Algorithms*. John Wiley & Sons, 2011.
- [41] A. D. Banasiewicz, *Marketing Database Analytics: Transforming Data for Competitive Advantage*. Routledge, 2013.
- [42] J. J. Faraway, *Linear models with R*. Chapman and Hall/CRC, 2016.
- [43] I. Pratama, A. E. Permanasari, I. Ardiyanto, and R. Indrayani, "A Review of Missing Values Handling Methods on Time-Series Data," in *International Conference on Information Technology Systems and Innovation (ICITSI)*. IEEE, 2016.
- [44] T. Kim, W. Ko, and J. Kim, "Analysis and Impact Evaluation of Missing Data Imputation in Day-ahead PV Generation Forecasting," *Applied Sciences*, vol. 9, no. 1, pp. 1–18, 2019.
- [45] L. L. Pipino, Y. W. Lee, and R. Y. Wang, "Data quality assessment," *Communications of the ACM*, vol. 45, no. 4, pp. 211–218, 2002.

# Design and Application of a Smart Diagnostic System for Parkinson's Patients using Machine Learning

Asma Channa<sup>1</sup>, Attiyah Baqai<sup>2</sup>  
Electronic Engineering, MUET  
Jamshoro, Pakistan

Rahime Ceylan<sup>3</sup>  
Electrical & Electronics Engineering  
Selçuk University Konya, Turkey

**Abstract**—For analysis of Parkinson illness gait disabilities detection is essential. The only motivation behind this examination is to equitably and consequently differentiate among sound subjects and the one who is forbearing the Parkinson, utilizing IOT based indicative framework. In this examination absolute, 16 distinctive force sensors being attached with the shoes of subjects which documented the Multisignal Vertical Ground Reaction Force (VGRF). Overall sensors signals utilizing 1024 window estimate around the raw signals, utilizing the Packet wavelet change (PWT) five diverse characteristics that includes entropy, energy, variance, standard deviation and waveform length were derived and support vector machine (SVM) is to recognize Parkinson patients and healthy subjects. SVM is trained on 85% of the dataset and tested on 15% dataset. Preparation accomplice relies upon 93 patients with idiopathic PD (mean age: 66.3 years; 63% men and 37% ladies), and 73 healthy controls (mean age: 66.3 years; 55% men and 45% ladies). IOT framework included all 16 sensors, from which 8 compel sensors were appended to left side foot of subject and the rest of the 8 on the right side foot. The outcomes demonstrate that fifth sensor worn on a Medial part of the dorsum of right foot highlighted by R5 gives 90.3% accuracy. Henceforth this examination gives the knowledge to utilize single wearable force sensor. Hence, this examination deduce that a solitary sensor might help in differentiation amongst Parkinson and healthy subjects.

**Keywords**—Parkinson patients; force sensors; machine learning; Wavelet Packet Transform (WPT)

## I. INTRODUCTION

Presently, every one needs panacea of each illness. Illness is simply another denomination of distortion that happen due to any inner or outer factor. Nowadays, the world is endorsing a growing demand on quality and quantity of healthcare due to rise of elderly population, chronic diseases and health maintenance of people. As Parkinson disease is one of the most prevailing disorder and affects around 6.3 million people in world. Parkinsons illness is the most natural issue of the sensory system [1] in which neurons are harmed and an individual is unfit to do its day by day life exercises. Parkinson's disease is cognitive impairment causing neurodegenerative disease that effects the dopamine produced in nerve cells and there is no therapeutic authoritative trial exist to analyze Parkinson's sickness. Indeed, even the single-photon outflow automated tomography (SPECT) examine named as a dopamine transporter (DAT) filter can not provide confirmation that the individual has Parkinson illness (PD). In spite of the fact that this can help to the odds and defines that the

subject may have Parkinson's infection, yet it is really the side effects and neurological surveillance that ultimately decide the right diagnosis. A number of people do not require a DAT examine. The principle side effects of Parkinson ailment are gait, tremor, hardened muscles, moderate advancement and trouble in walking because of which fall occurs in patients. As per [2] the crippling marvel is gait which considered as the most widely recognized side effect among the patients suffering from Parkinson. It is regularly a troublesome occasion that surprisingly assaults the subjects and shakes their steps toward the beginning of strolling even in unhindered fixing, amid going around or bending and subsequently irritates the personal daily life activities. Therefore this research aims to establish a gait detection device using IOT which is capable of detecting the gait using the biomedical signals from the sensors attached with body of Parkinson patients. The data in IOT will be analyzed using signal processing technique that may help in finding the gait features. Finally the extracted features are classified using machine learning algorithm.

## II. RELATED WORK

Recently number of research studies have been conducted on PD detecting system with the help of multiple types of sensors, feature sets and analysis methods. For gait examination, researchers in [3], [4] reasoned that the wearable technology is progressing decently by providing the better way to deal with pervasive, maintainable and adaptable monitoring of health. The results are more accurate because of their direct contact and rigid attachment with body, apart from this these wearables are lightweight and have good longevity. Distinctive calculations are implemented over wearable signals to explore, screen or perceive the Parkinson patients. The analysts [5] analyzed basic tremor and Parkinson infection utilizing particular singular value decomposition (SVD) to find highlights of intrinsic mode functions (IMFs) and SVM is proposed to recognize them. Hand quickened signals were gathered and pre-prepared by experimental mode disintegration (EMD) strategy and appropriated into various stationary IMF and contributed to SVM. For contrasting, they likewise utilized the particular esteem highlights of discrete wavelet transform (DWT) as contribution to the SVM. Cross-approved aftereffects of EMD-SVD highlights extricated gives 98%, 97.5% and 98% exactness, affectability and particularity, which are higher than Discrete Wavelet Transform-SVD. This research is basically focused on the collation of two approaches to overcome

misdiagnosis between essential tremor and Parkinson disease. Authors in [6] presented a novel methodology in which design acknowledgment of DTI information is performed utilizing AI. Information examination checks both level and dimension with respect to SVM order. The framework provides about 97.50% precision. The principle downside of this research is of few cases likewise the preparation and testing execution is on the equivalent dataset. Another issue is review nature of the present investigation. The specialists in [7] start an investigation for forecast of freezing of stride (FOG). The suspicion of this investigation is exclusively founded on the edge based model of FOG. Absolute six distinct highlights are siphoned from development signals recorded from wearable sensors and characterize calculation is created to anticipate FOG. The fundamental issue is few subjects and subjects having diverse sickness stages. The researchers in [8] put forward the framework consisting full body movement catch of six subjects is complied and utilized support vector machine classifier for segregating mellow against serious indications with a normal precision of around 90% for quantitative following of sickness movement. In any case, there are the confinements on various stances for recognizing the side effects. The exploration article [9] explicitly addresses smart shoe innovation using inertial sensors and Internet of things (IOT) to screen movement examples of subjects. This fundamentally serve as an analysis of Parkinson malady. Further developed calculations and test structures are needed for good results. The researchers in [10] proposed a movement checked framework to intently watch walking step in older subjects which comprises of body-worn labels and divider mounted sensors utilizing AI calculations so as to perceive explicit medical issue. Two kinds of studies are directed. In the possibility of programmed acknowledgment 12 labels, no commotion indicated k-closest neighbors and neural systems accomplished 100% exactness. Nonetheless, the second investigation depends on the effect of label arrangement and commotion level, this gives 99% precision utilizing AI calculation utilizing 8 additional labels with up to 15mm standard deviation of the clamor. So this demonstrates with more labels the classifiers perform more precisely. In [11] the Columbia University Robotics and Rehabilitation Lab introduced a versatile instrumented footwear named "SOLESOUND" which is equipped for estimating spatiotemporal walk parameters and dispatch activity related sound material appraisal. In the end, the execution of SOLESOUND under two alignments methodologies subject-explicit and conventional are estimated. With subject-explicit adjustment, the outcomes were increasingly precise. Consequently the gadget can possibly be utilized as quantitative walk investigation device. The analysts in [12] proposed a multivariate technique for breaking down stride utilizing gait influence graphs (GIDs). The specific case Weiner-Akaike-granger Schweder impacts estimates identified as 'Extended granger' causality, examination is utilized that are competent to recognize essentially the healthy subject from Parkinson patients. In this investigation, the recurrence related parameters helped in arrangement between PD subjects with various Hoehn and Yahr stages. Subsequently in this investigation analysts just presented GIDs that can be utilized for recognizing Parkinson individuals and healthy controls. In [13], creators presented a framework in which anomalous stride designs are identified in Parkinson patients. Information has been gathered from an absolute 16 drive sensors located in feet. Extricating specification from the information taken from

sensors performing foot T-test and receiver operating characteristics (ROC) bend strategies being utilized to dissect time and recurrence highlights. The outcomes accomplished within the tests obviously confirm the power appropriation around feet adjusts amongst subjects of various phases of PD. The investigation is centered around recognizing diverse phases of PD. In [14] the scientists used PHYSIONET dataset and applied statistical analysis of variance (ANOVA) test to separate subjects depending on their mean qualities and example characterization utilizing using linear discrimination analysis (LDA) calculation. The precision percentage is accomplished just for three highlights i.e. specific in step separation, position and swing stages which is 94.4%, 77.8% and 86.1%. In [15] the researchers recommended that FOG recognition is performed utilizing profound learning. The specialists utilized wearable unit over midsection of subjects comprising tri-pivotal accelerometer, gyroscope and magnetometer. Despite of the fact that in this methodology the execution accomplished is tantamount to aftereffects of condition of workmanship which is 88.6% sensitivity and 78% specificity. Adhering a quantifiable unit all over midsection might become oblique. The gait signal is really a development flag which we can get from the force sensitive resistor putting under the foot. The examination in [16] checked that recurrence spectra of left walk, right walk and left swing signs can be successfully inherit separate patients with amyotrophic sidelong sclerosis, Huntington infection or Parkinson's illness from sound control subjects. Recurrence range has been isolated in ten different balances of measurable parameters of mean, difference, skewness, kurtosis of every part has been utilized to delineate appropriation of coefficients. Execution of classifiers depends on three distinct kinds of AI classifiers. Executing three classifier increment the multifaceted nature of framework. The examination in [17] characterized another arrangement of highlights to improve execution of past strategies for FOG identification. Spatial and transient highlights of the walk with vitality and physiological highlights (EMG) result in an increasingly strong grouping answer for recognizing solidifying scenes. Characterization techniques give affectability of around 90% and particularity of 92%. Be that as it may, including increasingly biomedical signals, for example, pulse and galvanic skin reaction may expand the grouping exactness. The specialists in [18] executed counterfeit neural system and SVM for distinguishing walk highlights. Spatiotemporal, kinematic, active highlights are utilized in ordering PD stride and healthy subjects. Multiple kinds of standardization titled as intergroup and intragroup are utilized. In the fore-referenced two sorts are looked at out of which intragroup provides good precision. SVM provides 78.2% exactness, superior to ANN explicitly for combination of walk parameters. Fundamental spatiotemporal sacrifices as finest element for immaculate precision, explicitness and affectability. Three kinds of stride parameters are explored by creators in [19] from these progression lengths, strolling speed, knee edge and VGRF are affirmed as imperative highlights for PD subjects. The highlights are affirmed dependent on measurable examination and arrangement rate utilizing ANN classifier which gives around 95.63% exactness with utilizing four huge highlights determination through factual investigation. Consequently this exploration only centered around highlights identification and investigation. The creators in [20] proposed the framework which depends on Kinect sensor which is a 3D sensor that can extract complete step data from entire

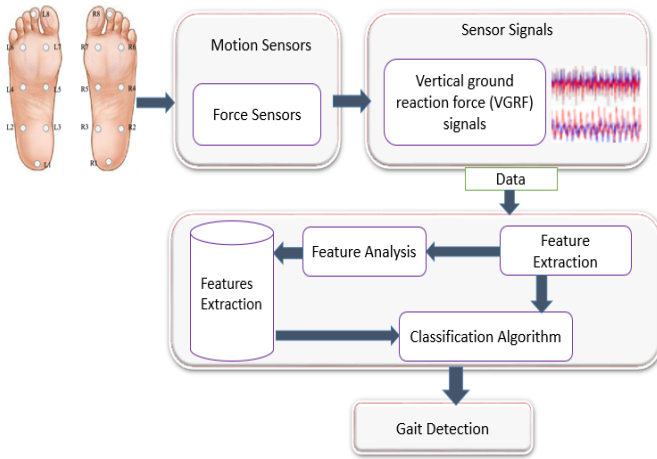


Fig. 1. Block diagram of proposed system.

body by estimating stride interims. Two analyses are directed, one for exactness and other for strength. In any case, the examination is performed on virtual skeleton as contribution in learned model. Henceforth following technique might help in additionally reaching out with estimating properties inclusive of lower limit rakish speeds and center stance. As previously research has been done on investigation of gait in Parkinson patients yet they all are either complicated, comprising of more than one inertial sensor and actualize different classifiers for the location and breaking down the walk parameters.

Given paper is being sorted out in 5 areas: Section 2 shows the proposed strategy and its portrayal, outcomes and exchanges are given in Section 3. While, Section 4 sum up the work and provides bearings for future work.

### III. MATERIALS AND METHODS

In this research work the inertial force sensors dataset is acquired from PHYSIONET [21] for Parkinson’s patients. The characteristics which are being isolated are entropy, energy, variance, standard deviation, and waveform length using WPT. Full scale eight sensors are attached to feet. Along this way, the 16 sensors’ outputs are investigated using machine learning algorithm. Fig. 1 shows the block diagram of proposed system.

#### A. Database Description

Dataset in this examination is secured from PHYSIONET [21]. Previously the research on relationship between hand predominance and Parkinson’s ailment is not being conducted in a systematic way. As in [22] research gives the conceivable relationship of handedness out of which 254 right-gave patients, 158 were right-sided while 96 patients had left-lateralized side effect strength. Right-handedness in this manner is by all accounts related with right-sided predominance of PD side effects, although the gathering of left-gave patients were too little to even think about drawing ends from. The dataset depiction has been provided in Table I.

The database comprises of absolute 199 documents of patients and almost 78 records of healthy subjects the description of dataset is cited in Table [23]

TABLE I. DATA DESCRIPTION

| Column       | Description  |
|--------------|--|
| Columns 1    | Time (in seconds)  |
| Columns 2-9  | VGRF values on each of 8 sensors fitted under the left foot      |
| Column 10-17 | VGRF values on each of the 8 sensors fitted under the right foot |
| Column 18    | Total VGRF under the left foot                                   |
| Column 19    | Total VGRF under the right foot                                  |

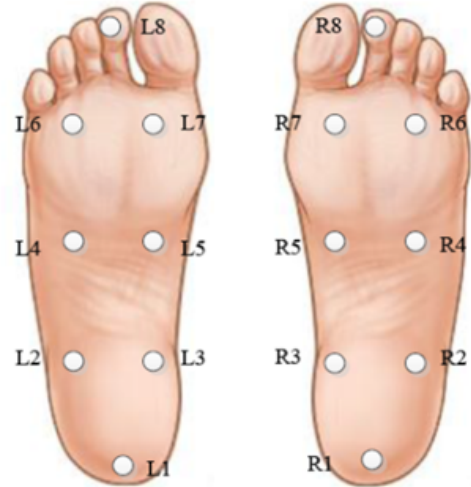


Fig. 2. Force sensors exact locations.

#### B. Force Sensor and Data Acquisition

There were 8 sensors situated on the lower portion of left and the right foot, separately. The surmised areas of the sensors have been mentioned in Fig. 2, and the precise areas of sensors are provided in Table II. The white dabs are indicating the force sensors (the sensors situated underneath the feet). The distinctive places of foot at which sensors are joined is shown in Fig. 3. The 16 channels of CDG (Computer Dyno Graphy, recording the powerful dissemination under the foot amid walk). The chronicle unit was carried on the abdomen amid the walk, and after the walk. Collected data was being recorded in a memory card that was transferred to a PC for additional investigation.

The forces summed over all sensors of one foot measured as a function of time are shown in Fig. 4. In this graph, a narrow calculation of force with respect to time values is shown by the Time Cursor. This is crucial for suppressing start and end effects. However the forces, selectable per sensor

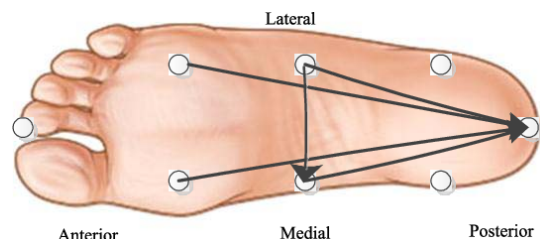


Fig. 3. Sensors at different positions of foot.

TABLE II. POSITION OF SENSORS WITHIN LEFT AND RIGHT FOOT

| Sensor | X    | Y    | Sensor | X   | Y    |
|--------|------|------|--------|-----|------|
| L1     | -500 | -800 | R1     | 500 | -800 |
| L2     | -700 | -400 | R2     | 700 | -400 |
| L3     | -300 | -400 | R3     | 300 | -400 |
| L4     | -700 | 0    | R4     | 700 | 0    |
| L5     | -300 | 0    | R5     | 300 | 0    |
| L6     | -700 | 400  | R6     | 700 | 400  |
| L7     | -300 | 400  | R7     | 300 | 400  |
| L8     | -500 | 800  | R8     | 500 | 800  |

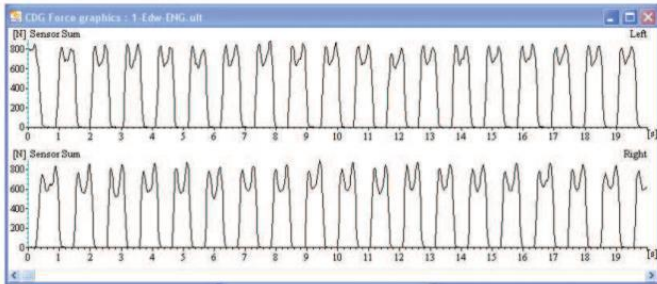


Fig. 4. Total summed up forces on one foot

displayed as a matter of time is shown in Fig. 5.

### C. Feature Extraction using Wavelet Packet Transform

Feature extraction is the most crucial part for machine learning algorithms. The question with respect to feature extraction and selection is which algorithm is best for feature extraction and the answer is it depends on what type of problem we are solving. However, it depends on few factors which are:

1. What kind of problem one is trying to solve? e.g. classification, regression, clustering, etc.
  2. Type of dataset.
  3. Is data having very high dimensionality?
  4. Is data labeled?
- After knowing this the next questions to deal with are
1. Either to perform feature extraction or feature selection?
  2. Have to use a supervised or unsupervised method?

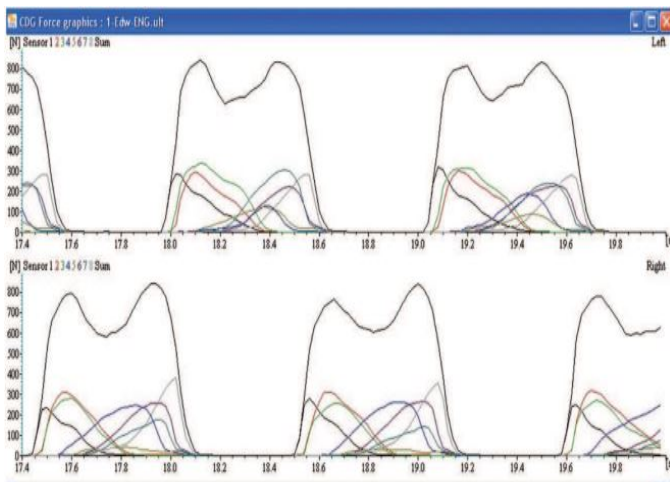


Fig. 5. The forces, selectable per sensor, displayed as function of time

Hence it is concluded that there is no generic feature extraction scheme which works in all cases. Lots of methods have been introduced for extracting features and their results may vary with respect to applications.

Fourier change is for the most part utilized for signal processing since 1950's, however latest change called wavelet transform in [24] brings another stage towards denoising, compression, and characterization. Wavelet change's fundamental objective is to personify a signal which might be dissected as superposition of wavelet. The DWT of signal x is determined by going through a number of filters. First, samples are gone through a low pass channel with impulse response bringing in convolution of two:

$$y[n] = (x * g)[n] = \sum_{-\infty}^{\infty} x[k]g[n - k]$$

The signal in a similar manner deteriorated almost at the same time managing a high-pass filter. The resulted signal provide complete information regarding coefficients (from the high-pass channel) and guess coefficients (from the low-pass). It is imperative that both channels are determined with one another and recognized as quadrature mirror filter. In spite of this, since a huge part of frequencies of the signal is now been expelled, majority of the portion of examples might be discarded of as determined by Nyquist's standard. The channel yield of the low-pass filter g is then sub sampled and further managed through a new low-pass filter g and a high-pass filter h with half off the cut of frequency of previous one i.e.

$$Y_{low} = \sum_{-\infty}^{\infty} x[k]g[2n - k]$$

$$Y_{high} = \sum_{-\infty}^{\infty} x[k]h[2n - k]$$

Wavelet Packet Transformer is used in this research with the aim to decompose the sensors data. The decomposition of level 3 is explained in Fig. 6. Fig. 7 depicts how wavelets packets are organized in form of tree where j defines depth and frequency n defines positions in tree. There are number of various wavelet families which are useful in different applications few of them are shown in Fig. 7 and in Fig. 8. Choosing a specific wavelet type for analyzing the data depends on what we want to do with the available dataset. This research requires the wavelet that finds the closely spaced features of interest. Hence 'db2' wavelet is preferred to detect gait intervals of Parkinson patients.

As in gait signal, a specific occasion comparatively happening at a moment can be exceptionally compelling. So WPT gives a bundle of vital signs that helped in the discovery of stride interims and concentrate their features. In this exploration wavelet packet transform change is utilized to decay signal.

The decay of information of subjects utilizing WPT is shown in Fig. 9. In flowchart first, data is served as an input to WPT a short time later the level is chosen. Additionally, the type of wavelet is selected i.e. 'db2'. Subsequently utilizing along these ways, we get various coefficients as clarified in [19].



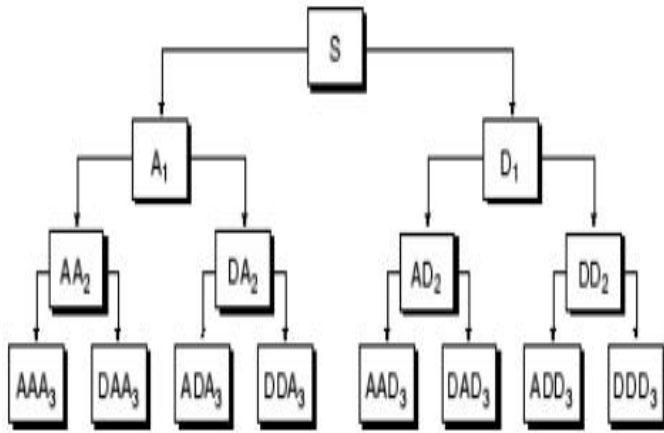


Fig. 6. Wavelet Packet Decomposition Tree at Level 3.

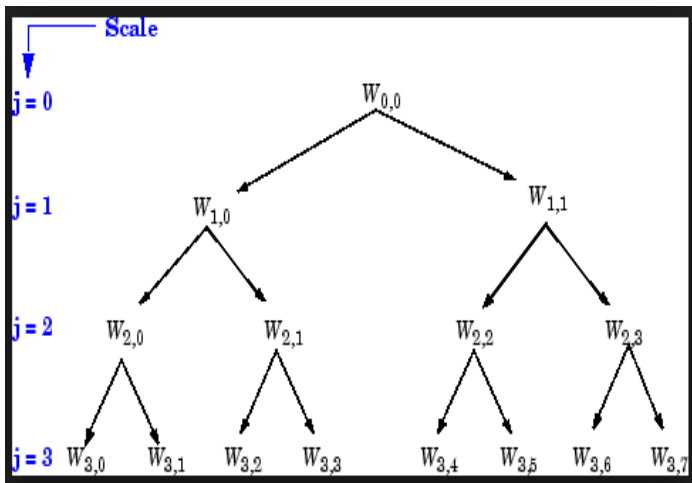


Fig. 7. Wavelet Packet organized in form of tree.

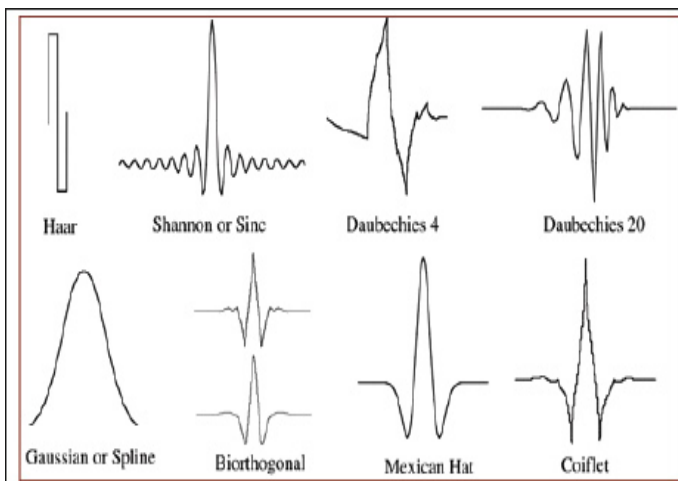


Fig. 8. Wavelet families.

#### D. Extracted Features

For identification of gait signs the information is processed utilizing WPT in [25][26]. The procedure is clarified in Fig. 9. In beginning window dimension and dispersion are selected i.e. 1024 and level is kept to  $J=7$  for better precision. Comprehensively, characteristics are extricated utilizing WPT.

#### E. Classification

Support vector machine is the standout amongst the ultimate considerate and straightforward calculations [27]. At the point when the information is tangled and can not be isolated effectively, SVM is the best alternative to pick. In Fig. 9 we have utilized SVM classifier. As all out of 8 sensors are utilized on each foot and our objective is to figure out which sensor identifies gait superior to the others. The WPT determined the highlights from every sensor. Utilizing these separated highlights, the SVM shown in [28] is trained utilizing classifier learner app in MATLAB.

#### F. Steps Performed In MATLAB Classifier Learner App

1. First, the data is prepared. We have  $N$  samples of training data and  $M$  samples of test data, the data was combined together to make it  $M \times N$  samples. The rows represent each sample and the columns the different types of features detected from a sample.
2. The next step was to add an extra column at First or Last of the data (preferably): This column represents the desired labels for the data. So, now the total number of columns = number of features + 1. While importing the data into the Classification Learner App, the data was supported as a table.
3. Then, data was fixed to be used by the Classification Learner App. By default, all columns are selected as predictors. The app prompts to select the responses. A response is the one which we added as an extra column (the label). So, we changed the label-column to make it point as a response.
4. Before starting the session, there was a need to set up the Cross Validation strategy adopted. A  $k$ -fold validation divides the total  $M \times N$  data into  $k$ -parts and begins by taking the first part of testing and rest  $k-1$  parts for training. Then, again it takes the second part for testing and rest  $k-1$  parts for training and so on. Finally, average of all the accuracy's obtained was taken as final accuracy. However the Holdout validation method asked to test the percent of the input data as testing data.
5. After selecting the validation method and choosing their rate start session, next was to select the classifier (i.e. SVM) that is used in this study and finally hit the training button.

## IV. RESULTS AND DISCUSSIONS

The extracted features were expelled from the sensors which were hooked to subjects feet. The essential target is to find the sensor that shows good exactness percentage.

At first initializing 8192 window measure utilizing dimension 5 and 'db2' type the precision of each wearable gotten by setting 20% holdout approval as shown in Table III. According to this table L2, L3 sensors and R7 sensor gives 81.9% accuracy using Cubic SVM classifier. While L3 and L5 give 81.9% accuracy using Quadratic SVM classifier. The R8 sensor also gives 81.9% accuracy using Fine Gaussian SVM. As the multiple sensors give same accuracy rate with different type of classifier so as to improve exactness rate the Wavelet packet

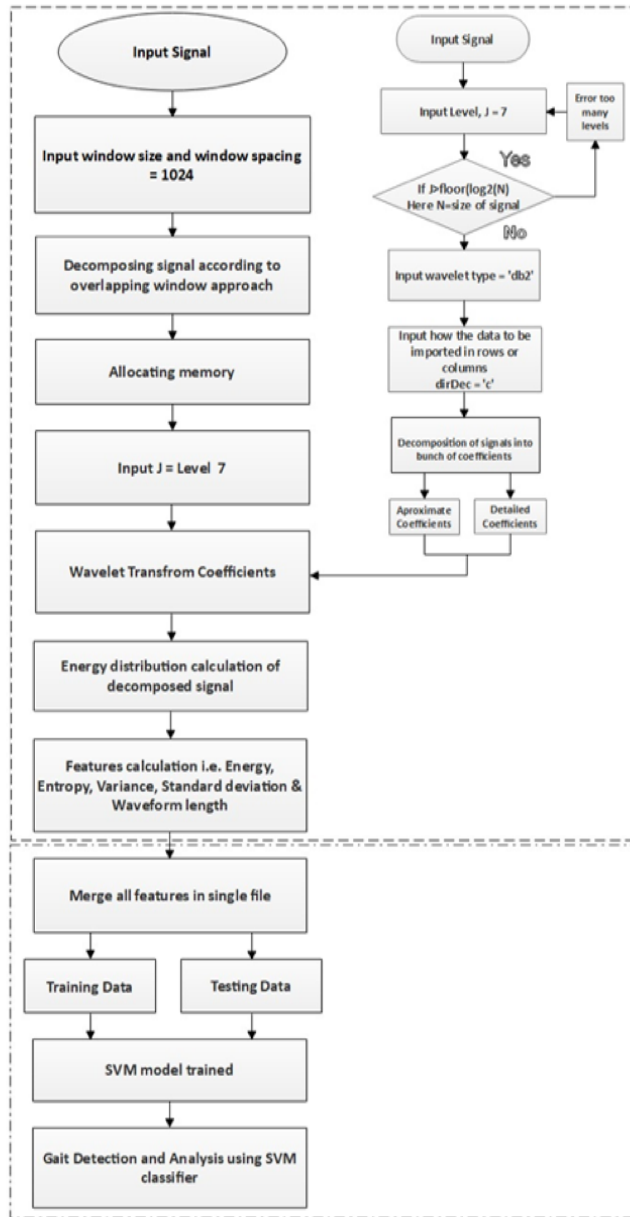


Fig. 9. Flow chart showing features extraction and classification.

transformers parameters are changed to Level = 7, wavelet = 'db2', window estimate = 8192 and holdout approval rate to 20% as appeared in Table IV. The results achieved shows R7 sensor gives 84.7% accuracy using cubic SVM. Eventually the accuracy is good but in order to validate it the validation method is changed to K-fold method and level = 7 is changed to level = 5. Then the trained model give 81.8% for L1, using Cubic SVM as shown in Table V. Hence this proves k-fold validation method does not give accurate results as compared to holdout validation method.

Other than setting 1024 window estimate keeping dimension 5 and 'db2' type the precision rates of sensors as appeared in Table VI, which depicts that L1 and L2 produce 84.9% precision with help of Cubic SVM classifier. To improve

the exactness rate the level is set to 7 as shown in Table VII where R5 produce 88.9% precision. Again the holdout endorsement kept to 15% and precision achieved is 90.3%. As the outcomes generated are progressively valid and more accurate, depicted in Table VIII. The R5 sensor compellingly in isolating between Parkinson persistent and solid subjects utilizing features separated with WPT.

TABLE III. ACCURACY OF ALL SVM CLASSIFIERS UTILIZING LEVEL=5,'DB2' WAVELET, WINDOW MEASURE = 8192 AND SETTING HOLDOUT APPROVAL TO 20%

| Sensor position | Linear SVM | Quadratic SVM | Cubic SVM | Fine Gaussian SVM | Medium Gaussian SVM | Coarse Gaussian SVM |
|-----------------|------------|---------------|-----------|-------------------|---------------------|---------------------|
| L1              | 72.2%      | 73.6%         | 80.6%     | 80.6%             | 72.2%               | 72.2%               |
| L2              | 69.4%      | 80.6%         | 81.9%     | 77.8%             | 72.2%               | 72.2%               |
| L3              | 79.2%      | 81.9%         | 81.9%     | 77.8%             | 79.2%               | 72.2%               |
| L4              | 70.8%      | 75.0%         | 75.0%     | 77.8%             | 70.8%               | 72.2%               |
| L5              | 75.0%      | 81.9%         | 80.6%     | 70.8%             | 80.6%               | 73.6%               |
| L6              | 77.8%      | 73.6%         | 69.4%     | 73.6%             | 68.1%               | 73.6%               |
| L7              | 79.2%      | 77.8%         | 72.2%     | 75.0%             | 73.6%               | 69.4%               |
| L8              | 73.6%      | 76.4%         | 69.4%     | 75.0%             | 73.6%               | 72.2%               |
| R1              | 76.4%      | 76.4%         | 76.4%     | 76.4%             | 70.8%               | 70.8%               |
| R2              | 70.8%      | 76.4%         | 72.2%     | 73.6%             | 73.6%               | 70.8%               |
| R3              | 69.4%      | 72.2%         | 70.8%     | 73.6%             | 73.6%               | 70.8%               |
| R4              | 68.1%      | 77.8%         | 77.8%     | 76.4%             | 70.8%               | 72.2%               |
| R5              | 73.6%      | 76.4%         | 80.6%     | 72.2%             | 79.2%               | 72.2%               |
| R6              | 80.6%      | 80.6%         | 75.0%     | 69.4%             | 77.8%               | 70.8%               |
| R7              | 79.2%      | 73.6%         | 81.9%     | 75.0%             | 75.0%               | 70.8%               |
| R8              | 80.6%      | 76.4%         | 76.4%     | 81.9%             | 80.6%               | 72.2%               |

TABLE IV. ACCURACY OF ALL SVM CLASSIFIERS UTILIZING LEVEL=7,'DB2' WAVELET, WINDOW MEASURE = 8192 AND SETTING HOLDOUT APPROVAL TO 20%

| Sensors position | Linear SVM | Quadratic SVM | Cubic SVM | Fine Gaussian SVM | Medium Gaussian SVM | Coarse Gaussian SVM |
|------------------|------------|---------------|-----------|-------------------|---------------------|---------------------|
| L1               | 73.6%      | 76.4%         | 70.8%     | 73.6%             | 72.2%               | 72.2%               |
| L2               | 76.4%      | 72.2%         | 73.6%     | 70.8%             | 72.2%               | 70.8%               |
| L3               | 72.2%      | 64.4%         | 70.8%     | 75.0%             | 72.2%               | 72.2%               |
| L4               | 75.0%      | 73.6%         | 69.4%     | 72.2%             | 72.2%               | 70.8%               |
| L5               | 73.6%      | 73.6%         | 72.2%     | 72.2%             | 79.2%               | 77.8%               |
| L6               | 76.4%      | 75.0%         | 75.0%     | 72.2%             | 76.4%               | 70.8%               |
| L7               | 80.6%      | 73.6%         | 68.1%     | 73.6%             | 73.6%               | 70.8%               |
| L8               | 77.8%      | 77.8%         | 70.8%     | 73.6%             | 76.4%               | 72.2%               |
| R1               | 73.6%      | 77.8%         | 80.6%     | 79.2%             | 72.2%               | 72.2%               |
| R2               | 72.2%      | 75.0%         | 66.7%     | 73.6%             | 73.6%               | 70.8%               |
| R3               | 75.0%      | 83.3%         | 79.2%     | 77.8%             | 73.6%               | 70.8%               |
| R4               | 65.3%      | 77.8%         | 80.6%     | 70.8%             | 75.0%               | 70.8%               |
| R5               | 76.4%      | 75.0%         | 75.0%     | 75.0%             | 76.4%               | 72.2%               |
| R6               | 70.8%      | 75.0%         | 75.0%     | 73.6%             | 76.4%               | 70.8%               |
| R7               | 79.2%      | 83.3%         | 84.7%     | 77.8%             | 77.8%               | 72.2%               |
| R8               | 79.2%      | 79.2%         | 66.7%     | 70.8%             | 76.4%               | 70.8%               |

The tested model portrayal of right foot sensor positioned at 5 is shown in Fig. 10. The model represents six kinds of SVM classifiers among these Cubic and medium Gaussian SVM classifiers give around 88% while Quadratic SVM gives 90.3% exactness utilizing kernel function with box requirement dimension of 1 and its training time is 6.1981 seconds.

A confusion matrix is fundamentally a table that gives performance of a classification model on a group of test data. It is given the name as confusion matrix since it is generally easy to see, however the related wording can be confusing. Subsequent to setting up the model, the disarray network in Fig. 11(a) shows the performance of a classifier. As lines of disorder arrange show true class and area addresses prescient

TABLE V. ACCURACY OF ALL SVM CLASSIFIERS UTILIZING LEVEL=5,'DB2' WAVELET, WINDOW MEASURE = 1024 AND SETTING K-FOLD APPROVAL TO 5

| Sensors position | Linear SVM | Quadratic SVM | Cubic SVM | Fine Gaussian SVM | Medium Gaussian SVM | Coarse Gaussian SVM |
|------------------|------------|---------------|-----------|-------------------|---------------------|---------------------|
| L1               | 72.5%      | 80.3%         | 81.8%     | 79.1%             | 78.5%               | 72.2%               |
| L2               | 75.6%      | 79.1%         | 79.5%     | 78.5%             | 77.7%               | 71.6%               |
| L3               | 71.6%      | 74.1%         | 77.1%     | 77.5%             | 73.4%               | 71.6%               |
| L4               | 78.4%      | 80.3%         | 79.7%     | 75.9%             | 79.1%               | 74.4%               |
| L5               | 78.3%      | 80.0%         | 78.9%     | 75.9%             | 78.7%               | 74.6%               |
| L6               | 77.0%      | 80.8%         | 79.5%     | 77.8%             | 79.3%               | 77.0%               |
| L7               | 76.3%      | 78.9%         | 79.9%     | 76.9%             | 77.7%               | 73.2%               |
| L8               | 76.4%      | 78.7%         | 79.5%     | 78.1%             | 77.0%               | 73.0%               |
| R1               | 72.5%      | 77.3%         | 78.5%     | 77.5%             | 75.1%               | 72.4%               |
| R2               | 72.5%      | 75.8%         | 78.6%     | 77.3%             | 74.4%               | 72.3%               |
| R3               | 71.6%      | 78.4%         | 78.4%     | 77.8%             | 75.9%               | 71.6%               |
| R4               | 74.1%      | 77.6%         | 78.9%     | 75.9%             | 76.7%               | 71.6%               |
| R5               | 75.5%      | 79.5%         | 79.4%     | 76.4%             | 77.7%               | 71.7%               |
| R6               | 76.2%      | 79.1%         | 79.4%     | 77.4%             | 78.1%               | 71.6%               |
| R7               | 76.4%      | 79.9%         | 79.8%     | 77.7%             | 79.2%               | 71.6%               |
| R8               | 77.0%      | 79.7%         | 80.5%     | 78.3%             | 78.3%               | 71.8%               |

TABLE VI. ACCURACY OF ALL SVM CLASSIFIERS UTILIZING LEVEL=5,'DB2' WAVELET, WINDOW MEASURE = 1024 AND SETTING HOLDOUT APPROVAL TO 20%

| Sensor position | Linear SVM | Quadratic SVM | Cubic SVM | Fine Gaussian SVM | Medium Gaussian SVM | Coarse Gaussian SVM |
|-----------------|------------|---------------|-----------|-------------------|---------------------|---------------------|
| L1              | 73.50%     | 83.20%        | 84.90%    | 79.20%            | 78.30%              | 73.40%              |
| L2              | 77.50%     | 81.20%        | 84.90%    | 78.10%            | 81.50%              | 72.80%              |
| L3              | 72.80%     | 74.00%        | 73.40%    | 76.30%            | 74.40%              | 72.70%              |
| L4              | 81.10%     | 83.00%        | 83.20%    | 75.00%            | 82.00%              | 75.30%              |
| L5              | 78.30%     | 81.90%        | 28.70%    | 77.70%            | 81.50%              | 74.30%              |
| L6              | 77.20%     | 81.10%        | 82.00%    | 81.30%            | 81.00%              | 77.50%              |
| L7              | 78.70%     | 81.10%        | 81.50%    | 77.00%            | 79.80%              | 73.90%              |
| L8              | 75.50%     | 77.30%        | 78.20%    | 79.20%            | 77.70%              | 74.90%              |
| R1              | 73.50%     | 77.20%        | 81.30%    | 78.10%            | 75.40%              | 73.50%              |
| R2              | 74.40%     | 76.60%        | 78.90%    | 78.50%            | 76.50%              | 74.10%              |
| R3              | 72.50%     | 77.20%        | 77.00%    | 77.30%            | 75.10%              | 72.50%              |
| R4              | 74.10%     | 77.60%        | 77.80%    | 76.60%            | 76.80%              | 72.70%              |
| R5              | 76.20%     | 78.10%        | 75.60%    | 77.20%            | 78.70%              | 72.80%              |
| R6              | 76.20%     | 77.20%        | 78.80%    | 76.90%            | 78.10%              | 72.50%              |
| R7              | 76.00%     | 78.40%        | 77.40%    | 77.50%            | 77.10%              | 72.50%              |
| R8              | 76.30%     | 81.50%        | 82.50%    | 78.60%            | 78.10%              | 73.20%              |

TABLE VII. ACCURACY OF ALL SVM CLASSIFIERS UTILIZING LEVEL=7,'DB2' WAVELET, WINDOW ESTIMATE = 1024 AND SETTING HOLDOUT APPROVAL TO 20%

| Sensors position | Linear SVM | Quadratic SVM | Cubic SVM | Fine Gaussian SVM | Medium Gaussian SVM | Coarse Gaussian SVM |
|------------------|------------|---------------|-----------|-------------------|---------------------|---------------------|
| L1               | 73.70%     | 78.60%        | 78.60%    | 76.80%            | 77.80%              | 72.50%              |
| L2               | 76.50%     | 79.10%        | 78.40%    | 75.60%            | 77.20%              | 72.50%              |
| L3               | 72.70%     | 76.50%        | 75.80%    | 74.20%            | 74.90%              | 72.50%              |
| L4               | 78.10%     | 79.60%        | 79.50%    | 75.40%            | 79.70%              | 76.80%              |
| L5               | 78.90%     | 78.10%        | 78.60%    | 74.00%            | 77.70%              | 75.90%              |
| L6               | 76.60%     | 83.30%        | 79.60%    | 77.00%            | 79.10%              | 74.40%              |
| L7               | 75.50%     | 77.10%        | 75.70%    | 75.20%            | 78.90%              | 74.20%              |
| L8               | 75.20%     | 77.20%        | 77.40%    | 74.50%            | 75.60%              | 74.20%              |
| R1               | 74.90%     | 78.30%        | 79.40%    | 75.90%            | 74.30%              | 74.70%              |
| R2               | 73.50%     | 77.10%        | 76.60%    | 73.70%            | 75.60%              | 73.70%              |
| R3               | 73.70%     | 77.10%        | 77.00%    | 74.60%            | 75.60%              | 73.70%              |
| R4               | 75.40%     | 82.50%        | 78.20%    | 74.60%            | 79.40%              | 73.70%              |
| R5               | 84.70%     | 87.20%        | 88.90%    | 77.10%            | 85.00%              | 78.90%              |
| R6               | 77.30%     | 78.70%        | 76.80%    | 75.10%            | 77.70%              | 72.50%              |
| R7               | 76.50%     | 81.70%        | 81.50%    | 74.40%            | 78.60%              | 72.70%              |
| R8               | 76.50%     | 79.80%        | 74.90%    | 74.90%            | 78.70%              | 72.50%              |

TABLE VIII. ACCURACY OF ALL SVM CLASSIFIERS UTILIZING LEVEL=7,'DB2' WAVELET, WINDOW ESTIMATE = 1024 AND SETTING HOLDOUT APPROVAL TO 15%

| Sensors position | Linear SVM | Quadratic SVM | Cubic SVM | Fine Gaussian SVM | Medium Gaussian SVM | Coarse Gaussian SVM |
|------------------|------------|---------------|-----------|-------------------|---------------------|---------------------|
| L1               | 73.10%     | 78.30%        | 78.40%    | 74.50%            | 76.20%              | 73.10%              |
| L2               | 77.00%     | 78.60%        | 77.90%    | 75.80%            | 78.30%              | 72.70%              |
| L3               | 72.70%     | 74.60%        | 74.60%    | 73.90%            | 73.90%              | 72.50%              |
| L4               | 80.70%     | 80.00%        | 78.90%    | 74.30%            | 78.90%              | 75.00%              |
| L5               | 75.70%     | 79.80%        | 78.90%    | 76.60%            | 80.00%              | 74.50%              |
| L6               | 78.00%     | 81.20%        | 81.60%    | 75.70%            | 78.30%              | 74.00%              |
| L7               | 77.00%     | 79.60%        | 75.90%    | 74.50%            | 78.90%              | 73.40%              |
| L8               | 73.40%     | 76.30%        | 76.80%    | 74.30%            | 74.70%              | 73.40%              |
| R1               | 73.60%     | 75.70%        | 81.00%    | 76.30%            | 74.00%              | 72.70%              |
| R2               | 72.70%     | 76.10%        | 80.70%    | 74.50%            | 76.30%              | 73.70%              |
| R3               | 72.70%     | 76.80%        | 78.40%    | 75.40%            | 74.50%              | 72.70%              |
| R4               | 74.70%     | 80.70%        | 82.60%    | 75.00%            | 78.00%              | 72.70%              |
| R5               | 88.40%     | 90.30%        | 87.60%    | 76.70%            | 87.80%              | 83.10%              |
| R6               | 77.30%     | 77.70%        | 76.80%    | 75.40%            | 78.00%              | 72.40%              |
| R7               | 76.10%     | 81.60%        | 78.70%    | 73.80%            | 78.70%              | 71.70%              |
| R8               | 75.05      | 79.30%        | 78.00%    | 75.40%            | 78.20%              | 72.90%              |

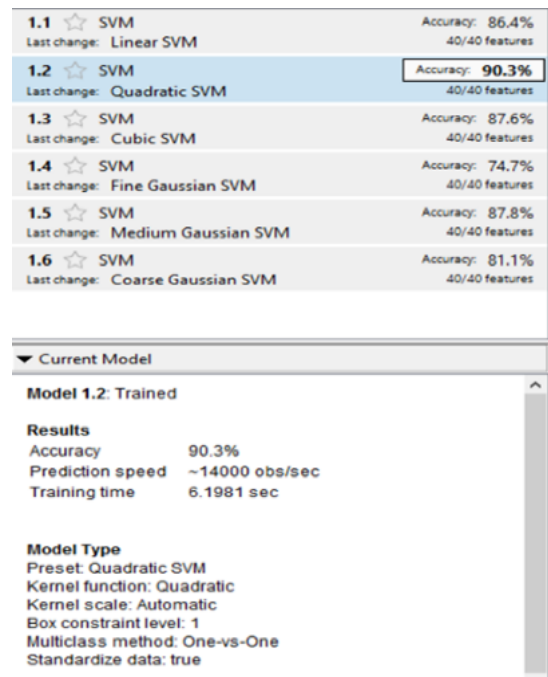


Fig. 10. Trained model descriptions.

class. The green boxes clearly exhibit good performance of classifier and pink boxes demonstrates incorrect execution. In class 1 the described impression of the correct class proves as 91 while mistaken expectations concludes 32. Be that as it may, for class 2 the arranged right perceptions are 301 and wrong perceptions are 10. Positive prescient qualities are shown in Fig. 11(b) the green boxes are for the effectively anticipated focuses in each class, which is 90% for each class.

The incorrect revelation measures are seeded pink for wrongly prediction appeared in Fig. 11(b). For both classes it is 10%. Classifier results reliant on each class is found in Fig. 11(c) exhibits True Positive Rates and False Negative Rates. The plot depicts genuine class in two segments on the right. The plot verifies for class 1 classifier classifies 74%

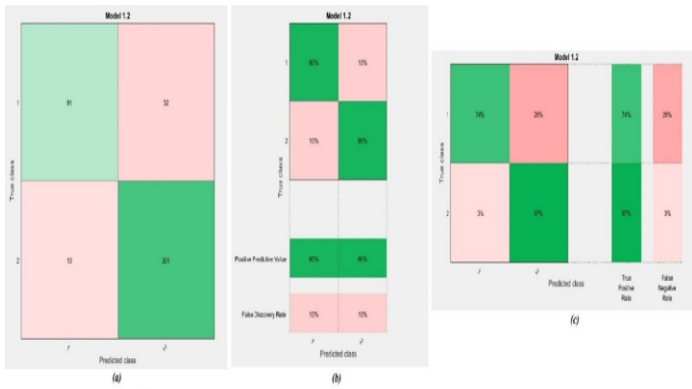


Fig. 11. (a) Confusion Matrix; (b) Positive Predictive Values and False Discovery Rates; (c) True Positive Rate and False Negative Rate.

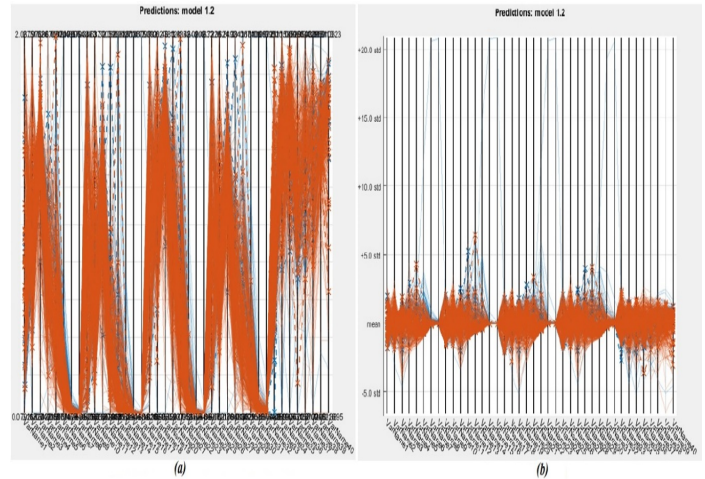


Fig. 13. (a) Model predictions in normalized scaling; (b) Model predictions in standardized scaling.

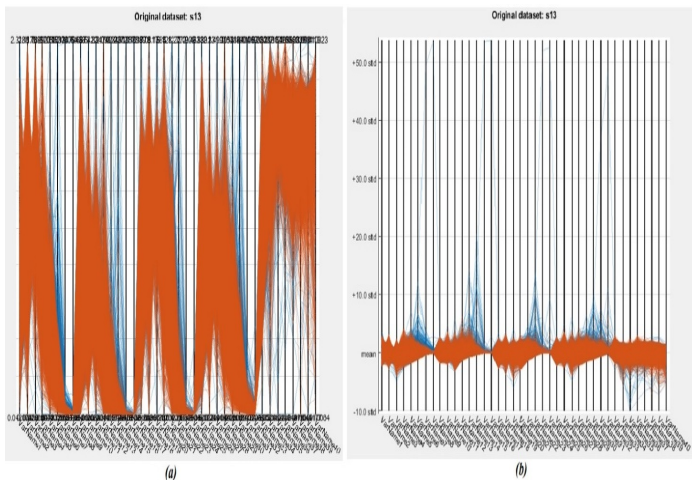


Fig. 12. (a) Original data in normalized scaling; (b) Original data in standardized scaling.

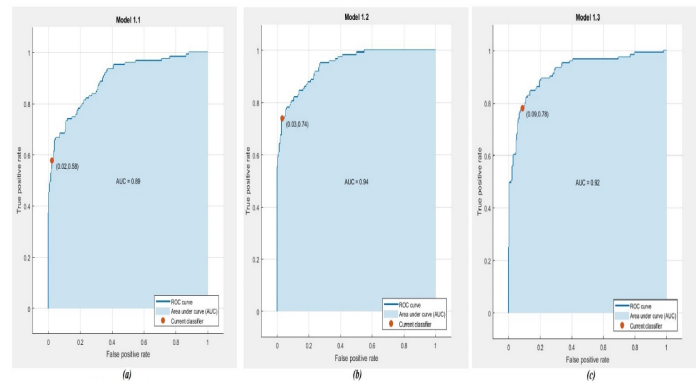


Fig. 14. (a) Linear SVM; (b) Quadratic SVM (c) Cubic SVM.

precisely and 26% erroneously and for class 2 it performs well 97% successfully while 3% mistakenly. Anyway regardless, the parallel co-ordinate show the components through which the model is arranged and checked. Fig. 12(a) and (b) exhibits the principal data in the normalized structure and standardized structure exclusively. Fig. 13(a) and (b) indicates exhibit the first information in the normalized structure and standardized structure individually. Blue shading addresses the class 1 and red shading addresses the class 2. The x-turn the factors (with-draw highlights) and the y-hub speaks to their potential. The cross defines the erroneous expectations of prepared model. The delayed consequences of Quadratic SVM are better than other SVM.

The results of Quadratic SVM are better than other SVM classifiers can also be verified using the ROC curves. Fig. 14 shows AUC of Linear, Quadratic and Cubic SVM classifiers and Fig. 15 shows AUC of Fine, Medium and Coarse Gaussian SVM classifiers. AUC of Quadratic SVM classifier is 0.94 which is greater than other SVM classifiers.

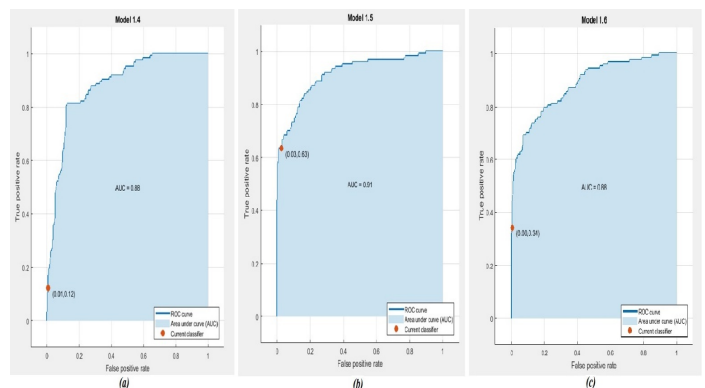


Fig. 15. (a) Fine Gaussian SVM; (b) Medium Gaussian SVM (c) Coarse Gaussian SVM.

## V. CONCLUSION

As Parkinson is dynamic ailment for that the gait examination is basic step. Gait is the method for strolling. It's an eccentricity which may adequately helps in location of Parkinson subject. As this examination was centered around exact and accurate investigation of gait that guides in separating between Parkinson patient and control subject. As most of the previous research uses kinect sensors or accelerometers for detecting gait and for recognition and processing multiple and complex algorithms are used this proposed system utilized the appropriate dataset of VGRF from feet. The features are extracted utilizing WPT. Five sorts of features are extracted. The amount of features depends on the window size and the level. For the best results level=7 and 1024 window size is used. The wavelet type preferred is "db2". For classification and comparisons of sensors SVM is used.

Assessment of the outcomes demonstrated that a solitary force sensor on right foot at position 5 evidently recognize persistent and sound subject by by analyzing gait features in Parkinson patient. The aftereffects of an examination demonstrated that SVM classifier shows 90.3% exactness that is superior to different classifiers being tested. Assessment of the outcomes demonstrated that a solitary constrain sensor located at right foot's medial portion conclusively recognize Parkinson's patient because of stride features incorporates into Parkinson patients. In future, the training of input features can be performed for the need of latest training algorithms. The resulted features can be trained utilizing deep learning to produce extensive results and making framework increasingly precise to manage substantial dataset and deliver progressively best outcomes.

## REFERENCES

- [1] M. Hariharan, K. Polat, and R. Sindhu, "A new hybrid intelligent system for accurate detection of parkinson's disease," *Computer methods and programs in biomedicine*, vol. 113 3, pp. 904–13, 2014.
- [2] M. Plotnik, N. Giladi, Y. Balash, C. Peretz, and J. M. Hausdorff, "Is freezing of gait in parkinson's disease related to asymmetric motor function?," *Annals of neurology*, vol. 57, pp. 656–63, May 2005.
- [3] W. Tao, T. Liu, R. Zheng, and H. Feng, "Gait analysis using wearable sensors.," *Sensors (Basel, Switzerland)*, vol. 12, no. 2, pp. 2255–83, 2012.
- [4] A. Godfrey, "Wearables for independent living in older adults: Gait and falls," *Maturitas*, vol. 100, pp. 16 – 26, 2017.
- [5] L. Ai, J. Wang, and R. Yao, "Classification of parkinsonian and essential tremor using empirical mode decomposition and support vector machine," *Digit. Signal Process.*, vol. 21, pp. 543–550, July 2011.
- [6] S. Haller, S. Badoud, D. Nguyen, V. Garibotto, K. Lovblad, and P. Burkhard, "Individual detection of patients with parkinson disease using support vector machine analysis of diffusion tensor imaging data: Initial results," *American Journal of Neuroradiology*, 2012.
- [7] L. Palmerini, L. Rocchi, S. Mazilu, E. Gazit, J. Hausdorff, and L. Chiari, "Identification of characteristic motor patterns preceding freezing of gait in parkinson's disease using wearable sensors," *Frontiers in Neurology*, vol. 8, p. 394, 08 2017.
- [8] S. Das, L. Trutoiu, A. Murai, D. Alcindor, M. Oh, F. De la Torre, and J. Hodgins, "Quantitative measurement of motor symptoms in parkinson's disease: A study with full-body motion capture data," in *Engineering in Medicine and Biology Society, EMBC, 2011 Annual International Conference of the IEEE*, pp. 6789–6792, 2011.
- [9] B. M. Eskofier, S. I. Lee, M. Baron, A. Simon, C. F. Martindale, H. GaBner, and J. Klucken, "An overview of smart shoes in the internet of health things: Gait and mobility assessment in health promotion and disease monitoring," *Applied Sciences*, vol. 7, no. 10, 2017.
- [10] B. Pogorelc, Z. Bosnić, and M. Gams, "Automatic recognition of gait-related health problems in the elderly using machine learning," *Multimedia Tools Appl.*, vol. 58, pp. 333–354, May 2012.
- [11] S. Minto, D. Zanotto, E. M. Boggs, G. Rosati, and S. K. Agrawal, "Validation of a footwear-based gait analysis system with action-related feedback," *IEEE Transactions on Neural Systems and Rehabilitation Engineering*, vol. 24, pp. 971–980, Sept 2016.
- [12] P. Ren, E. Karahan, C. Chen, R. Luo, Y. Geng, J. F. B. Bayard, M. L. Bringas, D. Yao, K. M. Kendrick, and P. A. Valdes-Sosa, "Gait influence diagrams in parkinson's disease," *IEEE Transactions on Neural Systems and Rehabilitation Engineering*, vol. 25, pp. 1257–1267, 2017.
- [13] R. Soubra, M. O. Diab, and B. Moslem, "Identification of parkinson's disease by using multichannel vertical ground reaction force signals," in *2016 International Conference on Bio-engineering for Smart Technologies (BioSMART)*, pp. 1–4, Dec 2016.
- [14] S. V. Perumal and R. Sankar, "Gait monitoring system for patients with parkinson's disease using wearable sensors," in *2016 IEEE Healthcare Innovation Point-Of-Care Technologies Conference (HI-POCT)*, pp. 21–24, Nov 2016.
- [15] J. Camps, A. Samà, M. Martín, D. Rodríguez-Martín, C. Pérez-López, S. Alcaine, B. Mestre, A. Prats, M. C. Crespo, J. Cabestany, À. Bayés, and A. Català, "Deep learning for detecting freezing of gait episodes in parkinson's disease based on accelerometers," in *Advances in Computational Intelligence* (I. Rojas, G. Joya, and A. Catala, eds.), (Cham), pp. 344–355, Springer International Publishing, 2017.
- [16] K. D. Das, A. J. Saji, and C. S. Kumar, "Frequency analysis of gait signals for detection of neurodegenerative diseases," in *2017 International Conference on Circuit ,Power and Computing Technologies (ICCPCT)*, pp. 1–6, April 2017.
- [17] P. Tahafchi, R. Molina, J. Roper, K. Sowalsky, C. Hass, A. Gunduz, M. Okun, and J. W. Judy, "Freezing-of-gait detection using temporal, spatial, and physiological features with a support-vector-machine classifier," 07 2017.
- [18] N. Tahir and H. Manap, "Parkinson disease gait classification based on machine learning approach," *Journal of Applied Sciences*, vol. 12, no. 2, pp. 180–185, 2012.
- [19] H. H. Manap, N. M. Tahir, and A. I. M. Yassin, "Statistical analysis of parkinson disease gait classification using artificial neural network," in *2011 IEEE International Symposium on Signal Processing and Information Technology (ISSPIT)*, pp. 060–065, Dec 2011.
- [20] M. Gabel, R. Gilad-Bachrach, E. Renshaw, and A. Schuster, "Full body gait analysis with kinect," in *2012 Annual International Conference of the IEEE Engineering in Medicine and Biology Society*, pp. 1964–1967, Aug 2012.
- [21] A. Goldberger, L. Amaral, L. Glass, J. Hausdorff, P. Ivanov, R. Mark, J. Mietus, G. Moody, C. Peng, and H. Stanley, "Physiobank, physiotoolkit, and physionet: Components of a new research resource for complex physiologic signals," *Circulation*, vol. 101, no. 23, pp. e215–e220, 2000.
- [22] A. van der Hoorn, A. L. Bartels, K. L. Leenders, and B. M. de Jong, "Handedness and dominant side of symptoms in parkinsons disease.," *Parkinsonism and related disorders*, vol. 17, pp. 58–60, Jan 2011.
- [23] "Infotronic.nl - infotronic resources and information", <http://www.infotronic.nl/cdg>,
- [24] Y. Rong, D. Hao, X. Han, Y. Zhang, J. Zhang, and Y. Zeng, "Classification of surface emgs using wavelet packet energy analysis and a genetic algorithm-based support vector machine," *Neurophysiology*, vol. 45, pp. 39–48, Jan 2013.
- [25] R. Polikar, *The wavelet tutorial*. 1996.
- [26] "Wavelet packets transform-mathswork," 2018.
- [27] "Support vector machine for binary classification," 2018.
- [28] "Train classification models in classification learner app," 2018.

# An Effective Framework for Tweet Level Sentiment Classification using Recursive Text Pre-Processing Approach

Muhammad Bux Alvi\*<sup>†1</sup>, Naeem A. Mahoto<sup>‡2</sup>, Mukhtiar A. Unar<sup>†3</sup> and M. Akram Shaikh<sup>‡4</sup>

\*Computer Systems Engineering, IUB, Bahawalpur, Pakistan

<sup>†</sup>MUET, Jamshoro, Pakistan

<sup>‡</sup>PASTIC National Center, Pakistan Science Foundation, Islamabad, Pakistan

**Abstract**—With around 330 million people around the globe tweet 6000 times per second to express their feelings about a product, policy, service, or an event. Twitter message majorly consists of thoughts. Thoughts are mostly expressed as a text and it is an open challenge to extract some insight from free text. The scope of this work is to build an effective tweet level sentiment classification framework that may use these thoughts to know collective sentiment of the folk on a particular subject. Furthermore, this work also analyses the impact of proposed tweet level recursive text pre-processing approach on overall classification results. This work achieved up to 4 points accuracy improvement over baseline approach besides mitigating feature vector space.

**Keywords**—Machine learning; recursive text pre-processing; sentiment analysis; sentiment classification framework; Twitter

## I. INTRODUCTION

The proliferation of Internet based micro-blogging social networks have opened new avenues to masses to express their response and reaction on variety of topics in real time. People discuss current affairs, complain about a policy, raise voice on a social issue or give feedback about any product or service. This scenario is instigating unremitting pouring of data from the users. It is estimated that till 2020 there will be about 44 ZB of digital data<sup>1</sup>. Another assessment reports that 80% of available data is unstructured today [1]. With around 330 million active user<sup>2</sup> and 6000 tweets per second, twitter has emerged as a popular medium among people to discuss currently trending topical issues to exhibit their tendencies [2], [3]. However, it is a tedious task to discover and summarize collective popular sentiment from this scaling twitter data. Manual monitoring and analysis of such a huge volume of data may be a highly impractical solution. Therefore, a computational method is the only rescue to this issue and opportunity i-e computer mediated sentiment classification [4] for user generated twitter text data.

To extract meaningful features from the acquired dataset(s), text data needs to be pre-processed properly because knowledge present in text data is not directly accessible. Text data requires two preliminary steps before its application to a machine learning algorithm: 1) removing trivial and non-discriminating data and 2) Text transformation. Text data especially twitter

text is notoriously prone to noise and data sparsity. Text data which already has its own inherent challenges to process and analyze, utilization of informal social media language has added more severity to it. For example informal short form (Internet slang), word-shortening, neologism, spelling variations and elongation [5].

The contribution of this work includes an effective tweet level sentiment classification (TLSC) framework that provides comprehensive steps for twitter sentiment classification and allows to discover sentiment orientation embedded in the tweets. Additionally, this work proposes a 19-step recursive text pre-processing approach, initial version proposed in [6], that results in 1) better data cleaning, and 2) reduction in feature vector space. The recursive pre-processing approach separates out redundant and irrelevant tweets and removes noisy data from the tweets to acquire a cleaner dataset. Cleaned dataset is then prepared for learning model to produce an analytic engine to perform tweet level sentiment classification. We have used Multinomial Naive Bayes, LinearSVC and logistic regression machine learning algorithms with six feature extraction techniques to experiment with baseline pre-processing methods and recursive pre-processing approach. This work consisted of 108 experiments for each machine learning algorithm comparing baseline and recursive approaches with hold-out and k-fold cross validation evaluation indexes. We found Multinomial Naive Bayes and LinearSVC algorithms consistently performing well with ngrams and TFIDF + ngrams feature extraction technique using recursive pre-processing approach.

The extracted results can help an non-government organization (NGO) to begin an awareness campaign or the government in policy making to cope with challenges or opportunities. Tweet level sentiment classification framework is presented in Fig. 1.

This work is organized as: 1) Introduction, 2) Related Work, 3) Methodology, 4) Performance Evaluation Indexes, 5) Results and Discussion, 6) Conclusion, and 7) Future Direction.

## II. RELATED WORK

Twitter has been largely used to know about people's choice and interest in politics, sports, social issues or global problems [7], [8]. Research on twitter data is recent. However, sentiment analysis, a broader area of study, is around for two decade which is an application of natural language

<sup>1</sup><https://www.emc.com/leadership/digital-universe/2014iview/executive-summary.htm>

<sup>2</sup><https://www.statista.com/statistics/282087/number-of-monthly-active-twitter-users/>

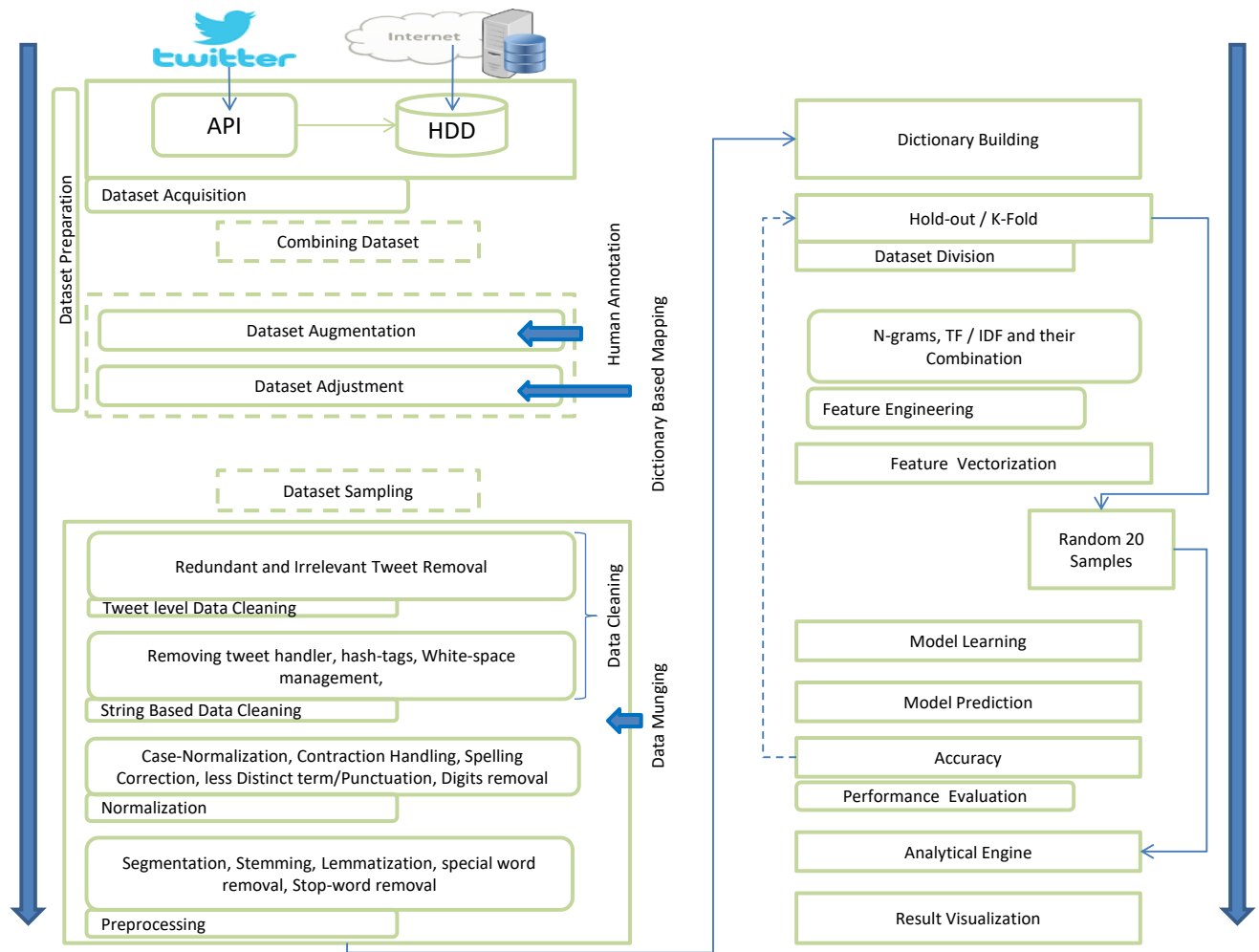


Fig. 1. Tweet Level Sentiment Classification Framework

processing. Most of the work in sentiment analysis, specially in twitter sentiment analysis, revolves around feature extraction. A few researchers have worked on developing a comprehensive framework for twitter sentiment analysis and data pre-processing techniques.

A document level unified framework for tweets classification has been proposed in [9]. The proposed method utilizes four classifiers to handle slang terms, emotions, term orientation and domain specific classifier. They claim to have achieved better results in comparison to other similar work.

In [10], authors reported about the significance of pre-processing and selection of correct pre-processing techniques in sentiment analysis. They have experimented on two datasets with 16 pre-processing techniques using four machine learning algorithms. They found lemmatization, removing digits and contraction handling beneficial and other pre-processing techniques trivial. Their further experiments encompass various combinations of basic pre-processing techniques.

In [11], authors demonstrated to elevate the importance of applying text pre-processing techniques before applying a

learning algorithm for twitter sentiment analysis. They have used 05 twitter datasets, 06 pre-processing techniques, two feature models and 04 classifiers including Naive Bayes, support vector machine, Logistic Regression and Random Forest. They have reported that classification efficiency increased by handling contractions and negation but no changes were observed with other steps.

Khan et al., in [12] have addressed the problems of feature vector space i-e data sparsity in tweets. They have concentrated on data pre-processing steps to mitigate data sparsity and to achieve better accuracy.

Kim J. et al. in [13] suggested collaborative filtering method to cope with challenge induced due to sparse data when predicting sentiments in twitter data. They tested their collaborative filtering model on two different datasets and reported it to be quite effective.

Prieto et al. in their work have collected location based tweets about public concern and disease information in Portugal and Spain with supervised signals. They have used regular expressions for feature selection and machine learning for

classification and have achieved F-measure values of 0.8 and 0.9 which are quite promising compared to baseline methods. They have disregarded slang in their work [14].

Many other studies have suggested frameworks for twitter sentiment analysis and assessed the impact of text pre-processing on overall accuracy increase. However, this study offers more practical and comprehensive approach for building twitter sentiment classification system. Additionally we have proposed an ordered recursive pre-processing approach that can handle twitter data well.

### III. METHODOLOGY: RECURSIVE PRE-PROCESSING APPROACH

The experimental methodology in this paper is organized as: 1) Dataset Preparation, 2) Data Munging, 3) Feature Engineering, 4) Feature Vectorization, and 5) Modeling.

#### A. Dataset Preparation

1) *Data Acquisition*: The twitter dataset can be acquired programmatically using twitter STEAMING API or REST API. Alternatively, a twitter dataset may be obtained from an online repository. Two datasets have been acquired externally from an online repository [15]. Global warming dataset describes people’s belief whether there is global warming or it is just a myth and over exaggerated matter. The other dataset is about people’s acceptability towards self drive cars. Table I represents some statistics about these two datasets. The obtained datasets have majorly two parts i.e. tweets and meta-data.

TABLE I. DATASET STATISTICS

| Dataset         | Total Tweets | Positive | Negative | Neutral | Missing Value | Duplicate |
|-----------------|--------------|----------|----------|---------|---------------|-----------|
| Global Warming  | 6090         | 3111     | 1114     | 1865    | 0             | 542       |
| Self Drive Cars | 7156         | 1904     | 795      | 4248    | 209           | 10        |

Once the dataset is acquired, the obtained dataset may be augmented with meta-data through human annotation if needed. In this case, the dataset is already annotated but the meta-data in the given dataset is inconsistent as shown in Table II. It consists of all variants for {Yes, Y, N, yes, Na}. Therefore, it needs dataset adjustment. Dataset adjustment process includes: A) Managing inconsistent categorical meta-data. B) Handling missing values.

TABLE II. RAW TWEET DATA

| No | Tweet  | Sentiment |
|----|--|-----------|
| 1  | Ocean Saltiness Shows Global Warming Is Intensifying Our Water Cycle <a href="http://bit.ly/bJsszY">http://bit.ly/bJsszY</a> | Yes       |
| 2  | RT @sejorg: RT @JaymiHeimbuch: Ocean Saltiness Shows Global Warming Is Intensifying Our Water Cycle                          | Y         |
| 3  | Top Climate Scientist Under Fire for 'Exaggerating' Global Warming <a href="http://bit.ly/9Pq0gQ">http://bit.ly/9Pq0gQ</a>   | N         |
| 4  | For #EarthDay Global warming could affect patient symptoms   | yes       |
| 5  | Great article.   | Na        |
| 6  | W8 here is idea. it is natural Climate change not human induced global warming.  | n         |

2) *Target Data Adjustment: Dictionary Based Series Mapping*: To align such inconsistent and object type data for computational purpose, dictionary based series mapping method has been used to remove inconsistency from the response vector data. An additional dictionary source is developed to handle these inconsistencies. Positive and negative labels are mapped to 1 and 0, respectively as shown in Table III.

TABLE III. CLEAN TWEET DATA

| No | Clean Tweet   | Sentiment |
|----|---|-----------|
| 1  | ocean saltiness shows global warming is intensifying our water cycle            | 1         |
| 2  | top climate scientist under fire for 'exaggerating' global warming              | 0         |
| 3  | earthday global warming could affect patient symptoms                           | 1         |
| 4  | wait here is idea: it is natural climate change human induced global warming    | 0         |
| 5  | wait here is idea it is natural Climate change not human induced global warming | 0         |

3) *Target Missing Values Management/Handling*: One way to handle tweets that do not have any supervising signal is to disregard them. This may be a feasible solution if the number of missing value tweets is low. Conversely, they may be annotated with an appropriate label.

Let Twitter Datasets (TDS) be the aquired dataset. The redundant, irrelevant and missing value tweets are removed initially to obtain Extracted Twitter Dataset (ETDS). Data cleaning methods are then applied on ETDS to determine Clean Twitter Dataset (CTDS) that is used as an input to learning algorithms after feature engineering and proper transformation.

a) *Definition 1*: Twitter Dataset TDS. Let ETDS be the extracted twitter dataset, then:

$$ETDS \in TDS \mid ETDS = \{tw_1, tw_2, tw_3, \dots, tw_n\} \quad (1)$$

Where  $tw_n$  represents individual tweet and is represented as;

$$tw = \{tk_1, tk_2, tk_3, \dots, tk_n\} \quad (2)$$

where  $tk_n$  is the individual token in the tweet

b) *Definition 2*: Clean Twitter Dataset CTDS may be defined as;

$$CTDS \subseteq ETDS \mid CTSD = \{feat_1, feat_2, feat_3, \dots, feat_n\} \quad (3)$$

where  $feat_n \in tk_n$  and represent selected feature(s) from ETDS

#### B. Data Munging

In this work, we have proposed recursive pre-processing twitter text pre-processing approach in a compact and structured form under the umbrella of Data munging as shown in Fig. 2. Data munging is an essential step to prepare noisy twitter data for text analyses because about 80% of the time and effort for text analyses is consumed for data munging<sup>3</sup>. Experimental work has shown that the proposed recursive

<sup>3</sup><https://www.forbes.com/sites/gilpress/2016/03/23/data-preparation-most-time-consuming-least-enjoyable-data-science-task-survey-says>



approach extracts cleaner dataset efficiently. Data Munging includes three major step. Each step involves multiple sub-steps. These three steps are:

- 1) Data Cleaning
- 2) Data Normalization
- 3) Data Pre-processing

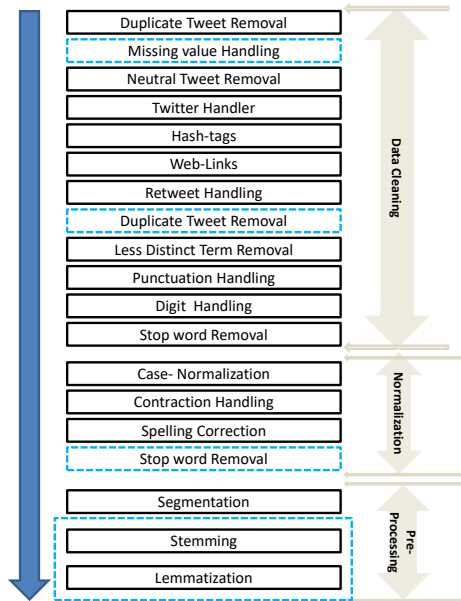


Fig. 2. Proposed Recursive Pre-Processing Approach

1) *Data Cleaning*: Cleaning of text data is a tedious but necessary step that requires a lot of care. In case of tweet level SA, which involves unprecedented word improvisations needs more attentions. Therefore, twitter data cleaning has become more challenging than traditional text pre-processing. Data cleaning is categorized as:

- 1) Tweet Level Data Cleaning
- 2) String Level Data Cleaning

a) *Tweet level Data Cleaning*: It includes 1) removal of redundant tweets, 2) removal of irrelevant tweets, and 3) removal of unintended tweets. As shown in Fig. 2, tweet level data cleaning is performed initially to get rid of redundant, irrelevant and unintended tweets to obtain CTDS at tweet level.

b) *String level Data Cleaning*: Twitter-handlers, hash tags, web-links and retweets are removed using regular expressions. Further processing include; word shortening (“w8”, “f9”, “gr8”), elongated terms (“Cooooool”), unusual acronyms (“ASAP”), neologism (“webinar”), etc. All of these challenges are handled by creating a dictionary in this work. Additionally punctuation, digits and dataset specific less distinct terms are evicted.

2) *Data Normalization*: Text Normalization is a multi-step procedure to standardize the tweets.

a) *Case-Normalization*: It is a non-reversible practice to avoid multiple copies of semantically similar terms. However, this step may be taken carefully with some datasets. For

example, case normalization of the term “United Nations” may negatively affect the performance of the learning model.

b) *Contraction Handling and Spelling Correction*:: Twitter short messages are written in an improvised language developed due to emergence of micro-blogging. Character bound tweets brings a lot of new challenges such as contractions which are informal shortened form of words as shown in Table IV. Contractions are avoided in formal writings but they are extensively used in informal way of expression.

TABLE IV. CONTRACTIONS

| No | Normal<br>Contraction | Actual           | Negated<br>tion | Contra-<br>tion | Actual           |
|----|-----------------------|------------------|-----------------|-----------------|------------------|
| 1  | he’s                  | he is            | can’t           |                 | can not          |
| 2  | She’d                 | She would        | was’nt          |                 | was not          |
| 3  | you’ll’ve             | you will<br>have | haven’t         |                 | have not         |
| 4  | y’all                 | you all          | ynt             |                 | why not          |
| 5  | y/n                   | yes or no        | idonno          | — idunno        | i do not<br>know |

3) *Data Pre-processing*: Some of data processing operations may have minimum incremental impact on the overall classification accuracy but these steps surely reduce feature vector space which is beneficial in improving estimation and execution time.

a) *Word Segmentation*: Given a tweet, splitting it into a list of words is referred as word segmentation or tokenization. We have used NLTK (version 3.2.5) tokenizer to segment the tweet into tokens.

b) *Stemming / Lemmatization*: It is a mapping task that maps different forms of verbs and nouns into a single semantically similar word. Stemming works on the principle of chopping off trailing character(s) from given word to reach base-form. Depending on the usage of stemmer genre, the converted base-form may be incorrect linguistically but works effectively for sentiment classification. Porter Stemmer algorithm [16], [17] has been used in this work for stemming. Optionally lemmatization may be used for this purpose with increased time complexity.

c) *Language stop words*: These terms rarely possess any sentiment significance, therefore they are discarded. We have used natural language toolkit (NLTK) library for this purpose [18], [19] has deeply observed the impact of stop word on twitter sentiment classification.

Fig. 3 represents six graphs in pair i-e (1a, 1b), (2a, 2b) and (3a, 3b). 1a, 2a, and 3a show dataset statistics before data munging while 1b, 2b, and 3b display statistics after applying recursive data pre-processing approach. In Fig. 3, 1(a) shows that few tweets in TDS have more than 140 characters that show lacking in data acquisition process. We infer that some unnecessary and irrelevant terms or characters have been padded into some tweets. 2(a) displays sentiment-wise distribution and 3(a) represents group wise distribution of tweets based on their frequency. 1(b), 2(b), and 3(b) show CTDS after applying recursive text pre-processing method i-e data munging. Extra characters have been deleted and there is no tweet having more than 140 characters as shown in 1(b), redundant tweets have been evicted as given in 2(b), and

3(b) shows group-wise tweet distribution and filtration. Fig. 3 graphically displays impact of recursive pre-processing on global warming dataset. Similar pre-processing is also applied on other dataset as well.

The resultant cleaned dataset needs to be split into training dataset and testing dataset for model learning and model evaluation purpose. There are two popular approaches to perform this division 1) Hold out Method, 2) K-fold method. These two strategies aim to determine the best model and the best parameters for the model and to estimate its suitability on out-of-sample data.

### C. Feature Engineering

Features are the distinct measurable attributes in each input data sample. Feature preparation or engineering is a process of feature extraction and feature selection. Feature extraction involves determination of all those input values that may describe the given object i.e. label. While feature selection results in the minimum feature set that may best describe the same object. Each term in the twitter dataset can be a candidate for being a feature. We have used ngrams and weighted versions of ngrams to test their suitability for tweet level sentiment classification with machine learning method as detailed in Table V and Table VI.

a) *Unigrams*: A single distinct term in the dataset is referred as unigram. However, all unigrams cannot be selected as the features. With ' $n$ ' actual number of unigram and ' $m$ ' selected unigrams, the following always stands true for unigrams feature selection method;

$$m_{Sel\_feat} \subseteq n_{Act\_feat} \mid m_{Sel\_feat} \leq n_{Act\_feat} \quad (4)$$

This is a common but most popular approach. The downside of this method is that it loses the order of the term and just count them but in practice it produces good results.

b) *N-grams*: An n-gram is a sequence of n-neighboring tokens. Bi-grams having two and tri-grams with three adjacent tokens. N-grams approach covers the disadvantages of unigram approach i.e. order is preserved, at least, at n-terms phrase level. This advantage, referred as capturing of partial contextual meaning, costs some complexity. For example, in case there are just 10000 tokens in the feature vector and bigrams approach is applied then we may end up with a huge number of tokens (all unigrams + bigrams). With trigram, the number of tokens may increase at least two-fold. The equation 5 calculates the number of ngrams produced given the selected features for  $n_{gram}S_{bigrams}$  and  $n_{gram}S_{trigrams}$ , respectively.

$$ngrams = \begin{cases} ngrams_{bigrams} = (2 * m_{Sel\_feat}) - 1 & ; m_{Sel\_feat} > 1 \\ ngrams_{trigrams} = (2 * m_{Sel\_feat}) + i & ; n > 2 \\ & i = \{0, 1, 2, \dots, n\} \end{cases} \quad (5)$$

c) *TF/IDF*: It is a weighted method that measures the significance of a feature in the document and in the dataset. N-grams approach is prone to overfit due to its capacity to increase the number of features exponentially. Usage of TFIDF handles high and low frequency ngrams implicitly. High frequency n-grams do not help to discriminate tweets while low frequency n-grams are likely to overfit. Medium

frequency n-grams are more likely to help in classification. The problem of sparse terms can be controlled by using n-grams approach with TF/IDF. It is mathematically denoted as:

$$tfidf(t, d, D) = tf(t, d) * idf(t, D) \quad (6)$$

Actually, equation 6 combines two techniques: 1) Term Frequency (tf), and 2) Inverse Document Frequency (idf).

d) *Term Frequency (tf)*: It is simply the count of the number of occurrences of a particular term in a document. Document here refers to a single tweet i.e. ( $f_{t,d}$ ). This gives higher weight to terms that are frequent in a tweet. The equation 7 represents term frequency in the normalized form.

$$tf = \frac{f_{t,d}}{\sum_{t' \in d} f_{t',d}} \quad (7)$$

e) *Inverse Document Frequency (idf)*: Document frequency ( $df$ ) is computed at dataset level. Document frequency is the ratio of total number of tweets where term "t" appear to the total number of tweets in the given dataset and is represented as:

$$df = \frac{|d \in D : t \in d|}{|D|} \quad (8)$$

Accordingly, the *idf* is the inverse of *df* and may be denoted as;

$$idf = \frac{|D|}{|d \in D : t \in d|} \quad (9)$$

And its normalized equation is given by;

$$idf = \log\left(\frac{|D|}{|d \in D : t \in d|}\right) \quad (10)$$

*idf* is biased toward unusual and more distinct terms in the dataset. Overall, a term achieves high weight using *tfidf* when its *tf* is high and its *df* is low. This method extracts more discriminating features in the tweet that are not so frequent in the whole dataset.

### D. Feature Vectorization

Tweets are unstructured data in nature. Unstructured features cannot be used as direct input to a machine learning algorithm for building a model. Feature vectorization is an important task that converts the extracted text features into numeric feature matrix to be used for model estimation and prediction. Feature vectorization replaces each piece of text i.e. tweet with a huge number vector. Each number dimension of that vector corresponds to a certain token in the dataset.

### E. Modeling

Modeling refers to model learning and model evaluation process. Supervised algorithms take a training subset and learn mapping of given feature to respective target values. In other words, the supervised learning algorithms learn by estimating their internal parameters from given examples. These parameters may then be used with out-of-sample data instances to predict the targets as shown in equation 11:

$$TSC : T_w \rightarrow C_{pos|neg} \quad (11)$$

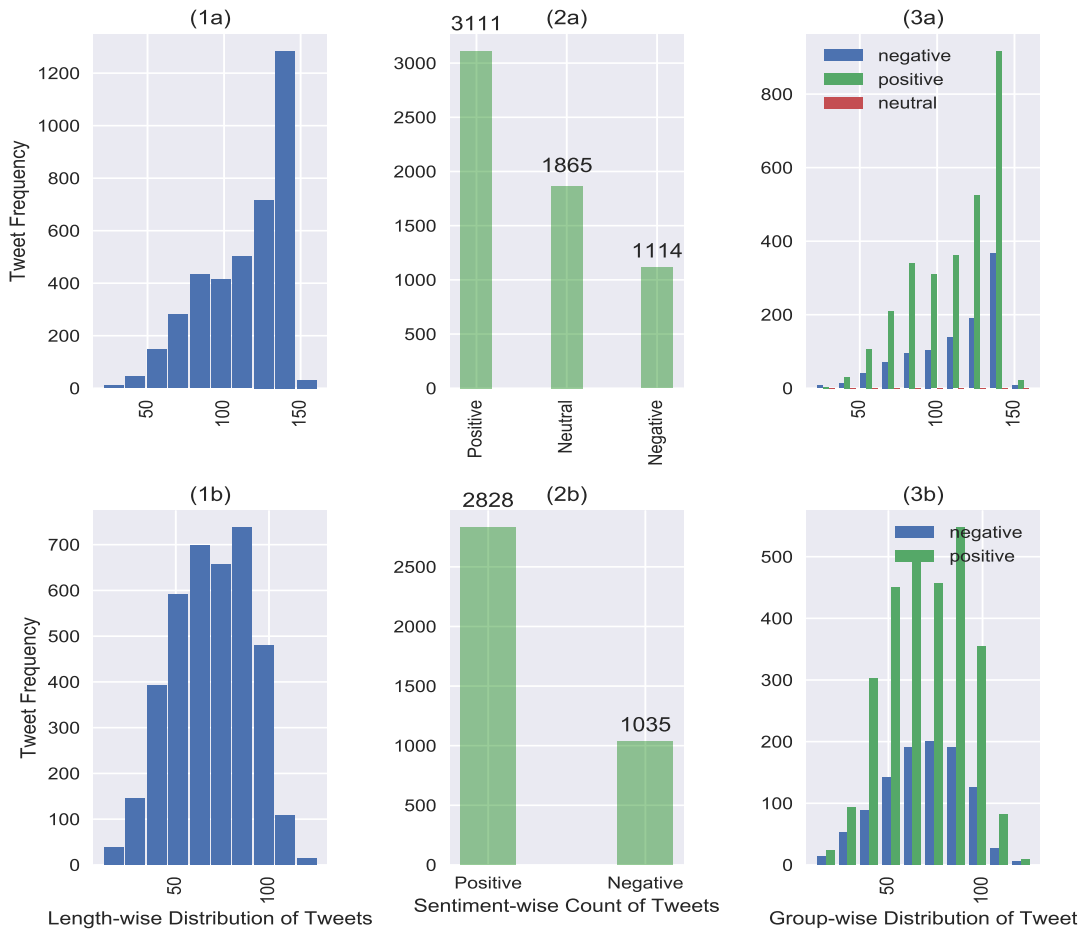


Fig. 3. Graphical representation of Impact of Recursive Text Pre-processing on Tweets - Global Warming Dataset

where TSC represents Twitter Sentiment Classifier,  $t_w$  is the input tweet to be assigned either class while  $C$  may be any of the two possible categories i-e positive or negative. Moreover, the input feature set must fulfill four prerequisites:

- 1) input features and the corresponding labels be stored separately,
- 2) both objects be numeric,
- 3) both be numpy array, and
- 4) their dimension must comply to each other.

1) *Learning Algorithm:* We have used Multinomial Naive Bayes, LinearSVC and logistic regression, most popular machine learning algorithms for text analyses, in this work [10], [11], [20], [21]. Multinomial Naïve Bayes is one of the most widely used probabilistic models. It takes into account the frequency of features in each twitter text communication ( $ttc_n$ ) and represents it as Vector Space Model. This technique outperforms the Bernoulli probabilistic model and all of its variations if the vector space is high. LinearSVC determines optimal decision boundary that is the hyperline having highest margin from the given sample in the extracted twitter data dataset (ETDS). All the  $tw_n$  with given margin form the hyperline are the support vectors that specify the correct location of the hyperline. If the  $tw_n$  are linearly inseparable then a hyperline is determined such that there is minimum

loss in accuracy. This technique is robust to high dimension datasets. Logistic Regression is another widely used dichotomous Machine Learning algorithms to describes and estimates the dependent variable using input feature vector. Logistic regression algorithm utilizes sigmoid function and learning is performed through maximum likelihood.

2) *Model Training:* Training dataset ( $T_rDS$ ) is used for model learning to develop a classifier. Model learning process refers to building up of patterns based upon extracted feature set and updating of learning algorithm's internal parameters. Given a supervised machine learning algorithm (S), trained on  $T_rDS$ , we build a sentiment classifier (F) such that

$$S(T_rDS) = F \quad (12)$$

3) *Model Prediction:* Model prediction refers to the process of predicting class labels for out-of-sample data of test data. This process is usually used as preliminary stage for model evaluation in which test data is normalized and features are extracted to be fed into trained classifier. The trained classifier receives out-of-sample tweet denoted as  $tw_{nd}$  and predicts its class  $c_{nd}$  based on previously learned patterns. While making prediction, the trained model will ignore all those tokens of the new tweet(s) that were not learned during model building process. This is the very reason that to have

more data during learning process is always recommended. Model prediction process may be represented as:

$$F(tw_{nd}) = c_{nd} \quad (13)$$

#### IV. PERFORMANCE EVALUATION INDEXES

We already have expert annotated true class labels for the test dataset  $T_eDS$ . Now with predicted class labels, we can compare true class labels and corresponding predicted class labels to evaluate the efficiency of the developed sentiment classification model using different model evaluation metrics such as Accuracy. There is no hard and fast rule for selection of an evaluation criteria. Actually it depends on the requirement of problem and the dataset.

##### A. Hold out Method

This strategy is computationally inexpensive and needs to run once only. Now given the clean twitter dataset, it is split into training dataset ( $T_eDS$ ) and testing dataset ( $T_rDS$ ) in a suitable proportions as shown in Table V and Table VI.

$$CTDS = \begin{cases} T_rDS = \{(tw_1, c_1), (tw_2, c_2), \dots, (tw_n, c_m)\} \\ T_eDS = \{tw_1, tw_2, \dots, tw_n\} \end{cases} \quad (14)$$

where  $tw_n$  and  $c_m$  denote individual tweet and corresponding label. The dataset subsets consisting of (80-20)% to (60-40)% train-test ratio are tested for suitability and their results are given in Table V and VI. This is more comprehensive approach but prone to test data leakage that may cause decrease in final classification model accuracy.

##### B. Cross Validation Method

In this division technique, feature set is divided into  $k$  equal parts. For the first iteration the model is fitted with  $k - 1$  parts of the given feature set and computes the fitted model prediction error on the  $k^{th}$  left out part. This process occurs  $k$  times and results are averaged to get the over all conclusion. This is computationally an expensive strategy but less biased method and not prone to data leakage. Furthermore, If k-fold split does not evenly separates the dataset, then one group will have remainder of the dataset.

a) *Accuracy*: Accuracy is a popular evaluation measure. Mathematical form for accuracy is given by

$$Accuracy = \frac{CorrectPredictionsMade}{TotalNo.ofPredictionsMade} * 100 \quad (15)$$

$$Accuracy = \frac{TP + TN}{(TP + FP + TN + FN)} * 100 \quad (16)$$

where  $TP$  denotes true positive,  $TN$  represent true negative,  $FP$  is false positive and false negative is given by  $FN$

#### V. RESULTS AND DISCUSSION

Table V and Table VI represent detailed experimental results for the two datasets using Multinomial Naive Bayes, LinearSVC and logistic regression algorithms. Various dataset division strategies for hold out and cross validation methods have been used to evaluate the impact of tweet level sentiment classification framework and recursive pre-processing approach by comparing accuracy achieved through baseline and recursive pre-processing technique.

As shown in Fig. 4, using global warming dataset, this work with recursive pre-processing approach, achieved about 4-points accuracy rise in comparison to baseline using ngrams features. Multinomial Naive Bayes and LinearSVC consistently shown better results. With TFIDF + ngrams models, Multinomial Naive Bayes algorithm outperformed other algorithms with most dataset division strategies.

Fig. 5, demonstrates that this work attained above 4-point accuracy increase using ngrams approach with self drive car twitter dataset. Here, Multinomial naive bayes algorithm was consistent to produce better results. With TFIDF + ngrams models, LinearSVC proved better. Trivial degradation in accuracy was also observed occasionally with this dataset

#### VI. CONCLUSION

In this work, we have proposed an effective and comprehensive tweet level sentiment classification framework with recursive twitter data pre-processing approach. This framework encompasses all the necessary steps involved from twitter dataset acquisition to classification results generation as shown in Fig. 1. Moreover, a 19-step recursive twitter data pre-processing approach is presented that covers all necessary twitter data munging operations in an ordered form. Couple of steps, duplicate tweets and stop word removal, may be required to be retaken for handling regenerated text segments. Moreover, it is observed that a few data munging step may not have significant impact on classification efficiency but they mitigate the issue of feature vector space that makes the process computationally efficient. For example, common punctuation, neologism and digits. Further investigation of this work concludes that Multinomial Naive Bayes and LinearSVC algorithms showed consistently better performance with ngrams and TFIDF + ngrams feature extraction methods using proposed recursive pre-processing approach, achieving up to 4 point accuracy improvement in comparison to baseline models.

#### VII. FUTURE DIRECTION

Future experimental investigation with this framework and proposed recursive pre-processing approach may include application of advanced machine learning algorithms to check their suitability. Furthermore, text pre-preprocessing techniques may be tested separately as well as combined together to determine the best text pre-processing pipeline configuration for sentiment classification.

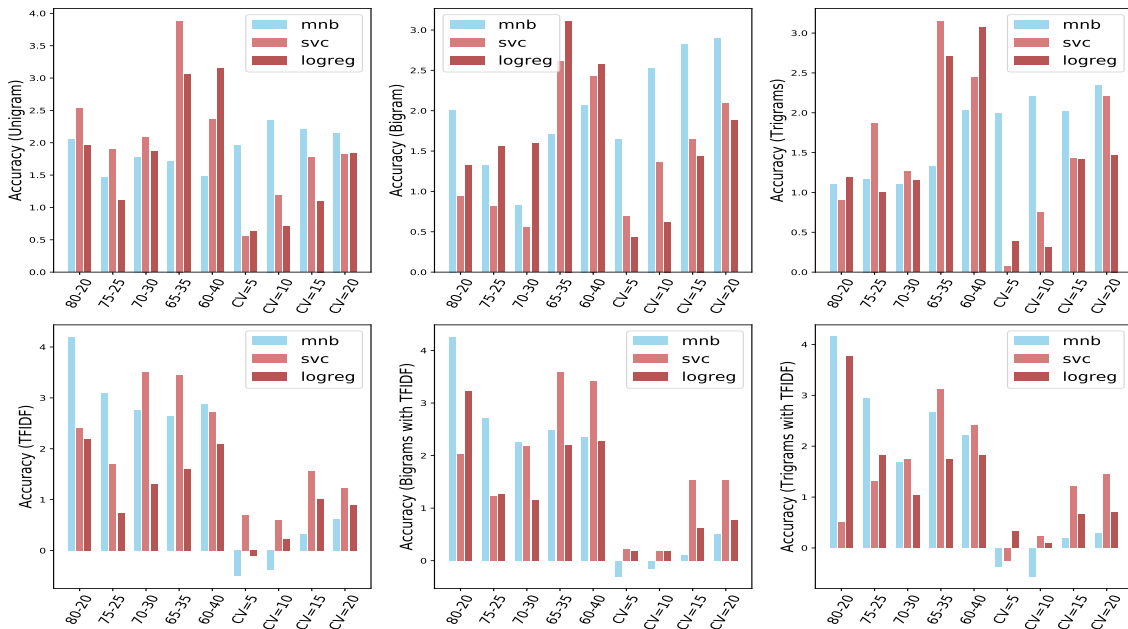


Fig. 4. Global Warming Twitter Dataset - Impact of Recursive Pre-processing approach using: (a) unigrams (b) bigrams (c) trigrams (d) tfidf+unigrams (e) tfidf+bigrams (f) tfidf+trigrams

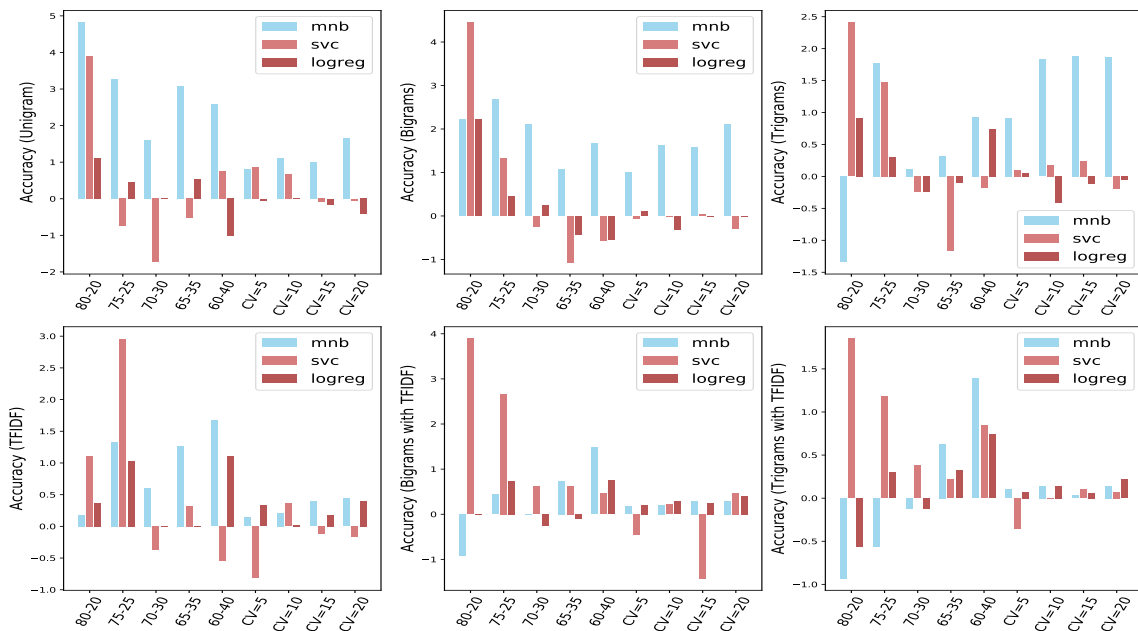


Fig. 5. Self Drive Car Twitter Dataset - Impact of Recursive Pre-processing approach using: (a) unigrams (b) bigrams (c) trigrams (d) tfidf+unigrams (e) tfidf+bigrams (f) tfidf+trigrams

TABLE V. DATASET1-GLOBAL WARMING: ACCURACY ANALYSIS OF TWEET LEVEL SENTIMENT CLASSIFICATION MODEL

|                | Hold-out          |          |          |          |          |                          |          |          |          |          | K-Fold Cross-Validation |       |       |       |       |                          |       |       |       |       |
|----------------|-------------------|----------|----------|----------|----------|--------------------------|----------|----------|----------|----------|-------------------------|-------|-------|-------|-------|--------------------------|-------|-------|-------|-------|
|                | BaseLine          |          |          |          |          | Recursive Pre-processing |          |          |          |          | BaseLine                |       |       |       |       | Recursive Pre-processing |       |       |       |       |
|                | (80-20)%          | (75-25)% | (70-30)% | (65-35)% | (60-40)% | (80-20)%                 | (75-25)% | (70-30)% | (65-35)% | (60-40)% | CV=05                   | CV=10 | CV=15 | CV=20 | CV=05 | CV=10                    | CV=15 | CV=20 |       |       |
| MNB            | Unigrams          | 81.50    | 81.88    | 82.13    | 81.44    | 81.95                    | 83.55    | 83.34    | 83.91    | 83.16    | 83.43                   | 77.58 | 77.80 | 78.01 | 78.37 | 79.54                    | 78.98 | 80.15 | 80.21 | 80.52 |
|                | Bigram            | 82.01    | 82.50    | 83.00    | 82.33    | 81.95                    | 84.02    | 83.82    | 83.83    | 84.04    | 84.02                   | 77.34 | 76.84 | 77.10 | 77.43 | 78.98                    | 79.37 | 79.92 | 80.33 | 80.33 |
|                | Trigram           | 82.92    | 83.12    | 82.65    | 81.96    | 81.75                    | 84.02    | 84.29    | 83.75    | 83.29    | 83.78                   | 74.55 | 74.67 | 74.54 | 74.60 | 76.54                    | 76.88 | 76.56 | 76.94 | 76.94 |
|                | TF/IDF (Unigrams) | 77.10    | 77.12    | 76.96    | 76.86    | 76.58                    | 81.30    | 80.22    | 79.73    | 79.51    | 79.46                   | 77.14 | 77.42 | 77.71 | 77.86 | 76.63                    | 77.04 | 78.03 | 78.48 | 78.48 |
|                | TF/IDF (Bigrams)  | 76.45    | 77.22    | 77.39    | 76.49    | 76.64                    | 80.71    | 79.94    | 79.65    | 78.97    | 78.99                   | 76.08 | 76.52 | 77.24 | 77.21 | 75.78                    | 76.37 | 77.34 | 77.72 | 77.72 |
|                | TF/IDF (Trigrams) | 76.32    | 77.01    | 77.48    | 76.64    | 76.84                    | 80.47    | 79.94    | 79.17    | 79.31    | 79.05                   | 75.69 | 76.39 | 76.80 | 77.19 | 75.33                    | 75.83 | 76.98 | 77.48 | 77.48 |
| SVC            | Unigrams          | 80.07    | 80.12    | 79.29    | 78.27    | 79.88                    | 82.60    | 82.02    | 81.38    | 82.15    | 82.24                   | 78.17 | 78.53 | 78.63 | 79.09 | 78.72                    | 79.71 | 80.40 | 80.91 | 80.91 |
|                | Bigram            | 80.59    | 80.74    | 80.75    | 79.60    | 79.81                    | 81.53    | 81.55    | 81.30    | 82.21    | 82.24                   | 79.21 | 79.10 | 79.10 | 79.38 | 79.90                    | 80.46 | 80.74 | 81.47 | 81.47 |
|                | Trigram           | 81.11    | 80.43    | 80.75    | 79.74    | 80.27                    | 82.01    | 82.30    | 82.01    | 82.89    | 82.72                   | 79.62 | 79.83 | 79.57 | 79.72 | 79.69                    | 80.58 | 81.00 | 81.92 | 81.92 |
|                | TF/IDF (Unigrams) | 81.37    | 81.26    | 81.19    | 80.33    | 81.17                    | 83.78    | 82.97    | 84.70    | 83.77    | 83.90                   | 79.26 | 79.72 | 79.75 | 80.36 | 79.95                    | 80.32 | 81.31 | 81.59 | 81.59 |
|                | TF/IDF (Bigrams)  | 81.75    | 82.40    | 82.05    | 81.07    | 81.56                    | 83.78    | 83.63    | 84.22    | 84.65    | 84.97                   | 79.47 | 79.98 | 79.65 | 80.21 | 79.69                    | 80.16 | 81.19 | 81.74 | 81.74 |
|                | TF/IDF (Trigrams) | 83.05    | 82.71    | 82.57    | 81.74    | 82.21                    | 83.55    | 84.01    | 84.30    | 84.85    | 84.61                   | 78.77 | 79.08 | 79.34 | 79.77 | 78.53                    | 79.31 | 80.55 | 81.22 | 81.22 |
| Log Regression | Unigrams          | 81.11    | 81.67    | 80.93    | 79.97    | 80.40                    | 83.07    | 82.78    | 82.80    | 83.02    | 83.55                   | 79.10 | 79.49 | 79.93 | 79.74 | 79.73                    | 80.20 | 81.03 | 81.57 | 81.57 |
|                | Bigram            | 81.75    | 81.88    | 81.53    | 80.93    | 80.98                    | 83.07    | 83.44    | 83.12    | 84.04    | 83.55                   | 79.80 | 80.11 | 80.11 | 80.47 | 80.23                    | 80.73 | 81.55 | 82.35 | 82.35 |
|                | Trigram           | 81.88    | 81.78    | 82.05    | 80.85    | 80.59                    | 83.07    | 82.78    | 83.20    | 83.56    | 83.66                   | 79.57 | 80.11 | 79.90 | 80.62 | 79.95                    | 80.42 | 81.31 | 82.09 | 82.09 |
|                | TF/IDF (Unigrams) | 79.81    | 80.53    | 80.24    | 79.45    | 78.97                    | 82.01    | 81.26    | 81.54    | 81.06    | 81.06                   | 77.71 | 78.07 | 78.14 | 78.43 | 77.60                    | 78.29 | 79.16 | 79.33 | 79.33 |
|                | TF/IDF (Bigrams)  | 78.78    | 79.81    | 80.15    | 79.08    | 78.91                    | 82.01    | 81.07    | 81.30    | 81.27    | 81.18                   | 76.41 | 76.96 | 77.27 | 77.39 | 76.59                    | 77.15 | 77.88 | 78.17 | 78.17 |
|                | TF/IDF (Trigrams) | 78.13    | 78.98    | 79.63    | 78.93    | 78.84                    | 81.89    | 80.79    | 80.67    | 80.66    | 80.65                   | 75.51 | 76.05 | 76.49 | 76.62 | 75.83                    | 76.14 | 77.15 | 77.32 | 77.32 |

TABLE VI. DATASET2-SELF-DRIVE CARS: ACCURACY ANALYSIS OF TWEET LEVEL SENTIMENT CLASSIFICATION MODEL

|                | Hold-out          |          |          |          |          |                          |          |          |          |          | K-Fold Cross-Validation |       |       |       |       |                          |       |       |       |       |
|----------------|-------------------|----------|----------|----------|----------|--------------------------|----------|----------|----------|----------|-------------------------|-------|-------|-------|-------|--------------------------|-------|-------|-------|-------|
|                | BaseLine          |          |          |          |          | Recursive Pre-processing |          |          |          |          | BaseLine                |       |       |       |       | Recursive Pre-processing |       |       |       |       |
|                | (80-20)%          | (75-25)% | (70-30)% | (65-35)% | (60-40)% | (80-20)%                 | (75-25)% | (70-30)% | (65-35)% | (60-40)% | CV=05                   | CV=10 | CV=15 | CV=20 | CV=05 | CV=10                    | CV=15 | CV=20 |       |       |
| MNB            | Unigrams          | 73.14    | 75.11    | 76.04    | 75.13    | 75.00                    | 77.96    | 78.37    | 77.65    | 78.20    | 77.59                   | 74.99 | 75.09 | 74.87 | 75.02 | 75.79                    | 76.20 | 75.86 | 76.67 | 76.67 |
|                | Bigram            | 73.14    | 73.92    | 75.06    | 75.76    | 75.55                    | 75.37    | 76.59    | 77.16    | 76.82    | 77.22                   | 73.69 | 73.69 | 73.28 | 73.35 | 74.68                    | 75.31 | 74.86 | 75.45 | 75.45 |
|                | Trigram           | 72.59    | 73.77    | 75.43    | 75.55    | 75.18                    | 74.25    | 75.55    | 75.55    | 75.87    | 76.11                   | 69.32 | 68.77 | 67.57 | 68.02 | 70.23                    | 70.60 | 69.45 | 69.89 | 69.89 |
|                | TF/IDF (Unigrams) | 70.37    | 71.11    | 71.85    | 71.95    | 71.66                    | 70.55    | 72.44    | 72.46    | 73.22    | 73.33                   | 71.13 | 71.32 | 71.32 | 71.28 | 71.27                    | 71.53 | 71.71 | 71.72 | 71.72 |
|                | TF/IDF (Bigrams)  | 70.37    | 70.96    | 71.72    | 71.64    | 71.20                    | 69.44    | 71.40    | 71.72    | 72.38    | 72.68                   | 70.58 | 70.65 | 70.65 | 70.61 | 70.75                    | 70.86 | 70.94 | 70.90 | 70.90 |
|                | TF/IDF (Trigrams) | 70.37    | 70.96    | 71.60    | 71.64    | 71.11                    | 69.44    | 71.40    | 71.48    | 72.27    | 72.50                   | 70.54 | 70.61 | 70.72 | 70.65 | 70.64                    | 70.75 | 70.75 | 70.79 | 70.79 |
| SVC            | Unigrams          | 73.14    | 77.18    | 77.28    | 76.08    | 75.37                    | 77.03    | 76.44    | 75.55    | 75.55    | 76.11                   | 73.87 | 73.54 | 73.84 | 73.99 | 74.72                    | 74.20 | 73.75 | 73.94 | 73.94 |
|                | Bigram            | 73.88    | 76.29    | 77.16    | 77.88    | 77.59                    | 78.33    | 77.62    | 76.91    | 76.82    | 77.03                   | 74.95 | 75.36 | 74.87 | 75.25 | 74.90                    | 75.35 | 74.90 | 74.97 | 74.97 |
|                | Trigram           | 73.70    | 74.96    | 76.29    | 77.46    | 76.66                    | 76.11    | 76.44    | 76.04    | 76.29    | 76.48                   | 73.32 | 74.28 | 73.73 | 74.69 | 73.42                    | 74.46 | 73.97 | 74.49 | 74.49 |
|                | TF/IDF (Unigrams) | 75.92    | 76.59    | 77.77    | 76.71    | 77.12                    | 77.03    | 77.92    | 77.40    | 77.03    | 76.57                   | 75.61 | 75.10 | 75.17 | 75.24 | 74.79                    | 75.46 | 75.05 | 75.08 | 75.08 |
|                | TF/IDF (Bigrams)  | 74.81    | 75.25    | 76.79    | 77.88    | 77.96                    | 78.70    | 77.62    | 77.40    | 78.51    | 78.42                   | 74.36 | 74.76 | 74.65 | 75.09 | 73.90                    | 74.98 | 75.23 | 75.56 | 75.56 |
|                | TF/IDF (Trigrams) | 74.07    | 75.25    | 76.41    | 77.24    | 77.03                    | 75.92    | 76.14    | 76.79    | 77.46    | 77.87                   | 73.47 | 73.50 | 73.21 | 73.46 | 73.12                    | 73.49 | 73.31 | 73.53 | 73.53 |
| Log Regression | Unigrams          | 74.81    | 76.29    | 77.03    | 77.24    | 77.96                    | 75.92    | 76.74    | 76.03    | 76.73    | 76.94                   | 74.36 | 74.95 | 74.54 | 75.21 | 74.31                    | 74.97 | 74.38 | 74.79 | 74.79 |
|                | Bigram            | 73.33    | 74.96    | 76.41    | 77.77    | 76.66                    | 75.55    | 75.40    | 76.66    | 77.35    | 76.11                   | 73.76 | 74.73 | 74.58 | 74.87 | 73.86                    | 74.42 | 74.57 | 74.86 | 74.86 |
|                | Trigram           | 73.33    | 74.81    | 75.55    | 75.76    | 75.64                    | 74.25    | 75.11    | 75.30    | 75.66    | 76.38                   | 73.10 | 74.13 | 73.95 | 74.24 | 73.16                    | 73.71 | 73.83 | 74.19 | 74.19 |
|                | TF/IDF (Unigrams) | 71.85    | 72.74    | 73.82    | 74.07    | 73.24                    | 72.22    | 73.77    | 73.82    | 74.07    | 74.35                   | 71.98 | 72.47 | 72.61 | 72.61 | 72.31                    | 72.49 | 72.79 | 73.01 | 73.01 |
|                | TF/IDF (Bigrams)  | 70.92    | 71.70    | 72.59    | 72.80    | 72.12                    | 70.92    | 72.44    | 72.34    | 72.69    | 72.87                   | 70.80 | 70.95 | 70.98 | 70.91 | 71.08                    | 71.23 | 71.23 | 71.31 | 71.31 |
|                | TF/IDF (Trigrams) | 70.74    | 71.55    | 72.09    | 72.06    | 71.66                    | 70.18    | 71.85    | 71.97    | 72.38    | 72.40                   | 70.61 | 70.69 | 70.61 | 70.61 | 70.68                    | 70.83 | 70.75 | 70.83 | 70.83 |

REFERENCES

- [1] G. Miner, J. Elder IV, A. Fast, T. Hill, R. Nisbet, and D. Delen, *Practical text mining and statistical analysis for non-structured text data applications*. Academic Press, 2012.
- [2] V. Kagan, A. Stevens, and V. Subrahmanian, "Using twitter sentiment to forecast the 2013 pakistani election and the 2014 indian election," *IEEE Intelligent Systems*, vol. 30, no. 1, pp. 2–5, 2015.
- [3] P. Burnap, R. Gibson, L. Sloan, R. Southern, and M. Williams, "140 characters to victory?: Using twitter to predict the uk 2015 general election," *Electoral Studies*, vol. 41, pp. 230–233, 2016.
- [4] B. Liu, *Sentiment analysis: Mining opinions, sentiments, and emotions*. Cambridge University Press, 2015.
- [5] S. Brody and N. Diakopoulos, "CoooooooooooooooooIIIIIIIIII-III!!!!!!!!!!!!: using word lengthening to detect sentiment in microblogs," in *Proceedings of the conference on empirical methods in natural language processing*. Association for Computational Linguistics, 2011, pp. 562–570.
- [6] M. B. Alvi, N. A. Mahoto, M. Alvi, M. A. Unar, and M. A. Shaikh, "Hybrid classification model for twitter data-a recursive preprocessing approach," in *2018 5th International Multi-Topic ICT Conference (IMTIC)*. IEEE, 2018, pp. 1–6.
- [7] A. Pak and P. Paroubek, "Twitter as a corpus for sentiment analysis and opinion mining," in *LREc*, vol. 10, no. 2010, 2010, pp. 1320–1326.
- [8] A. Agarwal, B. Xie, I. Vovsha, O. Rambow, and R. Passonneau, "Sentiment analysis of twitter data," in *Proceedings of the Workshop on Language in Social Media (LSM 2011)*, 2011, pp. 30–38.
- [9] M. Z. Asghar, F. M. Kundi, S. Ahmad, A. Khan, and F. Khan, "T-saf: Twitter sentiment analysis framework using a hybrid classification scheme," *Expert Systems*, vol. 35, no. 1, p. e12233, 2018.
- [10] S. Symeonidis, D. Effrosynidis, and A. Arampatzis, "A comparative evaluation of pre-processing techniques and their interactions for twitter sentiment analysis," *Expert Systems with Applications*, vol. 110, pp. 298–310, 2018.
- [11] Z. Jianqiang and G. Xiaolin, "Comparison research on text pre-processing methods on twitter sentiment analysis," *IEEE Access*, vol. 5, pp. 2870–2879, 2017.
- [12] F. H. Khan, S. Bashir, and U. Qamar, "Tom: Twitter opinion mining framework using hybrid classification scheme," *Decision Support Systems*, vol. 57, pp. 245–257, 2014.
- [13] J. Kim, J. Yoo, H. Lim, H. Qiu, Z. Kozareva, and A. Galstyan, "Sentiment prediction using collaborative filtering," in *Seventh international AAAI conference on weblogs and social media*, 2013.
- [14] V. M. Prieto, S. Matos, M. Alvarez, F. Cacheda, and J. L. Oliveira, "Twitter: a good place to detect health conditions," *PLoS one*, vol. 9, no. 1, p. e86191, 2014.
- [15] Datasets. [Online]. Available: <https://www.figure-eight.com/data-for-everyone>
- [16] M. F. Porter, "An algorithm for suffix stripping," *Program*, vol. 14, no. 3, pp. 130–137, 1980.
- [17] P. Willett, "The porter stemming algorithm: then and now," *Program*, vol. 40, no. 3, pp. 219–223, 2006.
- [18] E. Loper and S. Bird, "Nltk: the natural language toolkit," *arXiv preprint cs/0205028*, 2002.
- [19] H. Saif, M. Fernández, Y. He, and H. Alani, "On stopwords, filtering and data sparsity for sentiment analysis of twitter," 2014.
- [20] N. F. Da Silva, E. R. Hruschka, and E. R. Hruschka Jr, "Tweet sentiment analysis with classifier ensembles," *Decision Support Systems*, vol. 66, pp. 170–179, 2014.
- [21] A. Go, R. Bhayani, and L. Huang, "Twitter sentiment classification using distant supervision," *CS224N Project Report, Stanford*, vol. 1, no. 12, p. 2009, 2009.

# Competitive Algorithms for Online Conversion Problem with Interrelated Prices

Javeria Iqbal\*<sup>1</sup>

Department of Computer Science,  
International Islamic University, Malaysia

\*Corresponding Author

Asadullah Shah<sup>3</sup>

Department of Information Systems,  
International Islamic University, Malaysia

Iftikhar Ahmad<sup>2</sup>

Department of Computer Science and Information Technology,  
University of Engineering and Technology, Peshawar, Pakistan

**Abstract**—The classical uni-directional conversion algorithms are based on the assumption that prices are arbitrarily chosen from the fixed price interval  $[m, M]$  where  $m$  and  $M$  represent the estimated lower and upper bounds of possible prices  $0 < m \leq M$ . The estimated interval is erroneous and no attempts are made by the algorithms to update the erroneous estimates. We consider a real world setting where prices are interrelated, i.e., each price depends on its preceding price. Under this assumption, we derive a lower bound on the competitive ratio of randomized non-preemptive algorithms. Motivated by the fixed and erroneous price bounds, we present an update model that progressively improves the bounds. Based on the update model, we propose a non-preemptive reservation price algorithm  $RP^*$  and analyze it under competitive analysis. Finally, we report the findings of an experimental study that is conducted over the real world stock index data. We observe that  $RP^*$  consistently outperforms the classical algorithm.

**Keywords**—Time series search; one-way trading; online algorithms; update model

## I. INTRODUCTION

In an online problem setting, decisions are made with no or partial information about the future. A classic example is the *uni-directional conversion problem*, where a player wants to convert an asset in hand to a desired asset, say dollars to yens. The objective is to obtain the maximum amount of the desired asset (yens) at the end of a fixed length time horizon. The caveat is the unavailability of future conversion prices and the inability to accept a price from the past. The uni-directional conversion problem is an extension of time series search problem, which is a well-studied problem in computer science and operations research with applications in many financial domains, e.g., robust option pricing, secretary selection, job employee searches, and lowest price of goods [1].

Formally, we define online conversion problem as follows. Let  $m$  and  $M$  be the estimated lower and upper bounds of all price offers. Assume (w.l.o.g) that at the start of the investment horizon, the online player has  $D_0 = 1$  units of an asset and  $Y_0 = 0$  units of the desired asset. At each time point  $t = [1, T]$ , the online player is offered a price  $q_t \in [m, M]$  to convert  $D$  to  $Y$ . She has to make an irrevocable conversion decision, with the objective to maximize the amount of  $Y$  at the end of the investment horizon. If the online player accepts  $q_t$ , she converts  $D$  (whole or a portion) to  $Y$ . The game ends

when the player has converted all of  $D$  into  $Y$  or the last price  $q_T$  is revealed, which must be accepted. The player may convert all her wealth at one point of time (*non-preemptive conversion*) or may divide her wealth and spend little by little (*preemptive conversion*). In this work, we restrict to non-preemptive conversion.

Competitive analysis is the prevalent method for the design and analysis of online conversion algorithms. Competitive analysis measures the performance of an online algorithm against an optimum offline algorithm. Let  $\mathcal{ON}$  be an online algorithm for a profit maximization problem  $\mathcal{P}$ ,  $\mathcal{I}$  be the set of all inputs instances, and  $\mathcal{OPT}$  be an optimum offline algorithm for the same problem  $\mathcal{P}$ . Given any  $I \in \mathcal{I}$ ,  $\mathcal{ON}(I)$  and  $\mathcal{OPT}(I)$  denote the performance of  $\mathcal{ON}$  and  $\mathcal{OPT}$  on input  $I \in \mathcal{I}$  respectively.  $\mathcal{ON}$  is called  $c$ -competitive if  $\forall I \in \mathcal{I}$ ,

$$\mathcal{ON}(I) \geq \frac{1}{c} \cdot \mathcal{OPT}(I) \quad (1)$$

A considerable body of literature is devoted to online conversion problems [2], [3], [1], [4], [5]. To design online algorithms for uni-directional conversion problems with a bounded competitive ratio, it is imperative to assume a-priori information about the future [3]. For instance, the classical reservation price policy ( $RP$ ) of El-Yaniv [3] assumes a-priori knowledge of  $m$  and  $M$ , and calculates a reservation price  $q^* = \sqrt{Mm}$ . Any offered price which is at least  $q^*$  is accepted, if no such price is observed then the last price offer is accepted.  $RP$  guarantees a worst case competitive ratio  $\sqrt{M/m}$  [3]. The assumption of  $RP$  and other algorithms about a priori information is impractical when the real world applicability of online algorithms is considered.

In the real world; *i*) such information is either not available or is prone to errors. Algorithms presented in the literature (see Mohr et al. [6]) keep the estimated information fixed for the complete duration of the investment horizon and make no attempt to improve the quality of the assumed parameters. *ii*) The price fluctuation is bounded and is enforced by the circuit breaker rules (Chen et al.,[2]; Hu et al. [4]). The rules fix a minimum and a maximum permissible price movement and restrict the drastic change in stock prices. Most of the algorithms including  $RP$  consider the arbitrary price movement in the range  $[m, M]$ , which permits the inter-day price fluctuation to



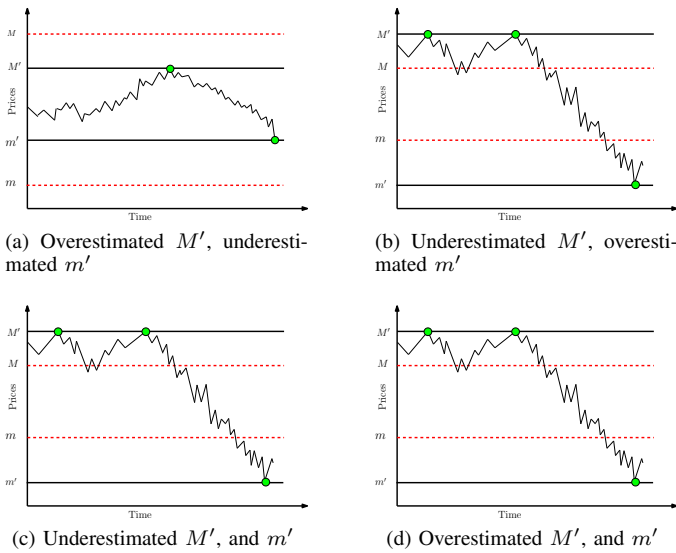


Fig. 1. Estimating the price interval  $[m, M]$  can lead to four types of errors; the green dots represent the true (observed) lower and upper bounds, whereas the red dotted line represents the estimated bounds

be  $M/m$ , i.e.,  $M$  can be followed by  $m$  and vice versa. These facts motivate us to study the problem of uni-directional non-preemptive conversion under the assumptions that the lower and upper price bounds are erroneous, fixed and arbitrarily drawn from the interval  $[m, M]$ . It must also be noted that source for acquiring the estimated values of  $m$  and  $M$  is not relevant as the values can be obtained by using a variety of forecasting techniques [7].

Let the true (exact) lower and upper bounds in a time series be represented by  $m'$  and  $M'$  respectively. The estimation errors in the values of  $m$  and  $M$  can be classified into four categories (see Fig. 1).

- i.  $m'$  is underestimated and  $M'$  is overestimated, i.e.,  $m < m'$  and  $M > M'$  (Fig. 1a).
- ii.  $m'$  is overestimated and  $M'$  is underestimated, i.e.,  $m > m'$  and  $M < M'$  (Fig. 1b).
- iii. Both  $m'$  and  $M'$  are underestimated, i.e.,  $m < m'$  and  $M < M'$  (Fig. 1c)
- iv. Both  $m'$  and  $M'$  are overestimated, i.e.,  $m > m'$  and  $M > M'$  (Fig. 1d)

This work is restricted to the type of error where  $M \geq M'$  and  $m \leq m'$ . Other cases are not considered as it is not possible to design an online algorithm with a bounded competitive ratio when  $M' > M$  (i.e.,  $M'$  can be infinity) and/or  $m' < m$  (i.e.,  $m'$  can be zero) [3], [6].

This work contributes towards the applicability of online conversion algorithms in the real world by considering the *bounded daily return model* [4] where the current price  $q_t$  depends on the previous price  $q_{t-1}$  as follows:

$$(1 - \gamma)q_{t-1} \leq q_t \leq (1 + \gamma)q_{t-1} \quad (2)$$

Note that  $\gamma \in ]0, 1[$ .

Rest of the paper is organized as follows: Section II briefly presents the relevant literature review. Next, based on the assumption that prices are interrelated, a lower bound on the competitive ratio for any randomized non-preemptive reservation price algorithm is derived in Section III. In Section IV, an update model is introduced that dynamically improves the erroneous bounds ( $m$  and  $M$ ) based on the inter-day price fluctuation. As an application, the update model is applied to the classical algorithm  $RP$  resulting in the modified policy  $RP^*$ .  $RP^*$  policy is analyzed under competitive analysis and minimum improvement in the competitive ratio is derived in relation to  $RP$ . Further, the extension of the update model and algorithm  $RP^*$  to the general price function of Chen et al. [2] is also discussed. In Section V,  $RP$  and  $RP^*$  are simulated over the real world stock index and the relative performance of each algorithm with respect to the optimum offline algorithm is reported. Section VI concludes the work and provides directions for future research.

## II. RELATED WORK

Besides the work of El-Yaniv [3], and El-Yaniv et al. [1], other major works includes that of Chen et al. [2], Hu et al. [4], and Schroeder et al. [5]. Chen et al. [2] observed that in the real world, the prices movement is not arbitrary but is restricted and governed by a set of rules. For example, in Bangkok stock market the current day price can fluctuate at maximum of 10% of the yesterday's price. Chen et al. [2] claimed, that the current day price  $q_t \in [\frac{q_{t-1}}{\alpha}, \beta q_{t-1}]$  with  $\alpha, \beta \geq 1$ . Hu et al. [4] simplified the Chen et al. [2] model by presenting a *bounded daily return* model of stock prices where each price offer depends on the yesterday's price with  $(1 - \gamma)q_{t-1} \leq q_t \leq (1 + \gamma)q_{t-1}$  for some fixed  $0 < \gamma < 1$ .

Iqbal and Ahmad [8] considered  $k$ -min search problem and proposed an optimum algorithm. The algorithm is based on reservation price and threat based algorithms of El-Yaniv et al. [1]. The authors validated the performance of their proposed algorithm against that of Lorenz et al. [9] by conducting experiments on the real world data. Wand and Xu [10] focused on a special case of the secretary problem where the number of applicants are not large, and there is a parameter to measure the ability of the applicant. The authors proved that their policy is better than that of Lorenz et al. [9]. Hasegawa and Itoh [11] considered multi-objective time series search problem (*MOTSS*) and put forth a modified version of competitive analysis for *MOTSS*. The authors presented an online algorithm called *Balanced Price Policy* for *MOTSS* and discussed that the presented policy is the best under the competitive analysis paradigm. Fung [12] considered two way trading problem, knowledge of  $m$  and  $M$  to derive a lower bound of  $\phi = M/m$  for a single trade problem. Further, the author generalized the work to  $k$ -trade problem and shown the competitive ratio to be  $\phi^{(2k+1)/3}$ .

Schroeder et al. [5] considered the time series search problem with inter-related prices and a profit function. The authors presented algorithms with bounded competitive ratio, and proved the optimality of the algorithms as well. For a detailed survey on online algorithm for conversion problems, the reader is referred to Mohr et al. [6].

To the best of our knowledge, there is no conclusive evidence of any study which examines the online algorithms

under the estimated values of parameters and suggests measures to improve the competitive ratio by improving the quality of the estimated parameters. Mahdian et al. [13] analyzed different online problems under estimated values of input parameters. One such problem is allocation of online advertisement space. In an online allocation of advertisement space, a search engine allocates an advertisement slot to a bidder based on the query term of the user. In order to optimally allocate the advertisement space, the estimated frequency of each search term is assumed to be known and the problem is solved using linear programming. However, the estimation can turned out to be completely wrong and the solution is no more optimal and competitive. Mahdian et al.[13] analyzed the problem under incorrect estimates but did not discuss any mechanism to improve the erroneous information in order to improve the performance of the algorithm.

### III. LOWER BOUND FOR RANDOMIZED ALGORITHM WITH INTER-DAY PRICE FLUCTUATION FUNCTION

Yao's minmax principle is used to obtain a lower bound on the competitive ratio of randomized algorithms [14]. In simple words, Yao's principle states that in order to obtain a lower bound on the competitive ratio of the best randomized algorithm, it is sufficient to calculate the performance of the best deterministic algorithm for a chosen probability distribution of input instances (see Borodin and El-Yaniv[14]; Lorenz et al. [9] for details). The same technique is employed to derive the lower bound of best uni-directional non-preemptive randomized algorithm when the prices are governed by the price function of Hu et al. [4](cf. Eq. (2)).

**Theorem 1.** *Assuming that prices follow the inter-day price fluctuation function as shown in Eq (2). Let fluctuation ratio  $\phi > 1$ , for online uni-directional non-preemptive conversion problem, no randomized algorithm can achieve a better competitive ratio than  $c$  where;*

$$c = \log \phi \frac{\gamma}{2(1+\gamma)\log(1+\gamma)}. \quad (3)$$

*Proof:* Let  $\mathcal{I}$  be the set of all input instances, we consider  $\mathcal{I}^\gamma \in \mathcal{I}$  such that all  $I \in \mathcal{I}^\gamma$  follows the price function of Hu et al. [4]. Let  $RAND$  be the best randomized algorithm for online uni-directional non-preemptive conversion problem. We need to show that competitive ratio achieved by  $RAND$ ,  $c(RAND) \geq c$ . Using the Yao's principle it will be sufficient to show that on the worst case probability distribution  $y(I)$ , the ratio of average optimum offline return to average return of any deterministic algorithm  $ON \in \mathcal{ON}$  is bounded below from  $c$  [15], [9], i.e.,

$$\left( \max_{ON \in \mathcal{ON}} E \left[ \frac{ON(I)}{OPT(I)} \right] \right)^{-1} \geq c \quad (4)$$

In order to prove Eq. (4), we consider the worst case sequences  $I_j \in S^\gamma$  such that  $S^\gamma \subset \mathcal{I}^\gamma$  denotes the worst case price sequences. We define our worst case input to be of the following form; ( $0 \leq j \leq N-1$ )

$$I_j = m(1+\gamma)^0, m(1+\gamma)^1, \dots, m(1+\gamma)^j, \\ m(1+\gamma)^j(1-\gamma), m(1+\gamma)^j(1-\gamma)^2, \dots, m$$

It shows that the worst case sequence  $I_j$  is increasing with a factor  $(1+\gamma)$  till time point  $j+1$ , after which it decreases

with a factor  $(1-\gamma)$ .  $I_j$  represents a worst case instance because if the only player accepts an offered price (too early error), adversary has the option to keep on increasing the price sequence to achieve a maximum profit. Similarly, if the online player keeps on rejecting offered price (too late error), the adversary can drop the offered price gradually to  $m$  and force the online player to accept the last offered price  $m$ .

Our distribution of sequences follows price function and we are only interested in price sequence which is in the form of  $I_j$ . We define the probability distribution  $y$  on  $\mathcal{I}^\gamma$  by

$$y(I) = \begin{cases} \frac{1}{N} & \text{if } I \in S^\gamma \\ 0 & \text{otherwise} \end{cases}$$

**Remark 1.** *The maximum fluctuation  $\phi$  of any price sequence in  $S^\gamma$  is bounded by  $(1+\gamma)^N$ .*

The above remark can easily be proved by considering the price sequence  $I_{N-1}$ ;

$$I_{N-1} = m(1+\gamma)^0, \dots, m(1+\gamma)^{N-1}, m(1+\gamma)^{N-1}(1-\gamma), \\ m(1+\gamma)^{N-1}(1-\gamma)^2, \dots, m$$

The maximum price observed is  $m(1+\gamma)^{N-1}$  and the minimum observed price is  $m$ . Therefore, the fluctuation ratio  $\phi = (1+\gamma)^{N-1} < (1+\gamma)^N$ .

Now we compute  $E \left[ \frac{ON(I)}{OPT(I)} \right]$  as under; Consider the last price sequence  $I_{N-1}$ ;

$$I_{N-1} = m(1+\gamma)^0, \dots, m(1+\gamma)^{N-1}, m(1+\gamma)^{N-1}(1-\gamma), \\ m(1+\gamma)^{N-1}(1-\gamma)^2, \dots, m$$

Assume (w.l.o.g) that,  $ON$  accepts  $m(1+\gamma)^p$  on  $I_{N-1}$ , it means that on all sequences where  $m(1+\gamma)^p$  appears,  $ON$  will accept  $m(1+\gamma)^p$ . This case corresponds to *too early error*. On all other sequences,  $ON$  will convert at the last offered price  $m$  which corresponds to *too late error*. As all worst case sequences are increasing up to time point  $j+1$ ,  $m(1+\gamma)^p$  appears in  $I_j$  where  $j = p$  to  $N-1$ . Therefore,  $E \left[ \frac{ON(I)}{OPT(I)} \right]$  will be;

$$E \left[ \frac{ON(I)}{OPT(I)} \right] = \frac{1}{N} \left( \sum_{0 \leq j \leq p-1} \frac{m}{m(1+\gamma)^j} + \sum_{p \leq j < N} \frac{m(1+\gamma)^p}{m(1+\gamma)^j} \right), \\ = \frac{1}{N} \left( \frac{(1+\gamma) - (1+\gamma)^{1-p}}{\gamma} + \frac{(1+\gamma) - (1+\gamma)^{p+1-N}}{\gamma} \right) \\ = \frac{(1+\gamma)(2 - (1+\gamma)^{p-N} - (1+\gamma)^{-p})}{N\gamma}. \quad (5)$$

To find the value of  $p$ , where maximum value of  $E \left[ \frac{ON(I)}{OPT(I)} \right]$  is observed, we take the derivative of Eq (5) with respect to  $p$ ;

$$\frac{d}{dp} \left( E \left[ \frac{ON(I)}{OPT(I)} \right] \right) = 0$$

$$\frac{d}{dp} \left( \frac{(1+\gamma)(2 - (1+\gamma)^{p-N} - (1+\gamma)^{-p})}{N\gamma} \right) = 0$$

We obtain,  $p = N/2$ . Replacing the value of  $p = N/2$  and  $N = \log_{(1+\gamma)}\phi$ , we obtain;

$$\max E \left[ \frac{ON(I)}{OPT(I)} \right] \leq \frac{1}{\log\phi} \left[ \frac{2(1+\gamma)\log(1+\gamma)}{\gamma} \right]$$

Applying the Yao's principle;

$$c(RAND) \geq \left( \max_{ON \in \mathcal{ON}E} E \left[ \frac{ON(I)}{OPT(I)} \right] \right)^{-1} \geq \log\phi \frac{\gamma}{2(1+\gamma)\log(1+\gamma)} \quad (6)$$

The proof follows. ■

Remember that  $\phi$  cannot be  $\infty$  as otherwise it will not be possible to design an online algorithm with bounded competitive ratio [3].

Lorenz et al. [9] showed that for online uni-directional non-preemptive conversion problem, no randomized algorithm can achieve a competitive ratio better than  $\bar{c} \geq \frac{\ln(\phi)}{2}$ . The authors assumed that the prices are arbitrarily drawn from the known interval  $[m, M]$  and did not enforce an inter-day price function. A  $\tilde{c} \geq \log\phi \frac{\gamma}{2(1+\gamma)\log(1+\gamma)}$  lower bound of is derived assuming that the inter-day price movement is bounded by the price function of Hu et al. [4]. Fig. 2 shows the ratio  $\bar{c}/\tilde{c}$  based on the increasing value of  $\gamma \in ]0, 1[$ . The results conform to the real world observation.

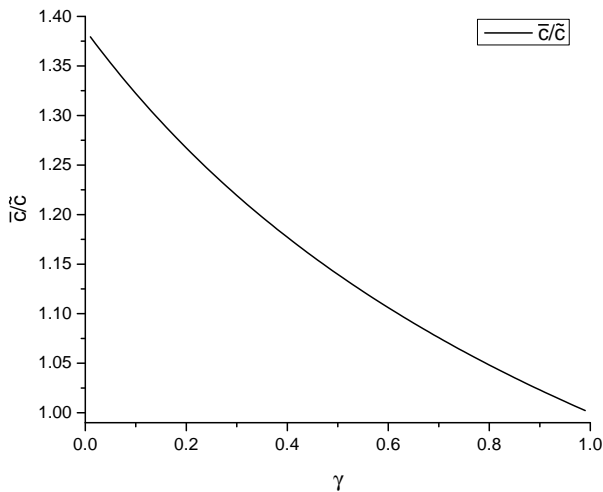


Fig. 2. Ratio of  $\bar{c}$  and  $\tilde{c}$

**Remark 2.** Intuitively speaking, the lower the inter-day price fluctuation, the lower the price movement and thus a better performance can be achieved. Our results confirms the same, for values of  $\gamma$  closer to 0,  $\tilde{c}$  is considerably lower than  $\bar{c}$ . As  $\gamma$  approaches 1,  $\tilde{c}$  approaches  $\bar{c}$ . However, our lower bound is lower than the lower bound shown by Lorenz et al. [9] for all values of  $\gamma \in ]0, 1[$ .

#### IV. PROPOSED MODEL AND ALGORITHM

In the following, the update model and the deterministic non-preemptive reservation price policy  $RP^*$  is presented and analyzed. The performance improvement of  $RP^*$  in comparison to  $RP$  is derived and the applicability of results for a general price fluctuation function is discussed.

#### A. Update Model

The basic purpose of the *update model* is to keep the initial estimated upper and lower bounds realistic based on the observed price, the inter-day price fluctuation and the remaining number of days. Further, the need of using the price function of Hu et al. [4] is discussed and the *update model* is presented.

A challenging aspect of any update mechanism is to model the stock prices. The behavior of stock prices is highly volatile and a plethora of work is dedicated to obtain an accurate view of stock price movement [16], [17]. Geometric Brownian Motion (*GBM*) is one of several attempts to model the random stock price movement in Black-Scholes model [18], [19]. However, it is hard to obtain an accurate GBM and the approximation of GBM is utilized [2].

In this work, the *bounded daily return* model of stock market introduced by Hu et al. [4] is considered. Recall that the price function restricts the price movement as under;

$$(1-\gamma)q_{t-1} \leq q_t \leq (1+\gamma)q_{t-1} \text{ with } 0 < \gamma < 1 \quad (7)$$

Eq.(7) is considered as an approximation to *GBM* [4] which can be used to model the stock price behavior.

El-Yaniv [3] assumed a fixed price interval in which all the prices must lie whereas Hu et al. [4] considered the bounds for inter-day price fluctuation. In this work, a dual approach is employed and the initial estimated bounds  $[m, M]$  as well as the inter-day price fluctuation factor  $\gamma$  are considered.

The update model computes the minimum and the maximum price bounds that can be achieved in the remaining number of days based on the current day price  $q_t$  and  $\gamma$ , as shown in Fig. 3. On each day  $t$  a price offer  $q_t$  is observed and compute:

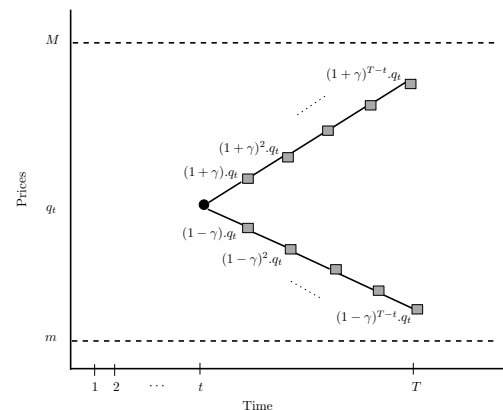


Fig. 3. Computing the achievable lower and upper bounds on day  $t$

- i. The minimum price (lower bound) that can be reached if prices keep on decreasing with a factor  $\gamma$  of which is  $q_t(1-\gamma)^{T-t}$ .
- ii. The maximum price (upper bound) that can be reached if prices keep on increasing with a factor  $\gamma$  of which is  $q_t(1+\gamma)^{T-t}$ .

Considering the type 1 error (Fig. 1a) i.e.,  $M \geq M'$  and  $m \leq m'$ , the update model should improve the upper bound in a non-increasing manner whereas the lower bound in a non-decreasing way. At time period  $t = 0$ , the initial estimated lower and upper bounds are  $m_0 = m$  and  $M_0 = M$  respectively such that  $m_0 \leq q_1 \leq M_0$ . For each price offer  $q_t$  where  $t \in [1, T - 1]$ , the price interval  $[m_t, M_t]$  is updated as follows:

$$m_t = \max\{m_{t-1}, q_t(1 - \gamma)^{T-t}\} \quad (8)$$

$$M_t = \min\{M_{t-1}, q_t(1 + \gamma)^{T-t}\} \quad (9)$$

It can be seen that  $M_t$  is non-increasing whereas  $m_t$  is non-decreasing with respect to time i.e.,  $M_t \leq M_{t-1}$  and  $m_t \geq m_{t-1}$ . The updated price bounds  $[m_t, M_t]$  are used for re-computing the reservation price for the proposed algorithm  $RP^*$ .

### B. Proposed Algorithm

The formal description of  $RP^*$  is given by Algorithm 1. It must be noted that the lower and upper bounds are updated

---

#### Algorithm 1 $RP^*$

---

**Require:**  $m, M, \gamma, T$

- 1: Set  $m_0 = m, M_0 = M$
  - 2: **for**  $t=1$  to  $T-1$  **do**
  - 3:   A new price  $q_t$  is observed.
  - 4:   Compute achievable lower bound  $m_t$ :  

$$m_t = \max\{m_{t-1}, q_t(1 - \gamma)^{T-t}\}$$
  - 5:   Compute achievable upper bound  $M_t$ :  

$$M_t = \min\{M_{t-1}, q_t(1 + \gamma)^{T-t}\}$$
  - 6:   Calculate new reservation price  $q_t^* = \sqrt{m_t M_t}$
  - 7:   **if**  $q_t \geq q_t^*$  **then**
  - 8:     Accept the offered price  $q_t$
  - 9:   **end if**
  - 10: **end for**
  - 11: If no price offer is accepted till the last day  $T$ , accept the last price  $q_T$  which may be the minimum.
- 

till  $T - 1$  as if the online player has not accepted a price till the last day, then she must accept the last offered price  $q_T$ . Therefore, updating the bounds on the last day is irrelevant.

### C. Competitive Analysis of $RP^*$

**Theorem 2.** Algorithm  $RP^*$  is  $c^w(RP^*)$  such that;

$$c^w(RP^*) = \sqrt{\frac{q_j(1 + \gamma)^{T-j}}{q_i(1 - \gamma)^{T-i}}} \quad (10)$$

where  $i$  and  $j$  are the time points where the last update occurs in the value of  $m$  and  $M$ , respectively.

*Proof:* Let  $q^*$  be the reservation price (threshold) for accepting a price. The player waits for an offer such that  $q_t \geq q^*$ . Two cases are possible.

*Too Early Error::* If the reservation price computed by  $RP^*$  is too low, the adversary offers  $q^*$  early in the price sequence and then raises the offered price to the maximum  $q_{max} = q_j(1 + \gamma)^{T-j}$ . Thus,  $RP^*$  converts at  $q^*$ , and  $OPT$  converts at  $q_{max}$  resulting in a competitive ratio as follows:

$$\begin{aligned} c_1^* &= \frac{OPT}{RP^*} \\ &= \frac{q_j(1 + \gamma)^{T-j}}{q^*} \\ &= \frac{q_j(1 + \gamma)^{T-j}}{\sqrt{q_j(1 + \gamma)^{T-j} * q_i(1 - \gamma)^{T-i}}} \\ &= \sqrt{\frac{q_j(1 + \gamma)^{T-j}}{q_i(1 - \gamma)^{T-i}}} \end{aligned} \quad (11)$$

*Too Late Error::* If the reservation price calculated by  $RP^*$  is too high, the adversary offers the prices such that  $q_{max} < q^*$ . The player waits  $q^*$  for which never occurs in the price sequence. Thus  $RP^*$  converts at  $q_{min} = q_i(1 - \gamma)^{T-i}$ , and  $OPT$  converts at  $q^* - \epsilon$  where  $0 < \epsilon \ll 1$ . Thus, the competitive ratio achieved by  $RP^*$  is as follows:

$$\begin{aligned} c_2^* &= \frac{OPT}{RP^*} \\ &= \frac{q^* - \epsilon}{q_i(1 - \gamma)^{T-i}} \\ &= \frac{\sqrt{q_j(1 - \gamma)^{T-j} * q_i(1 - \gamma)^{T-i}} - \epsilon}{q_i(1 - \gamma)^{T-i}} \\ &\leq \sqrt{\frac{q_j(1 + \gamma)^{T-j}}{q_i(1 - \gamma)^{T-i}}} \end{aligned} \quad (12)$$

In both too low and too high scenarios, the competitive ratio is no worse than  $c^w(RP^*)$ . The theorem follows. ■

### D. Improvement in Competitive Ratio

In this section, the minimum improvement in competitive ratio of  $RP^*$  in relation to  $RP$  is derived. It is pertinent to mention that improvement can only be observed when there is an update in the values of  $m$  and/or  $M$ , otherwise it is nonsensical to discuss improvement. The argument is inline with that presented in the literature related to online search problem such as that of Al-Binali [20]. Al-Binali [20] claimed that improvement in the competitive ratio can only be observed when the forecast is true. In the underlying case, the improvement in competitive ratio is restricted to cases, when an update in the bounds of  $m$  and/or  $M$  occurs, if no update occurs, it means that the estimated values of  $m$  and  $M$  were accurate enough and the update model is not required. Let,  $c^r$  be the restricted competitive ratio when an update in the  $m$  and/or  $M$  occurs.

**Lemma 1.** The minimum improvement observed in the competitive ratio of  $RP^*$  in relation to  $RP$  is as follows:

$$\Delta c = \min \left\{ \sqrt{\frac{q_1(1 - \gamma)^{T-1}}{m}}, \sqrt{\frac{M}{q_1(1 + \gamma)^{T-1}}}, \sqrt{\left(\frac{1 - \gamma}{1 + \gamma}\right)^{T-1}} \sqrt{\frac{M}{m}} \right\} \quad (13)$$

*Proof:* Depending on the modified value of  $m$  and/or  $M$ , there are three possible scenarios;

- i. *Update in the value of  $m$  only:* As there is an update in the value of  $m$ , the upper bound  $M$  remains unchanged. The restricted competitive ratio  $c_1^r(RP^*)$  is as follows:

$$c_1^r(RP^*) = \sqrt{\frac{M}{q_i(1-\gamma)^{T-i}}}$$

As  $M$  is constant, the maximum competitive ratio  $c_1^r(RP^*)$  is observed when the update occurs at day 1, i.e.,  $i = 1$ . The restricted competitive ratio observed is as follows:

$$c_1^r(RP^*) \leq \sqrt{\frac{M}{q_1(1-\gamma)^{T-1}}}$$

The minimum improvement in the competitive ratio of  $RP^*$  in comparison to  $c^w(RP)$  is as follows:

$$\begin{aligned} \frac{c^w(RP)}{c_1^r(RP^*)} &\geq \frac{\sqrt{M/m}}{\sqrt{\frac{M}{q_1(1-\gamma)^{T-1}}}} \\ &\geq \sqrt{\frac{q_1(1-\gamma)^{T-1}}{m}} \end{aligned} \quad (14)$$

- ii. *Update in the value of  $M$  only:* When an update in the value of only  $M$  is observed,  $c_2^r(RP^*)$  achieved is:

$$c_2^r(RP^*) = \sqrt{\frac{q_j(1+\gamma)^{T-j}}{m}}$$

To maximize  $c_2^r(RP^*)$ ,  $q_j(1+\gamma)^{T-j}$  must be maximized ( $m$  being constant).  $q_j(1+\gamma)^{T-j}$  is maximized at  $j = 1$ , and thus the competitive ratio  $c_2^r(RP^*)$  is achieved as follows:

$$c_2^r(RP^*) \leq \sqrt{\frac{q_1(1+\gamma)^{T-1}}{m}}$$

The improvement in the competitive ratio is:

$$\begin{aligned} \frac{c^w(RP)}{c_2^r(RP^*)} &\geq \frac{\sqrt{M/m}}{\sqrt{\frac{q_1(1+\gamma)^{T-1}}{m}}} \\ &\geq \sqrt{\frac{M}{q_1(1+\gamma)^{T-1}}} \end{aligned} \quad (15)$$

- iii. *Update in the value of  $m$  and  $M$ :* When an update in the value of  $m$  and  $M$  is observed,  $c_3^r(RP^*)$  is achieved such that

$$c_3^r(RP^*) = \sqrt{\frac{q_j(1+\gamma)^{T-j}}{q_i(1-\gamma)^{T-i}}}$$

To maximize  $c_3^r(RP^*)$ ,  $q_j(1+\gamma)^{T-j}$  must be maximized, whereas  $q_i(1-\gamma)^{T-i}$  must be minimized. The maximum value of  $q_j(1+\gamma)^{T-j}$  is observed for  $j = 1$ , whereas the minimum value of  $q_i(1-\gamma)^{T-i}$  is observed for  $i = 1$ . The restricted competitive ratio  $c_3^r(RP^*)$  is as follows:

$$\begin{aligned} c_3^r(RP^*) &\leq \sqrt{\frac{q_1(1+\gamma)^{T-1}}{q_1(1-\gamma)^{T-1}}} \\ &\leq \sqrt{\left(\frac{1+\gamma}{1-\gamma}\right)^{T-1}} \end{aligned}$$

The improvement in competitive ratio is as follows:

$$\begin{aligned} \frac{c^w(RP)}{c_3^r(RP^*)} &\geq \frac{\sqrt{M/m}}{\sqrt{\left(\frac{1+\gamma}{1-\gamma}\right)^{T-1}}} \\ &\geq \sqrt{\left(\frac{1-\gamma}{1+\gamma}\right)^{T-1}} \sqrt{\frac{M}{m}} \end{aligned} \quad (16)$$

The proof follows from Eqs. (14,15, and 16). ■

### E. Extending Results to a General Price Function

In this work, the price function of Hu et al. [4] is used, which is based on a constant price fluctuation factor  $\gamma$ . The results can be extended to the general price fluctuation function of Chen et al.[2] where the inter-day price fluctuation is bounded by two constants  $\alpha$  and  $\beta$ , i.e.,  $q_t$  can either decrease by a factor  $\alpha$  of  $q_{t-1}$  or increase by  $\beta$  times  $q_{t-1}$ . In the following, the competitive ratio achieved by  $RP^*$  using the price fluctuation function of Chen et al. [2] is discussed.

**Lemma 2.**  $c^w(RP^*)$  is valid for the general price function of Chen et al. [2].

*Proof:* Recall the price fluctuation function of Hu et al. [4] is given as follows:

$$(1-\gamma)q_{t-1} \leq q_t \leq (1+\gamma)q_{t-1}, \quad \text{with } 0 < \gamma < 1. \quad (17)$$

The price fluctuation function of Chen et al. [2] is given as follows;

$$\frac{q_{t-1}}{\alpha} \leq q_t \leq \beta q_{t-1}, \quad \text{with } \alpha, \beta \geq 1. \quad (18)$$

Comparing both Eq. (17) and (18) follows;

$$\begin{aligned} \alpha &= \frac{1}{1-\gamma} \\ \beta &= 1+\gamma. \end{aligned}$$

From Eq. (10), the competitive ratio  $c^w(RP^*)$  achieved by  $RP^*$  is as follows:

$$c^w(RP^*) = \sqrt{\frac{q_j(1+\gamma)^{T-j}}{q_i(1-\gamma)^{T-i}}}$$

Replacing  $(1+\gamma)$  by  $\beta$  and  $(1-\gamma)$  by  $1/\alpha$ ;

$$c^w(RP^*) = \sqrt{\frac{q_j(\beta)^{T-j}}{q_i(1/\alpha)^{T-i}}}$$

The proof follows. ■

## V. EXPERIMENTAL SIMULATION

The online algorithms for conversion problems are experimentally evaluated using real world data. For details, the reader is referred to Chen et al. [2], Hu et al. [4], Iqbal et al. [21] and Mohr et al. [6] (Section 5). In this section,  $OPT$ ,  $RP$ , and  $RP^*$  are simulated over the daily closing prices of *Deutscher Aktien Index* (DAX30) for ten years (01.Jan.2008 to 31.Dec.2017). Recall that  $OPT$  is the optimum offline algorithm that always converts on the maximum observed price.

### A. Methodology

As  $OPT$ ,  $RP$ , and  $RP^*$  perform only a single transaction, therefore, no transaction fee is considered. It is also assumed that the algorithms have the required a-priori information ( $\gamma$  and  $T$ ). However, in a real world setting, the true (exact) lower and upper bounds ( $m'$  and  $M'$ ) of prices are unknown. Therefore, it is assumed that there is error in estimation in the values of  $m'$  and  $M'$ . If true bounds are known, the reservation price calculated by  $RP$  is  $q^* = \sqrt{Mm}$ . The algorithms rely on the estimated bounds ( $m$ ,  $M$ ). Therefore, the reservation price  $q^*$  can either decrease or increase depending on the estimation error in bounds, i.e.,  $q^* = \delta\sqrt{Mm}$  where  $0 < \delta < \infty$ .

The estimation error  $\sigma$  in the lower and upper bounds are introduced such that the reservation price  $q^*$  (of  $RP$ ) is either decreased ( $\delta = 0.85$ ) or increased ( $\delta = 1.15$ ) by 15% of its exact value. The findings are based on the monthly as well as the yearly performance of algorithms. The dataset is partitioned into subsets where each subset represents an investment horizon of one month, thus resulting in 120 subsets for 10 years. The price fluctuation factor  $\gamma$  is extracted from each subset using Eq. (2).

On a given input  $\sigma$ , let,  $OPT(\sigma)$ ,  $RP(\sigma)$  and  $RP^*(\sigma)$  be the performance of  $OPT$ ,  $RP$ , and  $RP^*$  respectively. The performance of each algorithm ( $OPT$ ,  $RP$ , and  $RP^*$ ) is observed by executing them over 120 subsets of data. For ease of comparison, the performance ratios  $c^e(RP) = \frac{OPT(\sigma)}{RP(\sigma)}$  and  $c^e(RP^*) = \frac{OPT(\sigma)}{RP^*(\sigma)}$  is computed. As no algorithm can perform better than  $OPT$ , the performance ratios  $c^e(RP)$ , and  $c^e(RP^*)$  are at least one. The lower value of performance ratio (close to 1) indicates a better outcome. Further, the performance improvement of  $RP^*$  over  $RP$  by the improvement factor  $\frac{c^e(RP)}{c^e(RP^*)}$ , based on the varying values of the estimation error  $\sigma = [0.75, 1.25]$  is shown.

### B. Results

Fig. 4 summarizes the monthly competitive ratios by  $RP$  and  $RP^*$  for  $\sigma = 0.85$ . It is observed that on all 120 monthly data sets,  $c^e(RP^*) \leq c^E(RP)$ . On average,  $c^e(RP^*)$  is 2.5% better than  $c^e(RP)$ . It is noticed that on few instance, the experimental competitive ratio of  $RP$  is worse (greater) than the guaranteed worst case competitive ratio, i.e.,  $c^e(RP) > c^w(RP)$ . This behavior suggests that the estimation error can render the worst case guarantee useless. In contrast to  $RP$ , algorithm  $RP^*$  performs better by consistently achieving lower competitive ratio. On all 120 subsets,  $RP^*$  never performs worse than  $\sqrt{M/m}$ , thus ensuring that the worst case bounds are always respected. The worst (highest) value of  $c^e(RP)$

and  $c^e(RP^*)$  are 1.21 and 1.09 respectively. Similarly, for  $\sigma = 1.15$ ,  $RP^*$  outperforms  $RP$  as depicted in Fig. 5. Interestingly, the maximum (worst)  $c^e(RP)$  is 1.21 whereas the corresponding value of  $c^e(RP^*)$  is 1.09, i.e., the same values of  $c^e(RP)$  and  $c^e(RP^*)$  is observed when  $\sigma$  changes from 0.85 to 1.15.. It must be noted that for  $\sigma = 0.85$ , the worst (maximum) value is observed in Oct 2008, whereas for  $\sigma = 1.15$  the worst value is observed for Feb 2009.

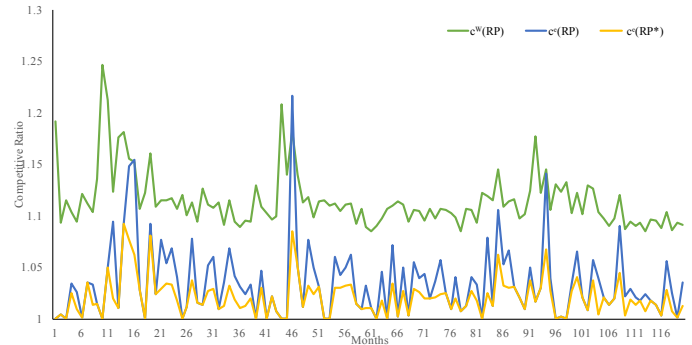


Fig. 4. Monthly Performance with Estimation Error  $\delta = 0.85$

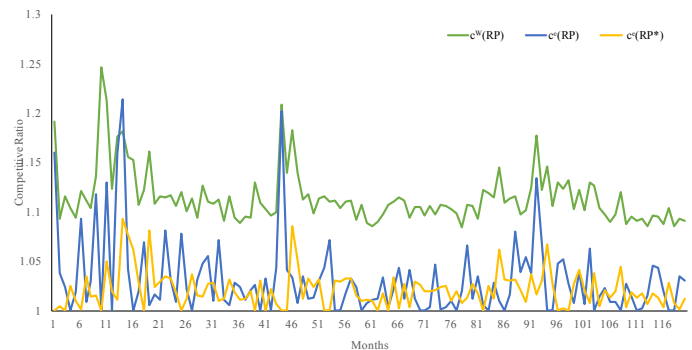


Fig. 5. Monthly Performance with Estimation Error  $\delta = 1.15$

The competitive ratios of  $RP$  and  $RP^*$  over yearly data with  $\sigma = 0.85$  are shown in Fig. 6. The worst  $c^e(RP)$  is 1.06 observed for year 2009. In contrast, the worst  $c^e(RP^*)$  over 10 years period is 1.04 also seen in year 2009.  $RP^*$  beats  $RP$  over all the years and never violates the worst case bound  $c^w(RP^*)$ . The performance of both algorithms with  $\sigma = 1.15$  is shown in Fig. 7. The same trends is observed for  $\sigma = 1.15$  as is seen for  $\sigma = 0.85$ . Again,  $RP^*$  outperforms  $RP$ .

In order to observe the improvement in experimentally achieved competitive ratio for varying values of  $\sigma$ , consider  $\sigma = \{0.75, 0.76, \dots, 1, \dots, 1.24, 1.25\}$ . For each value of  $\sigma$ , the average competitive ratio of  $RP$  and  $RP^*$  is computed over the 120 monthly subsets of data. Fig. 8 plots the improvement factor  $c^e(RP)/c^e(RP^*)$ . An improvement factor greater than 1 depicts that  $RP^*$  outperforms  $RP$ . For  $\sigma < 0$ ,  $RP^*$  performs better than  $RP$ . A constant improvement of 1.014 is observed when  $\sigma = [0.75, 0.9]$ . For  $\sigma = 1$ , both algorithms achieve a same competitive ratio. Over a small range when  $\sigma = [1.01, 1.04]$ , the performance of  $RP$  is better than  $RP^*$ .

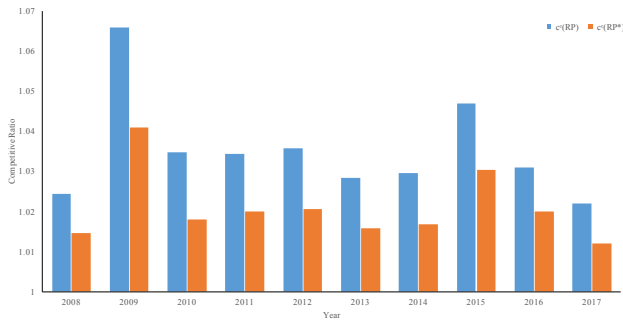


Fig. 6. Yearly Competitive Ratios with Estimation Error  $\delta = 0.85$

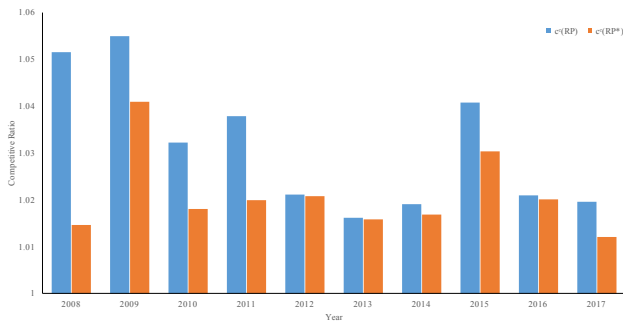


Fig. 7. Yearly Competitive Ratios with Estimation Error  $\delta = 1.15$

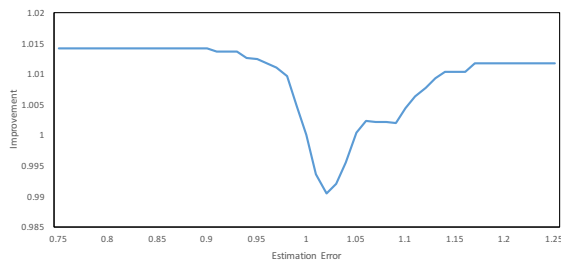


Fig. 8. Improvement Factor for  $\delta \in [0.75, 1.25]$

However, a consistent improvement is reported in competitive ratio of  $RP^*$  to that of  $RP$ , for  $\sigma > 1.04$ .

## VI. CONCLUSION

This work focused on bridging the gap between the theory and practice of online conversion problems by improving the quality of the estimated bounds using the update model. The model is a first step towards modifying the erroneous information for improving the performance of algorithms. A lower bound on the competitive ratio of randomized non-preemptive algorithms assuming the prices are interrelated is derived. Furthermore, algorithm is presented and evaluated using theoretical as well as experimental measures. The experimental simulation of algorithms over the real world data validated the approach of the update model. The work can be extended to investigate the preemptive algorithms under the update model. Further, the online algorithms under estimated values of the parameters can be studied in other areas such as job scheduling, cache algorithms, online advertisement space

allocation, etc.

## REFERENCES

- [1] R. El-Yaniv, A. Fiat, R. M. Karp, and G. Turpin, "Optimal search and one-way trading online algorithms," *Algorithmica*, vol. 30, pp. 101–139, 2001.
- [2] G. Chen, M. Kao, Y. Lyuu, and H. Wong, "Optimal buy-and-hold strategies for financial markets with bounded daily returns," *SIAM Journal on Computing*, vol. 31, no. 2, pp. 447–459, 2001.
- [3] R. El-Yaniv, "Competitive solutions for online financial problems," *ACM Computing Surveys*, vol. 30, no. 1, pp. 28–69, 1998.
- [4] S. Hu, Q. Guo, and H. Li, "Competitive analysis of on-line securities investment," in *Algorithmic Applications in Management*, ser. Lecture Notes in Computer Science, N. Megiddo, Y. Xu, and B. Zhu, Eds. Springer, 2005, vol. 3521, pp. 224–232.
- [5] P. Schroeder, R. Dochow, and G. Schmidt, "Optimal solutions for the online time series search and one-way trading problem with interrelated prices and a profit function," *Computers & Industrial Engineering*, vol. 119, pp. 465 – 471, 2018. [Online]. Available: <http://www.sciencedirect.com/science/article/pii/S036083521830127X>
- [6] E. Mohr, I. Ahmad, and G. Schmidt, "Online algorithms for conversion problems: a survey," *Surveys in Operations Research and Management Science*, vol. 19, no. 2, pp. 87–104, 2014.
- [7] J. Arroyo, R. Espínola, and C. Maté, "Different approaches to forecast interval time series: A comparison in finance," *Computational Economics*, vol. 37, pp. 169–191, 2011. [Online]. Available: <http://dx.doi.org/10.1007/s10614-010-9230-2>
- [8] J. Iqbal and I. Ahmad, "Optimal online  $k$ -min search," *EURO Journal on Computational Optimization*, vol. 3, no. 2, pp. 147–160, 2015.
- [9] J. Lorenz, K. Panagiotou, and A. Steger, "Optimal algorithms for  $k$ -search with application in option pricing," *Algorithmica*, vol. 55, no. 2, pp. 311–328, 2009.
- [10] S. Wang and Y. Xu, "Online  $k$ -max search algorithms with applications to the secretary problem," in *International Conference on Algorithmic Applications in Management*. Springer, 2016, pp. 209–221.
- [11] S. Hasegawa and T. Itoh, "Optimal online algorithms for the multi-objective time series search problem," *Theoretical Computer Science*, vol. 718, pp. 58–66, 2018.
- [12] S. P. Fung, "Optimal online two-way trading with bounded number of transactions," in *International Computing and Combinatorics Conference*. Springer, 2017, pp. 212–223.
- [13] M. Mahdian, H. Nazerzadeh, and A. Saberi, "Online optimization with uncertain information," *ACM Trans. Algorithms*, vol. 8, no. 1, pp. 2:1–2:29, Jan. 2012. [Online]. Available: <http://doi.acm.org/10.1145/2071379.2071381>
- [14] A. Borodin and R. El-Yaniv, "On randomization in on-line computation," *Information and Computation*, vol. 150, no. 2, pp. 244–267, 1999.
- [15] —, *Online computation and competitive analysis*. New York, NY, USA: Cambridge University Press, 1998.
- [16] R. Norvaiša, "Modelling of stock price changes: A real analysis approach," *Finance and Stochastics*, vol. 4, pp. 343–369, 2000. [Online]. Available: <http://dx.doi.org/10.1007/s007800050077>
- [17] R. Sollis, P. Newbold, and S. Leybourne, "Stochastic unit roots modelling of stock price indices," *Applied Financial Economics*, vol. 10, no. 3, pp. 311–315, 2000.
- [18] D. Duffie, *Dynamic Asset Pricing Theory*. Princeton University Press, 2001.
- [19] J. Hull, *Options, Futures, and Other Derivative Securities*. Prentice Hall, 1993.
- [20] S. al-Binali, "A risk-reward framework for the competitive analysis of financial games," *Algorithmica*, vol. 25, pp. 99–115, 1999.
- [21] J. Iqbal, I. Ahmad, and G. Schmidt, "Can online trading algorithms beat the market? an experimental evaluation," in *Proceedings of 3rd Student Conference on Operational Research (SCOR)*, ser. OASICS, vol. 22. Schloss Dagstuhl - Leibniz Zentrum für Informatik, 2012, pp. 43–52.

# Introducing Multi Shippers Mechanism for Decentralized Cash on Delivery System

Hai Trieu Le<sup>1</sup>, Ngoc Tien Thanh Le<sup>2</sup>, Nguyen Ngoc Phien<sup>\*3</sup>, Nghia Duong-Trung<sup>4</sup>,  
Ha Xuan Son<sup>5</sup>, Thai Tam Huynh<sup>6</sup>, and The Phuc Nguyen<sup>7</sup>

<sup>1,2,4,5</sup>Cantho University of Technology, Can Tho city, Vietnam

<sup>\*3</sup>Center for Applied Information Technology, Ton Duc Thang University, Ho Chi Minh city, Vietnam

<sup>\*3</sup>Faculty of Information Technology, Ton Duc Thang University, Ho Chi Minh city, Vietnam

<sup>4,5</sup>Can Tho University of Technology, FPT University, Can Tho city, Vietnam

<sup>6</sup>Transaction Technologies PTE. LTD., Singapore

<sup>7</sup>University of Trento, Trento, Italy

**Abstract**—One of the major problems of e-commerce globally is the selling and buying of goods among the parties over the Internet in which the traders may not trust their partners. Cash on delivery allows customers to pay in cash when the product is delivered to their home or a location they choose. This is sometimes called a payment system because customers receive goods before making a payment. This paper investigates a critical verification process issue in the cash on delivery system. In particular, we propose a multi shippers mechanism, which consists of blockchain technology, smart contracts and hyperledger fabric platform to achieve distributed and trustworthy verification across participants in the decentralized markets. Our proposed mechanism is given to not only ensure the benefits of the seller but also prevent shipper's fraudulent. The solution leverages the consistency and robustness of decentralized markets where trust is flexible and effectively controlled. To demonstrate the application and implementation of the proposed framework, we conduct several case studies on real-world transaction datasets from a local computer retailer. We also provide our sources codes for further reproducibility and development. Our conclusion is that the continued integration of multi-shipper mechanism and blockchain technology in the decentralized markets will cause significant transformations across several disciplines.

**Keywords**—Blockchain; smart contract; Cash on Delivery (COD); hyperledger fabric

## I. INTRODUCTION

A regular delivery transaction includes buyers and sellers. The seller needs to transport the goods to the buyer, while the buyer gives payment to the seller. However, both sellers and buyers can cheat. Specifically, the seller is skeptical that the buyer will receive the goods without payment, and the buyer will doubt that the seller will receive the money and not deliver the goods. In international transactions, this situation is exacerbated by a slow and complicated transaction process. Ordinary goods must be transported long distances and must go through import and export procedures. The payment must end up with barriers similar to currency changes and legal regulations of each country.

Cash on Delivery (COD) allows customers to pay in cash when the product is delivered to their home or a location they choose. This is sometimes called a payment system because customers receive goods before making a payment. COD has

become increasingly popular in recent years. However, most published documents about COD have appeared in reports or magazines or on the web, with a few scientific studies to date. Among research articles, most investigated payment methods in general, rather than focusing on COD in particular.

The commonly used transfer unit is postage, but usually, consumer and business shipments will be sent to COD by courier companies, commercial truck forwarders or organizations own delivery organizations. COD sales usually involve a fee charged by the shipping agent and is usually paid by the buyer. In retail and wholesale transactions, shipments are made on a COD when the buyer does not have a credit account with the seller and does not choose prepayment. The term is also often used when the small amount involved and the advance credit cost will be high in proportion to the size of the purchase.

The rest of the paper is organized as follow. Section 2 presents some related works. Section 3 briefly describes technical background. Section 4 presents our proposed COD transport process. Section 5-6 describes experimental results. Section 7 gives some conclusions.

## II. RELATED WORK

One of the major problems of e-commerce globally is the selling and buying of goods among the parties over the Internet in which the traders may not trust their partners. Krishnamachari *et. al.* [1] proposed the mechanism that executes a transaction with any kinds of assets by using the digital key and these processes do not need a trusted third-party. Additionally, the authors describe a transaction method which signs dual deposit for anti-fraud payment transactions and the delivery between two parties in which the trader can use the digital signature to verify. The seller and the buyer (customer) use a pair of symmetric keys to verify goods. They use smart contracts to decide and handle sellers and buyers by increasing deposits. But this paper has not yet analysis on a problem of shipping, if it is a physical product and the shipper fails to comply with the commitment, then the system is not resolved.

Hasan [2] proposes a delivery process in which participants (sellers, shippers and buyers) must mortgage an amount of



money. The mortgage is double the value of the goods shipped if the contract value will be returned to the parties. They provide a limited time solution to complete the contract. If the delivery time fails, the system will automatically resolve the dispute, based on the contract without the need for people.

Almost existing blockchain decentralized approaches still contain limitations that need to be improved to be effective and complete. Firstly, in [3], [4], [5] there is no incentive for any participating entities to act honestly. Sellers, buyers and carriers are fully believed. Secondly, [4], [5], [6], [7] depend on TTP or trusted arbitrator to act as a deposit and keep all the money from starting the sales process until the end. There is a TTP that holds money that can be considered as one focus point of failure. More, [2], [8] have no resolution mechanism dispute if any happens. Therefore, there will be a loss for the seller, buyer or both for any dishonest behavior.

Other researchers, Le *et al.* [9] has proposed a mechanism based on the Ethereum Blockchain [10] or Son *et al.* has introduced a mechanism [11] based on Hyperledger Fabric platform [12] that relates to product transportation between sellers and buyers. In their approach, the carrier plays an important role. In our article, it is recommended that the shipper join the system and mortgage a sum of money to ensure the reliability of the system. Our process is given to not only ensure the benefits of the seller but also prevent shipper's fraudulent. If the shipper has problems, such as loss of goods then the goods of the seller sent at the carrier will still be refunded in cash to the seller.

In this article, we review and summarize related work mentioning delivery solutions and technical implementation use blockchain technology. We also conducted decentralized surveys market based on blockchain. In addition, we use hyperledger fabric in the system to protect the rights of sellers.

### III. MATERIALS AND TECHNICAL BACKGROUND

#### A. Blockchain and Blockchain-based Smart Contracts

Blockchain is a list of developing logs, called blocks, linked by encryption. Each block contains the previous block's cryptographic hash function, timestamp, and transaction data. Each block has a block header and a body containing data and hash values of the previous block. The hash value is the result of a hash function. The hash function transforms data of any length into a fixed length string or numeric value, such as 256 bits (32 bytes) with SHA256. Blockchain is a technology that allows secure data transmission based on an extremely complex encryption system, similar to accounting books of a company where cash is closely monitored. In this case, the blockchain is an accounting ledger [13] that works in the digital field. A special feature of blockchain is that transactions are done at a high level of trust without disclosing information.

Blockchain-based smart contracts are proposed contracts that could be partially or fully executed without human interaction [14], [15], [16]. One of the main objectives of a smart contract is an automated escrow. An IMF (International Monetary Fund) staff discussion reported that smart contracts based on Blockchain technology might reduce moral hazards and optimize the use of contracts in general, but "no viable smart contract systems have yet emerged". Due to the lack

of widespread use, their legal status is unclear [17]. Smart contract based on blockchain is being considered for many different types of transactions, from ubiquitous devices to real-time operational management structures for industrial products and data transfer in some applications including transaction finance. All types of business and management can participate in the network and use the properties of the Blockchain system to ensure transparency of stakeholders.

#### B. Smart Contracts

A cryptocurrency is a decentralized platform that a distributed ledger is used to interact with virtual money. A contract is an instance of a computer program that executes on the Blockchain. Users transfer money by publishing transactions and interacting with contracts in the cryptocurrency network where information is propagated, data is stored among miners or network's nodes. An underlying cryptocurrency system supports the utilization of smart contracts. A smart contract contains program code, a stored file and an account balance. Any user can submit a transaction to an appendable-only log. When the contracted is created, its program code cannot be changed. An appendable-only log, called a blockchain, which imposes a partial or total arrangement on submitted transactions is the main interface provided by the cryptocurrency. Fig. 1 presents the idea of a decentralized cryptocurrency system and its components.

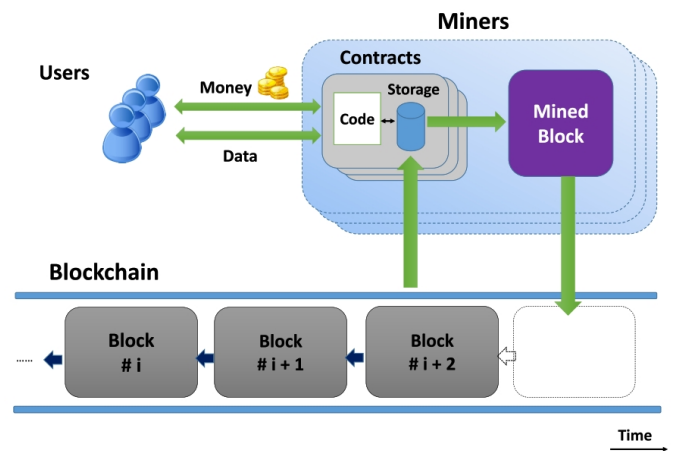


Fig. 1. An illustration of smart contracts and Blockchain in a decentralized cryptocurrency system [18].

#### C. Hyperledger Fabric

Hyperledger Fabric [19], [20], [21] is an open source distributed ledger platform, designed for developing permission application enterprise-grade. Fabric provides a platform to build instant, efficient and secure enterprise blockchain applications. Hyperledger Fabric is a platform for distributed ledger solutions underpinned by a modular architecture delivering high degrees of confidentiality, resiliency, flexibility, and scalability. It is designed to support pluggable implementations of different components and accommodate the complexity and intricacies that exist across the economic ecosystem.

#### IV. PROPOSED COD TRANSPORT PROCESS

In this section, the authors introduce a general overview of the architecture with a highlight of the idea of multi-shipper. Then, we discuss the proposed architecture in more details. Finally, we present an important algorithm that serves as the backbone of our proposed architecture.

##### A. General COD Process

The authors start this session by presenting a general description of COD transport process. The general procedure is illustrated in Fig. 2. First, buyers create an order and send to the seller (2), meanwhile the order details are encrypted and sent to the delivery company which and the seller began to agree on time constraints and delivery prices (3). Before the order can be delivered, the shipper of a delivery company will carry out identity verification by an ID and a hash code order (4). If the first step finishes successfully, the shipper authentication process is notified and verified to the delivery company and the buyer (5). Next, the order's goods will be shipped via a shipper and/or various shippers. Each time the carrier is changed, the two shippers carry out the authentication by an ID and a hash code of the order. The authentication information is returned to allow the next shipper or notify whether the order is illegally intervened. If the authentication process is successful, the next shipper continues to ship the order to another shipper (if any) (6). Finally, the remaining shipper will authenticate the order with the buyer by encrypting the details of the order. In addition, the buyer must verify the identity by the ID to prove that he or she has ordered (7).

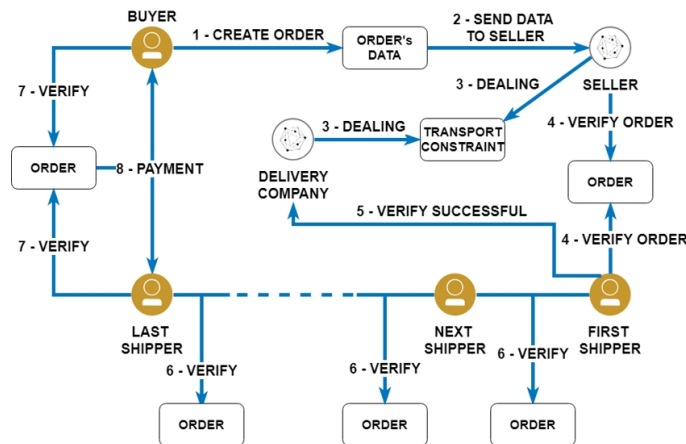


Fig. 2. General description of our proposed COD transport process.

##### B. Detailed COD Design

In this section, we describe how the authentication process between multi-shippers is done. The detailed procedure of multi-shippers authentication is illustrated in Fig. 3. The previous shipper will provide an ID and an asset hash code or each asset in the order (in the case of multiple asset orders) (1). The next shipper will enter the ID and the hash code into the system (2). Then, the system compares the hash code provided by the shipper with the hash code that has been previously stored in the database (3). If the hash code does not match, the system will store the authentication information with the

status "FAILED" (4) - (5.1) - (6). Consequently, the next shipper refuses such products (7) - (8.1). In case two hash codes match, the system will store authentication information with the status "SUCCESSFUL" (4) - (5.1) - (6). After that, the shipper continues to process the order delivery (7) - (8).

Algorithm 1 describes the authentication process between two shippers. First, the ID and hash of the asset are provided, the system checks the hash code stored in the database to make sure that it matches the hash code provided with the same ID of the asset. If the pair information does not match, the actual status will be immediately stored with "FAILED" state. Hence, the next shipper has the right to refuse the order's shipment. Otherwise, if the two hash codes match each other, the authentication information will be stored with the status "SUCCESSFUL", the next shipper accepts the assets and continues the order delivery process.

##### Algorithm 1 verifyShipper

```

1: for each asset given by the previous shipper do
2:   Get the asset to encrypt's data
3:   if The hash strings do not match then
4:     Store authentication information with "FAILED"
    status
5:     Next shipper refuses to get the asset
6:   else
7:     Store authentication information with "SUCCESS-
    FUL" status
8:     Next shipper gets asset
9:     Next shipper transports asset to the buyers or to
    another shipper(s) on the chain if any
10:  end if
11: end for

```

#### V. EXPERIMENTAL SETUP

##### A. Dataset Collection

The experimental datasets, see Table I, have been crawled from a local computer score that the authors use to demonstrate how the system works. There is one thing to note is that the price of products is in Vietnamese Dong (VND). The currency exchange rate when the paper is conducted is that 100 USD equals 2.300.000 VND.

##### B. Experimental Scenarios

1) *Scenario 1*: A buyer creates an order; successful verification between seller - shipper, shipper - shipper and shipper - buyer pairs.

Step 1: The buyer initiates the order information, the *createOrder()* function is called to perform this task and stores the information of the order into the distributed ledger. At this step, the *createAssetHash()* function is also called to encrypt the order and store the encrypted string into the database. An example of the *createOrder()* and *createAssetHash()* functions are presented in Tables II and III.

Step 2: Next, the process of verifying information between the seller and shipper begins. The *encryptAsset()* function is called to encrypt the commodity information. The encrypted string will be compared to the hash code and shipper holding

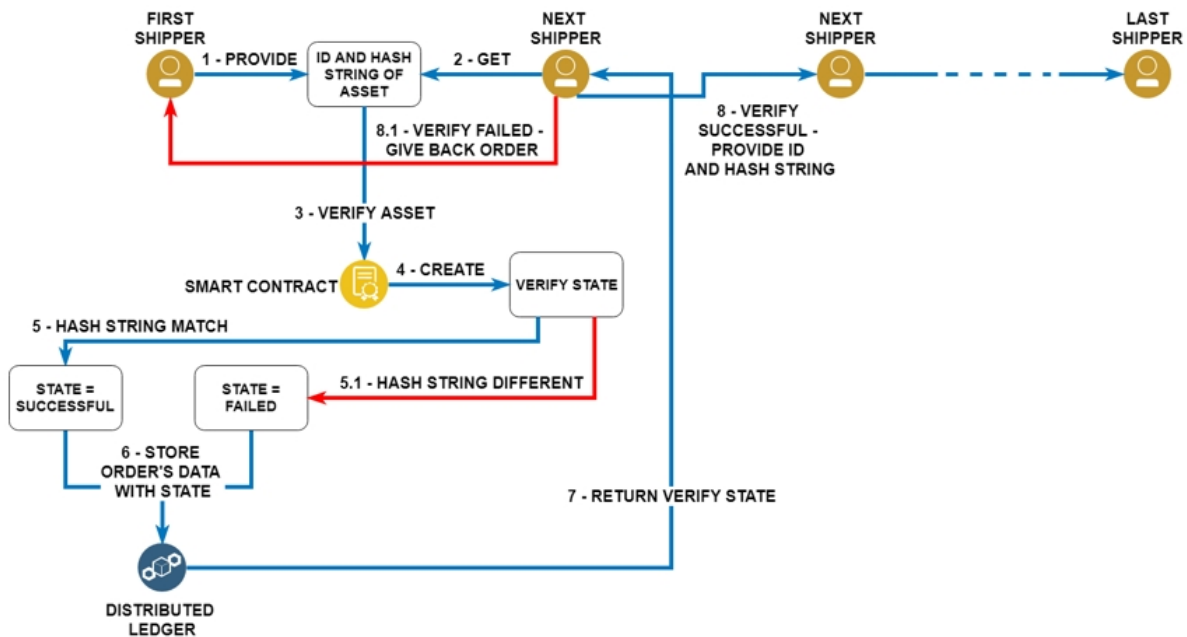


Fig. 3. Detailed design of our proposed COD transport process.

to confirm the order. The result of calling the *encryptAsset()* function is described in Table IV.

Step 3: After completing the authentication process with the seller, the shipper proceeds to authenticate each other during the shipment process. The *verifyshipper()* function is used to store the authentication information with “SUCCESSFUL” status from which the shipper can decide to continue shipping packages. The result of calling the *verifyShipper()* function is described in Table V.

Step 4: Delivery of the goods after being verified and shipped to the buyer. The shipper will eventually use the *encryptAsset()* function to encrypt the product information. The hash code after being generated coincides with the hash code that the buyer has. The authentication process is successful, and hence the buyer proceeds to pay for the delivered product. The result of calling the *encryptAsset()* function is presented in Table VI.

2) Scenario 2: A buyer creates an order; successful verification between seller - shipper pair; unsuccessful verification between shipper - shipper pair.

Step 1: The buyer initiates the order information, the *createOrder()* function is called to perform this task and stores the information of the order into the distributed ledger. At this step, the *createAssetHash()* function is also called to encrypt the order and store the encrypted string into the database. An example of the *createOrder()* and *createAssetHash()* functions are presented in Tables VII and VIII.

Step 2: Next, the process of verifying information between the seller and shipper begins. The *encryptAsset()* function is called to encrypt the commodity information. The encrypted string will be compared to the hash code and shipper holding to confirm the order. The result of calling the *encryptAsset()* function is described in Table IX.

Step 3: At this step, the shipper proceeds to authenticate orders together during exchanging the goods. The previous shipper will not be able to change the delivered items because this information is kept private. In addition, the shipper is completely unaware of the product inside the package. Any behaviors that deliberately change the details will cause the hash code to be generated because the last shipper’s hash code is completely different from the hash code held by the buyer. The shipper authenticates the items with the ID and hash code of the product. If the hash codes do not match, the system will store authentication information with the “FAILED” status. The next shipper will refuse to accept the goods. The process of calling the *verifyShipper()* function is presented in Table X.

3) Scenario 3: A buyer creates an order; unsuccessful verification between seller - shipper pair.

Step 1: The buyer initiates the order information, the *createOrder()* function is called to perform this task and stores the information of the order into the distributed ledger. At this step, the *createAssetHash()* function is also called to encrypt the order and store the encrypted string into the database. An example of the *createOrder()* and *createAssetHash()* functions are presented in Tables XI and XII.

Step 2: If the seller deliberately changes the product structure after the buyer has ordered, the hash code generated during the authentication period between the shipper and the seller will be different from the hash code that shipper is keeping (note that the seller does not know this hash code before). Since then, the shipper can determine that the product code has been changed by the seller and has the right to refuse to receive the package. The authentication information is also stored with “FAILED” status. The process of calling the *encryptAsset()* function is presented in Table XIII.

TABLE I. EXPERIMENTAL DATASET TAKEN FROM A LOCAL RETAIL STORE.

| No. | Product name                          | Product details   | Price (in VND) |
|-----|---------------------------------------|---|----------------|
| 1   | AsusX441MAN5000 (GA024T)              | display:14inch,HD; CPU:PentiumN5000,1.10GHz; RAM:4GB; HDD:1TB; graphics:IntelHDGraphics; OS:Windows10; DVD:no                                       | 7.190.000      |
| 2   | AsusVivoBookX441MAN5000 (GA004T)      | display:14inch,HD; CPU:PentiumN5000,1.10GHz; RAM:4GB; HDD:500GB; graphics:IntelHDGraphics; OS:Windows10; DVD:no                                     | 7.490.000      |
| 3   | AsusVivoBookX407UAI36006U (BV129T)    | display:14inch,HD; CPU:i3-6006U,2.0GHz; RAM:4GB; HDD:1TB; graphics:IntelHDGraphics; OS:Windows10; DVD:no  | 9.690.000      |
| 4   | AsusX407UAI37020U (BV351T)            | display:14inch,HD; CPU:i3-7020U,2.3GHz; RAM:4GB; HDD:1TB; graphics:IntelHDGraphics; OS:Windows10; DVD:no  | 10.090.000     |
| 5   | AsusX507UAI37020U (EJ727T)            | display:15.6inch,FullHD; CPU:i37020U,2.3GHz; RAM:4GB; HDD:1TB; graphics:IntelHDGraphics620; OS:Windows10,DVD:no                                     | 10.590.000     |
| 6   | AsusVivoBookX540UBi36006U (DM024T)    | display:15.6inch,FullHD; CPU:i3-6006U,2.0GHz; RAM:4GB; HDD:1TB; graphics:NVIDIAMX110,2GB; OS:Windows10; DVD:support                                 | 10.790.000     |
| 7   | AsusVivoBookA411UAI38130U (EB688T)    | display:14inch,FHD; CPU:i3-8130U,2.2GHz; RAM:4GB; HDD:1TB; graphics:IntelUHDGraphics620; OS:Windows10; DVD:no                                       | 11.290.000     |
| 8   | AsusA510UAI38130U (BR333T)            | display:15.6inch,HD; CPU:i3-8130U,2.2GHz; RAM:4GB; HDD:1TB; graphics:IntelUHDGraphics620; OS:Windows10; DVD:no                                      | 11.390.000     |
| 9   | AsusVivoBookX507UFI38130U (BR203T)    | display:15.6inch,HD; CPU:Corei3CoffeeLake,2.20GHz; RAM:4GB; HDD:1TBSATA3; graphics:NVIDIAMX130,2GB; OS:Windows10HomeSL; DVD:no                      | 11.990.000     |
| 10  | AsusVivoBookS15S510UAI38130U (BQ222T) | display:15.6inch,FHD; CPU:i38130U,2.2GHz; RAM:4GB; HDD:1TB; graphics:IntelHDGraphics620; OS:Windows10; DVD:no                                       | 12.890.000     |
| 11  | AsusA411UAI58250U (EB678T)            | display:15.6inch,FHD; CPU:i38130U,2.2GHz; RAM:4GB; HDD:1TB; graphics:IntelHDGraphics620; OS:Windows10; DVD:no                                       | 13.490.000     |
| 12  | AsusX407UAI58250U (BV485T)            | display:14inch,HD; CPU:Corei5CoffeeLake,1.60GHz; RAM:4GB; HDD:1TB; Optane16GB, graphics:IntelHDGraphics620; OS:Windows10Home                        | 13.690.000     |
| 13  | AsusA510UAI58250U (EJ1215T)           | display:15.6inch,FullHD; CPU:Corei5CoffeeLake,1.60GHz; RAM:4GB; HDD:1TB; graphics:IntelUHDGraphics620; OS:Windows10HomeSL                           | 13.790.000     |
| 14  | AsusX507UFI58250U4GB1TB (EJ121T)      | display:15.6inch,FullHD; CPU:Corei5KabyLakeRefresh,1.60GHz; RAM:4GB; HDD:1TBSATA3,supportSSDM.2; graphics:NVIDIAMX130,2GB; OS:Windows10HomeSL       | 14.590.000     |
| 15  | AsusVivoBookS15S510UAI58250U (BQ414T) | display:15.6inch,FullHD; CPU:i5KabyLakeRefresh,1.60GHz; RAM:4GB; HDD:1TB; graphics:UHDGraphics620; OS:Windows10; DVD:no                             | 15.490.000     |
| 16  | AsusVivoBookS510UNi58250U (BQ276T)    | display:15.6inch,FullHD; CPU:Corei5CoffeeLake,1.60GHz; RAM:4GB; HDD:1TBSATA3; graphics:NVIDIAMX150,2GB; OS:Windows10HomeSL; DVD:no                  | 16.790.000     |
| 17  | AsusVivobookS15S530UAI58250U (BQ290T) | display:15.6inch,FHD; CPU:i5-8250U,1.6GHz; RAM:4GB; HDD:1TB; graphics:IntelUHDGraphics620; OS:Windows10   | 17.390.000     |
| 18  | AsusZenBookUX433FAi58265U (A6061T)    | display:14inch,FullHD; CPU:Corei5CoffeeLake,1.60GHz; RAM:8GB; SSD256GBNVMePCIe; graphics:IntelUHDGraphics620; OS:Windows10Home                      | 22.990.000     |
| 19  | AsusFX504GEi58300H (E4138T)           | display:15.6inch,FullHD; CPU:Corei5CoffeeLake,2.30GHz; RAM:8GB; HDD:1TB, supportSSDM.2PCIe; graphics:NVIDIAGeForceGTX1050Ti,4GB; OS:Windows10HomeSL | 23.490.000     |
| 20  | AsusFX505GEi78750H (BQ037T)           | display:15.6inch,FullHD; CPU:Corei7CoffeeLake,2.20GHz; RAM:8GB; SSD128GBM2PCIe,HDD:1TBSATA3; graphics:NVIDIAGeForceGTX1050Ti,4GB; OS:Windows10Home  | 27.990.000     |

TABLE II. THE CREATEORDER() FUNCTION: A BUYER CREATES AN ORDER AND THE SYSTEM CREATES ORDER'S DATA.

| orderID  | buyerID     | sellerID  | deliverID   | Product name                      | Quantity | Price (in VND) | Status  | Execution time |
|----------|-------------|-----------|-------------|-----------------------------------|----------|----------------|---------|----------------|
| order001 | customer001 | seller001 | delivery001 | AsusX441MAN5000(GA024T)           | 1        | 7.190.000      | waiting | 1.008266524s   |
| order002 | customer002 | seller002 | delivery002 | AsusVivoBookX441MAN5000(GA004T)   | 1        | 7.490.000      | waiting | 1.003088932s   |
| order003 | customer003 | seller003 | delivery003 | AsusVivoBookX407UAI36006U(BV129T) | 1        | 9.690.000      | waiting | 1.006305223s   |
| order004 | customer004 | seller004 | delivery004 | AsusX407UAI37020U(BV351T)         | 1        | 10.090.000     | waiting | 1.003237888s   |
| order005 | customer005 | seller005 | delivery005 | AsusX507UAI37020U(EJ727T)         | 1        | 10.590.000     | waiting | 1.002595092s   |

TABLE III. CREATEASSETHASH(): THE SYSTEM CREATES ORDER'S HASH.

| orderID  | sellerID  | Product name                      | Quantity | Price (in VND) | Execution time |
|----------|-----------|-----------------------------------|----------|----------------|----------------|
| order001 | seller001 | AsusX441MAN5000(GA024T)           | 1        | 7.190.000      | 1.003257091s   |
| order002 | seller002 | AsusVivoBookX441MAN5000(GA004T)   | 1        | 7.490.000      | 1.002689831s   |
| order003 | seller003 | AsusVivoBookX407UAI36006U(BV129T) | 1        | 9.690.000      | 1.002950846s   |
| order004 | seller004 | AsusX407UAI37020U(BV351T)         | 1        | 10.090.000     | 1.003001433s   |
| order005 | seller005 | AsusX507UAI37020U(EJ727T)         | 1        | 10.590.000     | 1.002540695s   |

VI. REMARKS

The implementation of our approach is deployed on Ubuntu 19.04 machine with 2.53GHz CPU and 8GB of RAM. Tables

II, III, IV, V, and VI show the performance of functions in the Cash on Delivery system, in which the input data and

TABLE IV. ENCRYPTASSET(): THE SELLER ENCRYPTS ASSET TO VERIFY ORDER TO THE SHIPPER.

| sellerID  | Product name                      | Quantity | Price (in VND) | Execution time |
|-----------|-----------------------------------|----------|----------------|----------------|
| seller001 | AsusX441MAN5000(GA024T)           | 1        | 7.190.000      | 1.000282933s   |
| seller002 | AsusVivoBookX441MAN5000(GA004T)   | 1        | 7.490.000      | 1.000271937s   |
| seller003 | AsusVivoBookX407Uai36006U(BV129T) | 1        | 9.690.000      | 1.000289196s   |
| seller004 | AsusX407Uai37020U(BV351T)         | 1        | 10.090.000     | 1.000244656s   |
| seller005 | AsusX507Uai37020U(EJ727T)         | 1        | 10.590.000     | 1.000368499s   |

TABLE V. VERIFYSHIPPER(): THE SHIPPER ENCRYPTS ORDER'S DATA TO THE NEXT SHIPPER.

| orderID  | Hash   | Location  | Execution time |
|----------|--|-----------|----------------|
| order001 | bdd736bba7e3b336d5bed8b08fe503c7afeb1b6e21b1a439566ef6e46b96e30  | cityAlpha | 1.024215124s   |
| order002 | 5f2fe095759f31b2d91819f8df0602601758394d287fb63d92effa84e6679a02 | cityAlpha | 1.023620744s   |
| order003 | d873b49bc5ae5ee1d4e7cfff02aca09a91c739a72867e77eb70e5a8403499    | cityAlpha | 1.021422615s   |
| order004 | 21fbd6ee92b9ca5446409690136f65493572863fe8ea836df424d3328e0a1ac  | cityAlpha | 1.018266805s   |
| order005 | 00631c0bdd93ec1014bbf7290d0e43fa189c94b71af5ecf7ea187a548c2fc74  | cityAlpha | 1.016574424s   |

TABLE VI. ENCRYPTASSET(): THE SHIPPER ENCRYPTS ORDER'S DATA TO VERIFY TO THE BUYER.

| sellerID  | Product name                      | Quantity | Price (in VND) | Execution time |
|-----------|-----------------------------------|----------|----------------|----------------|
| seller001 | AsusX441MAN5000(GA024T)           | 1        | 7.190.000      | 1.000329441s   |
| seller002 | AsusVivoBookX441MAN5000(GA004T)   | 1        | 7.490.000      | 1.000292817s   |
| seller003 | AsusVivoBookX407Uai36006U(BV129T) | 1        | 9.690.000      | 1.000285833s   |
| seller004 | AsusX407Uai37020U(BV351T)         | 1        | 10.090.000     | 1.00029968s    |
| seller005 | AsusX507Uai37020U(EJ727T)         | 1        | 10.590.000     | 1.000230017s   |

TABLE VII. CREATEORDER(): THE BUYER CREATES ORDER AND THE SYSTEM CREATES ORDER'S DATA.

| orderID  | buyerID     | sellerID   | deliveryID  | Product name                         | Quantity | Price (in VND) | Status  | Execution time |
|----------|-------------|------------|-------------|--------------------------------------|----------|----------------|---------|----------------|
| order006 | customer006 | seller006  | delivery006 | AsusVivoBookX540UBi36006U(DM024T)    | 1        | 10.790.000     | waiting | 1.002387767s   |
| order007 | customer007 | seller007  | delivery007 | AsusVivoBookA411Uai38130U(EB688T)    | 1        | 11.290.000     | waiting | 1.002605573s   |
| order008 | customer008 | seller008  | delivery008 | AsusA510Uai38130U(BR333T)            | 1        | 11.390.000     | waiting | 1.002959993s   |
| order009 | customer009 | seller009  | delivery009 | AsusVivoBookX507Ufi38130U(BR203T)    | 1        | 11.990.000     | waiting | 1.002753797s   |
| order010 | customer010 | seller0010 | delivery010 | AsusVivoBookS15S510Uai38130U(BQ222T) | 1        | 12.890.000     | waiting | 1.002916293s   |

TABLE VIII. CREATEASSETHASH(): THE SYSTEM CREATES ORDER'S HASH.

| orderID  | sellerID   | Product name                         | Quantity | Price (in VND) | Execution time |
|----------|------------|--------------------------------------|----------|----------------|----------------|
| order006 | seller006  | AsusVivoBookX540UBi36006U(DM024T)    | 1        | 10.790.000     | 1.002827145s   |
| order007 | seller007  | AsusVivoBookA411Uai38130U(EB688T)    | 1        | 11.290.000     | 1.003145603s   |
| order008 | seller008  | AsusA510Uai38130U(BR333T)            | 1        | 11.390.000     | 1.003106346s   |
| order009 | seller009  | AsusVivoBookX507Ufi38130U(BR203T)    | 1        | 11.990.000     | 1.00231202s    |
| order010 | seller0010 | AsusVivoBookS15S510Uai38130U(BQ222T) | 1        | 12.890.000     | 1.002822286s   |

TABLE IX. ENCRYPTASSET(): THE SELLER ENCRYPTS ASSET TO VERIFY ORDER TO THE SHIPPER.

| sellerID   | Product name                         | Quantity | Price (in VND) | Execution time |
|------------|--------------------------------------|----------|----------------|----------------|
| seller006  | AsusVivoBookX540UBi36006U(DM024T)    | 1        | 10.790.000     | 1.000223568s   |
| seller007  | AsusVivoBookA411Uai38130U(EB688T)    | 1        | 11.290.000     | 1.000244662s   |
| seller008  | AsusA510Uai38130U(BR333T)            | 1        | 11.390.000     | 1.000268549s   |
| seller009  | AsusVivoBookX507Ufi38130U(BR203T)    | 1        | 11.990.000     | 1.000184843s   |
| seller0010 | AsusVivoBookS15S510Uai38130U(BQ222T) | 1        | 12.890.000     | 1.000358836s   |

TABLE X. VERIFYSHIPPER(): THE SHIPPER ENCRYPTS ORDER'S DATA TO VERIFY TO THE NEXT SHIPPER.

| orderID  | hash   | Location  | Execution time |
|----------|--|-----------|----------------|
| order006 | c40e97a57e66ed09388476a09571bfd513df6f2fd72dfc57b473fd5af2097a00 - a | cityAlpha | 1.015158103s   |
| order007 | 495f2a8e0e61732764c8b03e832cf0735bb07551b6388b89d2c20474e0ba094f - b | cityAlpha | 1.013581844s   |
| order008 | b85c9b9c7772b17b2c5641a75dc19bd448d386af5dbdeaca8fbbddeb3ca468 - c   | cityAlpha | 1.019617637s   |
| order009 | 29e869390120de9cda8bfd910701225a1ba0de37b9f5b77d5cf7fb1284570d48 - d | cityAlpha | 1.013978084s   |
| order010 | 08b640f9f41e83ce466de42251d19f80253b9af854688375f374f67ab7fa0581 - e | cityAlpha | 1.012554071s   |

TABLE XI. CREATEORDER(): THE BUYER CREATES ORDER AND THE SYSTEM CREATES ORDER'S DATA.

| orderID  | buyerID     | sellerID  | deliverID   | Product name                         | Quantity | Price (in VND) | Status  | Execution time |
|----------|-------------|-----------|-------------|--------------------------------------|----------|----------------|---------|----------------|
| order011 | customer011 | seller011 | delivery011 | AsusA411UAi58250U(EB678T)            | 1        | 13.490.000     | waiting | 1.003676700s   |
| order012 | customer012 | seller012 | delivery012 | AsusX407UAi58250U(BV485T)            | 1        | 13.690.000     | waiting | 1.001928328s   |
| order013 | customer013 | seller013 | delivery013 | AsusA510UAi58250U(EJ1215T)           | 1        | 13.790.000     | waiting | 1.001924617s   |
| order014 | customer014 | seller014 | delivery014 | AsusX507UFI58250U4GB1TB(EJ121T)      | 1        | 14.590.000     | waiting | 1.002541236s   |
| order015 | customer015 | seller015 | delivery015 | AsusVivoBookS15S510UAi58250U(BQ414T) | 1        | 15.490.000     | waiting | 1.002492703s   |

TABLE XII. CREATEASSETHASH(): THE SYSTEM CREATES ORDER'S HASH.

| orderID  | sellerID  | Product name                         | Quantity | Price (in VND) | Execution time |
|----------|-----------|--------------------------------------|----------|----------------|----------------|
| order001 | seller011 | AsusA411UAi58250U(EB678T)            | 1        | 13.490.000     | 1.002169191s   |
| order002 | seller012 | AsusX407UAi58250U(BV485T)            | 1        | 13.690.000     | 1.003219684s   |
| order003 | seller013 | AsusA510UAi58250U(EJ1215T)           | 1        | 13.790.000     | 1.003060215s   |
| order004 | seller014 | AsusX507UFI58250U4GB1TB(EJ121T)      | 1        | 14.590.000     | 1.003002701s   |
| order005 | seller015 | AsusVivoBookS15S510UAi58250U(BQ414T) | 1        | 15.490.000     | 1.002834664s   |

TABLE XIII. ENCRYPTASSET(): THE SELLER ENCRYPTS ASSET TO VERIFY ORDER TO SHIPPER.

| sellerID  | Product name                         | Quantity | Price (in VND) | Execution time |
|-----------|--------------------------------------|----------|----------------|----------------|
| seller011 | AsusA411UAi58250U(EB678T)            | 1        | 13.490.000     | 1.000232470s   |
| seller012 | AsusX407UAi58250U(BV485T)            | 1        | 13.690.000     | 1.000262189s   |
| seller013 | AsusA510UAi58250U(EJ1215T)           | 1        | 13.790.000     | 1.000224077s   |
| seller014 | AsusX507UFI58250U4GB1TB(EJ121T)      | 1        | 14.590.000     | 1.000301122s   |
| seller015 | AsusVivoBookS15S510UAi58250U(BQ414T) | 1        | 15.490.000     | 1.000283559s   |

execution time of the two main functions of the system (Verify and Encrypt) that describe in Tables IV, V, and VI. According to the measured data in the tables, we conclude that our method does not require high-configuration equipment for deploying but it still ensures system performance (approximately 1 second/function). In addition, the level of complexity algorithm *verifyShipper()* is  $n$  where  $n$  is the number of products in a package and that of *encryptAsset()* is 1, this function does not depend on the input data. Moreover, our proposed approach supports the decentralized architecture based on Blockchain, users do not need cryptocurrency units to execute transactions (such as Ethereum systems) that significantly reduce risks such as vector attack. The peer on the network verify the request by identity information of the users and it prevents the act of installing/launching malicious smart contracts to query illegal data. On the other hands, our proposal mechanism does not require complex encryption or authentication algorithms whenever verifying the information of the user, thus saving more than non-distributed Blockchain-based systems. Hence it easily deployed in an enterprise environment. We encourage further reproducibility and implementation by providing our sources codes freely accessed on our Github repository<sup>1</sup>.

## VII. CONCLUSION

As we have demonstrated, the introduction of multi-shipper mechanism applied in any cash on delivery systems is very beneficial. Our process is given to not only ensure the benefits of the seller but also prevent shipper's fraudulent. We have provided a transparent verification that works across participants. Several case studies have demonstrated the feasibility of the proposed mechanism in achieving trustworthy and transparent verification for the COD systems. The solution leverages the consistency and robustness of decentralized markets where

trust is flexible and effectively controlled. To the best of our knowledge, there have not been any research papers that exploit and implement a mechanism of multi-shipper in the COD system. We believe that the continued integration of multi-shipper mechanism and blockchain technology in the decentralized markets will cause significant transformations across several disciplines, bringing about new business applications and having us reconsider how the existing COD systems are developed.

## REFERENCES

- [1] A. Asgaonkar and B. Krishnamachari, "Solving the buyer and seller's dilemma: A dual-deposit escrow smart contract for provably cheat-proof delivery and payment for a digital good without a trusted mediator," *arXiv preprint arXiv:1806.08379*, 2018.
- [2] H. R. Hasan and K. Salah, "Blockchain-based solution for proof of delivery of physical assets," in *International Conference on Blockchain*. Springer, 2018, pp. 139–152.
- [3] "Two party contracts," Feb 2015. [Online]. Available: <https://dappsforbeginners.wordpress.com/tutorials/two-party-contracts/>
- [4] "How our escrow smart contract works," Oct 2017. [Online]. Available: <https://blog.localetereum.com/how-our-escrow-smart-contract-works/>
- [5] "Sites like ebay or etsy but decentralized - our features." [Online]. Available: <https://openbazaar.org/features/>
- [6] [Online]. Available: <https://www.syscoin.org/home.html>
- [7] J. Sidhu, "Syscoin: A peer-to-peer electronic cash system with blockchain-based services for e-business," in *2017 26th international conference on computer communication and networks (ICCCN)*. IEEE, 2017, pp. 1–6.
- [8] "Double deposit escrow." [Online]. Available: <https://bitbay.market/double-deposit-escrow>
- [9] N. T. T. Le, Q. N. Nguyen, N. N. Phien, N. Duong-Trung, T. T. Huynh, T. P. Nguyen, and H. X. Son, "Assuring non-fraudulent transactions in cash on delivery by introducing double smart contracts," *International Journal of Advanced Computer Science and Applications*, vol. 10, no. 5, 2019. [Online]. Available: <http://dx.doi.org/10.14569/IJACSA.2019.0100584>

<sup>1</sup><https://github.com/xuansonha17031991/CashOnDelevery-Chaincode>

- [10] "Ethereum project." [Online]. Available: <https://ethereum.org/>
- [11] H. X. Son, M. H. Nguyen, N. N. Phien, H. T. Le, Q. N. Nguyen, V. D. Dinh, P. T. Tru, and P. Nguyen, "Towards a mechanism for protecting seller's interest of cash on delivery by using smart contract in hyperledger," *International Journal of Advanced Computer Science and Applications*, vol. 10, no. 4, 2019. [Online]. Available: <http://dx.doi.org/10.14569/IJACSA.2019.0100405>
- [12] "Hyperledger fabric." [Online]. Available: <https://hyperledger-fabric.readthedocs.io/>
- [13] G. Wood *et al.*, "Ethereum: A secure decentralised generalised transaction ledger," *Ethereum project yellow paper*, vol. 151, pp. 1–32, 2014.
- [14] T. Hamid, "Cash on delivery the biggest obstacle to e-commerce in uae and region," May 2014. [Online]. Available: <https://www.thenational.ae/business/technology/cash-on-delivery-the-biggest-obstacle-to-e-commerce-in-uae-and-region-1.604383>
- [15] F. Idelberger, G. Governatori, R. Riveret, and G. Sartor, "Evaluation of logic-based smart contracts for blockchain systems," in *International Symposium on Rules and Rule Markup Languages for the Semantic Web*. Springer, 2016, pp. 167–183.
- [16] M. Alharby and A. van Moorsel, "Blockchain-based smart contracts: A systematic mapping study," *arXiv preprint arXiv:1710.06372*, 2017.
- [17] D. He, K. F. Habermeier, R. B. Leckow, V. Haksar, Y. Almeida, M. Kashima, N. Kyriakos-Saad, H. Oura, T. S. Sedik, N. Stetsenko *et al.*, "Virtual currencies and beyond: initial considerations," 2016.
- [18] K. Delmolino, M. Arnett, A. Kosba, A. Miller, and E. Shi, "Step by step towards creating a safe smart contract: Lessons and insights from a cryptocurrency lab," in *International Conference on Financial Cryptography and Data Security*. Springer, 2016, pp. 79–94.
- [19] E. Androulaki, A. Barger, V. Bortnikov, C. Cachin, K. Christidis, A. De Caro, D. Enyeart, C. Ferris, G. Laventman, Y. Manevich *et al.*, "Hyperledger fabric: a distributed operating system for permissioned blockchains," in *Proceedings of the Thirteenth EuroSys Conference*. ACM, 2018, p. 30.
- [20] P. Thakkar, S. Nathan, and B. Viswanathan, "Performance benchmarking and optimizing hyperledger fabric blockchain platform," in *2018 IEEE 26th International Symposium on Modeling, Analysis, and Simulation of Computer and Telecommunication Systems (MASCOTS)*. IEEE, 2018, pp. 264–276.
- [21] F. Benhamouda, S. Halevi, and T. T. Halevi, "Supporting private data on hyperledger fabric with secure multiparty computation," *IBM Journal of Research and Development*, 2019.

# Content-based Automatic Video Genre Identification

Faryal Shamsi<sup>1</sup>, Sher Muhammad Daudpota<sup>2</sup>, Sarang Shaikh<sup>3</sup>

Department of Computer Science  
Sukkur IBA University  
Sukkur, Pakistan

**Abstract**—Video content is evolving enormously with the heavy usage of internet and social media websites. Proper searching and indexing of such video content is a major challenge. The existing video search potentially relies on the information provided by the user, such as video caption, description and subsequent comments on the video. In such case, if users provide insufficient or incorrect information about the video genre, the video may not be indexed correctly and ignored during search and retrieval. This paper proposes a mechanism to understand the contents of video and categorize it as Music Video, Talk Show, Movie/Drama, Animation and Sports. For video classification, the proposed system uses audio and visual features like audio signal energy, zero crossing rate, spectral flux from audio and shot boundary, scene count and actor motion from video. The system is tested on popular Hollywood, Bollywood and YouTube videos to give an accuracy of 96%.

**Keywords**—Motion detection; scene detection; shot boundary detection; video genre identification

## I. INTRODUCTION

The word genre is defined as socially agreed category of content. So, the term content-based automatic video genre identification means, to recognize the category of a video on basis of its contents. The heterogeneous nature of video contents, makes the genre identification a challenging job. With the evolution of internet and social networking websites, content sharing is becoming a popular trend [1]. The level of facilitation provided to user by such websites leads to increase the information overload, while organization of the contents is becoming a challenging task [2]. The most popular form of content on social media is videos [3]. The nature of video contents is diverse as it combines all other types of media such as text, audio and image [4]. The top ranking social networking sites like Facebook, YouTube allow users to explore billions of videos per day. Proper organization of such videos is therefore a necessary operation to ensure efficient indexing and searching. In spite of all the progress in the field of multimedia mining and contents based filtering, still there is need of a system which can automatically understand the contents of a video. A reliable automatic video genre identification system which can categorize any type of video, is yet to be proposed.

The existing video indexing and searching mechanisms available are fully at mercy of the information provided by up-loader. On the other hand, an up-loader enjoys full autonomy while generating and sharing any type of contents. The up-loader is not bound to provide necessary information about the content so that it can be utilized for the purpose of indexing. Also, there is no check and balance to ensure the integrity of the information provided by the up-loader. For example, an up-loader has complete freedom to give any title to the video, no

matter how irrespective it is, with the actual contents of video. An up-loader might give his or her own name to a movie or can caption a talk show as a movie, in such cases a user may not be able to view these videos if his/her search string does not match with the information available with the video. So, there must be an identification system for video genre which considers its contents rather than the textual information provided by the up-loader.

This paper proposes a frame work to analyze contents of an input video and classify it in one of the five genres including music video, talk-show, movie/drama, animation and sports. We use audio and visual features to achieve this classification task.

Rest of the paper is organized as follows: Section II presents the literature review, Section III introduces different building blocks of the system, Section IV explains working of the audio classifier along with features used to work with audio of the input video, followed by discussion on video classifier in Section V. Finally, Section VI and Section VII report the results and conclude paper with discussion about future directions, respectively.

## II. RELATED WORK

Several attempts have been made in the recent years regarding video classification. Some of these attempts used text or audio based approaches while most worked on visual based or hybrid approaches. The text based approaches use the view-able text within a video to understand its contents [5]. A movie generally has textual information such as cast and subtitles which can give some insights about the video contents. Techniques extracting the text and TF-IDF (Term Frequency-Inverse Document Frequency) is discussed in [6].

Other than the text, audio contents within a video can also be used for video classification and genre identification. Various techniques are proposed in literature which uses audio information, like dialogues music or silence [7], [8]. This information can be captured through ZCR - Zero crossing rate as proposed in [9], [10], [11], [12] for video content analysis. Similar type of audio classification algorithms are proposed in [13], [14], using HZCR (high zero crossing rate), spectrum flux and time energy of an audio signal to classify an audio into four distinct classes - speech, music, environment sound or silence. Similar type of algorithm is proposed in [15] to extract musical sequences, in Bollywood movies, and uses ZCR and RMS (Root-Mean-Square) of an audio signal as classifying features.

Although a video has several textual and audio features that can be used for classification but among all these features,



visual features are most dominant within the video contents. The colors (i.e. RGB values) [16], shapes (i.e. Image histogram) [17], [18], luminescence [19] and motion [20] are some of the commonly used visual features used to analyze the contents of video, as proposed in literature. The color and shape information can be statistically analyzed by generating the color histogram and shape histogram of images extracted from the frames of video [21]. MPEG motion vectors [22], [23] are used as features to examine the motion information available in a video. HMM - Hidden Markov Model combines various features (e.g. color, shape and audio) and the Gaussian Mixture Model the probability distribution and many similar techniques use hybrid approaches for video classification [24], [25], [26], [27].

The features used for video classification by the above methods are low level. There are also further high level features for video classification e.g. Shot Boundary Detection, Scene Detection [10], Shot Duration [28], [29], [30], Motion Detection [10], [29], [31] and so on. Shot Boundary detection is a major building block for video processing activities. A shot boundary is defined as one or more frames in a video where one shot ends and other starts. For the purpose of shot boundary detection various audio and visual features can be used such as colors, edges, luminescence and motion information available within the frames [32]. One of the benchmark data-set for shot boundary detection is TRECVID, developed by NIST (National Institute of Standards and Technology in Gaithersburg, USA). TRECVID contains many subsets of video test data and ground truth information targeting the shot boundary detection which are widely used to evaluate the performance of different shot boundary detection algorithms [33]. Significant advancements are made by [34], [35], [36], [37], [38] [39], [40] to perform shot boundary detection to achieve optimal accuracy. Different accuracy ranges have been reported on TRECVID dataset from 94% to 96%.

Our proposed system use an algorithm inspired by [34] that attempts to identify the similarity between each consecutive frames. The algorithm uses the SAD function that calculates the sum of absolute differences between the RGB color values of the corresponding pixels of each two adjacent frames. To identify the shot boundary, the SAD value is compared to a predefined threshold. If the difference is greater than that threshold the later frame will be considered as shot boundary, otherwise as a continuous shot. The algorithm can be summarized as:

$$d_{sad}(f_{i-1}, f_i) = \frac{1}{|F|} \sum_{i=2}^F |f_{i-1}(r) - f_i| \quad (1)$$

Where F is the total number of pixel in a frame,  $d_{sad}$  is the function calculating the sum of absolute differences of each two consecutive frames and r represents the coordinates of pixels. The above algorithm is able to categorize the shots as cut, fades and dissolves by using the luminescence information.

For content based analysis, a video can also be broken down into scenes rather than shots. Although some authors refer the terms shot and scene interchangeably, most consider shots as a subset of scene. A scene is a temporal segment of a video with repetitive shots. A scene may also be defined

as continuous action with a specific event of a video. Scene detection is the process to automatically detect this repetitive pattern within a video. Scene detection is generally performed by using visual features like luminescence, motion detection and average length of shots to track the changes in lighting, environment and pace of the video in a movie [4]. Scene detection techniques may be rule based, where some predefined rule are constructed to analyze the frames and shots and decision is made if they belong to the same scene or not [5]. Some scene detection techniques may be graph based [41], stochastic based or cluster based [42], [43], [44] in contrast to the rule based [5], [45]. The accuracy of such algorithms range from 80% to 86% as reported these different attempts.

### III. VIDEO GENRE CLASSIFICATION

The proposed system is able to classify a video into five distinct classes, including Music Video, Talk Show, Sports, Animation and Movie/Drama. The abstract model of the system is given in Fig. 1.

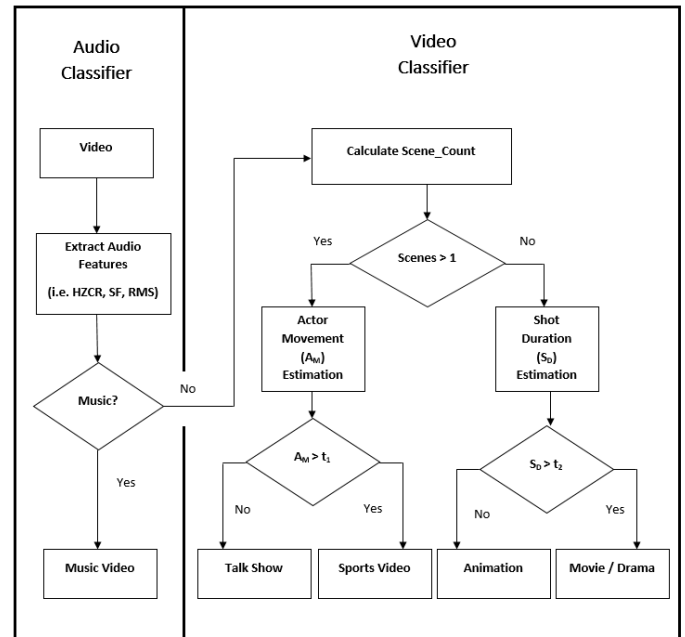


Fig. 1. Abstract Model of the Proposed System

The system is logically divided in two components, Audio Classifier and Video Classifier. The input video is fed to the Audio Classifier that extracts audio features to estimate music portion in the audio of input video. In case if majority of the frames are classified as having background music, the input video is classified as Music Video, else it is forwarded to the Video Classifier to check for the remaining genres of video.

The Video Classifier checks for the number of scenes in a video because it's a good indicator to separate Talk Show and Sports Video from Movies/Drama and Animations. As per video recording grammar, Talk Shows and Sports videos are comprising of only one scene i.e. for the whole duration of the video, all the shots belong to same scene, whereas for Movies/Drama and Animation there are multiple scenes

depending on the size of video file.

In case if there is only one scene in a video, we check for actor movement. If the actor movement is high with only one scene in the video, it is classified as a Talk Show, whereas, high actor movement results in a video being classified in Sport Video genre.

On the other hand, if there are multiple scenes in a video, we estimate shot duration in the input video. Usually, in order to increase excitement in Animation video, shot duration is kept very small, typically less than a second in many cases. Therefore, shot duration feature efficiently classifies input video in either Movie/Drama or Animation.

Rest of the paper describes working of Audio and Video Classifiers along with each components in both the classifiers.

#### IV. AUDIO CLASSIFIER

Classifying an audio input in music and non-music classes is an important task, many attempts have been made to use different audio features to accomplish this task [46], [47], [48], [49], [50], [51], [52], [53]. Lie Lu et al. [13] demonstrate that features like zero crossing rate, root mean square and spectrum flux are good at differentiating music signal from speech signal, however, the variations of these features in a defined window performs even better than the feature itself. They define high zero crossing rate ratio (HZCRR) as:

$$HZCRR = \frac{1}{2N} \sum_{n=0}^{N-1} [\text{sgn}(ZCR(n) - 1.5avZCR) + 1] \quad (2)$$

where  $avZCR$  is defined as:

$$avZCR = \frac{1}{N} \sum_{n=0}^{N-1} ZCR(n) \quad (3)$$

Where  $N$  represents total number of frames in a one second window,  $n$  is frame index,  $\text{sgn}[]$  is sign function and  $ZCR(n)$  is zero crossing rate of  $n^{th}$  frame in one second window.

Zero crossings in music signal are usually very low with almost zero variations, whereas in speech signal, due to sudden drop in energy, zero crossing variations are significantly high.

Similarly, Low Short Time Energy Ratio (LSTER) is defined as:

$$LSTER = \frac{1}{N} \sum_{n=0}^{N-1} [0.5avSTE - \text{sgn}(STE(n)) + 1] \quad (4)$$

and,

$$avSTE = \frac{1}{N} \sum_{n=0}^{N-1} STE(n) \quad (5)$$

Experiments suggest LSTER value is significantly lower in music signals compared to speech signal, therefore it performs well in differentiating between music and speech

signal.

Finally, Spectrum Flux (SF), which defines average variation value of spectrum between two adjacent frames in one second window is defined as:

$$SF = \frac{1}{(N-1)(K-1)} \sum_{n=1}^{N-1} \sum_{k=1}^{K-1} \quad (6)$$

$$[\log(A(n, k) + \delta) - \log(A(n-k, k) + \delta)]^2$$

Where  $A(n, k)$  represents Discrete Fourier Transform of  $n^{th}$  frame in a one-second window and defined as:

$$A(n, k) = \sum_{m=-\infty}^{\infty} x(m)W(nL - m)e^{j\frac{2\pi}{L}km} \quad (7)$$

Spectrum Flux values for speech are much higher than Music, therefore when combined with HZCRR and LSTER, it performs well for differentiating music from speech using SVM classifier.

In our task of genre identification, as we observe more seconds of music than speech, we classify input video in Music class. On the other hand, if there is low percentage of music seconds in the input video, the video is forwarded to Video Classifier for further processing.

#### V. VIDEO CLASSIFIER

This section of our genre identifier receives only those videos in which music portion is low. As per grammar of video recording, which although is not documented but if violated would result in an ambiguous video, all the video genres, except music video contains lower portion of music than pure speech or environment sound. For example, imagine a talk show discussing on recent political affair with a loud background music, obviously, such a recording would not make sense for the viewers. A non-music video can belong to any of the later four genres including Talk-Show, Sports, Animation and Movie/Drama.

A Talk-Show video generally has only one scene where there are 5-7 distinct shots frequently repeating. There is a shot of anchor person. Then, there are separate shots of each of the invited guests. There may be some shots showing more than one people at a time. There is also a shot of showing the environment from a distance. Another common observation in Talk-Show is that the actor movement is very low, as people are generally sitting and rarely moving during the discussion.

Similarly, a Sports video also usually has only one scene but the factor which can easily distinguishes between a Talk-Show and a Sports video is the actor movement. Unlike a Talk-Show, in a sports video actor movement is significantly high. Fig. 2 and Fig. 3 illustrates the patterns observed in Talk-Shows and Sports videos, as described above.

In order to differentiate Movie/Drama and Animation from Sports and Talk-Show videos, we use number of scenes feature. As discussed earlier, in Sports and Talk-Show videos, generally, there is only one scene, whereas in Movie/Drama and Animation, the number of scenes are many, depending on the video length.



Fig. 2. Consecutive frames in a Talk-Show, demonstrating only one scene and low actor movement.



Fig. 4. Frames in a Movie, demonstrating more than 1 scene and long shot duration.



Fig. 3. Consecutive frames in a sports video demonstrating only one scene and high actor movement.



Fig. 5. Frames in an Animation, demonstrating more than 1 scene and small shot duration.

Finally, if input video comprises of many scenes, there is a possibility that the input video is either a Movie/Drama or an Animation. In order to differentiate between these two video genres, we use shot duration. It has been observed that shot duration is high when input video is a Movie/Drama, whereas the value of shot duration is low, typically less than a second for many shots, when input video is an Animation. Fig. 4 and Fig. 5 show consecutive frames from two popular Bollywood movies and two animations. It can be observed that all the frames in movies are belonging to same shot, whereas in animation, all the frames are formulating different shots.

Table I summarizes differences in different video features

across all four genres.

In the next section, we describe different components of video classifier including shot detection, scene detection and actor movement.

#### A. Shot Boundary Detection

There are many attempts in the literature to detect shot boundary in video [33], [35]–[40]. Anil k. Jain et al. [54]

TABLE I. VIDEO GENRE IDENTIFICATION FEATURE VALUES

| Video Genre | Scene Count | Actor Movement | Shot Duration |
|-------------|-------------|----------------|---------------|
| Talk Show   | Low         | Low            | High          |
| Sports      | Low         | High           | Low           |
| Drama/Movie | High        | Low            | High          |
| Animation   | High        | High           | Low           |

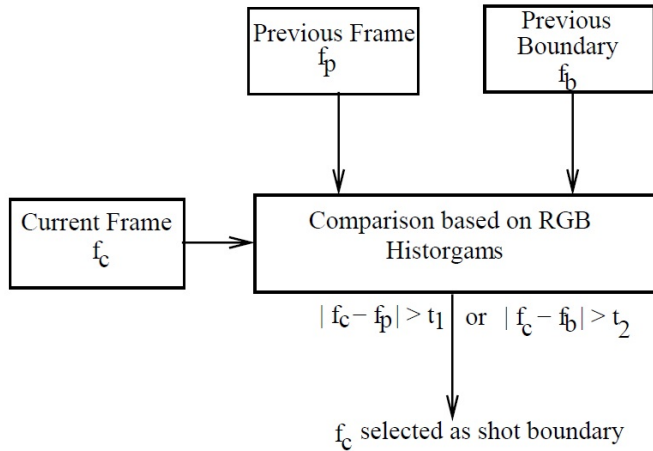


Fig. 6. Shot Boundary Detection [54]

proposed a method of shot boundary detection that is presented in Fig. 6.

A frame is defined as shot boundary if it is significantly different from either the previous frame or previous shot boundary. The different here refers to RGB histogram difference. One of the benchmark data-set for shot boundary detection is TRECVID, developed by NIST (National Institute of Standards and Technology in Gaithersburg, USA). TRECVID contains many subsets of video test data and ground truth information targeting the shot boundary detection which are widely used to evaluate the performance of different shot boundary detection algorithms [33].

One of the major issues in most of the shot detection approaches found in literature is requirement of learning threshold values for detecting shot boundary. Our experiments suggest that threshold values learned on a data-set do not perform well on other data-sets. For example, the threshold value for sum of absolute difference based on RGB color at pixel level learned on TRECVID 2007, as proposed by [34], does not perform well when used to detect shot boundaries from Bollywood movies. This might be because of different intensities in color values in two completely different data sets.

Inability of threshold values to make them independent of data-sets results in need of an algorithm that learns threshold values dynamically from the data set. Our approach of shot detection is based on clustering that eliminates the need of learning and applying static threshold values.

Suppose, we have a video  $V$  defined as set of  $n$  frames,

$$V = \{f_1, f_2, \dots, f_n\} \quad (8)$$

Simple sum of absolute difference  $d_{sad}$  between  $f_{i-1}$  and  $f_i$  is defined as [34]:

$$d_{sad}(f_{i-1}, f_i) = \frac{1}{|F|} \sum_{r \in F} |f_{i-1}(r) - f_i(r)| \quad (9)$$

Where  $F$  is the total number of pixel in a frame,  $d_{sad}$  is the function calculating the sum of absolute differences of each two consecutive frames and  $r$  represents the coordinates of pixels. A shot boundary is detected if,

$$d_{sad} \geq T \quad (10)$$

Where  $T$  is a threshold value learned through experiments. This approach of threshold value was tested on TRECVID 2007 and the precision and recall was reported to be 94.4% and 90.5%, respectively. In our approach, we use a set  $D$  consisting of  $d_{sad}$  for all the frames in a video  $V$ ,

$$D = \{d_{sad_1}, d_{sad_2} \dots d_{sad_{n-1}}\} \quad (11)$$

Our approach is based on two simple assumptions:

- 1) If two consecutive frames  $f_i$  and  $f_{i-1}$  belong to same shot, their  $d_{sad}$  would be relatively low
- 2) Consequently, if both the frames,  $f_i$  and  $f_{i-1}$  belong to two different shots, that is  $f_{i+1}$  is actually representing a shot boundary,  $d_{sad}$  would be high

Based on above two assumptions, different approaches in the literature have learned threshold values. We believe that learning threshold values could be avoided if we employ a clustering approach. We use simple K-Means clustering algorithm which is defined by a centroid for each cluster. Any point is assigned to its nearest centroid based on Euclidean distance. In our case, the value of  $K = 2$  which means two clusters.  $d_{sad}$  values in set  $D$  suggest that all the points are belonging to one of the two obvious clusters, suppose  $C$  is a set of centroids defined as:

$$C = \{c_i, c_j\} \quad (12)$$

Then each data point  $d_i$  in the set  $D$  is assigned to a cluster based on its squared distance from center  $c_i$ . Data suggests, the difference values fall in two distinct clustering categories:

- 1) The difference values are too low if consecutive frames are belonging to same shot.
- 2) The difference values are reasonably high if consecutive frames are belonging to two different shots.

Interestingly, in a video, non-representative frames to shot boundary are lower than the number of frames representing shot boundaries, thus, the cluster which holds lower number of frames is actually holding the shot boundaries. The advantage of our shot boundary detection over existing approaches is to avoid the need of learning threshold values. In a way, clustering mechanism is actually a dynamic threshold learning mechanism.

1) *Shot Detection: Post-Processing Step for Increasing System Precision:* Clustering based approach discussed in previous section, produces high recall values on TRECVID-2007, however, precision value is only 38%. It has been observed that simple clustering based algorithm is unable to distinguish well between two consecutive frames which are part of same shots but having high movement of high level objects like person, car, animal, etc. The absolute sum of difference as defined in previous section is high when there is significant movement between two consecutive frames belonging to same shot. In order to improve the system precision, we use RGB histogram values. No matter how much is the movement from one frame to next, RGB histogram remains almost same given both frames are belonging to same shot. We use this simple technique to eliminate false positives that are incorrectly clustered in the cluster which should hold shot boundary frames. With simple clustering algorithms for shot boundary detection followed by post-processing step, we achieved recall and precision of 97% and 92%, respectively on TRECVID-2007.

### B. Scene Detection

A scene is a temporal fragment of a video where shots are frequently repetitive. For example, in a talk-show. most of the shots are part of same scene. If observed closely, these shots are part of a frequently repetitive pattern. Same is the case with sports videos, where similar shots tend to repeat themselves and overall environment remains same. Contrasting, in case of a movie, drama or animation the repetition of same shot is not demonstrated throughout the video. Rather, this repetition is merely confined within a specific fragment of that video. A scene can be detected just by capturing this repetition of shots by using the Algorithm 1.

### C. Actor Movement Estimation

For video genre identification, actor movement is a strong predictor to classify between a talk-show and a sports video. In a talk-show the people and objects are generally stationary, while in a sports video, people and objects are continuously in moving state. The procedure followed to capture the actor movement is illustrated in Fig. 7. Here, two consecutive frames of video are broken down into 8x8 grid, resulting in 64 sub-images within each frame. The corresponding sub-images of both frames are compared. If there is low actor movement, many regions of the frame will remain same in both frames. On the other hand, if there is high actor movement, the sub-images will demonstrate significant level of dissimilarity.

Mathematically, actor movement  $A_m$  is defined as:

$$A_M = \frac{1}{n} \sum_{i=1}^n M_i \quad (13)$$

Where  $M$  represent average sum of difference between all the regions of a given  $Frame_i$  to its corresponding regions in  $Frame_j$  and defined as:

$$M = \sum_{i=1}^{64} |Frame_i - Frame_{i-1}| \quad (14)$$

---

### Algorithm 1 Scene Boundaries Detection Algorithm

---

**INPUT :** Set of Shot Boundaries  $S_h$   
**OUTPUT :** Set of Scene Boundaries  $S_c$

```

current ← 1, i ← 0, match ← 0
while current >= count(Sh) do
    current ← current + 2
    i ← current
    while current >= i do
        if Sh[current] == Sh[i - 2] then
            match ← 1
            break
        else
            match ← 0
            i --
        end if
    end while
    if match ← 0 then
        while (current - 1) >= (i - 3) do
            if Sh[current - 1] == Sh[i - 3] then
                match ← 1
                Sc ← current
                break
            else
                match ← 0
                i --
            end if
        end while
        if match ← 0 then
            Sc ← current - 1
        end if
    end if
end while

```

---

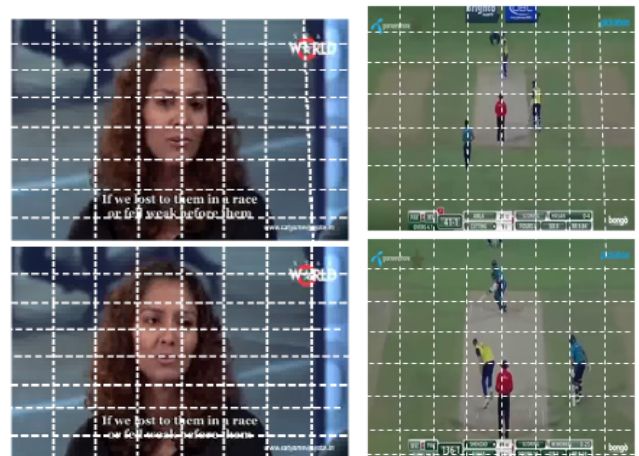


Fig. 7. Consecutive frames of 2 videos divided into 8x8 grid - on left are frames of a Talk Show (demonstrating low Actor Movement) and on right from a Sports Video (demonstrating high Actor Movement)

#### D. Shot Duration Estimation

To differentiate between a movie or drama and an animation, shot duration is used as a classifying feature. In a movie or drama, the shot duration is generally longer as compared to an animation. The proposed system performs shot boundary detection by using the cluster based approach as discussed earlier. The shot duration of  $i^{th}$  shot is defined as:

$$T_i = F_n - F_1 \quad (15)$$

Where  $F_n$  is last frame in a given shot and  $F_1$  is the first frame. The average shot duration in a video, that we use as feature to differentiate between movie/drama and animation genres, is defined as:

$$S_D = \frac{1}{n} \sum_{i=1}^n T_i \quad (16)$$

#### VI. EXPERIMENTAL RESULTS

The proposed system considerably depends on the intermediate procedures like shot detection, scene detection, motion detection and shot duration. Unfortunately, there is no benchmark data-set available with ground truth values recorded already. Therefore, for this study, a data-set comprising of 50 videos from the five desired genres (i.e. Music Video, Sports Video, Talk Show, Animation and Movie/Drama) was constructed. The number of scenes, and shot duration were observed manually to setup ground truth before applying the scene detection, motion detection and shot duration estimation. The manually calculated values were then compared to the values calculated by the system to evaluate its performance. The videos were selected carefully to avoid bias in the results. The data-set included 10 videos from each genre.

For music video, there is much signal variation even in case of pop, jazz and rock music and old classical songs or ballads. Thus the music videos were carefully selected to cover most of the possible classes. In this regard, the developed data-set included popular songs from Bollywood Movies and some international music channels from different categories.

The 10 sports videos in the data-set, all belonged to a distinct sports category: 1. Cricket, 2. Football, 3. Hockey, 4. Car Race, 5. Table Tennis, 6. Basketball, 7. Badminton, 8. Swimming, 9. Snooker and 10. Wrestling.

The 10 talk shows consisted 5 Pakistani shows, 3 talk shows from Indian TV channels and 2 American Talk shows. Similarly, the movies were selected both from Hollywood and Bollywood Industry, while the selected TV serials were taken from Pakistani, Indian as well as Turkish TV channels. The movies and dramas belonged to different genres like comedy, tragedy, romantic and action to cover the major variations of shot duration and camera movement. Also, the quality of graphics has drastically improved in past few decades, therefore to cover animations of all types, these were taken from old cartoons movies like pink panther to latest release of animated games like Assassin Creed and other animated movies in different foreign languages.

Table II shows the list of videos we have used in our data-set. The proposed system accurately predicts genre of 96% videos, the detailed results of genre identification are presented in confusion matrix of Table III. The results of scene detection are shown in Table IV.

TABLE II. SELECTED VIDEOS IN USER DEFINED DATA-SET FOR GENRE IDENTIFICATION

| Video                              | Genre       |
|------------------------------------|-------------|
| Capital Talk 29th May 2018         | Talk Show   |
| Capital Talk 31st May 2018         | Talk Show   |
| Live with Kelly 23rd April 2018    | Talk Show   |
| Live with Kelly 21st May 2018      | Talk Show   |
| Live with Kelly Priyanka           | Talk Show   |
| A+ Morning Show Hamid Mir          | Talk Show   |
| News Eye 29th May 2018             | Talk Show   |
| Coffee with Karan (Juhi & Madhuri) | Talk Show   |
| Satyamev Jayete (Dangal)           | Talk Show   |
| Comedy Nights with Kapil           | Talk Show   |
| Cricket                            | Sports      |
| Football                           | Sports      |
| Tennis                             | Sports      |
| Car Race                           | Sports      |
| Badminton                          | Sports      |
| Hockey                             | Sports      |
| Snooker                            | Sports      |
| Wrestling                          | Sports      |
| Basketball                         | Sports      |
| Swimming                           | Sports      |
| Big Buck Bunny                     | Animation   |
| Dreamworld - Ice Age               | Animation   |
| Memorable Moments - Rio            | Animation   |
| Tom and Jerry (Little Quacker)     | Animation   |
| Ferdinand - Escena Final Español   | Animation   |
| Mr. Bean -Nurse                    | Animation   |
| JAN on See TV                      | Animation   |
| Courage - The cowardly dog         | Animation   |
| Pink Panther                       | Animation   |
| Assassin's Creed Origin            | Animation   |
| Secret Super Star Part 1/6         | Movie/Drama |
| Andaz Apna Apna                    | Movie/Drama |
| Dhoop Kinare                       | Movie/Drama |
| Bulbulay                           | Movie/Drama |
| Diyar e Dil                        | Movie/Drama |
| Yaqeen Ka Safar                    | Movie/Drama |
| Dhamaal                            | Movie/Drama |
| Harry Potter                       | Movie/Drama |
| CID                                | Movie/Drama |
| Kosem Sultan                       | Movie/Drama |
| Everything I do, I do it for you   | Music Video |
| I am Alive, Stuart Little 2        | Music Video |
| It's my life, Bon Jovi             | Music Video |
| Kung fu fighting, Kung fu Panda    | Music Video |

Continued on next page

Continued from previous page

| Video                      | Genre       |
|----------------------------|-------------|
| Allah hi dega, Ubaid Rana  | Music Video |
| Sultan, Title Song         | Music Video |
| Challa, Jab tak hai jan    | Music Video |
| Hanikarak Bapu - Dangal    | Music Video |
| Khamaj, Shafqat Amanat Ali | Music Video |
| Tere bina zindagi, Andhi   | Music Video |

## VII. CONCLUSION

Different video genres have different recording rules, never documented but practiced so extensively that if violated, would result in a poor video. For example, imagine a movie action scene with high shot duration or low actor movement. Obviously, such videos won't inspire users. In this paper, we exploit these widely practiced recording rules for different genre videos and classify an input video in one of five genres including music, movie/drama, sports, talk-show and animation. Broadly, we use three visual features to achieve this classification task - 1) Shot Duration 2) Scene Count 3) Actor Movement along with three audio features including 1) High Zero Crossings Rate Ratio, 2) Spectrum Flux and 3) Low Short Time Energy Ratio. The audio features are used to separate music video from rest of the genres whereas scene count separates talk-show and sports video from movie/drama and animation. Finally, actor movement differentiates between talk-show and sports, and shot duration separates animation from movie/drama genre. We achieved classification accuracy of 96% on genre identification. Our shot boundary detection technique gives a precision and recall of 93.12% and 86.24%, respectively on TRECVID 2007 data-set. The advantage of our shot detection approach is elimination of need to learn threshold value for shot detection that varies in different data-sets.

## VIII. FUTURE WORK

The current video genre identification system can further be extended to identify sub-genres and sub-categories. A music video can be classified as ballad, classic, rock, pop and so on. Literature suggest many approaches of music genre identification based on music audio, whereas there is a possibility to classify musical video in any particular category. Similarly, by applying different speech recognition techniques a Talk show can be further classified as political, business, or entertainment categories. By applying shape identification techniques on objects within a video, the type of sports can also be identified in future. The shape and size of ball differs from one sports category to another. Presence of bat, racket, boundary rope or hockey sticks can also reveal more about the sports category. The current system classifies movie and drama as a same category, a future system can differentiate even between these two categories by assessing video size. Movie and dramas can also be sub divided into popular genres like comedy, action, tragic or romantic. An animation can be differentiated with a gaming video by using low level features like frame rate and motion rate, etc.

## REFERENCES

- [1] S. Asur and B. A. Huberman, "Predicting the future with social media," in *Proceedings of the 2010 IEEE/WIC/ACM International Conference on Web Intelligence and Intelligent Agent Technology-Volume 01*, pp. 492–499, IEEE Computer Society, 2010.
- [2] J. Tang, Y. Chang, and H. Liu, "Mining social media with social theories: a survey," *ACM SIGKDD Explorations Newsletter*, vol. 15, no. 2, pp. 20–29, 2014.
- [3] D. H. Park, I. Y. Choi, H. K. Kim, and J. K. Kim, "A review and classification of recommender systems research," *International Proceedings of Economics Development & Research*, vol. 5, no. 1, p. 290, 2011.
- [4] D. Brezeale and D. J. Cook, "Automatic video classification: A survey of the literature," *IEEE Transactions on Systems, Man, and Cybernetics, Part C (Applications and Reviews)*, vol. 38, no. 3, pp. 416–430, 2008.
- [5] S. Wang and Q. Ji, "Video affective content analysis: a survey of state of the art methods," *IEEE Transactions on Affective Computing*, no. 1, pp. 1–1, 2015.
- [6] A. G. Hauptmann, R. Yan, Y. Qi, R. Jin, M. G. Christel, M. Derthick, M.-y. Chen, R. V. Baron, W.-H. Lin, and T. D. Ng, "Video classification and retrieval with the informedia digital video library system.," in *TREC*, 2002.
- [7] U. Srinivasan, S. Pfeiffer, S. Nepal, M. Lee, L. Gu, and S. Barras, "A survey of mpeg-1 audio, video and semantic analysis techniques," *Multimedia Tools and Applications*, vol. 27, no. 1, pp. 105–141, 2005.
- [8] G. Lu, "Indexing and retrieval of audio: A survey," *Multimedia Tools and Applications*, vol. 15, no. 3, pp. 269–290, 2001.
- [9] S. M. Doudpota and S. Guha, "Mining movies to extract song sequences," in *Proceedings of the Eleventh International Workshop on Multimedia Data Mining*, p. 2, ACM, 2011.
- [10] L. Canini, S. Benini, and R. Leonardi, "Affective recommendation of movies based on selected connotative features," *IEEE Transactions on Circuits and Systems for Video Technology*, vol. 23, no. 4, pp. 636–647, 2013.
- [11] J. H. French, "Automatic affective video indexing: Sound energy and object motion correlation discovery," in *Southeastcon, 2012 Proceedings of IEEE*, pp. 1–6, IEEE, 2012.
- [12] M. Xu, J. Wang, X. He, J. S. Jin, S. Luo, and H. Lu, "A three-level framework for affective content analysis and its case studies," *Multimedia tools and applications*, vol. 70, no. 2, pp. 757–779, 2014.
- [13] L. Lu, H. Jiang, and H. Zhang, "A robust audio classification and segmentation method," in *Proceedings of the ninth ACM international conference on Multimedia*, pp. 203–211, ACM, 2001.
- [14] X. Ding, B. Li, W. Hu, W. Xiong, and Z. Wang, "Horror video scene recognition based on multi-view multi-instance learning," in *Asian Conference on Computer Vision*, pp. 599–610, Springer, 2012.
- [15] S. M. Doudpota, S. Guha, and J. Baber, "Shot-based genre identification in musicals," in *Wireless Networks and Computational Intelligence*, pp. 129–138, Springer, 2012.
- [16] Z. Cernekova, C. Kotropoulos, and I. Pitas, "Video shot segmentation using singular value decomposition," in *Acoustics, Speech, and Signal Processing, 2003. Proceedings.(ICASSP'03). 2003 IEEE International Conference on*, vol. 3, pp. III–181, IEEE, 2003.
- [17] R. W. Lienhart, "Reliable dissolve detection," in *Storage and Retrieval for Media Databases 2001*, vol. 4315, pp. 219–231, International Society for Optics and Photonics, 2001.
- [18] D. Lelescu and D. Schonfeld, "Statistical sequential analysis for real-time video scene change detection on compressed multimedia bit-stream," *IEEE Transactions on Multimedia*, vol. 5, no. 1, pp. 106–117, 2003.
- [19] J. Yu and M. D. Srinath, "An efficient method for scene cut detection," *Pattern Recognition Letters*, vol. 22, no. 13, pp. 1379–1391, 2001.
- [20] B. Lehane, N. E. O'Connor, and N. Murphy, "Action sequence detection in motion pictures.," in *EWMT*, Citeseer, 2004.
- [21] J. Mas and G. Fernandez, "Video shot boundary detection based on color histogram," *Notebook Papers TRECVID2003, Gaithersburg, Maryland, NIST*, vol. 15, 2003.

TABLE III. VIDEO GENRE IDENTIFICATION RESULTS

|        |             | Predicted |           |       |             |           |
|--------|-------------|-----------|-----------|-------|-------------|-----------|
|        |             | Music     | Talk Show | Sport | Movie/Drama | Animation |
| Actual | Music       | 10        | 0         | 0     | 0           | 0         |
|        | Talk Show   | 0         | 9         | 0     | 1           | 0         |
|        | Sports      | 0         | 0         | 10    | 0           | 0         |
|        | Movie/Drama | 0         | 0         | 0     | 10          | 0         |
|        | Animation   | 0         | 0         | 0     | 1           | 9         |

TABLE IV. RESULTS OF SCENE DETECTION ON 40 VIDEOS OF USER DEFINED DATA-SET, (AS. SCENE DETECTION NOT APPLIED ON 10 MUSIC VIDEOS)

| Video Name                   | Actual Scene Count | Predicted Scene Count | Precision | Recall |
|------------------------------|--------------------|-----------------------|-----------|--------|
| Capital Talk (Video 1)       | 1                  | 1                     | 100       | 100    |
| Capital Talk (Video 2)       | 1                  | 1                     | 100       | 100    |
| Live with Kelly (Video 1)    | 4                  | 9                     | 45        | 100    |
| Live with Kelly (Video 2)    | 12                 | 18                    | 50        | 82     |
| Live with Kelly (Video 3)    | 1                  | 1                     | 100       | 100    |
| A+ Morning Show              | 1                  | 1                     | 100       | 100    |
| News Eye (Dawn News)         | 1                  | 1                     | 100       | 100    |
| Coffee with Karan            | 1                  | 1                     | 100       | 100    |
| Satyamev Jayete              | 1                  | 1                     | 100       | 100    |
| Comedy Nights with Kapil     | 1                  | 1                     | 100       | 100    |
| Big Buck Bunny               | 5                  | 5                     | 100       | 100    |
| Dreamworld - Ice Age         | 19                 | 20                    | 83        | 74     |
| Memorable Moments - Rio      | 22                 | 30                    | 60        | 77     |
| Tom and Jerry                | 14                 | 17                    | 76        | 93     |
| Ferdinand                    | 8                  | 6                     | 100       | 75     |
| Mr. Bean                     | 12                 | 18                    | 60        | 100    |
| JAN on See TV                | 10                 | 8                     | 84        | 72     |
| Courage - The cowardly dog   | 20                 | 24                    | 83        | 98     |
| Pink Panther                 | 11                 | 10                    | 90        | 82     |
| Assassin Creed Origin        | 6                  | 6                     | 100       | 100    |
| Secret Super Star, Bollywood | 120                | 108                   | 75        | 60     |
| Andaz Apna Apna, Bollywood   | 40                 | 12                    | 90        | 41     |
| Bulbulay, ARY Digital        | 18                 | 35                    | 52        | 100    |
| Diyar e Dil, Hum TV          | 31                 | 26                    | 73        | 55     |
| Yaqaen Ka Safar, Hum TV      | 38                 | 26                    | 92        | 70     |
| Dhoop Kinare, PTV Classic    | 39                 | 32                    | 50        | 81     |
| Dhamaal, Bollywood           | 53                 | 102                   | 55        | 100    |
| Harry Potter, Hollywood      | 57                 | 113                   | 73        | 100    |
| CID, Sony Entertainment      | 27                 | 36                    | 60        | 78     |
| Kosem Sultan, Turkish        | 20                 | 26                    | 70        | 900    |
| Cricket Video                | 1                  | 1                     | 100       | 100    |
| Football Video               | 1                  | 1                     | 100       | 100    |
| Tennis Video                 | 1                  | 1                     | 100       | 100    |
| Car Race Video               | 1                  | 1                     | 100       | 100    |
| Badminton Video              | 1                  | 1                     | 100       | 100    |
| Hockey Video                 | 1                  | 1                     | 100       | 100    |
| Snooker Video                | 1                  | 1                     | 100       | 100    |
| Wrestling Video              | 1                  | 1                     | 100       | 100    |
| Basketball Video             | 1                  | 1                     | 100       | 100    |
| Swimming Video               | 1                  | 1                     | 100       | 100    |
| Overall                      | 504                | 615                   | 85.5      | 90.7   |

[22] V. Kobla, D. S. Doermann, K.-I. Lin, and C. Faloutsos, "Compressed-domain video indexing techniques using dct and motion vector information in mpeg video," in *Storage and Retrieval for Image and Video Databases V*, vol. 3022, pp. 200–212, International Society for Optics and Photonics, 1997.

[23] H. Wang, A. Divakaran, A. Vetro, S.-F. Chang, and H. Sun, "Survey of compressed-domain features used in audio-visual indexing and analysis," *Journal of Visual Communication and Image Representation*, vol. 14, no. 2, pp. 150–183, 2003.

[24] D. PEH, "Ro duda, pe hart, and dg stork, pattern classification, new york: John wiley & sons, 2001, pp. xx+ 654, isbn: 0-471-05669-3," *Journal of Classification*, vol. 24, no. 2, pp. 305–307, 2007.

[25] R. O. Duda, P. E. Hart, D. G. Stork, *et al.*, "Pattern classification. 2nd," *Edition. New York*, vol. 55, 2001.

[26] C. M. Bishop, "Pattern recognition and machine learning (information science and statistics) springer-verlag new york," *Inc. Secaucus, NJ, USA*, 2006.

[27] S. Fischer, R. Lienhart, and W. Effelsberg, "Automatic recognition of film genres," *Technical reports*, vol. 95, 1995.

[28] A. Yazdani, E. Skodras, N. Fakotakis, and T. Ebrahimi, "Multimedia content analysis for emotional characterization of music video clips," *EURASIP Journal on Image and Video Processing*, vol. 2013, no. 1, p. 26, 2013.

[29] M. Xu, C. Xu, X. He, J. S. Jin, S. Luo, and Y. Rui, "Hierarchical affective content analysis in arousal and valence dimensions," *Signal Processing*, vol. 93, no. 8, pp. 2140–2150, 2013.

[30] R. M. A. Teixeira, T. Yamasaki, and K. Aizawa, "Determination of emotional content of video clips by low-level audiovisual features," *Multimedia Tools and Applications*, vol. 61, no. 1, pp. 21–49, 2012.

[31] Y. Cui, S. Luo, Q. Tian, S. Zhang, Y. Peng, L. Jiang, and J. S. Jin, "Mutual information-based emotion recognition," in *The Era of Interactive Media*, pp. 471–479, Springer, 2013.

[32] C. Cotsaces, N. Nikolaidis, and I. Pitas, "Video shot boundary detection and condensed representation: a review," *IEEE signal processing magazine*, vol. 23, no. 2, pp. 28–37, 2006.

[33] A. F. Smeaton, P. Over, and A. R. Doherty, "Video shot boundary



- detection: Seven years of trecvid activity,” *Computer Vision and Image Understanding*, vol. 114, no. 4, pp. 411–418, 2010.
- [34] Y. Kawai, H. Sumiyoshi, and N. Yagi, “Shot boundary detection at trecvid 2007.,” in *TRECVID*, 2007.
- [35] Z. Li, X. Liu, and S. Zhang, “Shot boundary detection based on multilevel difference of colour histograms,” in *2016 First International Conference on Multimedia and Image Processing (ICMIP)*, pp. 15–22, IEEE, 2016.
- [36] T. Kar and P. Kanungo, “Video shot boundary detection based on hilbert and wavelet transform,” in *Man and Machine Interfacing (MAMI), 2017 2nd International Conference on*, pp. 1–6, IEEE, 2017.
- [37] C. Pingping, Y. Guan, X. Ding, and Z. Yu, “Shot boundary detection with sparse presentation,” in *Signal Processing (ICSP), 2016 IEEE 13th International Conference on*, pp. 900–904, IEEE, 2016.
- [38] S. Domic, “Walsh-hadamard transform kernel-based feature vector for shot boundary detection,” *IEEE Transactions on Image Processing*, vol. 23, no. 12, pp. 5187–5197, 2014.
- [39] J. Mondal, M. K. Kundu, S. Das, and M. Chowdhury, “Video shot boundary detection using multiscale geometric analysis of nset and least squares support vector machine,” *Multimedia Tools and Applications*, vol. 77, no. 7, pp. 8139–8161, 2018.
- [40] M. Yazdi and M. Fani, “Shot boundary detection with effective prediction of transitions’ positions and spans by use of classifiers and adaptive thresholds,” in *Electrical Engineering (ICEE), 2016 24th Iranian Conference on*, pp. 167–172, IEEE, 2016.
- [41] S.-B. Park, H.-N. Kim, H. Kim, and G.-S. Jo, “Exploiting script-subtitles alignment to scene boundary detection in movie,” in *Multimedia (ISM), 2010 IEEE International Symposium on*, pp. 49–56, IEEE, 2010.
- [42] M. Ellouze, N. Boujemaa, and A. M. Alimi, “Scene pathfinder: unsupervised clustering techniques for movie scenes extraction,” *Multimedia Tools and Applications*, vol. 47, no. 2, pp. 325–346, 2010.
- [43] V. T. Chasanis, A. C. Likas, and N. P. Galatsanos, “Scene detection in videos using shot clustering and sequence alignment,” *IEEE transactions on multimedia*, vol. 11, no. 1, pp. 89–100, 2009.
- [44] S. B. Needleman and C. D. Wunsch, “A general method applicable to the search for similarities in the amino acid sequence of two proteins,” *Journal of molecular biology*, vol. 48, no. 3, pp. 443–453, 1970.
- [45] A. Hanjalic, “Shot-boundary detection: Unraveled and resolved?,” *IEEE transactions on circuits and systems for video technology*, vol. 12, no. 2, pp. 90–105, 2002.
- [46] L. Lu, H.-J. Zhang, and S. Z. Li, “Content-based audio classification and segmentation by using support vector machines,” *Multimedia systems*, vol. 8, no. 6, pp. 482–492, 2003.
- [47] C. Panagiotakis and G. Tziritas, “A speech/music discriminator based on rms and zero-crossings,” *IEEE Transactions on multimedia*, vol. 7, no. 1, pp. 155–166, 2005.
- [48] E. Scheirer and M. Slaney, “Construction and evaluation of a robust multifeature speech/music discriminator,” in *Acoustics, Speech, and Signal Processing, 1997. ICASSP-97, 1997 IEEE International Conference on*, vol. 2, pp. 1331–1334, IEEE, 1997.
- [49] D. Li, I. K. Sethi, N. Dimitrova, and T. McGee, “Classification of general audio data for content-based retrieval,” *Pattern recognition letters*, vol. 22, no. 5, pp. 533–544, 2001.
- [50] H. Harb, L. Chen, and J.-Y. Auloge, “Speech/music/silence and gender detection algorithm,” in *In Proceedings of the 7th International conference on Distributed Multimedia Systems DMS01*, Citeseer, 2001.
- [51] A. Pirkakis, T. Giannakopoulos, and S. Theodoridis, “A speech/music discriminator of radio recordings based on dynamic programming and bayesian networks,” *IEEE Transactions on Multimedia*, vol. 10, no. 5, pp. 846–857, 2008.
- [52] L. Lu, S. Z. Li, and H.-J. Zhang, “Content-based audio segmentation using support vector machines,” in *Proc. ICME*, vol. 1, pp. 749–752, 2001.
- [53] J. Saunders, “Real-time discrimination of broadcast speech/music,” in *icassp*, pp. 993–996, IEEE, 1996.
- [54] A. K. Jain, A. Vailaya, and X. Wei, “Query by video clip,” *Multimedia systems*, vol. 7, no. 5, pp. 369–384, 1999.

# A Comparison of Sentiment Analysis Methods on Amazon Reviews of Mobile Phones

Sara Ashour Aljuhani<sup>1</sup>, Norah Saleh Alghamdi<sup>2</sup>  
School of Computing, Dublin City University (DCU)<sup>1</sup>  
Dublin, Ireland  
Department of Computer Science<sup>1,2</sup>  
Princess Nourah bint Abdulrahman University (PNU)  
Riyadh, KSA

**Abstract**—The consumer reviews serve as feedback for businesses in terms of performance, product quality, and consumer service. In this research, we predict consumer opinion based on mobile phone reviews, in addition to providing an analysis of the most important factors behind reviews being classified as either positive, negative, or neutral. This insight could help companies improve their products as well as helping potential buyers to make the right decision. The research presented in this paper was carried out as follows: the data was pre-processed, before being converted from text to vector representation using a range of feature extraction techniques such as bag-of-words, TF-IDF, Glove, and word2vec. We study the performance of different machine learning algorithms, such as logistic regression, stochastic gradient descent, naive Bayes and convolutional neural networks. In addition, we evaluate our models using accuracy, F1-score, precision, recall and log loss function. Moreover, we apply Lime technique to provide analytical reasons for the reviews being classified as either positive, negative or neutral. Our experiments revealed that convolutional neural network with word2vec as a feature extraction technique provides the best results for both the unbalanced and balanced versions of the dataset.

**Keywords**—Bag-of-words; TF-IDF; glove; word2vec; logistic regression; stochastic gradient descent; naive bayes; Convolutional Neural Network; log loss; lime

## I. INTRODUCTION

Purchasing a product is an interaction between two entities, consumers and business owners [1]. Consumers often use reviews to make decisions about what products to buy, while businesses, on the other hand, not only want to sell their products but also want to receive feedback in terms of consumer reviews. Consumers reviews about purchased products shared on the internet have great impact [2]. Human nature is generally structured to make decisions based on analysing and getting the benefit of other consumer experience and opinions because others often have a great influence on our beliefs, behaviours, perception of reality, and the choices we make [3]. Hence, we ask others for their feedback whenever we are deciding on doing something. Additionally, this fact applies not only to consumers but also to organizations and institutions. In the last few years, consumer ways of expressing their opinions and feelings have changed according to changes in social networks, virtual communities and other social media communities [4]. Discovering large amounts of data from unstructured data on the web has become an important challenge due to its importance in different areas of life [5]. To allow better information extraction from the plethora of data available,

sentiment analysis has emerged to be able to predict the polarity (positive, negative, neutral) of consumer opinion [6]. This in turn would help consumers to better analyse the textual data providing useful information. We study in this research sentiment analysis of mobile phone reviews taken from the Amazon<sup>1</sup> website, and how these reviews help consumers to have confidence that they have made the right decision about their purchases. Also, the research in this work aims to help companies understand their consumers' feedback to maintain their products/services or enhance them. In addition, giving them insights about them in providing offers on specific products to increase their profits and customer satisfaction.

### A. Problem Statement

Recently, electronic commerce websites use of the Internet has increased to the point that consumers rely on them for buying and selling [7]. Since these websites give consumers the ability to write comments about different products and services, huge amounts of reviews have become available [8]. Consequently, the need for to analyse those reviews to understand consumers' feedbacks has increased for both vendors and consumers. However, it is difficult to read all the feedbacks for a particular item especially for the popular items with many comments [9]. In this research, we attempt to build a predictor for consumers' satisfaction on a mobile phone product based on the reviews. We will also attempt to understand the factors that contribute to classifying reviews as positive, negative or neutral (based on important or most frequent words). This is believed to help companies improve their products and also help potential buyers make better decisions when buying products.

This paper is structured as follows, Section 2 discusses the required background of the work. The related work in the previous literature is discussed in Section 3. Section 4 and Section 5 explain both methodology and implementation respectively. Section 6 reports the experimental results of various settings while Section 7 discuss the limitations that could be leveraged as future directions. Lastly, Section 8 concludes the findings of the paper.

## II. BACKGROUND

Sentiment analysis involves a combination of natural language processing, computational linguistics and textual analy-

<sup>1</sup><https://www.amazon.com/>

sis in order to detect positive, negative or neutral feelings about the subject of the text [10]. It is used in different areas such as marketing, customer services, and amongst others. Sentiment analysis can be performed on both document-level or sentence-level depending on the unit of information being considered. In this project, sentence-level was considered [11]. Sentiment analysis has several applications in different areas including advertisement where sentiment analysis contributes in selecting specific advertisements to be shown on commercial and social media channels according to particular users opinions on particular products [12]. Sentiment analysis can also be utilized for opinion retrieval, i.e. build search systems to search for specific views on specific topics [13].

### III. RELATED WORK

Since this work is interested in studying the sentiments of mobile phones reviews on Amazon, the work related to analysing the sentiments of mobile phones or Amazon reviews have been considered in the review. In the following, these researches are reviewed in terms of pre-processing techniques, feature extraction methods, proposed methodologies, and evaluation metrics.

Various work in the literature have focused on the problem of identifying users opinions of different products using Amazon reviews of “Unlocked Mobile Phones” [14], [15]. The work by [14] focused on a specific Brand Name, ‘iPhone’, to examine algorithms’ validity in order to classify online reviews using a supervised model. On the other hand, [15] aggregated 400,000 reviews from various Brand Names. They did their experiments on two steps. First, they used balanced data which means that the number of negative reviews (1 and 2 star) is equal to the number of positive reviews (4 and 5 star), and they removed neutral reviews. Second, while using unbalanced data, they considered (1 and 2 star) as negative reviews and (3, 4, 5) as positive reviews. At the pre-processing phase, [14] did not take emoticon expressions into consideration, they rather focused on reviewers’ IDs, they assumed they must be unique and any duplications were eliminated. Also, names with @ sign and blank spaces were rejected. In addition, they applied feature reduction using a filter to remove stop words such as a, an, the, etc. After this reduction, the authors observed that the text was reduced by 8.68%. Moreover, after preprocessing step, the dataset contained 9,500 positive reviews and 9,500 negative reviews, and 2,500 neutral. On the other hand, [15] Used spaCy library to clean the data. They made stemming to utilize only the words roots. They also removed stop words to reduce the number of words, converted the words to lowercase, and removed both punctuation and whitespace. Unigram and weighted unigram were used in [14] as features, and the authors eventually concluded that weighted unigram gave the best results. On the other hand, word2vec [16], CBOW [17] and skip-gram [18] models were used to represent features. In terms of machine learning algorithms utilized, both [15] and [14] used naïve Bayes (NB) [19], [20] and support vector machine (SVM) [21], [22], but [15] added more algorithms such as logistic regression (LR) [23] and random forest (RF) [24]. In terms of results, [14] achieved the highest accuracy (81.20%) when using SVM and weighted unigram as features. On the other hand, random forest (RF) scored the highest accuracy (90.66%) when used with CBOW as features as reported in the experimental results by [15]. Other authors focused on

sentimental analysis of mobile phones reviews from different sources with different languages such as Chinese. The dataset used by [25] was obtained from jeng dong website which is specialized on mobile phone reviews. The authors collected a group of labelled data that consisted of 1,500 positive reviews and 1,500 negative reviews. They also collected real mobile application review. In a similar work proposed by [26], the dataset was gathered from ‘we chat’ over a span of three years. In addition, the review was scored from one to five where 1 and 2 were considered negative, 3 is considered neutral, while 4 and 5 were considered positive in terms of polarity. At the end, the dataset contained 109,901 positive reviews, 23,654 negative reviews, and 11,688 neutral reviews with percentages of 75.6%, 16.28%, 8.05% respectively. Also, the authors compared between various types of properties about mobile application reviews that made difference between mobile application reviews and PC reviews. Additionally, they used spare of length property which deals with the min and max size of chart. The minimum size is 1 chines chart while maximum size is 6,000 chines chart. Moreover, on short average length, the authors said that while they were reviewing the statistical features, they found that the average chines chart in mobile reviews was 17 while in micro blog it was 45 word. They started with feature selections in many approaches before establishing the algorithms. [25] mentioned variety of N grams. First, character ngram which is based on character sequence. Second, word ngram which considered words sequences. Third, POS (part-of-speech) ngram which considered part-of-speech types sequences. The authors discussed three types of n-POS-gram: i) Noun ngram, ii) a combination of noun and verb ngram, and finally, iii) a mixture of noun, adverb and adjective ngram. In their work, the authors focused on both n-char-gram and n-POS-grams. They developed a feature selection to document frequency method. After that, they used boolean weighted method (TF&IDF) [27] to calculate feature weight. On the other hand, [26] used word count in reviews to make sure there is no repetition within the same review and ngrams were used for features representation. In terms of the utilized machine learning algorithms, in their work [25] applied LIBSVM and SVM algorithms to analyse the sentiment polarity of the review. The result of this paper viewed ngrams using English language limited with one or two words. Yet in Chinese, they used ngram with higher values of n for more accurate results. A high performance was obtained when using 4-grams as reported in their results. In their conclusion, the authors reported that integrating noun, adverb and adjective ngram yields the best results. On the other hand, the authors of [26] showed that using SVM leads to more accurate results to identify positive reviews, and using naïve Bayes is more accurate with negative reviews. Furthermore, the best performance was obtained by using bigrams.

### IV. METHODOLOGY

In this section, we will present the methodology and techniques used in classifying mobile phone reviews that are adopted by most of the researchers in the field of sentiment analysis. Firstly, we will explain the steps followed during the experiments. Fig. 1 illustrates the phases of this work starting with the reviews dataset till the classification of each review into positive, negative, and neutral.

A. Preprocessing

In the preprocessing step, the reviews were tokenised, spelling mistakes were checked for, and all words were lower-cased. Also, stop-words such as “a, an, with etc.” were removed from the data. The tokens were returned to their roots by performing lemmatisation on all tokens. Each review in the dataset was labelled as positive, negative, or neutral based on its star rating in the same way adopted by [14]. The dataset was then split into 70% for training, 15% for development, and 15% for testing.

B. Feature Extraction

The employed dataset is textual, so it needs to be represented in numerical formats to be fed to the machine learning algorithms to build the desired classifiers. To achieve this, different vectorisation techniques are performed including term frequency which involves counting all the occurrences of all the terms in the document or sentence. A term can be expressed as a single word i.e. unigram, or any arbitrary number of words, namely, n-grams [28]. Fig. 2 illustrates how unigrams, bigrams, and trigrams can be formed from a sentence. Term frequency or count vectoriser (BOW) method suffer from a major pitfall, as it takes into account all the terms without taking into consideration the fact that some terms are very frequent in the corpus. Those terms do not capture document specific information since they occur in the majority of the documents. Such a drawback can be tackled by defining a maximum threshold for document frequency. However, the tuning of this threshold can be tricky, therefore, term frequency- inverse document frequency (TF-IDF) [27] is introduced. TF-IDF is a weighting scheme that works by giving low weight to the terms that occur frequently in the given corpus. Inverse document frequency (IDF) is the inverse of the number of times a specific term appeared in the entire corpus. It captures how a particular term is document specific, and when multiplied by term frequency (TF) the result should give a measure of how this term is of particular importance to the document at hand. Equation (1) demonstrates the main formula used for computing the TF-IDF for each term in each document.

$$TF - IDF = TF_{wd} * IDF_W \tag{1}$$

Although TF, and TF-IDF are popular feature representation techniques in various natural language processing tasks [27], they define the vocabulary over a given corpus as a set of unique words, ignoring the semantic and syntactic similarities between those words. For example, in both TF and TF-IDF extraction techniques, the words pretty and beautiful are represented as two different words although they are nearly synonyms. Therefore, distributed words representations, namely word-embeddings were introduced as an alternative features extraction technique [29]. Word-embeddings are extracted from huge corpora using different algorithms including deep learning algorithms [30]. The main idea behind word embeddings is to convert each word to a mathematical vector. In addition, each word will be represented by a vector, words with similar meaning have similar representations and this word is represented as positive and negative decimal number [31]. For example, the representation of Man = [1.0 2.9 0.9 -38 ...]. Therefore, we can find from this vector the similarity

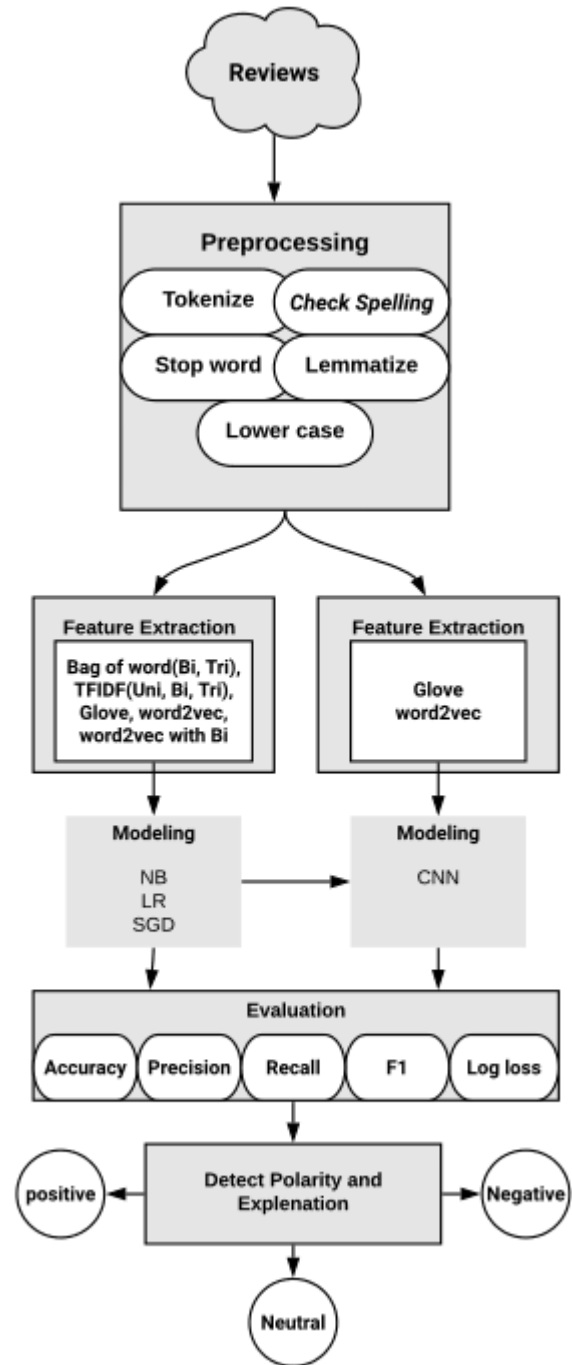


Fig. 1. Phases of the experiments of Amazon website dataset of mobile phone reviews sentiment analysis.

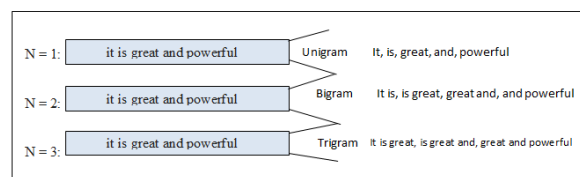


Fig. 2. Unigrams, bigrams, and n-grams extraction from a given sentence

between the words using mathematical equations. To illustrate, when word-embeddings are used to express the words as numerical vectors and different mathematical operations are performed on them as follows: Man + King – Woman = Queen. Egypt + Cairo – Saudi Arabia = Riyadh. Given the two examples above it is illustrated that the learned embeddings capture the information that a king is a man and a queen is a woman. Also that Cairo is the capital city of Egypt and Riyadh is its equivalent for Saudi Arabia. Two different types of word embeddings were included in this study, global vector for word representation (Glove) [32] and word2vec [33][34].

### C. Machine Learning Algorithms

In this work, different machine learning algorithms were applied to build a prediction model to assign a polarity for a given review. Logistic regression (LR), naive Bayes (NB), Stochastic gradient descent (SGD) [35], and convolutional neural network (CNN) [36] were experimented. Logistic regression (LR), assigns a probability to each class given an input vector it is originally a binary classification algorithm that can be extended to perform multi-class classification. Naive Bayes is a probabilistic classification algorithm that utilizes the properties of Bayes theorem hypothesis relationship between independent variables [37]. There are three types of naive Bayes classifiers: Gaussian, Bernoulli, and multinomial. Gaussian naive Bayes is used when the dataset is continuous, Bernoulli when the dataset is binary, and multinomial with count data. Bernoulli and multinomial naive Bayes are applied in text data classification [38]. Support vector machine (SVM) is a kernel based method, that attempts to find the optimal decision boundary by transforming non-linearly separable data samples to a higher dimension space where there exists a separation hyperplane [21]. Stochastic gradient descent (SGD) [39],[40] is a powerful technique applied to increase the speed and classification capability of SVM and LR. Therefore, it can be effectively applied to large datasets. Also, it works well with text classification and natural language processing. Stochastic gradient descent (SGD) classifier takes as input the sample before predicting the next value, and compares it with the actual value. In addition, it contains a loss function to measure the distance between the predictive and actual value. If the distance is high, then gradient descent (GD) changes the weight of each feature then compares it against each iteration until it reaches to a more similar value to the actual value. If the type of loss function is equal to 'hinge', that means it is used to optimise an SVM, while if loss is equal to 'log' then it is used to optimise an LR model. During the step of changing the weight of the feature, over-fitting problems may arise. So, the classifier compares the prediction value between training and development data. If the value of train is increasing and development is decreasing then an early stop function stops changing the weight. Convolutional neural network (CNN) [41] is a deep learning method which is effective for analysing images and text with huge data volumes. CNN is a supervised algorithm, so it needs labelled data to advance the weights of its convolutional filters. In addition, it receives the data from feature extraction as input then sends it to hidden layers called convolutional layers. These layers are the basis of CNNs. The first layer transforms the input, then the output from this layer sends it to the other layer. It is a sequence until the last layer. This process is called convolutional operation. Moreover, each

layer contains filters to detect the pattern. The size of the filter is determined at the beginning to monitor the algorithm and observe how it learns. The size of the filter is determined based on how many characteristics are needed to be detected. If it is large, it means that the size of the filter needs to be increased. Since machine learning models work as a black box, as they take the input, do some processing, then give the output. Lime (Locally interpretable models and effects) [42] is an incredible tool to clarify what classifiers predict. It works by making a line, separating the features and then seeing the strongest feature which are near to the line. Also, Lime adjusts a solitary input test by tweaking the element esteems and watching the subsequent effect on the output. In addition, the output from Lime is a list of interpretabilities. For example, In the medical domain where a patient goes to the doctor and the doctor enters the symptoms to the model, then the model predicts that the patient has flu based on some symptoms such as sneeze, weight, headache, feeling fatigue, age, etc. So, Lime explains why the model predicted flu and gives the reasons, which are sneeze and headache.

### D. Evaluation Parameters

In this work, the metrics used to test the performance of machine learning classifier are: accuracy, precision, recall, and F1-score [38]. Precision measures the percentage of positive reviews that predict truly divided by the total number of reviews that are classified positively as defined by Equation 2.

$$PR = \frac{tp}{tp + fp} \quad (2)$$

Recall on the other hand measures the percentage of the reviews that classify positively divided by the total number of reviews which are truly positive, as in Equation 3

$$RC = \frac{tp}{tp + fn} \quad (3)$$

F1-score combines both precision and recall as in Equation 4.

$$F1 - score = 2 * \frac{PR * RC}{PR + RC} \quad (4)$$

Lastly, accuracy is defined as the percentage of reviews that are classified correctly divided by the total number of reviews, Equation 5. Where tp, tn, fp, and fn are true positives, true negatives, false positives, and false negatives respectively.

$$ACC = \frac{tp + tn}{tp + tn + fp + fn} \quad (5)$$

Log loss<sup>2</sup> is also used to measure the performance of machine learning algorithms where the forecast input is a probability estimate somewhere in the range between 0 and 1. The objective of our models is to reduce the value of log loss. Therefore, the model performance can judge based on the log loss value, if the result is equal to 1 this means that the model is predicting value far from the actual value and it is not a good model. On the other hand, the model that provides values equal or near to zero is a better model. Moreover, it considers the vulnerability of your forecast dependent on the amount it fluctuates from the actual label. This gives us a more nuanced look into the execution of our model.

<sup>2</sup>[scikit-learn.org/stable/modules/generated/sklearn.metrics.log\\_loss.html](https://scikit-learn.org/stable/modules/generated/sklearn.metrics.log_loss.html)

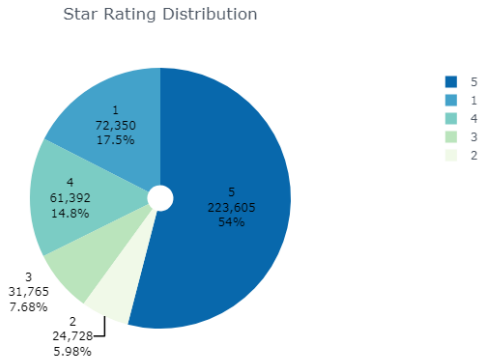


Fig. 3. Illustration of star rating distribution for Amazon website unbalanced dataset of mobile phone reviews.

## V. IMPLEMENTATION

### A. Data Collection

The dataset used for this research was obtained from Kaggle<sup>3</sup>. The data collected from Amazon it is about unlocked mobile phones. It consists of 400,000 reviews and it contains 6 columns: 1) Brand Name: it depicts the name of the organization, e.g. Nokia; 2) Product Name: e.g. Nokia Asha 302; 3) Price: the cost of the mobile; 4) Rating: star rating which the costumer gives to the product; 5) Reviews: the users opinion about each product; 6) Review Votes: the Number of consumers who voted the review. Moreover, to evaluate the model we divided the dataset to 70% for training data, 15% for developing data, and 15% for testing the data.

### B. Data Exploration

First, we want to examine the numbers of reviews each star rating contains. To represent this relationship, we used a 'pie chart' or a 'circle chart' diagram. Fig. 3 demonstrates the distribution. In this representation we used plotly and cufflink library. From the 'pie chart' of star ratings among the reviews, we notice that 54% of consumers gave 5, 7.68% gave 3, 17.5% gave 1, 14.4% gave 4, and very few gave a 2-star rating (5.98%).

We studied the distribution of Number of Reviews and the Brand Name. We concluded that Samsung received the highest number of reviews with 57,35k, while Blu and Apple got corresponding number of reviews 50,06K. The reviews are lower for LG. On the other hand, Sony, Posh mobile, and huawei acquired the least reviews. The rest of the brands obtained an average number of reviewers between 19K to 10K.

We also study the relationship between Review Length and Sentiment (Positive, Negative, Neutral). Fig. 4 shows that, negative reviews are longer in general. This is likely to be caused by consumers tending to elaborate in writing to express their feelings when they become angry from a product and tend to write less when they are happy. Moreover, from visualization we observed the distribution of the data is not normal. We evaluated the normality of the data (positive, negative,

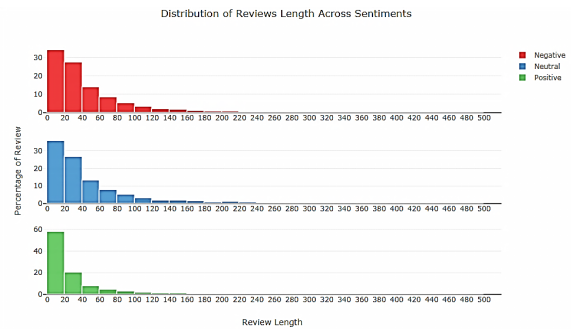


Fig. 4. The length of the review and the sentiment of review for Amazon website unbalanced dataset of mobile phone reviews.

neutral) using Shapiro test, and we found all classes do not follow normal distribution. So, we applied non-parametric test (Wilcoxon Rank Sum Test) from SciPy library to calculate the medians of the distributions, compare each two classes together and see if it is different than each other or not. Finally, we found 'p value' between (Negative, Neutral) classes = 0.0037, (Negative, Neutral) and (Neutral, Positive) = 0, that means the p value < 0.05. which clarifies it is a statistically significant variable to identify the polarity.

### C. Data Preprocessing

Each dataset needs to be prepared before entering it to the machine learning algorithms in order to achieve a high accuracy. Since we deal with textual dataset, it requires appropriate pre-processing. We carried out several steps to clean the data. First, we converted all "Brand Names" to lower case e.g. Samsung is written as "samsung". Second, we dropped the null value in "Reviews" (62 null values). Third, we replaced any "Asus computers" Brand Name to "Asus", "Lg electronics" to "Lg". After that, we used spaCy library, which is a machine learning library. spaCy is very powerful library in the domain of Natural language processing (NLP).

- 1) Tokenization: the purpose of Tokenization is to split the sentence into separate words based on white space. Each word is called a token. Fig. 5 show the review before and after tokenization.
- 2) Removing stop words: this involves cleaning stop words (e.g. a, the, about, etc.) that do not add meaning to reviews. There is another kind of stop word (e.g. cell phone, mobile, etc.) which is not built in to the library, specific for the dataset. We removed these special stop words because they are repeated a lot in the corpus, i.e. more than 50%. In addition, the words that repeated less than 4 times in the corpus.
- 3) Lemmatization of a word: this means returning words to their roots by eliminating all prefixes and suffixes. Fig. 6 illustrates before and after removing stop words and lemmetizing steps. As we can see the words and, the, would, not were removed as they are stop words. Moreover, the word dies is returned to its root die by removing 's' letter.
- 4) Lower casing: in this step we converted words from upper case to lower case.
- 5) Punctuation and special characters elimination: Such as coma, full stop, exclamation mark, etc.

<sup>3</sup><https://www.kaggle.com/PromptCloudHQ/amazon-reviews-unlocked-mobile-phones>

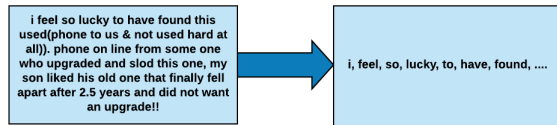


Fig. 5. Tokenization for Amazon website unbalanced dataset of mobile phone reviews.

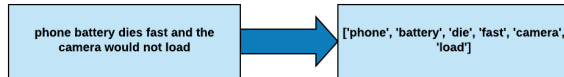


Fig. 6. Lemmatization for Amazon website unbalanced dataset of mobile phone reviews.

#### D. Features Engineering

In this step we take the "Ready Document" from preprocessing, then vectorize them using the following methods:

- Term frequency.
- TF-IDF.
- Glove.
- Word2vec.

The result from each method is a matrix that represents all documents in the dataset as vectors. These vectors can be fed to the machine learning algorithms to build classification models.

#### E. Classification Models

Using all four types of features mentioned in the previous section, LR models were trained. Using unigrams, bigrams, and trigrams for both TF and TF-IDF. NB and SGD models were also trained using all four types of features. Lastly, CNN was trained using documents represented using only word2vec and Glove. The parameters that define the structure of the CNN\_word2vec are specified as follows: First,  $n\_unique\_words = 10000$ , here we determined the most 10000 words that are repeated in the corpus. Second,  $max\_review\_length = 100$ , this shows the length of the vector for each review. Third,  $n\_dim = 100$ , we determined fixed length of the vector for each word. Fourth,  $drop\_embed = 0.5$ , it determines the number of neurons work, i.e. when word embedding starts to enforce all neuron to get the same number of jobs. So, in each step only the half of total number of neurons work. Fifth,  $k\_conv = 3$  it is about the dimension of the word, in our project it depended on the Trigram. Sixth,  $n\_conv = 256$  it is about the number of filters. Seventh,  $n\_dense = 128$  it is about the number of neurons on fully connected layers. After that, we used function sequence to convert each word to its index number. Then we applied `pad_sequences` function which fills the vector at the begin by zero then the values of the review at the end, it takes two parameters (sequence and max review length). Additionally, sentiment column contains positive, negative, and neutral in one column. However, in order for Keras library to work well, it must separate sentiment column to three columns (positive, Negative, Neutral). To do this step we used `np_utils.to_categorical` function. Then we used `encode` function to convert positive to 2, negative to 0, and neutral to

1. After that, we designed Neural Network layers: 1) sequential layers; 2) Embedding layers which take three parameters ( $n\_unique\_words$ ,  $n\_dim$ ,  $input\_length = max\_review\_length$ ); 3) SpatialDropout1D ( $drop\_embed$ ) for the purpose of the number of neurons work; 4) (Conv1D ( $n\_conv$ ,  $k\_conv$ ,  $activation = 'relu'$ )): it is about the dimension of the text and activation function `relu` it is about the mathematical process between neurons; 5) Global Max Pool layer to focus on the most power full words; 6) Dense ( $n\_dense$ ,  $activation = 'softmax'$ ) we mentioned it above and activation function `softmax` it is determine the final classes. In addition, to configure the model we used `adam` optimizer to calculate the distance between the prediction and actual value. `Adam` optimizer determines the learning rate based on the distance. If the distance large, then `adam` optimizer will increase the learning rate. Finally, we used 40 epoch to train the data. To build convolutional neural network with Glove as features engineering method we used same parameter we mentioned it in `word2vec` except we change the value of `drop_embed` to 0.25 and  $n\_conv$  to 512, to increase the complexity. Because under fitting problem appeared. Moreover, The same layers and discussed functions in `word2vec` are being used for the rest of the model to achieved the goal.

To get more insightful results, Lime was applied as follows: At the beginning we start using Lime library by importing `lime` text to take a review as a text and Lime text explainer to interpret the classifier prediction. Then, we defined variable name `class_name` that contains the sentiment label 'Negative', 'Neutral', and 'Positive'. After that, we applied `visualize_one_exp`. This function takes six parameters to visualize the result: First, `features`: the text we send it to lime. Second, `labels`: the label of the text. Third, `index`. Forth, `pipeline_obj`: it takes two inputs `Count` victories and our model. Fifth, `class_names = bigram_model.classes.tolist()`. Sixth, `top_labels=1`: how many interpretable classes are shown, `sit` explains only positive or negative or neutral or two labels together. Moreover, we used `explain_one_instance`. This function explains the lime with the same parameter (`instance`, `pipe_line_obj`, `class_names=bigram_model.classes._tolist()`, `top_labels= None`). Finally, we used variable `exp` to save the vale send it from `explainer.explain_instance` function, this function takes 4-parameter: (i) `instance`, (ii) `pipe_line_obj.predict_proba` which predicts the probability for each word in the sentence that effect on the prediction, (iii) `num_features= 6` which is about the highest word probability appear, and (iv) `top_labels=top_labels`).

## VI. EXPERIMENTS AND EVALUATION

In our research, each review has been classified as positive, negative, or neutral based on the star rating. So, four and five-star ratings are categorized as positive where two and one-star ratings are classified as negative. Finally, three-star rating is classified as neutral. We first, ran experiments on unbalanced data. Second, we applied our experiments to balanced data. Meaning that we took the same number of positive, negative, and neutral reviews. In our dataset, neutral reviews had the lowest number of reviews by 21,000 reviews. Therefore, we used this numbers for each sentiment balanced data.

TABLE I. RESULTS OF LOGISTIC REGRESSION FOR AMAZON WEBSITE UNBALANCED DATASET (DEVELOPMENT SPLIT) OF MOBILE PHONE REVIEWS.

|          | LL   | F     | RC    | PR    | ACC   |
|----------|------|-------|-------|-------|-------|
| BOW+B    | 0.29 | 91.21 | 91.71 | 91.42 | 91.71 |
| BOW+T    | 0.28 | 91.63 | 92.06 | 91.77 | 92.06 |
| TF-IDF+U | 0.39 | 84.29 | 86.63 | 85.55 | 86.63 |
| TF-IDF+B | 0.33 | 87.96 | 89.47 | 89.39 | 89.47 |
| TF-IDF+T | 0.34 | 87.34 | 88.90 | 88.76 | 88.90 |
| Glove    | 0.48 | 79.64 | 82.95 | 79.39 | 82.95 |
| word2vec | 0.44 | 81.36 | 84.56 | 81.79 | 84.56 |

TABLE II. RESULTS OF NAIVE BAYES FOR AMAZON WEBSITE UNBALANCED DATASET (DEVELOPMENT SPLIT) OF MOBILE PHONE REVIEWS.

|            | LL   | F     | RC    | PR    | ACC   |
|------------|------|-------|-------|-------|-------|
| BOW+B      | 0.67 | 87.00 | 87.87 | 86.98 | 87.87 |
| BOW+T      | 0.73 | 87.47 | 88.53 | 87.94 | 87.53 |
| TF-IDF+U   | 0.46 | 80.17 | 83.36 | 82.12 | 83.34 |
| TF-IDF+B   | 0.43 | 82.83 | 85.82 | 86.48 | 85.82 |
| TF-IDF+T   | 0.34 | 87.34 | 88.90 | 88.76 | 88.90 |
| Glove      | 0.75 | 54.61 | 67.66 | 45.78 | 67.66 |
| word2vec   | 0.71 | 54.72 | 76.71 | 68.81 | 67.71 |
| word2vec+B | 0.67 | 55.80 | 68.17 | 68.59 | 68.17 |

A. Results Obtained by Unbalanced data

Tables I, II, III and IV show the results for LR, NB, SGD, and CNN respectively using different features extraction techniques. Both BOW and TF-IDF have three variations depending on the number of grams used where U represents unigram, B represents bigram, and T represents trigrams. For logistic regression, bag-of-words with trigrams provided the highest accuracy and log loss value with 92.06%, 0.28 respectively. For naive Bayes we can observe that best performance is obtained by TF-IDF (Bigram) at 85.82% accuracy and 0.43 log loss. In contrast, Bag-of-words (Trigram) achieved higher accuracy at 88.53% but its log loss value is far from its actual value, it is 0.73. because when the value is near to zero, its near to actual value. However, Glove, Word2vec, and Word2vec with Bigram did not give good results because these methods study semantic between the word and measure similarity.

As shown in Table III, it can be observed the best performance for SGD is Bag-of-words (Trigram) with 89.61% accuracy. Moreover, we did not get any result from log loss since SGD is not a probabilistic algorithm. Table IV shows that CNN with word2vec achieved an accuracy of 92.73% and Log loss of 0.23. We can observe that the Log loss value is very near to zero. So, the performance of the model is very high, and probability of the error is very low. Additionally, CNN with Glove achieved 90.51% accuracy and 0.29 log loss value. A likely reason for this low result is that Glove has been applied on a per-trained model and the language is formal, while in reviews the language is informal. Finally, we found that CNN with word2vec achieved the best result comparing with Glove algorithms.

All the previous results were obtained using the development split of the dataset. Therefore, to obtain the test results, best settings of all of the four algorithms were applied on the test split, the results are illustrated in Table V. However, CNN achieved the best results with word2vec. In addition, all algorithms provided the lowest results with Glove feature extraction. As shown by Table V, CNN with word2vec achieved best result by 92.72 accuracy and 0.23 log loss.

TABLE III. RESULTS OF STOCHASTIC GRADIENT DESCENT FOR AMAZON WEBSITE UNBALANCED DATASET (DEVELOPMENT SPLIT) OF MOBILE PHONE REVIEWS.

|            | F     | RC    | PR    | AC    |
|------------|-------|-------|-------|-------|
| BOW+B      | 87.86 | 89.07 | 88.90 | 89.07 |
| BOW+T      | 88.56 | 89.61 | 89.43 | 89.61 |
| TF-IDF+U   | 81.14 | 84.74 | 82.82 | 84.74 |
| TF-IDF+B   | 81.59 | 85.13 | 84.66 | 85.13 |
| TF-IDF+T   | 81.43 | 85.00 | 84.58 | 85.00 |
| Glove      | 80.11 | 83.58 | 80.24 | 83.58 |
| word2vec   | 80.79 | 84.49 | 81.90 | 84.94 |
| word2vec+B | 81.21 | 84.70 | 82.91 | 84.70 |

TABLE IV. RESULTS OF CONVOLUTIONAL NEURAL NETWORKS FOR AMAZON WEBSITE UNBALANCED DATASET (DEVELOPMENT SPLIT) OF MOBILE PHONE REVIEWS.

|          | LL   | F     | RC    | PR    | AC    |
|----------|------|-------|-------|-------|-------|
| Glove    | 0.23 | 92.00 | 92.00 | 92.00 | 92.73 |
| word2vec | 0.29 | 90.00 | 90.00 | 90.00 | 90.51 |

B. Results Obtained by Balanced data

Tables VI, VII, VIII and IX show the results for LR, NB, SGD, and CNN respectively using different features extraction techniques. Both BOW and TF-IDF have three variations depending on the number of grams used where U represents unigram, B represents bigram, and T represents trigrams.

The best results of all of the four algorithms are reported in Table X. It is observed that We CNN with word2vec provided best accuracy with 79.60% and a log loss of 0.52.

C. Lime Results Analysis

To show positive reviews using Lime, Fig. 7 provides some insight into the possible reasons behind classifying the review as positive. We can notice that the model detects the words 'great' and 'love' with the highest probability effect by 0.09, the word 'nice' at 0.04. To illustrate, the words in dark green give higher effect than the words in lighter color. To represent negative reviews using Lime, Fig. 8 demonstrates why the model predicted the review as a negative one. The word mess with the highest probability is equal to 0.09, crack by 0.08, and the word damage with 0.04 probability. However, the light blue color in the figure means that it does not have effect as much as mess and crack. Also, there is neutral word with total probability 0.08 but the total probability of negative

TABLE V. FINAL RESULTS FOR AMAZON WEBSITE UNBALANCED DATASET (TEST SPLIT) OF MOBILE PHONE REVIEWS.

| Setting        | LL   | F     | RC    | PR    | ACC   |
|----------------|------|-------|-------|-------|-------|
| BOW+T → LR     | 0.3  | 91.24 | 91.72 | 91.44 | 91.72 |
| TF-IDF+B → NB  | 0.43 | 82.77 | 86.69 | 86.54 | 85.69 |
| BOW+T → SGD    | -    | 88.49 | 89.51 | 89.25 | 89.51 |
| word2vec → CNN | 0.23 | 92.46 | 92.37 | 92.37 | 92.72 |

TABLE VI. RESULTS OF LOGISTIC REGRESSION FOR AMAZON WEBSITE BALANCED DATASET (DEVELOPMENT SPLIT) OF MOBILE PHONE REVIEWS.

|            | LL    | F    | RC    | PR    | ACC   |
|------------|-------|------|-------|-------|-------|
| BOW+B      | 78.84 | 0.61 | 78.96 | 78.87 | 78.96 |
| BOW+T      | 79.37 | 0.60 | 79.52 | 79.44 | 79.52 |
| TF-IDF+U   | 71.27 | 0.67 | 71.53 | 71.20 | 71.53 |
| TF-IDF+B   | 75.89 | 0.62 | 76.04 | 75.88 | 76.04 |
| TF-IDF+T   | 76.90 | 0.61 | 77.01 | 76.89 | 77.01 |
| Glove      | 66.35 | 0.76 | 66.66 | 66.29 | 66.66 |
| word2vec   | 66.01 | 0.76 | 66.44 | 65.89 | 66.44 |
| word2vec+B | 66.44 | 0.75 | 66.73 | 66.33 | 66.73 |



TABLE VII. RESULTS OF NAIVE BAYES FOR AMAZON WEBSITE BALANCED DATASET (DEVELOPMENT SPLIT) OF MOBILE PHONE REVIEWS.

|            | LL   | F     | RC    | PR    | ACC   |
|------------|------|-------|-------|-------|-------|
| BOW+B      | 1.1  | 72.28 | 72.98 | 72.96 | 72.98 |
| BOW+T      | 1.3  | 70.79 | 72.10 | 72.99 | 72.10 |
| TF-IDF+U   | 0.72 | 69.82 | 69.84 | 69.83 | 69.84 |
| TF-IDF+B   | 0.63 | 74.08 | 74.34 | 74.18 | 74.34 |
| TF-IDF+T   | 0.62 | 74.42 | 74.90 | 74.94 | 74.90 |
| Glove      | 1.06 | 49.11 | 50.03 | 51.34 | 50.03 |
| word2vec   | 1.04 | 61.96 | 61.85 | 63.51 | 61.85 |
| word2vec+B | 1.01 | 64.05 | 63.93 | 65.20 | 63.93 |

TABLE VIII. RESULTS OF STOCHASTIC GRADIENT DESCENT FOR AMAZON WEBSITE BALANCED DATASET (DEVELOPMENT SPLIT) OF MOBILE PHONE REVIEWS.

|            | F     | RC    | PR    | AC    |
|------------|-------|-------|-------|-------|
| BOW+B      | 76.66 | 76.95 | 76.87 | 76.95 |
| BOW+T      | 76.92 | 77.18 | 77.12 | 77.18 |
| TF-IDF+U   | 70.05 | 70.74 | 70.28 | 70.74 |
| TF-IDF+B   | 73.90 | 74.47 | 74.33 | 74.47 |
| TF-IDF+T   | 74.74 | 74.74 | 74.58 | 74.74 |
| Glove      | 68.68 | 68.82 | 68.57 | 68.82 |
| word2vec   | 65.97 | 66.96 | 66.15 | 66.96 |
| word2vec+B | 69.60 | 70.15 | 69.70 | 70.15 |

words is highest. To highlight neutral reviews using Lime, we observed from Fig. 9 that the word ‘fine’ appeared as a positive with 0.17 probability, ‘freeze’ with 0.33 and ‘okay’ with 0.32 as a negative word. The words ‘freeze’ and ‘okay’ got also probability 0.43, 0.25 prospectively as neutral word. Hence, the total of neutral words is the highest so the model predicted it as neutral.

VII. BENCHMARKING

We also compare our work with some other work. In this paper, we involved dividing the data into three parts. First, training the data with 70%. Second, testing with 15%. Third, development with 15%. [15] has chosen to divided the data into two parts. Where, 80% of the data is training and the 20% left is for the testing, While, [14] has only worked on part of the dataset where only 21,500 were useful for training and 3,000 for testing. Moreover, our work and [15] both have worked on balanced and unbalanced data unlike [14]. A slight difference between our experiments and [15] is that our work categorized both the balanced and unbalanced into, five and four star ratings as positive, one and two as negative, and three as neutral. Meanwhile, [15] has categorized balanced and unbalanced data separately. Where, one- and two-star ratings as negative, four and five as positive, and three has been cancelled off for balance data. For unbalanced data comprised

TABLE IX. RESULTS OF CONVOLUTIONAL NEURAL NETWORKS FOR AMAZON WEBSITE BALANCED DATASET (DEVELOPMENT SPLIT) OF MOBILE PHONE REVIEWS.

|          | LL   | F     | RC    | PR    | AC    |
|----------|------|-------|-------|-------|-------|
| Glove    | 0.51 | 80.00 | 80.00 | 80.00 | 79.91 |
| word2vec | 0.60 | 76.00 | 76.00 | 76.00 | 76.51 |

TABLE X. FINAL RESULTS FOR AMAZON WEBSITE BALANCED DATASET (TEST SPLIT) OF MOBILE PHONE REVIEWS.

| Setting        | LL   | F     | RC    | PR    | ACC   |
|----------------|------|-------|-------|-------|-------|
| BOW+T → LR     | 0.66 | 77.27 | 77.47 | 77.34 | 77.47 |
| TF-IDF+T → NB  | 0.62 | 74.42 | 74.90 | 74.94 | 74.90 |
| BOW+T → SGD    | -    | 75.75 | 76.05 | 75.94 | 76.05 |
| word2vec → CNN | 0.52 | 79.57 | 79.55 | 79.55 | 79.60 |

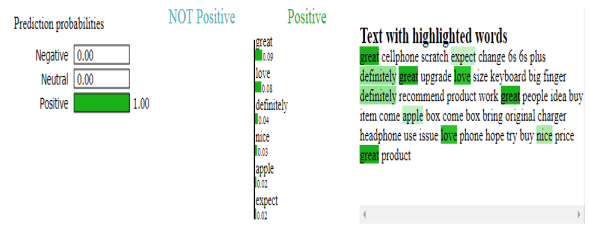


Fig. 7. Positive interpretation for Amazon website unbalanced dataset of mobile phone reviews.

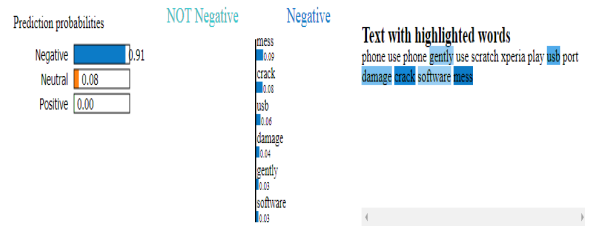


Fig. 8. Negative interpretation for Amazon website unbalanced dataset of mobile phone reviews.

one- and two-star rating as negative a three, four, and five as positive. Also, another point we have in common with one of the papers is that [14] and our work used the same algorithm (naive Bayes) with TF-IDF (unigram). On the other hand, [15] applied different deep learning methods such as, CBOW and skip-gram. To sum up, our work cannot be directly compared to either of the results because of the difference in the data division.

VIII. LIMITATIONS AND FUTURE WORK

In this study, we implemented four types of algorithms with a variety of feature extraction. Some algorithms that remain to be applied in future work include LSTM, KNN, and Maximum entropy. Then, we will compare the result to the result we performed in this current study. Also, we intend to add Arabic language to increase the scope of the research. Our research has some limitations: NLP is relatively a new topic, and highly advanced; hence, it needs a lot of research to understand the field and how it works. Furthermore, we faced some problems with computer memory causing experiments to be highly time consuming. We also used Google Colab to increase the performance, but it did not give us the expected speed.

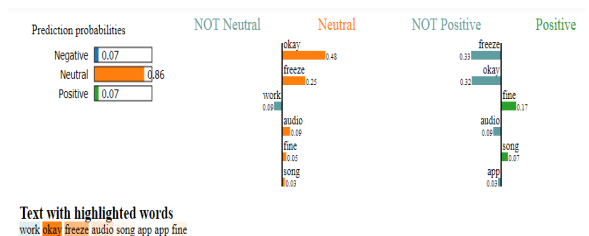


Fig. 9. Neutral interpretation for Amazon website unbalanced dataset of mobile phone reviews.

## IX. CONCLUSION

Reviews are essential for both individuals and companies. Consumers used them to make good decisions prior to buying a specific product and companies benefit from them to know their consumers' satisfaction about products. In this research we studied sentiment analysis of mobile phone reviews using different types of machine learning classifiers, such as Logistic Regression (LR), Naïve Bayes (NB), Stochastic Gradient Decent (SGD) and deep learning algorithms such as Convolutional Neural Networks (CNN). These algorithms are applied using different feature extraction approaches. For example, Bag-of-words with (Bigram, Trigram), TF-IDF with (Unigram, Bigram, Trigram), word2vec, word2vec with Bigram, and glove. We evaluated them with different classification methods such as bag-of-words revealing that when the size of 'n' in n-gram increases, the accuracy will also increase, and Log loss value will decrease. On the other hand, our Bigram approach provided best results with TF-IDF in unbalanced data, and Trigram in balanced data. Moreover, word2vec deep learning feature extraction provided better accuracy than Glove because glove used a pre-trained model, and the language the text written was formal, while in our corpus the reviews were written in informal language. Also, CNN with word2vec achieved the best accuracy (92.72%), and log loss value (0.23) compared to all other algorithms for unbalanced data. While in balanced data CNN with word2vec methods achieved the best result compared to other algorithms with (79.60%) accuracy and (0.52) log loss. Finally, we applied Lime technique to interpret the reasons behind classifying the reviews as positive, negative or neutral. From the statistical analysis, it was concluded that the length of a review is a significant variable to identify the polarity, therefore, it can be included as a feature to the machine learning algorithms.

## REFERENCES

- [1] C. Heller Baird and G. Parasnis, "From social media to social customer relationship management," *Strategy & leadership*, vol. 39, no. 5, pp. 30–37, 2011.
- [2] A. J. Flanagan, M. J. Metzger, R. Pure, A. Markov, and E. Hartsell, "Mitigating risk in ecommerce transactions: perceptions of information credibility and the role of user-generated ratings in product quality and purchase intention," *Electronic Commerce Research*, vol. 14, no. 1, pp. 1–23, 2014.
- [3] Y. Kim and J. Srivastava, "Impact of social influence in e-commerce decision making," in *Proceedings of the ninth international conference on Electronic commerce*, pp. 293–302, ACM, 2007.
- [4] R. Zhang and T. T. Tran, "Helping e-commerce consumers make good purchase decisions: a user reviews-based approach," in *International Conference on E-Technologies*, pp. 1–11, Springer, 2009.
- [5] R. Bolden and J. Moscarola, "Bridging the quantitative-qualitative divide: the lexical approach to textual data analysis," *Social science computer review*, vol. 18, no. 4, pp. 450–460, 2000.
- [6] B. Pang, L. Lee, et al., "Opinion mining and sentiment analysis," *Foundations and Trends® in Information Retrieval*, vol. 2, no. 1–2, pp. 1–135, 2008.
- [7] J. Riegelsberger, M. A. Sasse, and J. D. McCarthy, "Shiny happy people building trust?: photos on e-commerce websites and consumer trust," in *Proceedings of the SIGCHI conference on Human factors in computing systems*, pp. 121–128, ACM, 2003.
- [8] J. P. Singh, S. Irani, N. P. Rana, Y. K. Dwivedi, S. Saumya, and P. K. Roy, "Predicting the "helpfulness" of online consumer reviews," *Journal of Business Research*, vol. 70, pp. 346–355, 2017.
- [9] Z. Zhang, "Weighing stars: Aggregating online product reviews for intelligent e-commerce applications," *IEEE Intelligent Systems*, vol. 23, no. 5, pp. 42–49, 2008.
- [10] T. Wilson, J. Wiebe, and P. Hoffmann, "Recognizing contextual polarity in phrase-level sentiment analysis," in *Proceedings of Human Language Technology Conference and Conference on Empirical Methods in Natural Language Processing*, 2005.
- [11] C. Zhang, D. Zeng, J. Li, F.-Y. Wang, and W. Zuo, "Sentiment analysis of chinese documents: From sentence to document level," *Journal of the American Society for Information Science and Technology*, vol. 60, no. 12, pp. 2474–2487, 2009.
- [12] Y. Zhang, G. Lai, M. Zhang, Y. Zhang, Y. Liu, and S. Ma, "Explicit factor models for explainable recommendation based on phrase-level sentiment analysis," in *Proceedings of the 37th international ACM SIGIR conference on Research & development in information retrieval*, pp. 83–92, ACM, 2014.
- [13] J. Serrano-Guerrero, J. A. Olivas, F. P. Romero, and E. Herrera-Viedma, "Sentiment analysis: A review and comparative analysis of web services," *Information Sciences*, vol. 311, pp. 18–38, 2015.
- [14] A. S. Rathor, A. Agarwal, and P. Dimri, "Comparative study of machine learning approaches for amazon reviews," *Procedia computer science*, vol. 132, pp. 1552–1561, 2018.
- [15] B. Bansal and S. Srivastava, "Sentiment classification of online consumer reviews using word vector representations," *Procedia computer science*, vol. 132, pp. 1147–1153, 2018.
- [16] Y. Goldberg and O. Levy, "word2vec explained: deriving mikolov et al.'s negative-sampling word-embedding method," *arXiv preprint arXiv:1402.3722*, 2014.
- [17] T. Mikolov, K. Chen, G. Corrado, and J. Dean, "Efficient estimation of word representations in vector space," *arXiv preprint arXiv:1301.3781*, 2013.
- [18] D. Guthrie, B. Allison, W. Liu, L. Guthrie, and Y. Wilks, "A closer look at skip-gram modelling," in *LREC*, pp. 1222–1225, 2006.
- [19] A. McCallum, K. Nigam, et al., "A comparison of event models for naive bayes text classification," in *AAAI-98 workshop on learning for text categorization*, vol. 752, pp. 41–48, Citeseer, 1998.
- [20] I. Rish et al., "An empirical study of the naive bayes classifier," in *IJCAI 2001 workshop on empirical methods in artificial intelligence*, vol. 3, pp. 41–46, 2001.
- [21] T. Joachims, "Text categorization with support vector machines: Learning with many relevant features," in *European conference on machine learning*, pp. 137–142, Springer, 1998.
- [22] J. A. Suykens and J. Vandewalle, "Least squares support vector machine classifiers," *Neural processing letters*, vol. 9, no. 3, pp. 293–300, 1999.
- [23] R.-E. Fan, K.-W. Chang, C.-J. Hsieh, X.-R. Wang, and C.-J. Lin, "Liblinear: A library for large linear classification," *Journal of machine learning research*, vol. 9, no. Aug, pp. 1871–1874, 2008.
- [24] L. Breiman, "Random forests," *Machine learning*, vol. 45, no. 1, pp. 5–32, 2001.
- [25] L. Zheng, H. Wang, and S. Gao, "Sentimental feature selection for sentiment analysis of chinese online reviews," *International journal of machine learning and cybernetics*, vol. 9, no. 1, pp. 75–84, 2018.
- [26] L. Zhang, K. Hua, H. Wang, G. Qian, and L. Zhang, "Sentiment analysis on reviews of mobile users," *Procedia Computer Science*, vol. 34, pp. 458–465, 2014.
- [27] J. Ramos et al., "Using tf-idf to determine word relevance in document queries," in *Proceedings of the first instructional conference on machine learning*, vol. 242, pp. 133–142, Piscataway, NJ, 2003.
- [28] A. Tripathy, A. Agrawal, and S. K. Rath, "Classification of sentiment reviews using n-gram machine learning approach," *Expert Systems with Applications*, vol. 57, pp. 117–126, 2016.
- [29] M. Kusner, Y. Sun, N. Kolkin, and K. Weinberger, "From word embeddings to document distances," in *International Conference on Machine Learning*, pp. 957–966, 2015.
- [30] D. Bollegala, T. Maehara, and K.-i. Kawarabayashi, "Unsupervised cross-domain word representation learning," *arXiv preprint arXiv:1505.07184*, 2015.
- [31] M. Dragoni and G. Petrucci, "A neural word embeddings approach for multi-domain sentiment analysis," *IEEE Transactions on Affective Computing*, vol. 8, no. 4, pp. 457–470, 2017.
- [32] D. Mackay, "Glove.," May 7 1907. US Patent 852,972.

- [33] C. Cerisara, P. Kral, and L. Lenc, "On the effects of using word2vec representations in neural networks for dialogue act recognition," *Computer Speech & Language*, vol. 47, pp. 175–193, 2018.
- [34] A. Khatua, A. Khatua, and E. Cambria, "A tale of two epidemics: Contextual word2vec for classifying twitter streams during outbreaks," *Information Processing & Management*, vol. 56, no. 1, pp. 247–257, 2019.
- [35] L. Bottou, "Large-scale machine learning with stochastic gradient descent," in *Proceedings of COMPSTAT'2010*, pp. 177–186, Springer, 2010.
- [36] Y. Kim, "Convolutional neural networks for sentence classification," *arXiv preprint arXiv:1408.5882*, 2014.
- [37] H. Zhang, "The optimality of naive bayes," *AA*, vol. 1, no. 2, p. 3, 2004.
- [38] A. Tripathy, A. Agrawal, and S. K. Rath, "Classification of sentimental reviews using machine learning techniques," *Procedia Computer Science*, vol. 57, pp. 821–829, 2015.
- [39] S. Shalev-Shwartz, Y. Singer, N. Srebro, and A. Cotter, "Pegasos: Primal estimated sub-gradient solver for svm," *Mathematical programming*, vol. 127, no. 1, pp. 3–30, 2011.
- [40] S. Lu and Z. Jin, "Improved stochastic gradient descent algorithm for svm,"
- [41] I. Banerjee, Y. Ling, M. C. Chen, S. A. Hasan, C. P. Langlotz, N. Moradzadeh, B. Chapman, T. Amrhein, D. Mong, D. L. Rubin, *et al.*, "Comparative effectiveness of convolutional neural network (cnn) and recurrent neural network (rnn) architectures for radiology text report classification," *Artificial intelligence in medicine*, 2018.
- [42] M. T. Ribeiro, S. Singh, and C. Guestrin, "Why should i trust you?: Explaining the predictions of any classifier," in *Proceedings of the 22nd ACM SIGKDD international conference on knowledge discovery and data mining*, pp. 1135–1144, ACM, 2016.

# Virtualizing a Cluster to Optimize the Problems of High Scientific Complexity within an Organization

Enrique Lee Huamani<sup>1</sup>, Patricia Condori<sup>2</sup>, Avid Roman-Gonzalez<sup>3</sup>

Image Processing Research Laboratory (INTI-Lab)  
Universidad de Ciencias y Humanidades  
Lima, Perú

**Abstract**—The Image Processing Research Laboratory (INTI-Lab) of the Universidad de Ciencias y Humanidades has several research projects related to computer science needing high computational resources. Some of these projects are associated with climate prediction, molecule modeling, physical simulations, and others these applications generate a significant amount of data, regarding the big data issue, despite having excellent hardware features, the final result is obtained after hours or days of calculation depending on the algorithm complexity. For this reason, it is not possible to present optimal solutions at an ideal time. In this work, we propose the virtualization and configuration of a high-performance cluster (HPC) known commercially as a "supercomputer" that is composed of several computers connected to a high-speed network to behave like a single computer. The virtualization is used to run a scientific algorithm that will apply performance tests using four virtual computers to demonstrate that the reduction of time is achieved by using more machines and thus be able to be implemented in the laboratories of the institution.

**Keywords**—High-performance cluster; distributed programming; computational parallelism; supercomputer; high-efficiency computing

## I. INTRODUCTION

High-performance clusters (HPC) or also considered 'supercomputers' are potent computers that perform calculation tasks at high speeds compared to an ordinary computer [1]. These clusters are used in digital processing for scientific research, big data, data mining, bioinformatics, remote sensing, image processing, medical imaging, stage reconstruction, realistic simulations for computational chemistry, etc. [2] as new and emerging scientific findings, it is necessary to use the maximum performance of a computer so that these can give optimal results in an ideal time. By this necessity, it is possible to implement the HPC architectures where they use the Central Processing Unit (CPU) to obtain floating point operations per second (FLOPS) that are the processing capacity of a computer [3]. The use of several low cost machines that are interconnected through a network to have a unique behavior began with National Aeronautics and Space Administration (NASA) in 1994, where they used recycled computers for the creation of a supercomputer, this was called the Beowulf project which was realized in the Center for the Excellence in Data (CESDIS) [4]. The idea of the construction of low-resource computing supercomputers was disseminated worldwide to scientific and academic communities so they decided to use their computing resources without the need to

purchase assembled supercomputers due to the considerable costs that these generate by the specialized maintenance that can occur over time, making these unnecessary purchases in the future. The present work performs the virtualization of an HPC using four virtual machines to apply performance tests with a computational algorithm to prove its scalability and can be implemented in the institution. Due to the new proposal of projects, it is necessary to have equipment that uses the maximum computation resource; some universities use these architectures to carry out research. In Peru, there is the case of the Universidad Nacional de Ingeniería [5] that performs performance benchmarks to apply algorithms of high scientific complexity. Another university in Latin America is the Universidad de Quindío that uses HPC to carry out calculus of quantum-mechanical chemistry [6], there are also investigations related to urban traffic such as the case of [7] that performs simulations to allow researchers to address real-size traffic problems in large networks using powerful, precise approaches to network traffic. The use of this architecture is increasingly used worldwide as can be seen in the official page of supercomputers top 500, where it shows a list of the most powerful supercomputers in the world [8]. There is a significant increase in its implementation regarding the area of computer science; therefore, one must know the implementation, because it will be very required for the scientific community.

## II. METHODOLOGY

High-performance cluster virtualization consists of 4 virtual machines that will have the same open-source operating system and process distribution package. Virtualization will be made up of 2 or more computers that are interconnected by a network computer to use the SSH protocol that facilitates secure communications between systems [9]. The machine that manages the algorithm and distributes the processes is called the master node, and those that receive the information to be processed in parallel are the slave nodes that will have a single purpose that is to give the result to the master node, Fig. 1 shows its architecture.

### A. Master Node

It is in charge of administering and controlling the processes that will be sent to the receiving computers [3] its function is to distribute the tasks in equal parts to the desired amount of them that will use as a way of communication the Protocol Secure Shell (SSH). If one wants to see the ecosystem of the HPC graphical way, one can install monitoring

packages; therefore it is ideal that these have a graphical user interface, one can also access the public network to get updates of the operating system.

**B. Slave Node**

The computer that receives the algorithm and processes part of the problem is called the slave node. Its primary function is the processing of data designated by the master node [10] they are interconnected by a high-speed network where one has direct communication with the master node; it is recommended that the slave nodes do not have a graphical interface because they consume their computing resources. They do not need to be connected to the public network because their only function is communication with the master node it is recommended that all the computer that receives the algorithm and processes part of the problem is called the slave node. Its primary function is the processing of data designated by the master node [10]. They are interconnected by a high-speed network where one has direct communication with the master node. It is recommended that the slave nodes do not have a graphical interface because they consume their computing resources. They do not need to be connected to the public network because their only function is communication with the master node. It is recommended that all.

**C. Communication Network**

The interaction between the nodes is distributed through a communication network. In this virtualization is used a connector of Ethernet board thanks to this communication channel, the master node can spread the tasks to the slave nodes applying techniques of computational parallelism [11]. It is recommended that this network equipment does not include transit jobs outside the HPC operations because it can occur unbalanced at the time of obtaining results.

**D. Multiple Data Multi-Instruction**

The MIMD (multiple instructions, multiple data) is a technique that helps to achieve the parallelism between the nodes. Processors can run different instructions in different data [12]; it is recommended that this network equipment does not transit tasks outside the HPC operations because it can occur unbalanced at the time of obtaining results, in Fig. 2 its architecture is shown.

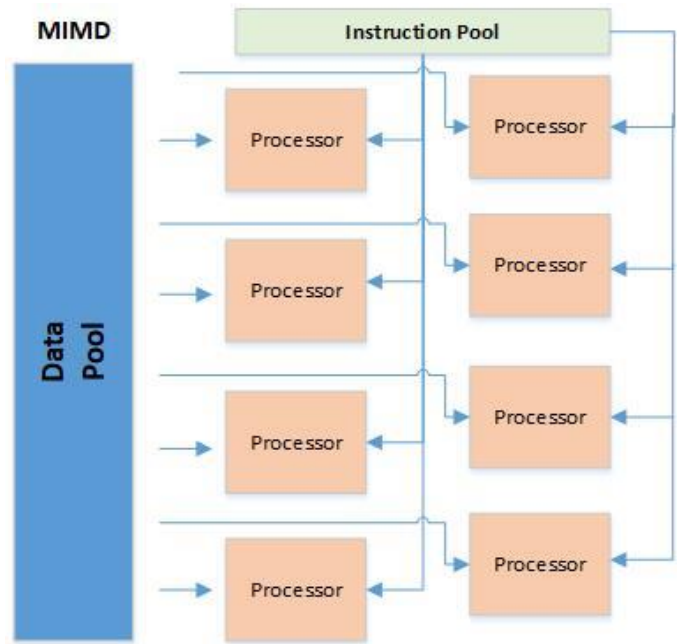


Fig. 2. Mingle Instruction Stream Multiple Data Stream (MIMD) Architecture.

**E. Message Passing Interface**

MPI (Message Passing Interface) is a specification for developers and users of message-passing libraries, mainly addressing the parallel message-passing programming model [13]. It is designed to be used in programs that exploit the existence of multiple processors. Different standards meet these techniques; among them, one has the MPICH, MVAPICH, and the Open MPI [14]. The tool used in this virtualization is Open MPI.

**F. Virtualization**

Virtualization is the most used in the world of computing, due to the advantage, it generates in saving energy, space, and management of the less physical machine. The virtualization tool used is Oracle VM Virtual Box, where four virtual machines are used, using one of them as a master node and the others as a slave node, as shown in Fig. 3.

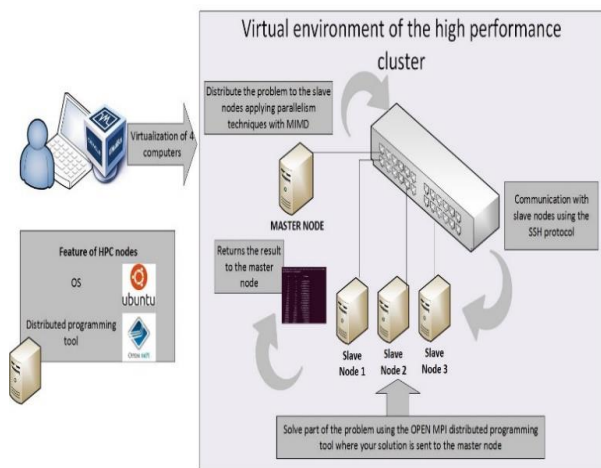


Fig. 1. Design of an HPC Architecture.

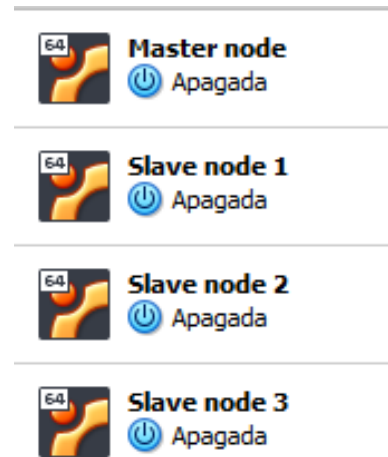


Fig. 3. HPC Node Virtualization.

### G. GNU/LINUX

All HPC nodes must have the same operating system that facilitates the interaction between the user and the project to be developed; an open-source operating system is used where modifications can be made without restrictions, in the Official supercomputer page [12] shows that most implementations are performed by open source operating systems, Fig. 4.

For the configuration, GNU/LINUX-Ubuntu was opted for having a friendly graphical interface and being open source, despite being one of the least used operating systems among HPC architectures, its scientific community compensates that one can always resort to having problems.

### H. High-Performance Cluster Configurations

For the use of HPC, there is an open-source tool called Open MPI. It is an open-source message step implementation that is maintained and developed by a large consortium of academic partners, research and industry. (To access to download the package that contains the installer go to its official page [www.open-mpi.org](http://www.open-mpi.org)) [13]. It is important to download the most stable version in this case `openmpi-4.0.1.tar.gz`, then use the following command from the terminal to decompress the package: `tar -xvzf openmpi-4.0.1.tar.gz`.

After uncompressing specify installation point: `./configure --prefix=$HOME/openmpi` then install: `make all install` and `sudo apt-get install openmpi-bin`, to conclude with: `sudo apt install libopenmpi-dev`.

When the installation is complete, the following is written to the terminal: `export PATH=$PATH:$HOME/openmpi/bin` and `export LD_LIBRARY_PATH=$LD_LIBRARY_PATH:$HOME/openmpi/lib`.

Then install the Secure Shell (SSH), this is a remote management protocol that allows you to launch commands and copy files from the master node to the slave nodes [14] with the command: `sudo apt-get install ssh` and the network file system is installed (NFS) which is the most used protocol for access to storage [15] with `sudo apt-get install nfs-common portmap`. From this point, the cloning of the nodes is started by assigning one of them as the master node.

Operating System System Share

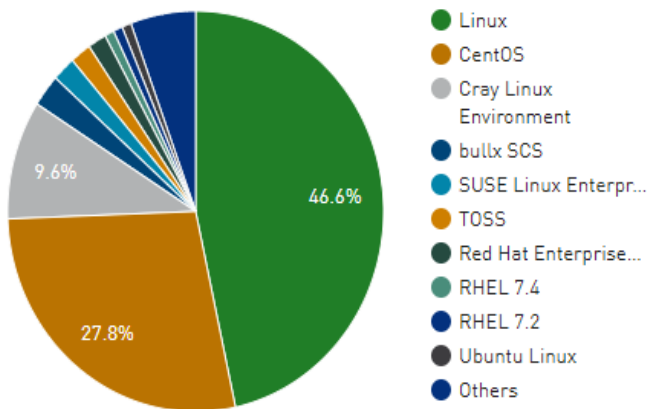


Fig. 4. Operating System Share.

From the master node the following command is entered: `sudo apt-get install nfs-kernel-server`, package that allows sharing the directory.

Each node has created a folder with the command: `mkdir clusterdir`, then a static IP is assigned with the same gateway, as shown in Table I.

An SSH key is generated from the master node where a copy is made to all the slave nodes in order not to ask for access at the time of processing; the following command is applied: `ssh-keygen`, where a unique key is generated as shown in Fig. 5.

Each of the slave nodes is accessed and a .SSH folder is created with: `mkdir .ssh`. The key is then copied from the master node to the slave nodes, as an example applies to the first node: `scp .ssh/id_rsa.pub cluster-uch@172.16.9.201:` Permissions are created. SSH with the command `chmod 700` then from all the slave nodes the copying of the `id_rsa.pub` is done: `mv id_rsa.pub .ssh/authorized_keys`. From the master node is accessed: `sudo nano /etc/hosts`, in it we add the static IPs of all the nodes of HPC with their respective prefix as explained in Fig. 6.

A modification is made to the export file with the command: `sudo nano /etc/exports` in it you enter the following: `/home/cluster-uch/Clusterdir 172.16.0.0/24(rw,no_subtree_check,async,no_root_squash)`.

TABLE. I. THE IP LIST USED IN THE CLUSTER

| Name         | IP           | Gateway      |
|--------------|--------------|--------------|
| Master node  | 172.16.9.200 | 172.16.9.254 |
| Slave node 1 | 172.16.9.201 | 172.16.9.254 |
| Slave node 2 | 172.16.9.202 | 172.16.9.254 |
| Slave node 3 | 172.16.9.203 | 172.16.9.254 |



Fig. 5. Getting SSH Key.

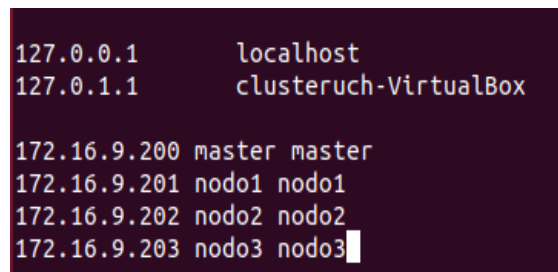


Fig. 6. Modification of the Hosts File.

The service is restarted with the command: /etc/init.d/nfs-kernel-server restart, rebooted the service applies the mount from each slave node: sudo mount-t nfs 172.16.9.200:/home/cluster-uch/clusterdir /home/cluster-uch/clusterdir.

As of last, a file is created from the master node with the following command: sudo nano .mpi\_hostfile, and the number of nodes to be used by HPC is selected. As shown in Fig. 7, the Nodo1, Nodo2, and Nodo3 are used. In this case a kernel is used where it is assigned from the slots.

In most cases, the slave nodes do not have monitors, keyboards or graphical interface because they want to avoid that the computing resources are consumed by the graphical user interface which is eliminated with the following command in each one of the nodes: sudo apt-get remove xserver-xorg-Core.

A computational algorithm is used that is programmed with the C programming language where MPI applies. This algorithm calculates the time it takes to find prime numbers [16]. Fig. 8 shows the description of the algorithm.

```
#Master node
#localhost slots=1
#Slave node 1
nodo1 slots=1
#Slave node 2
nodo2 slots=1
#Slave node 3
#nodo3 slots=1
```

Fig. 7. Enabling Slave Nodes with an Exact Amount of Kernels to use.

**PSEUDOCODIGO:** sum of prime numbers

```
** Start of parallel calculation

Main structure O {
** Declaration of variables
Number i, id, n, n_factor, n_hi, n_lo, p, primes, primes_part, master;
Decimal wtime;
** Declaration of values
n_lo=1; n_hi= 131072; n_factor= 2; master= 0;

** Initialization of MPI
Initialization_MPI(); p= amount_of_sloves (); id= call_processes_range();

If id is equal to master Do {
Samples the header and the number of slave nodes P to use }

**An initial value is assigned to make the journey
n = n_lo;
While n <= n_hi Do {
If id is equal to master Do {
** The current process time is assigned wtime = real_time_process()
** Send a message from a source process to the group send_message_group (n.Int.master)
** You get a part of the problem primes_part = prime_number(n.id,p)
** Reduce the problem from the root slaves Reduce_problem(primes_part, primes, master)
If id is equal to master Do {
** Apply time reduction wtime = real_time_process () - wtime;
Samples row of results : n , primes, wtime; }
** Multiply the route by the factor n=(n* nfactor);
}
} Ends the MPI
Ending_MPI();**End of parallel calculation
}
```

Fig. 8. Parallel Code for Calculating Prime Numbers.

To execute the code we will access the directory Clusterdir where the following command is entered: mpic++ primos.c++ -o primos. This way you get a compiled file for your use.

### III. RESULT

In this section, two performance tests are performed to make comparisons of scalability. The results of Table II are performed without the HPC architecture unlike Table III which uses 3 slave nodes and a master node, the final result shows three values where N is the number of processes performed, S the sum of the prime numbers and T the solution time, the following process is performed using the following command in its compiled directory: ./primos.

TABLE. II. RESULTS WITH A SINGLE COMPUTER

| N      | S     | T            |
|--------|-------|--------------|
| 1      | 0     | 0.000003693  |
| 2      | 1     | 0.0000001214 |
| 4      | 2     | 0.0000001077 |
| 8      | 4     | 0.0000001214 |
| 16     | 6     | 0.000000184  |
| 32     | 11    | 0.0000003319 |
| 64     | 18    | 0.0000007894 |
| 128    | 31    | 0.0000023744 |
| 256    | 54    | 0.0000095883 |
| 512    | 97    | 0.000282498  |
| 1024   | 172   | 0.003585893  |
| 2048   | 309   | 0.0260807    |
| 4096   | 564   | 0.0677598    |
| 8192   | 1028  | 0.196943     |
| 16384  | 1900  | 0.700947     |
| 36768  | 3512  | 0.700947     |
| 65536  | 6542  | 2.61356      |
| 131072 | 12251 | 10.1143      |

TABLE. III. RESULTS WITH THE HPC ARCHITECTURE

| N      | S     | T           |
|--------|-------|-------------|
| 1      | 0     | 0.0040071   |
| 2      | 1     | 0.000939131 |
| 4      | 2     | 0.00194287  |
| 8      | 4     | 0.00192809  |
| 16     | 6     | 0.00131488  |
| 32     | 11    | 0.00120115  |
| 64     | 18    | 0.000807047 |
| 128    | 31    | 0.000520945 |
| 256    | 54    | 0.000102179 |
| 512    | 97    | 0.000566006 |
| 1024   | 172   | 0.00029397  |
| 2048   | 309   | 0.000814915 |
| 4096   | 564   | 0.00234103  |
| 8192   | 1028  | 0.00741506  |
| 16384  | 1900  | 0.03195     |
| 36768  | 3512  | 0.101557    |
| 65536  | 6542  | 0.372828    |
| 131072 | 12251 | 1.33745     |

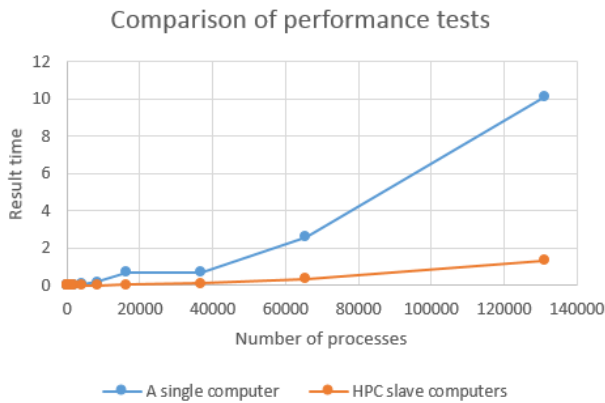


Fig. 9. Comparison of the Performance Test.

The algorithm is then executed using HPC virtualization within its Clusterdir folder with the following command: `mpirun -np 3 -hostfile ../mpi_hostfile ./primos`. The results are shown in Table III, where it is observed that the calculation of the last process takes 1.33745 seconds, which makes HPC virtualization meet the scalability and objectives defined.

Below is Fig. 9, where the comparison of an ordinary computer and the HPC virtualization is displayed, where it uses two axes that are the results time and the process numbers.

Fig. 9 shows a blue line that is the representation of a computer and the Orange Line of the HPC, as one can see, by using more number of slave nodes considerably reduces the time.

#### IV. DISCUSSION AND CONCLUSIONS

There are different ways to demonstrate scalability without resorting to virtualization, and one option would be the use of raspberry PI which is a low-cost computing platform, its configuration is similar to HPC virtualization in this case we have the work presented in [5] that performs benchmarks with its two raspberry PI cluster prototypes. It is always necessary to measure the number of FLOPs due to unbalance problem that may occur when a specific amount of slave nodes is used due to high-speed network bottlenecks. Some algorithms can give us FLOPs by using different amounts of nodes. A clear example is shown in [3] that use a package called Linpack that makes intensive use of the operations of floating per second applying basic linear algebra subroutines. These are applied by assigning different amounts of slave nodes when the FLOPs stop increasing; one must conclude that this is the ideal amount to use.

In this work, it is concluded that the virtualization of the cluster of high performance fulfills the reduction of time of the algorithmic processes thanks to the connection of computers that communicate using the protocol SSH. Therefore, this project performs as evidence for its implementation in the laboratories of the Universidad de Ciencias y Humanidades due to the results that show its scalability using the architecture to the comparison of a single computer. Also, it will contribute a benefit for the scientific community INTI-Lab that has thought in the accomplishment of machine learning applying techniques of Big Data using the architecture HPC that will use algorithms of high scientific complexity.

#### REFERENCE

- [1] G. Atul, G. Bhargavi, and K. Uditnarayan, "Study of Supercomputer 's Architecture , Application and Its Future Use," p. 2, 2014.
- [2] I. Ocampo and L. Exequiel, "Introducción A La Supercomputación En El Peru," vol. 39, no. 5, 2017.
- [3] A. S. Carranza Sánchez, J. A. Verduzco Ramírez, N. Farías Mendoza, F. Cervantes Zambrano, and F. Rodríguez Haro, "Plataforma de HPC portable de bajo consumo energético para aplicaciones de minería de datos," RECI Rev. Iberoam. las Ciencias Comput. e Informática, vol. 6, no. 11, pp. 16–24, 2017.
- [4] J. Fiestas, "Construcción e Implementación de un Clúster con máquinas PCs recicladas.," vol. 14, no. 1, pp. 9–13, 2014.
- [5] M. Cruz, "Medidas de rendimiento y comparación entre el Clúster Cruz I y el Clúster Cruz II," Rev. la Fac. Ciencias la UNI, vol. 17, no. 1, pp. 9–16, 2014.
- [6] D. Armando et al., "Computación De Alto Desempeño Para Cálculos De Química Mecano-Cuántica," p. 3, 2015.
- [7] W. Himpe, R. Ginestou, and M. J. C. Tampère, "High Performance Computing applied to Dynamic Traffic Assignment," Procedia Comput. Sci., vol. 151, no. 2018, p. 411, 2019.
- [8] "List Statistics." [Online]. Available: [www.top500.org](http://www.top500.org).
- [9] Massachusetts Institute of Technology, "Capítulo 20. Protocolo SSH." [Online]. Available: <https://web.mit.edu/rhel-doc/4/RH-DOCS/rhel-rg-es-4/ch-ssh.html>.
- [10] M. Brownell, "Building and Improving a Linux Cluster," 2015.
- [11] R. Samir and R. Caro, "Implementación De Un Clúster Experimental Bajo," p. 12, 2014.
- [12] TOP500.org, "Operating System System Share." [Online]. Available: [www.top500.org/statistics/list/](http://www.top500.org/statistics/list/).
- [13] The Open MPI Project, "A High Performance Message Passing Library," 2019. [Online]. Available: <https://www.open-mpi.org/>.
- [14] L. Alcántara, "Instalación y configuración de un cluster de alta disponibilidad con reparto de carga," p. 51, 2014.
- [15] D. Jiménez and A. Medina, "Cluster de Alto Rendimiento," pp. 16–17, 2014.
- [16] R. Francisco and A. Moreno, "Escalabilidad de Multiplataforma sobre OpenMPI," 2016.



# School Manager System based on a Personal Information Architecture

Elena Fabiola Ruiz Ledesma<sup>1</sup>, Elizabeth Moreno Galván<sup>2</sup>, Juan Jesús Gutiérrez García<sup>3</sup>, Chadwick Carreto Arellano<sup>4</sup>

Ciencias Básicas Department<sup>1</sup>

Instituto Politécnico Nacional. Escuela Superior de Cómputo and UPIICSA, Mexico, City<sup>1,3,4</sup>

Instituto Politécnico Nacional, Cecyt 9, UPIITA, Mexico, City<sup>2</sup>

**Abstract**—The current technological revolution has provided multiple benefits to human activities. For their part, organizations have had the need to make changes to their business requirements, which have led them to migrate to systems and services in more complex models. Educational institutions have experienced the impact of technological progress, because, regarding school management, information handling requires to be performed through automated processes that also protect data from any human or cyber-attack. The purpose of the paper herein is to show the development and integration of a system dedicated to manage personal information within a school environment, through the implementation of an information management architecture, whose main purpose is to create certified documents that can be shared with other information systems in the same trust environment. Research is descriptive in nature as it pretends to detect abnormalities in the characteristics of PIMS, describe their associations, and prove or reject the hypothesis in order to be compared to subsequent studies.

**Keywords**—Architecture; mobile computing; ubiquitous computing; information management system

## I. INTRODUCTION

Nowadays, data management represents an important part of information systems. It is important to consider that the value of information provision and handling does not only lie in corporate information, but also in every level where any kind of data is manipulated, whether sensible or publicly held. Therefore, currently, there are several software solutions available in the market that digitally manage information, so it can be used by different applications and systems, such as banks, social network, and databases, which have, in every case, some level of data protection and confidentiality. However, the development of systems that provide the possibility to share information, among them, in a transparent, controlled, and safe way is subject to study.

In this article, a system developed under an architecture that allows managing personal data from mobile system users is presented; such architecture considers several aspects focused on users being able to identify themselves, manage and validate their background, as well as to share and safely arrange such information, thus improving its mobility and ubiquity.

The paper is organized into four sections. The following section provides the related work on the subject matter that acts as the basis for the proposed framework. Section III

explains briefly the materials and methods used for the data analysis and elaborates on the framework. Finally, Section IV concludes the paper with a summary of the main findings and future works.

## II. THEORETICAL FRAMEWORK

### A. Related Work

There are several studies which have proved that there is interrelation between the length of time that has passed since the users previously accessed the data and perception of the difficulty of re-finding information [1]-[5].

The Personal Information Management Systems (PIMS) as organizations have the need to implement software systems to improve their information management, currently, the *Personal Information Management Systems (PIMS)* [1], [2], comprise an important part of any organizational system. The comparison of some current personal information systems [1]-[5], is shown in Table I.

### B. Research Problem

Software systems, from all current businesses and institutions, have, at least, one module dedicated to and focused on the information of one group of individuals. As systems for personal information management have not been confidentially and interoperably yet, the research problem lies in the development of systems capable of managing personal information that meet current needs of information storage, manipulation, distribution, and provision in a mobile environment, thus providing precision, coherence, safety, and ubiquity qualities.

### C. Hypothesis

It is required to follow the information management architecture as a guide for the development of an information system that ensures safe personal information exchange with other heterogeneous systems in the same trust environment.

### D. Rationale

In virtue of the increase in the development of personal information systems, the decision of developing a school management system applying an architectural scheme that might be referenced as one of the starting points for every organization at the time of being integrated to the digital technology world and adapting the advantages it can provide, especially regarding personal information management if it is seized with due responsibility, has been made.

TABLE. I. CHARACTERISTICS OF INFORMATION MANAGEMENT SYSTEMS I

| PIMS   | Inf. verification and validation | Information distribution channels | 24/7 information availability | Safety | Interoperability with other systems | Mobile computing | Ubiquitous computing |
|--|----------------------------------|-----------------------------------|-------------------------------|--------|-------------------------------------|------------------|----------------------|
| Business (web)   | X                                | X                                 | X                             | X      | X                                   | X                |                      |
| Multimedia content (photo and video album)                               |                                  | X                                 |                               |        | X                                   | X                | X                    |
| Tailor-made staff administrative management (incidence control, payroll) | X                                |                                   |                               | X      |                                     |                  |                      |
| Entertainment (coail media)  |                                  | X                                 | X                             |        | X                                   | X                |                      |

E. Definition of Architecture

Moreno [6], mention that “the architectural design, whose core component is information regarding the personal background of an individual, describes such background as a unique and unrepeatabe unit or object immersed in a series of computing elements that permit its creation, bearing, sharing, and management”. The structure of such object is presented in Fig. 1.

F. Architectural Model

Architecture has a series of layers that interact with those adjacent to them, thus allowing that the usefulness of a layer does not interfere with the usefulness of another. The way in which products generated in one layer are useful for the usefulness of an adjacent layer is shown in Fig. 2.

In order to exemplify that the architecture will be able to adapt itself to interoperability policies, according to applicable legislation of the geographical area where it is implemented, for current Mexican provisions, as pointed out in [7], the following guidelines shall be observed:

- Certificates.
  - Based on RFC5280 with X509 V3 structure, considering that, for electronic invoicing, FIEL certificates are based on such standard.
  - A length of 2048.
  - SHA2-256 cryptographic algorithm.
- Code generation based on asymmetric cryptography.
  - Private code (file.key).
  - Public code (file.crt).
- Electronic information maintenance.

In order to extend the validity of electronic documents and/or affirm their existence from a specific date, NOM-151-SCFI-2002, or simply NOM-151, specifies the technical elements to achieve such purpose, based on electronic time stamps.

G. School Management System

In order to show the benefits provided by the development of systems through the application of an architecture that organizes personal data of users, in mobile devices, a School Management Systems that showcases the implementation of personal information management architecture for its development has been developed.

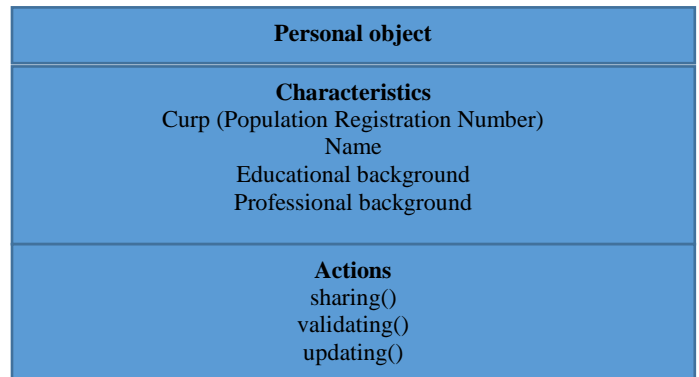


Fig. 1. Personal Object.

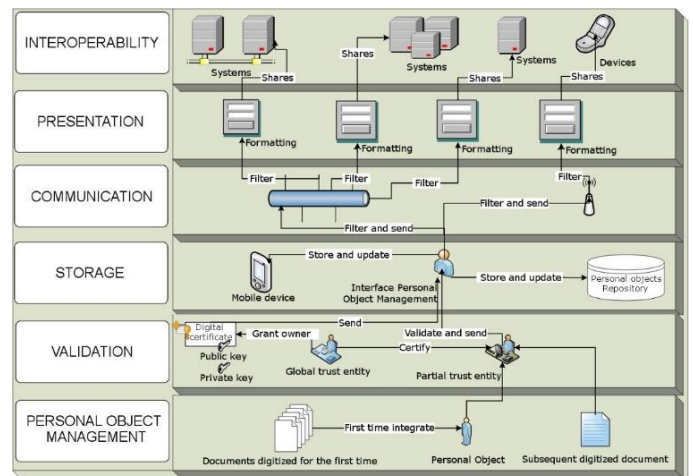


Fig. 2. Collaboration Model among Layers that Comprise the Architecture.

#### H. Project's basic Concepts

The computer system is in charge of automating several administrative and academic processes inside an educational institution, which are necessary for its management and operation. The system facilitates the approach, communication, and interaction among several elements in an educational institution (parents, students, teachers, administrative staff, and coordinators), thus allowing them to interact through it from any place, at any time, and at the most convenient moment.

Regarding safety and interoperability, the system considers information authentication and exchange through digital certificates, as well as digital signing and encryption schemes, besides XML document exporting.

### III. MATERIAL AND METHOD

Every software system has to be developed by following a methodology (cascade, spiral, XP agile, and SCRUM agile). For the case study here in, a RUP (abbreviation of Rational Unified Process) [8], methodology has been implemented, given the business nature and the need to implement the design architecture, which is robust and requires to be implemented in the appropriate stages.

#### A. Overview of the System Modules Development Starting Stage

- Project's definition and scope

The computer system is in charge of automating several administrative and academic processes through the implementation of a web site whose work will consist on solving problems in an academic environment, as well as managing personal data belonging to students and teachers, thus providing more comfort and safety to end users.

The system's scope is determined by the following tasks:

- 1) To facilitate the interaction among coordinators, teachers, students, and administrative staff.
- 2) To provide information availability regarding administrative and academic processes, so it is updated in real time.
- 3) To create a complete and agile form of performing daily activities in the institution, such as evaluating a group of students.
- 4) Online and in real time availability of the system's tools for those who require using them in the institution.
- 5) Registration processes of:
  - Personal data and documents of students and teachers in adherence with strict follow-up of the privacy and confidentiality notice.
  - Enrolments, subjects, groups, and teachers.

#### B. Creation Stage

- Artifacts

RUP methodology, in each stage, performs a series of artifacts that support a better comprehension of the study object and the tools needed to achieve both the system's

analysis and design (among others). Next, a description of the most representative artifacts is included:

- Definition of the requirements for the project's analysis.
  - Management of personal data from students, teachers, and school management administrative staff.
  - Subject management.
  - Schedule management.
  - Attendance management.
  - Automation of students' enrollment and re-enrollment process.
  - Report card, certificates, and completion certificates printing.
  - Enrolled students' list creation.
  - Regarding standards ISO(2017)[9], in order to evaluate software quality, the following shall be considered:
    - Usefulness. Uploading students in the school control system shall be made via web.
    - The systems shall cover more than 80% of the required usefulness, so it complies with every implicit and explicit need. It shall have a high degree of safety, which helps it ensure a good performance and operation of such system.
    - Reliability. The system shall be able of keeping its provision level under previously established conditions.
    - Usability. It shall be easy to use, user-intuitive, and that requires basic hardware and software knowledge so it can be used without problems.
    - Efficiency. The system shall always be ready to perform when a request is made; generating a response will not take too much time.
    - Ease of maintenance. When the system presents tolerable failures or unexpected defects, automating changes and system tests shall be easy to do.
    - Portability. The system does not require installing any extra tool, apart from default tools. It shall be multifunctional, i.e. it shall be executed from any device where it is needed to access the network.
- Hardware and Software requirements
  - Dedicated server.
  - Operational system: Windows or Linux centOS.
  - Openssl Win 32 or Linux.
  - Mysql 5.5 o higher, PHP 5 or higher.
  - Hard drive space: 20 GB available.
- Modeling for the project's design.

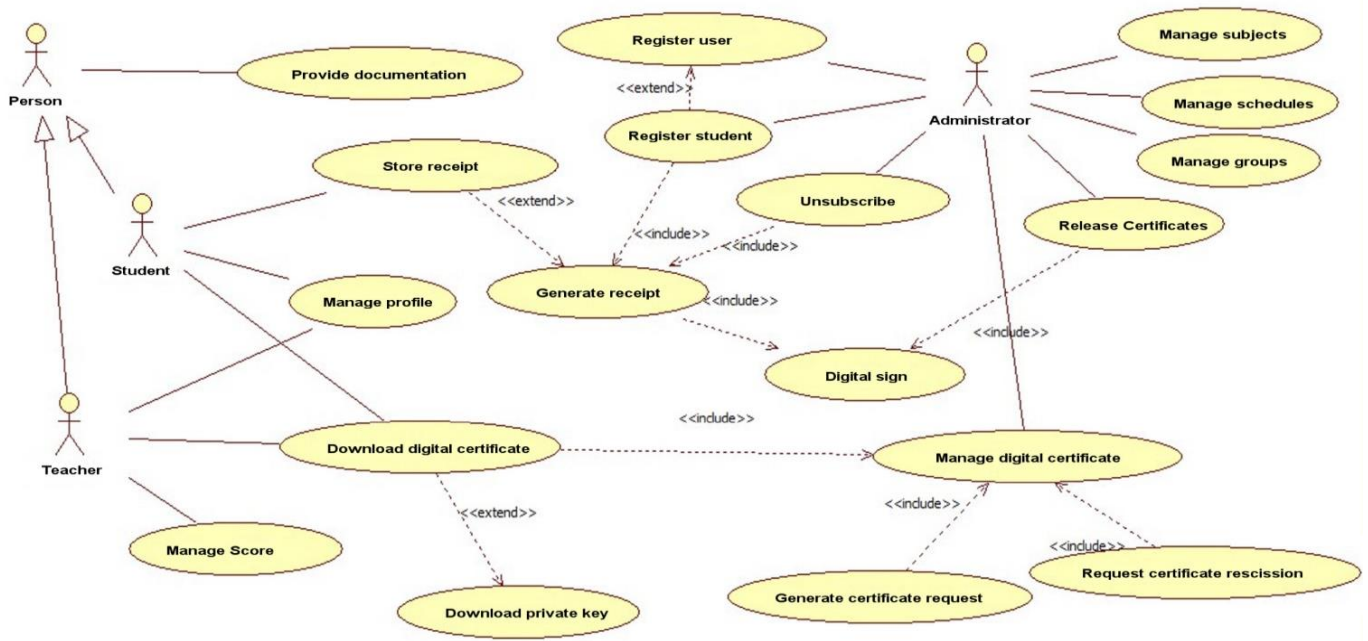


Fig. 3. High Level Case of use Diagram for the System.

RUP uses UML diagrams as system analysis and design tools. The case of use diagram shown in Fig. 3 constitutes a support model to obtain a global view of the system, showcasing actors, functions, and scope.

C. Construction Stage

Once the system’s analysis and design have been performed, it is possible to make decisions about implementation [10]. The elements that comprise the problem’s solution are presented in Fig. 4.

D. Transition Stage

This stage comprises the system’s implementation process, as well as functionality tests. The products per component represented in the display diagram are presented below.

- Registration entity (web application).
  - The entity in charge of receiving and verifying a person’s data and documents might have an interface, where the person’s necessary data is collected to create its personal object.
  - Once the person’s data has been collected, the Registration Unit might request the Global Certifying Authority (AC) the issuance of a digital certificate and private code, through an interface like the one shown in Fig. 5, where all the system’s users that still do not have a certificate are listed; once this is selected, a .csr file is created and it awaits for an answer from the AC.

E. Global Certifying Authority (AC)

- The AC shall have its own interface to perform activities related to digital certificates and private codes’ issuance, withdrawal, and management. In the web site, there is an interface, where the AC

manager can consult every csr certificate issuance requests made by registration entities within the trust environment, as well as issue such certificate.

When the csr request is signed, a digital certificate and private code is created for the client; those are placed in the server’s folder tree, which is created for such purpose; such files are available for the Biased Entity.

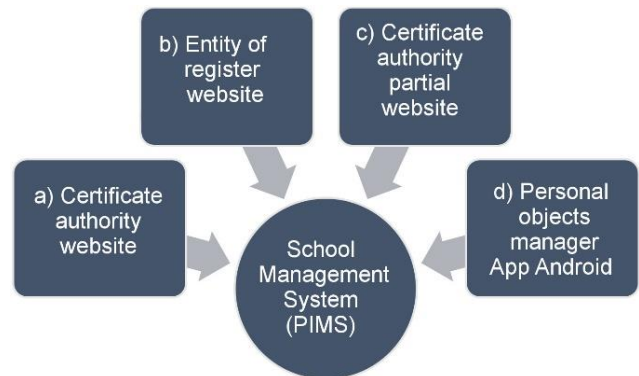


Fig. 4. System Components.

| Home       |              |           |                  | Request certificate |
|------------|--------------|-----------|------------------|---------------------|
| Register   | 101040001879 | Pedro     | Perez Lopez      | Request certificate |
| Management | 101040001807 | Sara      | Gonzalez Gomez   | Request certificate |
| Query      | 101040001893 | Santiago  | Tapia Valquez    | Request certificate |
| Upgrade    | 101040001828 | Karla     | Dominguez Aranda | Request certificate |
| Reports    | 101030001769 | Diego     | Duran Juarez     | Request certificate |
|            | 101030001901 | Elizabeth | Moreno Galvan    | Request certificate |
|            | 101040001991 | Carlos    | Fuentes Mora     | Request certificate |
|            | 201701073    | Cesar     | Cepeda Hernandez | Request certificate |
|            | 20170100617  | Daniel    | Rosendz Zamora   | Request certificate |
|            | 20170100203  | Juan      | Arcos Guerra     | Request certificate |

Fig. 5. Screen of the Certificate Issuance Request for a Student.

- Biased Entity (certificate and code management web site).
  - Both the AC and the Biased Certifying Entity have access to the certificate repository; therefore, when AC has signed a certificate request, the process status is updated, thus allowing the system manager to download the created certificate and private code.
  - Biased Certifying Entity (web site).
  - The Biased Certifying Entity has the quality of issuing documents that might be signed by such entity, which are accepted by every system from the same trust environment. The enrollment process interface, from which a certificate is created.

**F. Maintaining the Integrity of the Specifications**

The template is used to format your paper and style the text. All margins, column widths, line spaces, and text fonts are prescribed; please do not alter them. You may note peculiarities. For example, the head margin in this template measures proportionately more than is customary. This measurement and others are deliberate, using specifications that anticipate your paper as one part of the entire proceedings, and not as an independent document. Please do not revise any of the current designations.

When the data input process is finished, the receipts in PDF and XML formats, which are shown in Fig. 6, are issued. The latter is created under the structure determined by the architecture and it shall include the biased entity signature.

- Mobile application managing the personal object, management of signed documents [11] - [13].
- The objective of the architecture herein is to provide a ubiquity quality to the personal object; to this effect, such object can be carried through a mobile application, whose login and main menu are shown in Fig. 7.
- As aforementioned, a XML document that is required to be annexed to the personal object can be obtained from a server or the device storage external memory. The import process of a XML document to the personal object from the device external memory is presented in Fig. 8.

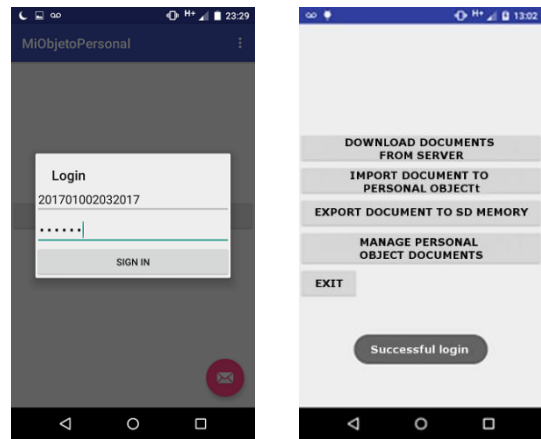


Fig. 7. Mobile Application Login and Main Menu.

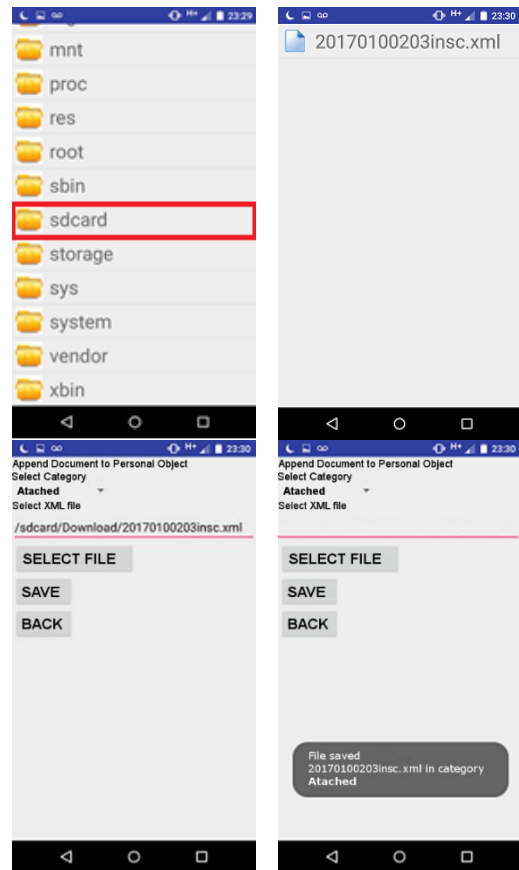


Fig. 8. Document Import to the Personal Object.



Fig. 6. Fragments of PDF and XML Documents Regarding Enrolment Receipts.

- All XML documents stored in the personal object shall have the label structured, established by the architecture, for their appropriate recovery. The process of visualizing a XML document, which is stored in the category Annex of the personal object, is shown in Fig. 9.
- Documents inside the personal object cannot be accessed through any application, as they are stored in the device internal memory. Therefore, in order to share them with other systems, it is necessary to create an external memory export route, where such

documents can be obtained and such route is accessed through other applications. The screens of the confirmation that a XML document, indicated by the owner (filtering process), has been exported to opExport in the device external memory are presented in Fig. 10.

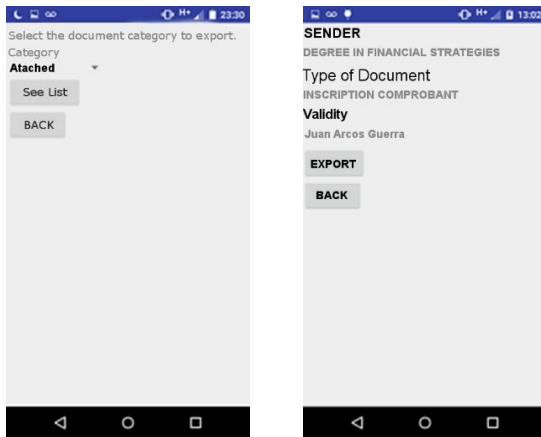


Fig. 9. Visualization of a Personal Object Document.

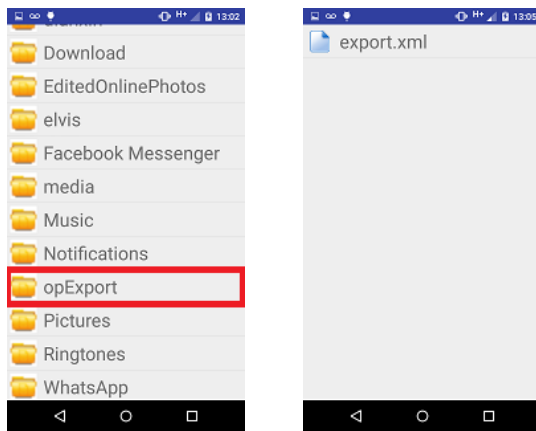


Fig. 10. Document Export from Personal Object to an External System.

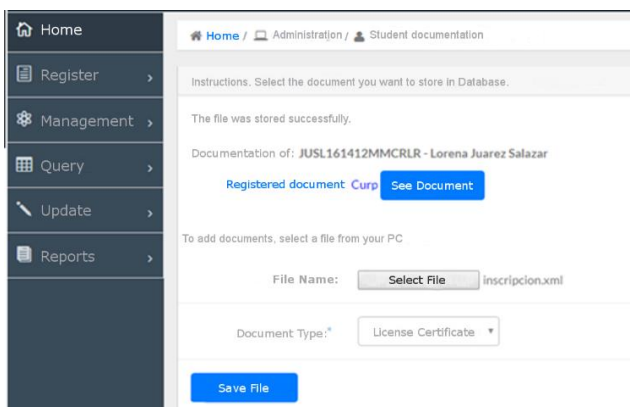


Fig. 11. Systems of Biased Entities that shall Provide an Interface.

### G. Document Export from Personal Object to External Memory

- Biased Certifying Entity, management of signed documents (web site).
- The systems of Biased Entities shall provide an interface (Fig. 11) in order to obtain documents exported by the owner from the personal object.

The reading of a document created under the structure defined by the architecture might be recovered in plain text or by applying a style sheet to facilitate visualization.

## IV. RESULTS AND DISCUSSION

Research, and data collection and analysis are basic procedures to achieve effectiveness of the efforts presented herein, justifying resource allocation and mobilization or the development of more advanced studies on this matter.

### A. Methodological Analysis

The applied research procedure is the technique of observational survey that implies data collection and creation of social interest, through the interrogation of members of the society, using the survey as a tool.

### B. Results

When performing ANOVA statistical analyses to data obtained through survey application, they indicate that users of existing PIMS are not completely satisfied with the quality of information exchange among such PIMS. The results overview, where a filled square represents total satisfaction with quality, an empty triangle represents dissatisfaction with quality, and no graphic represents any quality available for the PIMS are presented in Table II.

According to the following analysis, the opinion about the school management system shows a high degree of acceptance in the evaluated population, whose analysis overview is shown in Table III, where a filled square represents total satisfaction with quality, an empty triangle represents dissatisfaction with quality.

Results show that, currently, several trust gaps previously existing in electronic means to communicate, share information, and make operations such as online shopping have been overcome. Users are opened to new and innovating solutions that facilitate everyday activities and, on the other hand, developers have made great efforts to provide the same level of importance to the creation of intuitive interfaces and business processes.

According to the following analysis, the opinion about the school management system shows a high degree of acceptance in the evaluated population, whose analysis overview is shown in Table III, where a filled square represents total satisfaction with quality, an empty triangle represents dissatisfaction with quality.

TABLE. II. RESULTS OF SURVEY APPLIED TO PIMS USERS

| CUALITY              | a) System's ease of use (intuitive GUI) | b) Execution terminal or device configuration, required for the system's operation) (token) ease of use | c) Personal information management reliability (It provides safety services and mechanisms) | d) Information management ease of use | e) Management's ease of use of digital certificates and codes transport and distribution mechanisms | f) Information exchange, generated by the system with others, ease of use |
|----------------------|---|---|---|---------------------------------------|---|---|
| PIMS                 |   |   |   |                                       |   |   |
| Electronic invoicing | ■                                       |   | ■   | ■                                     | ■   | Δ   |
| Online banking       | ■                                       | ■   | ■   | ■                                     | ■   | Δ   |
| Electronic receipts  | ■                                       |   | ■   |                                       |   | Δ   |
| Digital documents    | ■                                       |   | ■   |                                       |   | Δ   |

TABLE. III. RESULTS OF THE SURVEY APPLIED TO THE USERS OF CASE STUDY PIMS ONT SIZES FOR PAPERS

| QUALITY                             | a) Use feasibility by users out of the information technology industry. | b) Feasibility of adding safety components, proposed by the architecture for systems' development | c) XML document management feasibility to create any type of document for systems' development. | d) Document exchange assurance in heterogeneous systems by XML document creation under the scheme established by the architecture. |
|-------------------------------------|---|---|---|--|
| Architecture implementation in PIMS | ■   | ■   | ▼   | ▼  |

### V. CONCLUSIONS

Results show that, currently, several trust gaps previously existing in electronic means to communicate, share information, and make operations such as online shopping have been overcome. Users are opened to new and innovating solutions that facilitate everyday activities and, on the other hand, developers have made great efforts to provide the same level of importance to the creation of intuitive interfaces and business processes.

Data obtained through surveys allowed confirming the general hypothesis and justifying why the design of an architecture that facilitates interoperability among systems is important, while the case study contributed to show that there are no obstacles, regarding technologies and computing tools, to implement the architecture, where the most restrictive identified factor is the organizational approach.

### ACKNOWLEDGMENT

We would like to thank SIP-IPN, COFAA and EDD for to support provided in the development of the research.

### REFERENCES

[1] M. Rustom, A. Nasar, M. Mohd, and M. Ali, M. A "Conceptual Framework for an Interactive Personal Information Management System". International Conference on User Science and Engineering (i-USEr), 2011a, pp. 100-105,  
 [2] M. Rustom, A. Nasar, M. Mohd, and M. Ali, M. "Personal Information Management Systems and Interfaces: An Overview". International

Conference on Semantic Technology and Information Retrieval, 2011b, pp.197-202, 28-29, Putrajaya, Malaysia.  
 [3] D. Elsweiler, M. Baillie, and I. Ruthven, "What makes re-finding information difficult? A study of email re-finding," Advances in Information Retrieval, 2011, pp. 568-579.  
 [4] Tyebjee, K. Charting a Mobility Roadmap Vol. 33 Issue 9, p42-43, 2p. Publisher: Cyber Media India Ltd.  
 [5] W. D. Srisamran. "The development of personal information system: A case study in the faculty of industrial education and technology". 2nd International Conference on Computer Technology and Development (ICCTD 2010), pp. 410-414. King mongkut's university of technology thonburi.  
 [6] S. Moreno. "Estudio de Arquitecturas de Software para servicios de Internet de las Cosas", thesis. Esc. Téc. Superior de Ingenieros de Telecomunicación, Universidad Politécnica de Madrid, 2015.  
 [7] A. Rodríguez. Publicación en internet y tecnología XML,. España: RAMA, 2004, pp. 44-123.  
 [8] G. Booch, J. Rumbaugh, and I. Jacobson. El proceso unificado de desarrollo de software. USA: Pearson Addison Wesley, 2000.  
 [9] Sitio oficial International Organization for Standardization [ISO]. (2017) ISO 2017, [Online] Available: <http://www.iso.org/iso/home.html>.  
 [10] R. Guzmán. "Arquitectura de Servicios Web Semánticos Sensible al Contexto para Dispositivos Móviles". M. Eng. thesis. CINVESTAV, febrero 2012.  
 [11] Medina, V. T. (2012). Análisis de la utilización de la Computación Móvil en diferentes procesos y actividades empresariales. Medellín: Universidad EAFIT.  
 [12] R. Evernden, and E Evernden. Third-generation information architecture. Communications of the ACM, 46(3) 95-98, 2003.  
 [13] P. Scifleet, S. Williams. "Constructing Digital Documents: Emerging Themes in Documentary Practice", Proceedings of the 44th Hawaii International Conference on System Sciences, 2011.

# Fusing Identity Management, HL7 and Blockchain into a Global Healthcare Record Sharing Architecture

Mohammad A. R. Abdeen<sup>1</sup>, Toqeer Ali<sup>2</sup>  
Islamic University of Madinah  
Madinah, Saudi Arabia

Yasar Khan<sup>3</sup>  
University of Kuala Lumpur,  
Malaysia

M. C.E. Yagoub<sup>4</sup>  
School of Electrical Engineering  
and Computer Science  
University of Ottawa, Canada

**Abstract**—Healthcare record sharing among various medical roles is a critical and challenging research problem especially in today's everchanging global IT solutions. The emergence of blockchain as a new enabling technology brought radical changes to numerous business applications, including healthcare. Blockchain is a trusted distributed ledger that forms a decentralized infrastructure. There have been several proposals regarding the sharing of critical healthcare records over blockchain infrastructure without requiring prior knowledge/trust of the parties involved (patients, service providers, and insurance companies). Another yet important issue is to securely share medical records across various countries for travelling patients to ensure an integrated and ubiquitous healthcare service. In this paper, we present a globally integrated healthcare record sharing architecture based on blockchain and HL7 client. Healthcare records are stored at the hosting country and are not stored on the blockchain. This architecture avails medical records of travelling patients temporarily and after performing necessary authentication. The actual authorisation process is performed on a federated identity management system, such as, the Shibboleth. Though there are similarities with identity management systems, our system is unique as it involves the patient in the permission process and discloses to them the identities of entities accessed their health records. Our solution also improves performance and guarantees privacy and security through the use of blockchain and identity management system.

**Keywords**—Healthcare; blockchain; electronic health record; identity management; Health Level Seven (HL7)

## I. INTRODUCTION

Healthcare record sharing systems (HRS) achieved significant maturity in the past couple of decades. Many works have been reported in the literature that used various techniques to securely store and retrieve Electronic Health Records (EHR) [1]. At the same time, an important aspect is to address the privacy concerns of the users such as the EHR should be made available to specific personnel within a specific time frame [2]. Storing EHR in a globally integrated database is also an open problem [3]. For example, retrieving a patient record, that is stored in a remote HRS system, from a local clinic currently being visited by a patient because HRS systems usually store health records in various non-standard formats. To anonymously store and retrieve records among two different HRS systems a standardized mechanism is provided with Healthcare Level Seven (HL7) standards [4]. Moreover, to release a health record to a specific medical

role in a given clinic requires further authorization. Federated Identity Management (FIDM) provides the required framework to achieve this objective. The FIDM systems provide authentication, authorization, and privacy of identity among various organizations that are accessing a specific resource. FIDMs consist of a Service Provider (SP), an Identity Provider (IdP) to provide access to a secure resource among various organizations, and a user that requests that specific resource. One of the critical issues we address in this research emerges from the fact that an attempt to integrate an FIDM and an HL7 system is that, once authorized to access an EHR, user activities will not be traceable. An example of this is when a patient visits a clinic/hospital that he/she is not registered in. Since the clinic is part of the federation, it is allowed to access a EHR of that patient after authorization by an identity provider (IdP). The SP then provides the EHR of the patient to the user. The physician can then make recommendation and prescription to the patient. In case of medication/prescription errors an investigation might be required and evidence can be gathered. The previous setup does not prevent recorded tampering of the HRS system which might result in an unresolvable dispute among parties involved. Fig. 1 shows a simplified sequence diagram for a non-blockchain healthcare record sharing system

The solution to this problem is to allow changes to healthcare records only upon consensus among all parties involved. Blockchains, which is an emerging technology, facilitates this objective. Blockchain is a trusted decentralized system that can perform a transaction among two unknown participants. Blockchains opened a new frontier to develop business applications and is adopted by many applications including healthcare. The aforementioned problem can be rectified by the Blockchain system as it provides a trusted ledger. The ledger keeps track of all the transactions performed by the Blockchain systems. It contains a smart contract, consensus and trusted ledger database. Each transaction on the smart contract is given to the consensus layer which upon agreement of each node in the Blockchain network stores the transaction. The transactions are secured with a hashing algorithm and chains all the previous records stored in the database. In parallel each transaction is stored on a normal database. However, the difference between a normal database and a Blockchain database is that a record cannot be deleted without the consensus of all nodes in the network. Any attempt to tamper with patient records, the system will immediately detect it.



In this work, the authors present a new architecture that employs the concept of federated identity management available by the FIDM and the security and immutability of the Blockchain. The HL7 provides a secure and trusted EHR sharing system. The proposed solution also provides a federation of healthcare systems globally. That is, if a patient is traveling across countries and if he/she requires healthcare service, they will be able to access their health records from anywhere. The remote service provider will be able to retrieve patient's EHR from his/her local database, while preventing tampering to those records. The HRS of the patient home country is known as Home\_Station(HS), the authorization provider is recognized as Identity Provider(IdP) and service provider at the remote clinic is RS in the presented solution. Each transaction is recorded on the Blockchain at the RS. The peer nodes in the Blockchain network belong to various organizations that are part of the federation.

We implemented a proof-of-concept of this architecture on the Shibboleth and Hyperledger composer. The necessary customizations are performed on the Shibboleth IdP and the HS. The HS is further integrated with HL7 to retrieve the EHR from the local HRS.

**Paper Organization:** In this paper we present a framework for global healthcare record retrieval by fusing FIDM, HL7, and Blockchain technologies for the purpose of achieving secure, standardized and tamper free transactions. A proof-of-concept of this framework is implemented on a Hyperledger composer Blockchain with use case scenarios. Section II gives an overview of the related work to the problem we are addressing. Section III gives a background information related to the topic. Section IV gives the implementation details including the architecture and the BNA.

## II. RELATED WORK

There has been various attempts to adopt the blockchain framework in healthcare to facilitate better data sharing among providers and replace the data silos model with a decentralized, more secure one. The following is a review of some of this work.

In [5], the author argued that the move to the blockchain platform in the healthcare sector will not be in the near future due to the fact that healthcare providers tend to keep the status quo, that is the technology they invested large amounts of cash for the past years. The authors argue that a more reasonable way is to gradually move from the current centralized healthcare system to the blockchain based one. This can be performed with one of three options, the easiest of which is that the patient be responsible for uploading the healthcare records to the blockchain each time they access the old system. This could result in an incomplete record if patient forgets to perform this manual step.

Ping Zhang et al. [6], demonstrated a blockchain based application - FHIRChain - for secure clinical data sharing and in light of the requirement defined by the "Office of National Coordinator for Health Information Technology" (ONC). The main objective is to achieve secure and scalable data sharing. The authors combined the objective of information sharing, through a blockchain based architecture, with security of personal sensitive information such as identity information

and medical records, via public key encryption based digital identity.

The authors implemented a decentralized application (DApp) based on the FHIRChain for a tumor board for the purpose of supporting collaborative clinical decision making. ONC requirements are achieved on this application using various techniques including storing metadata for medical records on the blockchain rather than storing the data itself for better security and scalability. The authors also used a double encryption public key encryption for authenticating access to patient medical records. Consistent medical data formatting is ensured by enforcing the FHIR standard. In [7] the authors proposed the use blockchain for the purpose of data sharing in pervasive social networks (PSN). Secure data sharing is achieved by implementing a modified version of the IEEE 802.15.6 to establish secure connections among wearable body sensors and other devices in the PSN.

In [8] the authors presented a software application, DASH, based on Ethereum platform for blockchain based healthcare to facilitate patient/doctor/provider interaction and grant required and necessary access to the parties involved. Software design patterns have been employed in this paper.

In [9] the authors presented a framework called MedRec that manages patient medical records while enables record sharing with authentication and fast editing. The main motivation is that the current electronic health record (EHR) system suffers from interoperability issues among various providers and does not allow patients to have access (read only) to their own records. There has been needs among care providers to share and transfer patient records for better healthcare. The proposed MedRec system is based on the blockchain model.

T.-T. Kuo et. al. [10] discussed health information prediction related to a patient for decision making purposes, such as, whether a patient should be admitted or not. Instead of transferring sensitive patient information, authors proposed the transfer of partially-trained models for the purpose of data prediction. Their proposed system minimizes both the transaction time and the chances of malicious attacks. In [11], the authors have presented a framework to securely share healthcare record among participants.

In [12] the authors proposed a blockchain based architecture for the purpose of achieving precision medicine and for a better clinical trials. The proposed architecture consists of a "new" blockchain built on top of the traditional blockchain.

## III. BACKGROUND

In this section we give an overview of the components of the presented global healthcare architecture.

### A. Blockchain

Blockchain is an emerging technology initially introduced by a group of researchers for timestamping digital document so that they can not be tampered with. The concept was redefined in 2008 by Satoshi Nakamoto and applied on the area of digital currency and created the first cryptocurrency project, the Bitcoin [13]. Blockchain is a decentralized, distributed ledger where transactions records are stored on a peer-to-peer network rather than a centralized system. This specific architecture

enabled blockchains to provide secure, immutable services with provenance. A blockchain consists of blocks representing transactions. Those blocks are chained together in the sense that each block carries a “fingerprint” of the previous blocks of the chain. Any attempts to change a block will render the whole chain invalid, unless in the case of the availability of an unusual immense computational power to reprogram the entire blockchain, which is nearly impossible. In blockchains, each node (or participant) approves, maintains, and updates new entries. Thus, validating the entries of the blockchain is not the responsibility of a single, centralized entity, but it is the responsibility of everyone participating in the network. This architecture therefore creates a trusted and secure ledger of members whom a priori trust does not necessarily exist [14].

Blockchains consist of the following main components:

- The node: is the hardware machine running the blockchain software
- The transaction: includes information about a specific transaction of the blockchain such as the originator, recipient and the nature of transaction (amount of money in exchange for example)
- The block: is a data structure and the basic building block of the blockchain that wrapped a transaction information and adds extra information about the previous blocks.
- The Miners: any nodes competing to find the required hash to validate a new transaction.
- Consensus: is a set of rules that are agreed upon between all participants for the purpose of approving new transactions.

Various flavors of Blockchains have emerged since its introduction. Initially public Blockchains served the purpose of providing anonymous service such as online retail of participating member of the network. While this had an advantage of flexibility and transaction security, it does not provide information about the identity of the participant. A new version of the Blockchains was introduced that are restricted to a set of users and are called private or permissioned Blockchains [15], [16]. This version is not public but it is restricted to specific users or user categories. Permissioned blockchains provides the advantages of security, immutability and provenance and at the same time provides user identification. Many notable private blockchain platforms exists such as Quorum and Hyperledger Fabric and [16]. Quorum is based on Ethereum which is itself a public blockchain platform. On the other hand, Hyperledger Fabric is a private blockchain that is specifically built for business transactions instead of only cryptocurrency exchange. Private blockchain enable support for general purpose business transactions, such as, Hyperledger Composer [17]. The system includes an access control mechanism to own various assets. In addition, the owners or participants are to be distinctly identified within the blockchain network. Composer provides Restful web services interface to connect third party applications with the blockchain.

The following sections briefly describe the most important aspects and terminology of blockchains:

1) *Consensus PoW, PoS*: Consensus is a central technique in the working of blockchains. It is a way to reach to a decision among the participants (which can be in tens of thousands) based on specific set of rules to perform/approve a given transaction. There exist several algorithms in the literature but the most known ones are the Proof-of-Work (PoW) and the Proof-of-Stake (PoS).

2) *Smart Contract*: A smart contract is a program that manages the transfer of assets or digital currency between parties when certain conditions are met. Smart contracts defines the rules and conditions under which this transfer occurs. They also can enforce those rules. Smart contracts can also perform transactions on a wide range of fields such as legal processes or insurance premiums. Smart contracts idea was solidified with the development of the cryptocurrency bitcoin and used the blockchain as a medium to store the terms of the contract. Smart contracts have been used recently to transfer and track property titles. Upon a transaction completion the buyer receives a digital token that can be used as a proof of ownership.

3) *Hyperledger Fabric*: The Hyperledger is an open source implementation of the blockchain and tools by linux foundation. The Hyperledger fabric is the permissioned blockchain infrastructure of the blockchain originally introduced by IBM.

4) *Hyperledger Composer*: The Hyperledger framework has several development tools. The Hyperledger composer is one of those tools that help developers build a blockchain business network and create smart contracts. The composer provide a GUI user interface that is called “Playground” which acts as a good starting point for prototyping proof of concept applications.

- **The Business Network Archive** The Business Network Archive (BNA) is a file that contains other file that includes the definition of the business network in the Hyperledger composer. These files include a set of model files, a set of JavaScript files written by the developer based on business analysis and a set of access control files that contains a set of rules that defines the permissions of participants of the network.
- **Restful Web Services** The Restful is an architectural style that defines a set of constraints to perform web services. A Restful web service is a service that complies with those constraints. The Hyperledger Composer avails a REST API to be consumed by HTTP or REST clients that participate in the network.

## B. Federated Identity Management System

Access to sensitive information/resource requires user authentication with usually username/password or through biometric systems. Healthcare systems, however, are designed to access its data locally or within their organizational boundaries. Most healthcare organizations have their own system for patient record keeping which might be shared by multiple individuals (physicians, laboratories, technicians) in multiple places. In places/countries receiving millions of tourists every year, accessing patient medical history from their home country is essential for safe, efficient, and swift healthcare service. Access to these health records by anonymous users is not possible in the traditional authentication model.

In this work, we are presenting a Federated Identity Management System (FIDM) where every home country is able to share health records of their citizens to other hosting countries where those citizens reside [18]. This system can also be utilized within one country and among several care providers.

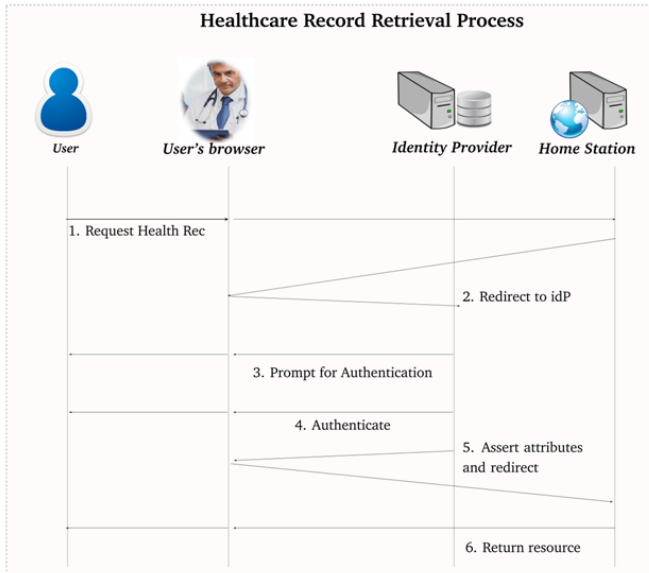


Fig. 1. Sequence Diagram for Healthcare Record Retrieval Process

Various models are suggested that provide integrity, authentication, authorization and attestation. However, each model addresses a particular aspect. A model is required which can address the aforementioned features all together. Federated Identity Management System (FIDMS) facilitates the confirmation, approval and conservation of identities. In FIDM case, a client demands a service or an asset from a Service Provider (SP). It is understood that the SP and the client don't have mutual earlier trust connection and that the SP requires some validation information to be able to provide the service. Every client might be related with at least one Identity Provider (IdP). The Identity providers can confirm the clients and give their related credentials to the SPs in view of the protection settings of the clients. These SPs give or deny access, in light of credentials and their set up (access policy as enforced by the service providers). The steps include the following: Step 1. clients submit credentials to IdP. Step 2. The privacy issues relating to a client are enforced/checked at IdP Step 3. SP trusts IdP while IdP provide clients' credentials. It is not necessary for the SP to know about the particulars of clients. It is pertinent to mention here that FIDM doesn't take into account the target's integrity. None of the current remote authentication procedures totally address the issues of security. The Identity Management Framework can be used to resolve such issues. We further incorporated trust enforced by using the blockchain infrastructure. This will be useful in addressing security issues and will measure patient's record integrity. The component layout proposed by Shibboleth is adopted for this purpose.

1) *Shibboleth Project*: The Shibboleth System (frequently called Shibboleth), offers a satisfactory answer for secure multi organizational access to web assets. The Shibboleth renders implementation of FIDM [18]. The versatile engineering of

the Shibboleth IdP combined with its particular structure and object oriented design makes it suitable for our target design. The four principle entities that constitute the Shibboleth system are the Service Provider (SP), the Identity Provider (IdP), the customer, and the Discovery Service (DS). In a normal login situation in Shibboleth, the customer asks for the SP for an asset. In the event of a secured asset, the SP diverts the customer to the DS, which gives the customer an interface to choose their IdP.

### C. Health Level Seven

Exchange of healthcare records presents a challenge to healthcare providers seeking integrated service. The Health Level Seven (HL7) is a standard that provides a comprehensive framework/structure/model for the exchange, integration, sharing, and retrieval of electronic health records of the patients [19]. The systems developed using HL7 specification, can share the medical information, such as, personal information, doctor's information, medications and healthcare records.

The author in [20] elaborates how the medical records/data from multiple sources is integrated and what is the importance of such integration in hospitals. The sharing of data among various platforms facilitate medical centers too who are attempting to find insights in the data. The HL7 has created an information system for the healthcare data known as HL7 RIM or Reference Information Model. In the research, they used HL7 RIM as an approach for the implementation of data model. Their approach, which combines elements of entity-relationship data modeling and entity-attribute-value data modeling, involves the modeling of base RIM classes, RIM inheritance, and RIM data types and incorporated the resulting data model into a way that enables medical experts to conduct clinical studies.

The customer framework inputs user's medical record, and incorporates them with HL7 message stream. HL7 messages in the customer framework transmitted over TCP/IP convention to the server framework. The server framework parses and approves this messages stream to the fragments and fields and afterward transmits affirmation to the customer framework through executing it in Java and JavaCC. The investigation of interface engine execution can be utilized genuinely in electronic wellbeing record, telemedicine framework, and medicinal data sharing among different social insurance foundations.

Our proposed global healthcare architecture is built around the concept of federated identity management (FIDM) to ensure scalability and interoperability between the service provider (i.e. the home station of the patient) and the identity provider (i.e. the healthcare provider accessing a patient's record in a given country). Typically, one of the goals of FIDMs is to ensure the privacy of the requesting entity through anonymization (by providing a delegated token). However, in our architecture, anonymization is not desired since the service provider should keep a record of all entities accessing a patient's health record. Other changes to the existing FIDM architecture are also required to fit the problem under investigation. In this section, we describe the complete architecture of the proposed system and the methodology for modifying the FIDM architecture to fit the new requirements with blockchain.

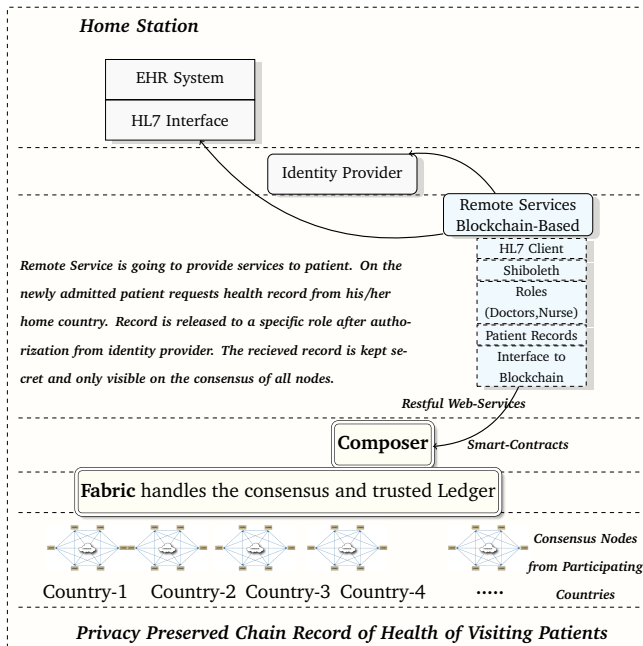


Fig. 2. Proposed Healthcare Record Sharing System

Our architecture is divided into three major modules: the service provider (SP), identity provider (IdP) and blockchain consensus/ledger. These FIDM terms are not quite applicable in the scenario addressed in this work. The service being provided to the patient is located in a remote country which requires that past health records be released by their home station. We therefore denote the patient’s healthcare record provider as Home Station (HS) and the clinic in a remote country offering services to the patient as Remote Service (RS). The identity provider (IdP), however, is responsible for authentication and authorization of the healthcare record to the role(Doctor/Technician). All request and response, that is, the remote service interaction with identity provider and home station is intermediated via blockchain for integrity, privacy and consensus of all the stakeholders. Fig. 2 shows a use-case of the interaction of these entities in the proposed architecture.

When a patient visits an RS location, their healthcare records need to be retrieved from their HS. The operator at the RS opens a web page corresponding to the HS that is set up by the patient home country. The HS cannot release sensitive information to unauthorized healthcare personnel, however. Therefore, the HS redirects the browser to a login page where the operator is displayed a list of IdPs recognized by the HS. This transaction is recorded on the blockchain via blockchain intermediary node. All the communication in the remote service and server is going via the intermediary node which is further connected with blockchain interface in Hyperledger composer. A list of IdPs are provided to all the registered HS’s which communicate via a signed XML document that contain (brief) metadata about registered RSs in that country. The HS redirects the request to the IdP server for authorization of the requesting role. The browser will then be redirected to the login page of the IdP. Since the HS only

needs to know which of the IdPs are authorized, it does not have to know which health personnel works at a given RS, it relies to the IdP to authorize the use of sensitive resource by the operator thus making system administration feasible and scalable for the HS. After the service provider logs in to the appropriate IdP using their credentials (or using two-factor authentication such as RFIDs or biometric tokens), they are redirected to the HS along with authorization tokens released by the IdP. The HS is now able to know that the operator has been authenticated at a valid IdP. However, the exact information of the SP is not known.

While the aforementioned procedure preserves the privacy of the entities consuming given health records, it waives the right of patient to obtain knowledge about those entities. To achieve this goal, a new step is added in this workflow. After getting the authorization token (termed as auth\_token) from the IdP, the HS further requests the IdP to release information about the RS requesting access to the patient’s record. The IdP releases the metadata of the RS, such as, their organizational ID, their role and job description, service expiration time etc. The IdP also releases a role identifier (such as nurse, doctor, surgeon, etc.). This helps the HS decide whether to release sensitive information of the patient. This metadata is released to the HS in the form of signed XML documents encrypted through a nonce. The metadata is then digitally signed using a hashing algorithm (such as Sha256) to ensure security properties such as freshness and non-repudiation. This ensures that the same messages cannot be used by a malicious party to request the data of the patient without proper authorization, by masquerading as the RS at a later time.

After the HS validates the the metadata using the protocols associated with these security properties, it releases the patient healthcare record in a standardized format. The presented architecture adopted the Fast Healthcare Interoperability Resources (FHIR) standard (HL7) which is currently used in many countries. The use of HL7 for exchange of healthcare records ensures that minimal effort is required for integration with the proposed system

By enabling this modular architecture and distributed deployment, we aim to ease the burden of deployment for all the involved parties thus ensuring a gradual and smooth transition to the new system.

#### IV. IMPLEMENTATION

Our model is based on three modules: the HL7 client, the Shibboleth framework to provide identity management and the Blockchain for providing trusted and immutable transactions. However, interfacing directly with Hyperledger Fabric is difficult. We used Hyperledger Composer to develop the HL7 client with our permissioned blockchain network. The HL7 client requests the HL7 server, that further, authorize with an IdP. There are node.js clients available that request and parse HL7 data from the server. In our proof-of-concept implementation, we connected with the composer-client npm module to create a business network archive(BNA). When the client receives the data, it distribute the clients data in various tables of couchdb. However, each transaction is chained with blockchain network. That brings novelty in our proposed work. Each healthcare transaction is recorded and any tempering to

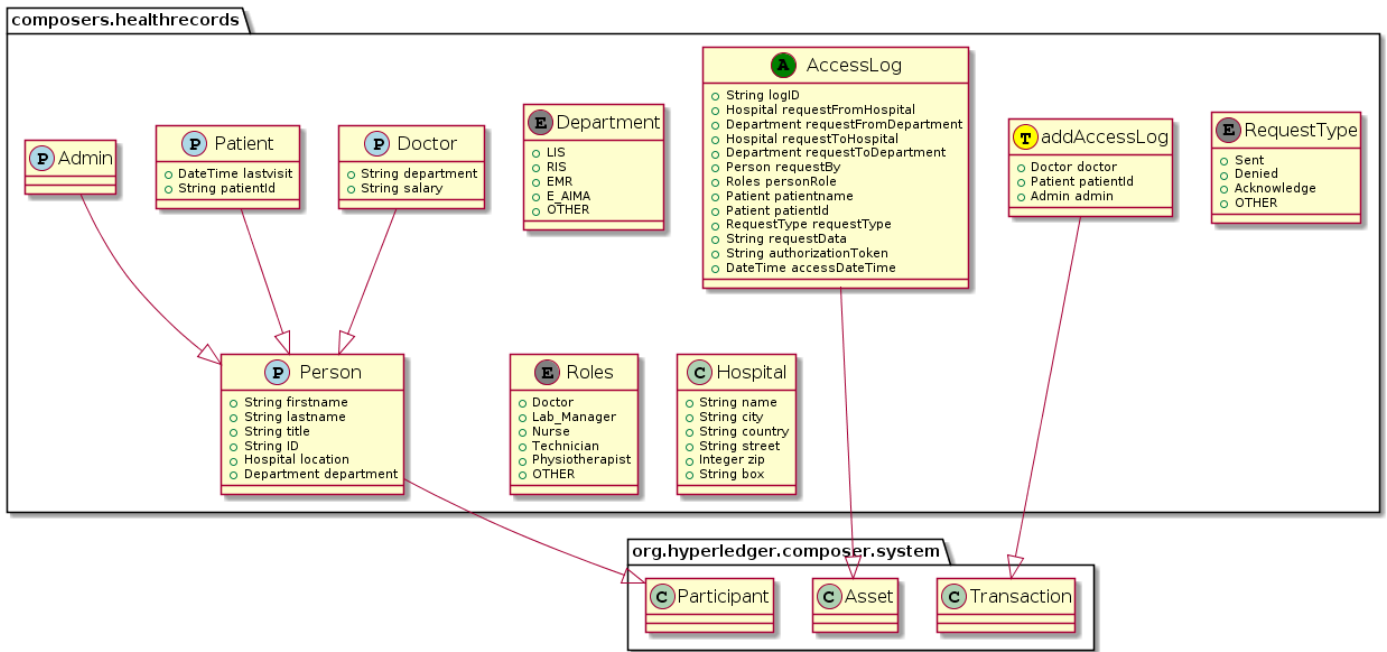


Fig. 3. BNA Data Model for the proposed blockchain section

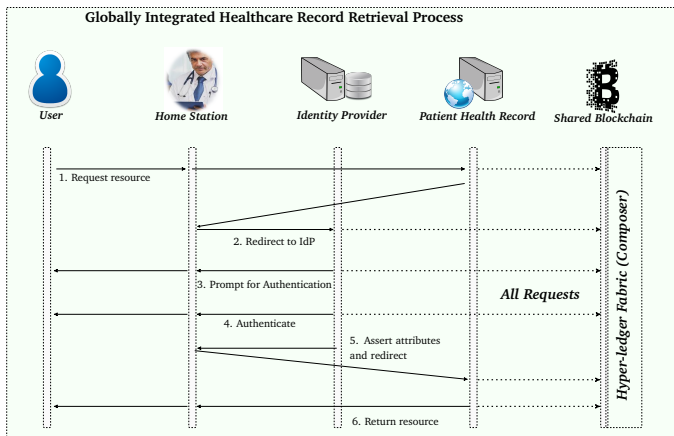


Fig. 4. Proposed Sequence Diagram for Globally Integrated Healthcare Record Retrieval Process

the records could be easily detected in database. The client, obtains the home\_station information using the user’s identity, such as, passport id. It then generates a request URL and communicates with the HL7 server to send/receive/parse HL7 messages.

Once the RS makes a request to the remote HL7 server for patient record extraction, it gets connected to the blockchain and the transaction is recorded. The request is then redirected to the Shibboleth module for authorization. The Shibboleth module then sends an authorization request to the HL7 client. The Shibboleth framework provides a demon process called **shibd** that runs on the Apache webserver. A web request to the Apache server is redirected to the *mod\_shib*. The Shibboleth framework uses Security Assertion Markup Language (SAML) language to communicate between the *IdP* and *shibd*. The

XML listing 1 below shows a portion of a SAML assertion containing the identity of the RS.

```

1 <saml:AttributeStatement>
2 <saml:Attribute Name="RS_client_id">
3 <saml:AttributeValue xsi:type="xs:anyType">
4 060D07777700SHZ</saml:AttributeValue>
5 </saml:Attribute>
6 <saml:Attribute Name="RS_id">
7 <saml:AttributeValue xsi:type="xs:anyType">
8 00DD00HHHH0F7P5</saml:AttributeValue>
9 </saml:Attribute>
10 </saml:AttributeStatement>

```

Listing 1: SAML request for authorization from HS to identity provider

Data Provenance is a very important aspect of our model. Each transaction for a specific user for HL7 data/message manipulation is registered on the Hyperledger composer Business Network Archive model (BNA). The BNA model uses the blockchain’s inherit append-only mode for recording all the transaction which are tamper-proofed. Authorized personal of a given organization can view the log on the ledger and can ensure their integrity.

In Fig. 3, the BNA Data Model deployment using Blockchain is elaborated. The model includes records related to three essential entities i.e. the participant, the asset and the transactions. A *participant* is a persons which may include the admin, a physician or a patient. Various data records are stored such as names, and departmental details their IDs and last date they had a medical checkup and which physician or healthcare clinic accessed the patient record. Similarly, to propose various health related authorized transactions to the blockchain and to represent various authorization levels for healthcare personnel different *Roles* are defined that includes limited to doctors,

lab managers, nurses, technicians, and physiotherapist. The *Asset* entity in records details of access logs pertaining various IDs. In addition, the requests made by various personnel or departments of particular hospitals regarding patient's history are also recorded. A complete workflow of our proposed solution is shown in Fig. 4.

## V. CONCLUSION

Many reports exist in the literature regarding healthcare record sharing system. However, most of them are standalone systems serving a single hospital/clinic. Few research findings, however, discussed a unified interface for health record sharing, such as, HL7. These systems are centralized, however. Recently, decentralized systems gained popularity which revolutionized the IT infrastructure. Some solutions exist based on decentralized system, such as, blockchain. Moreover, some are healthcare record sharing systems employing an order-execute architecture known as public blockchain while some of them are execute-order architectures. The proposed solution in this research is different from the traditional healthcare record sharing system. It presents a global healthcare record extraction solution depending on the patient's location. Our proposed solution authenticate/authorize the healthcare personnel at the remote service location (providing the current medical service to patients) by utilizing the blockchain, FIDM and HL7 technologies and standards. The HL7 server is at the home\_station which is located at the patient home country. Our solution shows that patients can share their healthcare records ubiquitously with various service providers. This Blockchain-based solution provides security, integrity and privacy to the patient record. All stake-holders (participating countries) are involved in the consensus process and keep copies of the health record of their home patients. Patient health records accessed by the remote service are temporary and get deleted upon patient disgorge. However, the blockchain ledger maintains an encrypted hash of that record for integrity verification and consensus process.

## REFERENCES

- [1] B. Fabian, T. Ermakova, and P. Junghanns, "Collaborative and secure sharing of healthcare data in multi-clouds," *Information Systems*, vol. 48, pp. 132–150, 2015.
- [2] A. Sajid and H. Abbas, "Data privacy in cloud-assisted healthcare systems: state of the art and future challenges," *Journal of medical systems*, vol. 40, no. 6, p. 155, 2016.
- [3] V. K. Omachonu and N. G. Einspruch, "Innovation in healthcare delivery systems: a conceptual framework," *The Innovation Journal: The Public Sector Innovation Journal*, vol. 15, no. 1, pp. 1–20, 2010.
- [4] T. Viangteeravat, M. N. Anyanwu, V. R. Nagisetty, E. Kuscu, M. E. Sakaue, and D. Wu, "Clinical data integration of distributed data sources using health level seven (hl7) v3-rim mapping," *Journal of clinical bioinformatics*, vol. 1, no. 1, p. 32, 2011.
- [5] D. Ivan, "Moving toward a blockchain-based method for the secure storage of patient records," 2016.
- [6] P. Zhang, J. White, D. C. Schmidt, G. Lenz, and S. T. Rosenbloom, "Fhirchain: applying blockchain to securely and scalably share clinical data," *Computational and structural biotechnology journal*, vol. 16, pp. 267–278, 2018.
- [7] J. Zhang, N. Xue, and X. Huang, "A secure system for pervasive social network-based healthcare," *IEEE Access*, vol. 4, pp. 9239–9250, 2016.
- [8] P. Zhang, J. White, D. C. Schmidt, and G. Lenz, "Applying software patterns to address interoperability in blockchain-based healthcare apps," *arXiv preprint arXiv:1706.03700*, 2017.
- [9] A. Ekblaw, A. Azaria, J. Halamka, and A. Lippman, "A case study for blockchain in healthcare: "medrec" prototype for electronic health records and medical research data," *white paper*, 2016.
- [10] T.-T. Kuo and L. Ohno-Machado, "Modelchain: Decentralized privacy-preserving healthcare predictive modeling framework on private blockchain networks," *arXiv preprint arXiv:1802.01746*, 2018.
- [11] A. Dubovitskaya, Z. Xu, S. Ryu, M. Schumacher, and F. Wang, "Secure and trustable electronic medical records sharing using blockchain," in *AMIA Annual Symposium Proceedings*, vol. 2017. American Medical Informatics Association, 2017, p. 650.
- [12] Z. Shae and J. J. Tsai, "On the design of a blockchain platform for clinical trial and precision medicine," in *2017 IEEE 37th International Conference on Distributed Computing Systems (ICDCS)*. IEEE, 2017, pp. 1972–1980.
- [13] A. M. Antonopoulos, *Mastering Bitcoin: unlocking digital cryptocurrencies*. "O'Reilly Media, Inc.", 2014.
- [14] T. Ali, M. Nauman, and S. Jan, "Trust in iot: dynamic remote attestation through efficient behavior capture," *Cluster Computing*, vol. 21, no. 1, pp. 409–421, 2018.
- [15] C. Cachin, "Architecture of the hyperledger blockchain fabric," in *Workshop on distributed cryptocurrencies and consensus ledgers*, vol. 310, 2016.
- [16] M. Vukolić, "Rethinking permissioned blockchains," in *Proceedings of the ACM Workshop on Blockchain, Cryptocurrencies and Contracts*. ACM, 2017, pp. 3–7.
- [17] V. Dhillon, D. Metcalf, and M. Hooper, "The hyperledger project," in *Blockchain enabled applications*. Springer, 2017, pp. 139–149.
- [18] E. Birrell and F. B. Schneider, "Federated identity management systems: A privacy-based characterization," *IEEE security & privacy*, vol. 11, no. 5, pp. 36–48, 2013.
- [19] G. J. Joyia, M. U. Akram, C. N. Akbar, and M. F. Maqsood, "Evolution of health level-7: A survey," in *Proceedings of the 2018 International Conference on Software Engineering and Information Management*. ACM, 2018, pp. 118–123.
- [20] T. J. Eggebraaten, J. W. Tenner, and J. C. Dubbels, "A health-care data model based on the hl7 reference information model," *IBM Systems Journal*, vol. 46, no. 1, pp. 5–18, 2007.

# An Efficient Machine Learning Technique to Classify and Recognize Handwritten and Printed Digits of Sudoku Puzzle

Sang C. Suh<sup>\*1</sup>, Aghalya Dharshni Manmatharaj<sup>2</sup>  
Department of Computer Science  
Texas A&M University-Commerce  
Commerce, Texas

**Abstract**—In this paper, we propose a convolutional neural network model to recognize and classify handwritten and printed digits present in Sudoku puzzle, which is captured using smartphone camera from various magazines, and printed papers. Sudoku puzzle grid is detected using various image processing and filtering techniques such as adaptive threshold. The system described in the paper is thoroughly tested on a set of 100 Sudoku images captured with smartphone cameras under varying conditions. The system shows promising results with 98% accuracy. Our model can handle more complex conditions often present on images that were taken with phone cameras and the complexity of mixed printed and handwritten digits.

**Keywords**—Convolutional Neural Network (CNN); Artificial Neural Network (ANN); Deep Belief Network (DBN); Optical character recognition (OCR), Open source computer vision (OpenCV); Convolutional Deep Belief Network (CDBN)

## I. INTRODUCTION

Profound Neural Network display arrangements have demonstrated exceptionally fruitful on digit acknowledgment. We thought of different explorations that tended to be the issues of perceiving Sudoku digits from paper pictures taken with an advanced camera, recognizing computerized numbers present in the Sudoku and distinguishing manually written numbers. The approach that we are attempting to address in this paper is whether such immense neural framework structures can manage the interpretation of both handwritten and computerized digits, present in Sudoku picture without separating them and classify into two characterizations.

The Sudoku baffle is a Japanese diversion. It is a rational, a number-based riddle. This paper centers around the standard number Sudoku played on a 9 x 9 network. Each cell should contain a digit between 0 and 10. The diversion starts with a halfway filled network and the objective is to fill each line, segment, and sub 3 x 3 square with numbers, so each number is available once [1][2][3][4][5]. In this work, we center around filled Sudoku, containing both transcribed and printed digits [6]. We employ different picture preparing procedures to acquire a commotion free Sudoku picture and use MNIST digits dataset to discover the digit's present in the picture [1][5][13]. The dataset is available and accessible online for everybody as a free of expenses. Fig. 1 shows one of the input images that we used as input.

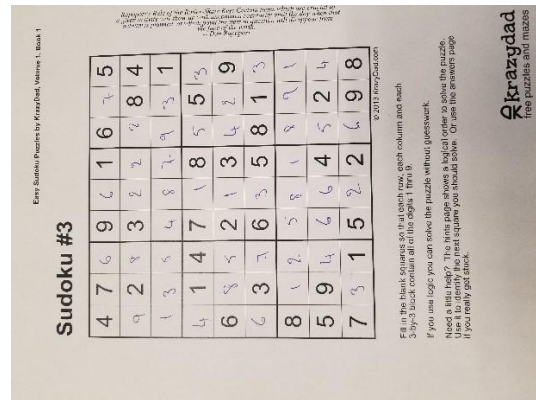


Fig. 1. Image of a Sudoku Puzzle Planned to be used.

The remainder of this paper is organized as follows. Section II gives the background of the problem and describes previous work achieved related to our research reported in this paper. Section III presents the methodology used to validate the proposed solution followed by the design of the project briefly described in Section IV. Section V describes the methods used and provides results of the system. Section VI presents the significance and scope of the study. Finally, the paper ends with conclusion with some ideas and suggestion for future work related to the problem.

## II. LITERATURE REVIEW

### A. Sudoku

Sudoku is a number game played on 9\*9 grid. The objective is to fill the blank squares with digits 1 to 9. When Sudoku is completed, each row and column must contain all digits from 1 to 9 exactly once [1][2][3][4][5]. Numbers from 1 to 9 must be affixed within each grid of 3\*3, no row and column can contain repeat of the instance [6][7][28]. In real life, we come across many Sudoku puzzles of varying difficulty levels in newspapers and other books.

### B. Sudoku Image Recognition

In the year 2012, A. Van Horn proposed a framework to perceive and fathom Sudoku puzzles dependent on the Hough change. Four corners of the lattice are identified dependent on the crossing point of the recognized lines. Van Horn proposed a framework to perceive and fathom a Sudoku confuse

\*Corresponding Author

dependent on the Hough change. Four corners of the network are identified dependent on the crossing point of the distinguished lines. Digits are centered in their cells and passed to an ANN [29][30]. The framework starts with a little arrangement of pictures. Versatile thresholding is connected, and segments associated with the fringes are expelled to lessen clamor and improve later advances. Utilizing another calculation, the biggest segment territory is distinguished as a network. At last, the digits are grouped according to straightforward format machine methodology. None of these techniques have been completely tried on characterized informational collections and no examination has been done on ordering Sudoku with combined printed and handwritten digits.

### C. Camera-based OCR

Content identification and recognition in pictures picked up from the scanners have been concentrated eventually with powerful courses of action proposed. Another hand, camera-based PC vision issues stay trying for a few reasons. Center in such gadgets are seldom flawless and optical zoom is of low quality. Pictures are taken under different conditions and different lighting conditions either normal or fake which presents shadows and slope of brightening [19]. The text from the Sudoku images, which have been taken from the scanner, has the perfect images than the distorted captured images from the camera. While thinking about the paper, a few different wellsprings of fluctuation contemplated the pictures from the paper results in twisted pictures. Font sizes and styles in a newspaper can also differ. The standard steps of image processing (normalization, text localization, enhancement, and binarization) are analyzed and different solutions are compared.

### D. Image Processing Techniques

By and large, picture preparation goes through such phases as picture import, examination, control and picture yield. Advanced (digital) and simple (analog) are the two strategies used for picture preparation [17]. Techniques which have been applied for image processing are image editing, image restoration, independent component analysis, anisotropic diffusion, linear filtering, and neural networks. In our research, the neural networks approach was investigated and used. The neural network techniques which we particularly focused on are Contour detection and Hough transform.

### E. Hough Transform

It is a technique which can be used to isolate features of the shape of an image because it requires the desired features to be specified in the parametric form. Generalized Hough transform can be employed in applications where an analytic description of features is impossible. The Hough method is especially helpful for figuring a worldwide portrayal of features where the quantity of arrangement classes need not be known from the earlier given (potentially uproarious) nearby estimations [14][20][22][26].

The motivating idea behind the Hough technique for line detection is that each input measurement (e.g., coordinate point) indicates its contribution to a globally consistent

solution such as the physical line which gives rise to an image point [1][5][8].

### F. Deep Belief Network (DBN)

A DBN is an unsupervised deep learning algorithm. It is composed of a multilayer of latent variables. Latent variables are binary, also called as hidden units. It is considered a hybrid graphical model. Top two layers are undirected. Lower layers have directed connections, with the arrows pointed towards the layer that is closest to data. Lower layers have acyclic connections that convert associate memory to observed variables. There are no intralayer connections. DBN is pre-trained using Greedy learning algorithm. This algorithm is fast and learns one layer at a time. In the year 2009, Lee et al. presented a new type of DBN, a CDBN [1]. This arrangement permits to scale the system to bigger picture sizes, allowing a CDBN to have the capacity to group full-sized normal pictures. They exhibited superb execution on visual acknowledgment tasks. Additionally, their network accomplished cutting edge on the MNIST dataset. Since then, Deep Belief Networks and Deep Architectures, in general, have been used in several domains such as face recognition, reinforcement learning, and handwritten characters recognition. They have demonstrated effective, frequently accomplishing cutting edge results by selecting a pattern in image.

### G. Digit Recognition

Digit acknowledgment utilizing OCR is done by identifying the length and broadness of the square matrix and isolating it into 9 a balance of yielding 81 littler squares. The corner to corner x and y co-ordinates of every little square are figured and re-allocated values from 1 to 9, determining the line and section number of each square. Therefore, the centroid estimations of every digit present in the riddle are resolved and these facilitate qualities are re-doled out qualities from 1 to 9 by over and again looking at the x and y directions of the centroid to the directions of each littler square. On the off chance that the centroid exists in the x and y directions of a square, it takes the estimation of the line and section number of that square. At that point the numbers present in the picture are perceived and arranged utilizing OCR [10][11]. The OCR yields exceedingly precise outcomes under the condition that the clamor present around the characters in the picture is insignificant. In this way, it is significant that the picture handling stages for commotion evacuation yield sharp and clear pictures for OCR location as appeared in Fig. 4. The recognized digits are put away in a 9x9 grid dependent on their new centroid esteems and empty spots are relegated zeros in the lattice.

## III. METHODOLOGY

We will be following the Agile Environment over our project. Agile is a theoretical structure for undertaking programming structure projects. Agile methods attempt to minimize risk by developing software in short time boxes, called iterations, which typically last one to four weeks. Every cycle resembles a smaller than usual programming venture of its own and incorporates every one of the errands important to discharge the scaled down addition of new usefulness: arranging, necessities investigation, plan, coding, testing, and



documentation. While iteration may not add enough functionality to warrant releasing the product, an agile software project intends to be capable of releasing new software at the end of every iteration. At the end of each iteration, the team reevaluates project priorities. Agile techniques underline continuous correspondence, ideally up close and personal, and overwritten archives. Most light-footed groups are situated in a warmup area and incorporate every one of the general population important to complete the product. At the very least, this incorporates developers and the general population who characterize the item such as item chiefs, business examiners, or real clients. The warmup area may likewise incorporate analyzers, interface planners, specialized scholars, and the board. Light-footed techniques additionally underscore working programming as the essential proportion of advancement. Joined with the inclination for eye to eye correspondence, coordinated techniques produce next to no composed documentation in respect to different strategies.

The reason for selecting this environmental model is because there are three unique phases. Each phase will provide an individual set of output.

#### IV. DESIGN AND APPROACH

##### A. Requirements and Planning

We used Python of version 3 and various libraries such as TensorFlow [12], Matplotlib, Keras, Convolutional [16], OpenCV 2, Numpy, Pylab. We used MNIST and Char74K dataset for training.

##### B. Design

Fig. 2 describes the design of the project.

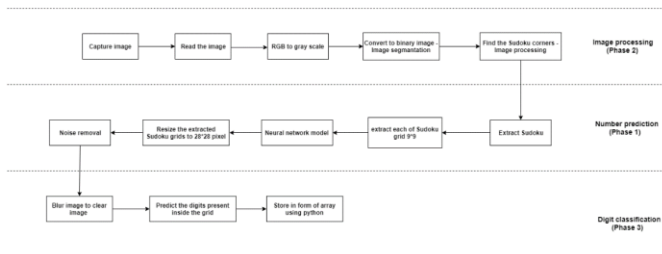


Fig. 2. Design of Mixed Handwritten and Printed Digit Recognition and Classification in Sudoku With Convolutional Deep Belief Network.

#### V. DEVELOPMENT AND RESULTS

##### A. Phase 1: Develop Handwritten Number Prediction Model

A Neural Network model is trained to predict numbers using MNIST dataset [13]. The training dataset is structured as a 3-dimensional array of the instance, image width, and image height. For a multi-layer perceptron model, we must reduce the images down into a vector of pixels. For this situation, the 28x28 estimated pictures will be 784-pixel input esteems. We can do this change effectively utilizing the reshape work on the NumPy exhibit. We can also reduce our memory requirements by forcing the precision of the pixel values to be 32 bits, the default precision used by Keras anyway [27]. The pixel values are grayscale between 0 and 255. It is quite often a smart thought to play out some scaling of info which esteems when neural system models can be utilized. Since the

scale is notable, we can rapidly standardize the pixel esteems to the range 0 and 1 by separating each incentive by the limit of 255. Fig. 3 shows the grayscale version of the image present in the MNIST database.

The yield variable is a whole number from 0 to 9. This is a multi-class classification problem. As such, it is good practice to use one hot encoding of the class values, transforming the vector of class integers into a binary matrix. We can undoubtedly do this by utilizing the inherent `np_utils.to_categorical()` method to support the work in Keras. We are presently prepared to make our straightforward neural system model. We will characterize our model in a capacity to training and testing. This is convenient in the event that you need to expand the precedent later and attempt and show signs of improvement score. The model is a basic neural system with one concealed layer which contains indistinguishable number of neurons. There are 784 inputs neurons present in the hidden layer. A rectifier actuation work is utilized for the neurons in the concealed layer.

A softmax activation function is used on the output layer to turn the outputs into probability-like values and allow one class of the 10 to be selected as the model's output prediction [15]. The logarithmic loss is used as the loss function called `categorical_crossentropy` in Keras and the efficient ADAM gradient descent algorithm is used to learn the weights [1][2][5]. We can now fit and evaluate the model. The model fits more than 60,000 training images in 10 epocs with 99 percent accuracy. The test data is used as the validation dataset, allowing you to see the skill of the model as it trains. A verbose value of 2 is used to reduce the output to one line for each training epoch. Fig. 4 shows the output of the epochs which finally gives a training accuracy of 99%.

The overall model follows Convolutional Neural Network. The architecture of our model is shown in Fig. 5.

Finally, the test dataset is used to evaluate the model and a classification rate is printed as shown in Fig. 6.

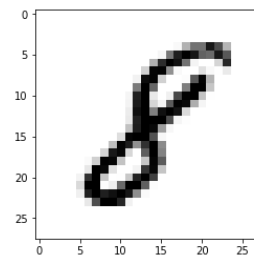


Fig. 3. The Grayscale Version of the Image Present in the MNIST Database.

```

Epoch 1/10
60000/60000 [-----] - 65s 1ms/step - loss: 0.1957 - acc: 0.9487
Epoch 2/10
60000/60000 [-----] - 61s 1ms/step - loss: 0.0829 - acc: 0.9747
Epoch 3/10
60000/60000 [-----] - 56s 933us/step - loss: 0.0553 - acc: 0.9819
Epoch 4/10
60000/60000 [-----] - 56s 927us/step - loss: 0.0448 - acc: 0.9861
Epoch 5/10
60000/60000 [-----] - 62s 1ms/step - loss: 0.0341 - acc: 0.9888
Epoch 6/10
60000/60000 [-----] - 81s 1ms/step - loss: 0.0285 - acc: 0.9902
Epoch 7/10
60000/60000 [-----] - 55s 921us/step - loss: 0.0248 - acc: 0.9922
Epoch 8/10
60000/60000 [-----] - 56s 926us/step - loss: 0.0215 - acc: 0.9928
Epoch 9/10
60000/60000 [-----] - 52s 875us/step - loss: 0.0197 - acc: 0.9934
Epoch 10/10
60000/60000 [-----] - 51s 851us/step - loss: 0.0188 - acc: 0.9939
    
```

Fig. 4. Training Epochs.

| Layer (type)                  | Output Shape       | Param # |
|-------------------------------|--------------------|---------|
| conv2d_1 (Conv2D)             | (None, 26, 26, 28) | 280     |
| max_pooling2d_1 (MaxPooling2) | (None, 13, 13, 28) | 0       |
| flatten_1 (Flatten)           | (None, 4732)       | 0       |
| dense_1 (Dense)               | (None, 128)        | 605824  |
| dropout_1 (Dropout)           | (None, 128)        | 0       |
| dense_2 (Dense)               | (None, 10)         | 1290    |
| Total params: 607,394         |                    |         |
| Trainable params: 607,394     |                    |         |
| Non-trainable params: 0       |                    |         |

Fig. 5. CNN Structure of our Model.

10000/10000 [=====] - 3s 273us/step

Fig. 6. Test Result.

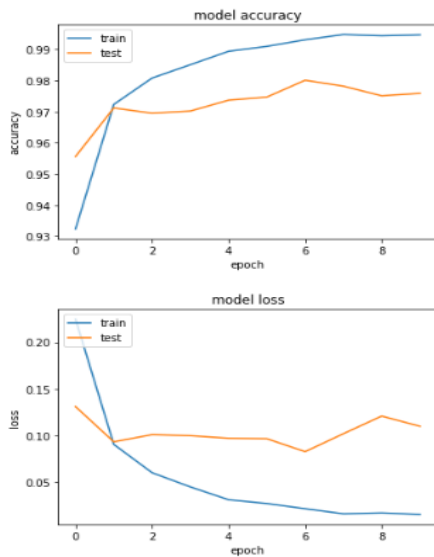


Fig. 7. Model Accuracy and Model Loss.

Model accuracy and model loss is shown in Fig. 7.

**B. Phase 2: Sudoku Grid Detection and Extraction**

We imported the camera captured Sudoku image into the model using Open CV which is one of the Open Source Computer Vision Library [25][9]. Red Green Blue scale image is converted into Grayscale image. Unwanted image background lighting is removed using the adaptive threshold method. The adaptive threshold module is used in uneven lighting conditions when you need to segment a lighter foreground object from its background. In many lighting situations, shadows or dimming of light cause thresholding problems as traditional thresholding considers the entire image brightness. Adaptive thresholding will perform binary thresholding (i.e. it creates a black and white image) by analyzing each pixel with respect to its local neighborhood. This localization allows each pixel to be considered in a more adaptive environment. The algorithm considers each pixel one at a time, calculate the mean of the local neighborhood 'window size' (x-windowSize/2, y-windowSize/2, x+windowSize/2, y+windowSize/2) and thresholds the current

pixel to white if the difference between the calculated mean and the current pixel value is lower than the 'mean offset' [18][23]. Fig. 8 shows the pre-processed image.

Each 9\*9 grid is separated using the image slicer technique as shown in Fig. 9. It is the one that slices an image into titles and rejoins them. A maximum number of tiles that can be produced is 9800. This can be an arbitrary limit which ensures that row and column number can be conveniently represented by two digits.

In the same manner, the remaining 3\*3 grids which have been separated from the 9\*9 grid are handled and separated into the single grids.

**C. Phase 3: Sudoku Grid Detection and Extraction**

In this phase each separated grid can be manually differentiated what are the handwritten and the printed digits by denoting the handwritten digits with 2, printed digits with 1 and the left part, the empty grid, can be taken as 0 and this has been done only once so that it is a onetime process. At the classification process we used the saved database to classify the digits for the other Sudoku pictures [24]. The result what we have considered for this project is classified as shown in Fig. 10.

The classified Sudoku image is to be stored in the form of an array as shown in Fig. 11.

We can get Sudoku logic as well if we pass Sudoku logic to it.

|   |   |   |   |   |   |   |   |   |
|---|---|---|---|---|---|---|---|---|
| 4 | 7 | 6 | 9 | 6 | 1 | 6 | 2 | 5 |
| 9 | 2 | 8 | 3 | 2 | 2 | 2 | 8 | 4 |
| 1 | 3 | 5 | 4 | 2 | 9 | 3 | 1 |   |
| 4 | 1 | 4 | 7 | 1 | 8 | 5 | 5 | 3 |
| 6 | 8 | 5 | 2 | 1 | 3 | 4 | 2 | 9 |
| 6 | 3 | 1 | 6 | 3 | 5 | 8 | 1 | 3 |
| 8 | 1 | 2 | 5 | 3 | 1 | 9 | 9 | 1 |
| 5 | 9 | 6 | 6 | 6 | 4 | 5 | 2 | 6 |
| 7 | 3 | 1 | 5 | 2 | 2 | 6 | 9 | 8 |

Fig. 8. Extracted Sudoku Grid.

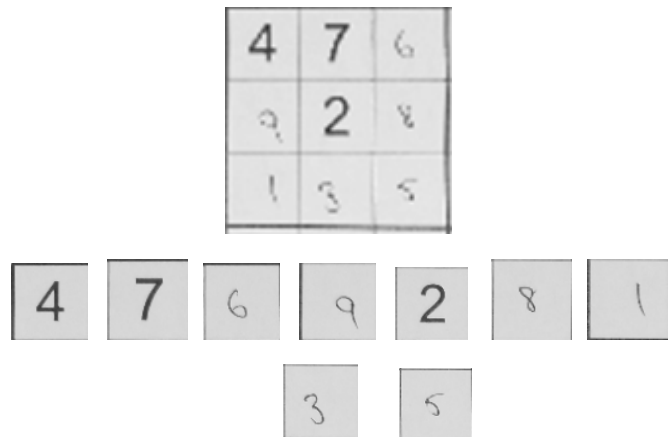


Fig. 9. Sliced Grids of Sudoku Image.

```
4 is digital number
7 is digital number
6 is handwritten number
9 is handwritten number
2 is digital number
8 is handwritten number
1 is handwritten number
3 is handwritten number
5 is handwritten number
9 is digital number
6 is handwritten number
1 is digital number
3 is digital number
2 is handwritten number
2 is handwritten number
4 is handwritten number
8 is handwritten number
7 is handwritten number
6 is digital number
```

Fig. 10. Recognized and Classified Handwritten and Printed Digits.

```
4,7,X,9,X,1,6,X,5
X,2,X,3,X,X,X,8,4
X,X,X,X,X,X,X,X,1
X,1,4,7,X,8,X,5,X
6,X,X,2,X,3,X,X,9
X,3,X,6,X,5,8,1,X
8,X,X,X,X,X,X,X,X
5,9,X,X,X,4,X,2,X
7,X,1,5,X,2,X,9,8
```

Fig. 11. Printed Digits are Stored in the Array Format.

## VI. SIGNIFICANCE AND SCOPE OF STUDY

The proposed model can be used for reducing manual work in education and merchant sectors. It may also play a crucial role in number recreations.

Nowadays, when the tip calculation is done manually, that may sometimes end with miscalculation. To avoid the miscalculation, the receipt can be scanned so that our model can predict the tip for automatically accurate total amount calculation. This may help with the reduction of profit loss for merchants.

In few education sectors, feedback and multiple-choice questions are still given in old paper writing format. To avoid manual correction and ranking, our model can be used for enhanced accuracy.

## VII. CONCLUSION AND FUTURE WORK

A model to recognize and classify both printed and handwritten digits was created using python version 3 in jupyter notebook. The process was split into three phases and the agile methodology was followed for the project to create a model. The CNN model and various image processing techniques were used to achieve 98% of accuracy.

The model created to recognize and classify both the handwritten digits and the printed digits separately was implemented by using various machine learning techniques and image processing techniques [21]. The significance of the work is that since the model can recognize the handwritten letters as well with the printed letters, it will be possible that both handwritten and printed sentences can be identified and classified as well.

## ACKNOWLEDGMENT

The authors would like to express special thanks to the Society for Design and Process Science for their support for this research.

## REFERENCE

- [1] H. Lee, R. Grosse, R. Ranganath, and A. Y. Ng, "Convolutional deep belief networks for scalable unsupervised learning of hierarchical representations," in Proceedings of the 26th Annual International Conference on Machine Learning, ser. ICML '09. New York, NY, USA: ACM, 2009.
- [2] B. Wicht and J. Hennebert, "Camera-based sudoku recognition with deep belief network," in Soft Computing and Pattern Recognition (SoCPaR), 2014 6th International Conference of, Aug 2014.
- [3] Bishop, M. Christopher. "Pattern Recognition and Machine Learning," 2006 Springer.
- [4] Berthier, Denis. "The Hidden Logic of Sudoku," 2007 International conference.
- [5] Boyer, Christian. "Supplément de l'article "Les ancêtres français du sudoku", " on December 10, 2006. Retrieved August 3, 2009.
- [6] Lewis, R (2007) "Metaheuristics Can Solve Sudoku Puzzles" Journal of Heuristics, vol. 13 (4), pp 387-401.
- [7] Perez, Meir, and Marwala, Tshilidzi (2008) "Stochastic Optimization Approaches for Solving Sudoku,".
- [8] <http://intelligence.worldofcomputing/brute-force-search> Brute Force Search, December 14th, 2009.
- [9] P. Simha, K. Suraj, and T. Ahobala, "Recognition of numbers and position using image processing techniques for solving sudoku puzzles," in Advances in Engineering, Science and Management (ICAESM), 2012.
- [10] S. M. Shamim, Mohammad Badrul Alam Miah, Angona Sarker, Masud Rana, and Abdullah Al Jobair "Handwritten Digit Recognition using Machine Learning Algorithms," in Global Journal of Computer Science and Technology: D Neural & Artificial Intelligence Volume 18 Issue 1 Version 1.0 Year 2018 Type: Double Blind Peer Reviewed International Research Journal Publisher: Global Journals Online.
- [11] Baptiste Wicht, Jean Henneberty "Mixed handwritten and printed digit recognition in Sudoku with Convolutional Deep Belief Network," in International Conference of August 2015.
- [12] M. Abadi et al., "TensorFlow: A System for Large-Scale Machine Learning TensorFlow: A system for large-scale machine learning", 12th USENIX Symposium on Operating Systems Design and Implementation (OSDI'16).
- [13] Y. Lecun, C. Cortes, C. J. C. Burges, The MNIST Database" Courant Institute NYU, 2014.
- [14] V. Nair, G. E. Hinton, "Rectified Linear Units Improve Restricted Boltzmann Machines", Proc. 27th Int. Conf. Mach. Learn.
- [15] R. Salakhutdinov, G. Hinton, "Replicated softmax: An undirected topic model", Adv. Neural Inf. Process. Syst. 22-Proc. 2009 Conf.
- [16] Y. LeCun, K. Kavukcuoglu, C. Farabet, "Convolutional networks and applications in vision", Circuits and Systems (ISCAS) Proceedings of 2010 IEEE International Symposium.
- [17] E. Alpaydin. "An Introduction to Machine Learning". The MIT press, Cambridge, Massachusetts, London, England, 2004.
- [18] T.CoverandP.Hart. "Nearest neighbor pattern classification". IEEE Transaction on Information Theory.

- [19] R.Duda, P.Hart, and D.Stork. "PatternClassification". Wiley Interscience, 2nd ed.
- [20] S. Eyheramendy, D. Lewis, and D. Madigan. "On the naive bayes model for text categorization". Proceedings Artificial Intelligence Statistics, 2003.
- [21] T. Mitchell. "Machine Learning". McGraw-Hill.
- [22] I. Rish. "An empirical study of the naive bayes classifier", 2001.
- [23] N. Roussopoulos, S. Kelley, and F. Vincent. "Nearest neighbor queries". International Conference on Management of Data, 1995.
- [24] K. Weise and W. Woger. "Comparison of two measurement results using the bayesian theory of measurement uncertainty". Measurement Science and Technology.
- [25] Q. J. Wu. "Machine Learning and Computer Vision". University of Windsor, Windsor, ON, Canada, 2007.
- [26] R. Deriche, "Using Canny's criteria to derive a recursively implemented optimal edge detector", Int. J. Computer Vision.
- [27] M. A. Nielsen, "Neural Networks and Deep Learning", Determination Press, 2015.
- [28] M. Perez and M., Tshildzi, "Stochastic Optimization Approaches for Solving Sudoku", 2008.
- [29] P. J. Simha, K. V. Suraj, and T. Ahobala, "Recognition of Numbers and Position using Image Processing Techniques for Solving Sudoku Puzzles", 2012.
- [30] B. Wicht and J. Hennebert, "Camera-based Sudoku recognition with Deep Belief Network", 2014.